

Are Long Leg Radiographs Necessary for Assessing Alignment Prior to Total Knee Arthroplasty?

*Anoop Chandrashekar - Vanderbilt - Nashville, United States of America

John Ryan Martin - Vanderbilt Health - Hendersonville, USA

Gregory Polkowski - Vanderbilt University Medical Center - Nashville, USA

Martin Faschingbauer - Department of Orthopedic Surgery, RKU, University of Ulm - Ulm, Germany

Courtney Baker - Vanderbilt - Nashville, USA

Stephen Engstrom - Vanderbilt University Medical Center - Nashville, USA

Introduction: Long leg radiographs (LLR) are the gold standard for the assessment of lower limb alignment in preparation for total knee arthroplasty (TKA). However, short leg radiographs (SLR) are more commonly collected in practice. The objective of this study was to determine if knee alignment could be accurately determined with landmarks from SLR using a machine learning model.

Methods: Long leg radiographs from 566 German patients with osteoarthritis of the knee were manually annotated to measure mechanical hip-knee-ankle (mHKA) angles, mechanical lateral distal femoral angle (LDFA), and mechanical medial proximal tibial angle (MPTA). A machine learning model was trained using 455 LLR to recognize anatomic landmarks necessary to measurement alignment. The model was then tested on 111 LLR. The LLRs were also annotated using landmarks available on a SLR to measure the same angles necessary for CPAK classification. Bland-Altman plots were used to measure agreement in the measurements obtained from the LLR and SLR.

Results: Of the 566 patient osteoarthritic knees included, 160 were classified under CPAK Group 1 and 406 were classified under CPAK Group 3. The mean difference in mHKA between the LLR and SLR was 0.481° with 95% upper- and lower- level of agreement of 3.75° to -2.79° . LDFA and MPTA measured from LLR and SLR did not vary given that the same landmarks were available.

Conclusion: We find that SLR and LLR differ minimally in measurement of mHKA. Thus compared to the gold standard of LLR, SLR may be a suitable alternative to determining knee alignment. Further is necessary to determine if the minimal angle differences observed have any clinical significance or effect on outcome.

Effect of Patient Specific Alignment Total Knee Arthroplasty on Joint Line Obliquity and Joint Line Restoration

*Ittai Shichman - Tel-Aviv Sourasky Medical Center - Tel Aviv, Israel

Aiden Hadad - Tel Aviv Sourasky Medical Center - Tel Aviv, Israel

Addy S. Brandstetter - Tel Aviv Sourasky Medical Center - Tel Aviv, Israel

Itay Ashkenazi - NYU Langone Health - New-York, United States of America

Yaniv Warschwaski - Tel Aviv Sourasky Medical Center - Tel Aviv, Israel

Aviram Gold - Tel Aviv Sourasky Medical Center - Tel Aviv, Israel

Nimrod Snir - Tel Aviv Sourasky Medical Center - Tel Aviv, Israel

Introduction:

In total knee arthroplasty (TKA), knee anatomical restoration including joint line height and

obliquity have shown improved knee kinematics and outcomes. We compared the joint line

alteration between manual mechanical alignment and robotic assisted patient specific alignment.

An intraoperative surgical decision based on calculated parameters pre and intraoperatively to

reach an alignment tailored for each individual patient.

Methods:

This retrospective study assessed patients who underwent single implant design TKA for primary

osteoarthritis, either mechanical alignment with manual instrumentation (maTKA) or patient

specific alignment assisted with imageless robotic TKA (psaTKA). Preoperative and postoperative long standing AP X-ray imaging were used to measure joint line obliquity formed

between the proximal tibial joint line and the floor. Joint line height restoration was measured as

the distance from the femoral articular surface to the adductor tubercle.

Results:

A total 101 patients were included in each group. Demographics between the two groups

including age, sex, ASA, laterality, and BMI did not significantly differ. For the maTKA group,

pre to postoperative joint line obliquity significantly changed (3.11 ± 2.04 vs. 2.33 ± 1.51

degrees, $p < 0.001$). No significant changes were found in joint line height from pre to

postoperative (40.77 ± 4.51 vs. 40.61 ± 4.79 mm, $p = 0.81$). For the psaTKA group, pre to

postoperative joint line obliquity did not differ (2.55 ± 1.84 vs. 2.30 ± 1.42 degrees, $p = 0.28$).

Additionally, no significant changes were found in joint line height (41.29 ± 6.83 vs. 42.5 ± 6.25

mm, $p = 0.18$). Joint line obliquity changes from pre to postoperative were significantly

lower in the psaTKA group when compared to maTKA ($p < 0.01$)

Conclusion:

PSA utilizing robotic assisted TKA allows accurate reconstruction of joint line height and obliquity compared to manual mechanical alignment. This alignment strategy may improve post TKA kinematics and outcomes.

Figures



[Figure 1](#)

Real-Time Intraoperative Alignment Feedback in Navigated Total Knee Arthroplasty

*Allan Maas - Aesculap - Tuttlingen, Germany

Adrian Sauer - Aesculap AG - Tuttlingen, Germany

Ingrid Dupraz - Aesculap AG - Tuttlingen, Germany

Raphael Renaudot - B.Braun New Ventures - Freiburg, Germany

Daniel Alberto Vazquez Urena - B.Braun New Ventures - Freiburg, Germany

Radek Hart - Masaryk University - Brno, Czech Republic

Ludger Gerdesmeyer - Orthopaedic and Trauma Surgery, Kiel Municipal Hospital - Kiel, Germany

Djordje Lazovic - University Hospital of Orthopedics and Trauma Surgery Pius-Hospital - Oldenburg, Germany

Thomas M. Grupp - Aesculap AG - Tuttlingen, Germany

Introduction

The increasing popularity of alternative alignment approaches in total knee arthroplasty (TKA) observed in recent years poses new challenges for implant system manufacturers of whether allowing those alignments or restrict the intended use to the existing gold standard of mechanical alignment.

To estimate the changes in implant loading due to alignment variations, a finite element (FE) analysis framework for use in pre-clinical testing of TKA- implant combinations was developed and validated with data from instrumented implants [1,2,3]. This standardized framework considers subject variables and uses standardized, dynamic loading conditions that can be scaled to the subject level. Although the approach used to develop the method is substantially more efficient than the traditional way of using musculoskeletal modeling, it still requires manual setup and analysis of the situation to be analyzed.

Aim of this work was the implementation of the FE- framework capabilities into the surgical navigation workflow to provide and display the limits defined for a chosen implant type and size combination with respect to alignment and subject parameters.

Methods

The existing FE- simulation pipeline was simplified and split into a theoretical part that calculates dynamic moment reactions under scaled standardized loading conditions and a parallel FE- pipeline to characterize the implant system and its mechanical reaction on changing loading conditions. The combination of system characterization and altered reaction moments allows to display whether the planned implant type and position remains in an appropriate corridor.

The definition of the limits and threshold values of the corridors were based on the results of reference systems with good long-term results [4,5]. These corridors were integrated into the next generation of TKA navigation software (OrthoPilot® Aesculap AG Tuttlingen Germany).

Systematic analyses were additionally set up to compare the results of the simplified real time approach to the standardized FE- framework used in preclinical testing.

Results

Within the range of validation given by the cohort with instrumented implants, the simplified and real-time capable framework produces results that are comparable to the fully finite element-based approach used in pre-clinical implant testing without the need of additional simulation runs. The determined limits for implant positioning are displayed to the user using a simple color-coded range (*Figure 1*).

Conclusion

A biomechanical simulation framework was developed and integrated into the TKA-navigation workflow. The framework calculates a biomechanical corridor depending on the implant system and size combination used, the hip-knee-ankle (HKA) and posterior tibial slope angle as well as the subject's bodyweight. This feature will support surgeons to perform personalized alignment.

Figures

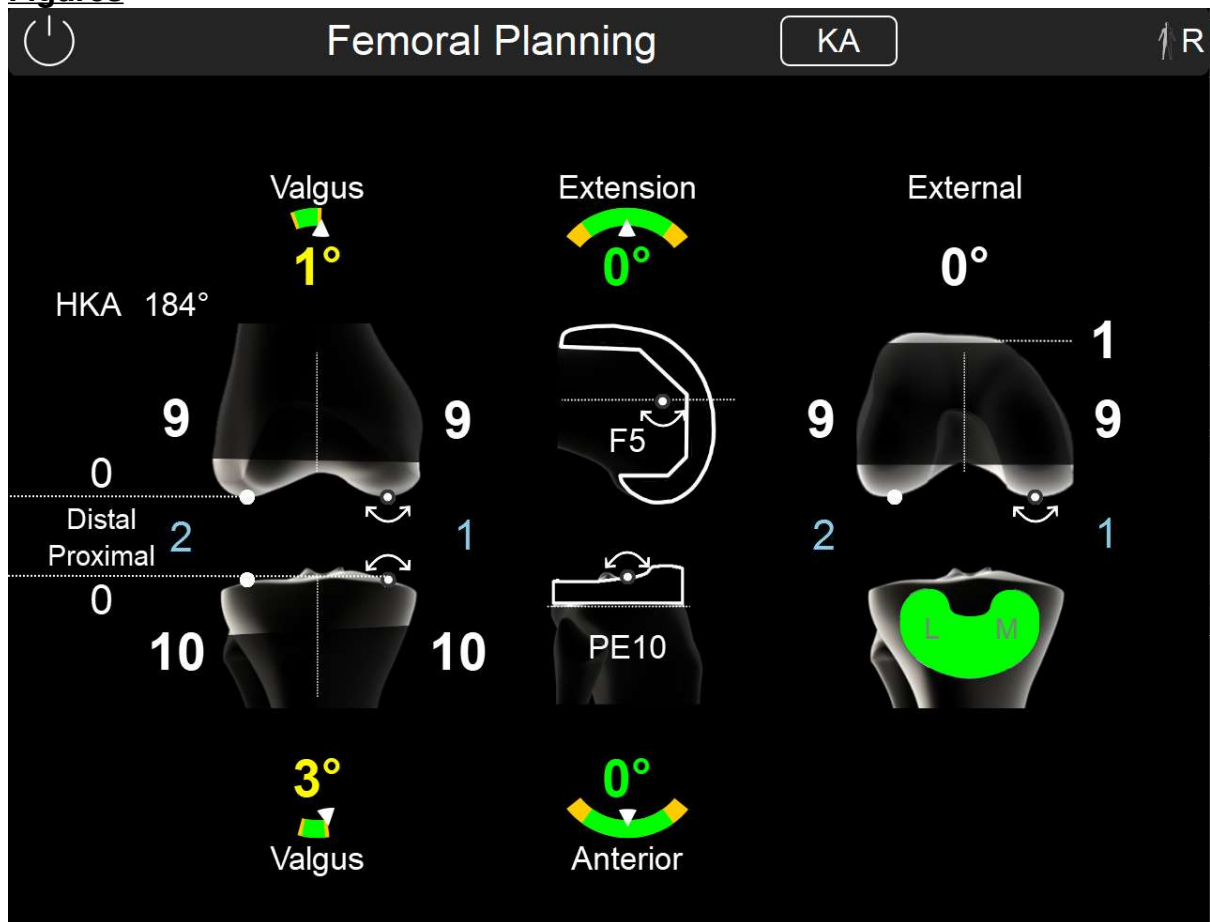


Figure 1

Measuring Static and Dynamic Frontal Plane Lower Limb Alignment Using Markerless Motion Capture

*Jacob Calderone - Queen's University - Kingston, Canada
Jereme Outerleys - Queen's University - Kingston, Canada
Kevin Deluzio - Queen's University - Kingston, Canada
Elise Laende - Queen's University - Kingston, Canada

Introduction

Lower limb alignment is typically measured from long-leg anterior-posterior radiographs. Static assessments, such as radiographs, do not appropriately capture potential alignment changes during dynamic weight-bearing movements [1]. Markerless motion capture is a computer-vision based tool that shows promise in quantifying lower limb alignment for both static and dynamic tasks. The objective of this study was to compare the frontal plane knee adduction angle (KAA) of patients during a quiet standing task and during the first half of stance of gait.

Methods

Patients diagnosed with knee osteoarthritis (OA) were recruited. During quiet standing, patients were instructed to stand still with their feet facing forward for thirty seconds. Gait was evaluated during over-ground walking at a self-selected speed for one minute. Theia3D (v. 2023.01.0.3161p7, Theia Markerless, Kingston, ON) processed the raw video data and biomechanical analysis was performed in Visual3D (v.2023.05.4, HAS-Motion, Kingston, ON). During quiet standing, the mean KAA was calculated over the first five seconds of the video recording. During gait, the peak KAA was identified in the first half of stance phase and averaged from all strides taken. A Bland Altman plot assessed agreement between alignment information from both tasks using R (v.2023.06.0).

Results

One hundred and twenty-eight subjects (45 male, 83 female, mean age 66 years (SD 9)) were analyzed in this study. The mean KAA from the quiet standing task (mean = 1.94°, SD = 3.7) and the peak KAA from the first half of stance of gait (mean = 4.3°, SD = 3.9) were highly correlated (Spearman's $r = 0.90$, $p < 0.0001$). The mean KAA from quiet standing explained 85% of the variance in the peak KAA during gait. The peak KAA during gait was on average 2.4 degrees more varus than standing (Figure 1).

Conclusion

Lower limb alignment measures from the static and dynamic tasks were found to be strongly correlated, which is consistent with previous work [1]. Similar to Zhang et al., we also found that dynamic lower limb alignment was on average more varus than static alignment [2]. Markerless motion capture is a minimally resource intensive tool to collect biomechanical data during both static and dynamic tasks and in turn shows potential to act as an additional assessment modality for the treatment of musculoskeletal diseases.

References

[1] Hunt et al., 2008. *Gait Posture*, vol. 27, no. 4, pp. 635-640. [2] Zhang et al., 2021. *Appl. Bionics Biomech*, vol. 2021, p. 6231406.

Figures

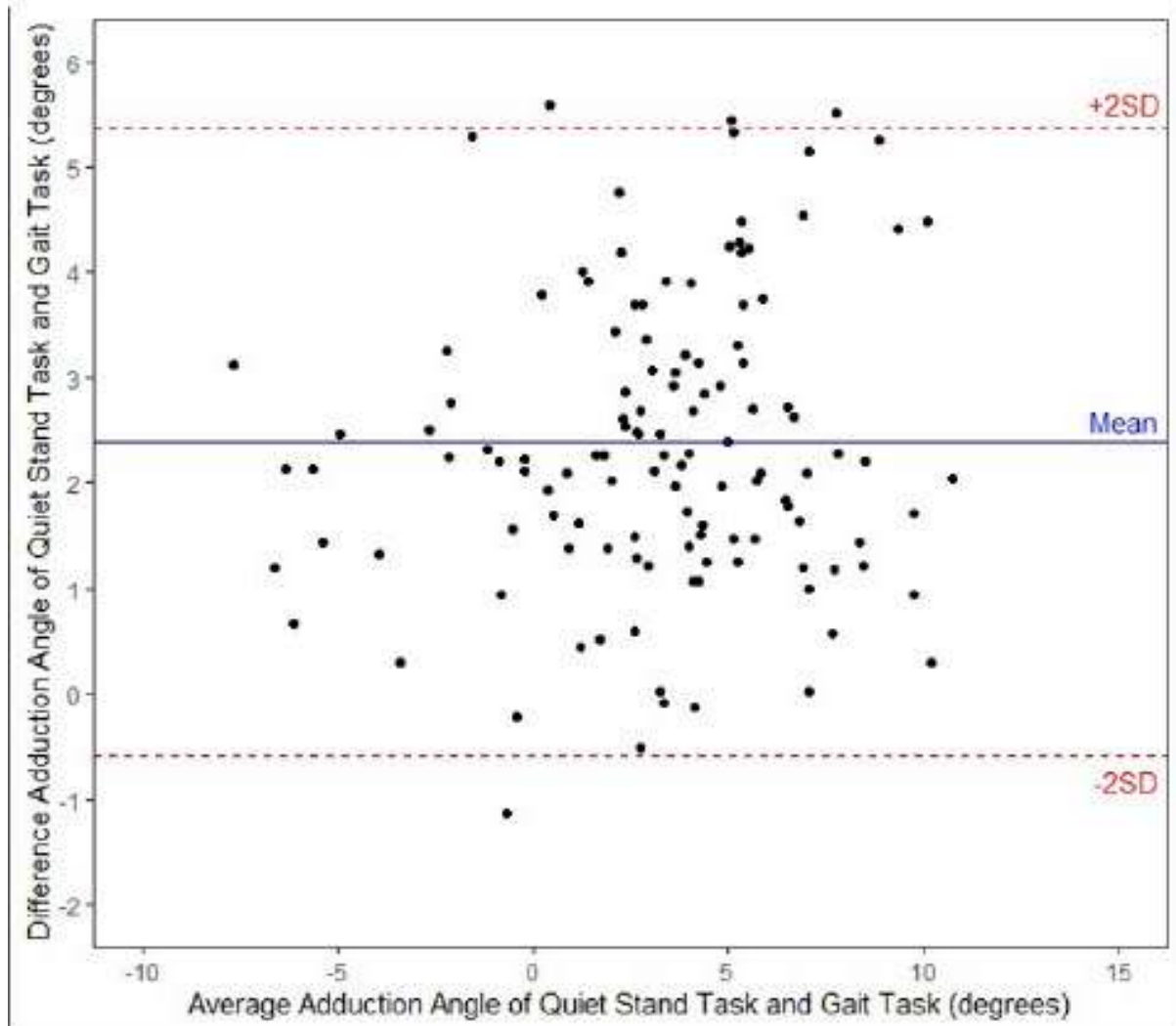


Figure 1: Bland Altman plot of the mean KAA from quiet stand and the peak KAA from the first half of stance of gait. Positive values represent varus alignment and negative values represent valgus alignment.

[Figure 1](#)

Analyzing the Effects of Tibial Plate Positioning on Patellofemoral Mechanics in TKA Subjects Using a Forward Mathematical Model of the Knee

*Caleb Chesney - University of Tennessee - Knoxville, USA

Michael LaCour - University of Tennessee - Knoxville, USA

Bradley Meccia - University of Tennessee - Knoxville, United States

Richard Komistek - The University of Tennessee - Knoxville, USA

INTRODUCTION

Robotic total knee arthroplasty (TKA) has undoubtedly improved the precision of component placement. Unfortunately, there remains a lack of consensus regarding “accurate” component placement, and the tibial component remains particularly vague [1]. It has been shown that femoral component positioning can yield abnormal kinematics and contact/ligament forces [2]. While various medially conforming systems aim to improve stability and recreate native kinematic patterns, the resulting patellofemoral mechanics are largely understudied, particularly in the cases of tibial misalignment. Thus, the objective of this study is to use mathematical modeling to investigate the effects of tibial tray position on the patellofemoral mechanics for three medially stabilized TKA systems.

METHODS

A single subject was virtually implanted with Medial Stabilized (DePuy Inc.), Medial Congruent (Zimmer Biomet Inc.), and Condylar Stabilized (Stryker Inc.) TKAs, all cruciate-retaining in Mechanical Alignment with 6° posterior tibial slope. Subjects underwent a deep knee bend to 120° flexion using a validated mathematical model [3]. Tibial alignment variations included $\pm 4^\circ$ adjustments to the varus/valgus (V/V) cut, 3° increments of the slope cut, and $\pm 5^\circ$ adjustments to I/E rotation (Figure 1). Parameters of interest include patellar rotation and translation with respect to the tibia as well as patellofemoral (P-F) force.

RESULTS

Varus/Valgus alignment changes seemed to have the largest effect on patellar kinematics, yielding approximately 4° of variability in patellar A/P rotations and 6mm of variability in patellar M/L translations (Figure 2). Interestingly, I/E rotations had a significant effect on the Medial Congruent TKA. The Medial Stabilized system appeared to yield more controlled motion patterns, demonstrating minimal I/E rotations and more gradual changes in kinematics throughout flexion, while the other systems had abrupt changes during the first 30° of flexion.

V/V alignment changes also had the largest effect on patellar kinetics, with valgus cuts shifting the force laterally and varus cuts shifting the force medially (Figure 3). The Medial Stabilized system appeared to experience improved biomechanics, maintaining the lowest overall P-F force, while the Condylar Stabilized system experienced the highest.

DISCUSSION

Component alignment variations can have unexpected consequences on patellofemoral biomechanics. As component positions change, patellar tracking follows trochlear groove guidance. However, the locations of the tibial tuberosity and quadriceps origins remain unchanged, so misalignments can yield unexpected patellar mechanics with respect to the bones. It is important for a system’s trochlear

groove to remain constrained enough to be stable yet robust enough to allow the patella to follow the path that the soft tissues guide.

REFERENCES

- [1] Indelli PF “Rotational alignment of the tibial component in total knee arthroplasty.” *Ann Transl Med.* 4(1):3. (2016 Jan). doi: 10.3978/j.issn.2305-5839.2015.12.03. PMID: 26855939; PMCID: PMC4716934.
- [2] Nishitani K, et al. “Excessive flexed position of the femoral component causes abnormal kinematics and joint contact/ ligament forces in total knee arthroplasty.” *Scientific Reports.* Volume 13, Article number: 6356 (2023). <https://doi.org/10.1038/s41598-023-33183-2>.
- [3] Khasian M, Meccia BA, LaCour MT, Komistek RD. “Effects of posterior tibial slope on a posterior cruciate retaining total knee arthroplasty kinematics and kinetics.” *The Journal of Arthroplasty,* 36 (7), 2379-2385 (2021). doi: 10.1016/j.arth.2020.12.007

Figures

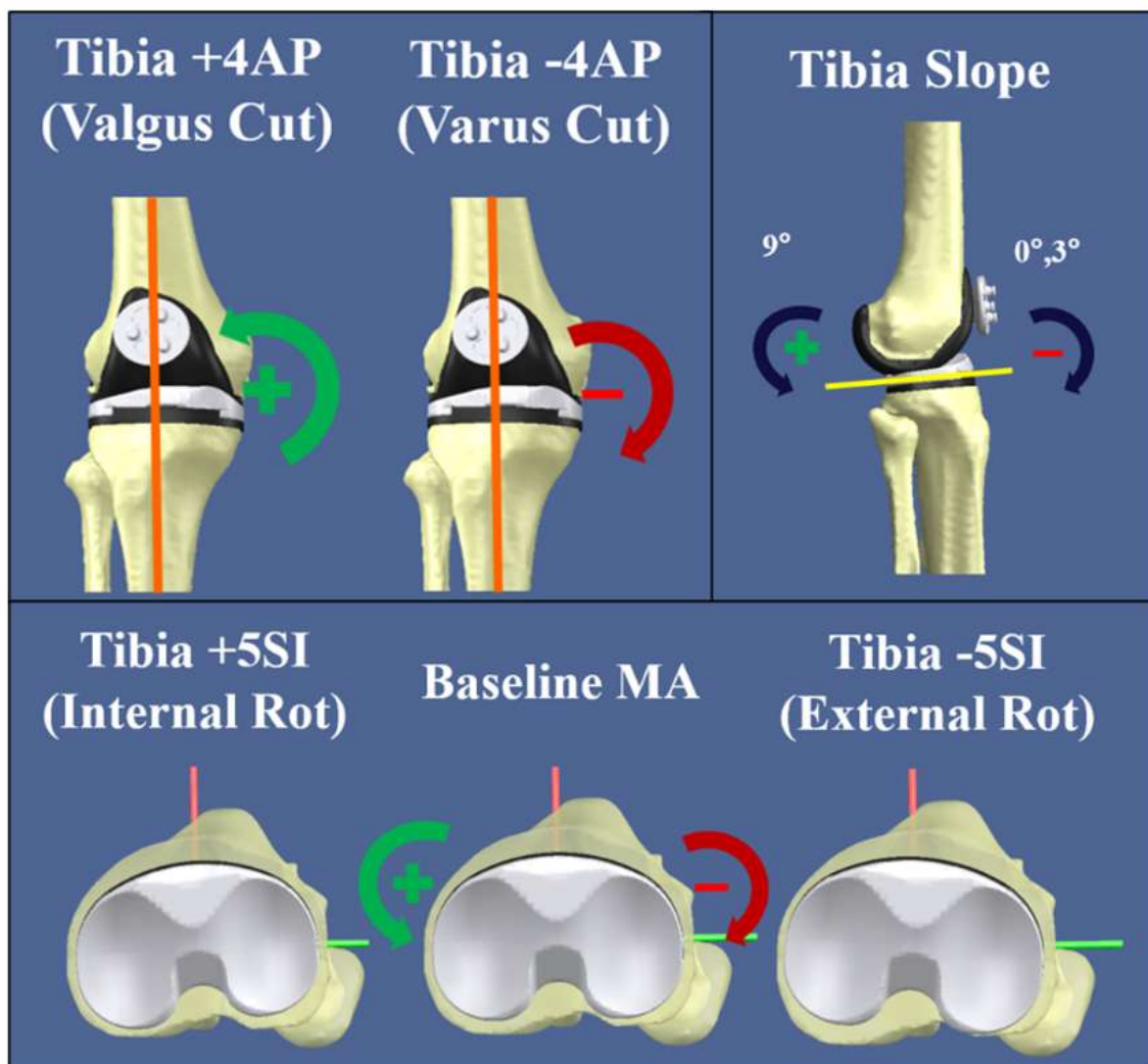


Figure 1: Visualization of all adjustments and directions made to the tibial tray.

[Figure1](#)

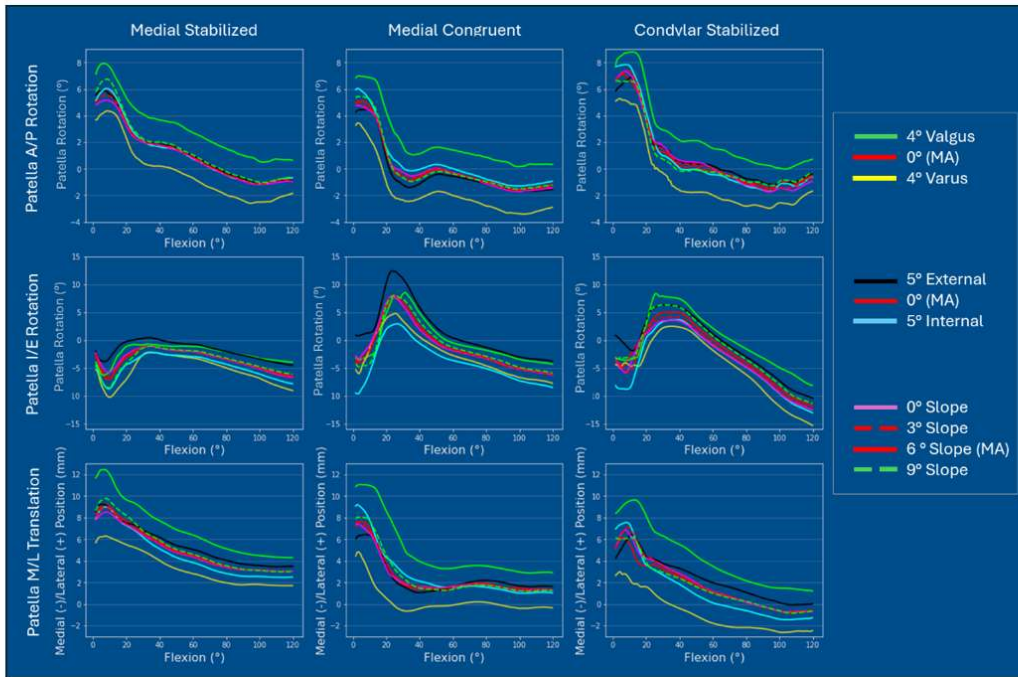


Figure 2. Primary Kinematic Outputs (Anterior/Posterior rotation, Internal/External rotation, and Medial/Lateral translation with respect to the tibia) versus Flexion. Positive A/P angles indicate the proximal aspect of the patella shifting laterally, positive I/E angles indicate internal rotation, and positive M/L translations indicate lateral positioning.

Figure 2

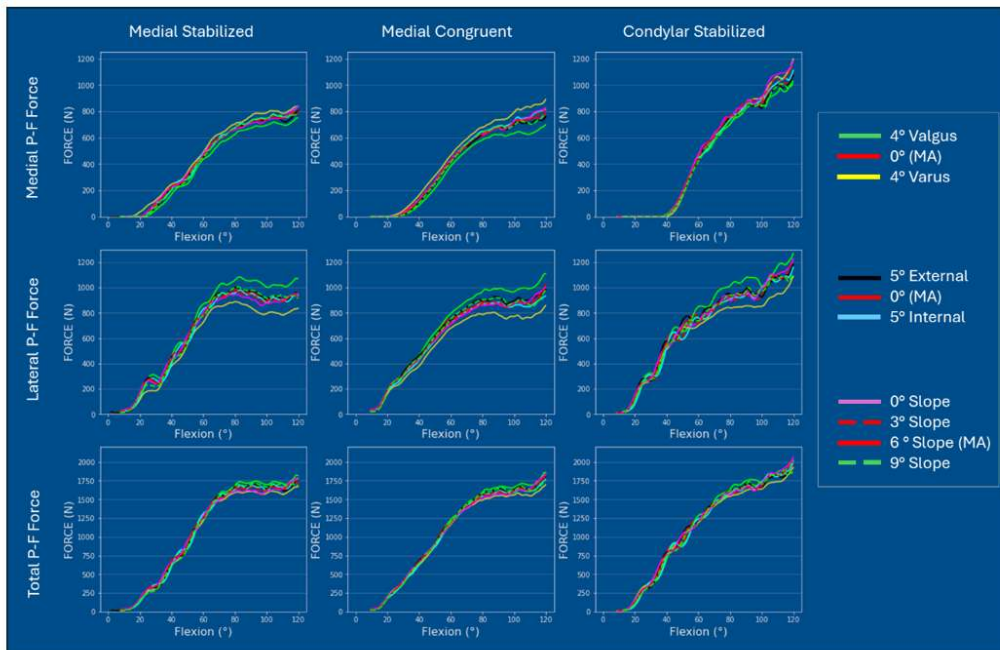


Figure 3. Patellofemoral (P-F) forces in Newtons. Plots are arranged with Medial P-F on the top row, Lateral P-F in the middle, and Total P-F on the bottom.

Figure 3

Variations in Bone Mineral Density After Joint Replacement: A Systematic Review Examining Different Anatomical Regions, Fixation Techniques, and Implant Design

*Domenico Alesi - IRCCS Istituto Ortopedico Rizzoli - Bologna, Italy

Davide Valente - Istituto Ortopedico Rizzoli - Bologna, Italy

Stefano Zaffagnini - Researcher Istituti Ortopedici Rizzoli - Bologna University Sports - Bologna, Italia

Giulio Maria Marcheggiani Muccioli - University of Bologna - Bologna, Italy

Laura Bragonzoni - University of Bologna - Bologna, Italy

Raffaele Zinno - University of Bologna - Bologna, Italy

Introduction

The aim of this study is to evaluate the postoperative periprosthetic bone mineral density (BMD) at various time points following joint replacement with different implant designs and fixation techniques, providing insights for future studies.

Methods

Database search was conducted on MEDLINE (PubMed), Scopus, Cochrane Central Register of Controlled Trials, Web of Science, and CINAHL according to the PRISMA guidelines for studies analyzing bone remodeling after joint replacement between March 2002 and January 2024. A Risk of bias critical appraisal of each article included in the review was conducted using the "Revised Cochrane risk-of-bias tool for randomized trials" for randomized controlled trial, and the Joanna Briggs Institute Critical Appraisal tools was used according to the specific study design.

Results

After the screening, 68 articles matched the selection criteria and were included in the study. Of them, 55 articles analyzed the hip joint, 12 the knee and only 1 the shoulder. The greatest bone resorption after total hip arthroplasty was recorded at the level of the proximal femur, with a negative peak at 6 months after surgery [Fig. 1]. Analyzing Gruen`s zones separately, it emerged how different patterns of load transfer produced greater bone resorption at the proximal femur, where there is a high strain energy density. The use of cemented implants and tapered stems induced more bone resorption than cementless implants and anatomical stems, with specific remodeling patterns [Fig. 2-3]. BMD around the acetabular component decreased in the first 6 months and then increased in the regions most subjected to loading forces. In total knee arthroplasty, an evident bone loss was reported in the anterior part of the distal femur and the medial tibial plateau [Fig. 4]. Cemented implants and posterior stabilized design showed higher bone loss than cementless implants and cruciate-retaining design [Fig. 5-6].

Conclusions

Specific patterns of bone remodeling emerged depending on the anatomical region, fixation technique, and implant design. However, gaps in knowledge still exist regarding the mechanisms governing this phenomenon. Future studies should focus on the metabolic activation state of periprosthetic bone, the influence of alternative, more biocompatible materials and of cementless implant for the knee joint.

Figures

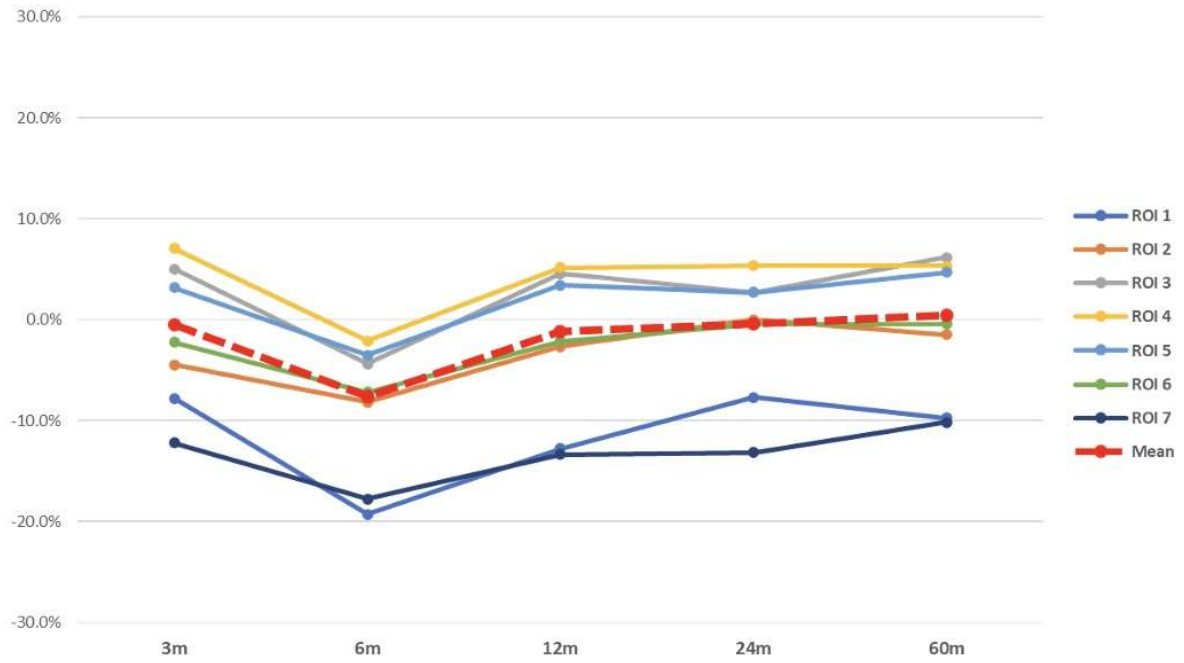


Figure 1. Temporal Variation (%) in femoral Bone Mineral Density across ROIs between the baseline and Follow-up.

[Figure1](#)

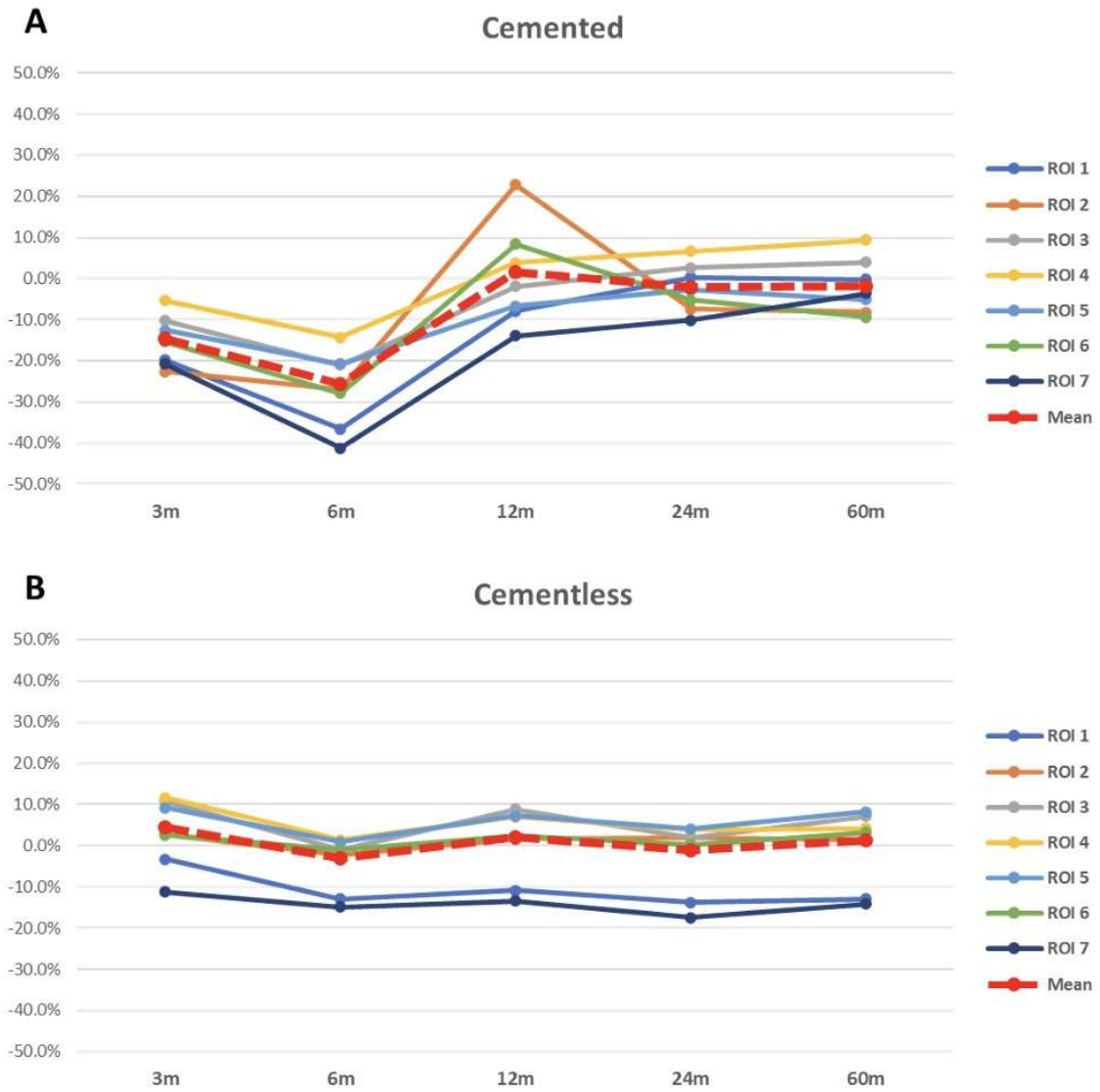


Figure 2. Femoral Bone Mineral Density comparison between Cemented and Cementless stems in THA across ROIs between the baseline and Follow-up times. Note: A, Cemented stems BMD; B, Cementless stems BMD.

[Figure2](#)

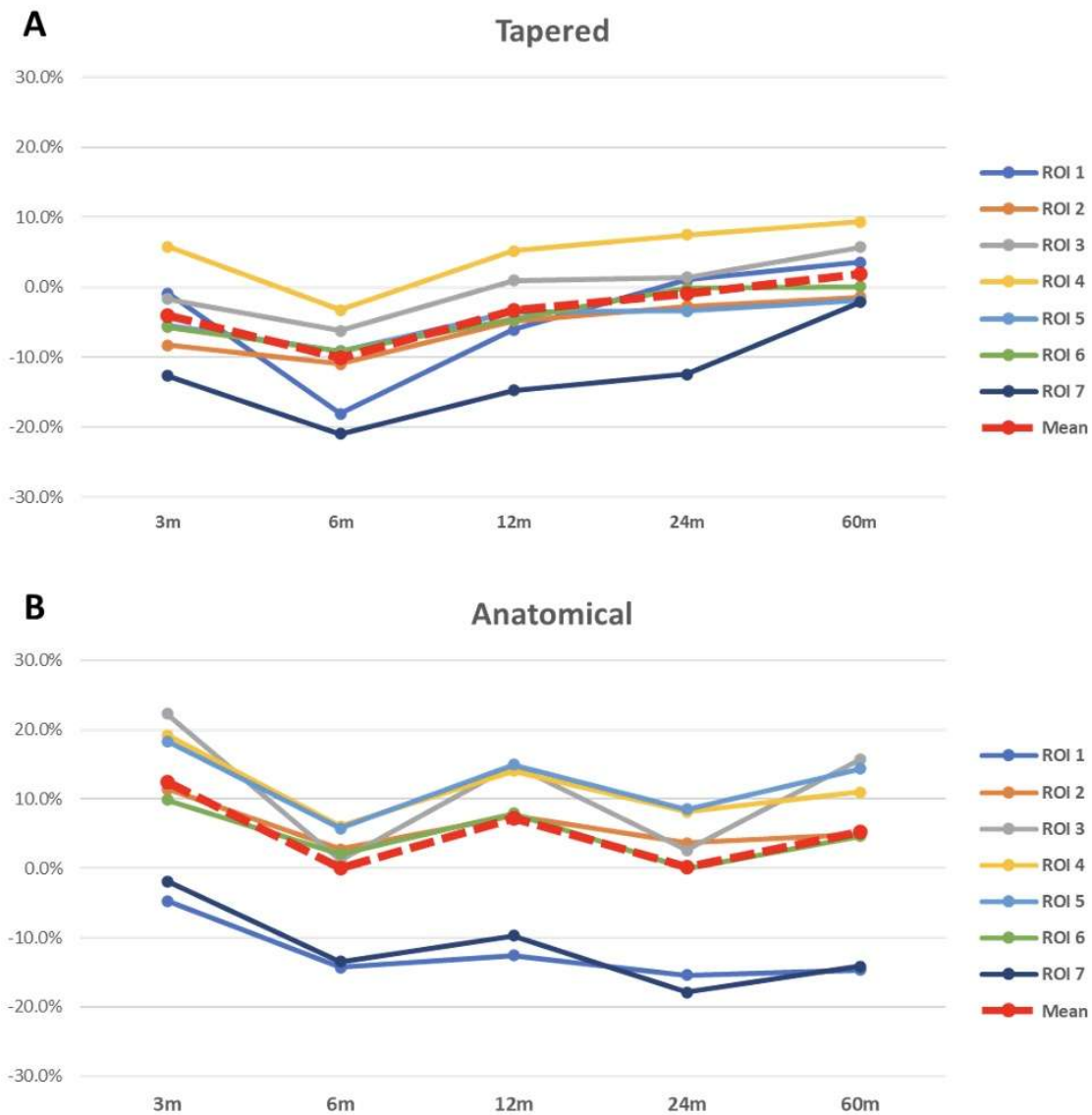


Figure 3 | Femoral BMD Comparison between Stem Designs THA across ROIs between the baseline and Follow-up times. Note: A, Tapered stems; B, Anatomical stems.

Figure3

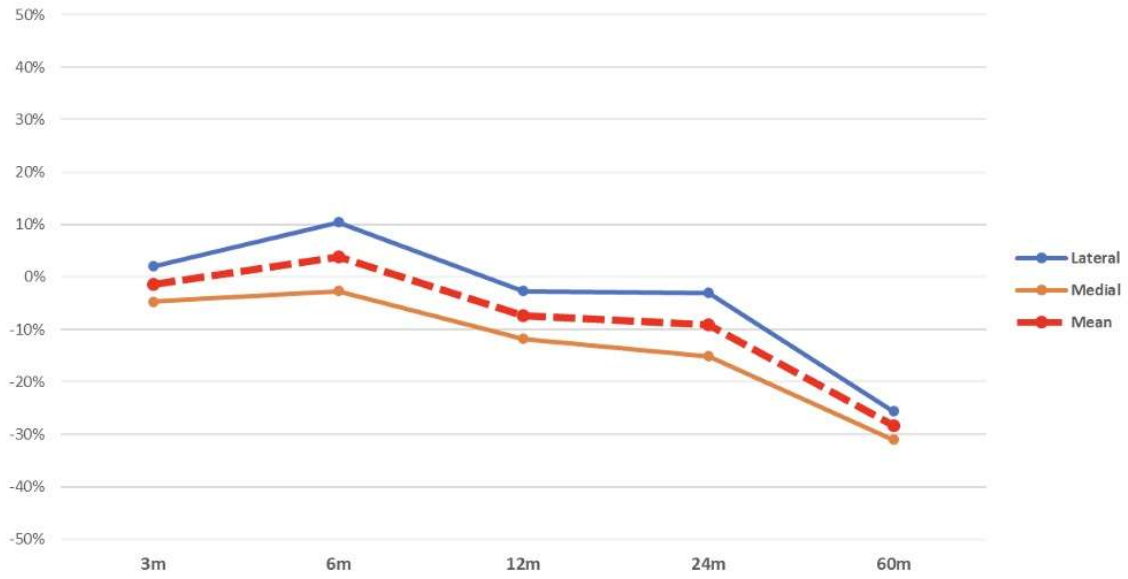


Figure 4. Temporal Variation (%) in tibial Bone Mineral Density across ROIs between the baseline and Follow-up times.

[Figure4](#)

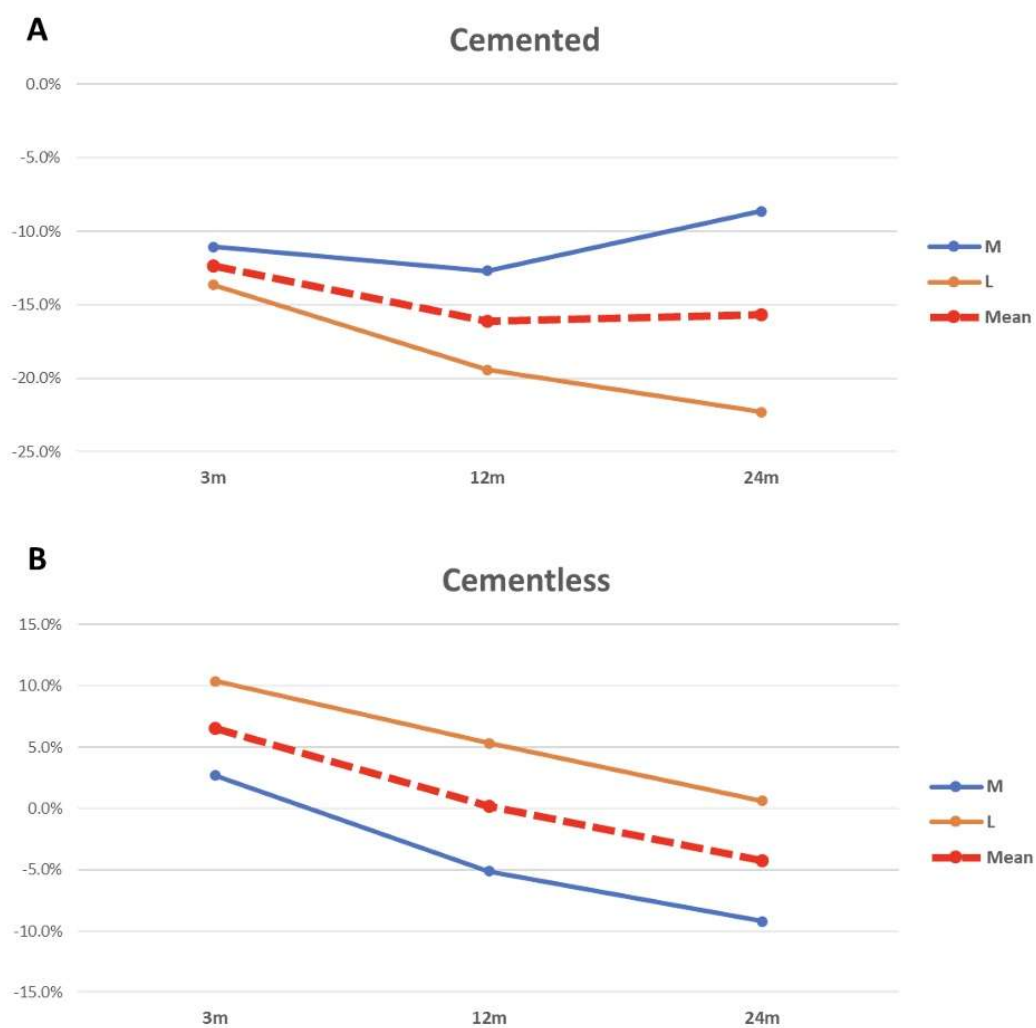


Figure 5. BMD Comparison between Cemented and Cementless TKR across ROIs between the baseline and Follow-up times. Note: A, Cemented knee prosthesis; B, Cementless knee prosthesis.

[Figure5](#)

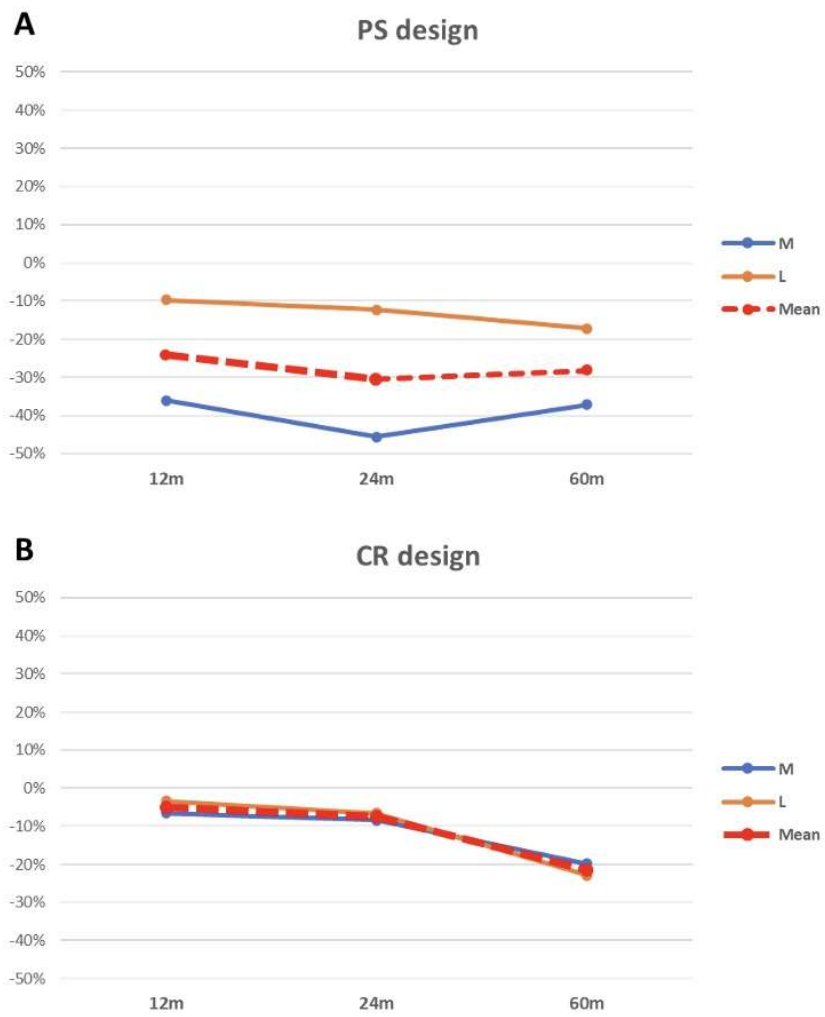


Figure 6. BMD Comparison between Knee prosthesis design across ROIs between the baseline and Follow-up times.

Note: A, Posterior stabilized design; B, Cruciate retaining design.

[Figure 6](#)

Effect of Zoledronic Acid on Femoral Periprosthetic Bone Mineral Density After Total Hip Arthroplasty: A Longitudinal Observational Study

*Wataru Ando - Osaka University Graduate School of Medicine - Suita, Japan

Nobuhiko Sugano - Osaka University Graduate School of Medicine - Suita, Japan

Masaki Takao - Osaka University Graduate School of Medicine - Suita, Japan

Hidetoshi Hamada - Osaka University - Suita, Japan

Keisuke Uemura - Osaka University - Suita, Japan

[Introduction] The well-established benefits of bisphosphonates on periprosthetic bone mass and bone strength contrast with the unclear impact of osteoporosis pharmacotherapy on improving stress shielding-induced bone loss following total hip arthroplasty (THA). Zoledronic acid, administered intravenously annually with high adherence, presents a potential solution. This prospective observational study aimed to assess the effect of zoledronic acid on post-THA bone mineral density (BMD) decline.

[Methods] BMD assessments were conducted on 60 hips of 47 patients who underwent THA utilizing Versys Fiber Metal® (Zimmer Biomet) between December 2000 and December 2003, with a follow-up duration exceeding 15 years. The bone mineral density (BMD) of these patients was examined. Initial BMD evaluations at surgery and 1-2 years post-surgery were available for 17 hips of 12 female patients (mean age at surgery 56.4 years), followed over 15 years. Patients exhibiting a YAM (young adult mean) value below 75% were diagnosed with osteoporosis/osteopenia and treated with zoledronic acid annually. Follow-up assessments were conducted up to 2 years post-administration. Changes in femoral BMD were examined in 12 hips of 8 female patients (mean age at administration 71.8 years).

[Results] Lumbar spine BMD exhibited an average decline to 74% 17 years post-surgery, with a comparable decline observed in Zones 3, 4, and 5 (Figure 1). Conversely, zones 1, 2, 6, and 7 exhibited more pronounced declines, notably Zone 7, which experienced a 72% reduction within 1-2 years post-surgery and a 32% decline over 17 years (Figure 1). Zoledronic acid administration led to an 8.3% increase in lumbar vertebral BMD two years post-administration, while femoral BMD in Zones 1-6 showed an increase compared to pre-administration levels (Figure 2). Zone 7 initially decreased to 95% six months post-administration but subsequently recovered to 99% by the two-year mark.

[Conclusion] Following THA, femoral BMD declines, particularly evident in Zone 7 over 17 years, while zoledronic acid effectively suppresses subsequent BMD decline across all zones. These findings indicate the potential of zoledronic acid as a therapeutic avenue in improving post-THA bone loss.

Figures

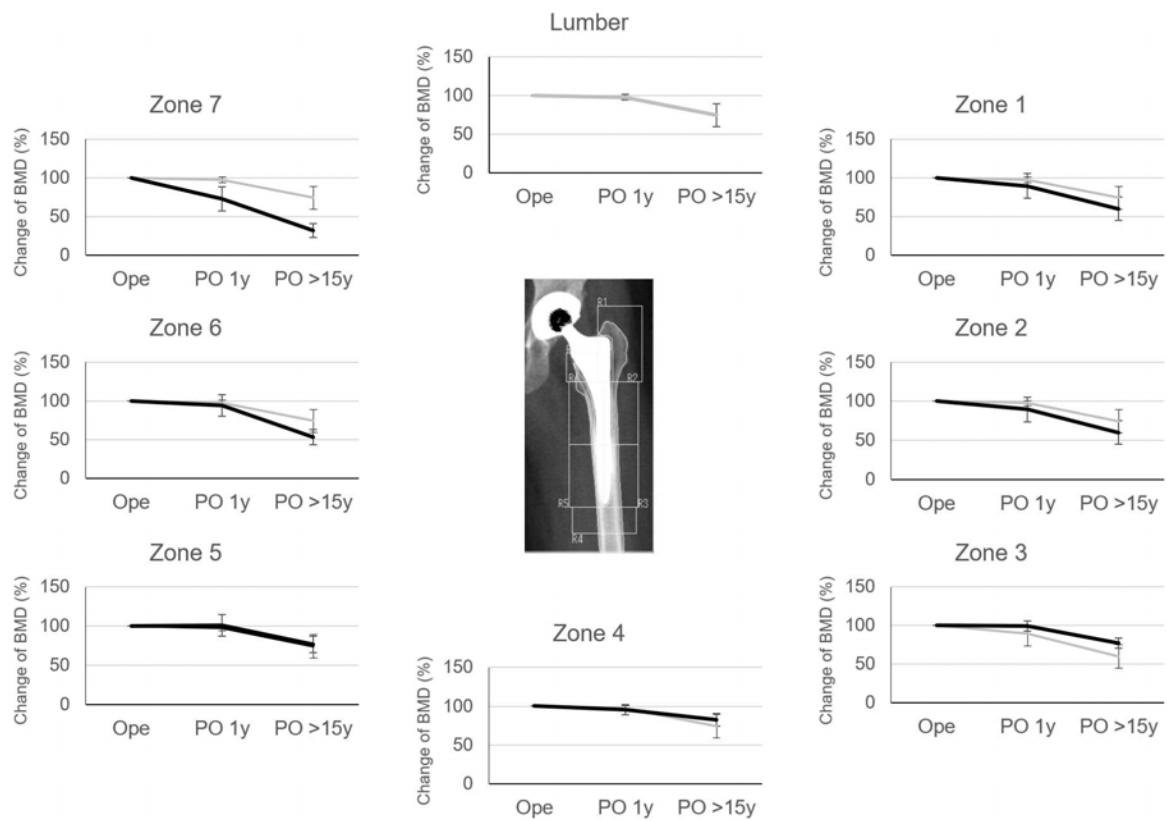


Figure 1

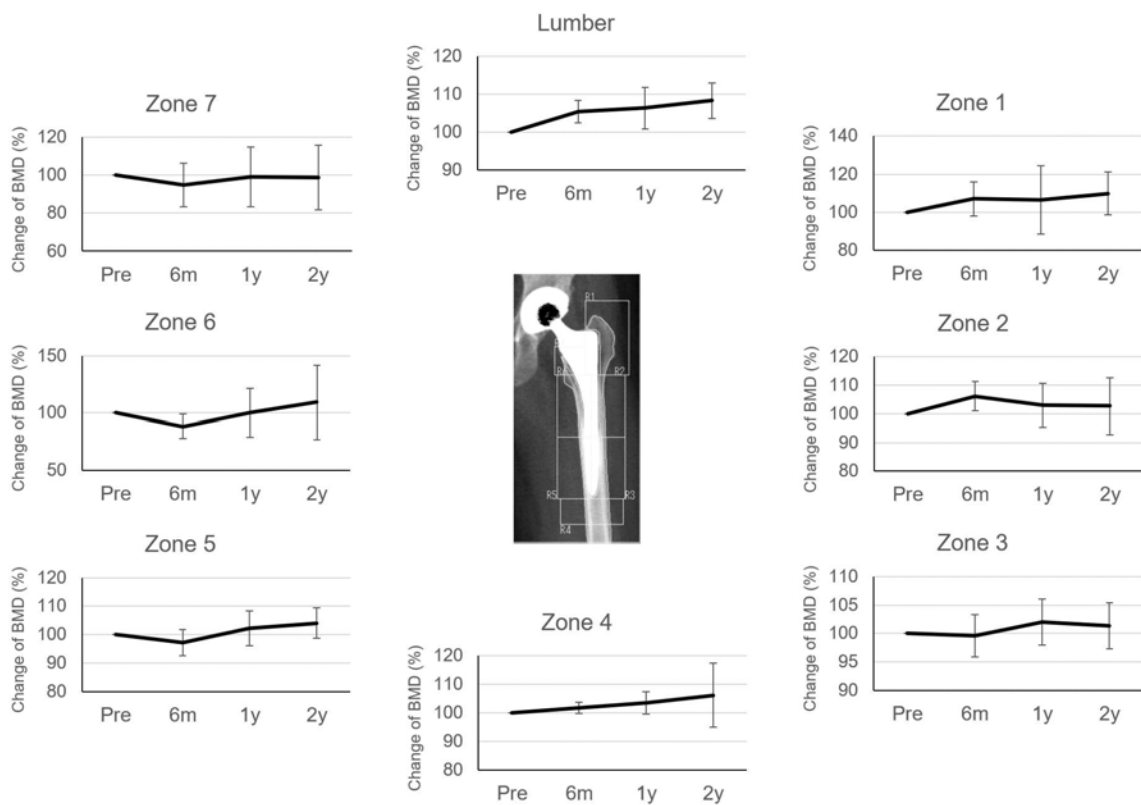


Figure 2

Does the French Paradox Cementing Technique Improve or Compromise Femoral Stem Stability? an *in Vitro* Cadaver Study

*Yizhao Li - Western University - London, Canada

Stefan George - London Health Sciences Centre - London, Canada

Jarrett Masse - Western University - London, Canada

Brent Lanting - London Health Sciences Centre - London, Canada

Ryan Willing - Western University - London, Canada

Introduction: Despite the success of total hip arthroplasty (THA), debate persists regarding the optimal femoral cementing technique. The French Paradox technique that consists of line-to-line cementing with a press-fit canal-filling stem has recently been applied to polished tapered stems with favorable results, despite that the resulting thinner thickness of cement mantle may fail to meet the minimum thickness of 2 mm suggested to mitigate mechanical failure and loosening of the implant. This study aims to compare the French Paradox (FP) with the standard (SD) cementing technique by comparing the resulting micromotions under clinically relevant loads in paired cadaveric femora.

Methods: Four pairs of fresh-frozen human cadaveric hip specimens were prepared for a single design polished tapered cemented THA stem. Specimens were CT-scanned pre-implantation to ensure no fractures or neoplasms, and to plan stem size. The left and right femora were randomly allocated to receive either the traditional 2 mm cement mantle or line-to-line cementing. Stems were implanted, and then a small (~1 cm diameter) hole was drilled through the bone and cement to the lateral surface of the stem at a distance of 25% stem's length from the stem's distal tip to access a pre-drilled threaded hole for an outrigger. Five Linear Variable Displacement *Transducers* (LVDTs) were mounted on the bone and employed to measure the real-time motions of the stem relative to the femur (Figure 1) (2 proximal LVDTs that measured anterior-posterior (AP) and medial-lateral (ML) motions, 3 distal that measured AP, ML and interior-superior (IS) motion of the outrigger). The specimens were potted and mounted onto a joint motion simulator (AMTI VIVO) and were then loaded for five thousand cycles of axial compression (0-1600 N) followed by five thousand cycles of internal torsion (0-15 Nm torsion and constant 1600 N compression). Migration was measured by the average change in length of each LVDT between the beginning to end of each experiment. Inducible motion was measured as the full range of motion of each LVDT over 20 loading cycles, evaluated at the beginning and end of each experiment.

Results: While no statistically significant differences were observed, four over the total five average migration measurements of stems trended greater with the FP for both axial and torsional loading scenarios (Fig. 2a and Fig.3a). Likewise, no statistically significant differences in initial and long-term inducible motion were observed, except for the greater distal initial ML micromotions ($p=0.036$) for the FP under axial loading (Fig. 2b and c, Fig.3b and c).

Conclusion: Based on the results of this *in vitro* cadaveric study, there are no statistically significant differences in stem migration resulting from using the FP cementing technique. This is based on a small number of specimens with high variability, and significant differences might emerge with larger samples. The trend of greater migration and inducible motion using the FP technique is interesting and warrants further study; however, the mean inducible motions were less than 100 μm

for either cementing technique, suggesting either approach results in well-fixed stems.

Figures

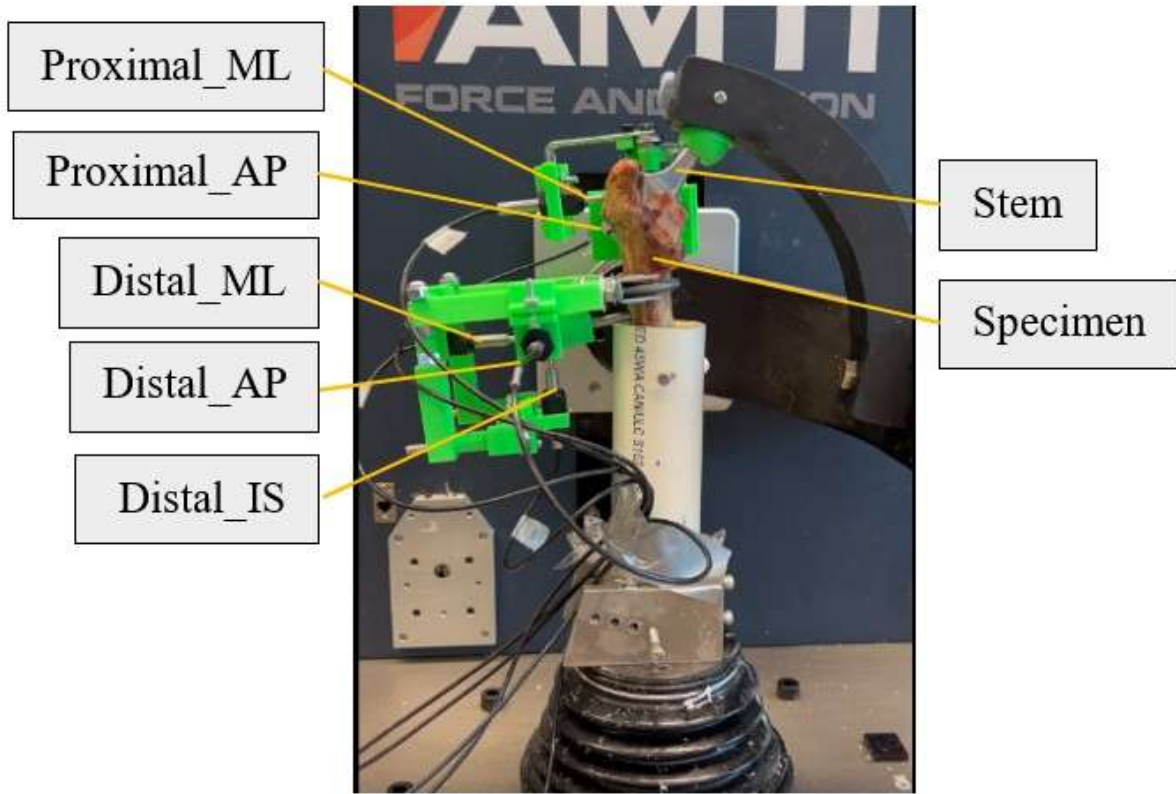


Figure1

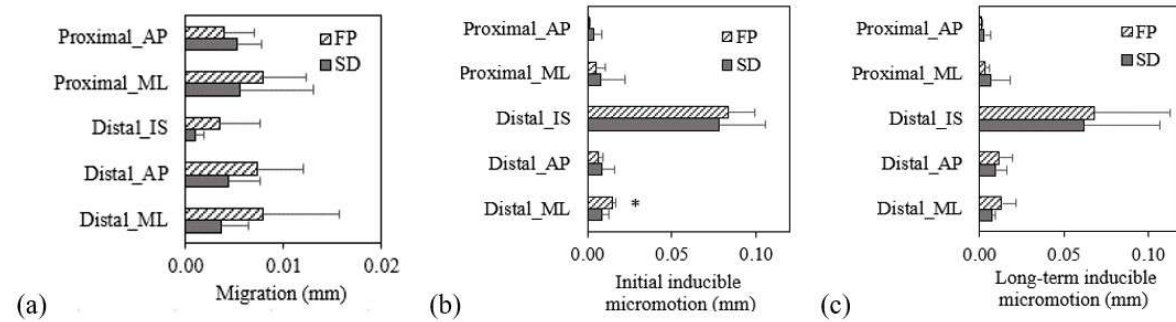


Figure2

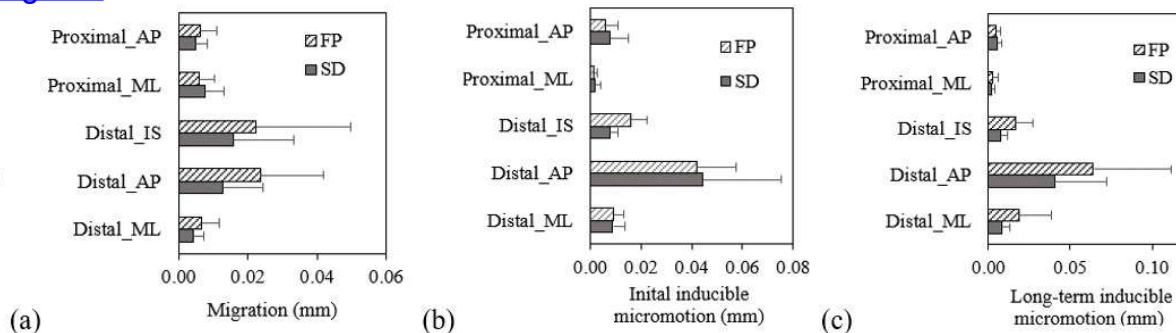


Figure 3

Plus 4 and Neutral Liners in Primary Total Hip Arthroplasty: Review of Survivorship and Clinical Outcomes From a Multi-Center Registry

*David Fawley - DePuy Synthes - Warsaw, USA

Kirk Kindsfater - Orthopaedic Center of the Rockies - Fort Collins, USA

David F Dalury - Baltimore, USA

Robert Gorab - Hoag Orthopedic Institute - Irvine, United States of America

William P Barrett - Renton, USA

Timothy Alton - Proliance Orthopedic Associates - Renton, USA

Donald Pomeroy - Arthroplasty foundation - Louisville, United States of America

John F Irving - New Haven, USA

Michael Swank - The Christ Hospital Health Network - Cincinnati, USA

Andrew Spitzer - Cedars-Sinai Medical Center - Los Angeles, United States of America

America

Sean Croker - Depuy Synthes - West Chester, USA

Introduction

During total hip arthroplasty (THA), if the cup has been medialized to gain coverage, it can be advantageous to use a lateralized liner to help restore proper center of rotation. Because the lateralized liner also adds offset it can help avoid bony impingement during range of motion. It also adds more polyethylene to the construct, which some surgeons might see as beneficial compared with the “worst-case” scenario liners where the poly is thinner. The objective of this evaluation is to review the long-term survivorship and outcomes for both neutral (+0) and 4mm lateralized (+4) polyethylene liners.

Methods

We conducted a retrospective multicenter registry case review from a company-sponsored registry. Clinical assessments were summarized at standardized registry visit windows. All primary THAs with a single acetabular cup were assessed and filtered by the liners of interest (+0 and +4). Kaplan-Meier (KM) survivorship was performed with revision of any component as the endpoint, with two separate censoring assumptions. First, unrevised subjects were censored at the last clinical follow-up [clinical assumption (CA)], and second at the date of database extract [registry assumption (RA)]. Survivorship was not calculated at timepoints where <40 hips were available for follow up.

Results

A total of 19,982 +0 hips, and 14,051 +4 hips were implanted between April 1999 and February 2024, all with the same acetabular shell. Primary diagnosis was osteoarthritis in 92.4% (+0) and 94.3% (+4) of cases. Mean age was 65.9 years for +0 and 66.1 years for +4; 56.79% in +0 and 53.78% in +4 were female and BMI averaged 28.2 for +0 and 29.6 for +4. Overall, 205 (1.03%) revisions were reported for +0 versus 185 (1.32%) for +4. The most common reasons for revision (N; % joints) were dislocation (51; 0.26%), infection (38; 0.19%), aseptic loosening (32; 0.16%), other (26; 0.13%), and periprosthetic fracture (25; 0.13%). For +4, most common reasons for revision (N; %) were dislocation (60; 0.43%), infection (34; 0.24%), other (33; 0.23%), and aseptic loosening (19; 0.14%). All-cause survivorship was 98.61% and 98.28% at 15 and 20 years for +0 and 98.28% at 15 and 20 years for +4 for the RA. KM estimates are presented in Figure 1 and Figure 2. Mean Harris Hip scores were not different and are presented in Figure 3.

Conclusion

While it is interesting to review the outcomes data for these liner components by style (+0 vs. +4), a limitation of this evaluation is a lack of stratification by poly material. There was a slight decrease of revision due to poly wear for +4 (0.04%) compared to +0 (0.08%), but reviewing potential differences between groups in poly materials, these results should be extrapolated with caution. There was a slight increase of revision due to dislocation with +4 liners (0.43%), compared with +0 (0.26%). HHS scores improved over pre-op and were similar between groups. Our study shows excellent long-term outcomes and survivorship for both +0 and +4 liners used in primary THA and obvious differences in terms of failure rate or modes of failure.

Figures

Figure 1 – Kaplan Meier Device Survivorship Estimates (Any component, any reason)

All +0 Hips (N=19,982)	2 Year	5 Year	10 Year	15 Year	20 Year
	KM Survivorship (95% CI) n with Later Follow-up				
All Cause Revision - CA	98.96% (98.75, 99.13%) n = 6986	98.11% (97.75, 98.41%) n = 3206	96.30% (95.49, 96.97%) n = 758	94.73% (92.54, 96.28%) n = 155	<40 Hips
All Cause Revision - RA	99.35% (99.22, 99.45%) n = 16424	99.07% (98.92, 99.21%) n = 12232	98.74% (98.55, 98.91%) n = 6130	98.61% (98.37, 98.82%) n = 2292	98.28% (97.85, 98.62%) n = 921
Cumulative Revised	121	161	194	198	203
All +4 Hips (N=14,051)	2 Year	5 Year	10 Year	15 Year	20 Year
	KM Survivorship (95% CI) n with Later Follow-up				
All Cause Revision - CA	98.54% (98.26, 98.77%) n = 4649	97.93% (97.52, 98.27%) n = 2270	95.69% (94.55, 96.59%) n = 489	92.57% (89.14, 94.95%) n = 71	<40 Hips
All Cause Revision - RA	99.01% (98.82, 99.16%) n = 11889	98.83% (98.63, 99.00%) n = 9944	98.51% (98.26, 98.71%) n = 5275	98.28% (97.97, 98.55%) n = 1363	98.28% (97.97, 98.55%) n = 552
Cumulative Revised	132	152	178	184	184

Figure 1

Figure 2 – KM Device Survival Estimates (Clinical and Registry Assumptions)

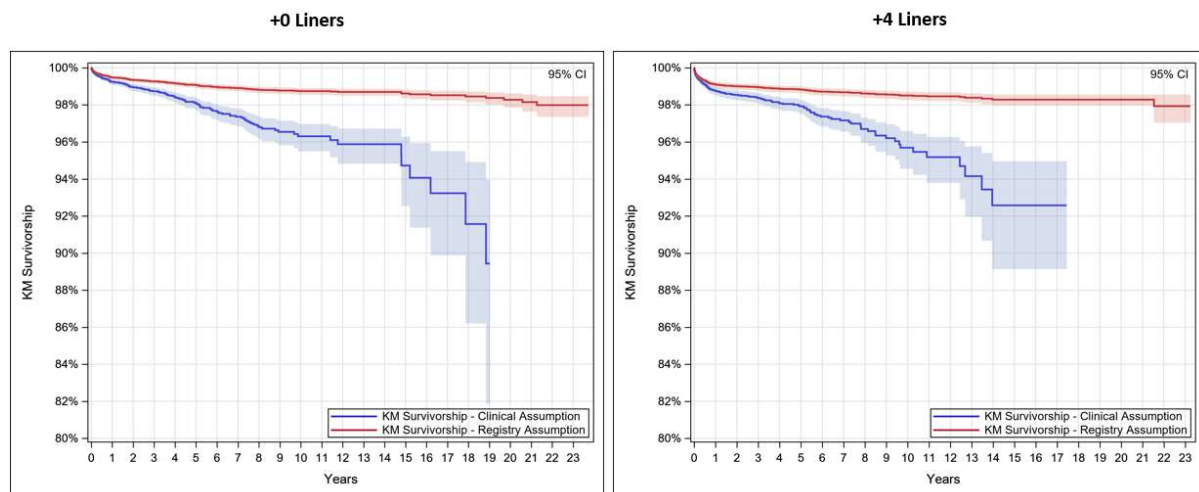


Figure2

Figure 3 – Harris Hip Total Scores (HHS)

	Mean Pre-op HHS Total Score (SD; n)	Mean 2 Year HHS Total Score (669-1034 days) (SD; n)	Mean 5 Year HHS Total Score (1765-2737 days) (SD; n)	Mean 10 Year HHS Total Score (2738-4562 days) (SD; n)	Mean 15 Year HHS Total Score (4563-6387 days) (SD; n)	Mean 20 Year HHS Total Score (6388-8212 days) (SD; n)
All +0 Hips (N=19,982)	52.5 (14.4; 13337)	94.5 (9.6; 4151)	93.0 (11.2; 2422)	91.3 (12.9; 1240)	89.7 (12.9; 284)	85.7 (13.9; 54)
All +4 Hips (N=14,051)	50.8 (14.6; 10629)	92.2 (10.8; 2146)	91.5 (12.4; 1580)	90.4 (12.7; 782)	89.4 (13.2; 145)	86.1 (14.0; 33)

Figure 3

Comparison Analysis of Direct Anterior Approach Versus Posterior Approach in Primary Total Hip Replacement: Evaluating Minimum 5-Year Outcomes and Clinical Important Thresholds

*Benjamin Domb - American Hip Institute - Des Plaines, USA

Roger Quesada-Jimenez - American Hip Institute Research Foundation - Chicago, USA

Yasemin Kingham - American Hip Institute Research Foundation - Chicago, USA

Ady Kahana - American Hip Institute Research Foundation - Chicago, United States of America

Elizabeth Walsh - American Hip Institute Research Foundation - Chicago, USA

Background: The direct anterior approach (DAA) has gained popularity in recent years for total hip arthroplasty (THA). Several authors have reported superior early outcomes for DAA patients, as compared to the posterior approach (PA).

The aim of the study is to compare the outcomes of the DAA and PA in patients undergoing primary THA at mid-term follow-up. The study also aims to provide a comprehensive interpretation of the clinical importance of the available patient-reported outcomes (PROs) based on approach.

Methods: A retrospective analysis was conducted on patients who underwent a primary THA between December of 2009 and November of 2018. Patients were included if they had completed pre- and postoperative patient-reported outcomes (PROs) and visual analog scale (VAS) questionnaires at a minimum of 5-year follow-up or had a documented endpoint. Patients were divided into two groups based on the approach (DAA and PA) and propensity-matched in a 1:1 ratio based on age at surgery, use of robotic assistance, sex, and body mass index (BMI). The analysis included comparisons of clinically significant thresholds for hip arthroplasty, complications, and revision rates.

Results: A total of 352 hips were included in the study, 176 hips in each matched group. Both groups demonstrated significant improvement in mHHS, HHS, VR-12 M, VR-12 P, SF-12 P, and VAS at a minimum of 5-year follow-up. Both groups experienced similar improvement and reached similar postoperative scores in all PROs and VAS. Both groups met MCID for mHHS, HHS, VR-12M, VR12-P, SF-12P, SF-12M and VAS at similar rates. Both groups met PASS for HOOS-JR, HHS and FJS at similar rates ($p > 0.05$). The overall complication rate was significantly higher in the PA group ($p < 0.05$).

Conclusion:

Both the DAA and PA groups reported positive outcomes at a minimum 5-year follow-up. Both groups achieved comparable postoperative scores for all PROs, VAS, and patient satisfaction, reaching the physical-based clinically significant thresholds at comparable high rates. However, MCID for the mental scales were reached at lower rates regardless of the approach. Importantly, the PA group faced a higher risk for complications, which may be considered when deciding on the surgical approach.

Evaluation of Two Stem Alignment Techniques Within the Femoral Canal Using a Preoperative Planning Tool: Could a Hybrid Approach Be Best?

*Michael LaCour - University of Tennessee - Knoxville, USA

Thang Nguyen - University of Tennessee - Knoxville, USA

Jarrod Nachtrab - University of Tennessee - Knoxville, USA

Richard Komistek - The University of Tennessee - Knoxville, USA

INTRODUCTION

As total hip arthroplasty (THA) expectations evolve with robotics, the need for precise component positioning remains, as not all THA involve robotics. While cup placement has been extensively studied, the three-dimensional (3D) positioning of the femoral stem remains less explored. The objective of this study is to use a novel 3D pre-operative planning tool to evaluate different stem alignments and evaluate fit quality.

METHODS

A 3D pre-operative planning tool was used to evaluate component position. The tool initially aligns the stem axis with the proximal canal axis. As the stem is inserted into the canal, a contact detection algorithm between the cortical wall and stem surface adjusts component positioning until the desired position is reached.

Two alignments philosophies were considered: a "canal fit" philosophy, which aims to minimize cortical bone removal and impacts the stem freely, and an "anatomical fit" philosophy, which prioritizes aligning the implanted femoral head center with the anatomical head center, possibly requiring more cortical bone removal.

Ten subjects were evaluated with three different THA systems (EMPHASYS™, Corail, and Tri-Lock® BPS, DePuy Synthes, Warsaw, IN). Parameters of interest include femoral head distance, stem version angle with respect to anatomical neck version, and cortical bone removal volume.

RESULTS

The average head distances for the anatomical fit approach were 2.0mm for EMPHASYS and 2.1mm for both Corail and Tri-Lock. Using the canal fit approach, the Tri-Lock head center relative to the anatomical head center averaged 6.0mm, while EMPHASYS and Corail averaged 3.0mm and 3.1mm, respectively (Figure 1). All three stems achieved accurate version (0 degrees) when aligned anatomically. With canal fit, EMPHASYS and Corail exhibited an average version malrotation of 2.0° and 3.0°, respectively, while Tri-Lock experienced 7.0° (Figure 2).

EMPHASYS and Corail exhibited similar outcomes when aligned anatomically, with an average cortical bone removal of 0.13cm³ and 0.14cm³, respectively. In contrast, the Tri-Lock stem necessitated higher bone removal, 0.46cm³, using anatomical fit. In the canal fit approach, the bone removal volumes were lower for all stems, averaging 0.02cm³ for EMPHASYS and Corail and 0.06cm³ for Tri-Lock (Figure 3).

CONCLUSION

The results from this study demonstrate the benefits of a hybrid approach, leveraging strengths of both philosophies through advanced 3D preoperative planning. There are a multitude of factors that influence stem position within the femoral canal. It is important to consider that the orientation of the canal may not accommodate

preoperative anteversion, potentially leading to misalignment and sub-optimal postoperative outcomes.

REFERENCES

1. LaCour MT, Ta DM, Komistek RD, "Development of a hip joint mathematical model to assess implanted and non-implanted hips under various conditions," Journal of Biomechanics, vol. 112, no. 9, 2020.

Figures

Patient	EMPHASYS								Corail								Tri-Lock							
	Anatomical Fit (mm)				Canal Fit (mm)				Anatomical Fit (mm)				Canal Fit (mm)				Anatomical Fit (mm)				Canal Fit (mm)			
	S/I	M/L	A/P	Total	S/I	M/L	A/P	Total	S/I	M/L	A/P	Total	S/I	M/L	A/P	Total	S/I	M/L	A/P	Total	S/I	M/L	A/P	Total
1	-2.7	-0.7	0.9	3.0	-2.3	0.4	1.8	2.9	-1.2	-1.5	0.9	2.1	-0.8	-0.4	2.2	2.4	-2.1	-0.7	0.7	2.3	-1.5	0.6	1.4	2.1
2	0.5	-0.1	-0.1	0.6	1.1	0.6	0.0	1.2	-1.0	-0.4	0.3	1.1	-0.8	-0.4	-0.1	0.9	0.8	0.3	-0.3	0.9	7.6	4.1	3.4	9.3
3	1.1	0.2	-0.4	1.2	0.9	-0.4	-0.8	1.2	1.3	1.7	-1.1	2.4	1.1	1.2	-1.2	2.0	1.5	-0.1	-0.4	1.6	4.0	1.7	2.5	5.0
4	1.4	1.3	-1.0	2.2	1.6	2.1	0.2	2.7	1.1	-0.6	0.0	1.2	1.1	-0.4	0.0	1.2	-0.3	-0.5	0.2	0.6	3.3	3.3	5.5	7.2
5	-1.4	1.3	-0.3	1.9	0.0	4.8	3.0	5.6	-1.2	-2.4	0.9	2.9	0.5	1.8	5.4	5.7	0.2	-2.2	0.5	2.3	5.5	1.3	6.8	8.8
6	-2.0	-3.2	1.3	4.0	-1.5	-1.9	1.4	2.8	-2.2	-3.5	1.7	4.5	-0.4	0.4	4.4	4.4	-3.0	-1.4	1.0	3.4	1.2	1.0	5.0	5.2
7	0.5	0.4	-0.3	0.7	1.6	3.3	1.0	3.8	-1.8	-0.7	0.6	2.0	0.7	4.8	4.0	6.3	-1.3	-2.2	1.2	2.8	4.7	0.9	3.4	5.8
8	-2.1	-0.7	0.6	2.3	0.0	3.9	4.0	5.6	-1.7	-0.9	0.6	2.0	0.1	3.2	3.8	5.0	-1.3	-1.3	0.9	2.1	7.6	2.6	4.8	9.4
9	2.0	2.7	-1.7	3.8	2.0	2.8	-1.4	3.7	-0.5	1.7	-0.8	2.0	-0.5	1.9	-1.0	2.2	0.3	-1.4	0.4	1.5	3.9	2.2	5.3	6.9
10	0.2	-0.8	0.2	0.9	0.3	-0.9	0.2	0.9	-0.5	0.7	-0.3	0.9	-0.6	0.6	-0.3	0.9	-0.8	-1.9	1.0	2.2	0.2	0.4	-0.2	0.4
Average	-0.2	0.1	-0.1	2.0	0.4	1.5	0.9	3.0	-0.8	-0.6	0.3	2.1	0.0	1.3	1.7	3.1	-0.6	-1.1	0.5	2.0	3.6	1.8	3.8	6.0
Std. Dev	1.7	1.6	0.9	1.2	1.4	2.2	1.7	1.7	1.2	1.7	0.8	1.0	0.8	1.7	2.5	2.1	1.4	0.9	0.5	0.8	3.0	1.2	2.1	3.0

Figure1

Patient	EMPHASYS		Corail		Tri-Lock	
	Anatomical Fit (degree)	Canal Fit (degree)	Anatomical Fit (degree)	Canal Fit (degree)	Anatomical Fit (degree)	Canal Fit (degree)
1	0	2	0	3	0	2
2	0	1	0	0	0	8
3	0	-1	0	-1	0	5
4	0	2	0	0	0	10
5	0	7	0	8	0	11
6	0	1	0	8	0	10
7	0	4	0	9	0	6
8	0	9	0	8	0	10
9	0	0	0	0	0	7
10	0	0	0	0	0	0
Average	0	2	0	3	0	7
Std. Dev	0	3	0	4	0	4

Figure2

Patient	Emphasys		Corail		TriLock	
	Anatomical Fit (cm ³)	Canal Fit (cm ³)	Anatomical Fit (cm ³)	Canal Fit (cm ³)	Anatomical Fit (cm ³)	Canal Fit (cm ³)
1	0.00	0.00	0.00	0.00	0.19	0.00
2	0.33	0.00	0.69	0.03	0.90	0.09
3	0.00	0.00	0.02	0.00	0.05	0.03
4	0.00	0.00	0.00	0.00	0.17	0.17
5	0.54	0.15	0.34	0.15	0.95	0.03
6	0.00	0.00	0.01	0.00	0.20	0.00
7	0.05	0.00	0.08	0.00	0.97	0.08
8	0.38	0.00	0.23	0.00	0.96	0.23
9	0.00	0.00	0.00	0.00	0.13	0.01
10	0.00	0.00	0.00	0.00	0.13	0.00
Average	0.13	0.02	0.14	0.02	0.46	0.06
Std. Dev	0.20	0.05	0.23	0.05	0.42	0.08

Figure 3

Hip Resurfacing Arthroplasty in Patients Younger Than 35: A Single-Surgeon Series of 184 Cases

*Dani Gaillard-Campbell - Midlands Orthopaedics & Neurosurgery - Columbia, USA

Thomas P Gross - Columbia, USA

Background: Hip arthroplasty in younger patients is known to carry higher failure rates. There are also few published outcomes on hip resurfacing arthroplasty (HRA) in patients younger than 35. This study aims to examine the clinical outcomes and implant survivorship of a single-surgeon series of HRA cases in patients under 35-years old at time of surgery.

Methods: Between December 2004 to February 2022, the primary surgeon performed 184 consecutive hip resurfacing surgeries in patients 35 or younger. We compared this study group to the 6523 cases performed in the same time period in patients over 35. All surgeries were performed using the Biomet Magnum-ReCap™ system, and all cases had a minimum 2-year follow-up.

Results: Kaplan-Meier implant survivorship at 15-years postoperative was 96.5% for the under 35 group and 97.6% for the over 35 group ($p=0.077$). Older patients were at an increased risk for reoperation fracture, while the younger patients were at an increased risk reoperation for early infection. Overall rates of failure and complications did not differ between the two cohorts. While pain scores were significantly greater for the under 35 group when compared with the control group ($p<0.0001$), mean HHS and UCLA activity scores did not differ significantly ($p=0.4$ and $p=0.5$, respectively). Whole blood metal ion levels did not differ significantly between the two groups.

Conclusions: Implant survivorship did not differ between age groups for this cohort of 6707 consecutive HRA cases. This study suggests hip resurfacing can be performed safely and with desirable clinical outcomes in patients under 35 when completed with proper perioperative protocols.

Figures

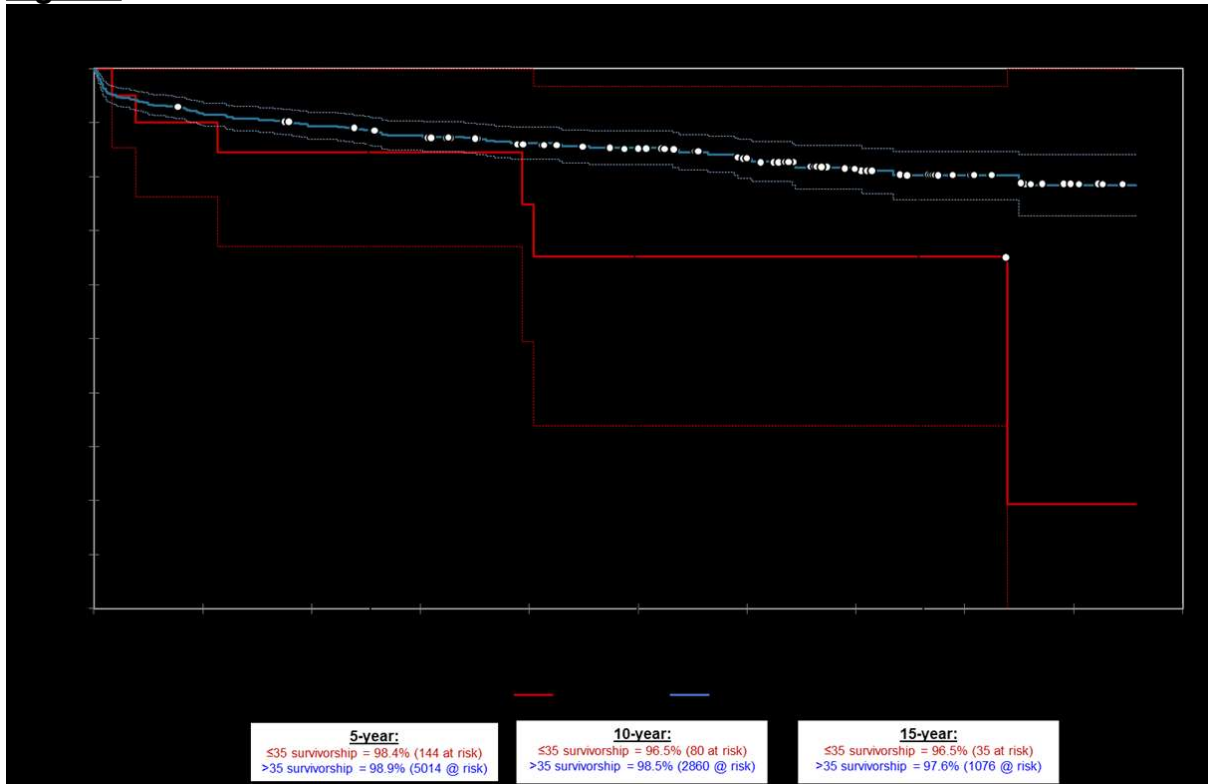


Figure 1

A Prospective Double-Blinded Randomised Controlled Trial Comparing the Direct Superior Approach Versus Posterior Approach for Total Hip Arthroplasty

*Mohammed Wazir - University College London University Hospitals - London, United Kingdom

Babar Kayani - University College Hospital London - London, United Kingdom

Sujith Konan - University College Hospital London - London, United Kingdom

Jenni Tahmassebi - UCLH - London, UK

Dia Giebaly - University College London Hospital - London, United Kingdom

Fares Haddad - University College London Hospital - London, United Kingdom

Introduction:

The direct superior approach (DSA) is a modification of the posterior approach (PA) that preserves the iliotibial band and short external rotators except for the piriformis or conjoined tendon during total hip arthroplasty (THA). The objective of this study was to compare postoperative pain, early functional rehabilitation, functional outcomes, implant positioning, implant migration, and complications in patients undergoing the DSA versus PA for THA.

Materials and Methods:

This study included 80 patients with symptomatic hip arthritis undergoing primary THA. Patients were prospectively randomised to receive either the DSA or PA for THA, surgery was undertaken using identical implant designs in both groups, and all patients received a standardized postoperative rehabilitation programme. Predefined study outcomes were recorded by blinded observers at regular intervals for two-years after THA. Radiosteriometric analysis (RSA) was used to assess implant migration.

Results:

There were no statistical differences between the DSA and PA in postoperative pain scores ($p=0.312$), opiate analgesia consumption ($p=0.067$), and time to hospital discharge ($p=0.416$). At two years follow-up, both groups had comparable Oxford hip scores ($p=0.476$); Harris hip scores ($p=0.293$); Hip disability and osteoarthritis outcome scores ($p=0.543$); University of California at Los Angeles scores ($p=0.609$); Western Ontario and McMaster Universities Arthritis Index ($p=0.833$); and European Quality of Life questionnaire with 5 dimensions scores ($p=0.418$). Radiographic analysis revealed no difference between the two treatment groups for overall accuracy of acetabular cup positioning within Lewinnek's safe zones ($p=0.687$) and femoral stem alignment ($p=0.564$). RSA revealed no difference in femoral component migration ($p=0.145$) between the groups at two years follow-up.

Conclusion:

There were no differences between patients undergoing the DSA versus PA for THA with respect to postoperative pain scores, functional rehabilitation, patient-reported outcome measurements, accuracy of implant positioning, and implant migration at two years follow-up. Both treatment groups had excellent outcomes that remained comparable at all follow-up intervals.

Femoral Stems Implanted Through a Direct Anterior Approach in THA Have Higher Anteversion Than Those Implanted Through a Posterior Approach

*Christopher Plaskos - Corin - Raynham, USA

Michael Solomon - Prince of Wales Hospital - Australia

Jim Pierrepont - Corin - Pymble, Australia

Introduction: Surgical approach has been reported to influence component positioning in THA [1]; however, this has not been investigated across many patients, surgeons, and stem designs. The purpose of this study was to investigate the influence of surgical approach on femoral stem version in THA.

Methods: This was a retrospective review of 830 THAs in 830 patients that had both preoperative and postoperative CT scans within the CorinRegistry. All patients underwent staged bilateral THAs and received CT-based 3D planning on both sides. Stem version was measured in the second CT-scan and compared to the native neck axis measured in the first CT-scan, using the posterior condyles as the reference for both. Cases were performed by 104 surgeons using either a direct anterior (DAA, n=303) or posterior (PA, n=527) approach and one of four stem designs: quadrangular taper, calcar-guided short stem, flat taper, fit-and-fill. Sub-analyses investigated changes in version for low ($\leq 5^\circ$), neutral ($5-25^\circ$) and high ($\geq 25^\circ$) native version subgroups and for the different implant types.

Results: Native version was not different between approaches (DAA = 12.6° , PA = 13.6° , $p = 0.16$). Overall, DAA stems were more anteverted relative to the native neck axis vs PA stems (5.9° vs 1.4° , $p < 0.001$), figure 1. This trend persisted in hips with high native version (3.2° vs -5.3° , $p < 0.01$) and neutral native version (5.3° vs 1.3° , $p < 0.001$), but did not reach significance in the low native version subgroup (8.9° vs 5.9° , $p = 0.13$), figure 2. Quadrangular taper, calcar-guided, and flat taper stem types had significantly more anteversion than native for DAA, while no differences were found for PA.

Conclusions: Stems implanted with a direct anterior approach had more anteversion than those implanted with a posterior approach.

References:

[1] Abe H, Sakai T, Takao M, Nishii T, Nakamura N, Sugano N. Difference in Stem Alignment Between the Direct Anterior Approach and the Posterolateral Approach in Total Hip Arthroplasty. J Arthroplasty. 2015 Oct;30(10):1761-6.

Figures

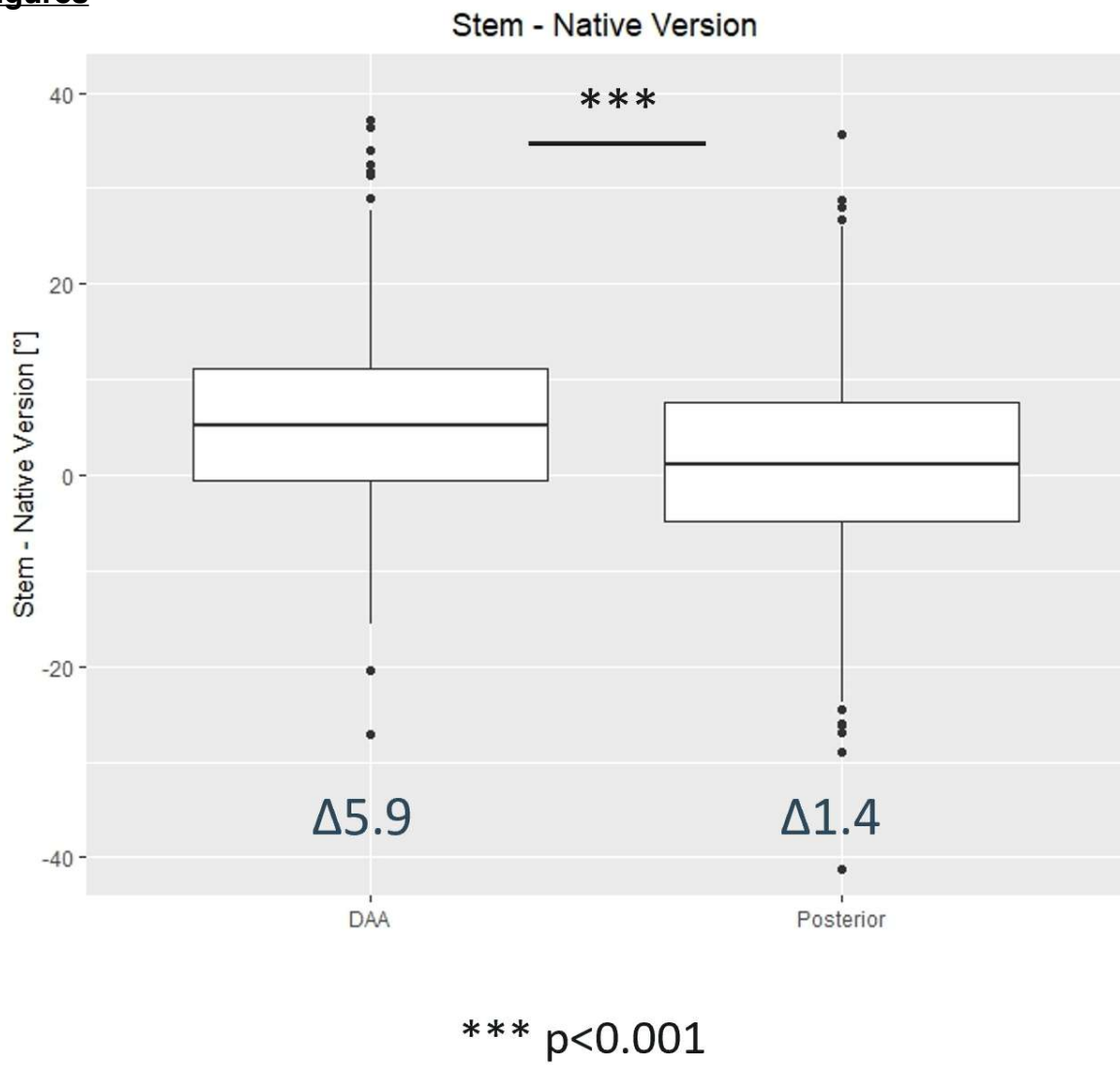


[Figure1](#)

Change in version from native for low, neutral and high native version groups

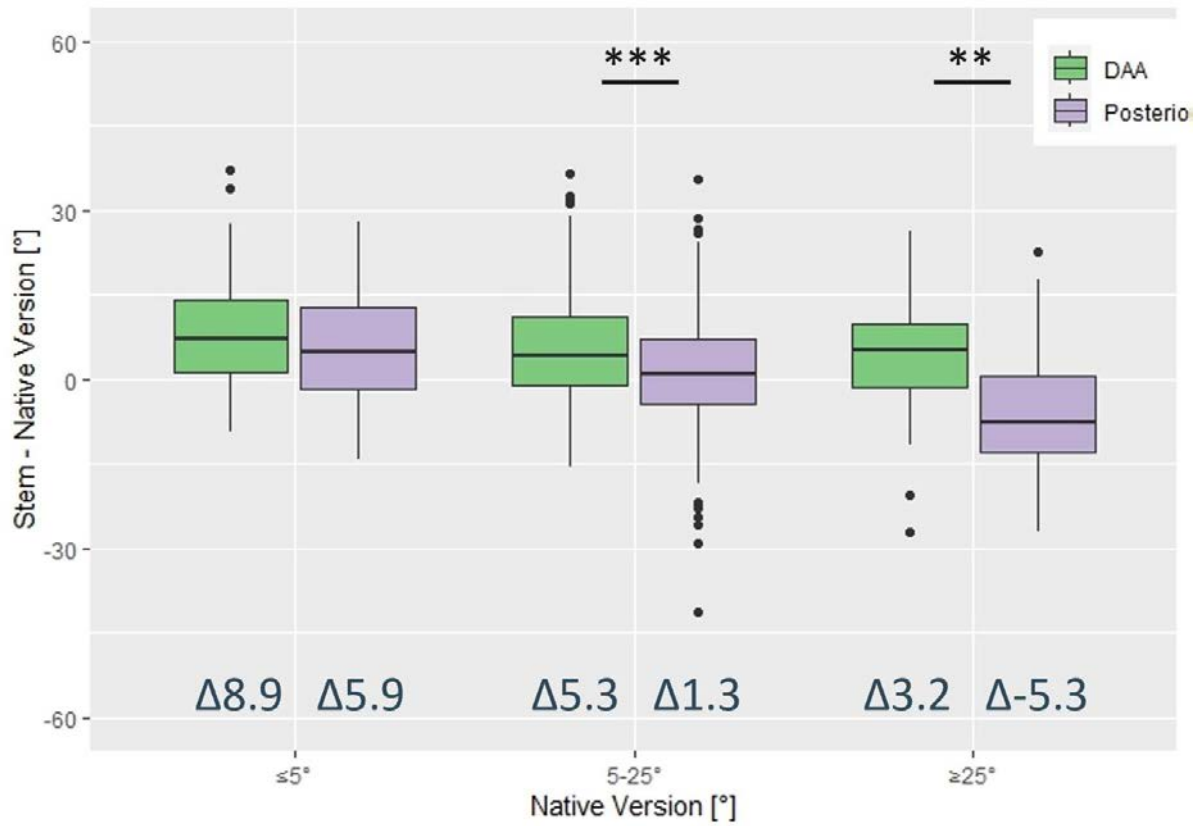


Figure 2

Implications of Functional vs Anatomic Femoral Anteversion on Combined Alignment Theories in THA

*Gerard Smith - Corin - Sydney, Australia

Christopher Plaskos - Corin - Raynham, USA

Jim Pierrepoint - Corin - Cirencester, United Kingdom

Richard Boyle - Royal Prince Alfred Hospital - Sydney, Australia

Precise alignment of prosthetic components is crucial for optimizing joint function and minimizing the risk of impingement and dislocation in THA. Traditionally, the posterior condylar axis of the distal femur is used to measure femoral anteversion for both the native and prosthetic femur. However, this static reference fails to consider dynamic variations in axial femur orientation which occur during activities of daily living. The authors propose that the functional position of the proximal femur should be considered, as well as in relation to the cup (combined anteversion), when considering clinical implications of stem anteversion. This study investigates the post-operative differences between anatomically-referenced and functionally-referenced stem and combined anteversion in the supine and standing positions.

58 patients underwent a THA procedure with OPSInsight™ 3D preoperative planning (Corin, Australia) performed by a single surgeon using the anterolateral approach. 57% of the patients were female, with a mean age (\pm SD) of 68 ± 10 years. Follow-up imaging was captured at an average of 13 ± 8 weeks post-op. Anatomic and functional stem anteversion in both the supine and standing positions were determined. The anatomic anteversion referenced the posterior condyles and was measured from the CT (RadiAnt, Poland), with supine functional anteversion was measured from CT and referenced to the coronal plane. Standing functional anteversion was measured by performing 2D-3D registration (Materialise Mimics, Belgium) of the implants to a weight-bearing AP X-ray. Correlation was quantified using the Pearson coefficient, and significant differences in means were assessed using a paired Student's t-test.

Mean functional femoral anteversion (\pm SD) differed significantly between supine and standing positions, both preoperatively (supine: $12.5^\circ\pm 10.3^\circ$ vs. standing: $10.8^\circ\pm 10.7^\circ$, $p=0.010$) and postoperatively (supine: $17.0^\circ\pm 11.1^\circ$ vs. standing: $12.4^\circ\pm 14.1^\circ$, $p=0.004$). Differences between anatomic and supine stem versions were significant ($p=0.0302$), as were preoperative and postoperative supine functional femoral anteversion ($p=0.0041$). A strong preoperative correlation (Figure 1A) between supine and standing FFA ($r=0.89$, $p<0.001$) decreased to a moderate correlation ($r=0.59$, $p<0.001$) postoperatively (Figure 1B), indicating increased internal femoral rotation under post-op weight-bearing conditions. Significant differences in anatomic femoral anteversion were identified between pre-op ($10.0^\circ\pm 7.0^\circ$) and post-op ($17.0^\circ\pm 11.1^\circ$) ($p<0.001$). In all but four cases, the pelvis rotated posteriorly in the sagittal plane from supine to standing, increasing functional acetabular anteversion by a mean of 5° ($p<0.001$).

Anatomic stem anteversion shows significant variability from functional stem anteversion in supine positions, underscoring differences in femoral rotation. The reduced correlation between pre- and post-operative supine and standing functional anteversions likely results from increased contraction of the gluteus medius during standing, promoting internal femur rotation. Suggesting that referencing femoral stem anteversion to the distal femur's native anatomy may be misleading in assessing the functional anteversion of the stem. These findings underscore the

importance of considering dynamic, patient-specific femoral rotations when determining the optimal combined anteversion alignment for total hip arthroplasty (THA), critical for enhancing joint functionality and reduced risk of dislocation.

How Variable Are Cup Angle Suggestions From Published Hip-Spine Analyses?

*Emily McIntosh - Intellijoint Surgical - Kitchener, Canada

Nathanael Heckmann - Keck School of Medicine of USC - Los Angeles, USA

Jonathan Vigdorichik - Hospital for Special Surgery - New York, USA

Introduction

The impact of spinopelvic mobility on dislocation risk following total hip arthroplasty (THA) is a topic which has been widely discussed. While the mechanisms are generally agreed upon, surgical management via the optimization of cup angles is still under debate. The purpose of this study was to compare cup recommendations from three published methods to see how they differ in patients with varying spinopelvic alignment and mobility.

Methods

This comparative model utilized pre-operative images from 9 THA patients that were gathered retrospectively from multiple sites. Patients were selected based on their alignment (anterior plane pelvic tilt, APpt) and mobility (delta sacral slope; dSS) so that there was a case representing each spinopelvic combination (anterior, posterior, and neutral pelvic tilt x stiff, normal, and hypermobile). The following parameters were measured using Intellijoint VIEW to calculate target angles: dSS, APpt, pelvic incidence (PI), lumbar lordosis (LL), and pelvic femoral angles (PFA). Targets were calculated for each patient in the standing radiographic plane using the methods from three different publications^{1,2,3} (see Figure 1A-C). A one-way ANOVA was used to compare the difference in anteversion values between each method and each target was assessed for dislocation risk using functional safe zone thresholds⁴. The range between the maximum and minimum target values for each patient was reported (Table 1) and a clinically relevant difference was defined as 5°.

Results

No statistical differences were observed between the anteversion recommendations from the three methods, but the range of values exceeded the clinically relevant difference in 56% of cases (see Figure 1A-C).

Conclusion

There is consensus in the literature of the importance of considering the hip-spine relationship when planning for cup positions, however, the targets suggested in the literature are not interchangeable. More discussion and long-term post-operative data should be considered for varying levels of spinopelvic mobility and alignment.

References

1. Vigdorichik JM, Sharma AK, Buckland AJ, Elbuluk AM, Eftekhary N, Mayman DJ, Carroll KM, Jerabek SA. 2021 Otto Aufranc Award: A simple Hip-Spine Classification for total hip arthroplasty : validation and a large multicentre series. Bone Joint J. 2021 Jul;103-B(7 Supple B):17-24.
2. Bodner RJ. The Functional Mechanics of the Acetabular Component in Total Hip Arthroplasty. J Arthroplasty. 2022 Nov;37(11):2199-2207.e1.
3. Grammatopoulos G, Falsetto A, Sanders E, Weishorn J, Gill HS, Beaulé PE, Innmann MM, Merle C. Integrating the Combined Sagittal Index Reduces the Risk of

Dislocation Following Total Hip Replacement. J Bone Joint Surg Am. 2022 Mar 2;104(5):397-411.

4. Tezuka T, Heckmann ND, Bodner RJ, Dorr LD. Functional Safe Zone Is Superior to the Lewinnek Safe Zone for Total Hip Arthroplasty: Why the Lewinnek Safe Zone Is Not Always Predictive of Stability. J Arthroplasty. 2019 Jan;34(1):3-8.

Pre- to Postoperative Spinopelvic Variability in Total Hip Arthroplasty Planning

*Joshua Twiggs - University of Sydney - Sydney, Australia

Max Hardwick-Morris - University of Sydney - Sydney, Australia

Brad Miles - 360 Knee Systems - Pymble, Australia

Tyson Doneley - Brisbane Orthopaedic Clinic - Spring Hill, Australia

Introduction: For decades, the Lewinnek safe zone was positioned as the gold-standard for cup orientation in total hip arthroplasty. However, this study had several limitations, and its conclusions were later dismantled by large-sample studies due to the variability of pelvic tilt (PT) and pelvic rotation between functional positions. These insights led to the use of functional radiographs to assist in templating. However, debate remains over which radiographs are best. Several papers have published algorithms that use relaxed seated and standing radiographs. Other planning protocols utilise flexed seated and standing radiographs. The aim of THA surgery should be to plan to the position the patient will assume postoperatively. Therefore, the aim of this study was to provide early results of the reproducibility of the sitting postures to determine which is more appropriate for templating.

Methods: All patients underwent pre- and postoperative functional imaging. Postoperative imaging was taken at least 12 months after surgery to ensure any postoperative postural changes from surgery had time to take place. The imaging protocol included standing, flexed seated, and relaxed seated radiographs. All standing radiographs were measured for lumbar lordosis (LL), sacral slope (SS), PT, and pelvic incidence (PI). All seated radiographs were measured for LL and SS. Lumbar flexion (Δ LL) and Δ SS between standing and each seated posture were calculated (Δ SS_{flexed} and Δ SS_{relaxed}).

Results: For the preoperative radiographs, mean Δ LL was 29.5° (18.8°-39.4°), mean Δ SS_{relaxed} was 15.8° (10.3°-20.8°), and mean Δ SS_{flexed} was 4.8° (-2.5°-16.6°). For the postoperative radiographs, mean Δ LL was 44.7° (33.9°-56.7°), mean Δ SS_{relaxed} was 9.5° (-1.2°-18.4°), and mean Δ SS_{flexed} was -7.9° (-31.7°-19.1°). Looking at the preoperative to postoperative changes in measurements, Δ LL changed by a mean of -15.3° (-33.4°-5.5°), Δ SS_{relaxed} changed by a mean of -6.4° (-19.5°-7.3°), and Δ SS_{flexed} by a mean of -12.7° (-39.1°-1.9°).

Conclusion: The jury is out on which preoperative radiographs provide the most informative spinopelvic assessment of patients. Our early results demonstrate volatility in both sitting postures from pre- to post-operative states. However, we observed greater change in flexed seated spinopelvic measurements and patients with conflicting flexed seated measurements. For example, one patient had a Δ SS_{flexed} of 4.4°, indicative of healthy spinopelvic behaviour, and Δ LL of 18.8°, indicative of pathologic spinopelvic behaviour. This patient's Δ SS_{flexed} also changed by 39.1° from pre- to postoperative states. In these patients, there may be ambiguity about the patient's spinopelvic condition, so it will be unclear if the cup position requires adjustment or not.

Verification of Usefulness of Subluxation Percentage According to the Crowe Classification in Cup Placement for Dysplastic Hip Osteoarthritis

*Keiji Otaka - Nagoya university - Nagoya, Japan

Yusuke Osawa - Nagoya University - Shizuoka, Japan

Yasuhiko Takegami - Nagoya University - Nagoya, Japan

Hiroki Iida - Nagoya University - Nagoya, Japan

Yuto Ozawa - Nagoya University - Nagoya, Japan

Hiroto Funahashi - Nagoya university - Nagoya, Japan

Hiroaki Ido - Nagoya University - Nagoya, Japan

Takamune Asamoto - Nagoya University - Nagoya, Japan

Shinya Tanaka - Nagoya university - Nagoya, Japan

Shiro Imagama - Nagoya university - Nagoya, Japan

Introduction: It is often difficult to achieve adequate bone coverage of the cup in total hip arthroplasty (THA) in cases of severe developmental dysplasia of the hip (DDH). We have reported a computer simulation study that it is difficult to achieve adequate cup coverage even when placed 15 mm and 25 mm from the inter-teardrop line in cases with subluxation percentage of Crowe classification $\geq 56.1\%$ and $\geq 73.6\%$, respectively. The purpose of this study was to investigate the position of cup placement after THA in patients with DDH and to evaluate the validity of our reported simulation study.

Methods: A total of 62 hips in 55 patients (male 9 hips, female 53 hips) comprising Crowe II/III (47 hips) and randomly selected Crowe I (15 hips) who underwent THA at our hospital between January 2018 and December 2023 were included in this study. The mean age at surgery was 64.7 years, and the mean BMI was 23.5 kg/m². Cases with subluxation percentage $< 56.1\%$, $\geq 56.1\%$ and $< 73.6\%$, and $\geq 73.6\%$ were classified as group I, II and III (24 hips, 21 hips and 17 hips), respectively. Vertical center of rotation (V-COR) was defined as the distance from the head center to the inter-teardrop line. Cup fixation methods, postoperative Cup-CE angle and V-COR were investigated in postoperative Xp.

Results: The cup fixation methods (cementless/cement with bone graft) were 19/4, 12/9 and 4/13 for group I, II and III respectively ($P < 0.001$). The mean postoperative cup-CE angles were 8.6°, 9.1°, 1.2° for group I, II and III respectively ($P = 0.22$). The mean V-COR were 20.1 mm, 21.7 mm, 25.4 mm for group I, II and III respectively ($P < 0.01$). The number of hips of V-COR ≥ 25 mm were 3 hips (12.5%), 7 hips (33.3%) and 10 hips (58.8%) for group I, II and III respectively. In cases of V-COR ≥ 25 mm, the mean postoperative cup-CE angles were 10.7°, 23.6°, 1.4° ($P = 0.021$) and the mean V-COR were 27.0 mm, 27.7 mm, 27.6 mm ($P < 0.96$) for group I, II and III respectively.

Conclusion: Even in clinical practice, almost all hips of group I could be placed 25 mm above from inter-teardrop line. On the other hand, group III was placed significantly higher than group I and II, did not provide adequate coverage despite the acetabular components being placed 25 mm above from inter-teardrop line.

Changes in Anteversion, Leg Length and Offset With Under- and Oversized Stems Are Patient Specific

David Liu - Gold Coast Centre for Bone and Joint Surgery - Tugun, Australia

Duncan Bakke - Formus Labs - Auckland, New Zealand

Lilian Lim - FormusLabs - Auckland, New Zealand

Thor F Besier - University of Auckland - Auckland, New Zealand

*Marco Schneider - Formus Labs - Auckland, New Zealand

James Germano - Northwell Health - Dix hills, United States of America

Introduction

Primary fixation of cementless femoral stems in Total Hip Arthroplasty (THA) depends on correct sizing [1], which can reduce the risk of subsidence post-operatively [2]. The three-dimensional position of the implant within the femur has implications for sizing as well as anteversion, leg length, and offset. This has secondary implications for musculoskeletal function, including changes in muscle length due to femoral offset and moment arms due to anteversion [3]. The aim of this study was to evaluate the effect of implant size on anteversion, leg length, and offset.

Methods

Preoperative CTs from 17 successful THA cases using Taperloc Complete stems (Zimmer Biomet, Warsaw IN), consisting of 12 females and 5 males aged 66 ± 11 years, were automatically segmented to obtain 3D models of the pelvis, femur, and femoral inner cortical surface (Formus Labs, NZ). 3D models of the actual implanted stem, as well as one size larger and one size smaller, were simulated for fit into the inner cortical surface of the femur. The simulated surgeries were used to generate estimates of stem anteversion, change in offset, and change in leg length. We identified relationships between implant size and changes in these measures due to undersizing and oversizing, as well as inter-subject variability in these relationships.

Results

Wilcoxon Signed Rank Tests showed that undersized implants were consistently less anteverted than the implanted ($-1.7 \pm 2.4^\circ$, $p=0.011$). Undersized implants also resulted in consistently shorter leg lengths than implanted by (-3.1 ± 6.9 mm, $p<0.001$). Offset did not appear to be consistently different between undersized and implanted stems (Figure 1A). No consistent change was observed for any of the measures between oversized and implanted stems (Figure 1B). Undersized stems were consistently less anteverted than oversized stems ($-0.99 \pm 9.8^\circ$, $p=0.040$), but also consistently more offset ($+1.3 \pm 4.2$ mm, $p=0.027$).

Conclusion

The near zero mean values and relatively large standard deviations demonstrates that the effect of size change on these measurements is non-linear and patient-specific, making it difficult to predict. Changes that registered as significant align with previous studies identifying undersized implants prone to changes in position [1,2]. Our findings demonstrate the variability of stem position if the size is altered by a single step. Intraoperative decision-making may benefit from patient-specific simulation of implant fit and its effects on surgical measures and potential effects on musculoskeletal function [3].

References

1. Kutzner, K., et al. (2022). Hip International. 32(2), 160-165
2. Hoskins, W. T., et al. (2020). J Arthroplasty. 35(4), 1074-1078

3. Petterwood, J., et al. (2023). In AOA Annual Scientific Meeting, Melbourne

Figures

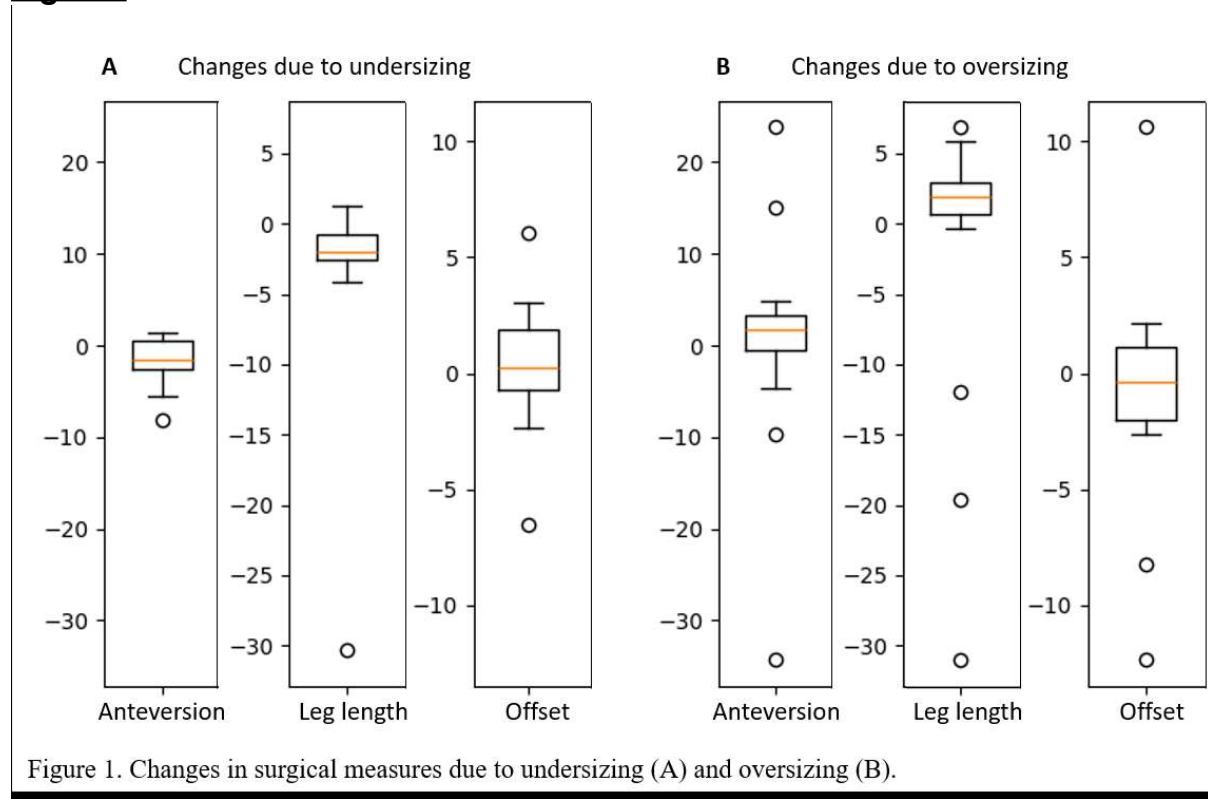


Figure 1. Changes in surgical measures due to undersizing (A) and oversizing (B).

[Figure 1](#)

Bone Ingrowth Fixation of Gription S Porous Coating

*Dustin Albert - DePuy Synthes - Warsaw, United States of America

Bryan Smith - DePuy Synthes - Warsaw, USA

Michael Frohbergh - Exponent Inc. - Philadelphia, USA

Ryan Siskey - Exponent - Philadelphia, USA

Celia Gupta - Glaxo Smith Kline - Philadelphia, USA

Bryan Smith¹, Celia Gupta¹, Dustin Albert¹, Michael Frohbergh², Ryan Siskey²

¹DePuy Synthes, Warsaw, IN, ²Exponent, Philadelphia, PA

INTRODUCTION: Porous surfaces designed for biological fixation are commonly evaluated using preclinical animal models to assess bone ingrowth. This study was performed to compare the cancellous and cortical bone ingrowth fixation of the Gription™ S porous coating to that of Porocoat™ and Gription™ porous coatings, which have a long record of successful clinical use. The Gription S coating was developed to maintain the coefficient of friction and interconnected porosity of Gription porous coating with reduced thickness.

METHODS: Test specimen implants were Ti6Al4V pins coated with either Gription S, Gription or Porocoat porous coating. Gription S is a new porous coating made by a powder metallurgy process from spherical and irregular CP Ti powders.

Pins were implanted bilaterally in six skeletally mature dogs for 6 weeks. Experiment 1 was a paired comparison of bone ingrowth fixation between Gription S and Porocoat-coated implants in cancellous bone of the proximal humerus. Experiment 2 was a paired comparison between Gription S and Gription-coated implants in cancellous bone of the distal femur and cancellous bone of a lower defect site in the proximal humerus. Experiment 3 compared bone ingrowth fixation among Gription S, Porocoat and Gription-coated implants that were rotated among four diaphyseal cortical bone sites per femur.

Implants in Experiments 1 & 2 were 6mm diameter x 16mm long and implanted with a line-to-line fit. Experiment 3 implants were coated to a 4.9mm diameter and implanted in one cortex with a slight press fit. For Experiments 1 & 2 a transverse cut was made through the implants at necropsy and the inner/medial half used for push-out testing and the outer/lateral half used for histomorphometry so that both tests had a sample size of 6. Experiment 3 had dedicated push-out and histomorphometry implants.

Bone ingrowth fixation was evaluated by histomorphometric measurements of bone in the porous coating and push-out testing of the strength of the implant-bone interface. Bone ingrowth was calculated as the percentage of the pore area within the porous coating region of interest that was filled with bone. ROIs extended inward from the porous coating-bone interface and were equal to the Gription S average thickness to avoid coating thickness bias in the measurements. For push-out testing, a threaded pin was placed in each implant to align it to the push-out fixture during potting and removed prior to testing. The push-out fixtures provided a 2mm diametrical clearance around the cancellous implants and, as described by Bobyń[1], a 0.5mm diametrical clearance around the cortical specimens.

RESULTS: No significant differences were found in bone ingrowth or bone-implant interface strength in canine cancellous or cortical bone between Gription S and Gription or Porocoat porous coatings as shown in Table 3.

CONCLUSION: The results suggest a thinner porous coating may help facilitate larger femoral heads in smaller acetabular shells, and consequently reduce the risk of dislocation, without compromising cup fixation.

REFERENCES: [1]Bobynd JD et al, JBJS 81(5):907-14, 1999

Figures

Implant Type	Coating	Volume Porosity (%)	Pore Intercept Length (mm)	Thickness (mm)
Cortical	Gription S	58 (1.0)	197 (4.2)	0.59 (0.01)
	Gription	61 (2.0)	233 (16.1)	0.90 (0.02)
	Porocoat	48 (1.9)	191 (3.8)	0.69 (0.01)
Cancellous	Gription S	55 (1.8)	187 (10.2)	0.60 (0.02)
	Gription	57 (1.3)	208 (7.6)	0.92 (0.03)
	Porocoat	44 (1.6)	171 (2.0)	0.69 (0.01)

Table 1. Comparative porous coating morphology measurements from cross section image analysis per ASTM F1854. Mean (std dev). Volume porosity and pore intercept length sample size was 3 representative test specimen implants from both implant types and coating groups. Thickness was measured by calipers and averaged across all prepared for each implant and coating type. WR150174

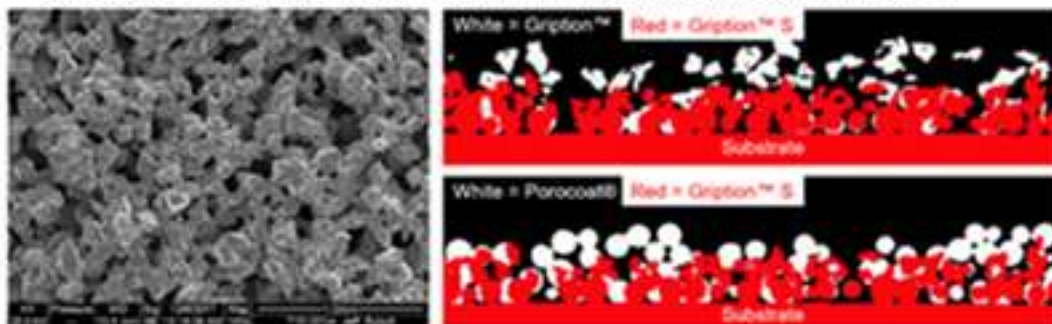


Fig. 1 (L) Image of Gription S surface. (R) Overlaid images of cross sections through Gription and Gription S (top) and Porocoat and Gription S coatings (bottom).

Figure1

Experiment #	Defect site (bilateral)	# Defects Per Animal	# Animals	Implant group
1	Lateral proximal / upper proximal humeral epiphysis	2	6	Gription S
				Porocoat
2	Lateral distal femoral epiphysis	2	3	Gription S
				Gription
	Lateral lower proximal humeral epiphysis	2	3	Gription S
				Gription
3	Lateral femoral diaphysis	8	6	Gription S
				Gription
				Porocoat

Table 2. Bone in-growth experiment design. Surgery, in-life, and necropsy were performed at NAMSA. Histomorphometric measurements were at NAMSA, and push-out testing was at Exponent.

Figure2

Experiment	Group (Sample Size)	Bone Ingrowth (%)		Push-Out Strength (MPa)	P value α 0.05
		Bone In Growth % Pore Area	P value α 0.05		
1 PHE / PHE Upper	Gription S (n=6)	29.8 (6.5)	0.904	2.61 (1.0)	0.892
	Porocoat (n=6)	30.3 (7.4)		2.68 (0.7)	
2 DFE / PHE Lower	Gription S (n=6)	28.5 (7.2)	0.577	3.08 (1.1)	0.414
	Gription (n=6)	31.9 (12.4)		3.60 (1.0)	
3 FMD	1 - Gription S (n=8)	53.3 (7.3)	1 vs 2 0.9216	20.7 (2.9)	1 vs 2 0.947
	2 - Porocoat (n=8)	55.1 (10.5)	1 vs 3 0.119	20.2 (3.7)	1 vs 3 0.991
	3 - Gription (n=8)	63.0 (9.9)	2 vs 3 0.2315	20.5 (2.9)	2 vs 3 0.981

Table 3. Bone ingrowth and push-out strength measurements for each of the three experiments (mean (standard deviation)). No significant differences between or among groups in any experiment. Two-sample t with α 0.05 for Experiment 1 and 2. Anova with post hoc α 0.05 for Experiment 3.

Figure 3

Are There Relevant Differences in Volumetric Wear Among Highly Crosslinked Polyethylene Brands in Total Hip Arthroplasty?

*Robin Pourzal - Rush University Med Ctr - Chicago, USA

Michel Schlppi - Cantonal Hospital Winterthur - Winterthur, Switzerland

Deborah Hall - Rush University Medical Center - Chicago, USA

Roman Heuberger - RMS foundation - Bettlach, Switzerland

Peter Wahl - Kantonsspital Winterthur - Winterthur, Switzerland

Introduction: Wear and the resulting periprosthetic tissue response remain one of the main issues in the long-term outcomes after total hip arthroplasty (THA). Highly cross-linked polyethylene (HXLPE) liners or cups may mitigate this issue. While the introduction of HXLPE has substantially reduced volumetric wear, the particles it produces are smaller and may induce a stronger cellular reaction compared to those from conventional polyethylene. Differences in the manufacturing process of HXLPE may have relevant consequences regarding long-term mechanical behaviour and wear performance. Therefore, this study aimed to quantify the volumetric wear of retrieved HXLPE liners and cups from various manufacturers.

Methods: An ongoing continuous series of retrieved HXLPE liners and cups were collected from revisions at a single center in Switzerland since August 2022.

Anonymized clinical data are prospectively collected from patient files. Volumetric wear was determined from retrievals with more than two years *in vivo* using an optical coordinate measuring machine (OrthoLux, RedLux). Due to limitations in case mix, preliminary results are presented solely for HXLPE liners and cups from two manufacturers.

Results: The current cohort included 18 implants of Type A and 9 implants of Type B with a median (range) time in situ of 8.1 (4.2 to 16.2) and 14.8 (11 to 22.1) years ($p < 0.001$), respectively. All liners exhibited an unworn area in the inferior aspect with original machining lines, thus making 3D reconstruction of the original sphere and measurement of wear volume possible. The median (range) wear volumes and wear rates were 116.8 (24.5 to 271.6) mm³ and 8.5 (2.01 to 43.9) mm³/year for Type A, and 106.4 (24.9 to 290.3) mm³ and 4.6 (2.0 to 14.5) mm³/year for Type B, respectively (Fig 1 & 2).

Conclusion: Preliminary results already demonstrate major differences in wear between the two implant types. Wear rates of Type A are almost double compared to Type B, and show a wide variability. Of note, revisions of Type A occurred after significantly shorter time *in vivo* compared to Type B, aligning with higher revision rates observed in both the Swiss and the Australian arthroplasty registries of THA for Type A brands compared to Type B. While the current findings are already significant, it is important to increase the study cohort to solidify the results and to compare with HXLPE liner and cups from other manufacturers. It is important to note that other potentially influential factors on wear (e.g., cup orientation, sex, BMI) could not be considered at this stage but will be incorporated as the cohort grows.

Figures

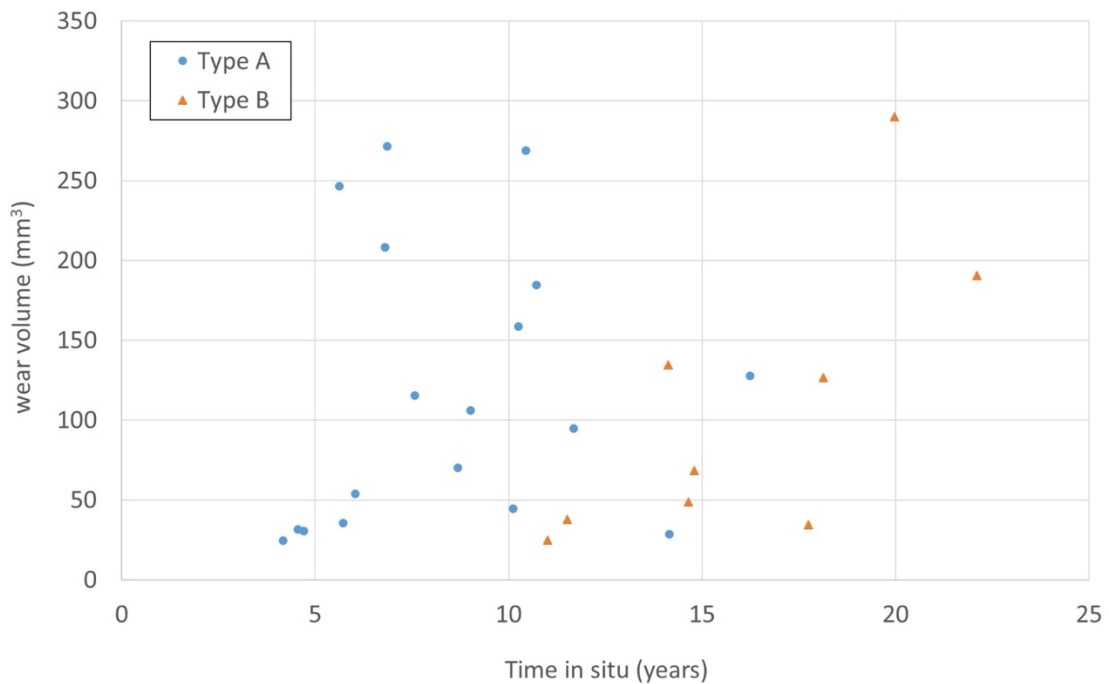


Figure 1 – Graph showing wear over time of individual liners and cups of Type A and Type B. It is of note that all Type B liners were retrieved after 10 years in situ, while most Type A liners were revised earlier.

Figure 1

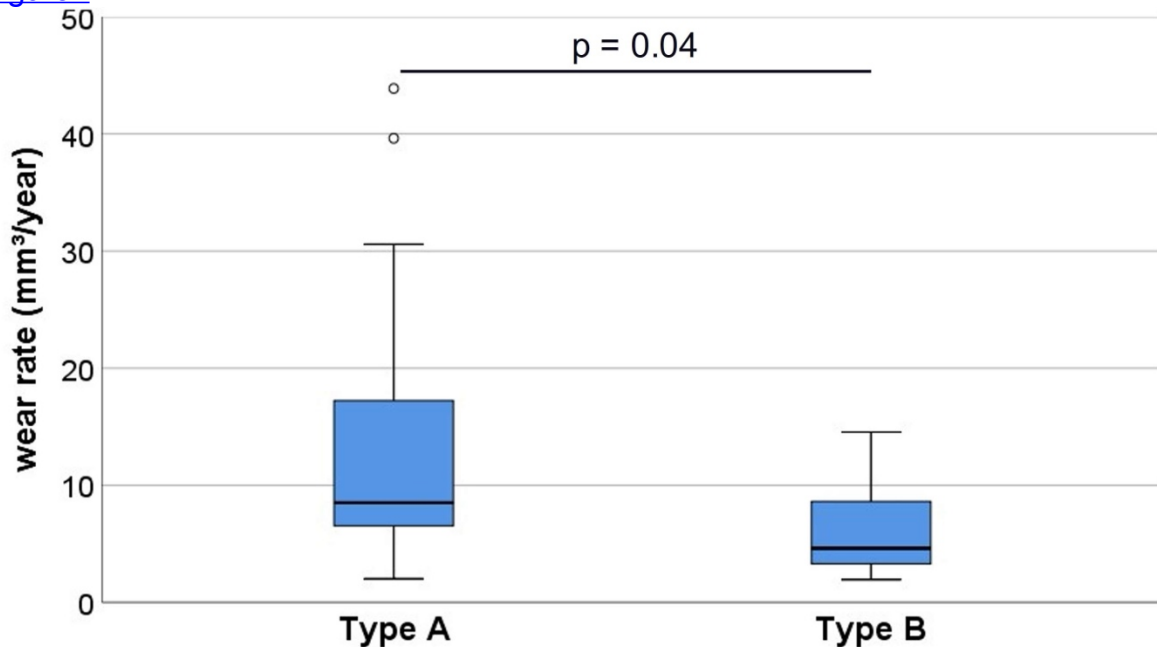


Figure 2 – Although there was no linear relationship between wear and time for either brand, the median individual wear rate was significantly higher for Type A compared to Type B.

Figure 2

Inspection of ISO 17853 for Investigating Wear Particles of THR Trunnions

*Charlotte Merrell - University of Leeds - Leeds, United Kingdom

Richard M. Hall - University of Birmingham - Birmingham, United Kingdom

Michael Bryant - University of Birmingham - Birmingham, United Kingdom

Andrew Robert Beadling - University of Leeds - Leeds, United Kingdom

Saurabh Lal - Zimmer Biomet - Swindon, United Kingdom

Imran Khan - Zimmer Biomet Inc - Swindon, United Kingdom

Introduction

Recent advances in hip replacement technologies highlight the significant role of fretting wear debris in prosthetic longevity and biocompatibility [1-5]. ISO 17853 standardises debris isolation and characterisation, yet debate surrounds its suitability for investigating metal particles, such as from modular tapers and other fretting contacts. [6-10]. Currently, metal debris morphology is not well documented, making it virtually impossible to relate debris texture to patient outcomes, necessitating improved morphology analysis [10]. This study investigated metal particle generation across fretting regimes and lubricants to identify current methodological limitations.

Methods

A fretting-corrosion tribometer simulated taper interface conditions across various lubricants: Ringer's solution., acidified Ringer's solution, and newborn calf serum with Ringers salts. Density gradient ultracentrifugation (outlined in CWA 17253-1 Joint Implants Part 1 [11]) was employed alongside Field Emission Gun Scanning Electron Microscopy and Energy Dispersive X-ray to surpass the traditional ISO 17853 methods [11]. Microscope resolution up to 1 pixel/nm allowed for detailed analysis of debris morphology, distribution, and chemical composition.

Results and Discussion

This study's methodology enabled a comprehensive comparison against the morphology categories in ISO 17853, scrutinizing their capability to accurately reflect characteristics of metal particles. Analysis revealed metal particles as small as 3 nm generated under partial slip conditions, which is potentially overlooked by ISO 17853 isolation methods due to its biases against nanosized debris [6, 8]. Significant shortcomings were noted in describing metal debris shape using length, width and their ratio per ISO 17853 as highlighted in Figure 1. This image displays two particles isolated from serum classified uniformly as 'oval' under ISO characterisation, despite possessing distinct textures. This oversimplification overlooks variations in debris morphology, which could influence cell internalisation pathways and biological impact, suggesting a need for more nuanced texture descriptors within standards. Classifying metallic debris by circularity, akin to polymer debris assessment per ISO 17853 and ASTM F1877-16, highlighted morphological differences - particles A and B resulted in values of 0.39 and 0.71 respectively [6, 12].

Conclusion

The study's findings advocate for a revision of ISO 17853 to include enhanced methods for debris isolation and more detailed categorizations for morphology. Considering circularity would provide a more robust description of debris, which may allow for investigation of its impact on bioreactivity and comparison between patient outcomes and retrieved debris [10]. By addressing these gaps, the standards can be

made more comprehensive, thereby improving the predictive accuracy of preclinical tests for implant safety and efficacy.

References

- 1) <https://journals.sagepub.com/doi/abs/10.1177/228080001000800101>
- 2) <https://pubmed.ncbi.nlm.nih.gov/25793158>
- 3) <https://pubmed.ncbi.nlm.nih.gov/19844976/>
- 4) <https://pubmed.ncbi.nlm.nih.gov/19583551/>
- 5) <https://pubmed.ncbi.nlm.nih.gov/27209084>
- 6) <https://www.iso.org/standard/57230.html>
- 7) <https://pubmed.ncbi.nlm.nih.gov/29505889/>
- 8) <https://etheses.dur.ac.uk/11402/>
- 9) <https://doi.org/10.1016/j.actbio.2016.07.004>
- 10) <https://pubmed.ncbi.nlm.nih.gov/25802639/>
- 11) <https://dps.gov.al/en/project/show/dps:proj:60268>
- 12) <https://www.astm.org/f1877-16.html>

Variability of the Porous Structure in 3D-Printed Acetabular Implants

*Arya Nicum - University College London - London, GB

Anna Di Laura - Royal National Orthopaedic Hospital and Dept. MechEng at UCL - London, United Kingdom

Harry Hothi - London Implant Retrieval Centre - Stanmore, United Kingdom

Klaus Schlueter-Brust - St. Franziskus Hospital - Köln, Germany

Johann Henckel - Royal National Orthopaedic Hospital - London, United Kingdom

Alister Hart - Royal National Orthopaedic Hospital - London, United Kingdom

Introduction:

3D-printing is rapidly being adopted for orthopaedic implant manufacture. Off-the-shelf acetabular implants are the most used 3D-printed orthopaedic implants, offering optimisation of the design of the bone-facing porous structure.

The lack of design standards for the lattice structure deemed to promote bone ingrowth has led to different approaches by manufacturers. It is important to understand the differences of the porous structures that currently exist to aid post-market surveillance and recognise which designs offer optimal clinical results.

This study aimed to characterise the porous structures of the bone-facing side of 3D-printed acetabular cups and compare the variability in their designs between manufacturers.

Study Design and Methods:

Five pristine commercially available 3D-printed off-the-shelf acetabular implants from five manufacturers were examined. Two had been printed using Electron Beam Melting (EBM) and three using Selective Laser Melting (SLM).

Light microscopy and scanning electron microscopy (SEM) were utilised to image the surface. Each cup was systematically studied across 4 regions of the bone-facing side (Figure 1(a)) through image analysis software. The outcome measures were: (1) strut thickness (μm), and (2) pore size (mm^2) (Figure 2(a)).

Results:

The lattice structure varied significantly across the 5 acetabular implants.

Two implants (Manufacturer 1 and 2) had a regular lattice which exhibited repeating unit cells, with a consistent strut thickness and pore size. Three implants (Manufacturers 3, 4 and 5) had irregular structures, with pores of varying sizes (Figure 1(b)).

1) The median strut thicknesses for the implants that exhibited a regular lattice structure (Manufacturer 1 and 2) were 523 and 501 μm , respectively. These ranged between 209-433 μm , for Manufacturers 3-5 (irregular lattice structure). All cups exhibited some degree of variation in strut thicknesses, independently from the lattice and manufacturing method (Figure 2(b(i))).

2) The median pore size for the implants with a regular lattice structure (Manufacturer 1 and 2) were 0.108 and 0.038 μm , respectively. Manufacturer 4 had a larger variation in pore size than Manufacturer 2 (both SLM); where the median(range) was 0.061(0.003-0.064) and 0.0378(0.0257-0.0597) mm^2 , respectively (Figure 2(b(ii))). The variation in pore size was affected by the regularity of the lattice structure.

Conclusion:

This study reports the wide variability that exists amongst 3D printed off-the-shelf acetabular implants. Currently, there is no recommended design nor long-term clinical results. Post-market surveillance and implant retrieval studies will help explain the impact of the lattice type on bony ingrowth and fixation to determine a recommended lattice design.

Figures

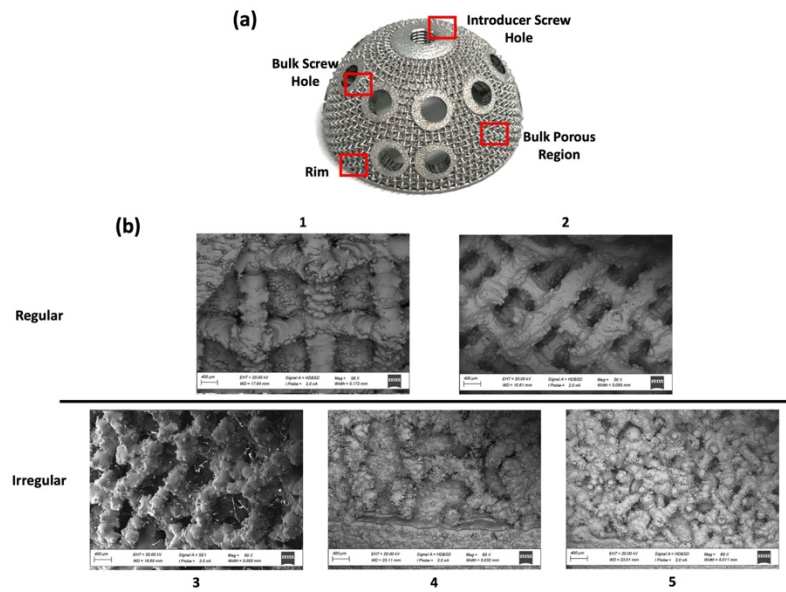


Figure 1

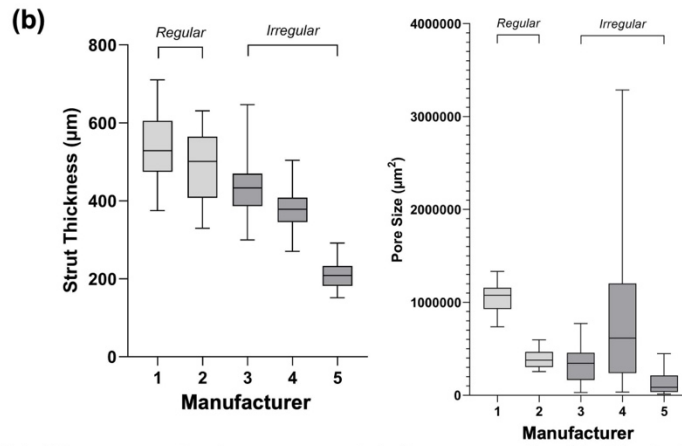
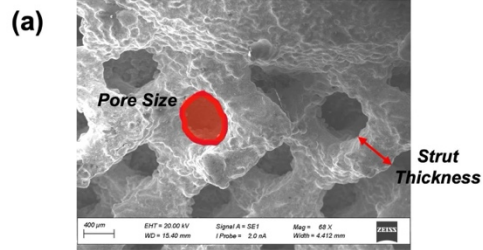


Figure 2: (a) An SEM of the porous structure on an acetabular cup examined in this study, indicating Pore Size and Strut Thickness. (b) A box plot to demonstrate the significant difference in (i) Strut Thickness and (ii) Pore Size between the cups with Regular and Irregular porous structure designs.

[Figure 2](#)

2-Octyl-Cyanoacrylate Mesh Dressings for Total Joint Arthroplasty: Dressing Design Influences Risks of Wound Complications

*John Cooper - Columbia University - New York, USA

Roshan Shah - Columbia University Medical Center - New York, USA

Alexander Neuwirth - Columbia University Medical Center - New York, USA

Carl Herndon - Columbia University Medical Center - New York, USA

William Levine - Columbia University Medical Center - New York, USA

Catelyn A. Woelfle - Columbia University Medical Center - New York, USA

INTRODUCTION

Recent liquid adhesive skin closure systems with a mesh patch and 2-Octyl cyanoacrylate liquid formula have shown promising results in total joint arthroplasty (TJA). Chemical accelerators are typically included to promote rapid polymerization of 2-Octyl cyanoacrylate. The goal of the current study is to distinguish designs and wound complication differences between two similar systems.

METHODS

An eighteen-week retrospective cohort study was conducted from July to December 2023, including 419 THA (49%) and TKA (51%) cases from four attending surgeons at a single institution that used one of two dressing designs. Both dressings had a 2-Octyl cyanoacrylate liquid adhesive formula that was applied topically to a polyester-based mesh overlaying the wound. Mesh A (used in 274 cases) included an accelerator, a quaternary ammonium salt, on the mesh patch, whereas Mesh B (used in 145 cases) included a similar accelerator within the liquid adhesive applicator.

RESULTS

Wound complications (3.2% vs. 7.6%; $X^2 = 3.86$; $df = 1$; $P = 0.049$), early periprosthetic joint infections (PJI) (0% vs. 2.8%; $X^2 = 7.63$; $df = 1$; $P = 0.006$), and 90-day reoperations for wound complication (0.4% vs. 3.4%; $X^2 = 6.39$; $df = 1$; $P = 0.011$) were all significantly lower in patients that received Mesh A versus B, respectively. There was no difference in superficial SSI (0.7% vs. 0%; $X^2 = 1.06$; $df = 1$; $P = 0.302$) or allergy rates (3.3% vs. 4.1%; $X^2 = 0.12$; $df = 1$; $P = 0.655$) between Mesh A and B, respectively.

CONCLUSION

We observed significantly different performance in wound complication, early postop PJI, and 90-day reoperation between the two designs. Having the accelerator in the applicator, rather than on the mesh patch, may lead to premature polymerization before bonding appropriately with the mesh to create the desired final wound closure and seal.

Bone Cement Abrasion Resistance of Titanium Nitride and Oxidized Zr_{2.5}Nb Surfaces

*Aline Elquist - Smith and Nephew - Memphis, United States of America

Amit Parikh - Smith & Nephew, Inc. - Memphis, USA

Bill Hurd - Memphis - Memphis, USA

Introduction: Surface hardening/coating is necessary to use titanium alloy as a bearing surface in total joint arthroplasty. While physical vapor deposition (PVD) and chemical vapor deposition (CVD) coatings have exhibited varied results due to coating durability challenges (adhesion/cohesion), technology continues to develop. One recently developed PVD technology utilizes ion beam assistance and reportedly creates a ballistically bonded zone between the coating and substrate to improve adhesion. The goal of this study was to compare abrasion resistance of this more recently developed, commercially available, TiN coating (applied to Ti6Al4V) to surface oxidized Zr_{2.5}Nb (OXINIUM™) material.

Methods: OxZr disks were manufactured from Zr_{2.5}Nb [1], and TiN coated disks were manufactured by coating Ti6Al4V using an ion beam assisted PVD process. Pin-on-disk abrasion testing was conducted to 1 million cycles using manufactured disks (n=5) and VERSABOND PMMA bone cement pins, which contain radiopaque zirconia particles. Vertical load was 24.5 N, pin radius was 6.35 mm, stroke length was approximately 10 mm, frequency was 2.25 Hz, and lubricant was lactated ringer's solution. After testing, contact profilometer traces were taken across the wear track at 0.5 mm intervals, and a software feature was used to calculate area under each profile. Wear volume was determined by averaging adjacent wear areas, multiplying by the distance between measurements, and summing values (i.e., using the midpoint rule). Further characterization included Knoop hardness measurements (50 g load) and cross-sectional metallography. Comparisons were made using Student's t-test ($\alpha=0.05$).

Results: OxZr disks appeared relatively pristine after testing while visible scratching was observed within the wear scars on TiN coated disks (Figure 1). Cross-sectional evaluation confirmed TiN coating breach and metallic substrate exposure (Figure 2). Mean volume loss of OxZr and TiN coupons was 0.01 ± 0.01 mm³ and 0.26 ± 0.02 mm³, respectively ($p<0.001$). Bone cement pins paired with TiN exhibited more wear than those paired with OxZr; as a result, contact stress for OxZr was significantly greater than for TiN by the end of testing. Mean Knoop hardness (50 g) for OxZr and TiN was 1061 ± 29 and 1147 ± 57 , respectively ($p=0.02$).

Conclusion: OxZr material has been used clinically for over 20 years and remains a benchmark for evaluating surface hardening/coating technologies. Test methodology used herein is applicable/relevant considering sources of third-body particulate present in the joint-space and has been successfully used to rank materials in the past. Compared to previous testing, OxZr and TiN coated coupons demonstrate better abrasion resistance than untreated (not coated) CoCrMo and titanium niobium nitride (TiNbN) coated CoCrMo (Figure 3) [2]. Despite having lower surface hardness, results indicate OxZr has superior bone cement abrasion resistance than the TiN coating applied using an ion beam assisted PVD process. If testing continued, wear of the TiN coated disks would likely accelerate due to the observed coating breach, resulting in further divergence with OxZr.

References: [1] Davidson et al, Biomed Mater Eng, 4(3), 1994: 213-229 [2] Elquist et al, Annual meeting of ORS, 2022:371

Figures



Figure 1: Representative images of OxZr (left) and TiN coated Ti6Al4V (right) disks after testing.

Figure 1

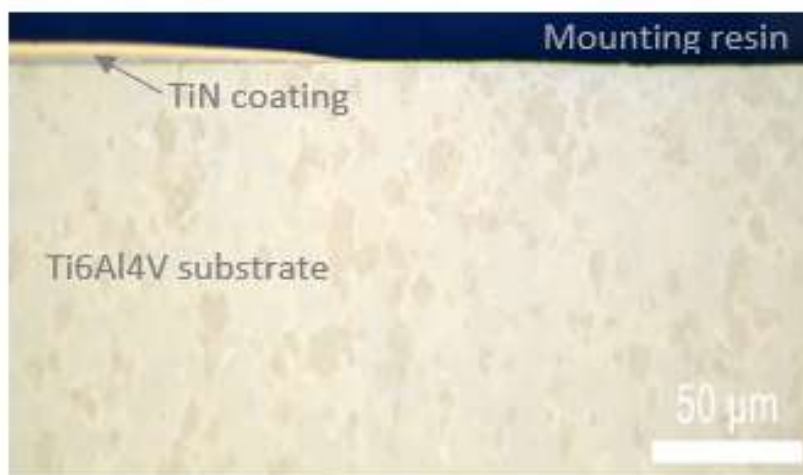


Figure 2: Cross-sectional image near edge of wear scar of TiN coated disk

Figure 2

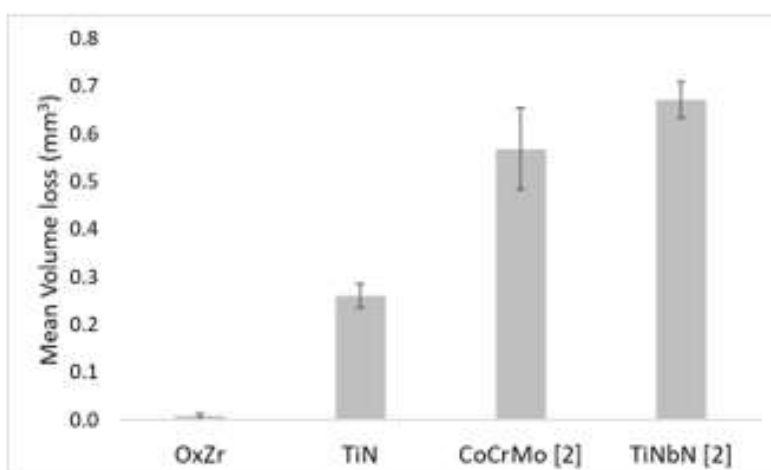


Figure 3: Mean volume loss of disks (error bars reflect standard deviation)

Figure 3

Retrieval Analysis of Fretting-Corrosion at the Stem-Head Interface of Total Hip Arthroplasty Implants Revised Within 5 Years: Preliminary Results

*Matheus Henrique Linhares da Silva - UFSC - Florianópolis, Brazil

Patricia Ortega Cubillos - Biomechanical Engineering Laboratory - Federal University of Santa Catarina - Florianópolis, Brazil

Eduardo Alberto Fancello - Mechanical Design and Analysis Group (GRANTE) - Florianópolis, Brazil

Lourenco Pinto Peixoto - INTO - Rio de Janeiro, Brazil

Marco Bernardo Cury Fernandes - Instituto Nacional de Traumatologia e Ortopedia

Jamil Haddad - Rio de Janeiro, Brazil

Adrielson Echamendi da Silva - Universidade Federal de Santa Catarina - Florianópolis, Brazil

Carlos Rodrigo De Mello Roesler - FAPEU - Florianópolis, Brazil

INTRODUCTION

The fretting-corrosion process in Total Hip Arthroplasty implants is of great interest as it may be responsible for component revision. There are several parameters that can affect the level of damage at the stem-head interface. This study aims to identify whether the fixation method influences this process.

METHODS

Eight explants were collected in an explant analysis center. They were all from the same manufacturer and evaluated for fretting-corrosion damage in both the stem taper and the head taper. Four regions were used for evaluation of each taper (anterior, posterior, medial, and lateral), with corrosion and wear scores assigned to each quadrant, following Goldberg's method. All explants had been implanted for up to 5 years and were divided into two groups: cemented ($n = 4$) and uncemented ($n = 4$). No distinction was made regarding the reason for revision or the design of the explants. Three operators conducted the evaluation. The resulting scores were used to correlate damage and the explant fixation method. Total damage in stem and head tapers was also correlated. Both correlations were conducted using the Spearman rank order test (with a limit of $p = 0.05$).

RESULTS

When correlating damage with fixation method, the p-values for wear were 0.154 for the head taper and 0.752 for the stem taper. For corrosion, the p-values were 0.572 for the head taper and 0.339 for the stem taper. The comparison of total wear damage between the stem taper and the head taper yielded a p-value of 0.001, while the comparison of total corrosion damage between the tapers resulted in a p-value of 0.02.

CONCLUSION

There was no correlation between damage and the fixation method of the evaluated explants. As expected, there is a strong correlation between the total damage of the head taper and the stem taper, as they are contacting surfaces. It is worth noting the study's limitation regarding the number of samples analyzed.

Survival Analysis of Total Hip Arthroplasty: Contribution of Cross-Linked Polyethylene and Bone Sparing Surgical Technique at a Minimum Follow-Up of Eleven Years.

*Masaaki Maruyama - Minaminagano Medical Center, Shinonoi General Hospital - Nagano, Japan

Hiroki Nomura - Minaminagano Medical Center, Shinonoi General Hospital - Nagano, Japan

Aims: Although total hip arthroplasty (THA) is a highly effective operation for hip disorders, the success is accomplished on the past failure. We aimed to evaluate the factors, such as prosthetic materials and surgical techniques, influenced on the long-term results of primary THA using survival analysis.

Methods: We included all patients who, between March, 1997 and July, 2009, had undergone a primary THA for hip disorders, at our hospital using a conventional (CON) or a highly cross-linked (XLP) polyethylene as materials of acetabular socket and a 22 mm ceramic femoral head. From a total of 544 hips (414 patients), 523 hips were available for evaluation (CON 79; XLP 444). Surgical technique of the bone grafting reconstruction methods for acetabular bone deficiency compared with morphologically normal acetabulum without bone grafting, XLP cases in THA were divided two subgroups: 1) group-1 with bone graft reconstruction for bone deficient hip (225 hips) and 2) group-2 without bone graft reconstruction for morphologically normal hip (219 hips), by classification of acetabular dysplasia.

Results: The cumulative implant survival, with loosening for polyethylene wear as the endpoint, was 45.7% (95% CI: 20.2–71.1) in the CON series at 25 years and 95.0% (90.1–99.9) in the XLP series at 20 years ($p = 0.0114$ in Log Rank test) (Fig.1), and, with revision as the endpoint, was 68.3% (95% CI: 50.2–86.3) and 98.7% (95% CI: 97.1–100), respectively ($p = 0.0052$) (Fig.2). The mean radiological linear wear of the CON socket was 0.168 mm/year compared with 0.027 mm/year for the XLP socket ($p < 0.0005$). The cumulative survival, with loosening for surgical technique as the endpoint, was 98.4% (95% CI: 95.9–100) in the group-1 at 20 years and 91.8% (95% CI: 82.5–100) in the group-2 at 20 years ($p = 0.6626$) (Fig.3), and, with revision as the endpoint, was 98.0% (95% CI: 94.9–100) and 99.5% (95% CI: 98.4–100), respectively ($p = 0.5966$).

Conclusion: This study shows that XLP sockets are associated with significantly less wear and a lower rate of loosening and revision THA than CON sockets, and THA with surgical technique for reconstruction acetabular bone deficiency provides good clinical results as compared with that of THA for morphologically normal acetabulum at long-term follow-up.

Take home message: The findings of this study highlight the clinical benefits of using XLP sockets and surgical reconstruction method for acetabular bone deficiency in THA in order to improve implant longevity and to decrease the number of patients needing revision for aseptic loosening.

Figures

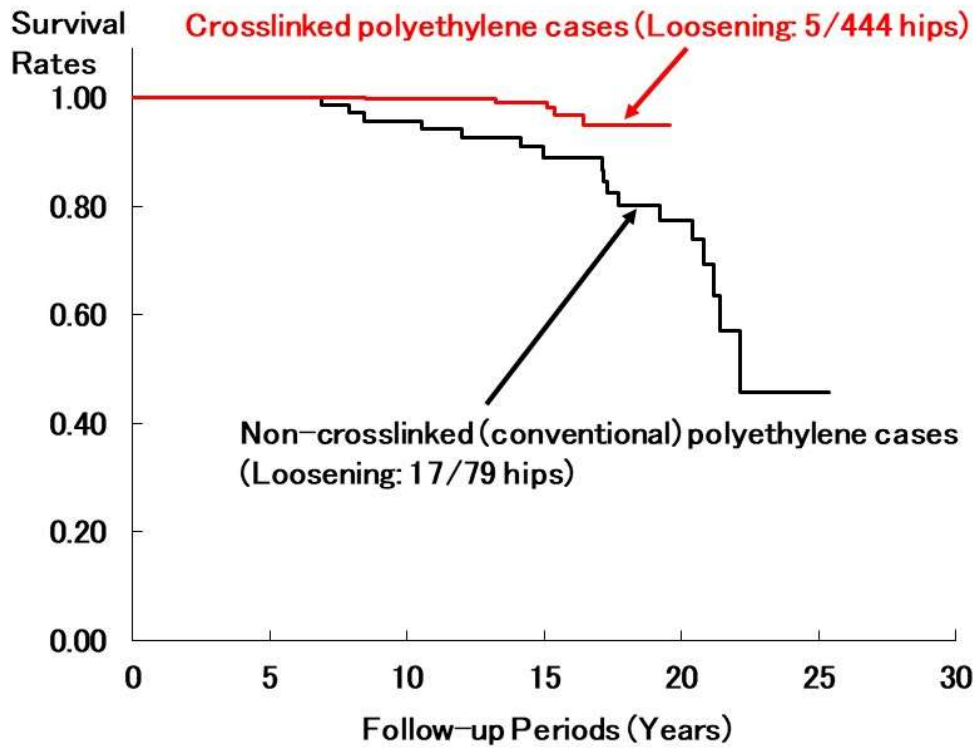


[Figure1](#)

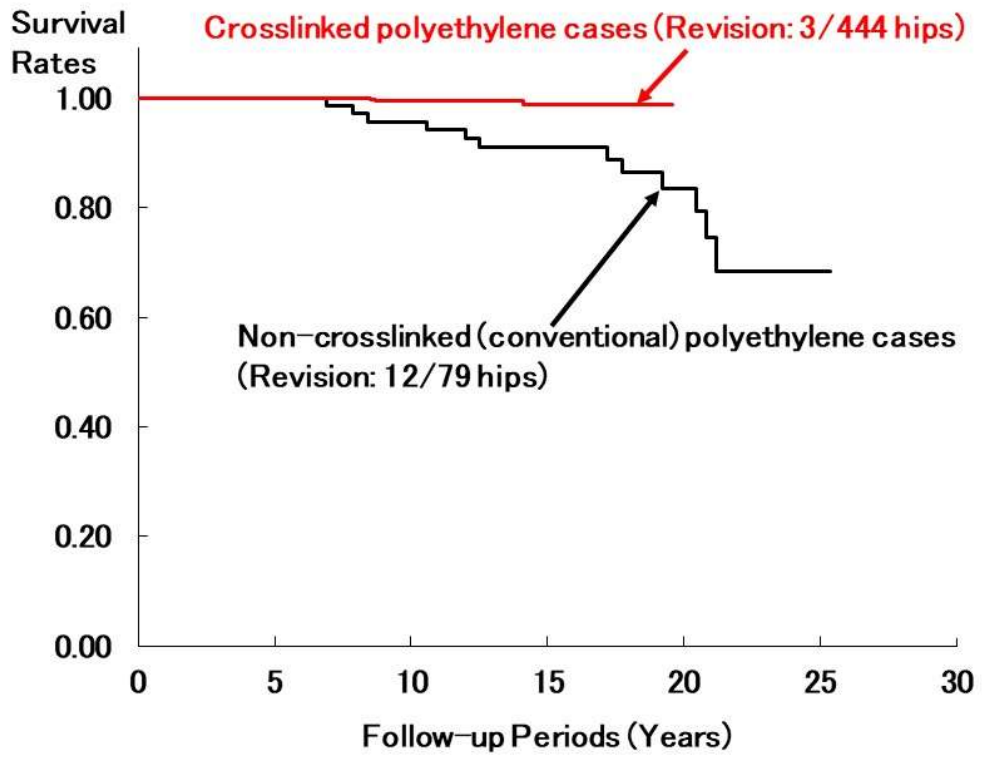


[Figure2](#)

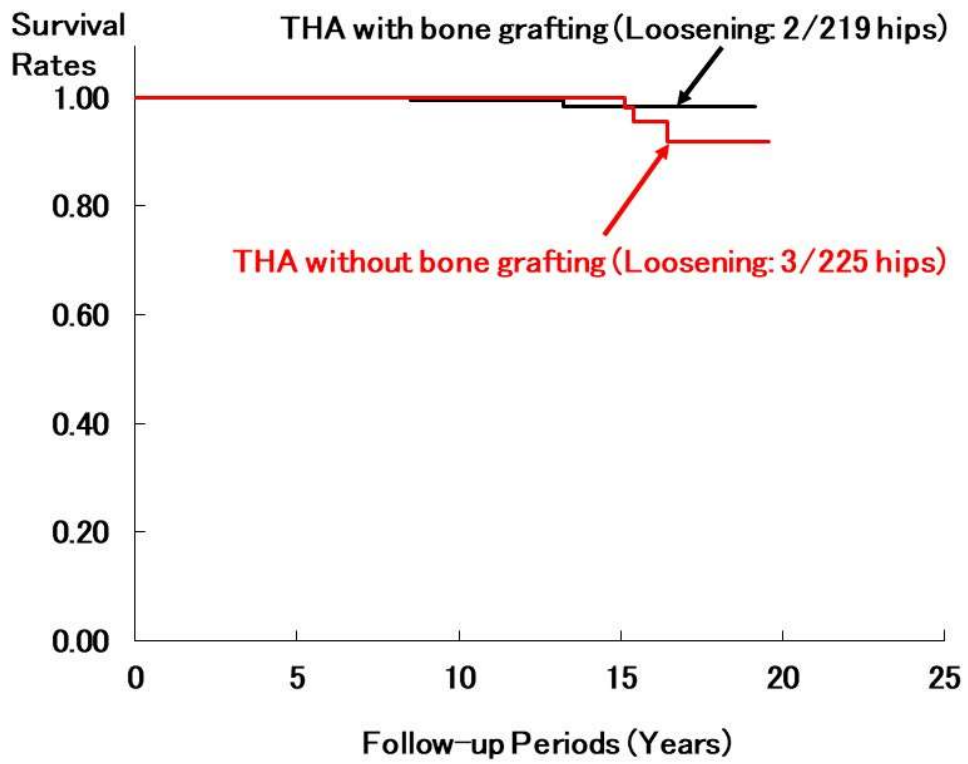


[Figure 3](#)

Effect of Spine Interbody Fusion Implant Surface Architecture on Fixation

*Sophia Sangorgio - Orthopaedic Institute for Children/UCLA - Los Angeles, USA

Edward Ebramzadeh - Orthopaedic Institute for Children/UCLA - Los Angeles, USA

Nicholas Lamb - Orthopaedic Institute for Children/UCLA - Los Angeles, USA

John Ehteshami - Additive Implants - Phoenix, USA

Matt Zoghi - Additive Implants - Phoenix, USA

Introduction: Spondylolisthesis, the anterior slippage of a vertebra, is a degenerative condition of the spine that is often associated with osteopenia or osteoporosis. Approximately 5-7% of the adults in the US alone have developed degenerative spondylolisthesis. Complex loading dynamics constitute the risk of migration of interbody fusion devices, increasing the likelihood of fusion failure. Therefore, fixation of fusion devices is of paramount importance. The present study evaluated three novel surface architectures to improve fixation for a novel additively manufactured interbody fusion device, using an in vitro model.

Methods: Three composite bone models simulating high density, low density, and a cellular model representing healthy, osteopenic, and osteoporotic bones respectively were included. Each bone model was tested with three implant types, two with 2mm serration height, one with a serration angle of 45° and the other with a serration angle of 60°. The third implant type had a serration angle of 45°, but a serration height of only 1 mm. Each synthetic bone block was preconditioned by applying a cyclic load profile with an amplitude of 100N, increasing the maximum force in increments of 100N after every 10 cycles at a rate of 0.5 Hz, in a step-wise fashion until failure. The outcome variables of each test included maximum force sustained at the interface prior to failure, sagittal migration at failure, and cyclic micromotion. Each architecture and bone model combination was tested three times with 3 new bone specimens at 30° of sagittal inclination, and separately three times at 45° (N=52).

Results: On average, sagittal migration of 2mm 60° implants were larger than other surface architectures. There was no statistically significant difference between the maximum forces with different architectures. Maximum force was highest in the healthy bone model followed by osteoporotic and then osteopenic models, but, with higher inclination, cellular and low density analogs were similar. Under 900N peak, cyclic micromotion was highest in low density bone analog, whereas cellular and high density analogs were similar.

Conclusion: Total sagittal migration was most heavily impacted by surface architecture, while cyclic micromotion and maximum force to failure were significantly less influenced by differing surface architecture. Bone quality and degree of sagittal inclination were important factors for all three measures of implant stability. For all combinations of synthetic bone quality and sagittal inclination, the 45° serrations provided greater or a similar amount of stability as the 60° serrations.

Figures



Figure 1

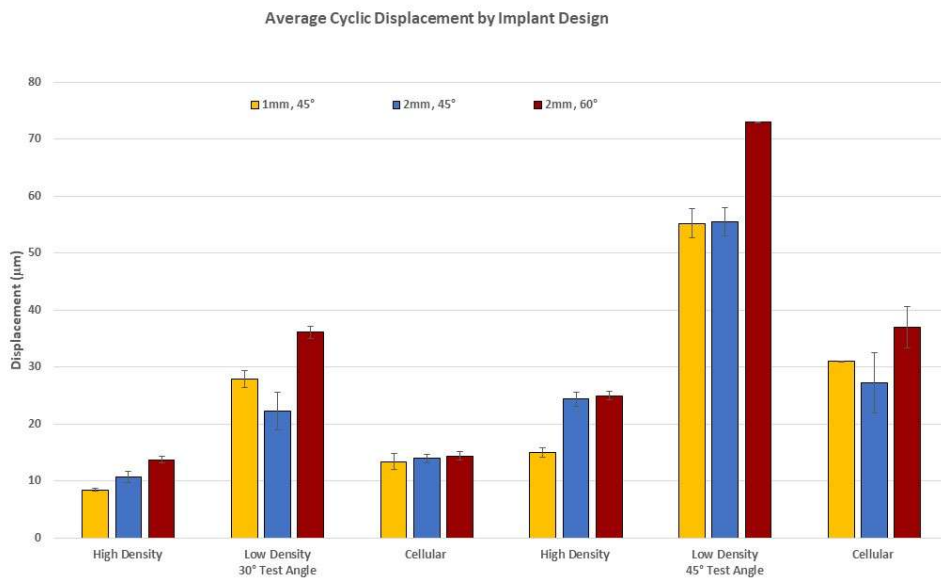


Figure 2

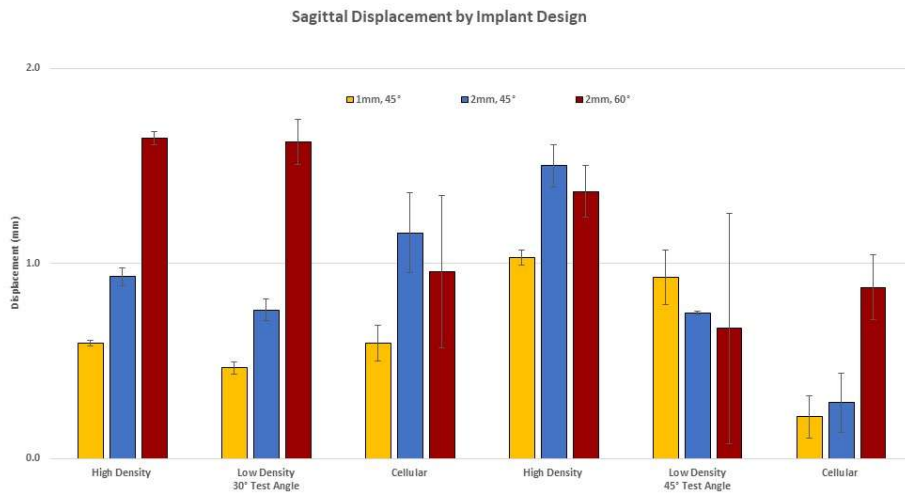


Figure 3

Surgical Outcomes of Bio-Integrative Fiber-Reinforced Implants (OSSIOfiber)

*Thellma Jimenez Mosquea - NYU Langone Health - New York, United States of America

Taylor Wingo - NYU Langone Health - NY, USA

Hugo Ubillus - NYU Langone Health - New York, USA

Raymond Walls - NYU Langone Health - New York, United States of America

INTRODUCTION: Hammertoe deformity is common and accounts for nearly half of all forefoot operations. Traditionally, Kirschner wire (K-wire) fixation has been used for correcting this deformity, but it is associated with several complications. Intramedullary implants are increasingly used due to better pain control, good union rates, and decreased infection risk. Bio-integrative fixation implants are novel and engineered from reinforcing mineral fibers bound by a bioabsorbable polymer matrix. This study aimed to evaluate radiological and clinical outcomes associated of OSSIOfiber implant.

METHODS: A retrospective cohort study was conducted on patients diagnosed with hammertoe deformities who underwent operative correction with OSSIOfiber fixation implant at a single large, urban, academic medical center between January 2022 and December 2023. Patient-Reported Outcomes Measurement Information System (PROMIS) and radiographic imaging were used to assess clinical outcomes and union rates, respectively. Data on patient characteristics and postoperative complications were collected.

RESULTS: The study included 11 patients and 21 operative toes. The mean follow-up was 5.7 months. Seventeen toes (81%) maintained deformity correction clinically and radiologically. All patients demonstrated significant improvement in Physical Function, Pain Interference, and Pain Intensity PROMIS domains. Successful union rate at final follow-up was 81%. However, the complication rate was 52.3%, with re-intervention due to painful malunion and non-union being the most common complication (19%). In 23.8% of cases, conversion into K-wire was reported.

CONCLUSION: The OSSIOfiber hammertoe fixation implant demonstrated satisfactory clinical and radiological outcomes, indicating a reliable and reproducible technique for maintaining PIP joint alignment in lesser toes. However, non-compatible implant size may require conversion into traditional fixation with K-wires, highlighting the importance of pre-operative planning before using this implant, to decrease its high complication rate. Long-term follow-up of this newly developed device is needed to establish its efficacy as a reliable alternative for lesser toes joint fusion.

Relationship Between Stem Taper Machining Line Height, Spacing, and Assembly Load for Total Hip Head-Neck Modular Junctions

*Hannah Lundberg - Rush University Medical Center - Chicago, USA

Mitchell Heacock - Rush University - Chicago, USA

Jonathan Rathjen - University of Illinois - Chicago - Chicago, USA

Robin Pourzal - Rush University Med Ctr - Chicago, USA

Brett Levine - Rush University Medical Center - Chicago, USA

Jonathan Gustafson - Rush University Medical Center - Chicago, USA

Introduction

Modular junctions in total hip replacement (THR) can be susceptible to fretting corrosion leading to adverse local tissue reactions. Fretting corrosion initiates mechanically via debris generated during micromotion between the femoral head and stem tapers. To stop fretting before it occurs, it is essential that the head-stem taper contact mechanics are optimized after assembly of the femoral head. In this study, we investigate the relationship between small changes in machining mark height and spacing, assembly force, and contact mechanics.

Methods

Two-dimensional axisymmetric finite element models representing a half cross-section of a femoral head and neck were used to investigate contact mechanics after head-neck assembly. The CoCrMo femoral head taper and Ti6Al4V stem taper dimensions represented a generic 12/14 taper with a distal locked junction (head taper larger than stem taper, angular mismatch of 0.016°). Machining lines of the head and stem tapers were modeled using a sine function, with amplitude and period corresponding to machining line height and spacing, respectively.

Elastic-plastic material properties were used for the head and stem tapers (CoCrMo head: $E=213$ GPa; $\nu=0.33$; yield stress= 1026 MPa / Ti6Al4V stem: $E=109$ GPa; $\nu=0.33$; yield stress= 941 MPa). Models were meshed using reduced integration linear hexahedral elements with an edge length of $\sim 1\mu\text{m}$ based on a prior convergence study. Contact was modeled using a surface-to-surface formulation with penalty contact and Coloumb friction ($\mu = 0.2$). To simulate the assembly of the femoral head, the distal stem taper was fixed, and a parabolic force was applied in a dynamic implicit step over 0.6ms . Models were run using Abaqus Standard (R2019). We parametrically varied the height and spacing of stem taper machining lines to span the first to third quartiles of retrieval measurements (height: $8, 11, \text{ and } 13\mu\text{m}$, spacing: $160 \text{ and } 239\mu\text{m}$). The dynamic assembly load varied between $6, 8, \text{ and } 10\text{kN}$ based on measured assembly loads applied by surgeons at our institution. Eighteen simulations were run in total. The model outcome variables included plastic strain, contact pressure, contact area, and displacement.

Results

Increased machining line height resulted in decreased contact area and increased plastic deformation. Increased machining line spacing resulted in an increase in the percentage of machining lines in contact at the end of the simulation, but decreased contact area, particularly for the lowest assembly load. Increased assembly load resulted in increased contact pressure, contact area, and plastic deformation. Fewer machining lines were in contact under a 6kN assembly load than under an 8 or 10kN assembly load. All machining lines underwent plastic deformation regardless of geometry or assembly load. Example simulations are shown in Figure 1.

Conclusion

This study aimed to investigate the relationship between machining line height and spacing and assembly load on contact mechanics during head-neck assembly. Moderate differences in contact mechanics were seen with height variation, and subtle differences were seen with spacing variation. Larger variation in contact mechanics were seen due to assembly load than machining line geometry.

Figures

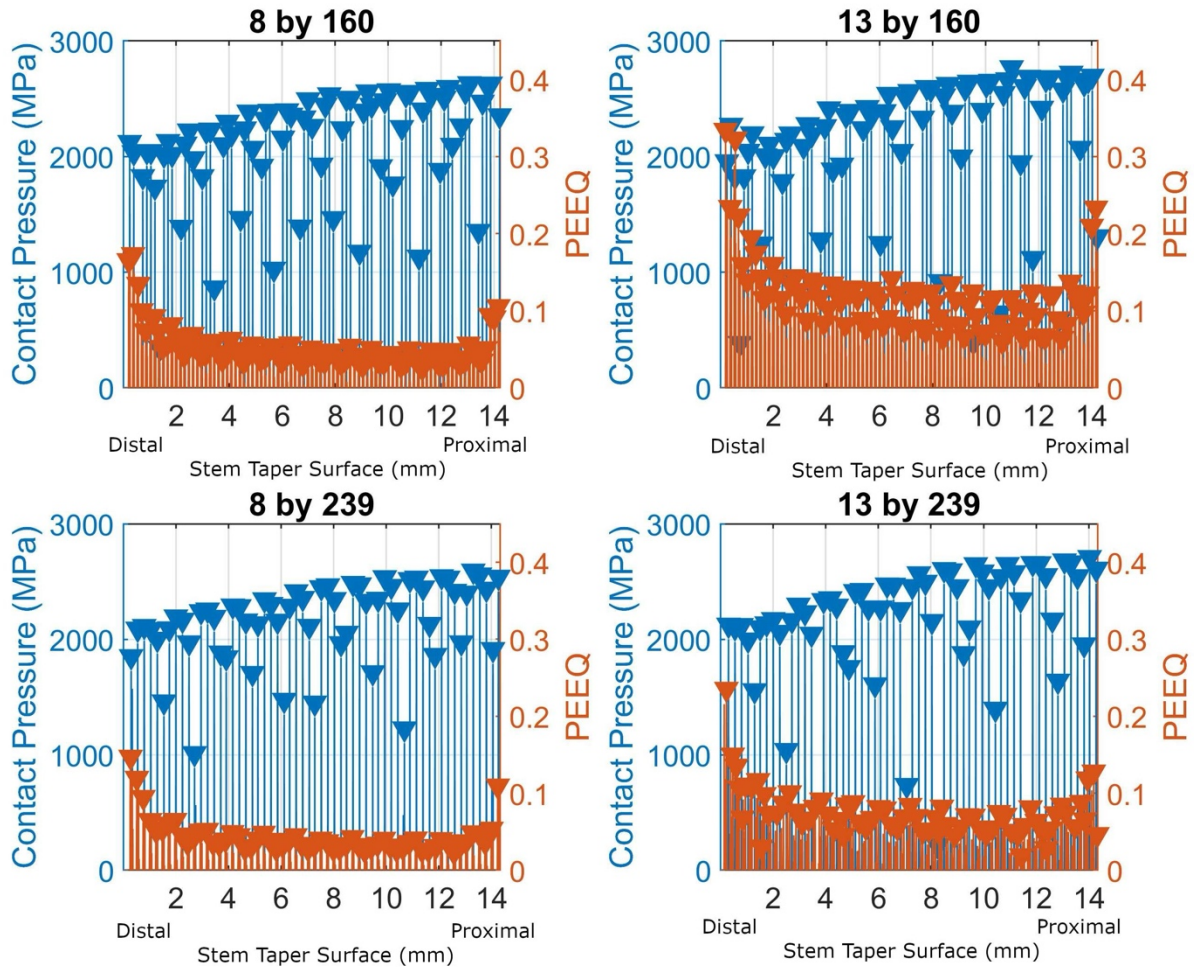


[Figure 1](#)

Assessment of Primary Implant Stability With Different Bone Graft Substitutes in an Acetabular Model Defect

*Ronja Schierjott - Aesculap AG - Tuttlingen, Germany

Georg Hettich - Aesculap AG - Tuttlingen, Germany

Luca Cristofolini - Alma Mater Studiorum-University of Bologna - Bologna, Italy

Martin Buttarò

Heiko Graichen - Asklepios Klinik Lindenlohe GmbH - Schwandorf, Germany

Volkmar Jansson - Hospital of the Ludwig-Maximilians-University of Munich - Munich, Germany

Maximilian Rudert - Orthopädische Klinik König-Ludwig-Haus Würzburg - Würzburg, Germany

Francesco Traina - Istituto Ortopedico Rizzoli di Bologna - Bologna, Italy

Thomas M. Grupp - Aesculap AG - Tuttlingen, Germany

Introduction

Aseptic loosening is one of the main reasons for revision in total hip arthroplasty (THA) [1] and can, among others, be caused by insufficient primary stability. Revision surgery is often associated with acetabular bone defects, whereby one treatment option is impaction bone grafting (IBG). However, the used cancellous bone chips are limited in supply and an infection risk remains. Synthetic bone graft substitute may represent an attractive alternative. The objectives of this study were to (1) use an especially developed reproducible surrogate model to assess the primary stability of a press-fit cup in combination with compacted bone chips (gold standard) (2) compare it to the primary stability achieved by two different bone graft substitutes.

Materials & Methods

Based on a quantitative acetabular defect analysis [2], a representative model defect was derived and implemented in an acetabular surrogate model made of polyurethane foam [3]. The mainly medial defect was filled with either bone chips (*bone chips*), bioactive glass granules in a polyethylene glycol-glycerol matrix (*b.a.glass+PEG*), or β -tricalciumphosphate tetrapods in a collagen matrix (*tetrapods+coll*) and combined with a press-fit cup (Figure 1).

Six specimens in each test group were loaded in direction of the maximum resultant force during level walking in a sinusoidal wave form. The maximum load was increased step by step from 600 N to 3000 N and relative motions between cup and acetabular model were analyzed using the optical measurement system GOM Pontos (GOM GmbH Braunschweig, Germany). It was distinguished between inducible displacement, i.e. reversible micromotion between maximum and minimum load in each load cycle and migration, i.e. permanent migration accumulated between the load steps. Statistical significance among the test groups was assessed using a Mann-Whitney U test.

Results

In all three test groups, relative motion increased with increasing load (Figure 2). Inducible displacement at the last load step was highest for *bone chips* ($113 \pm 3 \mu\text{m}$) and lowest for *b.a.glass+PEG* ($91 \pm 3 \mu\text{m}$), whereas migration was highest for *b.a.glass+PEG* ($881 \pm 95 \mu\text{m}$) and lowest for *tetrapods+coll* ($494 \pm 12 \mu\text{m}$). A statistically significant difference with $p < 0.05$ was found among the test groups at the last load step.

Conclusion

Three different defect filling materials could successfully be compared using a representative model defect. In terms of inducible displacements, *tetrapods+coll* showed a behavior comparable to *bone chips* and hence might represent an attractive alternative to the current gold standard. However, this should be further confirmed by tests in additional defect types and complemented by osseointegration assessments.

References

[1] AAOS American Joint Replacement Registry 2023 Annual Report

[2] Hettich et al, J Orthop Res, 37(1):181-189, 2019

[3] Schierjott et al., J Orthop Res, 38(8):1769-1778, 2020

Keywords: Acetabular bone defect, impaction grafting, press-fit cup, primary stability

Figure captions:

Figure 1: The three test groups bone chips, b.a.glass+PEG and tetrapods+coll in model defect (left) and exemplary specimen with press-fit cup and tracking points for optical relative motion analysis, dynamically loaded by a servo-hydraulic testing machine (right)

Figure 2: Mean (\pm SD) inducible displacement in the three test groups

Differences in Femoral Stress Distribution With Different Cement Mantle Thicknesses in the Same Type of Cemented Stem - a Thermoelastic Stress Analysis Study

*YASUNAGA SHOTA - University of Tsukuba Hospital - Tsukuba, Japan

Tomofumi Nishino - University of Tsukuba - Tsukuba, Japan

Koshiro Shimasaki - University of Tsukuba Hospital - Tsukuba, Japan

Ryunosuke Watanabe - university of tsukuba - Tsukuba, Japan

Sho Totsuka - University of Tsukuba, - Tsukuba, Japan

Tomohiro Yoshizawa - University of Tsukuba - Tsukuba, Japan

Hajime Mishima - University of Tsukuba - Tsukuba, Japan

Yoshihisa Harada - National Institute of Advanced Industrial Science and Technology - Tsukuba, Japan

Background

Bone resorption due to stress shielding and cortical hypertrophy due to stress concentration occur around the stem in the femur after total hip arthroplasty (THA), raising concerns about their impact on the long-term outcomes of the stem. Reports suggest that the shape, material, surface processing, and cement of the cement stem used in THA influence stress distribution and bone reaction, but there is no consensus. Thermoelastic stress analysis (TSA) is an experimental method that captures surface temperature changes on a simulated bone under load using an infrared camera, allowing for two-dimensional visualization of stress distribution.

Objectives

The aim of this study is to evaluate the femoral stress distribution of cement stems with different cement mantle thicknesses using TSA.

Methods

The study was divided into two groups based on cement mantle thickness: 0mm and 2mm. For each group, three C-Stem AMT (Depuy Synthes, 0mm group: stem size #4, 2mm group: stem size #3) were inserted into simulated femurs, and repeated vertical loads were applied. Temperature changes on the surface of the simulated bone were captured with an infrared stress imaging device and converted into stress distribution images. Stress values for each pixel along a line parallel to the bone axis were measured on both the lateral and medial sides and compared between the two groups.

Results

On the medial side, both groups showed compressive stress with peak values in Gruen zones 5 and 6, and the 0mm group exhibited higher values throughout the medial side. On the lateral side, both groups showed tensile stress with peak values in zones 2 and 3, but there were no clear differences in stress distribution and peak values.

Discussion

There has been no report on the comparison of stress distribution with different cement mantle thicknesses. In this study, it was observed that a thinner cement mantle showed greater compressive stress on the medial side. Conversely, in the group with the cement mantle set to the standard thickness of 2mm, stress was distributed both medial and lateral side, which is believed to have reduced the compressive stress on the medial side. Additionally, excessive stress concentration at the distal end of the stem was not observed in either group.

Conclusions

Differences in the thickness of the cement mantle resulted in variations in stress distribution on the medial side of the femur, but no difference was observed on the lateral side.

Promising Results and Removals in the First Year With a Redesigned Anatomically Shaped Meniscus Prosthesis

*Petra Heesterbeek - Sint Maartenskliniek - Nijmegen, Netherlands

Branco van Minnen - RadboudUMC - Nijmegen, Netherlands

K.C. Defoort - Sint Maartenskliniek - Ubbergen (near Nijmegen), The Netherlands

Pieter Emans - Maastricht University Medical Centre - Maastricht, Netherlands

Ewoud Van Arkel - Haaglanden MC - The Hague, Netherlands

Thijmen Struik - Atromedical - Uden, Netherlands

Liesbeth Jutten - Maastricht Medical Center - Maastricht, Netherlands

Saskia Susan - Sint Maartenskliniek - Ubbergen, Netherlands

Sebastiaan van de Groes - Radboudumc - Nijmegen, Netherlands

Nico Verdonschot - Radboudumc - Nijmegen, Netherlands

Tony van Tienen - Atro Medical BV - Nijmegen, Netherlands

Introduction

This interim analysis of a prospective single-arm clinical investigation aims to evaluate safety and feasibility of a redesigned, anatomically shaped medial meniscus prosthesis, including its fixation technique and the surgical procedure.

Methods

The meniscus prosthesis (*Figure 1*) was implanted arthroscopically in 10 patients suffering from medial post-meniscectomy pain syndrome and fixated to the tibial plateau by two fixation tapes and interference screws. Patient reported outcome measures (PROMs) were obtained at baseline, 6 weeks, 3 months, 6 months, and 12 months follow-up. The main clinical endpoint was KOOS Pain score at 12 months. Radiographs and MRI scans were obtained at baseline and after 12 months, to evaluate osteoarthritis progression and cartilage status.

Results

The surgical technique was found to be feasible, although the posterior horn was positioned suboptimal in three patients. In one case, this resulted in subluxation and removal of the prosthesis. Wear and breakage of one or more fixation tapes resulted in three additional explantations. Pain scores already started to improve 6 weeks after implantation and kept improving at three-, six- and 12-month follow-up. Five out of six patients who reached one-year follow-up reported an improvement of KOOS pain score exceeding the minimal clinically important difference (MCID) of 10 points, while the mean increase was 30.1 ± 25.8 (*Figure 2*). Imaging revealed no adverse effects of the meniscus prosthesis on osteoarthritis progression or cartilage condition.

Conclusion

The patients reaching one-year follow-up reported good clinical outcomes. The redesigned medial meniscus prosthesis was explanted in four out of 10 cases, due to fixation tape failure and discomfort. Improved positioning of the prosthesis and an enhanced fixation technique are needed to reduce the risk of failure, potentially making the anatomically shaped meniscus prosthesis a promising solution for patients suffering from post-meniscectomy pain syndrome.

Figures



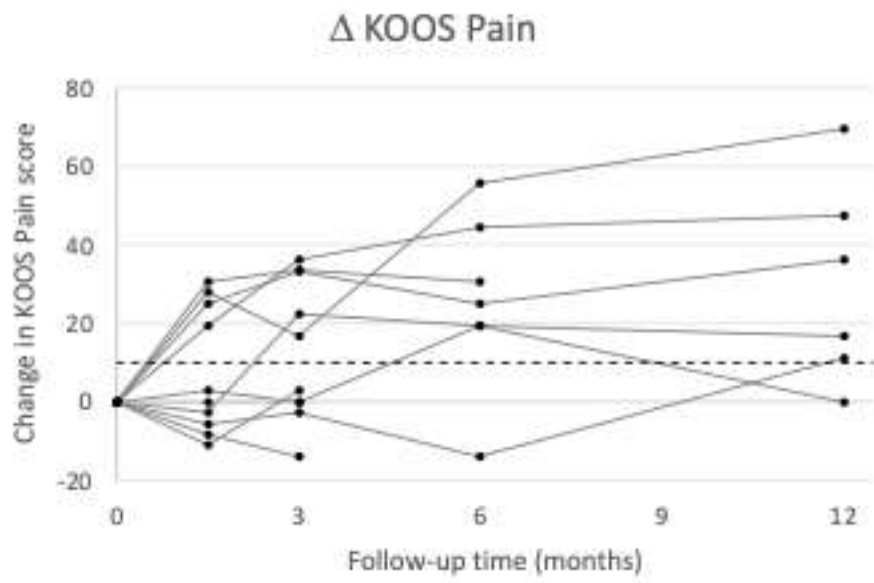


[Figure 1](#)
[Figure 2](#)

Clinical Outcomes Following Total Ankle Arthroplasty Over 18 Years at a Single Institution

*Kelly Dopke - Penn State College of Medicine - Hershey, USA

Michael Aynardi - Penn State College of Medicine - Hershey, USA

Luigi Sabal - Penn State - Hershey, USA

Zachary Koroneos - Penn State University - Hershey, USA

Introduction: The purpose of this study was to perform a retrospective review of all patients that underwent total ankle arthroplasty (TAA) procedures to assess cases resulting in failure or requiring revision. This work aims to contribute to the pre-existing data regarding TAA outcomes, providing a relatively large patient set at a single institution.

Methods: Following institutional review board approval, a database was obtained for patients that underwent TAA procedure for ankle arthritis between 2006 and 2024. The charts of 90 patients were reviewed for demographic, hardware, and clinical outcome data. The primary outcomes included implant survival, incidence of postoperative complications including infections, mechanical failures, and the need for revisions. Secondly, the implant manufacturer, hardware used in conjunction, and joint replacements of hips and knees on the ipsilateral and contralateral sides were noted with regards to their time relation to the TAA procedure.

Results: The cohort consisted of 53.8% males and 46.2% females, with a mean age at surgery of 63 years (range 33 – 82). Patients were predominantly white (91.2%) while 3.3% were African American, and 5.5% were noted as “other” or multi-racial. At the time of data extraction, 8.8% of patients were deceased. The percentages of implants from each company were the following: 45% Salto Talaris, 25% Zimmer, 11% Wright Medical Technology, 9% DePuy Agility, 6% Star Prosthesis, 2% Integra Salto, 1% Advanced Surgical, and 1% Prophecy Infinity. Additional surgical hardware included the use of additional screws (60.4%), plates (38%), locking screws (19%), and cortical screws (19%). Additional surgical interventions included osteotomies (37.4%), Achilles lengthening (47.3%), deformity correction frames (26.4%), and the removal of pre-existing hardware (22.0%). Readmissions were noted in 20.9% of patients, with causes related to both surgical complications and unrelated conditions such as abdominal pain and trauma. Of the related complications, 3.3% reported ankle pain, 4.4% had infections, and 3.3% had mechanical failure requiring revision. The revisions were performed at 74-, 21-, and 7-month post-initial-surgery, with the 7-month revision attributed to a failure in the Salto Talaris implant. Notably, two Salto Talaris implants were associated revision due to polyethylene wear. The remaining failure was the single Advanced Surgical implant. Amongst the patients, 42.2% had at least one other joint replacement of the hip or knee on either side. There was a total of 53 other (non-TAA) joint replacements across all patients. However, 81.1% of these were performed before the TAA. All three patients with revisions were still alive at the time of data extraction and had not been readmitted since their revision surgeries of at least 7 years ago.

Conclusion: Detailed information on the hardware being employed in TAA procedures, and long-term patient outcomes may contribute to our understanding of areas for improvement in these cases. This study aimed to provide a retrospective review of TAA patient outcomes and details on their procedures. This may contribute to pre-existing data on the outcomes of these patients and provides a groundwork for

more detailed analyses at our institution involving more complex statistical modeling and determining correlations.

Efficacy of Transfibular Total Ankle Arthroplasty Using a Tibial Pre-Cutting Technique for Severe Varus Deformity

*Koichiro Yano - Tokyo Women's Medical University - Tokyo, Japan

Katsunori Ikari

Ken Okazaki - Tokyo, Japan

Background

Coronal plane deformity greater than 15 degrees is considered a relative contraindication for total ankle arthroplasty (TAA). The authors have developed a novel technique to correct severe tibiotalar varus deformity in the ankle by pre-cutting the distal tibia, which helps to prevent impingement between the tibia and talus. The purpose of this study was to assess the radiographic and clinical outcomes following this innovative surgical procedure.

Methods

This study selected 17 cases with a preoperative coronal plane varus deformity greater than 15 degrees from patients who underwent transfibular TAA using the new technique between November 2019 and October 2023 (Fig. 1). The tibiotalar angle (TTA) was measured to assess the coronal angulation of the tibiotalar joint both before and after surgery. The position of the talus in relation to the tibia was evaluated using the tibiotalar ratio (TTR). The self-administered foot evaluation questionnaire (SAFE-Q) was employed preoperatively and at the latest follow-up to assess clinical outcomes.

Results

The median duration of follow-up was 12.3 months (Interquartile Range [IQR]: 6.4 to 28.8 months). The preoperative median TTA of 20.4 degrees (IQR: 19.7 to 24.6 degrees) significantly decreased to 1.9 degrees (IQR: 0.1 to 4.3 degrees) at the latest follow-up ($p < 0.01$) (Fig. 2). While there was no significant change in the TTR during the study period, the number of cases within the normal range increased from 8 (47.1%) preoperatively to 12 (70.6%) at the latest follow-up. All subscales of the SAFE-Q showed significant improvement at the latest follow-up.

Conclusion

The novel surgical technique for transfibular TAA can effectively correct severe coronal-plane tibiotalar varus deformity without additional interventions and leads to satisfactory clinical outcomes.

Figures

Figure 2. A posttraumatic osteoarthritis case who underwent the transfibular total ankle arthroplasty using this novel technique. a) Preoperative anteroposterior radiograph of the ankle. b) Postoperative anteroposterior radiograph of the ankle. Preoperative varus deformity was corrected.

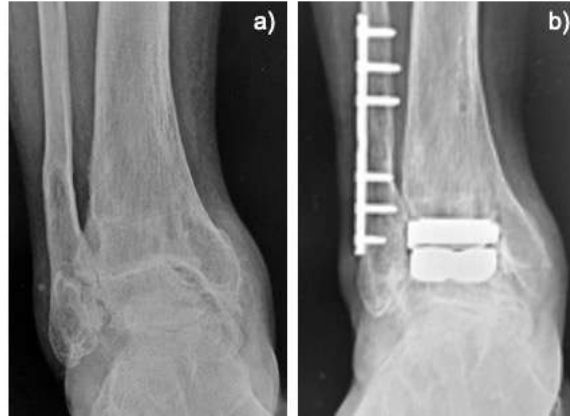


Figure 1

Figure 1. The result of the tibiotalar angle (TTA). Each box describes the interquartile range of values, with the bold horizontal lines within the boxes representing the median value. The vertical dashed lines describe maximum and minimum values within 1.5 box lengths.

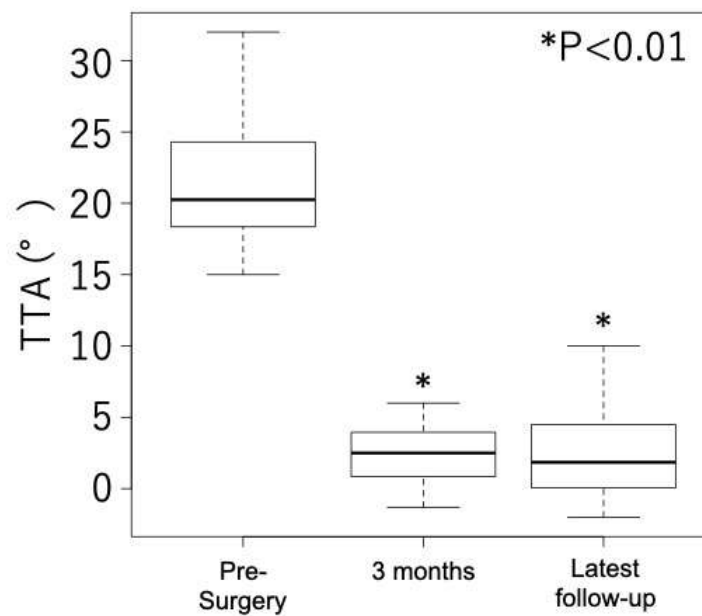


Figure 2

Mid to Long-Term Outcomes of Total Ankle Replacement: A Systematic Review

*Thellma Jimenez Mosquea - NYU Langone Health - New York, United States of America

Yasmeen Saeed - UMass Chan Medical School - Worcester, USA

Hugo Ubillus - NYU Langone Health - New York, USA

Raymond Walls - NYU Langone Health - New York, United States of America

INTRODUCTION: Total ankle replacements (TAR) are increasingly recognized as a viable alternative to ankle arthrodesis for treating end-stage ankle arthritis. Although initially marked by high rates of adverse events, newer generations of implants have led to improved outcomes. Reports on mid to long-term outcomes of TAR are still sparse. This study aimed to evaluate outcome across multiple TAR studies with an average follow-up between 5 to 10 years.

METHODS: A multi-database search was performed in April 2024 according to PRISMA guidelines. We included articles from the past 15 years involving patients who underwent TAR and had a minimum five-year follow-up, reporting clinical outcomes and complications. We collected American Orthopedic Foot and Ankle Society (AOFAS) and Visual Analog Scale (VAS) scores, along with range of motion at the final follow-up.

RESULTS: We included 31 studies involving a total of 3,111 patients and 4,043 ankles, with a mean follow-up of 116 ± 48 months. Mean age at the time of treatment was 59.3 years. The studies reported improvements in AOFAS score, from a preoperative mean of 33.6 to a postoperative mean of 76.6. The VAS also improved, decreasing from 8.1 preoperatively to 2.3 postoperatively. Additionally, there were enhancements in ankle mobility, with dorsiflexion increasing from 3.9° preoperative to 9° postoperative, and plantarflexion improving from 17.5° to 20.3° . There were 494 (16%) revisions, with an average of 29 per study. By final follow-up, the survival rate of the implants was 82%.

CONCLUSION: Outcomes following TAR are favorable, indicating improvement in clinical outcomes over mid to long-term follow-up. However, the revision and survival rates highlight challenges in the durability of TAR implants. Given the variance in outcomes and frequent revisions, future research should assess long-term effectiveness and refine patient selection criteria to identify those likely to achieve the best results.

Patient Perception of Artificial Intelligence Digital Medical Assistants for Postoperative Care

*Charles Lawrie - Baptist Health South Florida - Coral Gables, USA

Andrew McDaid - University of Auckland - Auckland, New Zealand

Introduction: Responding to patient messages and phone calls to the surgeon office in the postoperative period after hip and knee arthroplasty requires significant care team time and resources. Artificial intelligence powered digital assistants trained on surgeon specific protocols have the potential to handle these patient interactions. However, the patient perception of this technology remains unknown. In this study, we seek to determine patient willingness to use and perception of AI powered digital medical assistants for postoperative care after hip and knee arthroplasty.

Methods: Patients who had undergone primary total knee arthroplasty in a multi-surgeon practice were given a survey at their 6 week follow up visit to evaluate their perception and acceptance of digital assistants as their point of contact for questions and concerns postoperatively (Table 1 and Table 2).

Results: 76 responses were collected. Patient ages ranged from 40-80 years old. 46% of respondents identified as female gender. Survey results shown in table 1, and table 2 presents patients preference in response to concerns they may have. 54% would be “very likely” to use a digital medical assistant rather than trying to reach the surgeons office and 89% of people would trust a digital medical assistant. For all issues patients would rather chat to a digital assistant than any other existing option they currently have available, including calling the office. Digital orthopedic employees were built and successfully achieved a number of common tasks including answering common patient pre-/post-surgical questions and delivering accurate information on specific DME products prescribed to patients.

Conclusion: Patient perception of AI powered digital medical assistants is overall positive. Our findings support the use of such technology to improve patient care quality and efficiency.

Figures

Table 1. Survey results

How much would you trust a digital medical assistant to provide you with accurate information about your care?		
A great deal	15/76	19.74%
A lot	20/76	26.32%
A moderate amount	33/76	43.42%
A little	7/76	9.21%
None at all	1/76	1.32%
If a digital medical assistant were available today and it would give you answers within seconds, 24 hours a day 7 days a week, how likely would you be to use it instead of trying to reach the surgeons office?		
Extremely likely	18/76	23.68%
Very likely	23/76	30.26%
Somewhat likely	29/76	38.16%
Not so likely	5/76	6.58%
Not at all likely	1/76	1.32%
Would encouragement and reminders from the medical assistant regarding your postoperative care and physical rehab encourage you to be more engaged in your recovery?"		
Strongly agree	19/76	25.00%
Agree	30/76	39.47%
Neither agree nor disagree	25/76	32.89%
Disagree	1/76	1.32%
Strongly disagree	1/76	1.32%

Table 2. "If you had concerns about [issue] would you rather...?"

Issue	Call the office	Chat with a digital medical assistant	Internet search	Drive to the clinic	Drive to the Emergency Room	Do nothing
Wound care	26.32%	48.68%	18.42%	5.26%	0%	1.32%
Infection	35.53%	44.74%	1.32%	11.84%	5.26%	1.32%
Pain and medication	38.16%	43.42%	11.84%	5.26%	1.32%	0%
Activity	26.32%	51.32%	17.11%	5.26%	0%	0%

Figure 1

ChatGPT Is a Suitable Option for Common Patient Questions Regarding Total Joint Arthroplasty

*Hamza Raja - Henry Ford Hospital - Detroit, USA

Idris Nagarwala - Henry Ford Hospital - Detroit, USA

Hamza Kanchwala - Henry Ford Hospital - Detroit, USA

Noah Hodson - Henry Ford Hospital - Detroit, USA

Michael Charters - Henry Ford Hospital - Detroit, USA

Trevor North - Henry Ford Hospital - Detroit, USA

PURPOSE: This study investigates the quality and readability of ChatGPT responses to common patient questions regarding total hip and total knee arthroplasty compared to current reputable online information.

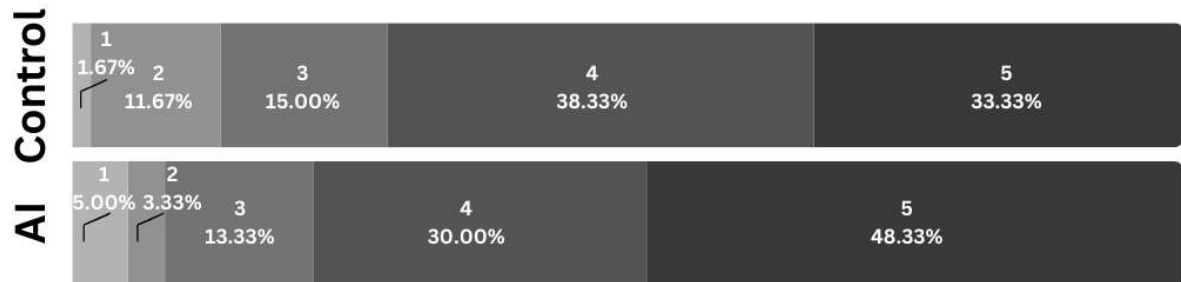
METHODS: A series of 30 common patient questions and responses (control) were taken from the “Frequently Asked Questions” webpages of various reputable academic institutions. These questions were asked to ChatGPT on November 15, 2023 and the responses were recorded (AI). The original questions, the blinded control responses, and the blinded ChatGPT responses were provided to 2 fellowship-trained orthopaedic adult reconstruction surgeons to grade for preference, medical accuracy, and appropriateness. Accuracy and appropriateness were graded using a Likert scale. Additionally, each response was graded for readability using the Flesch-Kincaid Grade Level.

RESULTS: Surgeons identified no significant preference between AI and control responses ($p > 0.05$). There was no significant difference in response accuracy or appropriateness between AI and control responses. Surgeons agreed (Likert 4 and 5) on the medical accuracy of $73.3 \pm 14.1\%$ of control responses and $68.3 \pm 11.8\%$ of AI responses. Additionally, they disagreed (Likert 1 and 2) on $18.3 \pm 16.5\%$ of control responses and $21.7 \pm 7.1\%$ of AI responses. Likewise, surgeons agreed (Likert 4 and 5) on the appropriateness of $71.7 \pm 21.2\%$ of control responses and $78.3 \pm 21.2\%$ of AI responses. Additionally, they disagreed (Likert 1 and 2) on $13.3\% \pm 18.9\%$ of control and $8.3 \pm 11.8\%$ of AI responses. Flesch-Kincaid Grade Level scores revealed both responses exceeded recommended reading levels (control: 10.04 ± 2.41 years; AI: 16.45 ± 2.40 years; $p < 0.05$).

CONCLUSION: Responses by ChatGPT were comparable in accuracy and appropriateness to responses by reputable academic institutions, offering a valuable alternative to information online. Patients should express caution with information presented and defer to surgeon counseling when making treatment decisions.

Figures

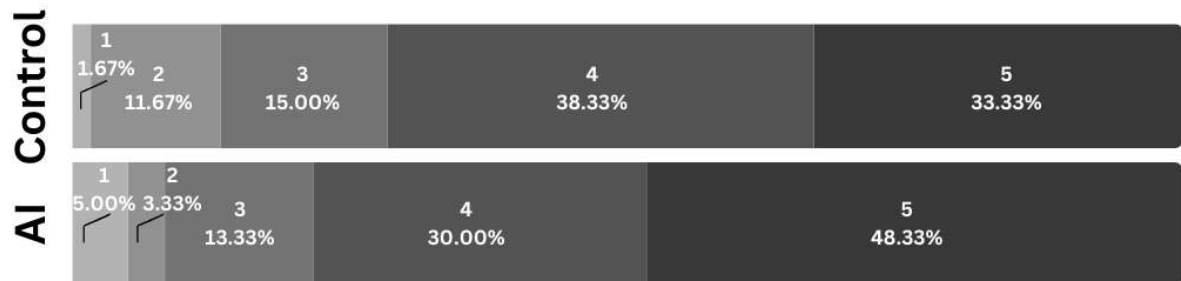
Appropriateness Likert Scale (mean)



1. Strongly Disagree: The response does not address the question at all.
2. Disagree: The response has significant deficiencies in addressing the question.
3. Neutral: The response is neither appropriate nor inappropriate.
4. Agree: The response is mostly appropriate with some minor issues.
5. Strongly Agree: The response is completely appropriate and directly addresses the question.

[Figure 1](#)

Appropriateness Likert Scale (mean)



1. Strongly Disagree: The response does not address the question at all.
2. Disagree: The response has significant deficiencies in addressing the question.
3. Neutral: The response is neither appropriate nor inappropriate.
4. Agree: The response is mostly appropriate with some minor issues.
5. Strongly Agree: The response is completely appropriate and directly addresses the question.

[Figure 2](#)

Mitigating Potential Retrieval Study Bias Through Multi-Institutional Study Design and Capture

*Rebecca Thomson - Dartmouth College - Hanover, United States of America

Kori Jevsevar - Dartmouth College - Hanover, USA

Alexander Orem - Dartmouth Health - Lebanon, United States of America

Matthew Abdel - Mayo Clinic - Rochester, USA

Douglas Van Citters - Dartmouth College - Hanover, USA

Introduction: Only a small fraction of revision arthroplasty devices is sent to retrieval laboratories for analysis. The additional effort associated with disinfecting, documenting, and transferring a retrieval to a laboratory has lower perceived value when that device appears “normal” or the reason for revision appears routine. Thus, retrieval laboratories have the potential to demonstrate selection bias based on the selection criteria exercised by their contributors. While this hypothesis is often stated at conferences and in limitation sections of manuscripts, the significance of the potential problem and its magnitude have not been established. This study seeks to test whether retrievals received from voluntary contributors demonstrate different damage scores when compared to retrievals from a group of partner institutions which contribute 100% of revised devices.

Methods: Analysis of Hood damage scores (a modification of Hood et al., 1983) from an IRB-approved database was performed to determine the difference in scores and potential for contribution bias. The retrieval laboratory receives 100% of the retrieved implants from multiple academic institutions, representing a non-biased control group (N=9672). Implants are also received from a variety of sources that may have selection bias due to the voluntary nature of contribution (N=10248). Implants with unknown explanting surgeons were excluded (N=2327). Averaged Hood damage scores were collected for all relevant areas of implants: articular metal components, non-articular polyethylene, and articular polyethylene components. Scores were aggregated across all joints in the collection including knees, hips, ankles, shoulders, and elbows. Statistical analysis for each location of damage was performed through Mann-Whitney tests.

Results: Overall, this study confirmed that the database shows statistically significant differences when comparing the damage scores of implants retrieved through the voluntary vs 100% capture routes. The implants retrieved through the compulsory collection pathway had lower average Hood damage scores. Only metal articular medial scratching had nonsignificant damage score differences. Both polyethylene articular and non-articular surfaces had higher damage scores when retrieved through voluntary routes.

Conclusion: Significant differences exist between implant appearance when contribution route is considered. While patient presentation at institutions designed to capture 100% of devices may be different, prior studies showed no difference in reason for retrieval between these different contribution sources. Studies must be engineered to address this potential contribution bias. Utilizing 100% capture and analysis across multiple institutions is one mechanism to build a more representative database.

Figures

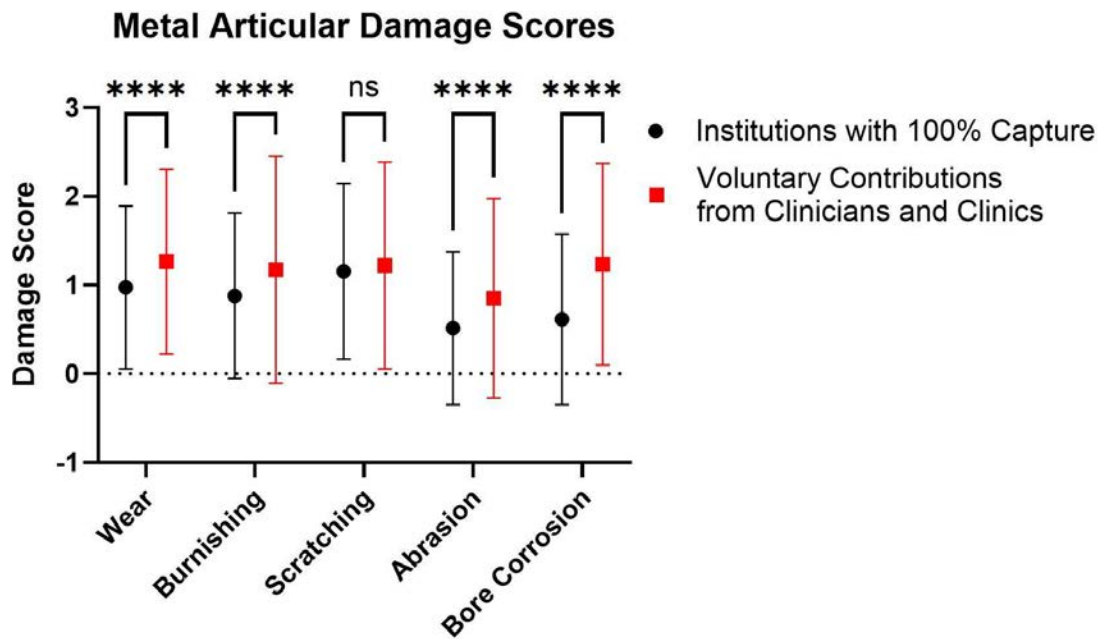


Figure 1: Average damage scores for metal articular surfaces comparing institutions with 100% capture with voluntary contributions. Statistical significance key: ns $P > 0.05$, $*P \leq 0.05$, $**P \leq 0.01$, $***P \leq 0.001$, and $****P \leq 0.0001$.

[Figure1](#)

Polyethylene Articular Damage Scores

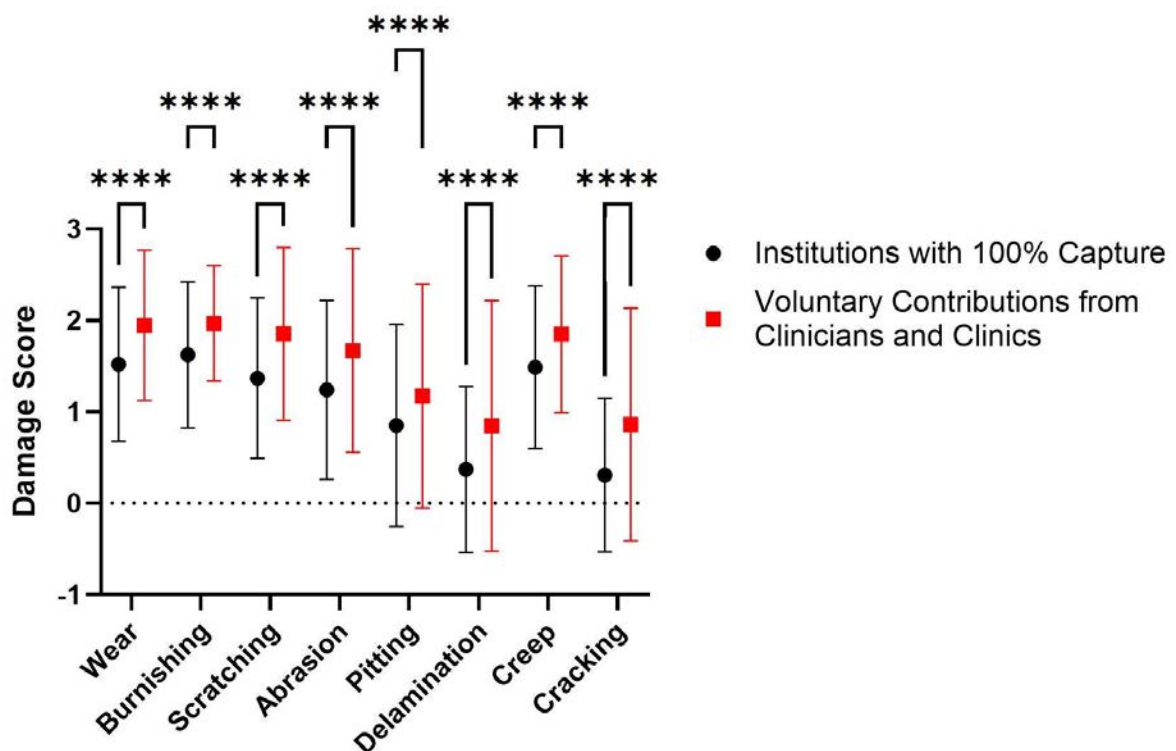


Figure 2: Average damage scores for polyethylene articular surfaces comparing institutions with 100% capture with voluntary contributions. Statistical significance key: ns $P > 0.05$, $*P \leq 0.05$, $**P \leq 0.01$, $***P \leq 0.001$, and $****P \leq 0.0001$.

[Figure2](#)

Polyethylene Nonarticular Damage Scores

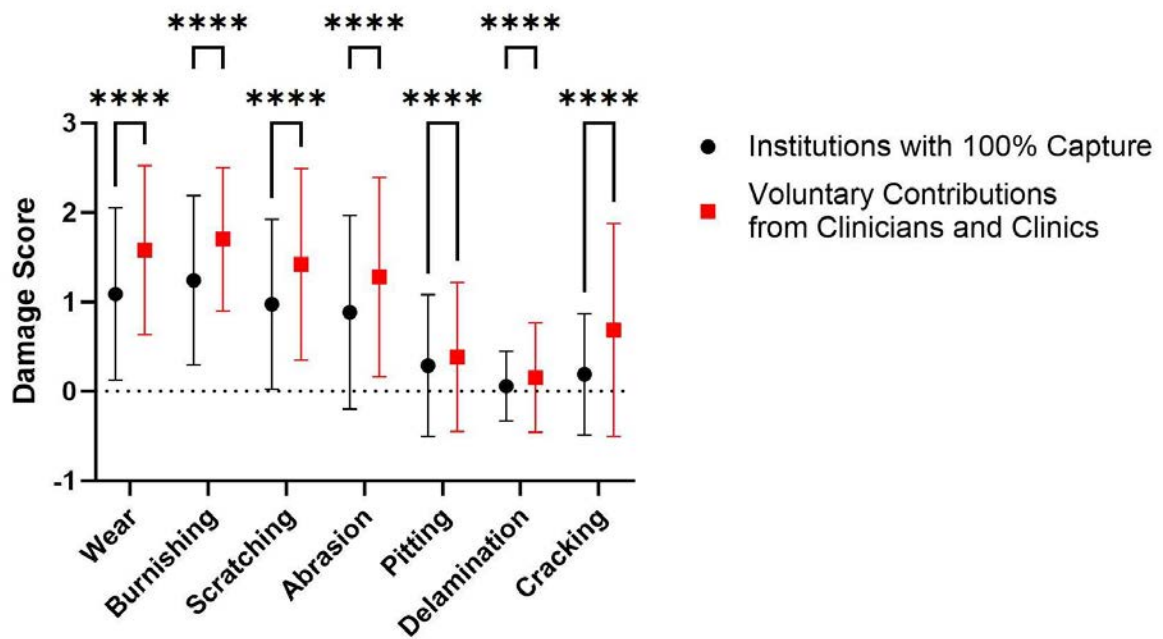


Figure 3: Average damage scores for polyethylene nonarticular surfaces comparing institutions with 100% capture with voluntary contributions. Statistical significance key: ns $P > 0.05$, * $P \leq 0.05$, ** $P \leq 0.01$, *** $P \leq 0.001$, and **** $P \leq 0.0001$.

[Figure 3](#)

Academic Lineage in Orthopaedics: Its How You Finish.

*Aleksander Mika - Vanderbilt Orthopedics

John Ryan Martin - Vanderbilt Health - Hendersonville, USA

BACKGROUND:

Orthopaedics is among the most competitive specialties included in the National Resident Matching Program (NRMP). Recent literature suggests that residents at the highest quartile of US orthopaedic residency are more likely to match at their most preferred choice for fellowship. The link between medical school rankings and residency training, however, has not yet been elucidated. Therefore, the purpose of this study was to determine if medical school rankings are predictive of obtaining a residency position at a top tier residency program and subsequently having the best opportunity to match at one's top choice for fellowship.

METHODS:

Data from 804 residents within the top quartile of US orthopaedic residencies, as per the 2023-2024 Doximity rankings were collected. Medical school rankings were sourced from the latest US News and World Report rankings. The investigation scrutinized acceptance trends, delineating the "academic lineage" at both program and individual levels. Differences in medical school rankings between quartiles were assessed through statistical tests, and prediction analyses were conducted using nonlinear coxvariates.

RESULTS:

When comparing quartiles amongst the top 24 programs, no significant difference in medical school ranking was found. However, for individuals, a resident's medical school ranking is a significant predictor of their residency ranking (Figure 1). This relationship appears to be non-linear and is strongest at the best ranking residency programs and medical schools (Figure 2). The COVID-19 pandemic provided an anomaly as individuals were more likely to become a resident at the same location as their medical school compared to non-COVID years.

DISCUSSION AND CONCLUSION:

This study sheds light on the intricate relationship between medical school rankings, residency training, and fellowship opportunities within orthopaedics. While individuals from higher-ranked schools were more likely to secure positions in top-tier residency programs, no significant differences were observed in medical school rankings among the top quartile of residency programs suggesting that programs maintain diversity and allow many to succeed outside of "traditional" pathways.

Figures

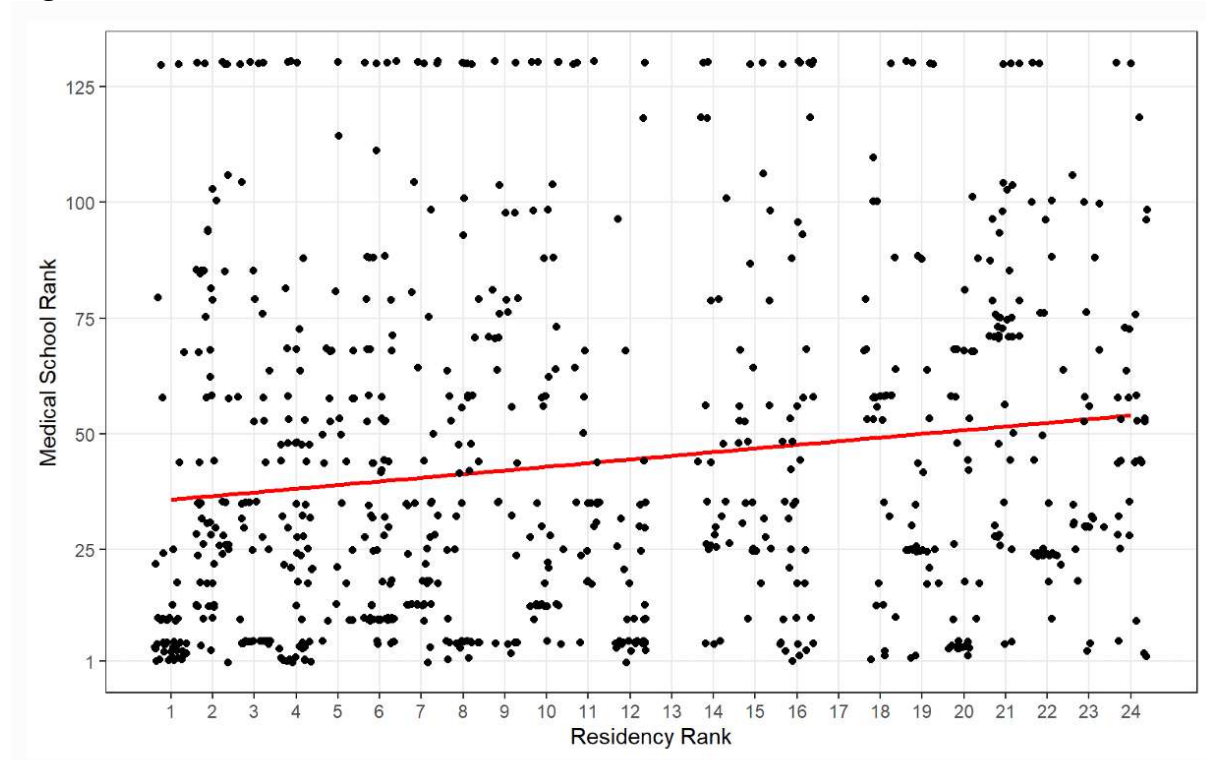


Figure 1

Non-linear Predictor (cubic spline)

For individuals at the top 24 residency programs, a resident's medical school ranking is a significant predictor of their residency ranking ($p < 0.001$), with residents at higher ranked medical schools attending higher ranking residency programs. This relationship appears to be non-linear (See significant "Nonlinear" term in ANOVA output: $p < .0001$).

The below graph plots predicted Residency Rank against Medical School rank. A visual inspection of the graph shows that this relationship seems to be strongest at the best ranking (i.e., numerically lowest ranks) residency programs and medical schools.

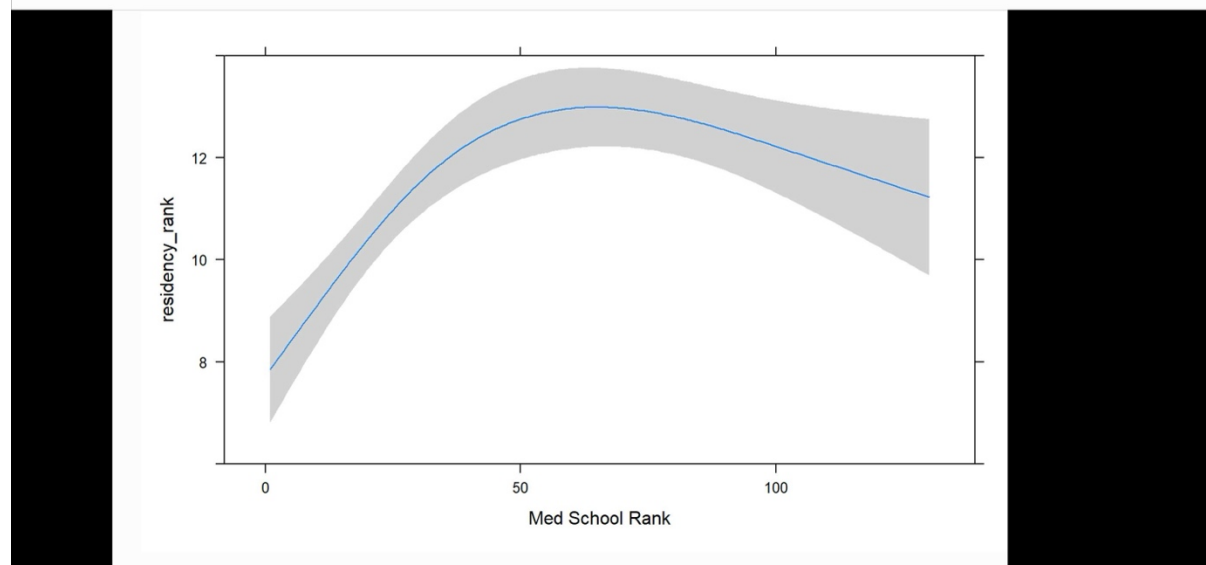


Figure 2

Accuracy and Outcomes of a Novel Cut-Block Positioning Robotic-Arm Assisted System for Total Knee Arthroplasty: A Systematic Review and Meta-Analysis

*Faseeh Zaidi - University of Auckland - Auckland, New Zealand

Michael Goplen - University of Alberta - Edmonton, Canada

Scott Bolam - University of Auckland - Auckland, New Zealand

Andrew Paul Monk - University of Auckland - Auckland, New Zealand

Introduction: The primary objective of this study was to determine the accuracy and precision of component positioning of the ROSA Robotic System for total knee arthroplasty (TKA).

Methods: A PRISMA systematic review was conducted using four electronic databases (MEDLINE, EMBASE, Pubmed and Cochrane Library) to identify all clinical and radiological studies reporting information about the use and results of the ROSA system. The criteria for inclusion were published research articles evaluating the accuracy of component positioning, learning curve, component alignment, complications, and functional outcomes in adults who underwent robotic-assisted TKA. The NIH Quality Assessment Tool was used to evaluate the quality of all included studies.

Results: A total of 26 studies were assessed for eligibility and 17 met the inclusion criteria. Nine studies reported on the accuracy and precision of component positioning. The ROSA platform for TKA had a cutting error of less than 0.6° for all coronal and sagittal parameters. Pooled analysis demonstrated accuracy within 0.61 - 1.87° and precision within 0.97 - 1.34° when the final intraoperative plan was compared to postoperative radiographs with fewer outliers. Four studies reported improved functional scores with ROSA-assisted TKA than conventional TKA within one year of surgery. There was no difference in overall complication rates when compared to conventional TKA.

Conclusion: The ROSA system is both highly accurate and precise with fewer outliers when analyzed at various time points including postoperative standing radiographs. Future studies with robust methodology and longer follow-up are required to demonstrate whether these findings have any clinical benefits in the long-term.

Are All Robotic Technologies Created Equal? Comparing One of the Latest Image-Free Robotic Technologies Against All Other Robotic Systems for Total Knee Arthroplasty

*Anshu Gupta - New Brunswick, United States of America

Philip Huang - OrthoIndy - Indianapolis, USA

Michael Cross - OrthoIndy - Indianapolis, USA

Dhara Intwala - Johnson & Johnson - New Brunswick, USA

Jill Ruppenkamp - Johnson & Johnson - New Brunswick, USA

Dan Hoeffel - Johnson & Johnson - New Brunswick, USA

Introduction

Robotic-assisted solutions have been developed for total knee arthroplasty (TKA) to increase surgical precision and reduce surgical variability [1]. Several different types of robotic systems have been introduced in the last decade for robotic TKA. The DePuy Synthes VELYS Robotic-Assisted Solution (VRAS) is one of the latest entrants in the rapidly evolving field of robotic technology in TKA. VRAS is an imageless system designed to eliminate the need for preoperative CT scans, which results in a reduction in preoperative planning time, cost, and radiation exposure to the patient [2]. There is currently limited evidence comparing this specific imageless robotic technology against other robotic-assisted systems [3,4].

Method

The Premier Healthcare Database [5] was analyzed for comparisons. Patients undergoing TKA using either VRAS or any other robotic-assisted surgery between January 1, 2022, and February 28, 2023, were identified. The primary outcomes for the study were hospital follow up visits (revisits) and readmission rates within 90-day post TKA. Secondary outcomes included operating room time, discharge status and hospital costs. To control for the differences between the VRAS and manual TKA cohorts, a fine stratification and weighing [6] methodology was used.

Results

A total of 827 VRAS TKA patients and 16,238 patients who had other robotic-assisted TKAs were included in the study with 90-day follow-up data. The rates of both all-cause and knee-related 90-day hospital revisits were significantly lower in the VRAS TKA cohort compared to the other class of robotic TKA cohort (14 vs. 22% and 2.8 vs. 5.4%, respectively, p -value <0.01). The readmission rates were also lower for VRAS cohort though this difference was not statistically significant. The index and 90-day follow-up costs were significantly lower for VRAS cohort compared to other robotic classes. The 90-day knee related cost for VRAS cohort was \$15,047 compared to \$16,867 for the class of other robotic technologies with mean difference and 95% CI of \$1,819 [\$1,444 to \$2,194]. Supply and operating room cost contributed more than 85% of total cost for both cohorts, with on average VRAS supply cost being lower by \$682 and operating room cost being lower by \$453. For both cohorts, 96% of patients were discharged to home or with home health services, and both groups had similar operating room times of around 137 minutes.

Conclusion

This database study demonstrated early post-operative readmission rates and total cost of care were significantly lower for VRAS compared to all other classes of robotic technologies while operating room time and discharge status were similar. These are important findings in the ever evolving and cost-conscious health care environment. Continued research with longer term follow-up is required to assess overall economic impact, efficiencies, and differences in patient outcomes.

No Difference in Patellar Resurfacing or Fixation Type in Robotic Total Knee Arthroplasty

*Alana Prinos - Langone Orthopedic Hospital - New York, USA

Akram Habibi - NYU Langone Orthopedic Hospital - New York, United States of America

Sophia Antonioli - NYU Langone - New York, USA

Matthew Hepinstall - NYU Langone Health - New York, USA

Morteza Meftah - NYU Hospital for Joint Diseases - New York, USA

Catherine Digangi - NYU Orthopedic Hospital - New York, USA

Introduction

The decision to resurface the patella in total knee arthroplasty (TKA) remains at the discretion of the surgeon. Different fixation techniques exist for patellar resurfacing, including cemented and cementless fixation, and each fixation type is associated with its own set of complications. The aim of this study was to assess short-term clinical and patient-reported outcomes between non-resurfaced, cemented, and cementless patella fixation in robotic-assisted TKA.

Methods

We retrospectively reviewed 590 primary, robotic-assisted (MAKO, Stryker) TKAs performed between November 2019 and June 2023. Bilateral cases and those without postoperative follow-up were excluded. Implant data was collected from operative reports; only cases with cruciate-retaining (CR) and posterior stabilized (PS) implants and a pressfit tibial baseplate were included. The cohort was divided by patellar component data into cementless (n=346), cemented (n=70), and non-resurfaced (n=174) groups. Patient-reported outcome measures (PROMs), including Knee injury Osteoarthritis Outcome Score for Joint Replacement (KOOS, JR.) and PROMIS Pain Interference scores, were collected; KOOS, JR. was further analyzed via individual patella-related questions. Various clinical outcomes were also collected, and data were analyzed using one-way ANOVA testing and chi-square analyses.

Results

At 6 weeks and 3 months following surgery, the mean change in KOOS, JR. score from prior to surgery showed the greatest trend in improvement for patients in the cemented cohort, though this improvement was not statistically significant (14.6, p=0.053 and 20.3, p=0.087, respectively). The non-resurfaced patella cohort showed the smallest trend in improvement over these same time intervals (9.1, p=0.053 and 15.2, p=0.087, respectively). The PROMIS Pain Interference scores from the preoperative to 6 week and 3 month intervals demonstrated a similar trend, with the greatest trend in improvements seen in the cemented cohort (-2.3, p=0.233 and -8.3, p=0.275, respectively), while the smallest improvement trends were seen in the pressfit cohort (-0.3, p=0.233 and -6.5, 0.275, respectively). The greatest percentage of patients who achieved a perfect AM-PAC score on postoperative Day 0 were in the non-resurfaced cohort, and the smallest percentage were in the pressfit cohort (33.9 vs. 15.9%, p<0.001).

Conclusion

In this study, the cemented cohort demonstrated the greatest trend in improvement in short-term PROMs, with similar improvement trends reflected in the pressfit and non-resurfaced cohorts. However, none of these differences between cohorts were statistically significant. While the pressfit cohort demonstrated the slowest functional

recovery, many of the other clinical outcomes measured showed no statistically significant differences between the three cohorts, and further studies with larger sample sizes are needed to assess whether a true difference exists between patella fixation techniques.

Figures

Table 1: KOOS, JR. Scores Stratified by Pressfit, Cemented, and Non-resurfaced Patella Resurfacing

	Pressfit Patella (n=834)		Cemented Patella (n=5880)		Non-resurfaced Patella (n=3033)		P-value
	M SD	Range	M SD	Range	M SD	Range	
Mean Preoperative KOOS, JR. Score	45.4±12.6	6.4 – 77.7	44.7±13.6	8.3 – 71	46.8±12.2	3.8 – 85	0.552
Mean 6-Week KOOS, JR. Score	54.7±11.2	0 – 85	59.3±11.6	34.2 – 100	55.9±11.7	0 – 92	0.053
Mean Δ Preoperative-6-Week KOOS, JR. Score	9.3±14.0	-34 – 45.5	14.6±14.8	-12.7 – 53.3	9.1±13.0	-28 – 34	0.053
	Pressfit Patella (n=136)		Cemented Patella (n=48)		Non-resurfaced Patella (n=94)		
	M SD	Range	M SD	Range	M SD	Range	P-value
Mean Preoperative KOOS, JR. Score	44.6±13.0	0 – 77.7	44.5±13.1	8.3 – 71	47.2±12.8	3.8 – 85	0.277
Mean 3-Month KOOS, JR. Score	63.1±11.4	27.2 – 100	64.8±10.7	42.0 – 100	62.3±12.7	0 – 92	0.502
Mean Δ Preoperative-3-Month KOOS, JR. Score	18.5±14.4	-10 – 60	20.3±14.2	-21 – 45	15.2±14.5	-29 – 48	0.087

Figure 1

Table 2: PROMIS Pain Interference Scores Stratified by Pressfit, Cemented, and Non-resurfaced Patella Resurfacing

	Pressfit Patella (n=189)		Cemented Patella (n=49)		Non-resurfaced Patella (n=109)		P-value
	<i>M SD</i>	<i>Range</i>	<i>M SD</i>	<i>Range</i>	<i>M SD</i>	<i>Range</i>	
Mean Preoperative PROMIS Pain Interference Score	65.6±6	50 – 84	65.3±6.5	51 – 78	65.9±5.6	48.3 – 78	0.812
Mean 6-Week PROMIS Pain Interference Score	65.4±6.4	39 – 84	62.9±6.7	39 – 74	65.2±6.9	47 – 84	0.064
Mean Δ Preoperative-6-Week PROMIS Pain Interference Score	-0.3±7.4	-25.4 – 25.5	-2.3±7.3	-25 – 11	-0.7±8	-22 – 17	0.233
	Pressfit Patella (n=167)		Cemented Patella (n=50)		Non-resurfaced Patella (n=100)		
	<i>M SD</i>	<i>Range</i>	<i>M SD</i>	<i>Range</i>	<i>M SD</i>	<i>Range</i>	<i>P-value</i>
Mean Preoperative PROMIS Pain Interference Score	65.8±5.8	54 – 84	65±6.5	52 – 78	65.8±5.8	48.3 – 78	0.673
Mean 3-Month PROMIS Pain Interference Score	59.3±5.9	39 – 78.3	56.7±7.2	39 – 69.5	58.9±6.8	39 – 78	0.038
Mean Δ Preoperative-3-Month PROMIS Pain Interference Score	-6.5±6.6	-28 – 11	-8.3±7.9	-24.5 – 9	-6.9±7.4	-27 – 8.7	0.275

[Figure 2](#)

Table 3: Clinical Outcomes Stratified by Pressfit, Cemented, and Non-resurfaced Patella Resurfacing

	Pressfit Patella (n=346)		Cemented Patella (n=70)		Non-resurfaced Patella (n=174)		P-value
	M SD	Range	M SD	Range	M SD	Range	
Mean Length of Stay (hours)	32.5±23	7 – 182	32±26.1	7 – 132	32.7±33.2	7 – 340	0.984
Implant - no. (%)							0.002
CR	311 (89.9)	-	66 (94.3)	-	171 (98.3)	-	
PS	35 (10.1)	-	4 (5.7)	-	3 (1.7)	-	
Achieved a Perfect AM-PAC Score on Postoperative Day 0 – no. (%)	55 (15.9)	-	19 (27.1)	-	59 (33.9)	-	<0.001
90-Day Readmissions – no. (%)	4 (1.2)	-	2 (2.9)	-	1 (0.6)	-	0.329
Days to 90-Day Readmission	13.3±15.9	4 – 37	17±5.7	13 – 21	19±.	19 – 19	0.914
Reason for 90-Day Readmission – no. (%)							0.247
Infection	1 (25)	-	1 (50)	-	0 (0)	-	
Pain	0 (0)	-	0 (0)	-	1 (100)	-	
Wound							
Issue	1 (25)	-	0 (0)	-	0 (0)	-	
Other	2 (50)	-	1 (50)	-	0 (0)	-	
Total Reoperations	2 (0.6)	-	2 (2.9)	-	1 (0.6)	-	
Septic Reoperations	0 (0)	-	1 (1.4)	-	1 (0.6)	-	0.141
Aseptic Reoperations	1 (0.3)	-	1 (1.4)	-	0 (0)	-	0.215
Extensor Mechanism Repair	1 (0.3)	-	0 (0)	-	0 (0)	-	0.702
Patellar Revisions	1 (0.3)	-	1 (1.4)	-	0 (0)	-	0.215
Days to Patellar Revision	91±.	91 – 91	187±.	187 – 187	±.	.-.	-

[Figure 3](#)

Robotic-Arm-Assisted Conversion of Unicompartmental Knee Arthroplasty to Total Knee Arthroplasty

*Matthew Magruder - Maimonides Medical Center - Brooklyn, USA

Tanner McClure - Ortho Rhode Island - Warwick, USA

Kevin Marchand - Ortho Rhode Island - South County, USA

Michael Mont - Sinai Hospital of Baltimore - Baltimore, USA

Robert Marchand - Ortho Rhode Island - South County, USA

Introduction: Unicompartmental knee arthroplasty (UKA) is a successful treatment for primarily single-compartment arthritis. The advent of new technologies has led to renewed interest in evaluating whether outcomes following the conversion of UKA to TKA can be improved. The purpose of this study was to describe a novel robotic-arm-assisted UKA to TKA conversion technique and evaluate the patient reported and clinical outcomes in these patients.

Methods: A retrospective review between 2017 and 2022 was conducted of patients that underwent robotic-arm-assisted UKA to TKA conversion. Charts were reviewed for patient demographics, indications for conversion from UKA to TKA, operative technique, implants used, postoperative complications, and patient-reported outcome measures (PROMs). The surgical technique resembles that of primary TKA, with the major exception of registering the robotic arm with retained UKA implants and removing the implants only when verification is complete. There were 44 robotic-arm-assisted UKAs in 41 patients were included in the study. Indications for UKA conversion to TKA included: 33 patients who had osteoarthritis progression (75%), 7 aseptic loosening (16%), 2 unspecified pain (4.5%), 1 polyethylene wear (2.3%), and 1 prosthetic joint infection (2.3%). Uncemented cruciate-retaining (CR) implants were used in 38 of the 44 robotic-arm-assisted TKAs (86.5%). The other six utilized cemented implants: four CR femurs (9.1%), six tibial baseplates (13.6%), four tibial stems (9.1%), and four medial tibial augments (9.1%).

Results: The PROMs significantly improved at 1-year follow-up, with the average KOOS JR score increasing from 48.1 to 68.7 ($P < 0.001$), and the r-WOMAC score decreasing from 25.7 to 10.6 ($P = 0.003$). Two patients developed prosthetic joint infections (4.5%), one developed aseptic loosening of the femoral component (2.3%), and one developed a superficial surgical site infection requiring superficial irrigation and debridement (2.3%). Overall survivorship was 93.18% at 1.8 years, and aseptic survivorship was 97.7%.

Discussion: Robotic-arm-assisted UKA to TKA conversion exhibited improved patient-reported outcomes and low revision and complication rates. While conversions from UKA to TKA are successful, the literature suggests that there is tremendous room to grow – some research suggests that these conversions have functional outcomes similar to revision TKA. Improved implant placement achieved with robotic-arm-assistance allowed us to decrease the use of revision components and use cementless implants in our cohort. Robotic-assisted technology will likely help surgeons improve the functional and clinical outcomes in our patients following UKA to TKA conversions.

Figures

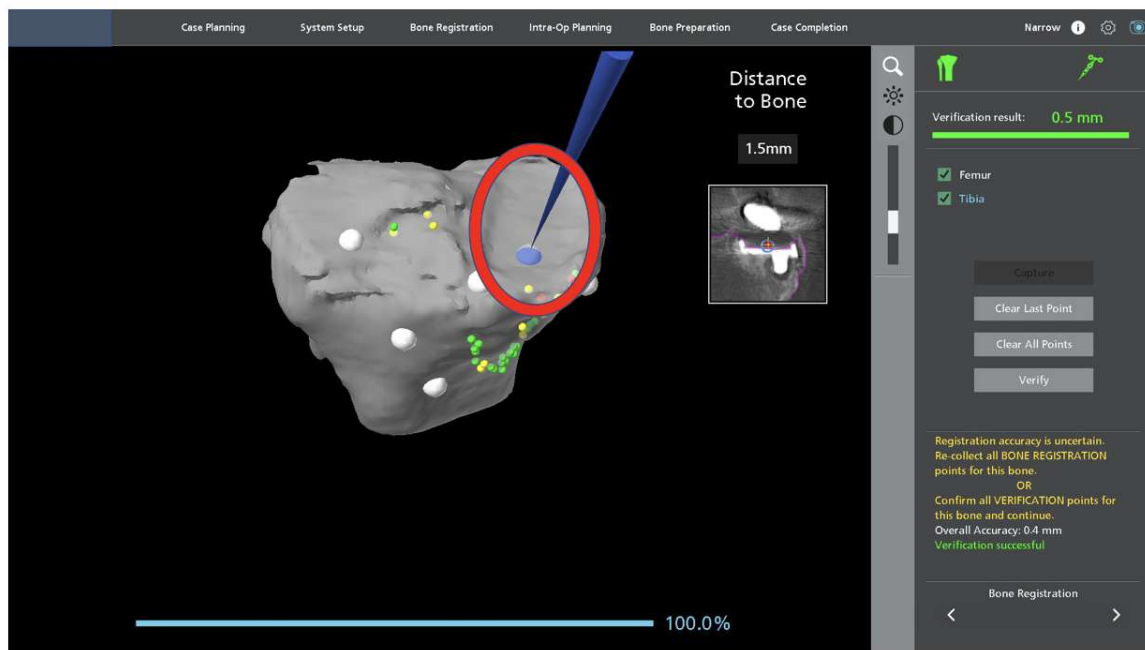
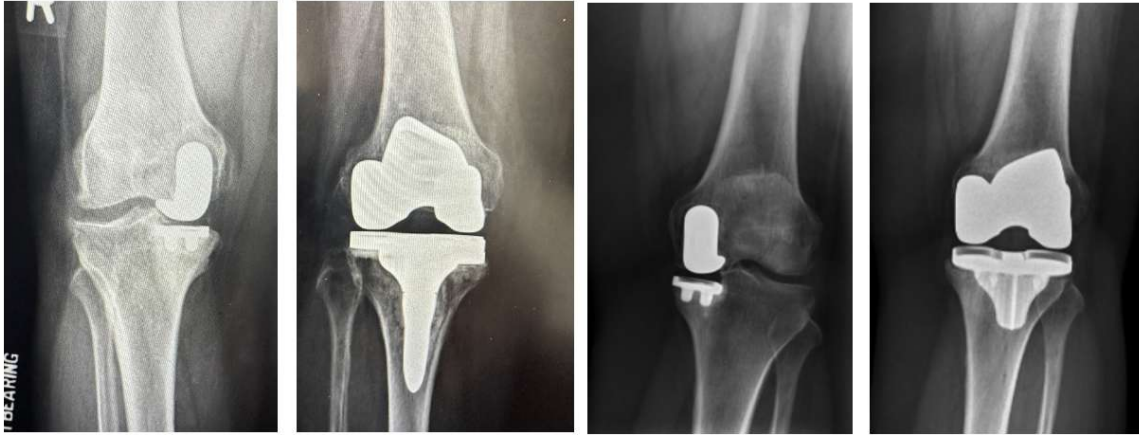


Figure 1: Verification screen using the MAKO Total Knee SmartRobotics™ System (Stryker, Mahwah, New Jersey, USA) demonstrating the verification probe adjacent to metal on the medial tibia.

[Figure 1](#)



A: 2017

B: 2022

Figure 2: Representative images of the evolution of robotic-arm-assisted medial unicompartmental knee arthroplasty to total knee arthroplasty. Panel (A) was performed on a patient in 2017 using mechanical alignment, tibial stem, and cemented technique. Panel (B) was performed on a patient in 2022 using functional alignment and a press-fit primary tibial component.

[Figure2](#)



Figure 3: Robot-arm-assisted case planning screen demonstrates A) the mechanical alignment technique used originally in the case series, and B) the functional alignment technique used in the latter part of the series.

[Figure 3](#)

The Conversion of Unicompartamental Knee Arthroplasty to Total Knee Arthroplasty With Non-CT Based Robotic Assistance: A Novel Surgical Technique and Case Series

*Hamza Raja - Henry Ford Hospital - Detroit, USA

Noah Hodson - Henry Ford Hospital - Detroit, USA

Phillip McKegg - Henry Ford Hospital - Detroit, USA

Luke Wesemann - Henry Ford Health - Detroit, USA

Michael Charters - Henry Ford Hospital - Detroit, USA

Trevor North - Henry Ford Hospital - Detroit, USA

Introduction: Robotic-assisted devices help provide precise component positioning in conversion of unicompartamental knee arthroplasty (UKA) to total knee arthroplasty (TKA). A few studies offer surgical techniques for CT-based robotic-assisted conversion of UKA to TKA, however no studies to date detail this procedure utilizing a non-CT based robotic assisted device. This paper introduces a novel technique employing a non-CT based robotic assisted device (ROSA® Knee System, Zimmer Biomet, Warsaw, IN) for converting UKA to TKA with a focus on its efficacy in gap balancing.

Case: We present three patients (ages 46 to 66) who were evaluated for conversion of UKA to TKA for aseptic loosening, stress fracture, and progressive osteoarthritis. Each patient underwent robotic-assisted conversion to TKA. Postoperative assessments at 6 months revealed improved pain, function, and radiographic stability.

Technique: Preoperative planning included biplanar long leg radiographs to determine the anatomic and mechanical axis of the leg. After arthrotomy with a standard medial parapatellar approach, infrared reflectors were pinned into the femur and tibia, followed by topographical mapping of the knee with the UKA in-situ. The intraoperative software was utilized to evaluate flexion and extension balancing and plan bony resections. Then, the robotic arm guided placement of the femoral and tibial guide pins and the UKA components were removed. After bony resection of the distal femur and proximal tibia, the intraoperative software was used to reassess the extension gap, and plan posterior condylar resection to have the flexion gap match the extension gap.

Conclusion: The use of a non-CT based robotic assisted device in conversion of UKA to TKA is a novel technique and a good option for surgeons familiar with robotic-assisted arthroplasty, resulting in excellent outcomes at 6 months.

Femoral Head Offset Effects on Abductor Muscle Function Vary Between THA Patients

J. Bohannon Mason - Orthocolorina - Charlotte, USA

Duncan Bakke - Formus Labs - Auckland, New Zealand

David Liu - Gold Coast Centre for Bone and Joint Surgery - Tugun, Australia

Atul Kamath - Cleveland Clinic - Cleveland, USA

Thor F Besier - University of Auckland - Auckland, New Zealand

*Marco Schneider - Formus Labs - Auckland, New Zealand

James Germano - Northwell Health - Dix hills, United States of America

Introduction

Femoral head-offset designation while performing total hip arthroplasty (THA) commonly occurs near the end of the procedure, and is subject to the surgeon's intuition, trialling, and feel, for example from the results of a shuck test. Beyond feel and qualitative testing, the unsuitability of a particular head-offset may not be evident until patients report abductor pain post-operatively. We investigated the effect of head-offset abductor and adductor muscle function.

Methods

Pelves and femurs of 12 THA patients (7F/5M; 50-83 years) were automatically segmented from preoperative CT and fitted with implants by Formus Hip automated THA planning software (Formus Labs, NZ), then fitted with an articulated shape model of the lower limb to create patient-specific musculoskeletal (MSK) models [1]. Post-operative models with varying head-offset were simulated by adjustment according to surgical plans, incorporating the range of available head-offset sizes (i.e. -3 to +6 mm). All models were used to simulate sit-to-stand motion, estimating moment arms and muscle lengths for abductors and adductors throughout, presented as percentage change from native. Muscle moment arms were multiplied by their respective peak isometric force and summed to calculate Moment Generation Capacities [2].

Results

Abductor moment generation capacity increased by $6.6\% \pm 1.2\%$ with head-offset across the range tested (mean $R^2 > 0.99$, $p < 0.001$), the equivalent of 0.7% increase per millimeter or 2.1% increase per size (Figure 1). There was no significant effect of head-offset on adductor moment generation capacity (Figure 2). Increase in head-offset led to increases in peak muscle length across all muscles, up to over 8% increase at maximal offset (gluteus minimus).

Conclusion

The effects of head-offset sizing on abductor muscle moment arms agreed with literature [3]. The values varied between subjects, even at the same femoral offset, by up to 15%. The relationship between increasing offset and increasing abduction moment arm was linear and positive for all subjects, but had a large relative standard deviation between subjects ($\pm 1.2\%$ compared to a mean of 6.6%). This reinforces the need for full-scale simulation of post-operative geometry when predicting effects on post-operative soft tissue function.

References

1. Rooks, N. et al. (2023). ISTA 2023 Annual Congress
2. Delp & Maloney (1993). J.Biomech 26.4-5
3. McGrory, B. J., et al. (1995) J.Bone & Joint Surgery 77-B.6

Figures

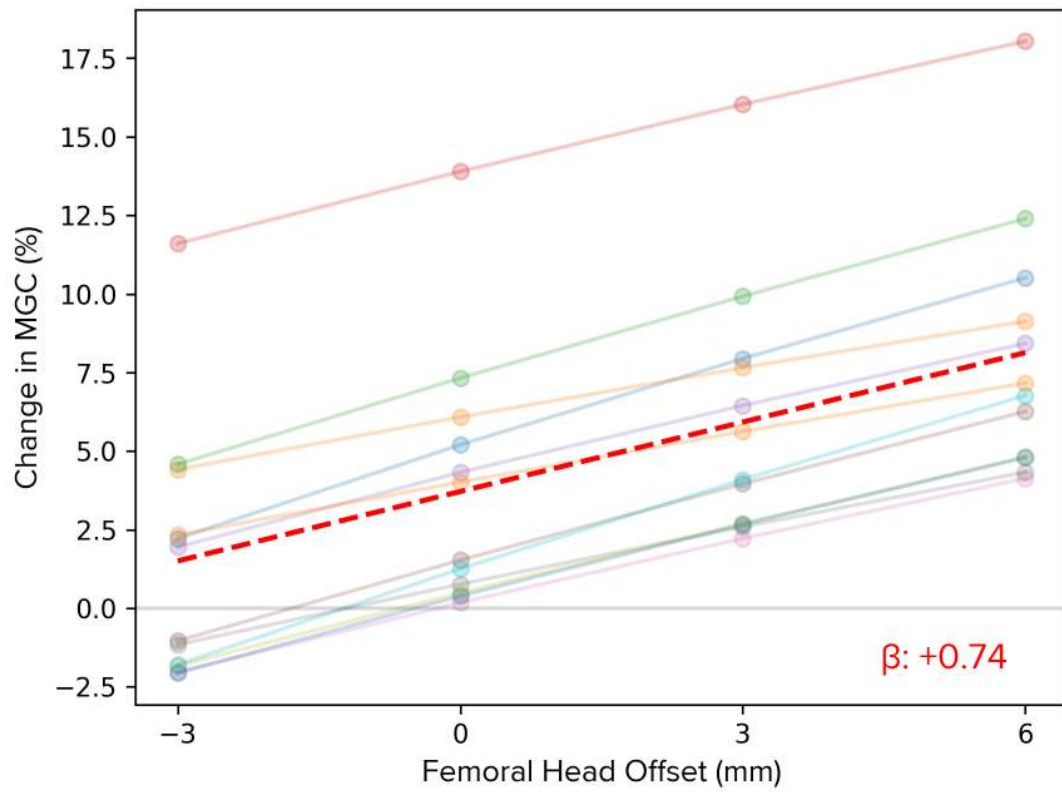


Figure 1. Effect of head-offset on hip abductor Moment Generation Capacity (MGC)

[Figure1](#)

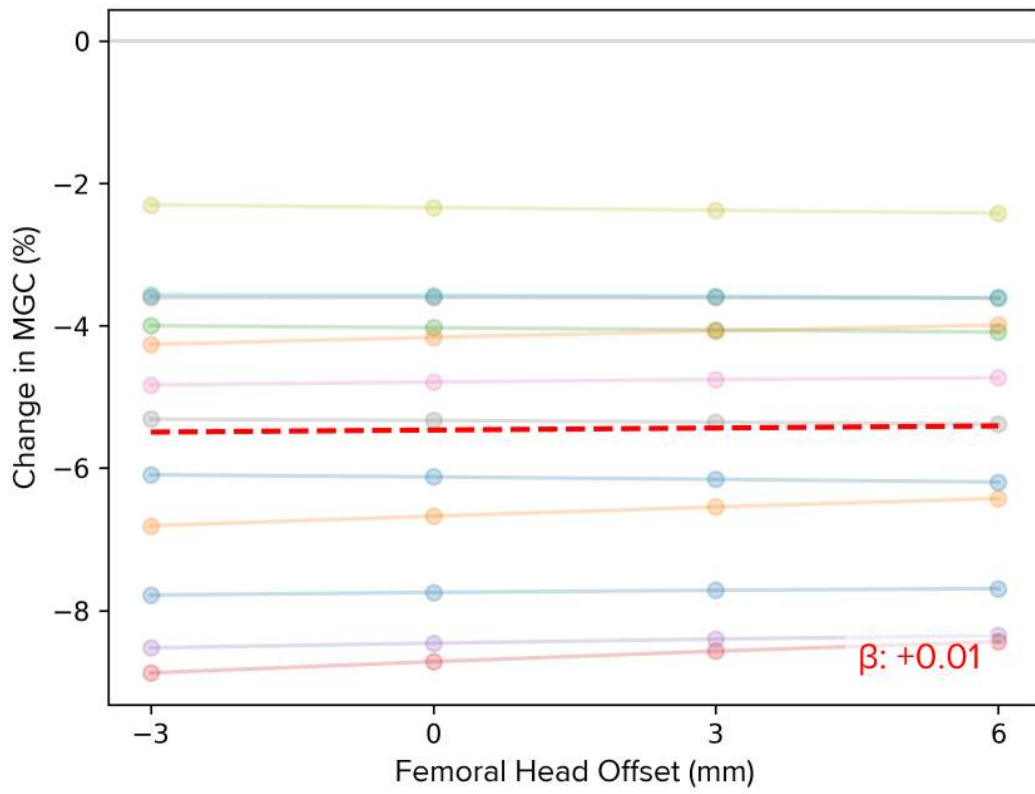


Figure 2. Effect of head-offset on hip adductor Moment Generation Capacity (MGC)

[Figure 2](#)

Intraoperative Recreation of Preoperative Pelvic Tilt: Is It the Key to Reliable Acetabular Component Positioning in Direct Anterior Total Hip Arthroplasty?

*Aleksander Mika - Vanderbilt Orthopedics

Peter Chan - UT Southwestern - Dallas, USA

Jacob Wilson - Vanderbilt - Nashville, USA

Courtney Baker - Vanderbilt - Nashville, USA

Anoop Chandrashekar - Vanderbilt - Nashville, USA

John Ryan Martin - Vanderbilt Health - Hendersonville, USA

Introduction: Proper positioning of components in total hip arthroplasty (THA) is vital to successful outcome. Pelvic tilt (PT) influences both acetabular component anteversion and inclination, and is therefore a critical factor for optimal functional acetabular component positioning during THA. We aimed to determine associations between preoperative, intraoperative, and postoperative radiographic PT and changes in acetabular component inclination and anteversion from intraoperative to postoperative in direct anterior (DA) THA.

Methods: We collected preoperative, intraoperative, and postoperative imaging from 63 consecutive DA THA procedures. The surgical technique utilized aimed to match the preoperative PT, based on a standing antero-posterior (AP) pelvis radiograph, with intraoperative fluoroscopy. The acetabular component was then positioned using this 'matched' view without technological assistance. PT, acetabular component anteversion and inclination calculated on pre-, intra-, and post-operative images. Descriptive and linear regression statistics were calculated to compare paired measurements between time points.

Results: Postoperative PT was not significantly different than preoperative PT (mean difference -0.05° ; $p = 0.48$). Intraoperative PT differed from pre- and post-operative PT by 3 degrees ($p < 0.01$). There was a significant difference between intraoperative and postoperative acetabular component inclination, median difference 3.5° ($p < 0.01$), but no significance difference in acetabular component anteversion from the intraoperative to postoperative images, median difference 1° ($p = 0.07$).

Conclusions: There is no change in pelvic tilt from preoperative to early postoperative standing AP pelvis radiographs after DA THA. "Recreating preoperative PT" during DA THA kept changes in acetabular component inclination and anteversion from intraoperative to postoperative on average < 4 degrees, which is anticipated to be clinically irrelevant.

Neurovascular Deviations and Factors in Fused Hips: Implications for Hip Arthroplasty

Chan Young Lee - Chonnam National University Hwasun Hospital - Hwasun-Gun, Jeollanam-Do, South Korea

TAEK-RIM YOON - Chonnam national university hwasun hospital - Gwang-ju, Korea (Republic of)

*Kyung-Soon Park - Center for Joint Disease, Chonnam National University Hwasun Hospital - Hwasun-gun, South Korea

Background

The purpose of this study was to compare the fused side and the normal side in patients with fused hips to determine the differences in neurovascular structures and factors that increase the risk of neurovascular injury.

Methods

We evaluated 38 patients who underwent total hip arthroplasty (THA) with a fused hip between 2003 and 2021. Excluding patients with bilateral lesions, the difference in neurovascular structure location was measured by comparing the fused side with the normal side. The position of neurovascular structures was measured by the distance from the acetabular rim and the shortest distance to the particular bony structure. In addition, the patient's sex, weight, body mass index (BMI), cause of fused hips, and preoperative range of motion were investigated to examine the differences and their correlation.

Results

Neurovascular distances for all the measured neurovascular structures were observed to be significantly reduced on the fused hip side compared with the normal side. Sex-based analysis revealed that females had significantly shorter distances to the femoral neurovascular bundle than males. Although height and body weight were associated with differences in neurovascular distances, BMI was not associated with significant differences except for the femoral nerve distance from the nearest bone. When classified by age of fusion onset, significant differences in neurovascular distances were found between the adolescent- and adult-onset groups.

Conclusion

The neurovascular structures in patients with fused hips are located closer to the bone than on the normal side. Moreover, patients in whom the fusion occurred before the completion of growth may exhibit a shorter neurovascular distance, thereby heightening the potential risk of direct injury.

The Outcomes of Repeat Two-Stage Revision Surgery for Previously Failed Two-Stage Revision Total Hip Arthroplasty

*Mohammed Wazir - University College London University Hospitals - London, United Kingdom

Babar Kayani - University College Hospital London - London, United Kingdom

Jenni Tahmassebi - UCL Hospitals NS Foundation Trust - London, United Kingdom

Fares Haddad - University College London Hospital - London, United Kingdom

Introduction:

Patients with persistent periprosthetic joint infections (PJIs) following failed two-stage revision arthroplasty may require repeat two-stage revision surgery. The longer-term survivorship and clinical outcomes of these patients remain unknown. The objective of this study was to report on the outcomes of repeat two-stage revision THA for persistent PJI following previously failed two-stage revision THA.

Methods:

This study included 58 patients who underwent repeat two-stage THA having undergone at least one previous two stage procedure for PJI. The study included 32 women and 18 men with a mean age of 65.1 years (range, 48 to 84 years) from two different treatment centres. All patients received minimum six weeks of intravenous antibiotics following the first stage revision procedure. Minimum follow-up time was five-years from the date of the revision two-stage revision THA.

Results:

Kaplan-Meier analysis revealed survivorship was 50.8% (95% CI [confidence interval]: 42.2 to 61.2%) when the end point was reoperation for any reason at ten-year follow-up. Reoperations were performed for infection (n=11), instability (n=5) and aseptic loosening (n=4). The mean patient satisfaction score was 64.8 ± 10.1 and the mean Forgotten Joint Score was 64.4 ± 12.2 at the final follow-up. The preoperative median University of California at Los Angeles score improved from 3 (IQR [interquartile range] 3 to 4) to 6 points (IQR 5 to 7) ($P < 0.001$), and the preoperative Oxford hip score improved from 12.1 ± 4.1 to 36.4 ± 4.6 points ($P < 0.001$) at the final follow-up.

Conclusion:

Repeat two-stage revision surgery for persistent PJI following previously failed two-stage revision arthroplasty is associated with high risk of recurrence and complications. Approximately, half of these patients will require reoperation within ten years of the revision two-stage THA. The most common reasons for reoperation include PJI, instability and aseptic loosening.

Radiographic Texture Features as Measures of Implant Fixation

*Mathew G Teeter - Schulich School of Medicine and Dentistry, Western University and London Health Sciences Centre - London, Canada

Sasha Hasick - Western University - London, Canada

Jennifer Polus - University of Western Ontario - London, Canada

Brent Lanting - London Health Sciences Centre - London, Canada

Edward Vasarhelyi - Western University - London, Canada

Introduction:

Tracking of implant osseointegration and diagnosis of aseptic loosening following total hip arthroplasty (THA) remains a challenge. Typically, qualitative visual observation of radiolucency around the femoral stem is performed across serial radiographs with scoring divided across different regions of the femur in seven Gruen zones. Bone mineral density has been shown to change across Gruen zones over time, but these measurements require dual x-ray absorptiometry (DXA) scans which are not standard of care. Texture features offer a quantitative approach to extract information from medical images. Texture feature analysis of standard x-rays might be a more readily available approach to quantify bone changes surrounding the femoral stem over time.

Methods:

Standard of care anterior-posterior x-ray images were acquired for 24 THA patients (12 male, 12 female) at 6 weeks, 1 year, and 5 years postoperatively. All participants had the same cementless THA femoral stem and were enrolled in a prospective trial using radiostereometric analysis (RSA). The seven Gruen zones were manually segmented on each x-ray image using 3D Slicer. Zones two and three were selected for analysis based on prior literature reports of bone mineral density changes in those regions with the analyzed stem. Texture features were then extracted from zones two and three using the PyRadiomics extension within 3D Slicer and included first order statistics, gray level co-occurrences matrices, and gray-level run-length matrices. Principal component analysis was used to reduce the 57 texture features to those that had the greatest variability. Statistical analysis of the remaining texture features in zones two and three over time was performed.

Results:

All participants displayed <0.2 mm/year of subsidence between one to five years post-operation indicating well-fixed stems. There were significant increases from six weeks to five years post-operation for three texture features: energy in zone two ($p = 0.0184$) and zone three ($p = 0.0026$), run length non-uniformity in zone 2 ($p = 0.0224$), and tenth percentile in zone three ($p = 0.006$).

Discussion:

Significant changes in texture features were observed in Gruen zones two and three on standard of care x-rays between six weeks and five years post-operation in patients who underwent cementless THA. This suggests the potential use of texture features as a quantitative means of assessing osseointegration and implant fixation. These findings align with existing literature indicating bone mineral density changes occur from six weeks to two years post-operation in zone 2 and 3 following THA with the same femoral stem measured with DXA. Future work should include analysis of

the remaining Gruen zones, evaluating the effect of implant and patient factors, and evaluating differences between well-fixed and loose stems requiring revision.

Revolutionizing 3D Bone Reconstruction: Introducing a Landmark-Less Workflow With Ultrasound Scanning

*Manh Ta - Stryker Corporation - Fort Lauderdale, USA

Daniel Sebald - JointVue. LLC - Knoxville, USA

Jarrold Nachtrab - University of Tennessee - Knoxville, USA

Steven MacDonald - London Health Sciences Centre - London, Canada

Richard Komistek - The University of Tennessee - Knoxville, USA

INTRODUCTION

In Computer-Assisted Orthopaedic Surgery (CAOS) systems, acquiring three anatomical landmarks for initial bone registration is conventional. However, this process is prone to human error, potentially compromising accuracy. Moreover, strict adherence to capturing these landmarks in a specific order is essential to maintain correspondence with predefined landmarks in a reference bone model. Landmarking using ultrasound is particularly challenging due to inherent imaging modality complexities. This study introduces a landmark-less workflow for bone registration and reconstruction using ultrasound imaging.

METHODS

Orthosonic™, developed by JointVue LLC, utilizes raw ultrasound radiofrequency (RF) signals and electromagnetic trackers for real-time reconstruction of patient-specific 3D bone models. Three pre-defined regions on the femur and tibia are scanned, allowing the user to capture these regions in any order. Noise filtering and k-means clustering algorithms segment the point cloud into three clusters. Spatial data from EM trackers and patella position classify clusters into medial, lateral, and rotational anchors. Centroids of these anchor point clouds enable initial registration, followed by fine-tuning using filtered point clouds. Subsequent scans generate point clouds representing bone surfaces, used to create patient-specific 3D bone models via a statistical shape model.

RESULTS

This research successfully implemented the landmark-less workflow within the Orthosonic™ suite, enabling efficient patient-specific 3D bone reconstruction using ultrasound imaging. Notably, the introduction of this innovative workflow significantly reduced total scanning time from 15 minutes to 5 minutes. Users provided overwhelmingly positive feedback, expressing substantial improvements in overall user experience. Despite the notable reduction in scanning time, the accuracy of bone reconstruction remained consistent. This outcome underscores the efficacy of the landmark-less approach in streamlining the bone registration process without compromising accuracy or quality. The successful implementation and positive user feedback highlight the potential of this workflow to enhance orthopaedic surgical procedures, paving the way for improved patient care and outcomes.

DISCUSSION

The landmark-less workflow presented here represents a significant advancement in bone registration and reconstruction using ultrasound within the Orthosonic™ suite. From its radiation-free nature to its expedited scanning process, Orthosonic™ is introducing revolutionary new technology to the orthopaedic industry. Within just 5 minutes, patient-specific 3D bone models are generated, enabling pre-

incision and pre-resection joint balancing and implant planning, thereby transforming total knee arthroplasty and improving patient outcomes.

Spine Flexibility in Patients Undergoing Total Hip Arthroplasty

*Alexander F Heimann - New England Baptist Hospital - Boston, USA

William Murphy - Harvard Medical School - Boston, USA

Patrick Lane - Surgical Planning Associates - USA

Andrew Amundson - Surgical Planning Associates - Medford, USA

Stephen Murphy - New England Baptist Hospital - Boston, USA

Introduction:

Spinopelvic characteristics are increasingly recognized as important factors in determining the ideal patient-specific implant positioning in total hip arthroplasty (THA) [1]. The quest for a better understanding of the relationship between spinal alignment, spinal flexibility and the resulting effects on the stability and impingement of THA has recently led to the development of new classifications [2]. However, dynamic changes in spinopelvic motion in patients undergoing THA are not yet fully understood. The aim of this study was to therefore to assess dynamic changes in a set of spinopelvic parameters in patients undergoing THA in our institution.

Methods:

One hundred and sixty consecutive patients underwent preoperative evaluation for THA including CT-imaging, as well as lateral conventional radiographs in the standing, seated, and forward bent position. Anterior plane pelvic tilt (APP-PT), sacral slope (SS), pelvic incidence (PI), lumbar lordosis (LL), pelvic femoral angle (PFA), acetabular anteinclination (AI), as well as central acetabular version (AV) and femoral anteversion (FV) were measured in all patients. Dynamic changes in APP-PT, SS, LL, PFA, and AI from standing to sitting, as well as from sitting to the forward bent position were analyzed. Patient history of spinal fusion was noted. In addition, the influence of demographic factors such as sex, age and body-mass-index on spinal flexibility was evaluated.

Results:

Preliminary results. Mean age at surgery was 65 ± 9 years (range 42 – 91). Mean supine APP-PT was $3.8 \pm 5.7^\circ$, mean standing APP-PT was $-1.5 \pm 7.7^\circ$, with a significant positive correlation of both (Pearson's $r = 0.66$). Mean change in LL when transitioning from the standing to the seated flexed position was $32 \pm 14^\circ$. Increasing age was significantly and negatively correlated with spinal motion ($r = -0.67$). Comprehensive stepwise, multiple regression analysis including all measured spinopelvic parameters not included in the preliminary results.

Conclusion:

There is a wide variation in pelvic position and spine flexibility between patients. A patient-specific approach based on dynamic preoperative imaging allows for a comprehensive analysis and subsequent planning of adjusted acetabular target orientations.

References

- [1] Ramkumar P, Pang M, Vigdorichik J, Chen A, Iorio R, Lange J. Patient-Specific Safe Zones for Acetabular Component Positioning in Total Hip Arthroplasty: Mathematically Accounting for Spinopelvic Biomechanics. *J Arthroplasty* 2023;38:1779–86. <https://doi.org/10.1016/j.arth.2023.03.025>.
- [2] Vigdorichik J, Sharma A, Buckland A, Elbuluk A, Eftekhary N, Mayman D, et al. 2021 Otto Aufranc Award: A simple Hip-Spine Classification for total hip arthroplasty?: validation and a large multicentre series. *Bone Jt J* 2021;103-B:17–24. <https://doi.org/10.1302/0301-620X.103B7.BJJ-2020-2448.R2>.

Validation of 2D to 3D Artificial Intelligence Templating for Total Knee Arthroplasty

*Nathan Whitsell - University of Kansas Medical Center - Wichita - Wichita, United States of America

Tarun Bhargava - The University of Kansas School of Medicine - Wichita - Wichita, USA

Introduction: Thorough preoperative planning allows for increased operating room efficiency and anticipation of component sizes in total knee arthroplasty (TKA). Digital templating is inconsistent and current three-dimensional (3D) imaging adds time and cost, and is associated with additional radiation to the patient. We tested the accuracy and learning capabilities of a novel artificial intelligence (AI) templating algorithm which converts two-dimensional (2D) radiographs to 3D bone models (Figure 1).

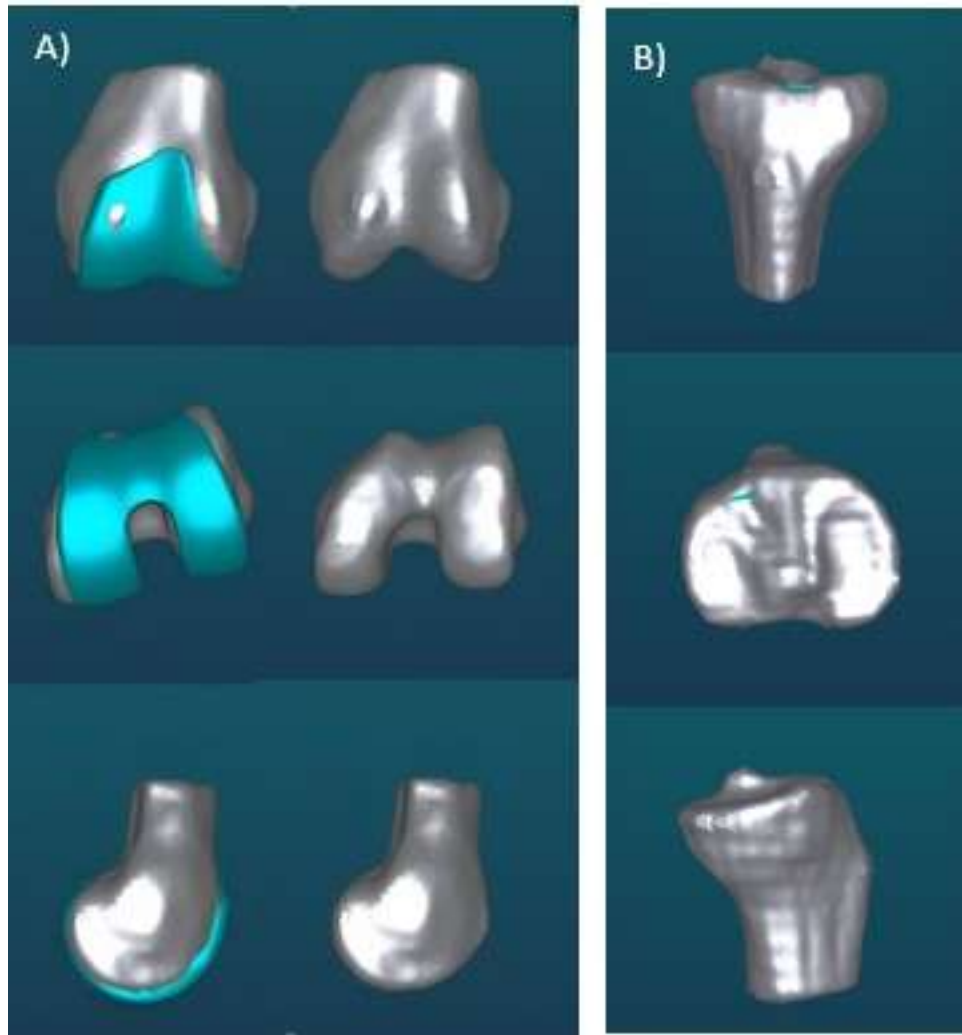
Methods: In this retrospective comparative cohort study, preoperative anteroposterior and lateral radiographs of 101 consecutive patients who underwent TKA between August 2022 to February 2023 were uploaded to the novel AI algorithm (PeekMed; Peek Health S.A; Braga Portugal). Accuracy of the algorithm was evaluated by comparing implanted femoral and tibial sizes to the AI predicted implant sizes. The potential for novel machine learning with improved predictive accuracy over time was evaluated by comparing the percentage of implanted components that were within one size (± 1) of the predicted size between the first 50 and last 51 patients in the study cohort.

Results: The AI algorithm was accurate in predicting the exact femoral and tibial implant sizes in 40% and 41.5% of cases, respectively. When allowing for (± 1) difference, the accuracy of the predicted femoral and tibial sizes improved to 90% and 87%, respectively (Table 1). The AI algorithm increased in accuracy over time for the tibial component (80% vs 94.1%, $P = 0.034$), and trended towards increased accuracy for femoral components (86% vs 94.1%, $P = 0.172$) (Figure 2).

Conclusions: 2D biplanar radiographs converted to 3D models by this novel AI-based modeling algorithm demonstrated high levels of accuracy when predicted TKA implant sizes were compared with component sizes implanted during surgery.

The AI-based algorithm was able to improve in accuracy over time and will keep improving with more data entry. This software has potential to increase efficiency and decrease costs associated with total knee arthroplasty and offers the surgeon information that may guide and improve intra-operative decision making.

Figures



		Comparison group	
		first 50	last 51
		Count	Count
absolute difference	.00	18	22
between implanted femoral	1.00	25	26
size and predicted femoral	2.00	5	3
size	3.00	2	0
absolute difference	.00	18	24
between implanted tibial	1.00	22	24
size and predicted tibial	2.00	7	2
size	3.00	2	1
	4.00	1	0

[Figure 1](#)

[Figure2](#)

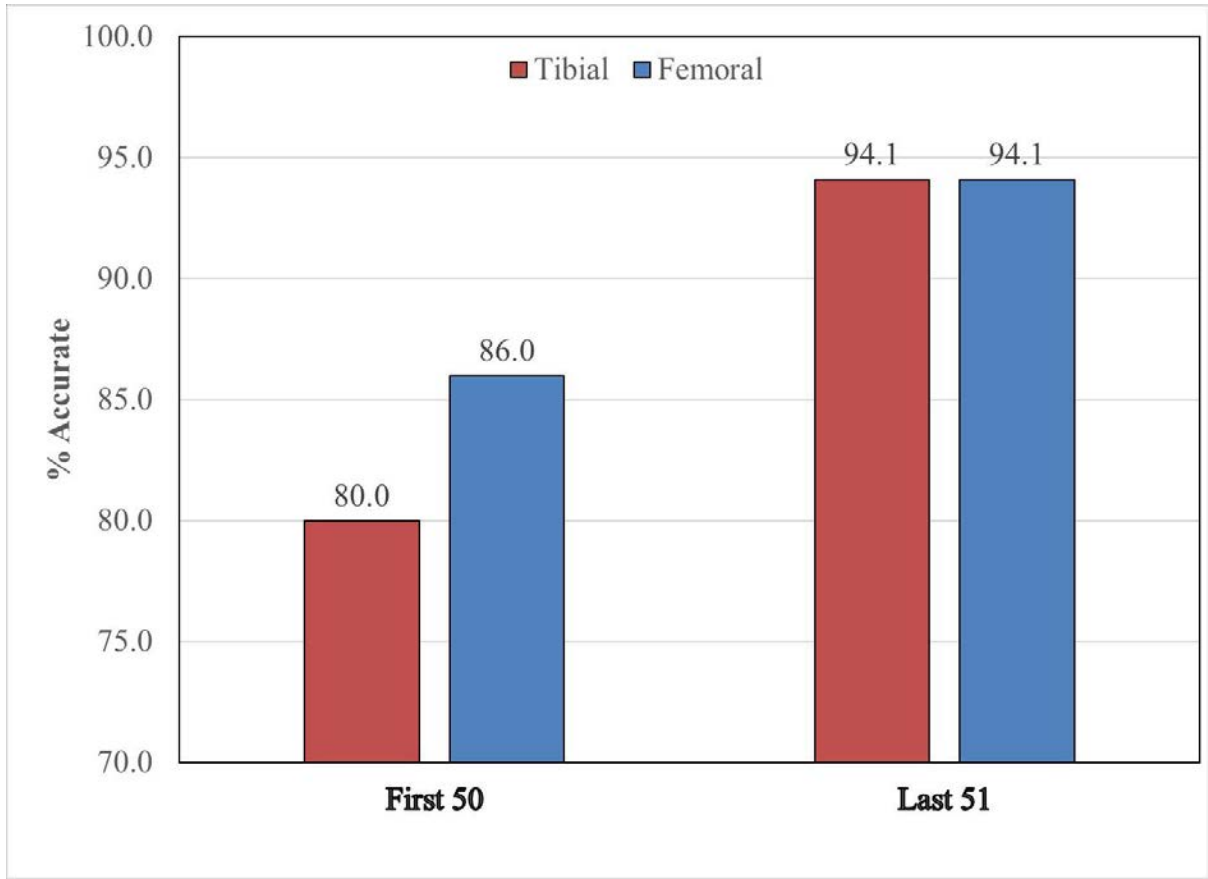


[Figure 3](#)

Cocktail of Ropivacaine, Morphine and Diprosan Reduces Pain and Prolongs Analgesic Effects After Total Knee Arthroplasty: A Prospective Randomized Controlled Trial

*Zhenyu Luo - West China Hospital, Sichuan University - Chengdu, China

Zongke Zhou - Sichuan University - Chengdu, China

Background: Local infiltration analgesia (LIA) provides postoperative analgesia for total knee arthroplasty (TKA). The purpose of this study was to evaluate the analgesic effect of a cocktail of ropivacaine, morphine, and Diprosan for TKA.

Methods: A total of 100 patients were randomized into 2 groups. Group A (control group, 50 patients) received LIA of ropivacaine alone (80 ml, 0.25% ropivacaine). Group B (LIA group, 50 patients) received an LIA cocktail of ropivacaine, morphine and Diprosan (80 ml, 0.25% ropivacaine, 0.125 mg/ml morphine, 62.5 µg/ml compound betamethasone). The primary outcomes were the levels of inflammatory markers C-reactive protein (CRP) and interleukin-6 (IL-6), pain visual analog scale (VAS) scores, opioid consumption, range of motion (ROM), functional tests and sleeping quality. The secondary outcomes were adverse events, satisfaction rates, HSS scores, and SF-12 scores. The longest follow-up was 2 years.

Results: The two groups showed no differences in terms of characteristics ($P > 0.05$). Group B had lower resting VAS pain scores (1.54 ± 0.60 , 95% CI = 1.37 to 1.70 vs. 2.00 ± 0.63 , 95% CI = 2.05 to 2.34) and active VAS pain scores (2.64 ± 0.62 , 95% CI = 2.46 to 2.81 vs. 3.16 ± 0.75 , 95% CI = 2.95 to 3.36) within 48 h postoperatively than Group A ($P < 0.001$), while none of the pain differences exceeded the minimal clinically important difference (MCID). Group B had significantly lower CRP levels (59.49 ± 13.01 , 95% CI = 55.88 to 63.09 vs. 65.95 ± 14.41 , 95% CI = 61.95 to 69.94) and IL-6 levels (44.11 ± 13.67 , 95% CI = 40.32 to 47.89 vs. 60.72 ± 15.49 , 95% CI = 56.42 to 65.01), lower opioid consumption (7.60 ± 11.10 , 95% CI = 4.52 to 10.67 vs. 13.80 ± 14.68 , 95% CI = 9.73 to 17.86), better ROM (110.20 ± 10.46 , 95% CI = 107.30 to 113.09 vs. 105.30 ± 10.02 , 95% CI = 102.52 to 108.07), better sleep quality (3.40 ± 1.03 , 95% CI = 3.11 to 3.68 vs. 4.20 ± 1.06 , 95% CI = 3.90 to 4.49) and higher satisfaction rates than Group A within 48 h postoperatively ($P < 0.05$). Adverse events, HSS scores and SF-12 scores were not significantly different within 2 years postoperatively.

Conclusions: A cocktail of ropivacaine, morphine and Diprosan prolongs the analgesic effect up to 48 h postoperatively. Although the small statistical benefit may not result in MCID, the LIA cocktail still reduces opioid consumption, results in better sleeping quality and faster rehabilitation and does not increase adverse events. Therefore, cocktails of ropivacaine, morphine and Diprosan have good application value for pain control in TKA.

Keywords Total knee arthroplasty; Local infiltration analgesia; Morphine; Diprosan

Reductions in Anxiety Following Total Joint Arthroplasty Are Most Closely Related to Lessening Pain

*Jason Cholewa - Zimmer Biomet - Warsaw, USA

Mike Anderson - Zimmer Biomet - Lehi, USA

Roberta Redfern - Zimmer Biomet - Pemberville, USA

Introduction

Research has begun to focus on whether mental health, particularly anxiety and depression, are impacted by arthroplasty procedures in patients with end-stage osteoarthritis. While studies suggest that anxiety is improved following surgical intervention, it is unclear what factors drive these changes. The aim of this study was to investigate baseline patient characteristics and changes in objective mobility to determine their association with changes in anxiety following arthroplasty.

Methods

This was a secondary analysis of a multicenter prospective observational cohort study. Patients undergoing partial knee arthroplasty (PKA), total knee arthroplasty (TKA) or total hip arthroplasty (THA) who owned a smartphone were eligible and were provided a smartwatch at least two weeks prior to surgery to allow for pre- and post-operative collection of gait metrics including step counts, gait speed, and walking asymmetry. Patients completed questionnaires including a numeric pain rating score and the Generalized Anxiety Disorder-7 instrument (GAD-7) pre-operatively and at 90-days post-operatively. Change in each of these variables was calculated from baseline and included in generalized linear models, including age, body mass index (BMI), and sex to quantify the impact on change in GAD-7 scores at 90 days post-arthroplasty.

Results

Evaluable data was available for 1,530 patients, including 260 (17%) PKA, 398 (26%) THA, and 872 (57%) TKA cases. The overall change in GAD-7 score was -0.68 ± 2.83 points, with the smallest change in TKA patients (-0.52 ± 2.9) and the largest in those undergoing THA (-0.97 ± 2.69 , $p=0.03$). On multivariable analysis, change in pain ($\beta=0.20$, 95%CI 0.03 – 0.67, $p=0.02$), sex ($\beta=-0.78$, 95%CI -1.44 – -0.12, $p=0.02$), and change in step count ($\beta=-0.0002$, 95%CI -0.0003 – -0.0001, $p=0.004$) were associated with change in GAD-7 in PKA patients. In the THA cohort, only change in pain ($\beta=0.23$, 95%CI 0.10 – 0.6, $p=0.0006$) and BMI ($\beta=0.10$, 95%CI 0.05 – 0.15, $p=0.0002$) were significantly associated with change in anxiety. In those undergoing TKA, change in pain ($\beta=0.16$, 95%CI 0.07 – 0.26, $p=0.0008$), BMI ($\beta=-0.04$, 95%CI -0.07 - -0.003, $p=0.03$), sex ($\beta=-0.59$, 95%CI -0.97 - -0.20, $p=0.003$), and change in gait speed at 90 days ($\beta=-2.45$, 95%CI -4.68 - -0.23, $p=0.03$) were associated with change in anxiety at 90 days post-operatively.

Discussion

Patients experience reductions in anxiety following knee and hip arthroplasty, which appears to be affected by baseline characteristics. Changes in objective gait metrics may impact anxiety in knee arthroplasty patients, however, changes in pain appear to be more strongly and consistently associated with anxiety reduction post-operatively.

Effects of Intravenous Dexamethasone on Postoperative Clinical Symptoms (Pain, Nausea and Vomiting) After Total Knee Arthroplasty According to Adrenal Function: Prospective, Observational Study

Sung Jun Jang - Seoul National University College of Medicine Boramae Medical Center (SMG-SNU Boramae Medical Center) - Seoul, Korea (Republic of)

*Hyung Min Lee - Seoul National University Boramae Hospital - Seoul, Korea (Republic of)

Hyunkwon Kim - SMG-SNU Boramae Medical Center - Seoul, Korea (Republic of)

Seung-Baik Kang - Boramae Medical Center/ Seoul National University College of Medicine - Seoul, South Korea

Moon Jong Chang - SMG-SNU Boramae Medical Center - Seoul, South Korea

Tae Woo Kim - Seoul National University College of Medicine, SMG-SNU Boramae Medical Center - Seoul, South Korea

Jisu Park - SMG-SNU Boramae Medical Center - Seoul, Korea (Republic of)

Cho min soo - Seoul, Korea (Republic of)

Background : The administration of intravenous (IV) dexamethasone in the perioperative period is commonly used as an effective method to reduce postoperative pain and postoperative nausea and vomiting (PONV) following total knee arthroplasty (TKA). However, a significant variability in the clinical effects of dexamethasone has been observed among patients. The relationship between the clinical effects of dexamethasone and preoperative adrenal function is not well described. This study aimed to investigate whether the clinical effects of dexamethasone administration differs based on the preoperative adrenal function in patients undergoing TKA.

Material & Methods : We included 304 patients undergoing TKA. Included patients were divided into two groups preoperatively based on the 30-minute cortisol levels from the rapid ACTH stimulation test: normal adrenal response as Normal group (Normal, n = 262) or decreased adrenal response as Adrenal fatigue group (AF, n = 42). All patients received IV dexamethasone according to the following schedule: 10mg one hour before surgery, 10mg on the morning of postoperative day (POD) 1, and 5mg on the morning of POD 2. Pain level, incidence of PONV and severity of nausea were assessed at postoperatively 0 to 6 hours, 6 hours to the night of the operation day, and daily on POD 1 to 5. ESR, CRP and Cortisol level were checked at preoperatively, POD 2, 4 and 6. Postoperative complications including delayed wound healing and surgical site infection were assessed within 90 days following surgery.

Results : Cortisol levels were significantly lower in the AF group on POD 2 ($p=0.003$), POD 4 ($p<0.001$) and POD 6 ($p<0.001$). However, there was no significant differences between the two groups in cortisol level on POD 1 ($p=0.13$). Postoperative pain levels were higher in the AF group from operation day to POD 2, then higher in the Normal group from POD 3 to POD 5, although no statistically significant differences were observed. There were no significant differences observed between the two groups regarding the severity of nausea and the incidence of PONV during the overall study period. There were no significant differences in wound complication and surgical site infection between two groups.

Conclusions : Cortisol levels were lower postoperatively in TKA patients with impaired adrenal function. However, no postoperative clinical differences were observed based on adrenal function when employing the same pain management protocol, including IV dexamethasone administration.

Predictive Modeling for Postoperative Pain Management in Total Knee Arthroplasty: Harnessing Artificial Intelligence for Personalized Care

*Julien Lebleu - moveUP - Brussels, Belgium

Andries Pauwels - moveUP - brussels, Belgium

Eduardo Vannini - moveUP - brussels, Belgium

Pierre-Antoine Absil - Université catholique de Louvain - Louvain La Neuve, Belgium

Philippe Anract - Hopital Cochin - Paris, France

Anissa Belbachir - Hopital Cochin - Paris, France

Philippe Van Overschelde - Hip & Knee Clinic AZ Maria-Middelares Gent - Sint-Martens-Latem, Belgium

Jared Weir

Introduction: The incidence of chronic postoperative pain following total knee arthroplasty (TKA) is approximately 20%. Early identification and prediction of chronic pain in patients after total knee arthroplasty can have a significant impact on treatment strategies and improve patient satisfaction. This study investigates severe postoperative pain and risk factors in patients undergoing TKA, and presents an innovative artificial intelligence (AI) model that predicts pain levels and pain progression after TKA, enabling practitioners to obtain information for personalized patient care

Methods: Pain intensity was measured using a visual analog scale on a mobile application in 1650 patients undergoing knee arthroplasty, one week before surgery and up to 12 weeks after surgery. They used an app to collect pre- and postoperative pain data, chronic pain risk factors, and analgesic usage. Patients were divided into two groups: those with pain $>40/100$ and/or using level 2 or 3 painkillers (D+), and those not meeting these conditions at three months postoperatively (D-). Statistical tests compared the groups' pre- and postoperative parameters. A training dataset was first used to identify patterns in the data that could better approximate pain trajectories. Confidence intervals were calculated to determine prediction accuracy. **Results:** 87% of patients were pain-free (D-), while 13% still had significant pain (D+). The pre-surgery characteristics more closely correlated with pain at 3 months were the number of comorbidities, patient reported high sensitivity, and higher preoperative rest pain ($p < 0.05$). The pain slope evolution in the first weeks post surgery was lower in the pain group.

Model accuracy was evaluated based on the percentage of predictions falling within 10% of true pain values. Two weeks after surgery, the model achieves a prediction accuracy of 67% for the pain experienced at six weeks. At four weeks postoperative, this prediction accuracy reaches 84% for the pain experienced at six weeks, and 69% for the pain at twelve weeks.

Conclusion: The proportion of patients with severe to moderate pain remained stable between 6 weeks and 3 months postoperatively. The AI model showed promising results in predicting pain progression, offering opportunities for personalized patient communication, guidance, and expectation management. Moreover, it could signal healthcare providers about deviations from the norm, allowing for timely intervention. This model enables care teams to adjust pain management strategies and supports effective telemonitoring, enhancing remote patient tracking. Integration of this technology into clinical practice can improve clinical outcomes and patient satisfaction.

Figures

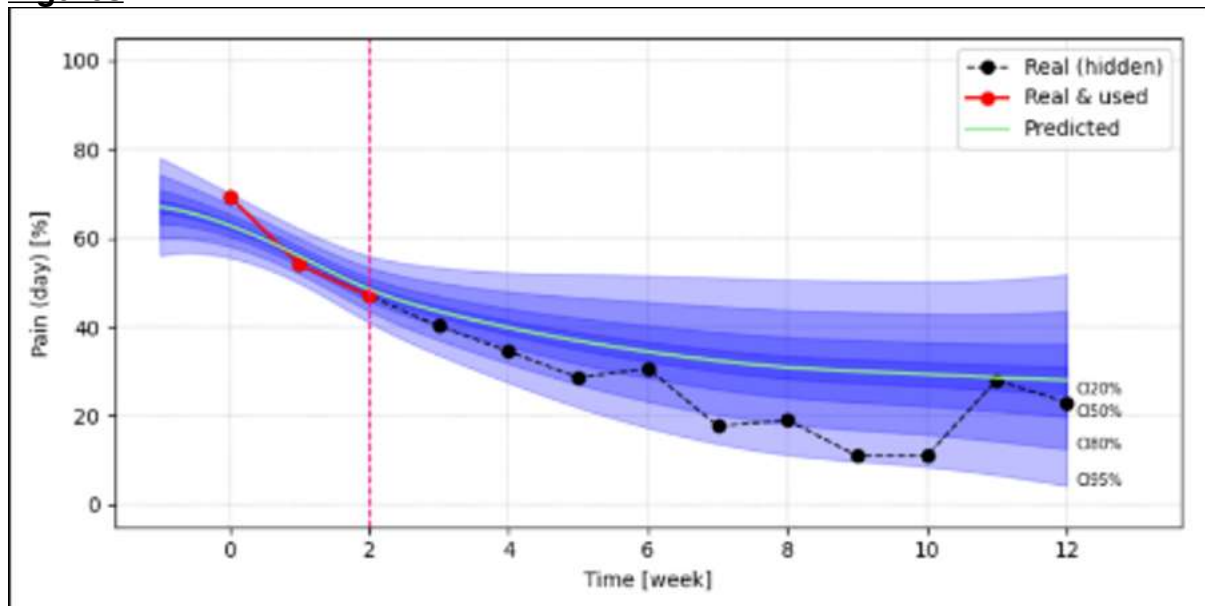
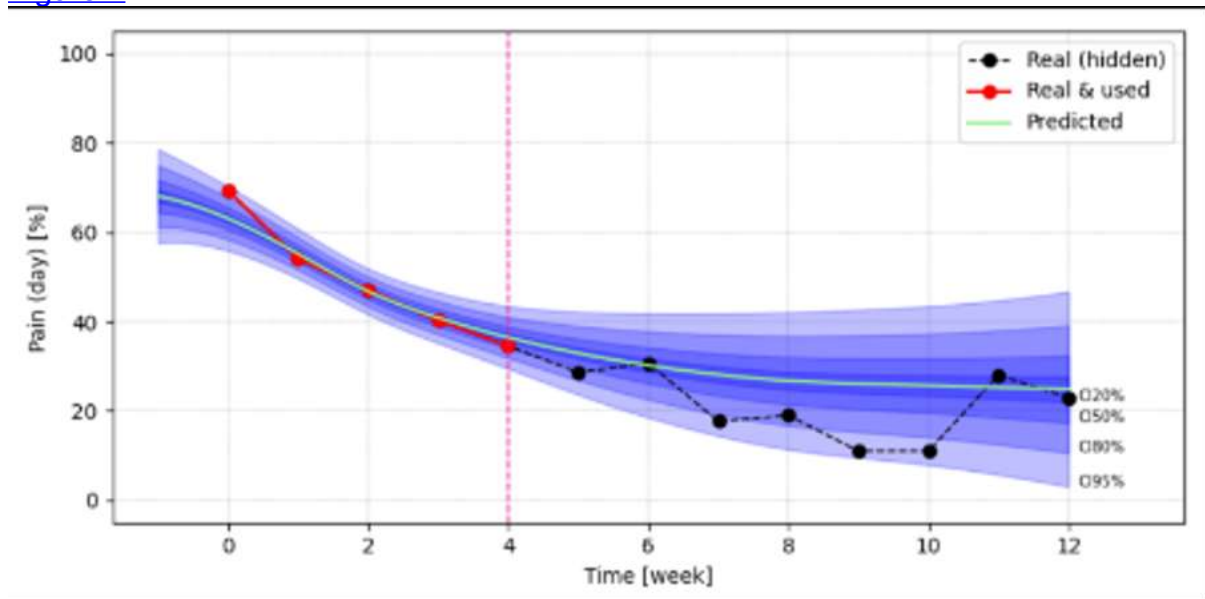
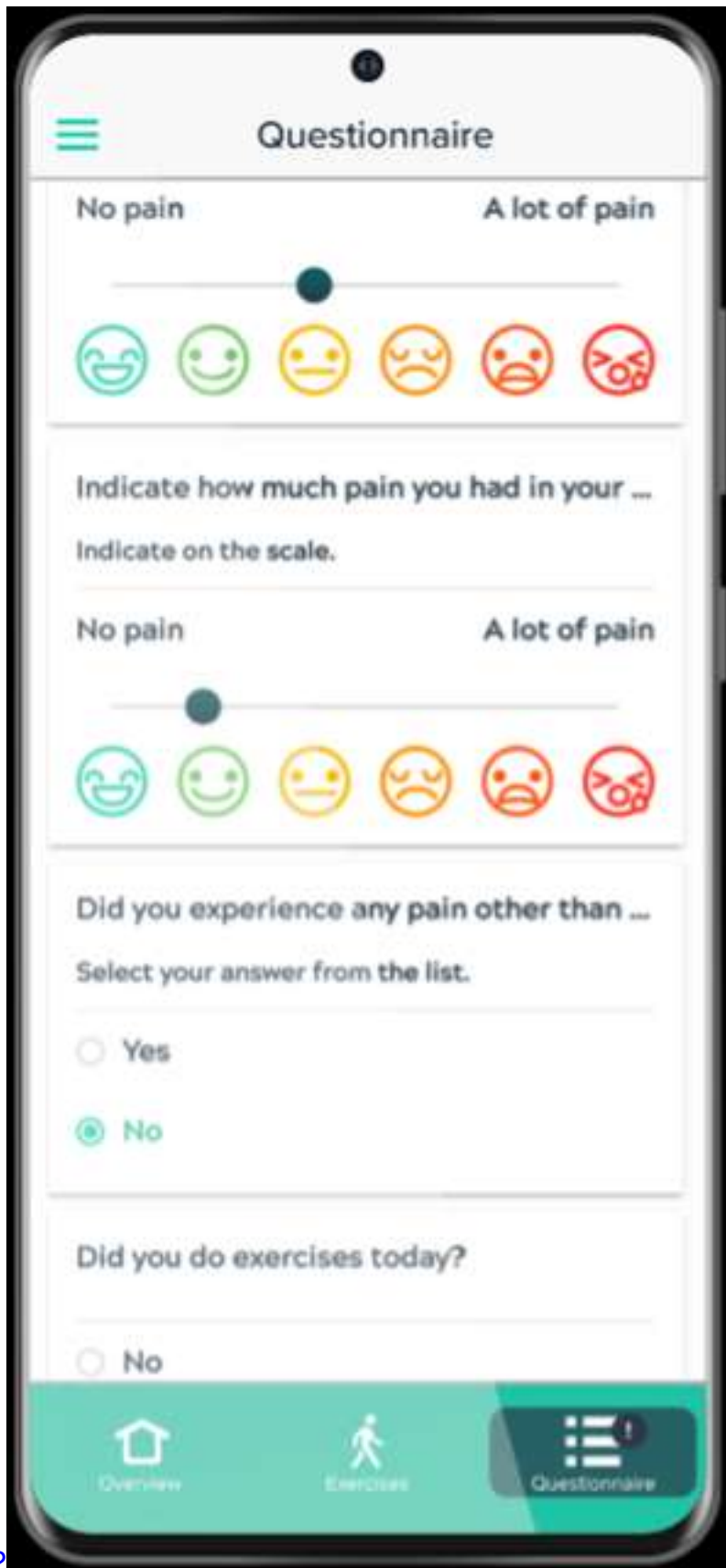


Figure 1





[Figure 2](#)
[Figure 3](#)

TKA Multimodal Swelling Intervention Protocol Shows Significant Reduction in BIA Values Compared to Baseline: A Pilot Study

*Louis Battista - Genesee Orthopedics - New Hartford, United States of America

Andrew Wickline

Richard Southgate - Northwestern Medical Group - Lake Forest, USA

Total knee arthroplasty (TKA) is the standard for treating end-stage knee osteoarthritis. However, patients recovering from a TKA can experience significant and prolonged swelling. This pilot study evaluated the effects of a multimodal intervention protocol to reduce postoperative swelling while monitoring patient satisfaction. The multimodal protocol utilized an anti-inflammatory bactericidal wash, cryocompression device, extended-duration oral tranexamic acid (TXA), and a novel, thigh-high compression stocking adapted from the lymphedema space. Swelling was monitored in patients using Single-Frequency Bioimpedance (SF-BIA) during the first 6 weeks of their recovery, and patients' answers to a satisfaction survey were recorded over the phone. Results indicated that the multimodal intervention decreased swelling by 11% ($p=0.005$) on POD 7 and 10% on POD 14 ($p=0.003$) when compared with the senior author's previous study baseline (Fig.1). In comparison to the previously published BIA reference chart, swelling was lowered by 18.7% and 19.4% at 7 and 14 days post-op, respectively (Fig. 1) (Loyd et al., 2019). This represents a 54% reduction in swelling at POD 7 and a 61% reduction in swelling at POD 14 when comparing this protocol to a protocol that likely represents the national standard. Additionally, post-op surveys showed 96% of patients being very satisfied with their recovery, and 100% of patients would recommend the multimodal protocol. These findings suggest that the integrated use of anti-inflammatory wash, cryocompression, extended length TXA, and novel compression stockings substantially mitigates postoperative swelling while maintaining high patient satisfaction rates and suggests the need for further research and validation.

Figures

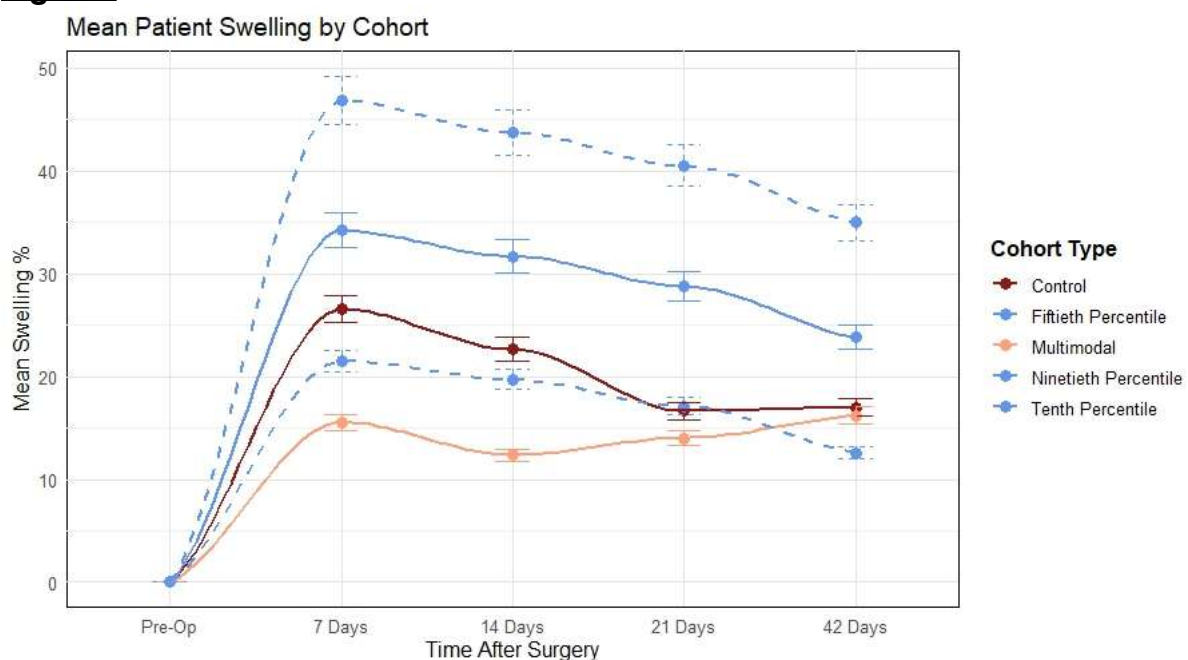


Figure 1

Risk Factors Associated With Increased Metal Sensitivity: A Retrospective Analysis Among 25,081 Pre- and Post-Operative Orthopedic Adults

Lauryn Samelko - Rush University Medical Center - Chicago, USA

Marco Caicedo - Orthopedic Analysis, LLC - Chicago, USA

*Nadim Hallab - Rush University - Chicago, United States of America

INTRODUCTION: Over >1 million total knee arthroplasties (TKA) are performed annually in the USA; however, patient-reported dissatisfaction post-TKA is as high as 10-20%, often leading to revision. The FDA acknowledges biological responses to metal implants including metal sensitivity as potential complications leading to poor clinical outcomes. Indeed, as many as 60% of patients with a poorly performing implant show metal sensitivity.¹ Although in vitro diagnostic tests are available and routinely performed to rule out metal sensitivity, it remains unknown which patient-specific characteristics are associated with higher odd ratios (ORs) for implant-related metal sensitivity. This retrospective analysis aimed to identify patient-specific risk factors associated with implant-related metal sensitivity among 25,081 all-comer primary and revision TKA patients suspected of metal sensitivity. **METHODS:** Blinded, de-identified diagnostic metal sensitivity data via lymphocyte transformation test (LTT)² from November 2009 to April 2023 from 25,081 adults were retrospectively reviewed including 11,903 pre- and 13,178 post-operative TKAs. Participants provided gender, age, implant-referable pain, implant time in situ, and history of cutaneous metal and drug allergy. The risk associated between each variable and 3 diagnostic ranges of metal sensitivity via LTT stimulation index (SI) to implant metal(s)² was assessed including mildly-, $SI \geq 4$; highly-, $SI \geq 8$; extremely-sensitive, $SI \geq 15$; OR with a 95% CI was calculated to determine the risk of metal sensitivity for each variable. Statistical significances were calculated with a student's t-test for demographic differences and Fisher's Exact Probability test for OR differences. **RESULTS:** Overall, women reported higher TKA-referable pain and rates of history of metal and drug allergy than males, Table 1. Of post-operative patients, women showed higher rates and severity of metal sensitivity than males, Table 1. The main significant risk factors for metal sensitivity across all three diagnostic SIs were women, patients with a self-reported history of cutaneous metal allergy, pre- vs post-operative patients, and patients with a high level of TKA-referable pain ($P < .05$; Table 2; Figure 1). The odds of extreme metal sensitivity ($SI \geq 15$) to implant metal(s) is 2.3 times more likely among women than men and 2.2 times more likely among patients with a history of cutaneous metal allergy ($P < .005$; Figure 1). Other significant risk factors for extreme metal sensitivity included pre- vs post-op patients and adults on anti-inflammatory medications ($P < .05$; Figure 1). **CONCLUSION:** This extensive cohort data review shows that specific demographic and clinical characteristics are associated with an increased risk of implant-related metal sensitivity, such as women, patients with a history of metal allergy, patients with a TKA, and those with high TKA-referable pain. Notably, a diagnosis of metal sensitivity is not a diagnosis of current or future implant failure but rather a diagnosis of higher risk for implant failure due to a potential adverse biological response. Understanding which patient populations have a higher risk of metal sensitivity is essential to mitigate implant complications associated with metal sensitivity and would be expected to contribute to greater patient satisfaction and clinical outcomes. **REFERENCES:** 1. Hallab NJ, et al. *J Bone Joint Surg Am.* 2001. 2. Caicedo MS, et al. *J Bone Joint Surg Am.* 2017.

Influence of Assembly Conditions of the Taper Junction of Modular Revision Hip Stems on Connection Strength

*Julius Boettcher - TUHH Hamburg University of Technology - Hamburg, Germany

Kay Sellenschloh - TUHH Hamburg University of Technology - Hamburg, Germany

Fenja Stiller - TUHH - Hamburg, Germany

Anna Strube - TUHH - Hamburg, Germany

Gerd Huber - TUHH Hamburg University of Technology - Hamburg, Germany

Michael Morlock - TUHH Hamburg University of Technology - Hamburg, Germany

INTRODUCTION

Revision total hip arthroplasty can be challenging due to the bone damage caused by implant removal [1]. Modular revision stems provide valuable customization options during surgery but are susceptible to fatigue fractures, primarily caused by corrosion and wear at the taper junction. Metal wear and corrosion products can also cause biological reactions [2,3]. The aim of this study was to investigate whether incorrect assembly and contamination of the modular taper surfaces reduces the strength of the taper connection.

METHODS

Modular revision stems designed for assembly with a pretension device and a locking screw were used (n = 48, MRP-TITAN®, PETER BREHM GmbH, Germany). Seven different situations were tested, differing in contamination (pristine, contaminated, cleaned, contaminated and coagulated) and assembly conditions (secured, pretensioned & secured). Contamination was achieved using porcine bone particles and bovine blood (Figure 1 A-D). A newly designed instrument was used for cleaning the taper surface of the cleaned groups with gauze bandages (Safety Wiper MRP-TITAN®, PETER BREHM GmbH, Figure 1 E). The number of rotations of the torque limiter during taper locking was recorded. Implants were subjected to cyclic loading in a material testing machine (10° lateral, 9° dorsal tilt, sinusoidal load curve, 1 Hz, 50-3000 N, 3600 cycles). Digital image correlation (DIC, GOM Zeiss, Germany) was used to determine axial rotation, micromotion and axial subsidence at the taper junction. Loosening torque of the locking screw and taper pull-off forces were determined after loading. Wear analysis was performed using a coordinate measuring machine (CMM, Mitutoyo, Japan, calibration accuracy < 3 µm, 0.1 mm measurement pitch) and evaluated iteratively. Qualitative wear patterns were evaluated using a high-resolution microscope (Keyence, Japan).

RESULTS

Contamination of the taper junction, especially in combination with improper assembly, significantly increased the axial rotation ($35.3 \pm 13.7^\circ$ vs. $2.4 \pm 4.4^\circ$; $p < 0.001$, Figure 2 A), axial micromotion ($67.8 \pm 16.9 \mu\text{m}$ vs. $5.1 \pm 12.1 \mu\text{m}$, $p < 0.001$, Figure 2 B) and axial subsidence ($-34.1 \pm 16.9 \mu\text{m}$ vs. $4.3 \pm 10.9 \mu\text{m}$; $p < 0.001$) of the neck piece relative to the stem. The number of rotations of the torque limiter required to tighten the locking screw was significantly increased in the contaminated and secured only groups (6.7 ± 2.5 rotations vs. 2.0 ± 1.4 rotations, $p < 0.001$). No taper wear was found for pristine or cleaned tapers after cyclic loading, while the contaminated groups exhibited varying levels of wear (Figure 3). Micromotion, component rotation and axial subsidence correlated strongly with taper wear ($p < 0.001$).

CONCLUSION

Contamination of the taper surface can be identified intra-operatively by an increased number of rotations of the torque limiter when tightening the locking screw. Cleaning of the taper in combination with correct assembly reduces relative motion and wear and therefore the risk of early failure and fatigue fracture of the modular taper junction.

ACKNOWLEDGEMENTS

Financial support from Peter Brehm is gratefully acknowledged.

REFERENCES

- [1] Buttaro 2007, J ARTHROPLASTY
- [2] Krull 2017, J ARTHROPLASTY
- [3] Krueger 2020, BONE JOINT J

Figures

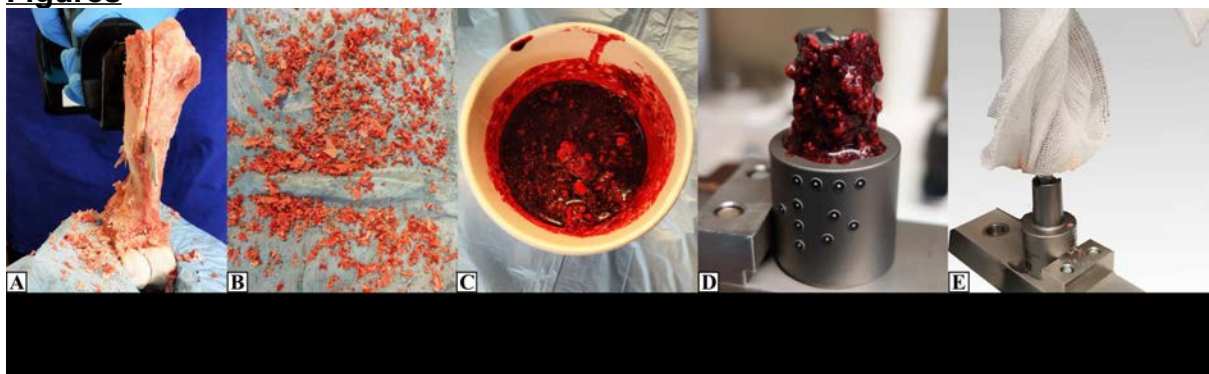


Figure 1

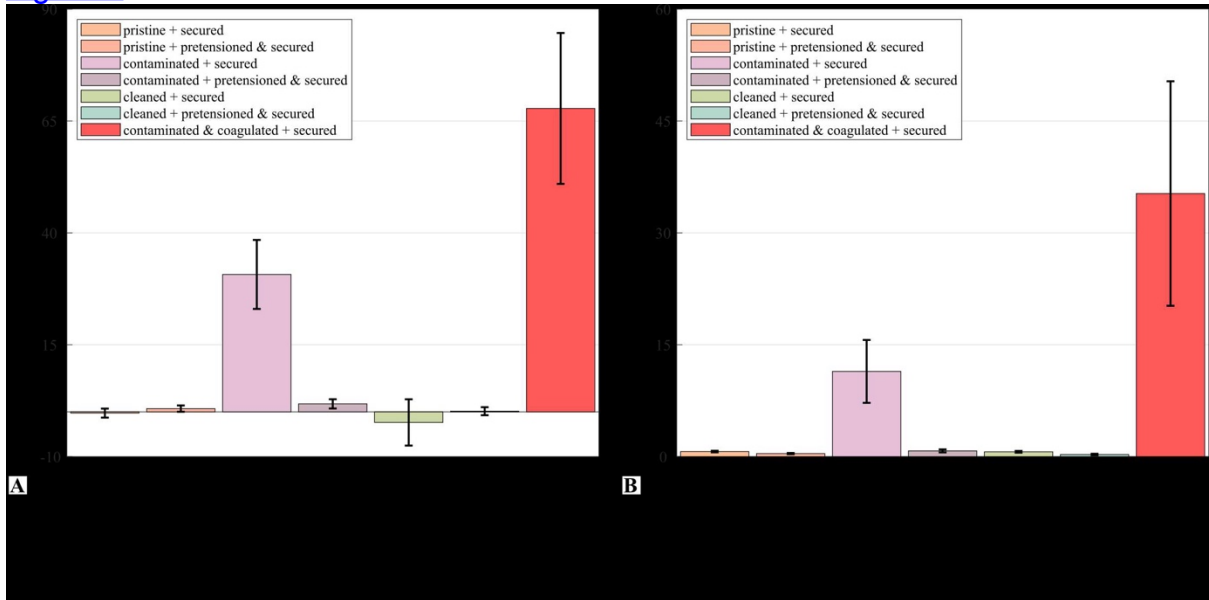


Figure 2

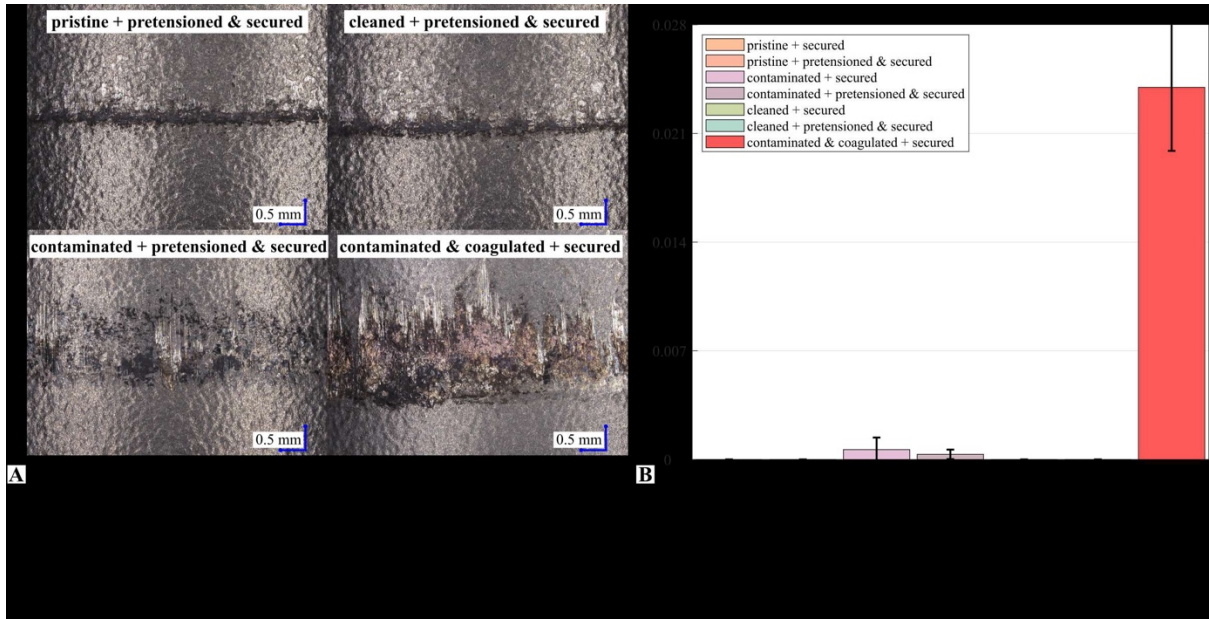


Figure 3

The Effects of Simulated CoCrMo Wear Particles on a Macrophage-Lymphocyte Co-Culture for Evaluating Cellular Corrosion

*Madison Brown - University of Tennessee Health Science Center - Memphis, USA

Danielle Bryant - University of Tennessee Health Science Center - Memphis, USA

Bailey Bond - University of Tennessee Health Science Center - Memphis, USA

Richard Smith - University of Tennessee Health Science Center - Memphis, USA

William Mihalko - University of Tennessee - Germantown, USA

Introduction: This study investigates the effects of simulated wear particles and proinflammatory activators on the cells involved in inflammatory cell-induced corrosion (ICIC). ICIC refers to the direct attack and corrosion of implant surfaces by phagocytic cells. During inflammation, these cells release reactive oxygen species which can negatively impact the corrosion susceptibility of cobalt-chromium-molybdenum. We hypothesized that TNF α and IL-6 levels would be higher in groups with CoCrMo particles and proinflammatory activators.

Methods: During the 30-day study, murine macrophages were grown on polished ASTM F1537 CoCrMo disks with suspended T-helper lymphocytes. Groups were either non-activated or activated with IFN γ and LPS. CoCrMo particles were added in 1:0 (none), 1:10, 1:100, or 1:500 cell-to-particle ratios. Supernatant was collected on day 10 of the experiment and cytokine levels were measured using ELISAs.

TNF α and IL-6 were measured to assess the pro-inflammatory response and overall activation of the macrophages. The number of viable macrophages was determined by an MTT assay at the conclusion of the study. Differences in cell counts and cytokine levels were determined using Welch's ANOVA with a Dunnett's post-hoc test and significance level of $\alpha=0.05$.

Results: There were fewer viable macrophages in groups with activators compared to groups without activators. Particle concentration resulted in a significant difference in macrophage viability only in the non-activated group with 1:100 particles, which had an unexpectedly high number of viable macrophages. For groups with 1:100 and 1:500 particles, TNF α and IL-6 levels were higher than no particle groups for both activated and non-activated groups. IL-6 levels were much lower in groups with 1:100 and 1:500 particles compared to groups with no particles for both activated and non-activated. While TNF α levels were relatively low, the groups with 1:100 and 1:500 particles had higher TNF α than groups with no particles for both activated and non-activated groups.

Conclusions: This study explores the mechanisms behind ICIC by evaluating the cytokine release of a macrophage-lymphocyte coculture on CoCrMo with CoCrMo simulated wear particles. Overall, endogenous and exogenous activators resulted in lower cell numbers and higher TNF α and IL-6 levels as expected. The increased TNF α in groups with 1:100 and 1:500 cell-to-particle ratios suggests that wear particles may increase inflammation and contribute to ICIC. IL-6 production may have been inhibited by the addition of the CoCrMo particles for the 1:100 and 1:500 cell-to-particle ratios. Future analysis will include imaging of the CoCrMo disks used during culturing to assess for damage to the disk surfaces. Future research will involve supernatant collection within 24-48 hours to gain insight to the initial cytokine release.

Figures

Macrophage Viability on Day 30

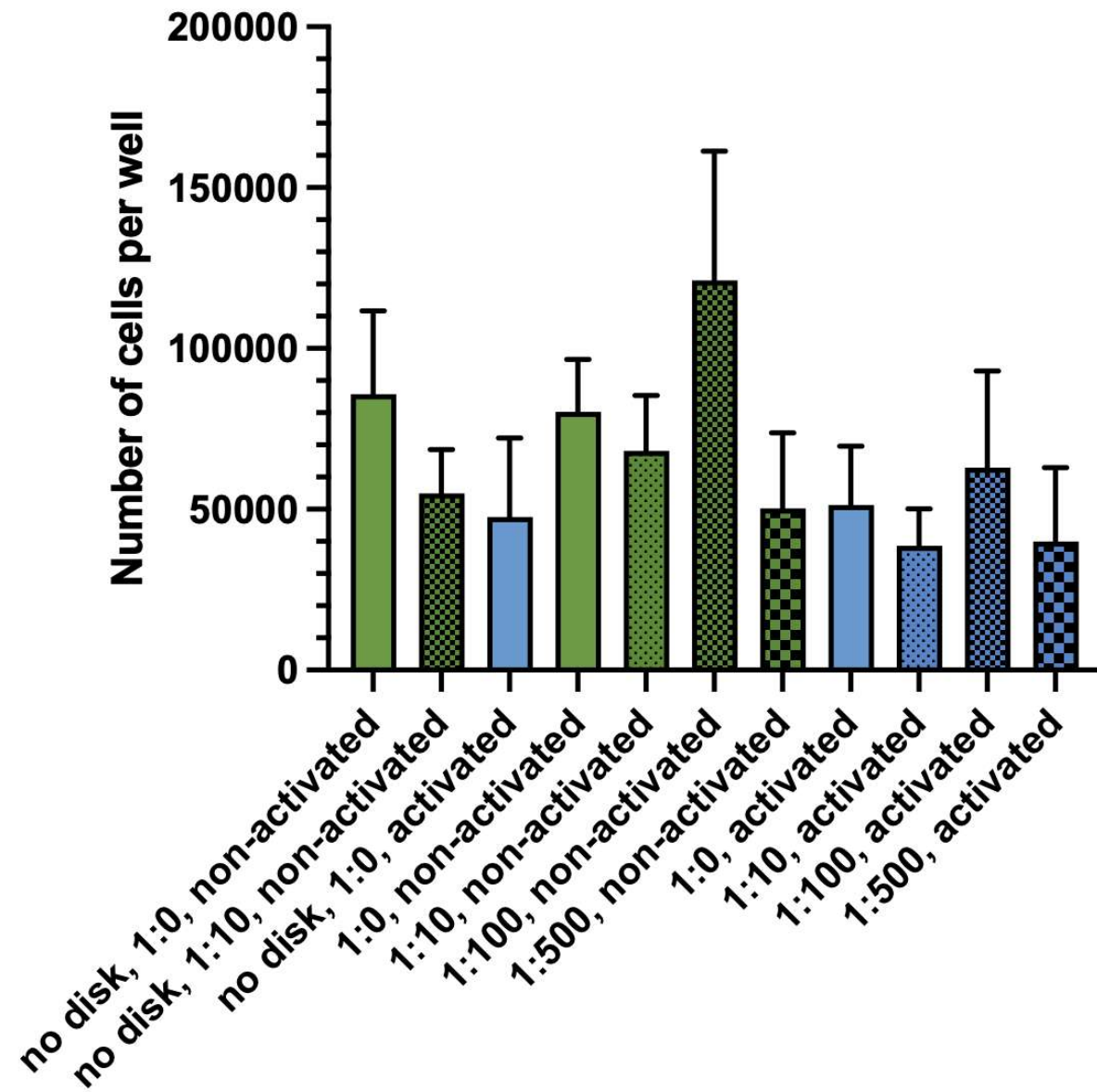


[Figure1](#)

TNFa Levels on Day 10

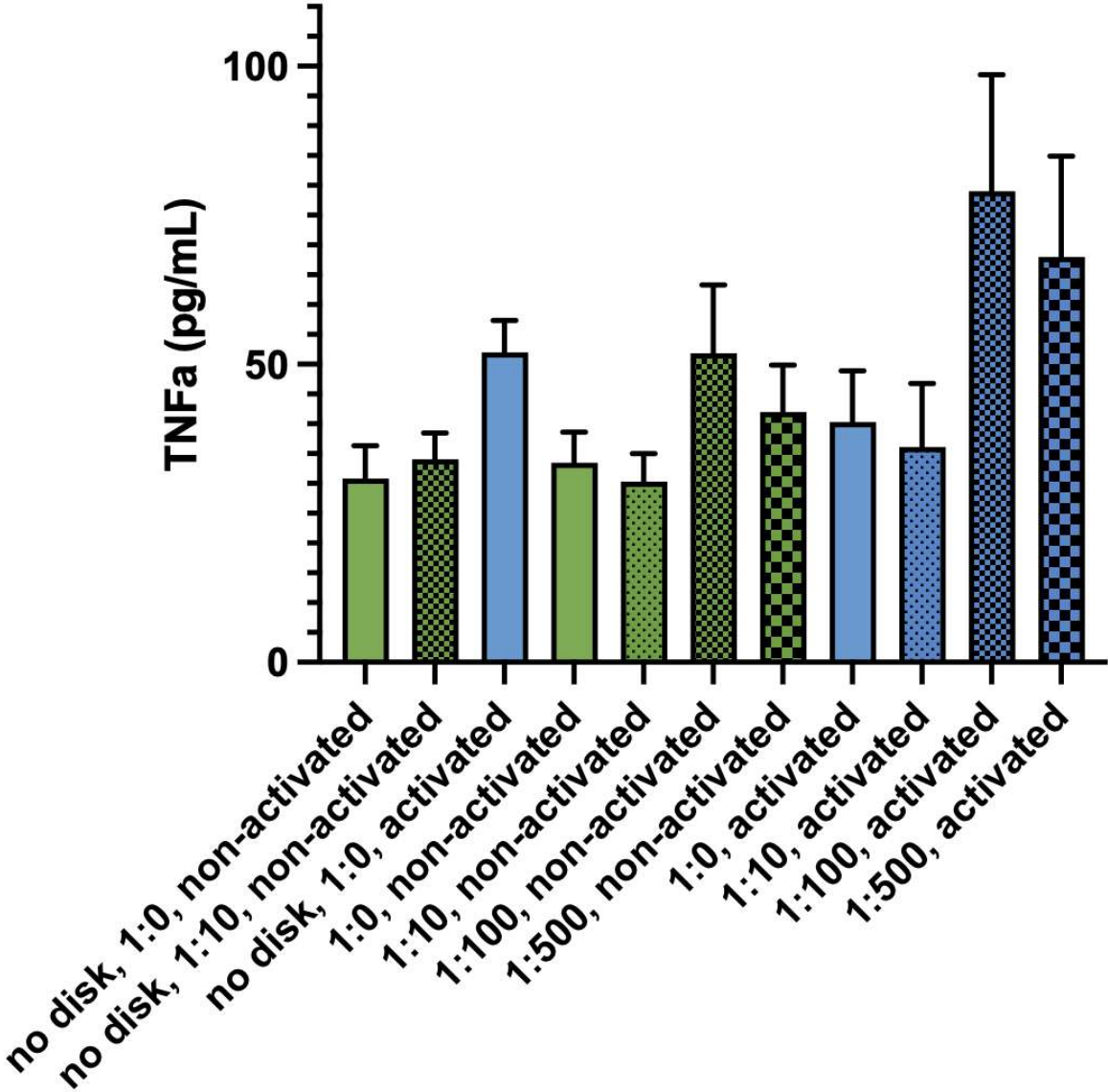
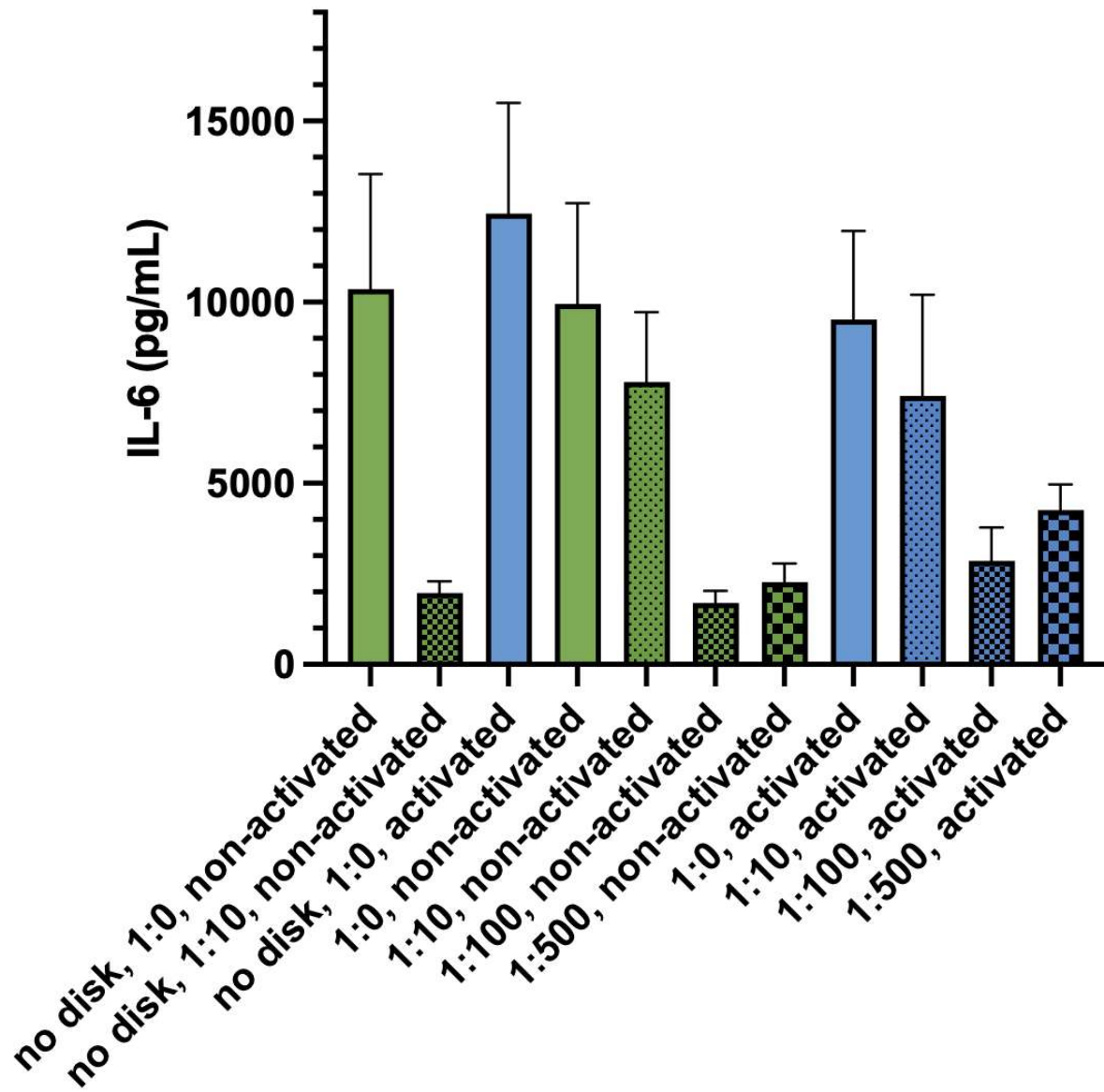


Figure2

IL-6 Levels on Day 10



[Figure 3](#)

Cobalt and Chromium Ion Levels in the Peri-Prosthetic Tissue of 42 Explanted CoCrMo Femoral Components Is Correlated With Surface Damage Score

Peter Kurtz - Clemson University - Charleston, USA

Shabnam Aslani - Drexel University - Philadelphia, USA

Michael Kurtz - Clemson University - Charleston, USA

Lilliana Taylor - Clemson University - Charleston, USA

Daniel MacDonald - Drexel University - Philadelphia, USA

Nicolas Piuizzi - Cleveland Clinic - Cleveland, USA

William Mihalko - University of Tennessee - Memphis, USA

Steven Kurtz - Drexel University - Philadelphia, USA

*Jeremy Gilbert - Clemson University - Charleston, USA

Introduction:

While total hip arthroplasty (THA) transitions away from the use of Cobalt Chrome Molybdenum (CoCrMo), total knee arthroplasty (TKA) continues to use cast CoCrMo in femoral components. In the past, CoCrMo has been associated with adverse local tissue reactions in metal-on-metal THA. Additionally, when comparing TKA to THA, there is a lag in patient satisfaction. For these reasons, as well as rising concerns about an association between CoCrMo components and cobalt toxicity, we investigated the ion levels in the peri-prosthetic tissue of 42 explanted CoCrMo femoral knee components. We hypothesized that increased damage to the implant's bearing surface (primarily based on a visual scoring system with wear scratches the dominant feature) would correspond with increased Co and Cr ion levels in the surrounding tissue of the explant.

Methods:

A total of 42 CoCrMo femoral components and associated peri-prosthetic tissue were collated from revision surgeries performed at the Cleveland Clinic (Cleveland, OH). The average implantation time was 6.8 ± 6.1 years. First, retrieved implants were given an overall damage score (1-4) based primarily on the severity of the wear scratches observed (1: Minimal, 2: Mild, 3: Moderate, 4: Severe). Then, tissues retrieved from the joint cavity were digested in 70% HNO₃ on a hot plate at temperatures 60-75 °C and prepared for ion measurement. To quantify Co and Cr ion levels, the digested samples were analyzed in ICP-MS (iCAP RQ, Thermo Fischer). A log₁₀ transformation was applied to the data for normalization. Student's T-tests ($\alpha = 0.05$) were used to compare the tissue ion levels from the undamaged implants (Score: 1) to the tissue ion levels of the damaged implants (Score: 2,3,4).

Results:

The damage score spanned the range of 1 (n=9), 2 (n=19), 3 (n=7) and 4 (n=7). There was a significant difference between the damaged and undamaged implants when observing cobalt and chromium ion levels in the surrounding tissue (see Figs. 1 and 2). Cobalt ion levels are higher for the implants with mild to severe damage when compared to the implants with minimal wear (Fig. 1) This was similarly shown when looking at chromium ion levels (Fig. 2). When looking at a plot of the cobalt and chromium levels for each specific tissue sample (Fig. 3), the cobalt ion levels are correlated with and proportional to the chromium ion levels.

Conclusion:

Tissue cobalt and chromium ion levels are higher in implants with more damage to the bearing surfaces due to wear and corrosion. The level of cobalt ions in the tissue of the more damaged implants may be cause for concern. The results of this study indicate the need for future investigation with increased sample size.

Figures

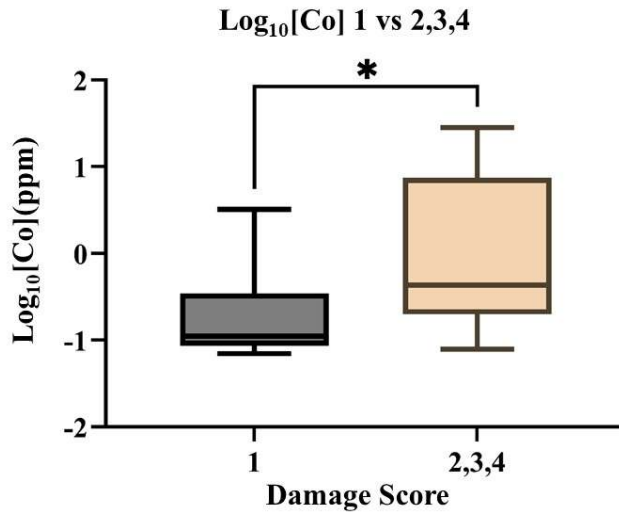


[Figure1](#)

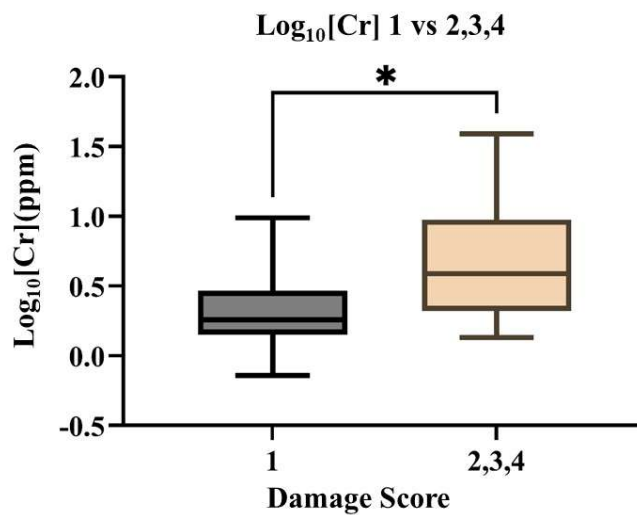


[Figure2](#)

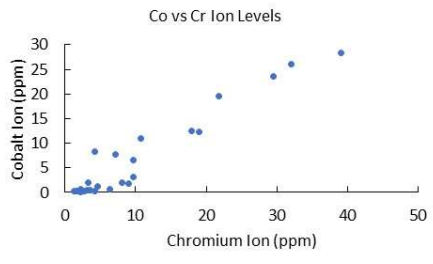


[Figure 3](#)

The Evolution of Pitting in Total Knee Arthroplasty

*Afton Limberg - Dartmouth College - Hanover, United States of America

Kori Jevsevar - Dartmouth College - Hanover, USA

Alexander Orem - Dartmouth Health - Lebanon, United States of America

David Jevsevar - OrthoVirginia - Richmond, USA

Douglas Van Citters - Dartmouth College - Hanover, USA

Introduction: Pitting is frequently reported on the articular surface of polyethylene bearings of total knee arthroplasty (TKA) at the time of revision surgery regardless of implantation date or polymer treatment. We hypothesize that the root cause of pitting has changed over the past two decades, with earlier observations related more often to oxidative degradation of the polyethylene bearing, and with polymer oxidative stability resulting in more recent observations being related to third body debris migrating to the articular space.

Methods: Using an IRB approved retrieval database a total of 2873 polyethylene components from TKAs were identified from a two-decade period. All devices were scored by an expert surgeon reviewer for pitting damage using a modified Hood method (1983). The pitting score was tested against the reason for retrieval as reported by the revising surgeon at the time of surgery. The era of revision was categorized by decade: 2000-2009 and 2010-2019. Chi-square tests were used to identify any association between reason for retrieval and decade for each score. Maximum ketone oxidation index was measured using FTIR; this was performed on a medial cross-section of the polyethylene <3 months post-explant. A two-way ANOVA was performed to compare between pitting scores and decade.

Results: The reasons for retrieval in the higher pitting scores of 2 and 3 change between the 2000s and the 2010s with polyethylene wear dominating earlier designs and loosening being more prominent in recent retrievals ($p < 0.001$, Figure 1A). An association between reason for retrieval and decade was noted for the lower pitting scores as well (both $p < 0.001$, Figure 1B). This highlights the dependence of reason for retrieval on decade regardless of the presence of pitting. The average maximum ketone peak showed significant increases with the higher pitting scores in both decades (both $p < 0.05$). Additionally, a significant decrease in average maximum ketone peak was observed between the 2000s and 2010s when looking at the higher pitting scores ($p < 0.001$, Figure 2). In general, a visual change in the presentation of pitting between the decades can also be appreciated (Figure 3).

Conclusion: The definition of pitting has evolved over the past two decades to include depressions in the articular surface in addition to the original focal material loss from contact fatigue. These results associate the new definition of pitting with loosening which can be clinically observed to be accompanied by generation of cement debris. This association does not imply that all cases of third body cement debris are loose, though this may contribute to other forms of bearing damage and wear.

Figures

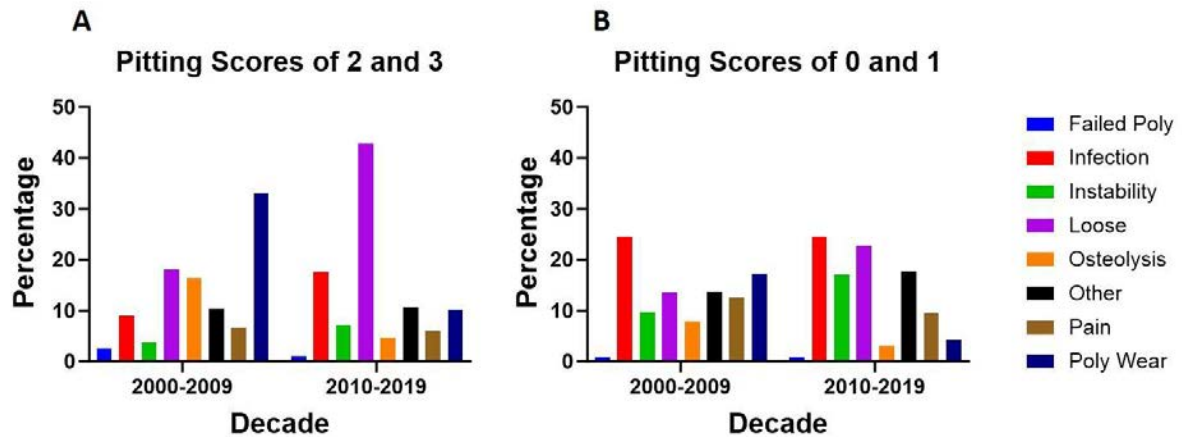


Figure 1: Reason for retrieval vs. decade for pitting scores. The pitting scores were grouped according to (2 and 3) and low (0 and 1),.

Figure 1

Max Ketone Peak

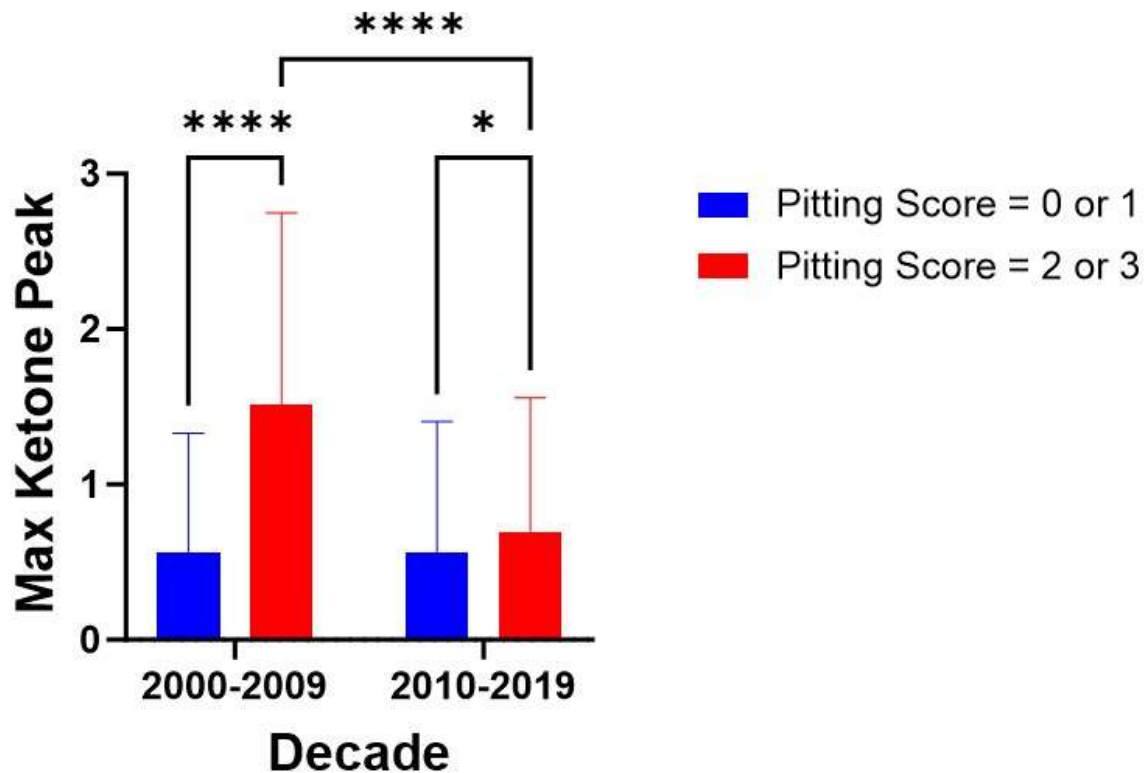


Figure 2: Maximum ketone peak for to low (0 and 1), and high (2 and 3) pitting scores separated by decade. Note: *: $p < 0.05$, ****: $p < 0.0001$.

Figure 2

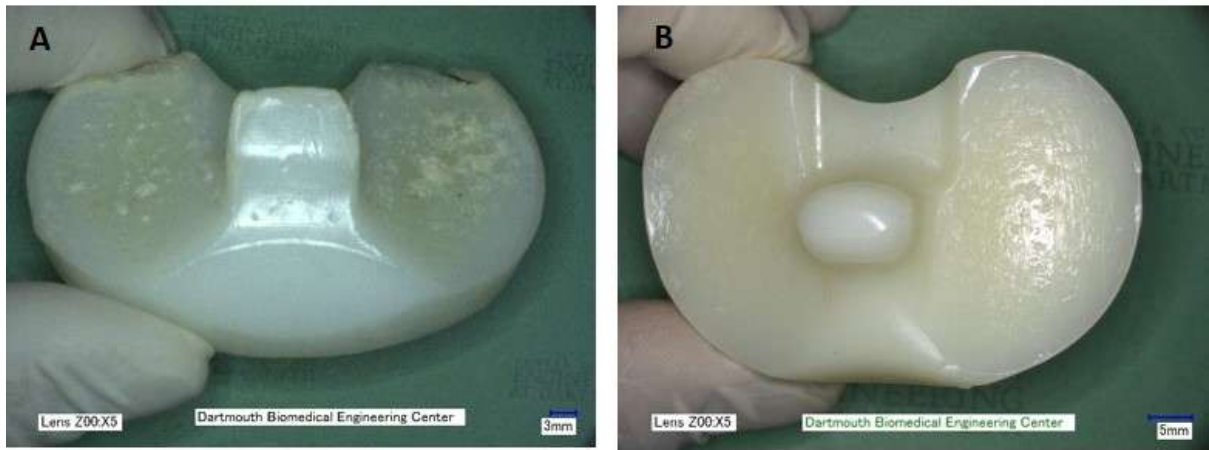


Figure 3: Representative images showing the differences in pitting between the decades 2000-2009 (A) and 2010-2019 (B).

[Figure 3](#)

Load and Scale Effects on Tribocorrosion Mechanisms in Biomedical CoCrMo Alloys

*Edona Hyla - University of Leeds - Leeds, GB

Andrew Robert Beadling - University of Leeds - Leeds, United Kingdom

Gregory deBoer - Institute of Thermofluids, University of Leeds - Leeds, United Kingdom

Richard M. Hall - University of Birmingham - Birmingham, United Kingdom

Michael Bryant - University of Birmingham - Birmingham, United Kingdom

Introduction

In the burgeoning global hip replacement market, set to be worth \$9.91 billion by 2028, understanding tribocorrosion in biomedical alloys is vital for implant success[1].

Engineering surfaces with microscopic roughness are commonly found at connecting surfaces such as modular taper and shell-liner interfaces and have been implicated in higher than acceptable revision rates.

Although engineering research has delved into the surface roughness-tribocorrosion domain, gaps persist in connecting cross-scale contact behaviour.

This study aims to bridge gaps between tribocorrosion, contact conditions (asperity geometry), and material properties to safely enhance implant design and manufacture. Thus, advancing implant technologies for better patient outcomes.

Methodology

Low Carbon CoCrMo discs were polished to a mirror finish with $R_a < 0.05 \mu\text{m}$, cleaned in an ultrasonic bath with acetone for 10 minutes and rinsed with deionized water before testing. To simulate abrasion processes commonly seen in vivo, a micro-tribometer was used.

Two diamond tips with a radius of $R_{\text{tip1}} = 100 \mu\text{m}$ and $R_{\text{tip2}} = 12.5 \mu\text{m}$ mimicking macro and micro contacts were employed in a sliding motion under a normal force varying from $F_n = 10$ to 200 mN with a displacement of 1.5 mm at 1.5 Hz for 2700 cycles.

To assess corrosion, a 3-electrode electrochemical cell was used. Current transients were recorded during sliding motion in PBS under potentiostatic polarization conditions (+100 mV vs Ag/AgCl). Post-analyses were conducted using vertical-scanning-interferometry (VSI) and field-emission-gun scanning-electron-microscopy (FEG-SEM).

Results and discussion

During the running-in phase, the coefficient of friction (COF) shown in Figure 1a reveals differences between macro and micro-contacts. Micro-tip-induced surface pressures led to a decrease of COF from 0.13 to 0.05. Conversely, for the macro-tip COF values start at 0.06 and increase to 0.1 (Figure 1b), consistent with prior studies[2].

Using the abrasive wear map (Figure 2), calculated shear stress and penetration depth (Table 1) a transition from cutting wear at 21 GPa to ploughing wear is shown, correlating low COF with unconstrained plastic flow. Considering the contact nature, it is highly unlikely that van der Waals forces contribute to COF increase; instead, such a response is attributed to shear stress approaching the bulk shear strength, therefore encountering heightened transversal resistance.

Volume loss analysis (Figure 3) indicates mechanical wear predominance at the microscale, with a transition to corrosive wear at the macroscale as shear stresses approach the bulk shear strength. A calculated penetration degree of 0.016, suggests disruption of the oxide layer; combined with an expanded contacting area it

increases surface exposure to corrosion aligning with Mischler and Munoz's findings[3].

Conclusion

This study underscores the significant influence of initial surface pressures and contact scales on the tribological behaviour of hip implants. The difference in pressure distribution between macro and micro contacts profoundly impacts the COF, wear mechanisms, and the dominance of mechanical/corrosive wear. Optimising the distribution of load to a larger real contact area, particularly those with considerable roughness such as the taper-head interface, would significantly reduce mechanical wear, leading to an extended implant lifespan. Underscoring the importance of surface design on the efficacy and durability of joint implants.

Founding:EU's Horizon-2020 programme, MSC grant No.956004.

[1]Fortune-Business-Insights,2023

[2]Martinez Nagues et al., TribolInt,2016

[3]S.Mischler and A.I.Munoz, Wear,2013.

Figures

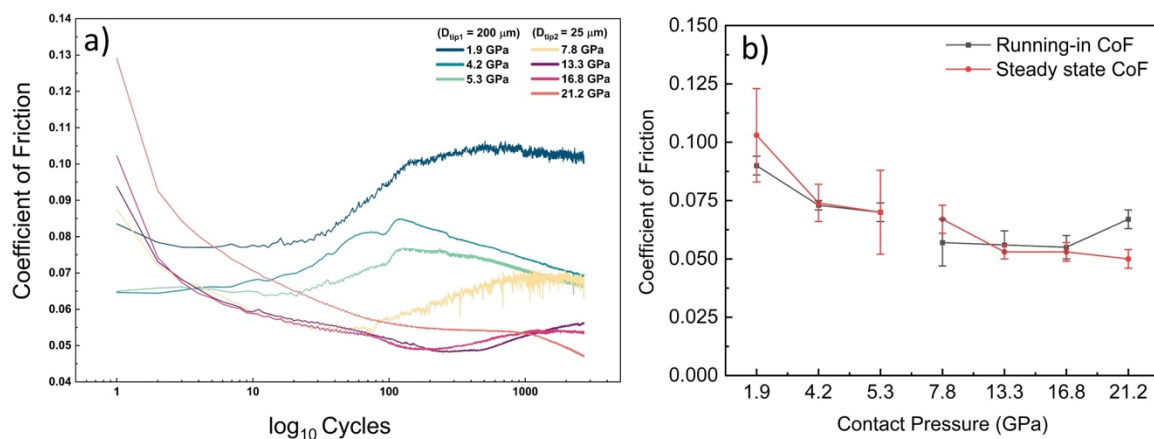


Figure 1 a) A logarithmic view of COF over cycles showing a change in shape with decreasing pressures during running in b) mean coefficients of friction during running-in and steady-state phases for all initial contact pressures.

[Figure 1](#)

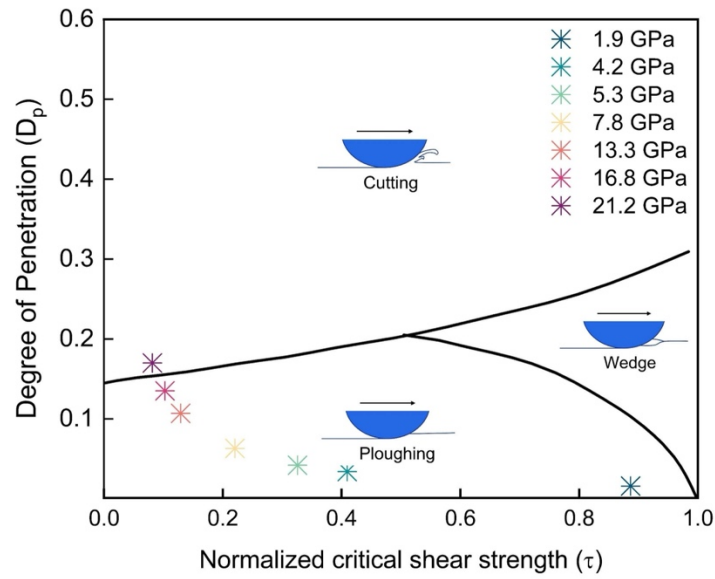


Figure 2. The wear map depicting ductile metals showcases three discernible mechanisms of abrasive wear. Each star symbolizes a predictive wear mechanism based on factors such as the normalized shear strength relative to the degree of penetration, bulk shear strength and initial contact pressure.

[Figure 2](#)

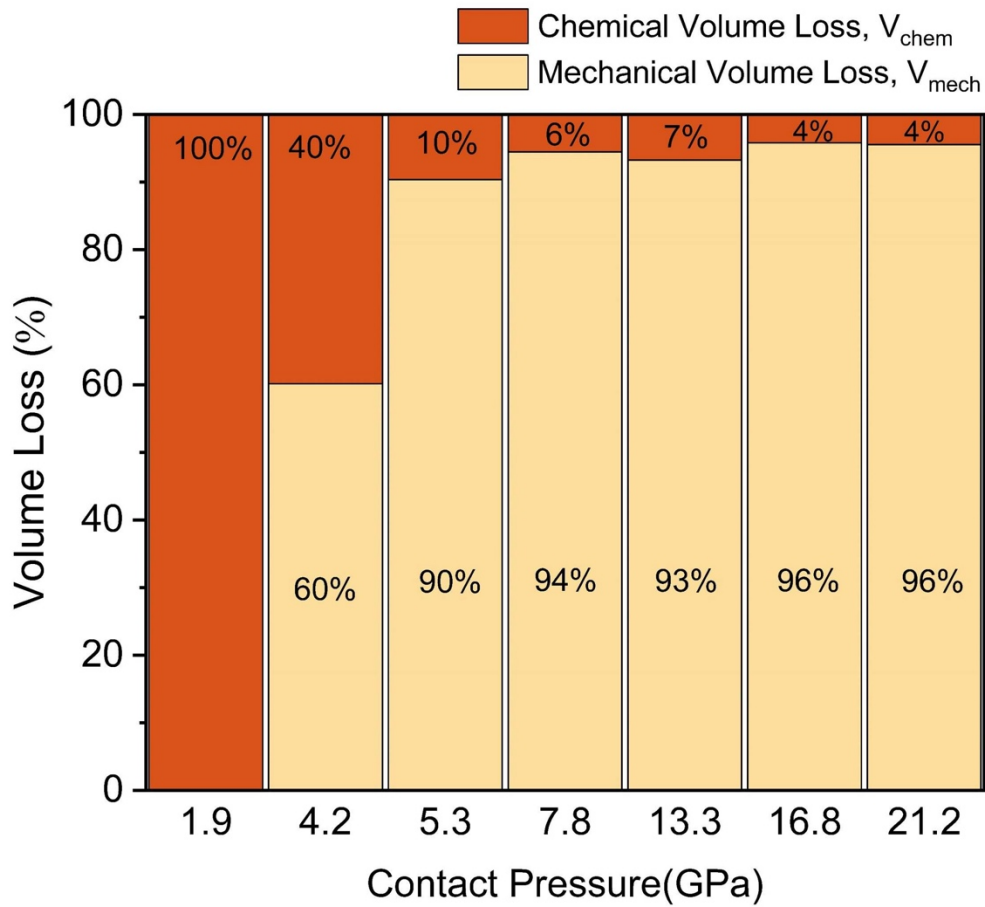


Figure 3. Graphs depicting the percentage dominance of mechanical and chemical wear across various initial contact pressures.

Figure 3

Tip Radius (μm)	Load (mN)	Radius of Contacting Area (μm)	Initial Contact Pressure (GPa)	Initial Penetration height (μm)	Degree of Penetration (Dp)	Shear Stress (GPa)	Shear strength (GPa)	Yielding (Tresca Criterion.)
100	10.0	1.57	1.95	0.02	0.016	0.97	0.86	YES
100	100.0	3.37	4.20	0.11	0.034	2.1	0.86	YES
100	200.0	4.25	5.29	0.18	0.042	2.64	0.86	YES
12.5	10.0	0.78	7.79	0.05	0.063	3.90	0.86	YES
12.5	50.0	1.34	13.33	0.14	0.107	6.66	0.86	YES
12.5	100.0	1.69	16.79	0.23	0.135	8.39	0.86	YES
12.5	200.0	2.12	21.15	0.36	0.170	10.58	0.86	YES

Table 1. The calculated results for various parameters, including the radius of the initial contacting area (a), Hertzian contact pressure (pmax), initial penetration height (h), degree of penetration (Dp), and shear stress at the contact between the tip and surface (τ_c) for different contacting geometries and loads. Additionally, values for bulk shear stress (τ_0) from the manufacturer's datasheet are provided, along with an indication if the material is yielding according to the Tresca criterion.

Figure 4

Formation of CoS₂ in the Tribological Taper Junction of Hip Implants

*Adrian Wittrock - TU Dortmund University - Dortmund, Germany

Christian Beckmann - TU Dortmund University - Dortmund, Germany

Alfons Fischer - Max-Planck-Institut fuer Eisenforschung - Duesseldorf, Germany

Saurabh Mohan Das - Max-Planck-Institut für Eisenforschung GmbH - Düsseldorf, Germany

Christian H. Liebscher - Max-Planck-Institut für Eisenforschung GmbH - Düsseldorf, Germany

Jörg Debus - TU Dortmund University - Dortmund, Germany

Markus Wimmer - Rush University - Chicago, USA

About 10 % of the hip and knee replacement surgeries in the US are revision surgeries. The reasons for the revision are often initialized by the release of wear products from a head-stem taper junction. Both retrieval studies and laboratory experiments have shown that the tribomaterial (e.g. 3rd-bodies generated through tribocorrosion) have an enormous influence on the tribological behavior. It has become clear that this nanostructured metallic-ceramic-organic composite consists of reaction products of the surrounding fluid and the materials in contact. From energy-dispersive X-ray spectroscopy analyses in the scanning electron microscope (SEM-EDS) on worn surfaces, we knew that there is some sulphur incorporated in areas where we also find molybdenum and cobalt. However, SEM-EDS does not allow for an unequivocal analysis of thin layers on such surfaces. To investigate the tribochemical reactions and the formation and constituents of tribomaterial, as it would appear inside a tapered joint of an implant, gross-slip fretting corrosion tests are performed. During such fretting tests, two CoCr29Mo6C0.03 pins (?12 mm x 7 mm) were pressed against a Ti6Al4V cylinder (?13 mm) that moved with an amplitude of 50 μ m at 37 °C. The experiments were run within a bovine calf serum (BCS) solution. Afterwards, the CoCr29Mo6C0.03 pins are studied by confocal Raman scattering combined with a microscope in air ambient environment. The pin surfaces were excited by the 532 nm emission of a single-frequency laser. Confocal Raman microscopy demonstrates that fretting corrosion gives rise to denaturation of albumin, associated with the availability of sulphur that reacts with metal ions released from the metal surfaces. To verify what kind of constituents have been generated destructive Raman spectroscopy measurements are performed using higher laser power, resulting in laser-induced oxidations. By this method, it was possible to identify amorphous/nanocrystalline CoS₂ as on constituent of tribomaterial sticking rigidly to and covering about 12 % of the CoCr29Mo6C0.03 contact surface. Further investigations using transmission electron microscopy and electron energy loss spectroscopy support this finding. Accordingly, self-generated CoS₂ acts like an extreme pressure additive, separates the direct metal-on-metal contact under fretting corrosion, and allows for ultra-mild wear rates below some ng/m wear path.

Extended in Vitro Wear of the Metal Glenosphere and Polyethylene Humeral Bearings of Reverse Total Shoulder Replacements Under Clean and Abrasive Conditions

*Hani Haider - UNMC - Omaha, USA

Joel Weisenburger - The University of Nebraska Medical Center - Omaha, USA

Ryan Siskey - Exponent - Philadelphia, USA

Ruth Heckler - DJO Surgical - Austin, USA

Nichole Plata - Enovis - Austin, United States of America

With loads reaching two-times-bodyweight and large spherical articular contact, Reverse Total Shoulder (RTS) wear has been reported clinically to raise osteolysis concerns. We tested RTS systems with worst-case physiologically realistic forces/motions in a wear simulator under both clean and abrasive conditions in a two-phase 10 million cycle (Mc) test.

We used a method, previously presented, and now the basis of an advanced draft ISO standard, with custom designed fixtures holding the RTS at compound angles in an adapted AMTI hip simulator such that the predominant shoulder force direction based on telemetry data aligned with the simulator compressive force axis. Multiple 3-D transformation iterations optimized the full-range of motion of all the simulator actuators to yield physiologically realistic shoulder motions with cross-shear. The motions elevated the shoulder 38°-79° in elevation planes 15°-45°, with a maximum force of 1,700 N at 79° maximum elevation angle and 170 N ($R=0.1$) at 38° elevation, in a double loading waveform (Fig. 1) cycled at 0.75 Hz frequency.

Two groups of RTS were tested ($N=3$ in each) with 32 mm cobalt chrome alloy (CoCr) glenospheres. One group had conventional GUR1050 ultra-high-molecular-weight-polyethylene (UHMWPE) humeral bearings and the other was highly cross-linked (HXL) (150 kGy) stabilized with vitamin-E. All bearings were secured into titanium humeral cups, lubricated with diluted bovine serum (30 g/L protein, 37°C) with testing conducted in a clean (standard) mode for 5 Mc.

Afterwards the CoCr glenospheres were intentionally scratched to simulate high abrasive conditions using titanium, titanium oxide, and aluminum oxide abrasive particles placed in separate (temporary) sacrificial UHMWPE humeral bearings with the same waveforms run dry for 75 shoulder cycles under a 500 N constant compression. This scratched the metal glenosphere surfaces ($R_a \sim 0.6 \mu\text{m}$), which were paired again with the original (tested) UHMWPE bearings and testing continued for another 5Mc. Wear of the UHMWPE bearings and metal glenospheres was measured at standard intervals and the UHMWPE wear was corrected with the weight gain of active load soak controls.

The average wear rates during the first 5Mc (Fig. 2) of conventional bearings was $23.5 \pm 6.57 \text{ mg/Mc}$ and 90% lower for HXL at $2.4 \pm 0.8 \text{ mg/Mc}$ ($p=0.029$). During the last 5Mc (scratched) the wear rate for the conventional poly increased 8-fold to $183 \pm 22 \text{ mg/Mc}$, and the HXL increased only 3-fold at $6.6 \pm 2.4 \text{ mg/Mc}$ which was 96% lower ($p=0.002$), and both increases after scratching were statistically significant ($p<0.05$).

During the first 5Mc the CoCr glenospheres wore similarly with conventional and HXL at 0.38 ± 0.17 and $0.36 \pm 0.18 \text{ mg/Mc}$ respectively ($p=0.895$) (**Fig. 3**). In the final 5Mc the scratched glenospheres wore $0.42 \pm 0.02 \text{ mg/Mc}$ with the conventional UHMWPE and half that ($0.22 \pm 0.04 \text{ mg/Mc}$) with HXL ($p=0.003$).

The RTS wear test method with physiologically realistic alignment, worst-case forces, motions, and cross shear, produced wear not dissimilar from RTS retrievals. HXL vitamin-E UHMWPE significantly reduced wear to a tenth with conventional UHMWPE, and 27 times lower after glenosphere scratching. Interestingly, the tiny amount of wear of the metallic glenospheres was half as much with HXL compared to conventional UHMWPE after scratching.

Figures

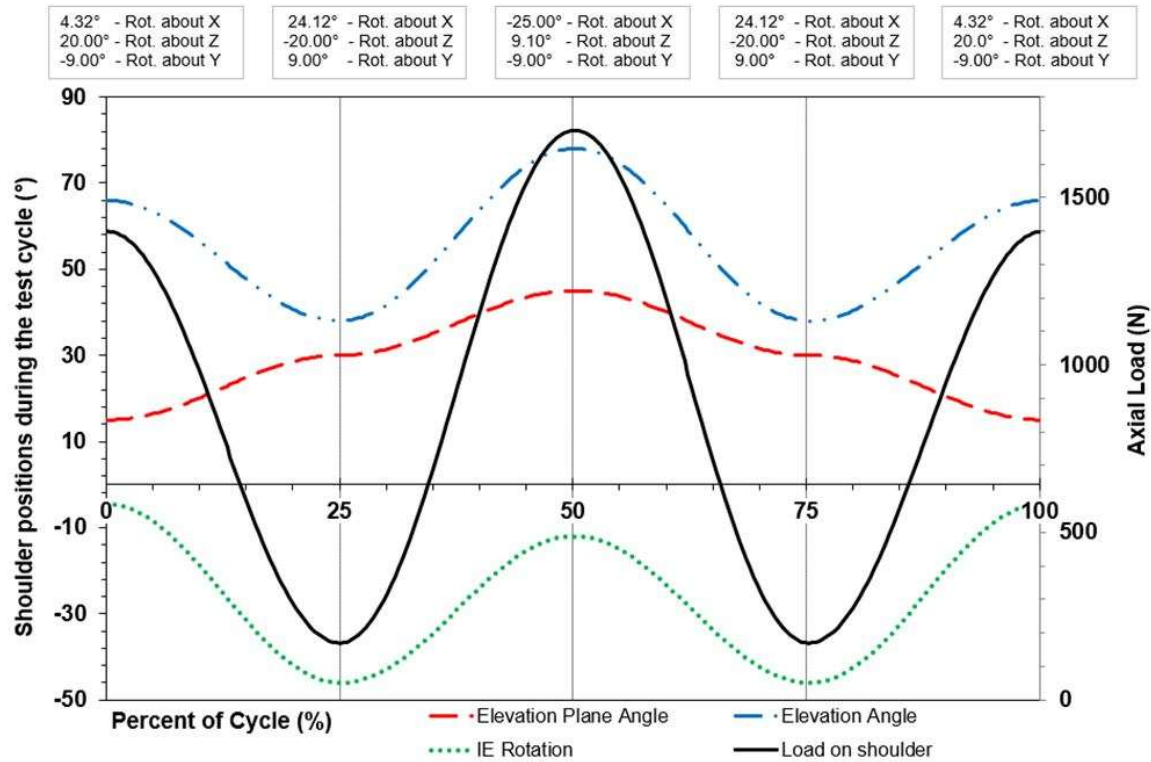


Fig. 1: Resulting shoulder motions (plotted curves) and in the text at the top are the corresponding AMTI Hip Simulator actuator positions.

[Figure 1](#)

Reverse Shoulder Wear Test - Average Wear of UHMWPE Humeral Bearings

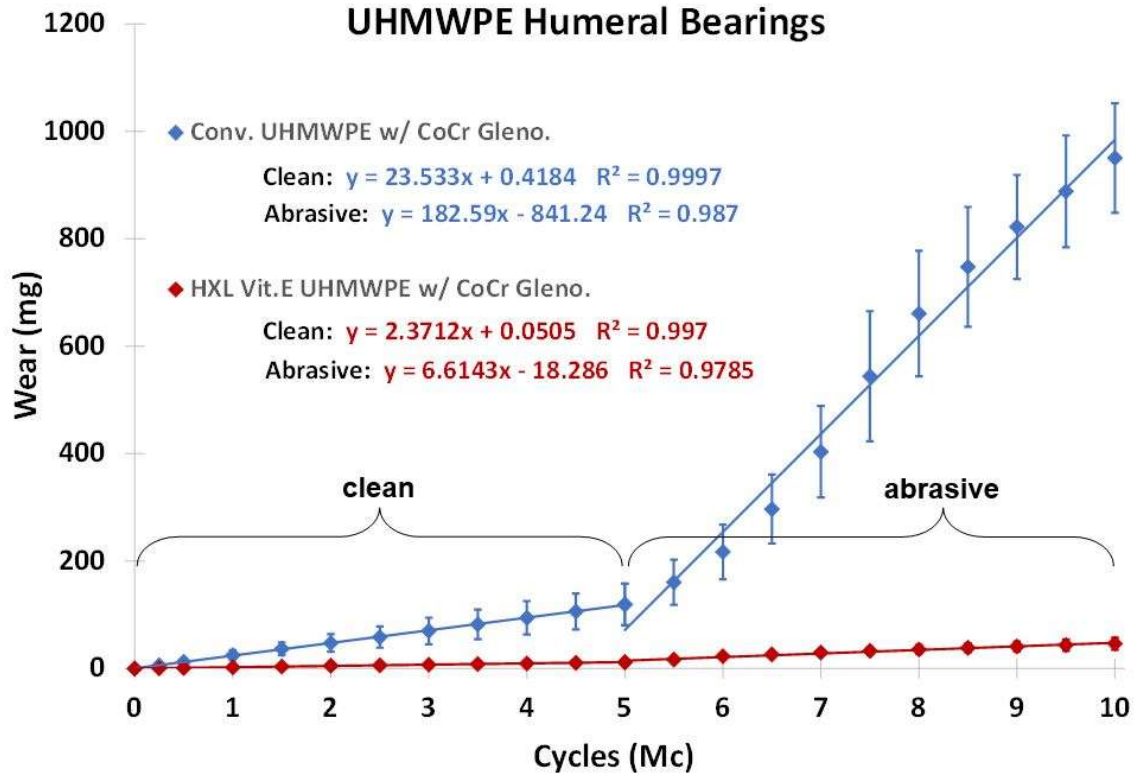


Fig. 2: Average wear of the UHMWPE humeral bearings over 10Mc, corrected with active soak control data (not shown). Wear rates calculated via least squares regression line with a free intercept. 95% confidence intervals are also shown.

Figure 2

Reverse Shoulder Wear Test - Average Wear of CoCr Glenospheres

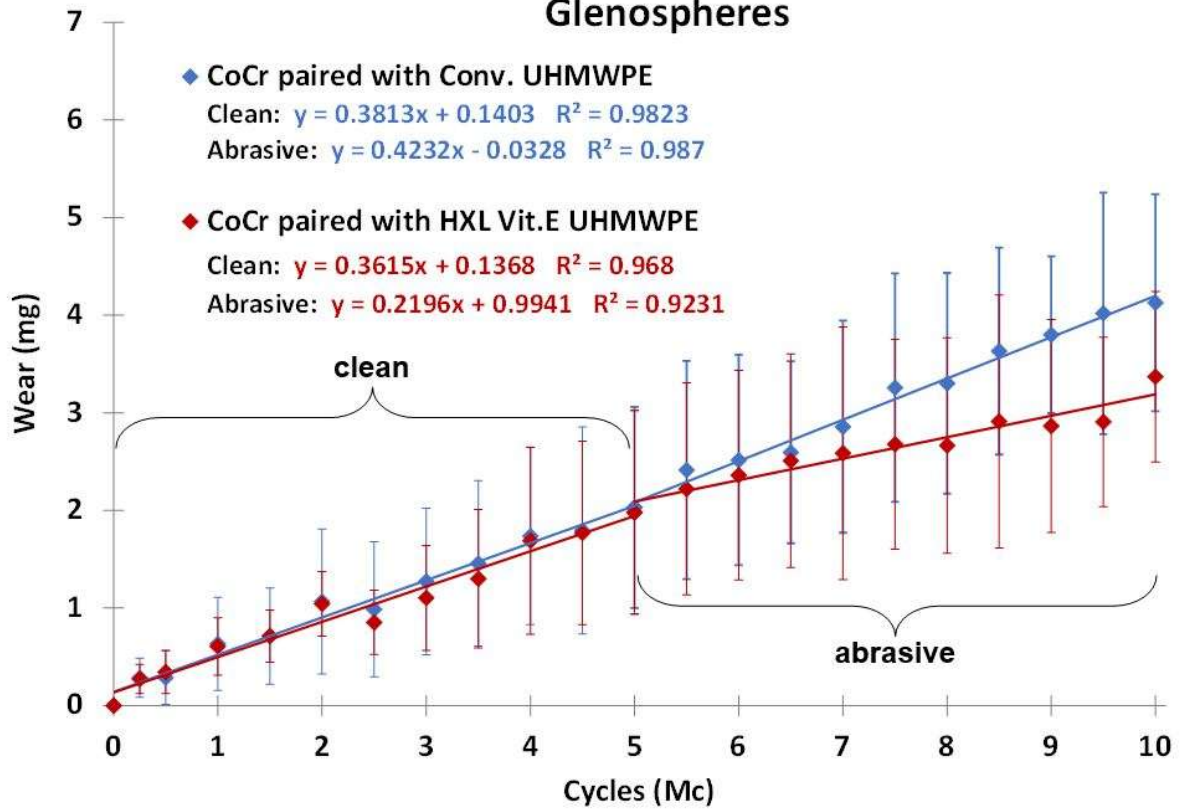


Fig. 3: Average wear of the CoCr glenospheres over 10Mc. Wear rates calculated via least squares regression line with a free intercept. 95% confidence intervals are also shown.

Figure 3

Validation of an MRi Technique for Measuring in-Vivo Glenoid Wear; a Tool for Understanding Glenohumeral Pain

*Ulrich Hansen - Imperial College London - London, UK

Hazimah Mahmud - Imperial College London - London, United Kingdom

Anthony Bull - Imperial College - United Kingdom

Sanjeeve Sabharwal - Imperial College London - London, United Kingdom

Roger JH Emery - Imperial College - London, United Kingdom

Andra Topan - Imperial College London - London, United Kingdom

Peter Reilly - Imperial College London - London, United Kingdom

Aim

To validate MR imaging for measurement of glenoid wear by comparison to high resolution micro-CT imaging.

Background

Glenohumeral pain and its relationship to rotator cuff function is not well understood but is one of the key reasons for revision of hemiarthroplasties. Glenoid wear is likely to be associated with glenohumeral pain. If MR imaging is able to assess glenoid wear, and thus arguably pain, this would make in-vivo studies of progressive glenoid wear and pain possible. Furthermore, such wear could even be related to simultaneous assessment of the rotator cuff to further the understanding of the relationship between rotator cuff function and pain. However, prior to this study it was unclear if MRi is able to assess glenoid wear.

Methods

Four cadaver glenoids were tested against a ceramic humeral head (simulating a hemiarthroplasty) within a dedicated shoulder joint wear simulator. The specimens were tested for 500,000 cycles simulating activities of daily living. The specimens were MRi and micro-CT scanned before testing and at the end of testing. Thus the thickness of the glenoid cartilage was assessed before and after testing, the difference being the wear due to testing. This assessment of cartilage thickness and wear was carried out using both MRi and micro-CT imaging and the measurements compared. The cartilage thickness varied across the glenoid surface and the measurements were separated into 4 quadrants providing a total of 16 data points when comparing MRi and micro-CT wear assessments. The micro-CT which has a resolution of 5 microns was considered the ground truth against which the MRi measurements were assessed.

Results

MRI underestimated cartilage wear by 0.15mm on average ($p=0.35$) and the maximum difference between the two techniques was 0.5mm.

Conclusion

MRi did underestimate the wear, on average by 0.15mm. However, comparing this difference, or even the maximum difference of 0.5 mm, to the thickness of glenoid cartilage of 2.2mm

Quantitative Polyethylene Wear Analysis and Scapular Notching Grade in Reverse Total Shoulder Arthroplasty

*Gabriel Landi - Dartmouth College - Hanover, United States of America
Douglas Van Citters - Dartmouth College - Hanover, USA

Scapular notching is a well-documented reverse total shoulder arthroplasty (rTSA) phenomenon characterized by the erosion of the inferior glenoid cavity, particularly initiated by repetitive contact with the implant system's polyethylene liner. Several other complications, including the generation of bioactive, microscopic polyethylene particles and liner instability, have also been observed to potentially have relationships with scapular notching, further driving the need to understand its full mechanism, including both its proposed 'abrasive impingement' and 'polyethylene-induced osteolytic' phases. Meanwhile, quantitative volumetric wear measurement has begun to rise in popularity throughout the field of arthroplasty, replacing qualitative and semi-quantitative methods of wear estimation like linear wear radiographic evaluation— however, up until now, they have lacked the precision necessary to evaluate the possible correlations with degree of scapular notching, represented by the Nerot-Sirveaux classification system that grades the notching's extent on a scale from 0 to 4. Therefore, this study aims to develop a tool that measures volumetric wear with sufficient precision to recognize these trends: more specifically, the relationships between scapular notching grade and grade over duration implanted (grade progression) with articular surface wear and the wear located around the liner's rim, the latter of which is directly associated with the polyethylene-scapula contact interface. A coordinate measuring machine (CMM)-based method was developed to measure 20 Zimmer Biomet rTSA polyethylene liners ranging from Nerot-Sirveaux grades 0 to 4, centered around the assembly of point clouds for each liner's articular and rim surfaces. The volumetric wear of these two regions were calculated independently, but in both cases, compared the volume of the 'worn' model to a retroactively generated 'unworn' mode in order to calculate wear; multiple algorithms and computational methods were utilized in conjunction with one another to render the unworn models, including bilinear interpolation, spherical linear interpolation, alpha shapes, and Savitzky–Golay smoothing. Subsequently, Kendall's tau correlation coefficients were computed to evaluate statistical significance, finding significant, consistent trends between scapular notching grade and articular wear, as well as grade progression and total wear. Therefore, both rim and articular wear seem to affect the rate of change of scapular notching grade with respect to implant duration, while the amount of articular wear in particular affects the grade itself; more importantly, this supports the proposed theory that polyethylene-induced osteolysis drives 'higher grade' scapular erosion by quantitatively evincing a relationship between articular wear and grade, despite the generally limited interaction between the joint's spherical socket and the scapula during articulation. This work ultimately intends to help inform rTSA prosthesis design, especially those modifications that reduce the volumetric amount of polyethylene wear and the rate of implant loosening.

Figures

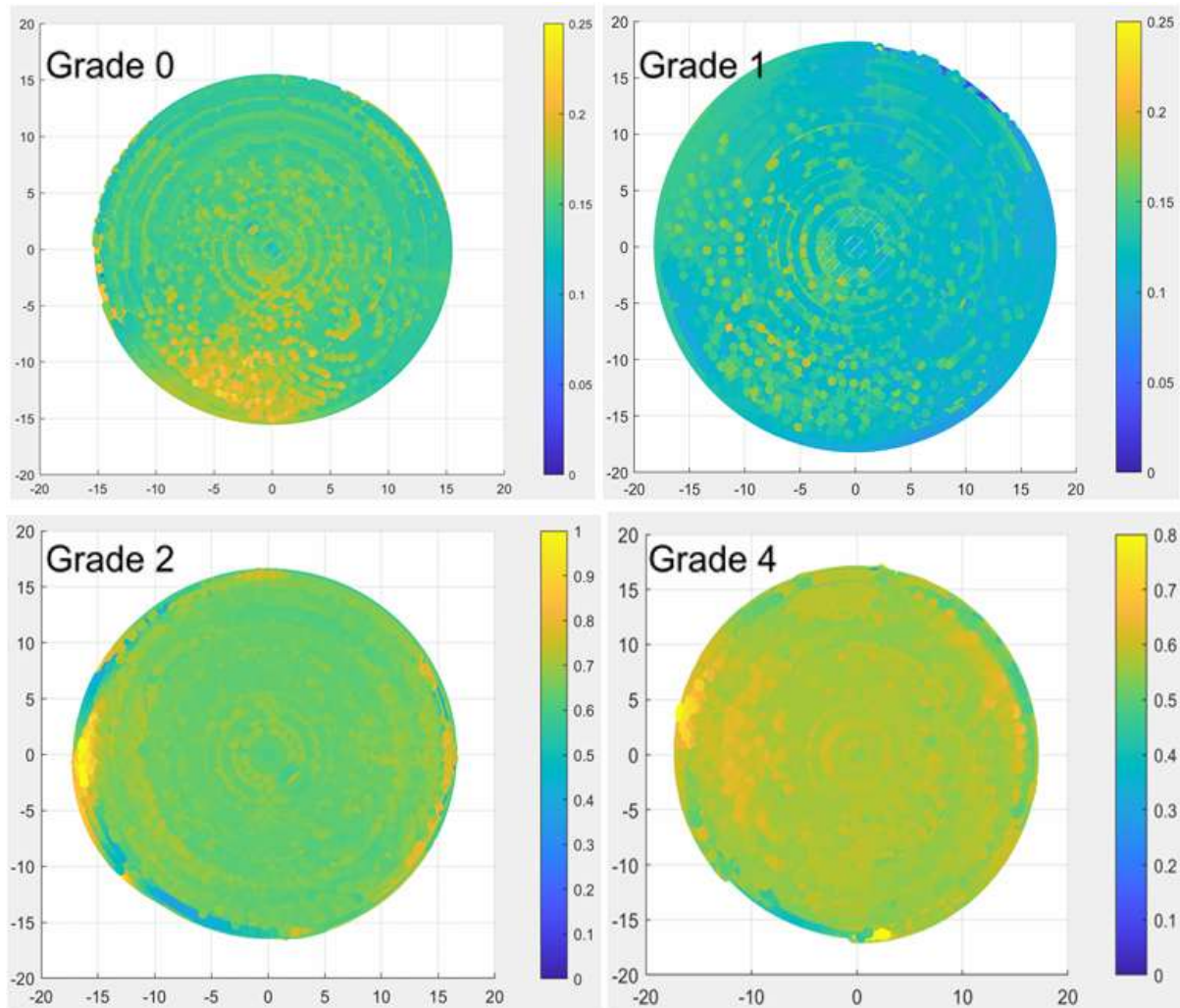


Figure 1: Normalized articular wear distribution heat maps for reverse total shoulder polyethylene liners retrieved from patients with Nerot-Sirveaux scapular notching grades 0, 1, 2, and 4.

[Figure 1](#)

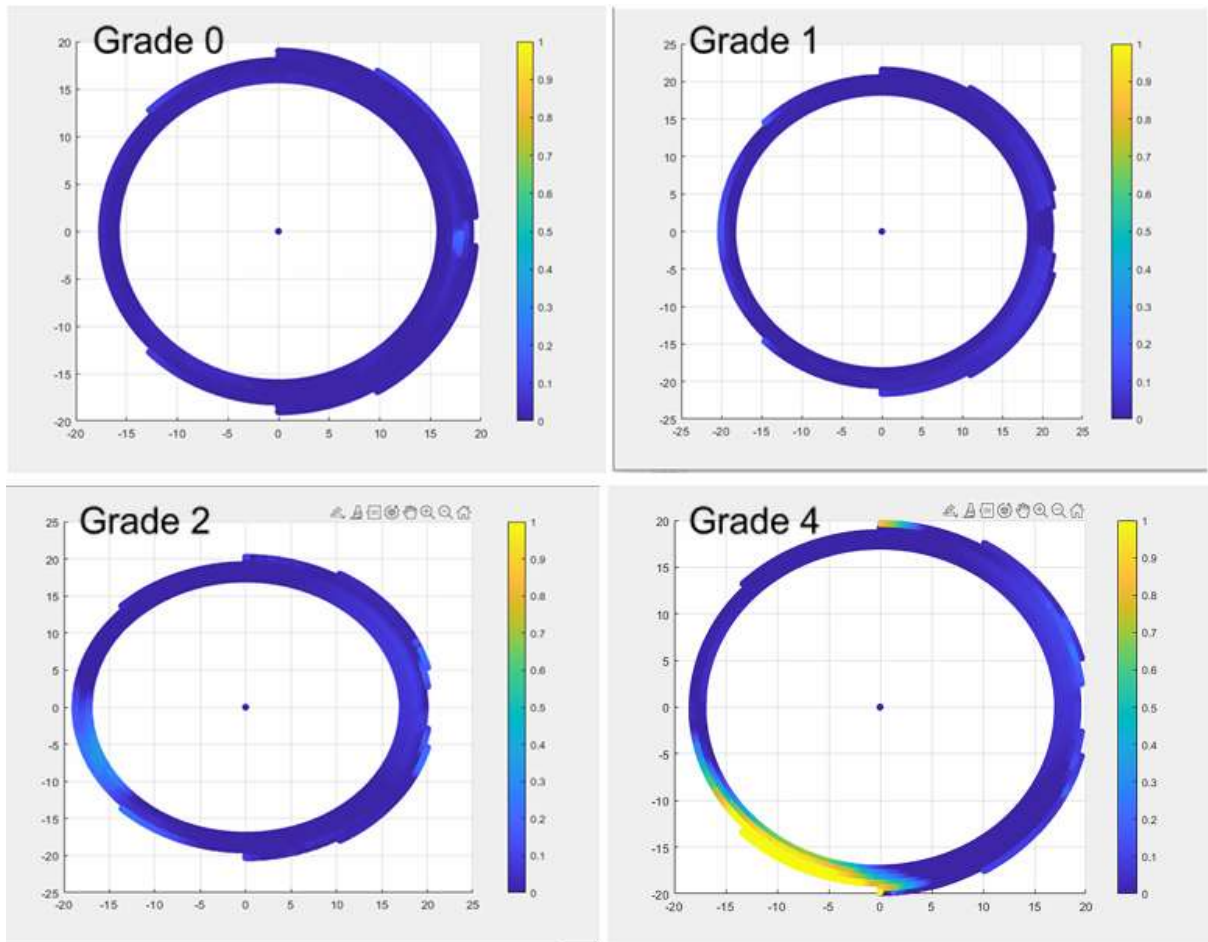


Figure 2: Normalized rim / ‘nonarticular’ wear distribution heat maps for reverse total shoulder polyethylene liners retrieved from patients with Nerot-Sirveaux scapular notching grades 0, 1, 2, and 4.

[Figure2](#)

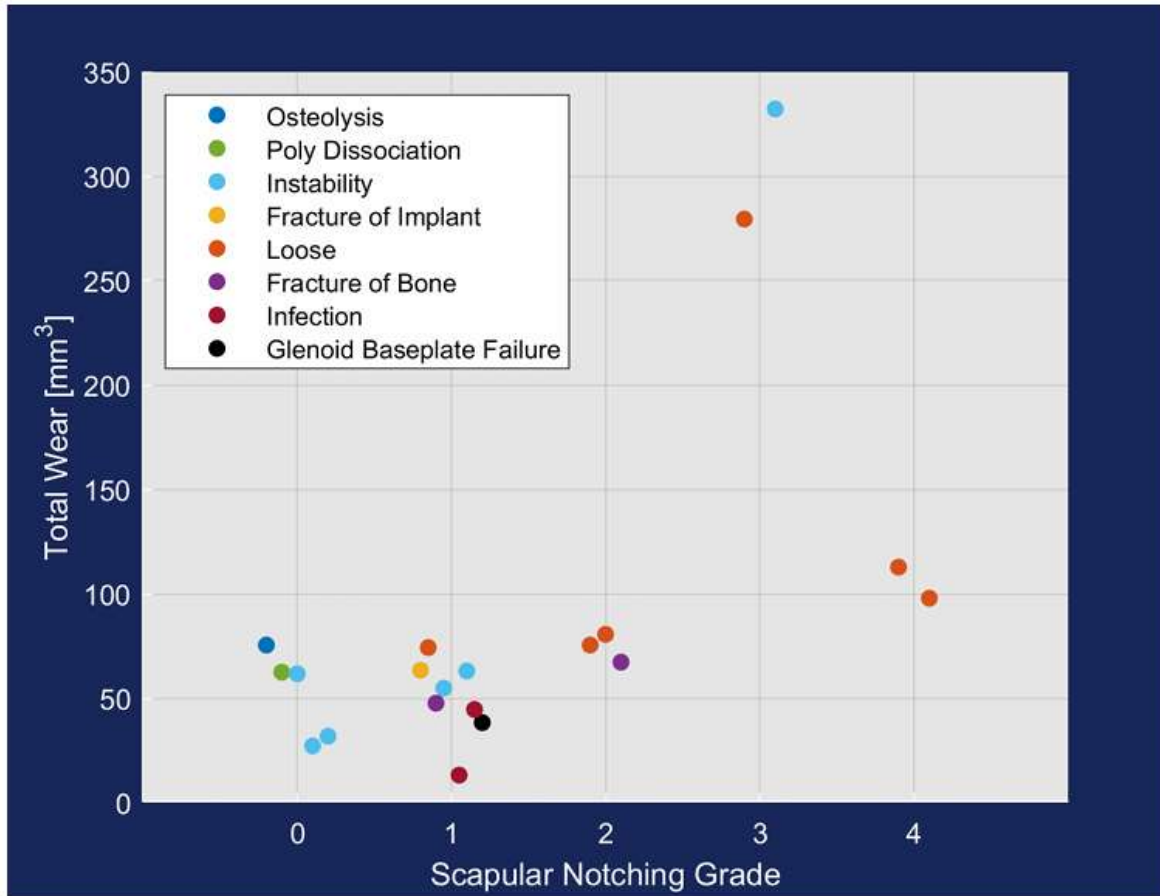


Figure 3: Total volumetric wear measurements for entire reverse total shoulder polyethylene liner cohort (n = 20), plotted against Nerot-Sirveaux scapular notching grades; retrieval reasons also included.

[Figure 3](#)

Can Subscapularis Deficiency Explain Glenoid Wear (Thus Possibly Glenohumeral Pain)

*Ulrich Hansen - Imperial College London - London, UK

Hazimah Mahmud - Imperial College London - London, United Kingdom

Andra Topan - Imperial College London - London, United Kingdom

Anthony Bull - Imperial College - United Kingdom

Roger JH Emery - Imperial College - London, United Kingdom

Sanjeeve Sabharwal - Imperial College London - London, United Kingdom

Peter Reilly - Imperial College London - London, United Kingdom

Aim

To investigate if abnormal shoulder joint loads, due to a deficient subscapularis, will lead to glenoid wear, which may in turn aid the understanding of glenohumeral pain.

Background

Glenohumeral pain is poorly understood but is of great clinical importance; notably, glenohumeral pain is a key reason for revision of hemiarthroplasties. The subscapularis is often reported to be compromised following a deltopectoral approach (the most common surgical approach during arthroplasty). The resulting abnormal shoulder joint loads may lead to increased wear of the glenoid. Glenoid wear may be related to glenohumeral pain. Thus this study which quantifies the wear during abnormal loads, aims to further the understanding of the relationship between surgical approaches, abnormal biomechanics and resulting joint pain.

Methods

A total of 14 cadaver glenoid specimens were tested to 250,000 cycles of daily activity in a dedicated shoulder joint wear simulator. The cadaver glenoids were articulated against a ceramic humeral head simulating a hemiarthroplasty situation. Eight (n=8) glenoids were tested simulating normal joint loads while n=6 were tested simulating abnormal (subscapularis deficient) joint loads. These loads were based on a musculoskeletal model calculation and in the abnormal case the subscapularis was removed from the model, thus representing the extreme case of a dysfunctional subscapularis case following a delto-pectoral approach during arthroplasty surgery.

Results

After 250,000 cycles the wear depth in the subscapularis deficient load case was more than double that of the normal load case, 0.85mm versus 0.3mm, respectively. However, this finding was not significant ($p>0.05$), a lack of significance seemingly related to a difference between male and female (small) glenoids which the study was not set up to address. An additional finding was that the wear pattern became more posterior in the subscapularis deficient load case.

Conclusion

The findings of this study suggests that subscapularis deficient loads may be related to glenohumeral pain and alternative surgical approaches may be warranted. However, while the results were notable they were not statistically

significant. The study found that subscapularis deficient loads led to posterior wear which is consistent with observed glenoid implant wear. Therefore our findings suggest that alternative surgical approaches leading to normal joint biomechanics may reduce implant wear.

The Impact of Augmented Reality Technology and Preoperative Planning on Patient Satisfaction and Perceptions After Shoulder Arthroplasty

*Garrett Jackson - Chicago, United States of America

Vani Sabesan - Cleveland Clinic Florida - Weston, USA

Aghdas Movassaghi - Michigan State University - East Lansing, USA

Julio Vandama - Charles E. Schmidt College of Medicine Florida Atlantic University - Boca Raton, USA

Carlos Fernandez - JFK / U Miami Orthopedic Surgery Program - Lantana, USA

Introduction

Intraoperative navigation (NAV) and augmented reality (AR) have emerged as promising new technologies in shoulder arthroplasty (SA). Previous research in these areas have focused on the use of these technologies by surgeons, but not around improved understanding of patient knowledge and perceptions. Little is known whether patients are aware or understand this technology and how it relates to their outcomes after SA. The purpose of this study was to see if direct patient education for the innovative technology used for SA would affect patient confidence in their surgeon and satisfaction following SA.

Methods

This was a prospective study that included 20 patients scheduled for SA with one fellowship-trained shoulder surgeon at a single institution from 2022-2023. During their preoperative visit, patients completed a survey regarding their perception of the use of technology for SA and were then shown a patient education video about the use of innovative AR technology for their surgery. Repeat survey testing was then performed to assess patient perception of this technology, effect of this technology on their outcome and satisfaction. The survey was again repeated postoperatively at 6 weeks and 3 months.

Results

Most patients were somewhat familiar with the use of 3D technology for preoperative planning (55%), had heard about it from their surgeon (60%), but had no preference about their surgeon using it for their surgery (60%). Additionally, most patients did think AR would lead to better results/outcomes (60%) and thought surgeons that utilize this technology are better than those that do not utilize it (60%). Many (90%) of the patients would prefer a high-volume surgeon that doesn't use 3D/AR technology compared to a low-volume surgeon that uses it. The 3 main concerns about this technology included lack of surgeon experience with it, increased costs, and increased surgery duration. Patients reported a 100% confidence level in their surgeon and satisfaction in knowing that their surgeon uses AR technology, which was unchanged by the patient education video. At 6 weeks, patients rated their satisfaction with knowing their surgeon used this technology at 78% and their satisfaction with their shoulder at 69%. At 3 months, these improved to 99% and 85%, respectively, with patients reporting they thought the use of AR technology and preoperative planning allowed for better results/outcomes.

Conclusions:

Our results demonstrated that patient perception of AR technology and preoperative planning was very positive, yet there are inconsistencies in how well patients understand the benefits of these technologies. Patient selection and confidence

levels were more impacted by surgeon volume and not the use of these innovative technologies, with most patients having no preference on whether their surgeon utilized it. Although technology may not impact patient selection of a surgeon it clearly positively impacts their confidence and satisfaction levels postoperatively.

Male Patients Experience Similar Improvement in Clinical and Functional Outcomes Despite Higher Revision Rates Following Reverse Shoulder Arthroplasty Compared to Female Patients: A Systematic Review

*Garrett Jackson - Chicago, United States of America

Colton Mowers - Rush Medical College - Chicago, United States of America

Devin John - HCA JFK/University of Miami Orthopaedic Surgery Residency Program - Atlantis, USA

Aghdas Movassaghi - Michigan State University - East Lansing, USA

Jacob Calpey - Charles E. Schmidt College of Medicine Florida Atlantic University - Boca Raton, USA

Vani Sabesan - Cleveland Clinic Florida - Weston, USA

Purpose: To compare patient-reported outcomes, range of motion, and rates of revision surgery following primary reverse shoulder arthroplasty (RSA) between male and female patients.

Methods: A systematic review was performed using the 2020 Preferred Reporting Items for Systematic Review and Meta-Analysis (PRISMA) guidelines. A literature search was performed on October 12, 2023, using the PubMed, Embase, and Scopus library databases for human clinical studies reporting postoperative outcomes and revision rates following RSA between male and female patients. Preoperative and postoperative outcome scores and revision rates were stratified by patient sex and quantitatively compared. The quality of the included studies was assessed using the Methodological Index for Non-Randomized Studies (MINORS) criteria.

Results: Nine studies consisting of 5,992 male (mean age, 78.1 years; mean follow-up, 48.6 months) and 20,031 female (mean age, 76.2 years; mean follow-up, 58.6 months) patients were included. At final follow-up, male patients reported significantly less improvement in postoperative American Shoulder and Elbow Society scores (ASES; Mean difference, -2.85; $p = 0.003$) and external rotation (Mean difference, -2.17° ; $p=0.03$), with no significant difference in Constant scores (Mean difference, -1.20; $p = 0.11$), forward flexion (Mean difference, -2.19° ; $p = 0.49$), or abduction (Mean difference, -1.40° ; $p = 0.58$) when compared to female patients. Revision rates were significantly higher in males when compared to females (6.9% vs. 4.9%, respectively; $p < 0.001$).

Conclusion: Males undergoing RSA report less improvement in postoperative ASES scores, as well as decreased external rotation values at a mean final follow-up of 48.6 months, with comparable Constant score, forward flexion, and abduction when compared to females with a mean final follow-up of 58.6 months. However, revision rates were significantly higher in males.

Preclinical Testing of Stemless Shoulder Implant Stability: How Much Complexity Is Necessary?

*Kyle Snethen - Zimmer Biomet - Warsaw, USA

Yang Son - Zimmer Biomet - Warsaw, USA

Christine Mueri - Zimmer Biomet - Winterthur, Switzerland

Marc Bandi - Zimmer GmbH - Winterthur, Switzerland

Introduction: Stemless total shoulder arthroplasty (TSA) is increasing in usage over the past decade. Adequate initial stability between implant surfaces and proximal humeral bone to support osseointegration is required for long-term fixation. There are currently no consensus technical standards for assessing the initial stability of stemless shoulder implants, leaving various options to perform static and/or dynamic tests to evaluate initial stability. With the goal of defining repeatable test methods that can produce clinically relevant results, the objective of the present study was to compare the ability of tests with varying levels of complexity to distinguish between different stemless shoulder implant designs when evaluating initial stability.

Methods: Three separate tests were executed including (1) static pull-out, (2) static lever-out and (3) dynamic micromotion (Fig. 1). Each test was performed on two different stemless shoulder designs; "Device A" and "Device B". Device A featured a 6-fin design, while Device B, similar in overall size, featured an asymmetric 6-fin configuration with unique fin shapes and a porous coating exhibiting a higher coefficient of friction. For each device, at least three samples were tested, inserted into 20PCF cellular polyurethane foam blocks using corresponding surgical instruments that provide similar press-fits. Static pull-out and lever-out tests quantified the maximum force required to remove the implant from the foam block under a purely tensile and shear force, respectively, without mating humeral head components assembled. The dynamic micromotion test measured humeral component-level micromotion during cyclic loading using digital image correlation as presented previously [1]. The output measures for Device A and Device B were compared for each of the three tests using a 2-sample t-test and F-test.

Results: Considering higher pull-out and lever-out forces and lower micromotion to be indicative of superior implant stability, the rank order between devices did not change between the 3 tests with Device B exhibiting superior stability (Fig. 2). The pull-out test produced the lowest percent difference between the two devices and was the only test that did not show significant differences ($p=0.180$). The lever-out test produced the highest percent difference but also the highest standard deviations, yet still determined statistically significant differences between devices ($p=0.025$). The micromotion test also determined significant differences between devices ($p=0.001$) yet significantly less standard deviation ($p=0.005$) despite added complexity regarding mating components and loading conditions.

Conclusion: When implant conditions are consistent, simple tests may suffice for evaluating initial stability; however, when considering differences in clinically relevant factors (e.g. surgical technique, mating components, etc.) between devices, conducting micromotion tests under full assembly conditions with physiological loading becomes crucial. The simplest pull-out test was limited in benchmarking implant stability between different designs while lever-out testing represents an extreme worst-case condition in the absence of mating components to resist motion and a purely shear applied load. The micromotion test was able to distinguish between devices while considering clinical factors influential to initial stability under

more physiologically relevant loading without compromising test method repeatability.

References:

[1] Snethen et al. ISTA, New York, USA. September 2023. Podium Abstract #8486

Figures

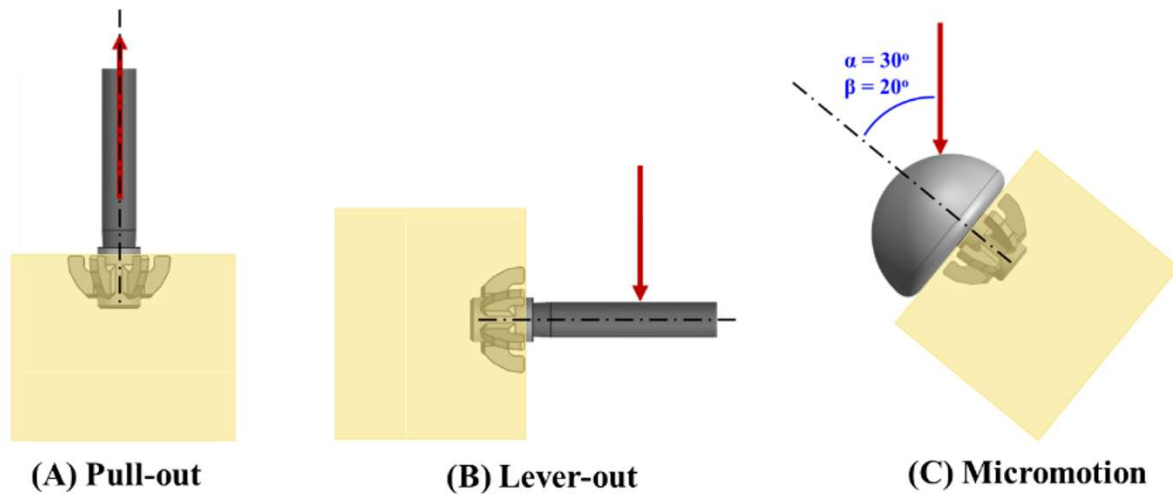


Figure 1. Illustrations of the three different stability tests performed.

[Figure1](#)

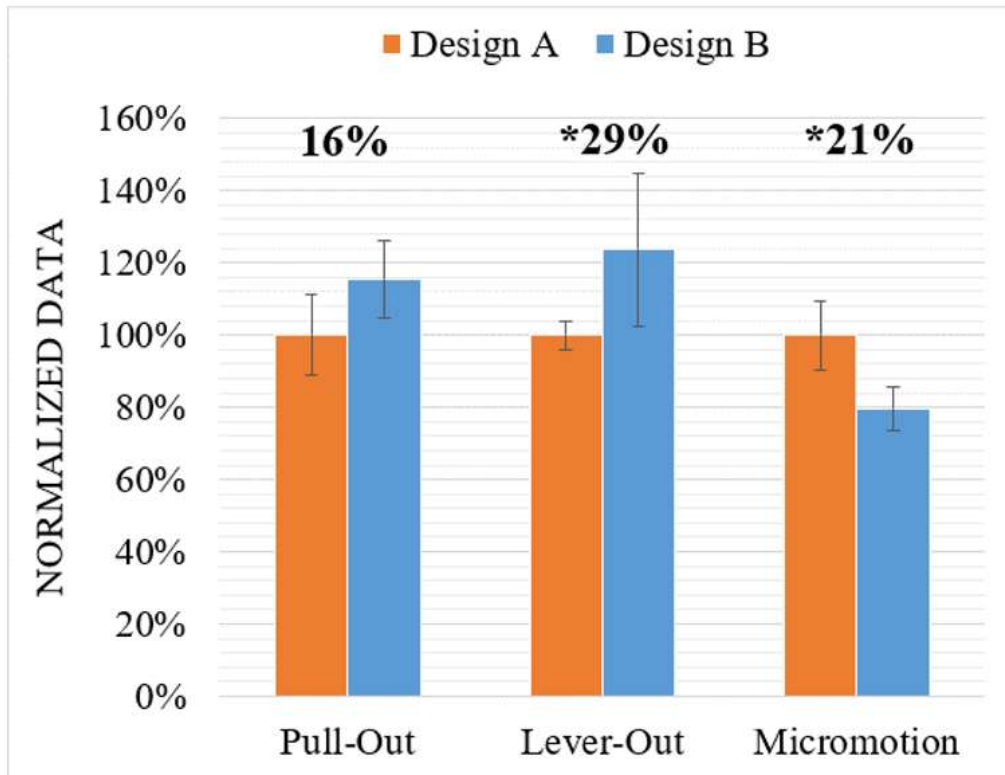


Figure 2. Results from each test normalized to the mean of Device A with percent difference listed above each tests and an asterisk “*” indicating a statistically significant difference ($\alpha=0.05$).

[Figure 2](#)

Technology Versus Technique: Will ChatGPT Replace Orthopedic Triage Nurses?

*Stephen Chenard - Vanderbilt University School of Medicine - Nashville, United States of America

Aleksander Mika - Vanderbilt Orthopedics

Gregory Polkowski

Stephen Engstrom - Vanderbilt University Medical Center - Nashville, USA

Jacob Wilson - Vanderbilt - Nashville, USA

John Ryan Martin - Vanderbilt Health - Hendersonville, USA

Introduction: Postoperative nursing triage remains a considerable financial and time burden following total joint arthroplasty (TJA). While the current system is effective, as reimbursement continues to decrease, fewer resources are available to deliver important perioperative care. An ideal triage method would be equally as safe as triage nurses, but more cost-effective and time-efficient. Therefore, this study aimed to see if ChatGPT could serve as a safe and effective method of postoperative triage in responding to potential patient concerns following TJA.

Methods: We compiled a list of ten potential concerns from post-operative arthroplasty patients and presented them to orthopaedic triage nurses (n=3) and ChatGPT (Table 1). The responses were rated by three blinded fellowship-trained arthroplasty surgeons using Likert scales ranging from 1-5 for safety and completeness. The mean scores for each group were calculated for each prompt and are presented as mean \pm standard deviation.

Results: There was no significant difference in average safety scores between ChatGPT responses (4.233 ± 0.473) and those of triage nurses (4.278 ± 0.382) ($p=0.68$) (Figure 1). Similarly, there was no significant difference in completeness scores between ChatGPT responses (3.933 ± 0.783) and those of triage nurses (4.044 ± 0.588) ($p=0.67$) (Figure 2). Furthermore, there were no significant differences in safety or completeness between ChatGPT and triage nurses for any of the individual prompts (all p -values >0.05).

Conclusions: As reimbursement for TJA continues to decrease, providing cost-effective clinical care is paramount. Postoperative triage is an important component of perioperative care but represents a substantial time and cost burden. Our study demonstrates that the use of an AI-enabled chatbot, even without specific orthopaedic training, can provide instantaneous, safe, and complete responses to common perioperative patient concerns.

Figures

Fig 1. AI vs TN: Safety

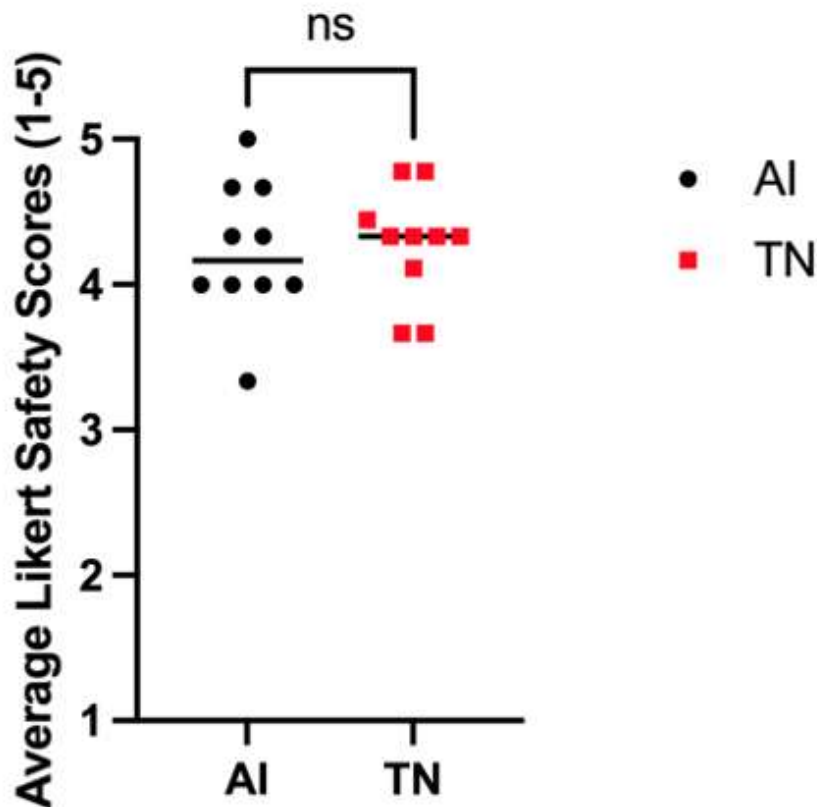


Figure 1. There is no significant difference in the average safety rating of ChatGPT and triage nurse responses. Fellowship-trained arthroplasty surgeons (n=3) rated the safety of responses of orthopedic triage nurses (TN) (n=3) and ChatGPT (AI). Each data point represents the average safety score for each of the ten prompts on a Likert scale from 1-5. Using a two-sided t-test, it was found that there was no significant difference in the average safety scores of ChatGPT responses (4.233 ± 0.473) and those of orthopedic triage nurses (4.278 ± 0.382) ($p=0.68$).

[Figure 1](#)

Fig 2. AI vs TN: Completeness

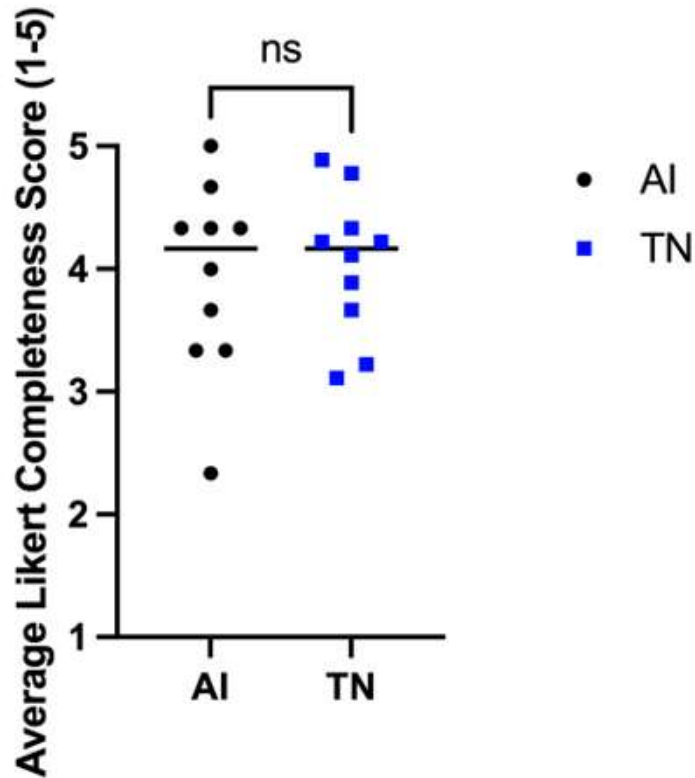


Figure 2. There is no significant difference in the average completeness rating of ChatGPT and triage nurse responses. Fellowship-trained arthroplasty surgeons (n=3) rated the completeness of responses of orthopedic triage nurses (TN) (n=3) and ChatGPT (AI). Each data point represents the average completeness score for each of the ten prompts on a Likert scale from 1-5. Using a two-sided t-test, it was found that there was no significant difference in average completeness scores between ChatGPT responses (3.933 ± 0.783) and those of triage nurses (4.044 ± 0.588) ($p=0.67$).

[Figure 2](#)

Table 1. List of prompts provided to ChatGPT and Orthopedic Triage Nurses.	
#:	Prompt Text:
1	"How much walking can I do?"
2	"My knee hurts. What should I do?"
3	"My incision is swollen and draining fluid. What should I do?"
4	"Can I put weight on my leg?"
5	"What medications can I take if my leg is sore?"
6	"Should I take my blood thinners?"
7	"Can I get my incision wet?"
8	"I suffered a fall and now my leg hurts. What should I do?"
9	"I just felt a snap and now my leg really hurts and I can't walk on it. What should I do?"
10	"My leg is throbbing and red, and I'm having trouble breathing. What should I do?"

[Figure 3](#)

AI Segmentation in Clinically Relevant Complex Orthopedic Cases: A Targeted Study on Developmental Dysplasia of the Hip

Lilian Lim - FormusLabs - Auckland, New Zealand

Chris Rapson - Formus Labs - Auckland, New Zealand

Duncan Bakke - Formus Labs - Auckland, New Zealand

Ju Zhang - Formus Labs - Auckland, New Zealand

Thor F Besier - University of Auckland - Auckland, New Zealand

*Marco Schneider - Formus Labs - Auckland, New Zealand

Introduction

Accurate segmentation of patient anatomy is critical for 3D preoperative planning of total hip arthroplasty (THA) surgery. AI-based segmentation of lower-limb bones has been shown to be robust to age, sex, and ethnicity [1], but given that THA is an intervention for many conditions, it also must be robust to atypical, pathological morphology. In this study, we evaluated the accuracy of the Formus convolutional neural network (CNN) (Formus Labs, NZ) in segmenting CT images from patients with developmental dysplasia of the hip (DDH).

Methods

Sixteen DDH hips were manually segmented by an experienced image analyst using Materialise Mimics (Materialise, Belgium) from nine CT scans (2 males and 7 females aged 35–77 years) of routine primary THA patients that were diagnosed with DDH to obtain 3D models of the hemipelvis, femurs, and the femoral inner cortical surface (ICS). The same DDH hips were automatically segmented using the Formus CNN which was not specifically trained on a DDH population. The differences between the automatically and manually segmented meshes were quantified by computing the surface-to-surface mean absolute distance (MAD), Dice score (an overlap index between 0 and 1), and Hausdorff distance (HD).

Results

The average Dice and MAD scores were greater than 0.9, and less than 1.5mm respectively (Figure 1/Table 1). ICS segmentations had the lowest mean HD and MAD. The highest mean HD was observed in the femur segmentations, despite highest mean Dice scores, indicating overall good fit with localised errors. Examining the spatial distribution of the absolute point-to-point distances in segmentations with the greatest HD indicated localisation of errors around the acetabular rim and femoral head (Figure 2).

Conclusion

These results demonstrate the high accuracy and robustness of the AI segmentation in automatically obtaining patient-specific morphologies, including those with developmental dysplasia of the hip. MAD and Dice scores of all bones, and the HD of the ICS were similar to segmentation errors in a generic dataset of a US population [1], indicating robustness for surgical templating applications.

References

1. Mason, J. B et al. (2024). AI segmentation in orthopedics: how accurate are the 3D models? AAOS 2024 Meeting.

Figures

Table 1. Average differences between automatically and manually segmented meshes

Bone	Dice	HD (mm)	MAD (mm)
Hemipelvis	0.95 ± 0.01	5.5 ± 2.7	1.3 ± 0.1
Femur	0.96 ± 0.01	6.0 ± 4.0	1.5 ± 0.2
ICS	0.93 ± 0.03	3.8 ± 2.2	1.2 ± 0.2

[Figure 1](#)

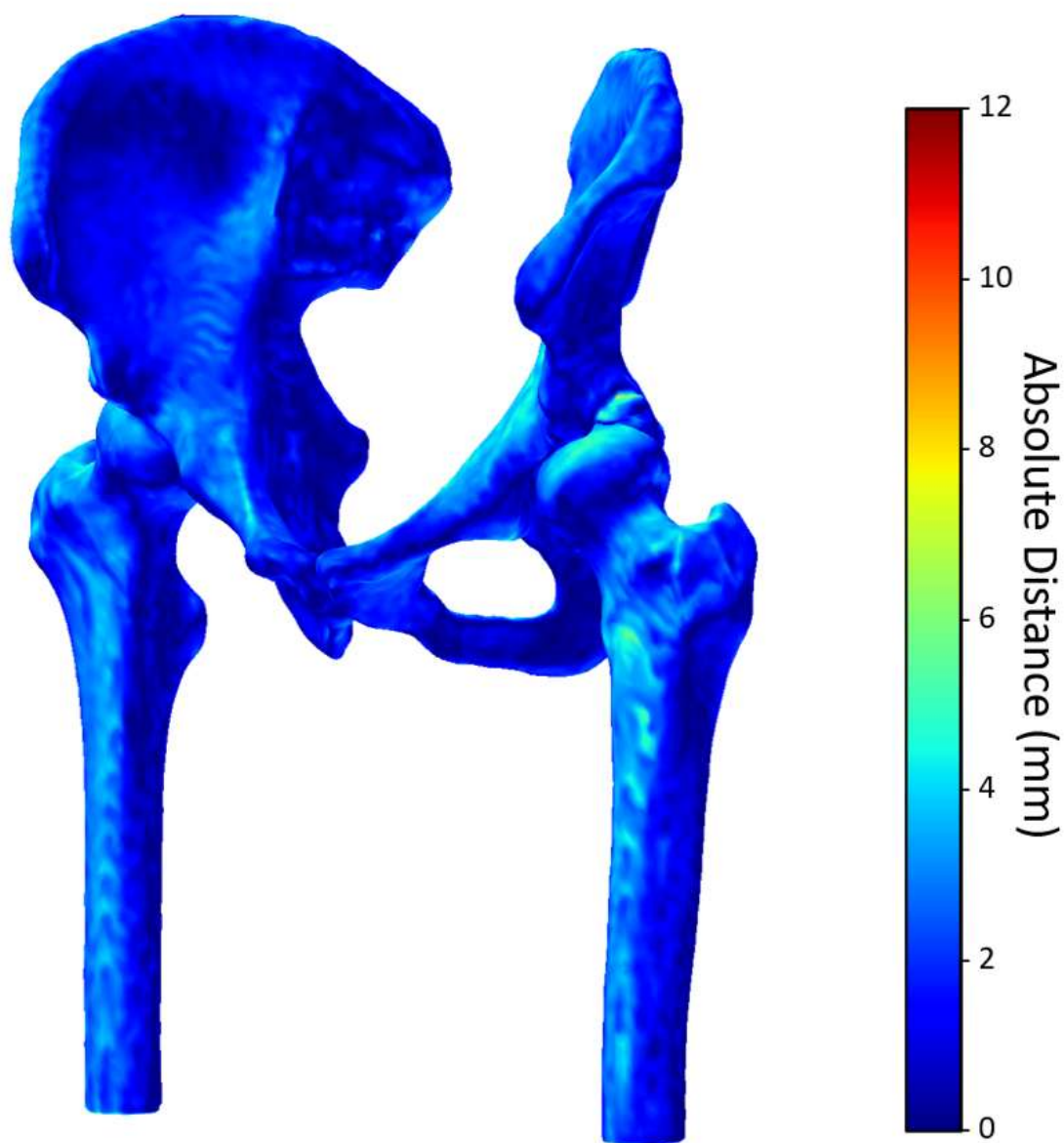


Figure 2. Exemplar segmentation and point-to-point distance of the hip with the highest HD.

[Figure 2](#)

Impact of 3D CT Reconstructed Deltoid Size, Shape, and Volume Measurements on Active Range of Motion Before and After Anatomic and Reverse Total Shoulder Arthroplasty

*Christopher Roche - Exactech - Gainesville, USA

Josie Elwell - Exactech, Inc - Gainesville, USA

Hamidreza Rajabzadeh-Oghaz - Exactech, Inc - Gainesville, USA

Bradley Schoch - Mayo - Jacksonville, USA

Bruno Gobbato - Est cio - Jaragu  do Sul, Brazil

William Aibinder - Michigan, United States of America

Anshuman Singh - University of California, San Diego - San Diego, USA

David Berry - University of California, San Diego - San Diego, USA

Vikas Kumar - Exactech, Inc - Gainesville, USA

Introduction

The deltoid is the primary elevator in the shoulder, and yet, few studies have quantified the 3-D size and shape of the muscle and no studies have correlated those measurements to active range of motion after anatomic (aTSA) and/or reverse (rTSA) total shoulder arthroplasty in any statistically/scientifically relevant manner. The goal of this study is to quantify the 3D CT reconstructed deltoid size and shape from 960 shoulder arthroplasty patients and determine the relationship of those image parameters to active range of motion measurements 2-years after aTSA and rTSA.

Methods

Preoperative CT images from 960 patients (584F/374M/2Unk), 700 rTSA (445F/253M/2Unk) and 260 aTSA (139F/121M) treated with a single platform shoulder arthroplasty prosthesis (Equinox; Exactech, Inc., Gainesville, FL) were analyzed in this study. A machine learning (ML) framework was used to segment the deltoid muscle and quantify 7 different muscle characteristics of size, shape, and volume. All patients had 2-year minimum follow-up, average = 37.8 ± 14.0 months; rTSA: 37.8, aTSA: 37.9). For all patients, active abduction and forward elevation were quantified pre-operatively and at latest follow-up. A multivariate analysis was conducted to compare deltoid image data associated with each aTSA and rTSA patient when classified by 3 different clinically relevant criteria: 1) bottom 25% or top 75% of preoperative abduction/forward elevation, 2) whether each patient achieved (or failed to achieve) patient acceptable symptomatic state (PASS) at latest follow-up for abduction/forward elevation, and 3) whether each patient achieved (or failed to achieve) minimally clinically important difference (MCID) improvement for abduction/forward elevation.

Results

The multivariate regression analysis identified several deltoid image measurements relevant to pre-operative (Table 1), post-operative (Table 2, PASS), and pre-to-post-operative measurements (Table 3, MCID) of abduction and forward elevation. Specifically, as described in Table 1, deltoid flatness ($p=0.042$) was identified for pre-operative forward elevation for aTSA patients and deltoid volume normalized by scapular bone volume ($p=0.042$) was identified for pre-operative abduction for rTSA patients. As described in Table 2, deltoid volume ($p=0.030$) was identified for achieving PASS for active abduction for aTSA patients. As described in Table 3, deltoid volume normalized by scapular bone volume was identified for achieving MCID for forward elevation ($p=0.032$) and abduction ($p=0.041$) for rTSA patients.

Conclusions

The results of this 960 patient shoulder arthroplasty study identified multiple 3D deltoid size, shape, and volume measurements that were statistically relevant to achieving clinically relevant active range of motion thresholds after aTSA and rTSA. Such data is useful to help better understand the relationship between deltoid morphology and functional performance after shoulder arthroplasty and the identification of specific clinically relevant deltoid measurements can be used to inform development of future clinical decision support tools which utilize CT image data to improve treatment decision making.

Figures

Table 1. Multivariate Analysis of Deltoid Image Size, Shape, and Volume Measurements Associated with aTSA and rTSA Patients who Failed to Achieve 25th Percentile of the Cohort's Pre-operative Forward Elevation (80°) and Abduction (60°) as Compared to Patients Exceeded this Pre-operative Active Range of Motion Threshold.

aTSA	Deltoid Image Measurement	Did not Achieve	Did Achieve	P-Value (univariate)	P-Value (multivariate)
Preop Forward Elevation (<80°)	Volume (cm ³)	320.19 ± 110.98	360.31 ± 121.05	0.053	
	Volume Normalized by Scapular Volume	3.75 ± 0.67	3.87 ± 0.64	0.352	
	Flatness	0.45 ± 0.03	0.46 ± 0.04	0.018	0.042
	Max Deltoid Width in Sagittal Plane (mm)	163.2 ± 16.51	164.16 ± 14.64	0.744	
	Max Deltoid Length in Sagittal Plane (mm)	127.63 ± 21.87	133.85 ± 19.95	0.117	
	Sphericity	0.45 ± 0.03	0.46 ± 0.03	0.647	
	Volume Normalized by Age and Gender	1.02 ± 0.16	1.03 ± 0.15	0.686	
Preop Abduction (<60°)	Volume (cm ³)	296.45 ± 99.91	362.13 ± 121.16	0.002	0.094
	Volume Normalized by Scapular Volume	3.57 ± 0.68	3.89 ± 0.63	0.020	0.418
	Flatness	0.45 ± 0.04	0.46 ± 0.04	0.082	
	Max Deltoid Width in Sagittal Plane (mm)	162.45 ± 14.44	164.17 ± 15	0.542	
	Max Deltoid Length in Sagittal Plane (mm)	127.02 ± 21.94	133.7 ± 20.05	0.117	
	Sphericity	0.45 ± 0.03	0.46 ± 0.03	0.036	0.686
	Volume Normalized by Age and Gender	0.98 ± 0.16	1.04 ± 0.15	0.050	*-
rTSA	Deltoid Image Measurement	Did not Achieve	Did Achieve	P-Value (univariate)	P-Value (multivariate)
Preop Forward Elevation (<80°)	Volume (cm ³)	303.13 ± 94.86	328.86 ± 109.42	0.001	0.497
	Volume Normalized by Scapular Volume	3.62 ± 0.66	3.77 ± 0.65	0.003	0.078
	Flatness	0.47 ± 0.04	0.47 ± 0.04	0.110	
	Max Deltoid Width in Sagittal Plane (mm)	157.65 ± 15.4	159.6 ± 15.69	0.109	
	Max Deltoid Length in Sagittal Plane (mm)	131.23 ± 19.73	135.37 ± 20.16	0.008	0.191
	Sphericity	0.45 ± 0.03	0.46 ± 0.03	0.032	
	Volume Normalized by Age and Gender	1 ± 0.18	1.04 ± 0.17	0.010	*-
Preop Abduction (<60°)	Volume (cm ³)	303.73 ± 91.87	328.51 ± 110.32	0.002	0.395
	Volume Normalized by Scapular Volume	3.58 ± 0.64	3.79 ± 0.65	0.000	0.042
	Flatness	0.47 ± 0.04	0.47 ± 0.04	0.422	
	Max Deltoid Width in Sagittal Plane (mm)	157.99 ± 15.38	159.47 ± 15.77	0.234	
	Max Deltoid Length in Sagittal Plane (mm)	133.61 ± 19.99	134.02 ± 20.29	0.798	
	Sphericity	0.45 ± 0.03	0.46 ± 0.03	0.002	0.412
	Volume Normalized by Age and Gender	0.99 ± 0.18	1.05 ± 0.17	<0.001	*-

*Note that a collinearity check removed volume normalized by Age and Gender from the multivariate analysis.

Figure 1

Table 2. Multivariate Analysis of Deltoid Image Size, Shape, and Volume Measurements Associated with aTSA and rTSA Patients who Failed to Achieve 2-year Minimum PASS for Forward Elevation (130°) and Abduction (104°) as Compared to Patients Exceeded PASS.

aTSA	Deltoid Image Measurement	Did not Achieve	Did Achieve	P-Value (univariate)	P-Value (multivariate)
2yr Min Forward Elevation PASS (130°)	Volume (cm ³)	323.39 ± 98.32	351.17 ± 121.26	0.211	
	Volume Normalized by Scapular Volume	3.8 ± 0.65	3.84 ± 0.65	0.781	
	Flatness	0.46 ± 0.03	0.46 ± 0.04	0.513	
	Max Deltoid Width in Sagittal Plane (mm)	161.05 ± 13.52	163.82 ± 15.04	0.354	
	Max Deltoid Length in Sagittal Plane (mm)	128.09 ± 22.01	132.89 ± 20.37	0.316	
	Sphericity	0.45 ± 0.03	0.46 ± 0.03	0.302	
	Volume Normalized by Age and Gender	1.02 ± 0.16	1.03 ± 0.15	0.664	
2yr Min Abduction PASS (104°)	Volume (cm ³)	302.17 ± 80.85	355.24 ± 122.27	0.004	0.030
	Volume Normalized by Scapular Volume	3.66 ± 0.72	3.86 ± 0.64	0.158	
	Flatness	0.46 ± 0.04	0.46 ± 0.04	0.422	
	Max Deltoid Width in Sagittal Plane (mm)	160.23 ± 12.99	164.05 ± 15.11	0.160	
	Max Deltoid Length in Sagittal Plane (mm)	130.87 ± 18.27	132.54 ± 20.9	0.660	
	Sphericity	0.45 ± 0.03	0.46 ± 0.03	0.209	
	Volume Normalized by Age and Gender	0.99 ± 0.19	1.03 ± 0.15	0.338	
rTSA	Deltoid Image Measurement	Did not Achieve	Did Achieve	P-Value (univariate)	P-Value (multivariate)
2yr Min Forward Elevation PASS (130°)	Volume (cm ³)	318.19 ± 96.05	318.1 ± 106.2	0.992	
	Volume Normalized by Scapular Volume	3.7 ± 0.65	3.73 ± 0.66	0.546	
	Flatness	0.47 ± 0.05	0.47 ± 0.04	0.854	
	Max Deltoid Width in Sagittal Plane (mm)	159.26 ± 14.6	158.77 ± 15.87	0.726	
	Max Deltoid Length in Sagittal Plane (mm)	131.61 ± 18.55	134.95 ± 20.5	0.062	
	Sphericity	0.45 ± 0.03	0.46 ± 0.03	0.633	
	Volume Normalized by Age and Gender	1.02 ± 0.18	1.03 ± 0.17	0.695	
2yr Min Abduction PASS (104°)	Volume (cm ³)	290.63 ± 94.85	328.01 ± 105.2	<0.001	0.304
	Volume Normalized by Scapular Volume	3.59 ± 0.65	3.77 ± 0.66	0.003	0.166
	Flatness	0.47 ± 0.04	0.47 ± 0.04	0.559	
	Max Deltoid Width in Sagittal Plane (mm)	154.97 ± 14.16	160.32 ± 15.83	<0.001	0.067
	Max Deltoid Length in Sagittal Plane (mm)	131.49 ± 19.8	135.09 ± 20.14	0.047	0.566
	Sphericity	0.45 ± 0.03	0.46 ± 0.03	0.070	
	Volume Normalized by Age and Gender	1 ± 0.17	1.04 ± 0.18	0.031	*-

*Note that a collinearity check removed volume normalized by Age and Gender from the multivariate analysis.

Figure 2

Table 3. Multivariate Analysis of Deltoid Image Size, Shape, and Volume Measurements Associated with aTSA and rTSA Patients who Failed to Achieve 2-year Minimum Pre-to-Post-operative MCID Improvement for Forward Elevation (16°) and Abduction (13°) as Compared to Patients Exceeded MCID.

aTSA	Deltoid Image Measurement	Did not Achieve	Did Achieve	P-Value (univariate)	P-Value (multivariate)
2yr Min Forward Elevation MCID (16°)	Volume (cm ³)	366.81 ± 125.99	341.65 ± 116.14	0.169	
	Volume Normalized by Scapular Volume	3.96 ± 0.68	3.8 ± 0.63	0.115	
	Flatness	0.46 ± 0.04	0.46 ± 0.04	0.767	
	Max Deltoid Width in Sagittal Plane (mm)	163.74 ± 13.65	163.67 ± 15.37	0.974	
	Max Deltoid Length in Sagittal Plane (mm)	130.56 ± 17.32	132.81 ± 21.53	0.413	
	Sphericity	0.46 ± 0.03	0.45 ± 0.03	0.106	
	Volume Normalized by Age and Gender	1.06 ± 0.16	1.02 ± 0.15	0.128	
2yr Min Abduction MCID (13°)	Volume (cm ³)	373.25 ± 133.08	341.15 ± 114.4	0.120	
	Volume Normalized by Scapular Volume	3.99 ± 0.7	3.8 ± 0.63	0.074	
	Flatness	0.46 ± 0.03	0.46 ± 0.04	0.700	
	Max Deltoid Width in Sagittal Plane (mm)	163.2 ± 14.12	163.81 ± 15.18	0.787	
	Max Deltoid Length in Sagittal Plane (mm)	130.66 ± 16.91	132.42 ± 21.5	0.538	
	Sphericity	0.46 ± 0.03	0.45 ± 0.03	0.139	
	Volume Normalized by Age and Gender	1.06 ± 0.16	1.02 ± 0.15	0.105	
rTSA	Deltoid Image Measurement	Did not Achieve	Did Achieve	P-Value (univariate)	P-Value (multivariate)
2yr Min Forward Elevation MCID (16°)	Volume (cm ³)	337.51 ± 106.23	313.01 ± 102.77	0.016	0.940
	Volume Normalized by Scapular Volume	3.86 ± 0.61	3.68 ± 0.66	0.002	0.032
	Flatness	0.47 ± 0.04	0.47 ± 0.04	0.429	
	Max Deltoid Width in Sagittal Plane (mm)	158.58 ± 15.02	159.09 ± 15.73	0.724	
	Max Deltoid Length in Sagittal Plane (mm)	137.17 ± 19.56	133.22 ± 20.09	0.037	0.244
	Sphericity	0.46 ± 0.02	0.45 ± 0.03	0.150	
	Volume Normalized by Age and Gender	1.06 ± 0.16	1.02 ± 0.18	0.003	*-
2yr Min Abduction MCID (13°)	Volume (cm ³)	335.91 ± 109.61	315.36 ± 102.25	0.056	
	Volume Normalized by Scapular Volume	3.89 ± 0.64	3.68 ± 0.65	0.001	0.041
	Flatness	0.47 ± 0.04	0.47 ± 0.04	0.784	
	Max Deltoid Width in Sagittal Plane (mm)	158.74 ± 15.4	159.22 ± 15.69	0.758	
	Max Deltoid Length in Sagittal Plane (mm)	136.01 ± 20.59	133.91 ± 19.99	0.301	
	Sphericity	0.46 ± 0.02	0.45 ± 0.03	0.004	0.352
	Volume Normalized by Age and Gender	1.07 ± 0.16	1.02 ± 0.17	0.001	*-

*Note that a collinearity check removed volume normalized by Age and Gender from the multivariate analysis.

Figure 3

Impact of CT Image Hounsfield Unit Based Measures of Deltoid Muscle Quality on a Patient's Ability to Elevate Their Arm Before and After Anatomic and Reverse Total Shoulder Arthroplasty

Josie Elwell - Exactech, Inc - Gainesville, USA

Hamidreza Rajabzadeh-Oghaz - Exactech, Inc - Gainesville, USA

Bradley Schoch - Mayo - Jacksonville, USA

Bruno Gobbato - Estıcio - Jaraguı do Sul, Brazil

William Aibinder - Michigan, United States of America

Anshuman Singh - University of California, San Diego - San Diego, USA

David Berry - University of California, San Diego - San Diego, USA

Vikas Kumar - Exactech, Inc - Gainesville, USA

*Christopher Roche - Exactech - Gainesville, USA

Introduction

The widespread clinical use of CT-based preoperative planning software for aTSA and rTSA has produced ample CT data that is readily available in existing clinical workflows to support clinical decision-making. However, it is currently unknown which CT data is useful for treatment decision making and relevant to clinical outcomes. The aim of this study is to quantify several Hounsfield Unit (HU) intensity-based measurements derived from 3D reconstructed CT images from 605 shoulder arthroplasty patients consisting of two convolution kernels (BONE and FC30) and determine their relationship to active range of motion 2-years after aTSA/rTSA.

Methods

Preoperative CT images from 605 patients (371F/234M) were treated with a single platform shoulder arthroplasty prosthesis (Equinox; Exactech, Inc., Gainesville, FL) were analyzed in this study. CT data was analyzed separately for 2 different convolution kernels: 226 FC30 kernels (131F/95M) and 379 BONE kernels (240F/139M); with prostheses distributions: FC30: 182rTSA/44aTSA and BONE: 261rTSA/118aTSA. A machine learning framework segmented the deltoid muscle and quantified 8 HU-based measurements of muscle quality by analyzing the distribution of gray-scale voxel intensities that compose the 3D deltoid muscle volume: All patients had 2-year minimum follow-up (average=37.4±13.3 months; BONE: 38.1, FC30: 36.3). A multivariate analysis compared deltoid HU-based image measurements for aTSA/rTSA patients for each convolution kernel when classified by: 1) bottom 25% or top 75% of preoperative abduction/forward elevation, 2) whether each patient achieved (or failed to achieve) patient acceptable symptomatic state (PASS) at latest follow-up for abduction/forward elevation, and 3) whether each patient achieved (or failed to achieve) minimally clinically important difference (MCID) improvement for abduction/forward elevation.

Results

The multivariate regression analysis identified several deltoid HU based image measurements relevant to pre-operative (Table 1), post-operative (Table 2, PASS), and pre-to-post-operative measurements (Table 3, MCID) of abduction and forward elevation for both CT convolution kernels. As described in Table 1, mean HU was identified for pre-operative forward elevation and abduction for both FC30 (p=0.025 FE & p=0.002 Abd) and BONE (both p<0.001) kernel patients and 90th percentile HU (p=0.001) was identified for pre-operative abduction for BONE patients. As described

in Table 2, deltoid fat percentage ($p=0.023$) was identified for achieving PASS for active abduction for FC30 patients and mean HU ($p=0.001$) and HU uniformity ($p=0.019$) were identified for achieving PASS for active abduction for BONE patients. As described in Table 3, mean HU ($p<0.001$) and 90th percentile HU ($p=0.039$) were identified for achieving MCID for forward elevation for BONE patients. HU skewness ($p=0.011$) was identified for achieving MCID for abduction for FC30 patients and mean HU ($p=0.024$) was identified for achieving MCID for abduction for BONE patients.

Conclusions

This 605-patient study quantified numerous HU-based deltoid image measurements for both kernels that were statistically relevant to achieving active range of motion after aTSA/rTSA. Kernels with greater noise, like the FC30 images, may interfere with HU threshold calculations of fat/muscle, potentially overstating the amount of fatty infiltration. Future HU-based analyses should separately assess convolution kernels and consider different HU intervals to characterize fat and muscle for each CT kernel.

Figures

Table 1. Multivariate Analysis of Deltoid HU-Based Measurements for FC30 and BONE Convolution Kernels Associated with aTSA/rTSA Patients who Failed to Achieve 25th Percentile of the Cohort's Pre-operative Forward Elevation (80°) and Abduction (60°) as Compared to Patients Exceeded this Pre-operative Active Range of Motion Threshold.

aTSA/rTSA, Kernel	FC30	Deltoid Image Measurement	Did not Achieve	Did Achieve	P-Value (univariate)	P-Value (multivariate)							
Preop Forward Elevation (<80°)		Fat Percentage	29.98 ± 3.73	27.87 ± 5.22	0.001	0.458							
		90 th Percentile HU	151.86 ± 13.41	155.03 ± 12.59	0.075								
		Entropy	3.97 ± 0.12	3.95 ± 0.17	0.233								
		Kurtosis	49.88 ± 409.18	32.93 ± 251.86	0.719								
		Mean HU	30.81 ± 8.94	35.61 ± 8.5	<0.001	0.025							
		Root Mean Squared HU	1035.53 ± 9.03	1040.85 ± 9.95	<0.001	*							
		Skewness	0.78 ± 3.87	0.41 ± 0.65	0.349								
		Uniformity	0.07 ± 0.01	0.07 ± 0.01	0.162								
Preop Abduction (<60°)		Fat Percentage	29.91 ± 4.47	28.17 ± 4.77	0.008	0.659							
		90 th Percentile HU	150.34 ± 13.9	155.33 ± 12.23	0.009	*							
		Entropy	3.96 ± 0.14	3.96 ± 0.15	0.957								
		Kurtosis	61.24 ± 467.11	29.78 ± 231.66	0.582								
		Mean HU	30.14 ± 9.25	35.32 ± 8.37	<0.001	0.002							
		Root Mean Squared HU	1034.76 ± 9.31	1040.52 ± 9.64	<0.001	*							
		Skewness	0.81 ± 4.41	0.45 ± 0.67	0.491								
		Uniformity	0.07 ± 0.01	0.07 ± 0.01	0.912								
aTSA/rTSA, Kernel	BONE	Deltoid Image Measurement	Did not Achieve	Did Achieve	P-Value (univariate)	P-Value (multivariate)							
							Preop Forward Elevation (<80°)		Fat Percentage	14.19 ± 5.4	12.11 ± 5.72	.002	0.485
									90 th Percentile HU	100.87 ± 18.98	104.9 ± 18.27	.071	
									Entropy	3.2 ± 0.34	3.16 ± 0.37	.308	
									Kurtosis	31.66 ± 109.21	23.06 ± 59.16	.462	
									Mean HU	32.85 ± 8.55	38.29 ± 8.06	<0.001	<0.001
									Root Mean Squared HU	1034.67 ± 8.5	1040.07 ± 7.83	<0.001	*
									Skewness	-0.07 ± 2.64	0.08 ± 2.12	.607	
	Uniformity	0.14 ± 0.03	0.14 ± 0.04	.175									
	Preop Abduction (<60°)		Fat Percentage	13.04 ± 5.32	12.49 ± 5.85	.383							
			90 th Percentile HU	97.78 ± 18.69	106.31 ± 17.91	<0.001	0.001						
			Entropy	3.12 ± 0.34	3.19 ± 0.37	.079							
			Kurtosis	18.33 ± 35.22	28.08 ± 86.18	.120							
			Mean HU	33.8 ± 8.9	38.13 ± 8.05	<0.001	<0.001						
			Root Mean Squared HU	1035.43 ± 8.85	1039.98 ± 7.76	<0.001	*						
			Skewness	0.26 ± 1.12	-0.04 ± 2.59	.119							
Uniformity			0.15 ± 0.03	0.14 ± 0.04	.154								

*Note that a collinearity check removed these variables from the multivariate analysis.

Figure 1

Table 2. Multivariate Analysis of Deltoid HU-Based Measurements for FC30 and BONE Convolution Kernels Associated with aTSA/rTSA Patients who Failed to Achieve 2-year Minimum PASS for Forward Elevation (130°) and Abduction (104°) as Compared to Patients Exceeded PASS.

aTSA/rTSA, FC30 Kernel	Deltoid Image Measurement	Did not Achieve	Did Achieve	P-Value (univariate)	P-Value (multivariate)
2yr Min Forward Elevation PASS (130°)	Fat Percentage	29.63 ± 4.76	28.4 ± 4.71	0.093	
	90 th Percentile HU	154.77 ± 9.5	154.14 ± 14.16	0.718	
	Entropy	3.99 ± 0.11	3.95 ± 0.16	0.076	
	Kurtosis	53.19 ± 346.17	9.58 ± 9.01	0.318	
	Mean HU	32.64 ± 10.13	34.38 ± 8.61	0.241	
	Root Mean Squared HU	1038.67 ± 12.79	1038.97 ± 8.57	0.867	
	Skewness	0.5 ± 0.7	0.36 ± 0.55	0.149	
	Uniformity	0.07 ± 0.01	0.07 ± 0.01	0.083	
2yr Min Abduction PASS (104°)	Fat Percentage	30.65 ± 3.55	28.32 ± 4.91	0.001	0.023
	90 th Percentile HU	154.26 ± 10.63	154.37 ± 13.4	0.952	
	Entropy	4.00 ± 0.08	3.95 ± 0.16	0.008	0.816
	Kurtosis	73.08 ± 422.47	9.9 ± 9.02	0.332	
	Mean HU	30.8 ± 9.63	34.59 ± 8.84	0.024	*-
	Root Mean Squared HU	1037.51 ± 14.03	1039.19 ± 8.71	0.459	
	Skewness	0.50 ± 0.74	0.37 ± 0.56	0.284	
	Uniformity	0.072 ± <0.001	0.075 ± 0.009	0.003	*-
aTSA/rTSA, BONE Kernel	Deltoid Image Measurement	Did not Achieve	Did Achieve	P-Value (univariate)	P-Value (multivariate)
2yr Min Forward Elevation PASS (130°)	Fat Percentage	15.42 ± 6.8	12.36 ± 5.37	0.007	0.160
	90 th Percentile HU	111.23 ± 20.71	103.46 ± 18.18	0.023	*-
	Entropy	3.33 ± 0.39	3.16 ± 0.35	0.009	0.866
	Kurtosis	13.26 ± 15.82	26.34 ± 78.7	0.010	*-
	Mean HU	35.32 ± 9.27	37.15 ± 8.08	0.224	
	Root Mean Squared HU	1037.49 ± 8.94	1038.91 ± 7.96	0.325	
	Skewness	0.36 ± 0.82	0.04 ± 2.34	0.084	
	Uniformity	0.13 ± 0.04	0.14 ± 0.04	0.013	*-
2yr Min Abduction PASS (104°)	Fat Percentage	12.99 ± 6.19	12.65 ± 5.46	0.651	
	90 th Percentile HU	98.53 ± 18.52	106.23 ± 18.34	0.001	0.213
	Entropy	3.12 ± 0.38	3.2 ± 0.35	0.068	
	Kurtosis	34.75 ± 89.98	21.64 ± 68.3	0.219	
	Mean HU	34.34 ± 9.23	37.74 ± 7.75	0.003	0.001
	Root Mean Squared HU	1036.07 ± 8.96	1039.57 ± 7.62	0.002	*-
	Skewness	0.12 ± 2.92	0.07 ± 1.94	0.870	
	Uniformity	0.15 ± 0.04	0.14 ± 0.04	0.045	0.019

*Note that a collinearity check removed these variables from the multivariate analysis.

Figure 2

Table 3. Multivariate Analysis of Deltoid HU-Based Measurements for FC30 and BONE Convolution Kernels Associated with aTSA/rTSA Patients who Failed to Achieve 2-year Minimum Pre-to-Post-operative MCID Improvement for Forward Elevation (16°) and Abduction (13°) as Compared to Patients Exceeded MCID.

aTSA/rTSA, FC30 Kernel	Deltoid Image Measurement	Did not Achieve	Did Achieve	P-Value (univariate)	P-Value (multivariate)
2yr Min Forward Elevation MCID (16°)	Fat Percentage	28.06 ± 4.72	29.04 ± 4.81	0.255	
	90 th Percentile HU	157.28 ± 9.45	153.53 ± 13.55	0.050	0.488
	Entropy	3.96 ± 0.13	3.96 ± 0.15	0.946	
	Kurtosis	81.59 ± 443.3	9.48 ± 8.9	0.316	
	Mean HU	36.74 ± 7.72	32.96 ± 9.44	0.012	
	Root Mean Squared HU	1043.46 ± 12.06	1037.61 ± 9.36	0.007	0.070
	Skewness	0.6 ± 0.77	0.36 ± 0.55	0.071	
	Uniformity	0.07 ± 0.01	0.07 ± 0.01	0.893	
2yr Min Abduction MCID (13°)	Fat Percentage	28.5 ± 4.1	28.91 ± 4.98	0.590	
	90 th Percentile HU	157.76 ± 8.99	153.3 ± 13.68	0.015	0.293
	Entropy	3.98 ± 0.11	3.96 ± 0.15	0.431	
	Kurtosis	76.75 ± 427.15	9.28 ± 8.84	0.312	
	Mean HU	36.36 ± 7.28	33 ± 9.58	0.017	0.188
	Root Mean Squared HU	1043.01 ± 11.63	1037.62 ± 9.47	0.008	*
	Skewness	0.63 ± 0.8	0.33 ± 0.53	0.026	0.011
	Uniformity	0.07 ± 0.01	0.07 ± 0.01	0.322	
aTSA/rTSA, BONE Kernel	Deltoid Image Measurement	Did not Achieve	Did Achieve	P-Value (univariate)	P-Value (multivariate)
2yr Min Forward Elevation MCID (16°)	Fat Percentage	11.82 ± 5.97	12.95 ± 5.41	0.114	
	90 th Percentile HU	109 ± 20.22	102.59 ± 17.7	0.008	0.039
	Entropy	3.18 ± 0.41	3.17 ± 0.34	0.844	
	Kurtosis	26.6 ± 83.14	24.29 ± 71.17	0.813	
	Mean HU	40.52 ± 6.78	35.76 ± 8.35	<0.001	<0.001
	Root Mean Squared HU	1042.39 ± 6.44	1037.54 ± 8.23	<0.001	*
	Skewness	0.07 ± 2.68	0.08 ± 2.04	0.958	
	Uniformity	0.14 ± 0.04	0.14 ± 0.04	0.882	
2yr Min Abduction MCID (13°)	Fat Percentage	12.22 ± 5.87	12.78 ± 5.5	0.455	
	90 th Percentile HU	107.5 ± 17.59	103.34 ± 18.75	0.074	
	Entropy	3.2 ± 0.37	3.17 ± 0.36	0.634	
	Kurtosis	26.46 ± 90.33	24.45 ± 69.49	0.858	
	Mean HU	38.87 ± 7.68	36.46 ± 8.32	0.019	0.024
	Root Mean Squared HU	1040.71 ± 7.31	1038.25 ± 8.22	0.013	*
	Skewness	-0.15 ± 2.84	0.14 ± 2.02	0.410	
	Uniformity	0.14 ± 0.04	0.14 ± 0.04	0.678	

*Note that a collinearity check removed these variables from the multivariate analysis.

Figure 3

Deep Learning-Based Predictions of Polyethylene Insert Wear in Total Knee Replacements

Mattia Perrone - Rush University Medical Center - Chicago, United States of America

*Steven Mell - Rush University Medical Center - Chicago, USA

Scott Simmons - Drury University - Springfield, USA

INTRODUCTION: Polyethylene wear remains a leading cause of long-term failure in total knee replacements (TKRs)¹. Studies leveraging finite element analysis (FEA) models have shown that variability of gait patterns can lead to significant variability in wear rates². However, FEA models can be resource-intensive and time-consuming to execute, hindering further research in this area. The aim of this study was therefore to develop a deep learning framework capable of predicting polyethylene wear starting from kinematic and kinetic gait patterns, significantly lowering both computational costs and processing time compared to traditional FEA models.

METHODS: A published method was used to generate 314 variations of ISO14243-3(2014) anterior/posterior translation, internal/external rotation, flexion/extension, and axial loading time series, and a validated FEA model was used to calculate linear wear distribution on the polyethylene liner². A deep learning model was then developed to predict linear wear, as an image, using gait patterns as input (**Figure 1**). Since predicting images from time series is a challenging task, we quantized each pixel value to fixed increments, transforming the problem from a regression into a pixel-wise classification task (**Figure 2A**). The dataset was then split into a training/validation/test set (60% - 20% -20%), and the model trained using categorical cross entropy as loss function.

Model performance on the test set was evaluated using mean absolute percentage error (MAPE) between the deep learning model and the FEA model predictions. For both the medial and lateral wear areas, we evaluated the length, width, area, and the location of the centroids of the wear scar areas (**Figure 2B**).

RESULTS: For the medial and lateral wear areas: MAPE values remained under 3% and 6% respectively for the wear scar's width and length measurements, below 6% for the area of the wear scar, and below 1% for the mean distance between wear scar centroids (**Table 1**).

CONCLUSION: This study presents a novel approach to rapidly predict polyethylene wear in TKR, using deep learning to generate a surrogate model from FEA simulations. Next steps include exploring methodologies that do not rely on a pixel-wise discretization approach, as well as the incorporation of patient data. This method could enable the early detection of gait patterns that would put a patient at high risk for implant failure, giving clinicians a chance for early intervention.

References:

1 AJRR. (AAOS), (2020)

2 Mell, S. P. et al. Journal of Orthopaedic Research 38, 1538–1549 (2020)

Figures

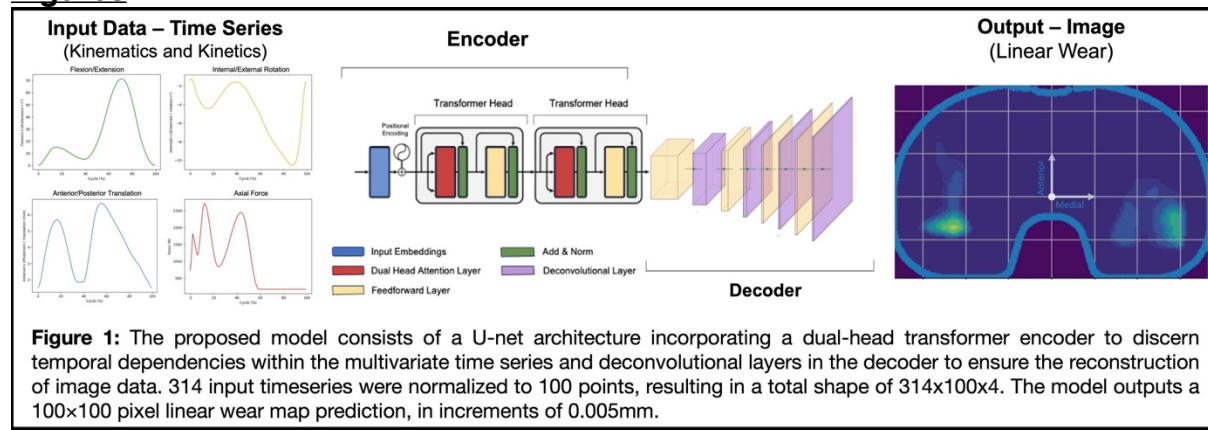


[Figure 1](#)

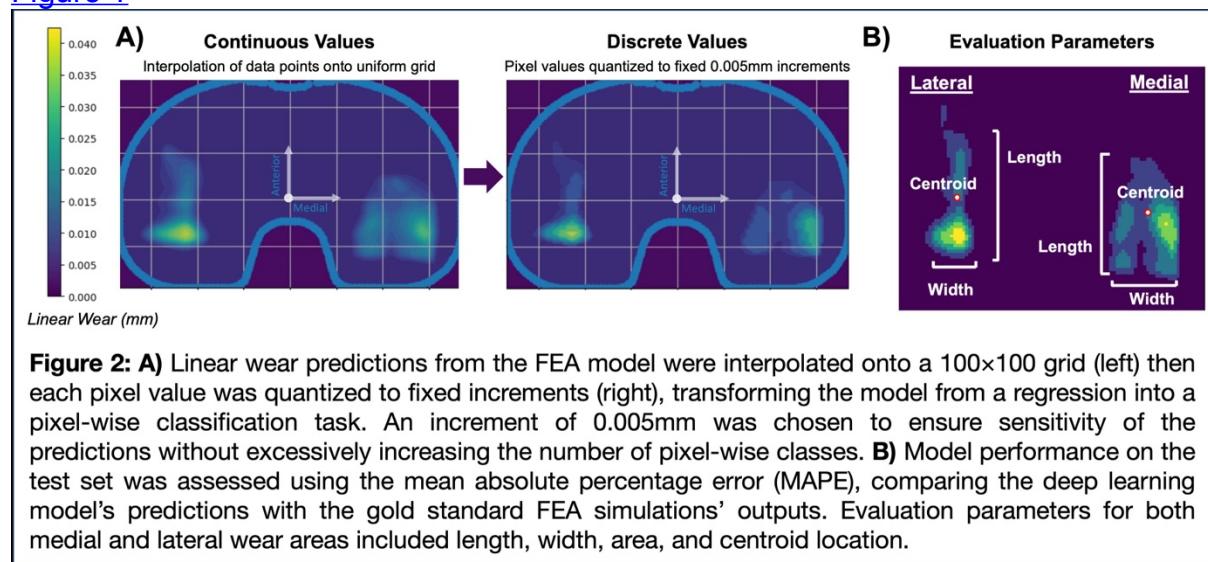


[Figure 2](#)

Table 1: Summary of mean average percentage error (MAPE) values for wear scar width, length, area, and centroid locations in medial and lateral wear scars.

Parameter	Mean Average Percentage Error (MAPE)
Width (Lateral)	2.92%
Length (Lateral)	5.26%
Area (Lateral)	5.35%
Centroid Location (Lateral)	0.39%
Width (Medial)	1.22%
Length (Medial)	2.28%
Area (Medial)	5.64%
Centroid Location (Medial)	0.57%

[Figure 3](#)

An Ultrasound-Based Method to Measure Knee Kinematics Enabled by Deep Learning

*Joshua Roth - University of Wisconsin-Madison - Madison, USA

Matthew Blomquist - University of Wisconsin-Madison - Madison, USA

Christopher Endemann - University of Wisconsin-Madison - Madison, USA

Introduction:

Medical imaging can reduce errors in knee kinematics measured in small-excision degrees of freedom (e.g., anterior-posterior (A-P) translation and varus-valgus (V-V) rotation) by enabling direct visualization of the bones. Direct visualization overcomes errors introduced by soft tissue motion relative to the bones. However, common imaging-based methods such as fluoroscopy and stress radiography are limited in their broad applicability because they require expensive equipment and data processing expertise, expose the participant to ionizing radiation, and/or are quasi-static. Accordingly, *our objective* was to develop and validate an ultrasound-based method to measure knee kinematics enabled by deep learning.

Methods:

In five fresh-frozen human cadaveric knees (1F/4M, 66.2 ± 3.4 years), we performed anterior, posterior, varus, and valgus laxity assessments at 0° , 20° , and 45° flexion using a six degree-of-freedom robotic testing system (**Figure 1**). The robot loaded each knee to ± 89 N at 4.5 N/s during A-P assessments and ± 15 Nm at 0.75 Nm/s during V-V assessments and measured the resulting kinematics. During each assessment, we placed an ultrasound transducer over the medial, lateral, or anterolateral aspects of the knee that recorded 40 B-mode frames per second. We trained custom, long short-term memory, convolutional neural networks (LSTM-CNN) (**Figure 2a**) to predict A-P and V-V kinematics. Our LSTM-CNNs took in an ultrasound cine loop and output the relative A-P or V-V motion between subsequent B-mode frames. Additionally, we augmented our dataset by adding random rotation, blur, and noise to the B-mode frames.

We implemented a five-fold, cross-validation to test our LSTM-CNNs using one specimen per fold as test data (**Figure 2b**). For each assessment, we computed the errors between the ultrasound-measured kinematics and the time-synched, robot-measured kinematics. We pooled errors across specimens and flexion angles, and computed the bias, precision, and root-mean-square errors (RMSEs) for each clinical assessment.

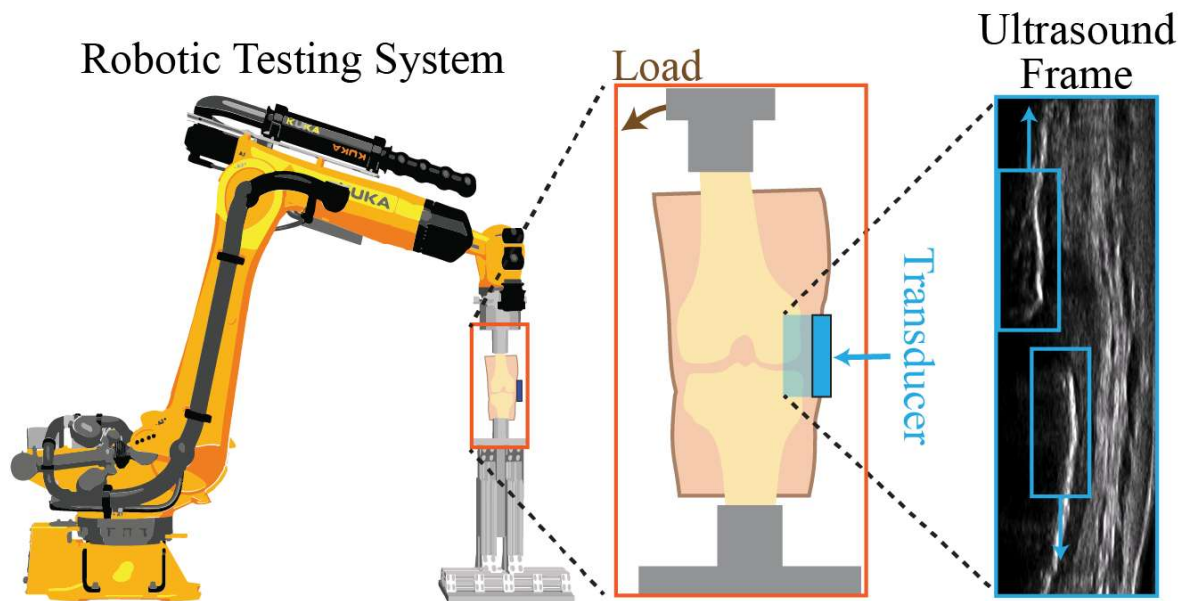
Results:

The RMSEs in measuring kinematics were 1.85 mm, 1.51 mm, 1.14° and 0.86° , for anterior, posterior, varus, and valgus, respectively (**Figure 3**). Our models tended to under-predict kinematic excursions in all degrees of freedom.

Conclusion:

This study showed that our ultrasound-based method is a promising approach to enhance measurements of knee kinematics because ultrasound is a safe, non-radiating imaging modality that is familiar to both clinicians and researchers. Because deep learning models are most accurate and robust when trained on a large, diverse dataset, our ongoing work is to expand our dataset to include more specimens from a more diverse population.

Figures



Ultrasound Transducer Placement Anterior

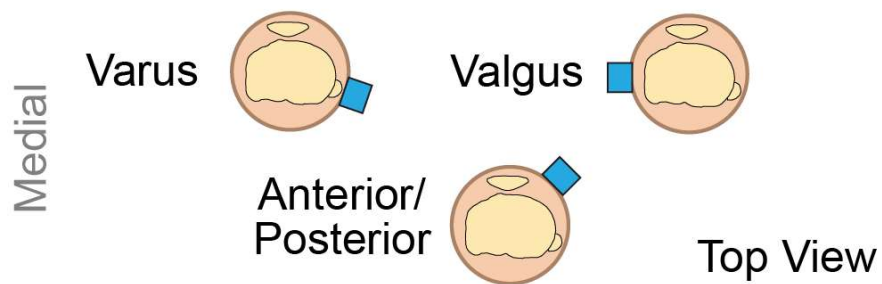


Figure 1: (*Top*) We performed clinical laxity exams and measured knee kinematics with a robotic testing system (KR300 2700-2, KUKA). During each assessment, we used an ultrasound transducer (F11-5H60-A3, ArtUS, TELEMED) to image bone motion. (*Bottom*) We placed the ultrasound transducer over the lateral, medial, or anterolateral aspects of the knee during varus, valgus, and anterior-posterior loading, respectively.

[Figure 1](#)

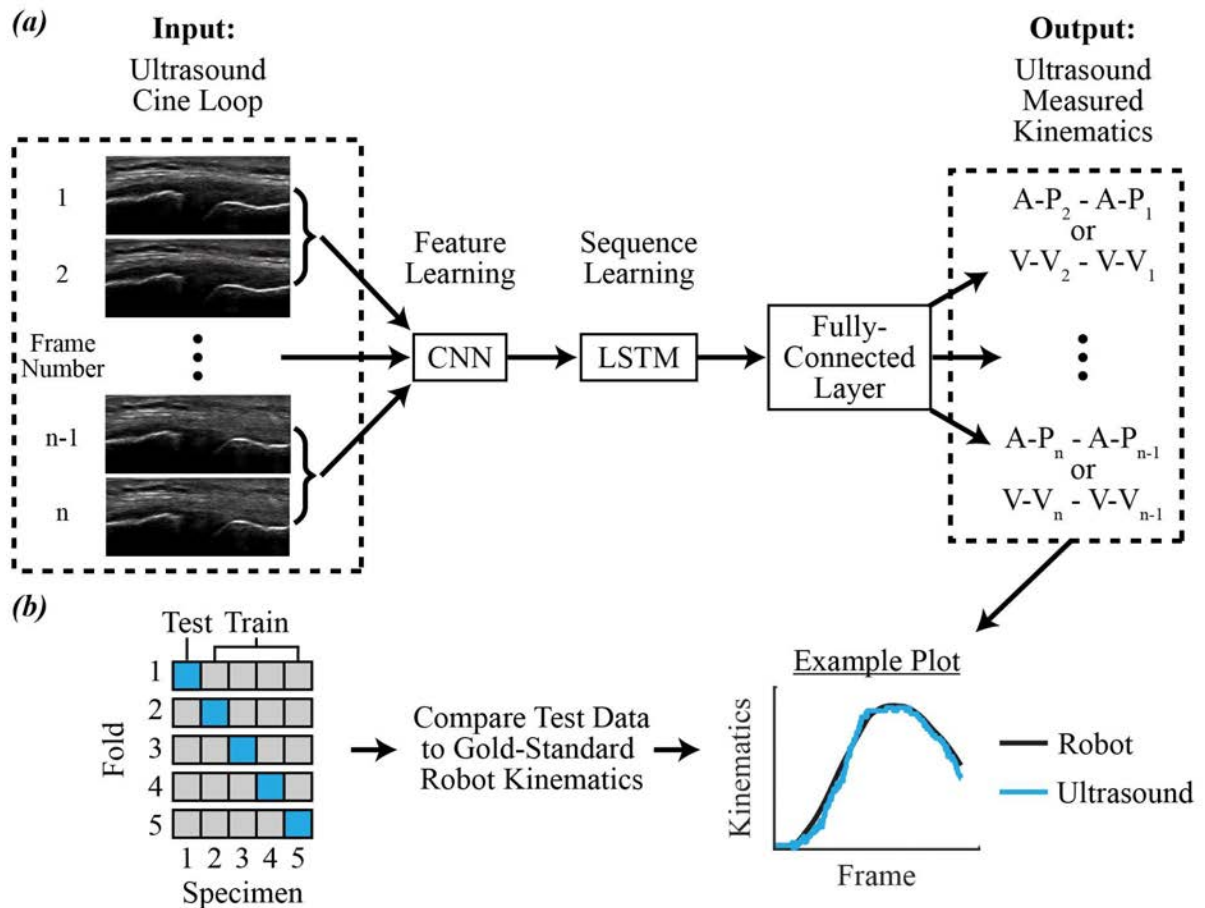


Figure 2: (a) We measured the change in anterior-posterior (A-P) or varus-valgus (V-V) kinematics throughout a B-mode ultrasound cine loop using a long short-term memory, convolutional neural network (LSTM-CNN). Our LSTM-CNN architecture consisted of convolutional layers, rectified linear units (ReLU), pooling layers, an LSTM layer, and a fully connected layer. Our LSTM-CNN took in a B-mode ultrasound cine loop, then fed consecutive frame pairs into the CNN and LSTM layers for feature and sequence learning, respectively. (b) We implemented a five-fold cross-validation to test our network. For each fold, we used one specimen as our test data and trained a LSTM-CNN with the other four specimens. For each laxity assessment in our test data, we computed the errors between the US-measured and robot-measured kinematics at each US frame.

[Figure 2](#)

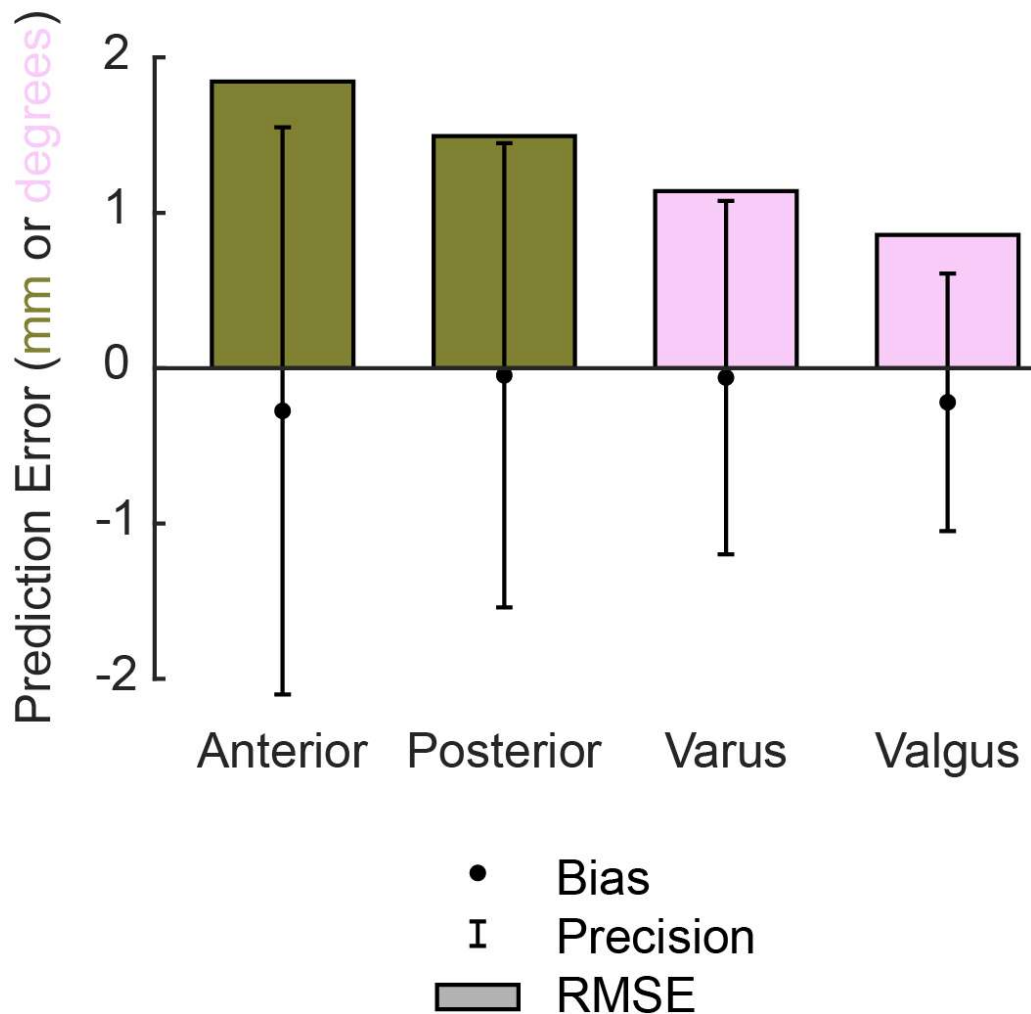


Figure 3: Bias (mean), precision (standard deviation), and root-mean-square errors (RMSE) for estimating kinematics during anterior, posterior, varus, and valgus laxity assessments. The average maximum excursions measured by the robot were 4.97 mm, 3.19 mm, 2.62°, and 2.59° for anterior, posterior, varus, and valgus assessments, respectively.

[Figure 3](#)

Phenotype Assessment in Three Dimensions

*Gokce Yildirim - Vent Creativity Corporation - Weehawken, USA

Dimitrios Georgopalis - Vent Creativity - Weehawken, USA

Rachel Alexander - Vent Creativity Corporation - Weehawken, USA

Introduction: Phenotypes have been increasingly relevant to orthopedics for bone alignment, joint alignment, and the potential for patient satisfaction with patient specific alignment strategies. CPAK is the current gold standard for assessment of phenotypes. However, recent publications¹ have pointed out the lack of sagittal considerations which may prevent the accuracy of classification from being clinically relevant.

Methods: CT data was used to generate previously validated intensity point clouds models². Three hundred and eighteen patients were analyzed for CPAK classification along with the new proposed method. Patient's primary, secondary and tertiary landmarks were analyzed for 3D clustering of femur and tibias. Primary landmarks were defined as identifiable locations such as the sulci, tubercle, eminence, malleoli for tibia, and posterior and distal femur, femoral neck and femoral head center for femur. (Figure 1). Secondary landmarks are lines generated from primary landmarks such as the sulci line, mechanical axis, etc. Tertiary landmarks are planes generated from points and lines combinations such as the posterior plane, sagittal plane, etc. An artificial intelligence system (Minerva, Vent Creativity, New York, USA) was used to segment, landmark, and measure landmark relationships for clustering of phenotypes. Resulting phenotypes were increased and decreased in cluster size for stability of the supervised machine learning.

Results: Compared to the CPAK classification system, 18 femoral and 20 tibial clusters were identified (Figure 2). The new proposed sagittal dimensions created an additional second dimension for each of the common 9 blocks. the lower right quadrants of the CPAK registered no patients (7,8,9) and the remaining groups had extra dimensions for sagittal planes.

Conclusion: While the phenotypes of bones for individual joints can vary in orientation and size, it is important to determine clinical significance associated with the variation. Sagittal plane and 3D morphology of patients add complexity to surgical outcomes and refined implant designs. Further studies are needed to tie phenotypes to functional kinematics and bone density related complexities.

Figures

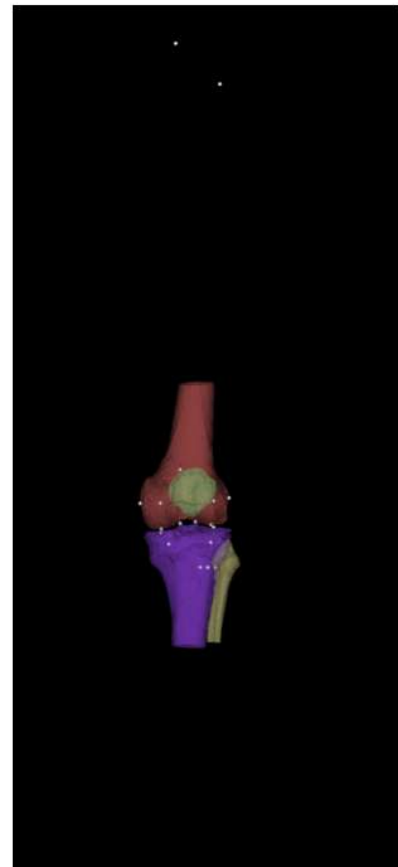
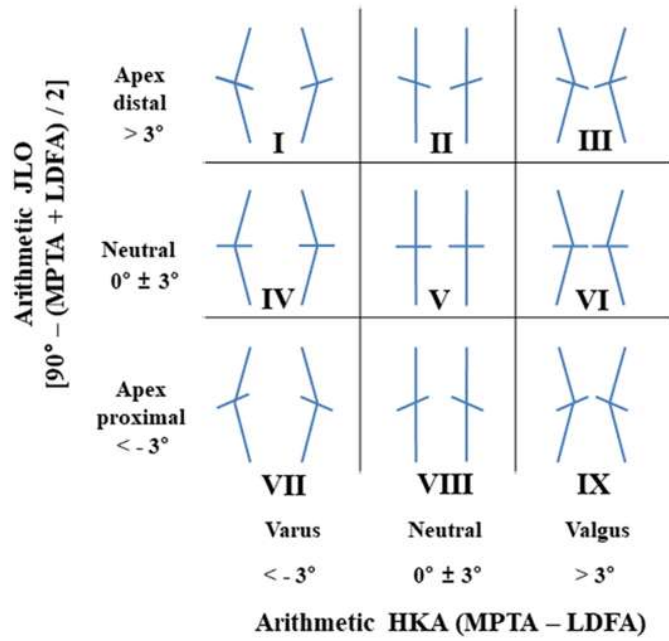


Figure 1

	A	B	C	D	E	F	G	H	I	J	K	L	M	N	O	P	Q	R	sum
1	10	4	10	2	0	3	1	0	0	0	3	4	5	1	2	0	4	1	50
2	8	17	23	2	1	14	3	4	0	1	5	10	13	0	4	1	5	1	112
3	5	6	9	2	0	3	1	1	1	1	3	1	6	0	2	1	3	1	46
4	3	1	8	0	0	1	1	0	0	0	1	4	6	1	4	0	1	0	31
5	2	9	12	0	0	6	1	0	0	0	5	2	4	0	6	1	2	0	50
6	3	1	8	0	0	2	3	0	0	0	5	0	3	0	2	0	1	1	29
7	0	0	0	0	0	0	0	0	0	0	0	0	0	0	0	0	0	0	0
8	0	0	0	0	0	0	0	0	0	0	0	0	0	0	0	0	0	0	0
9	0	0	0	0	0	0	0	0	0	0	0	0	0	0	0	0	0	0	0
sum	31	38	70	6	1	29	10	5	1	2	22	21	37	2	20	3	16	4	

Figure 2

Effect of Partial and Complete PCL Sectioning in Medial Congruent TKA on Femoral Rollback and Posterior Sag: A Computational Study

*Reza Pourmodheji - Hospital for Special Surgery - New York, United States of America

Cynthia Kahlenberg - Hospital for Special Surgery - New York City, USA

Brian Chalmers - Hospital for Special Surgery - New York City, USA

William Long - Hospital for Special Surgery - New York, USA

Timothy Wright - Hospital for Special Surgery - New York, USA

Eytan Debbi - Hospital for Special Surgery - NY, USA

Geoffrey H Westrich - Hospital for Special Surgery - New York, USA

David J. Mayman - Hospital for Special Surgery - New York, USA

Carl Imhauser - USA

Peter Sculco - Hospital for Special Surgery - New York, USA

Introduction: Medial congruent (MC) TKA involves adding an 'anterior lip' to the to the medial aspect of the tibial insert to increase conformity of the medial compartment [1,2]. Manufacturers suggest that this class of implants can be utilized in the presence or absence of the PCL. However, the biomechanical role of the PCL in MC- TKA is not well understood in terms of both preventing posterior sag of the tibia and facilitating femoral rollback [3]. Therefore, the purpose of this study was to determine the effect of partial and complete sectioning of the PCL on posterior sag of the tibia and femoral rollback in MC- TKA.

Methods: Computational models derived from ten independent cadaveric left knees (five males, five females; age: 63.7 ± 10.5 years) were virtually implanted with MC-TKA (Persona, Zimmer-Biomet). The knee model was tested with the PCL intact, with the AL bundle sectioned, and with the PCL completely sectioned. The knee was flexed from 0 to 90° under 500 N of compression and the femoral rollback of the medial and lateral compartments were determined. A test of posterior laxity was conducted by applying a posterior tibial force of 30 N at 90° of flexion (similar to force across knee joint seen in this position) for each condition of the PCL and the posterior tibial translation was calculated.

Results: Femoral rollback decreased medially by 1.3 [0.6 1.7] mm ($P=0.02$) and 2.3 [2.0 2.8] mm ($P<0.01$) on average with partial and complete sectioning of the PCL, respectively (Fig. 1). Posterior tibial translation under the posteriorly applied force increased by 1.8 [1.2, 3.1] mm ($P<0.01$) and 4.1 [2.8, 5.2] mm ($P=0.02$) on average with partial and complete sectioning of the PCL (Fig. 2).

Conclusion: Both femoral rollback and posterior tibial translation during a test of knee laxity are impacted by PCL sectioning. Addition of an anterior medial lip on the tibial insert does not compensate for the loss of femoral rollback and increased posterior sag in MC-TKA.

References: [1] Indelli, *Knee Surg. Sports Traumatol. Arthrosc*, 2023, [2] Fry, *Arthroplast. Today*, 2021. [3] Mahoney, *JOA*, 1994

Figures

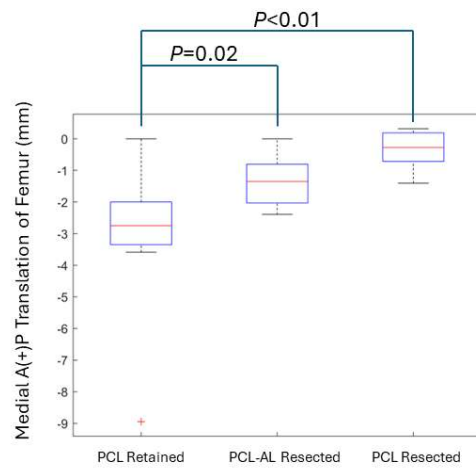


Figure 1: Boxplot of medial anterior-posterior (AP) translation of the femur with anterior positive at 90° of flexion for different posterior cruciate ligament (PCL) conditions. Red lines and boxes represent medians and quartiles, respectively. The whiskers extend to the most extreme data points not considered outliers. An outlier (red cross) is a value that is more than 1.5 interquartile range (IQR) away from the top or bottom edge of the box.

Figure 1

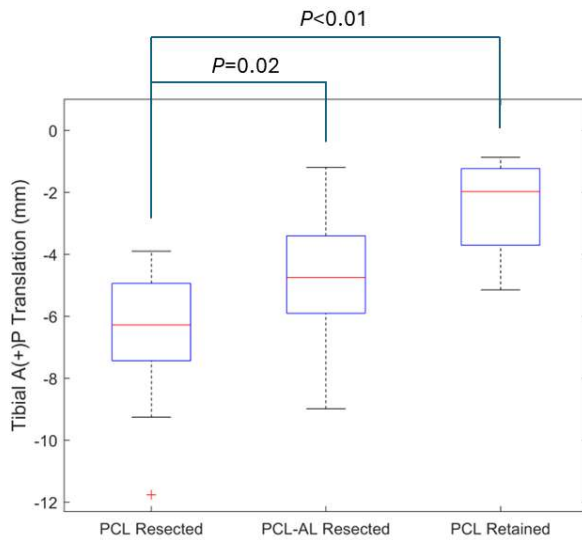


Figure 2: Boxplot of tibial anterior-posterior (AP) translation with anterior positive at 90° of flexion under posteriorly directed force on the tibia for different posterior cruciate ligament (PCL) conditions. Red lines and boxes represent medians and quartiles, respectively. The whiskers extend to the most extreme data points not considered outliers. An outlier (red cross) is a value that is more than 1.5 interquartile range (IQR) away from the top or bottom edge of the box.

Figure 2

The Location of Periprosthetic Femoral Fracture Corresponds to Areas of High Strain: A Finite Element and Cadaveric Experimental Study

*Clarisse Zigan - Hospital for Special Surgery - New York, United States of America

Ryan Helbock - Hospital for Special Surgery - New York, USA

Haena-Young Lee - Hospital for Special Surgery - New York, USA

Andrew Hughes - HSS - New York, United States of America

Joseph Lipman - Hospital for Special Surgery - New York, USA

Timothy Wright - Hospital for Special Surgery - New York, USA

Peter Sculco - Hospital for Special Surgery - New York, USA

Elizabeth B. Gausden - Hospital for Special Surgery - New York, USA

Sony Manandhar - Zimmer Biomet - Warsaw, USA

Jeffrey Bischoff - Zimmer, Inc. - Warsaw, USA

Fernando Quevedo Gonzalez - Hospital for Special Surgery - New York, USA

Introduction: Periprosthetic femoral fracture (PFF) is a prominent cause of revision for primary total hip arthroplasty (THA) [1]. As a biomechanical problem, PFF is dominated by the local mechanics of load transfer between implant and bone. Thus, to avoid PFF, we must understand how implant, surgical, and patient factors impact such load transfer. To achieve this goal, we compared experimentally derived fracture patterns against their respective computationally derived strain distributions under the same loading condition.

Methods: Four femur specimens (3 males and 1 female, ages 44-80 years, BMI 13.07-43.51 kg/m²) without prior trauma were pre-operatively CT-scanned, implanted [(2 collared and 2 collarless) Avenir, Zimmer Biomet] by a fellowship trained orthopaedic surgeon, and CT-scanned again to create post-operative renderings. Specimens were loaded to failure on a uniaxial servohydraulic load frame. Specimen-specific, 3D-printed guides were used to orient specimens such that loading would be representative of the most critical load from stumbling [2]. Specimens were painted with a speckle pattern to track the surface strains of the femur and displacement of the implant during loading using a digital image correlation system. Specimens were secured in the load frame and 3D scanned, allowing us to create finite element models that reproduce experimental testing conditions (Fig. 1). The maximum force recorded was considered the fracture load. In the computational models, meshing was performed with 0.8-3mm linear tetrahedral elements. Bone was assigned elastic, non-homogenous material properties using CT-scan data [3] and implants were considered titanium alloys ($E=110$ GPa, $\nu=0.33$). Line-to-line frictional contact was defined between the implant and bone (friction coefficient = 0.64) [4]. Models were simulated to the experimentally determined fracture load and the distribution of strains analyzed.

Results: Experimentally, we observed a range of failure loads (1530N, 4938N, and 8017N) with one specimen failing to achieve fracture altogether. Specimens with low BMI or poor tissue quality corresponded to lower failure loads while healthier or younger specimens were able to withstand higher loads. Computationally, we observed regions of high strain corresponded with experimental fracture locations (Fig. 2).

Conclusion: Our pipeline for creating specimen-specific finite element models of PFF demonstrated strains correspond to fracture patterns observed experimentally. Using additional matched specimens, we intend to investigate whether the addition of femoral component collars reduces the risk of PFF after primary THA.

References: [1] AJRR Annual Report, 2023; [2] Bergmann, et al., J Biomech, 2001; [3] Morgan, et al., J Biomech, 2003; [4] Biemond, et al., Arch Orthop Trauma Surg, 2011.

Figures

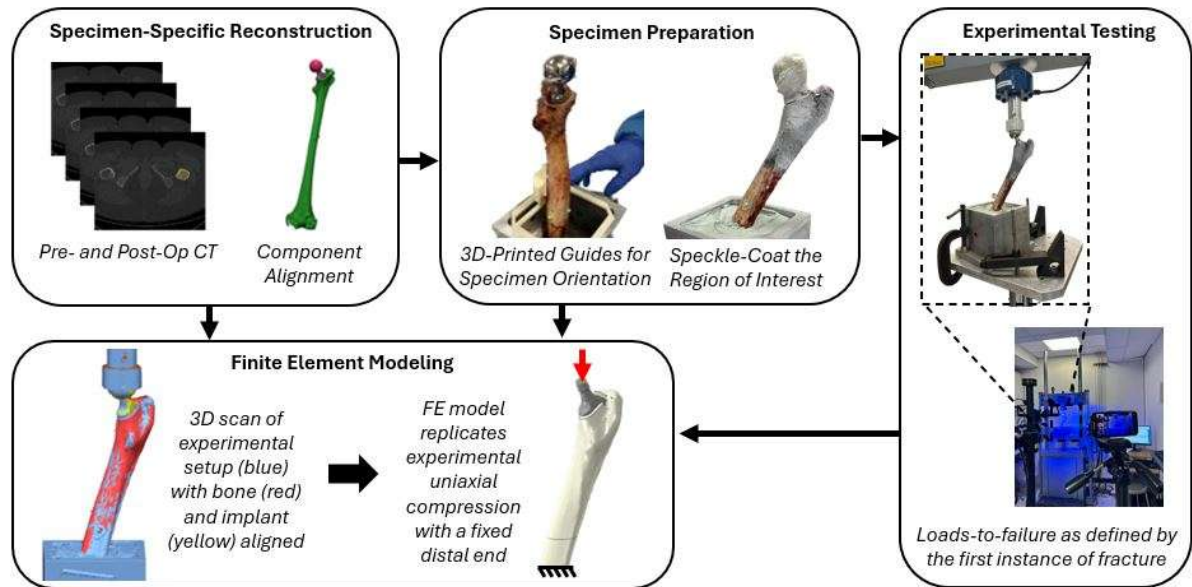


[Figure 1](#)

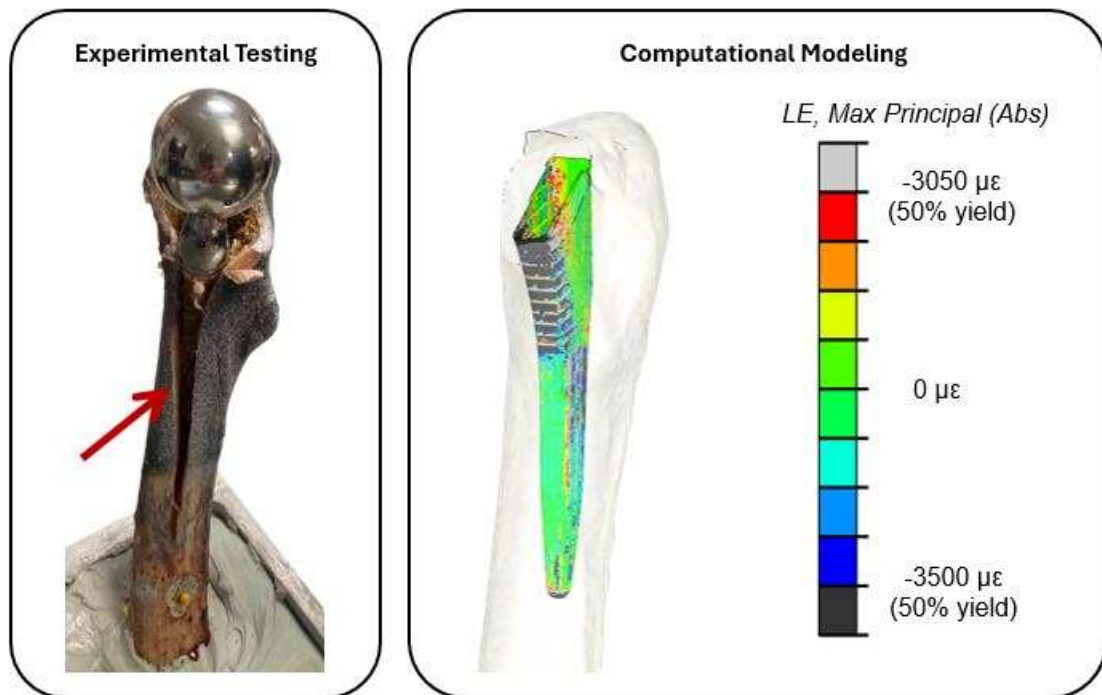


[Figure 2](#)

Femoral Condylar Geometry Is Related to MCL Force During Knee Flexion in Cruciate Retaining Total Knee Arthroplasty

*Reza Pourmodheji - Hospital for Special Surgery - New York, United States of America

Cynthia Kahlenberg - Hospital for Special Surgery - New York City, USA

Brian Chalmers - Hospital for Special Surgery - New York City, USA

Eytan Debbi - Hospital for Special Surgery - NY, USA

William Long - Hospital for Special Surgery - New York, USA

Timothy Wright - Hospital for Special Surgery - New York, USA

Geoffrey H Westrich - Hospital for Special Surgery - New York, USA

David J. Mayman - Hospital for Special Surgery - New York, USA

Peter Sculco - Hospital for Special Surgery - New York, USA

Carl Imhauser - USA

Introduction: The medial collateral ligament (MCL) plays a critical role in achieving knee stability following total knee arthroplasty (TKA) [1]. Numerous factors including femoral bony anatomy, and component design and placement can affect MCL tension through knee flexion.[2]. Recently, heterogeneity in femoral anatomy including the anterior-posterior (AP) offset of the medial condyle and the insertion location of the MCL has been recognized. Unfortunately, a knowledge gap remains as to how these anatomical variations relate to loading of the MCL. We previously defined a novel geometric ratio (the “MCL ratio”) to describe the anatomy of the medial femoral condyle accounting for these geometric features [3]. In this study, we asked two research questions: 1) What is the angle at which the MCL tension begins to carry force during passive knee flexion? 2) Is the MCL ratio related to this flexion angle?

Methods: Computational models derived from nine independent cadaveric left knees (five males, four females; age: 63.7 ± 10.5 years) were virtually implanted with CR-TKA (Persona, Zimmer-Biomet) using a measured resection technique. The computational model utilized 33 line-elements to represent the superficial MCL (sMCL), the PCL, lateral collateral, and capsular ligaments. The “MCL ratio,” was defined as the proportion of the distance of the femoral insertion of the anterior aspect of the medial sulcus of the femur, where the anterior fiber of the sMCL is located, to the posterior and to the distal cuts (Fig. 1). The knee was flexed from 0 to 90° under 500 N of compression to represent a test of passive flexion. Then the flexion angle at which the sMCL total force reached 20 N was identified for each knee. This tension target was selected because it results in a clinically acceptable medial extension gap of <1 mm [3]. The flexion angles vs. the MCL ratio was observed and fitted by an exponential function and coefficient of determination (r^2) was reported.

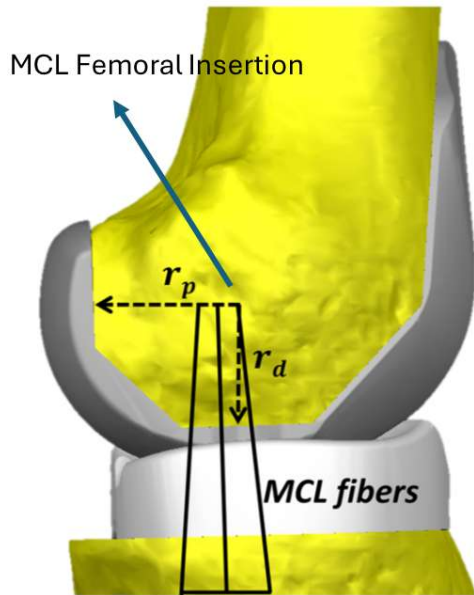
Results: From 0 to 90°, the flexion angle at which the sMCL tension reached 20 N was $62^\circ \pm 14.9^\circ$ ($n=7$). This flexion angle exponentially decreased as the MCL ratio increased ($r^2 = 0.89$) (Fig. 2). Two knees with the smallest MCL ratio did not achieve the MCL tension target.

Conclusion: The shape of the femoral condyle and placement of the femoral component with respect to the MCL femoral insertion may affect the MCL loading through a range of flexion. Interestingly, we found that no knee in the cohort regardless the shape of femoral condyle reached the target MCL tension (of 20 N) at less than 50° of flexion. Our findings also indicate that the MCL ratio may not

correlate with the MCL tension in flexion angles below 50° and other factors such as articular conformity, tibial insert thickness and femoral component curvature shape may affect the MCL tension in flexion. These findings may also inform surgical techniques for ligament balancing to address knee stability in mid-flexion.

References: [1] Kahlenberg, C., BJO, 2023, [2] Kia, M., 2018, [3] Elmasry, S., JOR, 2019

Figures



$$\text{MCL Ratio} = \frac{r_p}{r_d}$$

Figure 1: The anatomical description of the MCL ratio. r_p is the distance of the superficial medial collateral ligament (sMCL) from the posterior cut and r_d is the distance from the distal cut.

[Figure 1](#)

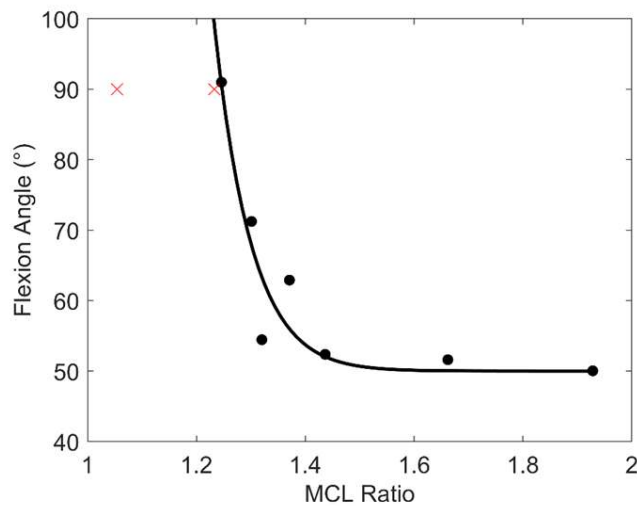


Figure 2: The scatter plot of the flexion angle at which the sMCL reaches 20 N of tension vs the MCL ratio. The black dots represent each knee that reached the 20 N of sMCL tension from 0 to 90° and red crosses are two knees that did not reach that certain sMCL tension within that flexion range. The solid curve is the exponential fit.

[Figure 2](#)

Computational Modeling of Implant Subsidence Over Heterogeneous Tissue Boundaries

*Remy Benais - University of Waterloo - Waterloo, Canada

Stewart McLachlin - University of Waterloo - Waterloo, Canada

Introduction

Computational modeling of implant subsidence has been extensively studied using the finite element (FE) method. However, the ability to predict implant subsidence remains limited, largely due to the size and complexity of existing image-based models. The meshless smoothed particle hydrodynamics (SPH) approach has shown benefits in representing the crushing and densification behaviour of bone indentation and has flexibility in simulating composite structures.

Clinical studies have shown that implant rotation can occur following interbody spinal fusion procedures, causing progressive changes in alignment and loss of surgical correction. Further, the vertebral body exhibits intra-site differences in mechanical properties across the vertebral endplate [1]. However, numerical studies have not yet investigated how implant subsidence occurs over these types of heterogeneous tissues.

The goal of this study was to examine a meshless SPH approach to model unconstrained, load-induced implant subsidence in a continuum-based trabecular bone model with asymmetric implant positioning over heterogeneous tissue boundaries.

Methods

Explicit FE simulations (LS-Dyna 12.1) were conducted using SPH elements of unconstrained load-induced rotational subsidence with asymmetric positioning over heterogeneous tissue boundaries. A generalized continuum-level approach was implemented with a crushable foam (CF) material model with isotropic hardening applied to the trabecular bone specimen. CF material parameters were calibrated to work from Soltanihafshejani et al. (2021) [2], where empirical relationships between the CF input parameters and trabecular bone mineral density (BMD) values were developed. Mechanical properties representative of bone specimens with BMD values of 102 and 187 mg/ml were assigned to adjacent sections of the trabecular bone specimen, respectively, defining a transition boundary between them. An interbody implant, meshed with Lagrangian elements, was placed on the trabecular bone specimen in five implant placement configurations: 0, 25, 50, 75, and 100% implant area initially placed over the higher density bone portion. Unconstrained compression up to 1 kN was applied to the bone-implant system.

Results and Discussion

The meshless continuum-based representation of trabecular bone was able to represent rotation of the implant into the lower-density portion of trabecular bone under unconstrained compression (Figure 1). Little implant rotation occurred in the 0% and 100% configurations where the material beneath the implant was near homogeneous. In the configurations where the implant was placed overtop the transition boundary, more rotational subsidence was induced (Figures 1 & 2). Minimal rotation occurred up to 0.4kN of applied force due to the bone system being loaded elastically with no plastic damage happening. A dip in the rotation was observed in each curve which is believed to be a result of the brief softening region in the stress-strain behaviour of the trabecular bone material models following ultimate stress.

Significance

The SPH method, coupled with a continuum-based representation of trabecular bone with a CF material model is effective at modeling the crushing and densification phenomena in bone indentation. By simulating unconstrained load-induced implant subsidence, this research advances comprehension of implant biomechanics and may improve future pre-clinical predictive modeling.

References

- [1] Kim D-G et al. *Ann Biomed Eng* 2007
- [2] Soltanihafshejani N et al. *Med Eng Phy* 2021.

Figures

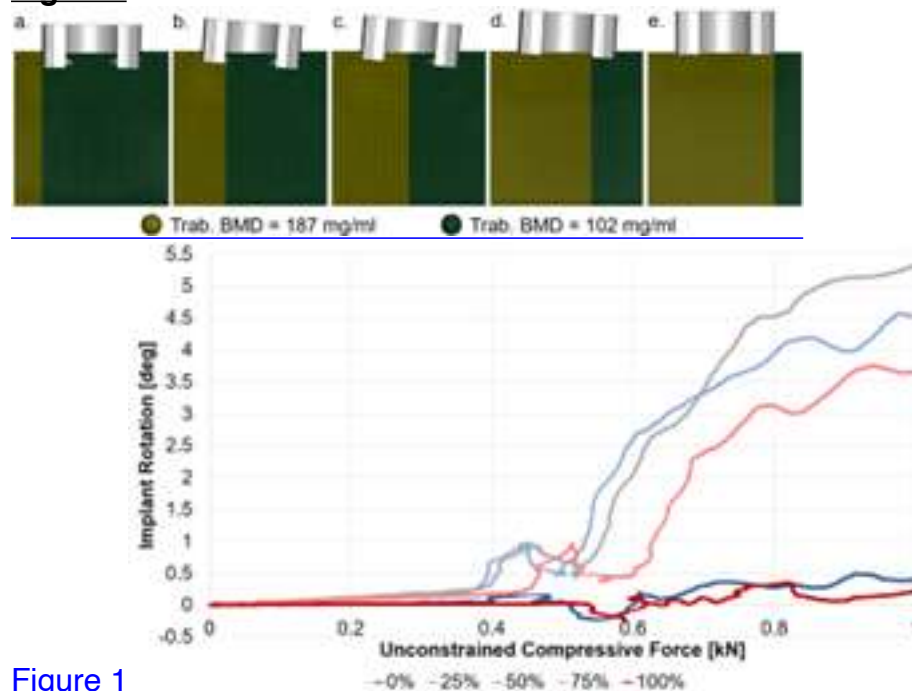


Figure 1

Figure 2

Particle-Based Simulation of Bone to Optimize Implant Fixation Features for Fracture Minimisation

*Jennifer Stoddart - Imperial College London - London, United Kingdom

Maxwell Munford - Imperial College London - London, United Kingdom

Jonathan Jeffers - Imperial College London - London, United Kingdom

Sloan Kulper - Lifespans - Wong Chuk Hang, Hong Kong

Erica Ueda - Lifespans, Ltd. - Wong Chuk Hang, Hong Kong

Katie Whiffin - Lifespans - Wong Chuk Hang, Hong Kong

Introduction: Cementless implants rely on a press-fit into bone to provide initial fixation before osseointegration can occur. Inherent in the use of a press-fit, where strain is put into the bone around the fixation features, is an increased risk of bone fracture. This risk is increased in smaller patients where the features required to provide sufficient initial fixation are relatively both larger and closer together when compared to a larger implant.

Methods: A subject-specific particle-based model (Alfonso, Lifespans, Hong Kong) of a small, female tibia was developed to simulate the implantation of a prototype titanium cementless UKA (Figure 1a). The bone model had heterogeneous material properties derived from a calibrated CT scan. A model of the implant was moved into the model of the prepared tibia with simulated mallet strikes until seated flush to the bone resections, at an implant velocity estimated according to the masses of the implant and mallet in a perfectly elastic collision. The friction coefficient between the bone and implant was tuned according to experimentally measured push-in and pull-out load data of the implant peg into Sawbones. A Taguchi methodology was used to test 5 different features on the implant (two keel, two peg and inter-peg) at three levels, and understand their effect on the damage calculated (ratio of failed:total particles, higher number indicates more damage) in 5 different regions of interest (Figure 1b). This resulted in 27 prototype implants, each with a unique combination of: peg diameter and interference, and keel width, length and interference.

Results: Across all the test implants, the regions of interest around the anterior peg and anterior to the keel were found to experience the most damage on average (Figure 2). The following factors were found to reduce the ratio of failed:total particles in each ROI: anterior keel - short keel length ($p = 0.002$); anterior peg - large peg taper angle ($p = 0.000$); inter-peg - small peg diameter ($p = 0.002$); posterior peg - large peg taper angle ($p = 0.000$); posterior keel - large peg taper angle ($p = 0.000$).

Conclusions: Particle-based simulations offer a powerful tool for quantitatively assessing bone damage and its link to fracture, particularly under impaction load cases. These can be used as a design tool in implant development. The factors found to significantly affect bone damage can then be used to define an acceptable design space for implant fixation features.

Figure 1: (a) Sagittal cross-section view of particle-based tibial model with implant in its final position (b) diagram showing the regions of interest in the tibia where bone damage during implantation was assessed

Figure 2: Mean damage (ratio of failed:total particles) in each region of interest over all simulated implants

Figures

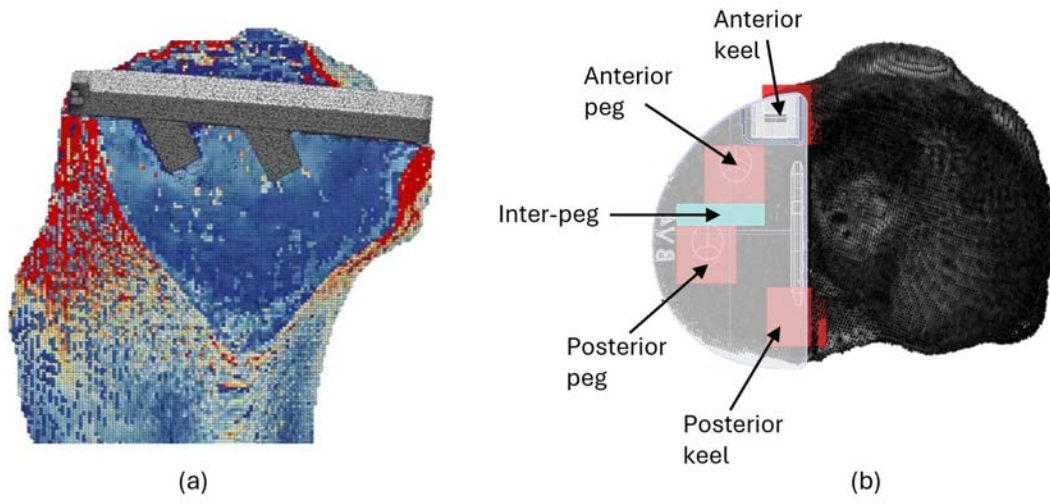


Figure 1

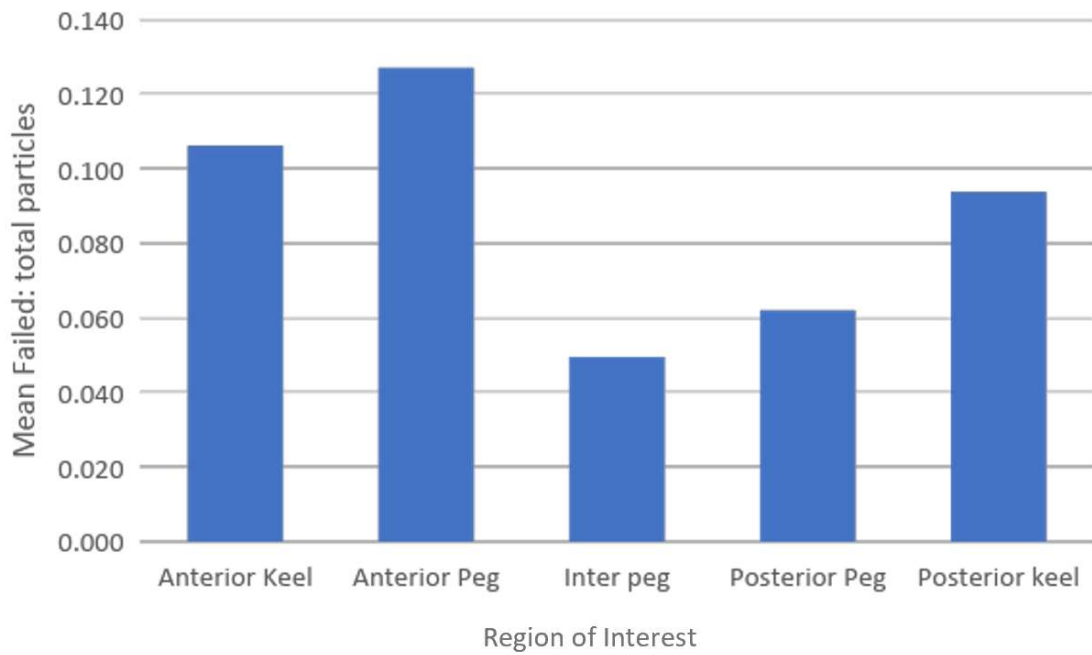


Figure 2

Finite Element Model of Patient-Specific Flanged Acetabular Components Highlights Biomechanical Effects of Bone Density and Cortical Shell Thickness

*Haena-Young Lee - Hospital for Special Surgery - New York, USA

Friedrich Boettner - Hospital for Special Surgery - New York, USA

Jason Blevins - Hospital for Special Surgery - New York, USA

Jose Rodriguez - Hospital for Special Surgery - New York City, USA

Joseph Lipman - Hospital for Special Surgery - New York, USA

Fernando Quevedo Gonzalez - Hospital for Special Surgery - New York, USA

Mathais Bostrum - Hospital for Special Surgery - New York, USA

Timothy Wright - Hospital for Special Surgery - New York, USA

Peter Sculco - Hospital for Special Surgery - New York, USA

Introduction: Patient-specific flanged acetabular components (FAC) are utilized to treat failed total hip arthroplasties with severe acetabular defects. Our previous work developed a finite element (FE) model that demonstrated the effects of hip joint center lateralization [1]. We have refined our model to examine how ischial cancellous bone density and cortical shell thickness affect the strain distributions in the implant and surrounding bone and the micromotions between implant and bone.

Methods: The FE model consisted of a FAC treating a superior-medial bone defect created in a standard pelvic bone geometry of a 54-year-old female (Fig. 1). The pelvis was loaded with the maximum hip contact force during gait and corresponding abductor force. Based on bone density analyses of our patient cohort and prior studies [2,3], we varied the ischial cancellous bone density (100% and 25%) and the thickness of the cortical shell (1.5, 1, and 0.75 mm). We compared the resulting bone strains against the fatigue strength of the bone (0.3% strain) [4] as a criterion for possible local bone failure and subsequent loosening and the micromotion against the threshold for compatibility with bone ingrowth (20 μm) [5].

Results: All configurations had similar strain distributions in the bone (Fig. 2). At 100% ischial cancellous density, halving the cortical thickness increased the areas at risk of bone failure at the ilial flange and screws, but did not impact the bone at the ischial flange and screws (Table 1). At 25% density, halving the cortical thickness resulted in a similar increase of areas at risk at the ilial flange and screws, with again no difference at the ischial flange. However, the combination of lower ischial cancellous bone density and a thinner cortex resulted in noticeably larger areas at risk at the ischial screws (6% to 38%). The areas compatible with bony ingrowth generally decreased with lower bone density and thinner cortices.

Conclusion: A combination of lower ischial cancellous bone density and a thinner cortical shell resulted in increased areas of bone at risk of failure, particularly at the ischial screws. This finding agrees with our previous clinical research, which found that compromised ischial bone and inadequate ischial fixation negatively impacted FAC survivorship [6]. Future studies with this model will examine a more sophisticated bone-screw interface. This series of FE studies establishes our systematic modeling approach of a robust computational model that can be utilized to guide the treatment of acetabular bone defects.

References: [1] Lee et al., ISTA 2022, [2] Watson et al., Med Eng Phys 2017, [3] Fallahnezhad et al., Comput Methods Programs Biomed 2023, [4] Dendorfer et al., J Biomech 2008, [5] Jasty et al., JBJS 1997, [6] Jones et al., Bone Joint J 2019

Keywords: hip, biomechanics, acetabular bone loss, finite element modeling, revision total hip arthroplasty

Figures

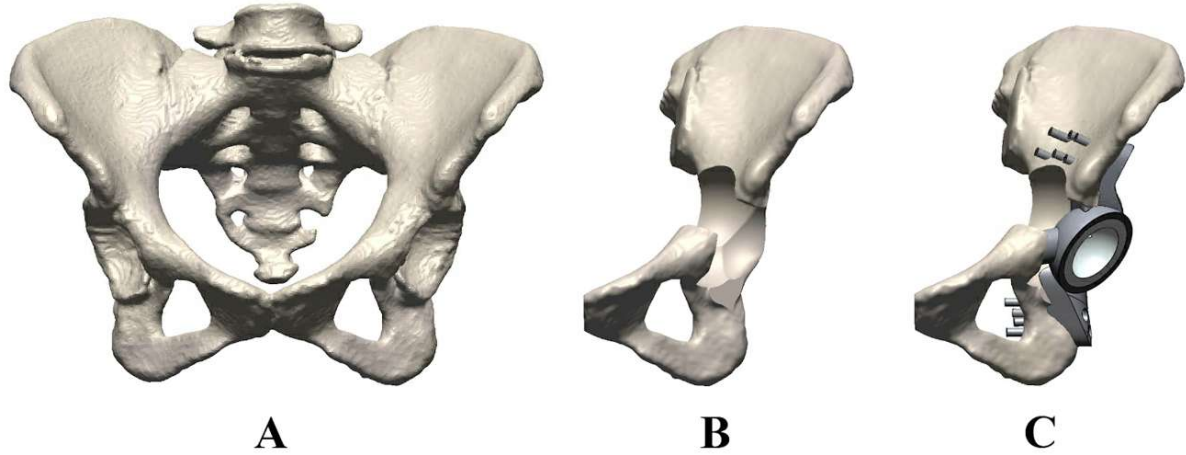


Fig. 1: Geometry of the (A) preoperative bone, (B) created defect, and (C) FAC and screws.

Figure 1

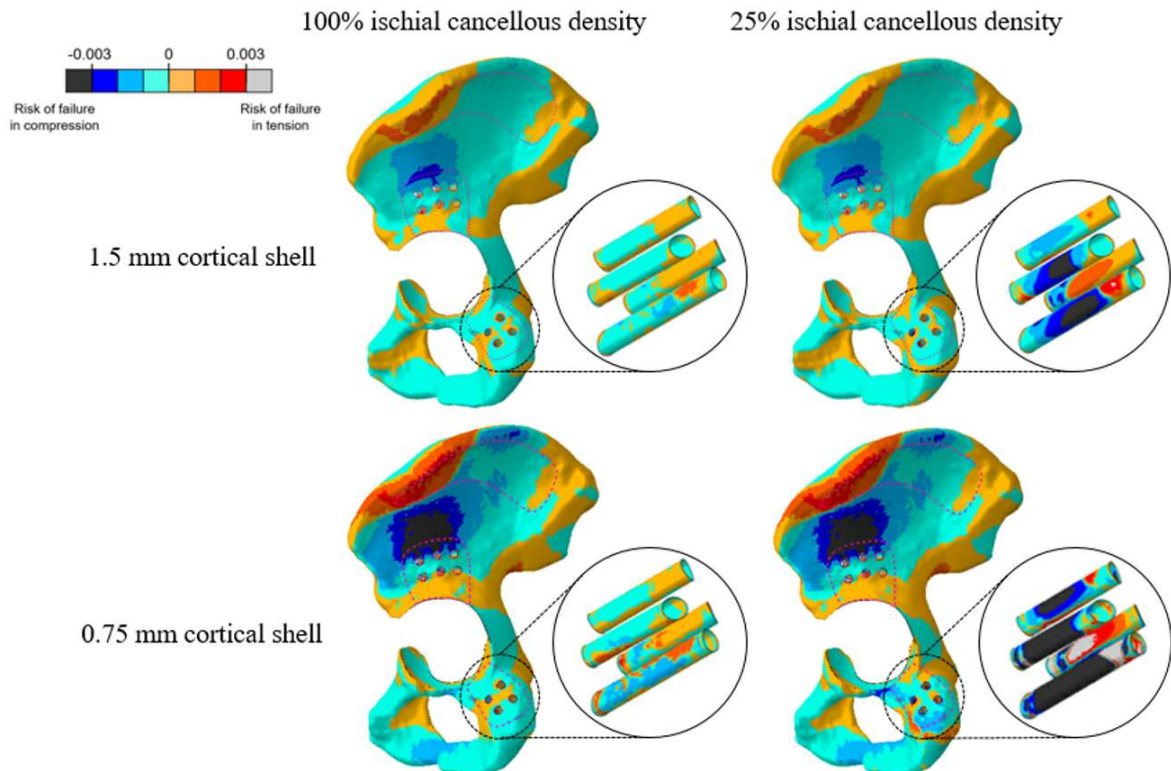


Fig. 2: Periprosthetic strain distributions for 100% and 25% ischial cancellous bone densities and 1.5 mm and 0.75 mm cortical shell thicknesses. Blue colors indicate bone in compression and red colors indicate bone in tension. Black and gray regions indicate bone with strain exceeding the bone fatigue strength in compression and tension, respectively.

Figure 2

Table 1: The percent areas of bone at risk of failure (strain > 0.3%) and the percent areas compatible with bone ingrowth (micromotion < 20 μm) for varying ischial cancellous bone densities and cortical shell thicknesses.

		100% ischial cancellous density			25% ischial cancellous density		
		1.5 mm shell	1 mm shell	0.75 mm shell	1.5 mm shell	1 mm shell	0.75 mm shell
% area of bone at risk of failure	Iliac flange	2	4	12	2	4	12
	Ischial flange	0	0	0	0	0	0
	Iliac screws	2	4	11	2	5	12
	Ischial screws	0	0	0	6	20	38
% area compatible with ingrowth	Iliac flange	100	99	85	100	99	89
	Ischial flange	95	90	85	87	82	78

[Figure 3](#)

How Does THA Impingement Risk During Activities of Daily Living Change With Pelvic Tilt and Spinopelvic Mobility?

*Alessandro Navacchia - Smith & Nephew - Broomfield, USA

Edward Davis - The Dudley Group NHS Foundation Trust - Dudley, United Kingdom

Bradford Waddell - Ochsner Clinic Foundation - New Orleans, USA

Stephen Duncan - University of Kentucky - Lexington, USA

Thorsten M. Seyler - Duke University - Durham, USA

Introduction

One of the most frequent causes for revision total hip arthroplasty is dislocation¹, which can be motivated by implant or bone impingement. Implant selection and placement determine post-operative range of motion and potential impingement. Both pelvic tilt (PT) and spine mobility play an important role in determining the patient's post-operative range of motion needs². This study investigated how impingement risk during activities of daily living (ADLs) is affected by PT and spine mobility.

Methods

A full-body skeletal computer model (LifeMOD[®]) was used to estimate hip kinematics for 12 ADLs from marker-based motion capture data: walking, stair climbing, stair descending, pivoting, twisting, chair rising, bending forward, sitting on a low chair, sitting with a crossed leg, seated reaching to floor, tying shoes, and a golf swing (Fig. 1). Hip kinematics was simulated for patients with normal and stiff spines.

Ten pre-operative CT scans were used to generate personalized 3D models of the patients' pelvises and femurs. Each model was virtually implanted with an R3[®] cup, a 0° liner, and a CATALYSTEM[®] (at time of submission, not FDA-cleared) (Smith+Nephew). Cup size, stem size, stem offset, and neck length were selected to match the patient's anatomy. For this initial planning step, a neutral tilt (PT=0°) and normal spine mobility were assumed.

Hip kinematics for the 12 ADLs were applied to each implanted model to estimate bone and implant impingement for both normal and stiff spine in 3 scenarios:

- PT=15° posterior.
- PT=0°.
- PT=15° anterior.

Results

Spine stiffness increased the number of impinging ADLs in 14/30 scenarios (47%) (Fig. 2). With a normal spine, the case simulation with the most impinging ADLs (5) had PT=15° posterior. The number of impinging ADLs changed when changing PT in 24/40 scenarios (60%), but importantly no consistent trend was observed. The case with most impinging ADLs (6) corresponded to a stiff spine with PT=15° anterior. A more posterior PT led to increased impingement in ADLs with high extension and external rotation, whereas a more anterior PT led to impingement in high flexion ADLs, especially in combination with a stiff spine.

Conclusions

PT and spine mobility affected the risk of impingement during ADLs and their influence was patient-specific. Personalized planning that accounts for the patient's spinopelvic condition and ADLs simulations is necessary to identify the risk of impingement and optimize planning because no linear trends exist.

References

1. UK National Joint Registry 2023
2. Vigdorichik, Bone Joint J, 2019

Figures

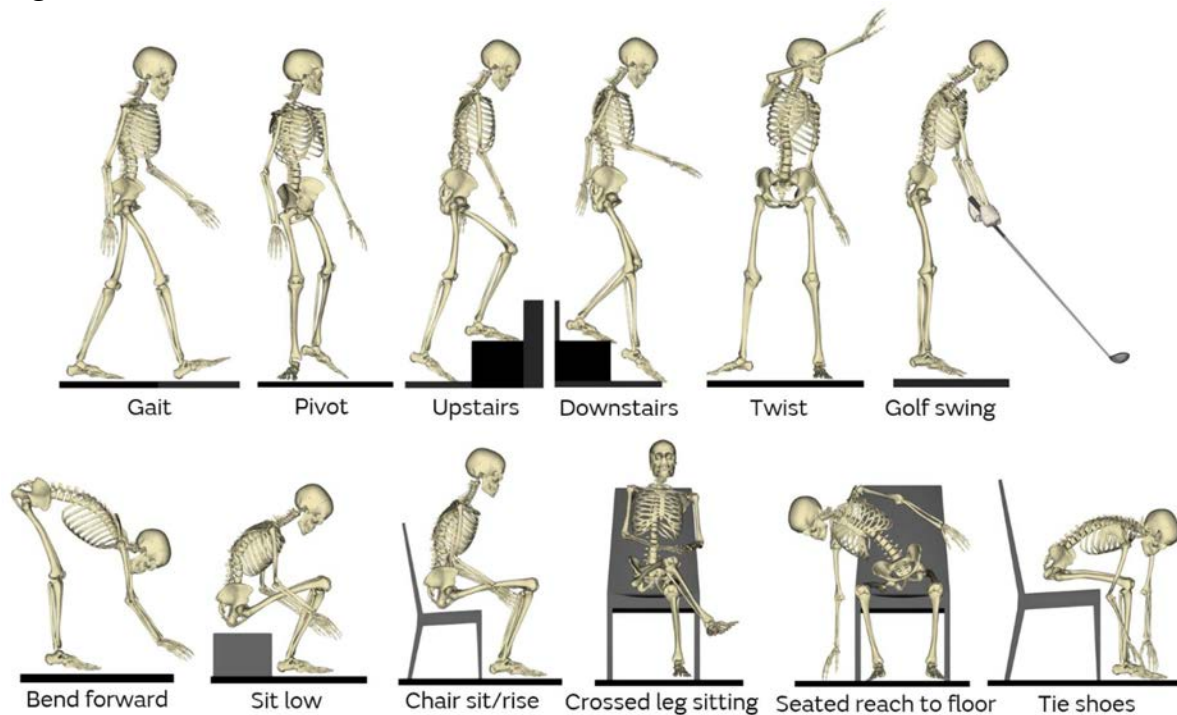


Figure 1: Full-body skeletal model used to estimate hip kinematics for the 12 ADL.

[Figure 1](#)

Patient #	Normal			Stiff		
	PT = -15	PT = 0	PT = +15	PT = -15	PT = 0	PT = +15
1	1	0	0	1	0	0
2	1	1	1	2	2	5
3	1	0	1	1	3	4
4	1	1	0	1	4	4
5	5	3	2	5	3	2
6	1	1	0	1	4	3
7	3	3	1	3	3	6
8	2	2	1	2	2	1
9	1	1	1	2	2	1
10	2	1	2	2	4	4

Figure 2: Number (out of 12) of impinging ADLs for each simulated scenario: normal vs stiff spine with PT variations (-15, 0, +15, with positive PT corresponding to anterior PT).

[Figure 2](#)

Digital Image Correlation for Ligament Balancing in Total Knee Arthroplasty Using Controlled Grid-Assisted Pie-Crusting Technique

Kristi Nguyen - University of Illinois College of Medicine - Chicago, United States of America

*Farid Amirouche - University of Illinois at Chicago - Highland Park, United States of America

Jason Koh - NorthShore University Health System - Evanston, USA

Nicole Tuoni - University of Illinois Hospital & Health Sciences System - Chicago, USA

Hristo Piponov - University of Illinois Hospital & Health Sciences System - Chicago, USA

Arash Rezai - University of Illinois Hospital & Health Sciences System - Chicago, USA

Introduction:

In total knee arthroplasty (TKA), ligament release is performed to balance flexion and extension gaps. Proper balancing is a significant indicator of postoperative joint stability, range of motion, and patient satisfaction. Among ligament balancing techniques, the pie-crusting technique is increasingly prevalent as a reproducible soft tissue lengthening method compared to conventional methods and approaches based on subjective surgeon assessment and experience. In pie-crusting, stiffness and elongation of the ligament are evaluated by measuring the medial femorotibial (MFT) space, which reflects global changes to the ligament but does not account for local changes in stiffness or elongation of the individual fibers that make up the heterogeneous collagen architecture of a ligament. This study investigated the efficacy and precision of using digital image correlation (DIC) to release the MCL during TKA balancing. We hypothesized that DIC testing will allow for a more controlled and precise release of the medial compartments by monitoring local fiber elongation and strain of individual MCL fibers in real-time.

Methods:

Nine frozen cadaver knees were dissected and underwent a TKA procedure, leaving the femur and tibia connected by an isolated MCL. The specimens underwent preloaded cyclic conditioning before mechanical testing was performed using an MTS machine (Criterion Electromechanical Test System, Model C44, MTS, Minnesota, United States) at a load of 120 N. During testing, a 3D-printed algorithmic pie-crusting grid was used to guide the release of the MCL. Horizontal perforations were made using an 18-gauge needle perpendicular to the MCL fibers. We used a DIC system to record local fiber displacement and deformation following needle punctures, collecting data after every 2 perforations until 8-12 holes, depending on specimen MCL width. Specimen MCLs were divided into 4-5 equal sections to observe spatial patterns of fiber strain. Stress-strain curve data and stiffness were calculated based on the cross-sectional area of the ligament in each specimen. Regression analyses were performed to determine the relationship between the number of perforations and the length and stiffness of the ligaments.

Results:

Ligament fibers preferentially stretched and elongated on the anterior and posterior aspects of the MCL instead of stretching uniformly across the ligament. Fiber bundles elongated inwards from either the anterior or posterior aspect of the MCL. No specimen experienced greater elongation in the center of the MCL compared to

either the anterior or posterior elements. These fiber changes are matched by the respective DIC mapping of local fiber strain at all perforations, with baseline DIC measurements demonstrating fiber strain incongruency despite cyclic conditioning. Conclusion:

DIC testing allowed for precise characterization of local fiber behavior in the MCL during pie-crusting, which improves current balancing methods that only evaluate global changes to ligament structures. Future studies should use DIC to assess and distinguish differences in baseline fiber behavior due to experimental, procedural, and physiologic variations.

Figures



[Figure 1](#)

Knee Sample

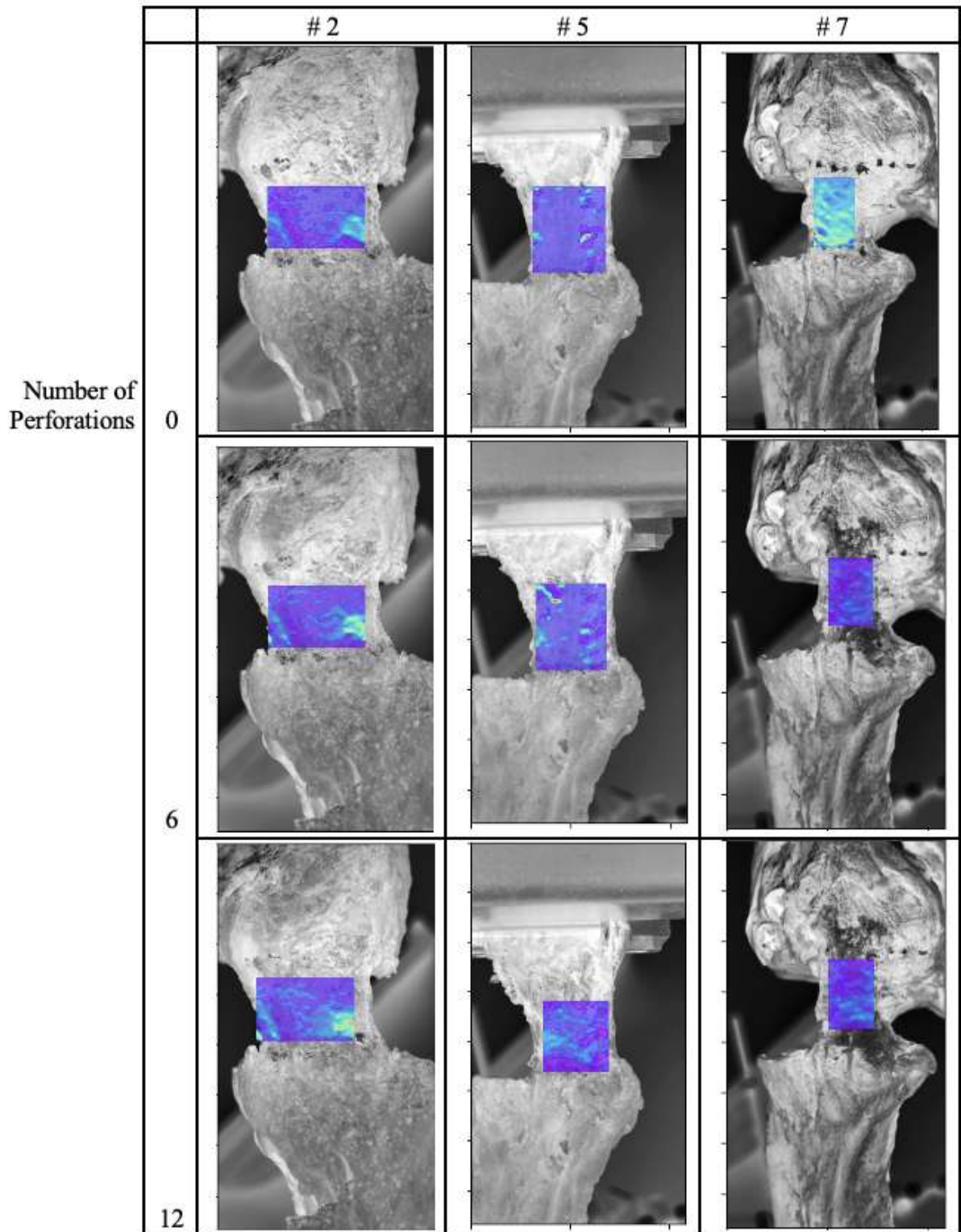


Figure 2

Evaluating Ligament Laxity Objectives Across Full Range of Motion in Total Knee Arthroplasty: A Focus on Tibia First Technique

*Prudhvi Tej Chinimilli - Exactech - Gainesville, USA

Laurent Angibaud - Exactech, Inc. - Gainesville, USA

Amaury Jung - Blue Ortho - La Tronche, France

James Huddleston

Introduction:

Alignment techniques in total knee arthroplasty (TKA) are constantly evolving, with modern approaches such as functional alignment providing clear recommendations for bone cutting parameters. However, the definition of ligament laxities remains unclear. In tibia first technique, the acquired joint gaps between proximal tibia cut and native femur used for femoral planning may vary depending on the tibia cut frontal orientation. This study evaluates the laxity signatures established by surgeons when defining femoral cut planning based on different tibia cut scenarios.

Methods:

A retrospective review analyzed 1762 TKA cases performed by 20 surgeons, each with a minimum of 15 cases, using a computer-assisted surgery (CAS) system. The cases were stratified based on the bearing type into three classes: posterior-stabilized (PS) with 15 surgeons, cruciate-retaining constrained (CRC) with 6 surgeons, and cruciate-retaining (CR) with 3 surgeons. Additionally, some surgeons were considered as hybrid, utilizing more than one type of bearing and thus included in multiple classes. The surgical technique allowed planning femoral cuts in terms of alignment, size, and ligament balance. Planned laxities for each case were referenced to the planned medial laxity at 10° flexion under two tibial cut scenarios: the actual tibia cut during surgery (Group A) and a simulated cut perpendicular to the mechanical axis (Group B). While the simulated cut alters lateral gaps due to tibia cut angles, medial gaps remain consistent across both groups. Relative planned laxities were calculated for full flexion arc from 10° to 120° flexion. A two-way ANOVA compared surgeon effect on laxity definition. If significant, Tukey's multiple comparisons analyzed pairwise laxity differences between surgeons.

Results:

ANOVA analysis indicated significant differences ($p < 0.05$) in relative laxities among the 20 surgeons in both groups, regardless of the bearing type class and compartment side. Box and whisker charts (Figures 1 and 2) illustrate the medial and lateral laxity curves for each surgeon in Group A and Group B across PS, CRC, and CR classes. The Tukey multiple comparison pairs results provided in Figure 3 revealed that the percentage of significant pairs in Group B lateral laxity across three bearing type classes (PS: 71.4%, CRC: 80%, CR: 66.7%) are nearly equal to or greater than those in group A lateral laxity (PS: 72.4%, CRC: 46.7%, CR: 66.7%). This suggests that the laxity definition during femoral planning depends on the surgeon, regardless of the tibial cut choice. Notably, 30% of the surgeons (6 out of 20) opted for tibial cut obliquity demonstrated a significant impact of the tibial cut on laxities.

Conclusion:

There is wide variability among surgeons in defining laxities, with preferences ranging from rectangular gaps to trapezoidal gaps or greater flexion gaps than extension. Regardless of the tibial reference, laxity definition for femoral cutting planning tends to be surgeon-specific. It is noteworthy that most of the surgeons in this study tend to prefer a tibial cut referenced to the mechanical axis, which reduces the difference between the two groups. As knee arthroplasty customization progresses, there is an opportunity to define patient-specific laxities.

Figures

Figure 1: Box and whisker plots for 15 PS surgeons (Group A on left and Group B on right)

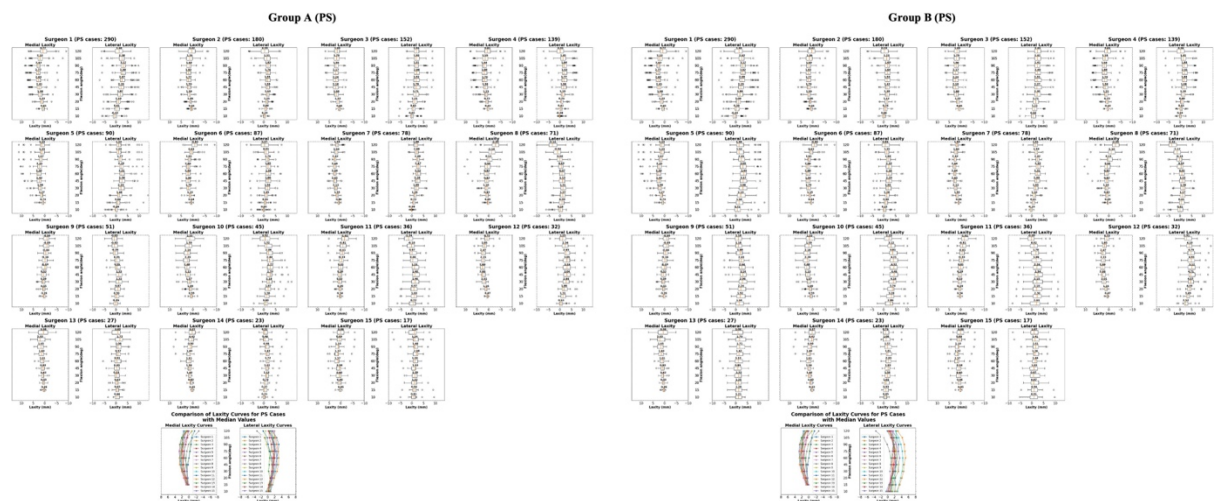


Figure 1

Figure 2: Box and whisker plots for 6 CRC surgeons and 3 CR Surgeons (CRC Group A: top left, CRC Group B: top right, CR Group A: bottom left, CR Group B: bottom right)

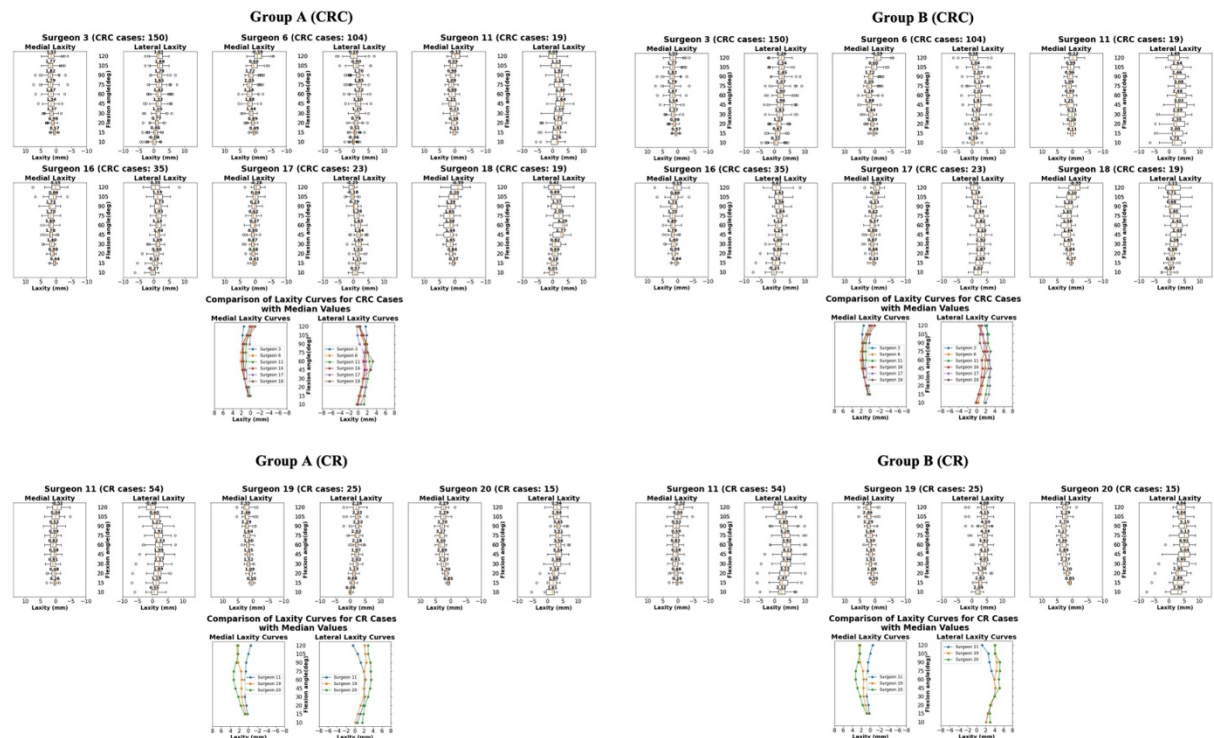


Figure 2

Figure 3: Tukey multiple comparisons results comparing pairwise laxity differences between 15 surgeons (PS), 6 surgeons (CRC), and 3 surgeons (CR)

Laxity	Number of surgeons*	Type of bearing	Number of cases	Total number of comparisons	Number of comparisons (p<0.05)	% comparisons (p<0.05)
Medial laxity (Group A & B)	15	PS	1318	105	77	73.3%
Lateral laxity (Group A)	15	PS	1318	105	76	72.4%
Lateral laxity (Group B)	15	PS	1318	105	75	71.4%
Medial laxity (Group A & B)	6	CRC	350	15	10	66.7%
Lateral laxity (Group A)	6	CRC	350	15	7	46.7%
Lateral laxity (Group B)	6	CRC	350	15	12	80%
Medial laxity (Group A & B)	3	CR	94	3	3	100%
Lateral laxity (Group A)	3	CR	94	3	2	66.7%
Lateral laxity (Group B)	3	CR	94	3	2	66.7%

*: Some surgeons were considered hybrid (i.e., used more than 1 type of bearing), explaining the sum being more than 20

Figure 3

Immediate Post-Operative Walking Asymmetry Affected by the Amount of Laxity in the Lateral Compartment in Flexion

*Roberta Redfern - Zimmer Biomet - Pemberville, USA

Mike Anderson - Zimmer Biomet - Lehi, USA

Jason Cholewa - Zimmer Biomet - Warsaw, USA

Joseph Brook - Zimmer Biomet - London, United Kingdom

Adam Henderson - Zimmer Biomet - Winterthur, Switzerland

Karl Surmacz - Zimmer Biomet - Swindon, United Kingdom

Introduction

It has previously been suggested that intra-operative data collected via robotics may provide answers to which surgical parameters affect outcomes in total knee arthroplasty. The purpose of this study was to evaluate if robotically assessed gap laxity was associated with objective post-operative activity measures.

Methods

Anonymized intra- and post-operative data from a commercial database of 4,354 patients were analyzed. The majority of patients were female (54%) and the mean age was 67 years. The mean body mass index was 31.2 kg/m². Data were captured from the robotic system's log files and a digital care management platform using a smartphone's gait metric analysis. We compared the change between the pre-operative and post-operative gait metrics between groups at 14-, 30-, and 90-days post-operative. Groups were categorized according to the degree of robotically measured gap laxity as follows: <0.5mm, 0.5 – 1.5, 1.5 – 2.5 mm, 2.5 – 3.5mm, ≥3.5mm. Measurements were taken in both the medial and lateral compartments and in 90° and 0° of flexion. Given that the data was not normally distributed, differences between the laxity groups were assessed using Kruskal Wallis tests.

Gait outcomes were considered clinically relevant if the differences in means between groups exceeded the following thresholds: gait speed ≥ 0.1m/s; steps ≥ 500; presence of walking asymmetry ≥ 0.141.

Results

Tight gaps, <0.5mm, in the lateral compartment in flexion demonstrated significantly greater presence of walking asymmetry at 14 days postoperative (p=0.037), where the <0.5mm group had a median walking asymmetry increase of 0.566 (IQR, 0.331 – 0.689, Figure 1). The change in percentage of time walking asymmetry was present in this group was clinically greater (>0.141) than both the 1.5mm – 2.5mm and 2.5mm – 3.5mm gap laxity groups at 14 days post-operative, but not at 90 days. Additionally, patients with ≥3.5mm of laxity in flexion in the lateral compartment had clinically greater increases in presence of walking asymmetry than those with 2.5mm – 3.5mm at 14 days post-operative. There was no difference in change in gait speed or step counts (p>0.05) at any time point between groups.

Discussion

These data present a signal in gap laxity, as measured by a robotic platform, and post-operative activity metrics, measured using a digital care management platform. There is potential for both tight and loose knees (≥3.5mm) to have greater increases in the percentage of time walking asymmetry is present immediately post-operative compared to their counterparts. Identifying targets intra-operatively that are associated with improved post-operative outcomes may be useful in future arthroplasty procedures, but more evidence is needed to substantiate these findings.

Figure 1. Violin plot demonstrating change in walking asymmetry at 14 days post-operative between lateral laxity groups at 0° final flexion.

Figures

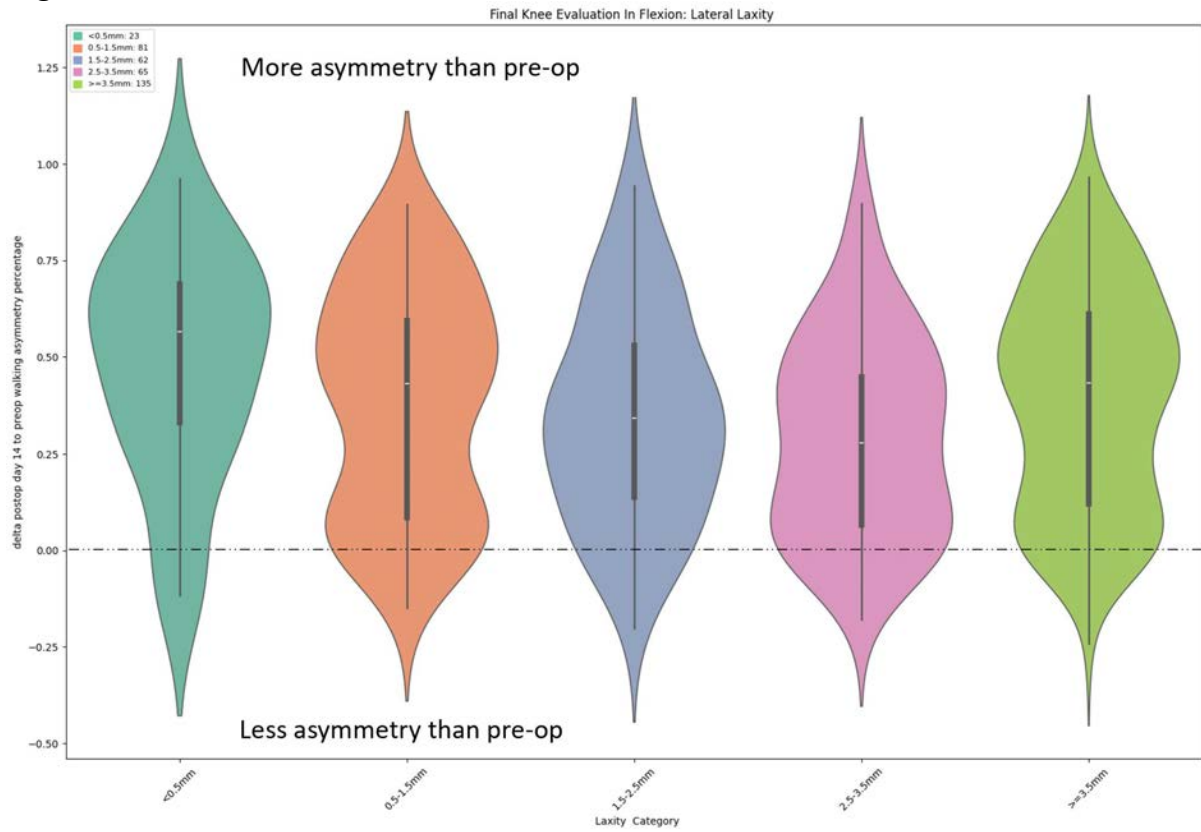


Figure 1

Surgeons' Expertise Does Not Prevent Complications in Technology Assisted TKA in Valgus Knees

*Shantanu Patil - SRM Medical College, SRM Institute of Science and Technology - Kattankulathur, India

Ashok Kumar P. S. - CHENNAI, India

Manideep Reddy - SIMS Hospital - Chennai, India

Anish Bharadwaj - SIMS Hospital - Chennai, India

Vijay C Bose - AJRI - chennai, India

Pichai Suryanarayan - India

Kalaivanan Kanniyar - Asian Joint Reconstruction Institute AJRI @SIMS Hospitals - Chennai, India

Introduction: TKA in subjects with a valgus knee deformity poses a challenge, requiring precise alignment and careful soft tissue management for optimal outcomes. Availability of state-of-the-art technology, while helpful, does not diminish the surgeon's role in achieving functional alignments with judicious soft tissue releases and favorable outcomes. This study aims to compare the efficacy of conventional, navigation-guided, and robotic-assisted TKA techniques in delivering a consistent result.

Methods: In this retrospective review of prospectively collected data between 2019-2022 at a tertiary care center, we compared three age and gender matched cohorts who presented with a valgus deformity and underwent total knee arthroplasty. They were labelled as Conventional total knee arthroplasty (cTKA) (n = 35) with navigation-assisted (nTKA) (n = 35), and image-free handheld robotic-assisted (rTKA) (n = 35). (**Table 1**) All patients were assessed as their one year follow up. Clinico-radiological, functional and patient-reported outcomes (PROMs) were also documented. Our primary objective was to compare clinical and knee-specific functional outcomes in each cohort, while secondary objectives included assessing general physical and mental health improvement, patient satisfaction, perioperative complications, and component alignment reliability in the sagittal and coronal planes, including implant alignment accuracy. PROMs studied included the Western Ontario McMaster University Arthritis Index (WOMAC), Oxford Knee Score (OKS), and Short Form 36 (SF-36).

Results: A total of 105 patients with valgus knee n=35 in each cohort of Conventional, Navigation, Robotic assisted TKA. Overall analysis indicates that both conventional and navigation-guided techniques demonstrated on par performance in achieving surgeon-guided functional alignment with minimal soft tissue releases compared to robotic-assisted TKA in valgus knee deformity cases.(Table 2). 2 patients in the rTKA cohort developed post-surgical neuropraxia with foot drop that recovered eventually. In spite of meticulous soft tissue releases, the use of a thicker tibial insert to achieve balance could have caused this complication. Figure 1 shows pre- and post- surgical correction of patient with severe valgus.

Conclusion: Our findings suggest that conventional and navigation-assisted techniques are equally effective as robotic-assisted TKA in achieving surgeon-derived functional alignment while minimizing the need for soft tissue releases. Although robotic-assisted TKA shows potential for various indications such as early recovery and precision, its current efficacy in addressing valgus knee deformity appears comparable to conventional and navigation methods. Our study

underscores the enduring importance of surgeon expertise in soft tissue management, which remains paramount even in the era of technology-assisted TKA.

Figures

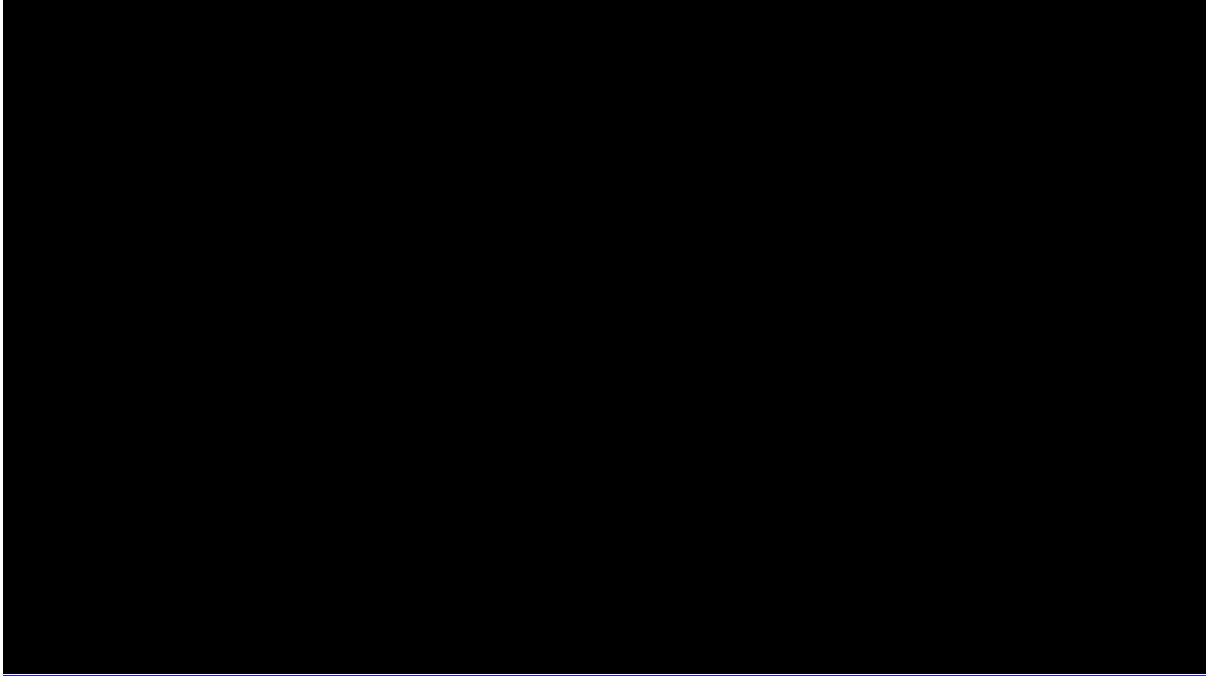


[Figure 1](#)



[Figure 2](#)

Pre & Post Static Alignment

Pre HKA
Left 11° Valgus
Right 15° Varus



Post HKA
Left 0°
Right 0°



Target was 0 to +/- 3°

[Figure 3](#)

The Effect of Bone Relaxation on the Simulated Pull-Off Force of a Cementless Femoral Knee Implant

*Thomas Gersie - RadboudUMC - Nijmegen, Netherlands

Thom Bitter - Raboud University Nijmegen Medical Centre - Nijmegen, Netherlands

Robert Freeman - DePuy International Ltd. - Leeds, United Kingdom

Nico Verdonshot - Radboudumc - Nijmegen, Netherlands

Dennis Janssen - Radboud University Nijmegen Medical Centre - Nijmegen, Netherlands

Introduction

Finite Element Analysis (FEA) allows for the investigation of the primary fixation of cementless implants. Simulation accuracy depends on various parameters, with a pivotal role played by the bone material model. Previous research has shown that both elastic and plastic bone models result in an overestimation of the initial stability of knee implants [1]. The overestimation is thought to result from a lack of substantial bone stress relaxation occurring around the implant [2]. This study integrates bone relaxation into FEA models to assess its impact on the compressive stresses after implantation and pull-off force (a measure of the initial stability) of a femoral component.

Methods

FEA model construction followed Berahmani et al. (2017) [1]. This study incorporated six simulated femoral reconstructions. Actual bone and implant surfaces were modeled to replicate realistic press-fit conditions observed in clinical practice, leading to a cut-dependent interference fit. The simulations contained three phases: Virtual implantation, a resting period, and a pull-off experiment (Figure 1). 54% Bone stress relaxation was implemented using a custom user subroutine, based on our 24-hours experimental measurements [2]. For each model, three situations were analyzed, considering the bone either as elastic, plastic, or plastic-viscoelastic. All simulations were performed using MSC.MARC.

Results

During the implantation phase, in the elastic-only models, bone stresses increased up to 1000 MPa. Incorporating plasticity ensured stresses remained below the local yield stress. Stress relaxation resulted in a reduction of compressive stresses between the bone and implant (Figure 2). During the pull-off phase, the elastic models showed an average pull-off force of 65 kN. Introducing plasticity alone resulted in a pull-off force of 5206 N, which was reduced by another 19% when combined with bone relaxation (Figure 3).

Conclusion

This is the first attempt to incorporate bone plasticity and relaxation in FEA for investigating the primary stability of cementless implants. In the elastic-only models, the pull-off force was highly overestimated. Introducing plasticity resulted in a decrease in pull-off force, while incorporating realistic bone stress relaxation further contributed to its reduction. Validation of our viscoelastic-plastic simulations through pull-off experiments is planned. Apart from its impact on pull-off force, we will assess the effect of bone relaxation on simulations of implant-bone micromotions, both in femoral and tibial reconstructions, with the goal of achieving a more realistic representation of the initial stability in FEA.

References

1. Berahmani et al, J Biomech 61:137-143, 2017.
2. Gersie et al, SSRN E-Journal, 2024.

Acknowledgements

This collaboration project is co-funded by the PPP allowance made available by Health~Holland, Top Sector Life Sciences & Health, to stimulate public-private partnerships, and DePuy Synthes (Leeds, UK).

Figures



Figure 1: On the left, the cutting plane in the coronal plane through the lateral condyle is shown. The cross sections in this article display the perspective towards the center of the femur. On the right, the simulation of the implant pull-off is shown.

Figure 1

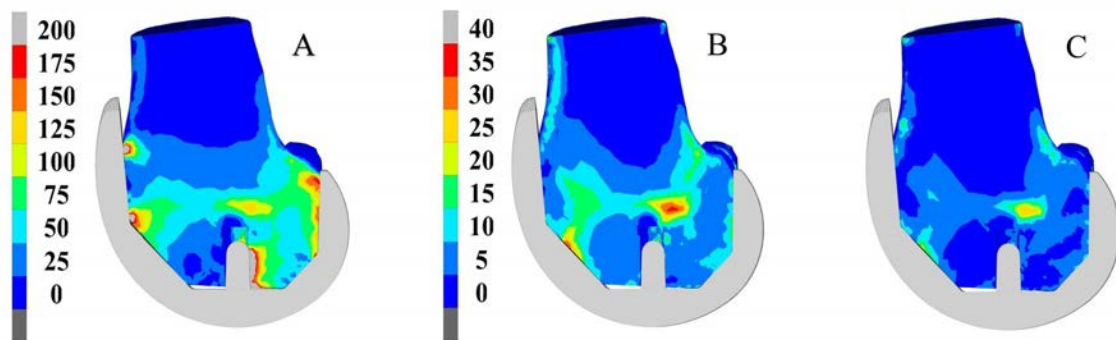


Figure 2: Equivalent von Mises stresses after virtual implantation when the model is sliced through the lateral condyle (visualized in Figure 1). A) Bone stresses when an elastic bone material model is used. B) Bone stresses for a plastic bone material model. C) Bone stresses after stress relaxation when the plastic bone material was considered. NOTE: When incorporating plasticity, the magnitude of bone stresses is one-fifth compared to using an elastic material model.

Figure 2

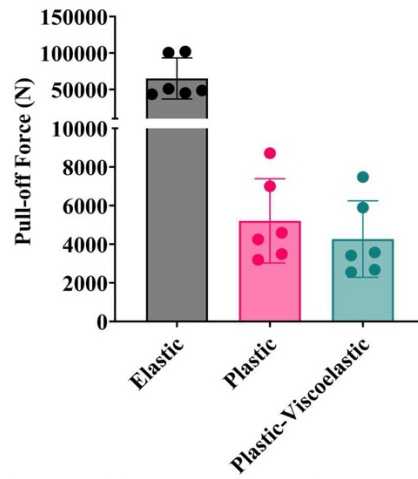


Figure 3: The effect of bone material model on the pull-off force for a femoral component. The pull-off force of an elastic-only material model is up to 8 times higher in comparison to a plastic model. The addition of stress relaxation to the plastic bone material model decreases the simulated pull-off force even more.

[Figure 3](#)

Migration of Cementless Tibial Baseplates Appears to Be Related to Bone Mineral Density

*Fernando Quevedo Gonzalez - Hospital for Special Surgery - New York, USA

Daniel Buchalter - HSS - New York, United States of America

Joseph Lipman - Hospital for Special Surgery - New York, USA

Peter Sculco - Hospital for Special Surgery - New York, USA

Cynthia Kahlenberg - Hospital for Special Surgery - New York City, USA

Eytan Debbi - Cedars-Sinai Medical Center - Los Angeles, USA

Timothy Wright - Hospital for Special Surgery - New York, USA

Jonathan Vigdorichik - Hospital for Special Surgery - New York, USA

David J. Mayman - Hospital for Special Surgery - New York, USA

Introduction

Bone mineral density (BMD) is one of the main determinants of bone's strength. [1] Consequently, BMD could be a useful surrogate for preoperative planning to achieve long-term cementless implant fixation. While our prior research characterized the BMD distribution in TKA patients,[2] the clinically relevant thresholds of BMD for TKA longevity have not been defined. In this way, the motion of the tibial implant in the bone during the first year postoperatively has been related to TKA longevity. Thus, our goal was to relate 1-year postoperative changes in tibial component position to BMD.

Methods

Four patients (1 male, ages 53-66 years, BMI 21.3-27.6 kg/m²) who underwent robotically assisted primary TKA using a cementless tibial baseplate had standard-of-care preoperative CT-scan with a bone density calibration phantom and standard-of-care biplane radiographs (EOS Imaging) at approximately 6 weeks and 1 year after TKA. The three-dimensional geometries of the bone, reconstructed from the CT scans, and the implant geometry, obtained from laser scans of retrieval implants of the same design and size, were projected and manually aligned to the 6-week and-1 year biplane radiographs (Fig. 1). We used a three-dimensional cubic phantom [3] to determine the accuracy of the manual alignment, which was 0.5 mm. To compute the BMD, we used the 6-week biplane radiograph as a reference to determine the implant position relative to the bone. Then, we utilized the calibration phantom to convert the CT-scan Hounsfield Units to mg/cm³ of potassium diphosphate. We limited our analysis to the bone underneath the baseplate (Fig. 2), which we related to the 6-week to 1-year changes in implant position relative to the bone.

Results

The 6-week to 1-year maximum total point motion (MTPM) of the implant from 1.1 mm to 1.5 mm. Patients who experienced greater MTPM had lower BMD under the medial half and anterior-medial quarter of the baseplate (Fig. 3). Interestingly, higher MTPM was associated with higher density under the lateral half as well as posterior-medial and posterior-lateral quarters of the baseplate.

Discussion

Our preliminary results highlight, for the first time, a relationship between BMD and implant migration. This relationship could be useful in establishing clinically relevant

BMD thresholds for preoperative planning. We expect this relationship to strengthen as we include more patients in the analysis.

References: [1] Van der Meulen et al., Bone, 2001; [2] Borsinger et al., JOA, 2024; [3] Knorlein et al., J Exp Biol, 2016

Figures

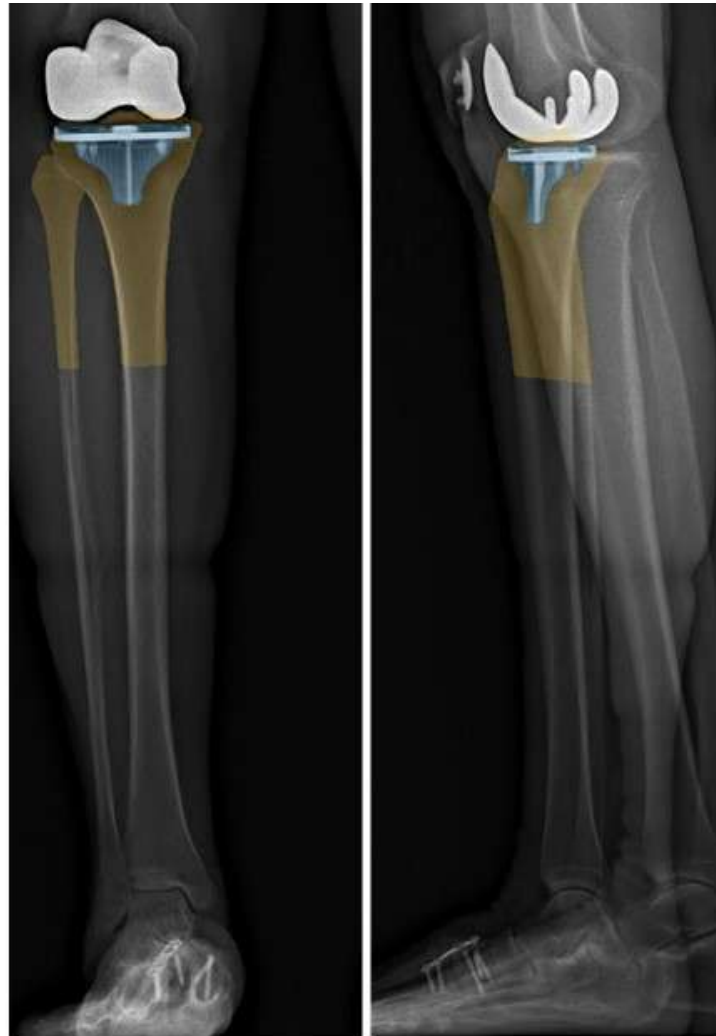


Fig. 1 – Projection and alignment of bone and implant onto biplane radiographs

[Figure 1](#)

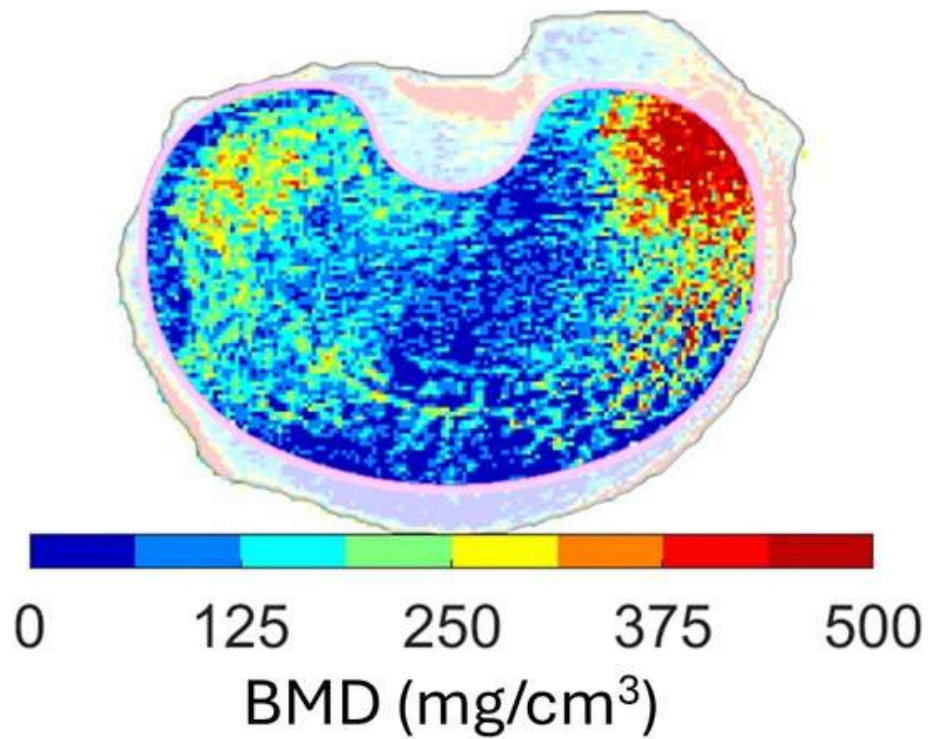


Fig. 2 – Evaluation of BMD underneath the implant baseplate

[Figure 2](#)

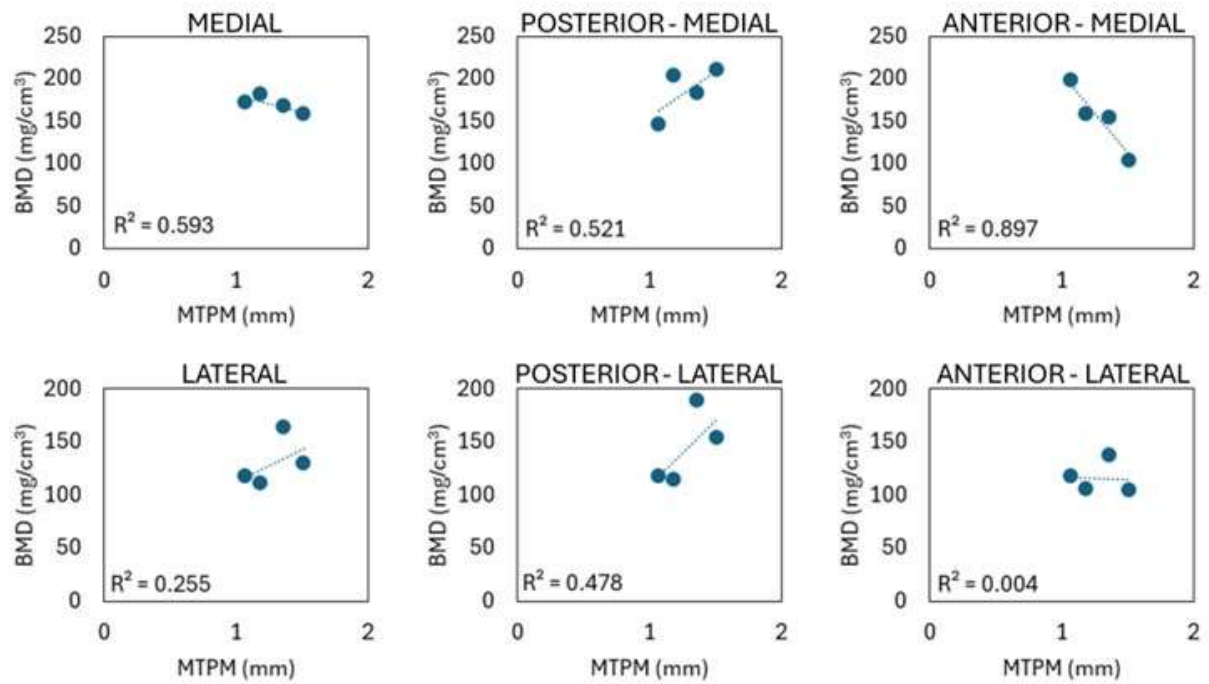


Fig. 3 – Maximum total point motion (MTPM) vs. Bone Mineral Density (BMD)

[Figure 3](#)

Osteoporosis May Not Be an Absolute Contraindication for Cementless TKA

*Ameer Tabbaa - x, United States of America

Gabriel Lama - Maimonides Medical Center - Staten Island, United States of America

Matthew Magruder - Maimonides Medical Center - Brooklyn, USA

Ariel Rodriguez - Maimonides Medical Center - Brooklyn, United States of America

Che Hang Jason Wong - Maimonides Medical Center - Brooklyn, USA

INTRODUCTION

Cementless total knee arthroplasty (TKA) has received growing interest, particularly in younger populations, due to potential long-term survivability and improved bone preservation. Poor bone stock, as seen in osteoporosis, is considered a contraindication for this technique. This study evaluated whether younger patients with osteoporosis undergoing cementless TKA demonstrate similar 1) implant-related complications, 2) medical complications, 3) readmission rates, and 4) 3-year implant survivability.

METHODS

A retrospective query of a national administrative claims database was performed between 2010 and 2022 for patients who have a diagnosis of osteoporosis and underwent primary TKA. Patients who were less than or equal to 75 years old and underwent uncemented TKA were propensity score matched to controls based on age, gender, obesity, and Charleston Comorbidity Index (CCI), which produced 7,923 patients (1,321 uncemented, 6,602 cemented). Multivariate logistical regressions were used to evaluate the following outcomes: 90-day and 2-year implant-related complications, 90-day post-operative medical complications, and 90-day readmissions. Kaplan-Meier survival analysis was conducted to assess 3-year all-cause revision implant survivability.

RESULTS

There were no statistically significant differences in implant-related complications, medical complications, readmissions, and lengths of stay between cementless and cemented TKA groups. Kaplan-Meier analysis demonstrated statistically similar 3-year survivability between cohorts (cemented = 97.6%, CI 96.6-98.5; cementless = 97.2%, CI 96.7-97.7; $p = 0.472$).

DISCUSSION AND CONCLUSION

Patients with osteoporosis have equivalent medical and implant-related complications as well as 3-year implant survival following cementless TKA compared with a cemented technique. Our results support cementless TKA as a viable option for younger patients regardless of prior diagnosis of osteoporosis. Intraoperative decisions regarding bone quality are still necessary to discriminate between those who are candidates for cementless TKA with those who are not.

Assessing Total Knee Arthroplasty Fixation Strength Using Inducible Displacement Measurements From Weight-Bearing CT-Based Radiostereometric Analysis

*Rebecca Hext - Western University - London, Canada

Bart Kaptein - LUMC - Leiden, Select Country

James Howard - London Health Sciences Centre - London, Canada

Brent Lanting - London Health Sciences Centre - London, Canada

Matthew Teeter - Western University - London, Canada

Introduction: Implant designs and surgical techniques have been improving, however aseptic loosening remains one of the top causes of revision total knee arthroplasty (TKA). Radiostereometric analysis (RSA) is the gold standard to assess for loosening and can be used to measure inducible displacement, defined as the magnitude of component micromotion between loaded and unloaded scans at a single time point. Inducible displacement is thought to relate to how well-fixed components are, therefore, these exams are useful in assessing instantaneous fixation strength. RSA has several limitations, restricting its use to research. Weight-bearing computed tomography (WBCT) has been increasing in availability and new methods have allowed RSA-like measurements to be performed with widely available clinical CT scanners, referred to as CT-RSA. The objective of this study is to validate the use of a novel WBCT-RSA approach compared to conventional RSA for inducible displacement measurements of TKA.

Methods: A prior RSA study recruited participants (n=16) to undergo a cementless TKA and return for imaging follow-ups up to 5 years post-operation. At 5 years post-operation, both supine and standing RSA exams, and seated (with leg extended) and standing WBCT exams were performed to enable inducible displacement measurements. Double examinations to measure precision were performed in the supine (for RSA) and seated (for WBCT-RSA) positions. RSA exams were measured with model-based RSA (MBRSA), and the WBCT exams were measured with CT-RSA software (V3MA). Translations, rotations, and maximum total point motion (MTPM) of the tibial component between loaded and unloaded exams were calculated and compared between RSA and WBCT-RSA.

Results: The mean yearly migration (MTPM) rate from one to five years post-operation was 0.08 ± 0.03 mm/year. For the tibial component, the mean \pm SD MTPM of precision measurements for the WBCT-RSA exams was 0.113 ± 0.070 mm and was 0.175 ± 0.069 mm for RSA ($p = 0.025$) (Figure 1). The mean \pm SD MTPM of inducible displacement measurements was 0.218 ± 0.197 mm for WBCT-RSA and was 0.638 ± 0.238 mm for RSA ($p = 0.0004$) (Figure 2).

Conclusions: WBCT-RSA displayed significantly better precision than RSA for the double examinations. WBCT-RSA also found a lower magnitude of inducible displacement of these well-fixed tibial components, potentially indicating superior accuracy as a diagnostic tool for aseptic loosening. This study is the first to compare inducible displacement measurements using WBCT-RSA to the gold-standard of conventional RSA. Further studies should examine loose components to establish a diagnostic threshold for loosening using WBCT-RSA.

The Stability of Cementless Tibial Trays During Functional Activities Is Explained by Variations in Bone Quality and Surgical Preparation

*Philip Noble - Institute of Orthopedic Research and Education - Houston, USA

Sabir K. Ismaily - UTHealth - Houston, USA

Shuyang Han - University of Texas Health Science Center at Houston - Houston, USA

Hugh Jones - UT Health Science Center at Houston - Houston, USA

Rikin Patel - Institute of Orthopedic Research & Education - Houston, USA

Jonathan E. Gold - UTHealth - Houston, USA

Introduction

Despite the overall success of total knee arthroplasty, failure rates approaching 20% are reported in patients under 55 years at 20 years after surgery. Attempts to improve these results via cementless tibial fixation have been met with mixed results. The underlying causes have not been elucidated using experimental and computational simulations that assume ideal surgical preparation and patient selection. To address this dilemma, we performed micromotion experiments using fresh cadaveric specimens prepared and tested under realistic conditions.

Methods

Eight experienced knee surgeons implanted a single design of cementless total knee replacement (Persona TM, ZimmerBiomet) in 16 fresh cadaveric knees using standard manual instruments. At each step of the procedure, factors potentially influencing cementless implant stability were monitored, including the flatness of the osteotomy, the alignment of the fixation holes within the tibia, and the orientation of the tray during impaction. The density of bone within the tibia and surrounding the pegs was measured using qCT. Each implant/bone construct was mounted in a multi-axial functional activity simulator and subjected to dynamic loads and motions simulating walking and stair descent. 3D motion at circumferential sites around the bone-tray interface was measured using digital image correlation.

After completion of micromotion testing, each implant-bone specimen was embedded in epoxy and sectioned to allow measurement of gaps over the implant-bone interface. Statistical analysis of our results was performed to isolate the effect of surgical technique and bone quality on interface micromotion.

Results

Large variations in migration and interface micromotion were observed between specimens, measurement sites and functional activities. The maximum value of tray-bone micromotion averaged 178 \pm 19 mm during stair descent and 149 \pm 22mm during walking. Step-wise multivariate regression showed that 85% of the variation in micromotion could be explained by 3 independent factors:

1. the flatness of the osteotomy surface ($r^2=0.462$, $p<0.001$).
2. the relative density of the medial and lateral tibial condyles ($r^2=0.250$, $p<0.001$), and
3. the degree of misalignment of the tray during impaction ($r^2=0.141$, $p=0.001$)

Conclusions

1. The stability of cementless tibial trays is primarily controlled by variations in the stiffness of cancellous bone across the tibial surface and the distribution of contact between the flat under-surface of each tray and the osteotomy.
2. Developments increasing bony contact, including robotic assistance, are expected to increase initial cementless stability.

Is the Tibia Mechanical Axis the Correct Landmark to Minimize Risk of Tibia Loosening?

*Nathan Lenz - Smith & Nephew - Memphis, USA

William Fugit - Bartlett, United States of America

Introduction:

Interest in kinematic alignment is growing seeking improved ligament balance and stability by preserving the native limb alignment and joint line and limiting ligament releases. Resecting the tibia more than 3° from mechanical alignment with kinematic alignment may increase the risk of loosening. This concern led to restricted kinematic alignment which limits the hip-knee-ankle angle and the deviation of the tibia and femur resections from their respective mechanical axes hoping to limit tibia bone-to-implant interface shear loads. Given the bodyweight load aligns with the leg mechanical axis from the hip to the ankle regardless of the hip-knee-ankle angle, we hypothesize that aligning implant resections perpendicular to the leg mechanical axis when preserving constitutional varus or valgus will cause less change in tibia medial-lateral shear than aligning the tibia perpendicular to the tibia mechanical axis.

Methods:

A computational analysis was performed simulating 0-120° knee flexion using previously validated software (LifeMOD/KneeSIM; LifeModeler Inc.). Scenarios for 0°, 5°, and 10° constitutional varus and valgus were created by moving the hip and ankle joints medial for varus and lateral for valgus from their mechanical alignment positions. The quadriceps origin was moved with the hip joint while all anatomy at the knee joint was unchanged for comparison purposes. Two PS TKAs were tested: one with a 3° asymmetric joint line and one with a symmetric joint line. Each constitutional alignment was evaluated with tibia perpendicular to the tibia mechanical axis and to the leg mechanical axis (Figure 1). The femur was aligned relative to the tibia for rectangular flexion-extension gaps. The tibia bone-to-implant medial-lateral shear load was compared for each analysis. The resulting tibia joint line orientation was calculated (Table 1).

Results:

Tibia bone-to-implant medial-lateral shear load increased in the medial direction with knee flexion for all scenarios and implant alignments. Tibia shear was more medial for constitutional varus and less medial for constitutional valgus when the tibia implant was aligned perpendicular to the tibia bone mechanical axis than when aligned to the leg mechanical axis (Figure 2). Tibia medial-lateral shear was similar for 0°, 5°, and 10° varus but increased with increasing valgus when the implant was aligned to the leg mechanical axis. The same trends were observed for symmetric and asymmetric joint line TKA. The femur and tibia joint line angles for the 5° varus and valgus leg mechanical alignment scenarios of the 3° asymmetric joint line TKA are similar to average constitutional varus and valgus population [1].

Conclusions:

When aligning a TKA in constitutional varus, the tibia bone-to-implant medial-lateral shear load is reduced by aligning the tibia implant perpendicular to the leg mechanical axis running between the hip and ankle centers, which is varus to the tibia mechanical axis. Furthermore, the resulting joint line when using an asymmetric joint line implant is close to average anatomical data when the tibia is

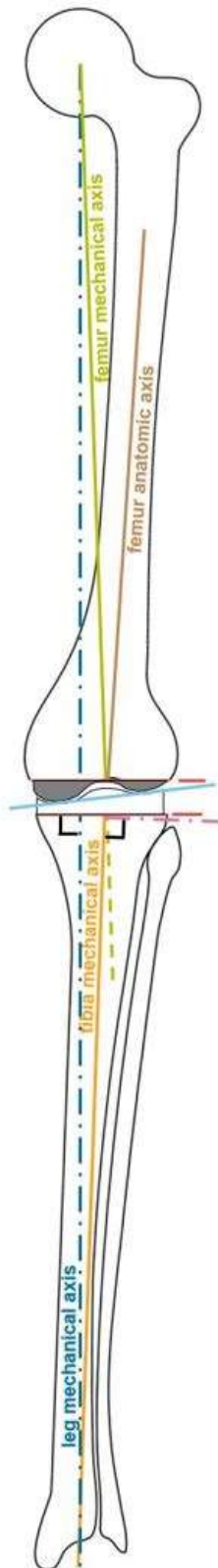
aligned to the leg mechanical axis suggesting that kinematic alignment of an asymmetric joint line implant could result in less risk of tibia loosening.

References:

1. Bellemans CORR. 2012;470(1):45-53.

Figures

(a)



(b)

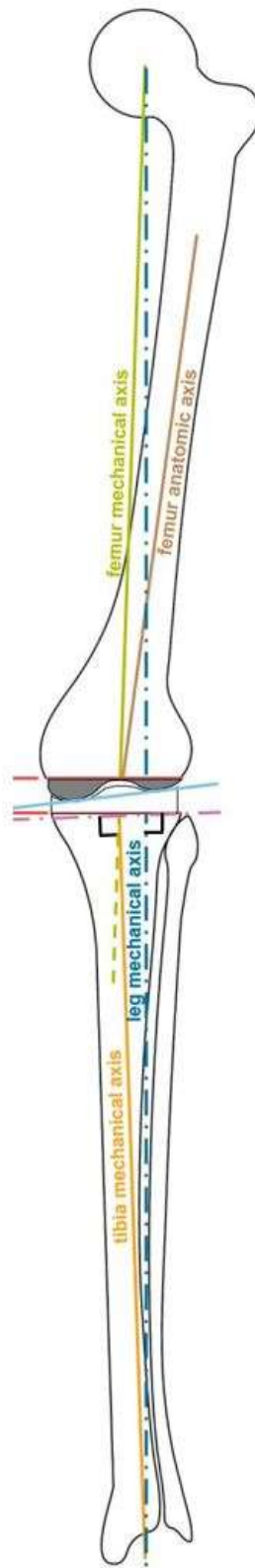


Figure 1: (a) Varus knee with tibia resection perpendicular to leg mechanical axis. (b) Valgus knee with tibia resection perpendicular to leg mechanical axis.

[Figure 1](#)

Table 1: Femur and tibia joint line angles for 10° varus to 10° valgus hip-knee-ankle scenarios when aligning the joint resections to the tibia mechanical axis or the leg mechanical axis for a 3° asymmetric joint line TKA

Scenario	Tibia Mechanical Aligned				Leg Mechanical Aligned			
	Mechanical Lateral Distal Femoral Angle (°)		Medial Proximal Tibia Angle (°)		Mechanical Lateral Distal Femoral Angle (°)		Medial Proximal Tibia Angle (°)	
	Asymm	Symm	Asymm	Symm	Asymm	Symm	Asymm	Symm
TKA design								
10° varus	97	100	87	90	92	95	82	85
5° varus	92	95	87	90	89.5	92.5	84.5	87.5
0°	87	90	87	90	87	90	87	90
5° valgus	82	85	87	90	84.5	87.5	89.5	92.5
10° valgus	77	80	87	90	82	85	92	95
Avg. varus 4.45° [1]					89.03		85.13	
Avg. valgus 3.56° [1]					85.45		89.06	

Figure 2

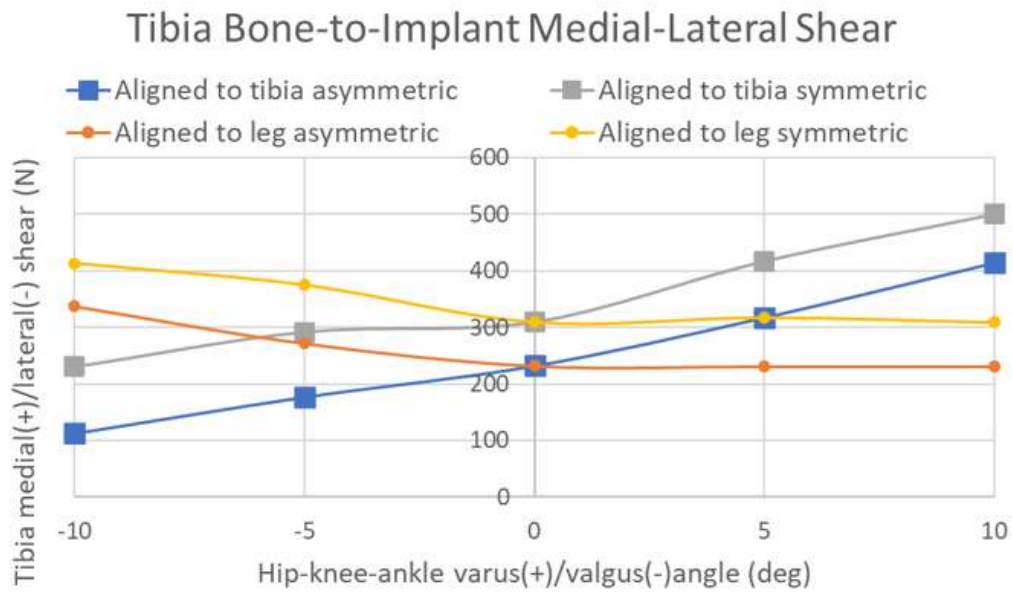


Figure 2: Tibia shear vs. hip-knee-ankle angle when aligning tibia resection to the tibia or leg mechanical axis

Figure 3

Radiographic Evaluation of Bony Ingrowth of Highly Porous Cups; a Study of 47 Patients Cadaveric Pelvises

*Jonathan Katzman - NYU Langone - New York, United States of America

Benjamin Schaffler - NYU Orthopedic Hospital - New York, USA

Akram Habibi - NYU Langone Orthopedic Hospital - New York, United States of America

Ran Schwarzkopf - NYU Langone Medical Center Hospital for Joint Diseases - New York, USA

Introduction: Highly porous, cementless acetabular components are reported to have high levels of osseointegration, and strong, long-lasting fixation in total hip arthroplasty (THA). No study has evaluated the degree of bony integration needed for successful acetabular component fixation that last the entirety of the patient's life. The purpose of this study was to radiographically evaluate osseointegration of acetabular implants in cadaveric specimens donated by patients who with well-fixed and well-functioning THAs at time of death.

Methods: 47 cadaveric pelvis specimens containing 47 THAs were donated as anatomical gifts from patients who previously underwent primary THA at a single institution over the last 30 years. All 47 specimens underwent a set of pelvic oblique radiographs, CT scans, and MRI which were reviewed by an orthopedic surgeon and a musculoskeletal radiologist. Percentage of bony contact with each cup was quantified. Linear regressions were performed to evaluate if there was a relationship between number of years implanted and percent of cup ingrowth.

Results: Acetabular implants were in place for an average of 10.1 years at time of death with a range of 1.18 to 25.47. Average bony ingrowth in the acetabular components was 82% with a range of 50-100%. Most common places for lucency or bone loss were medial wall with or without medial perforation (17 cases, 36%) and the posterosuperior quadrant (14 cases, 29.8%). Linear regression demonstrated that there was no correlation between implant years and the degree of lucency (95% CI -0.54, 0.84, $p=0.658$).

Conclusion: In a radiographic analysis of 47 well-fixed cups in donated cadaver pelvises, acetabular components remained well-fixed for the duration of the patient's life with a mean bony ingrowth of 82% and could remain well-fixed with as little as 50% bony integration. There was no correlation between years implanted and degree of osseointegration over a 1 to 25-year range.

Figures

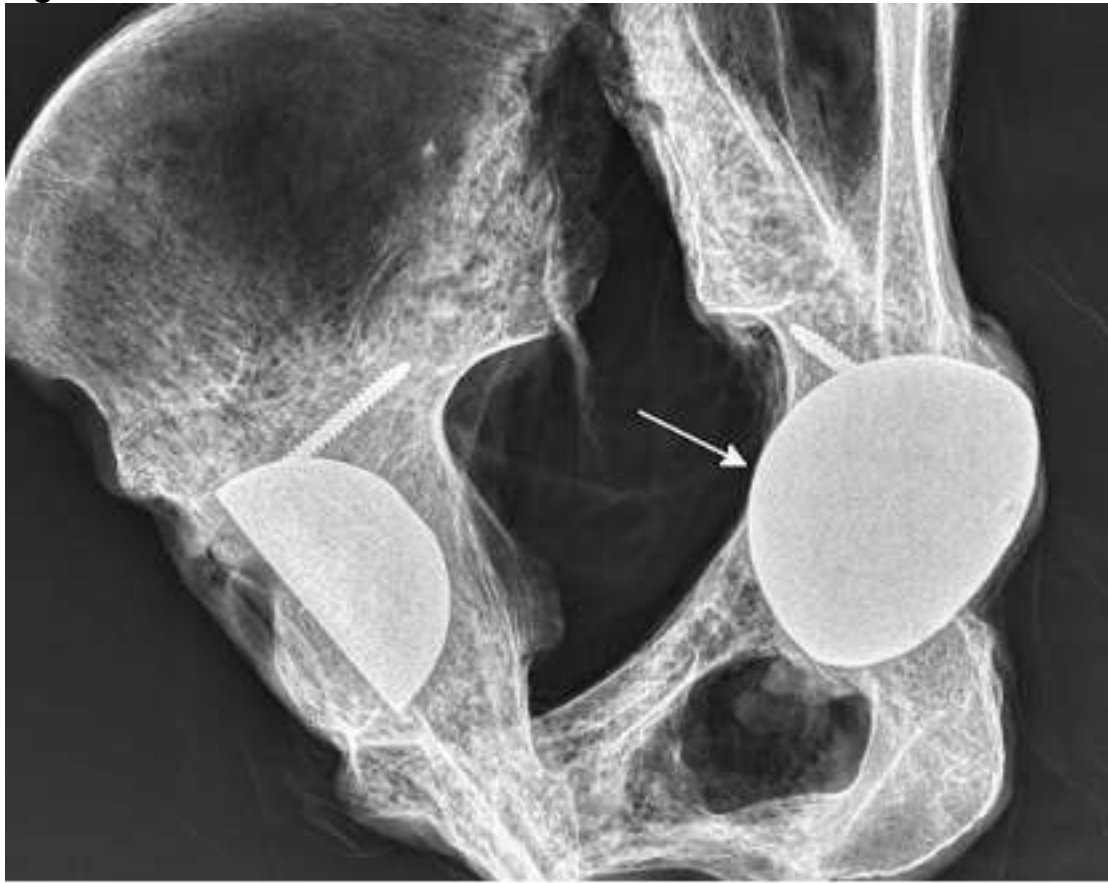


[Figure 1](#)

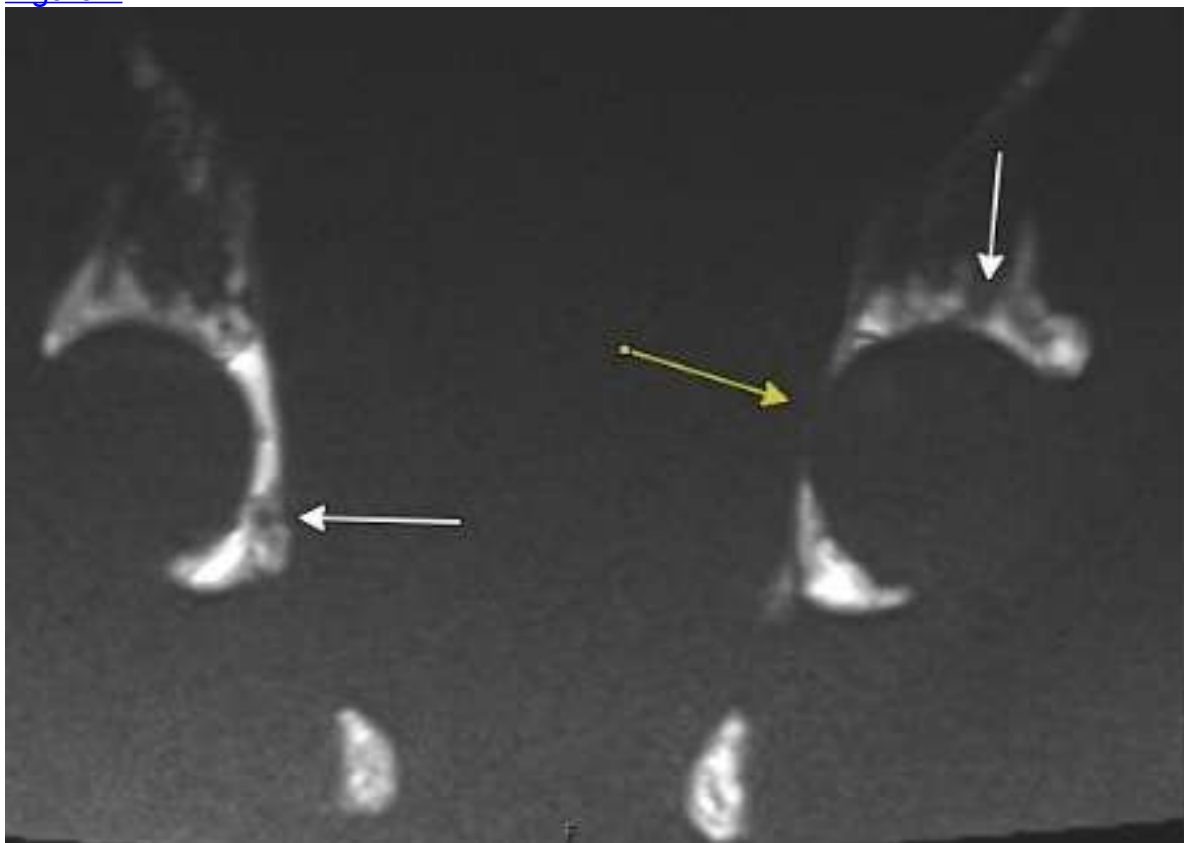


[Figure 2](#)

Targeted Rehabilitation Program Based on a Knee Kinesiography Exam Can Improve Outcomes and Accelerate Achievement of Patient Well-Being After Total Knee Arthroplasty

Pierre Ranger - Hopital Jean-Talon - Montreal, Canada

*Alix Cagnin - Emovi Inc - Montreal, Canada

Bianca Marois - Emovi - Montreal, Canada

Alex Fuentes - Emovi - Montreal, Canada

Introduction: Up to 20% of patients express dissatisfaction after total knee arthroplasty (TKA) surgery due to sub-optimal outcomes. While typical post-TKA rehabilitation programs emphasize on knee strengthening and mobility, studies suggest that targeting knee functional residual deficiencies should be a priority since knee biomechanical markers during weight-bearing activities have been linked to clinical outcomes and patient satisfaction post-TKA. Therefore, this study assessed the impact of a targeted rehabilitation program guided by a knee kinesiography exam on clinical outcomes after TKA.

Methods: Patients were contacted following their surgery at a private orthopaedic ambulatory surgical center (ASC) in Canada. They were invited to come back 3 months post-surgery for a one-hour session at the ASC during which a knee kinesiography exam with the KneeKG® system (Emovi, Canada) was performed to assess their knee function during walking (Figure-1). A home-based exercise program targeting the identified three-dimensional knee biomechanical markers was explained during the session and access to online instructional videos was provided. A follow-up call was planned after 2 weeks to adjust, if necessary, the exercise program. Patients who could not come back at the ASC followed standard rehabilitation which could include exercises and were asked to complete questionnaires as controls. All patients completed the Knee Osteoarthritis and Injury Outcome Score for Joint-Replacement (KOOS-JR) and a satisfaction level questionnaire 3 and 6 months after surgery. The patient acceptable symptom state (PASS) criteria was used on the KOOS-JR to identify patients who considered themselves well 6 months after TKA (i.e., $KOOS-JR \geq 71.0$). T-tests (paired and independent) were used to assess intra-/inter-group differences on the KOOS-JR and Chi-square tests for PASS and satisfaction levels.

Results: Sixteen (16) patients participated (rehabilitation: N=10, control: N=6). There was 75.0% of women (mean age: 68.9 years (95%CI:64.0;73.9), BMI: 30.8 kg/m² (26.2;35.3). Most patients who followed the rehabilitation program (80%) reported high adherence as they performed their home-based exercises minimum several times per week. They reported significant improvement on the KOOS-JR (+9.8, $p=0.001$) leading to higher scores compared to the control group at 6 months post-surgery (78.6 vs 69.3, $p=0.07$). Five out of the 8 questions from the KOOS-JR were significantly improved in patients who followed the targeted rehabilitation program (all $p \leq 0.05$). The proportion of patients who met the PASS criteria was significantly higher in the rehabilitation group as 90% already achieved the absolute level of patient well-being 6 months after TKA (vs 33% of patients following standard rehabilitation, $p=0.04$). Although the rehabilitation group demonstrated higher patient satisfaction, with 100% reporting being satisfied with their care, this difference did not reach statistical significance when compared to the control group (75%, $p=0.33$).

Conclusion: Findings suggest that a targeted home-based rehabilitation program, guided by a knee kinesiography exam, can improve outcomes post-TKA and

accelerate achievement of functional milestones and well-being. While future research with larger sample sizes and longer follow-up periods are needed to confirm these findings, these results highlight the added value of a knee kinesiography exam to provide patients with insights and personalized recommendations on their dynamic knee function following surgery.

Figures



Figure-1. A knee kinesiography exam in a clinical setting.

[Figure 1](#)

Controlling and Enhancing the Post Operative Care After Knee Arthroplasty: Insights From a Multi-Center Prospective Longitudinal Cohort Study of a Digital Rehabilitation Solution

*Julien Lebleu - moveUP - Brussels, Belgium

Andries Pauwels - moveUP - brussels, Belgium

Stefaan Van Onsem - Ghent University Hospital - Ghent, Belgium

Philippe Van Overschelde - Hip & Knee Clinic AZ Maria-Middelares Gent - Sint-Martens-Latem, Belgium

Jared Weir - DeepStructure - Saginaw, USA

Introduction: New surgical techniques, such as robotics and augmented reality, promise to increase the quality and reduce the variability of the surgical procedure. But the effect of these new developments could be altered by the variability of the post operative care. Rehabilitation following total knee replacement (TKA) traditionally involves in-person therapy, presenting challenges in terms of protocol adherence, reproducibility, and cost. Digital rehabilitation holds promise in addressing these issues, but existing systems often lack personalization, neglecting factors such as patient pain, participation, and recovery speed. Moreover, most digital platforms lack essential human support.

This study aimed to explore the engagement, safety, and clinical effectiveness of a personalized and adaptive app-based human-supported digital monitoring and rehabilitation program.

Method: Conducted as a prospective multi-center longitudinal cohort study, 127 patients were enrolled. A smart alert system managed undesired events, triggering physician interventions in case of suspected issues. The app collected data on dropout rates, complications, readmissions, Patient-Reported Outcome Measures (PROMS), and patient satisfaction.

Results: Results showed a 2% readmission rate, with smart alerts potentially preventing 85% of flagged issues through timely doctor interventions. Program adherence reached 77%, and 89% of patients endorsed the program's use.

Significant improvements were found at six months postoperative in all the KOOS sub-scales (14 points in KOOS Pain, 20 in KOOS-Symptoms, 22 in KOOS-Function, and 26 in KOOS-QoL). To the question: "Would you choose digital rehabilitation again?" 89% of the patients answered yes. Adherence to the exercise program was 79%.

Conclusion: The integration of personalized, human-backed digital solutions emerged as a transformative approach to standardize and enhance the rehabilitation journey post-TKA, while showing potential cost savings. Furthermore, when using this app-based digital rehabilitation program, a higher adherence rate to home exercises was reported than traditional rehabilitation, while patient-reported outcomes were still significantly improved. The implementation of this digital monitoring and rehabilitation program underscores its potential applicability within the framework of the Remote Therapeutic Monitoring (RTM) reimbursement system in the United States.

Is Markerless Motion Analysis a Valid Tool to Study Knee Joint Kinematics?

*Markus Wimmer - Rush University - Chicago, USA

Ariana Ortigas Vasquez - Aesculap AG - Tuttlingen, Germany

Christopher Knowlton - Rush University Medical Center - Chicago, USA

Michael Utz - Aesculap AG - Tuttlingen, Germany

Adrian Sauer - Aesculap AG - Tuttlingen, Germany

Camilla Antognini - University of Illinois Chicago - Chicago, United States of America

Introduction: Markerless motion analysis is a promising alternative to traditional marker-based motion capture to assess patients' function following total joint replacement. While allowing faster measurements with excellent repeatability, markerless measurements have shown kinematic differences when compared with marker-based technology. The possible influence of local frame orientation and position on the kinematic interpretation of the results hasn't been investigated. The aim of this study is to apply a reference frame alignment method ("REFRAME") to understand whether waveform inconsistencies between markerless and marker-based knee kinematics are related to differences in local frame orientation and position.

Methods: Ten healthy subjects (5/5 M/F, age 27 ± 8 , 22.16) were recruited to perform five walking trials each. Reflective markers were placed according to Qualisys' sporting full-body marker-set. Data was simultaneously recorded using eight video cameras (Miquis, Qualisys) for the markerless capture system (Theia3D), and twenty-four cameras (Oqus and Arqus, Qualisys) of the marker-based system (Qualisys). Both sets of processed data were exported for kinematic analysis in Visual3D (C-Motion). Joint angles were then compared using root mean square error (RMSE) before and after REFRAME optimization.

Results: After implementation of the REFRAME approach, the optimization of the markerless kinematics signals toward the marker-based led to an average rotation of the tibia coordinate system of 13.8° and 4.9° around the y- and z-axes, respectively, and of 5.3° , 5.8° and 7.9° for the femur coordinate system around the x-, y-, z-axes, respectively (Fig. 1). Results after REFRAME show improved agreement between markerless and marker-based capture data in all three planes, with a decrease in RMSE in the sagittal plane, from 3.9° to 1.7° , in the frontal plane, from 6.1° to 1.7° , and in the transverse plane, from 10.2° to 2.5° (Fig. 2).

Conclusion: To assess the function of knee prostheses, patient specific joint kinematics play an important role. Hence, valid measurement tools need to agree with each other. In this study, RMS errors between markerless and marker-based measurement systems dropped significantly after REFRAME optimization. This suggests that both markerless and marker-based kinematic waveforms represent the same underlying information, validating markerless motion capture for future studies of the knee joint.

Figures

Table 1: Rotations of the markerless femoral and tibial reference frames to minimize the RMSE between the markerless and marker-based rotational waveforms. The femoral flexion axes were fixed a priori.

	Femur	Tibia
Flexion Axis (+:extension)	$0 \pm 0^\circ$	$-5.3 \pm 2.8^\circ$
Anterior-posterior axis (+: Adduction)	$6.0 \pm 2.5^\circ$	$12.6 \pm 2.5^\circ$
Proximo-distal axis (+: internal rotation)	$-7.3 \pm 4.7^\circ$	$5.6 \pm 3.6^\circ$

Figure 1

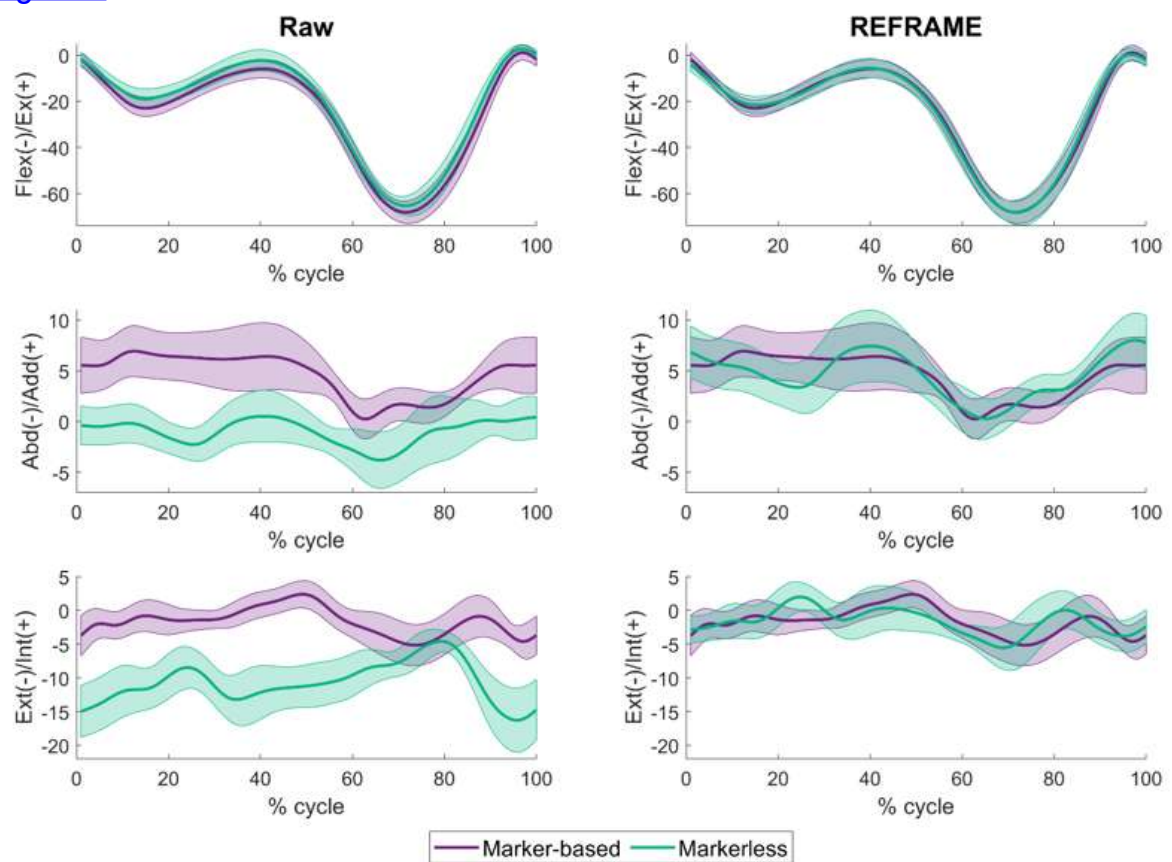


Figure 2: Rotational waveforms of the knee in all three planes for marker-based and markerless systems before (left column) and after (right column) REFRAME optimization.

Figure 2

Patient Characteristics and Pre-Operative Gait Speed as Useful Factors to Separate Recovery Curves Generated by a Smart Implant

*Roberta Redfern - Zimmer Biomet - Pemberville, USA

Karl Surmacz - Zimmer Biomet - Swindon, United Kingdom

Joseph Brook - Zimmer Biomet - London, United Kingdom

Mike Anderson - Zimmer Biomet - Lehi, USA

Jason Cholewa - Zimmer Biomet - Warsaw, USA

Adam Henderson - Zimmer Biomet - Winterthur, Switzerland

Introduction

Patients desire feedback to benchmark their recovery progress following joint arthroplasty procedures, requiring creation of similar cohorts of patients for accurate comparisons. Technological advances including smartphones and implantable sensors within the tibial stem that utilize accelerometers and gyroscopes for passive collection of data have the potential to give insight into a patient's progress following total knee arthroplasty (TKA). This analysis aimed to determine which patient characteristics can be used to separate recovery curves generated by the sensors within a tibial stem extension implanted during TKA.

Methods

Anonymized data from a commercial database were analyzed to investigate the ability to separate 2,472 patients into cohorts based on age, sex, body mass index (BMI, kg/m²), and pre-operative gait speed, as well as combinations of these factors. Gait metrics collected through 60-days post-operative by the tibial stem extension included knee range of motion (ROM), tibial ROM, cadence, gait speed, stride length, step counts, and average distance. Separation of these metrics by cohorts was measured by Kolmogorov-Smirnov test to investigate which defined cohorts could be best used to stratify patient recovery curves.

Results

Considering average knee ROM, the most impactful single cohort factor was sex, with the age/sex as the strongest cohort pair to separate ROM recovery over time ($p < 0.001$) and was not affected by the addition of pre-operative gait speed. Tibial ROM was well stratified by sex and BMI as separate factors for cohort creation, with age/sex pairing as the strongest significant cohort definer. Cohort pairs using sex/BMI and sex/age conferred similar results to separate cadence over time, however, were not significant for comparisons at most timepoints evaluated. Post-operative gait speed and stride length were both easily separated by all cohort factors alone, as well as all pairings ($p < 0.001$), with pre-operative gait speed providing a stronger impact than any other characteristic. Pre-operative gait speed was also the most impactful factor in separation of patients into cohorts considering recovery curves for cadence, step counts, and average distance walked.

Discussion

Patient gait recovery curves can be stratified based on demographic variables, which is strengthened by the addition of pre-operative gait speed considering post-operative cadence, gait speed, stride length, step counts, and average distance walked. Importantly, this analysis demonstrates the feasibility of collecting data from wearable devices in tandem with implanted sensors to better evaluate recovery following TKA, which may allow for improved patient progress feedback to clinicians and patients.

Variability of in-Clinic and Sensor-Based Free-Living Gait Outcomes in Total Knee Arthroplasty Candidates

*[Annemarie Laudanski - Dalhousie University - Halifax, Canada](#)

Michael Dunbar - Dalhousie University - Halifax, Canada

Glen Richardson - Dalhousie University & Capital Health - Halifax, Canada

Jennifer Leighton - NSHA - Dartmouth, Canada

Janie Wilson - Dalhousie University - Ancaster, Canada

Introduction

The outcomes of standardized surgical approaches currently utilized in total knee arthroplasty (TKA) for many reflect an inconsistency in restoring healthy in vivo function to the knee, with minimal improvements observed between pre- and post-operative biomechanical metrics and functional deficits in gait for the majority after surgery. Patient heterogeneity in these outcomes and advances in robotic-assisted arthroplasty support the need for evidence to incorporate patient-specific biomechanics into tailored surgical planning. Gait outcomes have primarily been measured in controlled environments over limited durations, and may not reflect in vivo gait biomechanics, nor their variability throughout the day. The objective of this study was to characterize the variability across and correlations among in-clinic and free-living gait metrics in patients awaiting TKA to inform efforts in knee arthroplasty patient phenotyping.

Methods

Patients with end-stage knee OA scheduled for robotic-assisted knee arthroplasty were recruited to perform a one-minute self-paced walking bout in-clinic. Stride length, gait speed, and frontal and sagittal plane knee angles during walking were calculated with a hallway-installed markerless motion capture system (Sony; Theia Markerless). A tri-axial accelerometer was attached to the pre-surgical shank (Axivity, AX6) to monitor free-living accelerations and physical activity (PA) outcomes over the subsequent seven-days. Free-living step counts and activity intensities across the central six-days were computed in addition to total shank accelerations and functionally aligned frontal plane accelerations for ten strides segmented from data collected during the second day. To characterize variability, a coefficient of correlation (CV, standard deviation / mean) was calculated for all in-clinic and free-living outcomes (Table 1) and these were compared to key clinic-based kinematic measures through Pearson's correlation coefficients (r).

Results

Twenty-two participants (8f/14m; 69.3 ± 6.29 years; 1.70 ± 0.13 m; 96.2 ± 19.8 kg) were included. Means, standard deviations, and CVs for all in-clinic and free-living gait metrics have been included in Table 1 in addition to the correlation results. In clinic, variability correlated with decreased flexion angle ranges, shortened strides, and slower gait, all measures traditionally associated with more severe OA. In free-living, variability in sedentary time increased with faster gait speeds (in clinic), total shank acceleration variability was associated with increased flexion and adduction joint angle ranges, while variability in stride time was associated with stiffer gait kinematics (in clinic), and frontal plane acceleration variability was associated with shorter stride lengths and slower walking speeds (in clinic).

Conclusions

The differences in variability across in-clinic and free-living gait measures emphasizes the need for caution when applying laboratory-based or in-clinic analyses to sensor-based measures. The impact of high stride-to-stride variability in free living gait on TKA outcomes is not currently known, yet is likely to influence the interpretation of traditional gait metrics collected outside of clinical settings. Therefore, future research into the influence of variability on surgical outcomes and its potential to complement in-clinic measures is required as we move towards patient-specific surgical planning.

Figures

Table 1. Pearson's correlation coefficients (*r*) between in-clinic gait knee metrics (flexion and adduction kinematics, stride length, and gait speed) relevant to patient total knee arthroplasty kinematic outcomes correlated with in-clinic and free-living coefficients of variation (CV). Bolded values represent moderate to strong correlations with significant results denoted by a * ($\alpha = 0.05$). Metrics have been defined during early stance (ES), stance (St), swing (Sw), from initial contact to peak acceleration (ICP), and across the entire stride cycle (Str). SD = standard deviation, Acc = acceleration.

	Mean (SD)	CV (%)	Peak Flexion ^{ES}	Flexion Range St	Peak Flexion ^{Sw}	Flexion Range ^{ICP}	Peak Extension ^{ES}	Peak Adduction St	Adduction Range St	Mean Stride Length (m)	Mean Gait Speed (m/s)
			16.9 (2.3)	11.9 (5.1)	56.3 (2.5)	52.6 (6.6)	7.7 (1.7)	4.9 (1.0)	3.5 (1.8)	1.2 (0.04)	1.1 (0.04)
Peak Flexion St (°)	15.5		-0.74*	-0.62*	-0.21	0.03	-0.44*	-0.27	-0.26	-0.18	-0.10
Peak Flexion ^{Sw} (°)	4.6		-0.34	-0.32	-0.66*	-0.49*	-0.22	0.12	0.30	-0.47*	-0.47*
Peak Extension ^{ES} (°)	24.8		-0.59*	-0.54*	0.04	0.15	-0.13	-0.17	-0.60*	-0.12	-0.14
Peak Adduction St (°)	13.3		0.00	0.00	-0.09	-0.01	0.01	0.33	-0.10	-0.05	0.12
Mean Stride Length (m)	3.5		0.08	-0.21	-0.18	-0.41	0.48*	-0.10	-0.18	-0.40	-0.45*
Daily Step Counts	6243.9 (1747.4)	31.2	0.05	0.24	0.12	0.27	-0.21	0.10	0.27	0.11	0.21
Average Daily % Sedentary	77.9 (5.2)	6.8	0.10	0.14	0.24	0.20	0.13	0.08	-0.17	0.26	0.45*
Free Living Stride Time (s)	1.4 (0.2)	13.3	0.33	0.12	-0.33	-0.48*	0.52*	0.08	0.13	-0.06	-0.17
Peak Total Shank Acc ^{ES} (m/s ²)	7.0 (2.3)	34.4	0.47*	0.48*	0.18	0.08	0.24	0.20	0.31	0.18	0.04
Peak Total Shank Acc St (m/s ²)	8.1 (1.9)	24.2	0.32	0.48*	0.03	0.06	0.10	0.28	0.38	0.35	0.29
Peak Total Shank Acc ^{Sw} (m/s ²)	9.0 (1.8)	20.0	0.26	0.41	-0.12	-0.03	0.03	0.32	0.48*	0.35	0.24
Range of Total Shank Acc ^{ICP} (m/s ²)	6.3 (2.3)	38.0	0.43*	0.41	0.12	0.02	0.25	0.12	0.31	0.09	-0.07
Peak FP Shank Acc ^{ES} (m/s ²)	2.9 (1.7)	68.3	0.07	0.03	-0.04	-0.04	0.38	0.01	-0.11	-0.20	-0.28
Peak FP Shank Acc St (m/s ²)	3.8 (1.5)	40.1	0.02	-0.07	-0.22	-0.26	0.45*	-0.09	-0.10	-0.33	-0.42
Peak FP Shank Acc ^{Sw} (m/s ²)	4.4 (1.4)	32.3	-0.14	-0.20	-0.19	-0.17	0.33	-0.29	-0.15	-0.52*	-0.57*
Range of FP Shank Acc ^{ICP} (m/s ²)	5.0 (2.1)	43.0	0.09	0.04	-0.06	-0.12	0.31	0.10	-0.06	-0.16	-0.36

Figure 1

Tibial AP Translation During Gait Correlates With Intraoperative Medial Mid-Flexion Laxity in Total Knee Arthroplasty Using a Robotic Ligament Tensioner

Takayuki Koya - Showa University Koto Toyosu Hospital - Tokyo, Japan

Alex Orsi - Corin - Raynham, USA

Chris Knowlton - Rush University Med Ctr - Chicago, USA

Christopher Plaskos - Corin - Raynham, USA

Vasili Karas - Rush University Medical Center - Chicago, USA

*Markus Wimmer - Rush University - Chicago, USA

Introduction: Knee joint instability leads to poor outcome after total knee arthroplasty (TKA). A better understanding of how intraoperative ligament tensioning affects postoperative gait kinematics and kinetics, may lead to better decisions in the operating room. This study investigates the relationship between intraoperative joint laxity measured with a robotic ligament tensioner and AP translation measured postoperatively during over-ground gait in the motion analysis lab.

Methods: For this IRB-approved study, twenty robotic-assisted TKA patients (BMI<35), who had received PCL retained, inverse kinematically aligned TKAs, were recruited from a single surgeon's clinic. In all surgeries, laxity was recorded using a robotic ligament tensioner (Figure 1). In particular, medial and lateral laxity were recorded throughout the entire flexion range, as the knee moved from flexion to full extension during final trialing. Laxity was defined as the tibial insert's thickness subtracted from the gap between the resected tibia and the femoral component. Eight to 14 months after surgery, patients were invited to participate in a gait assessment in the motion analysis lab. The point cluster marker set (PCT) was used to obtain knee joint kinematics and kinetics from this group, which were then compared with those of a healthy, elderly control group from our data repository. Passive reflective markers were placed on the skin and tracked with a multi-camera system. Simultaneously, ground reaction forces were collected during level and downhill walking. Subjects were instructed to walk at their usual pace. Level walking trials were completed over a horizontal surface with embedded force plates. Downhill walking trials were performed on a ramp with a 12.5% slope and an embedded force plate, and five trials were recorded for each activity. Knee kinematics and external moments were calculated and normalized to %bodyweight x height using inverse dynamics. Medial and lateral mid-flexion laxities were computed as the mean laxity between 40-50° for each patient. AP translation during gait was defined as the relative distance between the center of the epicondylar axis and the center of the tibia. For both level and downhill walking, statistical parametric mapping of the AP waveforms was performed. Pearson correlations were then obtained between laxity and AP translation for both the medial and lateral sides.

Results: The final demographics of the robotic TKA group comprised of 3/17 male/females, 66.3 ± 7.7 years, 27.3 ± 3.2 BMI, and 13/7 right/left knees and compared with 7/13 male/female, 57.1 ± 8.6 years, 25.6 ± 4.1 BMI, 9/11 right/left in the healthy group. The robotic group showed statistically lower AP translation during the swing phase compared to the healthy group in both level and downhill conditions. (p= 0.001) (Figure 2) It was found that AP translation during swing was associated with medial mid-flexion laxity for both level (p=0.024) and downhill (p=0.013) walking (Figure 3).

Conclusions: This observational study is one of the first to investigate the correlation between intraoperative mid-flexion laxity and tibial AP translation during level and downhill walking. Our results suggest that AP translation might be “normalized” in the operating room by adjusting joint laxity.

Figures

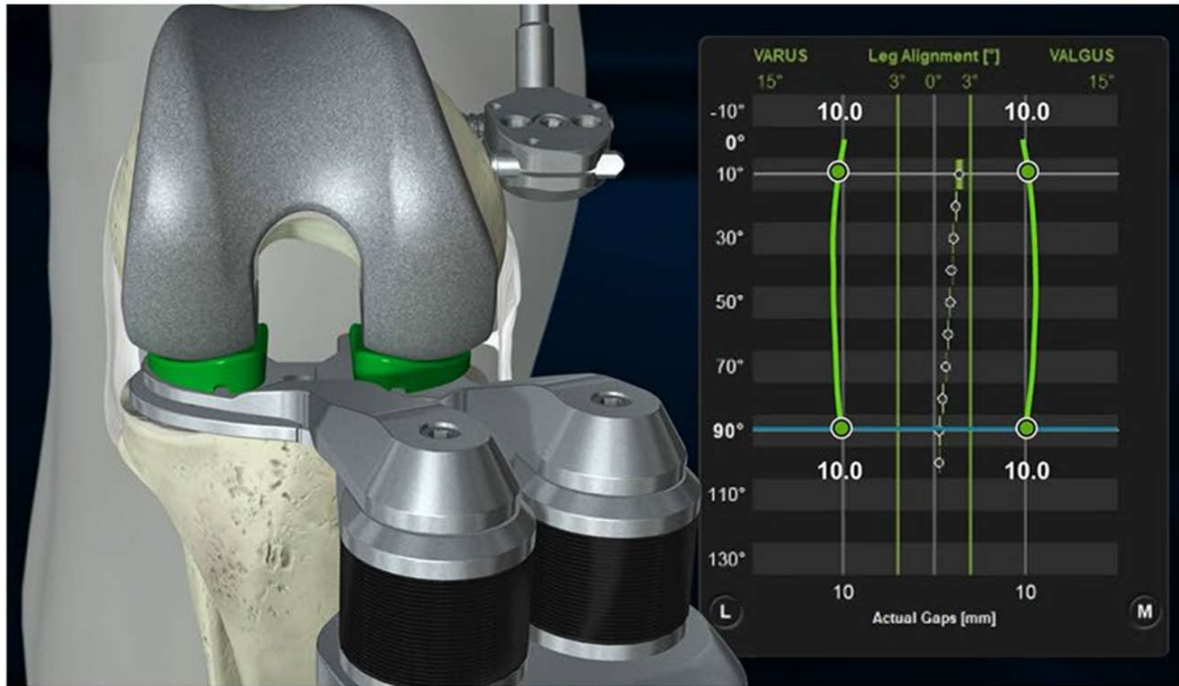


Figure 1: A robotic ligament tensioner is used to collect laxity data during final trialing. Laxity is defined as the tibial insert thickness subtracted from the gap between the resected tibia and the femoral component.

Figure 1

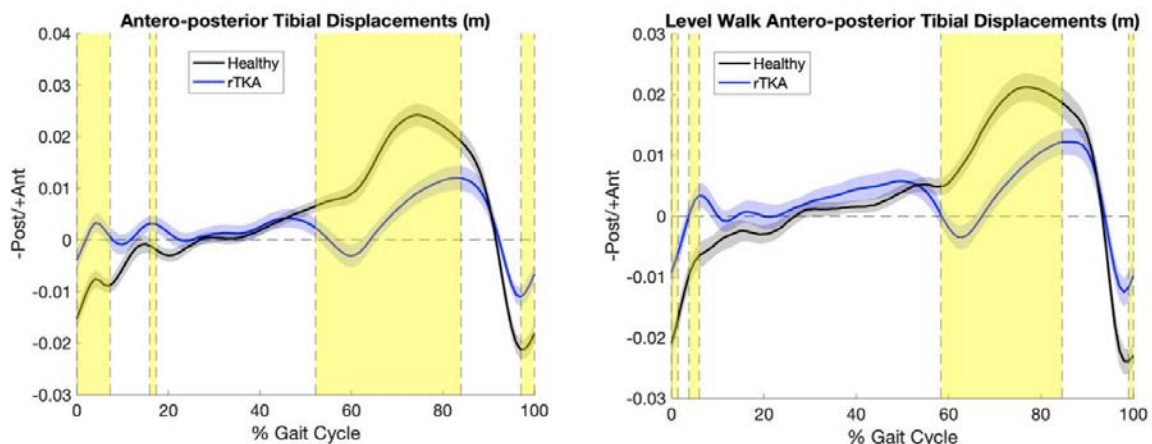


Figure 2: Antero-posterior tibial displacement relative to the center of the epicondylar axis of the femur during downhill and level walking. Yellowish shaded regions indicate significant differences between the robotic TKA group and an elderly healthy control group. Differences can be found during early swing phase when the knee flexes.

Figure2

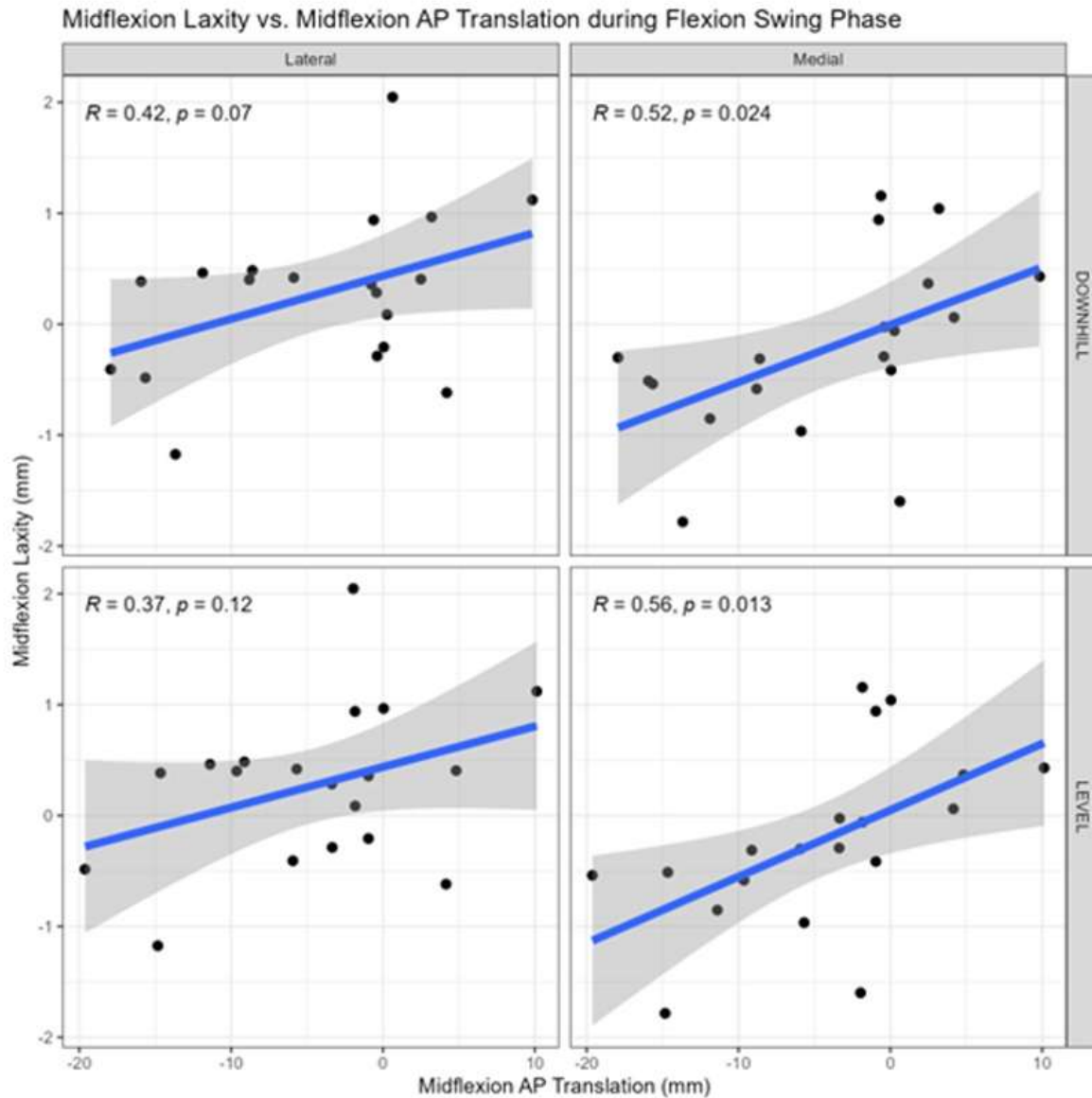


Figure 3: Pearson correlation plots comparing intraoperative medial and lateral midflexion laxity with postoperative AP translation during 40°-50° of initial swing while walking downhill or level ground.

[Figure 3](#)

Comparing TKA Implant Design for External Peak Knee Adduction Moments, Adduction Impulse and Movement Strategies During Stair Descent

*William Mihalko - University of Tennessee - Germantown, USA

Alexis Nelson - UTHSC - Memphis, Select Country

Nuanqiu Hou - Campbell Clinic - Memphis, United States of America

Marcus Ford - Campbell Clinic Orthopaedics - Germantown, USA

James Guyton - Campbell Clinic Orthopaedics - Germantown, USA

John Crockarell - Campbell Clinic Orthopaedics - Germantown, USA

Christopher Holland - Campbell Clinic - Memphis, USA

Douglas Powell - University of Memphis - Memphis, USA

Teri Ross - University of Tennessee Health Science Center - Memphis, USA

Introduction: Kinematically aligned (KA) surgical technique has reported to create better patient outcome scores by recreating natural knee joint movement post-surgery indicated by the patient's experience (Howell et al., 2013) and achieves better flexion scores compared to mechanical alignment surgical technique (Dossett et al., 2014). However, better patient reported outcomes do not indicate the biomechanical underpinnings of advantages or disadvantages of kinematically aligned TKA, which remain unclear. Therefore, our purpose was to analyze MA and KA TKAs on the effect of knee adduction moments (KAM) and knee adduction impulse during stair descent.

Methods: We included 28 patients who received a cruciate retaining Attune implant separated into two surgical alignment technique groups; MA (n=14) and KA (n=14). All patients underwent unilateral TKA and are at least one-year post-op. A three step instrumented staircase (1000Hz, AMTI Inc., Watertown, MA) and an 8-camera markerless motion capture system (200Hz, OptiTrack, NaturalPoint Inc., MA) were used to collect ground reaction forces and segment kinematics, respectively, during stair descent. An AI based reconstruction software (Theia Markerless, Inc., Version 2023, Kingston, ON) was used to identify segment kinematics. Visual3D Professional (HAS Motion, Version 2023.09.3, Canada) and MATLAB (The MathWorks, Inc., R2023b, Natick, MA) were used for data analysis. An independent sample t-test was used to compare surgical alignment techniques for the following variables: external peak KAM, mean KAM, knee adduction impulse and explanatory variables.

Results: There were no significant differences in age or BMI between MA and KA groups. Patients in both groups had compatible patient reported outcome scores. No significant differences were observed in peak KAM ($p=0.11$, Figure 1a) nor knee adduction impulse ($p=0.068$, Figure 1b) between the alignment groups. However, patients in the MA group demonstrated significantly larger lateral trunk lean towards the TKA limb compared to KA patients ($p=0.032$, Figure 1c). We did not observe any significant differences in peak ankle inversion angle ($p=0.524$) nor peak valgus knee angle ($p=0.388$) between the alignment groups.

Conclusion: We aimed to study the impact of surgical alignment techniques on knee joint biomechanics during stair descent. No significant differences were observed in KAMs or knee adduction impulse during stair descent between MA and KA groups. We observed a significant difference in lateral trunk lean towards the TKA limb between the alignment groups during stair descent. To further our understanding, future work will compare knee joint reaction forces and quadriceps activation patterns between alignment groups.

References

Dossett HG, Estrada NA, Swartz GJ, LeFevre GW, Kwasman BG. A randomised controlled trial of kinematically and mechanically aligned total knee replacements: Two-year clinical results. *Bone Joint J* 96-B(7):907-913, 2014.
Howell SM, Howell SJ, Kuznik KT, Cohen J, Hull ML. Does a kinematically aligned total knee arthroplasty restore function without failure regardless of alignment category? *Clin Orthop Relat Res* 471(3):1000-1007, 2013

Figures

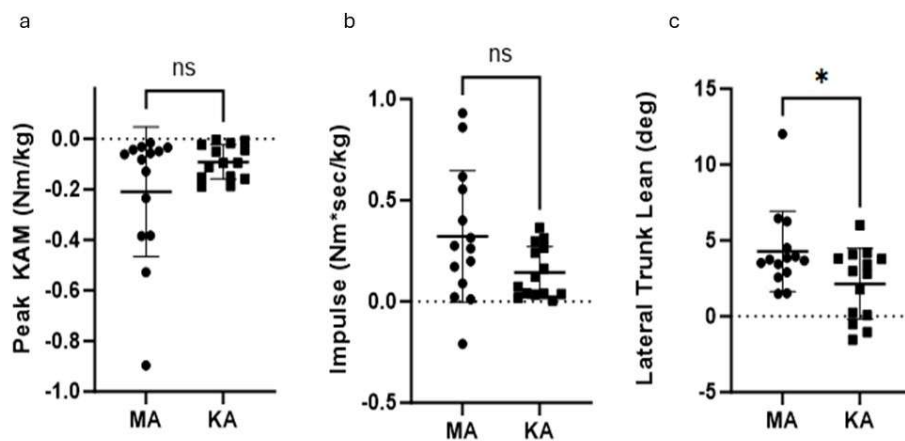


[Figure 1](#)

Femoral Resection Precision and Accuracy in Caliper-Verified Manual Kinematic Alignment Total Knee Arthroplasty vs. Robotic Arm Assistance and Patient-Specific Instrumentation

*David Scott - Spokane Joint Replacement Center - Spokane, USA

Lauren Holbrook - Orthopaedic Specialty Clinic - Spokane, USA

Introduction: Precise and accurate bone resections are essential for achieving proper component alignment and optimal patient outcomes in total knee arthroplasty (TKA). Poor implant positioning and alignment can lead to increased component wear, component loosening, pain, and/or instability, reducing patient satisfaction and implant survivorship. Patient-specific instrumentation (PSI) and robotic arm-assisted (RAA) TKA arose to enhance the reproducibility and accuracy of bone cuts by limiting the risk of human error; however, these potential benefits often come with increased time in the operating room and higher costs. Therefore, we evaluated the accuracy and precision of caliper-verified kinematic alignment (KA) performed with manual instrumentation against these technologies. We hypothesized that manual KA would achieve accuracy and precision comparable to RAA and PSI TKA.

Methods: 189 patients, including 88 women and 101 men, underwent primary unrestricted KA TKA performed with manual instrumentation by a senior orthopaedic surgeon. The thickness of the distal medial (DM), distal lateral (DL), posterior medial (PM), and posterior lateral (PL) femoral condyle resections were measured with a caliper and compared to a target value determined by the degree of cartilage loss, saw blade kerf, and thickness of the femoral component. We statistically compared the mean difference between the resected thickness and target thickness to the reported mean thickness difference and standard deviation of RAA and PSI TKA performed with a mechanical alignment technique using Welch's t-test and F-test analysis, respectively.

Results: The mean difference between the resected thickness and target thickness for the manual KA DM, DL, PM, and PL femoral resections were 0.1 ± 0.3 mm, 0.2 ± 0.3 mm, 0.2 ± 0.4 mm, and 0.2 ± 0.4 mm, respectively (mean \pm std. dev.). Most resections were within 0.5 mm of the target—97.9%, 94.2%, 85.3%, and 87.4% of DM, DL, PM, and PL femoral resections, respectively. The mean resection accuracy and precision (Table 1) of manual caliper-verified KA were equivalent to or significantly better than the reported accuracy of RAA and PSI.

Conclusion: Caliper-verified KA TKA performed with manual instruments achieved highly accurate and precise femoral resections that matched or exceeded the accuracy and precision of published RAA and PSI TKA data. If robotic and PSI technologies are unnecessary for achieving highly accurate and precise resections, it raises questions about the continued use of these more expensive and time-consuming options.

Key Words: total knee arthroplasty, robotic arm-assisted surgery, patient-specific instrumentation

Figures

Instrumentation	Knees	Distal Medial Accuracy \pm SD (mm)	Distal Lateral Accuracy \pm SD (mm)	Posterior Medial Accuracy \pm SD (mm)	Posterior Lateral Accuracy \pm SD (mm)
KA-Manual Instrumentation	189	0.1 \pm 0.3 (ref.)	0.2 \pm 0.3 (ref.)	0.3 \pm 0.4 (ref.)	0.3 \pm 0.4 (ref.)
RAA TKA #1	36	0.4* \pm 0.6*	0.5* \pm 0.7*	0.6* \pm 0.8*	0.7* \pm 0.8*
RAA TKA #2	71	0.3 \pm 1.0*	1.0* \pm 1.0*	0.2 \pm 0.9*	0.3 \pm 0.9*
RAA TKA #3	15	0.7* \pm 0.7*	0.7* \pm 0.7*	0.6* \pm 0.5*	0.6* \pm 0.5*
RAA TKA #4	75	0.8* \pm 0.6*	0.9* \pm 0.7*	0.4 \pm 0.6*	0.6* \pm 0.5*
Patient-Specific Instrumentation	118	0.9* \pm 1.3*	0.9* \pm 1.3*	1.5* \pm 2.1*	0.8* \pm 1.2*

Table 1. Mean Accuracy and Standard Deviation Comparison of Femoral Condyle Resections An F-test determined whether the standard deviations (SD) of RAA and PSI significantly differed from manual KA, and Welch's test determined whether the mean accuracy significantly differed (#* indicates $p < 0.05$).

Figure 1

Risk of Tibial Baseplate Loosening Is Low in Patients Following Unrestricted Kinematic Alignment Total Knee Arthroplasty Using a Cruciate-Retaining Medial Conforming Insert: A Study Using Radiostereom

*Maury Hull - University of California Davis - Sacramento, USA

Abigail Niesen - University of California, Davis - Davis, USA

Stephen Howell

Pranav Tirumalai - University of California, Davis - Davis, USA

Purpose: Assessing risk of tibial baseplate loosening in patients after unrestricted kinematically aligned (unKA) total knee arthroplasty (TKA) using a medially conforming insert is important because baseplates generally are aligned in varus which has been linked to an increased incidence of aseptic loosening following mechanically aligned TKA. Two limits that indicate long-term stability in patients are a change in maximum total point motion between 1 and 2 years (Δ MTPM) < 0.2 mm and anterior tilt at 2 years $< 0.8^\circ$. The purposes were to determine: (1) the number of patients with Δ MTPM > 0.2 mm, (2) the number of patients with anterior tilt $> 0.8^\circ$, and (3) whether varus baseplate and limb alignment were associated with migration.

Methods: Thirty-five patients underwent cemented, caliper-verified, unKA TKA using a medially conforming tibial insert with posterior cruciate ligament (PCL) retention (Fig 1). Biplanar radiographs acquired on the day of surgery and at 1.5, 3, 6, 12, and 24 months were processed with model-based radiostereometric analysis (RSA) software to determine migration and the number of patients with migration above the two stability limits. Medial proximal tibial angle (MPTA), hip-knee-ankle angle (HKAA), and posterior slope angle (PSA) were analyzed for an association with migration in six degrees of freedom and in MTPM.

Results: Thirty-two of 35 patients were available for analysis at 2 years. One patient exhibited Δ MTPM > 0.2 mm (Fig 2). The same patient exhibited anterior tilt $> 0.8^\circ$. Varus rotation ($p = 0.048$, $r \leq 0.34$) and medial translation ($p = 0.0273$, $r \leq 0.29$) increased with increased varus baseplate alignment.

Conclusion: The results indicate low risk of long-term baseplate loosening in patients. Although varus rotation and medial translation increased with increased varus baseplate alignment, the magnitudes of the migrations were minimal and did not increase Δ MTPM and anterior tilt.

Figures

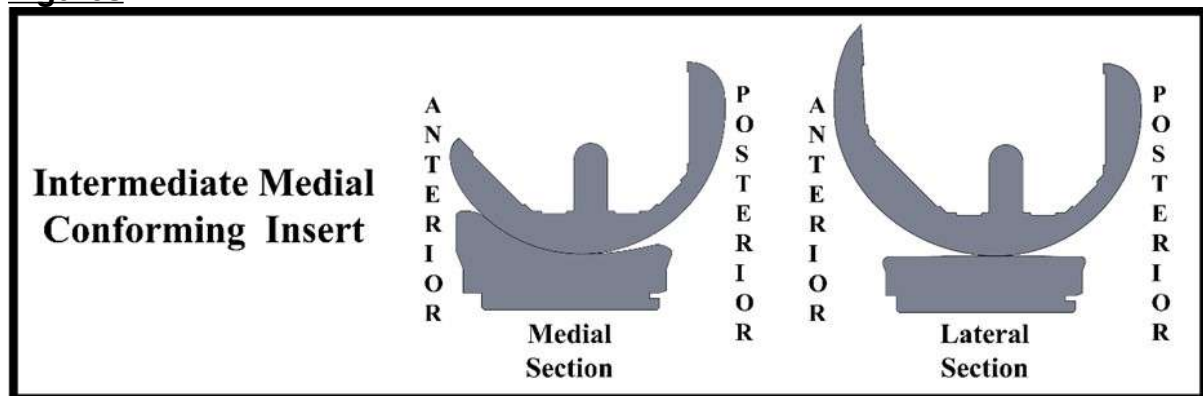


[Figure1](#)

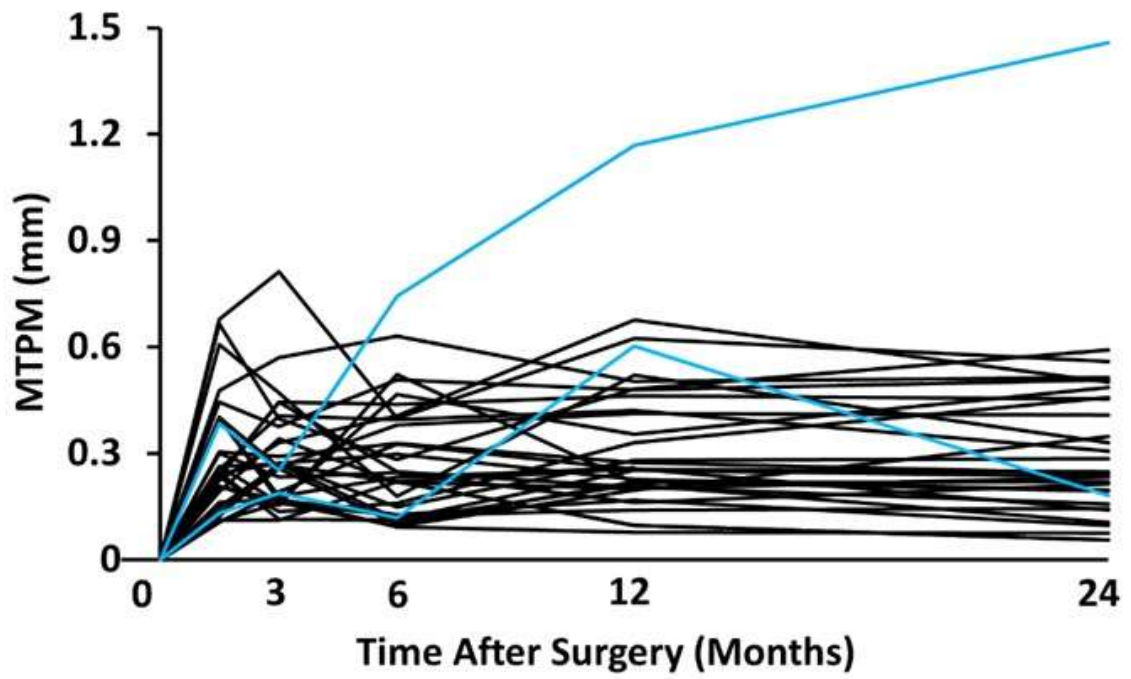


[Figure 2](#)

Perspectives in Navigated Total Knee Arthroplasty - Individual Alignments, Functional Phenotypes & Biomechanical Evidence

*Thomas M. Grupp - Aesculap AG - Tuttlingen, Germany

William Taylor - Swiss Federal Institute of Technology Zurich - Zürich, Switzerland

Ricardo Larrainzar-Garijo - Hospital Universitario Infanta Leonor, Orthopaedic & Trauma Department - Madrid, Spain

Peter E. Mueller - Hospital of the Ludwig-Maximilians-University of Munich - Munich, Germany

Bjoern Gunnar Ochs - Klinik für Unfallchirurgie, Handchirurgie & Orthopaedie, Orthopaedische Fachklinik Vincentius am Kli - Konstanz, Germany

Henning Windhagen - Hanover Medical School - Hannover, Germany

Gavin McHugh - Sports Surgery Clinic & National Orthopaedic Hospital Cappagh, Dublin Ireland - Dublin, Ireland

Allan Maas - Aesculap - Tuttlingen, Germany

Introduction

Primary total knee arthroplasty (TKA) is today a successful clinical treatment with excellent results over a 15 to 20 years period, but studies suggest that 15-20% of TKA patients were dissatisfied with their 1-year functional outcome [Gibon 2017]. In an empirical approach orthopaedic surgeons favor during the last years alternative knee alignment strategies, such as kinematic or restricted kinematic alignment [Rivière 2018], constitutional varus [Bellemans 2012] or dynamic coronal plane limb alignment [Larrainzar-Garijo 2017]. Keeping a focus on optimisation of knee soft tissue balancing, it has been demonstrated that for varus knees with neutral or apex distal joint line obliquity (CPAK Type I&IV) patients benefit from kinematic instead of mechanical alignment [MacDessi 2021]. Changing TKA patient's pre-operative functional limb & femoral phenotype [Hirschmann 2019] by two or more categories significantly lowers clinical outcomes (Forgotten joint score, WOMAC & OKS) after 1-year [Rak 2023]. In meta-analyses kinematic versus mechanical alignment has been in favor regarding some functional outcome scores with a short-term 1-year follow-up [Tian 2022, Wang 2023]. In contrast, most of today's TKA knee systems are designed & clinically validated for mechanical axis alignment ($180^{\circ} \pm 3^{\circ}$) and there is lack of clinical evidence, if a given TKA design is suitable for alternative knee alignment approaches in the long-term.

Methods

Multiple influencing factors on femoro-tibial contact stresses, such as patient bodyweight, frontal plane alignment, tibial slope, femur and tibia component rotation, implant design and size combination make it scientifically invalid to give a concrete global threshold value (i.e. ± 6 degrees) for a knee system. The sensitivity of polyethylene to high contact and sub-surface stress situations bears a substantial risk for increased abrasive-adhesive wear and delamination [Grupp 2009, Grupp 2017, MacDonald 2018], by applying alternative alignment philosophies in an empirical manner. Halonen et al. 2017 outlined the immanent limitations of a patient specific musculoskeletal modeling approach. To allow for evidence based biomechanical thresholds for patient-individual anatomical, kinematic & musculoskeletal TKA treatment strategies, a dynamic FEA-based Aesculap biomechanical knee model has been developed [Maas 2015, Maas 2024] and validated [Bergmann 2014, Taylor 2017] for intra-operative real-time usage in combination with orthopaedic knee navigation (Pheno4U-TKA[®] OrthoPilot[®] Aesculap

AG Tuttlingen Germany). During intra-operative surgical decision making the model predicts based on 58,000 setups for a single knee design if the given knee design in the chosen size combination, femur and tibia orientation, coronal and sagittal alignment is suitable considering implant fixation, contact mechanics and wear.

Results

Connecting for the first time musculoskeletal research, patient related factors, implant design related factors, articulating materials, surgical technique and intra-operative evaluation, allows for a comprehensive individual TKA clinical treatment with biomechanical evidence.

Conclusion

In a future perspective, the combination of patient specific anatomical and functional phenotypes with intra-operative tibio-femoral kinematic assessment and soft tissue balancing, enables a patients individual functional treatment build on up-coming primary TKA implant platform design developments and surgical expert knowledge (Figure 1).

Figures

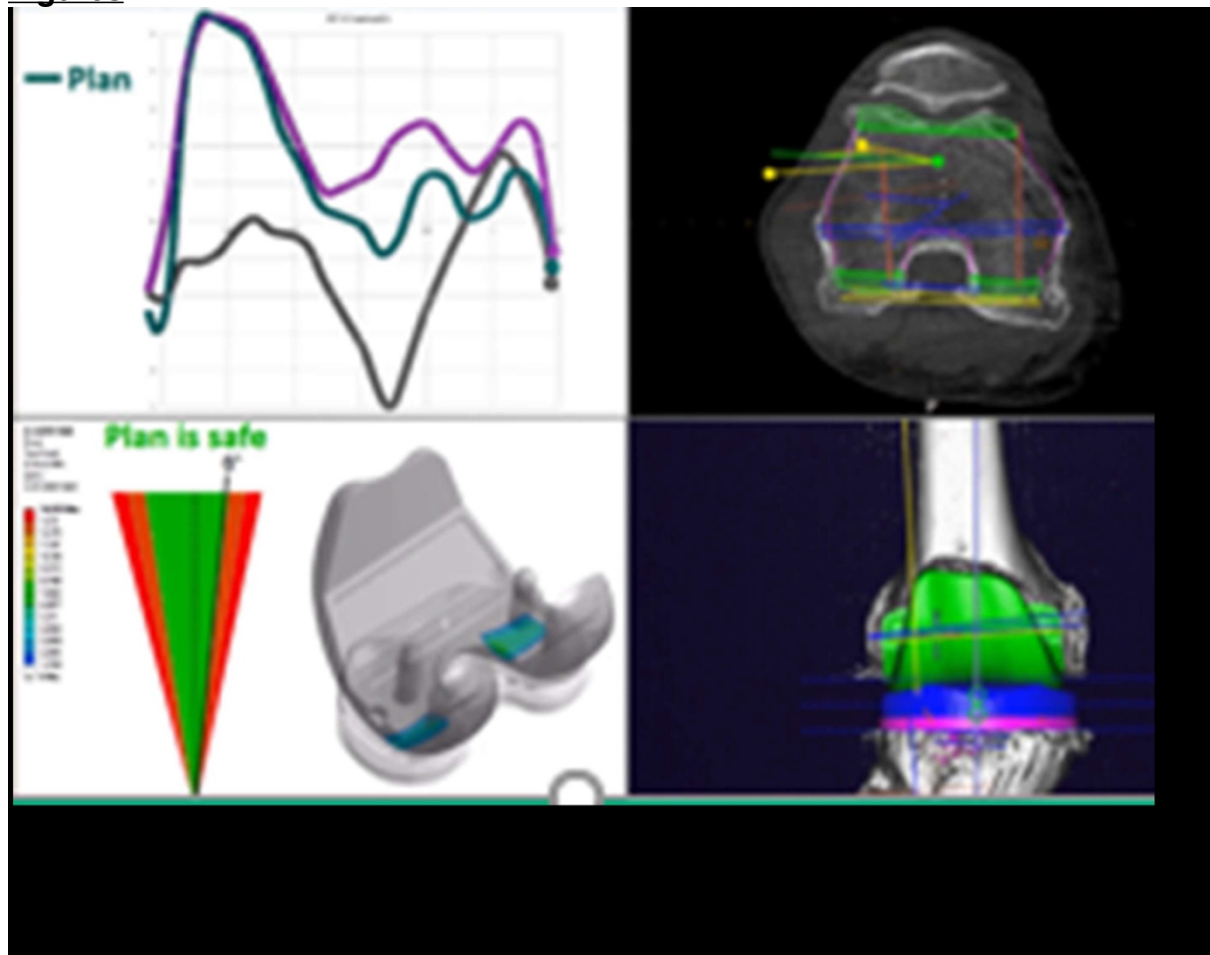


[Figure 1](#)

The Impact of Coronal Plane Alignment of the Knee (CPAK) Classification on Early Functional Outcomes After Primary Total Knee Arthroplasty

*Faseeh Zaidi - University of Auckland - Auckland, New Zealand

Michael Goplen - University of Alberta - Edmonton, Canada

Scott Bolam - University of Auckland - Auckland, New Zealand

Josh Petterwood - Calvary Hospital - Hobart, Australia

Peter McEwen - The Orthopaedic Research Institute of Queensland - Pimlico, Australia

Andrew Paul Monk - University of Auckland - Auckland, New Zealand

Introduction: The Coronal Plane Alignment of the Knee (CPAK) classification classifies alignments based on hip–knee–ankle (HKA) angle and joint line obliquity (JLO) to estimate constitutional limb alignment. This pragmatic classification system is thought to help guide target coronal alignment for patients undergoing TKA. However, it is not yet established if maintaining a patient’s preoperative CPAK status improves outcomes after TKA. The primary objective of this study is to determine if changing a patient's preoperative CPAK classification impacts early functional outcomes after TKA.

Methods: This was a retrospective cohort study of patients undergoing primary unilateral and bilateral robotic-assisted TKAs between January 2020 and March 2023. Standardized standing pre- and post-operative long-leg radiographs were obtained for each patient. Two reviewers independently measured lateral distal femoral and medial proximal tibial angles (LDFA and MPTA), and a third blinded review resolved any outliers. Pre- and postoperative CPAK classification was calculated by determining the arithmetic HKA and JLO by the sum or difference of the two coronal measurements. Validated functional outcomes were assessed using the Oxford Knee Score (OKS) at pre-operative baseline, and 3 months, 6 months and 1 year postoperatively.

Results: A total of 201 patients were included, with an average age of 66.6 years and mean BMI of 33. Of these, 28.4% were CPAK 1, 26.4% CPAK 2 and 16.9% CPAK 3 preoperatively, while 32.8% were classified CPAK 5, 29% CPAK 4, and 22% CPAK 2 postoperatively. Postoperatively, 23% of patients remained in the same preoperative CPAK classification, while 68% moved one CPAK classification and 9.5% moved 2. The mean change in MPTA was 0.66 ± 3.06 degrees, LDFA 1.63 ± 2.75 degrees, HKA 0.97 ± 3.91 , and JLO 2.29 ± 4.31 degrees when preoperative and postoperative values were compared. There were no differences when the change in OKS preoperative and 3 months, 6 months or 1 year postoperative scores were compared between patients that moved 0, 1, or 2 CPAK classifications. Improved OKS at 12 weeks was seen among patients with lower changes in their LDFA postoperatively when compared to preoperative OKS ($r^2 = 0.05$, $p=0.23$).

Conclusions: Coronal alignment can be shifted by one CPAK classification without an impact on early functional outcomes. However, increased changes in femoral component coronal alignment appear to negatively influence early functional outcomes after primary TKA. The impact of larger corrections and the direction of change on outcomes after TKA has yet to be established.

A Novel Ankle Joint Assessment Tool

*Gokce Yildirim - Vent Creativity Corporation - Weehawken, USA

Francois Lintz - Nouvelle Clinique de l'Union - Toulouse, France

Celine Fernando - Nouvelle Clinique de l'Union - Toulouse, France

Introduction: Ankle replacement surgery often relies primarily on the coronal plane of the patient to determine the implant position relative to the ground. Recent advances in standing CT scanning have allowed 3D assessment of bone morphology.

However, similar alignment heuristics are still utilized for the final implant position.

Methods: Standing CT data is used to generate previously validated intensity point clouds models¹. Fifty-eight patients were CT scanned. A fellowship trained surgeon assessed and diagnosed varus (21), valgus (17), or normal (20) ankle alignment.

The scanned bones were auto-segmented and auto-labelled. The resulting bones were assessed for intensity centroids in the axial plane. Resulting force vectors for the holistic bone structure of the entire ankle excluding toes, tibia, and fibula were calculated in three planes for the final assessment. The final vector was compared to the vertical ground reaction force vector.

Results: The Principal Density Analysis vectors were measured relative to the ground reaction forces for predictability of the conditions relative to each other.

Normal alignment was -6 degrees internal, 53 degrees posterior, and 8.5 degrees valgus (Figure 1). Varus ankles were differentiated in significantly reduced valgus angle from the normal only. Valgus ankles were significantly increased in posterior and valgus orientations (Figure 2)

Conclusion: It is important to understand the bone remodeling of the joints when addressing them with interventions such as joint replacements. Holistic approaches do not take bone density and forces acting on the joint into account. The Principal Density Analysis is a useful tool to determine force changes to the joint and the equivalent healthy versions to plan implant positions to recover the joint back to its original alignment and bone density distribution to potentially improve outcomes that can be negatively impacted by loosening or fractures.

Keywords: AI, Medical Imaging, Segmentation, Robotic Surgery, Navigation

Figures

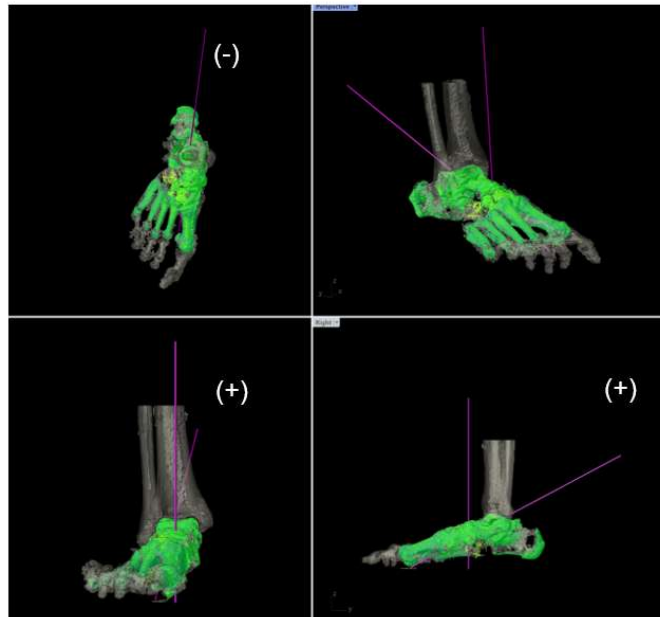


Figure 1. Representative output of raw data three standard views and an isometric view with the ground reaction force and the calculated Principal Density Analysis vector for the highlighted bone cluster

Figure 1

	Axial Angle (deg) external rotation positive	Sagittal Angle (deg) post positive	Coronal Angle (deg) int positive
Valgus Average	-11.36	58.91	17.67
Valgus std	7.35	3.40	10.51
Normal Average	-6.20	53.26	8.52
Normal std	7.44	2.83	8.95
Varus Average	-7.96	52.31	5.86
Varus std	8.79	4.28	12.27

Figure 2. Patient condition distribution

Figure 2

Accuracy and Precision Evaluation of Image-Based Computer Assisted Surgical System for Total Ankle Arthroplasty

*Matthew Rueff - Exactech - Gainesville, USA

Zachary Tupper - Exactech - Gainesville, USA

Prudhvi Tej Chinimilli - Exactech - Gainesville, USA

Scott Gulbransen - Exactech - Gainesville, USA

Laureline Prouvost - Blue Ortho - Grenoble, France

Edward Haupt - Mayo Clinic - Jacksonville, USA

Matthew Hamilton - Exactech - Gainesville, USA

Laurent Angibaud - Exactech, Inc. - Gainesville, USA

Introduction

Computer Assisted Surgical (CAS) systems have been used successfully in joint arthroplasty to improve the accuracy of resections. CAS usage leads to reduced outliers and improved targeted alignment of orthopedic implants. Total ankle arthroplasty (TAA) is a surgical treatment for end-stage ankle osteoarthritis, and the latest generation of TAA is associated with favorable clinical outcomes as a modern alternative to ankle arthrodesis. A TAA application for CAS system was developed using CT-based alignment alongside required fluoroscopy with the intent of facilitating the procedure and improving accuracy of bone resections. The objective of the study was to evaluate the accuracy and precision of the TAA CAS system.

Methods

TAA was performed by a board-certified, fellowship-trained orthopedic surgeon on twelve artificial ankle joint specimens (PN1132-3, Pacific Research) using a CAS system (ExactechGPS, Blue-Ortho) featuring a dedicated ankle application. Video tracking was performed to confirm surgical technique was standardized for all specimens. Scans of each of the twelve specimens were performed before TAA using a structured light industrial scanner (Comet L3D, Steinbichler) used for assessing surface profiles with an accuracy better than 50 μ m. From the initial scan, a DICOM series representative of the CAS system recommended CT scan protocol was created from each model was segmented, and a model coordinate system was created corresponding to the bony anatomy and mechanical axis of the specimen's tibia and talus. During the simulated surgery, active trackers were fixed to each specimen's tibia and talus to allow registration of the anatomical landmarks. Bone resections were individually virtually planned by the surgeon performing the operation using template software to choose appropriate implant position and size relative to the bony anatomy. Conventional cutting guides were then guided into place according to the template using the CAS system. Resections on the talus included a flat cut with three degrees of freedom (e.g. varus, slope, and cut height), whereas tibial resections included distal and medial cuts with five degrees of freedom (e.g. varus, slope, axial rotation, medial offset and cut height) (see Figure 1). Finally, the resected bones were scanned and overlaid with the initial model for assessment of the error relative to the original plan (see Figure 2).

Results

For all eight angular and positional cut parameters across both the tibia and the talus, the mean signed overall intraobserver error was less than 2mm and 2° relative to the plan, and the 95% confidence interval was less than 2mm and 2° (see Table

1). Both angular and positional overall errors on the tibia were less than 1mm and 1° relative to the plan according to the mean and 95% confidence intervals.

Conclusions

The results of the study show that the bone resections using the evaluated TAA application for CAS were associated with satisfactory accuracy level compared to conventional mechanical instruments and PSI blocks. Computer assisted TAA produced resections with errors of less than 2mm and 2° and therefore the system can offer both accurate and precise intraoperative surgical resection measurements.

Figures

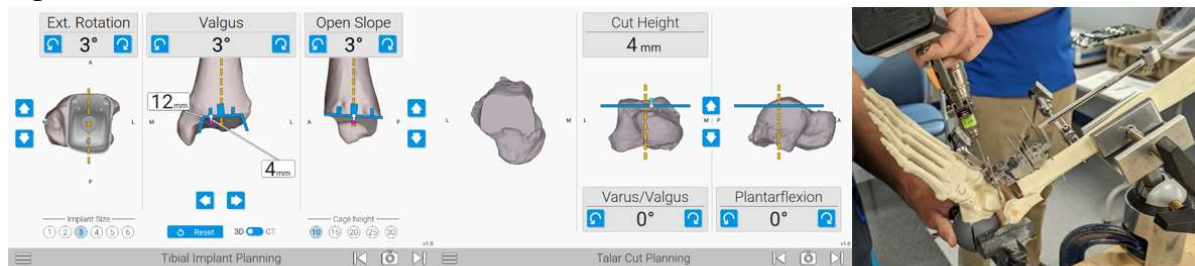


Figure 1: Example tibial and talar plans (left and middle respectively) and subsequent execution (right)

Figure 1

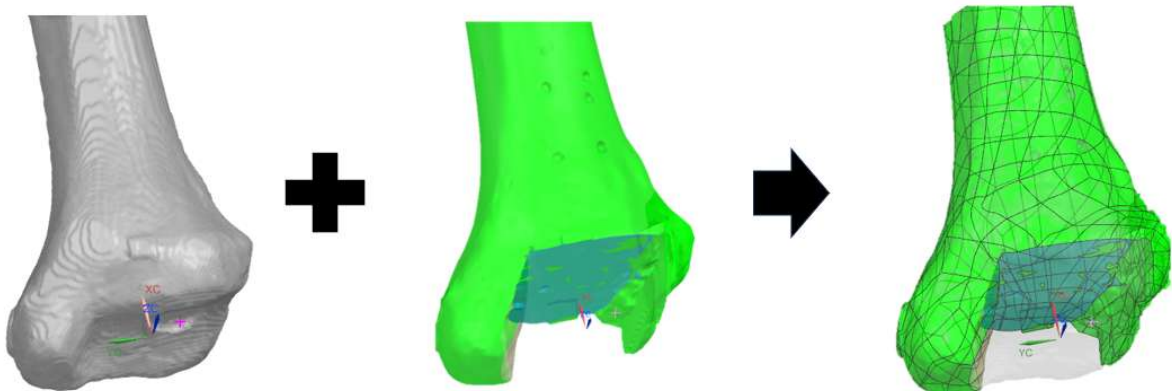


Figure 2: Overlay of segmented plan file with final cut

Figure 2

Table 1: Differences between planned resection and final measured resection, described as overall error

Parameter/Specimen	Tibial varus (°)	Tibial closed slope (°)	Tibial IR (°)	Tibial cut height (mm)	Tibial medial offset (mm)	Talar varus (°)	Talar slope (mm)	Talar cut height (mm)
Mean	-0.22	0.51	0.10	-0.14	-0.15	0.24	1.32	0.63
Lower CI (95%)	-0.79	-0.02	-0.58	-0.62	-0.74	-0.55	0.76	0.28
Upper CI (95%)	0.34	1.03	0.79	0.34	0.45	1.03	1.87	0.99
Specimen 1	-0.40	0.70	1.90	-0.07	-1.22	2.10	0.05	0.47
Specimen 2	1.50	1.70	0.01	0.73	0.34	0.95	0.40	0.24
Specimen 3	1	0.70	-0.90	-0.54	-0.13	2.18	2.57	1.28
Specimen 4	0.20	1.40	-0.05	0.11	-0.22	-1.15	1.80	0.64
Specimen 6	-1	1.35	-1.32	0.26	1.48	0.38	1.43	1.01
Specimen 7	-0.60	0.60	-0.01	1.05	0.08	-0.85	2.10	0.47
Specimen 8	-1.1	-0.70	0.21	-0.92	0.29	-1	0.88	0.52
Specimen 9	-0.20	0.20	-0.70	-0.08	0.38	0.38	0.85	0.96
Specimen 10	-1.10	-0.60	-0.60	-1.43	0.18	0.39	1.50	-0.19
Specimen 11	-0.55	0.10	1.50	-0.10	-1.35	0.16	0.60	0.02
Specimen 12	-0.20	0.10	1.1	-0.56	-1.44	-0.93	2.30	1.55

Figure 3

Tensile Forces Acting on the Posteromedial Meniscus Prosthesis Horn During Activities of Daily Living

Branco van Minnen - RadboudUMC - Nijmegen, Netherlands

Tony van Tienen - Atro Medical BV - Nijmegen, Netherlands

Nico Verdonschot - Twente - Nijmegen, Netherlands

Esmee Bosman - atro medical - Maastricht, Netherlands

*Albert van der Veen - Atro Medical B.V. - Nijmegen, Netherlands

Introduction: For patients with pain after a meniscectomy, a meniscus allograft transplant or an artificial meniscus implant can be used to delay a TKA. The loads on these meniscus replacements, during daily activities, are generally unknown. The purpose of the study was 1) to determine maximum tensile loads in the posterior horn of a medial native meniscus and meniscal prosthesis during various activities of daily living, and 2) to evaluate the influence of tibiofemoral joint forces and displacements on the posterior horn tension. The outcome of this study can be used to determine design loads and testing protocols for meniscal implants.

Methods: A six degrees of freedom joint simulator (AMTI-VIVO) was used to perform gait, stair descent, squat, and stand-to-sit cycles on a cadaveric knee joint. During these activities, the tensile forces acting on the posterior horn were measured by two force transducers, which were positioned at a known angle to enable the calculation of the resulting force (see fig1). First, the load in the posterior horn of the native meniscus was measured, next a meniscectomy was performed and an ATRO Medical meniscus prosthesis was implanted, after which the measurement was repeated. To prevent interaction of the lateral femoral condyle with the force transducers, the load-bearing structures, i.e. the lateral condyle and cruciate ligaments, were removed from the knee joint. Removal of these anatomic, load-bearing structures has a large effect on the stability of the cadaver knee. Therefore, the movements of the VIVO joint simulator were in displacement control instead of load control mode. Of the six degrees of freedom, only the vertical load was load-controlled all others were displacement-controlled. Maximum tensile forces obtained from the various daily activities were compared for each meniscus type.

Furthermore, correlations between applied tibiofemoral forces and displacements from the controlled axes and tensile forces acting on the meniscal horns were determined to see which degree of freedom had the most significant influence.

Results: The maximum tensile forces acting on the posterior meniscus horn were higher during walking and stair climbing compared to squatting and stand-to-sit simulations. For each activity, correlations were found between tibiofemoral force/displacements and tensile forces (comparison of the forces on the native meniscus with the applied loads on the knee joint during an average gait cycle: see fig2 and for the meniscusprosthesis: see fig 3). The posterior horn tension was higher in the meniscus prosthesis than in the native meniscus.

Conclusion: Maximum posterior horn tension varies among different simulated activities and is influenced by activity-specific complex combinations of force and displacements. The tension in the posterior meniscal horn depends on a combination of the applied external loads. Implementing a variety of daily activities in mechanical tests could optimize predictions of prosthesis survival in vivo.

Figures

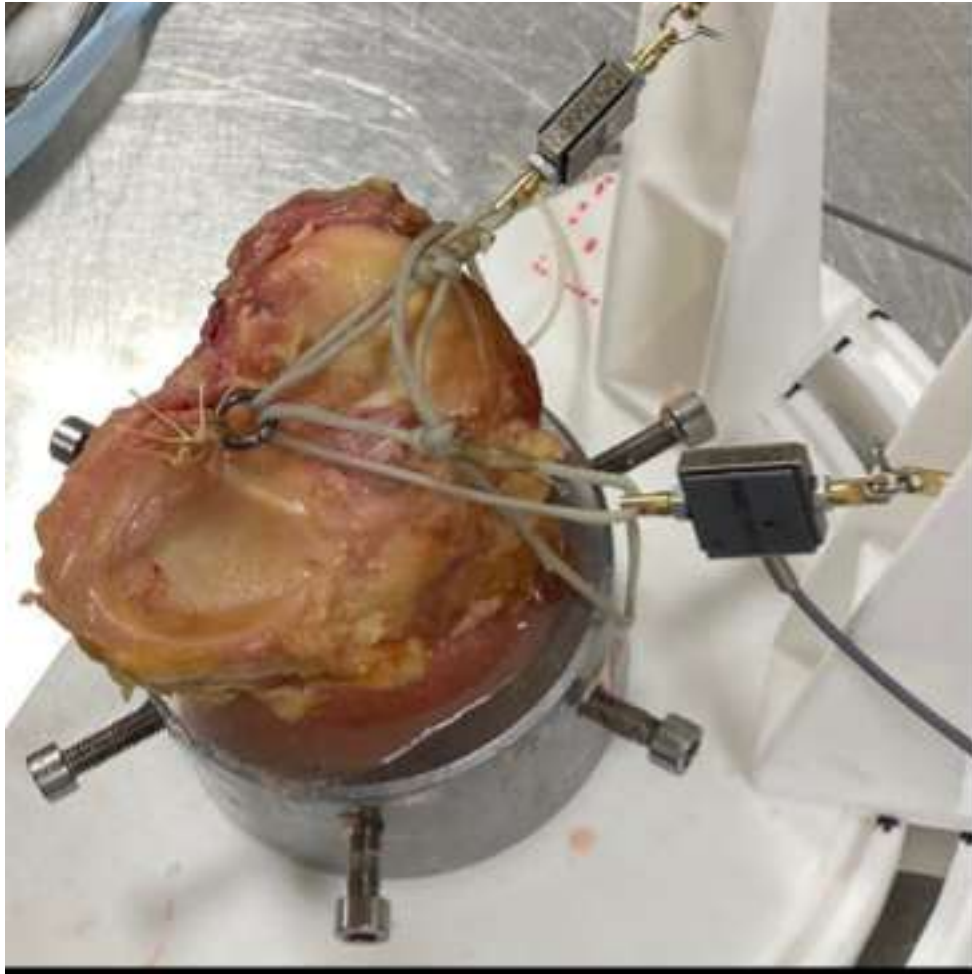


Figure 1

Native meniscus

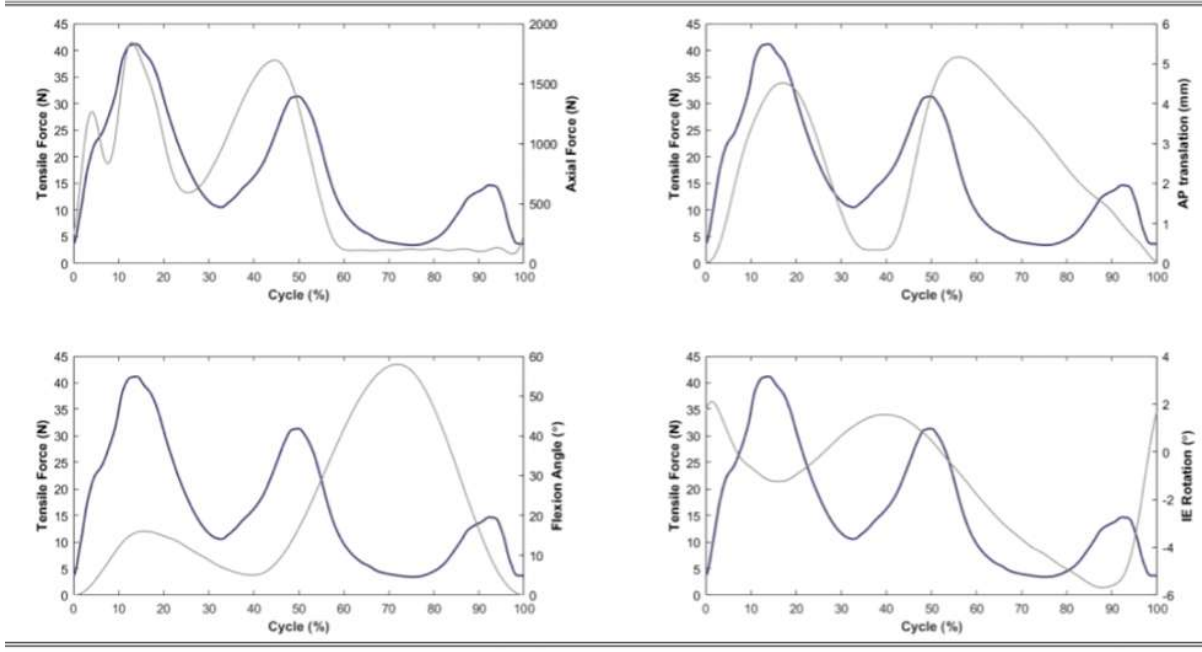
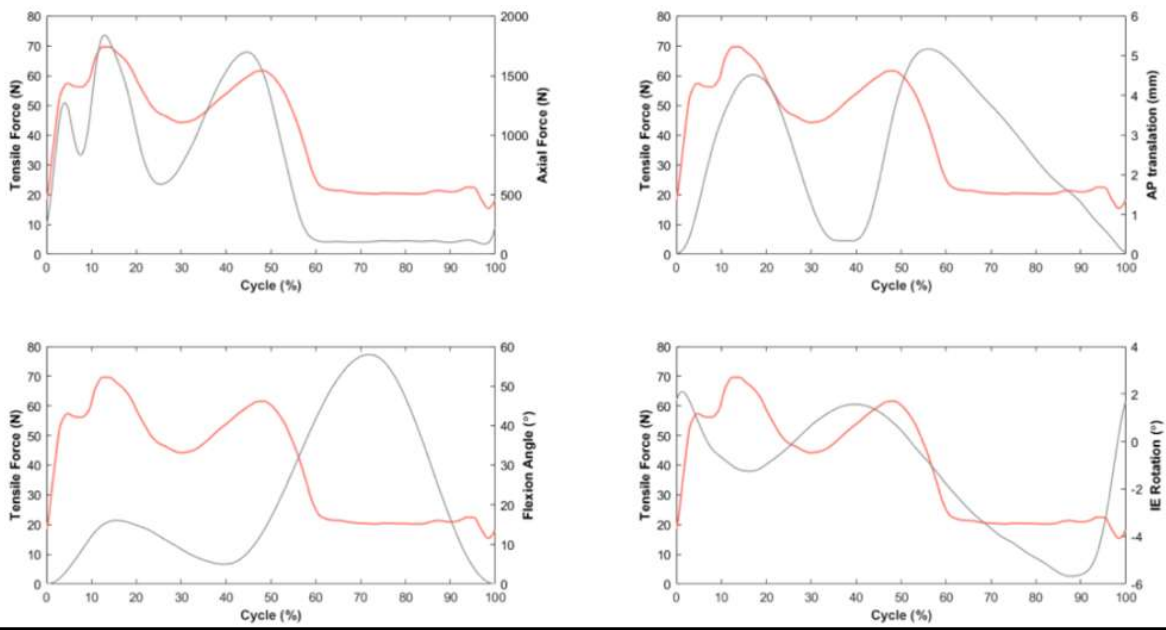


Figure 2

Meniscus prosthesis



[Figure 3](#)

Exploring 3D Joint Space Width and Its Relationship to Cartilage Loss Using MR and CT Images: Data From the OAI and IMI-APPROACH Cohorts

*Jared Weir

Michael Bowes - Imorphics - Manchester, United Kingdom

Philip Conaghan - University of Leeds - Leeds, United Kingdom

Sebastien Lustig - Hôpital de la Croix Rousse - Lyon, France

Alan Brett - Stryker - Newbury, United Kingdom

Introduction

Joint replacement surgery decisions involve an assessment of x-ray joint-space-width (JSW), a surrogate for cartilage loss. Usually, total knee arthroplasty (TKA) is performed. Partial knee arthroplasty (PKA) is considered when there is evidence of intact cartilage in medial (MedTF) or lateral (LatTF) compartments. However, x-ray JSW may be misleading due to variation caused by patient positioning. MR images provide an accurate assessment of cartilage status but are not usually available. Robotic surgery involves the use of 3D CT images for planning. We explored the relationship between cartilage loss and 3D JSW z-scores ("C-scores") using MR and CT images to determine the utility of C-score in TKA/PKA decisions.

Methods

We analyzed all Non-OA (age 45-50 years, no previous knee surgery, no pain, no functional impairment) baseline MRIs from the OAI using active appearance models (AAMs), an established machine learning method, to determine mean cartilage thickness in central MedTF or LatTF compartments. We explored the distribution of probable cartilage loss (Non-OA mean $-2SD$) in each compartment by C-score. Using AAMs with the entire OAI baseline MRI set, we established the C-score cutoffs for $\leq 5\%$ likelihood of probable cartilage loss or $\geq 50\%$ likelihood of severe cartilage loss (non-OA mean $-4SD$) in MedTF and LatTF compartments using cumulative probability distributions. Finally, we used the IMI-APPROACH cohort to compare paired MR and CT 3D JSW using Bland-Altman analysis.

Results

We found that a C-score of approx. ≥ -1 indicated probable no loss of cartilage and a C-score of approx. ≤ -2.5 indicated a $\geq 50\%$ chance of severe cartilage loss in each compartment (Figure 1). These thresholds may be used to differentiate treatment groups. CT and MRI 3D JSW differences were negligible in MedTF: bias [95%CI] = $+0.015$ [-1.228,+1.258] and LatTF: -0.063 [-1.625,+1.499] mm (Figure 2).

Conclusion

C-score identified knees with cartilage loss in only one or in both compartments, indicating that this may provide a

useful tool in PKA decision-making. C-score cutoffs for assessment of probable intact or lost cartilage are similar for compartments. Negligible bias between CT and MR means CT C-score should be effective as a substitute for MR. C-score utilizing CT images could be a valuable tool to aid PKA vs TKA surgical decision-making.

Figures

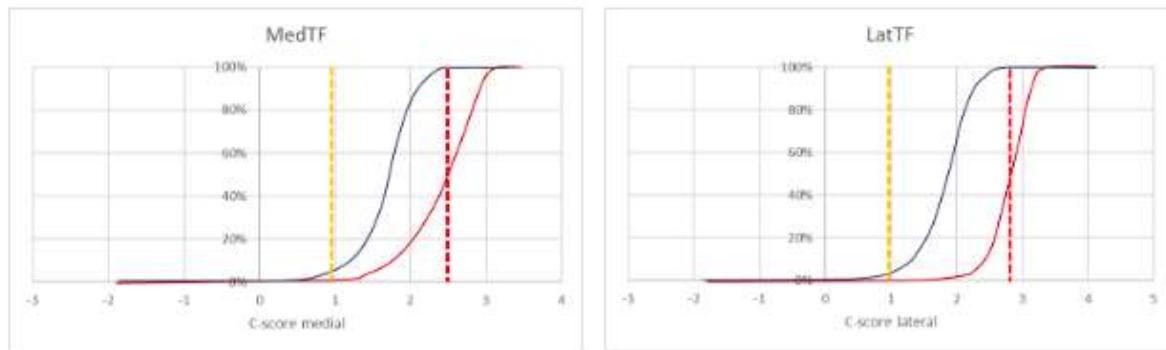


Figure 1: Cut-offs for C-score defined on cumulative probability distributions in the two compartments. Probable cartilage loss is defined at Non-OA mean -2SD (blue curve) and severe cartilage loss is defined as Non-OA mean -4SD (red curve). Yellow dashed cut-offs are at approx. 5th percentile of the -2SD curve, red dashed cut-offs are at the approx. 50th percentile of the -4SD curve.

[Figure 1](#)

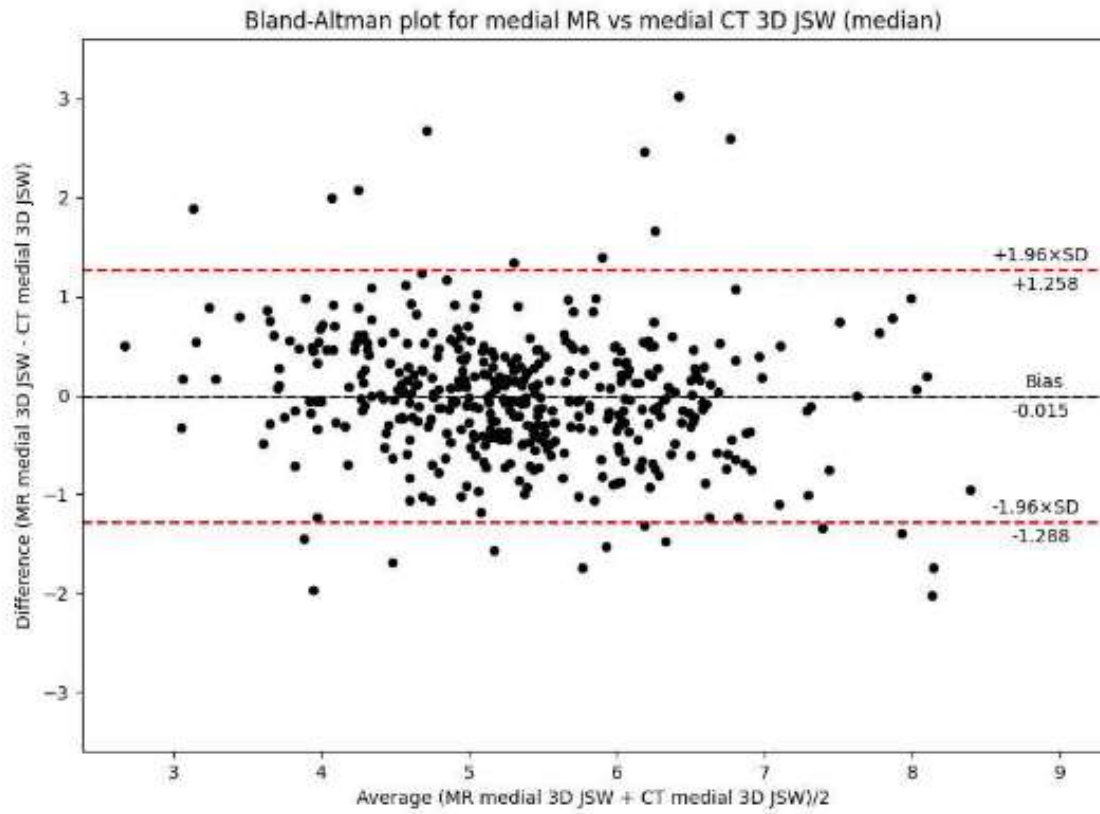


Figure 2: Bland-Altman plot illustrating MRI vs CT 3D JSW measures at the MedTF compartment.

[Figure 2](#)

Differences in Anterior Center-Edge Angle Using Conventional and Automated Planning for Periacetabular Osteotomy

*Nicholas Dunbar - Houston, United States of America

Shuyang Han - University of Texas Health Science Center at Houston - Houston, USA

James Baker - University of Texas Health Science Center - Houston, USA

Carey Clark - University of Texas Health Science Center - Houston, USA

Alexis Aboulafia - University of Texas Health Science Center - Houston, USA

Alfred Mansour III - University of Texas Health Science Center - Houston, USA

Philip Noble - Institute of Orthopedic Research and Education - Houston, USA

Introduction: Increased anterior center-edge angle (ACEA) is a known two-dimensional (2D) radiographic measure of anterior over-coverage in dysplastic hips. Periacetabular osteotomy (PAO) seeks to restore normal head coverage and to avoid excessive ACEA to decrease the risk of femoroacetabular impingement. However, acetabular repositioning can be challenging as restoring coverage can also restrict range-of-motion if acetabular flexion and anteversion are not carefully controlled. Three-dimensional (3D) preoperative planning may be able to maintain femoral head coverage and range-of-motion while minimizing anterior over-coverage and crossover sign compared to 2D radiographic planning. Therefore, the aim of this study was to compare ACEA and crossover sign using conventional 2D radiographic planning and automated 3D planning.

Methods: Patient-specific pelvis and femur bone models were reconstructed from computed tomography images for 17 retrospective PAO patients (22 hips) with hip dysplasia. Preoperative radiographs were digitally reconstruction by projection of the bone models onto the frontal plane. 2D radiographic planning was then performed by an experienced PAO surgeon while two distinct 3D plans were created by computer optimization: one weighted for femoral head coverage (3D area and lateral quadrant distribution) and one weighted for hip range-of-motion (maximum internal rotation at 90 degrees of flexion) without sacrificing lateral femoral head coverage. ACEA was measured and the presence of a positive crossover sign was recorded for all plans. Hips were considered over-covered anteriorly if the ACEA was greater than 40 degrees. Two-tailed, paired t-tests were used to compare ACEA between 2D and both 3D planning algorithms, with a significance level of 0.05.

Results: After 2D planning, coverage-weighted 3D planning, and range-of-motion weighted 3D planning 32% (7/22), 45% (10/22), and 23% (5/22) of hips remained over-covered anteriorly, respectively. No difference in ACEA was observed between 2D planning and coverage-weighted 3D planning ($p=0.56$, $0.8^{\circ}\pm 1.3^{\circ}$ mean \pm standard error) while a statistically significant difference was observed between 2D planning and range-of-motion weighted 3D planning ($p=0.046$, $-2.3^{\circ}\pm 1.1^{\circ}$ mean \pm standard error). A positive crossover sign was observed in 23% (5/22), 59% (13/22), and 14% (3/22) of patients using 2D planning, coverage-weighted 3D planning, and range-of-motion weighted 3D planning, respectively.

Conclusion: 3D planning for PAO surgery that prioritizes post-operative range-of-motion while maintaining normal lateral coverage may reduce anterior over-coverage.

Figures

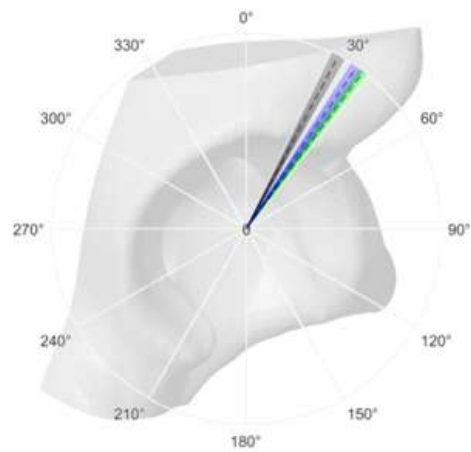


Figure 1. Comparison of the mean and standard error of ACEA for the dysplastic cohort (black), 2D plan (green), and range-of-motion weighted 3D plan (blue).

[Figure 1](#)

Sex Differences in Range of Motion After Eccentric Rotational Acetabular Osteotomy for Hip Dysplasia

*Hiroto Funahashi - Nagoya university - Nagoya, Japan

Yasuhiko Takegami - Nagoya University - Nagoya, Japan

Yusuke Osawa - Nagoya University - Shizuoka, Japan

Takamune Asamoto - Nagoya University - Nagoya, Japan

Keiji Otaka - Nagoya university - Nagoya, Japan

Hiroshi Asai - Nagoya university - Nagoya, Japan

Objective: To evaluate the pre- and post-operative acetabular coverage and hip range of motion (ROM) in eccentric rotational acetabular osteotomy (ERAO) for developmental dysplasia of the hip (DDH) by sex, and to clarify the sex differences in changes in acetabular coverage and ROM.

Methods: Among cases undergoing ERAO for DDH from 2016 to 2023, 19 males and 67 females with pre- and post-operative CT data were included. The mean age at surgery was 31 (± 12.9) years for males and 37 (± 11.9) years for females. Using ZedHip (Lexi Co.), the indicators of acetabular coverage such as anterior acetabular sector angle (aASA), posterior acetabular sector angle (pASA), and anterior superior acetabular coverage (ACEA) were measured, along with the ROM simulation for flexion, and compared between sexes.

Results: In pre-operative acetabular coverage, males showed only a lower value in pASA compared to females ($85.1^\circ \pm 9.4$ vs. $89.8^\circ \pm 7.1$, $p = 0.02$), with no significant gender differences observed in aASA, ACEA, or flexion range of motion. Post-operatively, males had higher values in aASA ($47.2^\circ \pm 14.6$ vs. $35.3^\circ \pm 10.1$), and ACEA ($55.8^\circ \pm 11.9$ vs. $46.0^\circ \pm 13.1$), but a lower value in pASA ($79.6^\circ \pm 20.8$ vs. $96.6^\circ \pm 13.7$) (all $p < 0.01$), and a decreased flexion range of motion ($112.1^\circ \pm 16.3$ vs. $103.0^\circ \pm 19.3$, $p = 0.03$) compared to females. The correlation between post-operative acetabular coverage and post-operative flexion range of motion was aASA ($r = -0.43$), pASA ($r = 0.40$), ACEA ($r = -0.61$) (all $p < 0.01$).

Discussion and Conclusion: Males showed an increase in anterior and anterosuperior acetabular coverage after ERAO and a decrease in flexion ROM compared to females. It is necessary for males to be cautious not to rotate the bone fragment too far anteriorly after ERAO to avoid flexion limitation.

Detecting Femoral Condylar Lift-Off With a Piezoelectric Joint Load Sensing Total Knee Replacement

Brandon Hines - Tennessee Technological University - Cookeville, United States of America

Ryan Willing - Western University - London, Canada

*Steven Anton - Tennessee Technological University - Cookeville, USA

Introduction: Smart implant technology seeks to aid in the diagnosis of potential failure mechanisms which are known to cause persistent postoperative pain. The lack of an *in vivo* method of tracking postoperative forces and alignment presents a gap that stands to be filled by smart implant technology. Piezoelectric sensing and energy harvesting systems offer a solution to this problem while also providing a means for self-powering the system. The sensing capabilities of these systems when subjected to clinically relevant loading scenarios have not been thoroughly investigated. This study evaluates the sensing capabilities of a piezoelectric load-sensing total knee replacement during simulated condylar lift-off using a joint motion simulator.

Methods: The smart implant evaluated in this study is a Stryker Triathlon size 3 right knee with a modified tibial insert that includes 6 piezoelectric transducers capable of measuring compartmental loads and contact points on the medial and lateral condyle. The implant components were cemented to femoral and tibial actuators of a six degrees-of-freedom joint motion simulator. To achieve condylar liftoff, the joint motion simulator applied cyclical alignment of 5°-0° varus and corresponding cyclical compressive joint loads of 100-800 N at a rate of 1.2 seconds/cycle, while holding ML and AP translations and flexion and IE rotations at zero. In this loading scenario, lift-off occurs as the joint is unloading. A single cycle of joint loads and kinematics as well as the voltage across each piezoelectric transducer was sampled at 1000 samples/second. Figure 1 shows the experimental setup. The measured voltages are converted to forces, and the forces are used to calculate compartmental contact locations.

Results: The study demonstrated the ability of the system to detect condylar lift-off. As seen in Figure 2, the measured load reveals the rapid transfer of load from the transducers embedded in the medial compartment (T1-3) of the tibial insert to the transducers in the lateral compartment (T4-6) as the femoral component comes into contact with lateral compartment of the tibial insert. The load is then rapidly transferred back to the transducers in the medial compartment as the femoral component lifts off the lateral compartment. Lift-off is also evident in the femoral contact location calculation, shown in Figure 3, which conveys that the lateral contact location moves from implausible coordinates during lift-off (i.e., those not located on the surface of the insert) to coordinates which reside on the lateral surface once joint contact is made. This demonstrates that the sensing system is able to recover the contact location even after lift-off has occurred.

Conclusion: This study indicates that piezoelectric transducers embedded in the tibial insert of a total knee replacement are capable of detecting condylar lift-off. The sensed load demonstrates the instants of condylar contact and lift-off by capturing the rapid change in load distributions. The calculation of contact location also

captures the location of the lateral contact location during the period of time the femoral component is in full contact. This study provides confidence in the sensing system as a method of detecting clinically relevant phenomena.

Figures

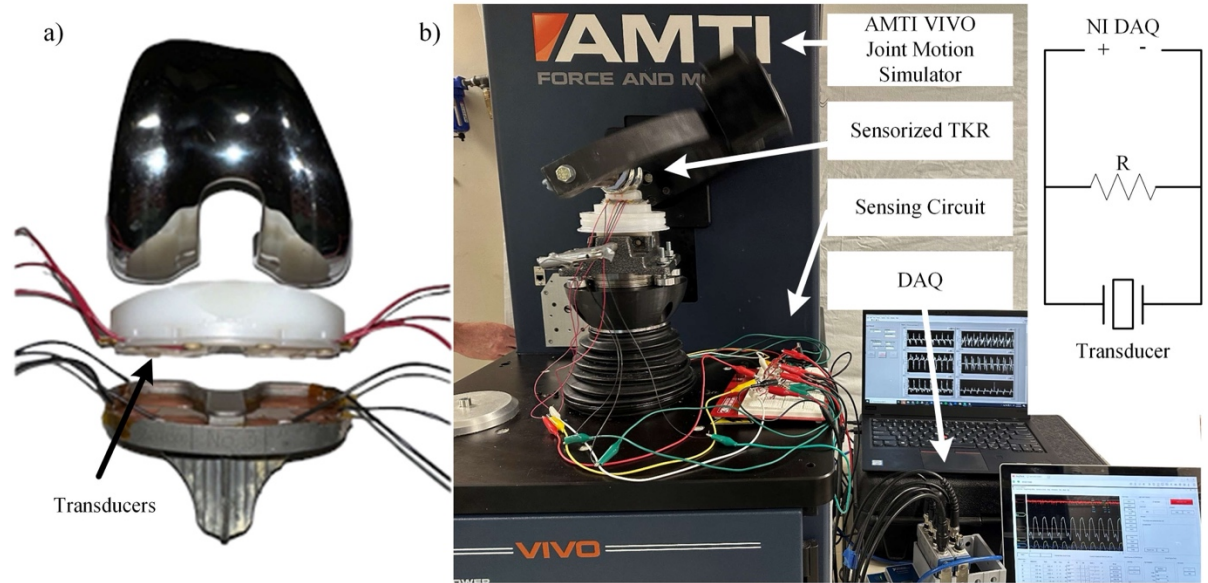


Figure 1

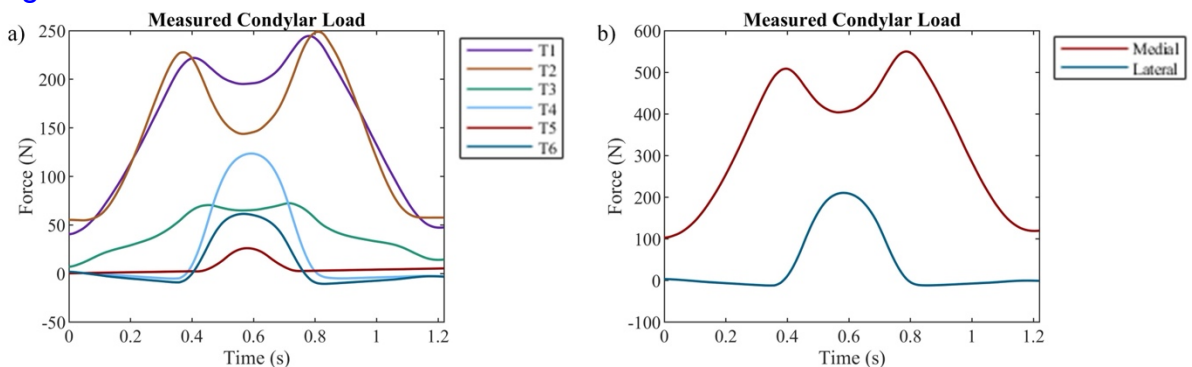


Figure 2

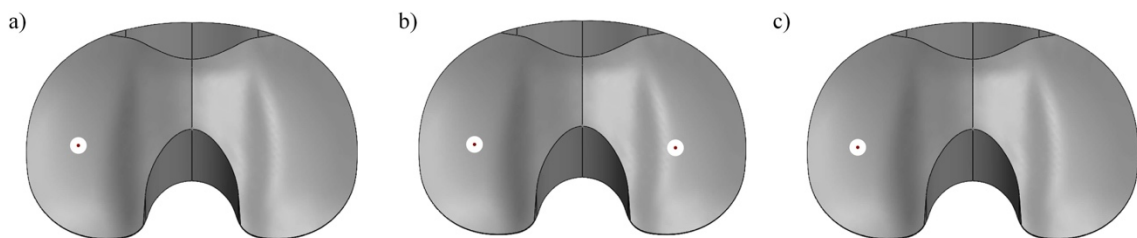


Figure 3

How Does Asymmetry Vary in Patients Undergoing Knee and Hip Arthroplasty?

*Jason Cholewa - Zimmer Biomet - Warsaw, USA
Mike Anderson - Zimmer Biomet - Lehi, USA
Roberta Redfern - Zimmer Biomet - Pemberville, USA

Introduction

Little research has focused on the level of asymmetry involved in the gait patterns of patients undergoing total knee arthroplasty, partial knee arthroplasty, or total hip arthroplasty. Advances in technology including wearables and smartphones allow for passive collection of this gait parameter in people with end-stage osteoarthritis prior to, as well as after, arthroplasty procedures. Our aim was to compare the pre-and post-operative gait asymmetry in patients undergoing TKA, PKA, and THA. We hypothesized that THA patients would exhibit the highest asymmetry pre-operatively, with the largest improvement following surgery.

Methods

This was a secondary analysis of a multicenter prospective longitudinal cohort study. All patients included in analysis downloaded a smartphone care management platform approximately two weeks prior to arthroplasty to allow for collection of pre-and post-operative gait metrics. Only patients who provided at least five days of walking asymmetry data in the two weeks prior to arthroplasty and four of seven days of data within each of the post-operative periods were included. Average asymmetry pre-operatively, and at one, three, six, and 12 months post-operatively were compared by procedure type using one-way ANOVA. Change in asymmetry from baseline was also compared by procedure type with ANOVA and post-hoc Tukey comparisons.

Results

In total, 3034 patients provided evaluable pre-operative asymmetry data; 1727 (56.9%) TKA, 524 (17.3%) PKA, and 783 (25.8%) THA. The average age of the entire cohort was 63.1 ± 9.5 years, where TKA patients were significantly older (64.3 ± 9.0) than those undergoing PKA (62.8 ± 8.8) or THA (60.6 ± 10.6). The majority of patients were female (51.5%). Prior to arthroplasty, THA and PKA patients exhibited similar asymmetry (11.7% vs 11.2%, respectively). TKA patients demonstrated greater asymmetry than other procedure groups before intervention (13.9%, $p < 0.0001$). This trend continued through one-year post-operatively, where TKA patients recovered to 9.3% asymmetry compared to 6.5% and 6.2% in PKA and THA cohorts, respectively ($p < 0.0001$). PKA and THA cohorts experienced greater improvements in asymmetry through 3 months, with non-significant changes between procedure types at one year (3.3% vs 4.3% vs 5.1%, $p = 0.08$).

Discussion

Patients with end-stage osteoarthritis undergoing TKA demonstrate greater walking asymmetry than patients indicated for PKA or THA. Over the entire cohort, PKA and THA patients appear to experience less asymmetry throughout one year following arthroplasty, however, absolute changes from baseline do not vary significantly between procedure types.

Combining Wearables and Implantable Sensors: Gait Metrics to Create Recovery Curve Cohorts

*Roberta Redfern - Zimmer Biomet - Pemberville, USA
Karl Surmacz - Zimmer Biomet - Swindon, United Kingdom
Joseph Brook - Zimmer Biomet - London, United Kingdom
Mike Anderson - Zimmer Biomet - Lehi, USA
Jason Cholewa - Zimmer Biomet - Warsaw, USA
Adam Henderson - Zimmer Biomet - Winterthur, Switzerland

Introduction

Feedback regarding recovery progress after total knee arthroplasty (TKA) is often requested by patients but requires benchmarking against similar patients for meaningful comparisons. Smartphones, consumer available wearables, and implantable sensors within the tibial stem that utilize accelerometers and gyroscopes for passive collection of mobility data may allow unprecedented ability to monitor recovery and provide valuable information regarding goals for mobility recovery after TKA. This analysis aimed to determine how pre-operative activity in combination with patient characteristics can be used to separate recovery curves generated by the sensors within a tibial stem extension implanted during TKA.

Methods

Anonymized data from a commercial database were analyzed to investigate the ability to separate 2,472 patients into cohorts based on age, pre-operative activity levels, and pre-operative gait speed as well as combinations of these factors. Pre-operative step counts were collected by smartphone and wearables. Patients were categorized by low activity (25th percentile) and high activity (75th percentile). Gait metrics collected through 60-days post-operative by the tibial stem extension included average cadence, gait speed, and step counts. Separation of these metrics by cohorts was measured by Kolmogorov-Smirnov test to investigate which pre-operative factors could be best used to stratify patient recovery curves, comparing the impact of the addition of pre-operative gait speed and pre-operative activity level.

Results

Pre-operative gait speed alone performed more strongly to separate cohorts than activity class alone, however, the combination of activity class and gait speed to stratify patients proved more effective than either alone or combined with age. The same trend was observed for post-operative gait speed, with pre-operative values providing better separation of cohorts than age or step count, and the most effective stratification was achieved combining gait speed and pre-operative activity class. However, pre-operative activity class better separated cohorts with regards to post-operative activity class than gait speed or age, with activity and gait speed combined as the best performing pairing of factors.

Discussion

Comparison of patient recovery of cadence, gait speed, and step counts following TKA require separation of patients into like groups for feedback to be meaningful. These results suggest that pre-operative activity level and pre-operative gait speed combined were the most impactful pairing for stratification of cohorts to compare recovery of these gait metrics. Most importantly, we demonstrate the feasibility of combining data from consumer wearables with implanted sensors for monitoring of recovery and better understanding of patient characteristics to be considered prior to comparison.

Going Faster Than PROMs: Early Assessment of Post-TKR/THA Recovery Through Physical Activity Markers

*Julien Lebleu - moveUP - Brussels, Belgium

Bruno BONNECHERE - U Hasselt - Hasselt, Belgium

Kim Daniels - PXL Hogeschool - Hasselt, Belgium

Andries Pauwels - moveUP - Brussels, Belgium

Hervé Poilvache - CHIREC - Braine L'alleud, Belgium

Philippe Van Overschelde - Hip & Knee Clinic AZ Maria-Middelares Gent - Sint-Martens-Latem, Belgium

Jared Weir - DeepStructure - Saginaw, USA

Introduction: The MCID (Minimal Clinically Important Difference) of PROMs (Patient Reported Outcome Measures) is an important criterion in studying the outcomes of total knee (TKA) and hip arthroplasty (THA), allowing for the evaluation of the intervention's effect as well as the speed of postoperative patient recovery. The development of smartphone-based physical activity measurement tools offers new possibilities, such as conducting unintentional walking tests, which can complement the collection of conventional PROMs. In this study, we propose the use of automatic activity measures in the postoperative period of TKA and THA in addition to the Forgotten Joint Score (FJS)

Methods: 1144 patients who underwent TKA (N=461) or THA (N=683) were followed up using a digital application for at least 6 weeks postoperatively. The average age was 62 years, with a body mass index (BMI) of 29. Physical activity data were collected using Garmin Vivofit 4 smartwatches, allowing for the extraction of several important parameters before and after the intervention: the number of steps per day, the peak cadence over 1 minute (P1M), and the peak consecutive cadence over 6 minutes (P6MC). Patients were divided into two groups based on the FJS MCID at 3 months postoperatively (TKA/MCID+: patients who underwent TKA and reached the MCID; TKA/MCID-: patients who underwent TKA and did not reach the MCID; THA/MCID+: THA patients who reached the MCID; THA/MCID-: THA patients who did not reach the MCID) to compare these two parameters.

Results: Patients in the THA/MCID- group (N=243) took longer to reach their preoperative activity level (THA/MCID+ (N=440): 33 days, THA/MCID-: 40 days). They also did not regain their preoperative P1M values during follow-up, while patients in the THA/MCID+ group reached it at 35 days postoperatively. Regarding P6MC, patients in the THA/MCID+ group had faster recovery (29 days, THA/MCID-: 32 days). Patients in the TKA/MCID- group (N=266) did not regain their preoperative activity level by the end of follow-up and took longer to normalize P1M (TKA/MCID+ (N=195): 38 days, TKA/MCID-: 50 days) and P6MC (TKA/MCID+: 29 days, TKA/MCID-: 39 days). We observed that P6MC and P1M, allowed for early identification of differences in comparison with the total number of steps per day.

Conclusion: The results of our study demonstrate the interest of P6MC and P1M in the study of postoperative recovery following THA or TKA and appear to be associated with FJS results at 3 months. These parameters have the advantage of being collected daily, without supervision, and automatically in the postoperative follow-up setting, offering new perspectives for postoperative monitoring and functional outcome assessment, in addition to PROMs.

Figures

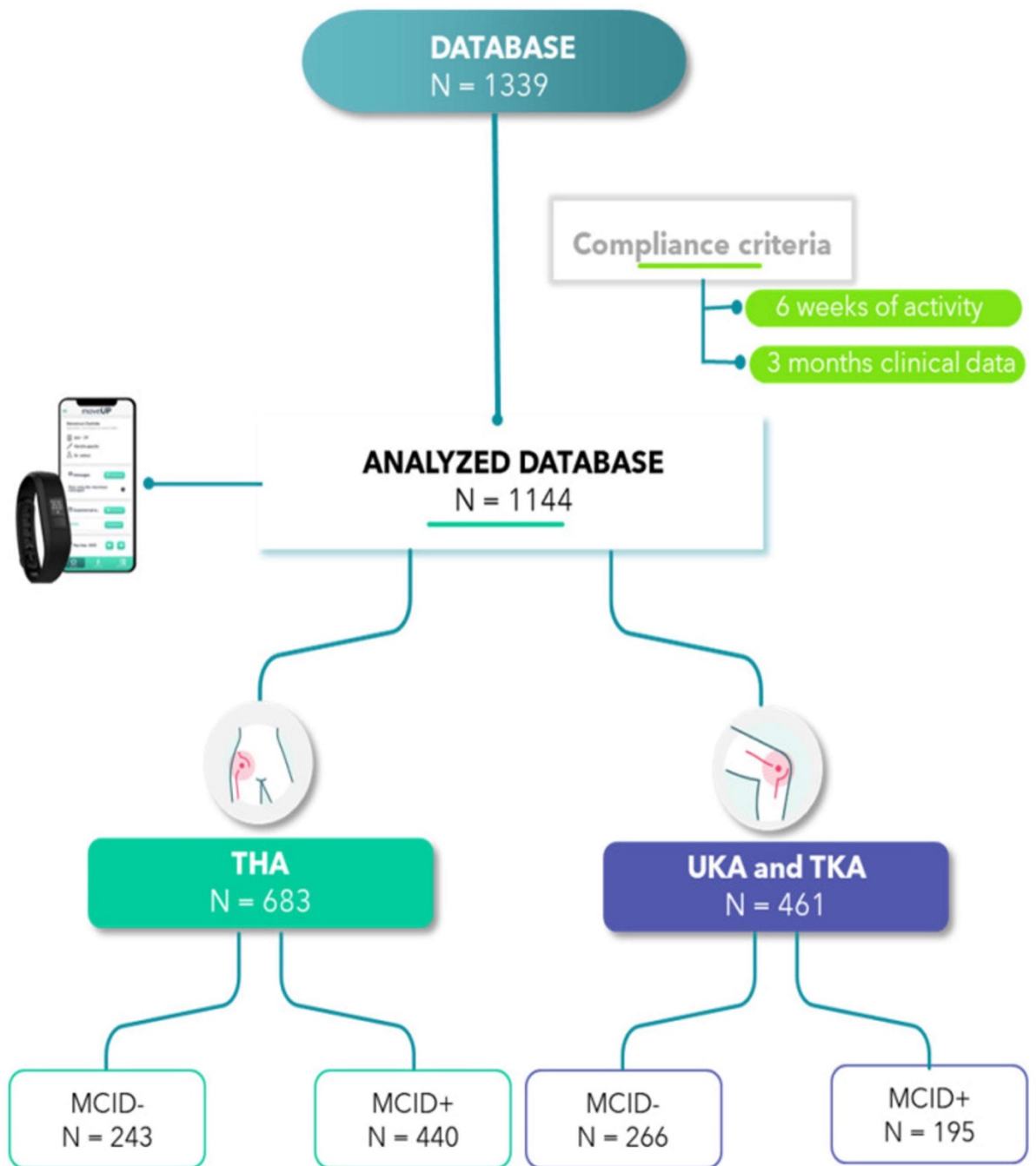


[Figure 1](#)

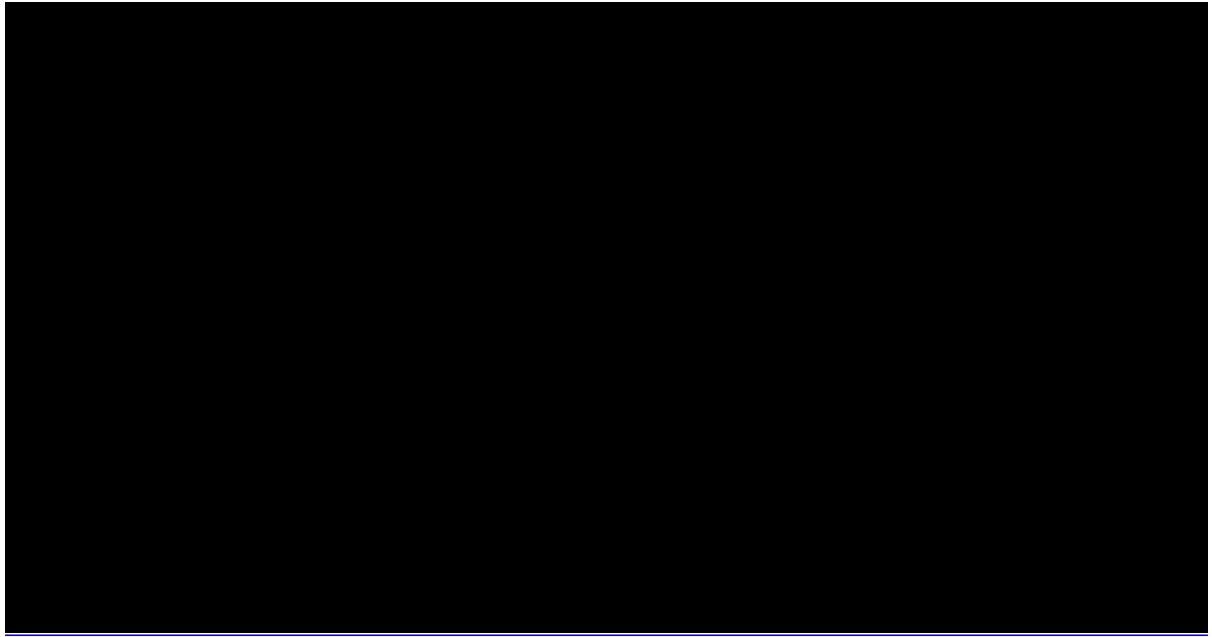


[Figure 2](#)

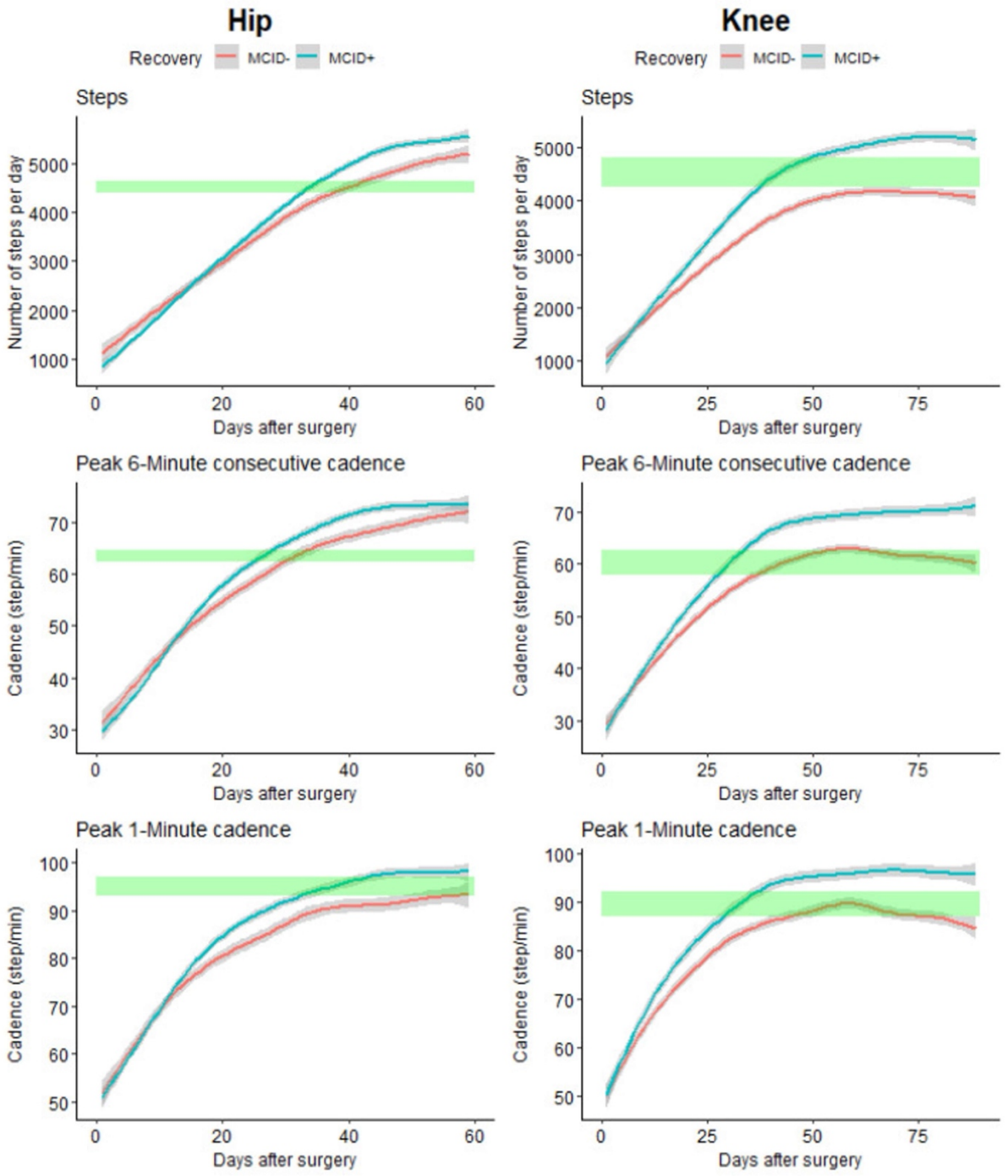


Figure 3

Unveiling Inaccuracy: A Comprehensive Analysis of Error Induced by Self Applying Wearable Sensors for Total Knee Arthroplasty Monitoring

Jocelynn Bechtel - University of Rhode Island - Kingston, USA

Jayson Hutchinson - University of Rhode Island - Kingston, USA

*Ryan Chapman - University of Rhode Island - Kingston, United States of America

Introduction: Post-total knee arthroplasty (TKA) monitoring historically involves discrete, goniometric or visual range of motion (ROM) estimates. These measures likely fail representing patient function outside well-controlled clinical settings. Commercially available wearable inertial measurement units (IMUs) are rapidly being adopted to mitigate these limitations. Most IMUs are self-applied, potentially yielding errors negatively impacting knee angle measures. Accordingly, evaluating IMU accuracy across sensor positions is crucial. Thus, we assessed IMU misplacement's impact on sagittal knee angle calculations.

Methods: This IRB approved prospective study compared sagittal knee angles during walking measured by one commercially available wearable IMU system and optical motion capture (MOCAP) in 10 healthy individuals. 3D lower extremity MOCAP data ($f_s=100\text{Hz}$; Figure 1A) were captured and passed to Visual3D computing sagittal knee angles (θ_{MOCAP}). Simultaneously, IMUs ($f_s=50\text{Hz}$; Figure 1B) adhered to the shin/thigh automatically estimated sagittal knee angles (θ_{IMU}). Simulating IMU misplacement, IMUs were moved in three anatomic planes (Figure 1C; sagittal/transverse physical rotations, frontal shims). Before each position, sensor-to-leg calibration was conducted per manufacturer algorithms. Each position's absolute value error (θ_{MOCAP} vs. θ_{IMU}) was computed and evaluated by error category (bony segment: shin, thigh; anatomic plane: sagittal, frontal, transverse; error type: flexion, extension, varus, valgus, internal rotation, external rotation).

Results: 10 healthy participants (5M, $22.3\pm 2.4\text{yrs}$) enrolled. Figure 2A highlights comparing MOCAP and correct/incorrect IMU placement. Across subjects/IMU positions, MOCAP/IMU angles were strongly correlated (Figure 2B, $R^2=0.85$) with 4.5° erroneous knee flexion. Error by segment (Figure 3A) was not a significant factor ($p>0.05$). Error by plane (Figure 3B) showed transverse IMU errors increased knee angle error versus neutrally aligned IMUs ($p=0.007$). Errors from internal rotation IMU misplacement were significantly greater than error from flexion/extension/varus IMU misplacement ($p<0.035$) and errors from external rotation IMU misplacement were significantly greater than extension/varus IMU misplacement ($p<0.01$).

Conclusion: Wearable IMUs could fundamentally transform post-TKA monitoring, yet their error is poorly described given IMU self-application could induce knee ROM computation errors. Herein, error was low ($\sim 2.5^\circ$) with sensors placed appropriately. Manufacturer supplied algorithms reduced error $\leq 5^\circ$ with flexion/extension/varus IMU misplacement. However, knee angle error was $>8^\circ$ with valgus/internal rotation/external rotation IMU misplacement. Perhaps most critically, transverse plane IMU misplacement was problematic, inducing greater knee angle error than flexion/extension/varus IMU misplacement. Given frontal plane IMU placement is largely dictated by patient anatomy, significant valgus deformity may not be indicated for use. Additionally, patient education on application/alignment are critical for proper use to reduce sagittal/transverse plane IMU misplacement.

Keywords: Wearable, Kinematics, Range of Motion, Motion Capture, Biomechanics

Figures

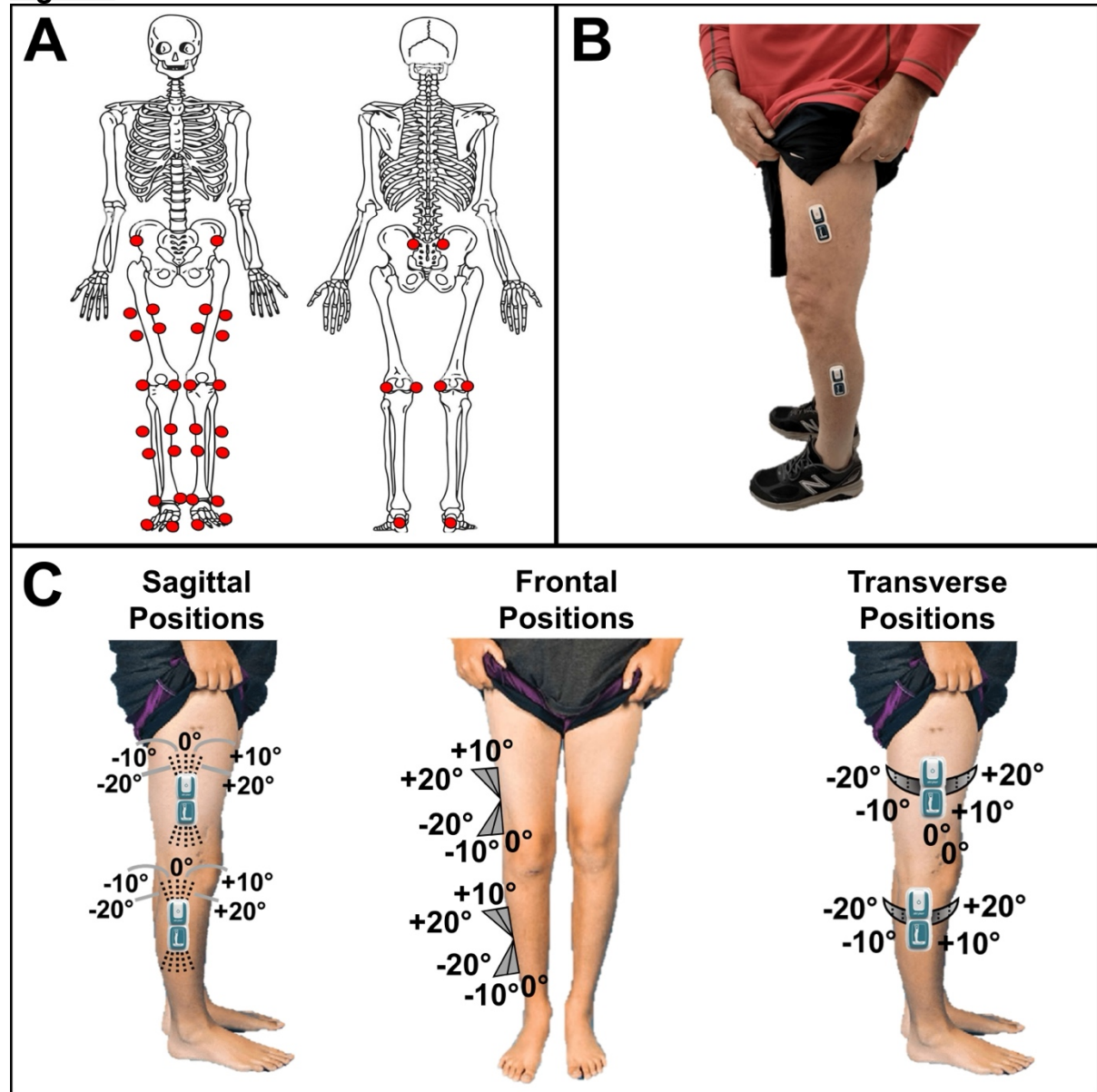


[Figure 1](#)

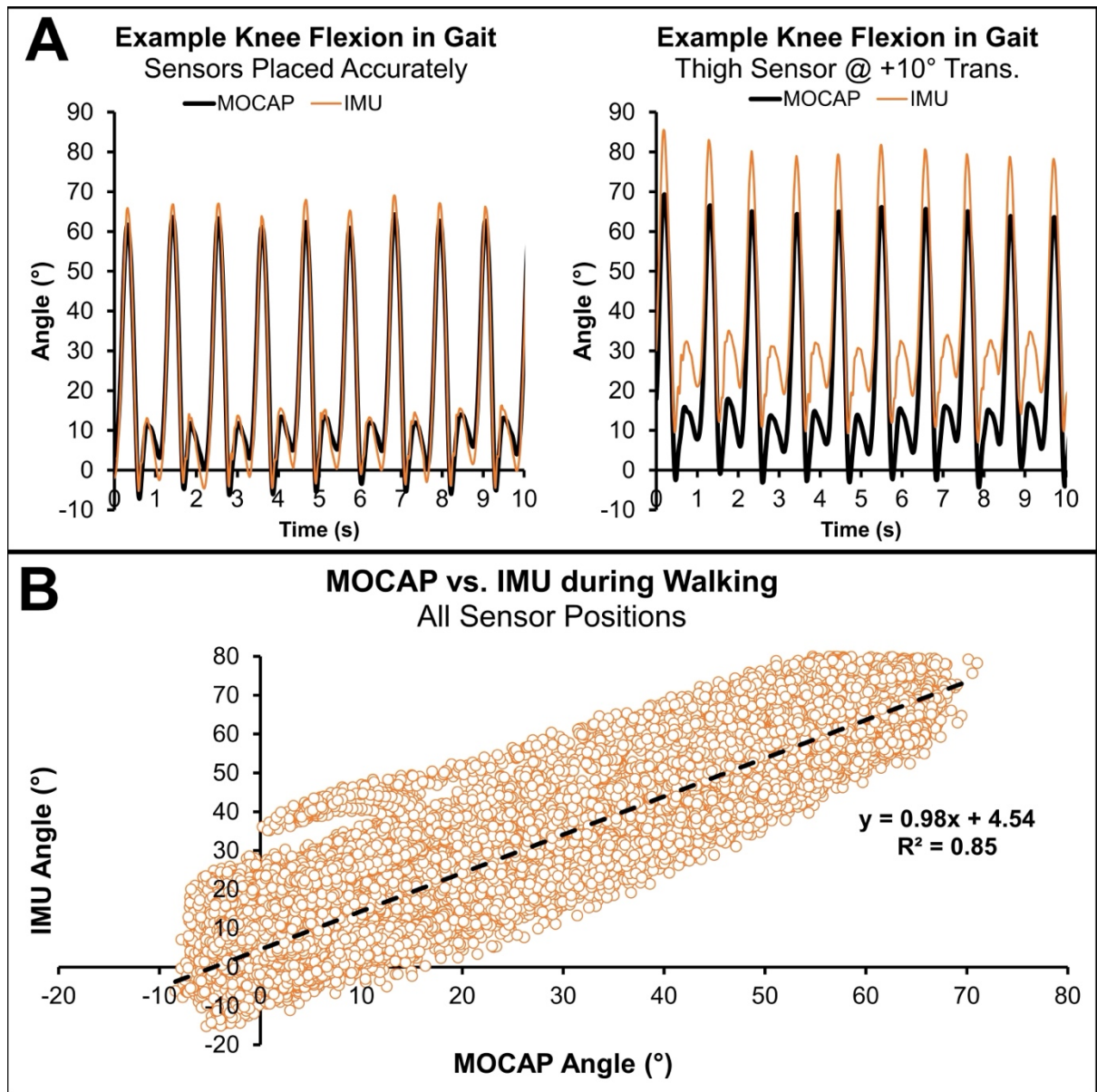


Figure 2

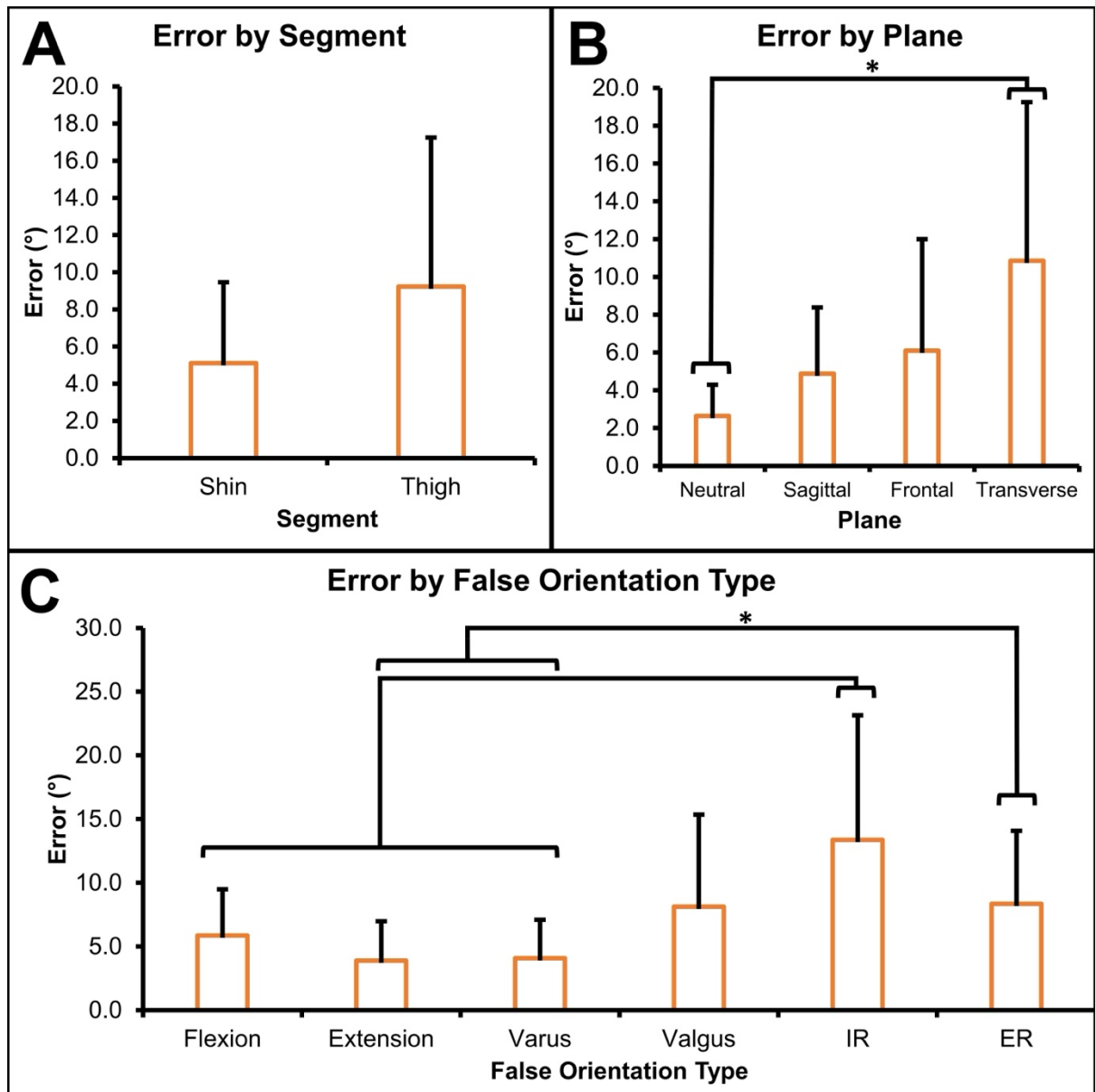


Figure 3

Variation in Wearable Sensor Functional Metrics During Early Recovery of Knee Arthroplasty Patients

*Ricardo Antunes - Stryker - Glasgow, GB

Paul Jacob - Oklahoma Joint Reconstruction Institute - Oklahoma City, USA

Robert Marchand - Ortho Rhode Island - South County, USA

Elaine Justice - Oklahoma Joint Reconstruction Institute - Oklahoma City, USA

Kelly Taylor - Ortho Rhode Island - South County, USA

Matthias Verstraete - Stryker - Fort Lauderdale, USA

Introduction: Adequate postoperative monitoring of TKA patients is necessary to detect complications, provide early treatment and ultimately contribute to a good outcome. Wearable and implantable devices are increasingly available and proposed to monitor patients at higher granularity than in-practice visits that are infrequent and can have low compliance. Also, the functional metrics such as collected by these systems have advantages over PROMs. Understanding variation of the metrics collected from these is necessary for benchmarking and their use for recovery assessment. We describe variation of wearable device metrics during early TKA patient functional recovery assessment and discuss implications for their use.

Methods: Functional metrics were remotely collected from 89 unilateral primary TKA patients using knee-worn wearable sensors including activities of daily living (ADL) knee active time, load bearing time, range-of-motion and step count, and gait range-of-motion and cadence. These metrics were summarized into weekly values and described for 12 weeks postoperative.

Results: The functional recovery is most pronounced during the first 6 weeks after surgery, during which significant weekly progression shall be expected (Fig. 1). Beyond this time, weekly comparisons are no longer expected to show significant progression though the patients are still improving albeit at a lower rate. Hence, progression shall be monitored and assessed over a longer time-period. Patients with lower pre-operative functional performance were more likely to return to their pre-operative level in the first 12 weeks prior to surgery compared to patients with higher pre-operative functional performance.

Conclusion: Remote monitoring of wearable functional metrics provides a good assessment of TKA patients functional recovery at a higher temporal resolution than can be achieved through practice visits alone. They can provide the basis for data driven feedback loops of patient care (e.g., physiotherapy responding to functional state of the patients) and engagement, and early detection of complications, ultimately contributing to better patient care.

Figures

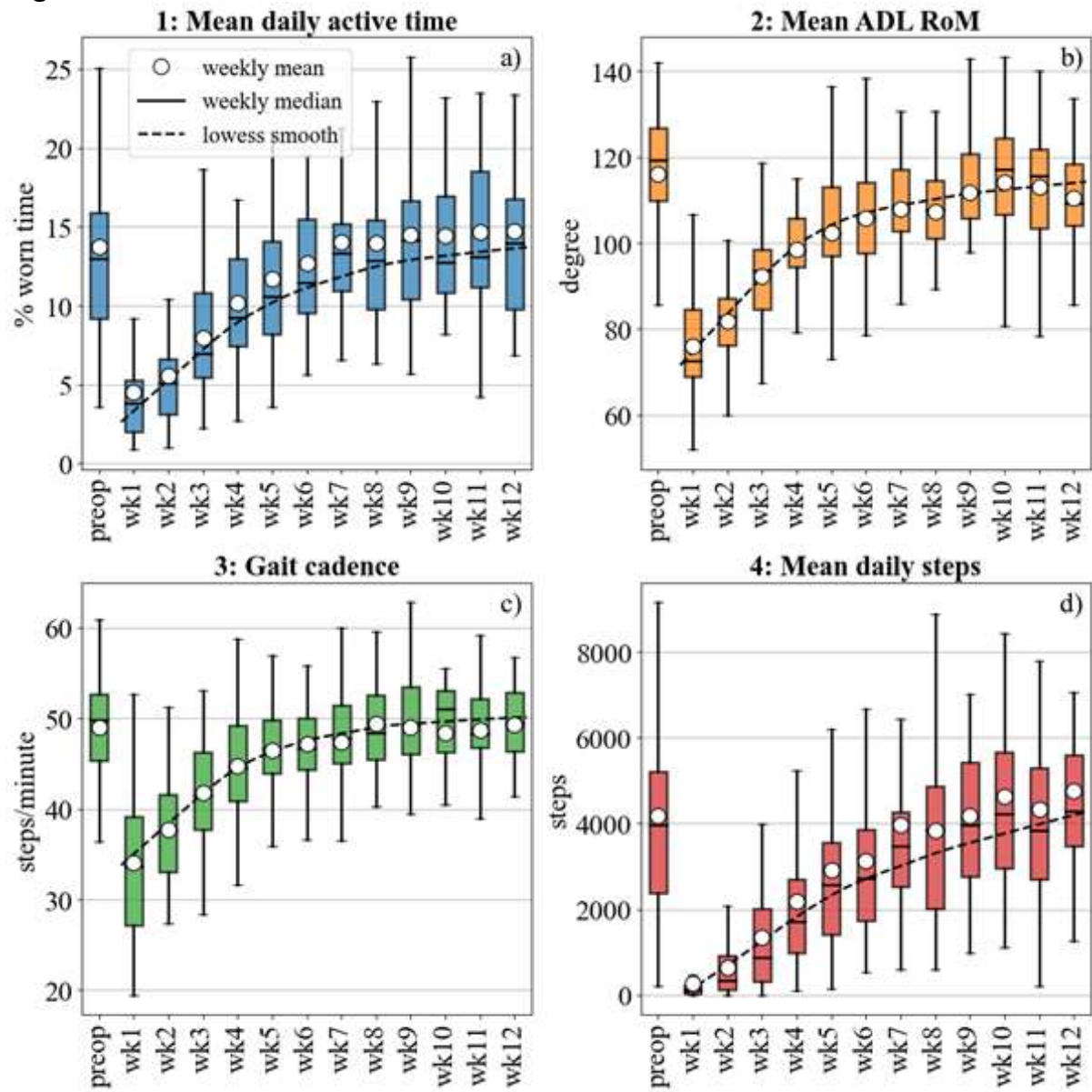


Figure 1

A PEEK-OPTIMA Femoral Component Articulating Against a Posterior Stabilized UHMWPE Gliding Surface Under Highly Demanding Activities Knee Wear Simulation

*Thomas M. Grupp - Aesculap AG - Tuttlingen, Germany

Adam Briscoe - Invibio Ltd - Lytham St. Annes, United Kingdom

Jens Schwiesau - Aesculap AG - Tuttlingen, Germany

Ian Revie - Invibio - Canada

Berna Richter - Aesculap AG - Tuttlingen, Germany

Ludger Gerdesmeyer - Orthopaedic and Trauma Surgery, Kiel Municipal Hospital - Kiel, Germany

William Mihalko - University of Tennessee - Germantown, USA

Ana Laura Puente Reyna - Ludwig Maximilians University Munich - Munich, Germany

Introduction

Total knee arthroplasty (TKA) is a well-established treatment for degenerative joint disease. However, complications may occur due to a biological response to polyethylene wear particles, as well as systemic and allergic hypersensitivity reactions triggered by metal ions such as chromium, cobalt and molybdenum. PEEK (poly-ether-ether-ketone) has been investigated in recent years as an alternative material to CoCr28Mo6, not only to avoid metal ion release, but also to improve patient satisfaction, as it is a material with a similar Young's modulus to that of bone, which could reduce stress shielding and bone resorption [Cowie2020].

Several studies have examined the wear performance of PEEK materials articulating against UHMWPE in basic pin-on-disc wear test set-ups or in standardized ISO 14243-3 (level walking only) knee wear simulation [Cowie2020,Cowie2019]. However, to further evaluate the robustness of this innovative PEEK/ UHMWPE articulation a more clinically realistic wear testing is mandatory in order to fully analyze the capabilities of PEEK as an appropriate TKA articulating material [Grupp2023].

Therefore, the purpose of the following study was to compare the wear characteristics and performance of a PEEK posterior stabilized femoral component against a clinically long-term established knee implant made out of CoCr28Mo6-alloy [Lee2023] under a highly demanding activities wear simulation.

Methods

Four medium size femoral components based on the VEGA System® posterior stabilized (PS) design (Aesculap AG) were manufactured out of PEEK-OPTIMA™ by injection molding (Invibio Ltd.). For the control group, four femur components from the clinically established casted CoCr28Mo6-alloy version of the implant were selected. UHMWPE gliding surfaces (VEGA® PS+, size T3, high 10 mm) and CoCr28Mo6 VEGA® tibial components were used in both test groups.

Wear simulation was performed on a load controlled 4 station Endolab knee wear simulator capable of reproducing loads and movement of highly demanding activities measured in vivo on 8 patients [Bergmann2014] and normalized to a patient weight of 100 kg [Schwiesau2014]. The UHMWPE gliding surfaces were evaluated for gravimetric wear. A roughness analysis of the articulating surfaces was performed through the whole test.

Results

An average wear rate of 2.6 ± 0.8 mg/million cycles was measured for the UHMWPE of the PEEK-group, whereas in the CoCr28Mo6-group it was 5.6 ± 1.2 mg/million cycles, which corresponds well to a previous ISO 14243-1 based study [Grupp2013]. The roughness of the UHMWPE gliding surface was similar for both groups through the whole test, showing similar wear patterns. On the femoral components slight scratches were seen following the direction of the articulating surface (Figure 1).

Conclusion

The wear rate of the UHMWPE gliding surfaces articulating against the PEEK PS-type femoral components was substantially lower in comparison to the articulation to the original CoCr28Mo6 femoral components and was in the range of a long-term clinically successful CR-type CoCr28Mo6 implant design [PuentesReyna2018, Schwiesau2021]. Furthermore, no cracks nor deformations were seen on the PEEK femoral cam, demonstrating to be a stable material during high flexion activities with frequent post-cam-bearing interaction. In conclusion, the PEEK femoral component shows promising wear results and represents an interesting alternative for a future metal free primary TKA solution.

Figures



Figure 1: Vega System® PS femoral component in CoCr28Mo6 (left) and made out of PEEK-OPTIMA™ (right) after 5 million HDA knee wear test cycles with slight scratches on the condylar bearing surfaces (both materials) and without any cracks or deformations on the cam of the PEEK femoral component

Figure 1

Investigating the Effects of Porous Geometries on the Interfacial Adhesion of UHMWPE-PEEK Structural Composites for Orthopedic Implant Applications

*James Smith - Drexel University - Philadelphia, USA
Cemile Basgul - Drexel University - Philadelphia, USA
Mark Allen - Orthoplastics Ltd - BACUP, United Kingdom
Steven Kurtz - Drexel University - Philadelphia, USA

Introduction: Ultra-high molecular weight polyethylene (UHMWPE) components, such as the patella and shoulder, have historically been integrated into metal backings by direct compression molding (DCM). However, metal backings are stiffer than cortical bone and may be associated with ion release *in vivo* and medical imaging distortion. DCM UHMWPE overmolded additively manufactured (AM) polyetheretherketone (PEEK) structural components could offer an alternative solution. However, an effective topology to adjoin the polymer interfaces remains unknown. In this study, we investigated different porous topologies on the interfacial force of UHMWPE overmolded AM PEEK. We asked: Can hybrid 3D printed PEEK-UHMWPE structural composites match the requirements of metal-backed UHMWPE components?

Methods and Materials: Cylindrical specimens (height = 18.5 mm and $\text{Ø} = 30$ mm) were printed from PEEK filament (M40® Evonik) on a medical material-extrusion printer (EXT 220 MED, 3D Systems). Grid, triangular, honeycomb, octahedral and gyroid porous infills with varying infill densities (20-60%) were implemented into the top third of the build, while the rest remained dense (Fig. 1). The porous PEEK specimens were then overmolded with GUR 1020 powder at industrially relevant DCM conditions. Pull-out tests ($n=3$) were performed on the specimens and compared to benchmark values (~ 3 kN) for overmolded UHMWPE-metal interfaces. Significance was determined by ANOVA ($p < 0.05$).

Results: Specimens with higher infill-densities typically (40-60%) recorded higher minimum pull-out forces, with failure occurring within the bulk of the UHMWPE (Fig. 2). By contrast, those with low infill-densities (20%) saw poorer performance and failure at the interface. Honeycomb (3.9 ± 0.2 kN) and gyroid (3.5 ± 0 kN) recorded the highest forces vs. grid (3.3 ± 0.1 kN), triangular (3.2 ± 0.2 kN) and octahedral (2.8 ± 0 kN) topologies. The honeycomb specimens benefitted from greater levels of internal friction between the UHMWPE and PEEK vs. grid and triangular, due to higher surface area availability within the porous structure to adhere to. The gyroid structure on the other hand additionally benefitted from UHMWPE ingress throughout the entirety of its internal structures (Fig. 3).

Conclusions:

UHMWPE overmolded AM PEEK specimens achieved a pull-out force of 3.9 kN, exceeding the historical benchmark for metal-polymer DCM interface components. This pilot study demonstrates the feasibility of hybrid-manufactured UHMWPE-PEEK structural composites for future orthopedic component design.

Figure Headings:

Figure 1 – Grid digital specimen (a-b) and printed PEEK at 20 (c), 40 (d) and 60 (e) infill-%. Triangular digital specimen (f-g) and printed PEEK at 20 (h), 40 (i) and 60 (j) infill-%. Honeycomb digital specimen (k-l) and printed PEEK at 20 (m), 40 (n) and 60 (o) infill-%. Octahedral digital specimen (p-q) and printed PEEK at 30 (r), 40 (s) and

60 (t) infill-%. Gyroid digital specimen (u-v) and printed PEEK at 20 (w), 25 (x) and 30 (y) infill-%.

Figure 2 – Pull-out forces of UHMWPE-porous PEEK specimens at low (a), medium (b) and high (c) infill-%.

Figure 3 – Cross-sections of UHMWPE-porous PEEK specimens: grid-20 (a), 40 (b), 60 (c), triangular-20 (d), 40 (e), 60 (f), honeycomb-20 (g), 40 (h), 60 (i), octahedral-30 (j), 40 (k), 60 (l), gyroid-20 (m), 25 (n) and 30 (o) infill-%.

Figures

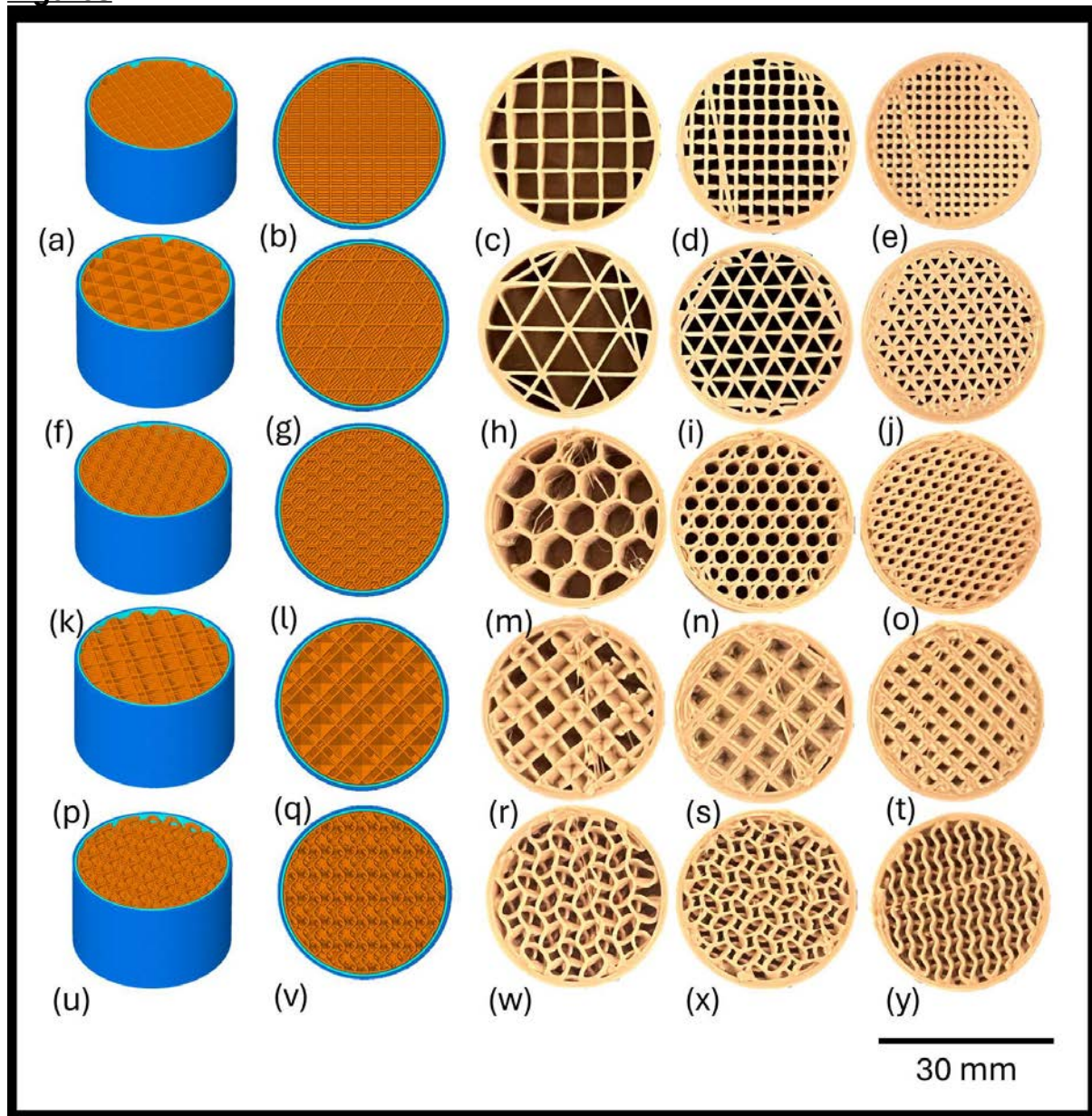


[Figure 1](#)

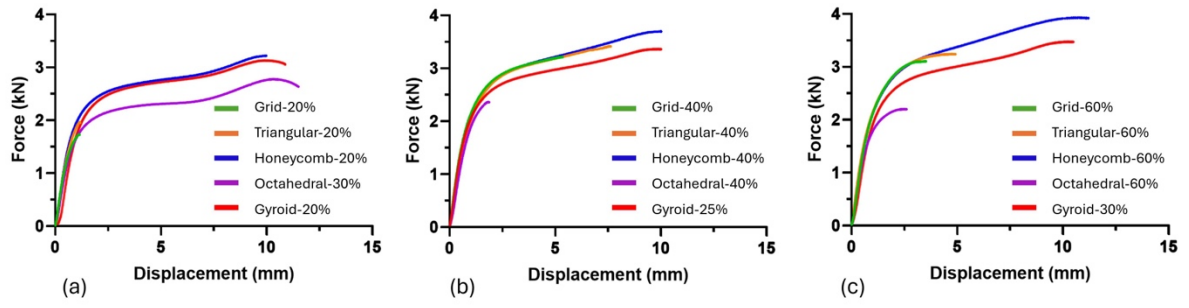
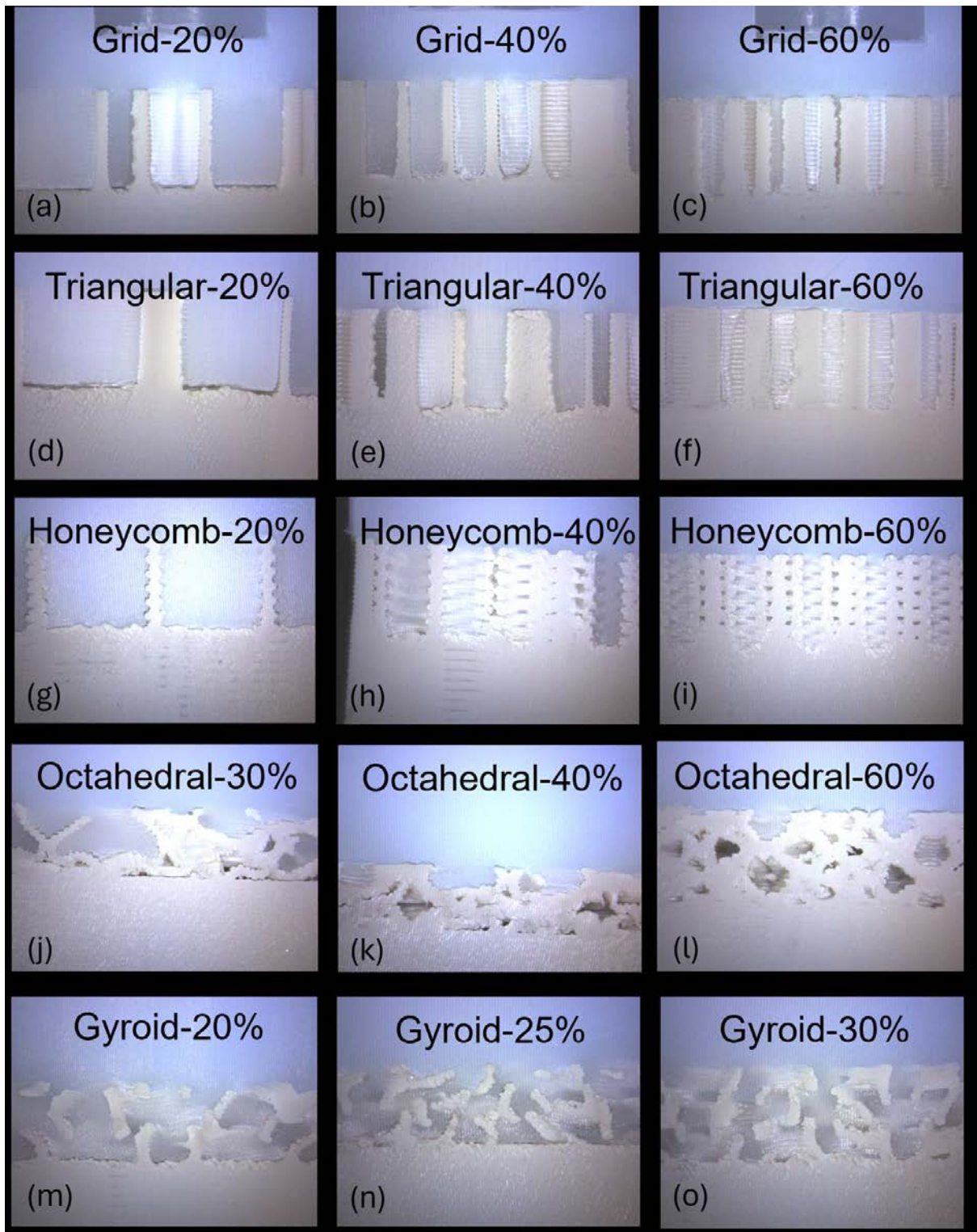


Figure 2



[Figure 3](#)

Revision Process With a Novel PEEK-OPTIMA Femoral Knee Replacement Prosthesis

*Asit Shah - Englewood Health - Englewood, USA

Harry Gaze - Invibio Ltd. - Thornton Cleveleys, United Kingdom

Ian Revie - Invibio - Canada

Adam Briscoe - Invibio Ltd - Lytham St. Annes, United Kingdom

Introduction

Revision of primary total knee prostheses is a challenging procedure and outcomes vary depending upon a number of factors. One aspect that can cause delay during the process, is the removal of a well-fixed femoral component. As well as extending the time taken to complete the operation, the removal of this component can cause significant damage to the underlying bone, increasing the challenge for the surgeon when implanting the revision component.

A novel PEEK-OPTIMA™ femoral component has been the subject of several studies over the last decade and is now in a clinical safety trial. Because this is a softer material than CoCrMo, an investigation was conducted into the possibility of removing well fixed components by resection and compared to removal of a CoCrMo component via conventional means.

Methods

Six fresh cadaver legs were implanted with Maxx Freedom cruciate retaining prostheses (three PEEK and three CoCr). Sizes were matched to the bone as per the surgical procedure. Palacos R cement was used for all components, mixed according to the manufacturers' instructions, under vacuum. Implantation wounds were closed and specimens kept at room temperature overnight to ensure that cement had fully polymerised.

Standard removal technique was used for removal of the CoCrMo components. This involved multiple different instruments, employed in a variety of ways. Time to remove the component was recorded.

Removal of the PEEK component, involved the use of an oscillating saw to section the implant along two lines, each at the chamfer cut of the implant, resulting in 5 pieces. These pieces were then prised from the bone/cement using an osteotome. Again, time to retrieve the components was recorded.

Assessment of the quantity of bone removed during the retrieval process was carried out by taking a cast of the dissected distal femoral bone, which were scanned using a GOM scanner. This produced a 3-dimensional model of the bone. By positioning a virtual component against this bone and calculating the gap a measure for the lost bone was made.

Results

Time taken to remove each of the implants are shown in Table 1 alongside the size of each implant. The average time to remove a metallic implant was 768 s, whereas the average time to remove a PEEK implant was 178 s.

The volume of bone lost in the removal process was calculated as 13812mm³ for the metallic group and 2605mm³ in the PEEK group. Figure 2 shows a view of the volume of bone lost from the femur, calculated as the gap between the implant and the femoral bone from the scanned replica.

Discussion

Removal of PEEK-OPTIMA™ components, using the proposed sectioning technique, took on average nearly 10 minutes less time than the removal of metallic components. Bone loss may be minimised, enabling reduced requirement for augmentation of the host bone for implantation of a revision component. If this technique can be employed, this may lead to improvements in infection control, rehabilitation time, due to reduced trauma during the removal process and improved outcomes of revision procedures.

Figures

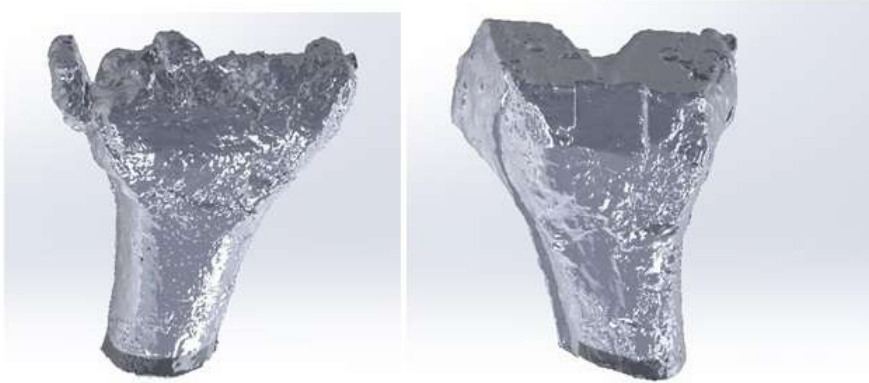


Figure 1 - Scans taken of dissected bone replicas following removal of femoral components

Figure 1

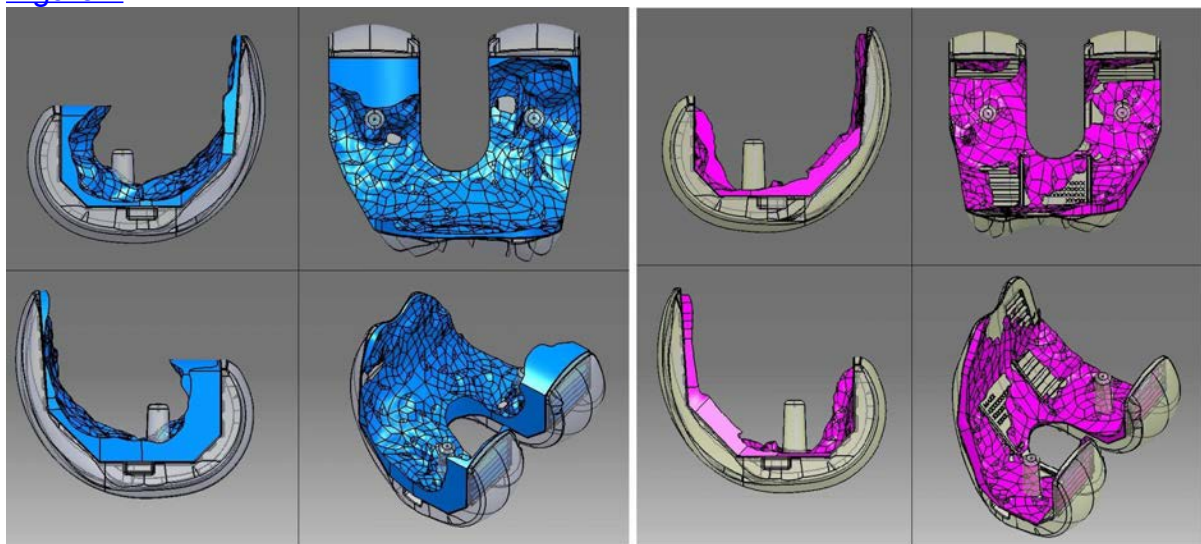


Figure 2 - Volume of bone lost after removal of femoral component (Left - CoCr using traditional removal technique, Right - PEEK using novel resection technique)

Figure 2

Implantation	Implant Material	Component size	Removal time (s)
1	PEEK-OPTIMA™	C	145
2	CoCr	C	625
3	CoCr	G	686
4	PEEK-OPTIMA™	G	231
5	CoCr	F	992
6	PEEK-OPTIMA™	F	158

Table 1 – Time to remove each component from bone

[Figure 3](#)

Challenges and Opportunities for Implant Fixation of PEEK Total Knee Arthroplasty: Lessons Learned From a Decade of Biomechanical Research

*Dennis Janssen - Radboud University Nijmegen Medical Centre - Nijmegen, Netherlands

Lennert de Ruiter - Radboud University Medical Center - Nijmegen, Netherlands

Corine Post - Radboud university medical centre - Nijmegen, Netherlands

Adam Briscoe - Invivio Ltd - Lytham St. Annes, United Kingdom

Thom Bitter - Raboud University Nijmegen Medical Centre - Nijmegen, Netherlands

Nico Verdonschot - Radboudumc - Nijmegen, Netherlands

Introduction

More than ten years ago our group started investigating the biomechanical implications of an all-polymer total knee arthroplasty system, consisting of an all-poly tibial component and a PEEK-Optima™ femoral component. PEEK (polyether ether ketone) is a high-grade polymer that has been used in several orthopaedic applications, such as screws, spinal cages, and fracture repair plates. PEEK is inert, biocompatible, radiolucent, and has a stiffness that is 25 to 50 times lower than metal alloys that currently are being used for TKA. The reduced material stiffness obviously has implications for the fixation biomechanics of PEEK components, but also for the load transfer across the joint to the underlying bone. In our research we initially investigated the biomechanical response of cemented femoral components, and subsequently expanded our focus to cementless femoral components and tibial baseplates, with a focus on implant fixation and periprosthetic load transfer.

Methods

A combination of experimental and computational analyses was adopted to evaluate the fixation of PEEK TKA components. The cemented femoral component was evaluated in pull-off experiments to determine the basic strength of the fixation, while computational modelling was used to investigate the fixation mechanics during activities of daily living. Similarly, fixation of cementless femoral and tibial components was investigated by evaluating interface micromotions.

The effect of PEEK components on periprosthetic load transfer was evaluated by studying changes in bone strains compared to conventional (metal) TKA components. Changes to bone surface strains were measured experimentally in cadaver experiments, while internal bone strain changes under physiological loads were simulated in computational models.

To further enhance the robustness of the computational modelling approach, analyses were performed on a larger population of models that was created based on CT data. The population-based analyses allow for evaluation of patient factors such as sex, age, and BMI.

Results

The biomechanical evaluations have demonstrated the feasibility of obtaining proper mechanical fixation of a cemented femoral PEEK component, through minor adjustments of the internal surface of the component to optimize the strength of the implant-cement interface (Figure 1). Cementless PEEK components generally displayed larger micromotions compared to metal implants. However, appropriate fixation can be achieved by adopting an adequate interference fit and surface coating. Using PEEK components it is possible to achieve more physiological

periprosthetic bone strains (Figure 2). Finally, simulations on a larger population of models demonstrated larger micromotions with increasing BMI, both for PEEK and metal TKA components.

Discussion

Changing the implant material for TKA components from metal (CoCr or titanium alloy) to PEEK presents new challenges and opportunities for patient care. All-polymer TKA systems can provide treatment options for patients suffering from metal hypersensitivity, but may also assist in preventing adverse peri-prosthetic bone changes. However, evaluating the implications of changing implant material on fixation is essential to ensure patient safety and longevity of the reconstruction. The research presented here has demonstrated the effect of using PEEK TKA components on the biomechanical response, and can assist in optimizing implant design to provide a robust solution for the entire patient population.

All-Polymer PEEK Knee Prosthesis: Radiologic Imaging Characteristics and Complication Detection

*Cedric Bohyn - AZ Monica Hospital - Antwerp, Belgium

Dennis Janssen - Radboud University Nijmegen Medical Centre - Nijmegen, Netherlands

Fedra Parnian Zaribaf - University of Bath - Bath, United Kingdom

Adam Briscoe - Invivio Ltd - Lytham St. Annes, United Kingdom

Introduction

Radiologic examination and follow-up of joint replacements have some limitations, primarily the result of metal artifacts. Weight-bearing arthroplasties have large metal components causing metal artifacts (Fig. 1), especially on CT and MRI scans, obscuring the areas adjacent to the metallic components. Therefore, certain complications such as cement fracture or implant loosening of joint replacements can be missed, especially in the early stage. The PEEK (Polyether Ether Ketone) Knee is a new concept for an all-polymer prosthetic joint replacement using material previously unseen by radiologists in the knee joint. The imaging (XR, CT, and MRI) characteristics of this material are known through the appearances in spinal applications but not in the context of intra-articular use. An all-polymer PEEK knee replacement has the advantage of being completely radiolucent and free of any metal components allowing better and earlier diagnosis of failure on radiologic follow-up (Fig. 2). This study aims to evaluate the characteristics of the PEEK knee under standard medical imaging protocols.

Methods

The all-polymer PEEK knee prostheses (Invivio, Thornton-Cleveleys, UK) were implanted in four cadaveric lower-limb specimens. The implanted PEEK knee prostheses were imaged using radiography, CT, and MRI applying standardized imaging protocols.

Subsequently, prosthesis complications were deliberately inflicted on the PEEK implants to simulate the following complications in the following order: implant loosening, cement fractures, implant migration, and prosthesis fracture. After each simulated complication, the joint was closed and filled with saline through a catheter. During the filling process, the knee was flexed several times and compressed manually to remove entrapped air from the joint. At each stage of complication simulation, the four specimens were again radiologically (XR, CT, and MRI) examined using the same standardized imaging protocols.

An experienced musculoskeletal specialized radiologist thoroughly studies all X-rays, CT, and MRI scans to compare the imaging appearances of a normal PEEK knee and each simulated prosthesis complication.

Results

All three image modalities (XR, CT, and MRI) allowed a clear depiction of the PEEK knee prosthesis and evaluation of its correct position. Radiography and especially CT accurately represented the entire bone-cement interface of the prostheses which is normally only partially visible in a metallic knee replacement.

Cement fractures were always detected on both CT and radiography. Subtle cement fractures were difficult to detect radiographically and needed careful comparison with the initial studies. On the other hand, cement fractures remained mostly undetected on MRI given the hypo-intense nature of cement, similar to the adjacent bone.

Prosthesis fracture and migration could be detected and were most obvious on MRI given MRI's superior demonstration of fluid in the widened bone-cement interface. In this cadaveric study, it was also possible to visualize the implant fractures and migration indirectly on radiographs due to the presence of interspersed gas. The interspersed gas obviously is an artifact of the cadaveric study and will not be present in the clinical situation.

Conclusions

The all-polymer PEEK knee enables early detection of complications on radiologic follow-up which are obscured in metal-based knee replacement.

Figures

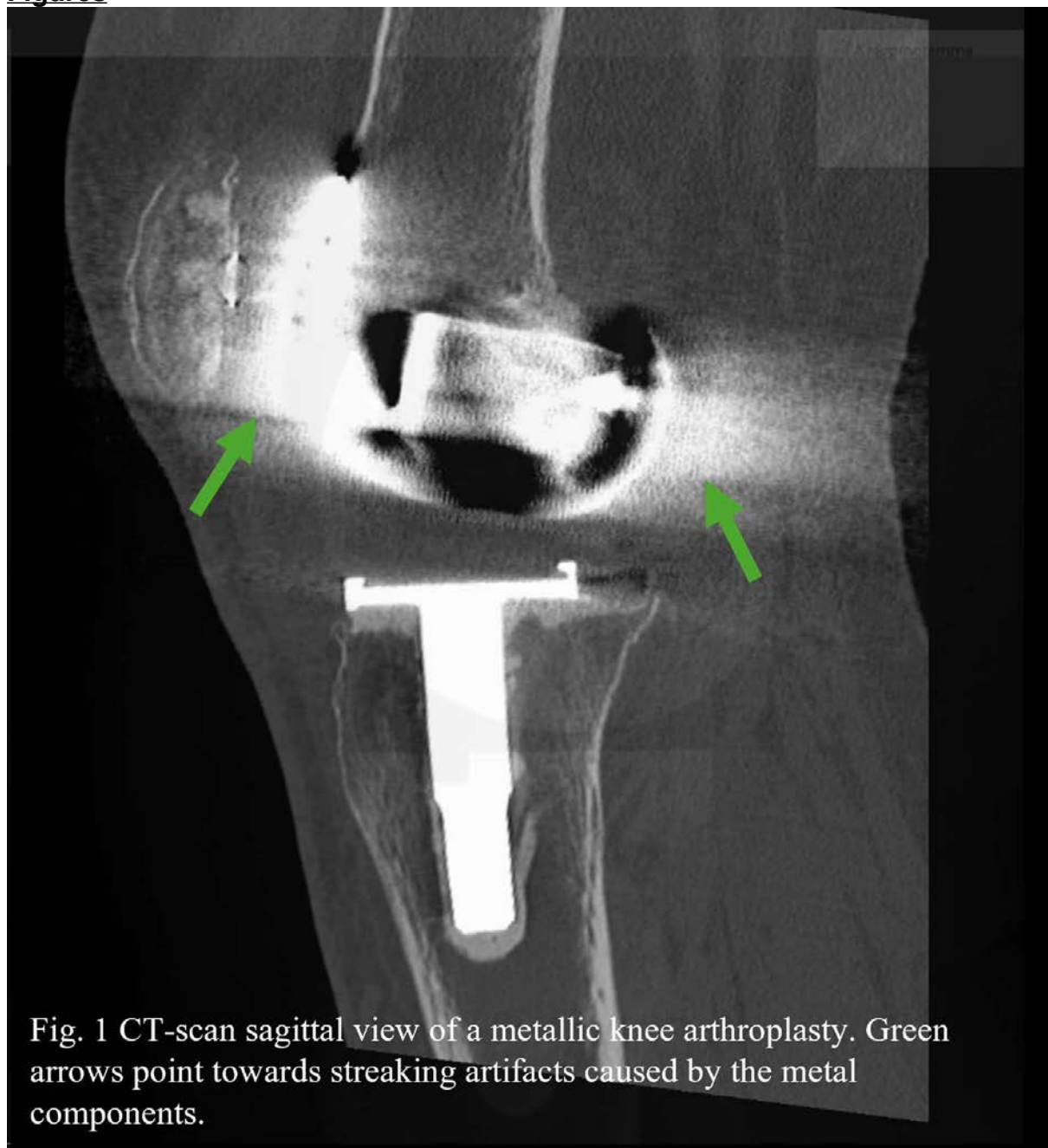


Fig. 1 CT-scan sagittal view of a metallic knee arthroplasty. Green arrows point towards streaking artifacts caused by the metal components.

[Figure1](#)

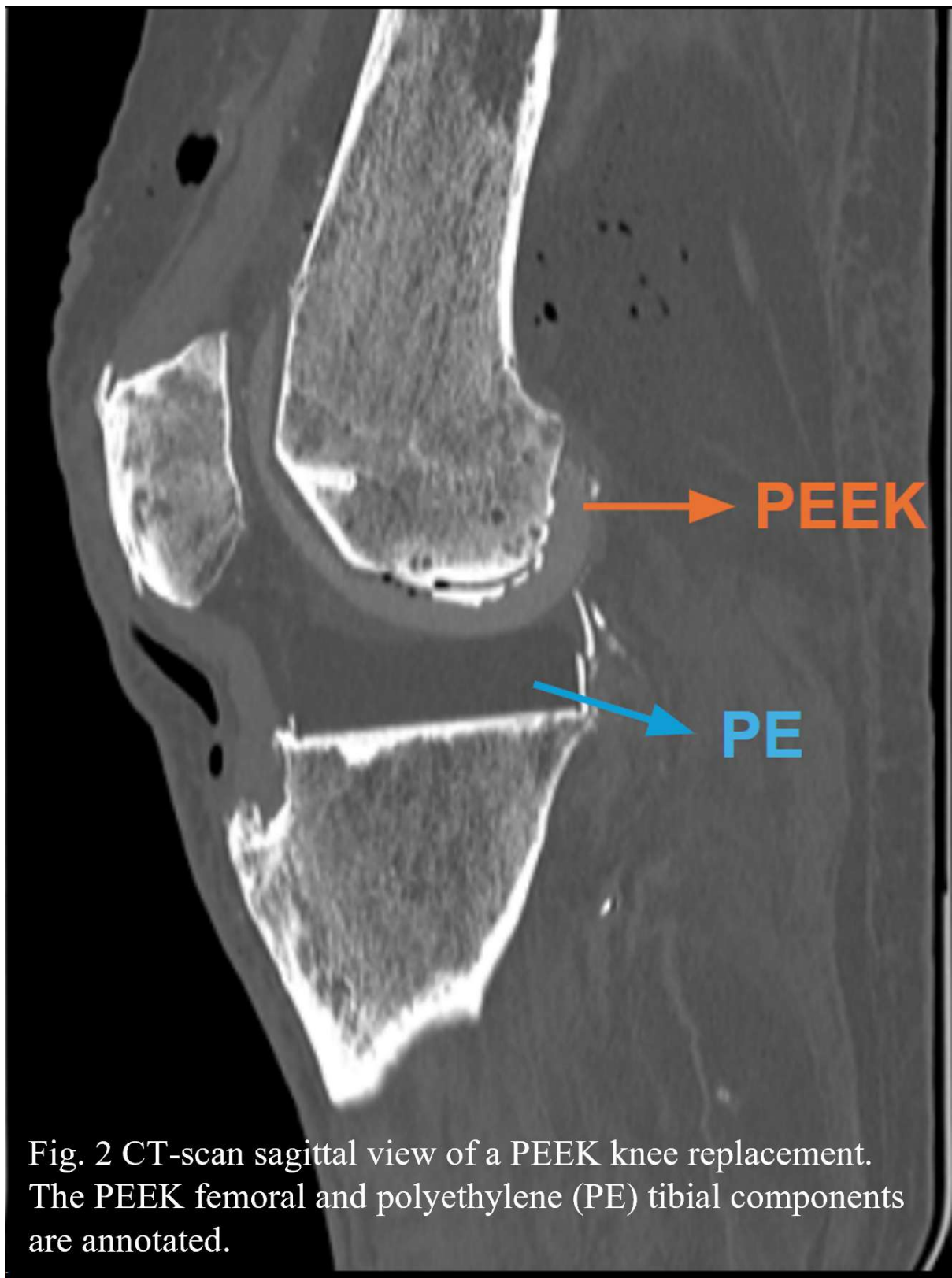


Fig. 2 CT-scan sagittal view of a PEEK knee replacement. The PEEK femoral and polyethylene (PE) tibial components are annotated.

[Figure 2](#)

PEKK Promotes Osteogenic Activity in Vitro Compared to PEEK in Solid 3D Printed Specimens

*Paul DeSantis - Drexel University - Philadelphia, United States of America

Tabitha Derr - Drexel University - Philadelphia, USA

Ryan Bock - SINTX Technologies - Salt Lake City, USA

Noreen Hickok

Steven M. Kurtz - Drexel - Philadelphia, USA

INTRODUCTION: Polyetheretherketone (PEEK), a high-temperature semicrystalline thermoplastic, has been considered as an alternative to CoCr for use in metal-free knee implants. PEEK implants have similar elastic modulus to bone, reducing stress shielding, but are also likely to fail at their interface due to their smooth surface and poor osseointegration. Polyetherketoneketone (PEKK), a relative of PEEK, differs in glass transition temperature and melt temperature, and its additional ketone group may influence its bioactivity. While research into coatings and composite materials of PEEK have aimed to overcome PEEK's poor osseointegrative properties, it is important to consider that PEKK may serve as a better starting point for use in arthroplasty due to its different surface properties. This work aims to explore how 3D printed PEEK and PEKK specimens perform *in vitro*, using a mouse pre-osteoblast model.

METHODS: PEEK and PEKK filaments were printed into solid discs with a 10 mm diameter and 1 mm height. Discs were sterilized, placed in an ultra-low-attachment (ULA) plate, pre-incubated in Minimal Essential Media Alpha (supplemented with 10% fetal bovine serum and 1% penicillin-streptomycin) for 24 hours, and seeded with 30,000 MC3T3 E1 mouse pre-osteoblasts. An empty ULA well acted as a control. After 7 days, media was supplemented with 5mM β -glycerophosphate and 50 μ g/mL of ascorbate to support osteogenic differentiation. After 24 and 72 hours, an MTT assay was performed to determine short term cell attachment and growth; at days 7, 14, and 21, an assay using fluorescein-diacetate (FDA) and 4-methylumbelliferone-phosphate (4-MUP) was used to determine normalized osteogenic activity; and at days 21 and 28, Alizarin Red stain was used to quantify cumulative mineralization on each surface. After 3 days, samples were also fixed with Karnovsky's fixative (2% paraformaldehyde, 2.5% glutaraldehyde), dehydrated in ethanol, and imaged using a scanning electron microscope to evaluate cell morphology. Statistical significance of quantitative data was determined using ANOVA with multiple comparisons ($\alpha=0.05$, $n=6$).

RESULTS: Short term cell attachment results were determined using an MTT assay (Figure 1), and PEKK was found to have significantly more cells attached when compared to PEEK after 24 and 72 hours of culture ($p<0.001$). PEKK was also found to have more normalized ALP activity, an indicator of osteogenic behavior (Figure 2), after 7, 14, and 21 days of culture ($p<0.001$). Figure 3 shows the morphology of fixed cells after 3 days of culture, where cells grown on PEEK have a more elongated shape when compared to the cells grown on PEKK. Cells grown on PEKK have a more typical, flat, fibroblast-like cell morphology with a larger number of attachments, possibly indicating a better surface for cell adhesion.

CONCLUSION: These *in vitro* results suggest that PEKK may be a more beneficial surface for cell attachment and osteogenic activity when compared to PEEK. With PEEK already being considered for use in non-metal knee implants, additional *in vivo* work is needed to evaluate whether PEKK should also be explored further for these novel devices.

Figures

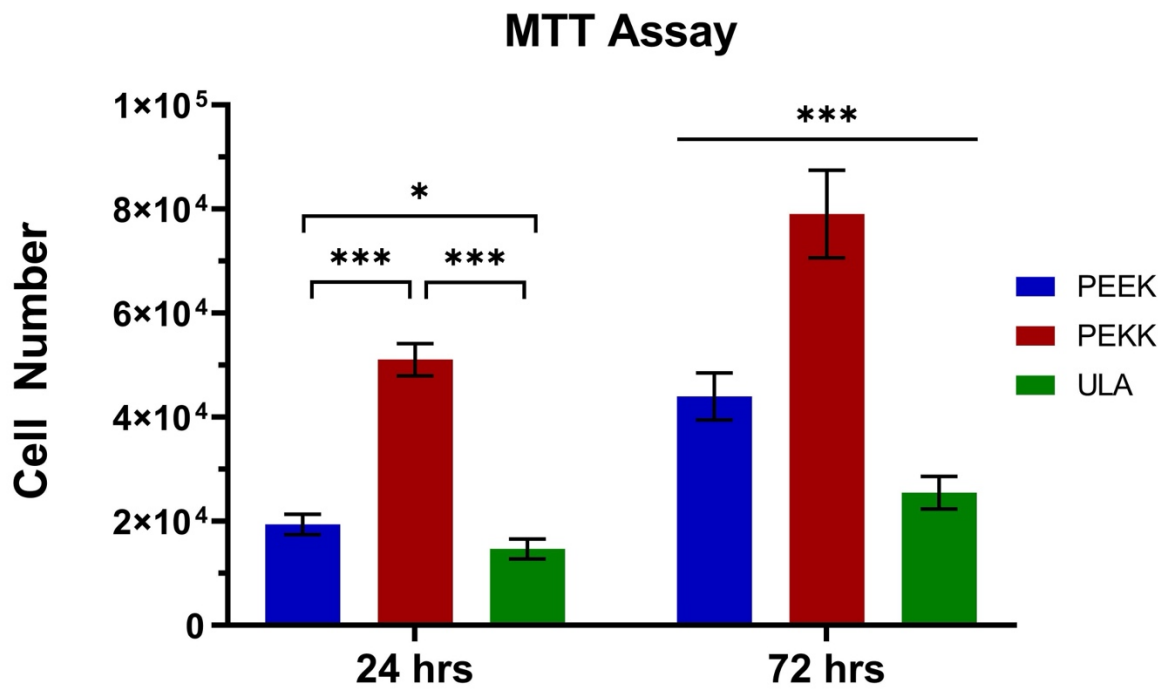


Figure 1

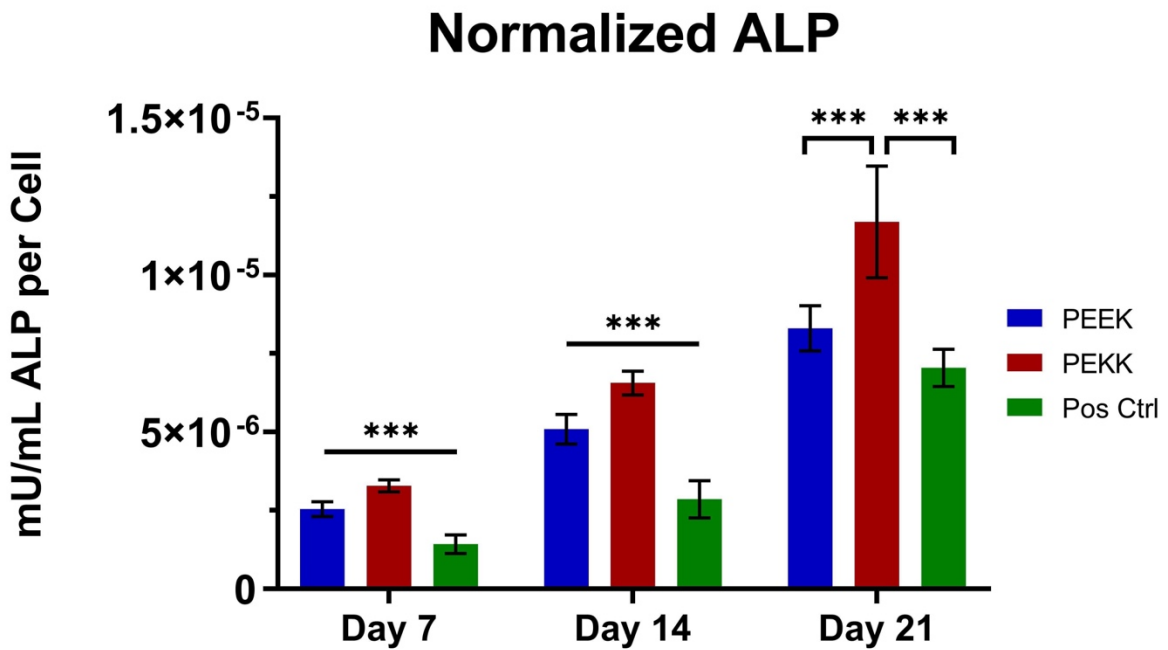
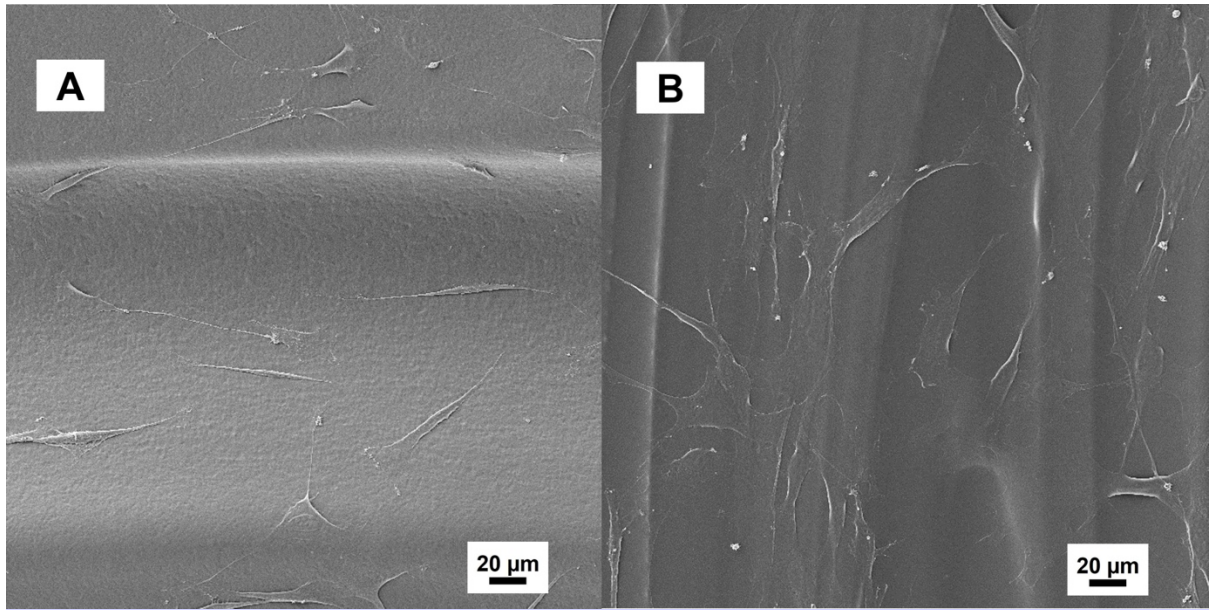


Figure 2



[Figure 3](#)

Taguchi Optimization of Additively Manufactured PEKK and Silicon Nitride Loaded PEKK for Medical Device Applications

*Tabitha Derr - Drexel University - Philadelphia, USA

Cemile Basgul - Drexel University - Philadelphia, USA

Paul DeSantis - Drexel University - Philadelphia, United States of America

Ryan Bock - SINTX Technologies - Salt Lake City, USA

Steven Kurtz - Drexel University - Philadelphia, USA

Introduction:

Periprosthetic joint infection remains a prevalent issue in modern joint arthroplasty. Silicon nitride, known to exhibit anti-bacterial properties and support osteoblast maturation, provides an effective method of combating infection. Incorporating silicon nitride with polyetherketoneketone (PEKK) enables it to exploit PEKK's favorable mechanical properties and advantageous manufacturability using extrusion-based additive manufacturing. Hence, silicon nitride loaded polyetherketoneketone (SN PEKK) composites may be of potential value in creating infection-resistant patient-specific medical implants. Our objective was to determine optimal fused filament fabrication (FFF) parameters for PEKK and SN PEKK.

Methods:

Taguchi optimization (L9 array, n=5) was performed on PEKK (IMPEKK® 3D-F, Seqens) and SN PEKK to assess the impact of printing parameters (layer height, nozzle temperature, bed temperature, and chamber temperature) on ultimate tensile strength (UTS). Z-directional tensile specimens were printed on a medical FFF printer (EXT 220 MED, 3D Systems). Specimens underwent tensile testing according to ASTM D638. Signal/noise ratios for UTS were calculated and ANOVA (Minitab 21.4.2) was used to assess statistical significance ($p < 0.05$).

Results:

Layer height had the greatest impact on UTS (signal/noise range: PEKK, 2.0 and SN PEKK, 4.4). Optimal nozzle and chamber temperatures were 400 °C and 130 °C for both materials, while optimal layer height was 0.1 mm for both materials. Optimal bed temperature for PEKK and SN PEKK were 150 °C and 170 °C, respectively. For PEKK, differences in all parameters were significant except bed temperature, while for SN PEKK all parameters were significant except nozzle temperature. Models with a layer height of 0.1 mm required 3 hours 23 minutes to print, while those with a layer height of 0.3 mm needed 1 hour 9 minutes. The specimens with optimum statistically significant parameters showed the highest UTS for both PEKK (91 ± 2 MPa) and SN PEKK (76 ± 3 MPa).

Conclusions:

Layer height is the most influential printing variable for both PEKK and SN PEKK; however, low layer height significantly increases print time. The optimal PEKK printing condition has a UTS comparable to that of injection molded specimens, but SN PEKK achieved only 84% of the injection molded value for neat PEKK. Further research is needed to understand SN dispersion in the composite tensile specimens and its potential implications on the behavior of medical implants.

The Effect of Component Lateralization in Reverse Total Shoulder Arthroplasty on Muscle Function and Scapular Strains During Simulated Active Motion: An Ex-Vivo Biomechanical Study

*David Axford - Western University - London, Canada

Robert Potra - Mathys Ltd Bettlach - London, Canada

Richard Appleyard - Macquarie University - Sydney, Australia

Janos Tomka - Macquarie University - Sydney, Australia

Desmond Bokor - Macquarie University Hospital - Sydney, Australia

*Sumit Raniga - Macquarie University - Sydney, Australia

Louis Ferreira - University of Western Ontario - London, Canada

Introduction

Implant lateralization in reverse total shoulder arthroplasty (RTSA) is used to balance several competing objectives. While glenoid and humeral lateralization can improve function and reduce the occurrence of complications associated with medialized designs, they can have adverse effects. With many commercially available RTSA implants, a comprehensive understanding of the biomechanical implications of implant lateralization is needed. Therefore, the purpose of this study was to use an ex-vivo shoulder motion simulator to investigate the effect of glenoid-sided lateralization, humeral-sided lateralization, and humeral-to-glenoid lateralization ratio on muscle function and scapular strains.

Methods

An ex-vivo shoulder motion simulator (Figure 1) performed scapular plane abduction (SPA) and internal rotation (IR) in eight cadaveric specimens (48 ± 14 years) for several joint conditions: intact; +0, +5, +10mm humeral lateralization; +0, +2.5, +5mm glenosphere lateralization; and 100%, 75%, and 50% lateralization ratio (humeral lateralization/glenoid lateralization) with constant global lateralization of +10mm. Four strain gauge rosettes were mounted to the acromion and scapular spine surface (Figure 2A, [1]) to measure strain throughout motion. Repeated measures analysis of variance was used to compare muscle function (excursion, force, and muscle work) and scapular strains across joint conditions.

Results

During SPA, compared to the intact state, RTSA implantation resulted in significant increases in deltoid function with decreases in rotator cuff function ($p < .05$). During IR, all RTSA states showed an increase in anterior deltoid function with decreases in inferior subscapularis and supraspinatus function ($p < .05$). Humeral lateralization was significantly associated with increases in superior subscapularis work ($p < .05$) as well as decreases in zones 2 and 3A strain ($p < .05$) (Figure 3 and 2B). Lateral deltoid force and work decreased while excursion increased with progressive humeral lateralization, although this was not significant. Glenosphere lateralization resulted in increases in deltoid and superior subscapularis force; however, these were not significant. Scapular strains were not significantly affected by glenosphere lateralization. Finally, increases in lateralization ratio resulted in increases in lateral and posterior deltoid excursion during SPA as well as decreases in superior subscapularis work, although not significant. An increase in lateralization ratio was significantly associated with decreases in strain in zones 2 and 3A ($p < .05$).

Conclusions

RTSA implantation significantly increased deltoid function during SPA and IR while decreasing rotator cuff function. Humeral lateralization restored rotator cuff function while decreasing scapular strain. Finally, constant global lateralization favoring

humerus lateralization over glenosphere lateralization showed small increases in deltoid recruitment with significant decreases in scapula strain.

References

[1] Kerrigan, A. M., Reeves, J. M., Langohr, G. D. G., Johnson, J. A., and Athwal, G. S., 2021, "The Influence of Reverse Arthroplasty Humeral Component Design Features on Scapular Spine Strain," *J Shoulder Elbow Surg*, 30(3), pp. 572–579.

Figures

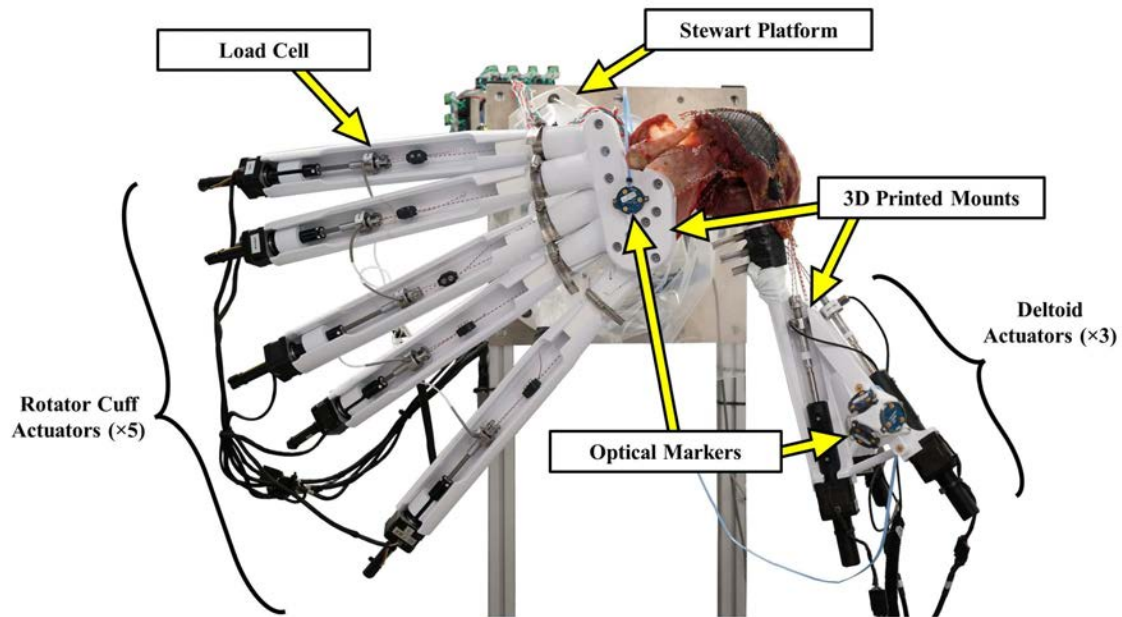


Figure 1: (A) Ex-vivo shoulder motion simulator. A specimen-specific 3D-printed scapular mount secured each specimen to a Stewart platform that simulated upward rotation of the scapula during motion. Three computer-controlled actuators were connected to the three aspects of the deltoid and five actuators were connected to five aspects of the rotator cuff. A load cell at the end of each actuator measured tendon load and optical markers tracked joint kinematics.

[Figure 1](#)

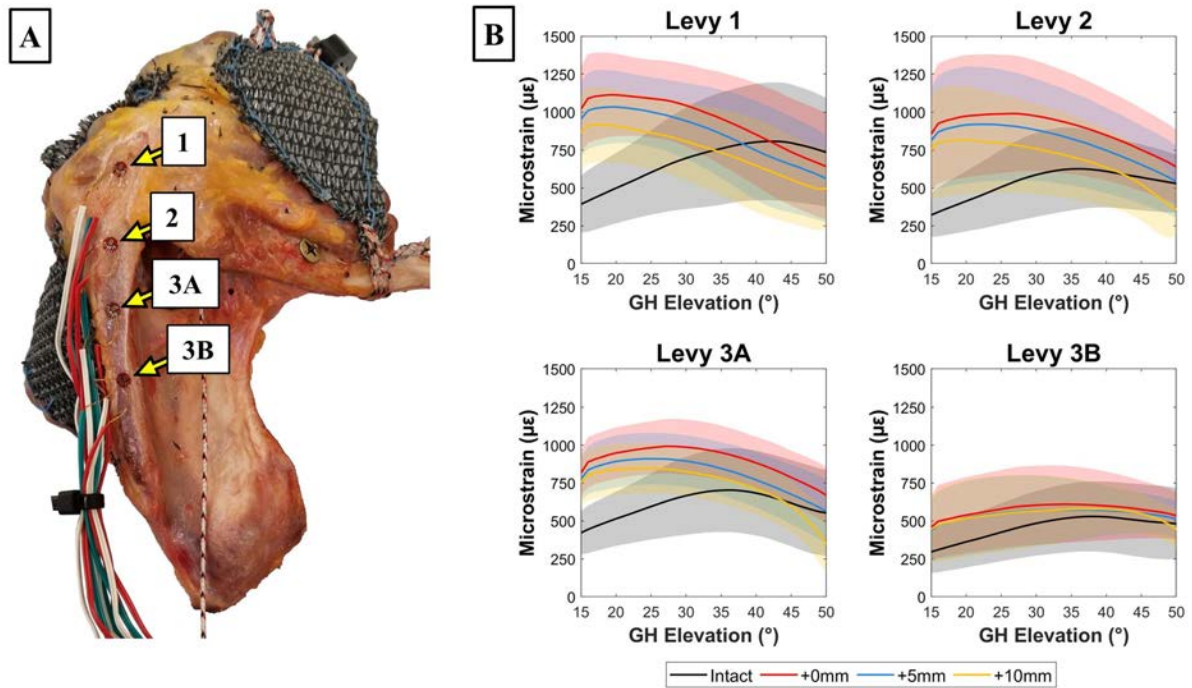


Figure 2: (A) Maximum principal strain was measured in four regions of the acromion and scapula spine as described by Kerrigan et al. [1] using triaxial strain gauge rosettes. (B) Maximum principal strains (N=8, Mean \pm SD) measured in each of the four regions (1, 2, 3A, and 3B) for each joint condition (intact, +0mm, +5mm, +10mm humerus lateralization) during scapular plane abduction.

Figure 2

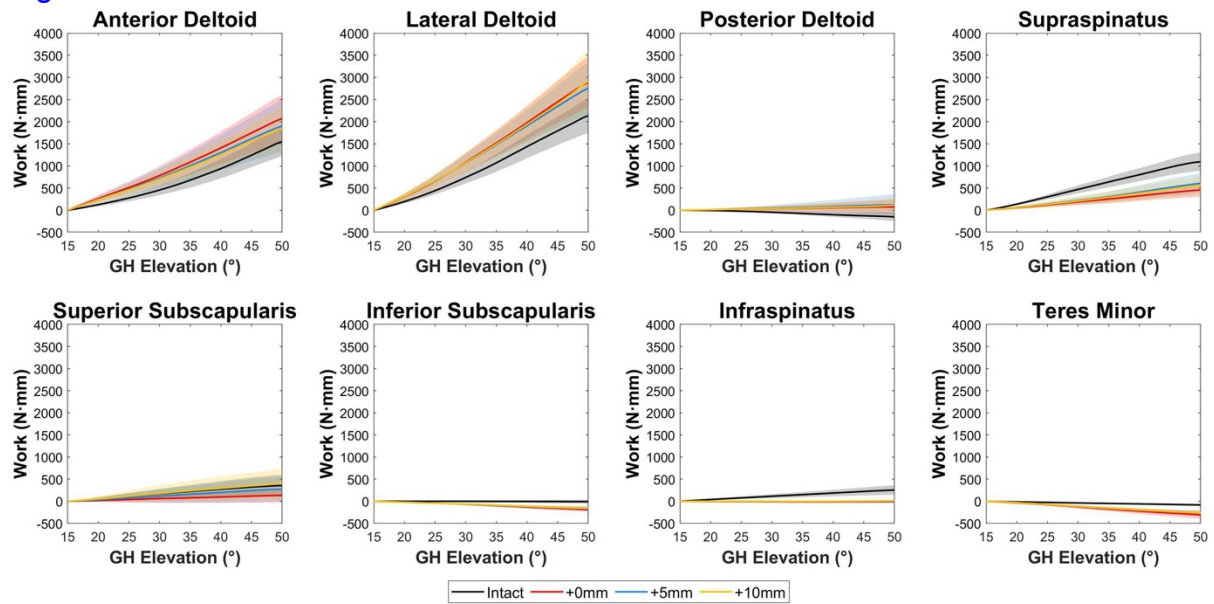


Figure 3: Average muscle work during scapular plane abduction (N=8, Mean \pm SD) for the intact joint and every progressive stage of RTSA humeral lateralization (intact, +0mm, +5mm, +10mm lateralization). Positive work means that the muscle is an agonist to the motion and negative work means that the muscle is an antagonist.

Figure 3

Semi-Inlay Type Reverse Shoulder Arthroplasty May Enhance Scapulohumeral Rhythm Compared to Inlay Type

*Itaru Kawashima - University of Florida - GAINESVILLE, United States of America

Norimasa Takahashi - Funabashi Orthopaedic Hospital - Funabashi, Japan

Keisuke Matsuki - Sports Medicine & Joint Center, Funabashi Orthopaedic Hospital - Funabashi, Japan

Kenji Kitamura - University of Florida - GAINESVILLE, USA

Hisato Watanabe - Funabashi Orthopaedic Hospital - Funabashi, Japan

Ryo Haraguchi - Funabashi Orthopaedic Hospital - Funabashi, Japan

Hayato Ryoki - Funabashi Orthopaedic Hospital - Funabashi, Japan

Thomas Wright - UFL - USA

Scott Banks - University of Florida - Gainesville, USA

Introduction

The scapulohumeral rhythm (SHR) refers to the 2:1 ratio of glenohumeral to scapulothoracic motion in the normal shoulder [1]. It has been recognized low but as crucial for improving shoulder joint elevation in shoulders undergoing reverse-type total shoulder arthroplasty (RSA) [2]. However, there is limited knowledge regarding kinematics, including SHR, in shoulders with the semi-inlay type of RSA, a relatively recent implant design situated between the inlay and onlay types. This study aimed to analyze SHR during glenohumeral joint abduction in postoperative shoulders with semi-inlay type RSA and compare it with inlay type RSA.

Methods

Eleven shoulders with semi-inlay RSA and 19 shoulders with inlay RSA over one year after surgery were analyzed. Shoulders underwent computed tomography and fluoroscopy during active scapular plane abduction. Using model-image registration techniques, poses of 3-dimensional implant models were iteratively adjusted to match their silhouettes with the silhouettes in the fluoroscopic images (shape matching), and 3-dimensional kinematics of implants were computed. SHR at each humeral elevation angle was calculated as $(\Delta H - \Delta S) / \Delta S$, where ΔH is the increment in humeral elevation angle and ΔS is the increment in scapular upward rotation angle. The mean SHR was assessed from 20 to 90° of humeral abduction. Additionally, the ratio of mean SHR ≥ 2 was also analyzed. Two-way repeated-measures analysis of variance (ANOVA) with post-hoc Bonferroni correction, student's t-test, and Fisher's exact test were used for statistical analysis. P values < 0.05 were considered statistically significant.

Results

SHR at each humeral elevation angle did not differ significantly between shoulders with semi-inlay RSA and inlay RSA (Fig. 1). Mean SHR until 90° of humeral abduction was also not significantly different between the two groups (Fig. 2). However, the proportion of shoulders with mean SHR ≥ 2 in shoulders with semi-inlay was significantly higher than that in inlay (4 of 11 [36.3%] vs 1 of 19 [5.3%], respectively; $p = 0.0472$).

Conclusion

The present study suggests the potential for the semi-inlay type RSA to enhance the SHR compared to the inlay type. Lateralizing the humerus could have influenced the observed results.

References

1. Inman VT, Saunders JB, Abbott LC. Clin Orthop Relat Res. 1996 Sep; (330):3-12.

Figures

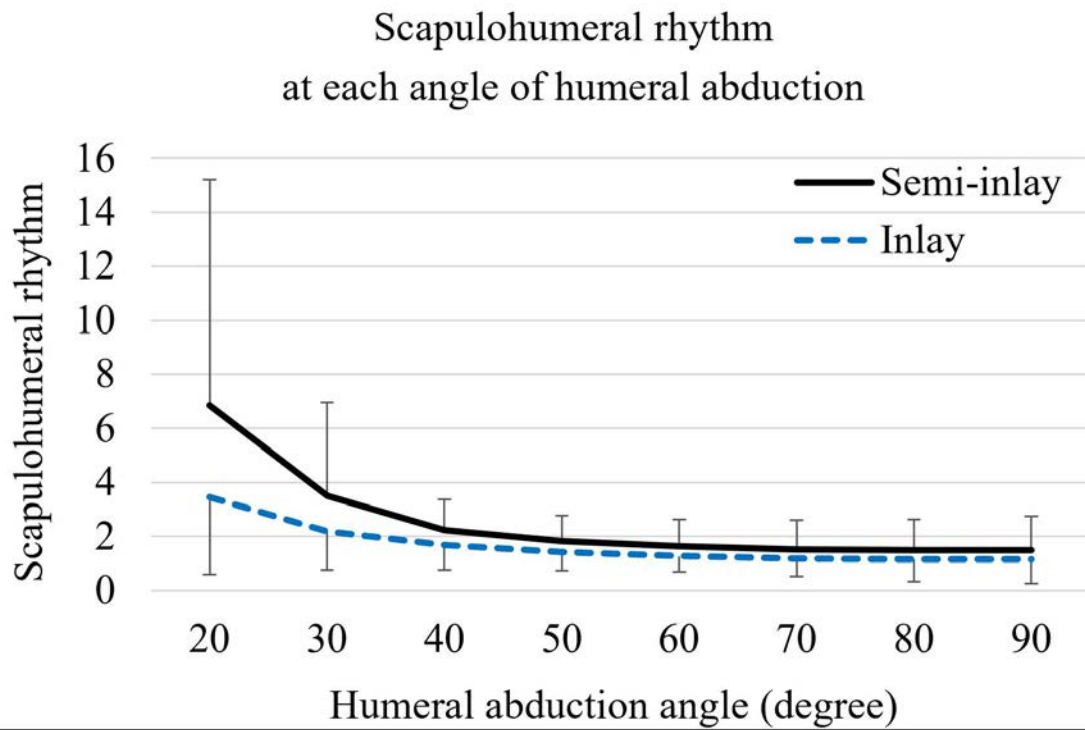


[Figure 1](#)

Mean scapulohumeral rhythm
until 90° of humeral abduction

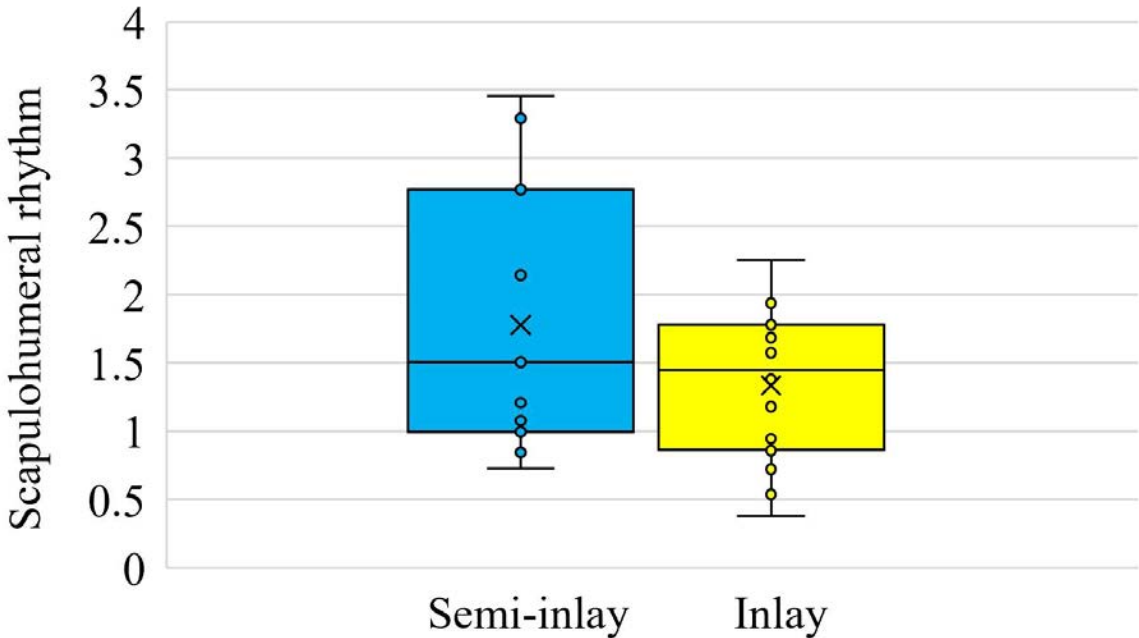


Figure 2

The ratio of mean scapulohumeral rhythm ≥ 2

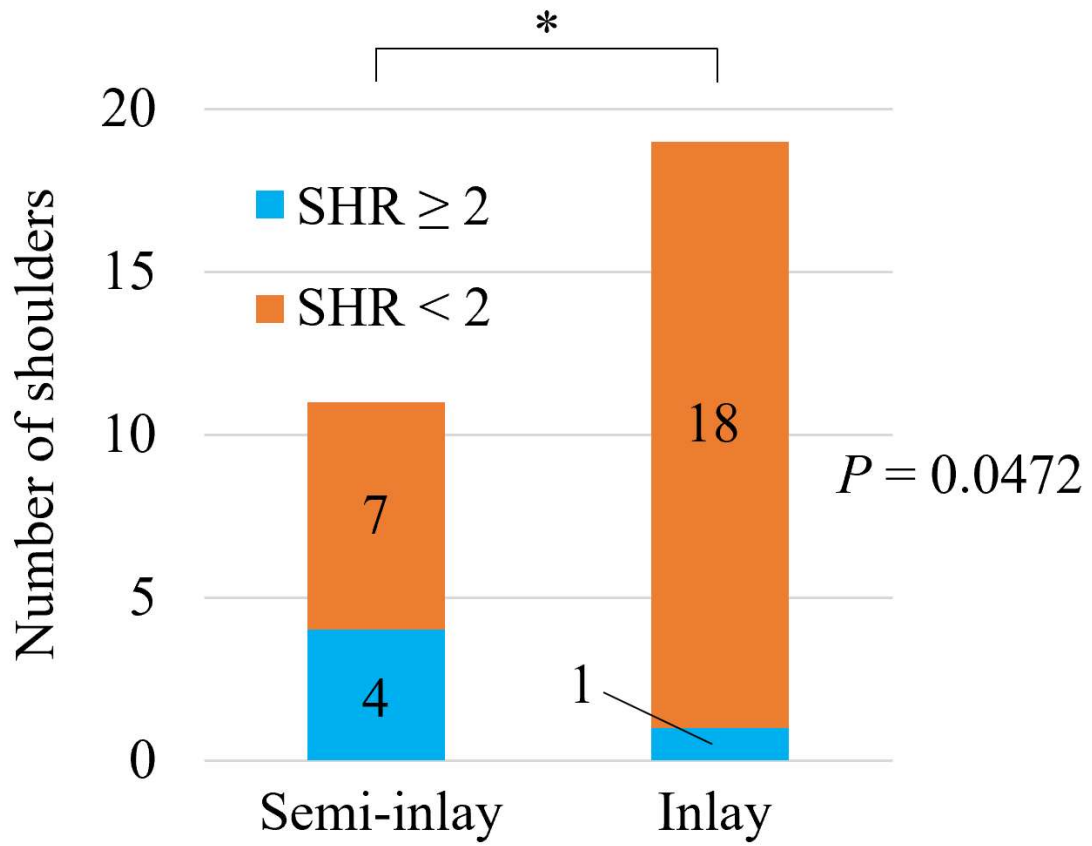


Figure 3

Enhancing Range of Motion in Reverse Total Shoulder Arthroplasty Through a Novel Dual Mobility Design

*Mercy Ombogo - University of Waterloo - Waterloo, Canada

Introduction

Reverse total shoulder arthroplasty (RTSA) has proven to be an effective treatment for various shoulder pathologies, particularly in cases of rotator cuff deficiency, serving as the go-to procedure to restore functional mobility and alleviate pain. Despite its widespread use, RTSA presents challenges such as restricted range of motion (ROM) thus driving ongoing exploration for refinements in implant designs. Traditional RTSA implants, which typically feature a polyethylene humeral cup and a metal glenosphere, often limit ROM at the extremes where impingement occurs, posing the risk of damage to both the implant and scapular bone (a complication known as scapular notching). To address this issue, we propose a novel approach by incorporating a second articulation into the bearing design, inspired by the successful application of dual mobility systems in total hip arthroplasty (THA). This innovative design aims to enhance ROM and minimize scapular notching through a unique articulation.

Methods

In our preliminary analysis, we incorporated a secondary articulation through a humeral eccentric liner (Fig 1), drawing on the principle used in well-established eccentric in Total Hip Arthroplasty (THA) dual mobility implants [1]. In such systems, a femoral head articulates within a mobile liner in the acetabular cup, employing a force-dependent self-centering mechanism driven by a geometric offset between the centers of the femoral head and mobile liner. Utilizing a mathematical model implemented in MATLAB, we examined the potential mechanical performance of this new RTSA implant design, focusing on the behavior of a self-centering liner due to its eccentricity relative to the glenosphere and humeral component. This model allowed us to analyze and predict relative movements, self-centering torque, and overall frictional torque during arm abduction, with particular attention to the eccentric offset parameter. Additionally, a manual assessment of a 2D implant model was conducted to preliminarily evaluate the concept's viability.

Results

Initial results from solid body modeling based on patient-specific CT scans, combined with our mathematical modeling, indicate that careful adjustment of the eccentric offset can substantially enhance shoulder function without compromising stability. The MATLAB-based analysis revealed that the self-centering liner could effectively reduce scapular notching while increasing ROM. The manual 2D implant assessments further supported the concept's feasibility, showing potential for improved performance in practical applications.

Conclusion

This novel dual mobility design represents a significant advancement in RTSA implant technology, offering a promising solution to the challenges of optimizing arthroplasty outcomes. Future research will focus on comprehensive experimental validation, including physical testing, to confirm these numerical predictions and ensure the implant's efficacy and reliability. This work highlights a potential path forward for improving ROM and reducing complications in RTSA, paving the way for enhanced patient outcomes.

Keywords: Reverse total shoulder arthroplasty, dual mobility design, range of motion, scapular notching, implant design, mathematical modeling, MATLAB.

References

[1] C. Fabry, C. Woernle, and R. Bader, "Self-centering dual-mobility total hip systems: Prediction of relative movements and realignment of different intermediate components," *Proc. Inst. Mech. Eng. Part H J. Eng. Med.*, vol. 228, no. 5, pp. 477–485, 2014, doi: 10.1177/0954411914531116.

Figures

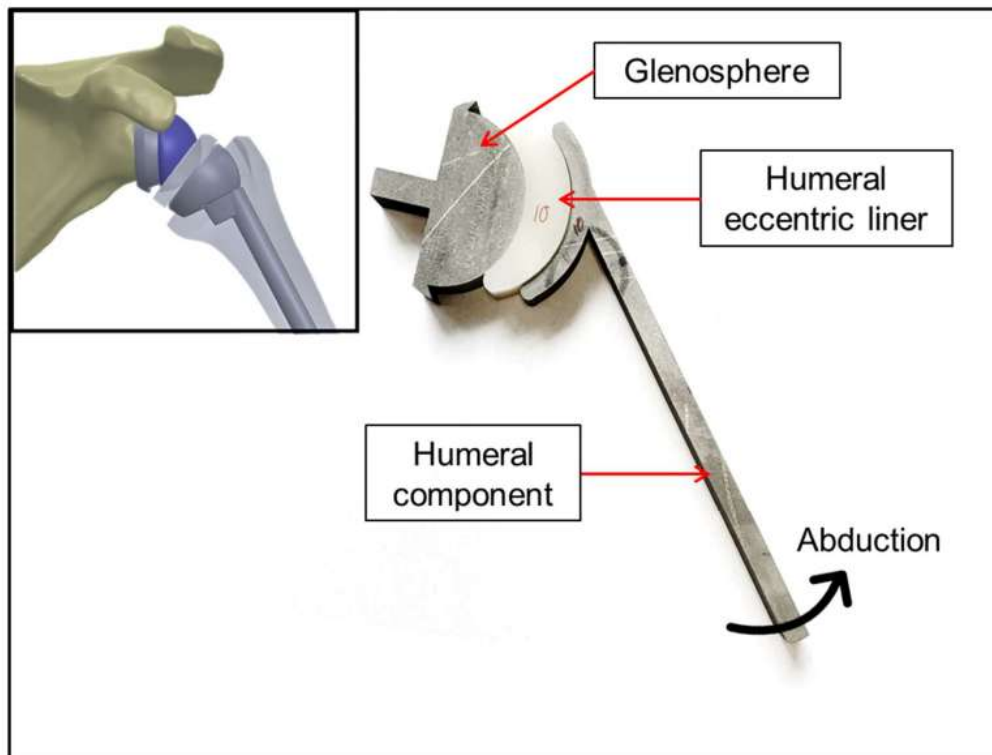


Fig 1: 2D image of proposed dual mobility RTSA implant

[Figure 1](#)

Differences in Scapulothoracic and Glenohumeral Coordination of Patients Undergoing Conventional and Lateralized RTSA

*Jonathan Gustafson - Rush University Medical Center - Chicago, USA

Talissa Generoso - Rush University - Chicago, USA

Joao Bonadiman - Instituto Brasil de Tecnologias da Saúde - Sao Paolo, Brazil

Vitor La Banca - Instituto Brasil de Tecnologias da Saude (IBTS) - Sao Paolo, Brazil

Felipe F Gonzalez - Rush University - Chicago, USA

Lucas Valerio Pallone - Rush University - Chicago, USA

Christopher Knowlton - Rush University Medical Center - Chicago, USA

Gregory Nicholson - Rush University Medical Center - Chicago, USA

Leonardo Metsavaht - Instituto Brasil de Tecnologias da Saude (IBTS) - Sao Paolo, Brazil

Gustavo Leporace - Instituto Brasil de Tecnologias da Saude (IBTS) - Sao Paolo, Brazil

Grant Garrigues - Rush University Medical Center - Chicago, USA

Introduction: Reverse Total Shoulder Arthroplasty (RTSA) represents a significant advancement in addressing shoulder arthropathy associated with compromised rotator cuff function. Recently, a notable surge in the use of RTSA has led to the development of new prosthesis designs (1). Research has highlighted that individuals who undergo conventional RTSA with a medialized glenoid/medialized humerus (MG/MH) prosthesis tend to exhibit reduced scapulohumeral rhythm ratios compared to their healthy counterparts (2). However, the impact of the lateralized glenosphere/medialized humerus (LG/MH) implant on shoulder kinematics remains largely unexplored in the existing literature. The objective of this study was to evaluate the differences in shoulder kinematics between patients receiving a conventional RTSA and those receiving a lateralized replacement.

Methods: This cross-sectional study included patients who underwent RTSA LG/MH procedure (DJO/Enovis) at least 6 months prior, with no movement limitations or complications. Patients were consented and asked to perform three repetitions of abduction in the coronal and scapular planes. Functional tasks were assessed using a 20-camera OptiTrack motion capture system (NaturalPoint, Inc., Corvallis, OR), with markers placed on subjects' upper limb, thorax and scapula---including a scapula marker cluster placed on the acromion. Scapulothoracic and glenohumeral joint angles were calculated in Visual 3D (C-Motion) following ISB guidelines(3). Scapulohumeral rhythm was calculated as the instantaneous change in glenohumeral angle relative to the change in scapulothoracic angle and binned between 0°-30°, 30°-60°, 60°-90°, and 90°-120° of humeral elevation. Student's t-test ($P < 0.05$) were used to compare range of motion differences in scapulothoracic and glenohumeral joint angles, in addition to scapulohumeral rhythm, between the convention (MG/MH) and lateralized implant groups (LG/MH).

Results: Preliminary analysis of our ongoing longitudinal study included 7 RTSA LG/MH (mean \pm SD age = 68.4 \pm 7 years) and 12 conventional MG/MH (mean \pm SD age = 69.8 \pm 6.7 years) implants. Average time of post-operative assessment was 15.9 months (6-49 months). The lateralized cohort showed near significant greater scapulothoracic upward rotation during scapular plane abduction as compared to the conventional group (47.5 \pm 11.1; 36.4 \pm 8.9, $P = 0.06$). We found significantly decreased scapulohumeral rhythm in the lateralized group as compared to conventional RTSA during both the 60-90 (1.1 \pm 0.6 vs 2.5 \pm 1.5) and 90-120 (3.5 \pm 1.6 vs 1.5 \pm 0.7) bins of scapular plane abduction.

Conclusion: This study highlights that there may be increased total scapulothoracic range of motion following a lateralized RTSA, but decreased scapulohumeral rhythm. We plan to isolate coordination differences between these two distinct implant-type groups in future work using combined MOCAP+EMG.

Acknowledgements: This study was funded by Rush Research Cohn Fellowship and the Instituto Brasil de Tecnologias da Saúde (IBTS) International Research Program.

References: (1) Routman et al., B Hosp Joint Diseases 2015. (2) Zaferiou et al., J Biomech 2021. Wu et al., J Biomech, 2005.

Figures

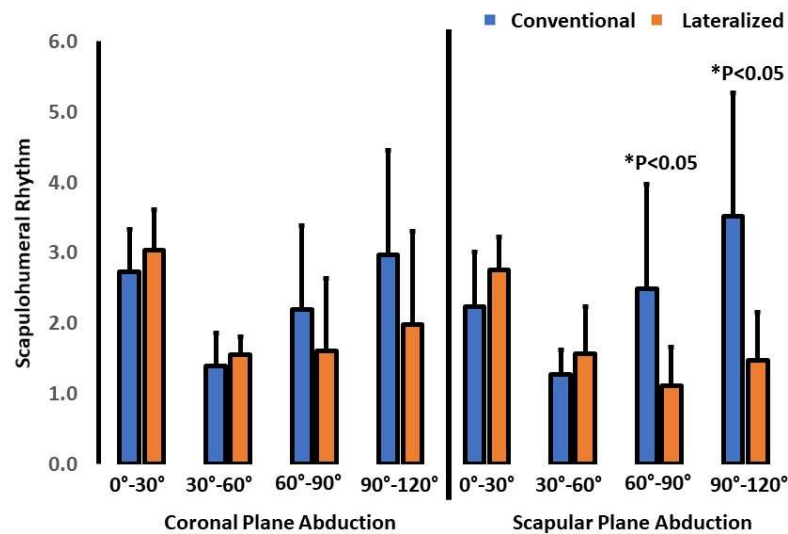


Figure 1. Scapulohumeral Rhythm for both conventional and lateralized RTSA patients during coronal plane abduction and scapular plane abduction across discrete humeral elevation angle ranges.

[Figure 1](#)

Design and Manufacturability of Compliant and Anatomically Optimized Spinal Implants Using Laser Powder Bed Fusion Additive Manufacturing

*Martine McGregor - University of Waterloo - Waterloo, Canada

Mihaela Vlasea - University of Waterloo - Waterloo, Canada

Stewart McLachlin - University of Waterloo - Waterloo, Canada

Introduction: Laser powder bed fusion (LPBF) is a metal additive manufacturing (AM) technology which enables the realization of latticed or porous structures, valuable in improving osseointegration and compliance in orthopaedic implant applications. Previous work has established the relationship between lattice AM design parameters such as pore size, feature thickness, lattice type, and lattice porosity relative to the mechanical performance of titanium and titanium alloy lattice structures (Figure 1).¹ While this data provides helpful guidance for implant design, it has not yet been translated into manufacturability considerations when attempting to optimize compliance and anatomical fit of latticed implant designs. The goal of this investigation was to design and manufacture multiple spinal implant designs that incorporate tailored lattice structures to improve compliance and anatomical fit.

Methods: The initial geometry for a lumbar interbody cage implant was reverse engineered using computer assisted design (CAD) software. Data for lumbar endplate geometries were then attained from literature, and the implant geometry was tailored for better sagittal endplate conformance.² Further, ultimate compressive strength of human lumbar endplates was attained from literature and a pre-established design tool was used to determine corresponding titanium lattice porosities.^{1,3} Lattice structures were applied to the medial, lateral, anterior and posterior regions of the implant geometry based on the endplate ultimate compressive strength using nTopology software. Implants had one of two lattice types: triply periodic minimal surface (TPMS) gyroid, superior for osseointegration, or stochastic Voronoi, for increased compliance. Voronoi lattices have known manufacturability challenges in LPBF AM due to the unpredictable down-skin surfaces presented. Final lumbar cage designs were manufactured in Ti6Al4V through LPBF. Manufacturability was evaluated through slice-by-slice comparison of the original CAD and post-manufacture micro-computed tomography (mCT) scans (Xradia 520 Versa, Zeiss).

Results: Six unique lumbar cages were manufactured. Three geometries were generated, two different tapers were added to the implant height, a 7 to 9 mm and a 9 to 11 mm to account for sagittal curvature of the endplate, as well as traditional straight cages (Figure 2). Designed lattice porosity ranged from 40% (posterior), 50% (medial), 60% (anterior) and 70% (lateral) for the two lattice structures applied, TPMS gyroid and Voronoi. All six lumbar cage designs were manufacturable. Analysis of post manufacture mCT showed under-printing not exceeding 0.5% for both lattice types, and over-printing not exceeding 1% and 2% for the TPMS gyroid and Voronoi lattice structures, respectively (Figure 3).

Conclusions: Current LPBF AM technologies allow for the successful manufacturing of compliance and anatomy optimized lattice implants. This technique has the potential to be adapted for other orthopedic implant applications to improve implant compliance and generate implant shapes unattainable by traditional manufacturing processes. Further evaluation of post-manufacture mCT was beneficial to evaluate print performance and comment on manufacturability of compliant and anatomically optimized orthopaedic implants produced through LPBF.

References:

- [1] McGregor et al. *Additive Manufacturing* (2021): 1;47, 102273.
 [2] Lowe, et al. *Spine* (2004): 29.21,2389-2394.
 [3] Lakshmanan, et al. *European Spine Journal* (2012): 21, 160-164.

Figures

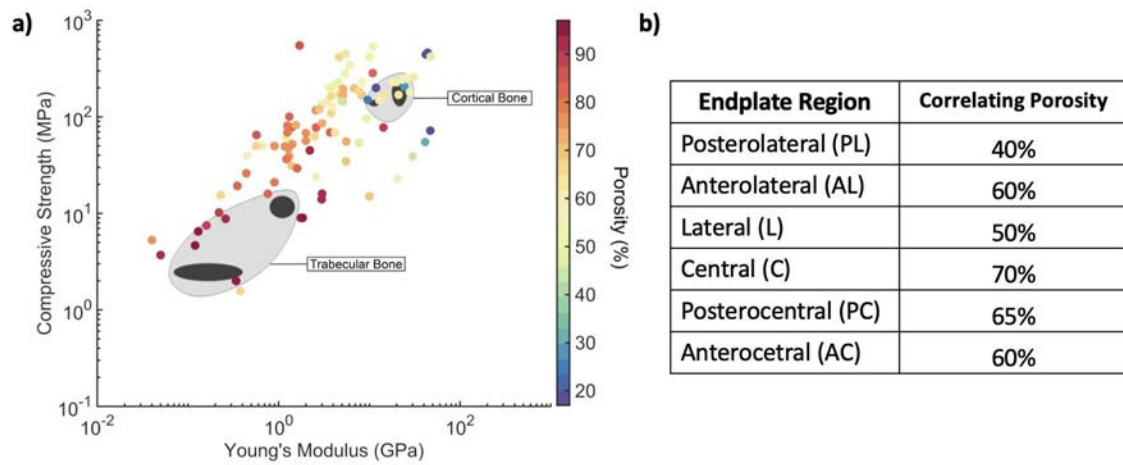


Figure 1: a) A pre-established design tool was leveraged to determine which titanium lattice porosities would best match endplate compressive properties while maintaining manufacturability.¹ b) Titanium lattice porosity for lumbar cages designs varied from 70% at the central endplate to 40% at the posterolateral endplate.

[Figure 1](#)

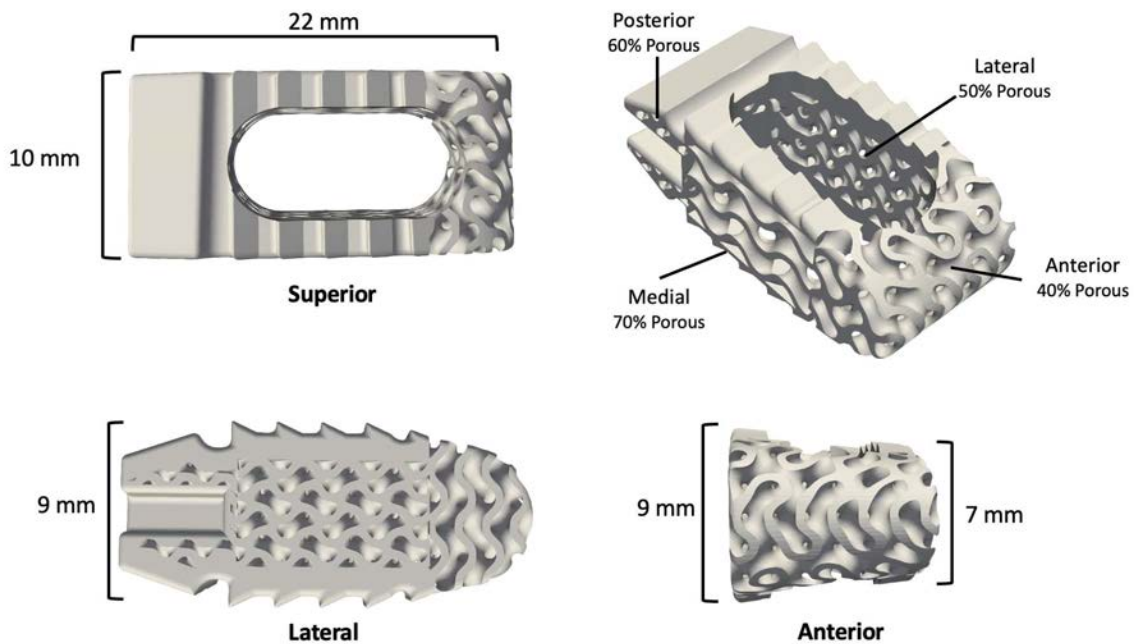


Figure 2: Six unique lumbar cages were manufactured (3 shapes x 2 lattice structures). The tapered cages have a greater height medially than laterally to account for the sagittal curvature of the endplate. The 9mm to 7mm tapered cages is describe in detail above.

[Figure 2](#)

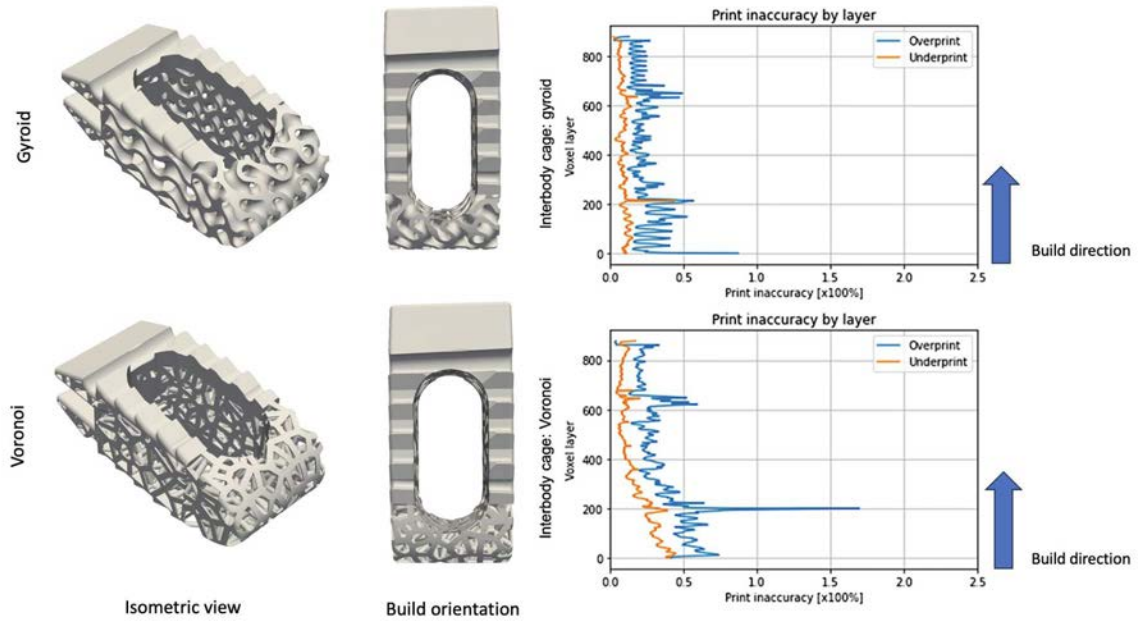


Figure 3: Manufacturability of the compliant, anatomically optimized lumbar spinal cages was evaluated using X-ray micro-computed tomography (mCT). mCT images were collected post-manufacture and final cage geometries were compared to CAD designs to quantify over and under-printed regions.

[Figure 3](#)

Early Monitoring of Polyethylene Wear Following Total Knee Arthroplasty Through Model Based Wear Measurement on Plain Radiographs

*Crystal Emonde - Hannover Medical School - Hannover, Germany

Christof Hurschler - Hannover Medical School - Hannover, Germany

Andre Breuer - Hannover Medical School - Hannover, Germany

Max-Enno Eggers - Leibniz University Hannover - Garbsen, Germany

Marcel Wichmann - Leibniz University Hannover - Garbsen, Germany

Max Ettinger - Hannover Medical School - Hannover, Germany

Berend Denkena - Leibniz University Hannover - Garbsen, Germany

Background:

Wear of the ultra-high molecular-weight polyethylene (UHMWPE) inlay in total knee arthroplasty (TKA) is a potential cause of implant failure. The main challenge in the detection of inlay wear is that it often goes undetected if pain or instability are absent. Current clinical methods of assessing inlay wear are unreliable and yield large errors (> 1 mm). Early monitoring through model-based wear measurement (MBWM) is a promising approach that could enable timely diagnosis and intervention. The aim of this study was to investigate the accuracy and precision of MBWM in an in-vitro setting. This novel technique utilizes 2D/3D registration (Fig. 1) to reconstruct the 3D pose of an implant from a plain radiograph, enabling the estimation of minimum inlay thickness and wear, based on the distance between the femoral and tibial components.

Methods:

Standard inlays ($n=6$) with mediolateral and anteroposterior measurements of 76 mm and 50 mm, respectively, and thicknesses of 10 mm, 14 mm, and 16 mm were milled from non-crosslinked UHMWPE1000. Each inlay was positioned in a phantom knee model and anteroposterior radiographs acquired at flexion angles 0° , 30° and 60° . MBWM accuracy was evaluated by comparing its estimations with reference values from a coordinate measuring machine. Three inlays underwent accelerated wear generation and were similarly evaluated for linear wear, which was regarded as the change in inlay thickness before and after wear testing. Double experiments were used to assess the technique's repeatability.

Results:

MBWM estimated minimum inlay thickness with medial and lateral accuracies of 0.13 ± 0.09 and 0.14 ± 0.09 mm respectively, and linear wear with an accuracy of 0.07 ± 0.06 mm. Thickness measurements revealed significant lateral differences at flexion angles of 0° and 30° (0.22 ± 0.08 mm vs. 0.06 ± 0.06 mm respectively, t-test, $p = 0.0002$) (Table 1), while linear wear measurements did not differ significantly across angles (one-way ANOVA, $p = 0.79$). Precision was high, with average differences of 0.01 ± 0.04 mm medially and laterally between double experiments.

Conclusion:

MBWM using plain radiographs presents a practical and promising approach for the detection of inlay wear in TKA clinically. It leverages readily available routine radiographs and 3D surface models of the implant components. Care should be taken to ensure consistent positioning of the knee joint between follow-ups to allow assessment at consistent points of contact.

Acknowledgements:

Funded by the Deutsche Forschungsgemeinschaft (DFG, German Research Foundation) – SFB/TRR-298-SIIRI – Project-ID 426335750.

Figures

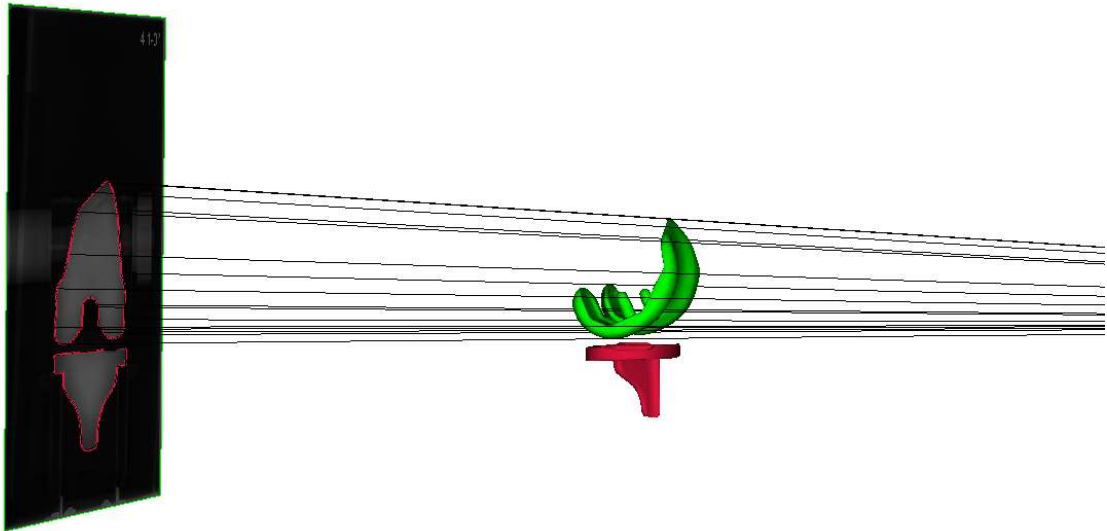


[Figure 1](#)

Flexion angle (°)	Condyle	Measurement error (mm)	SD	MAE (mm)	SD	MAE ± SD (both condyles)
0	med	-0.01	0.15	0.11	0.09	0.17 ± 0.08
	lat	-0.22	0.08	0.22*	0.08	
30	med	-0.21	0.14	0.21	0.14	0.22 ± 0.11
	lat	-0.05	0.07	0.06*	0.06	
60	med	0.02	0.10	0.08	0.05	0.14 ± 0.10
	lat	0.14	0.12	0.15	0.12	

[Figure 2](#)

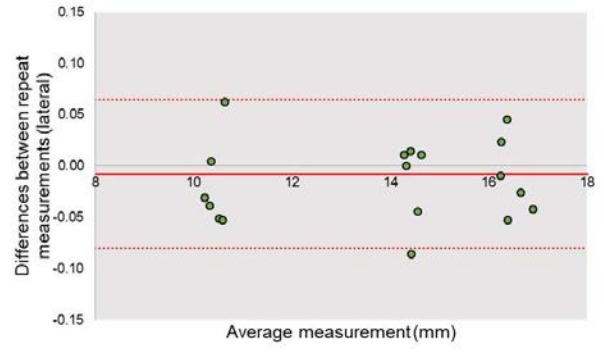
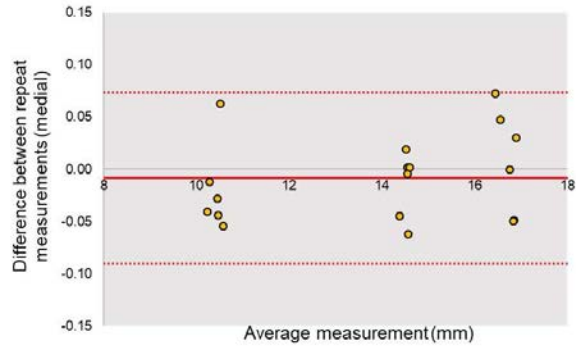


Figure 3

Radiation Sterilized and Crosslinked UHMWPE Loaded With Antibiotics

Nicoletta Inverardi - Massachusetts General Hospital - Boston, United States of America

Orhun Muratoglu - Massachusetts General Hospital - Boston, USA

Amita Sekar - Massachusetts General Hospital - Boston, USA

Keita Fujino - Massachusetts General Hospital - Boston, USA

Anthony Marzouca - Massachusetts General Hospital - Boston, USA

Maria Serafim - Massachusetts General Hospital - Boston, USA

Marcos Lora - Massachusetts General Hospital - Boston, USA

*Ebru Oral - Massachusetts General Hospital - Newtonville, USA

Introduction

Ultra-high molecular weight polyethylene (UHMWPE) is used in total joint replacement as the bearing component in light of its good mechanical and tribological performance. Recently, UHMWPE has also been proposed as a drug delivery vehicle for a wide array of drugs, including antibiotics to address peri-prosthetic joint infection, a severe complication of these surgeries¹. For a successful translation of this material technology to the clinic, feasibility of sterilization by irradiation is of paramount importance. In this study, we prepared and e-beam irradiated antibiotic-loaded UHMWPE. We studied the stability of the formulations after irradiation, the achievement of a crosslinked network, and their drug elution and antimicrobial properties.

Methods

The antibiotics vancomycin hydrochloride, VC or gentamicin sulfate, GS were blended into UHMWPE at a 10 wt.% loading by mechanical turbulence. The blends were compression molded (170°C, 20MPa, 10min) and vacuum packaged. Irradiation by e-beam was done at a total dose of 25 kGy or 100 kGy. Non-irradiated molded blocks were used as control (0 kGy). Prismatic samples (20x5x3 mm³) were machined and used for elution studies for all the conditions (i.e., 10% VC or 10%GS; radiation dose: 0, 25, or 100kGy). Drug elution was carried out in two conditions: i) the sample was eluted into 1.7 ml of deuterated water for 24h and the eluent and its control (unprocessed drug stock solution) were characterized by ¹H NMR; ii) the sample (n=6) was eluted into 1.7 de-ionized water, the release medium was collected at given timepoints (6h, 1, 2, 3 day(s), and every week until 6 months), and fresh water was replenished. The eluent concentration was obtained by UV-vis spectroscopy. Crosslink density was tested gravimetrically by swelling experiments in hot xylene. The antibacterial properties of eluted drugs as well as that of the pre-eluted material surfaces were tested against *S. aureus*, by optical density measurement, plating, and a luminescent viability assay².

Results

Irradiation did not affect the stability of the formulations: eluted drugs from irradiated UHMWPE were found to be stable as their NMR spectra did not show any significant difference with respect to that of the eluted drug from non-irradiated UHMWPE and to that of the unprocessed drug stock solutions. Swelling tests confirmed the achievement of a crosslink network, whose crosslink density increases along the radiation dose, regardless of the presence of the drug. High crosslink density is expected to indicate high wear resistance. Release rates for the eluted drugs were only marginally affected by the irradiation dose. The antibacterial properties of the eluents and of the pre-eluted surfaces were unchanged across the irradiation doses

and were found effective in inhibiting bacterial growth for at least one month (investigation up to 6 months ongoing).

Conclusion

Radiation was found to be a viable strategy for sterilizing and crosslinking antibiotic-loaded UHMWPEs. This finding is promising for further developing and translating this material technology, which may be of great clinical importance in preventing/treating infections in joint arthroplasty.

References

1. S. Lekkala et al., DOI: 10.1002/mabi.202300389
2. A. Sekar et al., DOI: 10.3791/64641

Can High-Tensile Sutures Contribute Significantly to Particle-Induced Tissue Response in Shoulder Arthroplasty?

*Deborah Hall - Rush University Medical Center - Chicago, USA

Songyun Liu - University of Illinois at Chicago - Chicago, USA

John Scanaliato - Rush University Medical Center - Chicago, USA

Gregory Nicholson - Rush University Medical Center - Chicago, USA

Grant Garrigues - Rush University Medical Center - Chicago, USA

Robin Pourzal - Rush University Med Ctr - Chicago, USA

Introduction: While implant loosening may be multifactorial, polyethylene wear-debris mediated osteolysis is felt to play a role in total shoulder arthroplasty. Evaluation of shoulder hemiarthroplasty (HA) specimens provide a unique opportunity to study the histopathologic response when a polyethylene-bearing surface was absent. We hypothesized that HAs would exhibit no significant inflammatory periprosthetic tissue response due to the absence of significant numbers of wear particles from the articulation.

Methods: HA components and periprosthetic tissues were retrieved from 13 patients. Damage to the implant bearing surfaces (1=mild to 3=marked) and head/stem taper junctions (1=minimal to 4=marked) were scored using stereomicroscopy. H&E sections of periprosthetic tissues were evaluated under white and polarized light microscopy and the extent and type of particulate debris and cellular response was semi-quantitatively scored (1=rare to 4=marked). Fourier Transform Infrared Spectroscopic imaging (FTIR-I) and scanning electron microscopy (SEM) with energy dispersive x-ray spectroscopy (EDS) were used to characterize debris present within tissue samples.

Results: The metal-bearing surface and head/stem taper damage was primarily mild, with average scores of 1.5 ± 0.7 , 1.7 ± 0.9 , and 1.7 ± 0.5 , respectively. The most prevalent histologic response was macrophage (3.1 ± 0.8) and foreign body giant cell (2.3 ± 1.1) infiltrates. Both cell types were associated with a foreign particle presence (Figure 1). Metal debris (91.7%) and suture debris (83.3%) were most predominate particles in the histiocytes. However the majority of cases with metal debris had no to minor amounts of metal particles within the tissues ($n=7$) whereas an extensive amount of polymeric particles involving greater than 50% of the tissue was seen in 5 cases. Cement debris was seen in 30.8% of cases. SEM/EDS revealed titanium alloy to be the most dominant metal particulate debris present, while FTIR-I scans suggested polyester to be the most commonly occurring type of suture debris (Figure 2).

Conclusion: Surprisingly, this surgically retrieved shoulder HA cohort exhibited a considerable macrophage and FBGC response within the periprosthetic environment. Interestingly, given the low amount of damage to metallic surfaces and the absence of a polyethylene bearing, the tissue response does not appear to be driven by wear particles from the metal-bearing surface or taper junction, but rather from suture and, to a much lesser degree, cement and metal debris. Overall, these findings highlight the potential impact that high-tensile suture material, frequently used in high quantities around shoulder arthroplasty, may have on the periprosthetic environment and identify these materials as a potential driver of osteolysis.

Figures

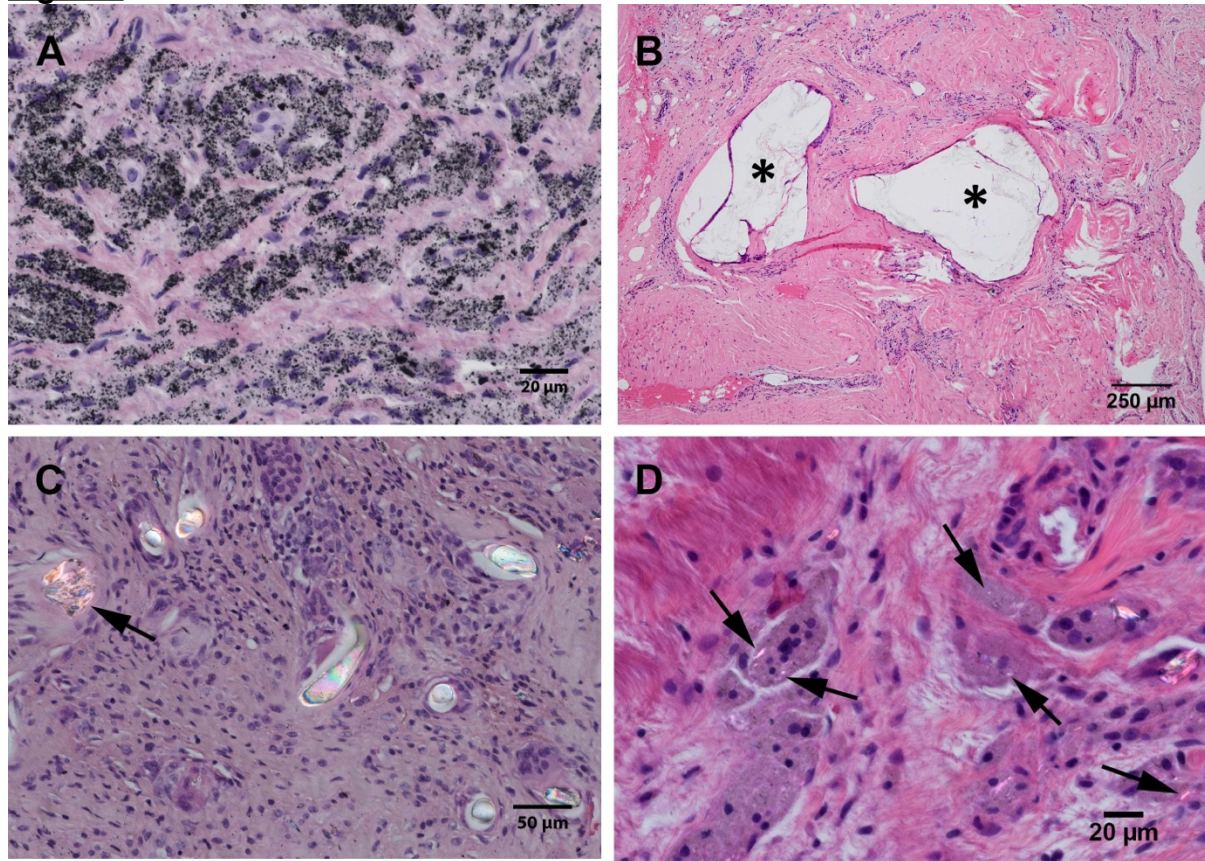


Figure 1. A) Marked macrophage response to abundant metal particles from a patient revised after 5 years for pain with arthrosis (H&E, x400). B) Two extremely large (> 850 μm) cement vacuoles (asterisks) encompassed by foreign body giant cells. The bone cement dissolved during histologic processing leaving scattered BaSO₄ radiopacity particles at the perimeters (H&E, x40). C) Suture fragments both in cross section and obliquely cut engulfed by macrophages and FBGCs. Frayed fragments (arrow) can also be seen within a larger giant cell (H&E with polarized light, x100). D) Very fine suture debris (arrows) within sheets of macrophages FBGCs (H&E with polarized light, original magnification x200).

[Figure 1](#)

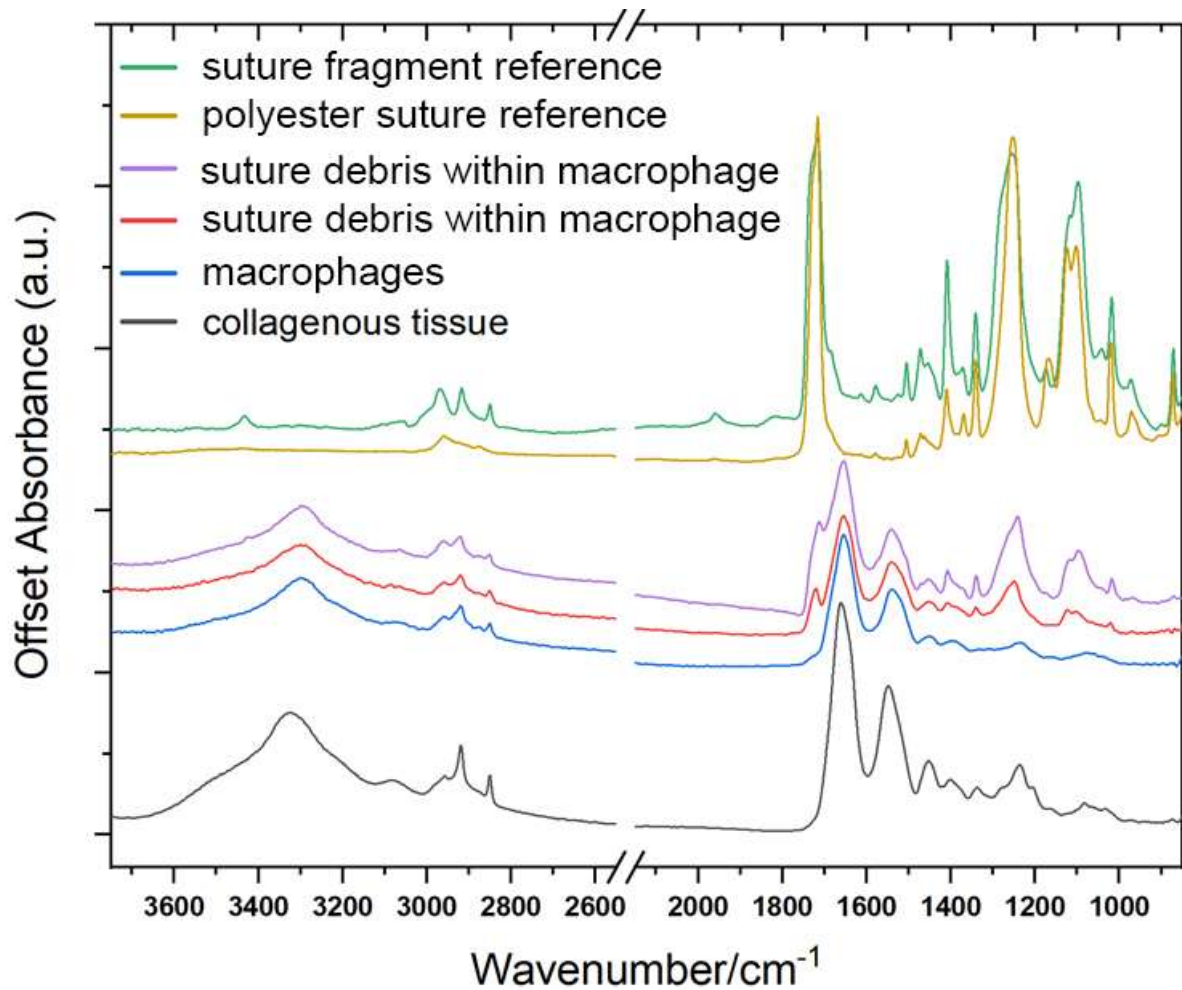


Figure 2. FTIR spectra illustrating suture debris internalized by macrophages (purple and red spectra) compared to wavenumber signatures of reference suture material (green and yellow spectra) and IR spectra of macrophages (blue spectrum) and collagenous tissue (black spectrum).

[Figure 2](#)

Surgical Alignment Techniques Comparisons for External Peak Knee Adduction Moments During Stair Descent

*Alexis Nelson - UTHSC - Memphis, Select Country

Nuanqiu Hou - Campbell Clinic - Memphis, United States of America

Douglas W. Powell - University of Memphis - Memphis, USA

Marcus Ford - Campbell Clinic Orthopaedics - Germantown, USA

James Guyton - Campbell Clinic Orthopaedics - Germantown, USA

John Crockarell - Campbell Clinic Orthopaedics - Germantown, USA

Christopher Holland - Campbell Clinic - Memphis, USA

Derek Dixon - Campbell Clinic Foundation - Germantown, USA

Teri Ross - University of Tennessee Health Science Center - Memphis, USA

William Mihalko - University of Tennessee - Memphis, USA

Disclosure: This study was funded by Medacta International

Introduction: Kinematically aligned (KA) surgical technique has reported to create better patient outcome scores by recreating natural knee joint movement post-surgery indicated by the patient's experience (Howell et al., 2013) and achieves better flexion scores compared to mechanical alignment surgical technique (Dossett et al., 2014). However, better patient reported outcomes do not indicate the biomechanical underpinnings of advantages or disadvantages of kinematically aligned TKA, which remain unclear. Therefore, our purpose was to analyze MA and KA TKAs on the effect of knee adduction moments (KAM) and knee adduction impulse during stair descent.

Methods: We included 28 patients who received a cruciate retaining Attune implant separated into two surgical alignment technique groups; MA (n=14) and KA (n=14). All patients underwent unilateral TKA and are at least one-year post-op. A three step instrumented staircase (1000Hz, AMTI Inc., Watertown, MA) and an 8-camera markerless motion capture system (200Hz, OptiTrack, NaturalPoint Inc., MA) were used to collect ground reaction forces and segment kinematics, respectively, during stair descent. An AI based reconstruction software (Theia Markerless, Inc., Version 2023, Kingston, ON) was used to identify segment kinematics. Visual3D Professional (HAS Motion, Version 2023.09.3, Canada) and MATLAB (The MathWorks, Inc., R2023b, Natick, MA) were used for data analysis. An independent sample t-test was used to compare surgical alignment techniques for the following variables: external peak KAM, mean KAM, knee adduction impulse and explanatory variables.

Results: There were no significant differences in age or BMI between MA and KA groups. Patients in both groups had compatible patient reported outcome scores. No significant differences were observed in peak KAM ($p=0.11$, Figure 1a) nor knee adduction impulse ($p=0.068$, Figure 1b) between the alignment groups. However, patients in the MA group demonstrated significantly larger lateral trunk lean towards the TKA limb compared to KA patients ($p=0.032$, Figure 1c). We did not observe any significant differences in peak ankle inversion angle ($p=0.524$) nor peak valgus knee angle ($p=0.388$) between the alignment groups.

Conclusion: We aimed to study the impact of surgical alignment techniques on knee joint biomechanics during stair descent. No significant differences were observed in KAMs or knee adduction impulse during stair descent between MA and KA groups. We observed a significant difference in lateral trunk lean towards the TKA limb between the alignment groups during stair descent. To further our understanding,

future work will compare knee joint reaction forces and quadriceps activation patterns between alignment groups.

Predicted Gait Speed Recovery and Patient-Reported Pain in Patients Requiring Additional Physical Therapy Following Hip and Knee Arthroplasty

*Roberta Redfern - Zimmer Biomet - Pemberville, USA

Joseph Brook - Zimmer Biomet - London, United Kingdom

Karl Surmacz - Zimmer Biomet - Swindon, United Kingdom

Mike Anderson - Zimmer Biomet - Lehi, USA

Jason Cholewa - Zimmer Biomet - Warsaw, USA

Adam Henderson - Zimmer Biomet - Winterthur, Switzerland

Introduction

Machine learning (ML) models have potential to predict which patients are at risk of poor outcomes or need for intervention following lower limb arthroplasty. This analysis aimed to investigate the performance of an ML model by examining which patients who were predicted to have performance deficits ultimately required additional intervention in the form of in-person physical therapy (PT) post-arthroplasty.

Methods

All patients were enrolled in a prospective randomized controlled trial investigating the use of a digital care management platform that provided education and exercise modules for self-directed rehabilitation following lower limb arthroplasty. At 90 days post-operatively, patients were asked to report pain on a numeric scale (0 – 10) and whether adjunct PT was required following surgery. An ML model was created based on commercial users and study patients of the platform. Patients were flagged if their post-operative gait speed was predicted to be in the lowest 15th percentile of similar patients (by age, gender, procedure, and body mass index). Additional flags were raised if gait speed recovery was slower than expected a drop in average gait speed in the first 90-days was observed, or if patients reported pain ≥ 7 . Flagged patients were then investigated to determine the proportion of predicted gait deficits who ultimately required PT.

Results

In total, 693 patients provided evaluable data; 594 (74.7%) reported use of in-person physical therapy. Of the 24 patients who were identified as predicted low gait speed, 87.5% required PT; of 67 patients who were identified as recovering slower than expected or 88.1% reported additional PT. Only 8.5% reported pain ≥ 7 in the overall cohort. Within the 87 total patients flagged for gait speed issues, 16.1% reported pain ≥ 7 ; all patients flagged for both pain and gait speed deficits reported use of in-person PT where flags for pain were more selective gait speed or pain notifications alone.

Discussion

Data from this analysis suggest that patients identified as being at risk of poor outcomes based on low predicted gait speed or slower than expected recovery of gait speed frequently required additional intervention. Addition of high pain to these predictions appears to improve selectivity. Use of gait speed data relative to similar patient cohorts may allow for prediction of patients at risk of poor gait outcomes in those who report pain and appears to agree well with the requirement for additional clinical intervention after arthroplasty.

3D-Printed Custom-Made Implants in Complex Revision Total Knee Arthroplasty

*Georg Hettich - Aesculap AG - Tuttlingen, Germany

Josef-Benedikt Weiß - Aesculap AG - Tuttlingen, Germany

Thomas M. Grupp - Aesculap AG - Tuttlingen, Germany

Introduction: In complex revision total knee arthroplasty (rTKA), where severe bone defects, peri-prosthetic fractures, or hypersensitivity to metal and/or bone cement components prevent the application of standard off-the-shelf implants, a custom-made implant is a highly appreciated solution. The aim of this study is to determine the regulatory, technical, quality assurance and clinical requirements for 3D-printed custom-made knee implants and to present two exemplary cases of severe rTKA where appropriate off-the-shelf implants are not available.

Method: A process for additive manufacturing (3D-printing) of custom-made knee implants by selective laser melting of Cobalt-Chromium-Molybdenum (CoCrMo) powder was developed (Fig.1). It considers the regulatory distinction between custom-made implants, patient-matched implants, and adaptable implants. Critical design features are determined in close cooperation between the responsible surgeon and engineers. Pre-clinical evaluation by finite-element analysis was applied to validate these features in a comparison to biomechanical hardware tests of a corresponding reference implant. These aspects are presented in two exemplary clinical cases. Case 1: Distal femur replacement for a patient with metal hypersensitivity. Case 2: Femur component for a patient with severe metaphyseal bone defects as well as hypersensitivity to metal and cement.

Results: The developed process for 3D-printed custom-made knee implants fulfil the regulatory, technological, and quality requirements for implantable medical devices. This prerequisite allows the treatment of patients, where off-the-shelf implants are unavailable. Case 1 was treated by an individually designed monobloc distal femur replacement with a zirconium nitride multilayer coating for reduction of metal ion release (Fig.2). Case 2 was treated with a monobloc femoral component with a sleeve, zirconium nitride multilayer coating as well as a porous coating for cementless fixation (Fig. 3).

Conclusion: 3D-printed custom-made knee implants allow adequate treatments for patients for whom an off-the-shelf implant is not available. Prerequisite is strict compliance with all state of the art regulatory, quality assurance and technological aspects, as well as close cooperation between surgeons and engineers.

Figures

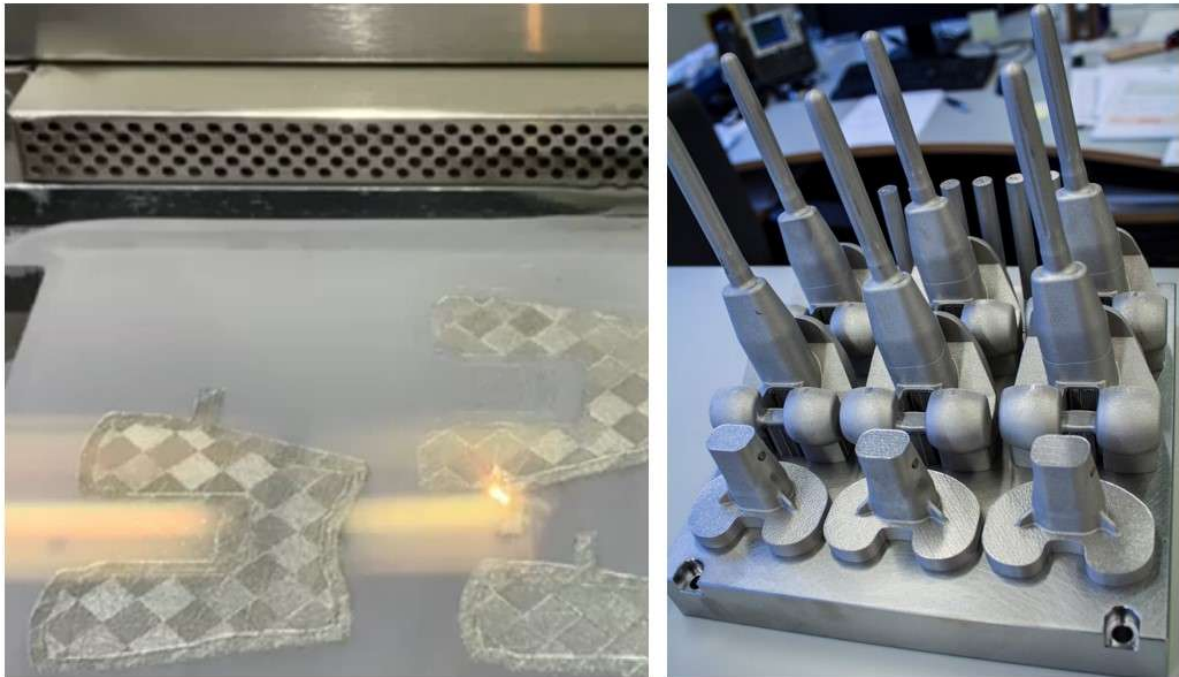


Fig.1: Additive manufacturing (3D-printing) by selective laser melting of Cobalt-Chromium-Molybdenum powder.

[Figure1](#)

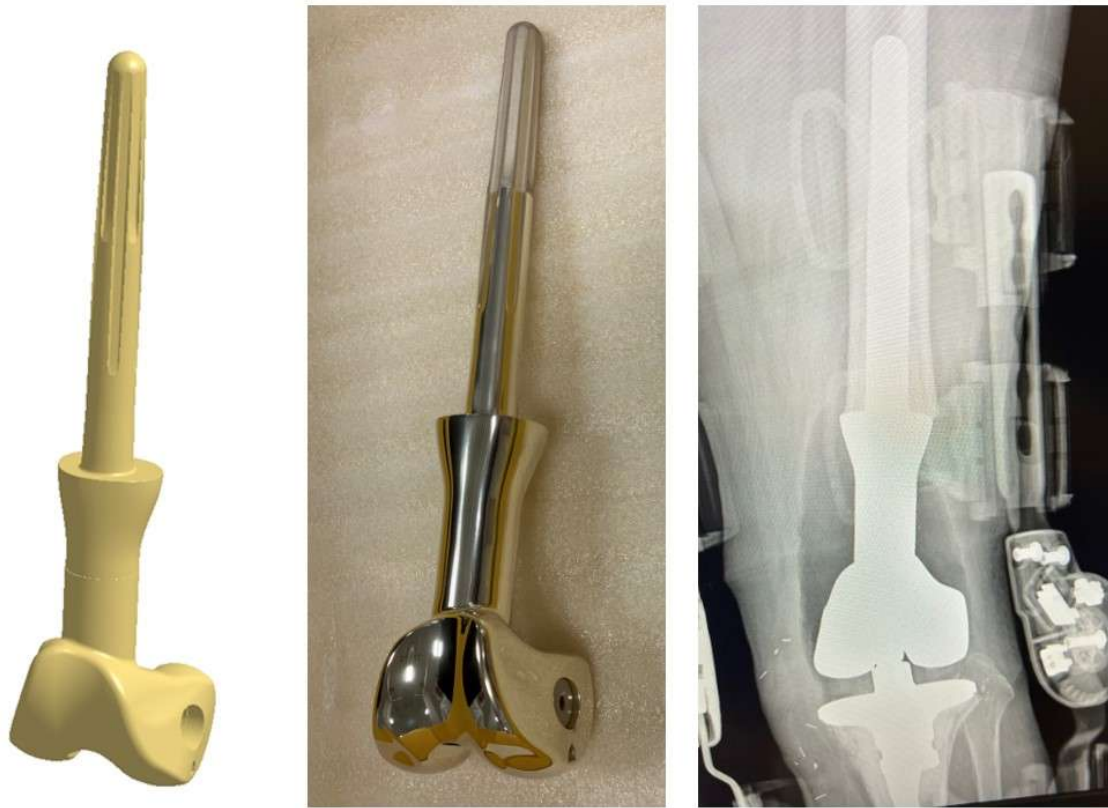


Fig.2: Monobloc custom-made distal femur replacement with zirconium nitride multilayer coating for reduced metal ion release.

[Figure 2](#)

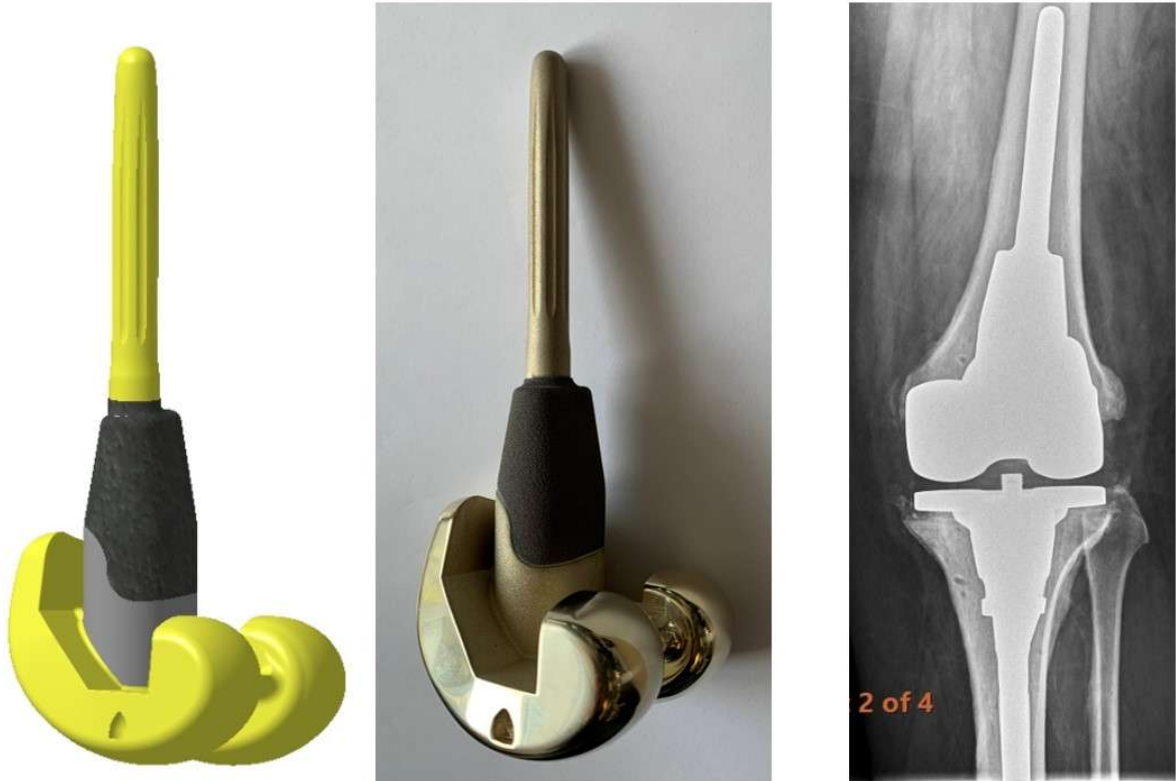


Fig.3: Monobloc custom-made femur component with metaphyseal cementless fixation and zirconium nitride multilayer coating.

[Figure 3](#)

Cementless 3D Printed Implants Match Conventional Cementless Implants in Micromotion Performance

*Colin Dudrey-Harvey - OSSTEC - London, United Kingdom

Arron Hughes - OSSTEC - London, GB

Maxwell Munford - Imperial College London - London, United Kingdom

Jonathan Jeffers - Imperial College London - London, United Kingdom

Jennifer Stoddart - Imperial College London - London, United Kingdom

Introduction: It is crucial that cementless unicondylar and total knee replacement (UKR and TKR) tibial trays have good initial fixation and stability to ensure longer-term osseointegration. Conventional cementless UKR implants rely on high interference press-fits for initial fixation, however this can lead to bone fracture during impaction and daily use. Additive manufacturing (AM) is of growing interest to improve cementless fixation of such implants by utilising lattice structures to achieve greater porosity for bone ingrowth. AM implants can also minimise any stress-shielding effects by matching the stiffness of the implant to the bone itself.

This study aims to compare the micromotion of a stiffness-matched AM UKR lattice tibial implant, designed with low interference on two pegs and no interference at the keel region, to a conventional cementless UKR with interference at the keel but with no pegs.

Methods: The AM lattice tibial implants were manufactured from a Ti alloy using powder bed fusion, and inserted into 15 PCF Sawbones with pre-prepared cavities to achieve a nominal radial interference fit of 0.25mm at the two pegs, with a zero-interference keel. The AM lattice was characterised to match the Sawbones modulus. A conventional cementless tibial implant was similarly inserted into 15 PCF Sawbones, achieving a nominal interference of 0.55 mm mediolaterally to the keel. The implants were modified with equidistant spheres to enable the measurement of varus/valgus and internal/external rotations and mediolateral translation using linear variable differential transformers (LVDTs).

The implants (n = 3 per group) were cyclically loaded at 2Hz for 10,000 cycles, with 900N peak load applied distally and an internal/external rotation between $\pm 8^\circ$. The load was positioned at the mediolateral centre of the implants, 16mm anterior to the posterior rim, and was applied through a 3mm thick polymer bearing. Eight LVDTs measured the displacement of the Sawbones and implants to evaluate the micromotion in 6 degrees of freedom, with an additional LVDT used to measure central inferior-superior displacement (Figure 1). Comparisons in the micromotion measurements between all samples were assessed using a one-way ANOVA.

Results: The AM lattice implant and the conventional implant achieve comparable peak average micromotion with no statistical difference ($107.95 \pm 7.37 \mu\text{m}$ vs $105.52 \pm 7.09 \mu\text{m}$, $p=0.093$) (Figure 2). Both implants achieved total implant micromotion results below $150 \mu\text{m}$, which is the threshold for osseointegration suggested in literature, despite the AM implant requiring a lower nominal interference.

Conclusions: AM lattice cementless UKRs can achieve comparable micromotion performance, and thus initial fixation and stability, to conventional cementless UKRs while reducing the risk of bone fracture by utilising a lower interference. The design-flexibility of AM allows an optimal implant design to be selected which can achieve suitable initial fixation while ensuring long-term bone ingrowth via matching implant and bone modulus.

Keywords:

Additive manufacturing
 Lattice Structures
 Cementless Fixation

Figures

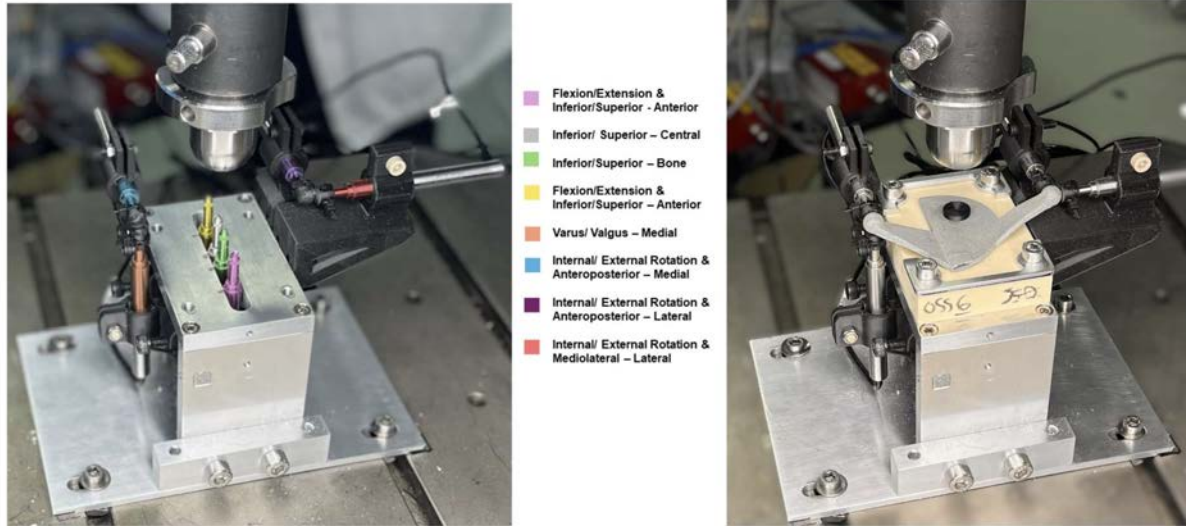


Figure 1: Placement of linear variable differential transformers (LVDTs) without implant (left) and with implant (right).

Figure 1

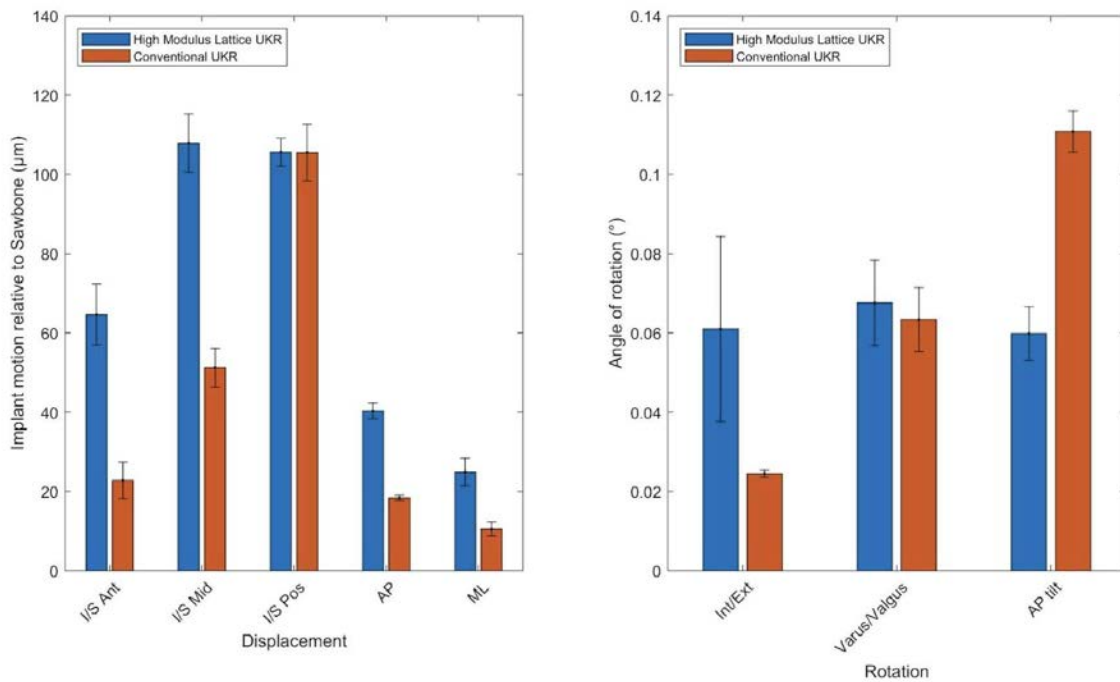


Figure 2: Peak average micromotion for displacement (left) and rotation (right) of all samples, for both AM lattice implants and conventional cementless implants.

Figure 2

The Impact of SLM and EBM 3D-Printers on Surface Adhered Titanium Particles on Acetabular Implants

*Arya Nicum - University College London - London, GB

Harry Hothi - London Implant Retrieval Centre - Stanmore, United Kingdom

Anna Di Laura - Royal National Orthopaedic Hospital and Dept. MechEng at UCL - London, United Kingdom

Johann Henckel - Royal National Orthopaedic Hospital - London, United Kingdom

Alister Hart - Imperial College - London, UK

Klaus Schlueter-Brust - St. Franziskus Hospital - Köln, Germany

Introduction:

Selective Laser Melting (SLM) and Electron Beam Melting (EBM) are the main 3D-printing techniques for orthopaedic implants. Both methods utilise high-energy beams to fuse metal powder layer-by-layer to construct the desired part but differ technologically.

During printing, some source titanium powder does not fully fuse with the component, leaving surface adhered particles within the porous structure. Despite manufacturers' post-processing, some particles may remain on the surface of the implant.

This study aimed to characterise the surface of the porous structure of off-the-shelf acetabular shells manufactured by SLM and EBM.

Study Design and Methods:

Nine pristine commercially available 3D-printed off-the-shelf acetabular shells from five manufacturers were examined. These were divided into two groups according to their manufacturing method: SLM (n= 6), EBM (n=3).

Their porous structures were analysed using light microscopy and scanning electron microscopy (SEM) across 4 cup regions at the surface and sub-surface level for a representative illustration, as indicated in Figure 1(a). Image analysis software was then used to evaluate the particles observed.

The outcome measures were (1) the number of particles per mm² and (2) the particle diameter.

Results:

Surface adhered particles were present on all shells examined (Figure 1(b)).

1) SLM shells had approximately twelve-fold the number of surface adhered particles than EBM; medians of 446 and 38.1 particles/mm², respectively (p<0.01), (Figure 2). This also increased further in SLM shells with an irregular bone-facing porous structure; a median of up to 517 particles/mm², compared with 10.9 particles/mm² for a repeating cell lattice (Designs 4 and 5 in Figure 2). Irregularity of the structure did not appear to have the same effect with EBM shells.

2) The SLM particles exhibited a smaller diameter than EBM particles; the median (range) particle diameters were 24.3 (5.05-71.5) μm and 53.8 (16.9-115) μm , respectively.

Surface adhered particles observed on SLM shells were more complete spheres and less fused to the main component, in contrast to the EBM shells, which were more hemispherical and adhered to the strut surface.

Conclusion:

We found surface adhered particles on all 3D-printed acetabular shells examined, despite the manufacture method. SLM shells had a significantly greater number of particles with smaller diameters compared to EBM shells, and also more loosely adhered to the implant. We recommend that the potential clinical impact of these particles breaking loose should be investigated using blood titanium level testing.

Figures

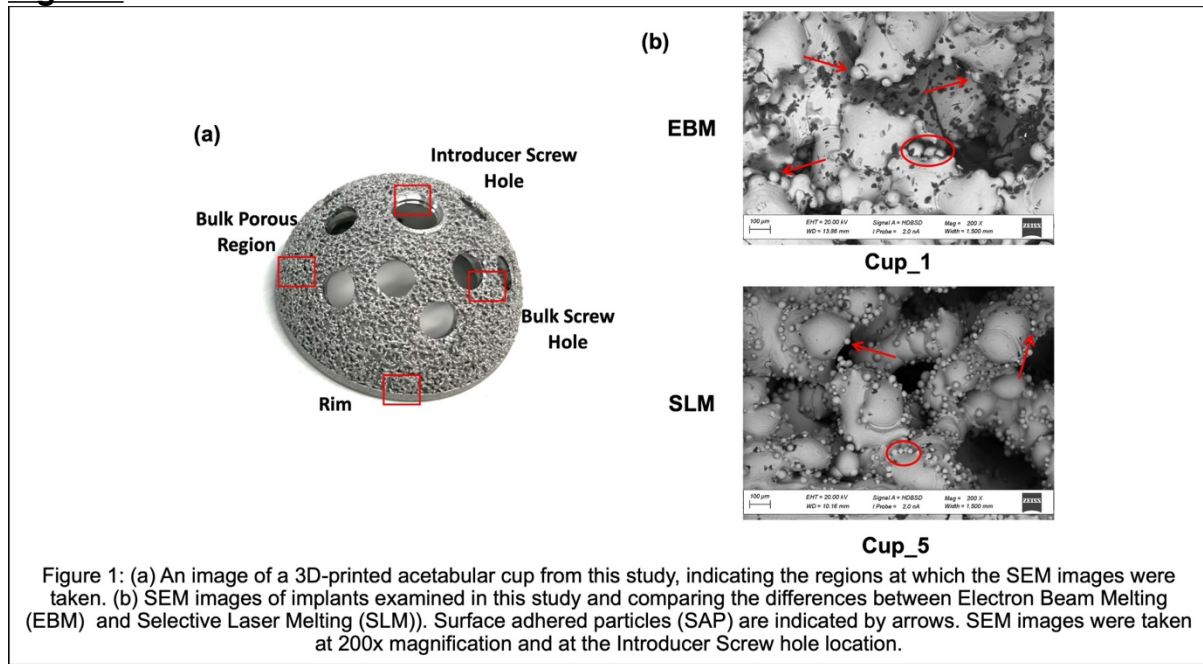


[Figure 1](#)

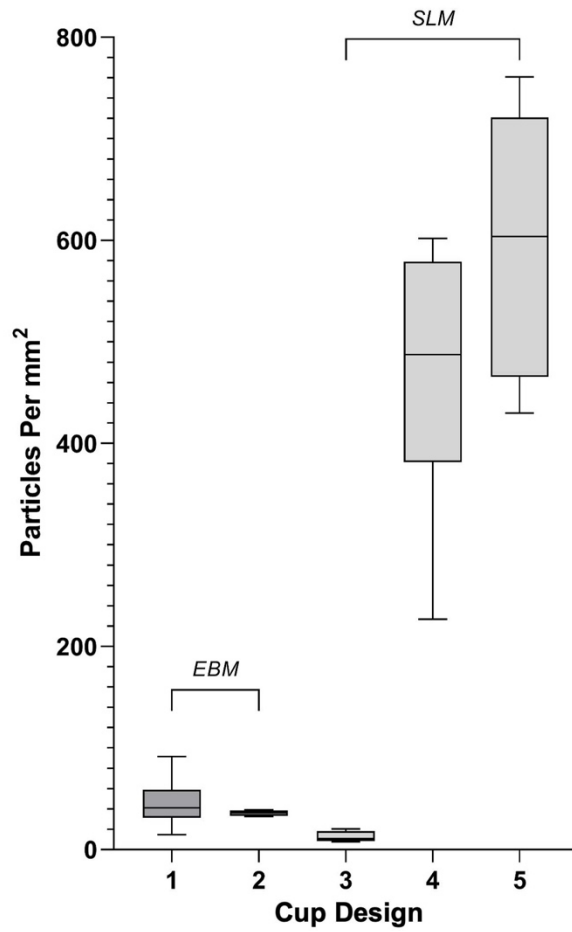


Figure 2: A box plot representing the significant difference in Particles per mm² at the surface level between cups manufactured by Electron Beam Melting (EBM) and Selective Laser (SLM).

[Figure 2](#)

Quantifying Bone Ingrowth in Additively Manufactured Titanium Alloy Baseplates

*Michael Kurtz - Clemson University - Charleston, USA

Hannah Spece - Drexel University - Philadelphia, USA

Paul DeSantis - Drexel University - Philadelphia, United States of America

Nicolas Piuze - Cleveland clinic - Cleveland, United States of America

Steven Kurtz - Drexel University - Philadelphia, USA

Introduction: In the last year, cementless total knee arthroplasty (TKA) increased to 18.8% of all primary procedures [1]. *In vivo*, cementless baseplates rely on keels, pegs, and porous surfaces for fixation. While various animal studies document bone ingrowth, data of human bone ingrowth within TKA devices remains limited. In this study, we characterize osseointegration on hybrid manufactured tibial baseplates using both manual and semi-automated methods. Our primary question was to what extent does bone grow into porous titanium surfaces of additively manufactured tibial baseplates?

Methods: Three representative tibial baseplates were selected from a multicenter implant retrieval program. Implants were revised for instability (1 year) and loosening (0.75 and 1.25 years). Devices were sectioned using an abrasive cut-off wheel and resulting samples were manually polished until the titanium reached a mirror finish. A section was stained with Alizarin Red to visually identify the bone ingrowth. Then, energy dispersive X-ray spectroscopy (EDS) was used to generate elemental maps. Bone ingrowth and surface area were measured on paired digital and scanning electron (SEM) micrographs acquired at 100x magnification. Ingrowth was determined by measuring from the base of the conventionally manufactured puck to the local maximum of the additively manufactured porous surface. Bone surface area was first manually segmented using digital optical microscopy (DOM). Next, using ImageJ, SEM micrographs were contrast thresholded and denoised to identify the area fraction of bone pixels. Differences between the two measurement methods (SEM, DOM) were assessed using a two-sample t-test ($\alpha = 0.05$, MATLAB 2023b).

Results: A digital image of a titanium alloy baseplate shows bone ingrowth around the additively manufactured keel and pegs (Figure 1A). After sectioning and staining, a micrograph identifies bone ingrowth from outside of the additively manufactured pores to the conventionally manufactured interface (Figure 1B). Paired digital micrographs (Figure 1 C-D) reveal bone at the porous interface of a bullet cruciform peg. Under backscattered electron SEM and EDS, the bone and titanium contrast (Figure 2A-B). Resulting elemental maps of calcium, oxygen, carbon, and phosphorus overlay the bone structure, while titanium and nitrogen overlay the porous metal (Figure 2 C-H). Paired digital (Figure 3A-B) and SEM (Figure 3C-D) micrographs show manual segmentation and contrast thresholding methodologies, respectively. Using SEM, we measured 1.07 mm of bone ingrowth and 2.37 mm² of bone surface area (Figure 3E-F). We found no significant difference between SEM analysis and manual labeling ($p > 0.05$).

Conclusion: Using SEM and DOM techniques, we meticulously identified and characterized bone ingrowth within additively manufactured porous titanium TKA components, revealing full interdigitation of the bone within the porous surface of each examined baseplate, extending to the conventionally manufactured puck. We found no significant differences between our two quantification methods (SEM, DOM). Contrast thresholding using SEM offered several advantages over manual

labeling including decreased user bias, rapid implementation, and the potential for automated area calculations. Future work will scale this study to a larger sample of retrieved devices.

References: [1] Hegde et al., *Arthroplasty Today* 2023;

Figures

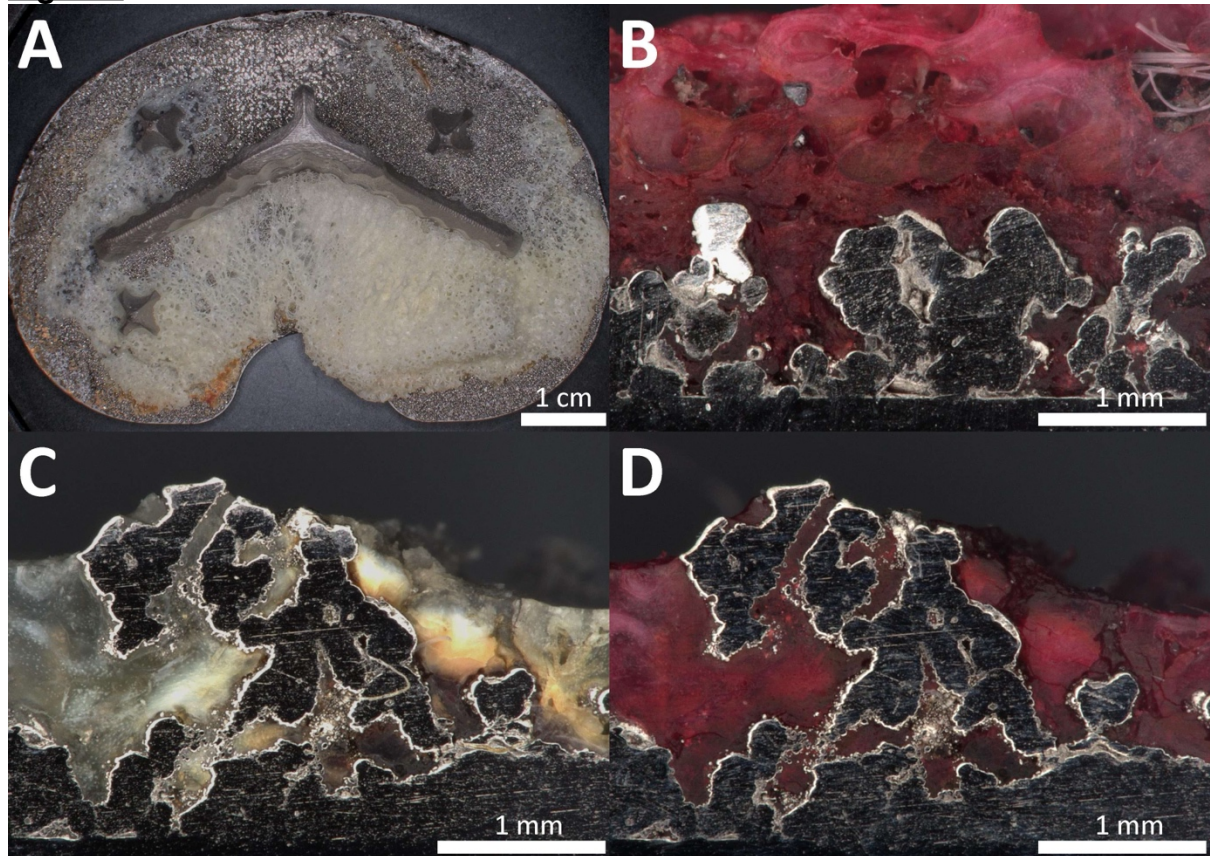


[Figure 1](#)

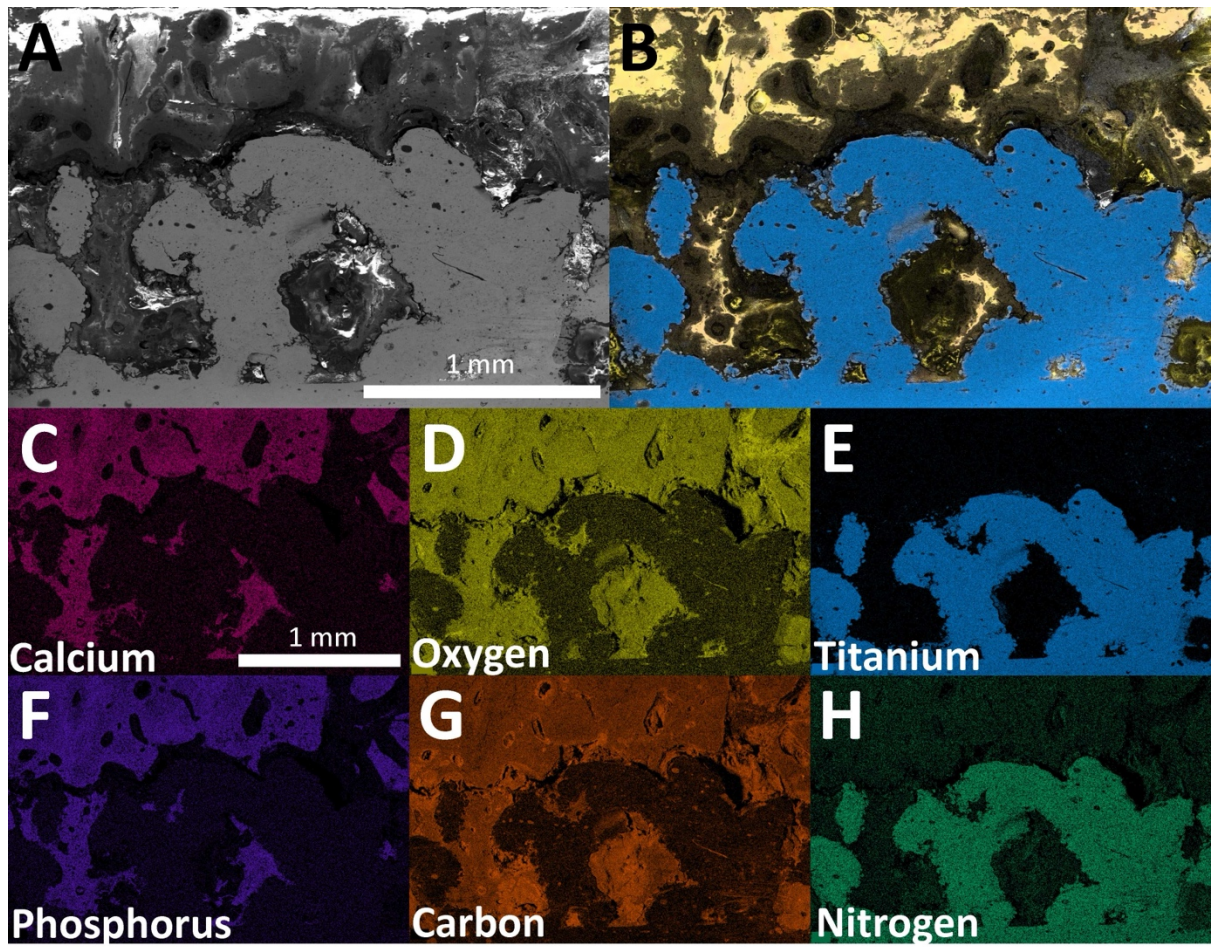


[Figure 2](#)

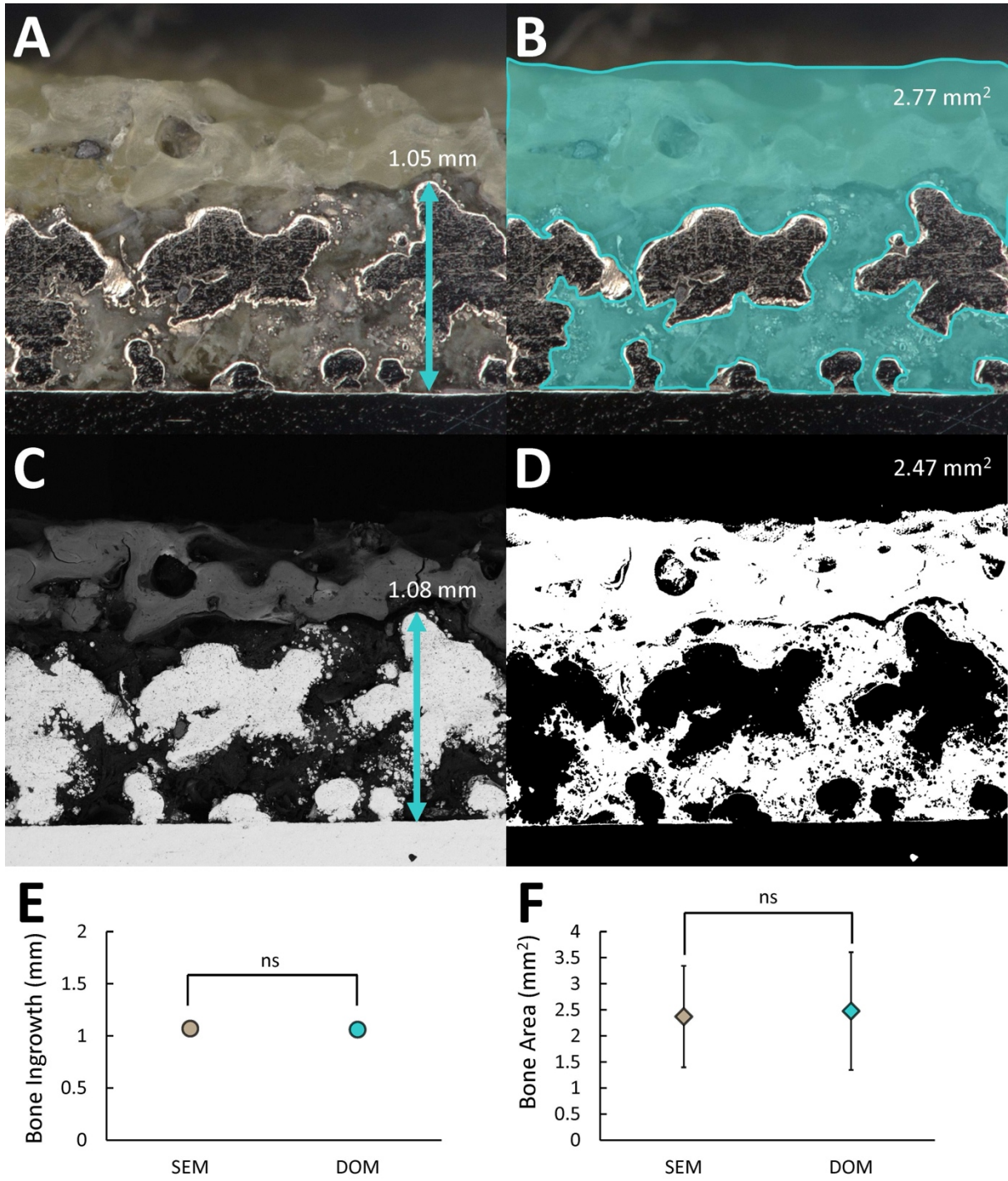


Figure 3

A Systematic Benchtop Construction and Deconstruction Study of Spinal Ligaments Using Novel 3D Printable Analogue Spine Models

*Siril Teja Dukkupati - McGill University - Montreal, Canada

Mark Driscoll - McGill University - Montreal, Canada

Introduction: Cadavers and finite element models are the two standard methodologies in today's spine biomechanical studies. Both these methods have their limitations in cost and time. These can be overcome by incorporating validated analogue models of the spine for biomechanical testing. To develop such models, it is essential to evaluate the effects of all the underlying soft tissues on the model biomechanical response. This study evaluated the effect of intertransverse and interspinous ligaments on the overall rotational stiffness of the lumbar spine by sequential construction of a previously validated 3D printed analogue L1-S1 spine model [Figure 1].

Methods: The analogue spine model consisted of vertebral bodies, intervertebral discs, intertransverse, interspinous ligaments. Stereolithography 3D printing was used to manufacture the model for its repeatability and consistency. Vertebrae and soft tissues were printed using Durable and Flexible 80A resins respectively (Formlabs, MA, USA) and were assembled by UV curing. The model construction involved three phases (P1, P2, P3) and after each phase, the corresponding model stiffness was evaluated by subjecting it to load-controlled pure bending load up to a cyclic amplitude of 5Nm at 1/60Hz in flexion-extension, lateral bending, and axial rotation along with a custom bending jig (Instron Electroplus E10000, MA, USA). P1 consisted of assembly of vertebral bodies and the corresponding intervertebral discs. P2 consisted of adding interspinous ligament to the P1 model. P3 completed the model construction by adding intertransverse ligaments to the P2 model. A follow-up study was also carried out to simulate a grade 3 ligament damage in the model. Specifically, an interspinous ligament tear was induced at the L4-L5 level, followed by similar tears in the left and right intertransverse ligaments at the same level. Rotational stiffness was then estimated and compared to that of the intact model.

Results: Hysteretic behavior during load-unload cycles was observed in the analogue spine model much like the human spine accounting for the underlying viscoelastic elastomers in the model. Addition of ligaments decreased the model rotation of motion (ROM) in flexion-extension motion (Flexion – P1=9.87±0.05°; P2=9.41±0.1°; P3=8.33±0.11° and extension – P1=8.99±0.09°; P2=6.7±0.05°; P3=7.12±0.04°). In lateral bending, there was no noticeable ROM change from P1 to P2 but an increase from P2 to P3 (left – P1=9.01±0.07°; P2=8.93±0.1°; P3=8.66±0.09° and right – P1=9.11±0.09°; P2=9.18±0.06°; P3=8.56±0.05°). There were no observable trends in the model ROM as construction progressed in axial rotation motion (left – P1=12.8±0.11°; P2=14.3±0.2°; P3=12.56±0.14° and right - P1=12.08±0.24°; P2=10.75±0.04°; P3=11.41±0.15°) [Figure 2]. Interspinous ligament tear at L4-L5 resulted in an ROM increase of 16% and 13.2% in flexion and extension respectively while Intertransverse ligament tear resulted in 6.11% ROM increase in lateral bending [Figure 3].

Conclusion: Interspinous and intertransverse ligaments contribute to flexion and lateral bending spine stiffnesses respectively. The current research quantified these effects using a cost and time effective opensource 3D printable platform demonstrating a proof-of-concept for 3D printable analogue spine models. Such

models hold potential as an effective research and educational tool to further investigate the lumbar spine structure.

Figures

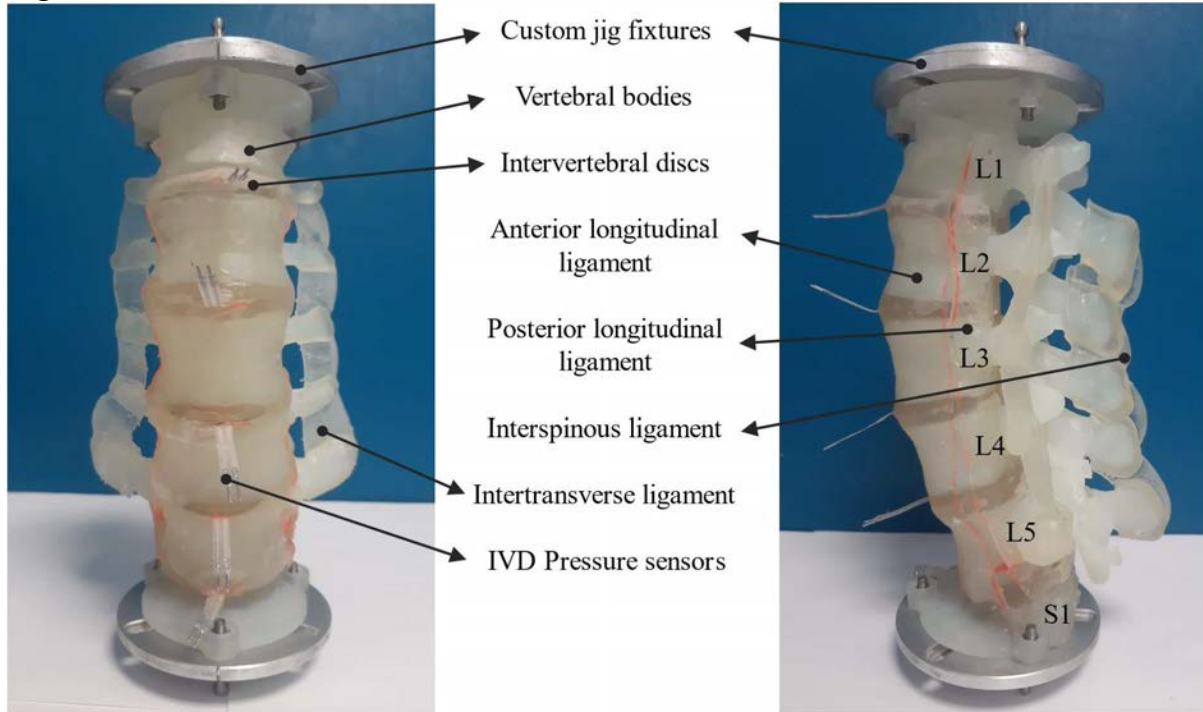


Figure 1: Developed novel 3D printable analogue lumbar spine segment.

Figure 1

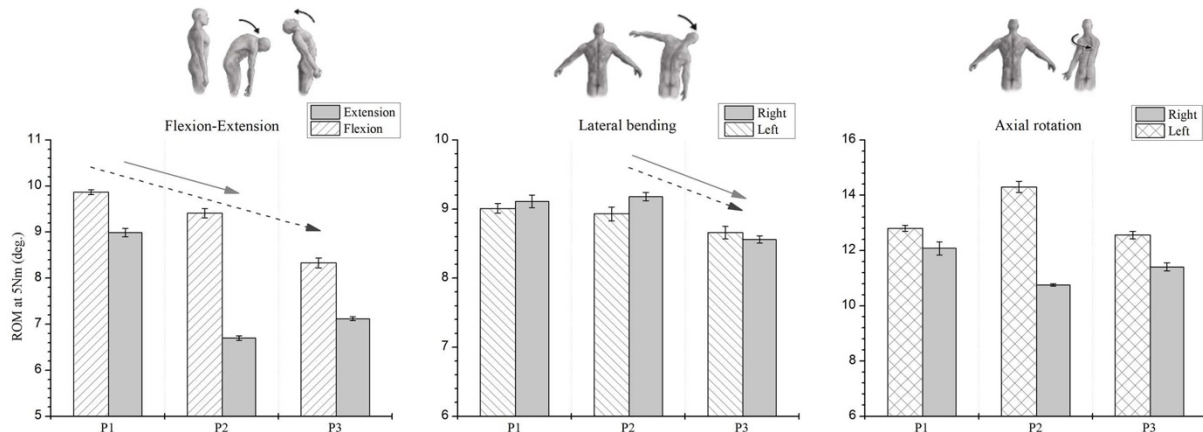


Figure 2: Progression of model rotation of motion (ROM) with the addition of interspinous (P2) and intertransverse ligaments (P3)

Figure 2

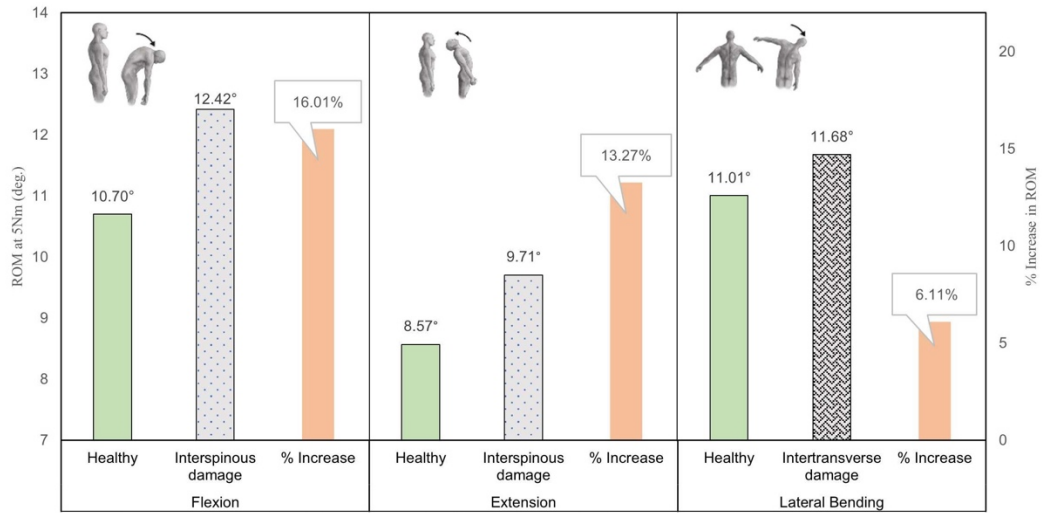


Figure 3: Progression of model rotation of motion (ROM) with introduction of ligamental tears in the model.

[Figure 3](#)

An Unconstrained Force-Control Testing Protocol for Evaluating Endplate Conforming Interbody Cage Designs

*Martine McGregor - University of Waterloo - Waterloo, Canada

Richard Barina - University of Waterloo - Waterloo, Canada

Stewart McLachlin - University of Waterloo - Waterloo, Canada

Introduction: Patient-specific and endplate conforming lumbar interbody cage designs have proven to decrease subsidence in biomechanical investigations.¹ However, current pre-clinical test methods are not well adapted to reliably measure performance of these tapered implant design. For example, compressive subsidence into engineered foam is a well-established in the pre-clinical ASTM F2267 test;² however, flat or partially curved foam does not allow for adequate evaluation of the potential benefits of patient-specific, endplate conforming cages. Typically, this must be done in cadaveric specimens, which is costly and has known limitations. As such, new test methodologies are needed for pre-clinical evaluation of implant subsidence with bone conforming geometry or features.

Methods: The geometry for a lumbar interbody cage implant was reverse engineered and adapted to improve endplate conformance. Two cage designs, traditional and endplate conforming, were manufactured through laser powder bed fusion additive manufacturing (LPBF-AM). Sawbones were machined at a 5° angle to better represent the profile of the endplate in the medial-lateral direction. Three of each lumbar cage design types (n=3) were compressed into Sawbones at 4kN at 25N/sec in force-control with all off axis maintaining zero force (Figure 1). Implant motion was measured through actuator displacement and subsidence was considered to have occurred at 2mm of displacement in the superior-inferior direction. Tests were continued past initial subsidence to ensure post-yield subsidence had occurred.

Results: Traditional implants reached 2 mm of subsidence at an average of 467.99 ± 330.70 N, while endplate conforming implants reached the same subsidence at an average of 718.24 ± 191.09 N, (Figure 2). During the initial 2mm of subsidence, the traditional shaped cage rotated about the anterior-posterior axis towards the medial direction by an average of 2.5°, followed by rotation in the lateral direction for the remainder post-yield test (Figure 3). In contrast, for the endplate conforming cages, there was an average of 2° of lateral rotation at 2 mm of subsidence, with no rotation seen in the medial direction.

Conclusions: This work describes an unconstrained force-control test methodology with the capacity to evaluate novel endplate conforming and patient-specific implants against current traditional designs. Use of the unconstrained loading approach allowed for the implants to freely rotate in response to the underlying foam substrate, used as a bone surrogate. The medial rotation initially seen for the traditional implant was needed to match the implant and foam surfaces. For both cages, there was lateral rotation of the implant seen due to the densification of the Sawbones foam from compression, resulting in implant rotation into less dense regions. Additional work is required to compare the proposed test methodology to the existing test standard and to further validate our findings with *in vitro* cadaveric study.

References:

[1] Fernandes et al. *Global Spine Journal* (2022): 21925682221134913.

[2] Fogalet al. *The Spine Journal* (2022): 22.6, 1028-1037.

Figures

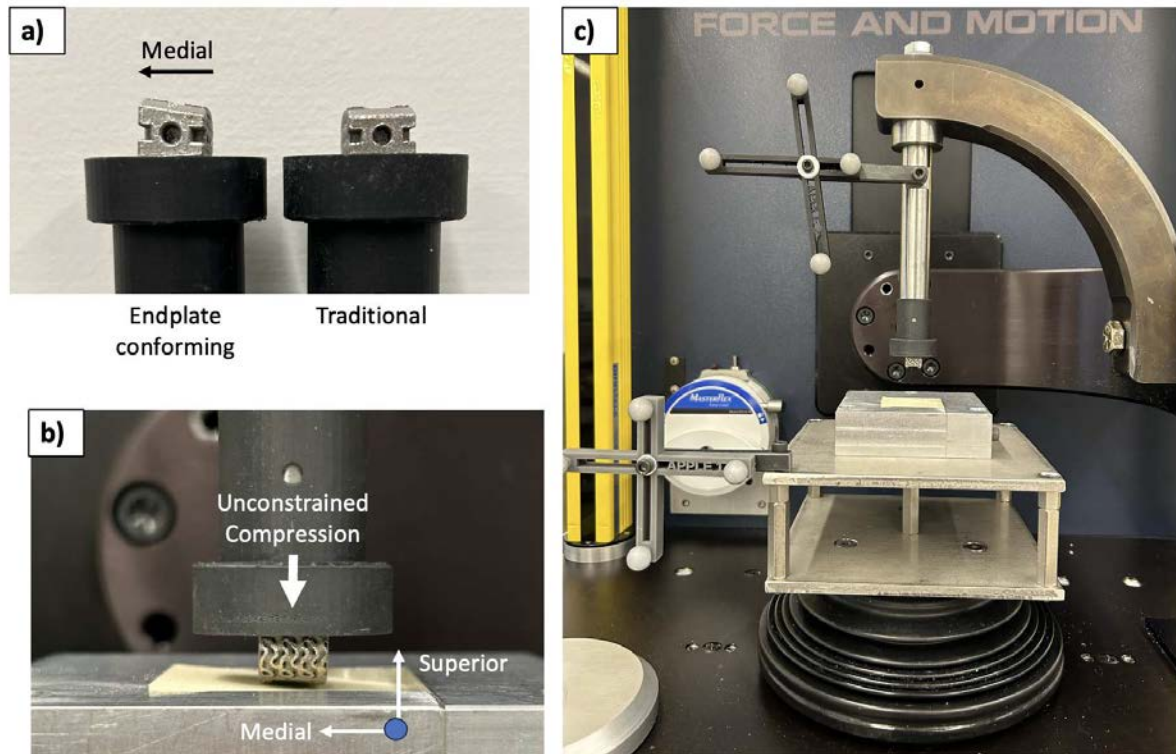


Figure 1: a) Two lumbar cages were tested: an endplate conforming cage and a traditional cage. (b) Implants were held in a fully constrained fixture and compressed into an engineered foam at 25N/sec to 4.5kN. (c) A force control joint motion simulator was used to apply unconstrained force with all off-axis actuators held at 0N load.

[Figure 1](#)

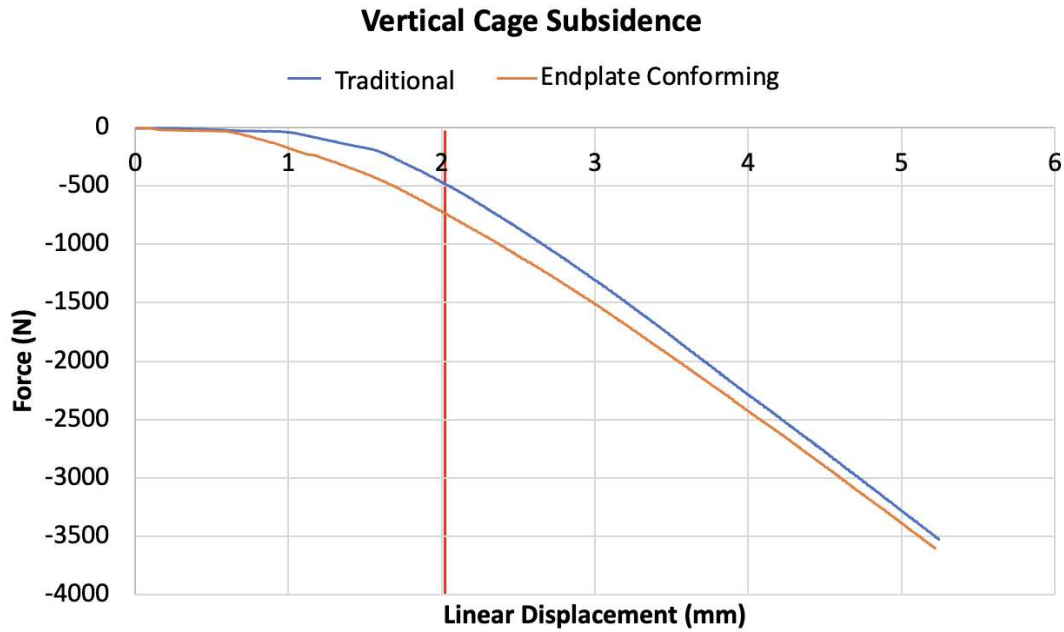


Figure 2: Vertical cage subsidence was considered to have occurred at 2 mm of vertical displacement (red). Subsidence occurred for both the traditional (blue) and endplate conforming implants (orange) at an average of 467.99 ± 330.70 N and 718.24 ± 191.09 N, respectively.

[Figure 2](#)

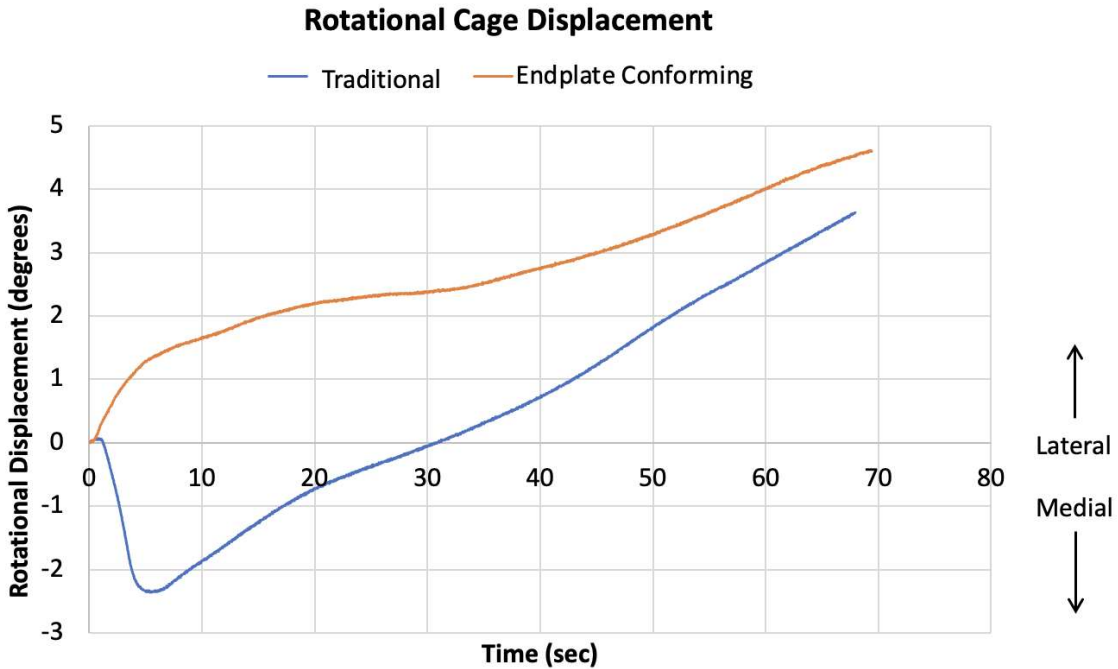


Figure 3: Both cage types rotated about the anterior-posterior axis throughout the unconstrained cage subsidence test. Straight cages rotated medially during the initial subsidence phase as they conformed to the angled sawbone surface, followed by rotation in the opposite direction similar to the endplate conforming cages.

[Figure 3](#)

Defining Phenotypes in Total Knee Arthroplasty Based on Intra-Operative Kinematics: a Multi-Center Cohort of 3915 Patients

Ingrid Dupraz - Aesculap AG - Tuttlingen, Germany

*[Raphael Renaudot - B.Braun New Ventures - Freiburg, Germany](#)

Ricardo Larrainzar-Garijo - Hospital Universitario Infanta Leonor, Orthopaedic & Trauma Department - Madrid, Spain

Bjoern Gunnar Ochs - Klinik für Unfallchirurgie, Handchirurgie & Orthopaedie, Orthopaedische Fachklinik Vincentius am Kli - Konstanz, Germany

Gavin McHugh - Sports Surgery Clinic & National Orthopaedic Hospital Cappagh, Dublin Ireland - Dublin, Ireland

Thomas M. Grupp - Aesculap AG - Tuttlingen, Germany

Introduction

Restoring patient function is key to a good Total Knee Arthroplasty (TKA). To account for the variability in patients' anatomy and function, phenotypes have been defined based on static and dynamic alignment [MacDessi2021, Larrainzar-Garijo2017]. The native kinematics of the patient should also be considered when choosing a specific implant design. The goal of this study was to define phenotypes based on the intra-operative kinematics during a neutral flexion.

Methods

3915 navigated cases were included in this study (Orthopilot®, Aesculap AG). After palpating the landmarks a neutral flexion of the knee joint was performed from full extension to full flexion. The position of the medial and lateral condyles at 0°, 30°, 60° and 90° of flexion was computed using an implant fit algorithm. The reference position of the femur to the tibia was defined at 0°. Phenotypes were defined based on the medial and lateral antero-posterior (AP) shift between 0° and 90°. Following thresholds were defined: small rollback AP shift <4mm, substantial rollback: AP shift >4mm. The distribution of the AP shift was analyzed between 0° to 30°, 30° to 60° and 60° to 90°.

Results

Half of the knees showed a medial pivoting pattern, with 49% having a posterior shift of the lateral condyle. 14% showed a lateral pivot, while 36% showed no pivoting or a central pivoting pattern (Figure 1). When looking at the distribution of the shift along the flexion angle, most of the knees were stable medially and most knees had the highest amount of lateral posterior shift between 0° and 30° (Figure 2). For the medial pivot phenotype, the most frequent patterns showed a strong pivoting motion between 0° to 30° and a low shift from 30° to 90° (Figure 3).

Conclusion

This study proposed a definition of phenotypes based on intra-operative kinematics during a neutral knee flexion. The majority of knees showed a medial pivot pattern, which is consistent with literature [Grassi2020]. The lateral rollback was strongest from 0° to 30° of flexion, followed by the rollback from 30° to 60° and 60° to 90°. The highest variability in AP shift occurred between 0° and 30°. Further analyzing the distribution of the rollback over flexion enabled to refine the medial pivot phenotype. This classification could support the choice of the implant system: patients with a medial pivoting pattern would benefit from a medial stabilized design. Patients with little or central pivoting patterns would benefit from posterior-cruciate retaining or sacrificing designs. Patients with a strong posterior rollback would benefit from posterior-stabilizing designs. The study had several limitations. The impact of the

chosen thresholds may be reduced by integrating further parameters such as rotation and pivoting point. The anterior cruciate ligament (ACL) was removed in some of the acquisitions. However its impact has been shown to be modest on passive knee flexion [Brendle2023]. Finally the transfer from passive to active kinematics remains unclear [Gasparutto2023]. To conclude, this study proposed a method to integrate intra-operative kinematics in the definition of phenotypes to better restore patient function after TKA.

Figures

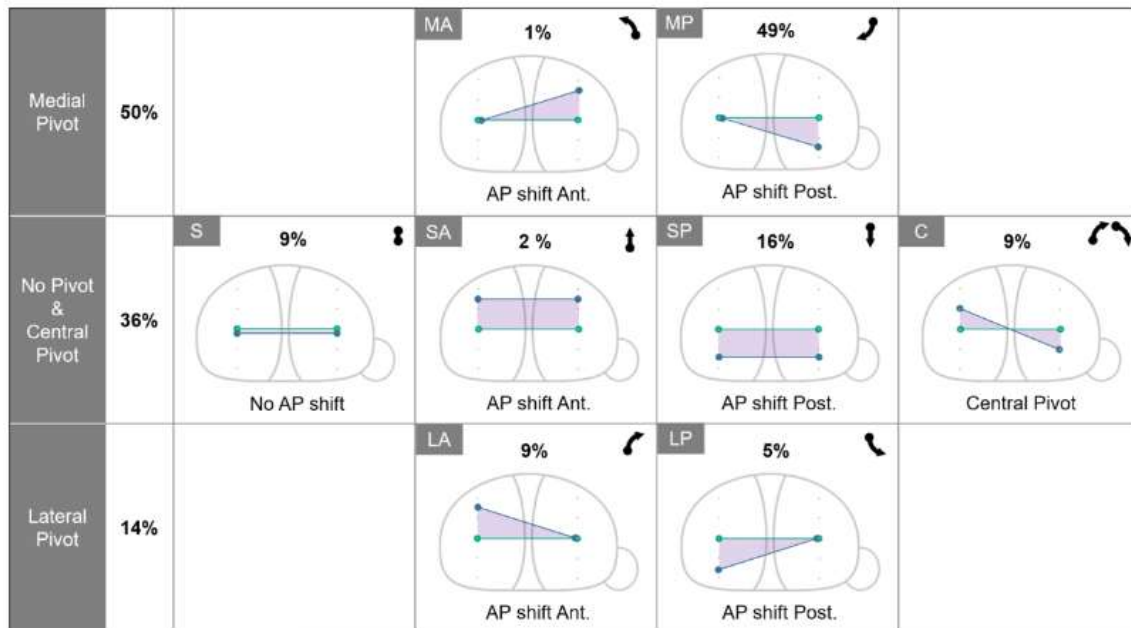


Figure1: Phenotypes based on the condylar AP shift between 0° (green) and 90°(blue) of flexion.

Figure 1

Medial Condyle Shift	From 0 to 30°	From 30 to 60°	From 60 to 90°	Lateral Condyle Shift	From 0 to 30°	From 30 to 60°	From 60 to 90°
> 8 mm Ant.	1%	2%	4%	> 8 mm Ant.	1%	2%	4%
> 4 mm Ant.	9%	10%	12%	> 4 mm Ant.	2%	6%	11%
[4 mm Ant. ; 4 mm Post.]	69%	71%	70%	[4 mm Ant. ; 4 mm Post.]	32%	62%	64%
> 4 mm Post.	16%	15%	11%	> 4 mm Post.	34%	27%	15%
> 8 mm Post.	5%	2%	3%	> 8 mm Post.	31%	4%	7%

Figure 2: Distribution of the AP Shift of the medial and lateral condyles from 0° to 90° of flexion.

Figure 2

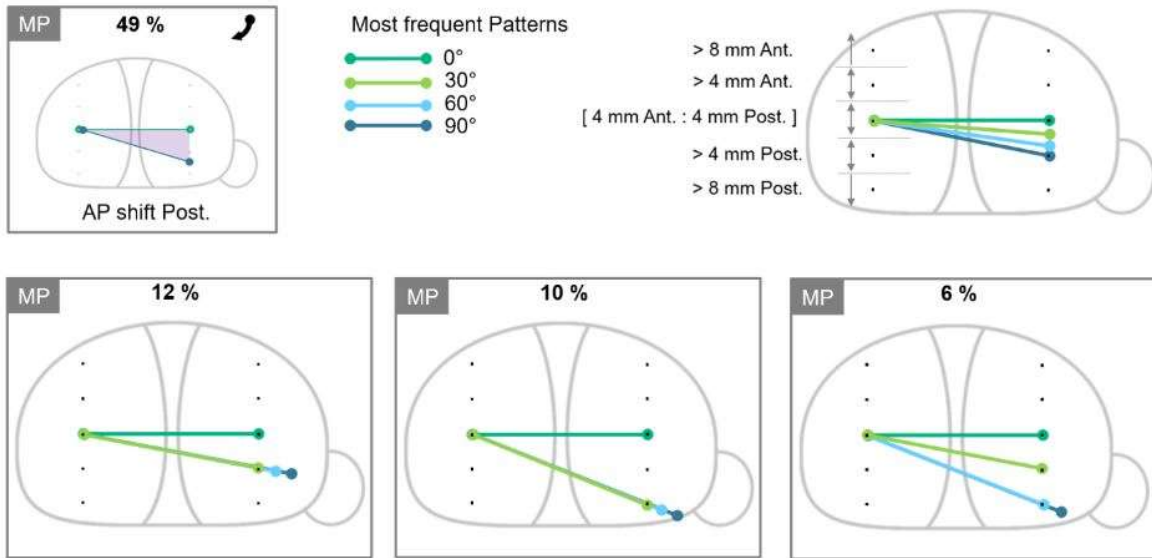


Figure 3: Medial Pivot Phenotype - distribution of the pivoting from 0° to 90° of flexion.

[Figure 3](#)

Bridging the Gap in Knee Arthroplasty: Validating Musculoskeletal Models for Functional Kinematics-Informed Surgical Planning

*Enrico De Pieri - ETH Zurich - Zurich, Switzerland

Sara Sarabadani - Zimmer Biomet - Winterthur, Switzerland

Pascal Schuetz - ETH Zurich - Zurich, Switzerland

William Taylor - Swiss Federal Institute of Technology Zurich - Zürich, Switzerland

Eik Siggelkow - Zimmer GmbH

Joern Seebeck - Zimmer Biomet - Winterthur, Switzerland

Marc Bandi - Zimmer GmbH - Winterthur, Switzerland

Introduction:

Knee arthroplasty seeks to restore mobility in osteoarthritis patients. Yet, current pre-surgical planning relies solely on static radiographs, lacking insights into patients' dynamic movements. Musculoskeletal (MSK) modelling has the potential to bridge this gap by incorporating physiological motion into pre-surgical planning, and by enabling the estimation of muscle activity, joint loads, and local joint kinematics in a non-invasive manner. Nonetheless, establishing sufficient model credibility through a thorough validation of these models is essential before clinical translation can be achieved.

The CAMS-knee datasets [1] currently represent the gold standard for MSK model validation, as they comprise knee loading data from 6 subjects fitted with instrumented implants, as well as simultaneous local joint kinematics obtained with moving video-fluoroscopy during different activities of daily living (ADLs; level and downhill walking, stair descent, squatting, sitting, and rising from a chair). The aim of this study was to compare predicted knee contact forces (KCFs) and local kinematics against *in vivo* measurements across different ADLs.

Methods:

Motion-capture data from the CAMS-knee datasets were used as input for a MSK inverse-dynamics analysis in the AnyBody Modeling System (AnyBody Technology A/S). Personalized models were built starting from the TLEM 2.2 lower-limb model while accounting for subject-specific anthropometrics and radiographic data. Virtual implantation of femoral and tibial components (INNEX FIXUC; Zimmer Biomet) was performed in the MSK models to match subject-specific post-operative implant alignment from CT data. An elastic-foundation contact model between implant components was defined and a balanced model of the ligaments was included. Tibiofemoral kinematics were determined by solving each instantaneous quasi-static equilibrium between external loads, muscle forces, and ligament constraints. These predicted kinematics were then compared against measurements from video-fluoroscopy, while predicted KCF magnitudes were compared against loading measurements from instrumented implants. For each subject, five trials per ADL were analysed. Root mean square error (RMSE) and coefficient of determination R^2 were computed across trials for each subject and ADL.

Results:

Predicted KCF magnitudes showed good qualitative agreement with the measured data across all ADLs (RMSE: 0.3–0.45 BW, Figure 1). The elastic-foundation contact model accurately predicted local implant kinematics during different ADLs (anterior-posterior translation RMSE: 1.61–2.77 mm, Figure 2), although some variability between subjects persisted.

Conclusions:

Recent literature suggests that kinematic and kinetic parameters during different ADLs might be best suited for identifying poor post-operative functionality and clinical outcomes [2,3]. While previous MSK modelling studies have mostly focused on validating predictions during level walking, the current study investigated a broader range of ADLs and subjects and represents the most extensive MSK quantitative validation for the prediction of knee loading to date. The development and validation of realistic MSK models will enable us to better understand how knee mechanics influence patient overall satisfaction and mobility during a broad range of real-life activities, while paving the way for dynamic, movement-informed, patient-specific surgical planning.

References:

- [1] Taylor WR et al. *J Biomech* **65**:32-39, 2017.
- [2] Banks SA et al. *J Arthroplasty* **13**:S0883-5403(24)00113-X, 2024.
- [3] Rao L et al. *The Knee* **34**:62-75, 2022.

Figures

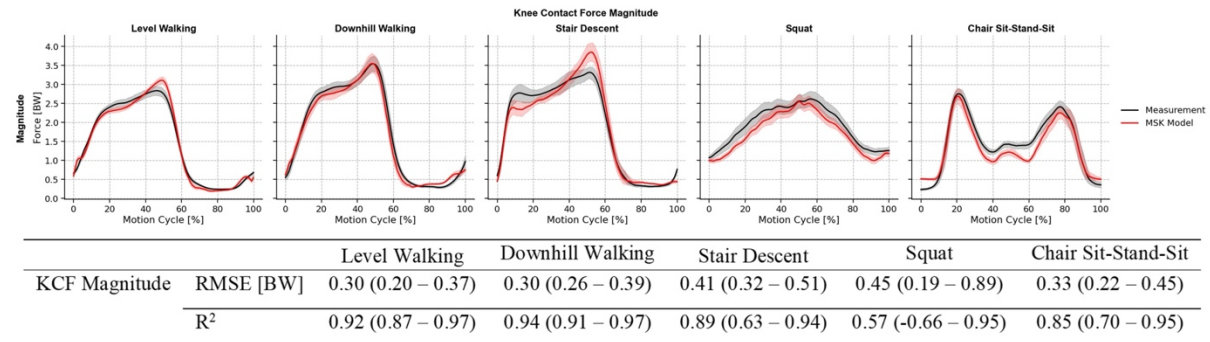


Figure 1: Mean (\pm 95% confidence intervals) predicted (solid red) and measured (dashed grey) KCF magnitudes, normalized against body weight (BW), computed for each ADL across all subjects, with corresponding RMSE and R² values (min–max range across subjects).

Figure 1

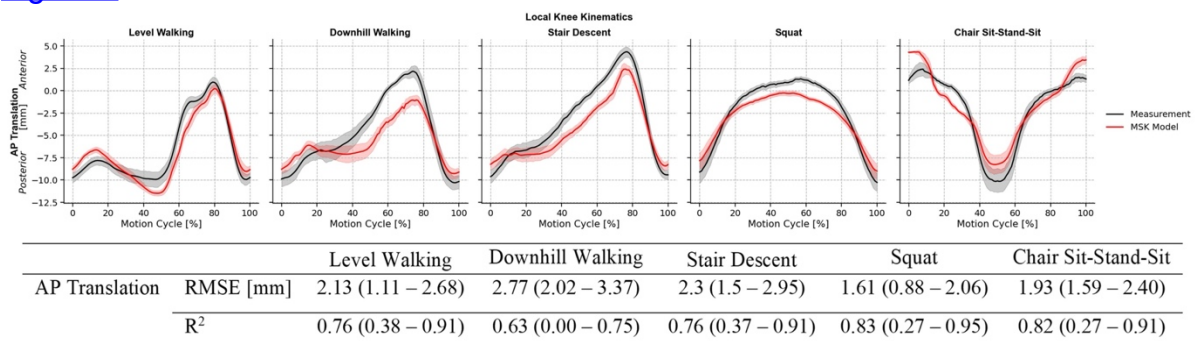


Figure 2: Mean (\pm 95% confidence intervals) predicted (solid red) and measured (dashed grey) local knee kinematics, defined as relative anterior (+) – posterior (-) translations of the femoral component with respect to the tibial baseplate, computed for each ADL across all subjects, with corresponding RMSE and R² values (min–max range across subjects).

Figure 2

Kinematic Phenotypes and Their Implications for Total Knee Implant Design

*Berna Richter - Aesculap AG - Tuttlingen, Germany

Brigitte Altermann - Aesculap - Tuttlingen, Germany

Allan Maas - Aesculap - Tuttlingen, Germany

Adrian Sauer - Aesculap AG - Tuttlingen, Germany
Sven Krueger - Aesculap AG Research & Development - Tuttlingen, Germany
Ingrid Dupraz - Aesculap AG - Tuttlingen, Germany
Alexander Giurea - Medical University of Vienna - Vienna, Austria
Masahiro Hasegawa - Mie University - Japan
Yukihide Minoda - Osaka City University Graduate School of Medicine - Osaka, Japan
Henning Windhagen - Hanover Medical School - Hannover, Germany
William Mihalko - University of Tennessee - Memphis, USA
Thomas M. Grupp - Aesculap AG - Tuttlingen, Germany

Introduction

For total knee arthroplasty (TKA) knee implant designs have been developed based on different indications and/or specific kinematic behaviours (CR: cruciate retaining, UC: ultra congruent, PS: posterior stabilized, MP: medial pivoting, LP: lateral pivoting, etc.) to restore the joint function.

Typically, there is currently no optimal match between patient's individual kinematics and the corresponding characteristics of the implant by default [1]. This is because the various implant systems are often incompatible with each other and give not the needed flexibility during surgery.

The aim of this work was to develop a total knee implant platform with different specific kinematic characteristics which can be easily chosen and evaluated intraoperatively.

Methods

Proven implants characteristics, indications and kinematic behaviours were first analysed and focused. As basic for the design process of the implant platform (oneKNEE®) the Aesculap dynamic knee model based on dynamic finite element analysis [2, 3] was used as kinematic simulation tool. Iteratively, design elements were adapted across all sizes and across different pattern of activities, like walking, climbing stairs, descend stairs, deep knee bending and chairs rising, always with respect to the kinematic behaviors. Referring to the overall kinematic input, implants that suite to individual phenotypes were devised and aligned with the important interfaces between the components.

For validation and comparison with proven implants a musculoskeletal multibody simulation (MMBS) model [4] of a dynamic squat motion and a well-established knee rig [5] with fresh frozen knee specimens were integrated.

Results

Specific knee implant design elements with a high degree of compatibility interfaces across all TKA components provide solutions for various indications and kinematic behaviors. Therefore, a platform can ensure flexibility in treating patients based on their individual kinematic profiles. Furthermore, the implant platform design considers alternative limb alignment, such as kinematic alignment, constitutional varus, functional alignment approaches.

Conclusion

Different knee implant designs address specific joint characteristics. To optimize patient care, we advocate for kinematic phenotyping, knee ligament analysis tools and knee implant platform designs that allow for patient specific treatment during surgery.

References

- [1] Dennis et al., Clin Orthop Relat Res., (416):37-57, 2003
- [2] Maas et al., 21th Eur Soc Biomech, Prague 2015
- [3] Maas et al., 29th Eur Soc Biomech, Edinburgh 2024
- [4] Kebbach et al., Materials (Basel), 13(10): 2365, 2020
- [5] Steinbruck et al., Arch Orthop Trauma Surg, 138:401–407, 2018

Effect of Postoperative Recovery Time on Joint Mechanics and Implant Fixation

*Fernando Quevedo Gonzalez - Hospital for Special Surgery - New York, USA

Jonathan Glenday - Hospital for Special Surgery - New York, USA

Joseph Lipman - Hospital for Special Surgery - New York, USA

Peter K. Sculco - Hospital for Special Surgery - NYC, USA

Cynthia Kahlenberg - Hospital for Special Surgery - New York City, USA

Eytan Debbi - Cedars-Sinai Medical Center - Los Angeles, USA

David J. Mayman - Hospital for Special Surgery - New York, USA

Jonathan Vigdorichik - Hospital for Special Surgery - New York, USA

Timothy Wright - Hospital for Special Surgery - New York, USA

Introduction

Achieving appropriate kinematics and sufficient implant fixation are common goals in total knee arthroplasty (TKA). However, the tradeoffs between joint kinematics and implant fixation are poorly understood. We previously developed a computational workflow to holistically assess knee joint biomechanics and implant fixation,[1] but the publicly available data used for validation consisted of outdated cemented designs. Thus, our goal was to apply the workflow to a new dataset with modern cementless implants. We asked: how do tibiofemoral joint mechanics (i.e., kinematics and kinetics) and implant fixation change with time after surgery?

Methods

Two patients who received robotically-assisted primary cementless TKA (MAKO, Stryker) and were enrolled on an ongoing IRB-approved study were analyzed with our workflow. We obtained their whole-body kinematics and ground reaction forces (GRF) at 6-weeks and 6-months postoperatively in our institution's gait lab. A generic musculoskeletal model [2] with a 12 degree-of-freedom knee joint and an enhanced static optimization algorithm (<https://simtk.org/projects/opensim-jam>) was adapted to each patient using the biplane radiographs (EOS Imaging) to calculate the patient-specific tibiofemoral joint forces and contact locations for each postoperative visit. We directly transferred the joint forces and contact locations to corresponding patient-specific FE models to evaluate the implant fixation. The implant and bone, reconstructed from the CT-scans, were meshed with linear tetrahedra. Materials were linear elastic. The non-homogeneous bone modulus (E) was derived from CT using relationships specific to the proximal tibia [3,4] and the Poisson's ratio (ν) was 0.3. The baseplate was solid titanium ($E=114.3$ GPa, $\nu=0.33$), except for the spikes and backside, which were 3D printed porous titanium ($E=1.1$ GPa, $\nu=0.3$). The insert was ultra-high molecular weight polyethylene ($E=463$ MPa, $\nu=0.46$). We considered frictional bone-implant interfaces (i.e., no ingrowth), with coefficients of 0.6 and 1.1 for the solid and porous titanium, respectively. Outcomes were the tibiofemoral kinematics, the joint forces in the medial and lateral compartments, the bone-implant micromotion, and the bone interfacial strains.

Results

At 6-months, contact forces were smoother and closer to a normal two-hump profile than at 6-weeks (Fig. 2A). For both patients, kinematics at 6-weeks were similar to 6-month (Fig. 2B). For both patients, the lateral compartment translated more than the medial compartment. However, the tibiofemoral contact points at the peak joint force

were less posterior at 6-weeks than at 6-months. In both cases, most baseplate micromotions were compatible with bone ingrowth; however, micromotion at 6 months was greater than at 6 weeks (Fig. 3A). Similarly, while the strains at the tibial cut remained low, 6 months exhibited higher strains than 6 weeks.

Discussion

In the postoperative recovery period, patients typically walk with more care. Our results indicate that such care creates favorable conditions for bone ingrowth at the bone-implant interface through less extreme tibiofemoral contact positions. We expect these observations to be confirmed as we continue to enroll patients.

References: [1] Glenday et al., J Biomech, 2024. [2] Arnold et al., Ann Biomed Eng, 2010. [3] Morgan et al., J Biomech, 2003. [4] Snyder & Schneider. J Orthop Res, 1991.

Figures

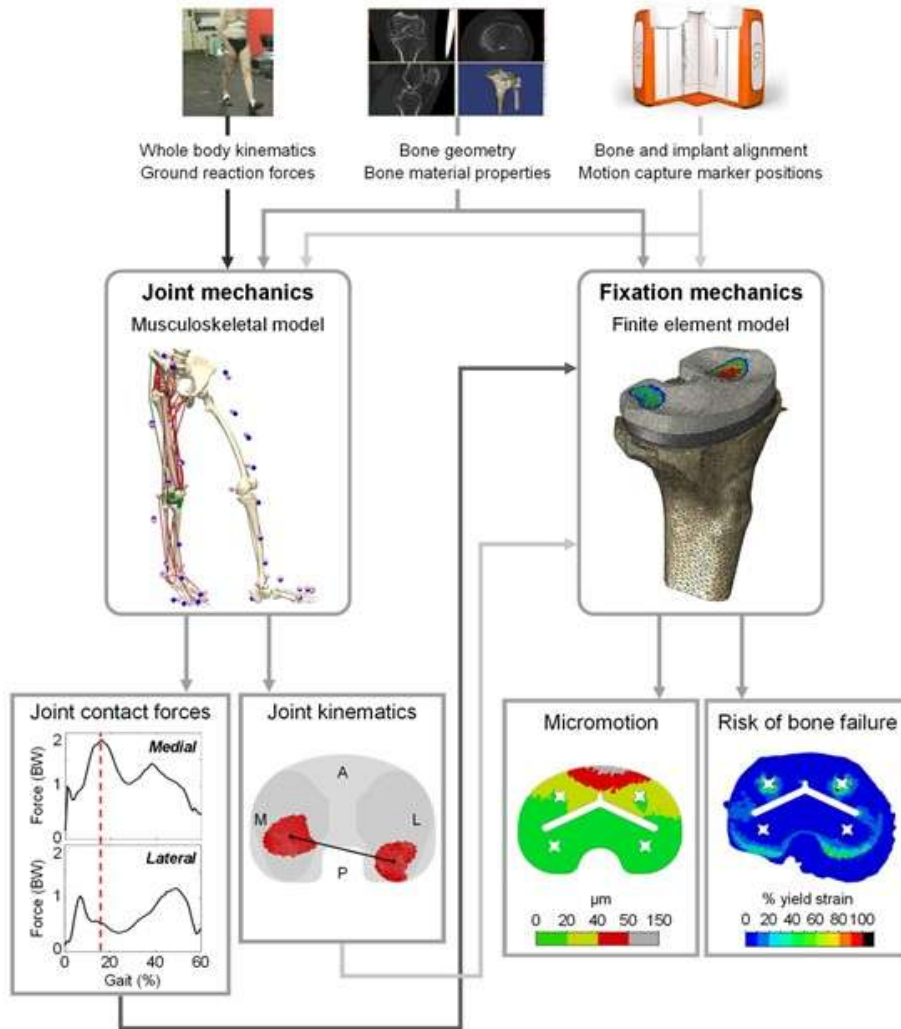


Fig. 1 – Overview of the workflow.

[Figure 1](#)

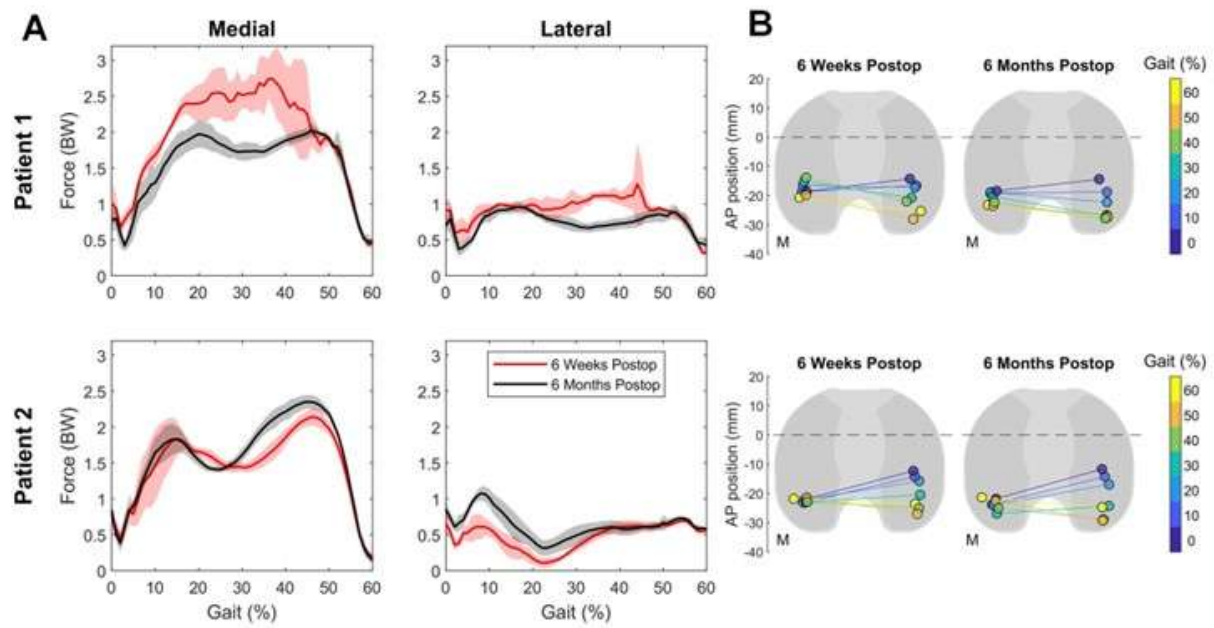


Fig. 2 – Joint kinetics (A) and tibiofemoral contact points (B)

[Figure 2](#)

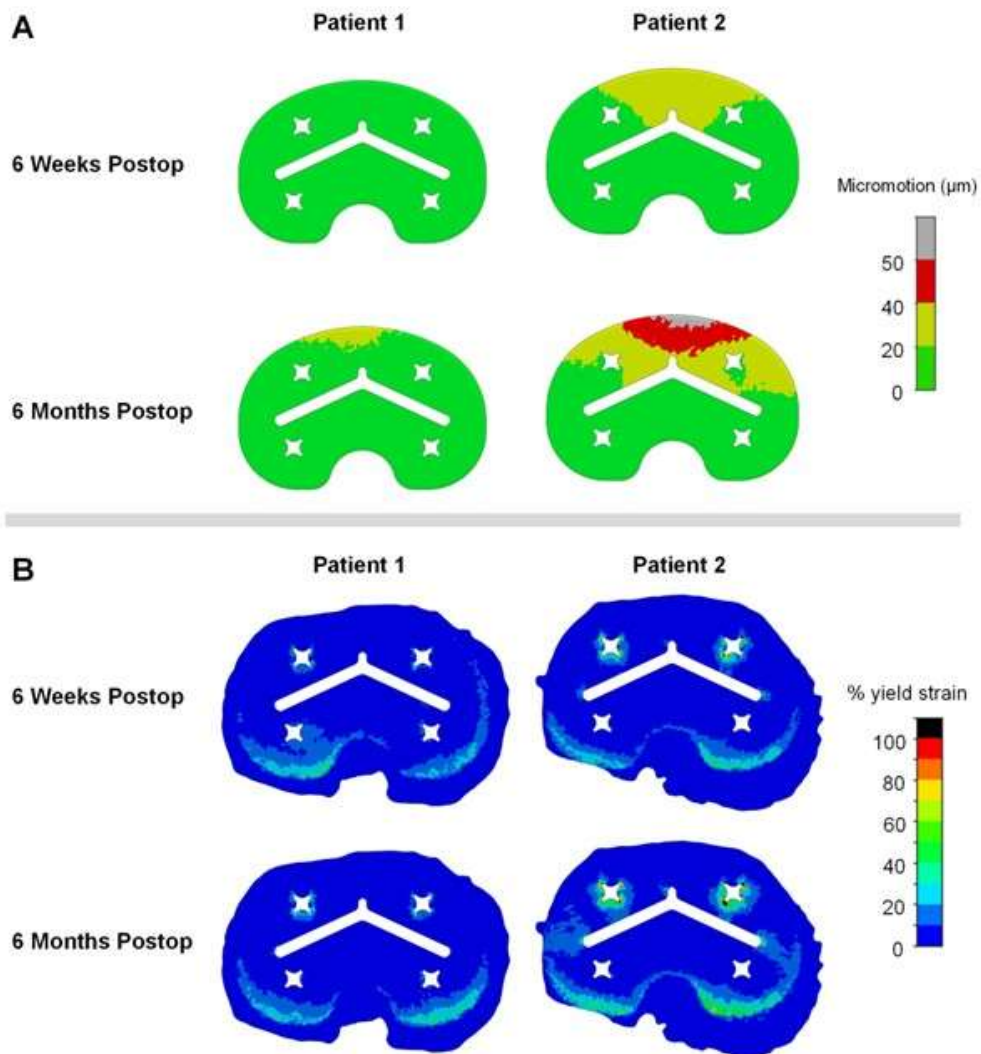


Fig. 3 – Micromotion at 6 weeks and 6 months (A) and bone strains at the same timepoints (B)

[Figure 3](#)

Optimization of Kinematics in Robotic Total Knee Arthroplasty: A New Classification for Functional Coronal Alignment

Catherine Digangi - NYU Orthopedic Hospital - New York, USA

*Morteza Meftah - NYU Hospital for Joint Diseases - New York, USA

Akram Habibi - NYU Langone Orthopedic Hospital - New York, United States of America

Sophia Antonioli - NYU Langone - New York, USA

Patrick Meere - NYU Hospital for Joint Diseases - New York, USA

Matthew Hepinstall - NYU Langone Health - New York, USA

Introduction

The Coronal Plane Alignment of the Knee (CPAK) classification method is a recently implemented tool that can be utilized to describe knee coronal phenotypes. The difference is determined by the arithmetic hip-knee-ankle (aHKA) and joint line obliquity (JLO) angles. With the recent increase in use of robotic-assisted total knee arthroplasty (TKA), where the bony cuts can be fine-tuned to avoid soft tissue release, the utility of this classification system remains unclear.

Methods

We retrospectively reviewed 530 primary MAKO (Stryker) TKA cases performed using restricted kinematic alignment technique from November 2022 to December 2023. Within this cohort, aHKA and JLO angles were obtained using MAKO software. In accordance with CPAK classification, neutral boundaries for aHKA were $0^\circ \pm 2^\circ$, with $< -2^\circ$ classified as varus and $> 2^\circ$ as valgus; Neutral boundaries for JLO were $180^\circ \pm 3^\circ$, with angles $< 177^\circ$ classified as apex distal and $> 183^\circ$ as apex proximal. Demographics, CPAK phenotypes, and planned resection values were collected and analyzed using Independent Sample t-tests and chi-square tests.

Results

In total, preoperative CPAK phenotypes were: 1 (31.7%), 2 (33.0%), 3 (19.1%), 4 (8.5%), 5 (5.1%), 6 (2.5%), and 7 (0.2%). Postoperative CPAK phenotypes were: 1 (4.0%), 2 (8.1%), 3 (0.8%), 4 (31.5%), 5 (49.2%), 6 (6.2%), and 7 (0.2%). Postoperatively, 64.7, 28.5, and 19.4% of cases retained their preoperative aHKA alignment, JLO alignment, and CPAK classification, respectively. However, of the 427 cases that changed CPAK, most varus and neutral cases remained in their preoperative aHKA alignment (60.4% and 72.7%), otherwise changing to neutral and varus respectively, while most valgus cases (72.5%) changed to neutral. Most (98.8%) preoperative neutral JLO cases retained their neutral classification, while a majority of apex distal (84.7%) cases became neutral. Cases that changed CPAK classification, when compared to those that retained their preoperative CPAK phenotype, were more neutral for aHKA (-0.7 vs. -2.3, $p < 0.001$) and more apex distal preoperatively (173.3 vs. 176.0, $p < 0.001$). Subgroup analysis revealed cases that retained their preoperative aHKA alignment for varus and valgus groups had larger native deformities as compared to those that changed to a neutral alignment. Based on these results, we classified the preoperative alignment according to the final functional coronal alignment that would reflect tibia and HKA angles (Figure 1). This new classification can guide the surgeon for optimizing kinematics of the knee using robotic-assisted technologies while avoiding soft tissue release.

Conclusion

This study highlights the ability of the MAKO robot to restore native knee phenotypes as well as describes instances in which the preoperative CPAK classification was changed. Based on this study we propose a simplified CPAK classification: Varus HKA/Varus tibia.

Figures

Table 1. CPAK Classifications

Remained in Same CPAK- no. (%)	N=103
1-1 (varus)	16 (15.5)
2-2 (neutral)	23 (22.3)
3-3 (valgus)	3 (2.9)
4-4 (varus)	34 (33)
5-5 (neutral)	25 (24.3)
6-6 (valgus)	2 (1.9)
Changed CPAK - no. (%)	N=427
Varus-Varus	99 (23.2)
1-4	97
1-7	1
7-4	1
Varus-Neutral	65 (15.2)
1-2	10
1-5	44
4-5	11
Varus-Valgus	-
Neutral-Varus	39 (9.1)
2-1	5
2-4	32
5-4	2
Neutral-Neutral	112 (26.2)
2-5	112
Neutral-Valgus	3 (0.7)
2-6	3
Valgus-Varus	1 (0.2)
3-4	1
Valgus-Neutral	79 (18.5)
3-2	10
3-5	59
6-5	10
Valgus-Valgus	29 (6.8)
3-6	28
6-3	1

Table 2. CPAK Characteristics, Stratified by Cases that Remained in Same CPAK vs. Changed CPAK Classification

	Remained in CPAK (n=103)		Changed CPAK Group (n=427)		P-Value
	<i>M</i> <i>SD</i>	<i>Range</i>	<i>M</i> <i>SD</i>	<i>Range</i>	
Implants- no. (%)					0.422
PS	11 (10.7)	-	35 (8.2)	-	
CS	92 (89.3)	-	392 (91.8)	-	
Mean Preop aHKA¹	-2.3±3.8	-12.3 – 12.5	-0.7±4.1	-12.8 – 10.7	<0.001*
Mean Postop aHKA¹	-2±2.2	-6.2 – 4.5	-1±2.2	-6 – 4.9	<0.001*
Mean Abs. Δ aHKA	1.6±1.6	0 – 8.5	2.4±1.7	0 – 10.8	<0.001*
Mean Preop JLO	176±4	164.1 – 182.6	173.3±2.8	164 – 184.1	<0.001*
Mean Postop JLO	177.9±2.5	171.5 – 182	178.7±1.5	172.1 – 184	<0.001*
Mean Abs. Δ JLO	2.4±2.1	0 – 12	5.5±2.7	0 – 15.6	<0.001*
Preop CPAK – no. (%)					<0.001*
1	16 (9.5)	-	152 (90.5)	-	
2	23 (13.1)	-	152 (86.9)	-	
3	3 (3)	-	98 (97)	-	
4	34 (75.6)	-	11 (24.4)	-	
5	25 (92.6)	-	2 (7.4)	-	
6	2 (15.4)	-	11 (84.6)	-	
7	-	-	1 (100)	-	
Remained aHKA - no. (%)	103 (100)	-	240 (56.2)	-	<0.001*
Pre-Postop aHKA alignment- no. (%)					<0.001*
Varus-Varus	50 (33.6)	-	99 (66.4)	-	
Varus-Neutral	-	-	65 (100)	-	
Neutral-Varus	-	-	39 (100)	-	
Neutral-Neutral	48 (30)	-	112 (70)	-	
Neutral-Valgus	-	-	3 (100)	-	
Valgus-Varus	-	-	1 (100)	-	
Valgus-Neutral	-	-	79 (100)	-	
Valgus-Valgus	5 (14.7)	-	29 (85.3)	-	
Remained JLO - no. (%)	103 (100)	-	48 (11.2)	-	<0.001*
Pre-Postop JLO - no. (%)					<0.001*
Distal-Distal	42 (62.7)	-	25 (37.3)	-	
Distal-Neutral	-	-	376 (100)	-	
Distal-Proximal	-	-	1 (100)	-	
Neutral-Distal	-	-	1 (100)	-	
Neutral-Neutral	61 (72.6)	-	23 (27.4)	-	
Proximal-Neutral	-	-	1 (100)	-	
Mean Femoral Rotation: TEA²	1.2±1.9	-3.9 – 5	2±1.9	-5.2 – 6.5	<0.001*
Mean Femoral Rotation: PCA²	3.9±2	-0.6 – 9.9	4.7±2.1	-1.2 – 10	<0.001*
Mean Sum of Resections: Extension					
Lateral	11.3±1.8	7.5 – 16.5	10.7±2.2	4.5 – 17.5	0.006
Medial	11.6±2	6 – 16.5	11.5±1.9	3.5 – 17.5	0.687
Mean Sum of Resections: Flexion					
Lateral	11.6±2.1	6 – 17	11.8±1.9	5.5 – 17.5	0.292
Medial	14±1.6	8.5 – 19	13.6±1.8	7 – 19	0.051

Abs=Absolute, aHKA=Arithmetic Hip-Knee-Ankle Angle, JLO=Joint Line Obliquity, PS=Posterior-Stabilized, CS=Condylar-Stabilizing, TEA=

Transepicondylar Axis, PCA= Posterior Condylar Axis

1. Valgus=+, Varus=-

2. External=+, Internal=-

Figure 2

Figure 1. Functional Coronal Alignment (FCA) Classification

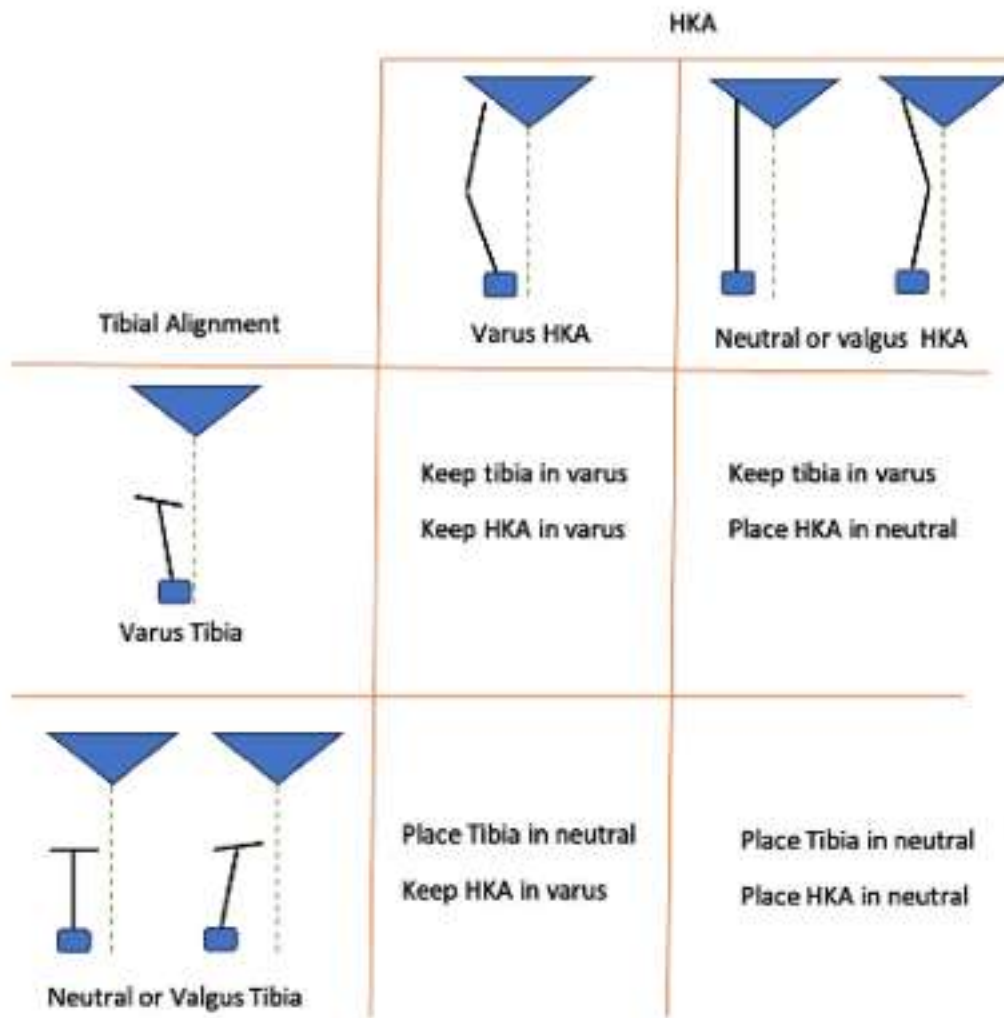


[Figure 3](#)

Are We Fulfilling Patient Expectations in Total Joint Arthroplasty? - a Review of a Large National Registry

*Tyler Madden - Corewell Health - Grand Rapids, USA

Kent Kern - Corewell Health/Michigan State University - Grand Rapids, United States of America

Karl Roberts - Corewell Health/Michigan State University - Grand Rapids, USA

Darby Dean - Michigan State University College of Human Medicine - Grand Rapids, USA

Shashank Chitta - Corewell Michigan State University Orthopedic Residency - Grand Rapids, USA

Tyler Janish - Corewell Health Michigan State University Orthopedic Residency - Grand Rapids, USA

Goal: The goal of this study is to describe fulfillment of patient reported expectations following elective total knee arthroplasty (TKA) and total hip arthroplasty (THA) using data gathered from a large national database of over 110,000 patients. We strive to establish a baseline of fulfillment rates of surgical and pain expectations at 10 weeks following TKA and THA, and to further stratify experiences based on primary and revision settings and age. We hypothesize that TKA and THA will meet patient expectations more commonly in the primary setting and in older patients.

Methods: This is a cross-sectional study using data gathered from over 110,000 patient responses across multiple institutions in the United States using a national registry. The primary survey asked patients to provide a rating on a 5 point scale asking if “the results of my surgery have met my expectations”, with 1 equaling “strongly disagree”, 2 equaling “disagree”, 3 equaling “neutral”, 4 equaling “agree”, and 5 equaling “strongly agree”. In addition, patients were surveyed on pain expectations by answering the question “after surgery, was your pain better or worse than you expected.” Responses were gathered using the same scale. Results were further stratified based on total hip arthroplasty (THA), total knee arthroplasty (TKA), primary and revision cases, and age (<50, 50-65, 67-80, and >80 years of age). The average patient response follow up time after surgery for all cases was 10 weeks.

Results:

For primary THA, 89.27% of patients either agreed or strongly agreed that the results of surgery met expectations, and were lowest in patients <50 years at 87.95%. This number decreased to 78.66% in all patients undergoing revision THA, and was lowest in patients >80 years old (Figure 1). After primary THA, 62.43% of patients agreed that pain was either better or much better than expected, and highest in patients >80 years at 65.71%. This number decreased to 53.85% in patients undergoing revision THA, and was lowest amongst those >80 years (Figure 2). For primary TKA, 81.58% of patients agreed or strongly agreed that the results of surgery met expectations, with those <50 years reporting lowest rates at 74.59% (Figure 3). For revision TKA, this number decreased to 74.8% overall, and was again lowest in patients <50 years at 67.5%. For primary TKA, 39.07% of patients agreed that after surgery, pain was either better or much better than expected, and was lowest in those <50 at 32.35% (Figure 4).

Conclusion

In this large nationwide database of over 110,000 patient responses, fulfillment of preoperative surgical and pain expectations at 10 weeks was highest in both primary and revision THA compared to TKA in all ages. Fulfillment rates were lowest in those aged <50 years undergoing primary and revision TKA. It is important to counsel all patients on the spectrum of postsurgical experiences, especially in patients 50 years or younger undergoing TKA who may experience the lowest fulfillment rates.

Figures

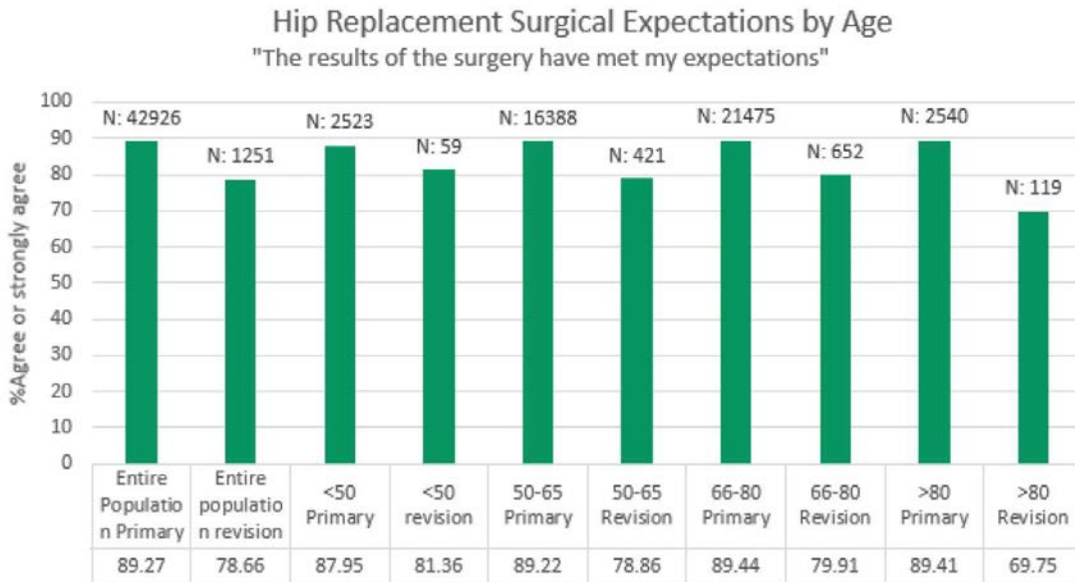


Figure 1

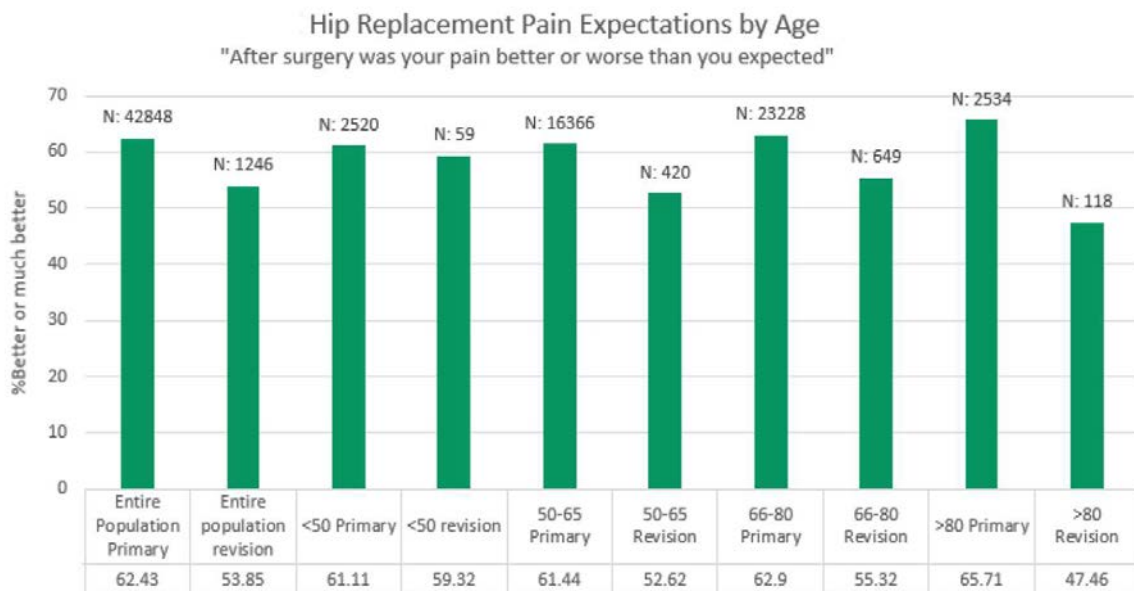


Figure 2

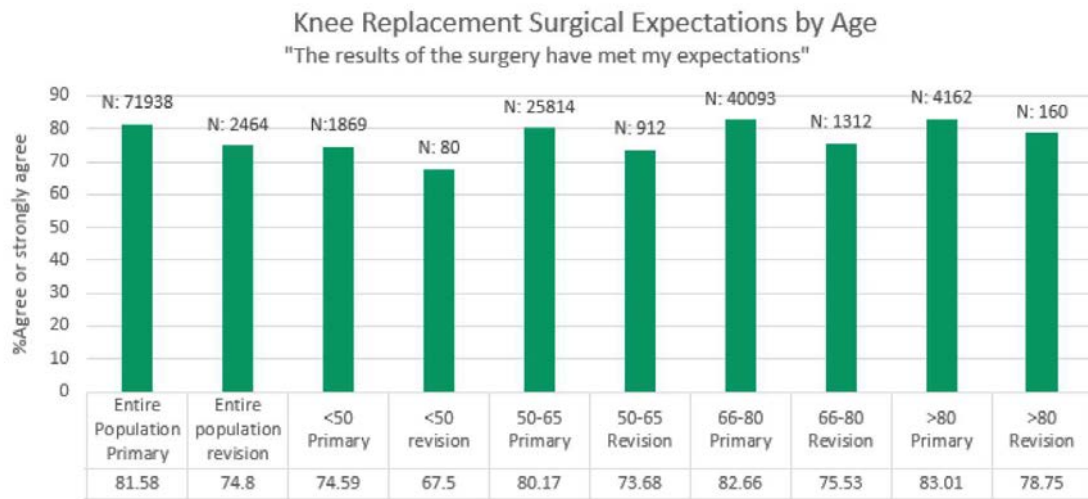


Figure 3

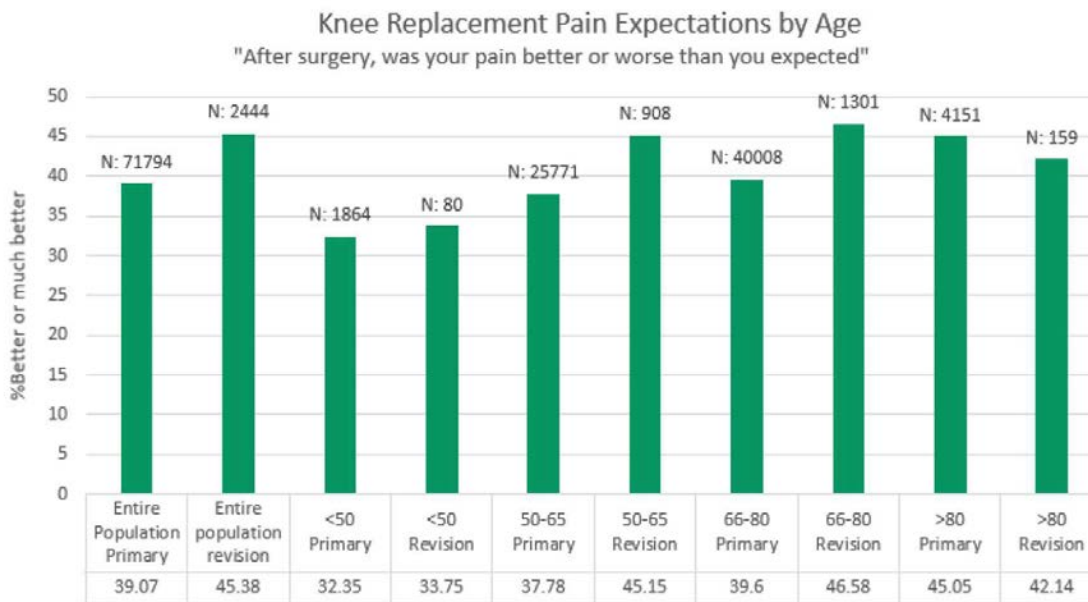


Figure 4

Clinical and Patient Reported Outcomes of a Novel Fully Cementless System Following Total Knee Arthroplasty

*Casey Cardillo - NYU Orthopedic Hospital - New York, USA

Ran Schwarzkopf - NYU Langone Medical Center Hospital for Joint Diseases - New York, USA

Joshua Rozell - NYU Langone Orthopedic Hospital - New York, USA

Muhammad Haider - NYU Orthopedic Hospital - New York, USA

Jonathan Katzman - NYU Langone - New York, United States of America

Akram Habibi - NYU Langone Orthopedic Hospital - New York, United States of America

Sophia Antonioli - NYU Langone - New York, USA

Catherine Digangi - NYU Orthopedic Hospital - New York, USA

Introduction

Cementless fixation in total knee arthroplasty (TKA) has gained popularity especially for younger, active patients to improve osteointegration and longevity of implants. This study aimed to evaluate the safety and efficacy of a novel cementless, porous TKA system.

Methods

A retrospective review of 135 consecutive cases of patients who underwent primary TKA using a novel cementless system (LEGION™ CONCELOC™; Smith & Nephew, Memphis, Tennessee) and had at least three months follow-up, was performed at a single academic health system. Study outcomes included 90-day emergency department (ED) visits and readmissions, as well as the rates of all-cause revisions and manipulations under anesthesia (MUA). Survivorship from all-cause revisions was also evaluated. The Knee Injury and Osteoarthritis Outcome Score, Joint Replacement (KOOS, JR) scores were assessed preoperatively and 3-months postoperatively.

Results

All 135 patients received both cementless femur and tibia components. A total of 78 patellas were resurfaced (57.8%), of which 66 were cementless (48.9%) and 12 were cemented (8.9%). The mean operative time was 97.8 (63-217) minutes, and the rates of 90-day ED visits and 90-day readmissions were 7.4% and 2.2%, respectively. Ten patients (7.4%) required a MUA. At the latest follow-up, two patients (1.5%) underwent a revision surgery, one for anterior knee pain due to unresurfaced patella and one for aseptic loosening; survival from all-cause revision was 98.5%. With a mean increase of 19.6 points in the KOOS, JR score from pre- to postoperative scores (39.7 and 57.3, respectively), the minimal clinically important difference was met at three months after surgery.

Conclusion

Clinical and patient reported outcome results of patients undergoing primary TKA with a novel cementless system show significant improvements in function and quality of life, with excellent performance and excellent survivorship. Increased rates of manipulation in younger patients requires further study to assess etiologies and mitigating strategies when using cementless fixation.

Clinical and Patient Reported Outcomes of a Kinematically Designed Cruciate Retaining Total Knee Arthroplasty With a Novel Medial Dished Insert Design

*Jonathan Katzman - NYU Langone - New York, United States of America

Casey Cardillo - NYU Orthopedic Hospital - New York, USA

Muhammad Haider - NYU Orthopedic Hospital - New York, USA

Mallory Ehlers - NYU Langone - New York, USA

Ran Schwarzkopf - NYU Langone Medical Center Hospital for Joint Diseases - New York, USA

Akram Habibi - NYU Langone Orthopedic Hospital - New York, United States of America

Catherine Digangi - NYU Orthopedic Hospital - New York, USA

Sophia Antonioli - NYU Langone - New York, USA

Introduction

Recent total knee arthroplasty (TKA) implant designs featuring innovative tibial inserts aimed at optimizing knee kinematics are being increasingly utilized to improve outcomes. This study evaluates the clinical efficacy and patient-reported outcomes (PROMs) associated with a kinematically designed Cruciate Retaining (CR) TKA, incorporating a novel, more constraining medial design.

Methods

A retrospective, single-center study was conducted to evaluate clinical outcomes and PROMs of patients undergoing primary elective TKA between 2022 and 2024, utilizing a novel kinematically-designed CR Knee System (JOURNEY™ II CR Medial Dished; Smith & Nephew, Inc., Memphis, TN). Patient demographics, surgical details, and outcome data were collected for individuals with a minimum 90-day follow-up.

Results

Of the 324 TKA patients, 60.2% were female, with an average age of 65.5 years. Primary osteoarthritis (97.8%) was the most common diagnosis. The mean surgical duration was 97.4 minutes, and the mean length of hospital stay was 1.3 days, with the majority of patients discharged home (97.2%). There were 15 (4.6%) 90-day emergency department visits, with 10 (3.1%) readmissions. Four patients required readmission due to TKA-related complications, including three for prosthetic joint infections (PJIs) and one for traumatic wound dehiscence. By latest follow-up, four patients (1.2%) required a revision surgery; one patient underwent femoral and tibial revision for arthrofibrosis and three patients required irrigation, debridement, and polyethylene insert exchange for PJI with one requiring further operations to manage the PJI. PROMs demonstrated significant improvements from preoperative measures, with a 16.8-point increase in KOOS, JR scores at six months postoperatively, and a 19.0-point increase at two years.

Conclusion

This study demonstrates favorable short-term outcomes associated with a novel CR medially constrained design, emphasizing its potential as a promising option in TKA procedures.

Leveraging Technology to Improve Patient Reported Outcome Measures (PROMs) Data Collection

*Danielle Edwards - Hospital for Special Surgery - Manhattan, United States of America

Mary Murray-Weir - Hospital for Special Surgery - New York, USA

Introduction:

Patient report outcome measures (PROMs) are valuable tools that allow for enhanced and individualized care. PROMs data can explore the clinical effectiveness of treatments and provides an opportunity for shared decision making.

Challenges arise when PROMs are not systematically integrated into an electronic health record (EHR) or inconsistently collected. Previously, our rehabilitation team used paper to collect PROMs for patients who arrived at their evaluation or follow-up visit without completing their PROMs. This process was time consuming and increased provider and patient burden. To improve PROMs data collection, decrease patient and clinician burden and allow for systematic collection of data we began using tablets for PROMs collection at the time of the rehabilitation visit.

Methods

For patients that arrived at their rehabilitation visit without previously completing their PROMs, we leveraged technology by using tablets that were designed to digitally collect PROMs data specific to their needs. The tablets were used at the initial evaluation and at subsequent visits every 21 days to collect series data. Within the EHR, we created a column that would notify our patient access team when a patient should be issued the tablet for PROMs completion. Providing the tablet at the time of the rehabilitation visit allowed the patient to complete the PROMs prior to the start of the visit, during or at the conclusion of the visit. Using the tablets allowed the patients responses to be automatically calculated and entered into the EHR for future analysis.

Results

As of September 2023, we implemented the use of tablets for PROMs collection in 4 rehabilitation departments. Using this technology has allowed us to increase the percentage of PROMs collected at evaluation to 85% and 89% when the PROMs series are started (figure 1). In addition, we were able to increase the overall number of patients for which we collected PROMs evaluation data to 3,226 (figure 1). Using this technology allowed decreased clinician burden as the therapist was allowed to have time back for clinical care, as PROM collection is now completely automated (figures 2 &3) therefore removing the need for manual collection and calculation of PROMs. The patient access team is more efficient, as they no longer need to scan the completed paper PROMs into the EHR.

Conclusion

PROMs data collected from specific patient populations provide information and understanding of how symptoms change over time. Digitally collecting PROMs allows for systematic data collection, while decreasing time associated with manual PROMs collection.

References

Keeney T, Kumar A, Erler KS, Karmarkar A. Making the Case for Patient-Reported Outcome Measures in Big-Data Rehabilitation Research: Implications for Optimizing Patient-Centered Care. Arch Phys Med Rehabil. 2022 May

Zigler CK, Adeyemi O, Boyd AD, Braciszewsk JM, Chevillie A, Cuthel AM, Dailey DL, Del Fiol G, Ezenwa MO, Faurot KR, Justice M, Ho PM, Lawrence K, Marsolo K, Patil CL, Paek H, Richesson RL, Staman KL, Schlaeger JM, O'Brien EC. Collecting patient-reported outcome measures in the electronic health record: Lessons from the NIH pragmatic trials Collaboratory. Contemporary Clinical Trials, Volume 137, 2024, 107426, ISSN 1551-7144.

Figures

Leveraging Technology to Improve Patient Reported Outcome Measures (PROMs) Data Collection

HSS

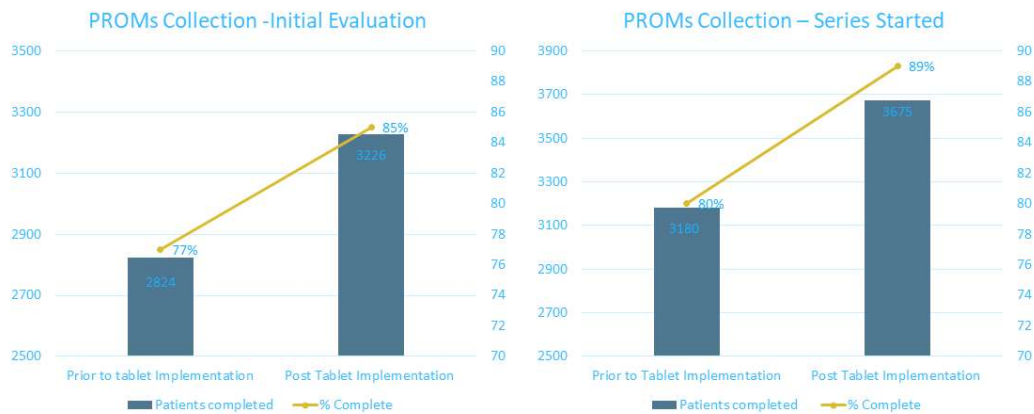


Figure1

Leveraging Technology to Improve Patient Reported Outcome Measures (PROMs) Data Collection



	For Evaluation	For Launching a Series
Ankle/Foot	FADI	FADI
Elbow/Forearm	Quick DASH	Quick DASH
Hip/Thigh	LEFS	LEFS
Knee/Lower Leg	LEFS	LEFS
Low Back/Pelvis	ODI	ODI
Neck/Upper/Mid-Back	NDI	NDI
Scoliosis/Kyphosis	SRS 22 + ODI + TAPS	SRS 22 + ODI + TAPS
Shoulder/Shoulder Girdle/Upper Arm	Quick DASH	Quick DASH
Wrist/Hand	Quick DASH	Quick DASH

Figure 2

Leveraging Technology to Improve Patient Reported Outcome Measures (PROMs) Data Collection



Department Appointments Report: Check In - Therapy Tablets_Sports

Refresh Settings Appt Desk Walk In Sign In Check In Check Out Orders/Follow-Ups Room

1 Full Appointment List 2 Appointment Totals

Date: 7/18/2023 1 Combined Departments

Last Used Ta...	HSS APPT H...	Referral Diag...	REHAB PROMs INCOMPLETE	Dept	W. P.	Ms Pa...
No DX			Patient must complete Rehab	Sports PT	N. R.	
Strain, cervical	Strain, cervical		Patient must complete Rehab	Sports PT	N.	
Medial	Medial		Patient must complete Rehab	Sports PT	X	
A1WELCOM...	Pain in left knee	Acute pain of	Patient must complete Rehab	Sports PT	N.	
	Other specified		Patient must complete Rehab	Sports PT	N. R.	
WELCOME03	Adhesive		Patient must complete Rehab	Sports PT	N. R.	
	Rupture of right	Rupture of right	Patient must complete Rehab	Sports PT	N. S.	
WELCOME03	Low back pain,	Chronic bilateral	Patient must complete Rehab	Sports PT	N. R.	
	Low back pain,	Low back pain,	Patient must complete Rehab	Sports PT	N. R.	
	Sprain of left	Sprain of	Patient must complete Rehab	Sports PT	N. R.	
	Bursitis of right	Rotator cuff	Patient must complete Rehab	Sports PT	N. R.	
	Pain in right	Left knee pain,	Patient must complete Rehab	Sports PT	N. R.	
	No DX		Patient must complete Rehab	Sports PT	N.	
K HSS	Unilateral		Patient must complete Rehab	Sports PT	N. R.	
SPWELCOM...	Lumbago with	Status post	Patient must complete Rehab	Sports PT	N. R.	
	Pain in right	Pain of right	Patient must complete Rehab	Sports PT	N.	
	Arthritis of ankle	Arthritis of ankle	Patient must complete Rehab	Sports PT	N. R.	
EWMREHAB	Sprain of	Rupture of	Patient must complete Rehab	Sports PT	N. R.	

© 2024 Epic Systems Corporation

Figure 3

Do Outcomes Following Total Joint Arthroplasty Differ by Objectively Measured Activity Performance?

Atul Kamath - Cleveland Clinic - Cleveland, USA

Karl Surmacz - Zimmer Biomet - Swindon, United Kingdom

*Roberta Redfern - Zimmer Biomet - Pemberville, USA

Dave Van Andel - Zimmer Biomet - Grand Rapids, USA

INTRODUCTION:

The desire for feedback regarding recovery progress, particularly in comparison to peers, has often been requested by arthroplasty patients. This study aimed to determine whether differences in clinically relevant outcomes were apparent by comparison of a patient's performance to peers based on walking metrics collected by wearable technology.

METHODS:

Mobility data was passively collected using a smartphone-based care management platform with smartwatch in patients undergoing joint replacement procedures. Subjects (n=3103) were divided into cohorts based on age, gender, BMI, and procedure. Patients were divided within these cohorts according to either step counts or walking sessions into performance groups compared to peers: low (<15th percentile); on-track (15th-85th percentile); high (>85th percentile). Outcomes including active flexion range of motion (ROM), KSS Satisfaction, NRS pain scores, and time to reach preoperative gait speed were compared between predicted performance groups by Kolmogorov-Smirnov two-sample tests. Principal component analysis (PCA) was applied to combine flexion, satisfaction, and pain outcomes to determine whether differences exist between predicted performance cohorts at 1 month.

RESULTS:

Differences in ROM were apparent at 1 month only between the low versus high-performance groups for both step counts or walking session groups with medians of distribution different by approximately 5° (p<0.001). Differences in ROM at 3 months were only observed between low- and high-performance groups based on walking sessions (p=0.005), but not step count predicted groups. Satisfaction at 3 months was significantly lower in the low step count performance group than on-track and high groups, while differences were significant only comparing on-track vs high-performance groups separated by walking sessions. Pain at 1 month was higher in the low-performance group compared to both on-track and high performers separated by either step count or walking sessions, while no differences were observed between any cohorts at 3 months post-operative. High performers, separated by either step count or walking sessions, returned to pre-operative gait speeds earlier than both on-track and low performance groups. PCA demonstrated a difference in outcome between high vs. on-track and high vs. low, but not on-track vs. low performance groups.

DISCUSSION AND CONCLUSION:

Patients can be meaningfully segmented into high, medium, and low progress compared to their peers using mobility data collected by wearables and smartphones. Differences in clinically important outcomes including ROM, satisfaction, pain, and gait recovery metrics were apparent between the highest and lowest performing groups based on these objective mobility metrics.

Rapidly Progressive Spinal Metastasis of Lung Cancer With Leukemic Transformation in Myelodysplastic Syndrome (MDS): A Case Report

*Takaaki Nakai - Itami city hospital - Itami, Japan

Atsunori Ohnishi - Itami city hospital - Itami, Japan

Tsuyoshi Nakai - Itami city hospital - Itami, Japan

Keisuke Kuroda - Itami City Hospital - Itami, Japan

Introduction: While there are many case reports of MDS secondly associated with lung cancer during chemotherapy, reports on lung cancer with primary MDS are rare. We report a rare case of lung cancer and bone metastasis diagnosed during the treatment course of MDS.

Methods: A 63-year-old male. During chemotherapy of MDS, a lung tumor was detected on a simple CT scan. One month later, magnetic resonance imaging (MRI) revealed a few spinal lesions which clinically diagnosed multiple bone metastasis of lung cancer. No therapy of lung cancer was provided because of poor prognosis. Although the lung lesions were not increased on imaging, the progression of leukemia was accompanied by new spinal metastases and lesions in the right ilium which increased rapidly.

Results: At the time of death, imaging diagnostics and pathological autopsy showed slight enlargement of the primary lung cancer and increased size of spinal and iliac bone metastases. The autopsy revealed that extensive infiltration of leukemia cells in the alveolus walls caused respiratory failure. The histopathological subtype of the lung cancer was adenocarcinoma. The thoracic vertebral lesions within leukemia-infiltrated bone marrow were diagnosed with bone metastases from lung adenocarcinoma.

Conclusion: Previous studies have suggested a correlation between the size and number of primary and metastatic lesions. In this case, the progression of leukemia coincided with rapid development of bone metastasis, though the untreated primary lung lesion did not increase significantly. It was suggested that bone metastasis developed more rapidly in leukemic bone marrow than normal bone marrow.

Pinnacle UHMWPE Liner Dissociation: An Investigation on the Movement Kinematics Based on Damaged Surface Evaluation

*Renir Reis Damasceno Neto - LEBm / UFSC - Florianopolis, Brazil

Patricia Ortega Cubillos - UFSC - Florianopolis, Brazil

Gean Vitor Salmoria - Universidade Federal de Santa Catarina - Florianópolis, Brazil

Lourenco Pinto Peixoto - INTO - Rio de Janeiro, Brazil

Osamu de Sandes Kimura - INTO - Instituto Nacional de Traumatologia e Ortopedia

Jamil Haddad - Rio de Janeiro, Brazil

Carlos Rodrigo De Mello Roesler - FAPEU - Florianopolis, Brazil

INTRODUCTION

The UHMWPE liner dissociation, although a relatively rare occurrence, poses a significant challenge for diagnosis and hip arthroplasty revision. This phenomenon, which still lacks a deep understanding of its mechanisms, has become increasingly evident in recent years. This increase is associated with the Pinnacle DePuy acetabular component, one of the most widely adopted worldwide for THA procedures, according to the National Registries. To properly evaluate the root cause of the failure of the fixation between the liner and the acetabular cup, there is a need to hypothesize and to investigate its movement mechanics.

METHODS

One sample of the Pinnacle liner was collected in an explant analysis center. Macroscopic and microscopic evaluations were conducted to discern liner movement relative to the acetabular cup, focusing on the region of fractured antirotational tabs. Macroscopic examination utilized a Leica M205 FA Stereo Microscope, while microscopic evaluation was carried out using a Tescan Scanning Electron Microscope post-golden coating preparation.

RESULTS

Initial observations revealed an elliptical plastic deformation altering the liner from its original circular shape, with a distinct longest axis indicating potential rotational movement within the acetabular cup, according to Figure 1. The shortest axis divides the portion of the three fractured antirotational tabs from the portion which still has the three other tabs.

Macroscopic analysis highlighted a deformed profile on the centrally fractured tab, contrasting with the smooth surfaces of adjacent tabs. The microscopic analysis confirmed the smooth and mirrored surface of those two tabs for approximately 65% of the area. The centered tab showed waved patterns along the tab area, with 3 main waves 0.6 mm apart from one another and smaller waves 20 μ m apart. The waved pattern indicates the direction of the brittle fracture, from the brim to the articular surface.

CONCLUSION

The ellipse-shaped plastic deformation of the dissociated liner indicated a hypothesized movement kinematics of it, while the analysis of the damaged surface confirmed it by the appearance and the direction of the waves. The probable kinematics is the rotation of the liner through the longest axis of the ellipse-shaped plastic deformation, firstly fracturing the tab on the opposite end (the centered tab 5), and then the adjacent ones. These findings prompt further exploration into the mechanisms underlying liner dissociation failures.

Figures

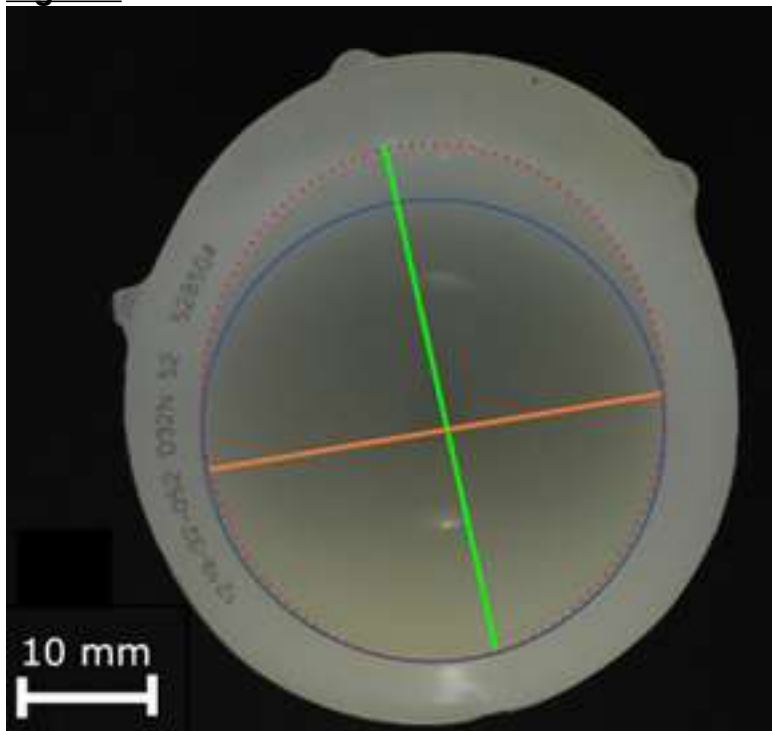


[Figure 1](#)



[Figure 2](#)

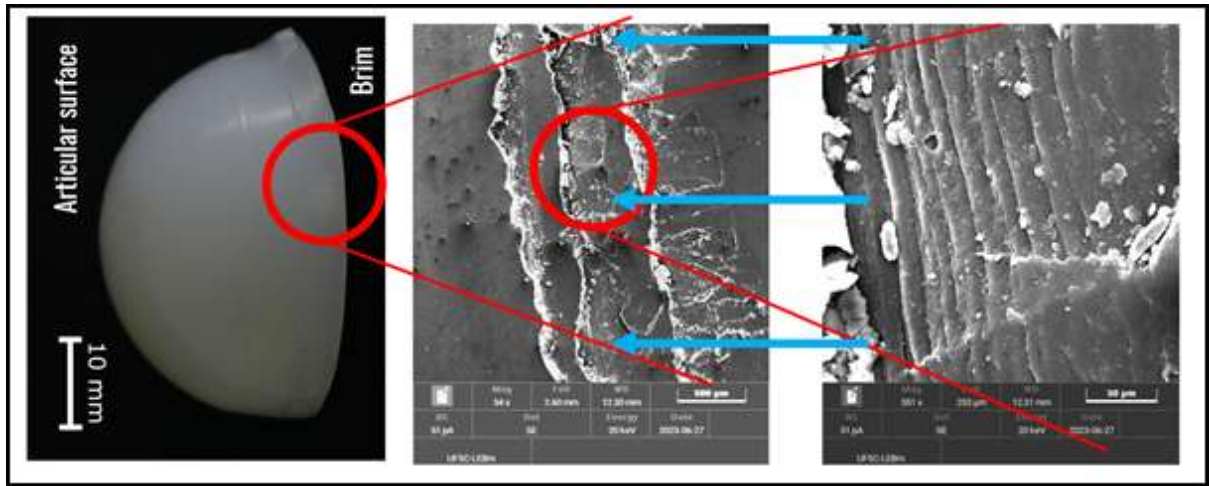


Figure 3

A Novel DM Component, Designed for Use in Young and Active Patients

***David Kirwan - Wirlinga, Australia**

Introduction:

Dual Mobility (DM) articulations were successfully developed for the elderly. Multiple complications were seen, especially in younger patients, with early iterations. The use of HXLPE bearings resulted in vast improvements, as did abandoning use of 22mm heads. However, the use of DM in THR is increasing at 20%+ per annum and, DM is often used in young patients today.

Methods:

A novel DM polyethylene component design is submitted for the Society's critical evaluation. The novel component is intended to reduce polyethylene wear and, improve locking mechanism strength, as well as increase pull-out and lever-out strength to prevent "neck notching" and both early and late "dissociation". Improved anterior soft tissue tensioning to enhance stability and flexor muscle strength is also claimed.

Results:

Locking mechanism deformation of DM components (further reducing pull-out and lever-out strength) is confirmed on head insertion. The novel design obviates this problem.

FEA studies on the novel component predict a >3 times greater resistance to dissociation (pull-out modelling), compared to a conventional DM bearing. These results are confirmed by "pull-out" and "lever-out" mechanical studies.

Conclusion:

It is recommended the novel DM bearing presented here-in, supplants the use of conventional DMs in any future THR.

Acknowledgements:

The author wishes to thank the following engineers: (to be disclosed in future)

Keywords:

Dual mobility, DM poly, dissociation, locking mechanism failure

Enhanced Surgical Outcomes

*Rami Kallala - NHS - London, United Kingdom

Rahul Singh - NHS - London, United Kingdom

1. **Introduction/Problem:** Corthotec, steered by a team of seasoned professionals including surgeon-founder Dr. Rami Kallala, targets the expansive market of orthopaedic surgery, particularly in arthroplasty. The existing bone graft market, valued at over £17bn, faces critical challenges with autografts and allografts—such as the risk of infection, and difficulties in harvesting sufficient bone. This is especially problematic in arthroplasty, where robust bone integration and healing are crucial, and surgery especially during revision procedures can result in bone voids.
2. **Solution:** Corthotec's synthetic bone graft addresses these arthroplasty issues head-on. It offers a novel solution that is both cost-effective and clinically superior to existing graft materials. Protected by a robust IP strategy that includes patents for its unique formulation and use, the product sets a new benchmark in orthopaedic surgery. This innovation is positioned to outperform competitors by reducing the operational complexities and risks associated with traditional bone grafts.
3. **Financial Data:** The product's pathway to market is underpinned by a clear regulatory strategy aimed at securing approvals from major health authorities like the MHRA and FDA. Financially, the product aligns with key reimbursement models and is competitively priced to penetrate the market effectively. The commercialisation roadmap is supported by both government grants and private investment, aimed at scaling up manufacturing and distribution capabilities rapidly.
4. **The Ask:** Corthotec's value proposition is compelling: it significantly improves patient outcomes in arthroplasty by enhancing the healing process and reducing complications associated with bone grafts. The company is seeking capital to accelerate clinical trials, obtain regulatory approvals, and launch a strategic market entry. Funds will be allocated to finalising product development, establishing manufacturing processes, and executing a targeted go-to-market strategy that includes collaboration with leading orthopaedic centres and specialists.

Outcomes Following Treatment of Symptomatic Accessory Navicular With Pes Planus Correction: A Systematic Review

*Thellma Jimenez Mosquea - NYU Langone Health - New York, United States of America

Hugo Ubillus - NYU Langone Health - New York, USA

Raymond Walls - NYU Langone Health - New York, United States of America

INTRODUCTION

The presence of an accessory navicular (AN) can disrupt the attachment of the tibialis posterior tendon (TPT), potentially resulting in a flattened medial longitudinal arch. The Kidner procedure aims to alleviate painful AN by correcting the abnormal TPT insertion, thus aiding in arch elevation. Subtalar arthroeresis (STA) serves to prevent excessive subtalar joint eversion, thereby averting arch collapse in flatfoot deformity. Conversely, the addition of a medial column reinforcement through osteotomy has been proposed to further stabilize the corrected foot shape. Literature on AN treatment often overlooks options for flatfoot deformity. This study compares outcomes of Kidner alone, Kidner with STA, and Kidner with medial column reinforcement for symptomatic AN with flatfoot, seeking to provide valuable treatment insights.

METHODS

In February 2024, a systematic review was conducted on the PubMed, Embase, and Cochrane Library databases to identify clinical studies investigating outcomes of the Kidner procedure alone, Kidner with STA, and Kidner with osteotomies for managing symptomatic accessory navicular (AN) with flatfoot deformity. The level of evidence (LoE) in the included studies was assessed according to the criteria set by the Journal of Bone and Joint Surgery. Information pertaining to subjective clinical outcomes, radiological findings, and complications was gathered and subjected to analysis.

RESULTS

This review included 19 studies, comprising one with Level II evidence, thirteen with Level III, and five with Level IV. Among 525 cases, 246 underwent Kidner procedure, 166 the Kidner + STA and 113 the Kidner + medial osteotomy. The weighted mean age was 15.7 ± 3.9 years for the Kidner cohort, 12.4 ± 2.7 years for the Kidner + STA and 25.29 ± 12.1 years for the Kidner + osteotomy, with weighted-mean follow-up of 67.8, 44.06 and 25.01 months, respectively. Pre-operative AOFAS mean scores were 46.0, 56.4 and 52.8, with post-operative scores of 85.5, 89.7 and 89.7, respectively. At final follow-up, Meary's angle improved 0.7 degrees in the Kidner, 13.2 degrees in the Kidner + STA and 10.86 degrees in Kidner + osteotomy.

CONCLUSION

This review highlights the effectiveness of different procedures in managing symptomatic accessory navicular with flatfoot deformity. The three approaches demonstrated improvements in subjective clinical outcomes and radiological parameters. Kidner alone experienced less radiologic improvement, suggesting that augmentation with either STA or osteotomy may provide better correction. Despite limitations in study design and heterogeneity among included studies, our findings underscore the importance of individualized treatment approaches. Further research

with larger sample sizes and longer follow-up periods is warranted to validate these findings and optimize treatment strategies for this challenging condition.

Is Combined Treatment Essential for Symptomatic Accessory Navicular in Flexible Flatfoot: A Study Comparing Kidner Procedure Alone Versus With Subtalar Arthroeresis

*Thellma Jimenez Mosquea - NYU Langone Health - New York, United States of America

Hugo Ubillus - NYU Langone Health - New York, USA

Raymond Walls - NYU Langone Health - New York, United States of America

Introduction:

The presence of an accessory navicular (AN) can alter the attachment of the tibialis posterior tendon (TPT), potentially leading to a flattened medial longitudinal arch. The Kidner procedure addresses painful AN by correcting the abnormal TPT insertion, facilitating arch elevation. Subtalar arthroeresis (STA) prevents excessive subtalar joint eversion, preventing arch collapse in flexible flatfoot (FF) deformity. Literature on AN treatment seldom explores options in FF deformity. This study compares outcomes of Kidner alone versus Kidner with STA for symptomatic AN with FF, aiming to offer treatment insights.

Methods:

During January 2024, the PubMed, Embase, and Cochrane Library databases were systematically reviewed to identify clinical studies examining outcomes following the Kidner procedure alone and the Kidner procedure with STA for the management of symptomatic AN with FF deformity. The level of evidence (LoE) of the included studies was evaluated using the Journal of Bone and Joint Surgery criteria. Data regarding subjective clinical outcomes, radiological outcomes, and complications were extracted and analyzed.

Results:

This review included 14 studies, comprising one with Level II evidence, ten with Level III, and three with Level IV. Among 362 cases of symptomatic AN, 246 underwent the Kidner procedure, while 116 underwent Kidner + STA. The weighted mean age was 15.7 ± 3.9 years for the Kidner cohort and 12.8 ± 3.0 years for the Kidner + STA cohort, with WM follow-up durations of 67.8 and 31.3 months, respectively. Pre-operative VAS scores were 6.4 for Kidner procedures and 4.4 for Kidner + STA, with post-operative scores of 1.6 and 1.7, respectively. Pre-operative AOFAS scores were 46.0 and 57.7, with post-operative scores of 85.5 and 89.2, respectively. At final follow-up, Meary's angle improved in the Kidner + STA cohort from 0.8 to 13.1 degrees.

Conclusion:

In conclusion, this review highlights the efficacy of both the Kidner procedure and its combination with subtalar arthroeresis (STA) in managing symptomatic accessory navicular (AN) with flexible flatfoot (FF) deformity. While the Kidner procedure effectively treats AN with flatfoot deformity, it carries a risk of arch collapse recurrence. Combining it with STA provides a more stable biomechanical construct for the tibialis posterior tendon (TPT), preventing arch collapse. Despite study limitations, personalized treatment approaches are crucial. Further research with larger cohorts and longer follow-ups is necessary to confirm and refine treatment strategies for this complex condition.

Should Orthopedic Surgeons Emulate Spiders or Martians in Their Approach to Total Hip Replacement Surgery

*Kambiz Behzadi - Behzadi Medical Device - Pleasanton, USA

In the rapidly evolving field of orthopedic surgery, the quest for innovation is perpetual, especially in procedures like Total Hip Replacement (THR) where failure rates persist at around 13% within a decade. Addressing these challenges requires a nuanced understanding of both technological advancements and the intricacies of surgical techniques. In this context, the debate arises: Should orthopedic surgeons emulate Spiders or Martians in their approach to THR surgery?

Spiders, known for their intricate webs and strategic adaptations, epitomize the concept of *extended cognition*. They leverage their environment to augment their capabilities, exhibiting a decentralized and distributed information-gathering system. Martians, on the other hand, symbolize immense processing power, often associated with *centralized control* and high computational capacity. In the realm of THR, where precision and efficiency are paramount, the choice between these two approaches holds significant implications for surgical outcomes.

Despite advocacy for the integration of robotic assistance in THR, its adoption remains limited, indicating persistent challenges and barriers within the orthopedic community. Surgeons must pay a heavy price for information with the extra workflow, bulk and time added to the operation, all of which overwhelm the surgeon's ability to process information. This necessitates a reassessment of surgical methods and the exploration of innovative approaches that strike a balance between human processing power and advanced technologies.

Central to addressing these challenges is the concept of decentralization. By shifting from centralized to decentralized and distributed information systems, surgeons can streamline decision-making processes and minimize cognitive overload. Embracing a modular approach to surgical tools, segregating tasks such as leg length and offset assessment from alignment evaluation, can enhance efficiency and precision. By strategically integrating sensors into instruments and the patient's body, surgeons can overcome the pitfalls of information saturation associated with robotic platforms, leading to more precise bone preparation and implant alignment.

Proposed decentralizing changes aim to address the limitations of current approaches and improve surgical outcomes:

1. "Electronic Signature Sizing of Bone Cavities" utilizes *analog electronics* to provide a quantitative assessment of the implant/bone contact conditions, reducing errors in sizing, implant fitting, and minimizing the risk of fractures or loosening.
2. Ultrasonic-assisted vibratory insertion tools reduce the force required during implant insertion by an order of magnitude, minimizing damage bone cells and vascularity and enhancing surgical control. This technology allows for precise and effortless alignment adjustments, improving the accuracy of implant placement.
3. Integration of screw sensors into patients' bodies provides real-time leg length and offset information to surgeons without cognitive overload. This distributed network of sensors streamlines decision-making and enhances surgeon's abilities during surgery.

In conclusion, the choice between emulating Spiders or Martians in THR surgery represents a fundamental shift in surgical philosophy. By decentralizing sensors from robots to surgical tools and patients' bodies, surgeons gain access to refined

information, enhancing sensitivity and reducing the risk of iatrogenic injuries. These advancements have the potential to significantly reduce THR failures by up to 80%, improving patient outcomes and surgical efficacy.

Figures

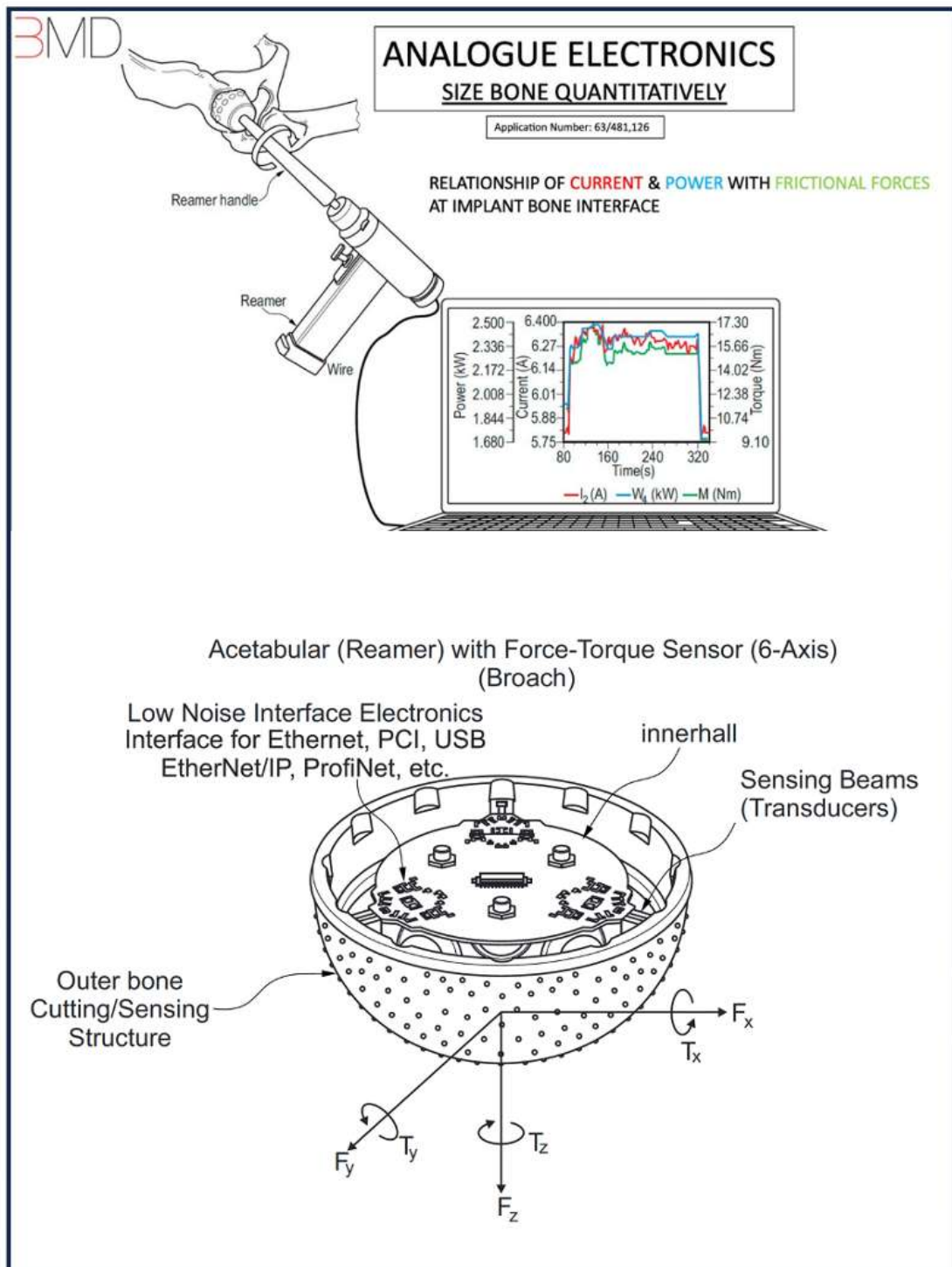


Figure1

TOTAL HIP REPLACEMENT
with
VIBRATORY INSERTION + LOCAL POSITIONING SYSTEM

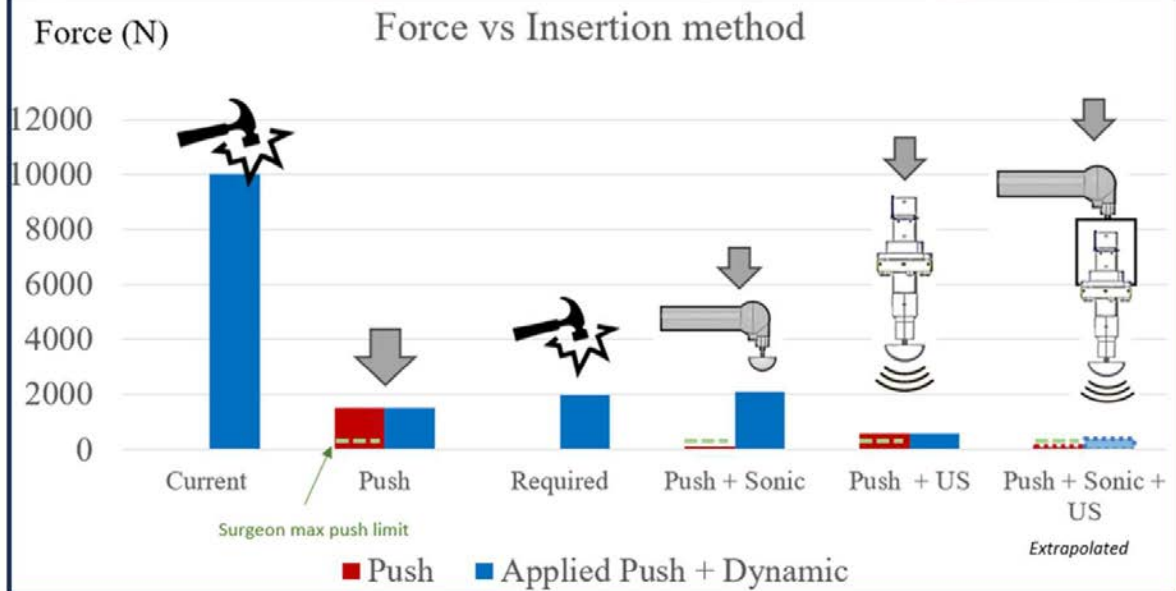


Figure 2

RELATED PATENTS

Vibratory Insertion of Orthopedic Implants

- US 11,234,840
- US 10,729,559
- US 10,610,379
- US 10,413,425
- US 10,245,160
- US 10,245,162
- US 10,172,722
- US 10,478,318
- US 9,168,154
- US 11,576,790
- EP 3089685

Vibratory Insertion + IMU Technology

- US 10,729,559
- US 10,478,318
- US 10,172,722

Vibratory Insertion with Ultrasonic Superimposition

- US 11, 234,840
- US 10,610,379

Screw-Sensors Local Positioning

- 16/819,092
- 16/945,908

Electronic Signature Sizing For Perfect Press Fit

- 63/481,126
- 63/528,591

[Figure 3](#)

Isolated Medial Patellofemoral Ligament Reconstruction Does Not Restore Normal Biomechanics of Patellofemoral Joint in Knees With Increased Femoral Anteversion: A Cadaveric Study

Jisu Park - SMG-SNU Boramae Medical Center - Seoul, Korea (Republic of)

Sung Jun Jang - Seoul National University College of Medicine Boramae Medical Center (SMG-SNU Boramae Medical Center) - Seoul, Korea (Republic of)

Hyunkwon Kim - SMG-SNU Boramae Medical Center - Seoul, Korea (Republic of)

Hyung Min Lee - Seoul National University Boramae Hospital - Seoul, Korea (Republic of)

Cho min soo - Seoul, Korea (Republic of)

Tae Woo Kim - Seoul National University College of Medicine, SMG-SNU Boramae Medical Center - Seoul, South Korea

Moon Jong Chang - SMG-SNU Boramae Medical Center - seoul, South Korea

Chong Bum Chang - Seoul National University College of Medicine - Seoul, South Korea

*Seung-Baik Kang - Boramae Medical Center/ Seoul National University College of Medicine - Seoul, South Korea

Background

Recurrent patellar dislocation is a challenging condition to treat because of varying contributing factors from patient to patient. Medial patellofemoral ligament (MPFL) reconstruction is the most widely used surgical procedure, but it can lead to unfavorable outcomes if not accompanied by correcting other risk factors. In case there is combined increased anteversion, femoral de-rotational osteotomy (FDO) is considered. Our study aimed to see (1) how changes in anteversion would affect normal patellofemoral (PF) joint contact pressure, (2) how PF pressure would change by releasing and reconstructing MPFL at normal femoral anteversion, and (3) if isolated MPFL reconstruction could restore normal PF joint contact pressure when femoral anteversion is increased.

Methods

Ten fresh-frozen human cadaveric knee specimens were mounted on a specially designed zig consisting of continuous passive motion (CPM) machine which bends knee from 0-degree to 90-degree. Three cycles of experiments were performed based on the state of the MPFL: MPFL in an intact state, after being released, and after being reconstructed. For each cycle, the anteversion was set as 0- (native), 10-, and 20-degree. At each point, contact pressures of medial and lateral facet of PF joint were measured.

Results

When MPFL was intact, lateral facet pressure increased and medial facet pressure decreased as femoral anteversion increased. At normal anteversion, lateral and medial facet pressure unchanged regardless of whether MPFL was released or reconstructed. At 10- and 20-degree increased anteversion, isolated MPFL reconstruction resulted in increased pressure of lateral facet and decreased pressure of medial facet compared to normal state (Fig. 1 and 2).

Conclusion

Lateral PF pressure increased and medial PF pressure decreased as femoral anteversion increased. At normal femoral anteversion, PF pressure did not change by releasing or reconstructing MPFL. Isolated MPFL reconstruction when femoral anteversion was increased was not enough to restore normal PF joint pressure.

Additional procedures like FDO are required to restore the normal PF joint pressure pattern.

Figures

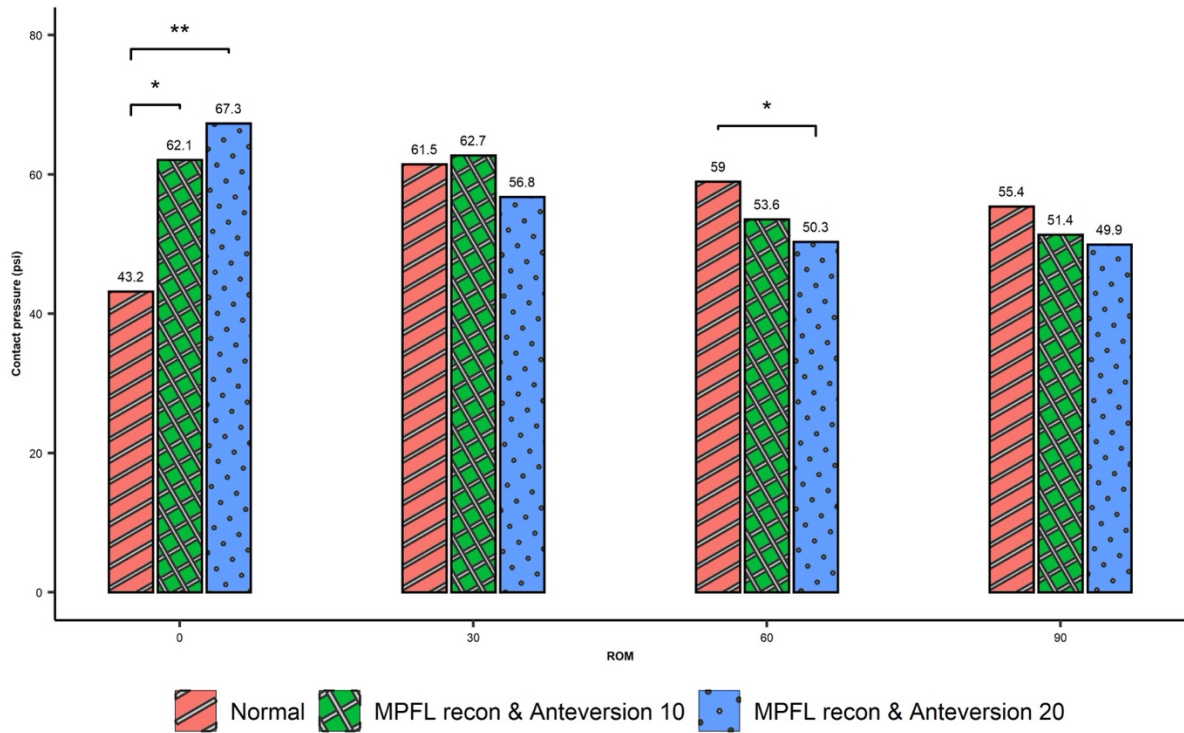


Figure 1

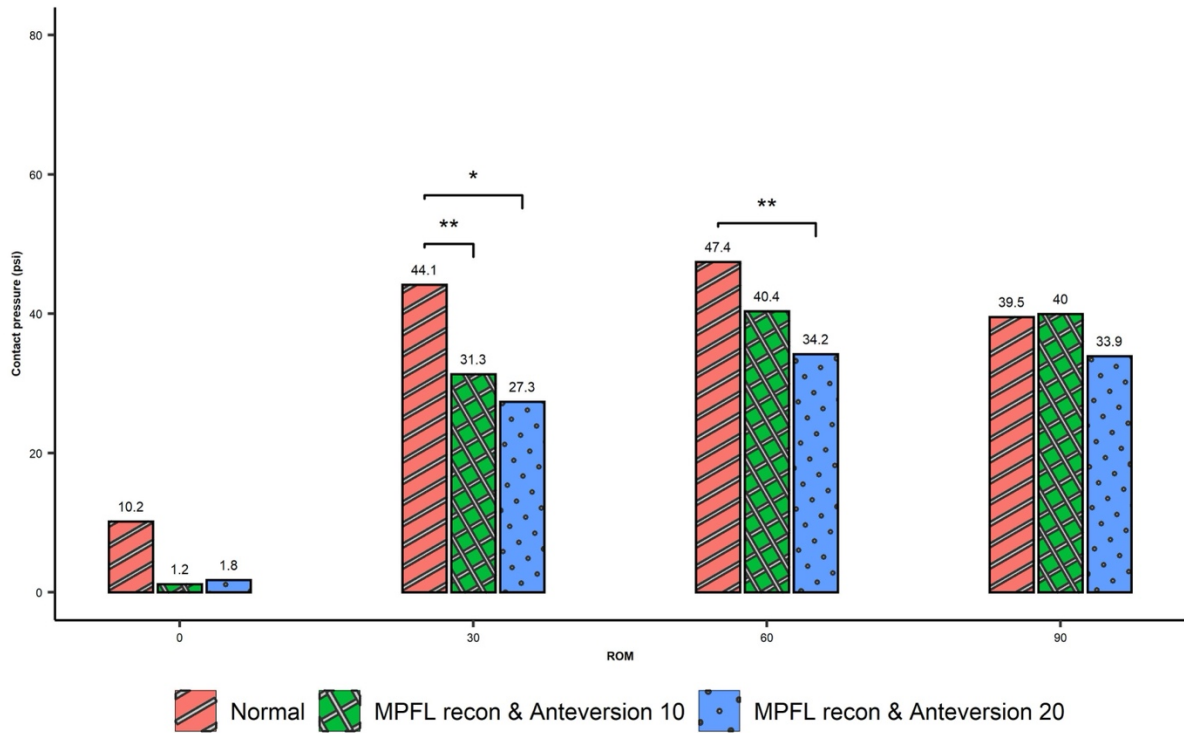


Figure 2

Surgical Draping for Shoulder Arthroscopy: Implications of Simplification

Srinath Kamineni - UK College of Medicine - Lexington, United States of America

*Anika Yadav - UK College of Medicine - Florence, United States of America

INTRODUCTION:

Over the last 30 years, healthcare spending per capita in the United States has risen at an alarming, unsustainable rate. The Centers for Medicare and Medicaid Services has found that healthcare spending has grown at twice the rate of GDP.

Several factors are responsible. We have chosen one small aspect, in this paper, for a safe but cost effective simplification: surgical draping for shoulder arthroscopy. We hypothesized that traditional shoulder arthroscopy draping is inefficient and costly, compared to a novel, simplified technique.

METHODS:

Two groups of orthopaedic shoulder arthroscopists were prospectively observed, group 1 (surgeons n=3 - patients n=20) using a traditional shoulder arthroscopy draping, and group 2 (surgeon n=1 - patients n=20) using a novel new simple draping technique. All patients were undergoing primary arthroscopic rotator cuff repairs. The operative parameters measured were time taken to prepare and drape the shoulder, and the number of drapes used; whilst post-operatively infection rates were measured at the two week follow-up consultation. Each drape used was costed from actual invoices from our purchased department. Statistical analysis was performed, to compare the two groups, with a t-test (significance <0.01).

RESULTS:

We found that utilizing our new draping method resulted in no nosocomial infections or wound related infections at the two week follow-up consultation, and was the same as the traditional draping group.

For the standard method (Group 1), the average time for draping was 580 seconds (25 seconds SD). The average time for the new draping method (Group 2) was 111 seconds (20 seconds SD). The new method reduced draping time by over 7 minutes, per case, of operating room time ($p < 0.0001$).

Group 1 used an average of 11 items during the preparation, including betadine, finger traps, drapes, with a total cost of

DISCUSSION AND CONCLUSION:

Based on population data from the Jain et. al. and the Colvin et. al. that estimated arthroscopic shoulder procedures in the year

2006, we were able to extrapolate the estimated number of procedures in 2012. This was the most recent US census data that we were able to access. There were an estimated 441,814 arthroscopic shoulder procedures performed in 2012.

By applying this new method to all arthroscopic shoulder procedures, we can save approximately \$327 million annually in North America alone. Our extrapolation data is almost certainly an under-

estimate for today's practice, but nevertheless, indicates a significant cost and time saving, without any added morbidity.

Figures

Standard Technique		Alternative Technique		Drape Supplier Costs	
Material	Cost	Material	Cost		
Finger trap	\$ -	1 Betadine layer	\$ 2.10	1010 Drape	\$ 1.58
2 plastic drapes	\$ 6.83	1 Extremity drape with fluid collection pouch	\$ 8.20	1015 Drape	\$ 5.25
1 Betadine layer	\$ 2.10	1 Betadine layer	\$ 2.10	U-Drape	\$ 8.25
1 down drape	\$ 6.50	Ioban	\$ 7.20	Down Drape	\$ 6.50
2 U drapes	\$ 16.50			Ioban	\$ 7.20
1 Impervious stockinette	\$ -			Extremity	\$ 8.20
1 Wrap	\$ -			Betadine (16 oz)	\$ 2.10
1 Extremity drape with fluid collection pouch	\$ 8.20				
Ioban	\$ 7.20				
Total Cost	\$ 47.33		\$ 19.60		

Table 3

[Figure1](#)



[Figure 2](#)

Treatment of Mild and Advanced Cases of Elbow OA With Arthroscopic Debridement and Intra-Articular Hyaluronic Acid Injections

Srinath Kamineni - UK College of Medicine - Lexington, United States of America

*Anika Yadav - UK College of Medicine - Florence, United States of America

Introduction: Intra-articular hyaluronic acid (HA) injections have demonstrated efficacy for osteoarthritis in joints such as the hip, knee, and ankle. As few published studies exist on the subject, HA injections for elbow OA have not been proven to be effective. This study investigates the efficacy of arthroscopic debridement with/without intra-articular hyaluronic acid (HA) injections with respect to pain relief, arc of movement, and functional improvement in 24 elbows with osteoarthritis.

Material & Methods: 24 elbows were treated for posttraumatic (n=11) or primary degenerative (n=13) osteoarthritis of the elbow by arthroscopic debridement. HA (Synvisc) injection protocol was either preoperative (n=5), postoperative (n=5), combined pre- and post-operative (n=5), or without HA injections (n=9). A clinical examination and Mayo elbow performance score was conducted at an average of 15 months (range 12-18 months) post-operation. The results were statistically analysed with the Mann-Whitney, Wilcoxon, and ANOVA tests.

Results: Intra-articular cartilage changes were observed to be mild fraying (n=5), significant fraying/fibrillation (n=6), and significant fibrillation with areas of bare bone (n=13). HA injections were associated with worse outcomes in patients with severe cartilage changes and exposed bone. A trend toward improved outcomes in patients without exposed bone was seen when treated with HA injection.

Discussion & Conclusions: These results support the use of HA in combination with elbow debridement in earlier stages of osteoarthritis with intact / frayed cartilage layer, but not in advanced cases with bone in communication with the synovial cavity. There is a symptomatic benefit in earlier stages (0-2) and a symptomatic detriment associated with HA in osteoarthritic joints with later stages (3-4), in the short term. Longer term studies are required to better understand the longevity of these results.

How Does Capsule Disorganization Correlate to the Range of Motion in Contracted Elbows?

Srinath Kamineni - UK College of Medicine - Lexington, United States of America

*Anika Yadav - UK College of Medicine - Florence, United States of America

INTRODUCTION: Stiffness is a common sequelae of trauma to the elbow joint. Previously, it has been demonstrated that contracted elbow capsules are thicker than cadaveric controls and lack normal collagen organization. Currently, there is little data on the degree of disorganization observed in these capsules. In this study, we use a semi-quantitative grading system, previously validated in tendinopathies, to grade this disorganization and correlate this with elbow motion loss.

METHODS: Twenty-three whole anterior elbow capsules were collected via open elbow release and were stored in 10% formalin. Measurements of each specimen's length, width and thickness were recorded. Each specimen was divided into four portions, two from the lateral side and two from the medial side. The medial and lateral portions were oriented at 90 degrees to each other, embedded in paraffin, sectioned and H&E stained. The tissue sections were graded using the modified Movin scale. Range of motion data was collected at three time points: pre-operative, immediately postoperatively, and at the final follow-up appointment.

RESULTS: Each specimen was assigned a Movin score equal to the average of the medial and lateral scores. There was no significant difference between the two scores based on laterality (12.9, 13.1, $p=0.69$). All capsules were scored as either abnormal or markedly abnormal. The average thickness (5.2cm) was comparable to previously published work (4.0cm, $p=0.47$) and was significantly greater than cadaveric controls (0.6cm, $p=0.01$). Average follow up was 6.9 months. Patients showed significantly increased extension at both postoperative measurements when compared to the preoperative measurement ($p=0.001$ and $p=0.00002$).

CONCLUSIONS: The thickness of our samples is comparable to previously published work and all of our samples are significantly thicker than cadaveric controls. Assessment of joint capsules from contracted elbows with a validated scoring system found that all samples scored either abnormal or markedly abnormal. Our data also suggests there is no difference in histological organization between the medial and lateral aspects of the capsule.

Figures

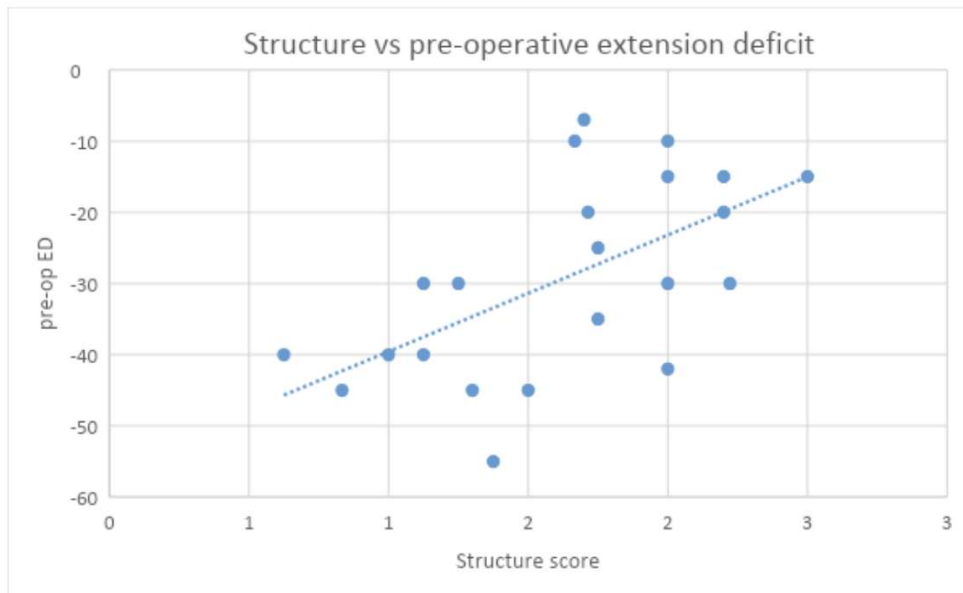


Figure ***. Pre-operative extension deficit (ED) vs. Movin sub-score of Structure. This graph demonstrates that the more organized a sample was in terms of structure, the larger extension deficit that the patient had. ($r=0.6$)

Figure 1

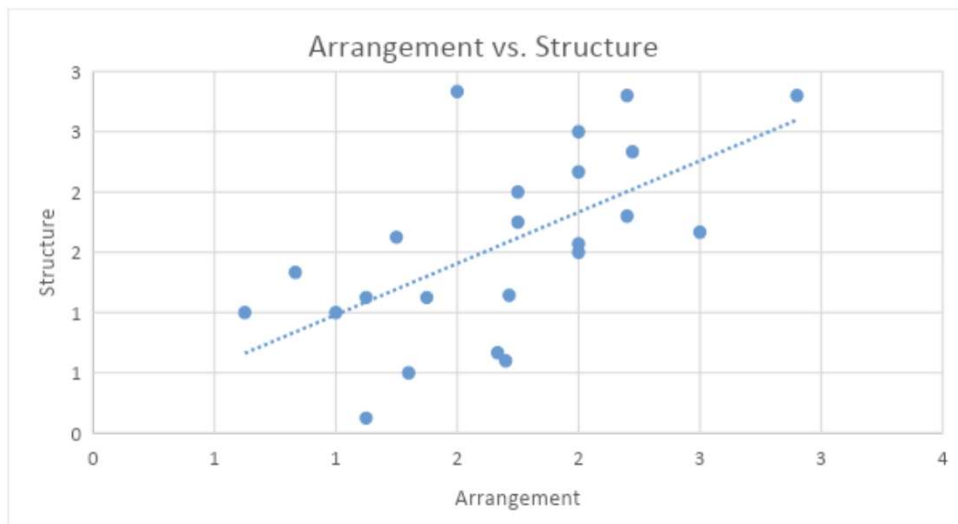


Figure ***. Average structure vs. average arrangement scores for each sample. As the structure becomes more abnormal (has a higher Movin score) the arrangement also becomes more abnormal. ($r=0.6$)

Figure 2

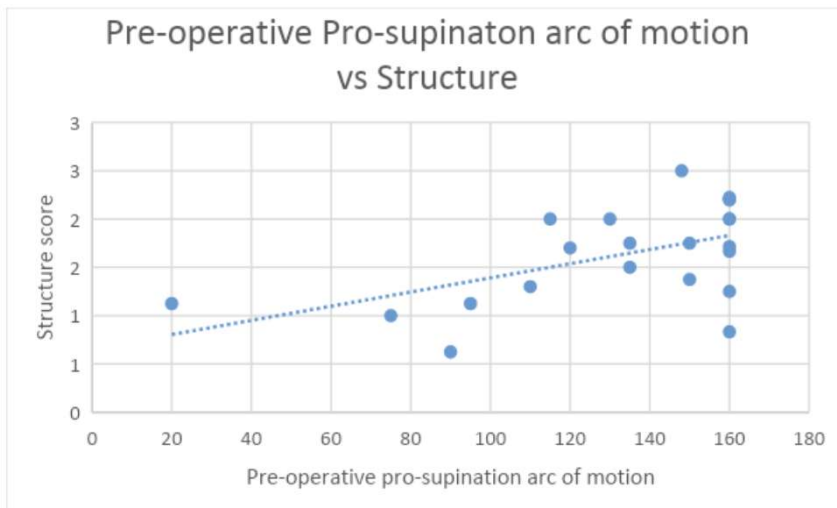


Figure *** Pro-supination arc of motion (AOM) vs. Structure score. As the structure score becomes more abnormal (has a higher Movin score), the more motion the patient has in the pro-supination arc.

[Figure 3](#)

Differential Collagen Isoform Expression in Post-Traumatic Stiff Elbow Anterior Capsules

Srinath Kamineni - UK College of Medicine - Lexington, United States of America

*Anika Yadav - UK College of Medicine - Florence, United States of America

Background: Posttraumatic elbow joint contracture produces functional limitations on activities of daily living. Very little is known about the structural properties of the elbow capsule, despite the critical role it plays in the pathogenesis of this condition. The type of collagen (notably I and III, II, V, VI, and X), and its organization in extracellular matrices, plays a critical role in determining the properties (structural strength / stiffness) of most biological structures.

Hypothesis: We hypothesized that several collagens are differentially expressed in response to elbow joint injury in addition to the better documented collagens I and III.

Methods: The anterior capsules of seven contracted elbows were removed at the time of elbow release surgery. These excised capsules were immediately preserved on dry ice and underwent basic histology and western blot analysis for collagen subtype analysis.

Results: Histology did not define a clear relationship between Collagen I and III in post-traumatic contracture elbow capsules. Western blot results indicated that type-I and III collagen levels, as well as lesser collagens II, V, VI and X, were detected at above and below normal levels, in a post-trauma time dependent relationship. The amalgamated data of the specimens showed a median maximum expression of all collagens at between 3 and 4 months from the traumatic event. Collagen I, VI and X demonstrated an up-regulation peak at 3-4 months and declined to normal levels at 18 months. Collagen II did not clearly demonstrate a pattern of expression. Collagen V demonstrated an up-regulation after trauma and sustained a level above normal at 18 months. Collagen III demonstrated an up-regulation peak between 3-4 months and then a down-regulation to sub-normal levels at 18 months.

Conclusions: Our data documents that there is a complex time dependent up- and down-regulation of collagens, from the time of injury to contracture formation, and this varies according to the collagen sub-type. There appeared to be three distinct patterns of time dependent collagen expression, with collagen II being unclear. This data may be useful for understanding elbow contracture at the molecular level, and a basis for future work into the complex interplay between collagen subtypes.

Figures

Figures

Fig 1.

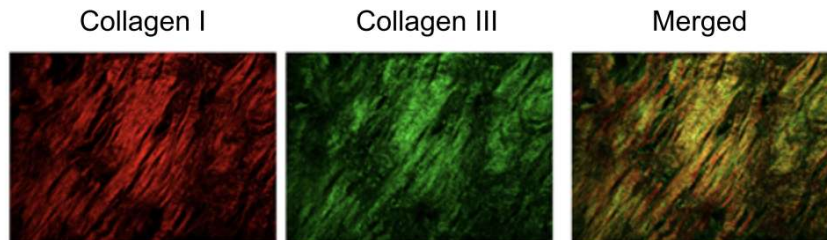


Fig 1. PSR staining under polarized microscope. Most thin fibers of collagens showed green polarization colors. Thick fibers of collagens showed yellow to red polarization colors.

Figure 1

Fig 2.

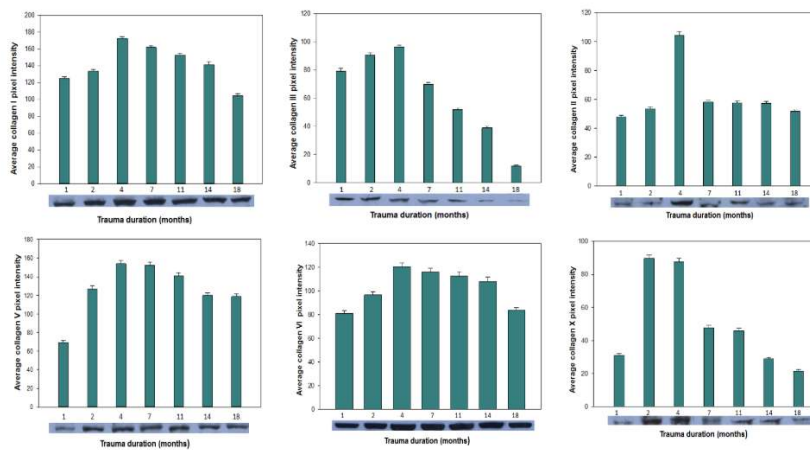


Fig 2. Semi-quantification of collagen subtypes using western blotting. The Y-axis corresponds to signal intensities (pixels): (a) collagen I (129 kDa), (b) collagen II (140 kDa), (c) collagen III (138 kDa), (d) collagen V (180 kDa), (e) collagen VI (140 kDa) and (f) collagen X (66 kDa).

Figure 2

Evaluating CPAK With Imageless Navigation Is Comparable to Computed Tomography

*Alex Orsi - Corin - Raynham, USA

Christopher Plaskos - Corin - Raynham, USA

Brett Fritsch - SORI - Sydney, Australia

INTRODUCTION:

Coronal plan alignment of the knee (CPAK) categorizes knee phenotypes, using joint line obliquity (JLO) and arithmetic hip-knee-ankle angle (aHKA). These are both determined using the medial proximal tibial angle (MPTA) and lateral distal femoral angle (LDFA). CPAK is traditionally measured using long leg radiographs, but recently other modalities have been used such as computed tomography (CT), and imageless navigation. The aim of this study is to understand how accurately imageless navigation with wear assumptions measures CPAK relative to CT.

METHODS:

Ninety-three TKAs performed using imageless navigation that also had preoperative CT were retrospectively reviewed (mean±SD age: 73±8, 57/93 (61%) female, preoperative coronal deformity 3.5±4.2° varus). MPTA and LDFA were measured from both the preoperative CT and the intraoperative imageless navigation landmark data. JLO was calculated as MPTA+LDFA, and aHKA was calculated as MPTA – LDFA.

Two articular cartilage wear assumption were applied to the imageless navigation data.

Assumption 1: Using these MPTA and LDFA thresholds:

- MPTA > 90: 2 mm lateral proximal tibia
- MPTA < 82.5: 2 mm medial proximal tibia
- LDFA > 90: 2 mm medial distal femur

Assumption 2: Using these preoperative coronal HKA thresholds (similar to previous studies):

- ≥3° Varus: 2 mm medial distal femur, 2 mm medial proximal tibia
- >3° Valgus: 2 mm lateral distal femur, 2 mm lateral proximal tibia

Mean absolute errors (MAE) were evaluated for MPTA, LDFA, JLO, and aHKA between CT and the imageless navigation with and without wear assumptions. CPAK distributions were also compared.

RESULTS:

The MPTA/LDFA based wear assumptions had the lowest MAE at 1.4 for MPTA, Figure 1. For LDFA both wear assumptions had MAE of 1.4, which was lower than that of the no wear assumption (1.6), Figure 1. Similarly, for JLO both wear assumptions had MAE of 2.2

CPAK percentages were most similar to CT measurements when using the MPTA/LDFA wear assumptions with the majority of patients in Type II, Figure 2.

CONCLUSIONS:

Imageless navigation can measure MPTA and LDFA with a mean error of <1.5° and <2° of CT when using generic wear assumptions based on MPTA/LDFA and HKA, respectively. Furthermore, MPTA/LDFA based wear assumptions may be applicable for determining CPAK from imageless navigation. These results indicate that imageless navigation effectively measures CPAK parameters, achieving comparable results to a CT-based approach.

Figures

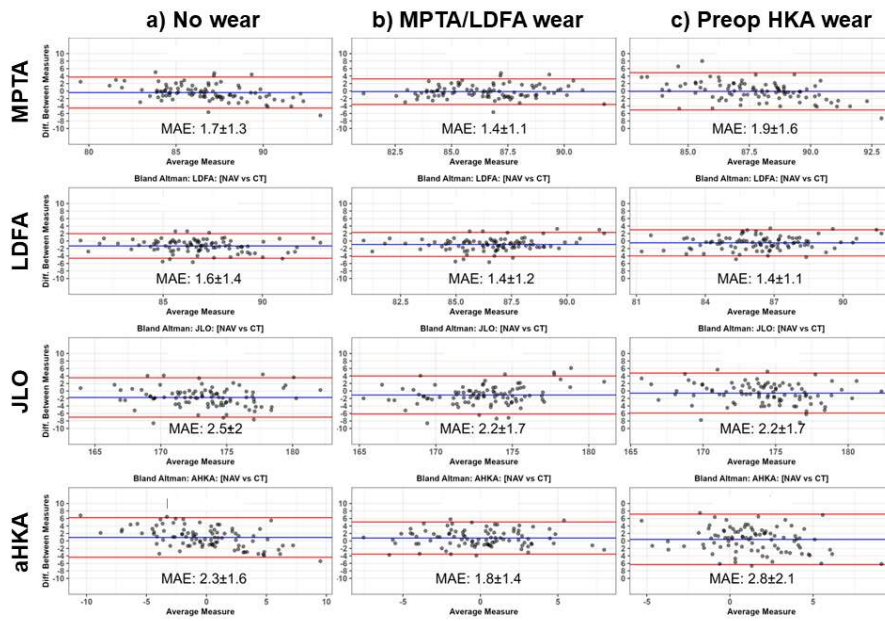


Figure 1: Bland-Altman plots with MAE comparing CT and imageless navigation. a) No wear correction applied, b) wear correction applied based on MPTA/LDFA, and c) wear corrections based on preoperative coronal HKA.

Figure 1

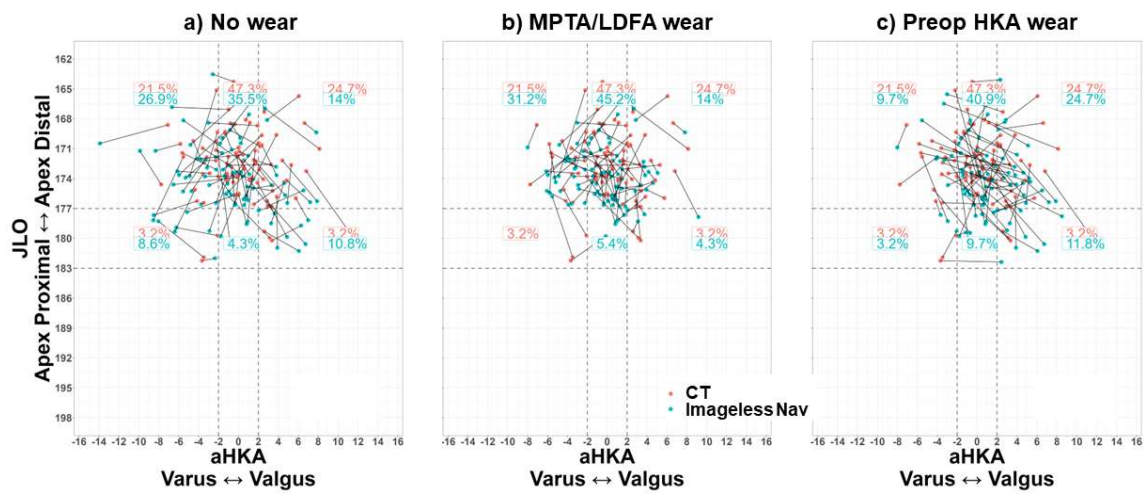


Figure 2: CPAK comparison between CT and imageless navigation. a) No wear correction applied, b) wear correction applied based on MPTA/LDFA, and c) wear corrections based on preoperative coronal HKA.

Figure 2

Natural History of the Sagittal Kinematics of the Hip-Spine

*Linden Bromwich - Corin Group - Sydney, Australia

Brett Biedermann - Keck School of Medicine of USC - Los Angeles, USA

Brandon Gittleman - Keck School of Medicine of USC - Los Angeles, USA

Gerard Smith - Corin - Sydney, Australia

Jim Pierrepoint - Corin - Cirencester, United Kingdom

Stephen McMahon - Monash University - Melbourne, Australia

Christopher Plaskos - Corin - Raynham, USA

Nathanael Heckmann - Keck School of Medicine of USC - Los Angeles, USA

Introduction:

Previous research into age-related degeneration of the hip-spine has identified increased risks of adverse spinopelvic mobility (SPM), in particular reduced lumbar flexion and hip flexion with increasing patient age [1].

This study aims to characterise the relationship between key SPM parameters for Total hip Arthroplasty (THA) and how they are influenced by patient age both pre- and post-operatively.

Methods:

A multicentre study was conducted involving patients undergoing THA from 9 Australian surgeons between May-2015 and July-2021 in the CorinRegistry. Patients received functional radiographs in standing and flex-seated pre-operatively, and at one year post THA. Anterior Pelvic Plane Tilt (APPTilt), Lumbar Lordosis (LL), Femur Flexion (FF) and the Pelvic Femoral Angle (PFA) were measured in each position (Figure 1). Changes in postural positions (?) and the Hip User Index (HUI) were calculated at each timepoint.

Patients were divided into four distinct Age Groups for inter-group statistical analysis of SPM parameters: “<60” (n=138), “60-70” (n=216), “70-80” (n=166), “>80” (n=35) years old.

A Spearman rank order correlation (ρ) analysis was performed to characterise the strength of the association between SPM parameters and patient age.

The Kruskal-Wallis rank sum test was used to compare the group distributions for each SPM parameter across the four patient age groups. Follow up post-hoc testing was performed using Dunn’s test to compare parameters between each of the age groups.

Results:

A total of 555 patients met the inclusion criteria with all required variables measurable. The mean age at surgery was 66 years old (range: 24 to 89), with 57% of the cohort females. The mean \pm SD follow-up time between surgery and post-op imaging was 13 \pm 2 months.

Strong ($0.5 < \rho \leq 0.8$) and Moderate ($0.3 < \rho \leq 0.5$) Spearman correlations were found for increasing patient age with pre-operative ?APPTilt ($\rho: 0.39$), Lumbar Flexion (?LL) ($\rho: -0.52$), HUI ($\rho: 0.50$) and post-operative Lumbar Flexion ($\rho: -0.45$), HUI ($\rho: 0.43$).

Figure 2 shows the distributions these parameters across each age-group.

Significant differences ($p < 0.05$) were found across the age groups in 13 of the 16 pre-op and 12 of the 14 post-op SPM parameters. A summary of these parameters, with the mean \pm [SD], the p-values (Kruskal-Wallis) and the significant intergroup associations highlighted (Dunn’s test) is shown in Figure 3.

Conclusion:

Multiple moderate to strong correlations were found between patient age and spinopelvic parameters, including decreasing lumbar flexion, increasing hip user

index, and increasing PFA/APP Tilt with increasing patient age. Each of these associations move the patient towards increased risk for adverse SPM [2, 3]. Inter age-group analysis showed significant variance between age groups in 25 out of 30 measurements in this study.

References:

1. Verhaegen, J.C.F., et al., Defining "Normal" Static and Dynamic Spinopelvic Characteristics: A Cross-Sectional Study. *JBJS Open Access*, 2022. 7(3).
2. Gu, Y.M., et al., The Effect of a Degenerative Spine and Adverse Pelvic Mobility on Prosthetic Impingement in Patients Undergoing Total Hip Arthroplasty. *Journal of Arthroplasty*, 2021. 36(7): p.2523-2529.
3. Vigdorchik, J.M., et al., Prevalence of risk factors for adverse spinopelvic mobility among patients undergoing total hip arthroplasty. *Journal of Arthroplasty*, 2021. 36(7): p.2371-2378.

Figures

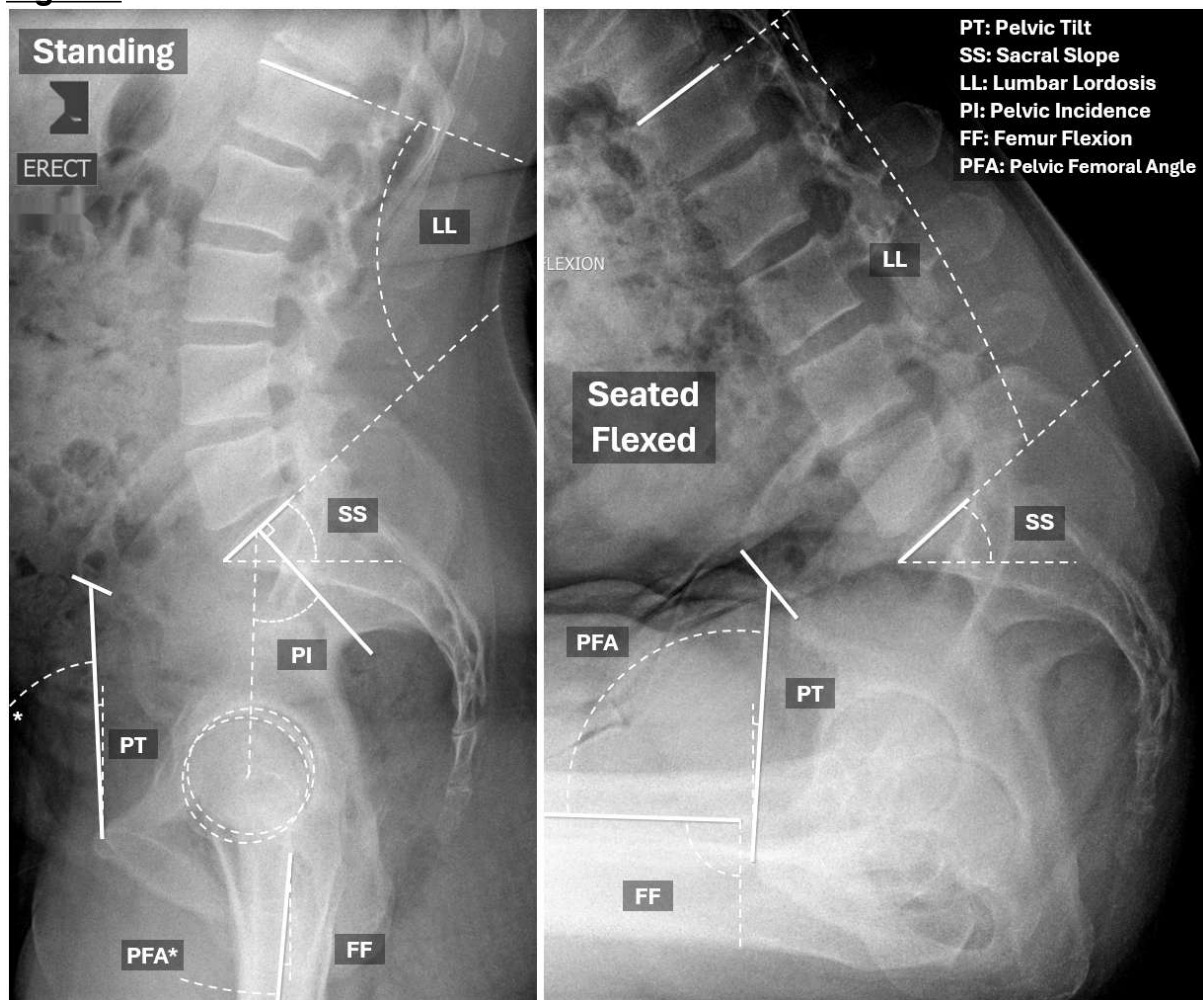


[Figure 1](#)

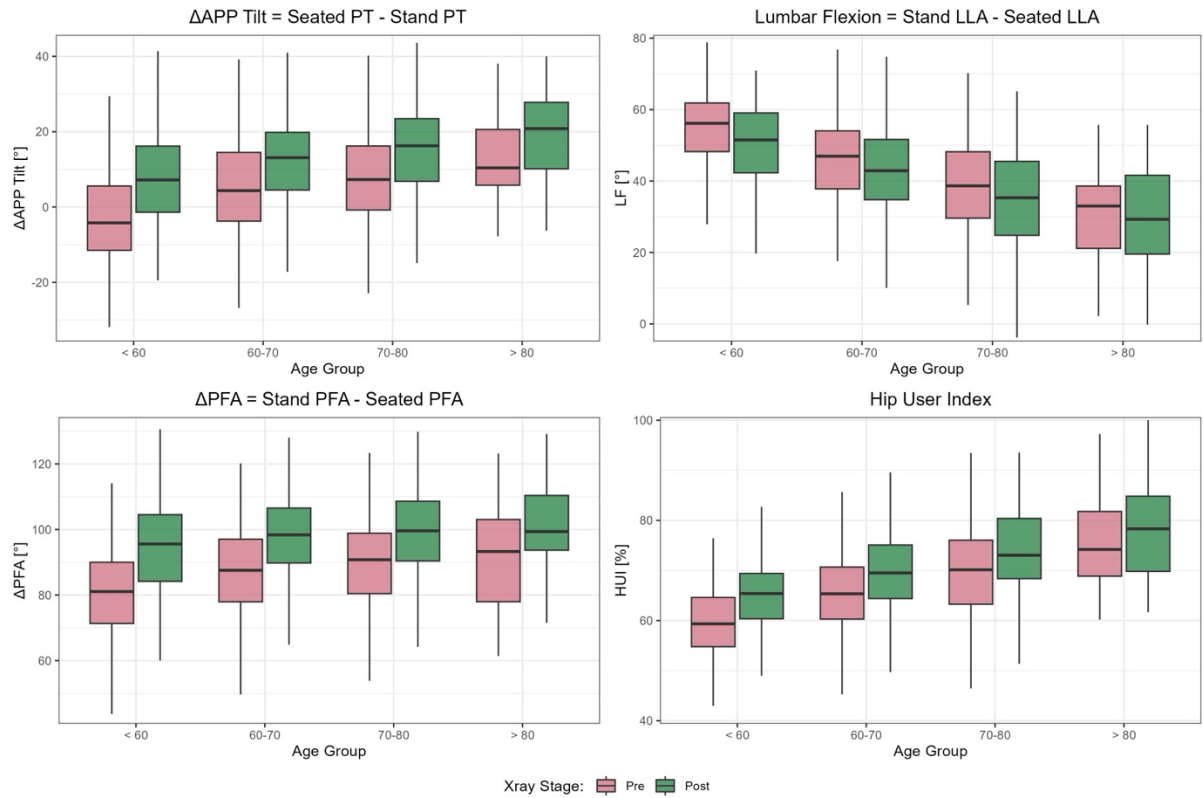


Figure 2

Measurement	Pre-Operative Measurements						Post-Operative Measurements					
	< 60	60-70	70-80	> 80	p value	*p < 0.05	< 60	60-70	70-80	> 80	p value	*p < 0.05
APP Tilt Supine	5 ± [6]	4 ± [6]	3 ± [6]	3 ± [6]	0.002	b,d	-	-	-	-	-	-
Pelvic Incidence	57 ± [12]	56 ± [11]	57 ± [11]	55 ± [10]	0.771		-	-	-	-	-	-
APP Tilt Stand	0 ± [6]	-2 ± [7]	-3 ± [7]	-5 ± [7]	<0.001	a,b,c,d,e	-2 ± [6]	-3 ± [7]	-5 ± [7]	-6 ± [7]	0.001	b,c,e
Lumbar Lordosis Stand	62 ± [12]	58 ± [13]	55 ± [12]	51 ± [17]	<0.001	a,b,c,d,e	61 ± [12]	57 ± [13]	55 ± [13]	50 ± [17]	<0.001	a,b,c,e
APP Tilt Seated	-4 ± [13]	3 ± [14]	5 ± [12]	9 ± [10]	<0.001	a,b,c,e	6 ± [13]	9 ± [12]	10 ± [13]	12 ± [13]	0.006	a,b,c
Lumbar Lordosis Seated	7 ± [13]	12 ± [13]	16 ± [15]	19 ± [13]	<0.001	a,b,c,d,e	11 ± [15]	14 ± [14]	19 ± [16]	21 ± [14]	<0.001	a,b,c,d,e
Femur Flexion Stand	7 ± [6]	9 ± [6]	10 ± [6]	11 ± [6]	<0.001	a,b,c,e	5 ± [5]	7 ± [5]	8 ± [5]	8 ± [5]	<0.001	a,b,c,d,e
Femur Flexion Seated	91 ± [6]	91 ± [6]	91 ± [6]	90 ± [5]	0.401		93 ± [6]	92 ± [6]	92 ± [6]	91 ± [7]	0.461	
Pelvic Femoral Angle Stand	172 ± [9]	173 ± [8]	174 ± [8]	174 ± [8]	0.850		176 ± [8]	177 ± [8]	177 ± [7]	178 ± [8]	0.734	
Pelvic Femoral Angle Seated	92 ± [13]	86 ± [14]	84 ± [12]	81 ± [11]	<0.001	a,b,c,e	81 ± [12]	79 ± [12]	78 ± [13]	77 ± [13]	0.039	a,b,c
Δ APP Tilt	-4 ± [13]	5 ± [14]	8 ± [13]	13 ± [11]	<0.001	a,b,c,d,e,f	8 ± [12]	12 ± [12]	15 ± [12]	18 ± [14]	<0.001	a,b,c,d,e
Lumbar Flexion	55 ± [11]	46 ± [13]	39 ± [13]	31 ± [12]	<0.001	a,b,c,d,e,f	50 ± [13]	43 ± [13]	35 ± [14]	30 ± [15]	<0.001	a,b,c,d,e
Sagittal Imbalance (PI-LL)	-5 ± [10]	-2 ± [11]	2 ± [11]	4 ± [17]	<0.001	a,b,c,d	-4 ± [10]	-1 ± [11]	2 ± [12]	5 ± [17]	<0.001	a,b,c,d
Δ Femur Flexion	84 ± [8]	82 ± [8]	81 ± [8]	79 ± [8]	0.001	a,b,c	87 ± [7]	85 ± [7]	84 ± [7]	83 ± [8]	0.001	a,b,c
Δ Pelvic Femoral Angle	80 ± [16]	87 ± [16]	89 ± [15]	92 ± [15]	<0.001	a,b,c	95 ± [14]	98 ± [13]	99 ± [14]	101 ± [13]	0.014	a,b,c
Hip User Index	59 ± [8]	65 ± [9]	70 ± [9]	75 ± [9]	<0.001	a,b,c,d,e,f	66 ± [8]	70 ± [8]	74 ± [9]	78 ± [10]	<0.001	a,b,c,d,e

Notes:

- Values vs Age Groups: p value calculated via Kruskal-Wallis Rank Sum Test
- *Dunn's Test multi pairwise comparisons. p-values expressed as P(|Z| ≥ |z|), reject Ho if p ≤ α, (α = 0.05)
- *Comparisons Pairs: a = <60 vs 60-70, b = <60 vs 70-80, c = <60 vs >80, d = 60-70 vs 70-80, e = 60-70 vs >80, f = 70-80 vs >80

Figure 3

Addressing Intraoperative Complications: Cementless Modular Revision Stem via Direct Anterior Approach for Iatrogenic via Falsa in Short Stem Arthroplasty

*Andrej Nowakowski - Kantonsspital Baselland - Bruderholz, Switzerland

Georg-Antonio Bernecker - Kantonsspital Baselland - Bottmingen, Switzerland

Introduction: Intraoperative complications are challenging, particularly when they disrupt standardised procedures. This case highlights the use of a cementless modular revision stem via the initial direct anterior approach as a remedy for a cortical perforation caused by a misplaced cement plug during a cemented short stem hemi-arthroplasty. The iatrogenic via falsa, characterized by femoral cortex weakening, prompts discourse on alternative solutions

Case presentation: An 89-year-old woman with a femoral neck fracture underwent an initial planned cemented hemi-arthroplasty via a direct anterior approach using an extension table and suffered an iatrogenic via falsa due to a misplaced cement plug resulting in femoral cortex weakening and procedural compromise. Treatment options including open reduction with internal plate fixation supplemented by cerclage to stabilize the short shaft or the additional use of a second approach using a revision stem were considered. These alternatives necessitate patient repositioning, further osteosynthesis material and a modified surgical approach. Upon consultation with the senior author (A.M.N.), a modular revision stem was chosen, preserving the anterior approach while mobilization was facilitated with the extension table.

Results: The patient received a cementless modular Revitan long stem 18/140 and Permedica head 50mm without much further release of the posterior capsule. Effectively covering the via falsa lesion with the stem through the direct anterior approach, ensuring stabilisation and minimising the risk of fracture. Removal of the cement plug via reaming of the femoral canal without cortical jamming was crucial. Mobilisation began on postoperative day 1 and the patient was allowed to bear full weight with the aid of crutches. Standardised follow-up radiographs at 4 days and 8 weeks postoperatively showed no evidence of subsidence or fissures. The patient regained pain-free independent ambulation with appropriate walking aid, without postoperative complications to date.

Conclusion: Regarding the intraoperative complication of iatrogenic via falsa during cemented hemi-arthroplasty using the direct anterior approach, the flexibility to modify the procedure is limited. However, conversion to a long revision modular stem offers a viable solution for patients who allow sufficient mobilisation with the extension table, obviating the need for additional surgical approaches and potentially time-consuming repositioning.

Multifunctional Mesoporous Polydopamine Near-Infrared Photothermal Controlled Release of Kartogenin for Cartilage Repair

*Zhenyu Luo - West China Hospital, Sichuan University - Chengdu, China

Zongke Zhou - Sichuan University - Chengdu, China

Improving chondrogenic differentiation while inhibiting hypertrophic differentiation of mesenchymal stem cells (MSCs) is of vital importance to effectively repairing cartilage injury. Accordingly, kartogenin (KGN) and antioxidants, which promote chondrogenic differentiation and inhibit hypertrophic differentiation, respectively, have shown great potential in promoting cartilage repair. However, KGN is poorly soluble in water, hindering efficient intracellular delivery. Near-infrared light (NIR)-responsive mesoporous polydopamine nanoparticles (MPDA) reportedly exert antioxidative effects by eliminating reactive oxygen species (ROS). In this study, we assessed whether KGN loaded in MPDA can accelerate cartilage injury repair in rats (See Figure 1). Specifically, a thermosensitive phase-change material (PCM, melting point 39°C) combined with KGN was loaded into MPDA as a gatekeeper (KGN@MPDA-PCM). The results showed that KGN@MPDA-PCM exhibited excellent photothermal properties under NIR irradiation, which induced PCM melting and consequent KGN release. In combination with antioxidative therapy, NIR-triggered KGN release enabled the nanocomposite to accelerate MSC chondrogenic differentiation and inhibit hypertrophic differentiation. Importantly, negligible damage to primary organs and satisfactory biocompatibility were observed in the rat model. RNA sequencing found that this MPDA-based platform promotes chondrogenic differentiation by promoting fibronectin-1 (Fn1) expression and activating the PI3K/Akt pathway. Collectively, these findings highlight the therapeutic potential of this MPDA-based platform for accelerating cartilage injury repair.

Figures

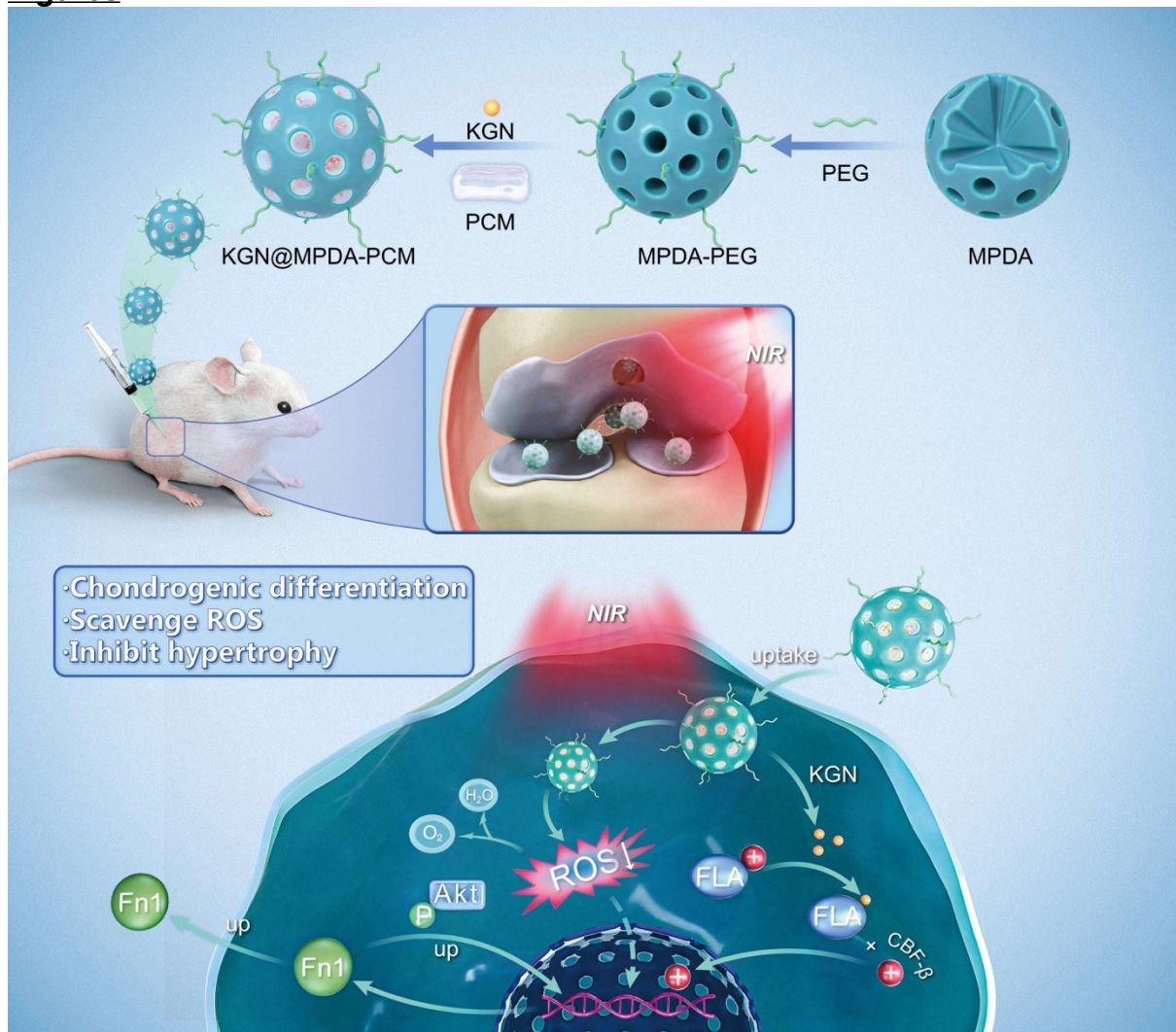


Figure 1

PCL Resection Increases Intraoperative Lateral and Medial Flexion Laxity During Total Knee Arthroplasty

Nathan Alloun - CHRU Lille - Lille, France

*Alex Orsi - Corin - Raynham, USA

Christopher Plaskos - Corin - Raynham, USA

Thomas Brosset - Alpillès Luberon Orthopédie - Cavaillon, France

Florian Boureau - Alpillès Luberon Orthopédie - Cavaillon, France

Sophie Putman - CHRU Lille - Lille, France

INTRODUCTION:

Understanding the impact of posterior cruciate ligament (PCL) resection on soft tissue laxity in total knee arthroplasty (TKA) is crucial for optimizing surgical outcomes. The PCL plays a crucial role in stabilizing the knee joint, and resecting this structure can significantly alter patient biomechanics, potentially compromising function due to postoperative instability. This study explores the relationship between PCL resection and soft tissue laxity throughout flexion using a robotically controlled ligament tensioner. Understanding this relationship is vital for enhancing TKA success rates and improving patient satisfaction and long-term functional outcomes.

METHODS:

55 robotic-assisted TKA were retrospectively reviewed from three surgeons (20 male, 35 female, mean age 70.3 ± 7.9 [54–86], BMI 29.7 ± 5.1 [19.6–43.5]). After an initial tibial resection, the robotic ligament tensioner was inserted to collect laxity data both before and after PCL resection for each case under a standardized load of 70–90N per side, Figure 1. Laxity is defined as the distance from the resected tibia to the femoral bone surface with the robotic ligament tensioner inserted and applying load. Gap opening was calculated as laxity before PCL resection minus laxity after PCL resection.

Medial and lateral coronal laxity were compared before and after PCL resection at 10° , 30° , 45° , 60° , 75° , and 90° flexion.

Gap opening was compared between preoperative coronal hip-knee-ankle (HKA) groups ($<2^\circ$ Valgus: 'Valgus' [n=12], and $\geq 2^\circ$ Valgus: 'Non-Valgus' [n=43]).

RESULTS:

Lateral laxity was significantly greater after PCL resection at 60° (12.7 ± 2 vs 11.5 ± 3 mm, $p < 0.05$), 75° (13.2 ± 2 vs 11.8 ± 3 mm, $p < 0.01$), and 90° (13.7 ± 2 vs 12.1 ± 3 mm, $p < 0.01$), Figure 2. Medial laxity was significantly greater after PCL resection at 90° (10.1 ± 2 vs 9 ± 2 mm, $p < 0.01$), Figure 2.

After PCL resection laxity in valgus patients increased significantly more laterally at 30° (1.2 ± 1 vs 0.3 ± 1 mm, $p < 0.05$), 45° (1.6 ± 1 vs 0.6 ± 1 mm, $p < 0.05$), and 60° (2.1 ± 2 vs 1 ± 1 mm, $p < 0.05$) compared to non-valgus, Figure 3. A similar, but non-significant trend was observed at 90° (2.7 ± 2 vs 1.5 ± 1 mm, $p = 0.09$).

CONCLUSIONS:

PCL resection increases flexion laxity laterally by up to 1.6 mm and medially by 1.1 mm, with coronal deformity playing an important role. The findings emphasize that surgeons should consider the interplay between PCL resection and coronal deformity when planning and executing TKA procedures. This relationship may be important when targeting patient specific soft tissue balance.

Figures



Figure 1: A robotic ligament tensioner collects laxity data before and after PCL resection.

Figure 1

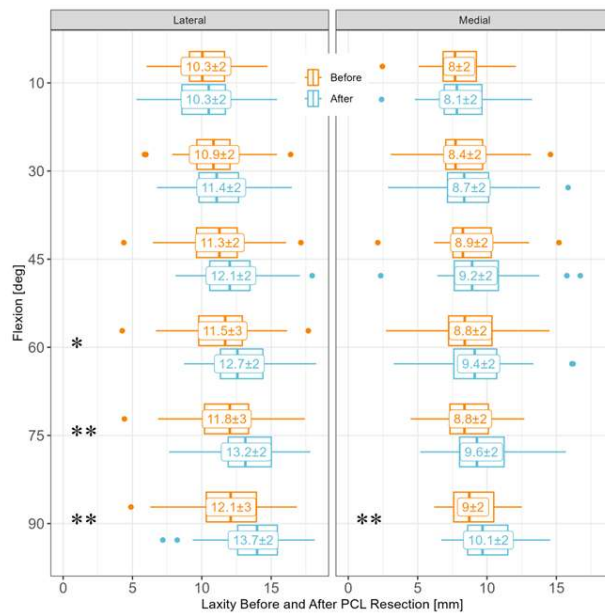


Figure 2: Ligament laxity comparison before and after PCL resection throughout the flexion range for both medial and lateral compartments. *, p<0.05, **, p<0.01, ***, p<0.001.

Figure 2

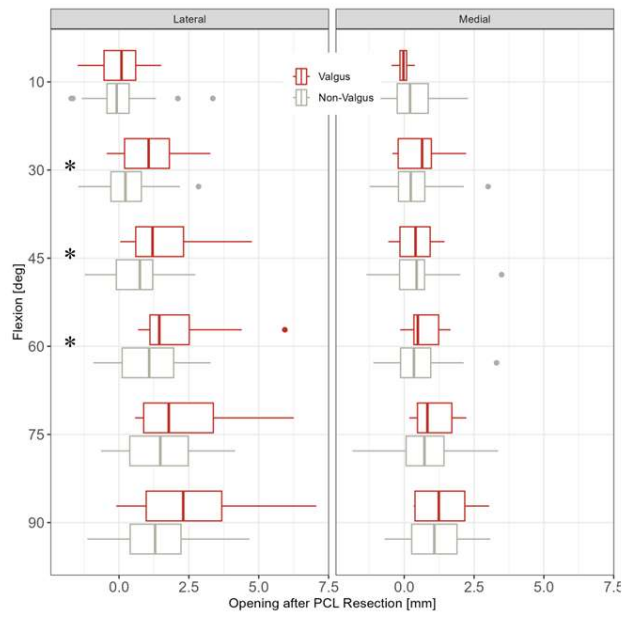


Figure 3: Preoperative coronal HKA comparison of gap opening due to PCL resection throughout the flexion range for both medial and lateral compartments. **: $p < 0.05$, ***: $p < 0.01$, ****: $p < 0.001$.

[Figure 3](#)

apollo™ - a Novel System for Pre-Resection Robotic Soft Tissue Assessment in Total Knee Arthroplasty - Accuracy and Efficiency of First Clinical Cases

*Alex Orsi - Corin - Raynham, USA

Christopher Plaskos - Corin - Raynham, USA

Andrew Lehman - Gundersen Health System - Viroqua, USA

Jeffrey Lawrence - Gundersen Health System - viroqua, USA

John Keggi - Orthopaedics New England - Middlebury, USA

INTRODUCTION:

Recent advancements in robotic assisted total knee arthroplasty (TKA) allow for pre-bone resection soft tissue assessment, as opposed to prior generations which required an initial tibial resection prior to soft tissue assessment. This is novel as it now facilitates a femur-first workflow along with the traditional tibia-first workflow. This study aims to compare predictive planning accuracy between pre- and post-bone resection assessments and analyzes the impact of femur- versus tibia-first workflows.

METHODS:

The first consecutive 82 cases performed by three surgeons using a novel pre-resection robotic ligament tensioner (Group A, Figure 1), were compared to the last 50 cases from each surgeon using a prior generation tensioner which required an initial tibial resection to fit the device into the joint and assess initial soft tissue laxity (Group B). Sub-analyses of Group A compared laxity accuracy between tibia-first (n=25) and femur-first (n=57) workflows, alongside a robotic surgical time analysis measuring the time from the start of the registration process to final trialing.

The robotic tensioner applied 70-90N per side and recorded joint laxity as the knee was moved from flexion to extension. A planning algorithm predicted final laxity using the recorded laxity data along with the planned component placement. Planned laxity was defined as the predicted distance between femoral and tibial components. Final laxity was measured using the robotic tensioner during a final soft tissue assessment during trialing. Mean absolute error (MAE) between planned and achieved laxity (medial and lateral) at 10°, 45°, and 90° was compared.

RESULTS:

Medial laxity MAE was similar between Group A and B at all flexion angles (MAE range for both: medial 0.9-1.1mm). Group A had similar lateral laxity MAE to B at 10° and 45° but was greater at 90° (1.4±1.1 vs 0.9±0.8 mm, p<0.01), Figure 2.

Within the pre-resection group (A), medial laxity MAE was greater in tibia-first workflows at 10° (1.6±1.2 vs 0.9±0.7 mm, p<0.05), 45° (1.4±1 vs 0.9±0.7 mm, p<0.05), and 90° (1.3±0.8 vs 0.9±0.6 mm, p<0.05), Figure 3. Lateral laxity MAE was greater in tibia-first workflows at 10° (1.9±1.2 vs 0.9±0.8 mm, p<0.01), Figure 3.

Femur-first had shorter robotic surgical time than tibia-first workflows (29±7 vs 34±10 min, p<0.05).

CONCLUSION:

Assessing soft tissues with a robotic tensioner before any bone resection resulted in accurate final gap balance. When using a pre-resection gap assessment workflow, performing an intermediate assessment after the tibial resection did not improve accuracy and took longer than a femur-first workflow. This study supports the integration of predictive planning using a novel pre-bone resection robotic soft tissue assessment tool and supports femur-first surgical protocols as a safe and effective means of optimizing soft tissue laxity.

Figures



Figure 1: A ligament tensing device which allows for soft tissue assessment prior to bone resections.

[Figure 1](#)

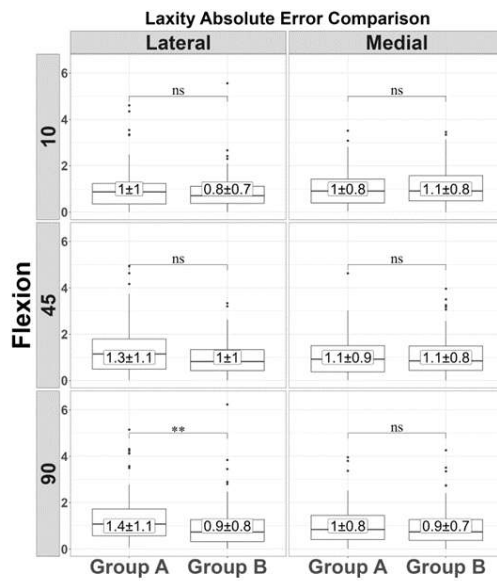


Figure 2: Boxplots comparing laxity absolute error between Group A and B throughout flexion for both medial and lateral compartments. Mean ± SD shown in bubbles. Statistically significant differences are indicated by **** = p ≤ 0.001; *** = p ≤ 0.01; ** = p ≤ 0.05; 'ns' = p > 0.05.

[Figure 2](#)

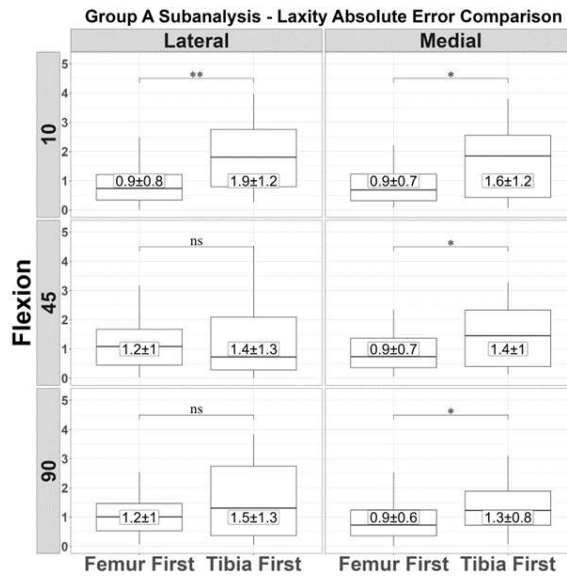


Figure 3: Sub analysis on Group A with boxplots comparing laxity absolute error between femur- and tibia-first workflows throughout flexion for both medial and lateral compartments. Mean ± SD shown in bubbles. Statistically significant differences are indicated by '**' = $p \leq 0.001$; '***' = $p \leq 0.01$; '**' = $p \leq 0.05$, 'ns' = $p > 0.05$.**

[Figure 3](#)

Variability and Similarity of Joint Balance Across CPAK Phenotypes

*Christopher Plaskos - Corin - Raynham, USA

Edgar Wakelin - OMNI Life Sciences - Raynham, USA

Gwo-Chin Lee - University of Pennsylvania - Philadelphia, USA

Introduction: The Coronal Plane Alignment of the Knee (CPAK) classification has been proposed to guide alignment strategy in total knee arthroplasty (TKA). However, the classification does not consider the variability of the soft tissue envelope unique to each knee. The purpose of this study is to 1) characterize the extension balance across each CPAK phenotype; 2) determine the proportion of overlap in ligament laxity and balance across CPAK phenotypes; and 3) evaluate the effects of a neutral and varus coronal tibial cut on the resulting knee balance across each CPAK phenotype.

Methods: Using the anatomic and ligament data acquired from 4515 robotic TKAs, the distraction of the medial and lateral joint spaces were simulated and classified across CPAK phenotypes I-VI. The distribution of joint balance for each CPAK phenotype was compared to determine the similarities across the various CPAK classes. Finally, the effects of a neutral and a varus tibial cut of 4 degrees were simulated to evaluate the resulting joint balance for each phenotype.

Results: When evaluating the joint balance of the native knee across the CPAK classification, there was significant but variable overlap between CPAK class I, II, IV and V (range 23-74%), Figure 1a. Dissimilarity was greatest between CPAK I and VI (8%), I and III (17%), and IV and VI (18%). Similarity was greatest between II and IV (74%), III and V (57%), and II and V (56)%. Neutrally aligned knees (Class II and V) were more similar to varus than valgus phenotypes. A neutral tibial resection in the coronal plane increased the joint balance similarities across all CPAK phenotypes with the concordance being greatest across knees having either all apex distal (CPAK I, II, III) or neutral (CPAK IV, V, VI) joint line orientations (range 82-87% for both), Figure 1b. A varus tibial cut of 4 degrees resulted in reduced imbalance in apex distal and variable balance change in neutral joint line knees, Figure 1c. Overlap of balance distribution in the neutral and varus cut group ranged between 47 – 87% between the different CPAK phenotypes.

Conclusions: The joint is complex and while the CPAK classification can help guide surgical decision making in TKA, it is not complete without incorporating the soft tissue envelope unique to each knee joint.

Figures

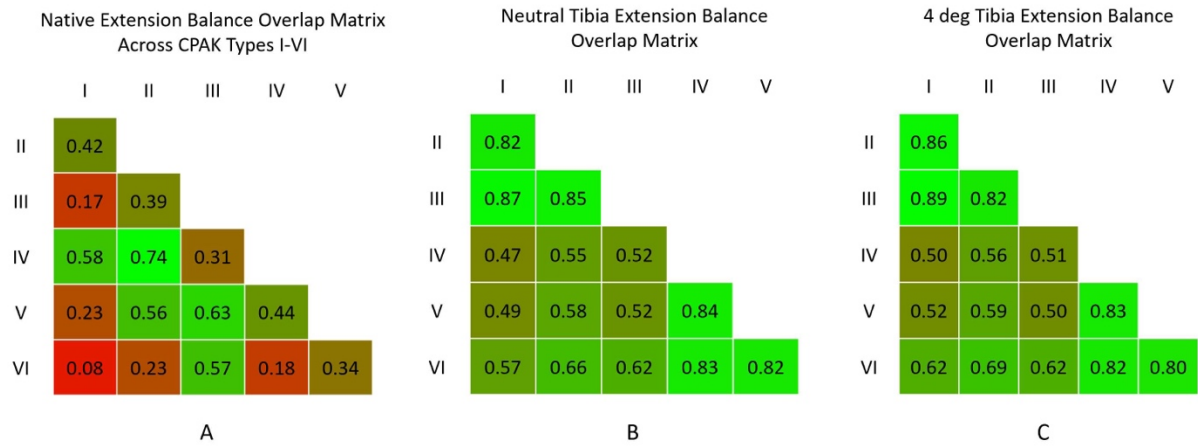


Figure 1

[Figure 1](#)

Detection of Prosthetic Joint Infection With an Implantable Sensor via Plain Radiography

*John DesJardins - Clemson University - Clemson, USA

Rong Wang - Clemson University - Clemson, USA

Caleb Behrend - OrthoArizona - Glendale, USA

Jeffery Anker - Clemson University - Clemson, USA

Introduction

A common complication of hip surgeries is post-surgery infections. These may be caused by bacterial contamination during surgery or subsequent adhesion of microorganisms onto the implant surface. If detected early, infections can be treated promptly with antibiotics and surgical debridement. Delayed diagnosis would lead to reduced function, increased morbidity and may require more complex surgeries. Therefore, early detection of infections is important for successful management of hip infections. Synovial fluid contains multiple infection biomarkers such as pH, lactate concentration, C-reactive protein, α -defensin etc. To detect these biomarkers, the joint is aspirated to collect synovial fluid. However, the procedure is painful, and is impractical for routine screening or serial monitoring during treatment. In this work, we present the development and testing of an X-ray based sensor that provides painless, non-invasive and inexpensive detection.

Materials and Methods

A hydrogel was developed that swells at high pH due to increased electrostatic repulsions between chains and osmotic pressure; while carboxylic acid groups are protonated at low pH and the smaller repulsions make hydrogel shrink. Figure 1 shows the calibration curve a sigmoidal shape with a dynamic range of pH 4-7 and pKa of 5.23, and high reversibility (exponential curve fit) between pH 6.5 and 7.5, which is the physiological pH range of hip infection.

An initial sensor design had a Ta bead glued at the end of thin hydrogel cylinder that attaches to the neck of a human hip prosthesis. The optimized sensor pins the hydrogel in the casing by the metal wire and prevents sensor migration over time. Instead of Ta bead, a metal wire crosses the embedded barb and equidistant reference positions are added. Therefore, both the stability and reproducibility are improved significantly. Figure 2 shows the schematic of pH sensing mechanism in casing with indicator in normal & infection states. A CAD drawing of sensor is shown attached to a hip prosthesis that is superimposed with a sheep femur radiograph from previous study and a final picture shows a hip prosthesis and sensor attached on the neck.

Discussion and Conclusion

Preliminary results show the feasibility of measuring local pH in synovial fluid at hip implants. It enables non-invasive early detection and monitoring of hip infection using plain radiography (X-ray imaging). Optimized sensor design can significantly improve the sensor reproducibility and stability.

Future Work will use the optimized sensors for animal studies and explore other infection biomarkers such as α -defensin and glucose.

Figures

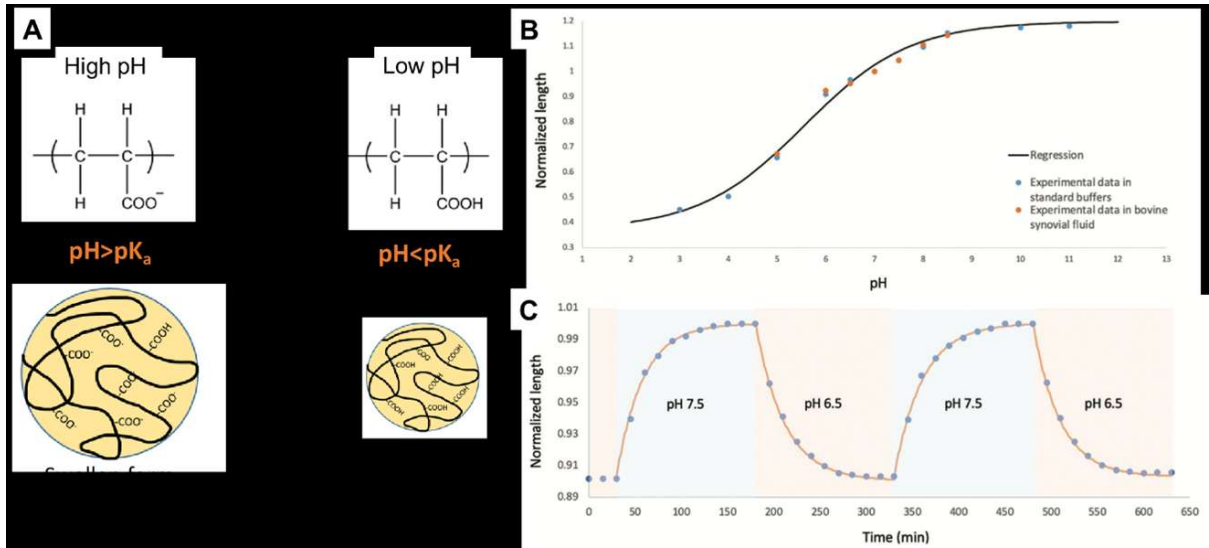


Figure 1

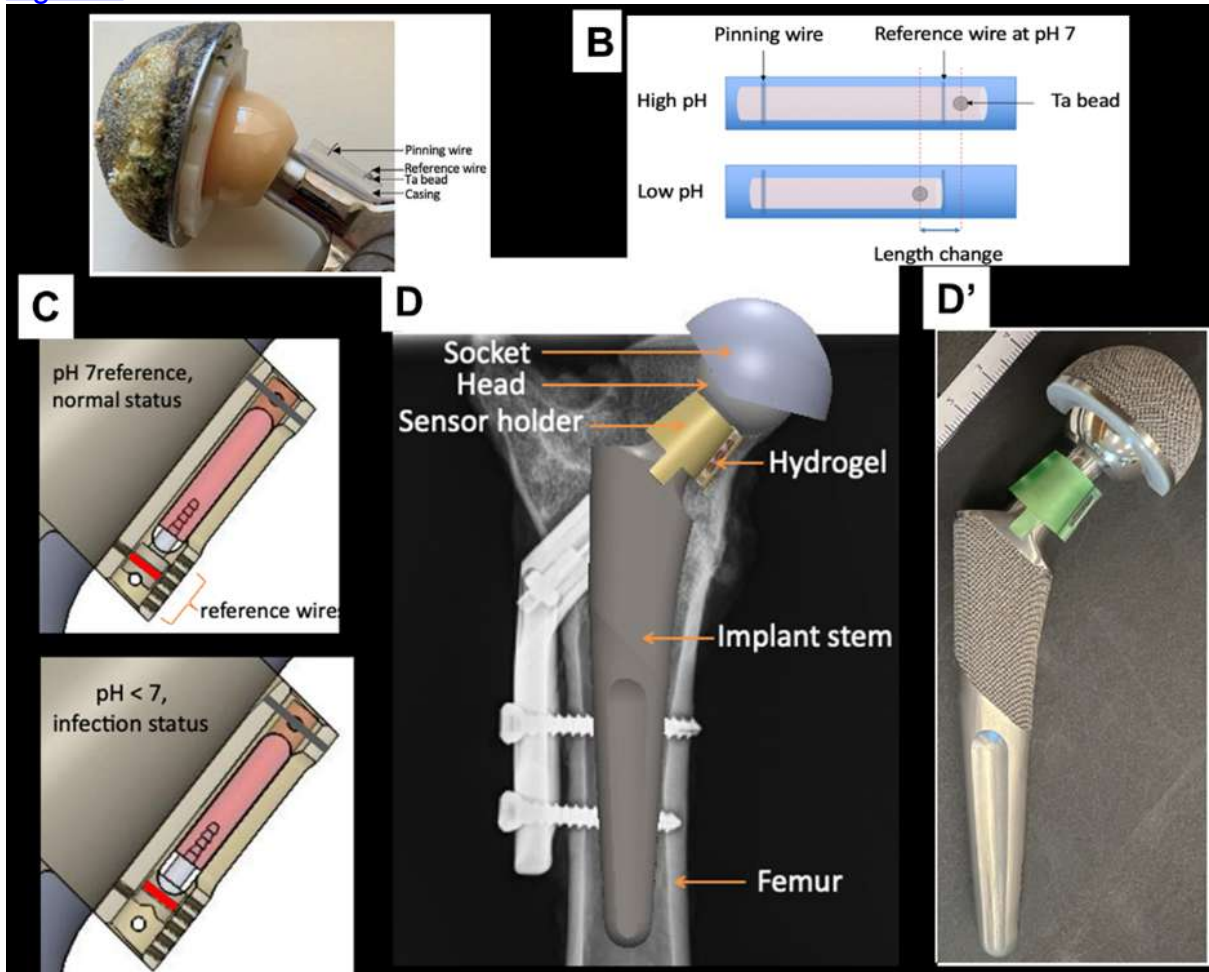


Figure 2

Social Determinants of Health Influence Clinical Outcomes of Patients Undergoing Total Ankle Arthroplasty: A Systematic Review

*James Butler - NYU Langone Health - New York, United States of America

Megan Calton - Royal College of Surgeons in Ireland - Dublin, Ireland

Amit Manjunath - NYU Langone Health - New York, USA

Amanda Mener - Albany Medical Center - Albany, USA

Andrew Rosenbaum - Albany Medical Center - Albany, USA

Michael Mulligan - Albany Medical Center - Albany, USA

Alan Samsonov - NYU Langone Health - New York, USA

John Kennedy - NYU Langone Health - New York, USA

Raymond Walls - NYU Langone Health - New York, United States of America

Introduction: Social determinants of health (SDOH) encompass environmental, institutional, and intrinsic conditions that can influence an individual's access to and utilization of healthcare over their lifespan. While SDOH effects are linked to disparities in patient-reported outcomes post hip and knee arthroplasty, their impact on total ankle arthroplasty (TAA) remains unclear. This study sought to examine how SDOH factors affect access to appropriate orthopedic treatment and their repercussions on patient-reported outcomes following TAA.

Methods: In January 2024, a systematic review of the PubMed, Embase and the Cochrane Library was conducted to identify studies reporting at least 1 SDOH and its effect on access to health care, clinical outcomes, or patient-reported outcomes following TAA.

Results: Fifty-eight studies, involving 212,944 patients, were analyzed. The INBONE system emerged as the most utilized Total Ankle Arthroplasty (TAA) system. Factors contributing to healthcare access delays included female gender, advanced age, worker's compensation claims, comorbidities, tobacco use, federally subsidized insurance, lower education, racial/ethnic minority status, low-income residence, low-volume surgery regions, unemployment, and preoperative narcotic use. Black patients experienced significantly worse postoperative clinical and patient-reported outcomes, along with heightened pain following TAA. Lower education level independently predicted poor surgical and patient-reported outcomes, increased pain, and lower patient satisfaction. Moreover, patients with federally subsidized insurance demonstrated significantly worse postoperative clinical and patient-reported outcomes.

Results: The impediments created by SDOH lead to worse clinical and patient-reported outcomes following TAA including increased risk of postoperative complications, TAA failure, higher rates of revision surgery, and decreased ability to return to work. Orthopedic surgeons, policy makers, and insurers should be aware of the aforementioned SDOH as markers for characteristics that may predispose to inferior outcomes following RCR.

No Superiority of Transfibular Approach Compared to Direct Anterior Approach for Total Ankle Arthroplasty: A Systematic Review and Meta-Analysis

*[James Butler](#) - NYU Langone Health - New York, United States of America

Ravneet Dhillon - Royal College of Surgeons in Ireland - Dublin, Ireland

Akram Habibi - NYU Langone Orthopedic Hospital - New York, United States of America

Andrew Rosenbaum - Albany Medical Center - Albany, USA

Michael Mulligan - Albany Medical Center - Albany, USA

Raymond Walls - NYU Langone Health - New York, United States of America

John Kennedy - NYU Langone Health - New York, USA

Introduction: The purpose of this study was to compare outcomes following transfibular approach and direct anterior approach for total ankle arthroplasty (TAA).

Methods: During January 2024, the PubMed, Embase and Cochrane library databases were systematically reviewed to identify clinical studies comparing outcomes between transfibular approach and direct anterior approach for TAA for the management of ankle osteoarthritis. Data regarding study characteristics, patient demographics, subjective clinical outcomes, radiological outcomes, complications, and failure rates were extracted and analyzed. In addition, the level of evidence and quality of evidence for each individual study was also assessed. Six studies were included in this review.

Results: There were 224 patients in the transfibular cohort and 273 patients in the direct anterior approach cohort. The mean follow-up time was 4.5 ± 2.1 years. There was no statistically significant difference in AOFAS scores, FAOS scores, talar tilt, prosthesis loosening, failures, complications and secondary surgical procedure rates between the 2 cohorts ($p > 0.05$ for all variables).

Discussion: This systematic review demonstrated no difference in outcomes between transfibular approach and direct anterior approach for TAA for the management of ankle osteoarthritis. However, this study is limited by the small patient cohorts, low number of studies and short-term follow-up, thus further studies with longer follow-up are warranted.

Relationship Between Mental Health Disorders and Outcomes Following Total Ankle Arthroplasty: A Systematic Review

*James Butler - NYU Langone Health - New York, United States of America

John Kennedy - NYU Langone Health - New York, USA

Alan Samsonov - NYU Langone Health - New York, USA

Raymond Walls - NYU Langone Health - New York, United States of America

Davis Hedbany - SUNY Upstate - Syracuse, USA

David Bloom - NYU Orthopedic Hospital - New York, USA

Andrew Rosenbaum - Albany Medical Center - Albany, USA

Michael Mulligan - Albany Medical Center - Albany, USA

Introduction: The purpose of this study was to evaluate the relationship between mental health disorders and outcomes following total ankle arthroplasty (TAA).

Methods: We searched PubMed, Cochrane, and Google Scholar from their inception till April 19, 2022. Studies exploring the association of mental health disorders and readmission risk following TJA were selected. The outcomes were divided into 30-day readmission, 90-day readmission, and readmission after 90 days. We also performed subgroup analyses based on the type of arthroplasty: total hip arthroplasty (THA) and total knee arthroplasty (TKA). A total of 12 studies were selected, of which 11 were included in quantitative analysis. A total of 1,345,893 patients were evaluated, of which 73,953 patients suffered from mental health disorders.

Results: In total, 6 studies (1124 patients) were included. Four studies found that pre-operative mental health disorders were associated with inferior clinical outcomes following TAA. Two studies reported no association between pre-operative mental health disorders. Pre-operative anxiety and depression were identified as significant risk factors for inferior clinical outcomes. Pre-operative mental health disorders were not associated with postoperative complications such as infection.

Discussion: This systematic review demonstrated that pre-operative mental health disorders were associated with inferior clinical outcomes following TAA. The evidence presented highlights the importance of addressing mental health considerations in the pre-operative assessment and management of patients undergoing TAA.

The Role of Patient Specific Instrumentation for Total Ankle Arthroplasty: A Systematic Review

*James Butler - NYU Langone Health - New York, United States of America

Kishore Konar - University of Buckingham - Buckingham, United Kingdom

John Kennedy - NYU Langone Health - New York, USA

Introduction: The purpose of this systematic review was to evaluate outcomes following the use of patient specific instrumentation (PSI) for total ankle arthroplasty (TAA) for the management of ankle osteoarthritis.

Methods: During January 2024, the PubMed, Embase and Cochrane library databases were systematically reviewed to identify clinical studies assessing outcomes in patients who underwent patient specific instrumentation for TAA implant. Data regarding surgical characteristics, subjective clinical outcomes, radiographic outcomes, failure rates and complications were extracted and analysed.

Results: Thirteen studies were included in this review. Overall, PSI resulted in satisfactory implant alignment with a low complication and failure rate. Due to significant heterogeneity between the included studies, robust meta-analytic models could not be run with regards to functional and radiographic outcomes between patients who underwent PSI and standard referencing TAA. There was no statistically significant difference in complication rates nor failure rates between the PSI and standard referencing cohorts.

Discussion: This systematic review and meta-analysis found satisfactory outcomes following PSI based TAA implants. However, due to the marked heterogeneity and under-reporting of data between the included studies, it was not feasible to robustly compare outcomes between the PSI and standard referencing cohorts, which limits the generation of any meaningful conclusions. Thus, further higher quality comparative studies are necessary to elucidate the superiority or otherwise of PSI based implants in comparison to standard referencing based TAA implants.

Rate of Improvement Following Reverse Shoulder Arthroplasty: A Comparison of Primary and Revision Reverse Shoulder Arthroplasty

*Garrett Jackson - Chicago, United States of America

Ali Mohamed - FAU - Boca raton, USA

Devin John - HCA JFK/University of Miami Orthopaedic Surgery Residency Program - Atlantis, USA

Aghdas Movassaghi - Michigan State University - East Lansing, USA

Vani Sabesan - Cleveland Clinic Florida - Weston, USA

Howard Routman - Atlantis Orthopedics - Atlantis, USA

Matthew McKinley - Florida Atlantic University, Charles E. Schmidt College of Medicine - Boca Raton, USA

Introduction: Incidence and revision rates for Reverse Shoulder Arthroplasty walk hand in hand, as expected. Despite this, little is known about postoperative recovery rates following revision RSA (rRSA). This study aimed to determine the rate of improvement for patients who underwent revision RSA (rRSA) compared to patients who underwent primary RSA (pRSA).

Methods: A retrospective review of 476 patients who underwent RSA by a single fellowship-trained shoulder surgeon was conducted. In this cohort, 386 patients underwent primary RSA (pRSA) and 90 patients underwent revision RSA (rRSA). Demographics, range of motion (ROM), and outcome scores including the Simple Shoulder Test (SST), Constant Murray Score (CMS), University of California at Los Angeles Shoulder Score (UCLA), Shoulder Pain and Disability Index (SPADI), Shoulder Function score, Shoulder Arthroplasty Smart score (SAS) and American Shoulder and Elbow Surgeon scores (ASES) following rRSA were collected preoperatively and postoperatively at 6 weeks, 3 months, 6 months, 12 months, and 24-months. The rate of improvement in each outcome measure was quantified and compared between pRSA and rRSA.

Results: Patients in the pRSA cohort were significantly older ($p < 0.001$) and had a greater number of females ($p < 0.011$) compared to the rRSA cohort. Patients who underwent pRSA had significantly greater postoperative SST ($p=0.0022$), UCLA ($p=0.0099$), ASES ($p=0.0077$), SPADI ($p=0.0140$), SAS ($p=0.0202$), and shoulder function scores ($p=0.0097$), and abduction ($p=0.0073$), forward elevation ($p=0.0068$), and external rotation ($p=0.0357$) compared to the rRSA group. When improvement was evaluated over time, the pRSA cohort had significantly greater improvements compared to the rRSA cohort as early as 3 months for the SPADI scores (0.0302), 6 months for forward elevation ($p=0.0358$), 12 months for SST ($p=0.0331$), CMS ($p=0.0354$), and abduction ($p=0.0108$), and 24 months for ASES ($p=0.0077$), UCLA ($p=0.0099$), SAS (0.0202), shoulder function scores ($p=0.0097$), and external rotation ($p=0.0357$). These differences in improvement for the SST, UCLA, SPADI, SAS, shoulder function score, abduction, forward elevation, and external rotation between pRSA and rRSA cohorts sustained significance at 24 months postoperatively.

Conclusions: Patients who underwent primary RSA or revision RSA demonstrated improvements across all outcomes in the immediate postoperative period of 6 weeks. However, an observable negative trend can be seen for most outcome measures between the 12 and 24-month period following rRSA. This study

establishes expectations regarding the rate of improvement following pRSA and rRSA for appropriate patient counseling and follow-up management.

Rate of Recovery Following Reverse Shoulder Arthroplasty

*Garrett Jackson - Chicago, United States of America

Howard Routman - Atlantis Orthopedics - Atlantis, USA

Ali Mohamed - FAU - Boca raton, USA

Aghdas Movassaghi - Michigan State University - East Lansing, USA

Carlos Fernandez - JFK / U Miami Orthopedic Surgery Program - Lantana, USA

Vani Sabesan - Cleveland Clinic Florida - Weston, USA

Antonio Da Costa - Florida Atlantic University, Charles E. Schmidt College of Medicine - Boca Raton, USA

Introduction: Reverse shoulder arthroplasty (RSA) has significantly grown over the last two decades due to its expanding indications. Given this increase, it is essential for the orthopedic surgeon to communicate the expected postoperative recovery timing to patients. The purpose of this study was to determine the rate of recovery following RSA and factors influencing this rate.

Methods: A retrospective review of 2132 patients who underwent RSA by a single surgeon was conducted. Data was collected preoperatively and postoperatively at intervals of 3-, 6-, 12-, and 24-months. At each follow-up period the cohort was divided into either a recovered or still recovering group. Patients with an American Shoulder and Elbow Score (ASES) of 70 or greater were defined as recovered, based on previously validated studies, compared to those with a score of less than 70 being defined as still recovering. Both the demographic and range of motion data were compared between the cohorts at each follow-up period.

Results: The recovered group included 36.4% at 3-months, 56.7% at 6-months, 71.8% at 12-months, and 70.5% at 24-months. At 6 months, the recovered and still-recovering groups had significantly more females (70.0% and 56.3% respectively; $p=0.02$). At 24 months, there was a significantly higher preoperative BMI for the recovered group compared to the still recovering group (30.15 versus 28.14 respectively, $p=0.04$). Previous shoulder surgery, preoperative injection, and subscapularis repair were comparable between groups at each follow-up period. Postoperative abduction was significantly greater in the recovered group at 12 months. Active forward elevation and external rotation were not significantly greater in the recovered group at 6-, 12-, and 24 months.

Discussion: It appears that perhaps female patients and those patients who gain postoperative abduction are more likely to reach recovery slightly faster than other cohorts. This information can allow clinicians to inform their patients of expected recovery times more accurately where more than a third of patients reach the recovery threshold by 3 months, and a majority by 12 months postoperative. Patients who had previous injections, variations in subscapularis management or prior shoulder surgery did not see an impact in their overall recovery rates for RSA.

Knee Pivot Motion During Gait After Total Knee Arthroplasty With an Asymmetric Conforming Bearing: Association of Posterior Cruciate Ligament Status With Patient-Reported Outcomes

*Alex Fuentes - Emovi - Montreal, Canada

Rémi Courteille - École de Technologies Supérieure - Montreal, Canada

Evan R Deckard - Indiana Joint Replacement Institute - Indianapolis, USA

Alix Cagnin - Emovi Inc - Montreal, Canada

Nicola Hagemester - Ecole de technologie superieure - Montreal, Canada

Laurence CHEZE - Université Claude Bernard Lyon 1 - Lyon, France

Scott Banks - University of Florida - Gainesville, USA

Michael Meneghini - Indiana School of Medicine - Fishers, USA

Introduction: Conforming bearing articulations in TKA aim to replicate native knee kinematics and guide knee center of rotation (COR) into certain pivot motions throughout motion. Interestingly, conforming kinematic bearings can be implanted with or without releasing the posterior cruciate ligament (PCL). This study purpose was to evaluate the relationship of knee COR during gait and outcomes in a dual-pivot conforming bearing TKA with and without the PCL.

Methods: Twenty-three (23) patients who underwent asymmetric dual-pivot congruent bearing TKA were included. Three-dimensional knee kinematics were evaluated during treadmill walking using the KneeKG™ system (Emovi, Canada) before surgery and at 4-month follow-up. Knee COR was assessed by projecting transepicondylar axis (TEA) in the transverse plane (i.e., tibial plateau) throughout the gait cycle. The COR location, corresponding to the intersection of two consecutive TEA projections, was determined through the gait cycle and used to characterize the pivot motion pattern (No pivot, Lateral, Medial, Central; Fig 1). The predominant pivot pattern was determined independently in seven gait cycle sub-phases. The proportion of patients exhibiting either a “Lateral/lateralized” (LL) pattern, consistent with a lateral pivot or shifting their pivot laterally or “Medial/medialized” (MM) pattern were compared. Clinical data and PCL status (full release [PCL-], intact/partial release [PCL+]) were extracted from medical records. The KOOS JR and ‘knee normal score’ from the modern Knee Society Score were evaluated at 4-month and 1-year follow-up.

Results: The cohort was 65.2% women, with a mean age of 67.3 years. Postoperatively, 63% of patients were categorized as LL pattern during stance (flexion typically $<20^\circ$) with the MM pattern being most prevalent during swing phase (knee flexion $>45^\circ$, Fig.2). Postoperatively, 72% of knees exhibited a predominantly lateral pivot during loading and mid-stance regardless of their PCL status. However, patients in the PCL- group continued to exhibit a predominant LL pivot at push-off (80.0% vs 33.3%) and early swing phase (44.4% vs 20.0%) compared to patients from the PCL+ group ($p=0.055$ and 0.259 respectively). KOOS JR scores were significantly higher in the PCL+ group at 4-month (75.8 vs 67.0, $p=0.017$), a difference not maintained at 1-year follow-up (87.7 vs 84.5, $p=0.617$). 91.7% of PCL+ patients reported their knee ‘sometimes or always’ felt normal compared to only 72.7% PCL- patients ($p=0.261$).

Conclusion: The dual-pivot conforming bearing appears to drive the knee to the intended motion for most patients post-TKA. Results also suggest that the PCL

status is associated with differences in knee COR during push-off and swing phases. In addition, a fully or partially intact PCL with minimal release may allow knees to feel more normal postoperatively and achieve higher overall knee joint health. Further research remains warranted with a higher sample size.

Figures

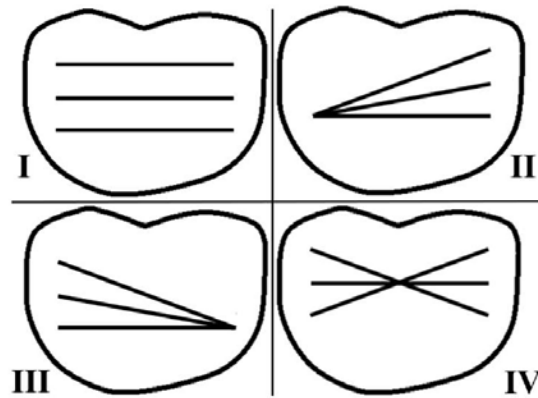


Figure 1 – Knee joint pivot patterns – Superior view of the transverse plane (anterior side at the top, left knee; I: translation, II: lateral pivot, III: medial pivot, IV: central pivot)

Figure 1

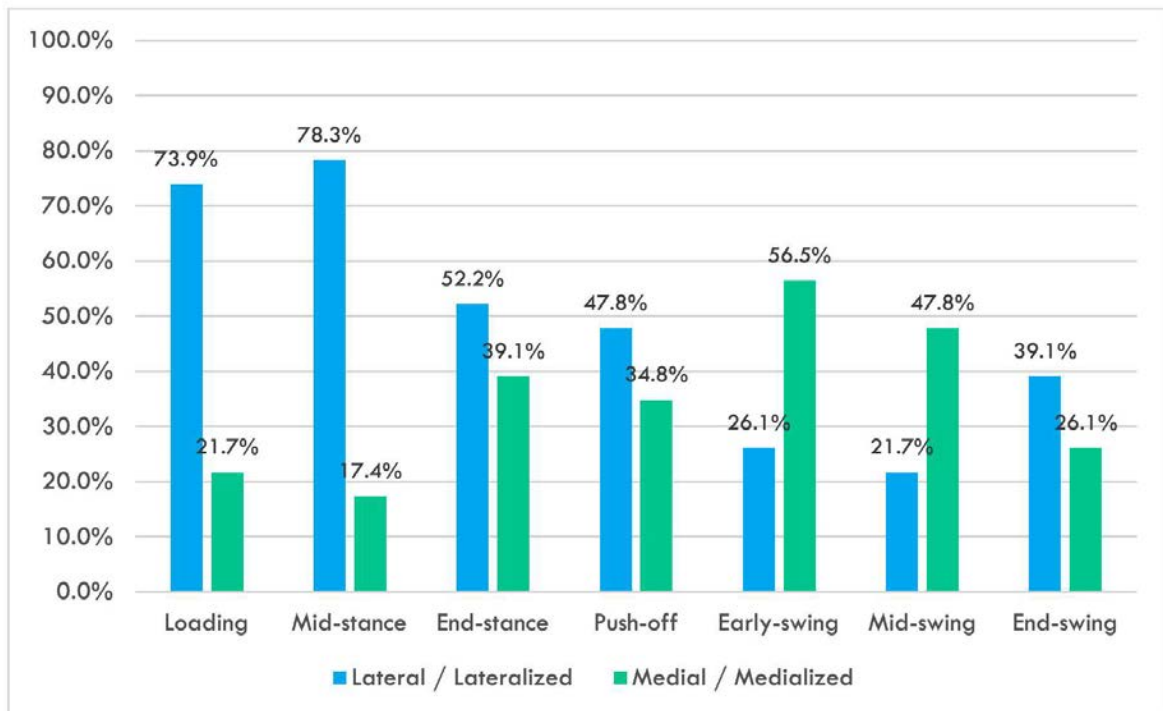


Figure 2 – Proportions of patients in LL and MM groups in each sub-phase of the gait cycle.

Figure 2

Does Sleep Comfort Predict Recovery After Primary and Revision Reverse Shoulder Arthroplasty?

*Garrett Jackson - Chicago, United States of America

Ali Mohamed - FAU - Boca raton, USA

Jared Kushner - Charles E. Schmidt Florida Atlantic University - Boca Raton, USA

Aghdas Movassaghi - Michigan State University - East Lansing, USA

Howard Routman - Atlantis Orthopedics - Atlantis, USA

Vani Sabesan - Cleveland Clinic Florida - Weston, USA

Matthew McKinley - Florida Atlantic University, Charles E. Schmidt College of Medicine - Boca Raton, USA

Jacob Calpey - Charles E. Schmidt College of Medicine Florida Atlantic University - Boca Raton, USA

Elisheva Kopf - Florida Atlantic University, Charles E. Schmidt College of Medicine - Boca Raton, USA

Introduction: The impact of sleep as a specific factor in surgical decision-making has not been studied. While the American Shoulder and Elbow Surgeon score (ASES) serves as the accepted benchmark, encompassing sleep as part of its evaluation of postoperative outcomes and recovery, this study aimed to examine and isolate the impact of sleep on patient's sense of recovery after primary reverse shoulder arthroplasty (pRSA) and revision reverse should arthroplasty (rRSA).

Methods: A retrospective review of patients who underwent RSA by a single fellowship-trained orthopaedic surgeon from 2015-2020 was conducted. Patients were separated into two groups: 1) pRSA and 2) rRSA. Demographic variables, composite ASES scores, and individual responses to the sleep component of the ASES score were collected at 3, 6, 12, and 24 months postoperatively. Patients rated their ability to comfortably sleep on a 0-3 scale (0="unable", 1="very difficult", 2="slightly difficult", 3="normal"). If a score of 0-2 was obtained, patients were considered to have "difficulty" sleeping. Utilizing the ASES score, patients were deemed "recovered" if they obtained a postoperative score of 70 or greater. Patients were further subgrouped into "not recovered" and "recovered" groups and statistically compared to their sleep scores using a chi-square analysis.

Results: A total of 476 RSA patients (pRSA=386, rRSA=90) were included in the final analysis. Patients who underwent pRSA had a mean age of 73 years, BMI of 29.2 kg/m² and consisted of 37% males. Patients who underwent rRSA had a mean age of 68 years, BMI of 29.7 kg/m² and consisted of 51.7% males. A majority of patients that recovered indicated "no difficulty" sleeping by 3 months (pRSA group = 61.1%, rRSA group = 63.6%) and this incrementally improved up to one year for both pRSA and rRSA patients (6 months (RSA group = 69.1%, rRSA group = 73.3%), 12 months (RSA group = 69.4%, rRSA group = 75%). The recovered patients demonstrated significantly higher rates of "no difficulty" sleeping when compared to their respective "not recovered" patients at each time point ($p < 0.001$).

Conclusion: This study establishes a significant association between the restoration of normal sleep and higher recovery rates following RSA. These findings hold vital implications for surgeons in patient counseling, emphasizing the importance of sleep and providing a timeline for the normalization of sleep patterns, specifically within 3 months post-RSA, as a key indicator for achieving complete recovery.

Influence of Age and Sex on Meeting MCID Following Reverse Shoulder Arthroplasty

*Garrett Jackson - Chicago, United States of America

Ali Mohamed - FAU - Boca raton, USA

Anna Redden - FAU - boca raton, USA

Aghdas Movassaghi - Michigan State University - East Lansing, USA

Vani Sabesan - Cleveland Clinic Florida - Weston, USA

Howard Routman - Atlantis Orthopedics - Atlantis, USA

Elisheva Kopf - Florida Atlantic University, Charles E. Schmidt College of Medicine - Boca Raton, USA

Introduction:

Patient-reported outcome measures (PROMs) are used to assess efficacy of reverse shoulder arthroplasty (RSA). Previous studies have assessed differences between age and gender following RSA. However, it is unknown if these differences are clinically significant. Thus, this study aimed to use the minimal clinically important difference (MCID) to determine the clinically relevant difference in outcomes between age and sex following RSA.

Methods:

A retrospective review of 227 RSA patients from 2007-2020 by a single fellowship-trained orthopedic surgeon was performed. Demographics, range of motion (ROM), and PROMs were collected preoperatively and at 6 weeks, 3, 6, 12, and 24 months postoperatively. PROMs included the Simple Shoulder Test (SST) score, American Shoulder and Elbow Surgeons (ASES) score, Shoulder Pain and Disability Index (SPADI) score, University of California at Los Angeles Shoulder (UCLA) score, and Shoulder Arthroplasty Smart (SAS) score. Logistic regressions determined the relationship between age and sex on reaching meeting MCID at each time point. MCID was determined using the anchor-based method, with MCID calculated from the preoperative visit to final follow-up.

Results:

MCIDs for SST, ASES, SPADI, UCLA, and SAS scores were 4.3, 30.2, -45, and 24.2 respectively. With every one-unit increase in age, patients were more likely to meet MCID for SPADI at 6 weeks (odds ratio [OR] 1.039, $p = .007$) and 6 months (OR 1.04, $p = .02$). At 3 months, patients were more likely to meet MCID for SST (OR 1.04, $p = 0.01$), ASES (OR 1.04, $p = 0.013$), UCLA (OR 1.04, $p = 0.004$), SPADI (OR 1.04, $p = 0.009$), and SAS (OR 1.04, $p = 0.006$) for each one-unit increase in age. Regarding ROM, patients were less likely to reach MCID for forward elevation at 6 weeks for each one-unit increase in age (OR 0.957, $p = 0.009$). Similarly, patients were less likely to meet MCID for external rotation at 1 year (OR 0.95, $p = 0.012$). When analyzed by gender, males were more likely to meet MCID for active abduction (OR 1.17, $p = 0.006$) and forward elevation (OR 1.038, $p = 0.041$) at 2 years.

Conclusion:

Increasing age and male gender were more predictive of meeting MCID for outcome scores and range of motion, respectively. These findings highlight the varying outcomes of RSA based on patient sex and age. Understanding these distinctions, in addition to identifying the points at which improvements in PROMs and ROM

measurements level off, can significantly enhance patient counseling and establish accurate postoperative expectations.

A Look at Postsurgical Complications for Outpatient Shoulder Arthroplasty

*Garrett Jackson - Chicago, United States of America

Vani Sabesan - Cleveland Clinic Florida - Weston, USA

Aghdas Movassaghi - Michigan State University - East Lansing, USA

Jacob Calpey - Charles E. Schmidt College of Medicine Florida Atlantic University - Boca Raton, USA

Matthew McKinley - Florida Atlantic University, Charles E. Schmidt College of Medicine - Boca Raton, USA

Elisheva Kopf - Florida Atlantic University, Charles E. Schmidt College of Medicine - Boca Raton, USA

Introduction: Healthcare systems seek safe and cost-effective alternatives to procedures that traditionally require inpatient (IP) stay. While total hip and knee arthroplasties have successfully transitioned from IP to outpatient (OP), shoulder arthroplasty (SA) lags as it continues to be predominantly performed in an IP setting. The purpose of this study was to compare IP versus OP postoperative complications in adult patients after SA to determine if the transition from IP to OP is feasible, given both degrees of safety and efficacy.

Methods: This cohort study utilized the National Surgical Quality Improvement Program (NSQIP) database to query all adults who underwent SA from 2011 to 2016. The primary independent variable was the type of patient status (IP, OP). The dependent variable was postoperative complications within 30 days of surgery. Multivariate logistic regression and propensity score matching were used to determine the association between patient status and postoperative complications while controlling for confounding factors.

Results: Of the 13,299 total SA sampled, 94.1% were IP. The IP cohort was significantly older with a significantly higher proportion of female patients and higher rates of hypertension. After matching, the frequency of complications was significantly higher in the IP group compared to OP (50.8% vs. 34.6%, respectively; $p=0.004$). The unadjusted odds of postoperative complications in the entire cohort were significantly higher in the IP group than in OP (OR 1.70, 95% CI 1.16 – 2.49). After propensity score matching analysis, the adjusted odds ratio (aOR) was similar (aOR = 1.84, 95% CI 1.14 – 2.98).

Conclusions: Patients with inpatient stay after SA were more likely to be female, significantly older, and have higher rates of hypertension. Notably, our findings indicate that IP SA is linked to increased postoperative complication rates compared to outpatient status, which can be attributed to the presence of more comorbidities and risk factors in this group. These findings have crucial implications for the implementation of outpatient SA programs, highlighting the need to consider age and gender when determining patient disposition after SA and assessing the risk for complications. There remains a need for the development of criteria for who is best suited for outpatient SA and protocols to minimize adverse risks for the IP and OP settings.

Artificial Intelligence Language Models Are Useful Tools for Patients Undergoing Total Ankle Replacement

Alan Samsonov - NYU Langone Health - New York, USA

James Butler - NYU Langone Health - New York, United States of America

*John Kennedy - NYU Langone Health - New York, USA

Raymond Walls - NYU Langone Health - New York, United States of America

Akram Habibi - NYU Langone Orthopedic Hospital - New York, United States of America

Introduction: Artificial intelligence (AI) large language models (LLMs), such as Chat Generative Pre-trained Transformer (ChatGPT), have gained traction as both augmentative tools in patient care but also as powerful synthesizing machines. The use of ChatGPT in orthopedic foot and ankle surgery, particularly as an informative resource for patients, has not been described to date. The purpose of this study was to assess the quality of information provided by ChatGPT in response to commonly-asked questions about total ankle replacement (TAR).

Methods: ChatGPT was asked ten frequently asked questions about TAR in a conversational thread. Responses were recorded without follow-up, and subsequently graded A, B, C, or F, corresponding with “excellent response,” “adequate response needing mild clarification,” “inadequate response needing moderate clarification,” and “poor response needing severe clarification.”

Results: Of the ten responses, two were grade “A,” six were grade “B,” two were grade “C,” and none were grade “F.” Overall, the LLM provided good quality responses to the posed prompts.

Conclusions: Overall, the provided responses were understandable and representative of the current literature surrounding TAR. This study highlights the potential role LLMs in augmenting patient understanding of foot and ankle operative procedures.

Risk Factors That Predispose Patients to Sub-Optimal After Reverse Shoulder Arthroplasty

*Garrett Jackson - Chicago, United States of America

Ali Mohamed - FAU - Boca raton, USA

Jake Goguen - New York, United States of America

Anna Redden - FAU - boca raton, USA

Aghdas Movassaghi - Michigan State University - East Lansing, USA

Howard Routman - Atlantis Orthopedics - Atlantis, USA

Vani Sabesan - Cleveland Clinic Florida - Weston, USA

INTRODUCTION

Reverse shoulder arthroplasty (RSA) has become an increasingly popular treatment option for many shoulder pathologies. Because RSA is associated with many complications and high failure rates, undergoing these procedures based on pathological indication alone is insufficient. The MCID is a valuable measurement that can be used to evaluate PROMs to determine patient improvement following surgery. The purpose of this study was to identify characteristics associated with failure to meet the MCID following reverse shoulder arthroplasty.

METHODS

A retrospective analysis was conducted from a prospectively collected database to identify patients who underwent shoulder arthroplasty from 2007-2020. Patients were categorized as either having underwent standard RSA (sRSA) or augmented RSA (aRSA). Preoperative and postoperative range of motion as well as PROMs were collected included the SST, CMS, UCLA, SPADI, SAS, and the ASES. The MCID was determined using the anchor-based method, and logistic regressions were used to determine the relationship between risk factor and meeting MCID.

RESULTS

576 patients (sRSA = 379, aRSA = 197) were analyzed. The sRSA group demonstrated a significantly greater number of females ($p < 0.001$) and the aRSA group demonstrated a significantly greater number of patients who use tobacco ($p = 0.045$). For patients who underwent sRSA, there were no risk factors that correlated with decreased likelihood of meeting the MCID for PROMs or ROM. For aRSA, risk factors included 71% less likely to meet the MCID for CMS if they used injections ($p = 0.023$; odds ratio = 0.293, C.I 0.102-0.843), 81% less likely to meet the MCID for SPADI if they had hypertension ($p = 0.016$; odds ratio = 0.209, C.I 0.059-0.744), 57% less likely to meet the MCID for SAS if they had a rotator cuff tear ($p = 0.033$; odds ratio = 0.43, C.I 0.198-0.935), and 54% less likely to meet the MCID for forward elevation if they had a rotator cuff tear ($p = 0.050$; odds ratio = 0.457, C.I 0.208-1.001). Patients within the aRSA group did not demonstrate any significant likelihood regarding meeting or not meeting the MCID for SST, ASES, UCLA.

CONCLUSION

Patients who underwent standard RSA were not found to have any risk factors associated with failure to meet the MCID for any PROMs or ROM. Patients were less likely to meet the MCID following augmented RSA for the CMS if they had previously used injections, for the SPADI if they had hypertension, and for the SAS as well as measurements of forward elevation if they had a rotator cuff arthropathy.

What Factors Impact a Patients Feeling of Recovery After Shoulder Surgery?

*Garrett Jackson - Chicago, United States of America

Anna Redden - FAU - boca raton, USA

Ali Mohamed - FAU - Boca raton, USA

Aghdas Movassaghi - Michigan State University - East Lansing, USA

Vani Sabesan - Cleveland Clinic Florida - Weston, USA

Antonio Da Costa - Florida Atlantic University, Charles E. Schmidt College of Medicine - Boca Raton, USA

Introduction

The American Shoulder and Elbow Surgeons (ASES) score is a well-validated patient-reported outcome measure (PROM) used daily in to evaluate shoulder problems in patients. It is comprised of many components such as pain and activities of daily living (ADLs) but yet no prior study has evaluated the impact of specific individual factors on a patient's feeling of recovery. Specifically sleep, ADLs and driving are common factors reported by patients in terms of recovery after shoulder surgery, but there is limited research in this area. The purpose of our study was to evaluate the influence of specific factors, including sleep, ADLs, and driving, on a patient's assessment of recovery after shoulder surgery.

Methods

An anonymous survey was administered to participants above the age of 18 in Palm Beach County, Florida. Patients were asked to rank pain, shoulder function, sleep, driving, and self-care activities to assess the importance and impact of these factors on their assessment of recovery. Patients were also asked to predict the time to recovery of these activities. Descriptive statistics and Kruskal-Wallis analyses were conducted.

Results

The cohort consisted of 101 participants with 51.4% identifying as male. The mean age of the cohort was 38.7 with the majority (68.2%) being Caucasian. Participants were asked about considerations for undergoing shoulder surgery and pain relief in terms of ranking of importance of specific activities for recovery. As for ADLs, the most important factor in the feeling of recovery was sleeping on the affected side (73.8%), followed by toileting (67.3%), driving (60.7%), and ability to do usual work (32.1%). The time patients expected to return to normal sleep on the affected side was 5.3 weeks, ADLs 5.2 weeks, and driving 3.9 weeks after surgery.

Conclusion

Although pain was ranked as the most important factor, it is not the only factor to consider for a patient's feeling of recovery after shoulder surgery. The ability to perform ADLs, sleep without difficulty, and driving are also important factors to consider for patients to feel they have recovered from shoulder surgery. Shoulder specialists should take these patient perceptions into account in order to optimally meet patient expectations and personalize care when discussing recovery after shoulder surgery.

Custom 3D-Printed Cups for Acetabular Reconstruction: A 3-Year CT Implant Migration Study

*Anna Di Laura - Royal National Orthopaedic Hospital and Dept. MechEng at UCL - London, United Kingdom

Johann Henckel - Royal National Orthopaedic Hospital - London, United Kingdom

Alister Hart - Royal National Orthopaedic Hospital - London, United Kingdom

Intro

The use of custom 3D printed titanium implants is increasing in the complex revision scenario. It has been showed tha initial migration can occur without eventual construct failure, if present on radiologic follow-up, it is advised that more frequent imaging is performed to monitor the patients until implant stabilization and ingrowth are achieved.

We aimed to assess component migration 3 years post acetabular reconstruction surgery by bone-to-bone registration of sequential CT imaging.

Our primary and secondary objectives were to: 1. Assess implant position 3-year post surgery in comparison with the 1-year post-operative CT imaging; 2. Assess clinical outcome.

Methods

This was a single-centre cohort study of 20 patients from a single surgeon. All patients had massive acetabular defects Paprosky type 3B and were treated with single-manufacturer 3D printed custom made acetabularup

Using 3D software solutions, the CT images were rendered to produce 3D reconstructions of the patients' bony pelvis for relative comparison of the two imaging timepoints (1-year and 3-year post-operative). Bone-to-bone registration allowed for the assessment of implant movement over time, this was studied in terms of difference in centre of rotation (CoR) in X (medial-lateral, ML), Y (inferior-superior, IS) and Z (anterior-posterior, AP) planes. Meticulous patient follow-up by the operating surgeon to monitor for complications was undertaken. Serial oxford hip scores were recorded.

Outcome measures: 1. The change in centre of rotation (CoR) between CT scans carried out 1-year and 3-year post-operatively. 2. Clinical outcomes.

Results

All 20 patients had Paprosky type-3B defects. Pelvic discontinuity was confirmed intraoperatively in 3 patients. The mean follow-up time was 71 months (range 52 to 93 months).

One year post-operatively, the deviation of CoR was a mean (\pm SD) of -0.1 ± 1.5 mm (min = -3.0 mm, max = 3.0 mm) in the ML plane, $1.5 (\pm 1.5)$ (min = 0 mm, max = 5 mm) in the IS plane and $1 (\pm 1.5)$ (min = -2.0 mm, max = 4 mm) in the AP plane.

Three years post-operatively the deviation of CoR was a mean (\pm SD) of 0.3 ± 0.9 mm (min = 0 mm, max = 3 mm) in the ML plane, $0.7 (\pm 0.8)$ (min = 0 mm, max = 3 mm) in the IS plane and $0.5 (\pm 0.8)$ (min = 0 mm, max = 2 mm) in the AP plane.

Overall, the migration was lower 3 years post-op compared to year 1 post-op in the three planes, significantly lower in the IS plane (inferior-superior direction), $p=0.0073$.

Postoperative sequential imaging revealed no fractures, there was no evidence of implant loosening or failure of metalwork. The Oxford Hip Score improved significantly, from a median of 8 (range, 2 to 21) preoperatively to 33 (range, 16 to 47) at the last follow-up, $p=0.0001$.

Conclusion

Clinically well-fixed 3D printed custom implants used to reconstruct massive acetabular defects commonly exhibit small degrees of migration 1 year post-operatively, the degree of movement lowers over time as the construct further stabilises. Surgeons and engineers should be aware when monitoring these patients.

Fatigue Strength of an Additively Manufactured Ti-6Al-4V Porous Patellar Implant With Comparison to Commercially Available All-Polyethylene and Metal Porous Patellar Implants

*Bradley Elliott - Zimmer Biomet, Inc. - Warsaw, USA

Kimberly Mimnaugh - Zimmer Biomet, Inc - Warsaw, USA

Introduction

Additive manufacturing (AM) holds promise for developing more complex and economical joint replacement components. However, AM may have a negative effect on the fatigue strength of the devices. In this study, the median fatigue strength (MFS) of a Ti-6Al-4V AM porous (AMP) patella was determined under two dynamic loading conditions designed to simulate in vivo fractures from literature^{1,2}. Performance of the AMP patella was compared to that of a commercially available all-polyethylene (AP) patella in peg shear and to a commercially available metal porous (MP) patella in the under-supported loading condition.

Methods

Test parameters are summarized in Table 1.

Patella Peg Shear Fatigue Test

A load applicator constrained the patellar implant (Figure 1A) while a static compressive load and cyclic shear load were applied for three million cycles (3Mc) or until fracture occurred. An accelerated life test (ALT) with cyclic shear forces ranging from 1200 N to 1600 N was performed to determine MFS.

Under-Supported Patella Bending Fatigue Test

A femoral implant applied cyclic compressive loading to a patellar implant that was minimally supported at the superior and inferior poles (Figure 1B). An ALT with cyclic compressive loading ranging from 600 N to 900 N was conducted to determine MFS.

Results

The AMP patella had better fatigue performance than either of the comparator devices in their respective tests, with 22.5% increase in peg shear fatigue strength over the AP patella and 25.5% increase in bending fatigue strength over the MP patella.

Patella Peg Shear Fatigue Test

The AMP and AP patellae both fractured in a similar manner to that observed clinically¹, with cracks initiating at the peg-base interface and propagating in the direction of shear loading until complete fracture occurred (Figure 2A-2B – AP patellar implant, Figure 2C-2D – AMP patellar implant).

Under-Supported Patella Bending Fatigue Test

Fractures typically initiated at the peg interface and propagated transversely for the MP patellae, similar to the fracture pattern observed clinically². The AMP patellae had fatigue fractures that initiated on the outer rim of the base, with no evidence of complete transverse fractures (Figure 3B-3C).

Conclusion

In conclusion, this study demonstrated that an AM Ti-6Al-4V porous patella can be at least as strong as commercially available MP and AP patellae when subjected to different fatigue loading scenarios. It was also demonstrated that clinically observed patellar fractures could be simulated with in-vitro fatigue testing.

References

1. Shafi M, Kim YY, Lee YS, Kim JY, Han CW. Patellar polyethylene peg fracture: a case report and review of the literature. *Knee Surg Sports Traumatol Arthrosc.* 2005

Sep;13(6):472-5. doi: 10.1007/s00167-004-0566-9. Epub 2005 Feb 22. PMID: 15726329.

2. Chun KA, Ohashi K, Bennett DL, El-Khoury GY. Patellar fractures after total knee replacement. AJR Am J Roentgenol. 2005 Sep;185(3):655-60. doi: 10.2214/ajr.185.3.01850655. PMID: 16120913.

Figures

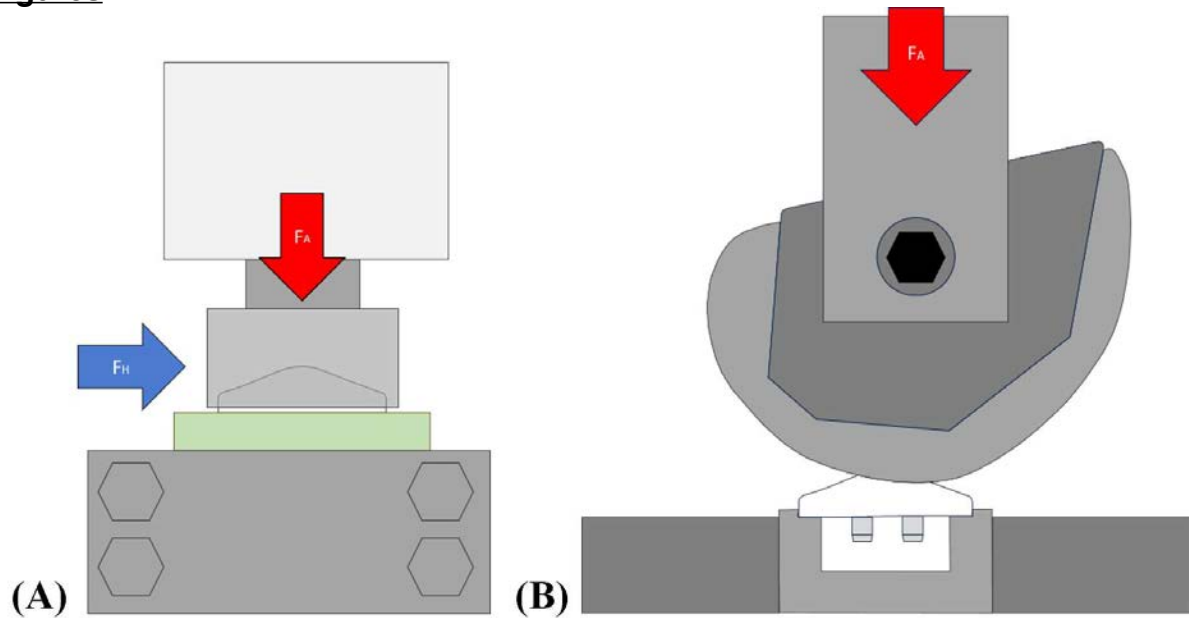


[Figure 1](#)

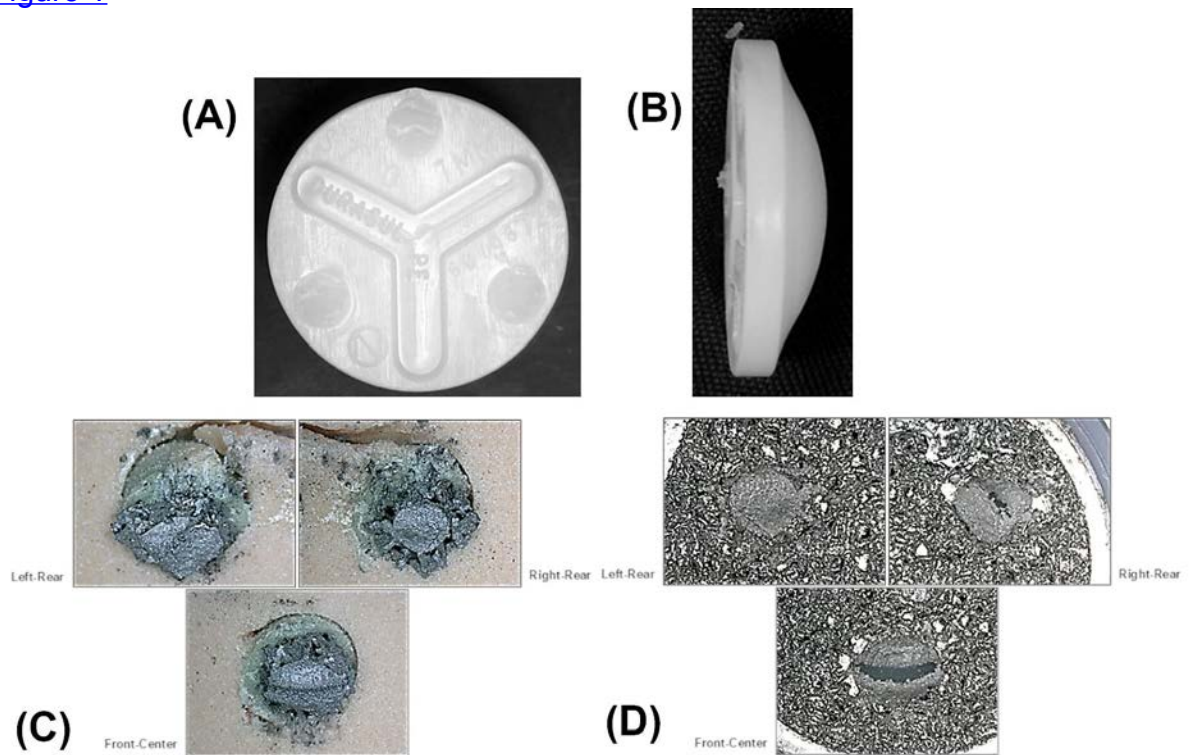


[Figure 2](#)

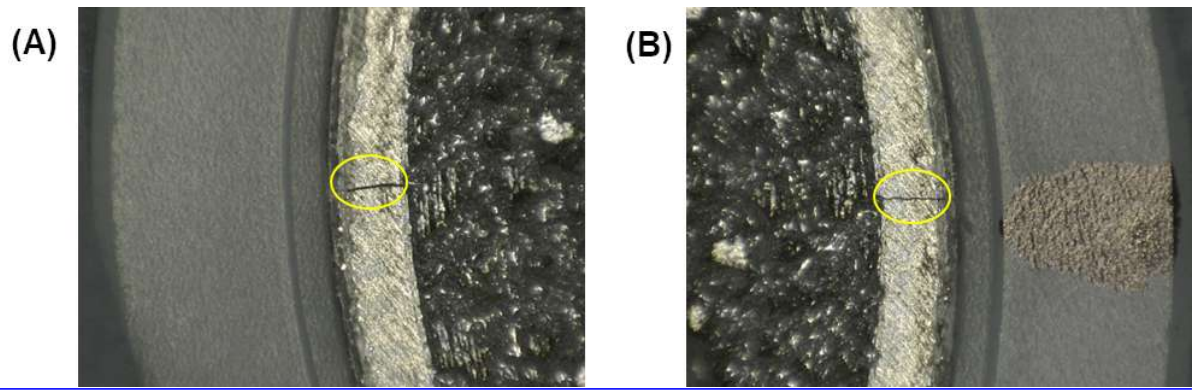


[Figure 3](#)

Table 1. Test Method Parameters

Peg Shear Fatigue Test		Under-Supported Bending Fatigue Test	
Parameter	Value	Parameter	Value
Static Compressive Force (N)	500	Peak Cyclic Compressive Force (N)	Up to 900
Peak Cyclic Shear Force (N)	Up to 1600	Frequency (Hz)	3
Frequency (Hz)	3	Environment	Ambient
Environment	Ambient	Test Endpoint (Cycles)	3,000,000
Test Endpoint (Cycles)	3,000,000	Sample Size (n)	15 each
Sample Size (n)	15 each		

[Figure 4](#)

3D Printed Prosthesis for Appropriate Reconstruction of Massive Acetabular Bone Defects in Multiple Failed Total Hip Arthroplasty a Functional Outcome Study

*Raghav Arora - MAX SUPERSPECIALITY HOSPITAL, SHALIMAR BAGH, DELHI - Delhi, India

satya narain - max superspeciality hospital - delhi, India

mannu bhatia - max superspeciality hospital, Shalimar Bagh - delhi, India

HYPOTHESIS:Reconstructive procedure following failed Total Hip Arthroplasty pose a huge challenge for all arthroplasty surgeons. Complicated and large acetabular bone defects in such cases leave the surgeon with very limited options. This case report aimed to explore the advantages of three-dimensional (3D) printing technology in the reconstruction of such acetabular bone defects and study their functional outcome

METHOD:We present 1 year follow up functional outcome of a patient with severe bone defects around the acetabulum due to four failed surgeries who was treated using 3D printing technology. The patient presented with a 3-year-old history of fracture acetabulum, followed by fixation and total hip arthroplasty which later had to be removed due to loosening and later revised thrice. The patient presented with pain over his hip and inability to bear weight. X-rays showed that the patient had been operated for Total Hip Arthroplasty with reconstruction of the acetabulum with Burch- Schneider Cage which had now displaced postero-centrally. Various radiographs(Fig. 1), CT scan were done along with a three phase bone scan to rule out infection. All the blood parameters were within normal limits.Reconstruction of bone defect by using conventional methods of bone restoration was not possible in this patients. To tackle this problem, we reconstructed a virtual model for planning and estimation of bone defects using GEO – Magic and D2P software. A virtual model of the pelvis was created and assessed for coverage of bone defects, stability of the joint and placement and fixation of implants. Based on these findings a 3D printed customised prosthesis was made using porous titanium alloy with a pore diameter of 300–400 mm with a trabecular structure to promote ingrowth of bone and provide stability.

Intraoperative procedure included fixation of the prosthesis using preplanned sites of screw fixation followed by placement of cemented cup in the designed space of the prosthesis followed by reduction of the joint.

RESULT:Post-operative period was uneventful and xrays were satisfactory(Fig.2).

The patient underwent regular physiotherapy for a period of 6 months. A follow up examination along with Harris hip score was obtained at 3,6 and 12 months to evaluate limb function. Weight bearing was allowed at 2 months with brace with a walker and at 4 months the patient was able to bear full weight without any brace or support. 1 year follow up x-ray (Fig.3) when compared to immediate post-operative x-rays showed no signs of loosening or osteolysis. The same was confirmed with a good functional outcome using the Harris hip score of 81 at 12 months as compared to 40 before surgery.

CONCLUSION: 3D printed prosthesis in cases with complex and large bone defects could be used by arthroplasty surgeons in cases of revision of Total Hip Arthroplasty. **Figures**

Study Time: 16:29:4



Pre Op

Figure 1



Figure 2



[Figure 3](#)

Optimization of Fused Filament Fabrication (FFF) Process Parameters for PEEK and PEKK Biomaterials for Orthopedic Medical Device Application

*Abigail Tetteh - Drexel University - Philadelphia, USA

Daniel Porter - US Food and Drug Administration - Silver Spring, USA

Matthew Di Prima - Food and Drug Administration - Silver Spring, USA

Steven Kurtz - Drexel University - Philadelphia, USA

The disparity in mechanical properties between materials used in joint arthroplasty and bone has been linked to stress shielding and bone loss. As a result, aseptic loosening continues to be one of the frequently reported causes of revisions. High-performance thermoplastics like Poly-ether-ether-ketone (PEEK) and Poly-ether-ketone-ketone (PEKK) exhibiting mechanical properties comparable to surrounding bone can be used to fabricate 3D printed orthopedic load bearing devices. Therefore, this study aims to optimize fused filament fabrication (FFF) process parameters for PEEK and PEKK.

A Taguchi L9-orthogonal array (4 factors and 3 levels) with 4 replicates was employed as the experimental design. PEEK (VESTAKEEP® i4 3DF-T, Evonik) and PEKK (IMPEKK® 3D-F, Sequens) were evaluated to determine optimal process parameters (print temperature, chamber temperature, layer height, print speed) that maximize compressive mechanical properties (compressive strength, modulus, and yield strength). Cylindrical samples were printed in the z-direction on a high-temperature 3d printer (EXT 220 MED, 3D Systems). Compression testing was performed following ASTM D695 standard on an Instron testing machine (Instron 68FM-100) at 1.3mm/min crosshead speed. Minitab 21.4.3 software was utilized to calculate signal-to-noise ratios for optimal parameters and to conduct ANOVA for assessing statistical significance at $p < 0.05$.

Compressive strength ranged from 136-173 MPa, compressive modulus from 2.6-3.5 GPa, and 0.2% yield strength from 85-94 MPa for PEEK samples. Compressive strength ranged from 108-120 MPa, compressive modulus from 2.8-3.4 GPa, and 0.2% yield strength from 80-93 MPa for PEKK samples. The four process parameters (Figure 1) investigated had varying effects on the two materials and their compressive properties. For PEEK, print temperature impacted compressive strength ($p = 0.013$) and yield strength ($p = 0.048$), layer height impacted compressive modulus ($p = 0.000$), print speed impacted yield strength ($p = 0.048$) and compressive modulus ($p = 0.000$), and chamber temperature showed no significant effect on any of the output metrics. For PEKK on the other hand, all process parameters significantly affected yield strength ($p < 0.05$), and chamber temperature impacted compressive strength ($p = 0.003$) and compressive modulus ($p = 0.047$). The main effects plots for signal-to-noise ratios highlighting optimal process parameter levels for PEEK and PEKK are shown in Figure 2 and 3 respectively. Due to the intended application of both materials for orthopedic devices, compressive yield strength was chosen as the failure criterion.

Print temperature, print speed and layer height influenced the compressive properties of PEEK while all process parameters influenced the properties of PEKK. The optimal process parameters for yield strength (the chosen material strength metric) were; the highest tested print temperature (410°C PEEK, 410°C PEKK); the

highest tested chamber temperature (210°C PEEK, 150°C PEKK), and the lowest tested layer height (0.1mm PEEK, 0.1mm PEKK). However, unlike the preceding parameters where the optimal levels were similar for both materials, the optimal print speed differed for both materials. Specifically, the optimal print speed was 2000mm/min, the highest tested for PEEK, and 1500mm/min, the middle speed tested for PEKK. The current results can be used to guide the design and printing process for FFF medical devices.

Figures

Process Parameter - Factor	PEEK Process Parameter - Level	PEKK Process Parameter - Level
Print Temperature (°C)	390, 400, 410	390, 400, 410
Chamber Temperature (°C)	170, 190, 210	110, 130, 150
Layer Height (mm)	0.1, 0.2, 0.3	0.1, 0.2, 0.3
Print Speed (mm/min)	1000, 1500, 2000	1000, 1500, 2000

Figure 1: FFF process parameters (factors and corresponding levels) for PEEK and PEKK used in the study.

Figure 1

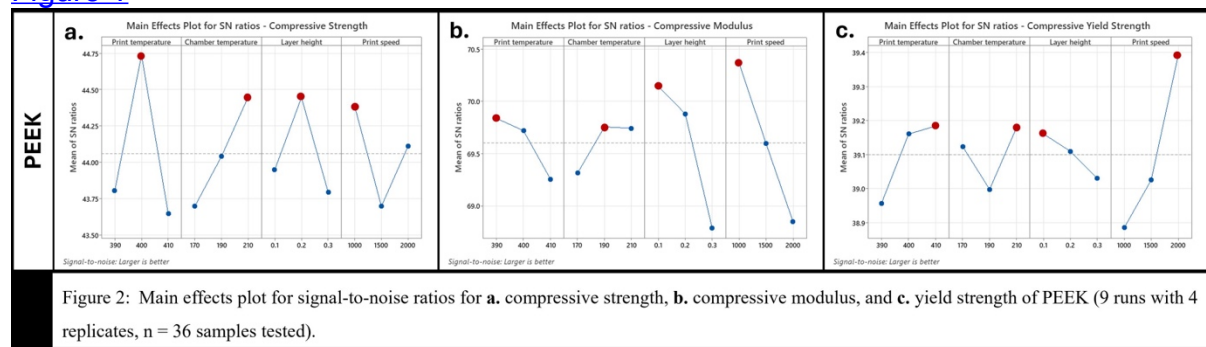


Figure 2

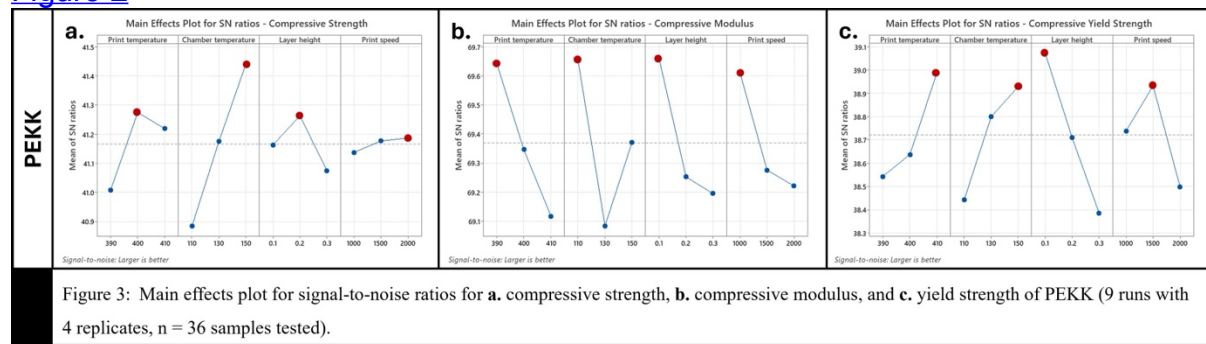


Figure 3

PROMs Are Becoming SoC. a Novel Approach to Mitigate Their Limitation

*Julien Lebleu - moveUP - Brussels, Belgium

Andries Pauwels - moveUP - brussels, Belgium

Philippe Van Overschelde - Hip & Knee Clinic AZ Maria-Middelares Gent - Sint-Martens-Latem, Belgium

Jared Weir - DeepStructure - Saginaw, USA

Charles-Eric Winandy - moveUP - Brussels, Belgium

Introduction: Patient-Reported Outcome Measures (PROMs) collection is continuing to become mandatory in more countries. They not measure the quality of care from patients' point of view, but can also be used to manage expectations, benchmark quality, and assess recovery speed. Even so, PROMs lack crucial variables such as physical activity, post-surgery expectations, prior treatments, comorbidities, and BMI. This study presents a novel index designed to address these limitations by incorporating the missing variables and assess if these new formulas enable to better differentiate between candidates for surgery.

Method:

We developed a new index overcoming the limitations of traditional PROMs such as KOOS JR and FJS in accounting for key variables (Comprehensive score). This new score is given through a proprietary formula on a scale from 0 to 100. A cohort of 1580 patients, suffering from degenerative knee pain completed the index pre-consultation with an orthopedic surgeon, either remotely via personal devices or in the clinic's waiting rooms using tablets. The surgery decision was recorded for all patients, with 125 cases selecting surgical treatment (TKA) as the best option. Descriptive statistics were utilized to analyze the distribution of the comprehensive score and the traditional PROM score, with a focus on the impact of overlooked factors on the distribution of surgery decision.

Results

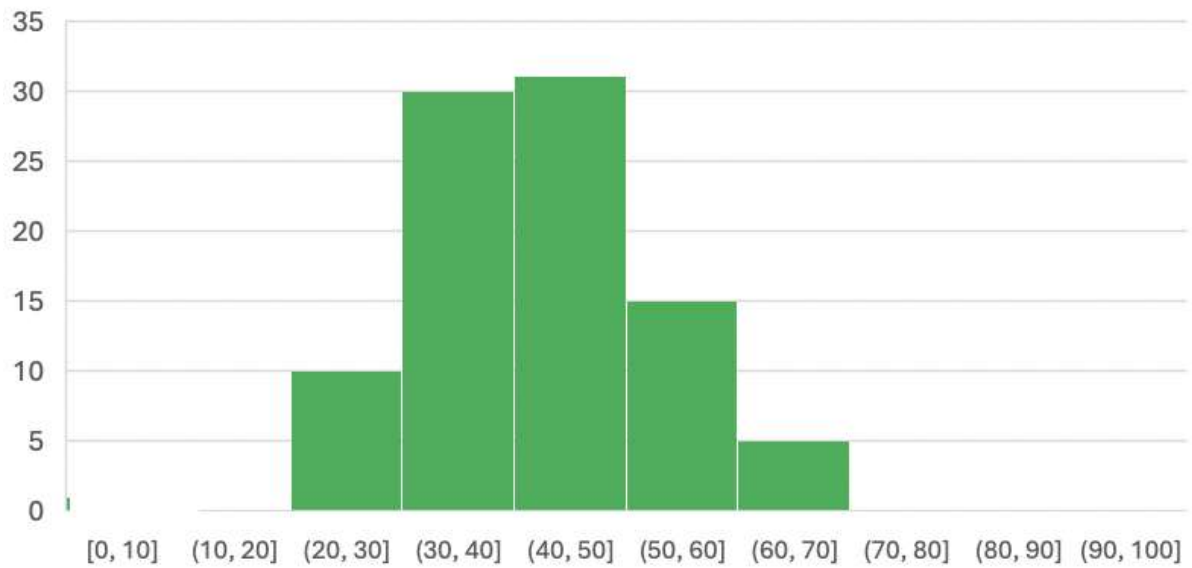
The PROM score which did not include the overlooked factor was 42 (+-10) for surgical patients, vs 52 (+-12) for non-surgical patients. The score which included the overlooked factors was 49 (+-18) for surgical patients and 70 (+-21) for non-surgical patients. Hence, including the overlooked factors, the distribution shifted operated patients by 7 points and non-operated patients by 18 points. The shift was significantly higher for non-operated patients, showing a better segmentation of patients with the comprehensive score.

Conclusion

Patients who underwent TKA displayed lower average scores compared to non-operated counterparts, indicating the utility of the comprehensive score in distinguishing between surgical candidates. Importantly, the inclusion of overlooked factors significantly shifted the score distributions towards higher values, showing that surgery decision should include more comprehensive variables. In conclusion, the novel index offers an improved tool for orthopedic surgeons, facilitating informed decision-making and patient education. Leveraging a web-based platform, the index enables seamless integration into clinical workflows, thereby streamlining triage processes and optimizing patient care in knee arthroplasty.

Figures

Operated patients index not modified



Non operated patients index not modified

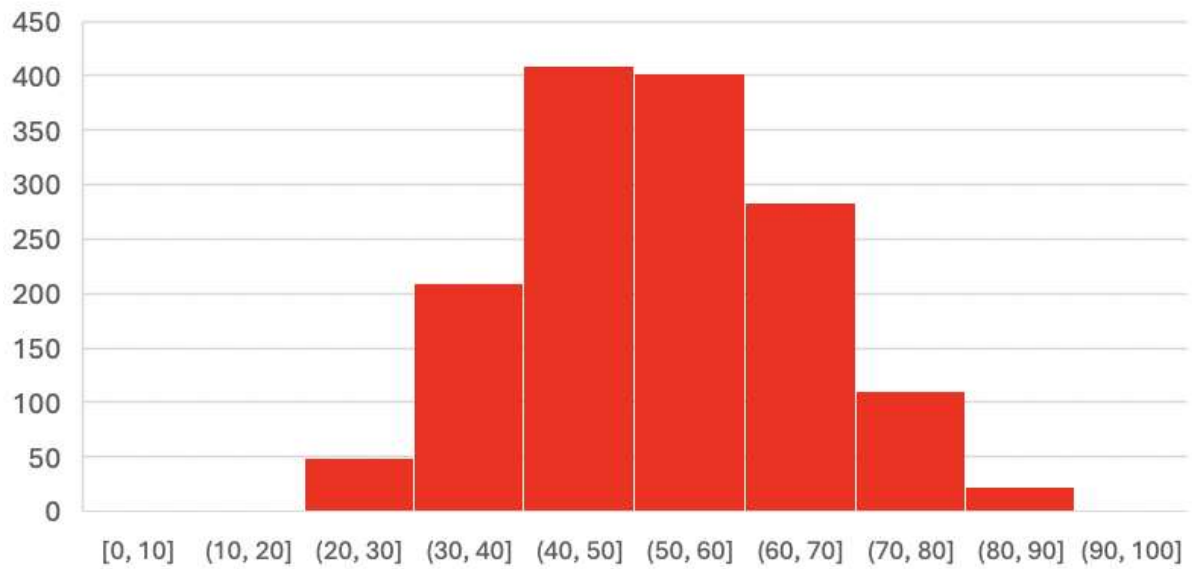


[Figure 1](#)

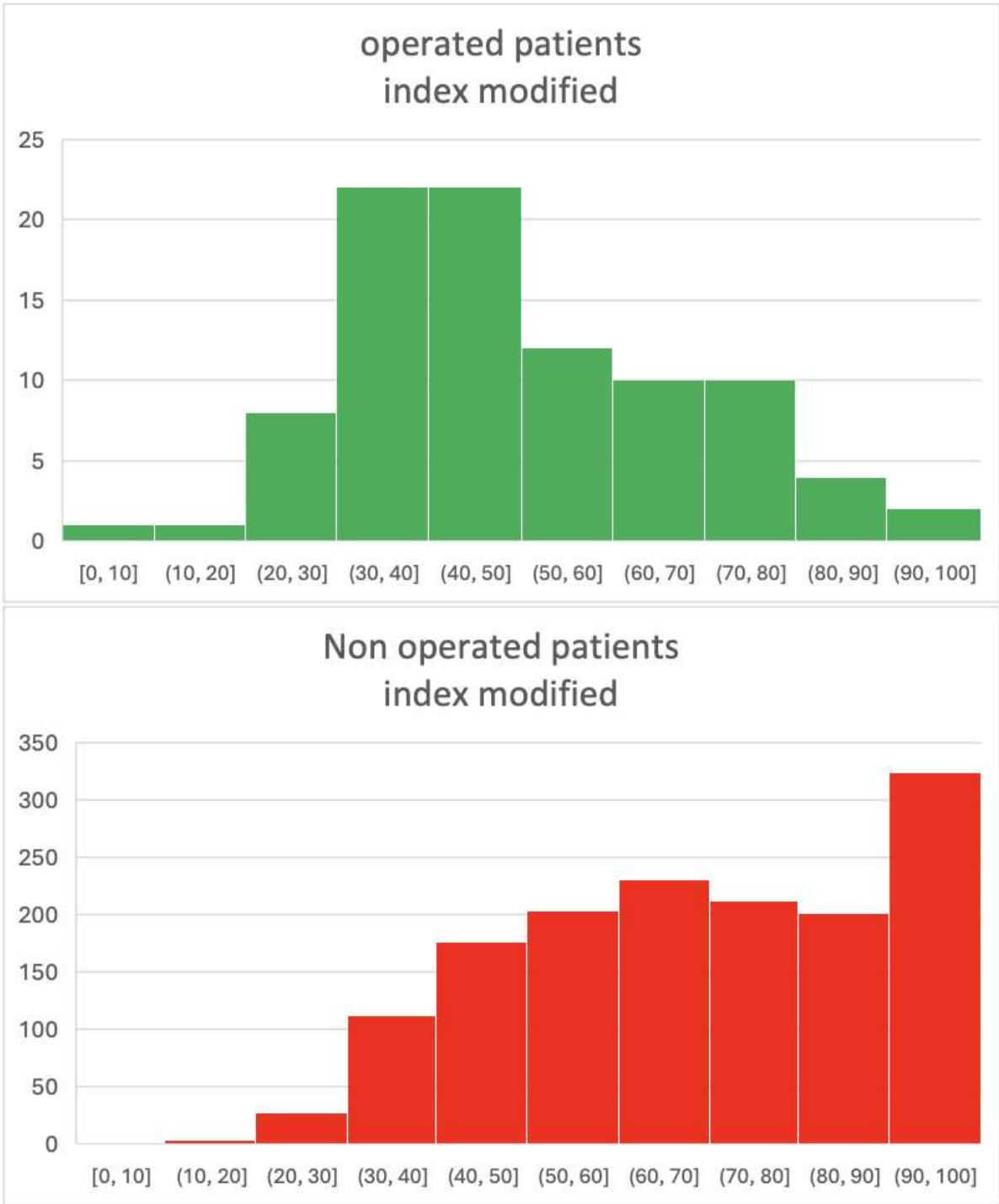


Figure 2

Total Knee Arthroplasty Recovery in Patients Above Patient Acceptable Symptom State Preoperatively

*Roberta Redfern - Zimmer Biomet - Pemberville, USA

Mike Anderson - Zimmer Biomet - Lehi, USA

Dave Van Andel - Zimmer Biomet - Grand Rapids, USA

Jason Cholewa - Zimmer Biomet - Warsaw, USA

Introduction

Patient acceptable symptom state (PASS) thresholds have been used as a marker of good functional outcome following total knee arthroplasty (TKA) but have not been applied to pre-operative subjective function. This study aimed to compare outcomes of patients above and below PASS thresholds prior to TKA.

Methods

Secondary analysis of a multicenter prospective observational study of patients prescribed a smartphone-based care management platform following TKA. Patient demographics, pain, satisfaction, and KOOS JR were compared between those above and below PASS pre-operatively (63.7 points) by student t-test. Logistic regression was used to quantify odds of decline or no improvement on KOOS JR at 1 year.

Results

Pre-operative and 1-year KOOS JR scores were available in 1,182 patients; 191 (16.2%) were above PASS prior to TKA. Those above PASS pre-operatively were older (66.5 ± 8.0 vs 63.9 ± 8.7 , $p=0.0002$) with lower BMI (29.9 ± 6.0 vs 31.9 ± 6.3 , $p<0.0001$) and lower pain scores (3.7 ± 1.9 vs 6.0 ± 1.9 , $p<0.0001$). Patients above PASS also demonstrated higher KSS satisfaction scores pre-operatively (20.7 ± 7.9 vs 12.1 ± 6.7 , $p<0.0001$). Those above PASS pre-operatively exhibited less pain reduction (-1.4 ± 2.5 vs -3.2 ± 2.6 , $p<0.0001$) and smaller improvements in satisfaction (9.9 ± 10.6 vs 16.5 ± 11.2 , $p<0.0001$) at 90 days. A greater proportion of those who presented above PASS experienced a decline or no improvement in KOOS JR at 1 year (13.1% vs 3.1%, $p<0.0001$). On logistic regression, considering baseline characteristics, those above PASS pre-operatively were 4.7 times more likely to report decline or no improvement in KOOS JR at 1 year (OR 4.71 95%CI 2.22 – 9.96, $p<0.0001$). Considering only those who reported no improvement or a decline in function, fewer of those who were above the PASS threshold pre-operatively experienced a knee-related event with the potential to impact patient reported function (14.3% vs 34.3%, $p=0.009$).

Conclusions

These findings suggest that patients above previously defined PASS thresholds who present for TKA appreciate less improvement in pain and satisfaction and are less likely to demonstrate improvements on KOOS JR post-operatively. Application of PASS thresholds pre-operatively may be useful for patient selection or guidance of patient expectations.

Can Patient Reported Outcome Measures Predict Length of Stay and Discharge Disposition Following Total Hip Arthroplasty?

*Jonathan Katzman - NYU Langone - New York, United States of America

Casey Cardillo - NYU Orthopedic Hospital - New York, USA

Muhammad Haider - NYU Orthopedic Hospital - New York, USA

Catherine Digangi - NYU Orthopedic Hospital - New York, USA

Akram Habibi - NYU Langone Orthopedic Hospital - New York, United States of America

Sophia Antonioli - NYU Langone - New York, USA

Ran Schwarzkopf - NYU Langone Medical Center Hospital for Joint Diseases - New York, USA

Joshua Rozell - NYU Langone Orthopedic Hospital - New York, USA

Introduction:

Patient-reported outcome measures (PROMs) offer clinicians valuable insight into patients' perceptions of their health and treatment outcomes. This study seeks to evaluate the predictive capability of various preoperative PROMs for prolonged hospital stays and discharge disposition following total hip arthroplasty (THA).

Methods:

A retrospective analysis was conducted on patients undergoing primary, elective unilateral THA at an urban academic center between 2017 and 2023, with at least 90 days of follow-up. Patients lacking preoperative Hip Injury and Osteoarthritis Outcome Score for Joint Replacement (HOOS JR) or Patient-Reported Outcomes Measurement Information System (PROMIS®) scores were excluded. Short-term outcomes, including length of stay (LOS) and discharge status, were collected. Receiver operating characteristic (ROC) curves and univariate logistic regression models were utilized to assess the predictive capacity of various preoperative measures (CCI, Risk Assessment Prediction Tool [RAPT] score, HOOS JR, and PROMIS).

Results:

In total, 2,725 THA patients with complete PROM data were analyzed. ROC curves indicated that RAPT (AUC: 0.734; 95% CI: [0.712, 0.755]), CCI (AUC: 0.643; 95% CI: [0.619, 0.666]), PROMIS Physical Health (AUC: 0.660; 95% CI: [0.637, 0.683]), and PROMIS Mental Health (AUC: 0.640; 95% CI: [0.617, 0.663]) were the most predictive of extended LOS (>2 days). ROC curves also revealed that RAPT (AUC: 0.863; 95% CI: [0.828, 0.899]), CCI (AUC: 0.721; 95% CI: [0.678, 0.764]), PROMIS Physical Health (AUC: 0.729; 95% CI: [0.685, 0.772]), and PROMIS Mental Health (AUC: 0.710; 95% CI: [0.666, 0.755]) were the strongest predictors of facility discharge. Univariate logistic regression models identified all demographic variables and preoperative PROM scores as significant predictors of both extended LOS and facility discharge, except for BMI.

Conclusion:

The findings of this study demonstrate the predictive potential of physical and mental health PROMs for short-term outcomes post-THA. PROMs may enhance risk stratification in THA planning.

Figures

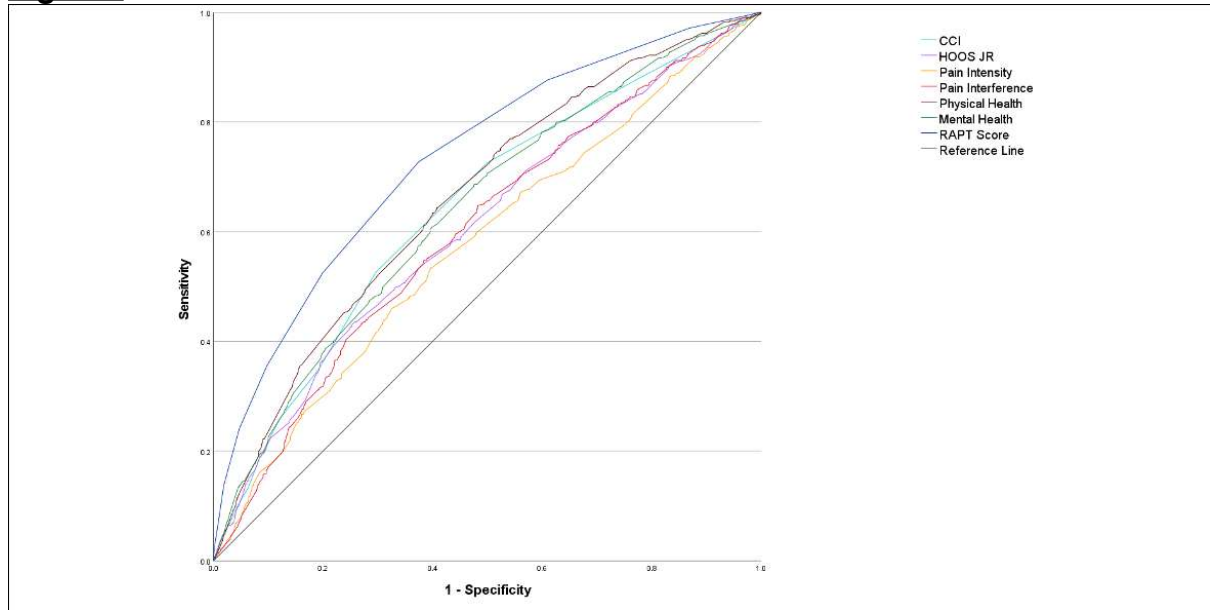


Figure 1

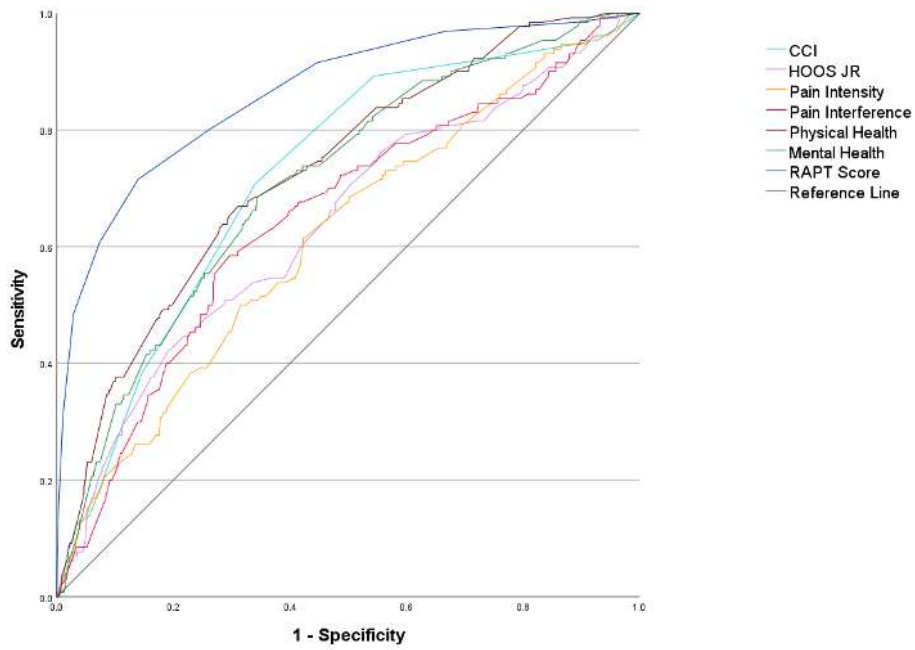


Figure 2

Serial Changes in Patient-Reported Outcome Measure at Long-Term Follow-Up After Total Knee Arthroplasty: A Systematic Review and Meta-Analysis

Jisu Park - SMG-SNU Boramae Medical Center - Seoul, Korea (Republic of)

Sung Jun Jang - Seoul National University College of Medicine Boramae Medical Center (SMG-SNU Boramae Medical Center) - Seoul, Korea (Republic of)

Hyunkwon Kim - SMG-SNU Boramae Medical Center - Seoul, Korea (Republic of)

Hyung Min Lee - Seoul National University Boramae Hospital - Seoul, Korea (Republic of)

Cho min soo - Seoul, Korea (Republic of)

Tae Woo Kim - Seoul National University College of Medicine, SMG-SNU Boramae Medical Center - Seoul, South Korea

Moon Jong Chang - SMG-SNU Boramae Medical Center - seoul, South Korea

Chong Bum Chang - Seoul National University College of Medicine - Seoul, South Korea

*Seung-Baik Kang - Boramae Medical Center/ Seoul National University College of Medicine - Seoul, South Korea

Background

Total knee arthroplasty (TKA) is a highly successful surgery for knee osteoarthritis patient. Long-term survival of primary TKA has been proven to be good. Nowadays, besides prosthesis survival and radiologic outcome, patient-reported outcome measure (PROM) is getting attention in evaluating the result of TKA. There are several studies reporting that PROM remained above preoperative state at long-term follow-up (f/u) after TKA, but its serial change has not been reported. Our study aimed to see the serial change of PROM after TKA during long-term f/u.

Methods

A systematic review and meta-analysis were performed to evaluate the serial change of PROM after TKA with at least seven years of f/u. PROM was subdivided into following subscales: function, pain, quality of life and objective. The f/u periods were divided into three groups: up to 1 year as short-term; up to 5 years as mid-term; up to 10 years as long-term. The focus was on the changes between each time period. Quality appraisal and data tabulation were performed using the predefined criteria. Data were synthesized by narrative review and multilevel random-effects meta-analysis using standardized mean differences. Heterogeneity was assessed with the τ^2 and I^2 statistics.

Results

Thirteen studies were included in the review, and ten studies were used for meta-analysis. The overall PROM remained constant until mid-term f/u, but tended to decline at long-term f/u. The multilevel meta-analysis revealed a decline of PROM at long-term f/u compared to mid-term f/u ($d_+ = -0.16$; 95% CI [confidence interval], -0.32 to -0.00). When analyzed by subscale, pain score improved from short-term to mid-term f/u ($d_+ = 0.22$; 95% CI, 0.09 to 0.35) and function score decreased from mid-term to long-term f/u ($d_+ = -0.27$; 95% CI, -0.49 to -0.06). Patient satisfaction remained relatively constant throughout the whole period of time.

Conclusion

Pain score showed improvement by mid-term f/u and it was maintained through long-term f/u. Functional score and total PROM score decreased after mid-term f/u, but most patients remained satisfied during long-term f/u.

Figures

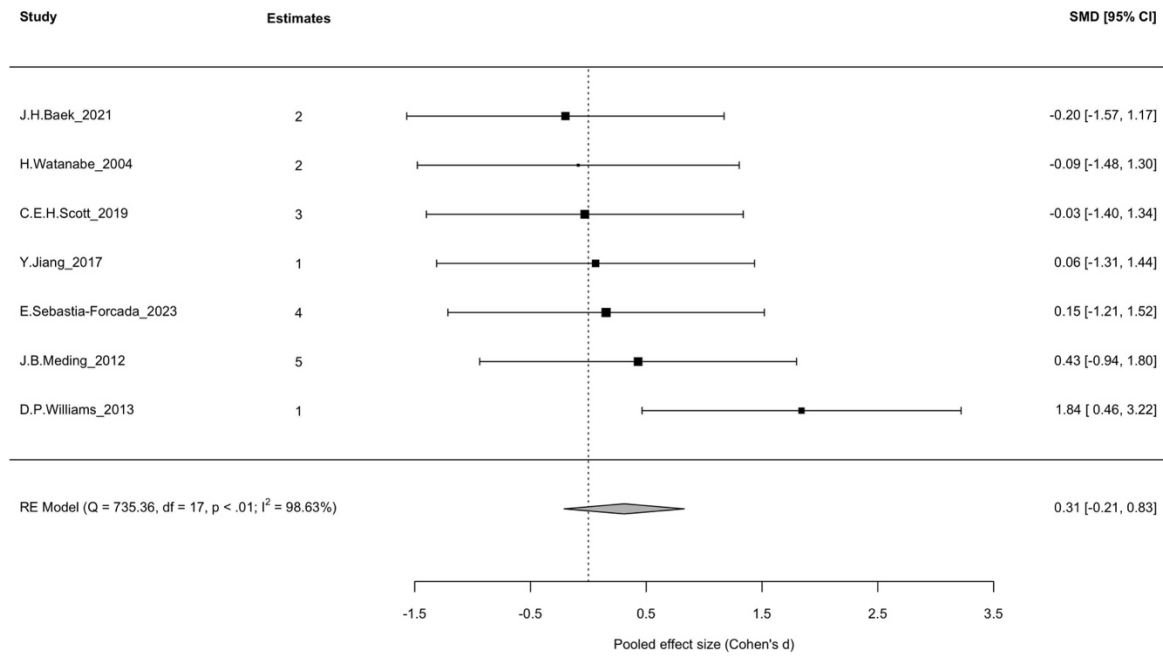


Figure 1

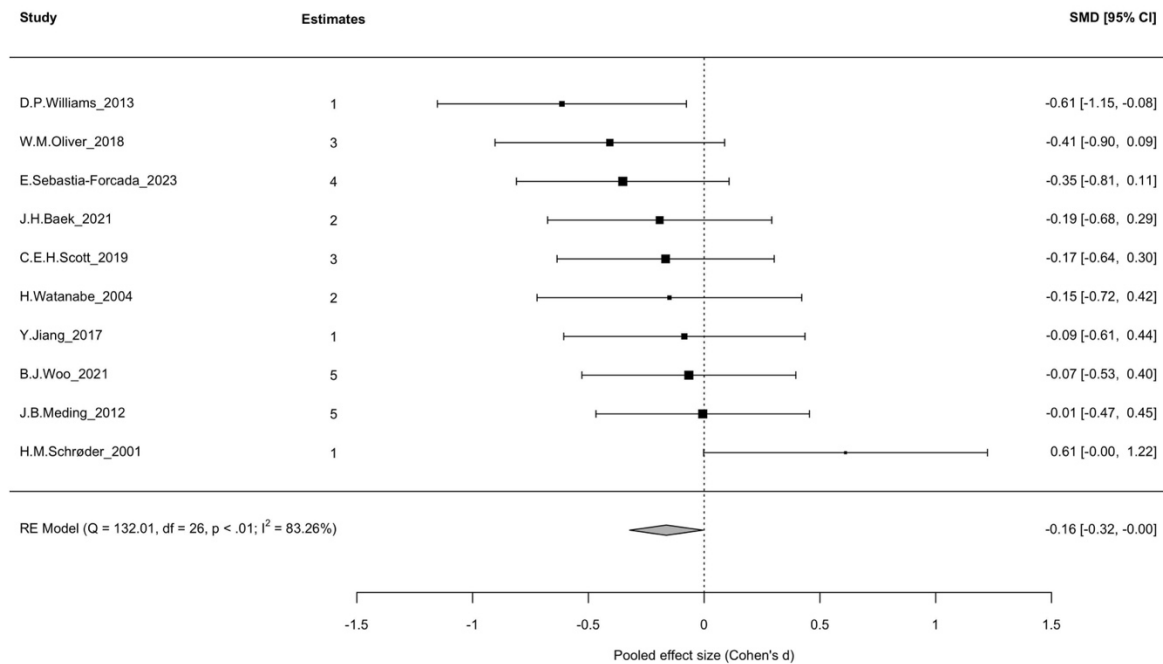


Figure2

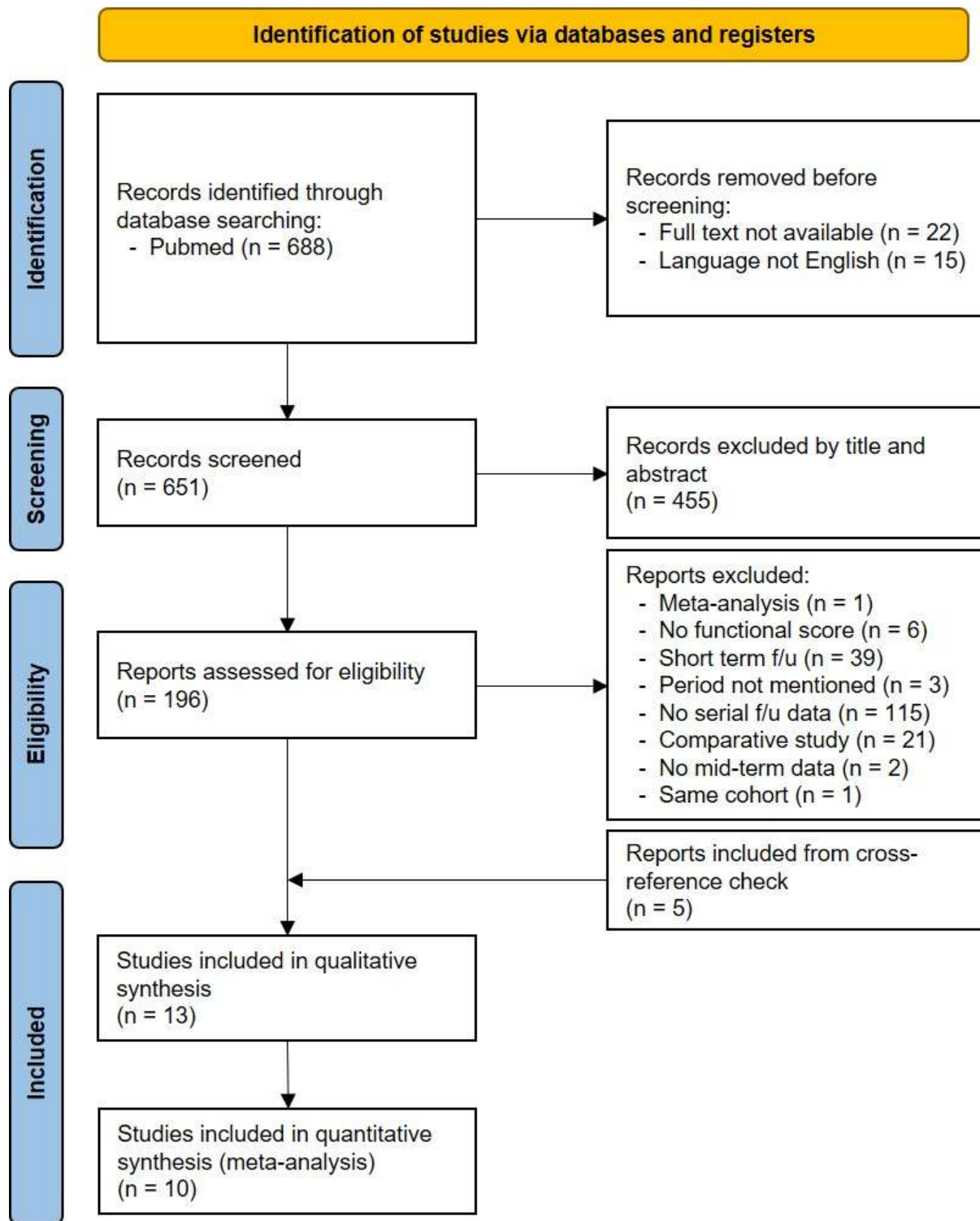


Figure 3

Lack of Standardization in TKA Kinematics Studies Hinders Big Data Analysis: A Call for Unified Protocols

*Andrew Jensen - University of Florida - Gainesville, USA

Scott Banks - University of Florida - Gainesville, USA

Introduction: Total knee arthroplasty kinematics have been studied and measured in research settings for over three decades, allowing unparalleled exploration of joint-level dynamics to assist with implant design, wear prediction, and post-operative outcome. However, despite its utility in limited studies (typically involving fewer than 50 patients), TKA kinematics data has not been widely incorporated into large-scale datasets suitable for advanced machine learning algorithms.

Methods: Hand-labeled data from nine different TKA kinematics studies comprising 123 patients was collected and analyzed. Image sequences were paired by movement description (lunging, walking, sit-to-stand, etc) and each kinematics measurement was filtered and interpolated to provide 100 data points for signal analysis. Dimensionality reduction techniques were employed to simplify the feature space, enabling the use of basic classification and regression algorithms. However, at this point, it was found that the data were not sufficiently standardized to provide meaningful interpretation across different studies and research groups.

Results: Three main issues were encountered while attempting to process this data, all stemming from a lack of standardization in kinematics measurements:

1. Different research groups giving the same or similar names to categorically different movements. Additionally, some papers do not explicitly mention the protocol used for each movement, instead providing only the name.
2. There are no standardized set of movements to measure. Among the nine studies explored, for any given movement, at most two studies both measured the same movement.
3. Different groups are reporting kinematics at different resolutions. A denser sampling of the flexion arc, particularly in the ambulatory range, has revealed significant variation of kinematics with specific activities.

Discussion: The first issue likely comes from the fact that different movements are in fact, ambiguous. For example, using regular language, the distinction between a deep knee bend and a deep lunge can be slightly arbitrary. A standardized set of descriptions and protocols for kinematics studies would need to be established and followed to mitigate these issues. The second issue arises from the fact that kinematics measurements do not form any part of a standard of care. The movements to measure and the data to report are entirely up to the discretion of the researcher. To overcome this, a standard set of movements and activities to measure could be reported and followed. The last issue stems likely stems from the time required to generate a kinematics report. Manual methods of kinematics measurement are extremely time consuming, and the potential upside for reporting extremely detailed dynamics might not seem worth the necessary time investment. The adoption of rapid, automated measurement tools could help address this problem.

Conclusion: For TKA kinematics to be effectively utilized in the realm of "big data," enabling powerful algorithms to identify more precise and predictive correlations between joint dynamics and clinical outcomes, the research community might adopt a standardized set of measurements and activities to ensure data homogeneity. To

overcome the time-consuming nature of measuring this data, novel methods of autonomous kinematics measurement can be used.

Lateral and Medial Laxity, but Not Gap Balance, Is Associated With Objectively Measured Post-Operative Gait Quantity and Quality

*Roberta Redfern - Zimmer Biomet - Pemberville, USA

Joseph Brook - Zimmer Biomet - London, United Kingdom

Mike Anderson - Zimmer Biomet - Lehi, USA

Adam Henderson - Zimmer Biomet - Winterthur, Switzerland

Karl Surmacz - Zimmer Biomet - Swindon, United Kingdom

Jason Cholewa - Zimmer Biomet - Warsaw, USA

Introduction

Evidence has suggested that intra-operative data collected by robotic systems during total knee arthroplasty (TKA) may be associated with post-operative outcomes. The study aimed to determine whether gap laxity and balance were associated with post-operative gait quantity and quality in patients who were provided a smartwatch for accurate collection of pre- and post-operative step counts.

Methods

A commercial database including anonymized data of 2,820 patients who underwent TKA with robotic assistance and utilized a digital care management platform with smartwatch prior to and following surgery were analyzed. Intra-operative data were captured from the robotic system; pre- and post-operative gait data was collected by a smartphone and smartwatch. Groups were categorized according to the degree of robotically measured gap laxity in 90° and 0° of flexion as follows: <0.5mm, 0.5 – 1.5, 1.5 – 2.5 mm, 2.5 – 3.5mm, ≥3.5mm. Balance was categorized in similar fashion considering the difference in gaps between compartments. Changes in step counts, gait speed, and presence of gait asymmetry from pre-operative were compared between groups at 14-, 30-, and 90-days post-operative by Kruskal Wallis tests. Median changes and interquartile ranges (IQR) are reported.

Results

Knees that were tight (<0.5mm) at 0° final flexion in the lateral compartment demonstrated the smallest reduction in step counts (-1378, IQR 2163, p=0.03, Figure 1), while those that were tight in the medial compartment had the largest reduction (-1948, IQR 2187, p=0.02) at 14 days. Medial compartment tightness continued to be associated with reduction in step counts throughout 90 days, where those with tight medial spaces did not reach pre-operative activity levels, and those with 2.5-3.5mm gap demonstrated the largest improvement in step counts (542, IQR 2889, p=0.005, Figure 2). Gait speed reduction at 14 days was greatest in those with tight medial spaces (-0.267, IQR 0.185, p=0.003) and increase in presence of asymmetry was greatest in those with tight and loose (≥3.5mm) lateral spaces at 14 days post-operative (0.532, IQR 0.458, p=0.03), but these trends did not continue through 90 days. Balance between compartments was not associated with gait metrics at any timepoint.

Discussion

Recent studies have focused on determining whether intra-operative decisions impact TKA outcomes. Our study demonstrates the ability of an integrated system to link intra-operative robotic data with objectively measured post-operative gait metrics. The findings of this analysis suggest that tightness of the medial and lateral compartments may be associated with gait quantity and quality post-operatively, though further research is needed to confirm these findings.

Figure 1. Violin plot demonstrating change in step count at 14 days post-operative between lateral laxity groups at 0° final flexion.

Figure 2. Violin plot demonstrating change in step count at 90 days post-operative between medial laxity groups at 0° final flexion.

Figures

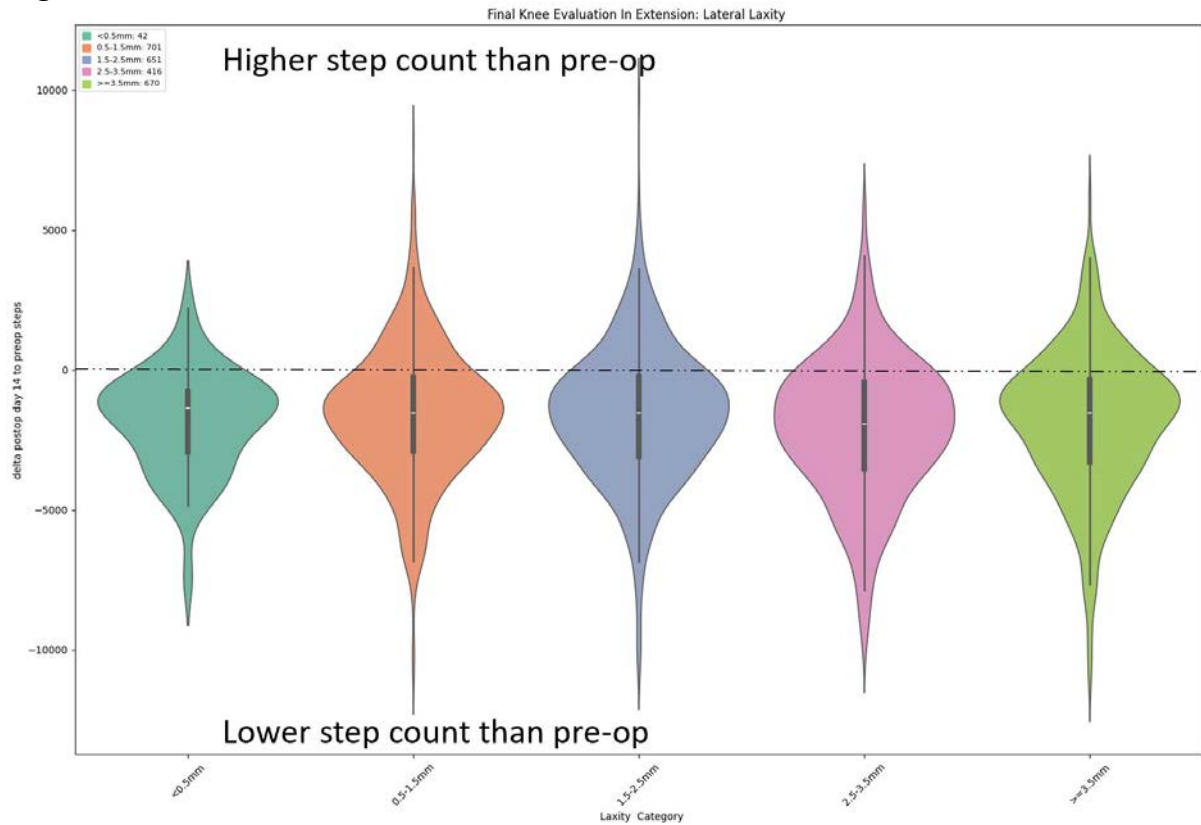


Figure 1

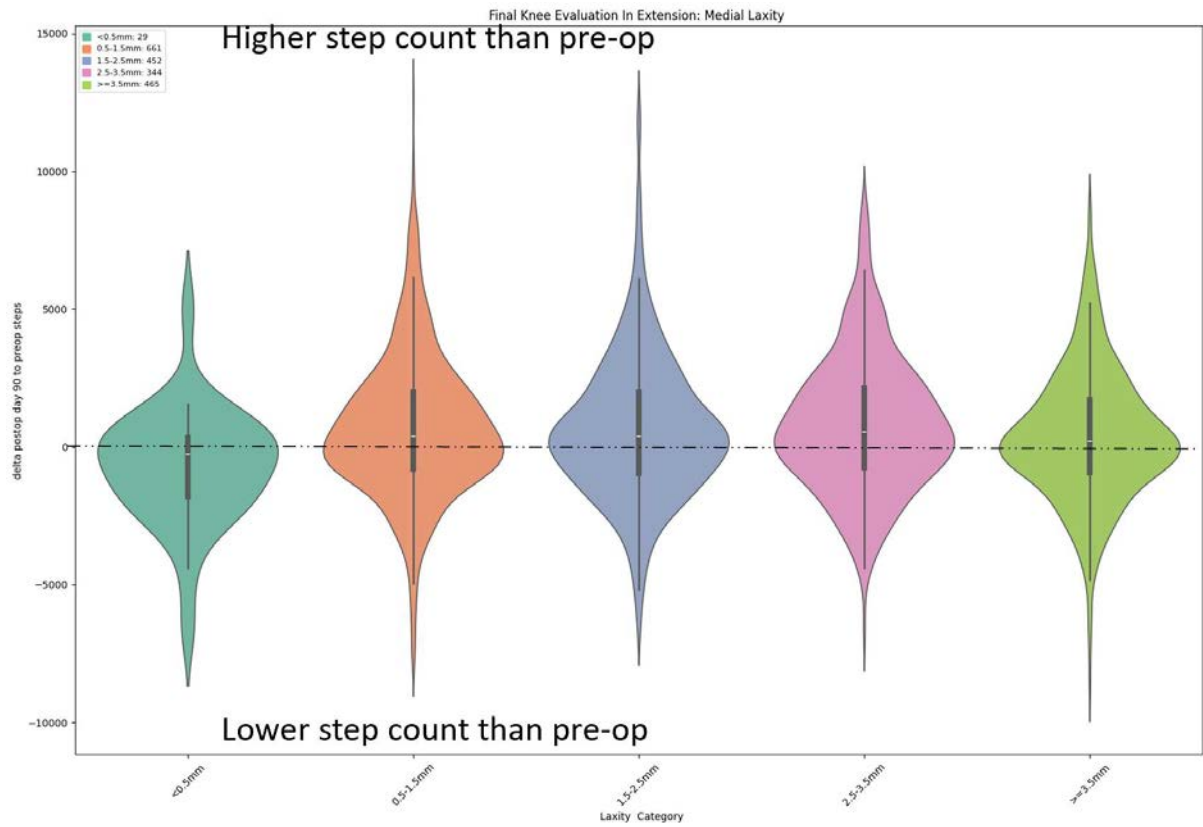


Figure 2

Robotic Tensioning Provides a More Reproducible Assessment of Soft Tissue Laxity and Balance Compared to Manual Methods

*Alex Orsi - Corin - Raynham, USA

Christopher Plaskos - Corin - Raynham, USA

John Keggi - Orthopaedics New England - Middlebury, USA

Paramjeet Gill - UCSF-Fresno - Fresno, USA

Simon Coffey - Nepean Hospital - Sydney, Australia

INTRODUCTION:

Balancing the soft tissue envelope during total knee arthroplasty (TKA) plays a critical role in achieving optimal joint stability and functional outcomes. Robotically controlled ligament balancing in TKA allows for precise and reproducible measurements; however manual soft-tissue assessment remains the standard of care. This manual process is known to be subjective due to several factors such as surgeon preferences, assessment technique, hand dominance, and variation in patient factors such as native soft tissue laxity and stiffness, patient weight, and BMI. This study aims to compare these two modalities with the goal of understanding which measurement technique is more reliable.

METHODS:

100 consecutive robotic-assisted TKA were retrospectively reviewed from six surgeons (600 total). During final trialing laxity and mediolateral (ML) balance was assessed manually and using the robotic ligament tensioner seen in Figure 1. ML balance is calculated as medial – lateral laxity. The manual and robotic data relative to the plan were compared for each surgeon. For both robotic and manual assessments, differences in ML balance and Δ ML (manual-robotic) balance were compared between right and left knees. Comparisons were performed at 10°, 30°, 45°, 60°, 75°, and 90°

RESULTS:

All surgeons had poorly correlated (ICCs<0.46) and significantly different ML balance between manual and robotic from 45° to 90° flexion, Figure 2. Four surgeons manually measured more relative medial laxity, while two surgeons manually measured more lateral laxity compared to the robot, Figure 2. Five of six surgeons showed significant differences between operative leg side manual assessments throughout flexion ($p<0.05$). Two surgeons showed significant differences between right and left leg robotic assessments at 10° and 30° ($p<0.05$). Five surgeons had significant differences in Δ ML balance between operative leg sides ($p<0.05$), Figure 3. Surgeon-specific variations were evident in terms of relative medial or lateral laxity.

CONCLUSIONS:

Manual ML balance assessment is poorly correlated with robotic assessment, is significantly different and further from the surgical plan than robotic assessment, and less reproducible side to side. Individual surgeons exhibit unique patterns in how these measurements differ. This indicates that robotic balance assessment provides a more reproducible and reliable measurement and should be recommended as standard of care to help standardize ligament laxity and balance measurements.

Figures

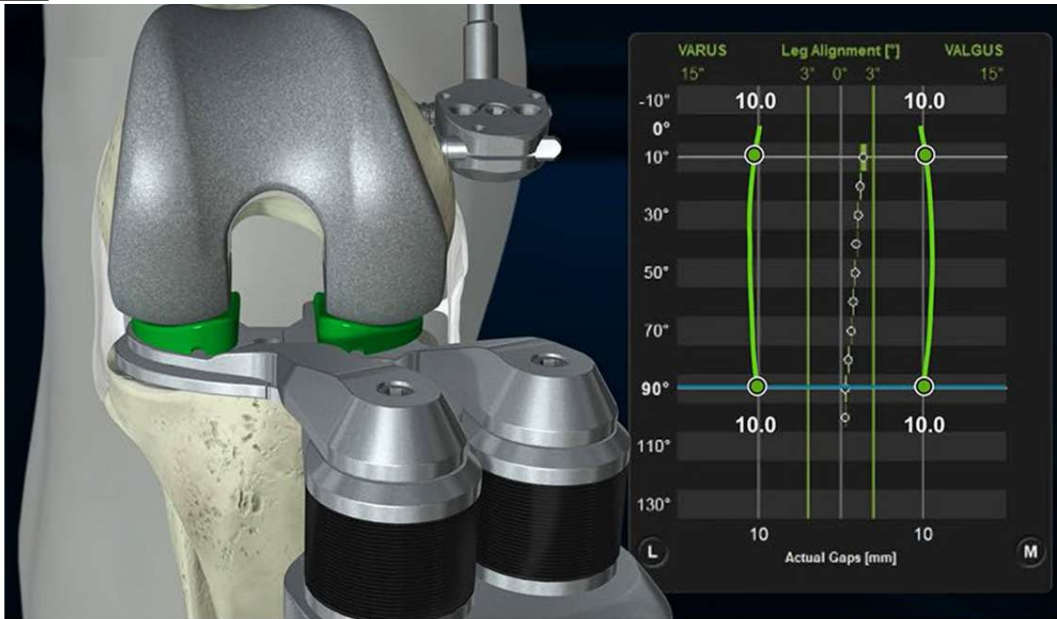


Figure 1: A robotic ligament tensioner is used to collect laxity data during final trialing. Mediolateral balance is calculated as medial - lateral laxity.

Figure 1

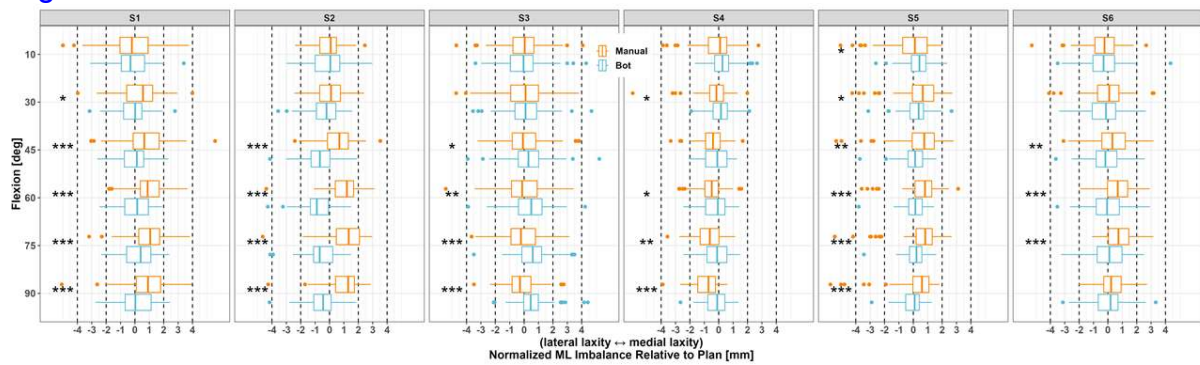


Figure 2: Manual (orange) and robotic (blue) comparisons throughout flexion for all surgeons of ML imbalance relative to the plan. Statistically significant differences are indicated by '***' = $p \leq 0.001$; '**' = $p \leq 0.01$; '*' = $p \leq 0.05$.

Figure 2

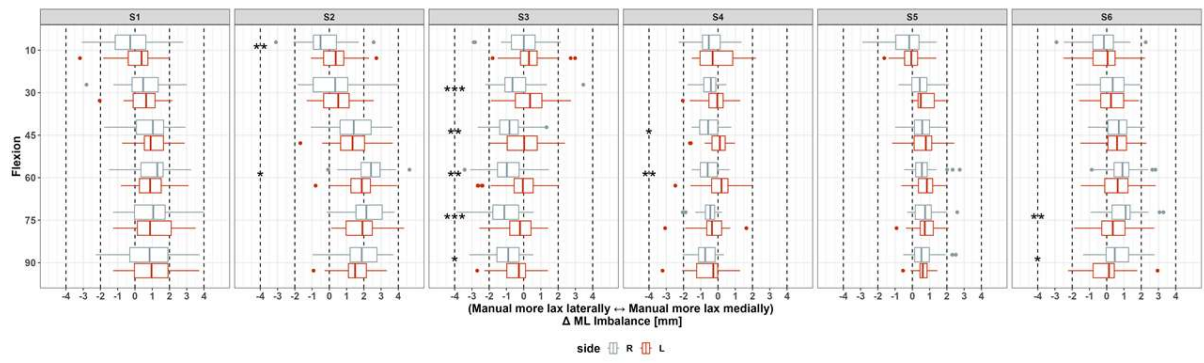


Figure 3: Comparing ΔML balance (manual – robotic) between operative leg side throughout flexion for all surgeons. Statistically significant differences are indicated by ** = $p \leq 0.001$; *** = $p \leq 0.01$; ** = $p \leq 0.05$.**

[Figure 3](#)

Does Patient Phenotype Predict Knee Laxity in Total Knee Arthroplasty?

*Azhar Ali - Stryker Orthopaedics - Mahwah, USA

Yogesh Mittal - The Orthopaedic Center - Tulsa, USA

Paul Jacob - Oklahoma Joint Reconstruction Institute - Oklahoma City, USA

Robert Marchand - Ortho Rhode Island - South County, USA

Introduction: Patient-specific surgical planning remains a challenge in total knee arthroplasty (TKA) due to variation in patient anatomy and soft tissue balance. While methods have been established to classify patient phenotype using CPAK [1], the relationship between patient's anatomy and initial soft tissue knee laxity remains unknown. The goal of this study was to classify the phenotype of patients who have undergone robotic-assisted surgery using CPAK and a novel JLO classification, and to evaluate the relationship between patient phenotype and initial knee laxity prior to bone resection.

Methods: 777 patients underwent robotic-arm assisted TKA surgery. Using CT, patient phenotypes were classified according to CPAK (Figure 1a). Like CPAK, nine phenotypes were established, but defined according to extension/flexion joint line obliquity (JLO) and extension/flexion hip-knee-ankle (HKA) angle (Figure 1bc). Extension JLO was defined by the proximal tibial angle (MPTA) and distal femoral angle (LDFA) (varus(+), valgus(-)). Flexion JLO was defined by MPTA and the femoral posterior condylar axis. While CPAK computes the arithmetic HKA (MPTA – LDFA), extension and flexion HKA alignment were determined using the varus-valgus angle between the femur and tibia mechanical axes during intra-operative assessment at 0° and 90° with no surgeon-applied stress. Initial knee laxities were recorded as bone-to-bone joint distances in medial and lateral compartments at extension (10°) and flexion (90°) during maximum varus-valgus applied stresses. Patient phenotype, extension and flexion JLO were correlated to intra-operative knee laxity assessments.

Results: Patient phenotype, according to JLO and mechanical HKA alignment, had a strong linear relationship in comparison to CPAK ($R^2=0.69$ extension, and $R^2=0.59$ flexion, $p<0.05$), indicating JLO and limb alignment are correlated (Figure 1). When comparing extension knee laxity assessments to extension JLO, there were weak correlations between the anatomy and initial knee laxity in the medial and lateral compartments (Figure 2). Similarly, there was a weak correlation between flexion knee laxity assessments and flexion JLO across the patient population for both compartments.

Conclusion: The current study evaluated an alternative method for patient classification to CPAK, which showed that JLO can be predictive of the mechanical HKA alignment in extension and flexion. Mechanical HKA alignment has implications on the distribution of joint loading, which may be an important consideration for a well-balanced knee. Patient phenotypes had no correlation to initial knee laxity, indicating anatomy may not be predictive of soft tissue laxity. This finding highlights the importance of intra-operative balancing assessments to address variations in initial knee laxity for patient-specific surgical planning.

Figures

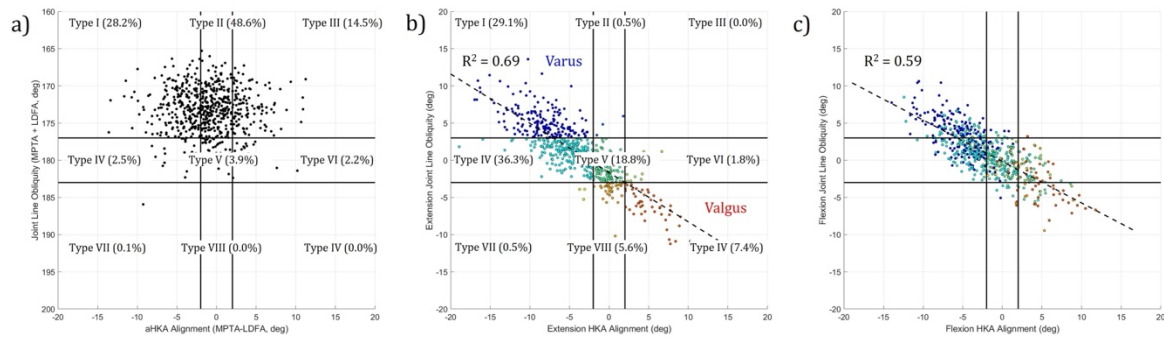


Figure 1: a) Patient phenotypes described according to CPAK classification, b) extension JLO vs. extension HKA alignment (middle), and c) flexion JLO vs. flexion HKA alignment. Individual cases are color-coded for nine phenotypes according to extension JLO-extension HKA relationship (varus to valgus)

Figure 1

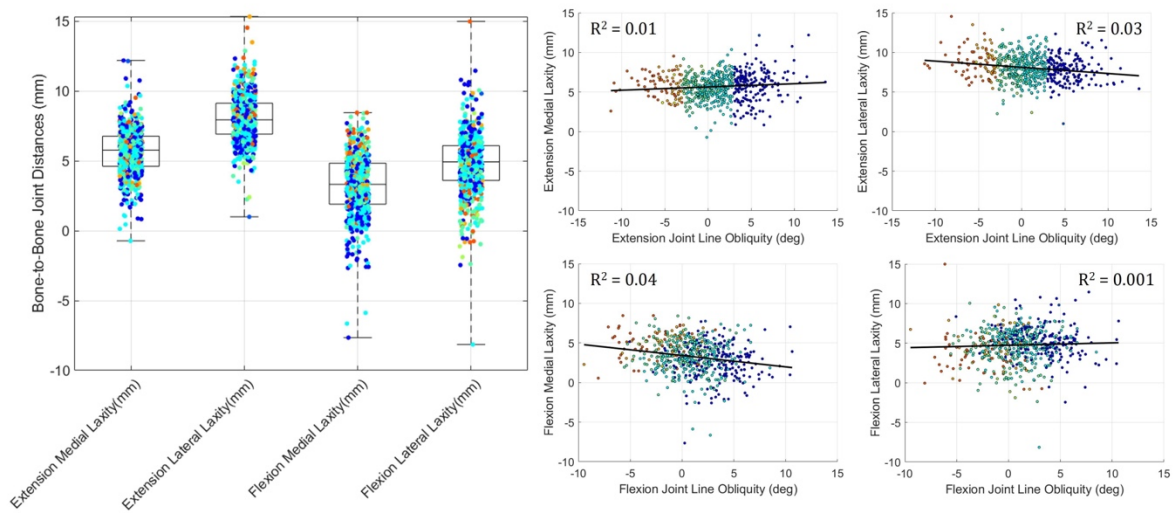


Figure 2: Box plot representing bone-to-bone joint distances during intra-operative knee laxity assessment prior to bone resections (left), and relationship between extension and flexion JLO, and intra-operative initial knee laxity assessments (right). Individual cases are color-coded for nine phenotypes according to extension JLO-extension HKA relationship (varus to valgus)

Figure 2

Effect of Simulated PCL Fiber Release on Compartmental Contact Forces in Cruciate Retaining Total Knee Arthroplasty: A Computational Study

*Reza Pourmodheji - Hospital for Special Surgery - New York, United States of America

Cynthia Kahlenberg - Hospital for Special Surgery - New York City, USA

Brian Chalmers - Hospital for Special Surgery - New York City, USA

Eytan Debbi - Hospital for Special Surgery - NY, USA

William Long - Hospital for Special Surgery - New York, USA

Timothy Wright - Hospital for Special Surgery - New York, USA

Geoffrey H Westrich - Hospital for Special Surgery - New York, USA

David J. Mayman - Hospital for Special Surgery - New York, USA

Peter Sculco - Hospital for Special Surgery - New York, USA

Carl Imhauser - USA

Introduction: In cruciate retaining (CR) total knee arthroplasty (TKA), partial or total release of the PCL is often used intraoperatively to reduce excessive PCL tension in flexion. The effect of complete or selective PCL release on femoral rollback was recently elucidated in a computer model; however, the effect of releasing the PCL on contact forces acting on the medial and lateral compartments of the tibia is not well understood. Therefore, we employed a computational model to quantify how releasing the PCL fibers affects the articular contact forces at the medial and lateral compartments at 90° of the knee flexion.

Methods: Computational models derived from nine independent cadaveric left knees (five males, four females; age: 63.7±10.5 years) were virtually implanted with CR-TKA (Persona, Zimmer-Biomet). The model utilized 33 spring elements to represent the geometry and nonlinear stiffness of the following major ligaments: PCL and the collateral and capsular ligaments. The PCL was represented by seven spring elements: four for the posteromedial bundle (PMB) and three for the anterolateral bundle (ALB). Passive flexion was simulated for the PCL-retained condition and after serially releasing each fiber of the PCL starting from the most anterior fiber of the ALB to the most posterior fiber of the PMB (Fig. 1). The contact force on the medial and lateral compartments of the tibial insert was calculated after releasing each fiber and reported as median and quartiles. Outcomes were compared for each condition using Kruskal-Wallis with Bonferroni post hoc correction ($\alpha = 0.05$)

Results: The largest reduction in contact force occurred after sectioning the ALB together with the most anterior fiber of the PMB (i.e., selective release of the PCL central fibers) by 22 N [20.2, 36.4] ($P=0.02$) medially and 11.0 N [8.2 39.5] ($P=0.04$) laterally (Fig. 2). The computational model demonstrated that releasing the PCL created an asymmetric reduction of contact forces.

Conclusion: Releasing the PCL fibers reduced both medial and lateral contact forces. The largest reduction in contact forces occurred after resecting the central fibers of the PCL. Interestingly, the reduction in contact force was asymmetrical with twice the reduction on the medial compartment. Based upon this study, after complete or selective release of the PCL, surgeons should consider reassessing knee balance of the medial and lateral compartments in 90° of knee flexion.

Figures

Cadaver image from Cousin et. al. (2021) *Orthop. Traumatol-Sur*

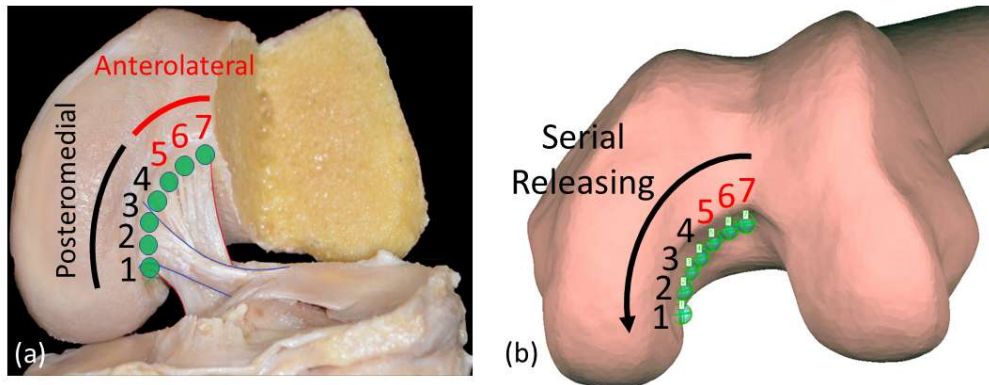


Figure 1: Femoral insertions of PCL fiber numbered from 1 to 7 where fibers 1-4 represent the posteromedial and fibers 5-7 represent the anterolateral bundle (a). The serial release of the fibers in the computational modeling was performed from fiber 7 to fiber 1.

Figure 1

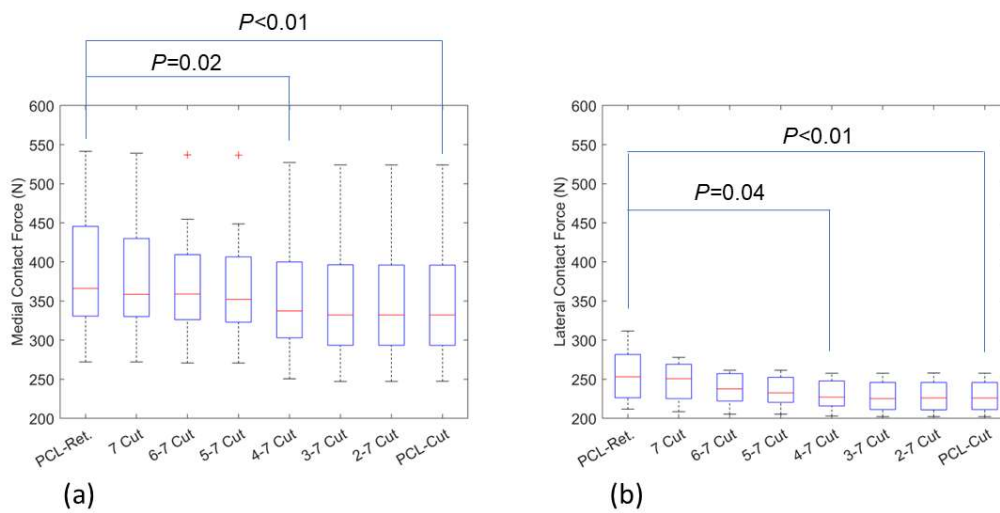


Figure 2: Boxplots of the contact forces for each posterior cruciate ligament (PCL) fiber release for (a) medial compartment, (b) lateral compartment. PCL-Ret is PCL-retained. Red lines and boxes represent medians and quartiles, respectively. The whiskers extend to the most extreme data points not considered outliers. An outlier (red cross) is a value that is more than 1.5 interquartile range (IQR) away from the top or bottom edge of the box.

Figure 2

The Impact of Surgical Workflow on Bone Cut Parameters Evolution in Total Knee Arthroplasty - Transitioning From Measured Resection to Gap Balancing Surgical Workflow

*Laurent Angibaud - Exactech, Inc. - Gainesville, USA

Prudhvi Tej Chinimilli - Exactech - Gainesville, USA

Amaury Jung - Blue Ortho - La Tronche, France

François Boux de Casson - Blue-Ortho - Meylan, France

INTRODUCTION

A goal of total knee arthroplasty (TKA) is to achieve balanced gaps, however, there exists debate regarding the proper surgical workflow to achieve such an objective. These workflows vary based on the order of bone cuts as well as the definition of the references. For example, the femur-first measured resection (MR) workflow relies on anatomical landmarks, whereas the tibia-first full gap balancing (GB) workflow leverages collateral ligament tension to define the bone cuts. This study highlights variations in targeted implant position and orientation for surgeons transitioning from MR to GB workflow.

METHODS

This study involved 8 surgeons using a dedicated TKA enabling technology, who transitioned their surgical workflow from MR to GB. A total of seven targeted femoral cut parameters were considered for both workflows. Four parameters were related to position: distal resection, posterior medial resection, posterior lateral resection, and anterior offset, while three other parameters were related to orientation: flexion/extension, varus/valgus, and axial rotation. The evaluation was conducted at three timepoints: the last 20 TKAs with MR workflow (MR proficient), the first 20 TKAs with GB workflow (GB learning), and the last 20 TKAs with GB workflow (GB proficient). Comparing MR proficient and GB learning groups shed light on the technique change, while comparing GB learning and GB proficient groups revealed the impact of gaining experience. Non-parametric Fligner-Killeen (FK) test assessed variances, yielding corresponding p-values. Post FK-test, Wilcoxon signed-rank tests enabled pairwise comparisons between groups to identify significant differences. Finally, standard deviations (SDs) within each surgeon for each parameter were compared to evaluate linear transition of cut parameters range, assessing if GB learning group SD surpassed MR proficient group SD and if GB proficient group SD exceeded GB learning group.

RESULTS

Among the 8 surgeons, it was found that between 3 and 4 exhibited statistically significant variance differences for position parameters, while 7 showed significant differences for flexion/extension and varus/valgus angles. Results from Wilcoxon signed-rank tests highlighted a notably significant difference in group distribution for orientation parameters, particularly femoral implant axial rotation. Overall, both position and orientation parameters demonstrate a trend: surgeons generally had lower standard deviation (SD) in the MR proficient group compared to the GB groups (learning and proficient). When comparing GB learning and GB proficient groups, 4 and 5 surgeons had higher SD in the GB proficient phase for position and orientation parameters, respectively.

DISCUSSION

The study observes that as surgeons shift from MR to GB groups, there's a tendency to widen both position and orientation cut parameter ranges. Notably, about half of the surgeons continue this trend with experience, evident in the SD values of the GB learning and GB proficient groups. This underscores the significant influence of surgical technique on femoral cut parameters, highlighting the importance of awareness for surgeons transitioning from MR to GB. However, the study's limitation lies in the relatively small sample size in each group, suggesting that a larger sample would provide more comprehensive insights.

Figures

Figure 1: Position parameters mean and SD for the 8 surgeons. Pairwise comparisons statistical significance: NS ($p > 0.05$), * ($p \leq 0.05$), ** ($p \leq 0.01$), *** ($p \leq 0.001$)

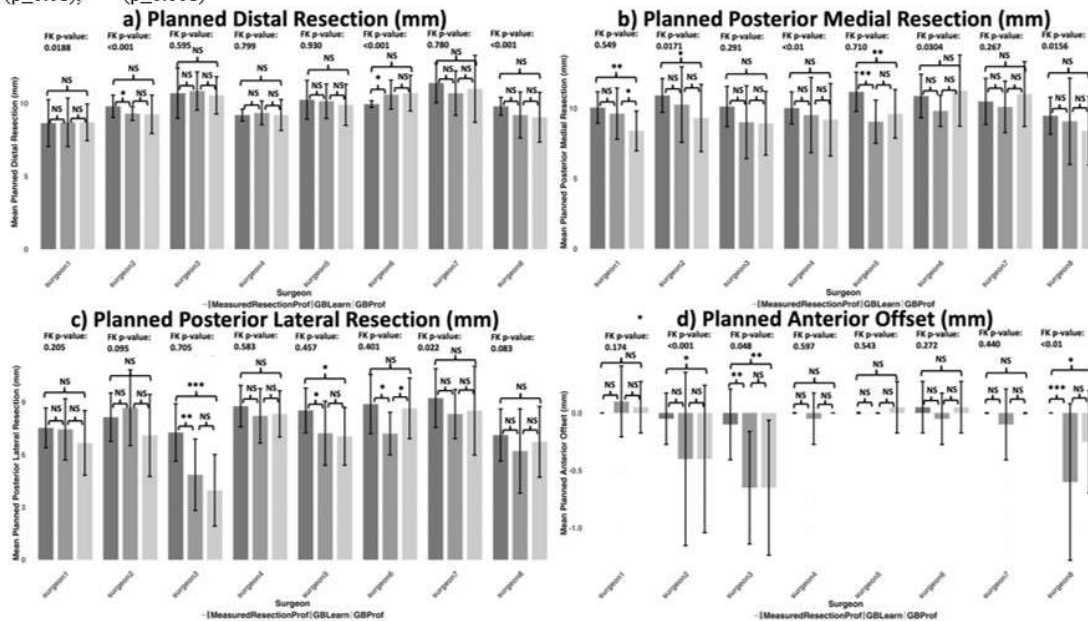


[Figure 1](#)

Figure 2: Orientation parameters mean and SD for the 8 surgeons. Pairwise comparisons statistical significance: NS ($p > 0.05$), * ($p \leq 0.05$), ** ($p \leq 0.01$), *** ($p \leq 0.001$)

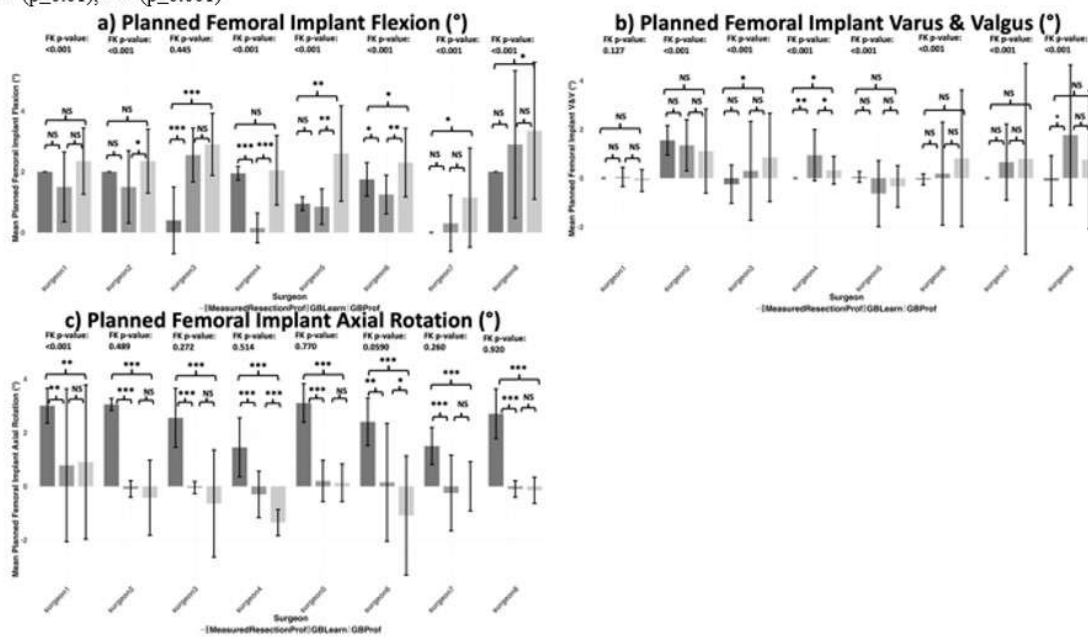


Figure 2

Role of Femoral Condylar Geometry in Loading of the MCL and PCL in Cruciate Retaining Total Knee Arthroplasty: A Computational Approach

*Reza Pourmodheji - Hospital for Special Surgery - New York, United States of America

Cynthia Kahlenberg - Hospital for Special Surgery - New York City, USA

Brian Chalmers - Hospital for Special Surgery - New York City, USA

Eytan Debbi - Hospital for Special Surgery - NY, USA

William Long - Hospital for Special Surgery - New York, USA

Timothy Wright - Hospital for Special Surgery - New York, USA

Geoffrey H Westrich - Hospital for Special Surgery - New York, USA

David J. Mayman - Hospital for Special Surgery - New York, USA

Peter Sculco - Hospital for Special Surgery - New York, USA

Carl Imhauser - USA

Introduction: Appropriately tensioning the medial collateral and the posterior cruciate ligaments (MCL and PCL, respectively) are critical to achieving knee stability in cruciate retaining (CR) total knee arthroplasty (TKA) [1]. Femoral anatomy including the geometric features of the medial condyle like its anterior-posterior (AP) offset and the insertion location of the MCL are highly variable; yet, a knowledge gap remains as to how these anatomical variations relate to loading of the MCL and PCL in flexion. We previously defined a novel geometric ratio (the “MCL ratio”) to describe the anatomy of the medial femoral condyle accounting for these geometric features and the posterior and distal femoral bony cuts. Then, we asked: Is the MCL ratio related to MCL and PCL force at 90° of flexion?

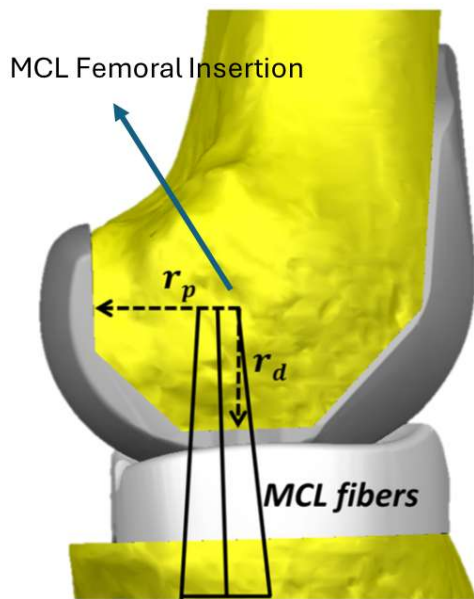
Methods: Computational models derived from nine independent cadaveric left knees (five males, four females; age: 63.7±10.5 years) were virtually implanted with CR-TKA (Persona, Zimmer-Biomet). The computational model utilized 33 line-elements to represent the superficial MCL (sMCL), the PCL, lateral collateral, and capsular ligaments. The “MCL ratio,” was defined as the proportion of the distance of the femoral insertion of the anterior aspect of the medial sulcus of the femur, where the anterior fiber of the sMCL is located, to the posterior and to the distal cuts (Fig. 1). The knee was flexed from 0 to 90° under 500 N of compression to represent a test of passive flexion.

Results: The sMCL force at 90° of flexion was positively correlated with the MCL ratio ($r^2 = 0.96$, $P < 0.01$) (Fig. 2a), but the PCL force was not ($p > 0.05$) (Fig. 2b).

Conclusion: The MCL ratio is strongly associated with the force carried by the sMCL but not by the PCL in a computational model of CR TKA. This finding can help explain the surgical challenge in simultaneously balancing both the MCL and PCL in CR-TKA [3]. These findings may inform surgical techniques for MCL balancing. Future clinical studies are needed to determine optimal tension target of the MCL, but utilization of this ratio for implant placement may help surgeons achieve this target.

References: [1] Kahlenberg, C., JBJS, 2024, [2] Kia, M., CORR, 2018, [3] Mihalko, W., JAAOS, 2009.

Figures



$$\text{MCL Ratio} = \frac{r_p}{r_d}$$

Figure 1: The anatomical description of the MCL ratio. r_p is the distance of the superficial medial collateral ligament (sMCL) from the posterior cut and r_d is the distance from the distal cut.

Figure 1

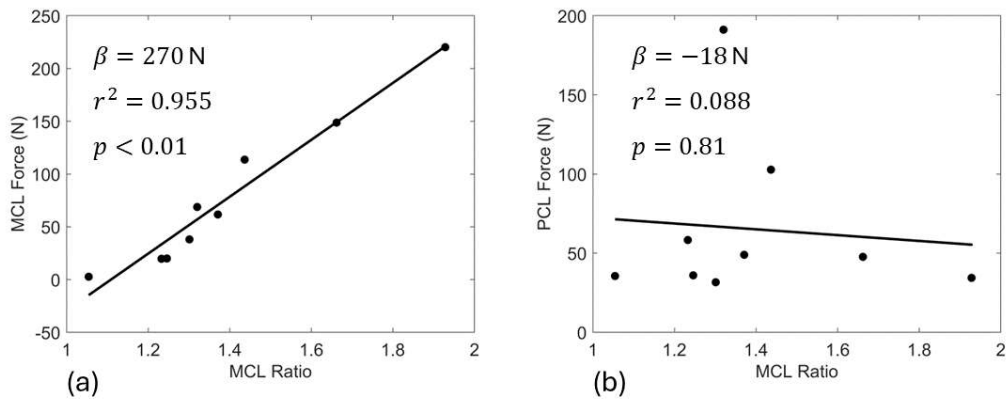


Figure 2: The scatter plots of the (a) superficial medial collateral ligament (sMCL) and (b) the posterior cruciate ligament (PCL) force at 90° vs. the MCL ratio.

Figure 2

Coronal Knee Laxity in Total Knee Arthroplasty and Patient Reported Outcomes: Awake Versus Anaesthetised

*Ishaan Jagota - 360 Med Care - Sydney, Australia

David Liu - Gold Coast Centre for Bone and Joint Surgery - Tugun, Australia

Willy Theodore - Flinders University - Adelaide, Australia

Joshua Twigg - University of Sydney - Sydney, Australia

Brad Miles - 360 Knee Systems - Pymble, Australia

Introduction

Intraoperative ligament laxity assessments in total knee arthroplasty (TKA) are subjective but can heavily influence the component alignment decision-making process. Few studies compare intraoperative ligament laxity assessment against standardised preoperative and postoperative assessments. This study compares coronal knee laxity in TKA patients awake and anaesthetised, both pre- and post-prosthesis implantation, examining its impact on patient-reported outcome measures (PROMs)

Methods

A retrospective analysis of 49 primary TKA joints was conducted. Preoperatively and postoperatively, patients received a long-leg computer tomography scan and 2 stress radiographs (1 each with a standardised varus and valgus stress applied), which were obtained using the Telos SD-900. Patients also completed the Knee injury and Osteoarthritis Outcome Score (KOOS) questionnaire preoperatively and 12-month postoperatively. The imaging was used to assess functional laxity (FL) in awake patients, while computer navigation measured intraoperative surgical laxity (SL) preimplantation and postimplantation, with patients anaesthetised. Varus and valgus stress states were measured along with their difference, joint laxity. A summary of the preoperative and postoperative imaging and analysis process is displayed in Figure 1.

Results

As displayed in Figure 2, SL exceeded FL both preimplantation (8.1° (interquartile range [IQR] 2.0°) and 3.8° (IQR 2.9°), respectively) and postimplantation (3.5° (IQR 2.3°) and 2.5° (IQR 2.7°), respectively). Preoperatively, SL was more likely than FL to categorise knees as correctable to $\pm 3^\circ$ of the mechanical axis. Preoperative FL correlated with KOOS Symptoms ($r=0.33$, $p=.02$) and Quality of Life (QOL) subscores ($r=0.38$, $p=.01$), while reducing medial laxity with TKA enhanced postoperative QOL outcomes ($p=.02$).

Conclusion

Intra-operative laxity measurements can be subjective and are performed with patients in an anaesthetised state. Despite limited reliability and correlation to functional laxity, many clinicians rely on intra-operative measurements for TKA alignment guidance. In this study, functional coronal knee laxity assessment of awake patients was observed to generally be lower than intraoperative surgical assessments in anaesthetised patients. The use of preoperative SL to guide TKA alignment may result in over-correction of coronal alignment during TKA, while preoperative FL better predicts postoperative patient outcomes and may be more representative of the patients' native and tolerable knee laxity.

Figures

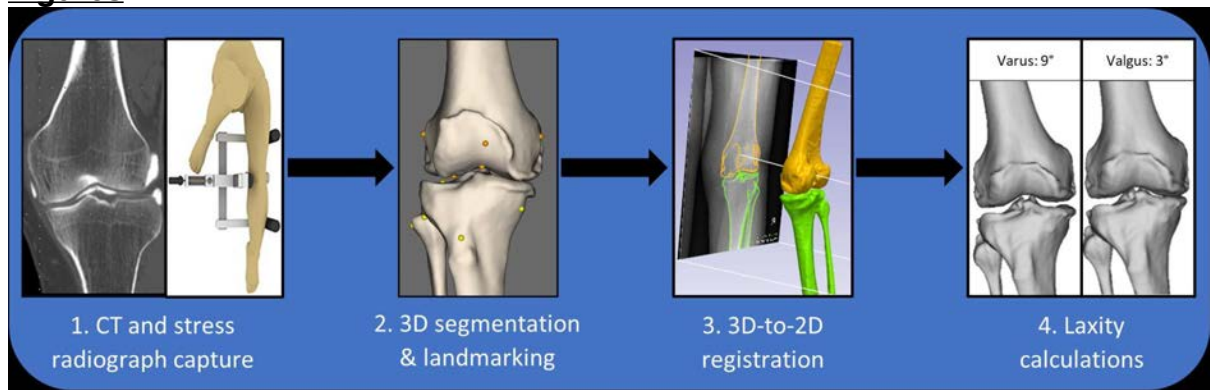


Figure 1

Joint Laxity Comparison

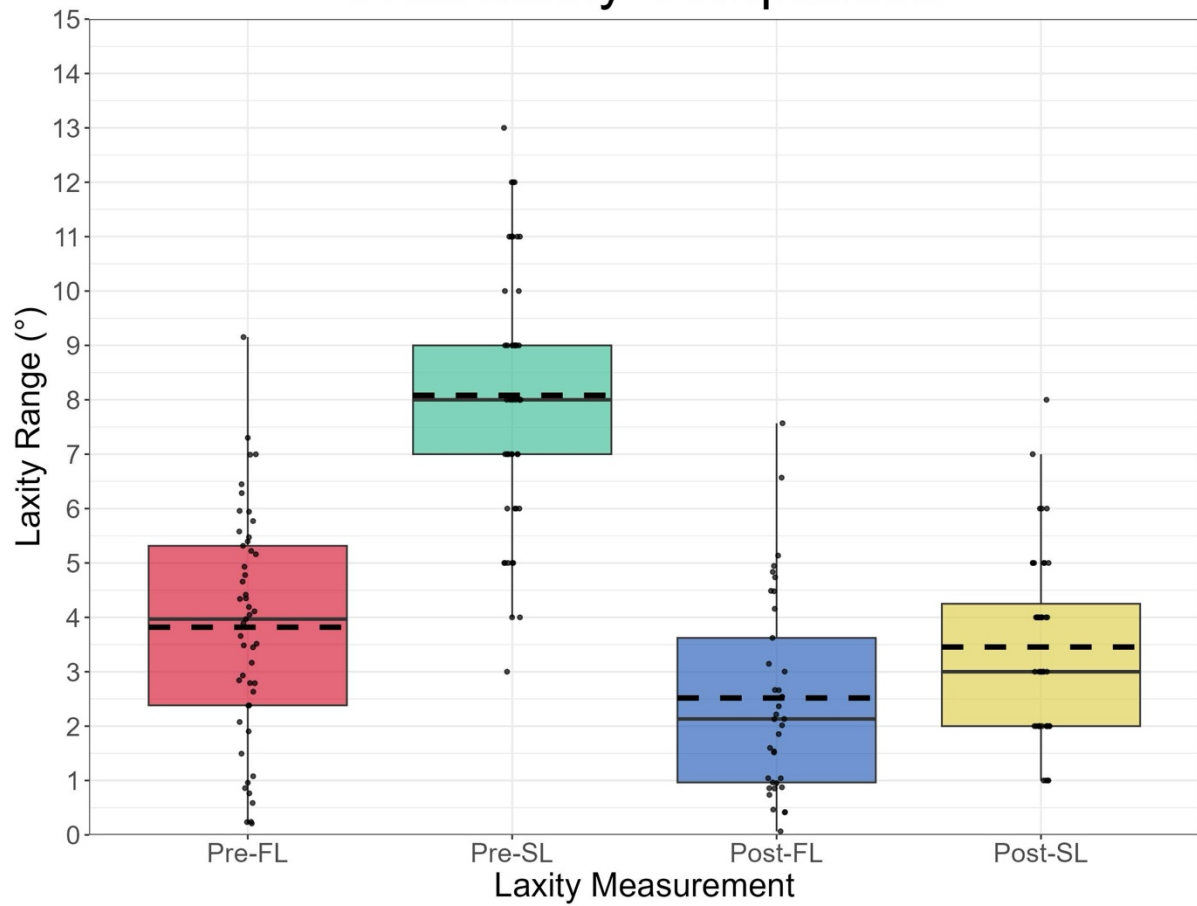


Figure 2

Patients Having Primary Total Joint Arthroplasty at ASC's Have Lower Readmissions and ER Vists Than Those at HOPDs or Hospitals.

*Simarjeet Puri - Detroit, United States of America

Harjot Uppal - Ascension Providence - Southfield, USA

Martin Weaver - Ascension Providence Hospital - Southfield, USA

Giresse Melone - University of Michigan - Ann Arbor, USA

Richard Hughes - University of Michigan - Ann Arbor, USA

Elizabeth Dailey - University of Michigan - Ann Arbor, USA

David Markel - Providence Hospital and Medical Center - Southfield, USA

Introduction: More primary total joint arthroplasty (TJA) is moving from hospitals to ambulatory surgery centers (ASCs) and hospital outpatient departments (HOPDs). As part of a Michigan Arthroplasty Registry Quality Collaborative Initiative (MARCQI) study, we compared rates of 30- and 90-day readmissions, 30-day Emergency Room (ER) visits, periprosthetic joint infection (PJI), periprosthetic hip fracture, and dislocations after primary total hip (THA) or knee (TKA) arthroplasty performed at ASCs, HOPDs and inpatient hospitals.

Methods: All MARCQI primary THAs and TKAs performed between July 1st, 2021 and June 30th, 2022 (n=43,454) were reviewed. Of the 17,108 THAs: 9.5% (1,630) were performed in ASCs, 4.7% (798) in HOPDs, and 85.8% (14,680) in hospitals. Of the 26,346 TKAs: 9.9% (2,617) were performed in ASCs, 4.2% (1,110) in HOPDs, and 85.9% (2,2619) in hospitals. Cohorts were not significantly different in terms of age, sex, or body mass index. However, the inpatient hospital cohort had more patients with American Society of Anesthesiology Class 3 and 4 ($p<0.001$) as well as lower rates of private health insurance ($p=0.04$).

Results: For THAs, ASCs had the lowest readmission rates at 30 days (ASC 0.98%, HOPD 1.75%, Hospital 3.36%, $p<0.001$) and 90 days (ASC 1.66%, HOPD 3.38%, Hospital 5.44%, $p<0.001$) postoperatively. ASCs also had the lowest 30-day ER visits (ASC 1.84%, HOPD 3.51%, Hospital 5.33%, $p<0.001$). Similarly, for TKAs, ASCs had the lowest 30-day (ASC 1.18%, HOPD 1.35%, Hospital 3.14%, $p<0.001$) and 90-day readmission rates (ASC 2.1%, HOPD 2.25%, Hospital 5.15%, $p<0.001$). Likewise, 30-day ER visit rates were significantly lower at the ASC (ASC 3.02%, HOPD 6.76%, Hospital 6.33%, $p<0.001$) postoperatively. Interestingly, rates of PJI and hip dislocation were not significantly different, but differences in periprosthetic hip fracture rates (ASC 0.43%, HOPD 0.64%, Hospital 1.18%, $p<0.001$) were noted.

Conclusion: Primary TJA performed at ASCs had significantly lower 30- and 90-day readmission as well as 30-day ER visits but relatively similar complications compared to arthroplasties performed at HOPDs and hospitals.

Revolutionizing Total Knee Arthroplasty Inventory Management: Seamless Integration of Ultrasound-Based Bone Reconstruction Into Robotic-Assisted Surgery

*Manh Ta - Stryker Corporation - Fort Lauderdale, USA

Riddhit Mitra - Smith and Nephew - Pittsburgh, USA

Russell McKissick - Tennessee Orthopaedic Alliance - Murfreesboro, USA

Steven MacDonald - London Health Sciences Centre - London, Canada

Richard Komistek - The University of Tennessee - Knoxville, USA

INTRODUCTION

Inventory management poses a significant challenge in Ambulatory Surgery Centers (ASCs), often resulting in unnecessary expenses. Total knee arthroplasty (TKA) surgeries, in particular, demand extensive implant and instrument inventory. JointVue LLC has developed innovative technology allowing surgeons to reconstruct patient-specific 3D bone models from ultrasound, streamlining implant size identification and reducing ASC inventory. This study aims to seamlessly integrate the Orthosonic™ software suite (JointVue, LLC) into a robotic-assisted surgery system (CORI, Smith & Nephew) for pre-operative bone reconstruction and surgical planning, intra-operative bone registration and preparation, evaluating its efficacy in producing implant sizes comparable to those determined using CT or MRI models.

METHODS

The Orthosonic™ software suite, comprising 3D Echo for ultrasound-based bone reconstruction and jFit for pre-operative surgical planning, was employed in this study. Two datasets were collected to assess its efficacy. In the first dataset, 22 TKA candidates underwent ultrasound scans with Orthosonic™ and subsequent surgical planning, followed by implantation of Journey II BCS implants by a single surgeon. The selected implant sizes were compared to those determined by the surgeon. In the second dataset, a cadaver was scanned using ultrasound-based reconstruction and robotic-assisted surgery. The 3D bone models generated by Orthosonic™ were then transferred seamlessly to the CORI robot for planning and intra-operative bone registration and preparation. The implant sizes determined using Orthosonic™ were compared to those derived from MRI-derived models using controlled planning software within the surgical robot.

RESULTS

In the first dataset, 20 out of 22 subjects exhibited implant sizes within one deviation of those selected by the surgeon, despite challenges in landmarks and posterior condyle acquisition in two cases. In the second dataset, Orthosonic's 3D bone models seamlessly integrated into a surgical robot, marking a milestone in ultrasound system integration into a robot-assisted surgery system. Implant sizes determined by Orthosonic™ matched those from the controlled surgical planning software used by the surgical robot. Also, alignment was within 0.5 mm compared to MRI derived 3D bones.

DISCUSSION

This study demonstrates successful Orthosonic™ integration into robotic-assisted surgery, facilitating pre-operative planning, intra-operative bone registration and preparation. Orthosonic™ reliably produces implant sizes comparable to existing robot-assisted surgery systems, promising reduced ASC inventory requirements and significant operational cost savings.

Why Do Total Hip Arthroplasties Get Canceled on the Day of Surgery?

*Jonathan Katzman - NYU Langone - New York, United States of America

Sophia Antonioli - NYU Langone - New York, USA

Akram Habibi - NYU Langone Orthopedic Hospital - New York, United States of America

Carlos Sandoval - NYU Langone - New York, USA

Eric Grossman - Rothman Orthopaedic Institute - Philadelphia, USA

Armin Arshi - New York University Langone Health - New York, United States of America

Ran Schwarzkopf - NYU Langone Medical Center Hospital for Joint Diseases - New York, USA

Catherine Digangi - NYU Orthopedic Hospital - New York, USA

Introduction

Same-day cancellations of elective surgeries present challenges to patients, providers, and healthcare institutions. This study aimed to investigate the frequency and predictors of same-day cancellations for elective total hip arthroplasty (THA).

Methods

A retrospective review was conducted on 13,744 scheduled primary, elective THAs at an urban academic center from September 2017 to August 2023. Cases that experienced same-day cancellations were identified. Same-day cancellations were then grouped based on the reasoning for cancellation into health-related (active medical concerns or lack of medical clearance), operative-related (concerns with patients' preoperative preparation or qualification for THA), and logistic-related (absence of the surgeon or patient for non-medical reasons or administrative concerns such as facility or financial clearance issues) categories. Patient demographics were compared between the cancellation and underwent surgery cohorts. Demographic differences and reschedule rates were also assessed between the categorical reasons for cancellation.

Results

Out of the 13,744 scheduled THAs, 179 cases (1.3%) underwent a same-day cancellation. Patients who experienced a same-day cancellation were more likely to be male (58.1% vs. 43.2%, $P < 0.001$), Black or Latino (28.4% vs. 16.5%, $P < 0.001$), current or former smokers (55.8% vs. 46.9%, $P = 0.006$), and have a higher BMI (30.8 vs. 29.4, $P = 0.002$). There were no differences in age or Charlson Comorbidity Index (CCI) between the cancellation and underwent surgery groups. Health concerns accounted for 54.2% of the cancellations, operative concerns accounted for 19.6%, and administrative or logistical concerns accounted for 26.2%. Patients who canceled due to medical or operative concerns were older and had a greater CCI compared to patients who canceled due to logistical concerns. 74.9% of all same-day cancellations were ultimately rescheduled and rescheduled cases occurred at a median of 20.5 days (range, 1 to 425 days) after cancellation. There were no significant differences in rescheduling rates and time to rescheduled cases between the reasons for cancellation.

Conclusion

A sizable subset of patients experienced a same-day cancellation of their elective THA, most of which occurred due to health concerns. These findings may guide the development of tailored preoperative optimization strategies aimed at reducing the occurrence of same-day cancellations for high-risk patients, thereby maximizing the utilization of operating room resources and enhancing care for THA patients.

Incidence of Surgical Indications From Orthopedic Source

*Ira Kirschenbaum - Bronx-Lebanon Hospital - Bronx, USA

Katelyn DCosta - BronxCare Health System - Bronx, USA

Alec Ralph - BronxCare Health System - Bronx, USA

Jonathan Metellus - BronxCare Health System - Bronx, USA

Millie Rouffiac - BronxCare Health System - Bronx, USA

Chelyn Park - BronxCare Health System - Bronx, USA

Emelia Ohnmacht - BronxCare Health System - Bronx, USA

Francesca Vecchio - BronxCare Health System - Bronx, USA

Isaiah Dolphin - BronxCare Health System - Bronx, USA

Jaiden Stokes - BronxCare Health System - Bronx, USA

Anthony Kang - BronxCare Health System - Bronx, USA

Erik Kim - BronxCare Health System - Bronx, USA

Introduction

Efficiency and accuracy in surgical referrals are crucial for optimizing patient care and resource allocation. Understanding the percentage of indications and subsequent surgery requests from referring doctors provides valuable insight into the effectiveness of a practice or hospital system. We aimed to examine the referral process leading to surgery between a senior former joint replacement surgeon and two junior joint replacement surgeons.

Methods

In this study conducted in a closed urban community in the Bronx, NY, a senior former joint replacement surgeon referred patients to two junior surgeons for evaluation and surgical indication. A cohort of 200 patients from 2019 to 2022 was utilized to gather relevant data. The senior surgeon sent two types of referrals: one using the term “surgical evaluations” and one using the term “indicated for surgery.” The results from the junior surgeon's first visit were recorded, including recommendations for alternative treatment, patient opting for alternative treatments, surgery refusal, surgery request, inability to proceed with surgery due to medical issues, or delayed surgery. “Patients opting for alternative treatments” was classified as patients wanting to try alternative treatments with surgery as a final option while “surgery refusal” was patients refusing to ever get surgery. We also documented whether the patient eventually received a joint replacement with the junior surgeon, along with the corresponding date.

Results

Out of 200 patients, 47 were referred for only a surgical evaluation, and 153 were referred as being indicated for surgery. The results indicate that 45.8% of a non-operating senior surgeon's evaluations were converted into surgical requests on the patient's first visit with a junior surgeon, and 58.1% of non-operating senior surgeon's indications were converted into surgical requests on the patient's first visit with a junior surgeon. Overall, 55.44% of a senior surgeon's referrals, whether an indication or evaluation, resulted in a surgery request. The complete results of the treatment plan for patients referred for surgical evaluation or indication are shown in Graphs 1 and 2.

Discussion

Clearly, the numbers shown here represent a high efficiency in the use of experienced non-operative orthopedic surgeons in referring surgical indications to arthroplasty surgeons in a community-based practice. In this changing healthcare environment, where resource allocation represents an important goal, using high-priced arthroplasty surgeons efficiently is a goal.

Making Sense of Data: Creating Actionable Information From Remote Monitoring Technology

*Richard Bolander - TracPatch - Orland Park, United States of America

Victor Hernandez - University of Miami Hospital - Miami, USA

S. David Stulberg - Northwestern Memorial Hospital - Chicago, USA

Michele D'Apuzzo - University of Miami Miller School of Medicine - Miami, USA

Introduction

The recent introduction of remote monitoring technologies has allowed for the ability to measure performance and outcomes associated with a patient's recovery. These innovations are timely with additional challenges in the healthcare industry including decreased human resources, rising costs, and the need for subjective and objective information.

In conjunction with increased clinical burden for patient management, providers can be apprehensive about utilizing new technologies because of the perceived effort to manage a patient day to day or experiencing data overload. To address these concerns, it is important for developers and researchers to create metrics to simplify the patient monitoring experience. This abstract provides an example of a simple system to classify patients as normal or atypical to direct which patients may need the most attention from clinicians.

Method

A cohort of 566 participants undergoing total knee arthroplasty wore the TracPatch and had an average daily wear time of 12 hours (± 4) for a total of 45 days (± 27). Daily means and standard deviations were calculated for achieved flexion, extension and total daily step counts. Recovery was nonlinear, where the greatest gains in the first 3 weeks post-surgery for all metrics. Real patient data is presented against these bounds.

Result

In Figure 1, patient total daily step counts follow the expected trajectory within the bounds.

In Figure 2, a patient was outside side of the lower bound but returned to within bounds by day 50.

In Figure 3 the patient had significant extension leg pre-surgery but fell within the bounds post-surgery.

Conclusion

This abstract presents an application to identify patients outside of the norms for multiple metrics associated with the recovery following total knee arthroplasty. To reduce clinical load, methods such as these can be used to classify which patients should require additional resources and which require minimal intervention. For example, if a system has 100 active patients, methods such as these can identify the non-conformers and direct staff to only focus on a subset of these patients at any given time. To be fully applicable to a clinician, the specific rule sets, such as amount of deviation from the norm for so many specific days as well as sufficient data cleansing are required for clinical applicability.

Figures

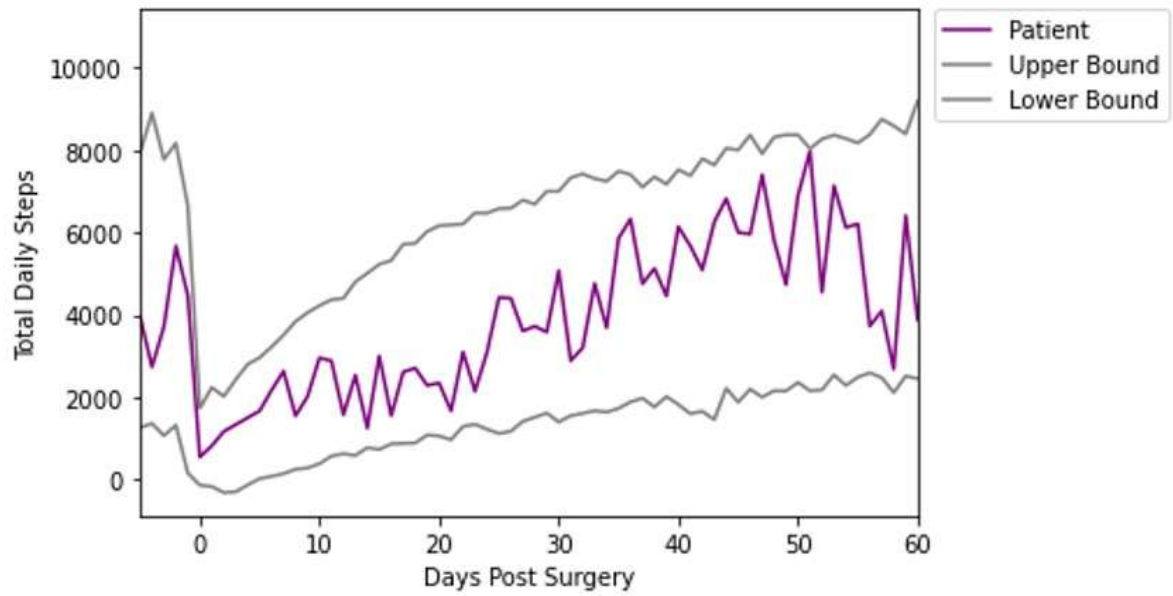


Figure1

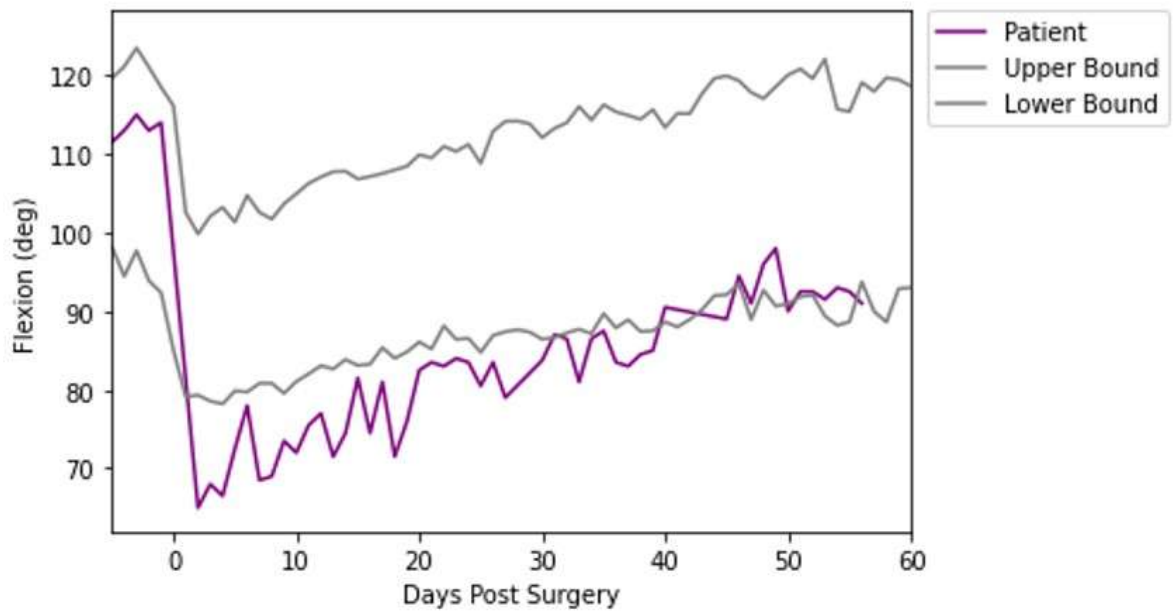
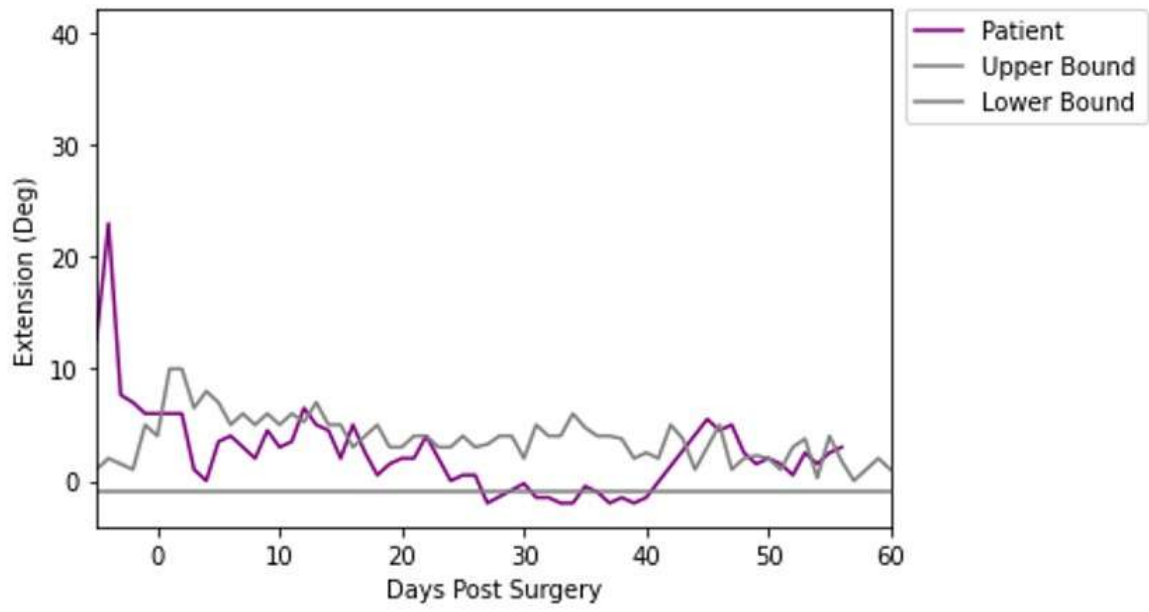


Figure2



[Figure 3](#)

Relationship Between Area Deprivation Index and Patient Reported Outcomes Following Total Knee Arthroplasty

*Gregory Laborde - LSUHSC - New Orleans, USA

Gregory Benes - LSUHSC - New Orleans, USA

Introduction

In recent years, research on total knee arthroplasty (TKA) outcomes has gained prominence due to its impact on patient well-being and provider reimbursement. Research has established that black patients are at increased risk for worse outcomes following TKA. Because socioeconomic disadvantage and non-white race are related, it is not clear to what extent socioeconomic disadvantage may mediate racial disparities in TKA outcomes. Recently, the area deprivation index (ADI) has emerged as a measure to help elucidate the relationships between race, socioeconomic disadvantage, and outcomes in TKA patients.

The purpose of this study is to quantify the significance of social deprivation on post-TKA outcomes. By doing so, additional steps can be taken amongst socially deprived populations to prevent post-TKA adverse events. For example, by identifying high risk populations, clinicians will be aware of which patients may need additional care post-TKA. They can use this knowledge to know when to allocate additional resources to these patient. Furthermore, by identifying significant risk factors of post-TKA adverse events, further studies can be conducted to test solutions oriented to these specific factors.

Methods

This is a retrospective chart review study. 900 patients who had TKA surgery between 1/1/16 and 12/31/23 were included. Patient population involved Ochsner-Kenner patients. Patients under the age of 18 were excluded. Knee injury and osteoarthritis outcome score (KOOS) was taken 3 and 6 months post-operative TKA. Patient-Reported Outcomes Measurement Information System (PROMIS) was also taken at 3 and 6 months post-op. These scores are compared with specific patient ADI.

Results:

Data analysis is currently undergoing. Estimated completion by May 1.

Conclusion:

It is hypothesized that patient's with lower socioeconomic status will have worse outcomes following TKA regardless of race. In order to decrease poor outcomes following TKA, specific risk factors must be identified. This study will help determine the significance of social deprivation's effect on post-surgical outcomes. By doing so, additional steps can be taken amongst socially deprived populations to prevent post-TKA adverse events.

Influence of a Post-Cam Mechanism on Femoral Rollback of Human Cadaveric Knees

*Saskia Anna Brendle - Aesculap AG / LMU Munich - Tuttlingen, Germany

Sven Krueger - Aesculap AG Research & Development - Tuttlingen, Germany

Joachim Grifka - Regensburg University Medical Center - 93077 Bad Abbach, Germany

Peter E. Mueller - Hospital of the Ludwig-Maximilians-University of Munich - Munich, Germany

William Mihalko - University of Tennessee - Germantown, USA

Berna Richter - Aesculap AG - Tuttlingen, Germany

Thomas M. Grupp - Aesculap AG - Tuttlingen, Germany

For posterior cruciate ligament (PCL)-deficient total knee arthroplasty (TKA), surgeons can choose between inlay designs with or without a post-cam mechanism. Previous studies show that both inlay designs provide similar stability but more potential complications with the post-cam mechanism. In addition, the post-cam mechanism could have an effect on tibiofemoral kinematics and result in a more pronounced femoral rollback. However, it is not clear how the kinematics of these two designs differ within the same ligamentous situation. For this reason, this study investigated the femoral rollback of two different inlay designs in the same knee during passive knee flexion.

Within the scope of this in vitro study, thirteen fresh-frozen human cadaveric knees were tested on a six-degrees-of-freedom joint motion simulator (VIVO, Advanced Mechanical Technologies Inc., Watertown, USA). Before testing, each specimen underwent cruciate-sacrificing TKA by an experienced orthopaedic surgeon using oneKNEE TKA components (Aesculap AG, Tuttlingen, Germany). This TKA system allows the use of an inlay with or without a post-cam mechanism (CR/CS or PS). The neutral path of motion of each knee was recorded with both inlays by applying continuous knee flexion from 0° to 90° with 200 N compression force, and all other forces/moments maintained at 0 N/Nm (Figure 1). In order to track the relative position of femur and tibia during testing, each specimen underwent a complex 3D fitting process (ARAMIS 12M, Carl Zeiss GOM Metrology GmbH, Braunschweig, Germany). Knowledge of the relative positions of femoral and tibial coordinate systems, their according bone geometries and the position of the implants relative to the bones allowed the projection of the flexion axis and medial and lateral flexion facet centres (MFC and LFC) of the femoral component onto the tibial plane at different flexion angles and therefore the measurement of condylar motion throughout the arc of flexion. Anterior-posterior (AP) translation of the MFC and LFC of each specimen was calculated with both inlay designs and normalized to the CR/CS positions at 0° flexion. Paired t-tests were used to compare the AP translation between CR/CS and PS in 5° flexion intervals ($p \leq 0.05$).

Up to 50° of flexion, the specimens show a stable AP position at approximately 1 mm for both, CR/CS and PS inlays (Figure 2 and 3). Starting from 55° of flexion, the PS inlays show a markable increase in AP translation which significantly differs from the CR/CS inlays. The mean difference between both inlays was approximately 1 mm for medial and lateral condyles at 55° of flexion, growing up to a mean difference of 7.2 mm medial and 8.0 mm lateral at 90° of flexion.

The post-cam mechanism of the PS inlay induces femoral rollback, while the CR/CS inlay is less constraining in the same ligament situation. This should be taken into account when deciding whether to use a CR/CS or PS inlay design.

Figures



Figure 1. Experimental setup with an instrumented knee specimen mounted on the six-degrees-of-freedom joint motion simulator at 0° flexion.

Figure 1

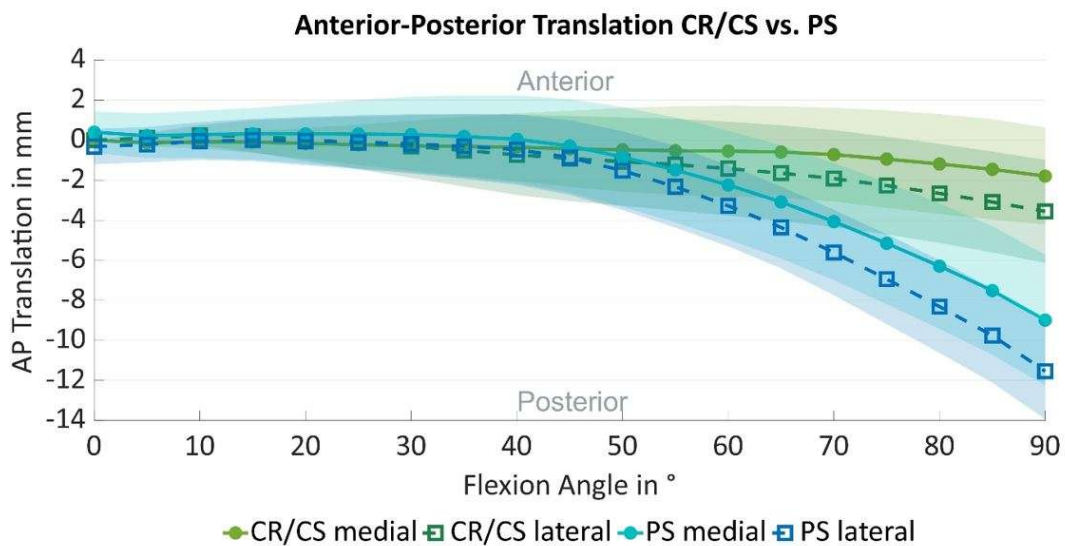


Figure 2. Mean normalized medial (solid line) and lateral (dashed line) anterior-posterior (AP) translation (n=13) and standard deviation throughout the range of flexion (0° to 90°) with CR/CS (green) and PS inlays (blue).

Figure2

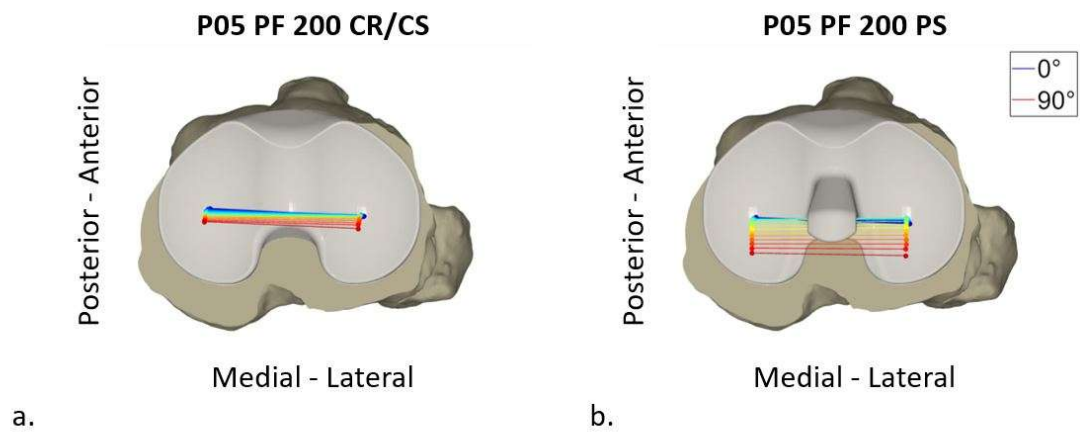


Figure 3. Projection of the flexion axis and medial and lateral flexion facet centers (MFC and LFC) of the femoral component onto the tibial plane at different flexion angles showing condylar motion throughout the arc of flexion with (a) a CR/CS inlay and (b) a PS inlay in specimen P05.

[Figure 3](#)

Comparison of Kinematics Between Bi-Cruciate Stabilized and Medial Stabilized Total Knee Arthroplasty Cohorts

*Garett Dessinger - Center for Musculoskeletal Research - Knoxville, USA

Peter Thadani - Illinois Bone & Joint Institute, Libertyville Division - Libertyville, USA

Andrew Gaetano - Loyola University Chicago - Chicago, USA

Richard Komistek - The University of Tennessee - Knoxville, USA

Michael LaCour - University of Tennessee - Knoxville, USA

Introduction:

A common goal of total knee arthroplasty (TKA) is to recreate the weight-bearing kinematics of the non-implanted knee. Unfortunately, TKA typically fall short of this goal via postoperative losses in range of motion, paradoxical kinematic patterns, and instability. To overcome this, a variety of options exist for surgeons, ranging from different cam-post mechanisms, changes in bearing conformity, asymmetrical surgical techniques, and more. This study investigates bi-cruciate stabilized (BCS) with anatomical alignment built into the implant and medially stabilized (MS) TKA designs implanted using a kinematic alignment (KA). The objective of this study is to evaluate differences between weight-bearing kinematics and patient reported outcome measures (PROMs).

Methods:

Twenty-eight TKA patients (BCS: n=14, MS: n=14), all implanted by the same surgeon, were analyzed using 3D-to-2D fluoroscopic image registration while performing a deep knee bend (DKB) activity. Range of motion (ROM), anterior/posterior position of the medial (MAP) and lateral (LAP) condyles, and axial rotation were determined from fluoroscopy. KOOS Jr scores were also collected for both cohorts prior to the collection of fluoroscopic data.

Results:

Both implants exhibited high ROM and excellent KOOS scores. The BCS ROM was $117.0 \pm 15.9^\circ$ while the MS ROM was $114.1 \pm 19.6^\circ$. The average KOOS Jr score for the BCS cohort was 90.5 while the average for the MS cohort was 94.9. The BCS lateral condyle started 8.0 ± 3.9 mm anteriorly of the midline in extension, and the medial condyle started 3.5 ± 2.5 mm anterior. Throughout flexion, both condyles rolled posteriorly, 19.2 ± 5.5 mm for LAP and 7.4 ± 3.5 mm for MAP, yielding $14.7 \pm 8.2^\circ$ of external femorotibial rotation. The MS lateral condyle started 0.9 ± 3.8 mm anteriorly of the midline, and the medial condyle started 3.5 ± 1.6 mm posteriorly. Throughout flexion, the lateral condyle rolled posteriorly by 9.0 ± 5.0 mm and the medial condyle stayed largely stable, rolling 1.0 ± 3.3 mm posteriorly. This generated $9.7 \pm 8.4^\circ$ of external femorotibial rotation. These patterns are shown in Figures 1-3.

Conclusion:

Despite excellent PROMS, the two cohorts revealed distinct kinematic differences. The anterior cam of the BCS cohort was evidenced by the anteriorized starting femoral condyles, which enabled greater rollback throughout flexion than the MS cohort. Conversely, the increased conformity on the medial side for the MS implant was successfully stabilizing the condyle, generating progressive external femorotibial axial rotation. These results suggest favorable functional outcomes for patients in both groups, and both implant designs appear to be functioning as their designs

intended. These findings underline the importance of kinematic analysis in TKA design evaluation and decision-making.

Keywords: arthroplasty, TKA, kinematics, fluoroscopy, BCS, PCS, PROMs

Figures

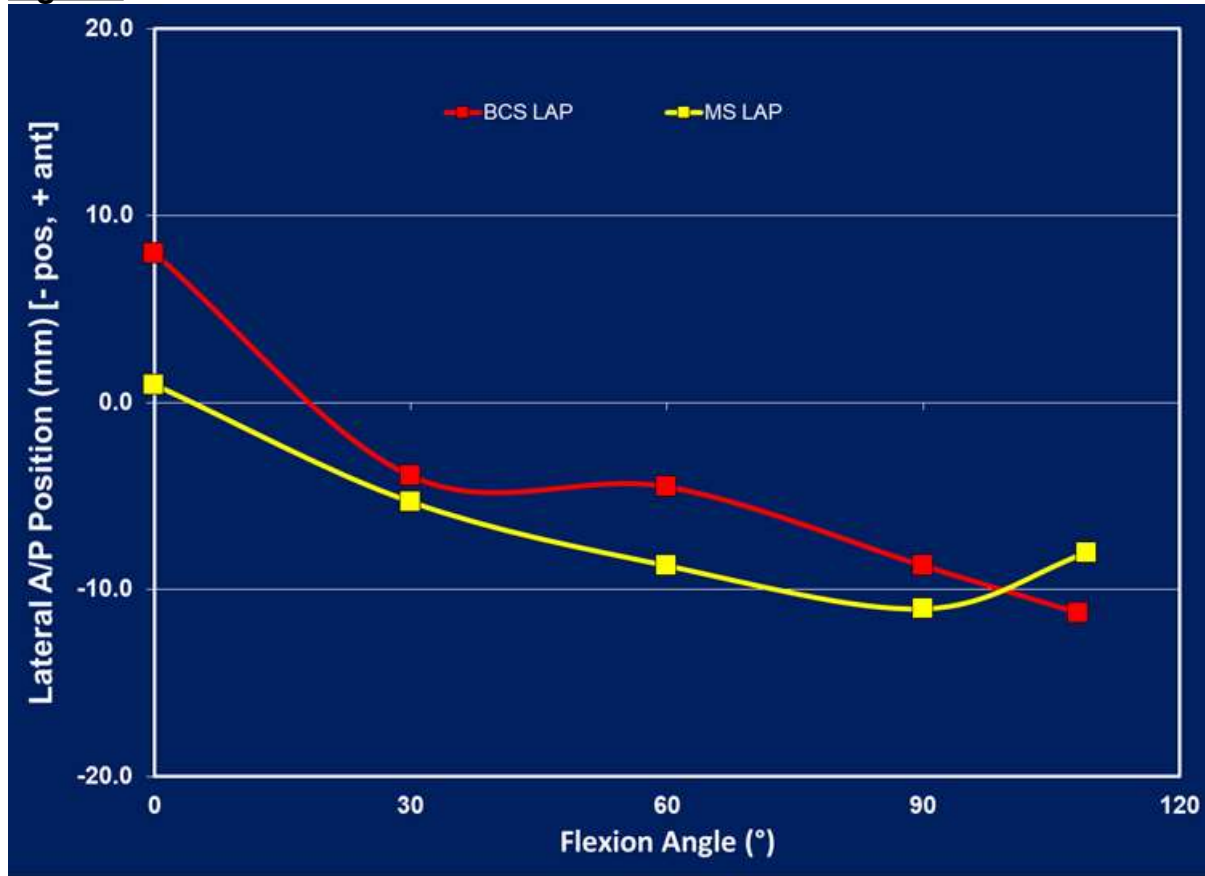


[Figure 1](#)

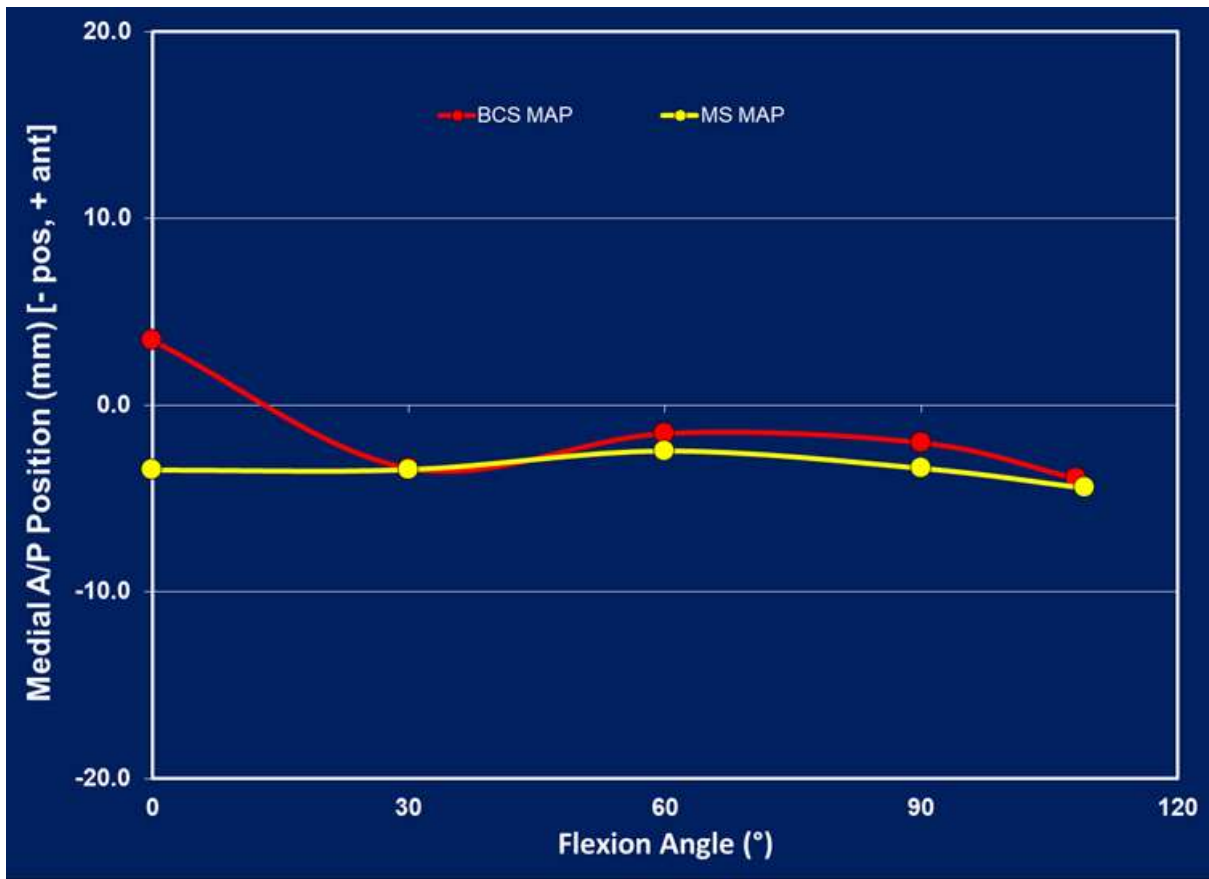


Figure 2

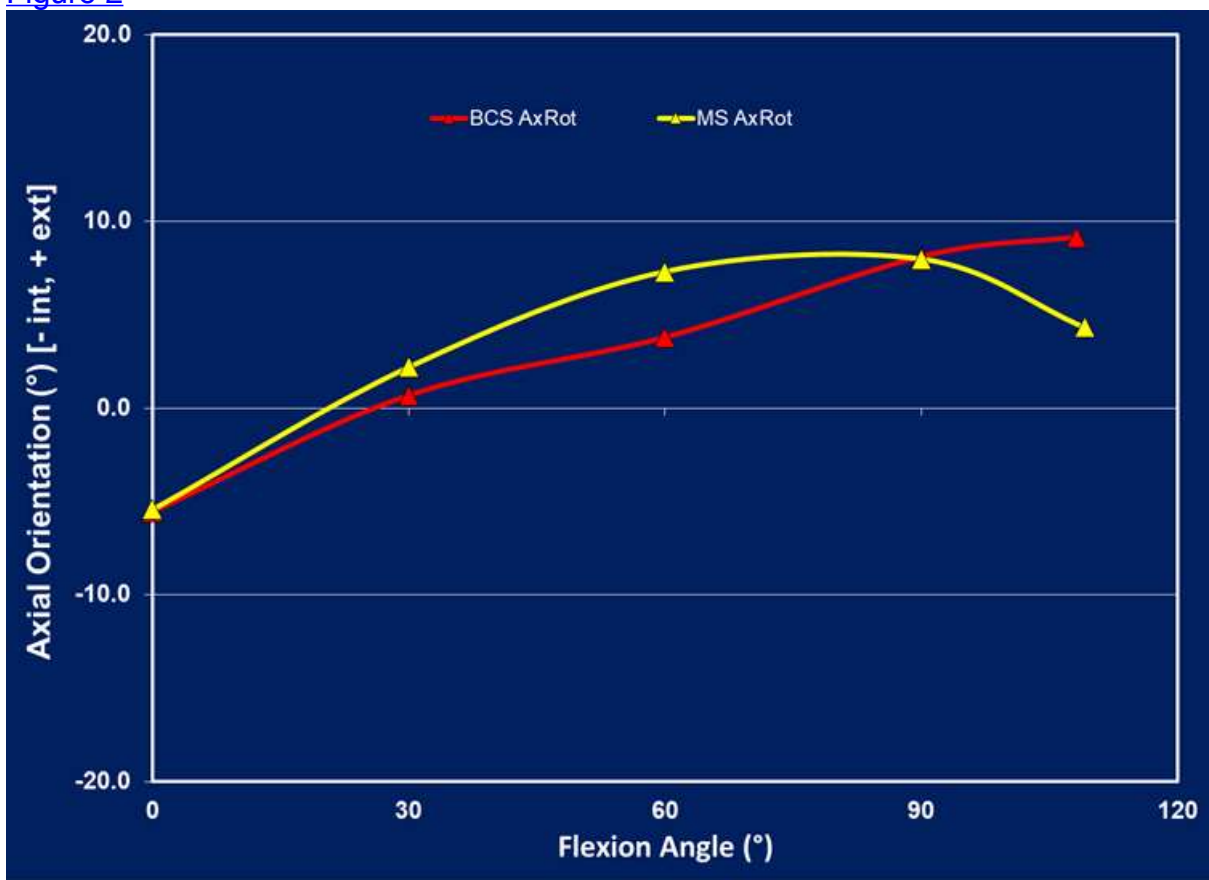


Figure 3

Does Robotic Assistance Improve Success of Component Fixation in Cementless Total Knee Arthroplasty?

*John Cooper - Columbia University - New York, USA

Jeffrey Geller - Columbia University Medical Center - New York, USA

Alexander Neuwirth - Columbia University Medical Center - New York, USA

Nana Sarpong - Columbia University Medical Center - New York, USA

Roshan Shah - Columbia University Medical Center - New York, USA

Catelyn A. Woelfle - Columbia University Medical Center - New York, USA

INTRODUCTION

New cementless implant designs in total knee arthroplasty (TKA) have begun to shift the longstanding practice of cemented fixation. With aseptic loosening a leading cause for revision of cementless implants, initial osteointegration is critical for component survivorship. Robotic-assisted TKA (RA-TKA) has shown promising results in recent literature at improving component accuracy. The current study aims to evaluate if RA-TKA affects the rate of aseptic loosening of cementless components.

METHODS

All cementless primary TKA components from one manufacturer implanted by five surgeons between June 2018 and October 2022 with minimum one-year follow-up were retrospectively reviewed. Femoral and tibial components were reviewed separately and grouped based on whether manual or RA-TKA was performed. A Chi-Squared test was used to analyze if aseptic loosening rates were different between the two techniques.

RESULTS

319 cementless components from a single knee system were included. 123 femoral and 92 tibial components were implanted using RA-TKA, while 50 femoral and 54 tibial components were implanted manually. At a mean follow-up of 18.7 months (range, 12 to 48 months), successful fixation was achieved in 97.8% of all components. No femoral components from either group were revised due to aseptic loosening. Four manually implanted vs. no robotically assisted tibial components were revised due to aseptic loosening (7.4% vs 0.0%; $X^2 = 6.86$; $df = 1$; $P = 0.009$).

CONCLUSION

The performance of modern cementless femoral components was excellent with or without robotic assistance, however the survivorship of the same system's cementless tibial component was improved with RA-TKA.

Image Free Robotic-Assisted System for Total Knee Arthroplasty Associated With Reduced and More Consistent Surgical Times Versus Manual Instrumentation: A Retrospective Controlled Single Surgeon Study

*James Lesko - DePuy Synthes Joint Reconstruction - warsaw, USA

Ian Leslie - DePuy Synthes Joint Reconstruction - Leeds, United Kingdom

Timothy Alton - Proliance Orthopedic Associates - Renton, USA

Introduction

Robot-Assisted (RA) total knee arthroplasty (TKA) has gained popularity due to its ability to improve component positioning accuracy and facilitate patient specific techniques. One reported drawback is the potential increase in surgical time, especially during the adoption phase. The impact on surgical time may vary with surgeon experience and specific RA system. The VELYS Robotic-Assisted Solution (VRAS) may offer efficiency advantages based on its combination of image free registration and direct guidance of the saw. Prior studies have demonstrated that VRAS can be time neutral after a short learning curve, but these were limited to relatively small sample sizes (<100). Even after the initial learning phase, further improvements in workflow efficiency may offer continued time savings. This study aimed to assess surgical time mean and variance for VRAS versus manual instrumentation from a single surgeon with a large sample size.

Methods

This was a retrospective review of 600 single surgeon TKA cases in a company sponsored registry (DOTS): final 300 cases prior to adoption of VRAS, and first 300 VRAS cases. Surgical time was from the initial skin incision to closure. Surgical time means were compared via t-test, and variances were compared with Bartlett's test. To address potential OR efficiency changes over time which may vary even among manual cases due to OR team work flow improvements and changes in surgical technique, both groups were stratified into time sequential groups of 100 procedures.

Results

Surgical time was assessable for 291 manual and 299 VRAS procedures. Mean (SD) surgical time for VRAS was 74 (18) minutes, a significant reduction from manual which was 88 (29) minutes ($p < 0.0001$) (Figure 1). Consecutive groups of 100 procedures showed a downward trend in surgical time for both manual and VRAS groups (Figure 2), with the most recent 100 VRAS procedures having a mean (SD) of 58 (12) minutes. Variances were heterogeneous among manual case strata ($p = 0.006$), but more homogeneous among VRAS cases ($p = 0.051$).

Conclusions

This single surgeon study demonstrated that VRAS had lower, and more consistent surgical time versus manual instrumentation, even in light of apparent OR efficiency improvements also seen for manual cases. This finding contrasts with prior literature which suggests RA TKA may increase surgical time, or at best be time neutral. Additionally, this study demonstrates that improvements in efficiency may continue well after the initial adoption phase. Further investigation with larger sample sizes is warranted to determine if VRAS is generally more efficient than manual.

Figures

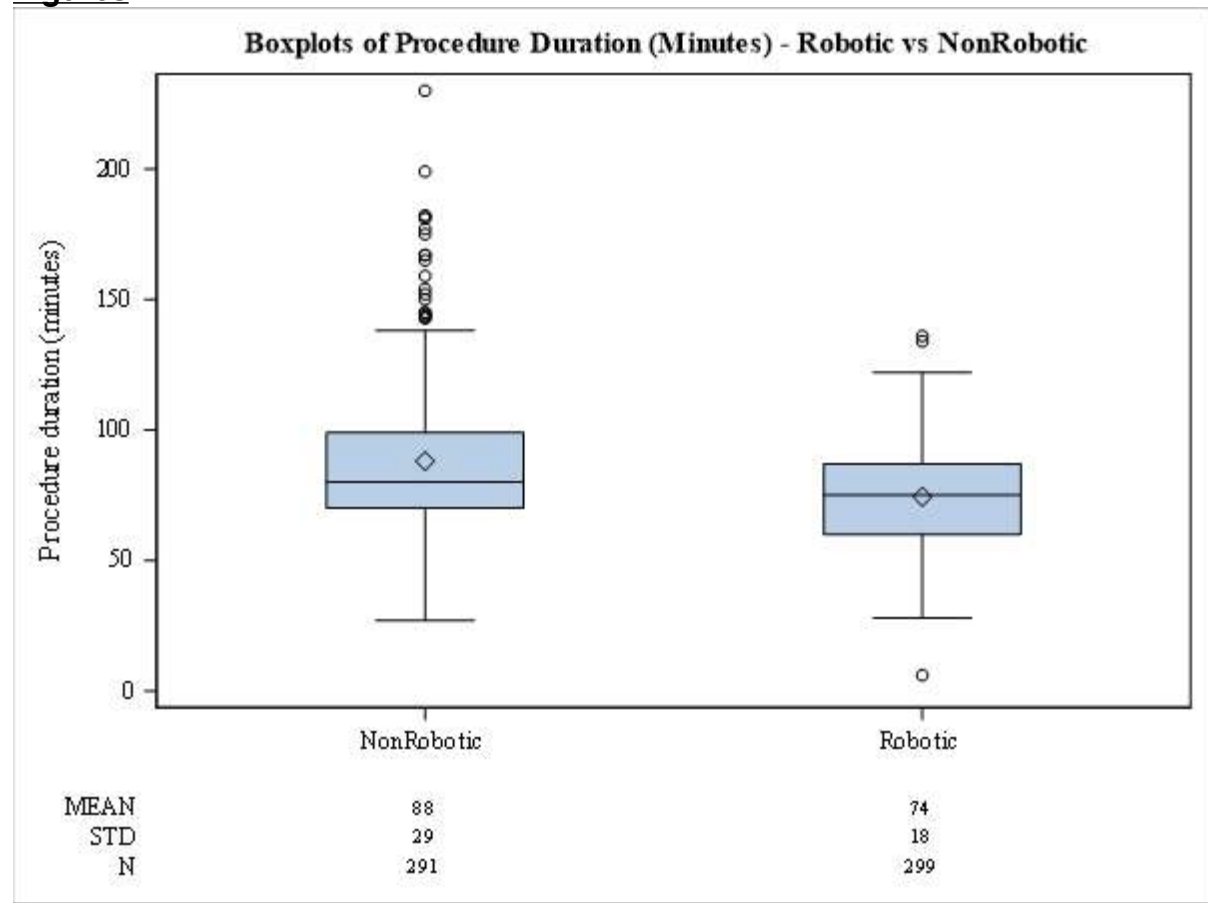


[Figure 1](#)

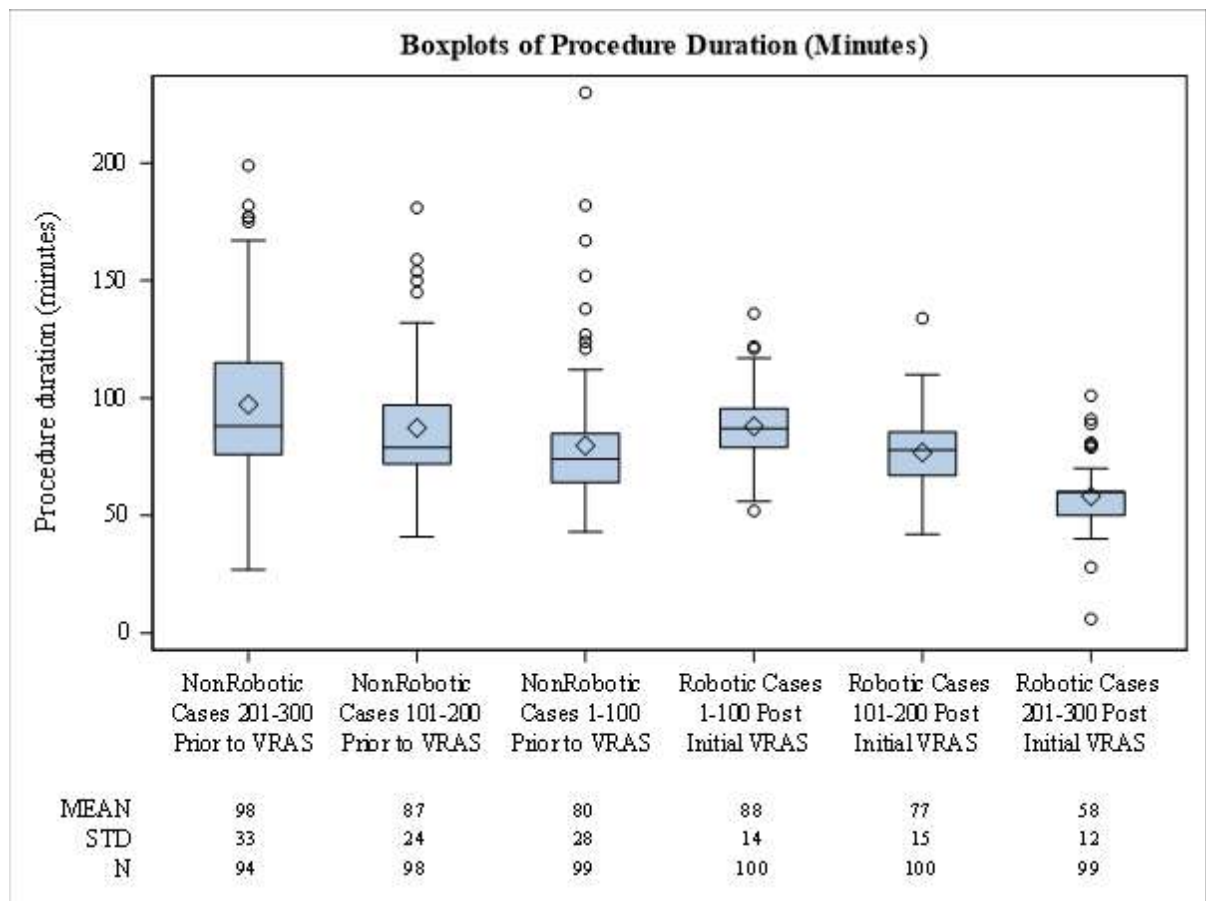


Figure 2

Clinical and Patient Reported Outcomes of a Novel Robotic System in Total Knee Arthroplasty

*Muhammad Haider - NYU Orthopedic Hospital - New York, USA

Michelle Zabat - NYU Langone Orthopedic Hospital - New York, USA

Casey Cardillo - NYU Orthopedic Hospital - New York, USA

Akram Habibi - NYU Langone Orthopedic Hospital - New York, United States of America

Sophia Antonioli - NYU Langone - New York, USA

Ivan Madrid - NYU Langone Orthopedic Hospital - New York, United States of America

Morteza Meftah - NYU Hospital for Joint Diseases - New York, USA

Joshua Rozell - NYU Langone Orthopedic Hospital - New York, USA

Ran Schwarzkopf - NYU Langone Medical Center Hospital for Joint Diseases - New York, USA

Catherine Digangi - NYU Orthopedic Hospital - New York, USA

Background: Even though bony resection and balancing may be more accurate, the effect of robotic assistance (RA) on clinical and patient reported outcome measures (PROMs) in total knee arthroplasty (TKA) is still unclear. The purpose of this study was to compare robotic and manually instrumented TKAs using a novel robotic system.

Methods: A retrospective review was conducted on 8,633 patients who underwent TKA from January 2021 to October 2023. Surgical information and operative notes were utilized to identify 114 patients who underwent primary, elective, unilateral TKA with the Smith & Nephew CORI robotic system. Robotic patients were 1:1 propensity-score matched to conventional TKA for patient demographics, surgeon identity and implant variables (Journey II vs. Legion, CR vs. PS, liner type, fixation). Perioperative and clinical outcomes including surgical time, length of stay (LOS), discharge disposition, 90-day readmissions, revisions, manipulation under anesthesia (MUA) and postoperative range of motion (ROM) were collected and analyzed. PROMs analyzed included Knee Injury and Osteoarthritis Outcome Scores (KOOS JR) and Patient Reported Outcome Measurement Information System (PROMIS) scores.

Results: RA-TKA patients demonstrated significantly longer mean surgical time from incision to closure compared to conventional TKA patients (113.8 vs. 101.2 mins, $P < 0.001$). Both groups demonstrated comparable LOS ($P = 0.119$) and discharge dispositions ($P = 0.469$). Each group had four 90-day readmissions, but the RA-TKA group had four readmissions due to stiffness, all undergoing MUA, versus the conventional group with four 90-day readmissions due to infection ($P = 0.014$). The conventional group had five revisions during the study period (4.4%) for prosthetic joint infection (PJI), compared to one (0.9%) in the RA group for arthrofibrosis ($P = 0.048$). While the RA group had six MUAs (5.3%), compared to zero in the conventional group ($P = 0.015$), ROM at latest follow up was comparable ($P = 0.531$). The RA group showed significantly improved KOOS, JR. scores (24.79 vs. 13.61, $P = 0.009$) at one year postoperatively compared to the conventional group.

Conclusions: The present analysis demonstrated superior 1-year PROMs, lower revision rates, and comparable postoperative ROM for this novel RA system when compared to a propensity-matched conventional group. The RA system was associated with longer surgical times, potentially reflective of a learning curve, and higher MUA rates, potentially reflective of higher patient expectations and surgeon bias. Further study is required to elucidate the benefits of robotic-assisted TKA.

Figures

Table 1. Baseline Characteristics

Demographic	RA (n=114)	Conventional (n=114)	P-Value
Mean Age (years) [range]	66.96 [29-94]	67.45 [32-85]	0.675
Sex, n (%)			0.999
Men	42 (36.8)	42 (36.8)	
Women	72 (63.2)	72 (63.2)	
Race, n (%)			0.681
White	56 (49.1)	54 (47.4)	
African American	19 (16.7)	26 (22.8)	
Asian	9 (7.9)	10 (8.8)	
Hispanic/Latino	7 (6.1)	5 (4.4)	
Middle Eastern	0 (0.0)	1 (0.9)	
Other	23 (20.2)	18 (15.8)	
Mean BMI (kg/m ²) [range]	32.5 [16.5-54.4]	32.7 [16.8-62.3]	0.806
Smoking Status, n (%)			0.382
Never	76 (66.7)	76 (66.7)	
Former	37 (32.5)	34 (29.8)	
Current	1 (0.9)	4 (3.5)	
ASA Class, n (%)			0.557
1	8 (7.0)	7 (6.1)	
2	75 (65.8)	74 (64.9)	
3	31 (27.2)	31 (27.2)	
4	0 (0.0)	2 (1.8)	
Primary Indication, n (%)			0.215
OA	113 (99.1)	109 (95.6)	
Post-Traumatic OA	1 (0.9)	3 (2.6)	
Rheumatoid Arthritis	0 (0.0)	2 (1.8)	
Procedure Laterality, n (%)			0.447
Right	50 (43.9)	52 (45.6)	
Left	64 (56.1)	62 (54.4)	

RA; Robotic-Assistance, BMI; Body Mass Index, ASA; American Society of Anesthesiologists, OA; Osteoarthritis

Figure 1

Table 2. Implant Data

Variable	RA (n=114)	Conventional (n=114)	P-Value
Fixation, n (%)			0.131
Cemented	110 (96.5)	114 (100.0)	
Cementless	2 (1.8)	0 (0.0)	
Hybrid	2 (1.8)	0 (0.0)	
Design, n (%)			0.363
Cruciate-Retaining	96 (84.2)	93 (81.6)	
Posterior Stabilized	18 (15.8)	21 (18.4)	
System, n (%)			0.791
Journey II	55 (48.2)	58 (50.9)	
Legion	59 (51.8)	56 (49.1)	

RA; Robotic-Assisted

Table 3: Perioperative and Clinical Outcomes

Demographic	RA (n=114)	Conventional (n=114)	P-Value
Surgical Time (Mins)	113.8	101.2	<0.001*
Length of Stay (Hours)	33.7	41.5	0.119
Anesthesia Type, n (%)			0.223
Regional	112 (98.2)	109 (95.6)	
General	2 (1.8)	5 (4.40)	
Discharge Disposition (n, %)			0.469
Home	111 (97.4)	107 (93.9)	
SNF	2 (1.8)	6 (5.3)	
ARF	1 (0.9)	1 (0.9)	
90-Day Readmissions (n, %)	4 (3.5)	4 (3.5)	0.999
Readmission Cause (n)			0.014*
Infection	0	4	
Stiffness	4	0	
Revisions (n, %)	1 (0.9)	5 (4.4)	0.106
Revision Cause (n)			0.048*
Arthrofibrosis	1	0	
PJI	0	5	
MUA (n, %)	6 (5.3)	0	0.015*

[Figure 2](#)

Table 4. Patient-Reported Outcome Measures

	RA (n = 114)	Conventional (n=114)	P-Value
Mean KOOS, JR (SD)			
Preoperative	43.30 (16.73)	43.89 (17.02)	0.834
2 weeks	55.20 (11.22)	54.67 (6.43)	0.936
3 months	63.90 (13.13)	73.50 (16.26)	0.268
1 year	68.09 (16.85)	57.50 (21.92)	0.444
Δ Preop to 2 weeks	11.90 (13.98)	10.78 (11.73)	0.172
Δ Preop to 3 months	20.60 (14.93)	29.61 (16.64)	0.268
Δ Preop to 1 year	24.79 (16.79)	13.61 (19.47)	0.009*
Mean PROMIS Pain			
Interference (SD)			
Preoperative	65.74 (8.33)	65.31 (6.90)	0.731
2 Weeks	64.28 (7.65)	64.00 (3.92)	0.942
3 Months	58.18 (7.65)	58.67 (12.70)	0.918
1 Year	57.79 (7.04)	64.83 (6.71)	0.052
Δ Preop to 2 weeks	-1.46 (7.99)	-1.31 (5.41)	0.942
Δ Preop to 3 months	-7.56 (7.99)	-6.64 (9.80)	0.714
Δ Preop to 1 year	-7.95 (7.69)	-0.48 (6.81)	0.661

RA; Robotic-Assisted, KOOS, JR; Knee Disability and Osteoarthritis Outcome score, SD; Standard Deviation, PROMIS; Patient Reported Outcome Measurement Information System

[Figure 3](#)

Introduction of ROSA Robotic-Arm System for Total Knee Arthroplasty Is Associated With a Minimal Learning Curve for Operative Time

*Faseeh Zaidi - University of Auckland - Auckland, New Zealand

Scott Bolam - University of Auckland - Auckland, New Zealand

Mei-Lin Tay - University of Auckland - Auckland, New Zealand

Michael M Hanlon - Auckland City Hospital - Auckland, New Zealand

Jacob T Munro - University of Auckland - Auckland, New Zealand

Andrew Paul Monk - University of Auckland - Auckland, New Zealand

Introduction: The introduction of robotics for total knee arthroplasty (TKA) into the operating theatre is often associated with a learning curve and is potentially associated with additional complications. The purpose of this study was to determine the learning curve of robotic-assisted (RA) TKA within a multi-surgeon team.

Methods: This prospective cohort study included 83 consecutive conventional jig-based TKAs compared with 53 RA TKAs using the Robotic Surgical Assistant (ROSA) system (Zimmer Biomet, Warsaw, Indiana, USA) for knee osteoarthritis performed by three high-volume (> 100 TKA per year) orthopaedic surgeons. Baseline characteristics including age, BMI, sex and pre-operative Kellgren-Lawrence graded and Hip-Knee-Ankle Axis were well-matched between the conventional and RA TKA groups. Cumulative summation (CUSUM) analysis was used to assess learning curves for operative times for each surgeon. Peri-operative and delayed complications (infection, periprosthetic fracture, thromboembolism, and compromised wound healing) and revisions were reviewed.

Results: The CUSUM analysis for operative time demonstrated an inflexion point after 5, 6 and 15 cases for each of the three surgeons, or 8.7 cases on average. There were no significant differences ($p=0.53$) in operative times between the RA TKA learning (before inflexion point) and proficiency (after inflexion point) phases. Similarly, the operative times of the RA TKA group did not differ significantly ($p=0.92$) from the conventional TKA group. There was no discernible learning curve for the accuracy of component planning using the RA TKA system. The average length of post-operative follow-up was 21.3 ± 9.0 months. There was one revision for instability in the conventional TKA group and none in the RA TKA group. There was no significant difference ($p > 0.99$) in post-operative complication rates between the conventional TKA and RA TKA groups.

Conclusions: The introduction of the RA TKA system was associated with a learning curve for operative time of 8.7 cases. Operative times between the RA TKA and conventional TKA group were similar. The short learning curve implies this RA TKA system can be adopted relatively quickly into a surgical team with minimal risks to patients.

Examining the Associations Between Morphologic Knee Features With Demographics and Walking Gait Kinematics in Patients Awaiting Robotic-Assisted Knee Arthroplasty.

*Nadim Ammoury - Dalhousie University - Halifax, Canada

Stephanie Civiero - Dalhousie University - Halifax, Canada

Michael Dunbar - Dalhousie University - Halifax, Canada

Glen Richardson - Dalhousie University & Capital Health - Halifax, Canada

Jennifer Leighton - NSHA - Dartmouth, Canada

David Wilson - NSHA - Halifax, Canada

Janie Wilson - Dalhousie University - Ancaster, Canada

INTRODUCTION: Patients suffering from end-stage knee osteoarthritis (OA) have significant limitations in joint kinematics during walking, generally characterized by reduced ranges of knee motion (ROM) in the sagittal and frontal planes¹. While knee arthroplasty aims to restore joint dynamics, many patients continue to experience deficits after surgery² making this a key target for innovative approaches to knee arthroplasty using robotic surgery³. Knee joint morphology varies highly among individuals⁴, yet there is minimal evidence on the associations between knee morphological features and in vivo joint function, which is important to inform personalized surgical planning to improve knee function. We aimed to examine the associations between distal femur morphology and knee joint gait kinematics in patients awaiting robotic-assisted knee arthroplasty.

METHODS: Computed tomography images of the affected knee joint for patients with end-stage knee OA awaiting robotic-assisted arthroplasty were segmented (Mimics; Materialise) to obtain 3D models of the distal femur. Anatomical landmarks, axes and planes of interest were manually placed⁵ for measuring morphological distances and angles. A 10-camera (Sony RX0 II) markerless motion capture system (Theia3D Markerless) was used to capture and model the 3D limb segment poses during walking to define 3D knee joint kinematics (Visual3D; C-motion). Pearson's correlations were used to examine associations between distal femur morphologic variables (Table 1) with gait kinematic outcomes and demographics. T-tests were used to examine sex differences in morphology.

RESULTS: Twelve patients were recruited to date. Statistically significant correlations were found (Table 2) including: speed was negatively correlated with VZX ($r=-0.67$; $p<0.05$), with trends identified with MZX ($r=-0.53$; $p<0.097$); knee flexion range of motion (Figure 1) was positively correlated with CTA ($r=0.65$; $p<0.05$) and negatively correlated with LZX ($r=-0.62$; $p<0.05$). The ML*AP dimension, which is a measurement of the general size of the distal femur, was smaller for female patients than it was for male patients ($p<0.01$).

DISCUSSION: Patients whose lateral femoral condyle was elevated in the anterior direction (LZX) and who had a smaller condylar twist angle (CTA) had smaller knee flexion range of motion during walking, and a more elevated intercondylar groove anteriorly (MZX) was associated with slower walking speeds, both findings pointing toward the potential importance of the intercondylar groove shape with gait kinematics. Sex differences in the overall size of the distal femur were consistent with literature^{4,5}. These are preliminary findings on a small sample, and therefore should not be overinterpreted. However, evidence points to interrelationships among gait mechanics and knee joint morphology which should be further investigated with larger samples and more multivariable analyses to fully characterize.

CONCLUSION: These results suggest relationships among knee joint morphology and gait kinematics in knee arthroplasty patients that should be investigated further to inform how surgical variables may influence post-operative in vivo joint mechanics, with an ultimate goal of reducing the continued burden of post-operative functional deficits for patients.

REFERENCES:

- ¹Outerleys et al., Journ. Applied Biomechanics,2021 ;31:130-138.
- ²Hatfield et al., Journal of Arthroplasty,2011;26(2):309-318.
- ³Kenneth et al., Orthopedics,2016;39(5):e822-e827.
- ⁴Mahfouz et al., Clin Orthop Relat Res,2012;470:172–185.
- ⁵Mahfouz et al., Comp Methods Biomech Biomed Eng,2007;10(6):447-456.

Figures

Table 1: Definitions of the gait kinematic outcomes and anthropometric measurements.

Anthropometric measurements	ML/AP	Ratio of width (mediolateral distance) and height (anteroposterior distance) of distal femur. Closest to 1 indicates a more square shape.
	ML*AP	Measure of the general size of the distal femur.
	AP angle	Angle between the line joining the most anterior aspects of the medial and lateral condyles and the posterior plane. The posterior plane passes through the most posterior aspects of both condyles and is parallel to the mechanical axis.
	CTA angle	Condylar twist angle. Angle between the most lateral aspects of the condyles and the posterior plane.
	LZX	Elevation of the lateral anterior condyle relative to the most anterior aspect of the femoral shaft proximal of the condyles (AP sizing point) in direction normal to posterior plane.
	VZX	Elevation of anterior portion of intercondylar groove relative to AP sizing point in direction normal to posterior plane.
	MZX	Elevation of medial anterior condyle relative to AP sizing point in direction normal to posterior plane.
Gait kinematic outcomes	FxROM	Total knee flexion range of motion. The minimum is taken after weight acceptance during the stance phase of the cycle (20-62%) and the maximum, throughout the cycle.
	FxROMStance	Knee flexion range of motion during stance. The minimum is taken after weight acceptance during the stance phase of the cycle (20-62%) and the maximum during weight acceptance (0-20%).
	AddROMStance	Knee adduction range of motion during stance. The minimum is taken after weight acceptance during the stance phase of the cycle (20-62%) and the maximum during weight acceptance (0-20%).
	AvgFxStance	Average of the knee flexion angle during stance (0-62%).
	AvgAddStance	Average of the knee adduction angle during stance (0-62%).

[Figure 1](#)

Table 2: Patient demographics, anthropometric measurements and gait kinematics.
 Values for Pearson's r correlation coefficient are indicated for gait speed and Knee flexion range of motion.

Variables	Mean (Std)	Correlation with gait speed (r)	Correlation with knee flexion ROM (r)
Number of subjects (m, f)	(4, 8)	-	-
BMI (kg/m ²)	32.2 (5.4)	-0.76a	-0.38
Age (years)	68.7 (7.3)	-0.12	0.12
ML/AP	1.44 (0.07)	-0.03	-0.13
ML x AP	4770 (625)	0.16	-0.12
AP angle (deg)	4.6 (2.5)	0.36	-0.40
CTA angle (deg)	5.1 (1.5)	0.35	0.65b
LZX (mm)	7.4 (1.2)	-0.22	-0.62b
VZX (mm)	1.9 (1.0)	-0.67b	-0.30
MZX (mm)	4.6 (1.6)	-0.53c	-0.05
Gait speed (m/s)	0.9 (0.2)	-	0.53c
FxROM (deg)	43.3 (10)	0.53c	-
FxROMStance (deg)	6.8 (3.4)	-0.03	0.58c
AddROMStance (deg)	2.3 (1.5)	0.47	0.48
meanFx (deg)	14.2 (6.1)	0.01	-0.50
meanAdd (deg)	2.1 (6.2)	-0.05	-0.29

Statistically significant correlations are indicated by subscripts a : $p < 0.01$, b : $p < 0.05$ and c : $p < 0.10$.

[Figure 2](#)

Figure 1: Average and standard deviation of knee flexion (top) and adduction (bottom) angles during a gait cycle.

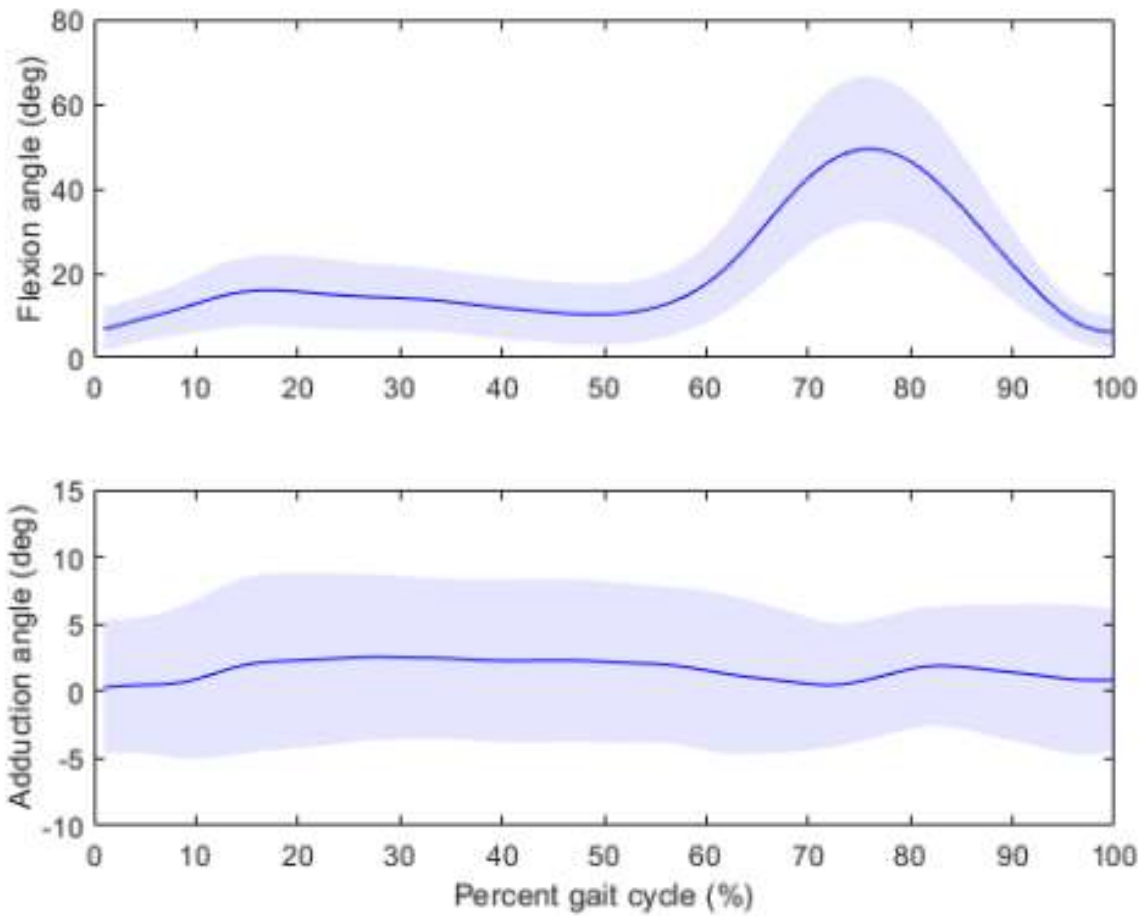


Figure 3

Consistency in Robotic-Assisted Total Knee Arthroplasty Case Time Between Different Patient Preoperative Deformities

*Laura Yanoso-Scholl - Stryker Orthopaedics - USA

Radhakrishnan Rambatla - Stryker - Fort Lauderdale, USA

Todd Gutkowski - Stryker - Mahwah, USA

Introduction: Surgical time is routinely considered since it has been shown to have an impact on concerns such as healthcare costs, length-of-stay, and risk of post-operative infection. Surgeon case volume, implant design, patient age and BMI have all been shown to influence operative time. Coronal and sagittal preoperative deformities provide an intraoperative challenge to the surgeon, requiring them to carefully adjust implant placement and sizing to correct for these deformities. Robotic-assisted TKA has been shown to result in improved outcomes for patients with preoperative deformities but there is less focus on understanding how this technology influences surgical time for complex cases. The purpose of the current study is to determine how patient preoperative coronal and sagittal deformity influences robotic case time.

Methods: A retrospective study was performed on 837 RATKA cases performed by 3 high-volume surgeons. Intra-operative timestamps were collected for bone registration, bone preparation, implant planning, ligament laxity assessment, and trialing, for each case. Pre-operative coronal and sagittal deformities were assessed using a 3D CT. Coronal deformity was defined using hip-knee-ankle angle (HKA), separating varus and valgus cases. Sagittal deformities were defined as $>10^\circ$ of flexion being a flexion contracture. Statistical analysis was performed using a two-way ANOVA with $\alpha=0.05$.

Results: Coronal deformity did not have statistically significant impact on surgical time ($p>0.05$, Figure 1 and 2). Flexion contracture did statistically significant increase surgical time ($p<0.05$) where neutral cases (19 minutes 55 seconds \pm 7 minutes 36 seconds) had, on average, a 3 minutes 55 seconds shorter surgical time compared to flexion contracture cases (23 minutes 50 seconds \pm 10 minutes 52 seconds). Majority of this difference in time was due to implant planning (+58 seconds), bone preparation (+56 seconds), and trialing (+74 seconds) times.

Discussion: The current study found no statistical difference in surgical time based on coronal deformity, indicating consistency in surgical timing regardless of deformity. Correction of flexion contractures were shown to increase operative time on average less than 4 minutes which when considering obesity can have upwards of 15 minute surgical increase for manual TKA. The additional time for the flexion contracture cases was spent during implant planning, bone preparation and trialing, which are all critical steps when properly balancing a TKA. Understanding differences in surgical time and reducing variability in time between cases, may lead to a more predictability and efficiency in the OR.

Accuracy of a Novel Imageless Guided Robotic System Using Patient-Specific Alignment

*Ittai Shichman - Tel-Aviv Sourasky Medical Center - Tel Aviv, Israel

Amer Hallak - Tel Aviv Sourasky Medical Center - Tel Aviv, Israel

Amit Benady - Tel Aviv Sourasky Medical Center - Tel Aviv, Israel

Yaniv Warschwaski - Tel Aviv Sourasky Medical Center - Tel Aviv, Israel

Aviram Gold - Tel Aviv Sourasky Medical Center - Tel Aviv, Israel

Nimrod Snir - Tel Aviv Sourasky Medical Center - Tel Aviv, Israel

Keywords: Patient Specific Alignment, Total Knee Arthroplasty, Imageless Navigation-Assisted Robot

Background

The rise of imageless navigation-assisted total knee arthroplasty (TKA) over the last decade can be attributed to refining precision and reproducible intraoperative measurements relative to traditional manual instrumentation. Robotic assisted TKA have been associated with higher precision of bone resections and Target alignment.

Objectives

This study examined the accuracy of bony resections using a novel imageless robotic arm system to achieve patient specific alignment (PSA); an intraoperative surgical decision based on calculated parameters preoperatively and intraoperatively to reach an alignment tailored for each individual patient.

Study Design & Methods

This prospective study assessed 105 patients who underwent imageless navigation-assisted robotic patient-specific alignment TKA using a single implant design for primary osteoarthritis between January 2022 and July 2023. Intraoperative planned angles for the lateral distal femoral angle (LDFA) and medial proximal tibial angle (MPTA), as well as achieved arithmetic HKA after implant positioning were compared to postoperative angles measured on full-length standing anterior-posterior X-ray. The desired postoperative alignment was deemed as being within ± 2 standard deviations (STD). Difference greater than two STDs was considered an outlier.

Results

Between the validated and planned angles for the LDFA the mean difference was $0.14^\circ \pm 1.80^\circ$ with 102/105 (97.1%) of cases achieving desired alignment. Between the validated and planned angles for the MPTA the mean difference was $0.79^\circ \pm 1.29^\circ$ with 102/105 (97.1%) of cases achieving desired alignment. The proportion of outliers was 2.9% (3/105) of cases across both LDFA and MPTA angles. The mean difference between intraoperative achieved HKA measured by the robotic imageless navigation system and final postoperative HKA as measured on full-length standing anterior-posterior (AP) X-ray at 6 months postoperatively was $0.66^\circ \pm 2.16^\circ$.

Conclusions

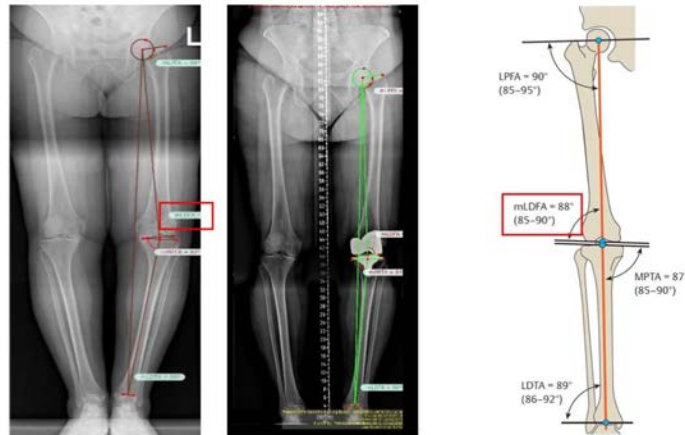
The use of a Novel imageless navigation robotic assisted TKA system to achieve PSA conferred with high accuracy of bony cuts for both MPTA and LDFA with adequate coronal alignment postoperatively. These findings suggest that the use of

imageless navigation robotic assisted system is a valid tool to surgeons who seek contemplating PSA in TKA.

Figures

METHODS – Angle measurement

- Lateral distal femoral angle (LDFA)

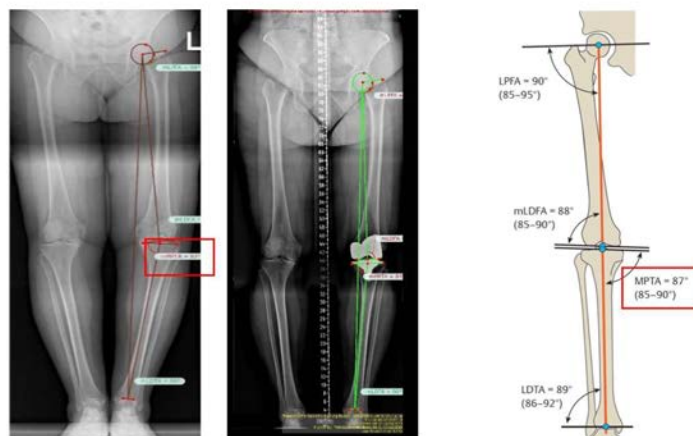


Radiologykey.com 10.1055/s-0034-92241

Figure 1

METHODS – Angle measurement

- Medial proximal tibial angle (MPTA)



Radiologykey.com 10.1055/s-0034-92241

Figure 2

METHODS – Measurements

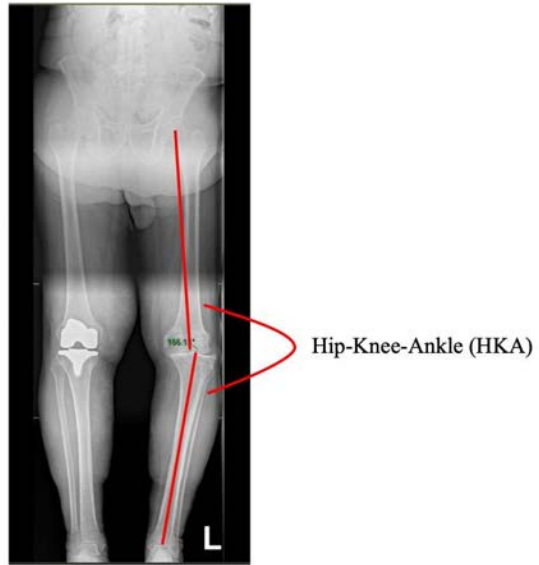


[Figure 3](#)

Effect of Tibial Slope on Knee Mechanics for PCL Deficient Cruciate-Retaining Total Knee Arthroplasty

*Kyle Snethen - Zimmer Biomet - Warsaw, USA

Marc Bandi - Zimmer GmbH - Winterthur, Switzerland

Eik Siggelkow - Zimmer GmbH

Craig Silverton - Henry Ford Hospital - Detroit, USA

Nicholas Frisch - Ascension - Bloomfield Hills, United States of America

Introduction: Continuing debate exist over the optimal tibial slope for a cruciate-retaining (CR) total knee arthroplasty (TKA) versus a cruciate-sacrificing TKA. Recently introduced CR-TKA systems accommodate both posterior cruciate ligament (PCL) retention or sacrifice, thus further compounding the debate; specifically, how to address the tibial slope if bone cuts were already performed for a CR-TKA and the PCL becomes compromised during the surgical procedure. The objective of this study was to determine the effect of tibial slope on knee mechanics during CR-TKA with a deficient PCL with the intention of informing surgical decisions regarding if the tibial slope should be adjusted.

Methods: A robotic simulator performed passive laxity tests and simulated lunge on seven fresh-frozen cadaveric knee specimens in the natural state and following TKA (Persona®Medial-Congruent®, Zimmer Biomet, Warsaw, IN, USA) with the PCL completely resected at tibial slopes of 0°, 3°, 5° and 7°. Laxity assessments were performed at 15°, 30°, 45°, 60°, and 90° knee flexion by applying ±6 Nm internal-external (IE) torque, ±12 Nm varus-valgus (VV) torque, ±100 N anterior-posterior (AP) force, and ±100 N medial-lateral (ML) force in each direction. Rapid prototyped tibial bearings were used to modify the tibial slope without performing any additional bone cuts or rebalancing the knee. Two-way ANOVA ($\alpha=0.05$) with post-hoc pairwise multiple comparison was used to compare laxities between the different tibial slopes at each knee flexion angle tested.

Results: The tibial slope did not have a significant ($\alpha=0.05$) effect on IE, VV, AP or ML knee laxity over the entire arc of knee flexion. VV laxity decreased with increased slope (Fig. 1), but the overall maximum difference between slopes was only 1.4°. There was no clear trend in AP laxity with a change in tibial slope; however, the joint shifted posteriorly by an average of 2.2mm with each incremental slope increase (Fig. 2) The tibial slope also did not have a significant effect on lunge kinematics (Table 1).

Conclusion: Increasing tibial slope did not significantly affect varus-valgus laxity throughout flexion suggesting slope should not be adjusted to correct for flexion/extension gap balancing. An increase in tibial slope shifts the dwell point of the knee slightly posteriorly, but without an intact PCL, had no significant effect on knee laxity or joint kinematics. In conclusion, in the event the PCL is compromised during a CR-TKA procedure, it is not necessary to recut the tibial slope.

Figures

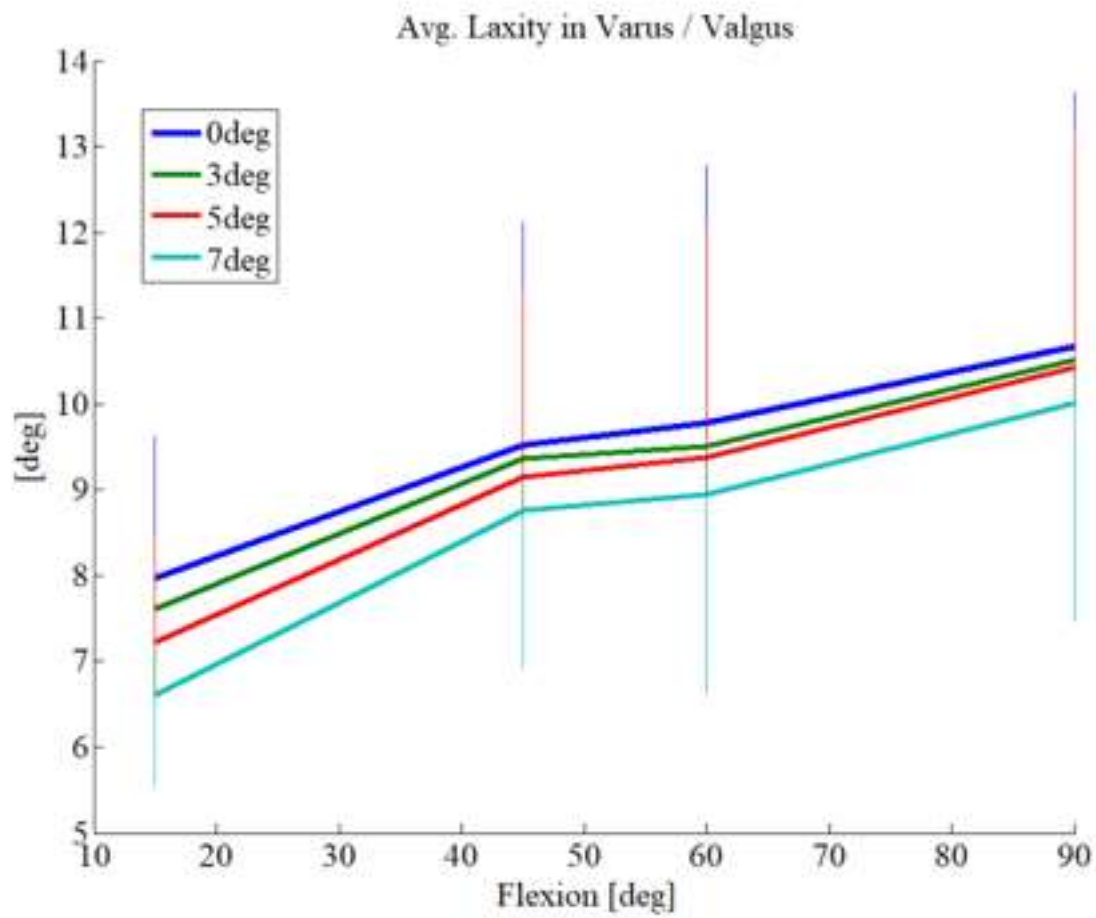


Figure 1. Averaged VV laxity over the range of flexion for each tibial slope.

[Figure 1](#)

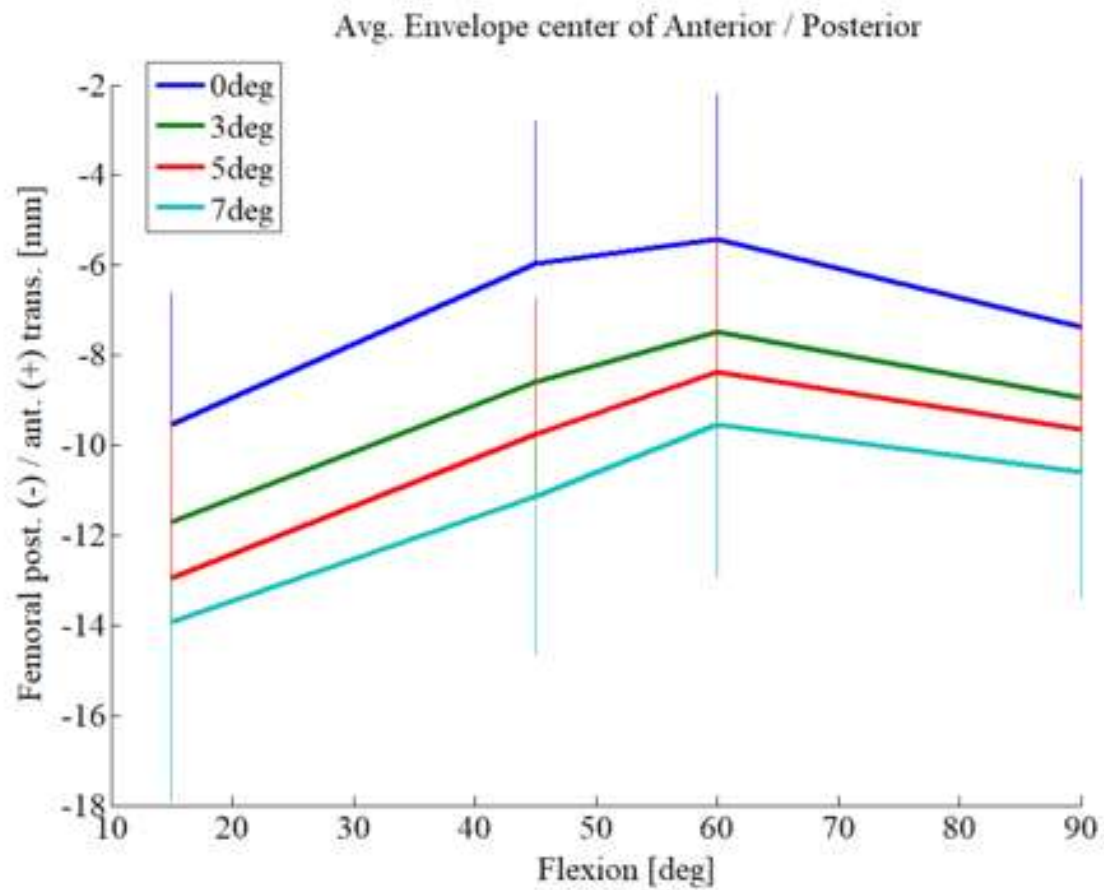


Figure 2. The average mid AP positions from the envelope of motions determined during AP laxity simulations for each tibial slope.

Table 1. Root mean square error (RMSE) between lunge kinematics for 0° and 7° tibial slopes in each degree-of-freedom (DOF)

DOF	RMSE
Flexion	1.4
ML	1.0
VV	0.9
AP	3.6
IE	3.1
PD	0.6

[Figure 2](#)

[Figure 3](#)

TKA Joint Line Obliquity Post-Op Comparisons for External Knee Adduction Moments During Stair Ascent

*William Mihalko - University of Tennessee - Germantown, USA

Nuanqiu Hou - Campbell Clinic - Memphis, United States of America

Alexis Nelson - UTHSC - Memphis, Select Country

Douglas Powell - University of Memphis - Memphis, USA

Marcus Ford - Campbell Clinic Orthopaedics - Germantown, USA

James Guyton - Campbell Clinic Orthopaedics - Germantown, USA

John Crockarell - Campbell Clinic Orthopaedics - Germantown, USA

Christopher Holland - Campbell Clinic - Memphis, USA

Teri Ross - University of Tennessee Health Science Center - Memphis, USA

Derek Dixon - Campbell Clinic Foundation - Germantown, USA

Introduction: A TKA joint line can be placed either in a mechanical or kinematic alignment. Achieving a femorotibial mechanical axis of $180^\circ \pm 3^\circ$ has been shown to produce optimal clinical outcomes (Fang et al., 2009). However, placement in the mechanical axis does not maintain patient's natural knee joint alignment nor account for patient-specific differences in gait dynamics which could lead to differences in PROs compared to kinematic alignment. Our aim was to understand whether the difference between preoperative and postoperative knee joint alignment impacts biomechanical variables during stair ascent.

Methods: We included 58 patients who received cruciate retaining implants. All patients underwent unilateral TKA and are at least one-year post-op. A three step instrumented staircase (1000Hz, AMTI Inc., Watertown, MA) and an 8-camera markerless motion capture system (200Hz, OptiTrack, NaturalPoint Inc., MA) were used to collect ground reaction forces and segment kinematics, respectively, during stair descent. An AI based reconstruction software (Theia Markerless, Inc., Version 2023, Kingston, ON) was used to identify segment kinematics. Joint line convergence angle was measured using anteroposterior weight bearing radiographs. Visual3D Professional (HAS Motion, Version 2023.09.3, Canada) and MATLAB (The MathWorks, Inc., R2023b, Natick, MA) were used for data analysis. An independent sample t-test was used to compare external peak and mean knee adduction moment and impulse between patients who had a change in knee joint alignment and those who maintained the same knee joint alignment postoperative.

Results: A change in knee joint alignment was observed in 34 patients. 24 patients maintained their natural alignment postoperative. There were no significant differences in age or BMI between groups. We did not observe a significant difference in external peak knee adduction moments (Figure 1a, $p=0.379$), mean knee adduction moment (Figure 1b, $p=0.317$), and adduction/abduction impulse (Figure 1c, $p=0.491$).

Conclusion: We aimed to understand the impact that knee joint alignment changes had on knee joint biomechanics during stair ascent. Whether patients' natural knee joint alignment was maintained did not significantly impact external peak and mean knee adduction moment.

References:

Fang, D. M., Ritter, M. A., & Davis, K. E. (2009). Coronal alignment in total knee arthroplasty: just how important is it? *J Arthroplasty*, 24(6 Suppl), 39-43.

Howell, S. M., Papadopoulos, S., Kuznik, K. T., & Hull, M. L. (2013). Accurate alignment and high function after kinematically aligned TKA performed with generic instruments. *Knee Surg Sports Traumatol Arthrosc*, 21(10), 2271-2280.

Niki Y, Nagura T, Nagai K, Kobayashi S, Harato K. Kinematically aligned total knee arthroplasty reduces knee adduction moment more than mechanically aligned total knee arthroplasty. *Knee Surg Sports Traumatol Arthrosc*. 2018;26(6):1629-1635.

Figures

C2A

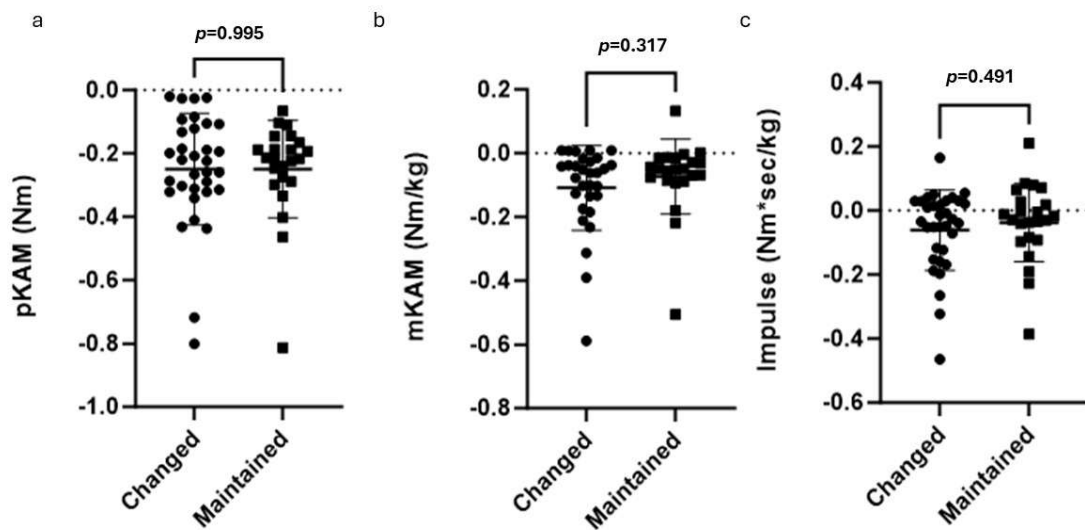


Figure 1

Impacts of Medial-Lateral Implant Placement in TKA

*Nathan Lenz - Smith & Nephew - Memphis, USA

Introduction:

Anterior knee pain related to the patellofemoral joint is one of the more common complaints following TKA. Tight lateral retinaculum structures and associated poor patella tracking are potential contributors to anterior knee pain. Medializing the patella implant, lateralizing the femoral implant, and lateralizing the tibia implant has been suggested to improve patella tracking [1]. This study seeks to understand the individual and combined effects of medial-lateral (M-L) placement of the femoral, tibial, and patellar implants on the resected bone throughout the flexion range.

Methods:

A computational analysis was performed simulating 0-120° knee flexion of a PS TKA with a 3° asymmetric joint line using previously validated software (LifeMOD/KneeSIM; LifeModeler Inc.) that includes MCL, LCL, popliteal-fibular ligament, iliotibial band, iliopatellar band, and medial retinaculum. A three-level factorial DOE was performed (Stat-Ease 360, Stat-Ease Inc.) for ± 2 mm M-L placement of the femoral, tibial, and patellar implants on the resected bone surfaces for a simulated TKA surgery. Iliotibial band (ITB) strain, iliotibial-patellar band (ITB-pat) strain, medial retinaculum strain, patella M-L shift, patella M-L tilt, and patella interface M-L shear were measured throughout flexion for a deep knee bend activity. Linear regression coefficients for implant position variables were calculated for every 10° knee flexion with the DOE software.

Results:

ITB and ITB-pat strain were reduced by medialized patella and lateralized femur with the effect increasing with knee flexion while medial retinaculum strain was increased by medialized patella and lateralized femur with a reduced effect on the femur in flexion and both femur and patella in mid-flexion (Figure 1). The ITB effects are fairly insignificant at 0.1-0.3% strain/mm for the femur and 0-0.4% strain/mm for the patella while ITB-pat effects are 0.5-1.2% strain for the patella and 0.2-0.8% strain/mm for the femur at $\geq 30^\circ$ knee flexion and medial retinaculum effects for the femur range 0.5-1.2% strain/mm and 0.7-1.5% strain/mm for the patella. Patella tracks more lateral for medialized patella and lateralized femur with both approaching regression coefficients of -1mm/mm and 1mm/mm respectively while lateral patella tilt is reduced by lateralized patella, lateralized femur, and medialized tibia with patella effects generally larger than femur and tibia effects although all effects are less than 0.4°/mm (Figure 2). Patella interface lateral shear is reduced by medialized patella and lateralized femur and tibia with larger effects for patella than femur and tibia and larger effects in flexion than extension (Figure 3).

Conclusion:

Patella tracking, lateral retinaculum strain, and patella shear forces were improved by medializing the patellar and lateralizing the femoral. Only patella tilt was improved by lateralizing the patella, but at less than 0.4°/mm the effects on patella tilt are not likely to be clinically relevant. The tibial implant M-L position effects were minimal. Given beneficial effects of medializing the patella and lateralizing the femur on patella tracking with no apparent downsides, these results support this as a good practice although lateralizing the tibia may not be necessary.

References:

1. Shervin et al. World J Orthop. 2015; 6(10):795-803.

Figures

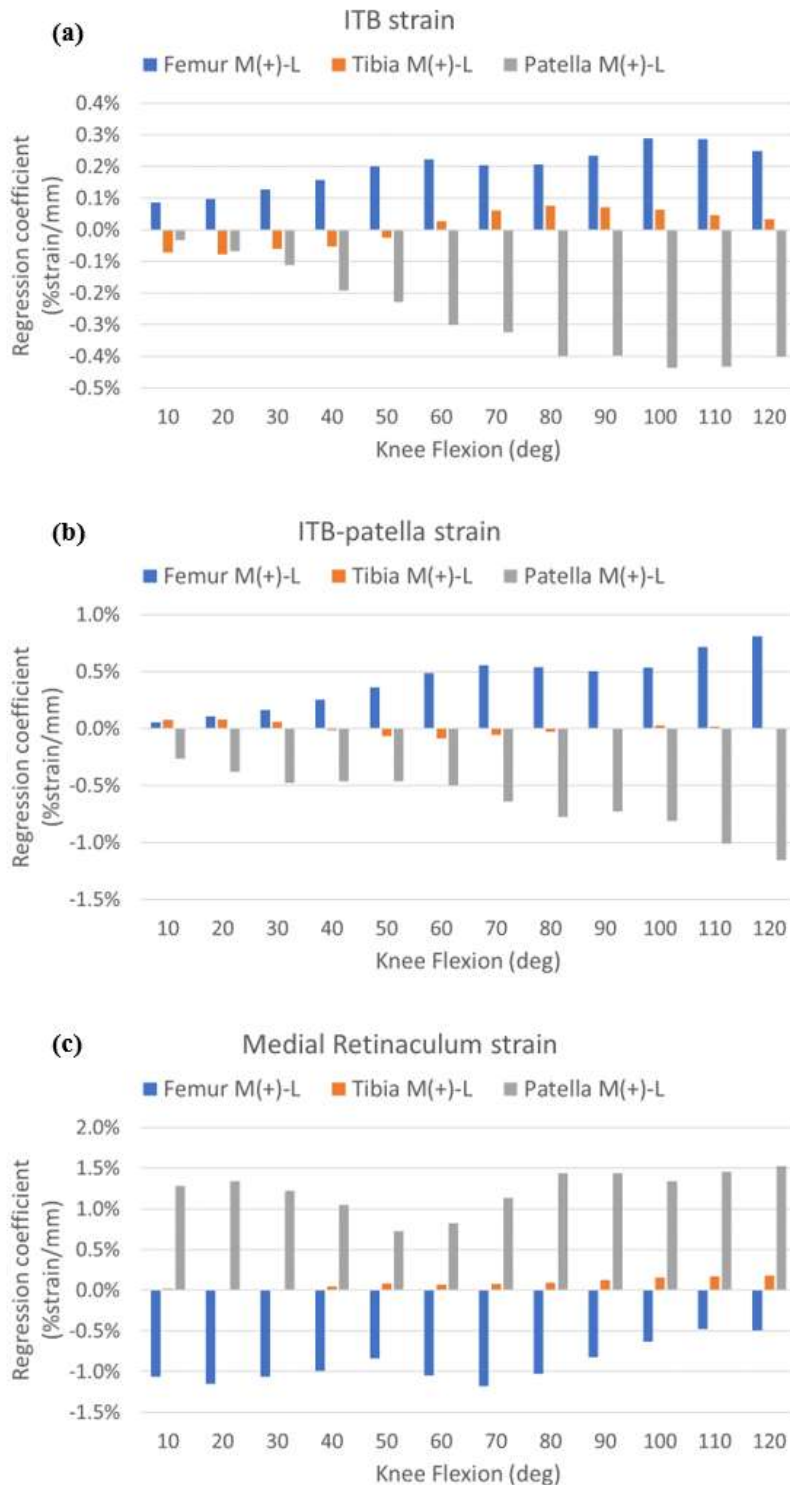


Figure 1: Ligament strain regression coefficients indicating change in % ligament strain per 1mm M-L change in femur, tibia, and patella implant position for (a) iliotibial band, (b) iliotibial-patellar band, and (c) medial retinaculum throughout flexion.

[Figure 1](#)

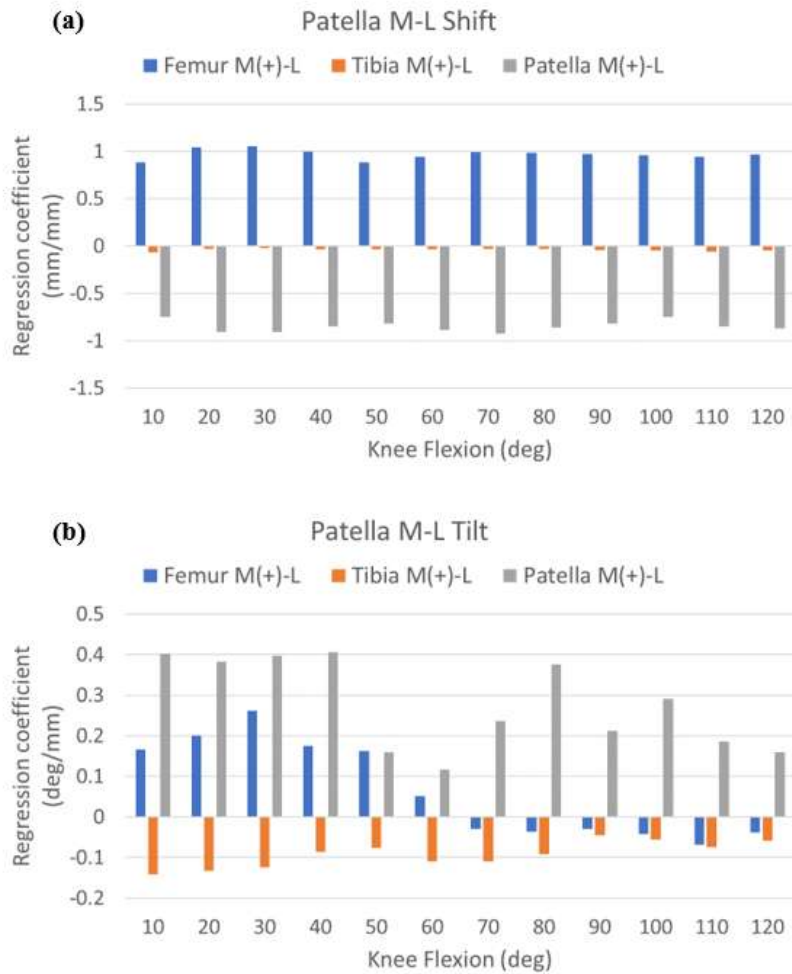


Figure 2: Patellofemoral kinematics regression coefficients indicating change in position per 1mm M-L change in femur, tibia, and patella implant position for (a) patella M-L shift and (b) patella M-L tilt throughout flexion.

[Figure 2](#)

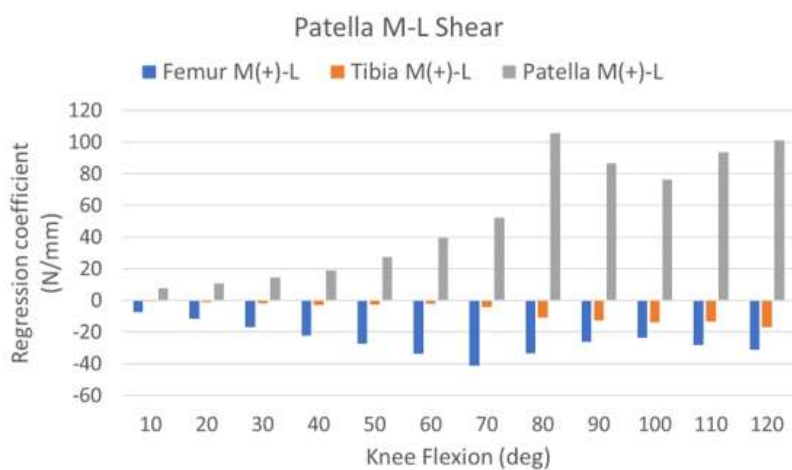


Figure 3: Patella interface M-L shear regression coefficients indicating change in shear load per 1mm M-L change in femur, tibia, and patella implant position throughout flexion.

[Figure 3](#)

Interfacial Motion Comparison Between 1-Peg and 3-Peg Cementless Patellar Implants During Simulated Patellofemoral Kinematics and Kinetics

*Bradley Elliott - Zimmer Biomet, Inc. - Warsaw, USA

Kimberly Mimnaugh - Zimmer Biomet, Inc - Warsaw, USA

Introduction

Small interfacial motions (micromotion) may disrupt the stability of cementless implants and prevent bony ingrowth. As little as 150 μ m of cyclic motion has been shown to disrupt bone formation and compromise implant stability.¹ Cementless patellar implants often feature pegs that anchor the implant while ingrowth occurs. However, the relationship between peg layout and its effects on initial stability of the implant has been rarely considered. The purpose of this study was to compare the ability of two different cementless patellar implant designs to resist interfacial motion when subjected to patellofemoral loading conditions.

Methods

A summary of the test parameters can be found in Table 1. Specimens were coupled with a cruciate retaining (CR) femoral implant (Fig. 1) on a 6-axis joint simulator, where each specimen was subjected to simulated walking and squat loads and motions.

A digital image correlation (DIC) system was used to record superior-inferior (S/I) motion of the patellar implants relative to the foam blocks. Tracking markers were affixed to the patellar implants and foam blocks, and displacement of the patellar implant markers relative to those on the foam blocks was measured.

Raw displacement data was filtered and mean peak-to-peak amplitude for each signal was calculated. ANOVA statistical analysis was conducted with implant design (1-peg, 3-peg) as the main effect in the model affecting micromotion magnitude.

Results

The average micromotion was below the 150 μ m threshold for bony ingrowth for both patellar implant designs (Fig. 2). The highest average motion was measured in the 1-peg patellar implants during the squat activity (55.8 \pm 6.7 μ m). In comparison, the 3-peg patellar design had an average micromotion of 38.4 \pm 7.2 μ m during the simulated squat activity. ANOVA showed that implant design made a small but statistically significant contribution to the motion measured ($p = 0.004$), and Tukey analysis demonstrated that the 1-peg patellar implant had statistically significantly higher average motion than the 3-peg patellar implant ($p = 0.004$).

Conclusions

In conclusion, the peg layout on cementless patellar implants has been shown to have a small but statistically significant effect on interfacial motion between the implant and bone foam during simulated walking and squat activities. A cementless patellar implant with one central peg showed less ability to resist interfacial motion compared to a cementless 3-peg patellar implant. However, neither patellar implant had micromotion that exceeded the common 150 μ m threshold for bony ingrowth.

References

N. Kohli, J. C. Stoddart, and R. J. van Arkel, "The limit of tolerable micromotion for implant osseointegration: a systematic review," *Sci. Rep.*, vol. 11, no. 1, p.10797, Dec. 2021, doi: 10.1038/s41598-021-90142-5.

Figures

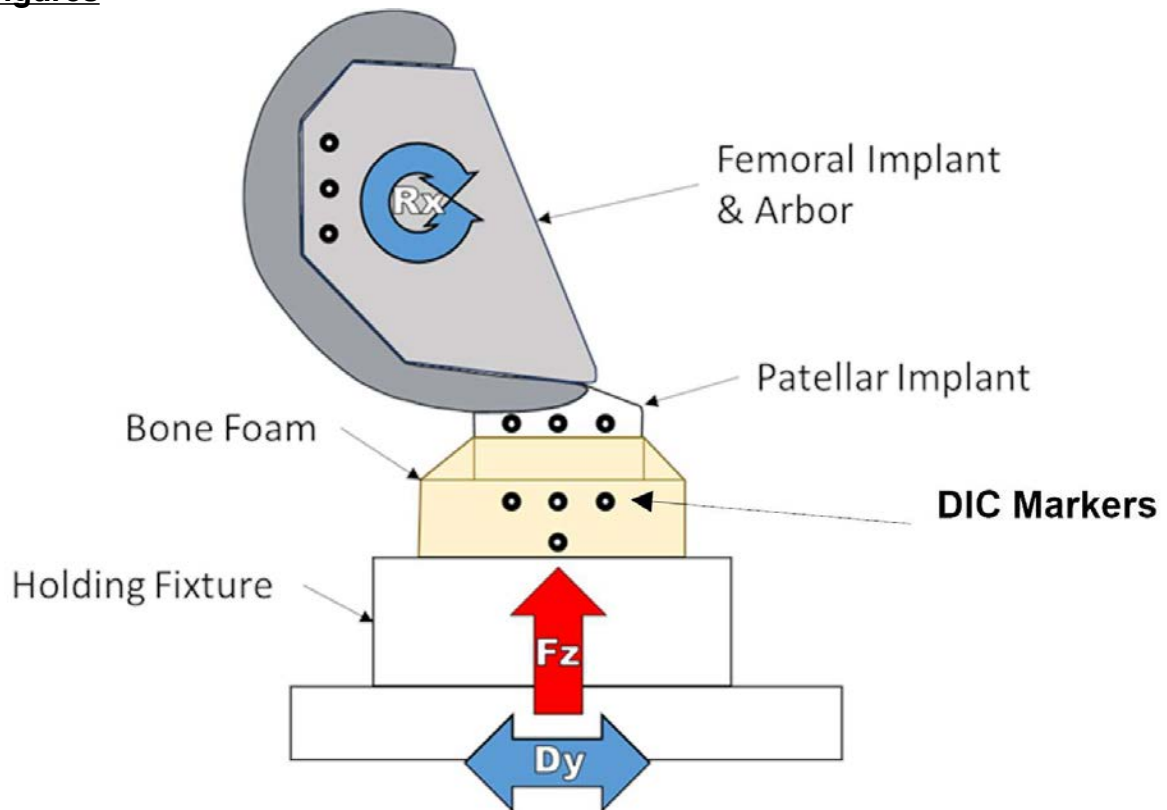
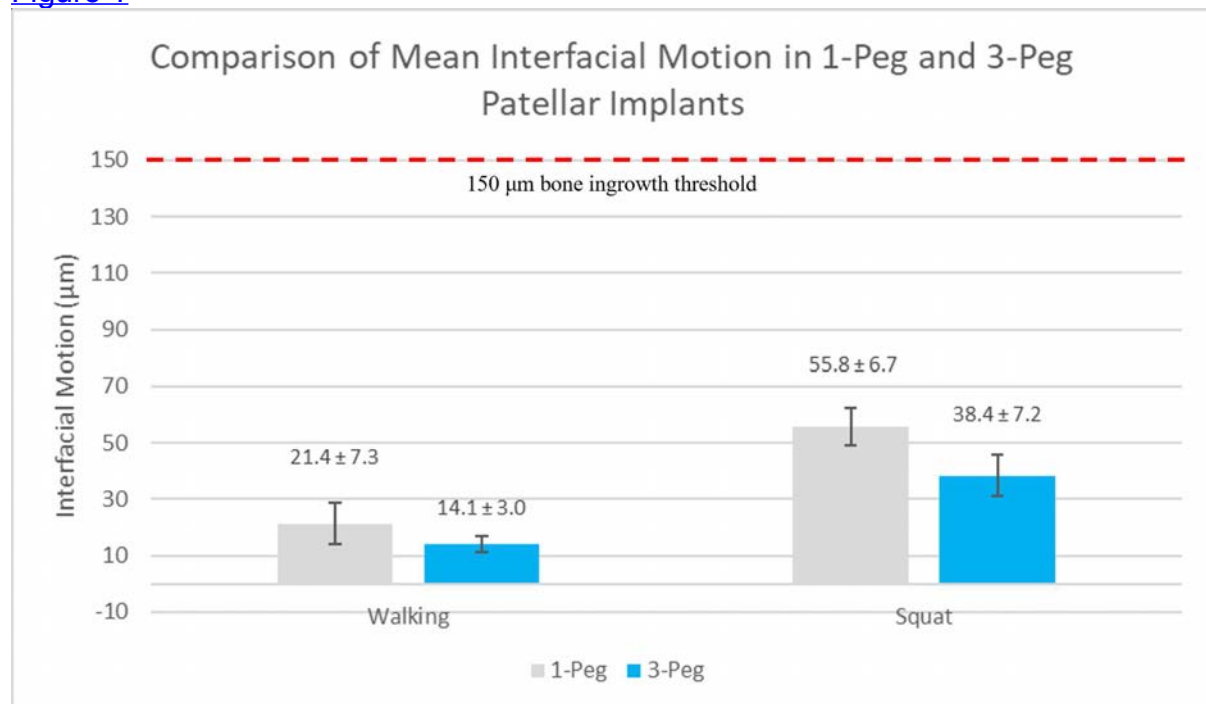


Figure 1



[Figure 2](#)

Table 1. Test Method Parameters

Parameter	Simulated Walking	Simulated Squats
Peak Compressive Force, Fz (N)	525	3150
Peak M/L Displacement (mm)	1.8	4.9
Peak S/I Displacement (mm)	12.6	30
Max PF Flexion Angle (°)	40.6	84
Frequency (Hz)	1.1	0.33
Bone Foam Density (lbf/ft ³)	30	30

Parameter	1-Peg Patella	3-Peg Patella
Environment	Ambient	Ambient
Sample Size	8	15
Peg Orientation	Centralized	Variable

[Figure 3](#)

The Pendulum Knee Drop Test as a Means to Distinguish Balance in a Total Knee Arthroplasty Model

*Kevin Abbruzzese - Stryker - Mahwah, USA

Scott Logan - Stryker Orthopaedics - Mahwah, USA

Michael Dunbar - Dalhousie University - Halifax, Canada

Jared Weir

Michael Mont - Sinai Hospital of Baltimore - Baltimore, USA

Sally LiArno - Stryker Orthopaedics - Bergenfield, USA

Introduction:

Soft-tissue balance is an important aspect of a successful total knee arthroplasty (TKA) procedure. Standard soft-tissue balancing techniques utilized in TKA are often subjective, centered around a surgeon's feel of ligament laxity [1]. A pendulum knee drop (PKD) technique offers a quantifiable and reproducible approach to reliably estimate the soft-tissue laxity of the knee joint based on passive motion. This study evaluated laxity and motion in three different total knee arthroplasty models by utilizing this PKD test with an inertial measurement unit (IMU) to characterize soft-tissue balance.

Methods:

An advanced knee simulator model was used to assess robotic-assisted TKA surgical parameters for three surgical plans: A,B,C [2]. The native proximal femur and distal tibia were designed as modular end caps and replaced after each procedure. Robotic software was used to position components and balance the knee using a size four cruciate-retaining femur and a 9mm thick polyethylene insert. The PKD test was performed on each specimen to assess knee laxity changes. Compartmental resection depths were captured as the summation of the distal femur and proximal tibia resection depths in extension and the posterior femur and proximal tibia resections in flexion. Knee range of motion (ROM) was measured with an IMU system and the log decrement value was estimated for each plan to characterize the degree of laxity with larger reported values indicating greater stiffness [3]. Three trials were performed for each surgical plan and the final implanted surgical plans were ranked by each surgeon in terms of laxity and assessed for significance with a Kruskal-Wallis test.

Results:

Surgeons ranked plan A as the stiffest and plan C as having the greatest laxity. The pendulum knee drop technique was able to determine differences between surgical plans based on laxity values (Figure 1). Significant differences were detected in laxity between surgical plan A and surgical plan C ($p < 0.05$). Medial extension resection depth values demonstrated a reciprocal pattern with smaller resections resulting in greater log decrement values ($R^2 = 0.91$). Increased femoral flexion demonstrated a positive correlation with increased log decrement values ($R^2 = 0.91$). No other significant trends were observed for other surgical planning parameters. The PKD demonstrated reproducible results for log decrement estimations (SD 0.028).

Discussion:

Surgical planning is a static three-dimensional process that relies on bony resections and component placement for soft-tissue balance. The PKD technique objectively assessed laxity changes across multiple surgical plans. Plan A demonstrated the greatest stiffness, preserving more bone medially in extension and exhibiting greater

femoral flexion. Plan C resulted in increased laxity, observed by a smaller log decrement coefficient and greater medial resections in extension with less femoral flexion. Plan B displayed intermediate laxity based on medial extension resection parameters and femoral flexion. The PKD test discerned simulated soft-tissue conditions and laxity variations between plans, offering a reproducible means to evaluate effects of resection depths and component rotations on knee laxity.

Figures

JR-GSNPS-ARTI-1029367

Table 1. Robotic-assisted total knee arthroplasty surgical planning parameters

	Extension Resection Depth (mm)		Flexion Resection Depth (mm)		Femur (deg)			Tibia (deg)	
	Medial	Lateral	Medial	Lateral	Varus	Internal	Flexion	Varus	Slope
Surgical Plan A	13.5	15	14	13	0	1	5	2	3
Surgical Plan B	14	13.5	15	14	0	1	4	4	3
Surgical Plan C	14.5	15	14.5	15.5	-0.5	2	3	3	5

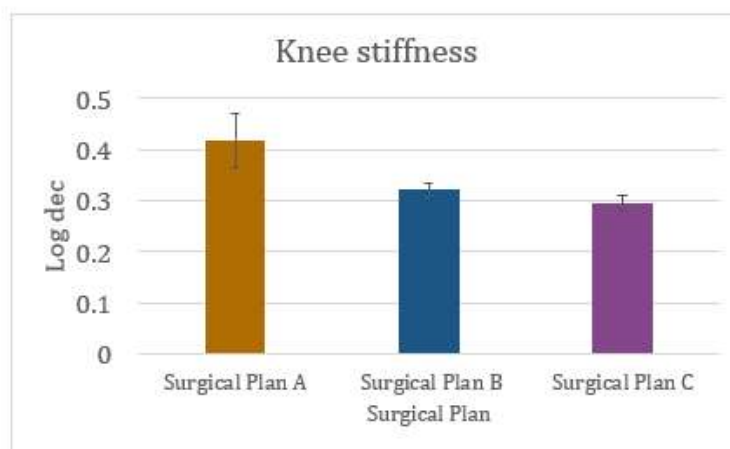


Figure 1. Mean log decrement coefficients for all surgical plans

References:

1. Kwak DS, Kong CG, Han SH, Kim DH, In Y. Development of a pneumatic tensioning device for gap measurement during total knee arthroplasty. *Clin Ortho Surg.* 2012;4(3):188-192. doi:10.4055/cios.2012.4.3.188
2. Faizan, A. (2023). An Advanced knee simulator model can reproducibly be used for ligament balancing training during TKA. *ORS 2023.*
3. Abbruzzese, K. (2023). Knee Stiffness Evaluations Using an Advanced Total Knee Arthroplasty Simulator Model for Loaded Ligament Assessments. *ISTA 2023*

Figure 1

Impact of Asymmetric Tibial Inserts on Multi-Planar Kinematics During Pendulum Knee Drop Test

*Kevin Abbruzzese - Stryker - Mahwah, USA

Michael Dunbar - Dalhousie University - Halifax, Canada

Jared Weir

Michael Mont - Sinai Hospital of Baltimore - Baltimore, USA

Sally LiArno - Stryker Orthopaedics - Bergenfield, USA

Introduction:

Achieving optimal outcomes in total knee arthroplasty (TKA) relies on restoring the physiologic balance in the soft-tissue envelope surrounding the knee joint. A novel technique known as the pendulum knee drop (PKD) offers a reliable means to assess soft-tissue laxity by measuring oscillation parameters when the leg is passively swung. This study aims to evaluate laxity and passive motion in a TKA model using the PKD test with an inertial measurement unit (IMU). Additionally, it seeks to assess multi-planar compartmental changes with precise 1-millimeter (mm) thickness increments to enhance the characterization of soft-tissue measurements.

Methods:

The PKD test was conducted on a mechanical bone model that underwent robotic assisted total knee arthroplasty (RATKA). Utilizing a two-sensor IMU system, knee range of motion (ROM) was recorded by placing femoral and tibial sensors approximately 0.75 meters apart. Three trials were performed for various insert thicknesses, ranging from 10 to 14 mm with 1 mm increments. The medial compartment was evaluated with 1 mm changes, while the lateral compartment maintained a fixed 10 mm insert. The test was repeated for the lateral compartment with 1 mm increments, while the medial compartment had a fixed 10 mm insert. ROM was measured and the log decrement ratio was computed for each of the 15 trials conducted [1]. Analyses of variance tests were employed to assess significance of log dec values between insert groups at a 95% confidence level.

Results:

Significant differences in sagittal and coronal plane kinematics were observed based on log decrement estimates. Medial stiffness exhibited an increasing trend in the sagittal plane, with significant differences among inserts except for 11-mm and 12-mm inserts. No significant differences were noted in the lateral compartment for sagittal plane kinematics, Figure 1. Knee ROM was influenced by insert thickness changes, notably with the 14 mm medial insert resulting in reduced flexion and extension movements. A similar increasing trend in coronal medial stiffness was observed across all inserts, with significant differences except for the 10-mm and 11-mm inserts. Significant differences in coronal plane kinematics were detected between inserts in the lateral compartment, particularly with the 14 mm insert resulting in stiffer knee ROM compared to the 10 mm and 11 mm inserts.

Discussion:

The study revealed a significant increase in knee stiffness with thicker implant trial thicknesses, particularly in the medial compartment across sagittal and coronal planes. Interestingly, the lateral compartment exhibited less sensitivity to asymmetric increases and greater laxity. While previous examinations focused on compartmental pressures and ligament tension, these metrics serve as surrogate endpoints rather than direct measures of construct laxity. Dynamic multi-planar soft tissue

assessments may offer a complementary approach to understanding the impact of TKA decisions on kinematics.

Figures

JR-GSNPS-ARTI-1029399

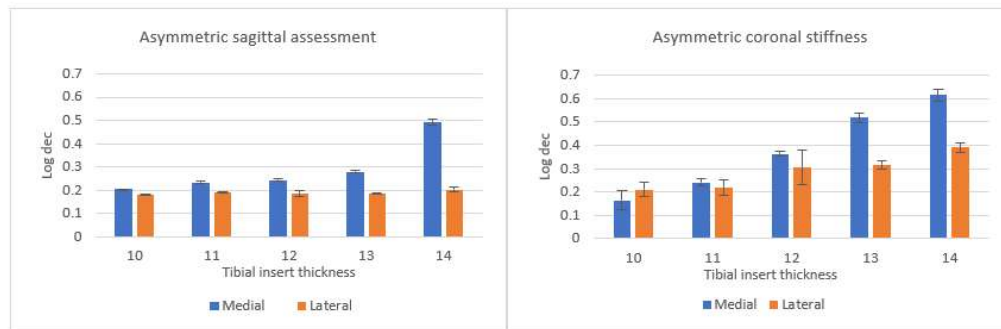


Figure 1. Average log decrement estimates per asymmetric tibial insert for both medial and lateral compartments

References:

Abbruzzese, K. (2023). Knee Stiffness Evaluations Using an Advanced Total Knee Arthroplasty Simulator Model for Loaded Ligament Assessments. ISTA 2023

Figure 1

Press-Fit Tibial Tray Micromotion Is Similar During Loading in High Flexion Between Manual and Robotic-Assisted Total Knee Arthroplasty

*Ana Figueroa - University of Iowa Orthopedic Biomechanics Laboratories - Iowa City, USA

Ayobami Ogunsola - University of Iowa - Iowa City, USA

Michael Marinier - University of Iowa

Marc Brouillette - University of Iowa Orthopedic Biomechanics Laboratories - Iowa City, USA

Jacob Elkins - University of Iowa - Iowa City, USA

Introduction: Most studies comparing robot assisted TKAs (rTKA) to manual TKAs (mTKA) focus on revision rates [1], implant positioning [2], and patient satisfaction [3]. However, tibial implant stability is another key factor for successful TKA, and initial implant stability is perhaps even more critical in the setting of modern press-fit components. The objective of this study was to determine differences in relative motion of the posterior edge of a press-fit tibial component when the surgery was performed with and without use of a surgical robot.

Methods: 10 fresh-frozen lower-body cadaveric specimens were implanted with Attune press-fit Cruciate Retaining Knee Systems (DePuy Synthes, Warsaw, IN). One side of each specimen was randomized to a mTKA with a traditional gap-balancing technique, and the contralateral underwent rTKA with a VELYS Robotic-Assisted Solution (DePuy Synthes, Warsaw, IN). Specimens were axially loaded with 250 N (replicating initial post-operative, protected weightbearing standing) to seat the implants. Specimens were then rotated to a 60° angle from vertical and cyclically loaded from 10 N to 600 N for 10 cycles to represent stair climbing. Displacement of the posterior edge of the implant relative to the tibia was measured using a digital image correlation system (ARAMIS, GOM, Braunschweig, Germany). Average displacement within each loading cycle (between 10 N and 600 N) and maximum displacement of the implant under load were calculated independently for the medial and lateral sides of the implant.

Results: Data from n=2 mTKA specimens was not available due to software failure during data capture (n=1) and to a tibia fracture (n=1). Within-cycle implant displacement for rTKAs and mTKAs averaged 0.32 ± 0.18 mm and 0.20 ± 0.11 mm respectively, which was significantly different ($p = 0.018$), but of a negligible magnitude. Maximum displacement on the lateral side of the implant averaged 1.07 ± 0.60 mm for mTKA and 1.38 ± 0.86 mm for rTKA. Similarly, maximum implant displacement on the medial side averaged 1.00 ± 0.56 mm for mTKA and 1.30 ± 0.80 mm for rTKA. Maximum displacement did not correlate with the percentage of the posterior implant overhanging the tibia ($r = 0.36$).

Conclusion: This study determined that there was no significant difference in press-fit tibial implant motion between rTKAs and mTKAs when loaded in high flexion. The wide variation in implant displacement for both rTKA and mTKA and could be the result of large variation in bone density among cadaveric specimens.

Acknowledgments: The authors would like to acknowledge DePuy Synthes and the Roy and Linda Crowninshield Fund for Biomechanics Research for supporting this work.

References: [1] Sione AO., et al., *Arthroplasty Today*, 6(4), 2020. [2] Song EK., et al., *Clin Orthop Relat Res.*, 471(1), 2013. [3] Khlopas A, et al., *J Knee Surg*, 33(07), 2020.

Figures

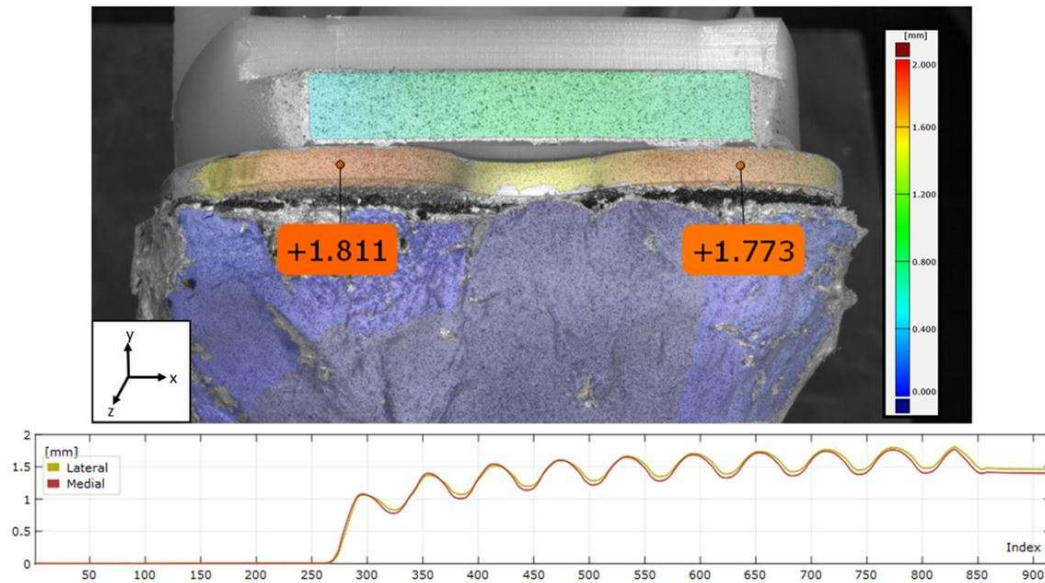


Figure 1. Digital image correlation analysis was conducted for each specimen to track the displacement (mm) of the posterior-most edge of the tibial implant relative to the tibia which was set to be a rigid reference frame (blue). Implant displacements are shown in both heat map and graph form.

[Figure 1](#)

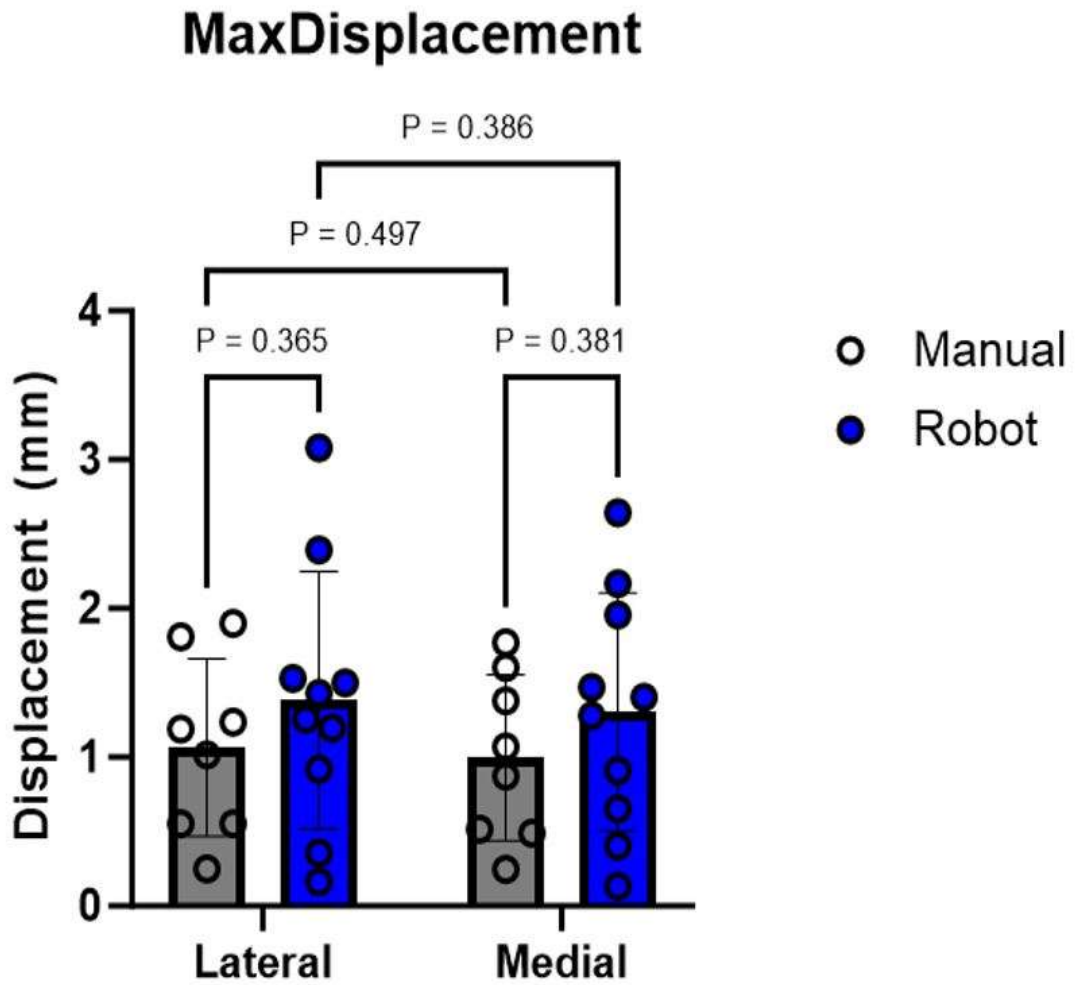


Figure 2. Maximum displacement of the posterior tibial implant edge relative to the tibia.

[Figure 2](#)

Cementless vs Cemented Robotic-Assisted Total Knee Arthroplasty Outcomes: A Single Center MARCQI-Based Study

*Alexander Ziedas - Ascension Providence Hospital - Southfield, USA

Simarjeet Puri - Detroit, United States of America

William Kesto - Ascension Providence Hospital - Southfield, USA

David Knesek - Ascension Providence Hospital - Southfield, USA

Jefferey Michaelson - Ascension Providence Hospital - Southfield, USA

Todd Frush - Ascension Providence Hospital - Southfield, USA

David Markel - Providence Hospital and Medical Center - Southfield, USA

Introduction

Robotic-assisted total knee arthroplasty (RA-TKA) has become increasingly popular and can be performed with either a cementless or cemented implants. The purpose of this study was to determine whether a difference exists between cementless and cemented RA-TKA techniques with regards to revision rate and 90-day outcomes. We hypothesized that cementless RA-TKA would have comparable survivorship and 90-day complications to cemented RA-TKA.

Methods

A prospectively maintained statewide arthroplasty registry, the Michigan Arthroplasty Registry Collaborative Quality Initiative (MARCQI), was queried for all primary RA-TKAs from January 2018 to July 2023 performed at a single hospital. Cementless and cemented RA-TKA cohorts were compared for revisions and 90-day complications including emergency department visits, readmissions, and returns to the OR. Chi-square and Fisher's exact tests were used for categorical data and t-tests for continuous data.

Results

Of 1003 RA-TKAs identified (mean age 65.8 ± 9.1 years, 53% female), 730 were cementless and 273 were cemented. There were no statistically significant differences between cementless and cemented cohorts relative to age, BMI, gender, race, 90-day events or revision rate. Similarly, the specific nature of the 90-day events did not correlate with technique (Table 1). Logistical regression modeling showed no difference in odds of a 90-day event based on patient factors (Figure 1). Cemented RA-TKA had longer mean surgical time (111.8 ± 30.4 vs 91.2 ± 19.8 minutes, $p=0.0001$) and mean length of stay (40.6 ± 26.8 vs 30.8 ± 22.0 hours, $p=0.0001$). Twenty-two revision surgeries were performed (thirteen cementless, nine cemented) for a revision rate of 1.7% and 3.2%, respectively ($p=0.1514$). Mean time to revision was shorter for cementless RA-TKA (0.80 ± 0.46 vs 1.4 ± 1.1 years, $p=0.0001$). Cumulative percent revision (CPR) at five years was 1.8% for cementless and 3.9% for cemented RA-TKA ($p=0.1671$, Figure 2).

Conclusion

Cementless and cemented RA-TKA had comparable revision rates and 90-day complications. Cementless RA-TKA had a shorter mean surgical time, length of stay, and time to revision compared to cemented RA-TKA. The overall RA-TKA revision rate herein was comparable to that of conventional TKA reported in MARCQI.

Figures

Outcome	Cementless (n=730)		Cemented (n=273)		P-Value
	Count	%	Count	%	
Revision	13	1.7	9	3.2	0.1514
Aseptic Loosening	5	<1	1	<1	0.5567
Fracture	1	<1	1	<1	0.4721
PJI	4	<1	5	1.8	0.0685
Instability	2	<1	2	<1	0.3014
Arthrofibrosis	1	<1	0	0	0.5395
Total 90-Day Events	139	19.0	55	20.1	0.7196
Joint Related 90-Day ED Visits	34	4.6	18	6.5	0.2618
Fracture	1	<1	0	0	0.5406
Wound Issue	6	<1	6	2.1	0.099
Pain	21	2.8	10	3.6	0.5403
DVT/PE	6	<1	2	<1	0.8874
Joint Related 90-Day Readmission	12	1.6	7	2.5	0.4338
PJI	1	<1	0	0	0.5406
Aseptic Loosening	1	<1	0	0	0.5406
I&D for Wound Issues	9	<1	6	2.1	0.2549
DVT/PE	1	<1	1	<1	0.4705
MUA	35	4.7	6	2.1	0.0731
Non-Joint Related 90-Day ED Visits	45	6.1	18	6.5	0.6557
Non-Joint Related 90-Day Readmission	13	1.7	6	2.1	0.6128

[Figure 1](#)

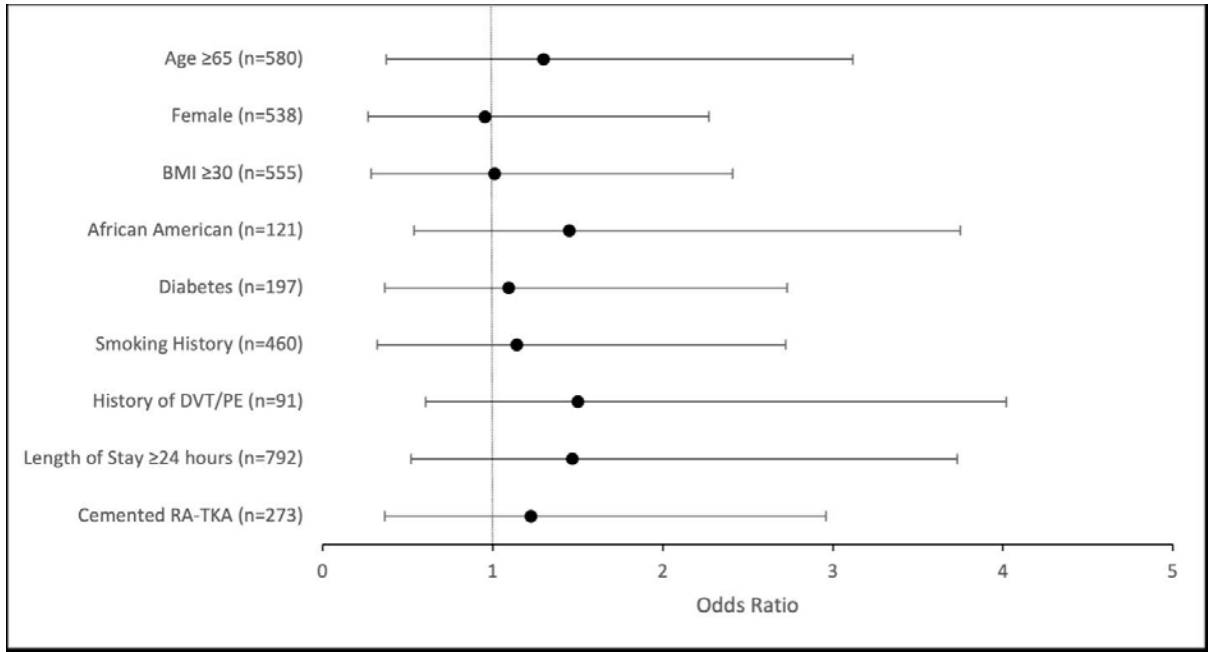
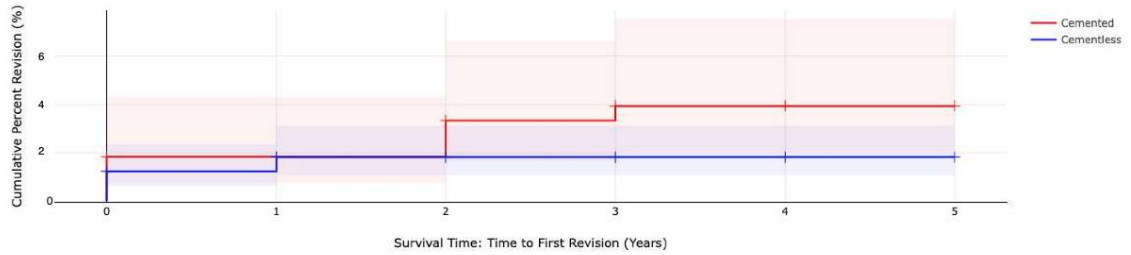


Figure 2



	N	1 year	3 years	5 years
CPR All RA-TKA	1,003	1.39 (0.82, 2.34)	2.25 (1.46, 3.43)	2.47 (1.61, 3.77)
CPR Cementless RA-TKA	730	1.23 (0.64, 2.35)	1.82 (1.06, 3.12)	1.82 (1.06, 3.12)
CPR Cemented RA-TKA	273	1.83 (0.76, 4.34)	3.33 (2.00, 6.61)	3.94 (2.04, 7.53)

Figure 3

Walking Aid Use Has Significant Impact on Gait Parameters During TKA Recovery

*Ricardo Antunes - Stryker - Glasgow, GB

Andrew Meyer - Stryker - Mahwah, USA

Paul Jacob - Oklahoma Joint Reconstruction Institute - Oklahoma City, USA

Robert Marchand - Ortho Rhode Island - South County, USA

Elaine Justice - Oklahoma Joint Reconstruction Institute - Oklahoma City, USA

Kelly Taylor - Ortho Rhode Island - South County, USA

Matthias Verstraete - Stryker - Fort Lauderdale, USA

Introduction: Remote postoperative monitoring using wearable devices has been gaining influence when measuring total knee arthroplasty (TKA) outcomes. In particular, gait metrics post-TKA from wearable sensors could provide valuable insights into patient recovery. However, these metrics might be significantly altered in patients using walking aids. Here we describe the use of walking-aids during recovery of TKA patients and effects of their use on gait parameters remotely collected using wearable devices.

Methods: Functional metrics were remotely collected from unilateral primary TKA patients using two knee-worn IMU sensors up to 12-week postoperative. Patients were regularly asked to walk for 1-minute during which knee flexion angles were recorded from the operated leg. Patients reported the use of walking aids (walker/cane/unaided) after each session. Angles were segmented into discrete gait steps using custom algorithms, and gait cadence and range-of-motion was averaged across all steps. A generalized additive model (GAM) with a smooth term for days since surgery and a random effect for walking aid use was fitted to cadence and range-of-motion.

Results: Gait data from 42 patients were analyzed. The proportion of patients reporting the use of walker/cane/unaided progressed from 74/10/16% on week one, to 0/7/93% on week five and to 0/0/100% on week ten (Fig. 1). The cadence GAM model showed a significant effect ($p < 0.001$) for time since surgery. Also, a significant effect ($p < 0.001$) of walking aid use was apparent, indicating lower cadence (by ≈ 5 steps \cdot minute $^{-1}$) due to the use of walker and cane, relative to unaided walking (Figs. 2 and 3). The GAM model for range-of-motion also showed a significant recovery effect but the effect of walking aids was not significant.

Conclusion: Wearables devices are increasingly used to remotely monitor TKA patients' functional recovery with advantages over traditional in-clinic visits. When tracking recovery progress using gait parameters it is important to account for the use of walking aids.

Figures

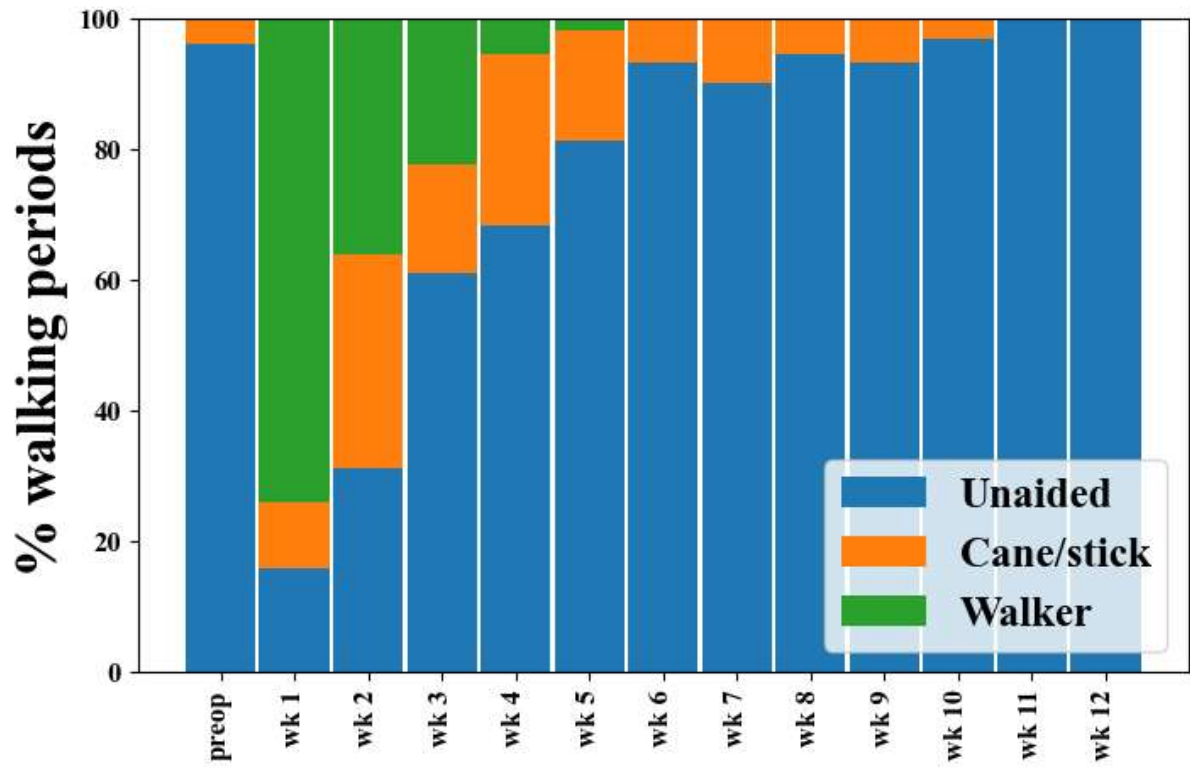


[Figure 1](#)

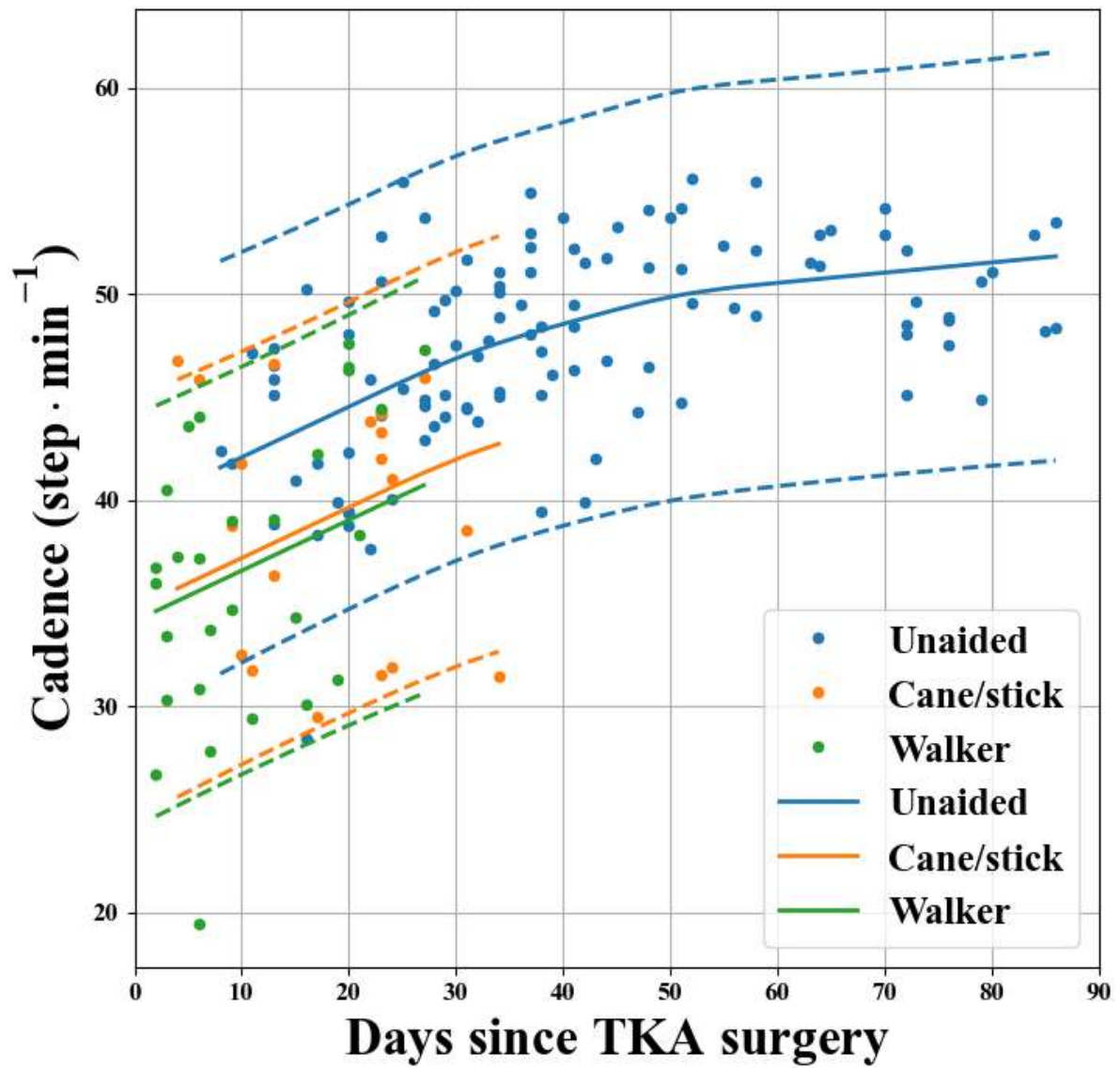
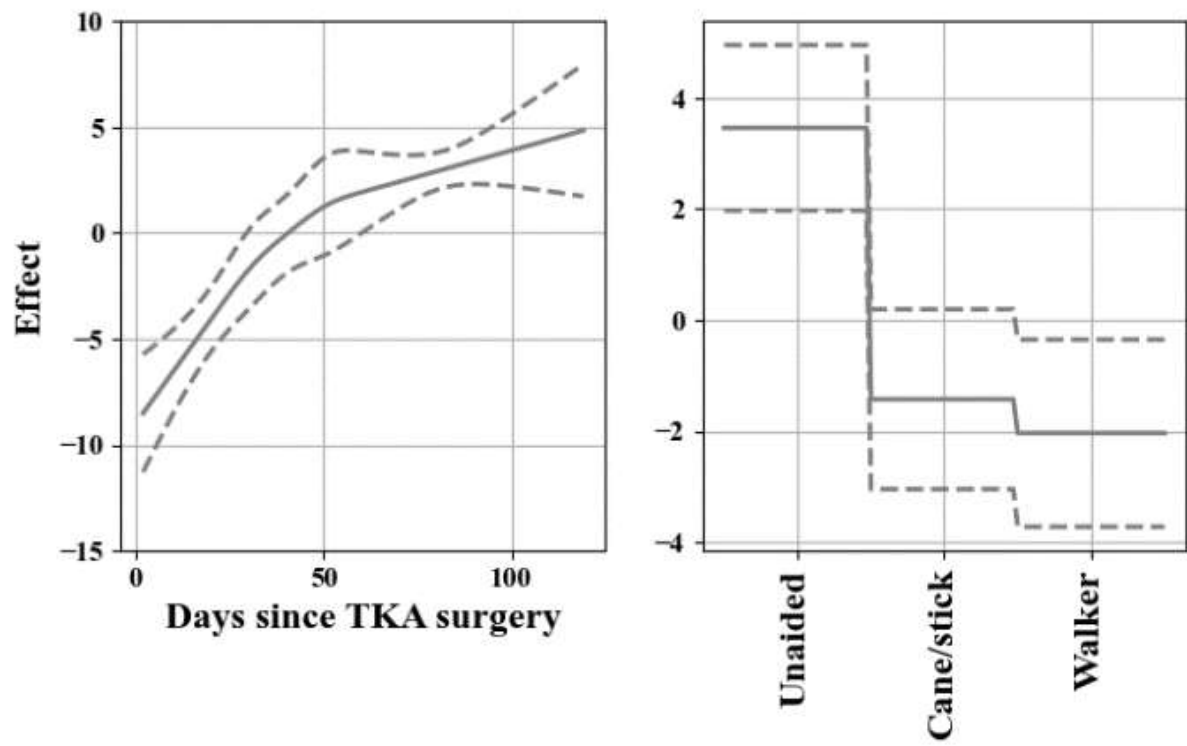


Figure 2



[Figure 3](#)

What Factors Affect Patients Perception of Changes in Mobility Following Knee Arthroplasty Procedures?

*Roberta Redfern - Zimmer Biomet - Pemberville, USA

Mike Anderson - Zimmer Biomet - Lehi, USA

Jason Cholewa - Zimmer Biomet - Warsaw, USA

Introduction

Patient reported outcomes measures have often been used to measure the success of arthroplasty procedures, which often include patient perceptions of mobility. The general health-related quality of life (QoL) questionnaire, Euro-Qol 5-Dimensions 5-Levels (EQ-5D-5L), contain a mobility dimension as measure of QoL. The aim of this analysis was to investigate factors that impact the change in patient responses to the mobility dimension following knee arthroplasty.

Methods

Patients undergoing total knee arthroplasty (TKA) or partial knee arthroplasty (PKA) who were enrolled in a multicenter prospective observational cohort study were included in this secondary analysis. Patients were eligible if they owned a smartphone and were provided a smartwatch at least two weeks prior to surgery for pre- and post-operative collection of gait metrics, including step counts, gait speed, and walking asymmetry. Change in mobility dimension on the EQ-5D-5L was calculated over baseline pre-operative reports at 90 days post-operatively. Generalized linear models including patient characteristics (age, sex, and body mass index (BMI)), change in anxiety as reported on the generalized anxiety disorder 7 (GAD-7) instrument, change in pain, and change in gait metrics at 90 days from baseline were calculated to evaluate variables affecting patient perception of mobility changes.

Results

Data was available 1,066 patients, including 250 (23.5%) PKA and 816 (76.5%) TKA cases. Generalized linear models suggest that in those undergoing PKA, only change in anxiety ($\beta=0.003$, 95%CI 0.0002 – 0.006, $p=0.04$) and change in gait speed ($\beta=-0.12$, 95%CI -0.21 – -0.03, $p=0.008$) were associated with change in patient perception of mobility as reported in the EQ-5D-5L. Within the TKA cohort, only change in gait speed ($\beta=-0.06$, 95%CI -0.11 – -0.01, $p=0.01$) was significantly associated with patient report of mobility, considering age, BMI, sex, change in anxiety, change in pain, change in step counts, and change in walking asymmetry.

Discussion

Gait speed has frequently been considered a measure of patient function and capacity in healthy and diseased individuals, however, objective measures of gait rarely correlate strongly with patient reported outcome measures. This analysis suggests that patient perception of mobility, as measured by the mobility dimension of the EQ-5D-5L alone, may be associated with passively measured gait speed, rather than other factors, such as demographics, anxiety, or pain.

Survivorship and Clinical Outcomes for a New and Legacy All Polyethylene Tibia Used in Primary Total Knee Arthroplasty: A Multi-Center Registry Review

*David Fawley - DePuy Synthes - Warsaw, USA

David F Dalury - Baltimore, USA

Kirk Kindsfater - Orthopaedic Center of the Rockies - Fort Collins, USA

Robert Gorab - Hoag Orthopedic Institute - Irvine, United States of America

William P Barrett - Renton, USA

Donald Pomeroy - Arthroplasty foundation - Louisville, United States of America

John F Irving - New Haven, USA

Sean Croker - Depuy Synthes - West Chester, USA

Introduction

Although metal-backed tibial components are used more frequently in total knee arthroplasty (TKA), all polyethylene tibias (APT) have performed as well or better in many clinical studies. A new APT design was launched within a large implant system. The aim of this evaluation was to assess survivorship and outcomes of new (nAPT) and legacy (IAPT) designs utilizing a retrospective outcome review.

Methods

We conducted a retrospective multicenter registry case review from a company-sponsored registry. Clinical assessments were summarized at standardized registry visit windows. Kaplan-Meier (KM) survivorship was performed with revision of any component as the endpoint, with two separate censoring assumptions. First, unrevised subjects were censored at the last clinical follow-up [clinical assumption (CA)], and second at the date of database extract [registry assumption (RA)]. Survivorship was not calculated at timepoints where <40 knees were available for follow up.

Results

A total of 6,443 (6,003 CR) IAPT, and 796 (536 CR) nAPT knees were implanted between November 1995 and July 2023. Primary diagnosis was osteoarthritis in 98.0% (IAPT) and 87.6% (nAPT) of cases. Mean age was 76.8 years (R 32-99) for IAPT and 77.7 year (R 47-94) for nAPT; 65% in IAPT and 61% in nAPT were female and BMI averaged 29.2 (R 15 to 57) for IAPT and 28.3 (R 16-44) for nAPT. Overall, 51 (0.8%) revisions were reported for IAPT. Reasons for revision (N; %) were infection (23; 45.1%), instability (8; 15.7%), pain/stiffness (6; 11.8%), aseptic loosening (4; 7.8%), and other (10; 19.6%). Only 1 revision was reported for the nAPT group, for instability. All-cause survivorship was 99.15% at 10 and 15 years for IAPT and 99.73% at 2 years for nAPT for the RA. KM estimates are presented in Figure 1 and Figure 2. Mean knee society total scores (pre-2011) are presented in Figure 3.

Conclusion

One advantage of APTs is the single surface for generation of wear debris. In this series there were no reports of revision due to osteolysis and only four due to aseptic loosening (0.06%) in IAPT. KSS scores were lower in the nAPT cohort, but authors determined that discrepancies in reporting of the alignment were impacting the score and corrections are currently underway to address this. Our study shows excellent outcomes and survivorship for a legacy APT used in primary TKA, and positive 1- and 2-year survivorship for a new APT design. Continued study of the new design would be beneficial.

Figures

Figure 1 – Kaplan Meier Device Survivorship Estimates (Any component, any reason)

All <i>APT</i> Knees (N=6,443)	1 Year	2 Year	5 Year	10 Year	16 Year
	KM Survivorship (95% CI) n with Later Follow-up				
All Cause Revision - CA	99.70% (99.51, 99.82%) n = 4,421	99.20 % (98.87, 99.43%) n = 3,422	98.78 % (98.36, 99.09%) n = 1,817	98.19% (97.40, 98.74%) n = 446	98.19 % (97.40, 98.74%) n = 40
All Cause Revision - RA	99.76 % (99.61, 99.86%) n = 6,300	99.46 % (99.25, 99.61%) n = 6,158	99.26 % (99.02, 99.45%) n = 5,482	99.15% (98.89, 99.36%) n = 3,884	99.15% (98.89, 99.36%) n = 1,476
Cumulative Revised	15	34	46	51	51
All <i>nAPT</i> Knees (N=796)	1 Year	2 Year	5 Year	10 Year	16 Year
	KM Survivorship (95% CI) n with Later Follow-up				
All Cause Revision - CA	100% (100, 100%) n = 157	<40 knees			
All Cause Revision - RA	100% (100, 100%) n = 583	99.73 (98.13, 99.96%) n = 288	<40 knees		
Cumulative Revised	0	1	<40 knees		

Figure 1

Figure 2 – KM Device Survival Estimates (Clinical and Registry Assumptions)

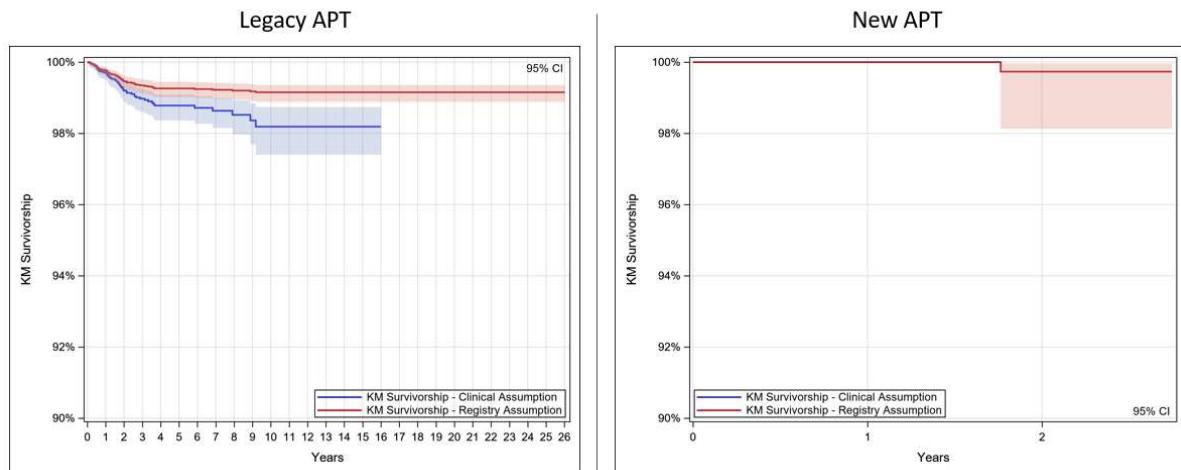


Figure 2

Figure 3 – American Knee Society (pre-2011) Total Scores

	Mean Pre-op KSS Total Score (SD; n)	Mean 1 Year KSS Total Score (304-668 days) (SD; n)	Mean 2 Year KSS Total Score (669-1034 days) (SD; n)	Mean 5 Year KSS Total Score (1765-2737 days) (SD; n)	Mean 10 Year KSS Total Score (2738-4562 days) (SD; n)	Mean 15 Year KSS Total Score (4563-6387 days) (SD; n)
All IAPT (N=6,443)	38.4 (15.5; 3373)	91.6 (10.8; 3677)	91.8 (10.1; 2214)	92.2 (10.1; 1531)	91.6 (10.6; 818)	93.9 (10.6; 154)
All nAPT (N=796)	41.0 (17.1; 602)	88.3 (12.9; 251)	81.8 (11.4; 33)	N/A	N/A	N/A

[Figure 3](#)

A Failed Trial of Selective Patellar Resurfacing During Primary Total Knee Arthroplasty

*John Cooper - Columbia University - New York, USA

Catelyn A. Woelfle - Columbia University Medical Center - New York, USA

INTRODUCTION

Routine patellar resurfacing remains controversial in primary total knee arthroplasty (TKA). With an abundance of conflicting literature regarding this decision, surgeons are left to their own judgement, with significant variability in practice. The current study reports the experience of a high-volume arthroplasty surgeon who stopped routinely resurfacing patellae for a two-year period.

METHODS

All primary TKAs performed by a single surgeon between January 2018 and September 2022 with a minimum one-year follow-up were retrospectively reviewed. Data were first analyzed between two cohorts – non-resurfaced and resurfaced patellae – and second between two phases – universal and selective resurfacing. Outcomes included reoperation, patellar complications, and patient-related outcome measure (PROM) scores at one-year. Chi-Squared tests and Independent Samples t-tests were used for analysis.

RESULTS

504 primary TKAs, with a mean 24-month follow-up, were included. Patellar resurfacing was performed in 77% of the overall cohort, including 58% of the selective resurfacing phase and 100% during the universal resurfacing phases. Reoperation (7.6% vs 0.3%; $P < 0.001$) and patellar complications (8.4% vs 1.3%; $P < 0.001$) were significantly higher in the non-resurfaced versus resurfaced cohort, respectively. Eight of the nine reoperations in the non-resurfaced group were for secondary resurfacing, and all were female ($P = 0.017$). Mean SF-12 Physical Health ($P = 0.037$) and WOMAC Pain scores ($P = 0.002$) were significantly better in the resurfaced cohort. The phase of selective resurfacing also demonstrated a significantly higher reoperation rate (3.3% vs 0.4%; $P = 0.022$) and worse WOMAC Pain ($P = 0.026$) and Knee Society Knee Functional scores ($P = 0.042$) compared to the phases of universal resurfacing.

CONCLUSION

Cessation of routine patellar resurfacing by an experienced, high-volume arthroplasty surgeon led to inferior clinical results and an unacceptably high reoperation rate within two years, specifically among women. Universal patellar resurfacing has been re-adopted.

Reproducibility of Coronal Plane Alignment of the Knee (CPAK) Using Restricted Inverse Kinematic Alignment

*Ittai Shichman - Tel-Aviv Sourasky Medical Center - Tel Aviv, Israel

Amer Hallak - Tel Aviv Sourasky Medical Center - Tel Aviv, Israel

Itay Ashkenazi - NYU Langone Health - New-York, United States of America

Yaniv Warschwaski - Tel Aviv Sourasky Medical Center - Tel Aviv, Israel

Aviram Gold - Tel Aviv Sourasky Medical Center - Tel Aviv, Israel

Nimrod Snir - Tel Aviv Sourasky Medical Center - Tel Aviv, Israel

Keywords: CPAK, Coronal Alignment, Total Knee Arthroplasty, Restricted Inverse Kinematic Alignment, Patient Specific Alignment

Background

The Coronal Plane Alignment of the Knee (CPAK) classification categorizes knee phenotypes based on constitutional limb alignment and joint line obliquity (JLO). Restricted inverse kinematic alignment (riKA) is an intraoperative surgical decision based on calculated parameters preoperatively and intraoperatively to reach an alignment tailored for each individual patient using a tibia first cut.

Objectives

This study investigated the reproducibility of restoring preoperative CPAK knee phenotypes by applying the riKA concept in total knee arthroplasty (TKA) using a novel imageless robotic arm system.

Study Design & Methods

This prospective study assessed 118 patients who underwent riKA TKA using a novel imageless navigation-assisted robotic arm using a single implant design for primary osteoarthritis between January 2022 and July 2023. Preoperative and postoperative angles for the lateral distal femoral angle (LDFA) and medial proximal tibial angle (MPTA) were measured from full-length standing anteroposterior X-ray imaging. Arithmetic HKA (aHKA) was defined as $MPTA - LDFA$ and JLO was outlined as $MPTA + LDFA$ to classify each knee into one of nine CPAK phenotypes. CPAK boundaries for neutral aHKA and JLO were $0^\circ \pm 2^\circ$ and $180^\circ \pm 3^\circ$, respectively.

Results

The mean pre and postoperative aHKA were -2.81° (SD $\pm 5.0^\circ$) vs -3.19° (SD $\pm 2.96^\circ$), respectively. The most common preoperative CPAK phenotypes were 1 (n=49, 41.5%) and 2 (n=28, 23.7%), respectively. Among type 1 phenotypes, 14/49 (28.6%) patients preserved their composition postoperatively, but a noteworthy 29/49 (59.2%) patients converted into type 4. Among Type 2 phenotypes, 16/28 (57.1%) knees preserved their alignment, with only 4/29 patients (13.8%) shifting to type 5. In preoperative types 4 and 5, 9/10 (90%) and 12/17 (70.6%) knees preserved their original phenotypes, respectively. Regarding valgus categories 3,6 and 9, 12/14 knees (85.7%) changed into neutral phenotypes 2 and 5. CPAK types 7, 8, and 9 were rare throughout this study.

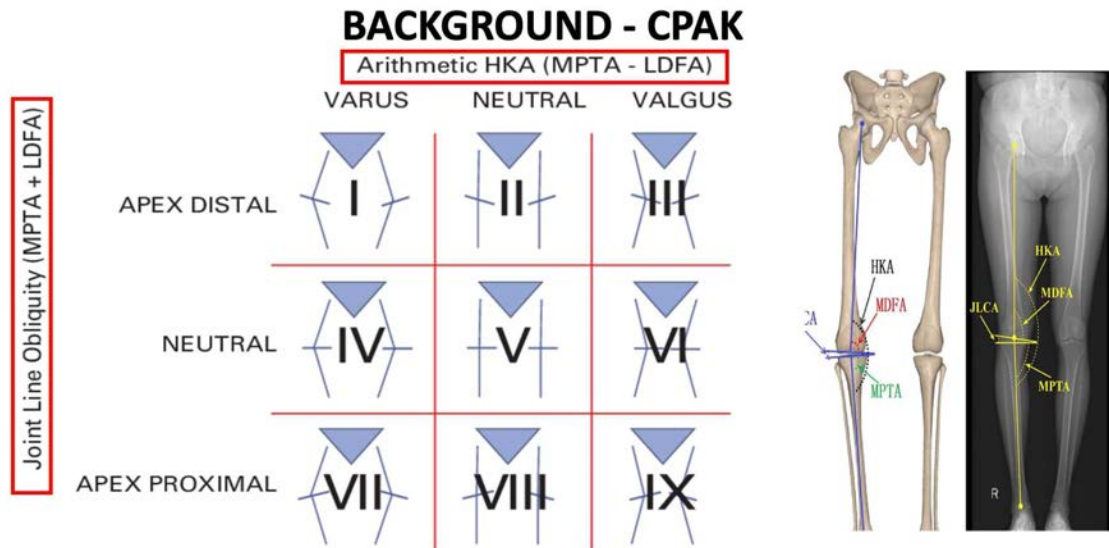
Conclusions

Achieving balance in extension using riKA technique requires adjustments on the coronal plane in order to compensate for equal medial and lateral gaps. Due to tibia

first technique mimicking the MPTA, more adjustments are made on the femoral side. JLCA (derived from lateral laxity and lateral meniscus height) is compromised by this technique.

The use of a novel imageless navigation robotic assisted TKA to achieve riKA conferred with adequate preservation of the native coronal alignment postoperatively. These findings suggest that the use of imageless navigation robotic assisted system is a valid tool to surgeons who seek contemplating riKA in TKA.

Figures



MacDessi SJ, Griffiths-Jones W, Harris IA, Bellemans J, Chen DB. Coronal Plane Alignment of the Knee (CPAK) classification. Bone Joint J. 2021 Feb;103-B(2):329-337. doi: 10.1302/0301-620X.103B2.BJJ-2020-1050.R1. PMID: 33517740; PMCID: PMC7954147.

Figure 1

BACKGROUND - RESTRICTED INVERSE KINEMATIC ALIGNMENT

- Anatomical tibia-first, gap balancing technique restoring the native tibial joint line obliquity (JLO)
- No - minimal soft tissue releases
- Kinematic alignment with minimal adjustments
- HKA , tibial alignment with Boundaries (5 deg)
- Balanced in extension (M=L)
- Rectangular in flexion (M<L)

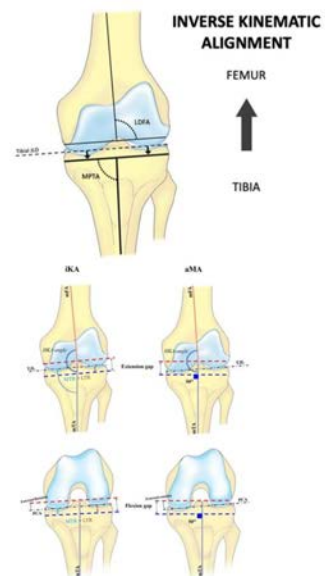


Figure 2

METHODS

- Pre and post-operative AP standing weight-bearing full-body low-dose imaging and
- A total of 131 patients
- Patients were then categorized into one of the nine CPAK groups
- Min 1-year follow-up

Pre and post - op full standing radiographs with limb alignment analysis

Angle(°)	Pre	Normal	Post
mLPA	14	85-95	
mLGA	21	85-90	
mBPFA	82	85-90	
mLDTA	11	85-90	
JLCA	7	5-2	
Length (mm)			
MAD	54		
Femur	495		
Tibia	373		
Total Length	877		



[Figure 3](#)

Preoperative Flexion Contracture Influences Magnitude of Planned Resections in RA-TKA

*Catherine Digangi - NYU Orthopedic Hospital - New York, USA

Alana Prinos - Langone Orthopedic Hospital - New York, USA

Patrick Meere - NYU Hospital for Joint Diseases - New York, USA

Sophia Antonioli - NYU Langone - New York, USA

Morteza Meftah - NYU Hospital for Joint Diseases - New York, USA

Matthew Hepinstall - NYU Langone Health - New York, USA

Akram Habibi - NYU Langone Orthopedic Hospital - New York, United States of America

Introduction

Varying degrees of knee flexion contracture appear commonly in total knee arthroplasty (TKA) patients. Increasing distal femoral bone resection during TKA facilitates correction of contracture, but can result in midflexion laxity. Robot-assisted gap balancing seeks to improve ligament balance through bone optimized resections. The aim of this study was to evaluate the influence of preoperative flexion contracture on the magnitude of resections surgeons perform to balance the knee in robotic TKA.

Methods

This was a retrospective cohort of 365 primary robotic TKAs from April to December 2023 using a single cruciate-retaining (CR) implant design. Native flexion and alignment, as well as the final planned bony resection data, was collected from intraoperative screen captures. The cohort was divided by native flexion deformity into three cohorts: < 0 degrees flexion (“hyperextension”, n=70), 0 to 9.9 degrees flexion (“minimal contracture”, n=212), and ≥ 10 degrees flexion (“high contracture”, n=83). The arithmetic hip-knee-ankle (aHKA) angle was used to determine native deformity groups for additional subanalyses, with neutral defined as -2 to 2 degrees, valgus as less than -2, and varus as greater than 2. Demographics, implants, and intraoperative data was collected and analyzed using Chi-Square and ANOVA tests.

Results

Mean preoperative flexion was -3.6, 4.2, and 13.2 degrees for the hyperextension, minimal contracture, and high contracture cohorts, respectively. Significant differences were found between cohorts for mean lateral and medial distal femur resections as well as lateral and medial proximal tibia resections, with the high contracture group having the largest resections. After accounting for implanted polyethylene thickness, significant differences were noted between flexion deformity cohorts in the sum of extension resections, both laterally and medially. Subanalysis for varus knees found the high contracture group was associated with the greatest values for both medial distal femur resection and the sum of medial resections in extension, but no change in lateral resections. In the valgus group, there was a significant difference between cohorts on both the lateral and medial side for distal femur resections and sum of resections in extension.

Conclusion

Surgeons using robotic-assistance planned slightly larger bone resections for patients with more severe flexion contractures. Varus knees with flexion contracture were treated with larger distal medial femoral cuts, while valgus knees were treated with larger distal lateral and medial femoral cuts. This may reflect increasing

surgeon tolerance of slight varus alignment for soft tissue balance. Additional work should explore if this reduces the risk of symptomatic midflexion laxity.

Figures

Table 1. Planned Resection Values, Stratified by Native Flexion Deformity

	Hyperextension (n=70)		Minimal Contracture (n=212)		High Contracture (n=83)		P-value
	M SD	Range	M SD	Range	M SD	Range	
Age at Surgery	64.9±8.5	45 – 84	69±8.5	43 – 89	67.4±9.2	42 – 88	0.003
BMI	31.6±5.9	22.5 – 45.9	31.1±5.4	18.2 – 46.3	33.4±5.5	21.5 – 47.5	0.009
Native Deformity- no. (%)							0.096
Varus	21 (30)	-	87 (41)	-	35 (42.2)	-	
Neutral	25 (35.7)	-	85 (40.1)	-	30 (36.1)	-	
Valgus	24 (34.3)	-	40 (18.9)	-	18 (21.7)	-	
Native Flexion (°)	-3.6±2.7	-12 – -1	4.2±2.9	0 – 9	13.2±3.1	10 – 24	<0.001
Preoperative aHKA (°)	-0.2±4	-7.8 – 8.8	1.2±4	-10.7 – 12.8	1.1±4	-8.8 – 9.9	0.032
Planned Coronal Alignment (°) ¹							
Limb	0.5±2.1	-3 – 5	1.2±2.3	-4 – 6	1.4±2.3	-4.5 – 6	0.020
Distal Femur	-0.7±1.4	-4.5 – 2	-0.2±1.5	-4.5 – 4	-0.1±1.4	-3 – 3	0.020
Proximal Tibia	1.2±1.4	-1 – 4.2	1.4±1.4	-1.5 – 4.4	1.5±1.5	-1.5 – 5.1	0.306
Planned Transverse Rotation (°) ²							
Femoral TEA	1.8±1.9	-2 – 5	1.7±2.1	-4.6 – 6	2.1±2	-2.5 – 6.5	0.357
Femoral PCA	4.9±2.2	-0.6 – 9.5	4.7±2.2	-0.8 – 9.9	4.7±2.3	-0.7 – 10	0.710
Planned Sagittal Alignment (°)							
Femoral Flexion ³	4.1±1.4	0.1 – 8	3.9±1.4	0.5 – 8	4±1.5	0.5 – 7	0.697
Tibial Slope ⁴	3.2±0.7	2 – 5	3.3±0.7	2 – 5.8	3.4±0.6	2.5 – 5.5	0.513
Distal Femur Resection (mm)							
Lateral	3.8±1.6	1 – 7	4.7±1.5	0.5 – 9.5	5.1±1.6	2 – 9	<0.001
Medial	6.7±1.3	3.5 – 10	6.9±1.4	2 – 11	7.6±1.3	5 – 11	<0.001
Posterior Femur Resection (mm)							
Lateral	5.5±1.6	2.5 – 10.5	5.7±1.9	1 – 11.5	5.5±1.9	0.5 – 10	0.657
Medial	9.4±1.5	5.5 – 12.5	9.5±1.7	4 – 14.5	9.4±1.7	6 – 13.5	0.787
Tibia Resection (mm)							
Lateral	5.8±1.3	2 – 8	6.1±1.3	2 – 10	6.4±1.4	2.5 – 10	0.022
Medial	4.1±1.5	0.5 – 7.5	4.2±1.3	1 – 9	4.6±1.5	1 – 8	0.039
Sum of Extension Resections (mm)							
Lateral	9.6±1.9	5.5 – 13.5	10.7±2.1	4.5 – 17.5	11.5±2	7 – 17	<0.001
Medial	10.8±1.8	7 – 15	11.1±1.8	3.5 – 16.5	12.3±1.9	8 – 16.5	<0.001
Sum of Flexion Resections (mm)							
Lateral	11.3±1.7	7 – 15.5	11.7±2	5.5 – 17	11.9±1.9	6.5 – 17.5	0.125
Medial	13.5±1.6	10.5 – 18	13.7±1.8	8 – 19	14±1.5	9 – 17	0.152
Tibia Resection: Corrected* (mm)							
Lateral	4.4±1.7	-1 – 8	5±1.8	-1 – 9	5.4±2	0.5 – 10	0.007
Medial	2.7±1.8	-2 – 7.5	3.2±1.9	-6 – 7	3.7±2.2	-1.5 – 8	0.014
Sum of Extension Resections: Corrected* (mm)							
Lateral	8.3±2.1	3.5 – 13	9.7±2.3	2.5 – 16.5	10.5±2.2	6.5 – 17	<0.001
Medial	9.4±2	4.5 – 13.5	10.1±2.4	-3.5 – 16.5	11.3±2.5	3.5 – 16	<0.001
Sum of Flexion Resections: Corrected* (mm)							
Lateral	10±1.9	5.5 – 13.5	10.7±2.3	3.5 – 16	10.9±2.4	3 – 16	0.023
Medial	12.1±1.7	8.5 – 15.5	12.6±2.2	1.5 – 18	13±1.9	9 – 16	0.032

M, mean; SD, standard deviation; BMI, body mass index; mm, millimeters; aHKA, arithmetic hip-knee-ankle; TEA, transepicondylar axis; PCA, posterior condylar axis

¹ Varus measurements are greater than 0; valgus measurements are less than 0. ² External measurements are greater than 0; internal measurements are less than 0. ³ Flexion measurements are greater than 0; extension measurements are less than 0. ⁴ P slope measurements are greater than 0; a slope measurements are less than 0. *Corrected = Polyethylene thickness accounted for by subtracting absolute difference from 9 millimeters from measurement.

Figure 1

Table 2. Planned Resection Values for Preoperative Varus Knees, Stratified by Magnitude of Native Flexion

	Hyperextension (n=21)		Minimal Contracture (n=87)		High Contracture (n=35)		P-value
	M	SD	Range	M	SD	Range	
Native Flexion (°)	-3.4±2.7		-10 - -1	4.7±3.1		0 - 9	<0.001
Preoperative aHKA (°)	4.5±1.5		2.5 - 8.8	4.9±2.4		2.1 - 12.8	0.677
Planned Coronal Alignment (°)¹							
Limb	2.2±1.8		-2 - 5	3.1±1.8		-2 - 6	0.095
Distal Femur	0.2±1.1		-2 - 2	0.7±1.4		-3.5 - 4	0.208
Proximal Tibia	2±1.2		0 - 4.2	2.3±1.1		-1 - 4.4	0.417
Planned Transverse Rotation (°)²							
Femoral TEA	2.9±1.5		-0.5 - 5	2.2±1.9		-3 - 6	0.288
Femoral PCA	5.8±1.8		1.9 - 9.5	5±2.1		-0.8 - 9.2	0.188
Planned Sagittal Alignment (°)							
Femoral Flexion ³	3.5±1.6		0.1 - 6	3.9±1.3		0.5 - 7	0.437
Tibial Slope ⁴	3.3±0.8		2 - 5	3.3±0.6		2 - 5	0.729
Distal Femur Resection (mm)							
Lateral	5.1±1.2		3 - 7	5.3±1.3		0.5 - 9.5	0.209
Medial	6.4±1.2		3.5 - 8	6.8±1.7		2 - 11	0.014
Posterior Femur Resection (mm)							
Lateral	5.4±1.5		2.5 - 8	5.8±1.7		1 - 10	0.597
Medial	10±1.2		7.5 - 12.5	10±1.7		6 - 13.5	0.857
Tibia Resection (mm)							
Lateral	5.9±1.2		3.5 - 8	6.3±1.2		2 - 10	0.432
Medial	3.4±1.2		0.5 - 5.5	3.7±1.2		1 - 7	0.254
Sum of Extension Resections (mm)							
Lateral	11±1.4		8.5 - 13.5	11.5±1.8		6.5 - 17.5	0.084
Medial	9.7±1.3		7.5 - 12.5	10.5±2.1		3.5 - 16.5	0.003
Sum of Flexion Resections (mm)							
Lateral	11.3±1.9		7 - 14	12.1±1.9		5.5 - 16	0.221
Medial	13.4±1.5		10.5 - 16	13.7±1.8		8 - 16.5	0.704
Tibia Resection: Corrected* (mm)							
Lateral	4.5±1.9		1.5 - 7.5	5±1.9		-1 - 9	0.479
Medial	1.9±1.9		-2 - 5	2.4±1.9		-6 - 7	0.433
Sum of Extension Resections: Corrected* (mm)							
Lateral	9.5±1.8		5.5 - 13	10.3±2.4		4.5 - 16.5	0.163
Medial	8.3±1.9		4.5 - 12.5	9.2±2.9		-3.5 - 16.5	0.041
Sum of Flexion Resections: Corrected* (mm)							
Lateral	9.9±2.3		5.5 - 13.5	10.9±2.4		3.5 - 15	0.259
Medial	12±1.9		9 - 14.5	12.5±2.5		1.5 - 16.5	0.629

M, mean; SD, standard deviation; mm, millimeters; aHKA, arithmetic hip-knee-ankle; TEA, transepicondylar axis; PCA, posterior condylar axis
¹ Varus measurements are greater than 0; valgus measurements are less than 0. ² External measurements are greater than 0; internal measurements are less than 0. ³ Flexion measurements are greater than 0; extension measurements are less than 0. ⁴ P slope measurements are greater than 0; a slope measurements are less than 0. *Corrected = Polyethylene thickness accounted for by subtracting absolute difference from 9 millimeters from measurement.

[Figure 2](#)

Table 3. Planned Resection Values for Preoperative Valgus Knees, Stratified by Magnitude of Native Flexion

	Hyperextension (n=24)		Minimal Contracture (n=40)		High Contracture (n=18)		P-value
	M	SD	M	SD	M	SD	
Native Flexion (°)	-4.2±2.9	-12 - -1	3.6±2.8	0 - 9	13.2±3.2	10 - 21	<0.001
Preoperative aHKA (°)	-4.8±1.8	-7.8 - -2.3	-4.6±2	-10.7 - -2.1	-4.6±1.9	-8.8 - -2.1	0.888
Planned Coronal Alignment (°) ¹							
Limb	-1.4±1.3	-3 - 1	-1.2±1.5	-4 - 2	-1.6±1.4	-4.5 - 1	0.600
Distal Femur	-1.8±1.1	-4.5 - 0	-1.3±1.3	-3 - 2	-1.6±0.9	-3 - 0	0.146
Proximal Tibia	0.4±1.3	-1 - 3.5	0±0.9	-1.5 - 2.5	0±1.1	-1.5 - 3	0.315
Planned Transverse Rotation (°) ²							
Femoral TEA	0.4±1.7	-2 - 4	0.5±2.3	-4.6 - 5	0.9±1.6	-2.5 - 4	0.663
Femoral PCA	3.6±2	-0.3 - 6.8	3.6±2.1	0.1 - 9.3	4.1±2.2	-0.2 - 10	0.647
Planned Sagittal Alignment (°)							
Femoral Flexion ³	4.5±1.3	1.6 - 8	4.1±1.2	1.5 - 6.5	4±1.9	0.5 - 6	0.476
Tibial Slope ⁴	3.3±0.6	2 - 5	3.4±0.6	3 - 5.5	3.2±0.5	2.5 - 4	0.500
Distal Femur Resection (mm)							
Lateral	2.8±1.1	1.5 - 5.5	3.4±1.2	1.5 - 6.5	4.3±1.2	2.5 - 7	<0.001
Medial	7±1.2	4.5 - 9.5	7±1.1	5 - 11	7.8±1.2	6 - 10	0.036
Posterior Femur Resection (mm)							
Lateral	5.8±1.7	3 - 9.5	5.7±1.9	2.5 - 9.5	4.9±1.6	1.5 - 8	0.184
Medial	8.6±1.4	5.5 - 12	8.5±1.3	5.5 - 11.5	8.3±1.3	6 - 10.5	0.797
Tibia Resection (mm)							
Lateral	5.3±1.5	2 - 8	5.3±1.4	2.5 - 7	6.3±1.5	3.5 - 10	0.039
Medial	4.5±1.7	1 - 7.5	4.8±1.1	1.5 - 6.5	5.6±1.5	2.5 - 7.5	0.071
Sum of Extension Resections (mm)							
Lateral	8.1±1.4	5.5 - 11	8.7±1.8	4.5 - 12.5	10.6±1.7	7.5 - 14	<0.001
Medial	11.5±1.4	9.5 - 14	11.8±1.1	8 - 14	13.4±1.7	10.5 - 16.5	<0.001
Sum of Flexion Resections (mm)							
Lateral	11.1±1.9	8 - 15.5	11.1±1.9	7 - 15	11.2±1.8	6.5 - 14	0.945
Medial	13.1±1.7	10.5 - 16	13.3±1.6	9.5 - 18	13.9±1.6	10.5 - 16	0.224
Tibia Resection: Corrected* (mm)							
Lateral	4.2±1.9	-1 - 8	4.5±1.6	0.5 - 7	5.8±1.8	2 - 9	0.011
Medial	3.5±1.8	0 - 7.5	4±1.5	0.5 - 6.5	5.1±1.9	1.5 - 7.5	0.006
Sum of Extension Resections: Corrected* (mm)							
Lateral	7±1.7	3.5 - 11	7.9±1.9	2.5 - 11	10.1±1.8	7 - 13.5	<0.001
Medial	10.5±1.4	8 - 13	10.9±1.4	7 - 14	12.9±2	9 - 16	<0.001
Sum of Flexion Resections: Corrected* (mm)							
Lateral	10.1±2	6 - 13	10.2±2.1	5 - 14	10.7±1.9	6.5 - 13.5	0.556
Medial	12±1.8	8.5 - 15.5	12.4±1.8	8.5 - 17	13.4±1.9	9.5 - 16	0.047

M, mean; SD, standard deviation; mm, millimeters; aHKA, arithmetic hip-knee-ankle; TEA, transepicondylar axis; PCA, posterior condylar axis
¹ Varus measurements are greater than 0; valgus measurements are less than 0. ² External measurements are greater than 0; internal measurements are less than 0. ³ Flexion measurements are greater than 0; extension measurements are less than 0. ⁴ P slope measurements are greater than 0; a slope measurements are less than 0. *Corrected = Polyethylene thickness accounted for by subtracting absolute difference from 9 millimeters from measurement.

Figure 3

Infection Prevention Strategies for Extensor Reconstruction Synthetic Meshes

Alisina Shahi - University of Texas Health Science Center at Houston - Bellaire, USA

Samantha Gardner - University of Texas Health Science Center at Houston - Bellaire, USA

Annabelle Lin - University of Texas Health Science Center at Houston - Bellaire, USA

*Hugh Jones - UT Health Science Center at Houston - Houston, USA

David Rodriguez - University of Texas - Houston, USA

Introduction

In the realm of total knee arthroplasty, the use of synthetic meshes for extensor reconstruction presents a unique set of challenges, particularly concerning the prevention of postoperative infections. These infections can significantly impact patient outcomes, leading to increased morbidity and healthcare costs. Thus, innovative strategies to minimize bacterial colonization and infection are paramount. This study investigates the efficacy of various infection prevention strategies applied to polypropylene meshes, comparing standard meshes with those modified either by antibiotic-loaded calcium sulfate (CaSO₄) beads or by direct antibiotic embedding.

Methods

The tested groups included a polypropylene mesh (Marlex), polypropylene with antibiotic loaded calcium sulfate beads (Marlex), and an antibiotic embedded polypropylene mesh (Ariste). Each mesh was prepared in their clinical configuration by folding it in upon itself and securing with a running locking stitch. Each construct was then cut lengthwise into five 25mm sections and housed inside 6-well plates. CaSO₄ beads were prepared by mixing 20g of CaSO₄, 1g vancomycin, and 6ml of saline. The mixture was pushed into a form to mold 3mm diameter spheres weighing 0.05g each. A total of six beads were placed inside the inner folds of each mesh section (n=5). The antibiotic mesh was embedded with minocycline and rifampin by the manufacturer (Ariste)(n=5).

Each mesh set was inoculated with 4.8×10^7 *Staphylococcus aureus* and incubated for five days. After incubation, the meshes were rinsed in PBS, sonicated, and vortexed in Dey-Engley neutralizing broth to detach any bacteria cells. The suspensions were serially diluted and plated for colony counting. Prior to sonication, five of the ten plain polypropylene mesh samples were treated with a PVP-I solution for three minutes. The remaining five plain mesh samples served as controls for calculation and comparison.

Results

The plain polypropylene group had an average bacterial population of 2.5×10^8 (range: 6×10^7 – 7.9×10^8). SEM imaging showed attachment occurred on both the mesh and suture (Figure 1). After treating with PVP-I, there was a 96.8% reduction. The mesh loaded CaSO₄ group had minimal bacteria attachment (261 average; range: 0 – 1.1×10^3) while the embedded mesh group had no bacteria attachment. When comparing the groups in terms of log reduction, the loaded CaSO₄ and embedded mesh groups were both significantly different than the iodine washed group ($p < 0.001$, $p < 0.001$), but not when comparing each other ($p = 0.107$) (Figure 2).

Conclusion

The results of this study demonstrate that both antibiotic-loaded and antibiotic-embedded polypropylene meshes significantly reduce bacterial colonization compared to standard polypropylene meshes treated with PVP-I. Particularly,

meshes with embedded antibiotics showed the highest efficacy in preventing bacterial attachment, suggesting that this method could be the most effective strategy for infection prevention in extensor reconstruction surgeries. Future studies could further explore the long-term effects of these modifications on mesh integrity and patient outcomes. This research supports the integration of antibiotic modifications as a standard practice in the preparation of synthetic meshes for surgical applications.

Figures

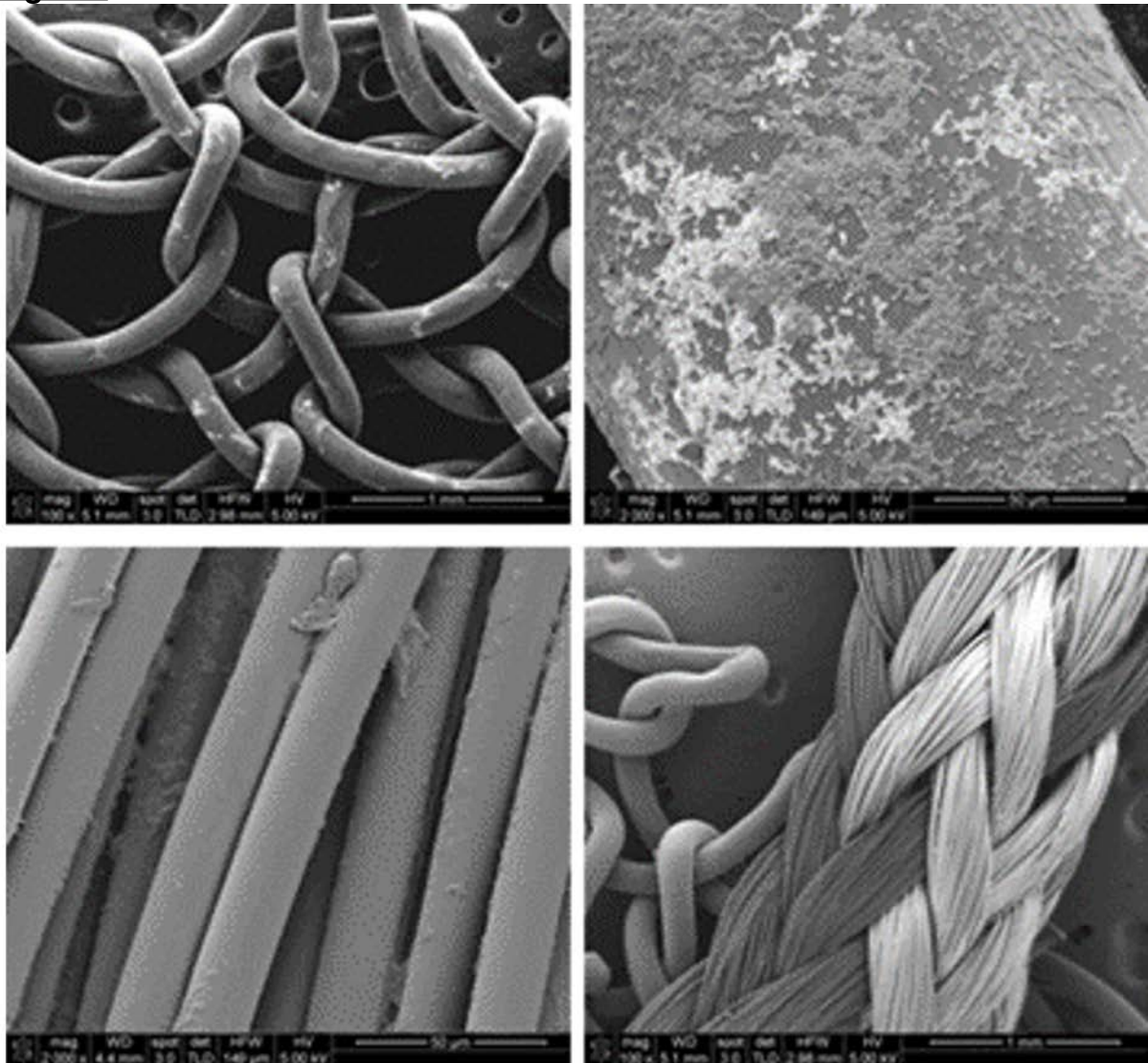


Figure1. SEM images of mesh filament (top) and suture fibers (bottom).

[Figure 1](#)

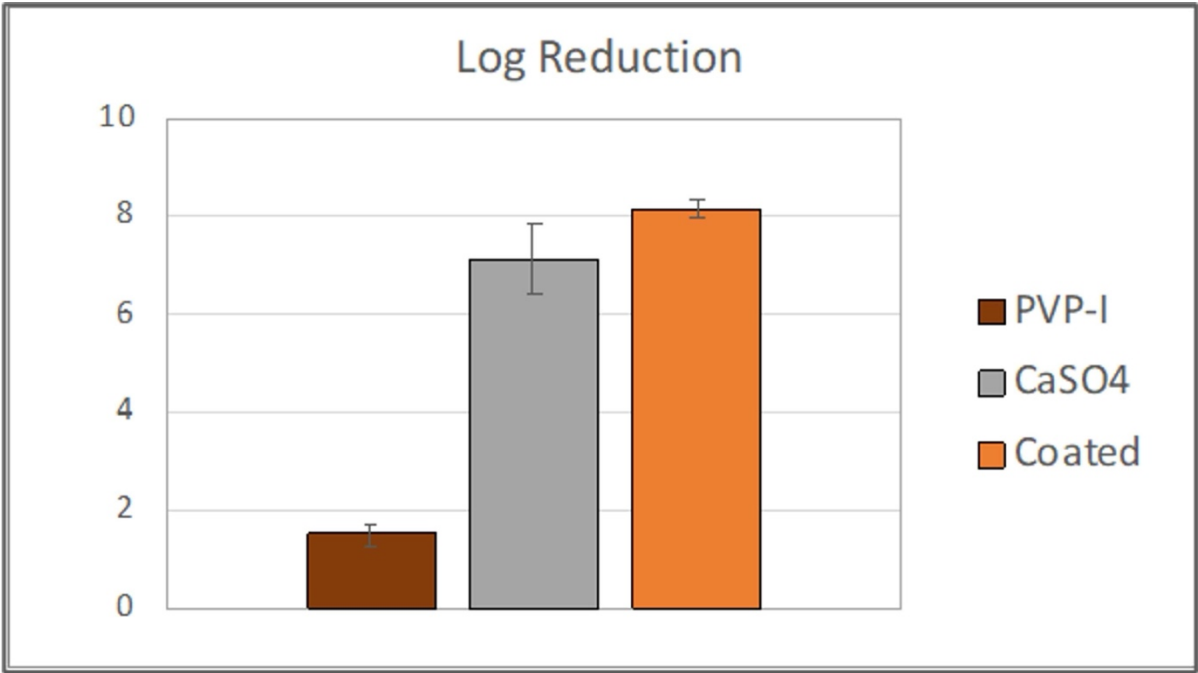


Figure2. Chart showing log reduction comparisons

[Figure 2](#)

Achieving High Weight-Bearing Flexion With an ACL Retaining TKA: Is Inclusion Criteria a Difference Maker?

*Lauren Smith - University of Tennessee, Knoxville - Knoxville, USA

Michael LaCour - University of Tennessee - Knoxville, USA

Richard Komistek - The University of Tennessee - Knoxville, USA

Michael Ries - Reno Orthopedic Clinic - Reno, USA

Jan Victor - Ghent University - Gent, Belgium

Introduction:

Various fluoroscopic studies have focused on determination of kinematic differences between total knee arthroplasty (TKA) designs, highlighting various amounts of weight-bearing flexion. However, what defines a successful TKA? Is it patient satisfaction, overall range-of-motion, normal-like kinematics, or a combination? Additionally, can patient inclusion criteria affect overall implant success? This research study investigates the influence that various inclusion criteria can have on post-operative kinematics of patients implanted with a Bi-Cruciate Retaining (BCR) TKA, aiming to highlight the importance that preoperative morphology have on knee kinematics of ACL-retaining knees.

Methods:

The in vivo 3D kinematics were determined for 19 subjects having a BCR TKA implanted by two different surgeons. The first surgeon uses only ACL integrity as their inclusion criteria, while the second uses additional criteria as well. While an intact ACL/PCL was a requirement for both surgeons, Surgeon #1 required minimal knee deformity not exceeding 5° varus/valgus while Surgeon #2 required not exceeding 10° varus/valgus. These knees were also compared to 10 non-implanted subjects. All knees were deemed well-functioning by their respective surgeons. All subjects were asked to perform a weight-bearing deep knee bend (DKB) under fluoroscopic surveillance. The kinematic parameters assessed for each subject can be seen in Figure 1.

Results:

During DKB, Surgeon #1 exhibited the largest ROM ($129.1 \pm 6.8^\circ$) overall ($p=0.0004$), with Surgeon #2 displaying a statistically lower ROM ($104.7 \pm 13.8^\circ$). Both cohorts demonstrated a significantly more posteriorized initial position of the lateral condyle than the normal knee ($p<0.0001$). Surgeon #1 cohort displayed noticeably more lateral rollback from full extension to maximum flexion while Surgeon #2 displayed an overall anterior motion of the medial condyle during the same flexion range. Mid-flexion highlights small amounts of anterior sliding for all cohorts, as one can expect to see in any implanted TKA. Detailed kinematics and motion patterns can be found in Table 1 and Figure 2.

Discussion:

The results of this study demonstrate that inclusion criteria seem to have an influence on post-operative TKA kinematics, as pre-operative morphology, varying patient ligament stiffnesses, and the difficulty of this procedure may altogether contribute to the diverse kinematic profiles yielded from this study. Nonetheless, despite some initial variability, both implanted cohorts typically experienced progressive rollback and kinematic patterns similar to the normal knee. Despite

different inclusion criteria, retaining both the ACL/PCL appears to yield overall kinematic patterns that are similar to the normal knee for patients in this study, indicating the importance of ACL functionality postoperatively.

Figures

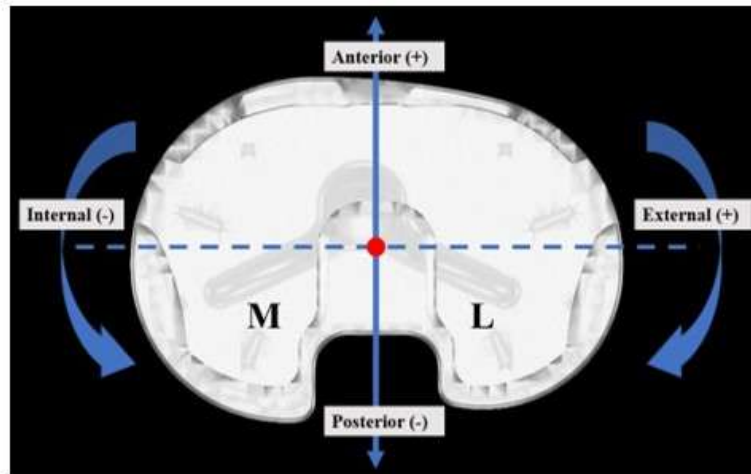


Figure 1: Schematic diagram showcasing the defined directions used for analysis of the kinematic variables.

Figure 1

Table 1: Average Kinematics for all BCR TKAs & the Normal Knee.

			0° - MAX°
Implant Type	Surgeon #1	LAP (mm)	-6.3 ± 5.1 (-15.7 to 1.3)
		MAP (mm)	-1.4 ± 4.7 (-13.0 to 6.7)
		Axial Rotation (°)	6.5 ± 4.1 (-2.9 to 17.3)
	Surgeon #2	LAP (mm)	-2.9 ± 6.3 (-10.9 to 8.8)
		MAP (mm)	1.2 ± 3.5 (-4.5 to 6.9)
		Axial Rotation (°)	5.3 ± 6.0 (-5.8 to 12.6)
	Normal Knee	LAP (mm)	-17.8 ± 6.0 (-25.4 to -6.2)
		MAP (mm)	-9.1 ± 4.9 (-14.4 to -3.2)
		Axial Rotation (°)	23.7 ± 7.8 (8.1 to 30.7)

Figure 2

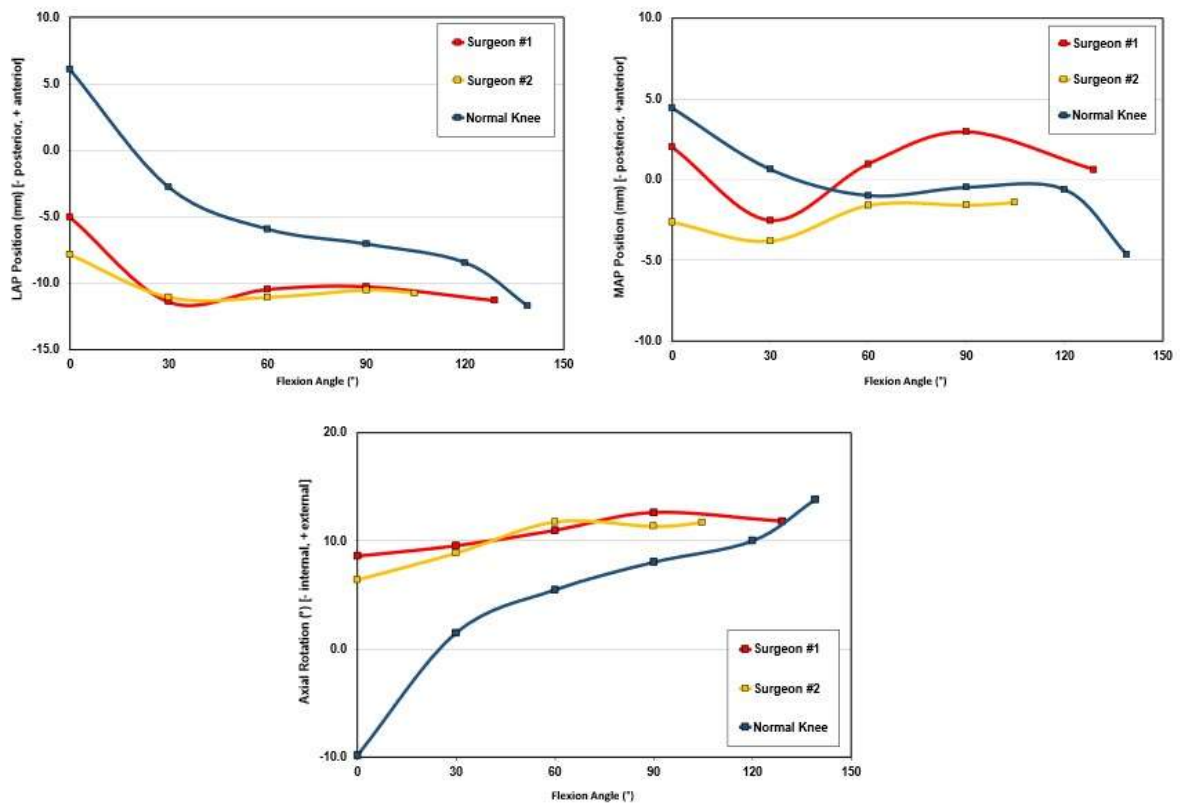


Figure 2: Average LAP (top, left), MAP (top, right), Axial Rotation (bottom) positions during a deep knee bend for low point analysis. All motions are representative of the femur with respect to the tibia.

Figure 3

Cost-Effectiveness of a Patient Centered Digital Platform After Elective Orthopaedic Surgery- Experiences at a District Hospital

Gagandeep Mahi - Kettering General Hospital - Coventry, GB

*Faizal Rayan - Kettering General Hospital - Kettering, United Kingdom

Srinivasan Shyamsundar - Kettering General Hospital - Kettering, United Kingdom

Myrto Vlazaki - University Hospitals of Leicester NHS Trust - Leicester, United Kingdom

Hamidreza Khairandish - Kettering General Hospital - Kettering, United Kingdom

Introduction:

In the UK, the National Health Service (NHS) provides medical care free at the point of delivery, with the country spending about 10% of its GDP on healthcare, amounting to £181.7 billion over the past five years.

This study evaluates the potential savings for healthcare and society through the implementation of a digital application called 'Post Op', which connects post-operative patients with their surgical teams for remote interactions. Initially trialled at a UK-based District General Hospital, the app. encourages patients to use it in the post-operative period to contact their surgical teams, exchange multimedia including pictures of the surgical site for assessment of healing and infection, receive prompts and post-operative advice, and track patient progress against the typical milestones expected for their type of operation and demographic group.

Building upon these findings, our paper simulates populations of orthopaedic post-operative patients providing estimates for resource savings associated with the digital surgical follow-up app. Figure 1 outlines four areas where cost-effectiveness can be enhanced: reducing inappropriate medical care-seeking episodes, preventing deterioration of postoperative complications, mitigating environmental costs related to excessive hospital resource and transport use, and alleviating patient-borne expenses.

Methodology:

We collected preliminary data from patient survey through a questionnaire to assess patients' views of Post Op app. We calculated the estimates for NHS services cost using reports citing unbiased and systematically reported mean nationwide costs. Table 1 provides a summary of the mean cost per event for different NHS-provided services. We also estimated the travel-associated costs and mean distance from the patients' homes to the hospital and used this figure to calculate the mileage saved and we also assessed associated reduction in carbon emission levels. We used a conservative modelling approach simulating different patient groups with varying levels of postoperative anxiety/complications as detailed in Table 2.

Results:

This study focused on evaluating costs associated with avoidable deterioration of post-operative complications.

For the purposes of our simulation, we proposed that early detection of SSIs can prevent deterioration without the need for further surgical procedure. Our calculation showed that each early SSI detection equates to saving £5,845/100 patients. There is clear proposed co-relation between usage of this digital pathway and avoidable antimicrobial resistance/tolerance as well as possibility of saving approximately 0.32 metric tons of CO₂, which is equal to £49 . Costs that could be saved due to lost

productivity and access to hospital per 100 patients as a result of time spent seeking unnecessary medical care, we that would be equal to £2,547 and £560 per 100 patients respectively.

Conclusion:

We have shown that the Post Op application provides excellent support for most patients in the immediate postoperative period and is likely to result in a significant reduction in the number of contacts patients make with the GP or hospital, and with the Emergency Department, thereby resulting in significant cost saving for both the service and the patients. Our findings contribute valuable insights into the potential of digital tools to enhance postoperative care and generate significant savings for the healthcare system.

Lateral UKA in Patients With Greater Than 14 Degrees Valgus Deformity

Martin Redish, MD - ParkRidge Bone & Joint - Chattanooga, USA

*Robert Eberle - Maxx Orthopedics - Apex, USA

INTRODUCTION / PURPOSE

The indications for use of lateral unicondylar knee arthroplasty (UKA), and especially in the presence of significant valgus with deformity are controversial. The purpose of this retrospective study was to review the results of single surgeon series of consecutive lateral UKAs performed in patients with $>14^\circ$ of valgus deformity.

METHODS

Between January 2019 and October 2022, twenty-two (22) consecutive lateral UKAs were performed by the author on patients with $>14^\circ$ of valgus deformity. Patients were recommended a lateral UKA procedure if the joint line could be corrected utilizing a stress radiograph without narrowing of the medial compartment. There were 19 (86%) females and 3 (14%) males, with an average age at surgery of 75.6 ± 7.1 years (range: 64.1 to 86.7). Of the knees indicated for surgery, there were 9 (41%) left and 13 (59%) right. A minimally invasive lateral approach with excision of part of the lateral patellar facet was used to improve lateral compartment access. All knees were implanted with a resurfacing UKA and an all polyethylene, inlaid tibial component ranging in thickness from 6.5mm to 9.5mm (Biomet Repicci II® UKA: n=1, Maxx Orthopedics Renew™ Partial Knee Replacement: n=21). All patients were evaluated radiographically to measure pre- and post-operative valgus angle using weight bearing AP views to measure alignment. Adverse events, and patient satisfaction were recorded.

RESULTS

All patients were post-operatively evaluated, without loss to follow-up, at an average of 37.6 ± 16.2 months (range: 17.4 to 62.3). Any incidence of early post-operative swelling was quickly resolved, and there were no further adverse events or subsequent revisions for any reason. Valgus correction to a pre-deformity alignment was obtained in all patients. The average pre-operative valgus was $17.7^\circ \pm 2.6^\circ$ (range: 15° to 27°) and was corrected to $7.4^\circ \pm 2.2^\circ$ (range: 4° to 12°) ($p < 0.001$). The average percent change in valgus correction was $58.6\% \pm 10.0\%$ (range: 35.3% to 75%). At the most recent follow-up all patients were satisfied with their partial knee.

CONCLUSIONS

From this small, single surgeon review of a consecutive series of patient candidates for lateral UKA presenting with valgus deformities $>14^\circ$, we believe that minimally invasive resurfacing lateral UKA may be a safe and viable option as an alternative to total knee arthroplasty (TKA). However, we recommend that it is necessary all patients that deformity corrections be verified utilizing stress radiography without loss of medial compartment joint space. We also believe that avoiding TKA, in especially the elderly population (>75 years old), allows for quicker recovery, avoidance of complications common to TKA, and return to expected activities of daily living (ADL). While this is a small single surgeon retrospective series, further use of a resurfacing / inlay UKA component and study is warranted in this specific patient population.

The Impact of Surgeon Volume on UKA Survivorship: A MARCQI Database Analysis

*Muhammad Abbas - Henry Ford Hospital - Detroit, USA

David Markel - The CORE Institute - Novi, USA

Brian Hallstrom - University of Michigan - Ann Arbor, USA

Huiyong T Zheng - MARCQI Coordinating center - Ann Arbor, USA

Michael Charters - Henry Ford Hospital - Detroit, USA

Introduction: Utilization of unicompartmental knee arthroplasty (UKA) has remained low when compared to total knee arthroplasty (TKA) possibly due to reports of higher rates of revision and reoperation. This study aims to quantify surgeon UKA case-volumes and measure the effect of surgeon volume on early revision. We hypothesized that surgeons with high case volumes would have lower revision rates compared to medium and low volume surgeons.

Methods: Primary UKAs performed between February 2012 to November 2021 and associated revisions were identified utilizing Michigan Arthroplasty Registry Collaborative Quality Initiative (MARCQI). Surgeon information including total cases and annual UKA volume was collected. Case volume per year was stratified as High (≥ 35 cases/year), Medium (15 – 34 cases/year), low (< 15 cases/year).

Results: There was a total of 15,542 UKA performed. Of these, 701 (4.51%) were revised and 412 (58.8%) of revisions occurred within 2 years. Of the 287 surgeons who performed an UKA in the registry, 237 (82.6%) were low volume surgeons; 36 (12.5%) were medium volume, and 14 (4.9%) were high volume. High volume surgeons were more likely to operate on older patients ($p < 0.01$), Medicare patients ($p < 0.01$), ASA scores of III/IV ($p < 0.01$), and less likely to utilize a medial parapatellar approach ($p < 0.01$). High volume surgeons had significantly lower 5-year revision rates compared to medium and low volume surgeons (high: 4.26% (95% CI: 3.70, 4.90), medium: 5.22% (4.44, 6.12), low: 7.15% (6.37, 8.02); $p < 0.001$). At 2 years post-operatively, high volume surgeons had revision rate 2.13% (95% CI: 1.79, 2.54), medium: 2.71% (95% CI: 2.23, 3.30) and low: 4.05% (95% CI: 3.52, 4.65). In comparison, the 5-year revision rate for TKA in Michigan was 2.99% (95% CI: 2.90, 3.08) and the 2-year revision rate for TKA in Michigan was 1.74% (95% CI: 1.68, 1.80).

Conclusion: When UKA were performed by high volume surgeons in the state of Michigan there was better survivorship when compared to low volume and medium volume surgeons. High volume surgeons were more likely to perform UKA on older patients, Medicare patients, ASA scores of III/IV, and less likely to utilize a medial parapatellar approach. The revision rate for the high-volume surgeons still exceeded the 5 year revision rate for total knee replacement in Michigan.

Safety, Efficacy and Validation of AMF Heating on a Primary Prosthetic Knee Implant and Surrounding Tissues Using Human Cadaver and Digital Knee Models

*Bibin Prasad - Solenic Medical - Addison, USA

Varun Sadaphal - Solenic Medical - Addison, USA

Luke Gritter - AltaSim Technologies - Columbus, USA

Joshua Thomas - AltaSim Technologies - Columbus, USA

Jose Guzman - Solenic Medical, Inc - Addison, USA

John Tepper - Solenic Medical - Addison, USA

Haley Alegria - Solenic Medical, Inc - Addison, USA

Rajiv Chopra - Solenic Medical - Addison, USA

Introduction: Metal implant infections are a devastating problem due to the formation of biofilm which impairs the effectiveness of antibiotics and leads to surgical replacement as definitive treatment. Exposing implants to Alternating Magnetic Fields (AMF) generates surface heating where biofilm tends to reside. However, the use of AMF heating on implants to eradicate biofilm must be accurate and safe to surrounding tissues, in order to be practical. In this study the validation, safety, and efficacy of AMF heating in a knee implant and surrounding tissues is investigated using Solenic's AMF treatment device (Sola 2) on a human cadaver and digital knee models [Fig. 1].

Methods: In a cadaver leg real time temperature measurements using fiber optic sensors were performed on a primary knee implant and surrounding tissues including, medial and lateral collateral ligaments, patella, muscle, and skin [Fig. 2 (a)]. To efficiently deliver AMF treatment to the implant C-Arm X-Ray imaging was performed to position the cadaver with Sola 2 transducer. Simulations were performed on a cadaver equivalent digital knee model to compare the temperatures that were measured from the cadaver [Fig. 2 (b)]. To ensure safety due to the AMF treatment thermal dose levels on surrounding tissues were calculated based on CEM43 and Arrhenius tissue damage models. To determine the efficacy of AMF treatment, mathematical models of biofilm eradication with heat were created based on *in vitro* experiments using different gram positive (*S. aureus*) and gram-negative (*P. aeruginosa*) bacterial strains.

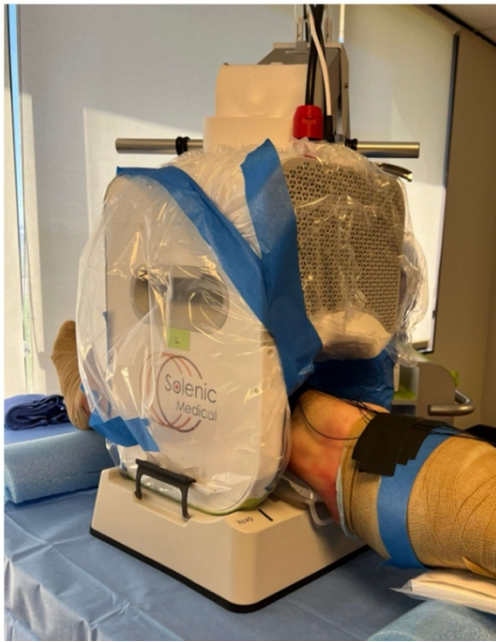
Results: Results show <10% of uncertainty variation between simulations and experiments [Fig. 3]. Using the treatment strategy of achieving an average surface temperature of 75°C in single 80s exposure, no significant irreversible tissue damage was observed to surrounding tissues. 2logCFU reduction of bacteria was quantified on >85% surface area of the implant. This heating scheme has also been shown to be effective at eradicating biofilm in our *in vitro* and *in vivo* studies.

Conclusion: Overall, this study indicates accurate heating, safe and effective implementation of AMF treatment in clinics for primary knee implants.

Figures

Fig 1

Cadaver model



Digital knee model

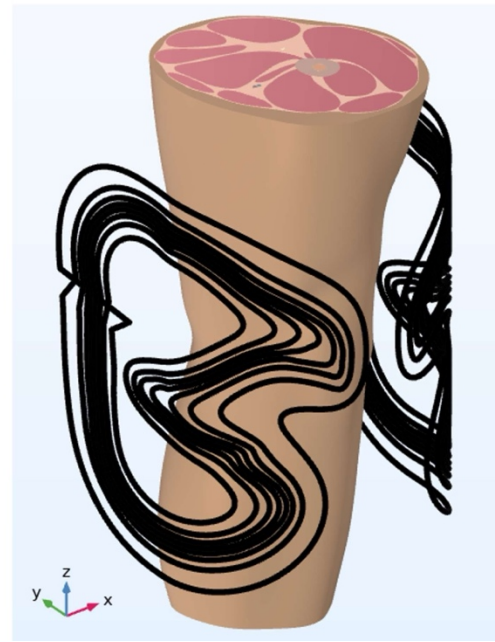
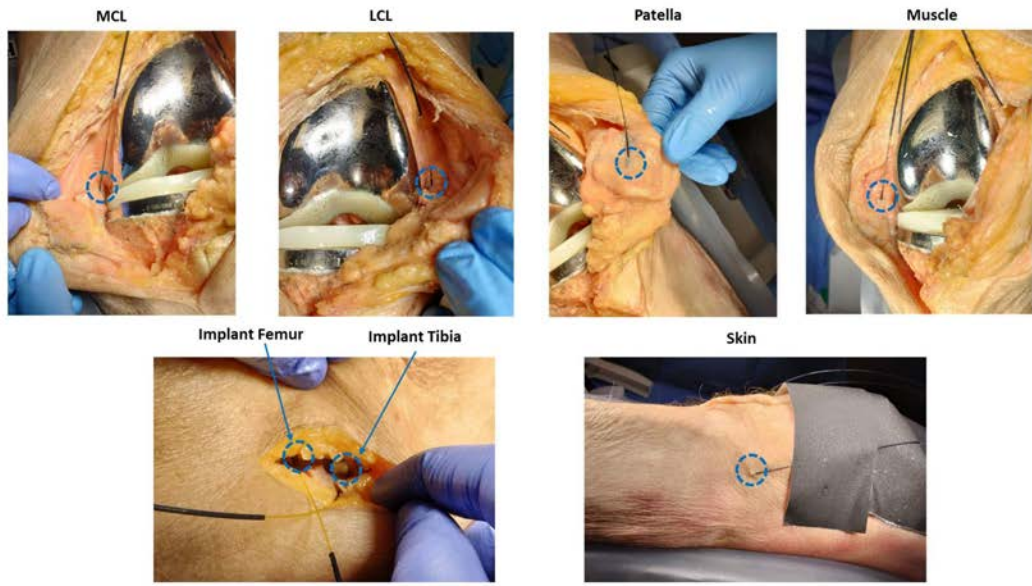
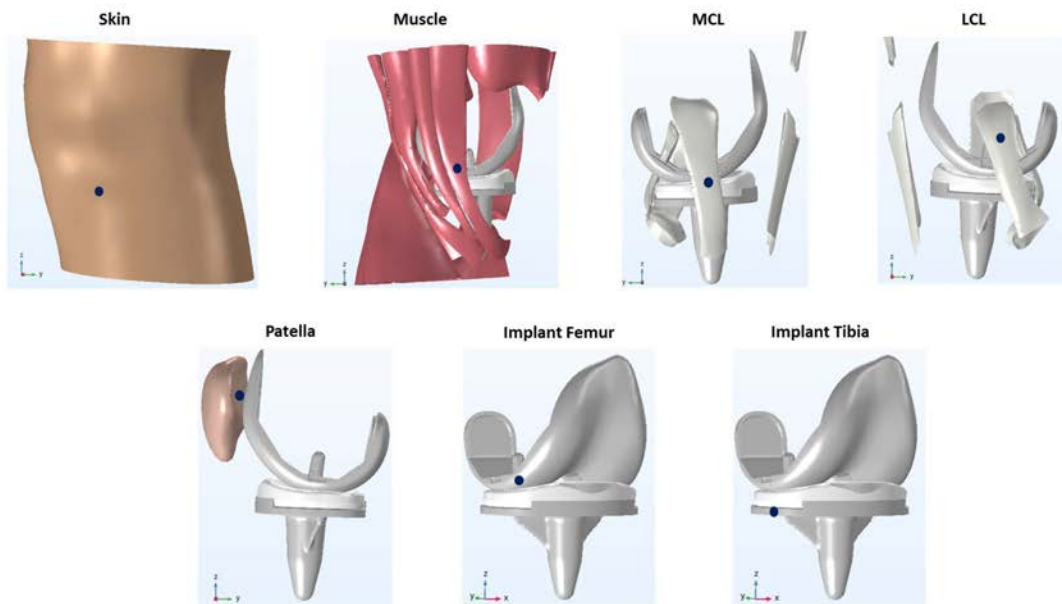


Figure 1

Fig 2 (a) Sensor positions in cadaver



(b) Sensor positions in digital knee model



[Figure 2](#)

Comparison of temperature form cadaver and digital knee model

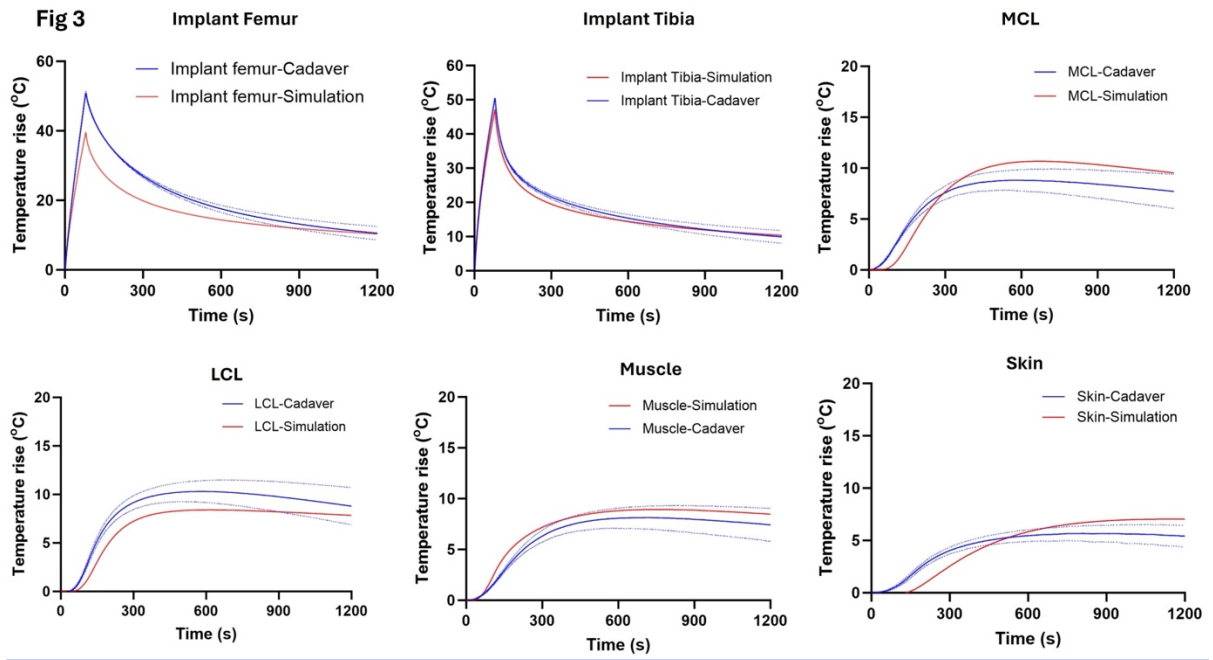


Figure 3

Integrating Virtual Reality in ACL Rehabilitation: A Novel Approach for Enhanced Neuromuscular Connectivity Following Arthroscopic Reconstruction

*Cadence Lee - University of Illinois College of Medicine at Chicago - Chicago, USA
Farid Amirouche - University of Illinois at Chicago - Highland Park, United States of America

The anterior cruciate ligament (ACL) is pivotal in maintaining knee stability, chiefly by limiting excessive tibial rotation and anterior tibial translation. Management of ACL injuries encompasses both arthroscopic surgical reconstruction and non-surgical rehabilitation strategies. Integrating Virtual Reality (VR) technology may offer an innovative approach to enhancing post-operative neuromuscular coordination, facilitating an earlier return to athletic activities and baseline function. Common post-injury complications such as inadequate squat mechanics, anterior pelvic tilt, and compromised single-leg stance necessitate corrective rehabilitation measures. Here, we define a Virtual Reality (VR) protocol using VAST. Rehab software to improve functional outcomes following ACL reconstruction. A cohort of 9 healthy volunteers collected data on balance, range of motion, functional mobility, divided attention, reaction time, and memory retention. Each participant was subjected to two separate workout sessions, each spanning 15 minutes, modeled after the traditional rehabilitation strategy defined by Massachusetts General Brigham Sports Medicine. Throughout the VR sessions, subjects performed gamified tasks within an immersive virtual environment designed to engage both motor and cognitive tasks. At the same time, motion sensors captured real-time data related to both physical movements and relayed them in a feedback panel. Results were found for functional movement scores as a percentage of task success in the following exercises: standing lateral balance (77%), lateral leg raise (71%), left/right leg kick (64%/62%), seated lateral foot swing (82%), standing left/right hip abduction (83%/98%), standing knee raise (85%), seated knee raise (95%), standing left/right lateral leg raise (67%/76%), and planted standing torso balance (48%). Additionally, we observed the range of motion for left/right lateral leg raise (88°/86°), divided attention task success (53.4%), standing left/right cross-body kick reaction time (1347/1200 msec), and squat symmetry (0.54 cm right-lean). Our findings validate proof of concept for the protocol's ability to data track and provide real-time feedback on functional metrics, underscoring the need for further technological involvement in post-ACL injury strength and conditioning protocols. This protocol also highlights the potential advantages of integrating VR into conventional physical therapy by transitioning from isolated muscle training to a more holistic approach emphasizing neurological connectivity. Not only does VR technology have the potential to improve functional outcomes following arthroscopic reconstruction, but it can also be modified for home-based applications, diminishing dependence on continuous

From Theory to Practice: Integrating Wearable Technology Into Clinical Environments

*Richard Bolander - TracPatch - Orland Park, United States of America

Sarah Bolander - Exhibitor: TracPatch - USA

Victor Hernandez - University of Miami Hospital - Miami, USA

Michele D'Apuzzo - University of Miami Miller School of Medicine - Miami, USA

From Theory to Practice: Integrating Wearable Technology into Clinical Environments

Introduction:

- The increased accessibility of remote monitoring technologies (RMT) has the potential outpace the desire for these technologies to be used within clinical environments due to factors such as usability for patients and providers, clinic re-training and reimbursement potential.
- For these technologies to be incorporated at scale, a strategy needs to be developed to address the entire eco-system for which these technologies will need to be integrated.
- The purpose of this abstract is to present on the efforts conducted by a major University Health system to integrate wearable technology designed for remote patient monitoring of total knee arthroplasty patients.

Methods and Results:

- For successful clinical integration, the value proposition of using a new technology must outweigh the costs associated with using and implementing the RMT for multiple stake holder groups.
 - Executive management: Does the inclusion of RMT advance the mission of the health system while either being cost neutral or net positive?
 - Cyber security and IT: Does inclusion of RMT unduly burden the IT department for integration? Does inclusion increase risk to the organization's data security strategy?
 - Value and cost analysis purchasing teams: Does the inclusion of RMT result in a net benefit to the organization?
 - In department champions: Who will be the primary promoter or champion of the technology and do they believe in the value that the data can create?
 - Devices users: Can the RMT be used efficiently within day-to-day clinical work flows?
 - Billing departments: Is there a mechanism and process that allows for the capture of reimbursement and is the process to capture the reimbursement overly burdensome?
 - Research coordination: Can the RMT be used for research?
 - Patient: Is the RMT something that a patient will actually want to use?
- Some of the keys to implementation success include:
 - Develop protocols that define roles and responsibilities with the clinic.
 - Clearly define patients' roles and responsibilities and provide appropriate levels of education and enthusiasm for the process.
 - Understand that not every patient is a candidate for RMT.
 - Start small with a growth and learning mindset.

Conclusion:

- RMT provides a level of patient tracking that was not available previously. In order for implementation within a healthcare system to be successful, buy-in needs to occur across multiple key stake holder groups within a system and concerns addressed quickly.
- Protocols must be developed, and clinical integration time needs to be minimized.
- Finally, sufficient patient education and strong provider motivation are critical for patient adoption.

Remote Therapeutic Monitoring: What to Consider for Meaningful Clinical Integration and Reimbursement Potential

*Richard Bolander - TracPatch - Orland Park, United States of America

Sarah Bolander - TracPatch Health - Orland Park, United States of America

Introduction:

Remote patient monitoring was first introduced as a service based intervention using FDA approved medical devices to collect, store, and distribute medical device data to healthcare providers in 2019. The initial focus was on physiologic parameters and only accessible to healthcare providers who work and bill under the evaluation and management code sets associated with the outpatient physician fee schedule.

In 2021, CPT expanded remote monitoring and included a new code set for remote therapeutic monitoring. These code sets followed the same guidelines but were introduced within the general medicine category of the outpatient physician fee schedule which allow them to be initiated and utilized by other Qualified Health Professionals.

As with any innovative technology, the process of re-defining appropriate regulatory, coding and payment guidelines continues to evolve. In this talk, we will consider key questions, including when and how to use these codes for a provider's practice

Method:

This talk will consider the following:

An FDA approved medical device is required to facilitate a healthcare provider to engage in a remote monitoring plan for their patients.

- Defined as adjunct medically qualified services different from traditional or telehealth-based treatment.
- The reimbursement pathways outside traditional durable medical devices

An overview of the basic architecture of the remote monitoring code set evaluation and structure

- Requirements
- Initial Education, data supply, and intra service work
- code set valuation

Similarities and differences between remote physiologic monitoring and remote therapeutic monitoring

- Scope of Practice, Billing Provider and Supervision Requirements
- Variability of coverage and payment, private versus Medicare insurers

Current 2024 PFS (Physician Fee Schedule) rules and guidelines

- How to apply remote monitoring to a 90 day Global in 2024.

Conclusions and Looking Ahead:

- Advocacy efforts required within the MSK/ Orthopedic space to support more opportunity for use of RTM (Remote Therapeutic Monitoring) as an adjunct to standard of care to develop a new "gold standard of care".
- Providers need to own their remote monitoring plan and the effective management of the resources required to care for their patients and produce desired outcomes.

Survivorship and Clinical Outcomes for a Short Stem Used in Shoulder Arthroplasty: A Multi-Center Registry Review

*David Fawley - DePuy Synthes - Warsaw, USA

Amon Ferry - Arizona Sports Medicine Center - Scottsdale, USA

Rudolf Hoellrich - Slocum Research & Education Foundation - Eugene, USA

Jacob Stueve - Kansas City Orthopaedic Institute - Leawood, USA

Sean Croker - Depuy Synthes - West Chester, USA

Introduction

A short stem for use in shoulder arthroplasty was recently released. The proximal biological fixation and stability are the same as the legacy standard length stem, but bone preservation is possible due to the shortened stem geometry. The aim of this evaluation was to retrospectively assess early complications and revisions of this short stem used in shoulder arthroplasty.

Methods

We conducted a retrospective multicenter registry case review from a standard of care company-sponsored registry. Clinical assessments were summarized at standardized registry visit windows.

Results

A total of 92 short stem shoulders were implanted across 3 US sites. Five (5) were hemiarthroplasties, 59 were primary anatomic total shoulders, and 28 were reverse shoulder arthroplasties. Mean age was 64.2 years (R 41-88), 26 (28.6%) were female and BMI averaged 29.7 (R 19.7 to 42.5). Primary diagnoses and additional demographic detail are presented in Figure 1. No revisions or complications were reported.

Conclusion

Our study showed no revisions to date and low complications for a short stem used in shoulder arthroplasty. While early follow up results are promising, continued study of this design would be beneficial.

Figures

Figure 1 – Patient Demographics

	All cases	Hemiarthroplasty	Primary TSA	Reverse
N	92	5	59	28
Age	64.2	44.6	62.7	71.0
Mean (range)	(41 to 88)	(43 to 47)	(41 to 80)	(52 to 88)
Gender – Female [n (%)]	26 (28.6%)	0 (0%)	14 (24.1%)	12 (42.9%)
BMI	29.7	26.3	30.8	28.0
Mean (range)	(19.7 to 42.5)	(24.3 to 28.9)	(23.5 to 42.5)	(19.7 to 36.6)
Indication for Surgery [n (%)]				
Avascular Necrosis	1 (1.1%)	0	0	1 (3.6%)
Complete Cuff Tear	17 (18.5%)	0	0	17 (60.7%)
Osteoarthritis	66 (71.7%)	4 (80.0%)	58 (98.3%)	4 (14.3%)
Partial Cuff Tear	6 (6.5%)	0	0	6 (21.4%)
Post Traumatic Arthritis	2 (2.2%)	1 (20.0%)	1 (1.7%)	0

[Figure 1](#)

Mid-Term Recovery of Range of Motion and Function Similar in Revision and Primary Knees

*Emily Hampp - Stryker - Mahwah, USA

Sarah Shi - Stryker - Mahwah, USA

Introduction: The number of global total knee arthroplasty (TKA) cases is projected to continue increasing. As primary TKA cases increase, so does the frequency of revisions. Clinical objectives for TKA cases include alleviating pain and improving overall knee function. This study aimed to compare the change in outcomes as measured by the Knee Society Score (KSS), between primary and revision TKA systems. Additionally, this study sought to analyze the outcomes of low-activity (LA) and high-activity (HA) subgroups of patients receiving primary or revision TKA systems.

Methods: Data was collected as part of two prospective, post-market, multicenter studies comparing preoperative to 1, 2, and 5-year data. A total of 584 patients were stratified into two groups based on indication and type of knee device: Primary TKA Posterior Stabilized (PS) group (n = 404) and Revision TKA Total Stabilized (TS) group (n = 180). PS and TS patients were further divided into two groups based on preoperative activity level using the Lower Extremity Activity Scale. Patients scoring between 1 and 7 were classified as “Low Activity” (LA) and patients scoring 8 to 18 were classified as “High Activity” (HA). The change in KSS scores preoperative to 1, 2, and 5-year postoperative was compared between PS and TS groups, as well as low-activity [PS-LA (n = 141) vs. TS-LA (n = 104)] and high-activity [(PS-HA (n = 261) vs. TS-HA (n = 75)] groups. Demographics and changes in PROMs were compared using t-tests and Chi-squared tests with a significance level of $\alpha=0.05$.

Results: There were no significant differences in baseline characteristics for BMI (kg/m^2 ; mean \pm SD) or sex (male; %), between the PS and TS groups (30.8 ± 4.6 , 42.3% and 30.8 ± 4.4 , 44.4%, respectively; $p > 0.05$). PS patients were younger age (years; mean \pm SD) compared to TS patients (65.1 ± 8.6 vs. 67.1 ± 9.7 , respectively; $p = 0.0147$). The improvement in range of motion was similar across all groups (all $p > 0.05$). The KSS Pain/Motion score improved significantly more in the PS, PS-LA, and PS-HA groups at each timepoint, compared to the respective TS groups (all $p < 0.0001$). Within the KSS Pain/Motion section, the PS group demonstrated greater pre- to post-operative reduction in pain and correction in alignment, while the TS group had greater pre- to post-operative reduction in anteroposterior and mediolateral instability (all $p < 0.0001$). The improvement in KSS Functional scores were similar between all groups: PS vs. TS, PS-LA vs. TS-LA, and PS-HA vs. TS-HA (all $p > 0.05$).

Conclusion: Revision TKAs typically exhibit lower functional outcomes, which may be due to surgical technique complexity and patient indications. The revision TS TKA demonstrated comparable functional scores to the primary PS TKA, suggesting its potential efficacy in addressing challenges associated with revision TKAs. Further, this finding was consistent for patients with high and low preoperative activity levels, highlighting the versatility and potential of the TS TKA system for patients undergoing knee revision procedures.

Multi-Center RSA Study of a Novel Cementless Total Knee Replacement

***Mathew G Teeter - Schulich School of Medicine and Dentistry, Western University and London Health Sciences Centre - London, Canada**

Trevor Gascoyne - Orthopaedic Innovation Centre - Winnipeg, Canada

Brent Lanting - London Health Sciences Centre - London, Canada

Eric Bohm - Concordia Joint Replacement Group - Winnipeg, Canada

Thomas Turgeon - Concordia Joint Replacement Group - Winnipeg, Canada

Douglas Naudie

Purpose:

Cementless total knee arthroplasty (TKA) is increasing in popularity as a definitive treatment for end-stage osteoarthritis. Purported advantages to cementless TKA are shorter surgical time and improved long-term survivorship compared to cemented TKA. The purpose of this study is to determine the risk of aseptic loosening of a novel cementless TKA based on micromotion analysis of implants with respect to bone using radiostereometric analysis (RSA).

Methods:

Thirty patients requiring primary TKA were enrolled at two Canadian academic joint replacement centres. All patients received a porous CONCELOC tibial baseplate paired with a cruciate-retaining LEGION porous (n=24) or LEGION cemented (n=6) femoral component (Smith & Nephew, Memphis, TN). The patella was selectively resurfaced based on surgeon preference, and was resurfaced using either a cementless CONCELOC (n=10) or a cemented GENESIS inset biconvex patella (n=6). During surgery, RSA beads were inserted into the tibia, femur, and patella (when a cementless CONCELOC patellar implant was employed). Patients received supine RSA imaging at six weeks (baseline), and six and 12 months following surgery. The primary study outcome was change in maximum total point motion (MTPM) of the tibial baseplate between six and 12 months. A secondary outcome was to characterize migration patterns of the tibial baseplate over the follow-up period. Patient reported outcome measures (PROMs) from pre-operative to post-operative time points using Oxford-12 Knee Score (OKS), European Quality of Life (EQ-5D), Forgotten Joint Score (FJS), and visual analogue scale (VAS) for satisfaction with surgery were also collected.

Results:

Our patient cohort (16 females, 14 males) had a mean age at surgery of 66 years (range: 53-79) and a mean body mass index of 30.6 kg/m² (standard deviation: 3.8). The pattern and magnitude of baseplate migration remained stable between six and 12 months with mean change in baseplate subsidence and MTPM of 0.02 mm and 0.18 mm, respectively. Similarly, femoral and patellar component migration was stable between six and 12 months with mean change in MTPM of 0.14 mm (n=15) and 0.01 mm (n=5). Patients reported substantial improvement in functional (OKS, FJS) and health-related (EQ-5D) PROMs following surgery. Patients reported 83.8% and 84.1% satisfaction VAS at six and 12 months, respectively. One patient was revised due to persistent stiffness after completing their 12 month follow-up. This patient received a new tibial insert and a resurfaced patella while the baseplate and femoral components were retained.

Conclusion:

This study provides valuable early data on the fixation of this novel cementless TKA implant. Implant migration patterns for this patient cohort did not indicate any concerns for future aseptic loosening of any component of the TKA. A further assessment will be performed at 24 months to confirm this finding.

Preoperative Abnormal Posture Due to Knee Osteoarthritis Could Improve With Total Knee Arthroplasty as Knee-Hip-Spine Syndrome

*Yasushi Oshima - Nippon Medical School - Japan

Nobuyoshi Watanabe - Kyoto Kujo Hospital - Kyoto, Japan

Toru Takeoka - Kyoto Kujo Hospital - Kyoto, Japan

Yoshiteru Kajikawa - Kyoto Kujo Hospital - Kyoto, Japan

Tadahiko Yotsumoto - Kyoto Kujo Hospital - Kyoto, Japan

Tokifumi Majima - Nippon Medical School - Tokyo, Japan

Background:

Global body posture is an important factor to keep body balance and to walk smoothly, in which spinal, pelvic, and lower extremity alignment is crucial for maintaining a healthy posture. However, with aging, this posture becomes challenging to maintain due to muscle weakness and skeletal degeneration. Abnormal body posture leads to fall, which results in fracture and is associated with increased morbidity and mortality, especially in older population. Thus, the prevent of falls is critical issue in an aging society. Osteoarthritis (OA) of the hip and knee can also lead to abnormal posture, known as hip–spine and knee–spine syndrome. Total knee arthroplasty (TKA) can help relieve pain and improve lower extremity alignment, therefore, this may also improve abnormal posture, which is called as knee–hip–spine syndrome. However, we hypothesized that the condition of the contralateral knee may affect this improvement. This study evaluated the effects of TKA on clinical outcomes and radiographic body posture. The hospital's Institutional Review Board approved this study, and all the patients provided written informed consent prior to performing any study-related activities.

Methods:

Patients scheduled for primary one-sided TKA were divided into two groups: the unilateral group comprised patients with contralateral knee OA conditions. The bilateral group included patients with prior contralateral TKA. Knee range of motion (ROM), the Knee Injury and Osteoarthritis Outcome Score (KOOS), radiographic lateral femorotibial angle (FTA), hip and knee flexion angles, and sagittal vertical axis (SVA) while standing were measured 24 months after TKA.

Results:

Both groups showed improved knee extension, KOOS, FTA, and hip and knee flexion angles 24 months after TKA. SVA also improved six months after TKA in both groups and was maintained in the bilateral group, while it deteriorated again in the unilateral group 24 months after TKA (Fig.).

Conclusion:

TKA can improve abnormal body posture due to knee OA as a knee–hip–spine syndrome. However, a contralateral knee's condition can affect TKA outcomes. Therefore, for the 2-stage TKAs in bilateral knee OA, the contralateral TKA should be performed 24 months after the first TKA before the improved body posture by the one-sided TKA deteriorate again.

Fig.: SVA Variations

In the unilateral group, the SVA significantly improved 6 months after TKA but deteriorated again 24 months after TKA. However, in the bilateral group, the SVA was significantly improved at 6 months and remained stable until 24 months after TKA.

Timing From Admission to Debridement, Antibiotic and Implant Retention (DAIR) Affects Treatment Success in Total Knee Arthroplasty Prosthetic Joint Infection

*Simon Garceau - The Ottawa Hospital - Ottawa, Canada

Samuel Morgan - University of Ottawa - Ottawa, Canada

Paul E. Beaulé - The Ottawa Hospital - Ottawa, Canada

Hesham Abdelbary - Canada

George Grammatopoulos - The Ottawa Hospital - Ottawa, Canada

Sophie Henke Tarnow - The Ottawa Hospital Research Institute - Ottawa, Canada

Introduction:

Prosthetic joint infection (PJI) represents a devastating complication associated with increased patient morbidity, mortality and a decreased quality of life. DAIR is an attractive treatment option in patients presenting with acute PJI due to its relative simplicity, reduced morbidity and cost. Little is known on the influence that timing from admission to DAIR has on treatment success. We developed a study to assess the association of factors associated with failure of DAIR in total knee arthroplasty (TKA).

Methods:

This is a retrospective, consecutive series from a single academic, tertiary referral centre specializing in the treatment of PJI. A search of our institutional PJI registry was conducted between 2008 and 2021 for patients having undergone DAIR following TKA at a minimum 2-year follow-up. Baseline patient and surgical characteristics were collected. The primary outcome assessed was reoperation for recalcitrant PJI. Secondary outcomes assessed were: 90-day readmission, 90-day and 1-year mortality, post-operative complications, and use of chronic suppressive antibiotic therapy. Multivariate regression analysis was performed to determine the effect of variables on outcomes.

Results:

A total of 121 patients satisfied final inclusion criteria for this study. Multivariate regression analysis of our primary outcome demonstrated that time from admission to DAIR > 48 hours was associated with a substantial increase in risk for reoperation for PJI (OR: 8.7, CI95% 1.5-51.1, $p = 0.017$). Post-operative complications were positively associated with DAIR >48 hours from admission (OR: 47.7, CI95% 2.7 – 827.1, $p = 0.008$). 90-day readmission was associated with lower preoperative Hb (OR: 1.04, CI95% 1.01 – 1.07, $p = 0.014$). Similarly, 1-year all-cause mortality was associated with lower preoperative Hb (OR: 1.06, CI95% 0.99 – 1.14, $p = 0.082$).

Conclusion:

The results of this study suggest that the timing of hospital admission to DAIR has both a significant impact on reoperation for recalcitrant PJI and post-operative complications. Akin to the treatment of hip fractures, care should be provided within 48 hours of admission to reduce treatment failure. Surgeons should advocate for rapid OR access when performing DAIR in the treatment of TKA PJI. Further research is required to delineate more specific time cut-offs in DAIR for TKA PJI.

The Impact of Previous Lumbar Spine Surgery on Primary Total Hip Arthroplasty: Minimum 2- Outcomes Controlling for Approach and Technology

***Benjamin Domb - American Hip Institute - Des Plaines, USA**

Roger Quesada-Jimenez - American Hip Institute Research Foundation - Chicago, USA

Andrew Schab - American Hip Institute Research Foundation - Chicago, USA

Ady Kahana - American Hip Institute Research Foundation - Chicago, United States of America

Elizabeth Walsh - American Hip Insitute Research Foundation - Chicago, USA

Background: Prior lumbar spine surgery (LSS) can limit spine mobility, potentially increasing hip motion requirements. This study aimed to assess the influence of LSS on primary THA.

Methods: Retrospective analysis was conducted on patients who underwent THA with prior LSS. Included patients completed PROs and VAS questionnaires or documented revision surgery with a minimum 2-year follow-up. Patients were propensity matched to a benchmark control group of patients without previous spine pathology, in a 1:3 ratio controlling for age at surgery, surgical approach, use of advanced technology, sex, and BMI. The analysis included comparisons of hip arthroplasty thresholds and complications. Sub-analysis based on the type of lumbar surgery, and type of approach were also conducted.

Results: 244 hips were included in the study. The LSS group reported comparatively lower postoperative scores on mHHS, FJS, SF-12 M, SF-12 P, VR-12 M, VR-12 P, VAS, and patient satisfaction. However, the LSS group experienced similar magnitude of improvement. The LSS group met PASS for FJS at a significant lower rate. The LSS had a higher frequency of complications leading to revision THA with a relative risk of 24 and a relative risk of 20.77 for revision THA due to instability. Comparing patients by type of LSS, PROs, the percentage of patients reaching hip arthroplasty thresholds, and the revision THA rates were similar. There was no significant difference in complications considering type of approach.

Conclusion: Patients with prior LSS who underwent primary THA demonstrated equivalent improvements in PROs but achieved lower overall postoperative scores and met hip arthroplasty thresholds at lower rates. Furthermore, patients undergoing primary THA with prior LSS had higher risk of complications leading to revision surgery, including a 24-fold relative risk for complications leading to revision and a 20.77-fold relative risk of revision due to instability.

Effect of Duration of Wound Drainage on Treatment Success After Prosthetic Joint Infection Surgery: How Long Is Too Long?

*Simon Garceau - The Ottawa Hospital - Ottawa, Canada

Alberto Telias - The Ottawa Hospital - Ottawa, Canada

Sanjula Costa - The Ottawa Hospital Research Institute - Ottawa, Canada

George Grammatopoulos - The Ottawa Hospital - Ottawa, Canada

Hesham Abdelbary - The Ottawa Hospital - Ottawa, Canada

Introduction: Periprosthetic joint infection (PJI) following primary total hip arthroplasty (THA) is a catastrophic complication with a reported incidence ranging from 0.3 to 2.9% (1). Such complications are associated with an increase in patient morbidity, mortality (2) and reduced quality of life (3). Persistent leaking wounds are a concern following THA. Expert recommendations and cohort studies recommend performing a surgical intervention if a primary hip or knee continues draining after 5-7 days (4). For persistent wound leakage following PJI surgery, there are currently no clinical studies or guidelines addressing when persistent leakage mandates repeat surgery, which is associated with increased morbidity and mortality. The aims of this study were to evaluate for temporal association of persistent drainage and treatment failure, and for factors associated with persistent drainage after PJI revision surgery in THA.

Methods: A retrospective cohort study of PJI patients was conducted at our tertiary PJI referral center from March 2019 to December 2022, with a minimum follow-up of 1 year. Patients with PJI of the hip who received DAIR, 1st stage treatment, single-stage or resection arthroplasty were included. Regression analysis was performed to assess for association of treatment failure with the following covariates: BMI, malnutrition, anemia, ASA score, number of previous surgeries, and type of PJI surgery performed. Additionally, analysis was performed for association of prolonged wound drainage with patient and surgery related factors. Definition of a dry wound was when dressing changes were no longer required, as evaluated by the latest nursing notes, or uploaded wound images in the patients' charts. Persistent leaking was defined as >14 days. Failure of treatment was defined as the need for repeat surgery for persisting PJI, the presence of a chronic fistula, or death related to the infection.

Results: 174 cases in 103 patients were identified within our institutional PJI database for inclusion in this study: 103 females (59%) and 71 males (41%), with a mean age of 68.7 ± 13.8 years. PJI treatment had a 46.7% failure rate after the first surgical procedure at our tertiary PJI specialty referral center. 55 (53.3%) patients required only one, 33 (32%) two, 6 (5.8%) three, 5 (4.8%) four and 2 (1.9%) five PJI surgeries. The mortality rate was 9.7% at 1 year, and five (4.8%) patients persisted with a chronic PJI without further intervention. Logistic regression demonstrated that persistent wound leakage was significantly associated with treatment failure (coefficient = -1.42, SE=0.44, z=-3.208 p=0.00134). Wound drainage was significantly associated with the use of VAC dressings (p = 0.048).

Conclusion: Prolonged wound drainage after PJI surgery for THA is common compared to primary THA. Wound drainage >14 days is associated with an elevated risk of failure after any PJI surgery. Surgeons should consider optimization of reversible factors perioperatively to prevent prolonged drainage and consider early repeat surgery on patients with persistent wound leakage prior to 2 weeks after PJI

revision surgery due to elevated risk of treatment failure. Earlier intervention may optimize healthcare resource utilization.

Long-Term Radiographic and Clinical Outcomes of the Mayo Conservative Hip for Developmental Dysplasia of the Hip in Young Patients: Mean Follow-Up of More Than 10 Years

*Masanori Nishi - Showa University School of Medicine - Tokyo, Japan

Takashi Atsumi - Showa Univ. Fujigaoka Hosp. - Yokohama, JAPAN

Yasushi Yoshikawa - Showa University School of Medicine - Tokyo, Japan

Ryosuke Nakanishi - Showa Univ. Fujigaoka Hosp. - Yokohama, JAPAN

Minoru Watanabe - Showa University Fujigaoka Hospital - Yokohama, Japan

Yuki Usui - Showa University School of Medicine - Tokyo, Japan

Yoshifumi Kudo - Showa University School of Medicine - Tokyo, Japan

Introduction: Total hip arthroplasty (THA) for secondary osteoarthritis due to developmental dysplasia of the hip (DDH) can be challenging. There have been few studies about short-stem THA in young patients with DDH, and no reports on long-term outcomes. The purpose of this study was to evaluate the radiographic and clinical long-term outcomes of Mayo conservative hip, which has one of the longest track records among short stem devices in young patients with DDH.

Methods: A retrospective analysis involved 50 joints from 42 patients (man:7,woman:35) who underwent total hip arthroplasty (THA) using the Mayo conservative hip in patients less than 55 years old with DDH, excluding cases with a follow-up of less than 5 years. Radiographic evaluation was conducted by comparing immediate postoperative antero-posterior images with those at final follow-up.

Clinical evaluations utilized the Japanese Orthopaedic Association (JOA) Hip score (100-point scale) and postoperative major complications, including revision surgery.

Results: The mean age of patients was 48.8 years (31–54) with the mean follow-up of 11.6 years (5 - 17). According to Crowe classification, 35 cases were graded as type I, 11 cases as type II, and 4 cases as type ?. According to Dorr classification, 29 cases were graded as type A and 21 cases as type B. Radiographically, spot welds were observed in 98% of joints in zones 2 or 6, while stress shielding was evident in 94% (zone 1) and 54% (zone 7). Stem sinking ?3mm was observed in two joints. There were no periprosthetic femoral fracture, dislocation, and infection. The final mean JOA score was 96.2. One case underwent cup revision due to loosening, however, none of the stem was revised. The 7-year implant survival rate was 100% and 10-year was 84.1% with all revisions as the endpoint using the Kaplan–Meier method.

Conclusion: The use of Mayo conservative hip in young patients with DDH exhibited favorable long-term outcomes, including long-term stability and bone preservation. The use of this stem is considered an effective treatment strategy in young patients with DDH with long term.

Endoscopic Iliopsoas Fractional Lengthening as a Treatment for Refractory Iliopsoas Impingement After Total Hip Arthroplasty: Functional Outcomes With Minimum 2-Year Follow-Up

*Benjamin Domb - American Hip Institute - Des Plaines, USA

Roger Quesada-Jimenez - American Hip Institute Research Foundation - Chicago, USA

Andrew Schab - American Hip Institute Research Foundation - Chicago, USA

Tyler McCarroll - American Hip Institute Research Foundation - Chicago, USA

Itay Perets - Hadassah Medical Center - Jerusalem, Israel

Ady Kahana - American Hip Institute Research Foundation - Chicago, United States of America

Background: Iliopsoas impingement is a common, but under-recognized, source of hip pain after total hip arthroplasty (THA). When conservative treatment fails, endoscopic iliopsoas fractional lengthening (IFL) can be performed. The aim of the study was to assess clinical outcomes after IFL in patients with previous THA.

Methods Data was prospectively collected from 2014 to 2020 for patients who underwent IFL following primary THA as part of the institutional hip outcomes registry. Patients were included if they had completed preoperative and minimum 2-year follow-up questionnaires for the modified Harris Hip Score (mHHS) and, visual analog scale (VAS). Available preoperative and post-operative data for: International Hip Outcomes Tool (IHOT-12), and patient satisfaction was also analyzed. Patients included in the study reported irritation of the iliopsoas tendon following cementless THA, refractory to conservative treatment methods. IFL was recommended after workup which included ruling out infection and aseptic loosening, and a positive iliopsoas diagnostic injection.

Results: There were 20 patients identified to have THA with subsequent IFL. Seventeen patients completed a minimum 2-year follow up. Mean age at IFL was 56,81 (34,42-81,29). The mean interval between THA and IFL was 4,56 (24,0-108,1) months. There was significant improvement in all PROs, with 14 (87.50%) patients meeting the minimal clinically important difference (MCID) for mHHS, and 15 (88,25%) for VAS. No patient reported weakness or impact on range of motion. Preoperatively, flexion was 106,33° (85,0°-120,0°), and post-operatively was 106° (90,0°-120,00).

Conclusions: Iliopsoas tendinitis is an entity that should be considered as a differential diagnosis of anterior hip pain after THA. We report significant improvements in all PROs in the short-term follow-up, with no reported complications. This procedure did not have a significant negative impact on hip range of motion.

Obtaining an Accurate Intraoperative Leg Length and Offset Measurement During THA Using 3-D Imaging and a Novel Computer Software Program

*Wenchao Tao - University of California, Los Angeles - Los Angeles, USA

Brad Penenberg - Cedars Sinai Medical Center - Los Angeles, USA

Michelle Riley - Arthritis & Joint Replacement Institute of Southern California - Beverly Hills, USA

Rebecca Burr - Cedars-Sinai Medical Center - Los Angeles, USA

INTRODUCTION: Achieving precise and consistent limb length and offset measurements during total hip arthroplasty (THA) is challenging due to patient positioning and parallax from intraoperative radiographs. This study aims to assess a method for achieving accurate intraoperative limb length and offset measurements utilizing 3-D imaging in conjunction with an innovative computer software program.

METHODS: Patients undergoing THA with pre-operative 3-D imaging using a novel computer software program were evaluated. A 3-D model of the pelvis with the operative femur was acquired from either an intraoperative computed tomography (CT) scan in the operating room immediately prior to patient positioning or a preoperative CT scan. Intraoperative limb length and offset measurements were obtained using a 3-D overlay technique applied on trial radiographs with computer assistance during surgery, including cases with significantly malrotated pelvis radiographs. These measurements were then compared with limb length and offset measurements from two-week postoperative radiographs.

RESULTS: The cohort comprised 150 patients. This abstract reports preliminary data from a subset of 50 patients. The complete dataset will be available and presented by the time of the conference. There was no statistical significance difference between intraoperative 3-D overlay measurements and postoperative radiographs for leg length and offset changes ($p = 0.29$ and 0.07 , respectively). 98% of cases had postoperative leg length measurements within 2mm of intraoperative measurements based on 3-D overlay, and 96% had postoperative offset within 2mm of intraoperative measurements. Among patients with malrotated trial radiographs, there was no statistically significant difference between intraoperative 3-D overlay measurements and postoperative radiographs.

CONCLUSION: Utilizing intraoperative 3-D imaging combined with this novel software program may enable surgeons to achieve accurate intraoperative limb length and offset measurements while reducing the need for repeated X-rays.

The Distance Between Scapular Neck and Polyethylene Insert During Active External Rotation in Shoulders With Semi-Inlay Reverse Shoulder Arthroplasty

***Itaru Kawashima - University of Florida - GAINESVILLE, United States of America**

Norimasa Takahashi - Funabashi Orthopaedic Hospital - Funabashi, Japan

Keisuke Matsuki - Sports Medicine & Joint Center, Funabashi Orthopaedic Hospital - Funabashi, Japan

Kenji Kitamura - University of Florida - GAINESVILLE, USA

Hisato Watanabe - Funabashi Orthopaedic Hospital - Funabashi, Japan

Ryo Haraguchi - Funabashi Orthopaedic Hospital - Funabashi, Japan

Hayato Ryoki - Funabashi Orthopaedic Hospital - Funabashi, Japan

Thomas Wright - UFL - USA

Scott Banks - University of Florida - Gainesville, USA

Introduction

In shoulders with inlay reverse total shoulder arthroplasty (RSA), the mean distance between the neck and insert was approximately 1 mm throughout the activity during active external rotation, with eleven out of 18 (61%) shoulders showing <1 mm separation over the entire rotation. Additionally, it has been reported that inlay RSA clinically caused scapular notching in more than half of the cases.² However, it remains unclear what the distance between the neck and insert in shoulders after semi-inlay RSA is.

The purpose of this study was to measure the distance between the scapular neck and the humeral polyethylene insert in shoulders after semi-inlay RSA during active external rotation at the side.

Methods

Fourteen shoulders from 13 patients who underwent surgery with semi-inlay RSA at a single institution were included in the study. The shoulders underwent computed tomography (CT) and fluoroscopy. Fluoroscopic images were acquired during the activity, starting from internal rotation at the side and progressing to maximum external rotation, while keeping the shoulder adducted. Using model-image registration techniques, poses of 3-dimensional implant models were iteratively adjusted to match their silhouettes with the silhouettes in the fluoroscopic images, and 3-dimensional kinematics of implants were computed. Based on the calculated kinematics of the implants, the closest distance between the scapular neck and polyethylene insert was computed using the combined glenosphere and scapular neck model and the humeral implant model with the insert. The distance was computed at each 5° increment of humeral internal/external rotation, and the data from 15° internal rotation to 45° external rotation were used for analysis. Linear mixed-effects models were calculated to examine the change of the distance during the activity. P values < 0.05 were considered statistically significant.

Results

The distance significantly decreased when the arm was externally rotated ($P < 0.001$) (Fig. 1). Two out of 14 (14.3%) shoulders were observed to approach within 1mm of distance during activity (Fig. 2).

Conclusion

The distance between the scapular neck and polyethylene insert during active external rotation in semi-inlay RSA appeared to be greater than that previously reported in inlay RSA. Furthermore, the distance significantly decreased as the external rotation angle increased. Therefore, surgeons could take note of the limit of

external rotation to avoid scapular notching by assessing the maximum external rotation during surgery.

References

1. Matsuki K, et al. Clin Biomech (Bristol, Avon). 2021.
2. Lévigne C, et al. Clin Orthop Relat Res. 2011.

Figures

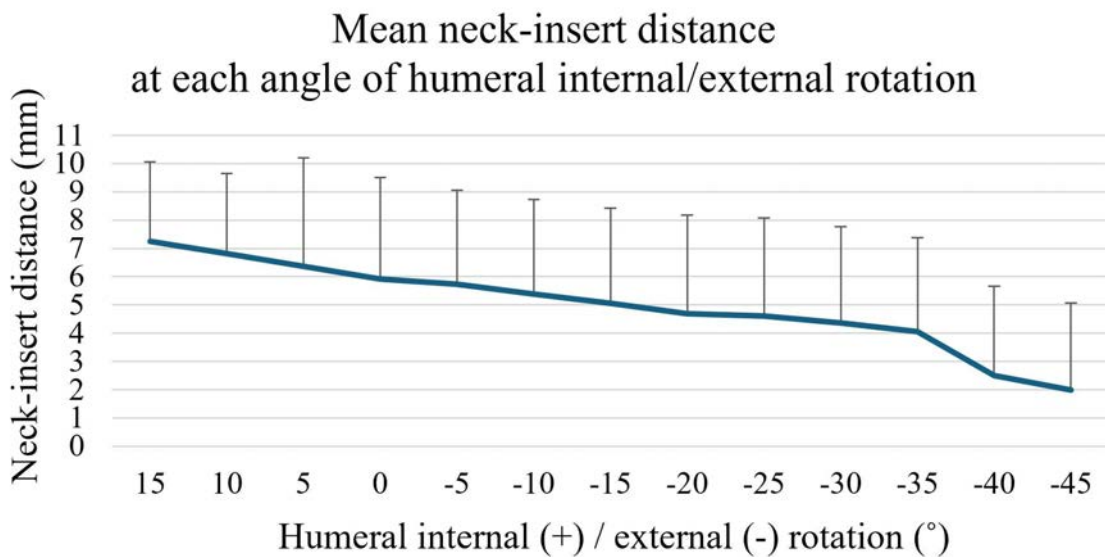


[Figure 1](#)

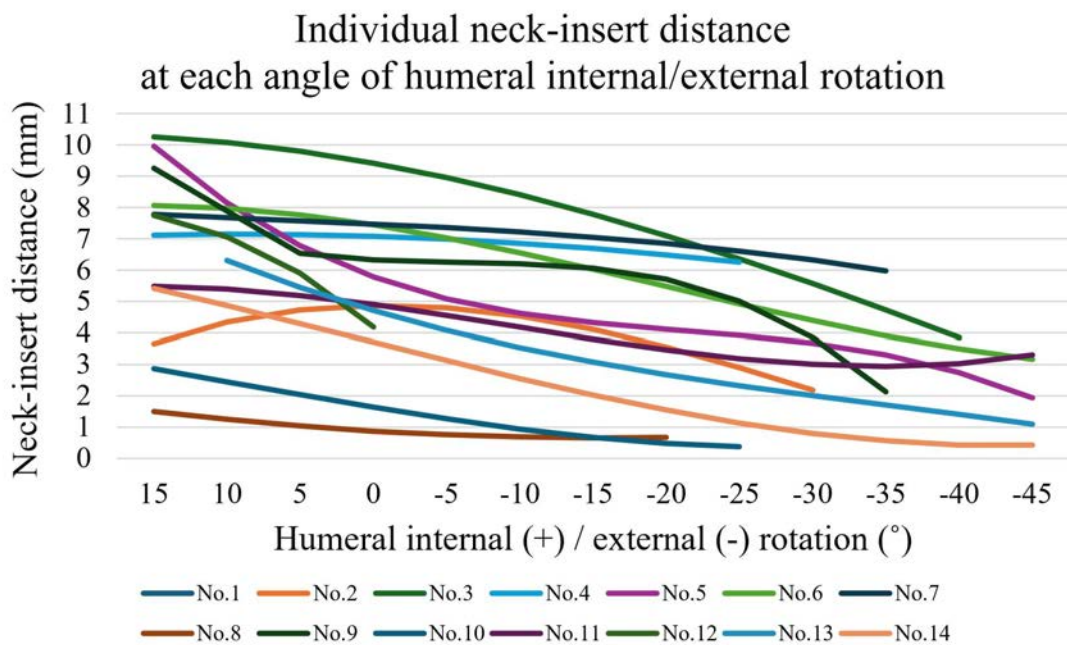


[Figure 2](#)

Better Outcomes? Rotator Cuff Repair Versus Reverse Shoulder Arthroplasty for Massive Rotator Cuff Tears in Elderly Population

*Garrett Jackson - Chicago, United States of America
Anna Redden - FAU - boca raton, USA
Aghdas Movassaghi - Michigan State University - East Lansing, USA
Vani Sabesan - Cleveland Clinic Florida - Weston, USA

Introduction: Despite advances in surgical technology with rotator cuff repairs (RCR), there is as high as a 90% re-tear rate for large and massive rotator cuff tears (RCT). An alternative and more recent treatment option for elderly patients with massive RCTs (MRCTs) is reverse shoulder arthroplasty (RSA). This study aimed to provide preliminary evidence to better understand the role of RSA in large rotator cuff tears without rotator cuff arthropathy by comparing patient-reported outcomes, opioid usage, and pain scores for patients treated with RCR versus RSA for MRCT without evidence of arthropathy.

Methods: All patients who underwent primary reverse shoulder arthroplasty or primary rotator cuff repair for MRCT from 2017 to 2019 by two fellowship-trained shoulder surgeons at a single institution were retrospectively identified through a prospectively collected database. Range of motion, opioid usage, and outcomes scores, including the American Shoulder and Elbow Surgeons (ASES) score, Penn (PSS) score, Constant score (CS), and Subjective Shoulder Value (SSV) were compared between RCR and RSA patients at baseline, 6 weeks, 3 months, and 12 months postoperatively.

Results: A total of 46 patients were analyzed. Twenty-two patients were treated with RCR (mean age, 61.9 years) and 24 underwent RSA (mean age, 67.1 years). No significant differences between preoperative ASES, PSS, CS, or SSV scores were appreciated between groups. At 6 weeks postoperatively, mean PSS ($p < 0.001$), ASES function ($p = 0.003$), and CS scores ($p = 0.005$) were significantly higher in the RSA group compared to the RCR group. No significant difference in patient-reported outcomes at 3 months or final follow-up was appreciated between groups. At final follow-up, internal rotation was significantly higher in the RCR group ($p = 0.049$).

Conclusion: Our results demonstrated that both RCR and RSA showed significant improvements in all pain and functional scores for patients with MRCTs. Those patients treated with RSA showed better initial recovery with significant difference seen only at 6 weeks postoperatively while the RCR group showed slightly better final ROM. RSA is comparable to RCR, suggesting that both options are good solutions for the treatment of MRCTs. However, surgeons should be aware of the tradeoffs associated with each option. Further studies are needed to examine long-term functional outcomes, re-tear rates and cost-effectiveness in these patients.

Auto-Planning in Anatomic Total Shoulder Arthroplasty Improved Placement and Precision in Preoperative Surgical Planning

Sarah Lammers - Stryker - Fort Wayne, United States of America

*Arthur De Gast - Stryker Orthopedics - Amsterdam, Netherlands

Emile Ducrocq - Stryker - Plouzane, France

Claudia Beimel - Stryker - Kiel, Germany

Gilles Walch - Jean Mermoz Private Hospital - Lyon, France

Mike Coronel - Stryker - Phoenix, USA

David Fitch - Stryker - Memphis, USA

Introduction: Accurate glenoid implant placement is vital in total shoulder arthroplasty (TSA) for desired outcomes, impingement-free range of motion and joint stability.^{1-2, 5-9} Preoperative planning tools, offering 3D measurements, assist surgeons in precise implant positioning.^{1-4, 9-11} Recent advancements include auto-planning software, which streamlines the process and potentially saves time. This study compares manual and automated preoperative planning in TSA, hypothesizing that auto-planning decreases the number of clicks and reduces travel distance in achieving the final virtual implant placement during surgeon planning.

Methods: In a limited user release (LUR) for Anatomic Total Shoulder Arthroplasty (aTSA) Auto-planning (Blueprint® v4.0.2, Tornier SAS, a subsidiary of Stryker Corp, Montbonnot, France) 28 surgeons participated, contributing 441 cases between October 2022 and May 2023. Analyses focused on the impact of the pre-operative planning algorithm on virtual implant distance traveled, number of clicks, and software accuracy in predicting the surgeon's final implant selection. All aTSA-planning algorithm cases (n=441) were included for the number of clicks analysis, while validated cases (n=421) were used for distance traveled and implant selection analyses. The statistical methods included paired analysis for distance traveled and independent group comparison for the number of clicks.

Results: In the study encompassing 441 Anatomic Total Shoulder Arthroplasty (aTSA) cases, primary indications were recorded for 440 cases (99.77%), with Primary Glenohumeral Osteoarthritis being the leading cause in 88.21% of cases. Glenoid types were identified for 165 (42.42%) cases with Primary Glenohumeral Osteoarthritis using the Walch classification. There were 68 B2 (41.21%) and 56 A1 (33.94%) glenoids. The use of auto-planning statistically significantly decreased the distance traveled to final placement in 78.62% (331/421) cases and reduced the median distance traveled by 0.39 mm compared to the use without auto-planning (Wilcoxon W Test $p < 0.001$). The rounded upper 99% percentile for the number of clicks with auto-planning was significantly lower with 162, compared to 376 clicks when used without auto-planning (Mann-Whitney U Test $p < 0.001$). The auto-planning feature precisely selected the implant size matching the surgeon's choice in 321 out of 421 cases (76.25%), with almost all instances demonstrating a maximum one-size difference (419 out of 421, 99.52%). This marked a statistically significant improvement compared to the previous version of the software.

Conclusions: The results of this study demonstrate that the use of the Blueprint auto-planning software can improve implant selection, in this study accurately identifying exact implant size in 76.25% of cases, compared to the 62.00% of the previous aTSA software version without auto-planning. Moreover, it notably reduced both the virtual implant's median distance traveled, and the number of clicks made in the graphical user interface by the surgeon. The study highlights the Blueprint auto-

planning software's improved placement and precision by aligning with surgeons' preferences during surgical planning. Nevertheless, further research and refinement of the algorithm, as well as clinical studies, are essential to harness its full potential and as a tool for improved virtual planning and real-world implant positioning for enhanced patient outcomes.

Robotic-Assisted Surgery Does Not Decrease Prosthetic Impingement in Total Hip Arthroplasty

*Sara Sacher - Hospital for Special Surgery - New York, United States of America

Jeffrey O'Donnell - HSS - NYC, United States of America

Elexis Baral - Hospital for Special Surgery - New York, USA

Eytan Debbi - Hospital for Special Surgery - NY, USA

Douglas E Padgett - Hospital for Special Surgery - New York, USA

Timothy Wright - Hospital for Special Surgery - New York, USA

Introduction: Implant-related impingement is a main contributor to THA instability^{1,2}. THA impingement is multifactorial, influenced by acetabular liner position, femoral stem positioning, head-neck ratio, and head size^{3,4}. Robotic-assisted surgery, increasingly utilized in THA, aims to improve implant positioning and restore native hip mechanics with the goal of reducing hip instability. The purpose of the present study was to determine if robotic surgery for THA reduces impingement rates. To answer this question, we determined the prevalence and severity of acetabular liner impingement in robotic-assisted THA liners compared to non-robotic assisted controls.

Methods: From our IRB-approved institutional implant retrieval system, 18 acetabular liners from robotic-assisted surgical procedures (Stryker MAKO) and 11 acetabular liners from non-robotic surgical procedures matched for head size, length of implantation (LOI), and revision indication were collected from revision surgeries performed between 2018-2023. The presence and severity of impingement was scored by two independent graders based on a previously published scoring system,⁵ where impingement was defined as wear or surface deformation on the rim of the liner based on visual examination (Fig. 1). Chi-squared tests, Fishers exact tests, and likelihood ratios were used to assess differences between the MAKO and control groups in impingement presence and severity with categorical variables. T-tests were used to compare means of numeric variables.

Results: 61% of the 18 MAKO THA liners showed impingement (7 none, 9 mild, 2 severe), and 45% of the non-robotic-assisted liners showed impingement (6 none, 4 mild, 1 severe). Within the MAKO group, 3/3 (100%) 32mm heads had impingement (2 mild, 1 severe), 7/12 (58%) 36mm heads had impingement (6 mild, 1 severe), and 1/3 (33%) 40mm heads had impingement. Within the control group, 1/4 (25%) 32mm heads had impingement (1 mild) and 4/7 (57%) 36 mm heads had impingement (3 mild, 1 severe) (Fig. 2). LOI did not differ between liners with impingement vs. those without (MAKO: impingement = 2.7 years, no impingement = 3.5 years; Controls: impingement = 3.3 years, no impingement = 2.5 years) (Fig. 3). Impingement presence and severity were not related to revision indication or radiographic measurements. No comparisons were statistically significant.

Conclusion: Acetabular liner impingement presence and severity did not differ between robotic-assisted MAKO liners and those placed without robotic assistance, suggesting current robotic technology may not improve impingement rates. Nevertheless, further investigation with larger cohorts, longer implantation lengths, and newer implants is required for a comprehensive understanding of the impact of robotic-assisted surgery on impingement rates.

References: 1. Malik et al J Bone Joint Surg Am 2007; 2. Gwam et al. J Arthroplasty 2017.; 3. Wadell et al HIP international 2019; 4. Scott et al JOA 2018; 5. Shon et al. J Arthroplasty 2005.

Figures

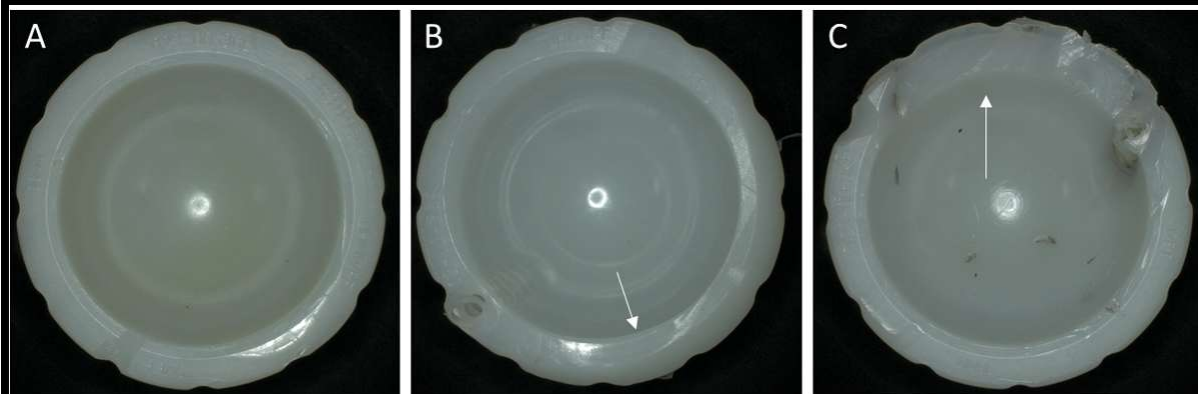


Figure 1. Representative liners exhibiting categorizations of the extent and severity of impingement A) none (no evidence of impingement); mild (minimal evidence extending ≤ 1 mm into the rim); and severe (damage extending >1 mm).

Figure 1

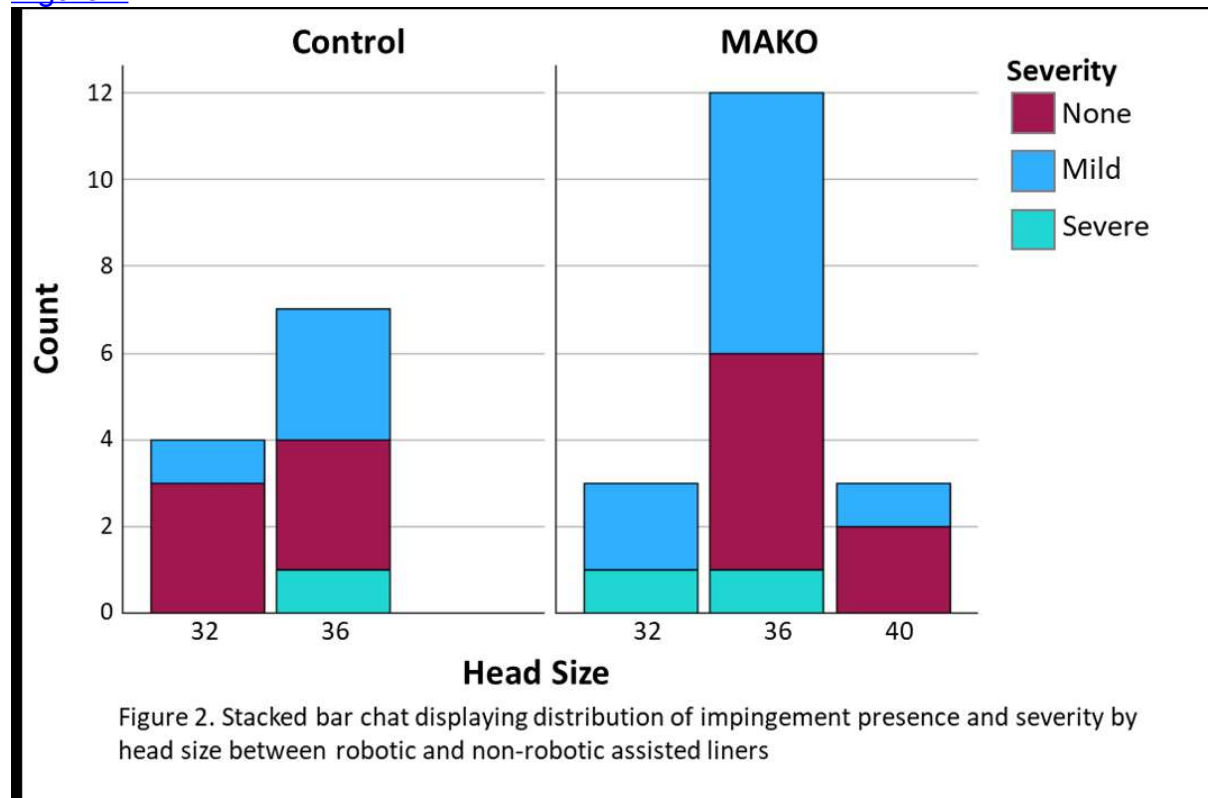


Figure 2. Stacked bar chart displaying distribution of impingement presence and severity by head size between robotic and non-robotic assisted liners

Figure 2

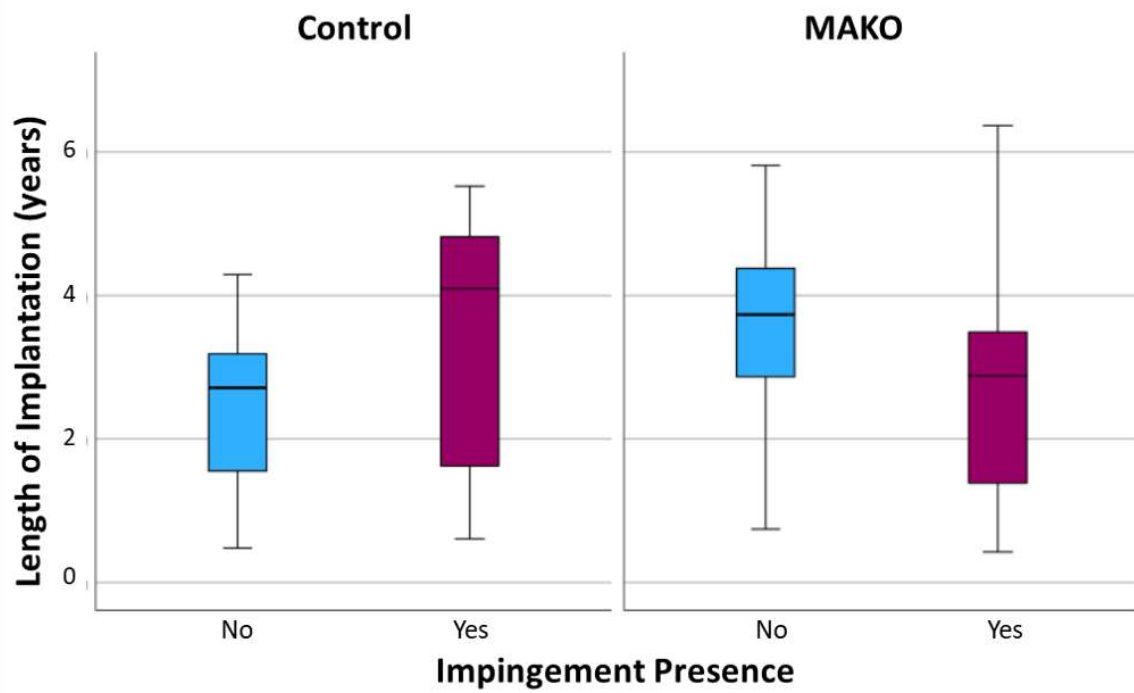


Figure 3. Box plot of length of implantation vs. impingement presence in robotic compared to non-robotic assisted liners

[Figure 3](#)

Long-Term Outcomes of Robotic Assisted Total Hip Arthroplasty With Nested Comparison to Conventional Total Hip Arthroplasty

*Benjamin Domb - American Hip Institute - Des Plaines, USA

Ady Kahana - American Hip Institute Research Foundation - Chicago, United States of America

Drashti Sikligar - American Hip Institute Research Foundation - Chicago, USA

Roger Quesada-Jimenez - American Hip Institute Research Foundation - Chicago, USA

Benjamin Kuhns - American Hip Institute Research Foundation - Chicago, USA

Mark Schinsky - American Hip Institute Research Foundation - Chicago, United States of America

Background: Robotic-assisted primary total hip arthroplasty (rTHA) has been shown to provide more precise and accurate acetabular component placement than manual total hip arthroplasty (mTHA). However, it is still unclear if there is an increased long term clinical benefit.

Purpose: The purpose of this study is to compare minimum 10-year radiographic and clinical outcomes between a propensity matched primary rTHA and mTHA group.

Methods: Prospectively collected patient data was retrospectively reviewed for robotic-assisted primary THA recipients from October 2008 to January 2014. Patients with complete minimum 10-year follow up were considered eligible. Clinical, radiographic, and Patient Reported Outcomes (PROs) were collected. Radiographic variables included acetabular component version, inclination, and leg length discrepancy. Clinical outcomes included complications and revision rates. Lewinnek and Callanan safe zones were used to evaluate acetabular component position. A propensity matched subgroup analysis with mTHA patients was also performed to identify differences in functional or radiographic outcomes between the two groups.

Results: 57 rTHAs were matched to 57 mTHAs. There were no significant differences in Harris Hip Score, Hip dysfunction and Osteoarthritis Outcome Score, Forgotten Joint Score-12, or Visual Analog Scale ($p > 0.05$). rTHAs were 74% less likely to have acetabular implant placement outside the Callanan safe zone (relative risk, 0.26; $p < 0.01$). The time to revision arthroscopy for mTHAs was significantly longer than time to revision arthroscopy for rTHAs at 33.34 months ($p < 0.05$), for aseptic loosening and instability.

Conclusion: Patients who underwent rTHA reported favorable outcomes at minimum 10-year follow-up. When comparing matched cohorts, rTHAs reported similar PRO scores and a reduced risk of acetabular cup placement beyond established component safety zones. Revision arthroscopy occurred further away from surgery for mTHAs, for aseptic loosening and instability.

Two-Dimensional Versus Three-Dimensional Pre-Operative Planning in THA: Results From a Randomized Controlled Trial

*Adam Yasen - University College Hospital London - London, United Kingdom
Andreas Fontalis - University College London Hospital - London, United Kingdom
Babar Kayani - University College Hospital London - London, United Kingdom
Tianyi David Luo - Wake Forest Baptist Medical Center - Winston-Salem, USA
Ricci Plastow - University College London Hospitals NHS Foundation Trust - London, United Kingdom
Fares Haddad - University College London Hospital - London, United Kingdom

Objectives

Pre-operative planning in THA, involves utilizing radiographs or advanced imaging modalities, including computerized tomography (CT) scans, for precise prediction of implant sizing and positioning. This study aimed to compare 3D versus 2D pre-operative planning in primary THA with respect to key surgical metrics including restoration of the horizontal and vertical COR, combined offset and leg length, as well as the accuracy in predicting the size of implants used.

Materials and Methods

This study included 60 patients undergoing primary THA for symptomatic hip osteoarthritis randomly allocated to either robotic-arm assisted or conventional THA. Digital 2D templating and 3D planning using the robotic software were performed for all patients. All measurements to evaluate the accuracy of templating methods were conducted on the pre-operative CT scanogram, using the contralateral hip as a reference. Sensitivity analyses explored differences between 2D and 3D planning in patients with predominantly supero-lateral or medial osteoarthritis patterns.

Results

Compared to 2D templating, 3D templating was associated with less medialization of the horizontal COR (-1.2 mm vs -0.2 mm, $P=0.002$) and more accurate restoration of vertical COR (1.63mm vs 0.6mm, $P<0.001$) with respect to the contralateral side. Furthermore, 3D templating was superior for planned restoration of leg length (+0.23 mm vs -0.74 mm, $P=0.019$). Sensitivity analyses demonstrated that in patients with medial osteoarthritis, 3D planning resulted in less medialization of horizontal COR and less offset reduction. Conversely, in patients with supero-lateral osteoarthritis, there was less lateralization of horizontal COR and less offset increase using 3D planning. Additionally, 3D planning showed superior reproducibility for femoral stem and acetabular cup sizes and stem neck angle, while 2D planning often led to undersized implants.

Conclusions

Our findings indicated a higher accuracy in planned restoration of native joint mechanics using 3D planning, as well as in predicting the sizes of implants used. Additionally, this study highlights distinct variances between the two planning methods across different osteoarthritis pattern subtypes, offering valuable insights for clinicians employing 2D planning methods.

Robot-Assisted Acetabular Reconstruction in Revision Total Hip Arthroplasty: A Clinical Study With Minimal 2-Year Follow-Up

Hao Tang - Beijing Jishuitan Hospital - Beijing, China

Wang Deng - Beijing Jishuitan Hospital - Beijing, China

Xiangdong Wu - Beijing Jishuitan Hospital - Beijing, China

Hongyi Shao - Beijing Jishuitan Hospital - Beijing, China

Zhaolun Wang - Beijing Jishuitan Hospital - Beijing, China

Dejin Yang - Beijing Jishuitan Hospital - Beijing, China

Yong Huang - Beijing Jishuitan Hospital - Beijing, China

*Yixin Zhou - Beijing Jishuitan Hospital - Beijing, China

Introduction: Recent studies have discussed the advantages of robot-assisted technology for primary total hip arthroplasty (THA). However, no previous studies reported the use of modern robotic systems in revision THA. This study aimed to report the surgical techniques and early clinical results of robot-assisted acetabular reconstruction in revision THA.

Methods: Between October 2019 and May 2021, we used the Mako robotic system to perform 62 revision THAs at our hospital. This study included 54 single-surgeon patients who underwent robot-assisted revision THA for acetabular reconstruction. Surgical techniques using the robotic system to reconstruct the acetabulum, including preoperative planning, intraoperative registration, and the accuracy of different registration methods, have been reported. The accuracy between the target cup orientation and final orientation was evaluated. The latest follow-up Harris Hip Score (HHS) and radiographs were analyzed.

Results: Among the 54 cases included, four types of intraoperative registration methods with different surfaces were developed and registered 65 times. The overall success rate of the registration process was 98.5%. The mean accuracy of successful registration was 0.375 mm (ranges 0.2–0.5 mm). The median difference between the target and final cup orientations assessed by Mako was 1.0° for inclination and 0.0° for anteversion. Four cases were classified as outliers in the cup orientation. The reconstructed centers of rotation (CORs) were slightly lower than the anatomical CORs by 4.72 mm and shifted laterally by 3.92 mm on postoperative radiographs. The median HHS improved significantly from 46.00 preoperatively to 89.00 postoperatively ($p < 0.001$). The overall satisfaction rate was 86.00%. No radiographic failures occurred at the latest follow-up visit.

Conclusion: In revision THA, robotic system provides valuable information to analyze bone defect and form reconstructing strategies. Robotic-arm assisted reaming and cup/augment positioning greatly eases operation and improve cup position and orientation. The radiographic and preliminary clinical results of the robotic revision THA were satisfactory.

Figures

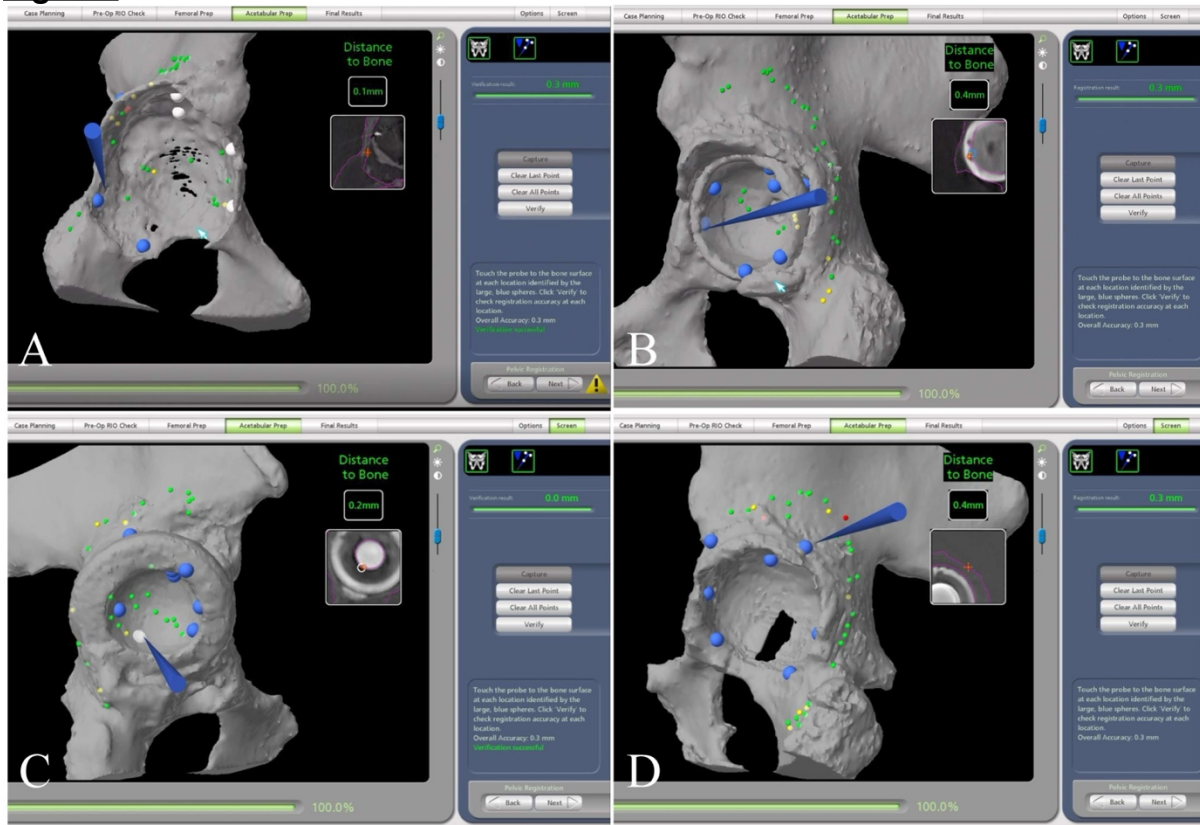


Figure 1

Inducible Displacement of the Femoral Stem Measured Using Computed Tomography-Based Radiostereometric Analysis (CT-RSA)

*Mathew G Teeter - Schulich School of Medicine and Dentistry, Western University and London Health Sciences Centre - London, Canada

Jennifer Polus - University of Western Ontario - London, Canada

Bart Kaptein - LUMC - Leiden, Select Country

Edward Vasarhelyi - Western University - London, Canada

Brent Lanting - London Health Sciences Centre - London, Canada

Introduction: Diagnosis of aseptic loosening following total hip arthroplasty (THA) remains a challenge. Radiostereometric analysis (RSA) is the gold standard for implant migration tracking, but its clinical adoption has been limited due to the need for embedded bone marker beads and specialized imaging equipment. New developments have made computed tomography-based RSA (CT-RSA) available, which leverages conventional CT scanners and does not require bone marker beads. A type of CT-RSA exam that measures the inducible displacement of the implant between back-to-back scans with different joint loading may be a viable diagnostic tool for suspected aseptic loosening. The objective of this study was to investigate the validity of CT-RSA for inducible displacement measurements of the femoral stem in comparison to RSA.

Methods: Patients (n=48) from a previous cementless THA RSA study returned at five-years post-operation to be re-examined for femoral stem implant stability using CT-RSA and RSA imaging. Migration between two- and five-years post-operation was calculated using RSA migration as a measure of implant stability. Double examinations were taken for both CT-RSA and RSA to calculate the precision of measurements. For CT-RSA, inducible displacement was measured between CT examinations with the leg externally versus internally rotated. For RSA, inducible displacement was measured between supine and weight-bearing examinations. Inducible displacement measurements in each axis of translation and rotation were compared between CT-RSA and RSA. Inducible displacement measurements were also compared with double examination results to determine if the measured displacement in each axis was greater than measurement error.

Results: All stems were well-fixed with subsidence <0.2 mm/year. Precision for CT-RSA ranged from 0.049mm-0.130mm in translation and 0.061° - 0.220° in rotation and for RSA ranged from 0.093mm-0.262mm in translation and 0.118° - 0.678° in rotation. Inducible displacement of the stem was lower for CT-RSA than RSA for distal translation (mean difference=0.122 mm, $p<0.0001$), total translation (mean difference=0.139 mm, $p<0.0001$), and total rotation (mean difference=0.449 $^{\circ}$, $p<0.0001$). For CT-RSA, inducible displacement and the double examination were only significantly different for total translation and total rotation. For RSA, inducible displacement and the double examination were different for medial, distal, and total translation, and total rotation.

Conclusion: CT-RSA demonstrated superior precision for inducible displacement measurements compared to RSA. Measurements of rotationally loaded inducible displacement from CT-RSA were minimal, consistent for a patient cohort with well-fixed implants. These findings are encouraging, and future work should explore the reliability of CT-RSA in patients with suspected aseptic loosening prior to undergoing revision surgery.

Accuracy of 3D/2D Registration for Determining Cup Position and Leg Length in Fluoroscopy Guided THA

*Christopher Plaskos - Corin - Raynham, USA

Jim Pierrepont - Corin - Cirencester, United Kingdom

Junfen Shi - University of Southampton - Southampton, United Kingdom

Gerard Smith - Corin - Sydney, Australia

Linden Bromwich - Corin Group - Sydney, Australia

Jevan Arulampalam - University of Sydney - Sydney, Australia

Arjun Saxena - Rothman Orthopaedic Institute - Philadelphia, USA

Eric M Slotkin - Reading Hospital, Orthopaedic Associates of Reading, - West Reading, Pennsylvania, USA

Moritz Ehlke - Corin - Saarbrücken, Germany

Introduction:

The aim of this study was to evaluate the accuracy of a new system for measuring cup position, leg length and offset on intraoperative fluoroscopy images using 3D/2D registration.

Methods:

Four users made a total of 128 measurements on 96 unique digital reconstructed radiographs (DRRs). DRRs were generated to simulate intraoperative 2D fluoroscopic images from preoperative CT scans of 8 THA patients with virtually positioned implants. Images were simulated for the following surgical stages: cup insertion, femoral trialing, final implants. For each stage, different views were simulated by rotating the image intensifier by $\pm 5^\circ$ about the mediolateral and superior-inferior axes. The 3D/2D registration was initialized by selecting predefined landmarks on the pelvis and femur, Figure 1. The algorithm then generated an initial registration using a contour matching algorithm. The user was then able to refine the registration by adjusting the position of the bone, cup and femoral head overlay models while visually evaluating the correspondence on the display, Figure 2. Accuracy was determined as the mean absolute error for the initial and final registration relative to the ground truth values.

Results:

Cup inclination, anteversion and medialization/superiorization accuracy was within 1 degree and mm across all users for both the initial and final registration, with maximum errors of 1.6 degrees and 1.9mm, Figure 3. Leg length and offset accuracy with trials were 1.5 and 2.4 mm initially, and 1.4 and 2.1 mm after adjustment. With implants, leg length and offset were within 2.9 and 2.5 initially and 2.4 and 2.1 after adjustment, with final maximum errors of 7.2 and 4.7 mm. Inter-user differences in accuracy were within 1 mm.

Conclusions:

3D/2D registration of 3D preoperative CT and implant models with 2D fluoroscopic images provides an accurate and robust means of measuring cup position, leg length and offset intraoperatively.

Figures

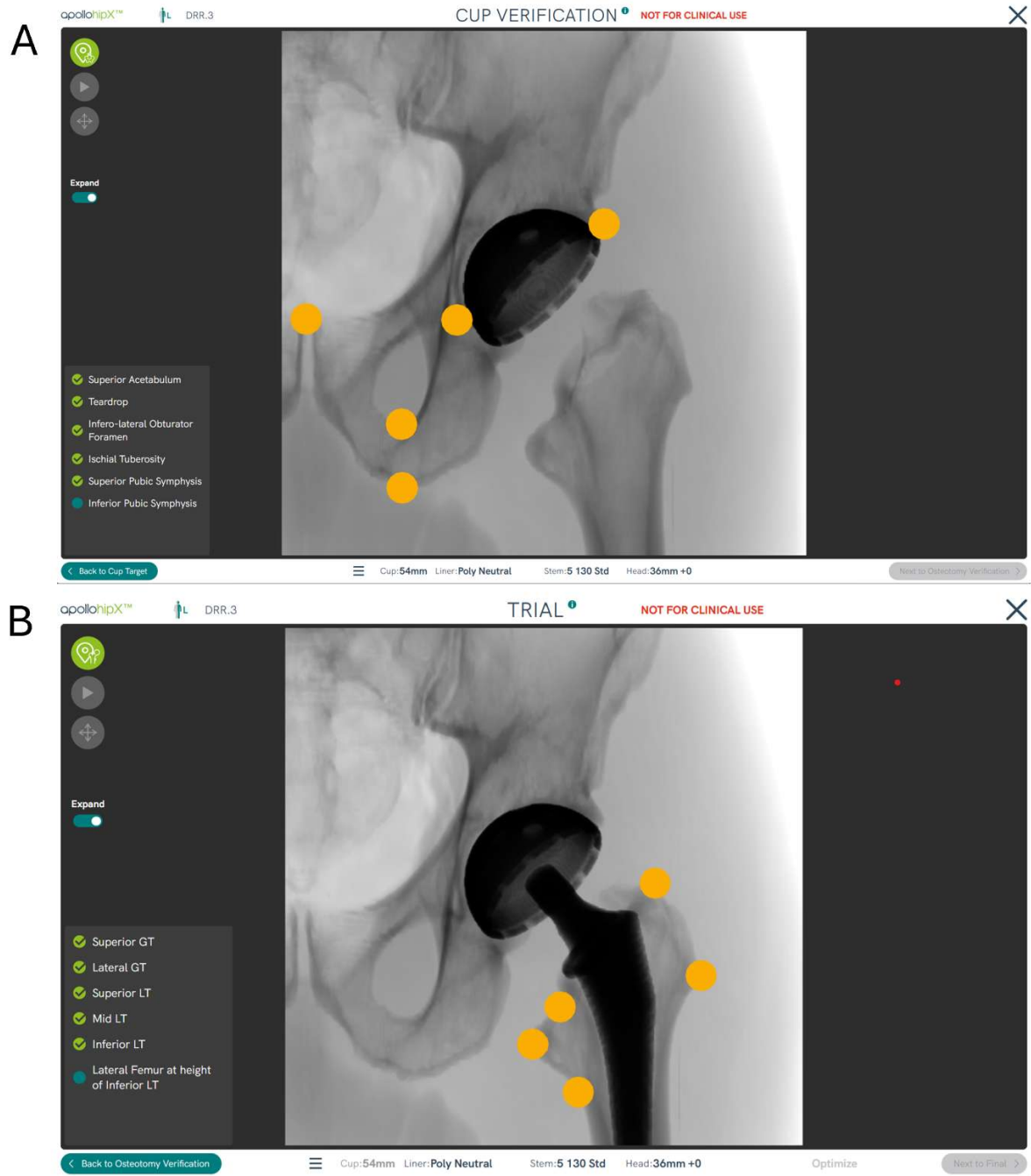


Figure 1

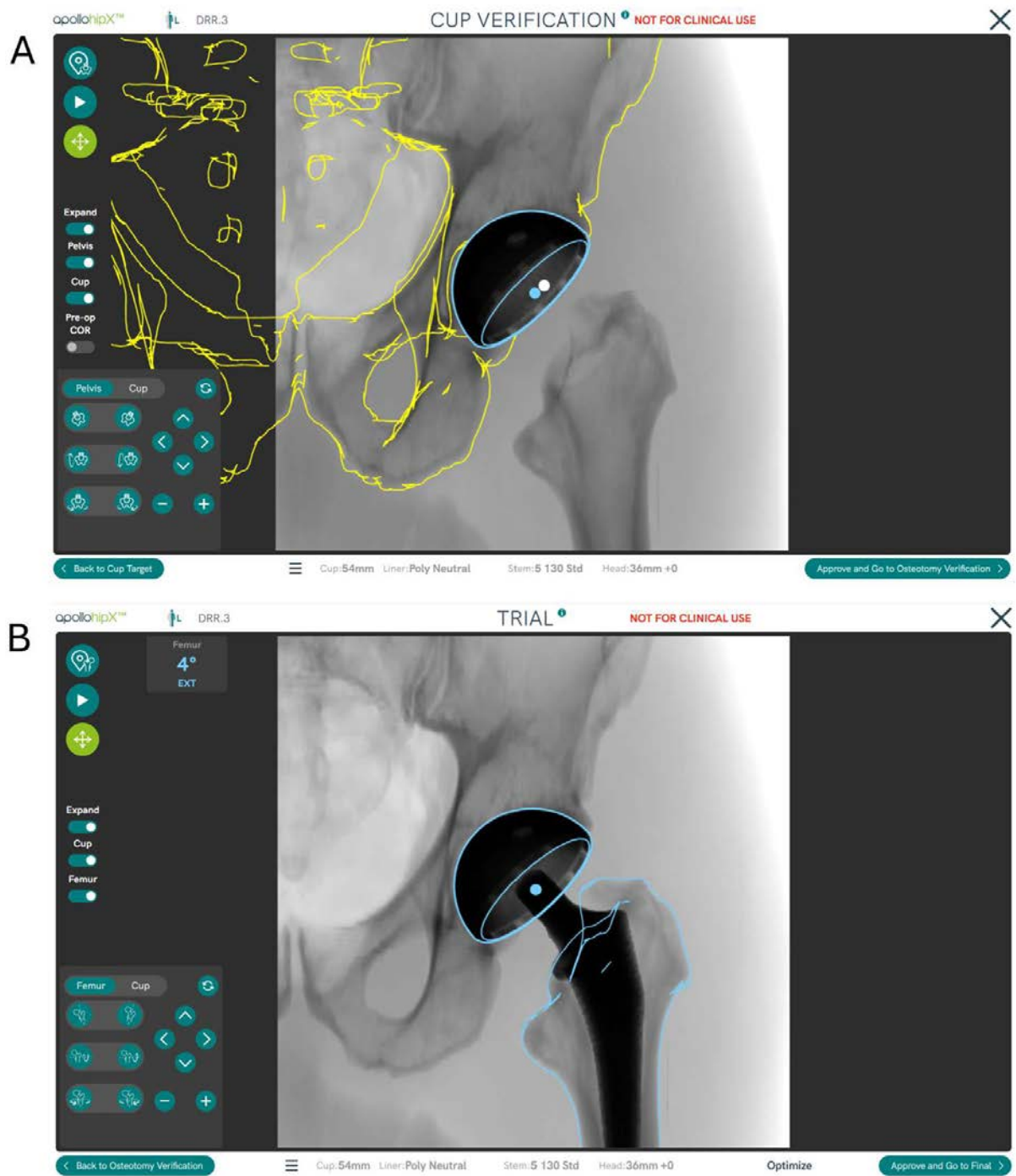
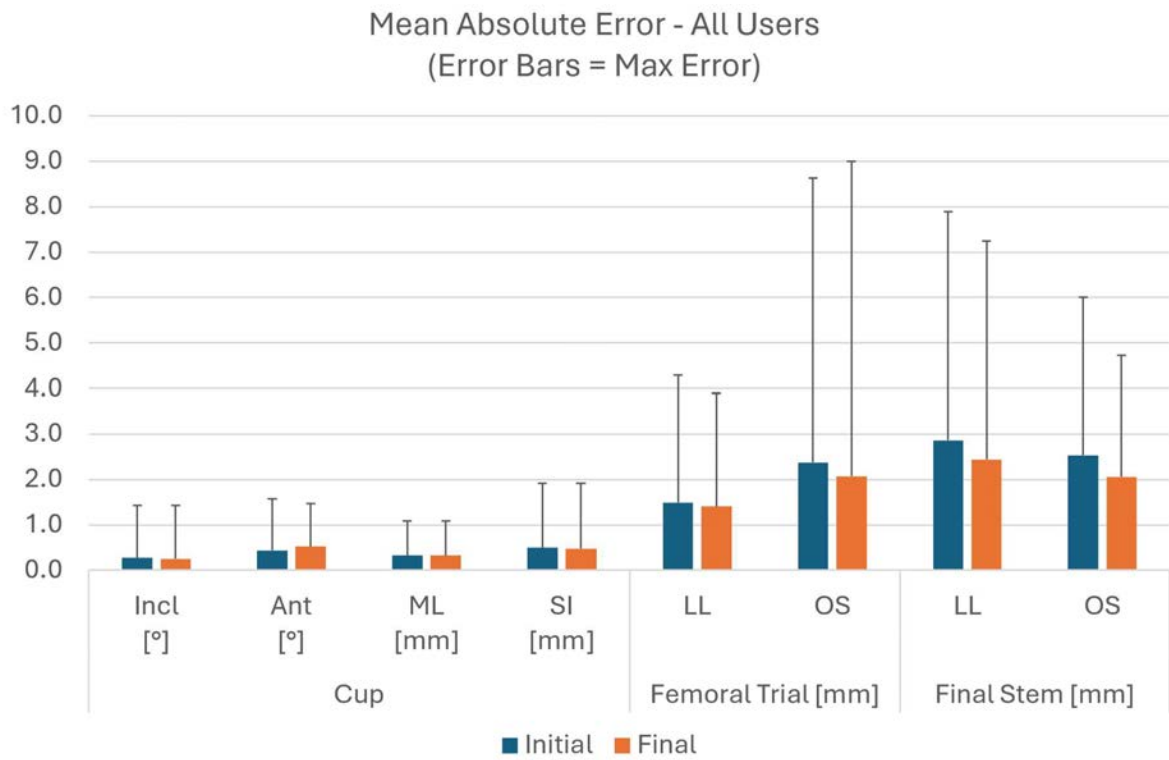


Figure 2



[Figure 3](#)

A Novel Radiographic Methodology to Measure Knee Adduction Moment

*Fernando Quevedo Gonzalez - Hospital for Special Surgery - New York, USA

Drake Lebrun - Hospital for Special Surgery - New York, USA

Theofilos Karasavvidis - Hospital for Special Surgery - New York, USA

Cale Pagan - Hospital for Special Surgery - New York, United States of America

Edward Grabov - Hospital for Special Surgery - New York, USA

Joseph Lipman - Hospital for Special Surgery - New York, USA

Peter K. Sculco - Hospital for Special Surgery - NYC, USA

Cynthia Kahlenberg - Hospital for Special Surgery - New York City, USA

Eytan Debbi - Cedars-Sinai Medical Center - Los Angeles, USA

Timothy Wright - Hospital for Special Surgery - New York, USA

David J. Mayman - Hospital for Special Surgery - New York, USA

Jonathan Vigdorchik - NYU Langone Hospital for Joint Diseases - New York, USA

Introduction

Most failures of total knee arthroplasties (TKA) have a mechanical origin.[1] Since knee replacements most often experience loads during walking, understanding the alignment and forces across the knee during gait is critical. The knee adduction moment (KAM) indicates the load distribution between the medial and lateral knee compartments. However, measuring KAM requires a highly specialized test in a gait laboratory, limiting its routine clinical use. We sought to develop a radiographic-based static KAM to routinely evaluate TKA patients and assess its relationship with implant alignment and a patient-reported outcome (KOOS JR).

Methods

Under IRB approval, we evaluated the whole-body kinematics and ground reaction forces (GRF) of seven patients (age 47–76 years, BMI 22.6–31.6 kg/m²) preoperatively and 6-weeks postoperatively in our institution's gait lab. We simultaneously measured whole-body kinematics by tracking skin surface reflective markers with 12 cameras at 100 Hz and ground reaction forces (GRF) with four floor-embedded force plates (AMTI; Bertec) at 2,000 Hz. At the same timepoints, the same patients underwent biplanar radiographs (EOS Imaging) while standing on a force plate (ACS Dual, AMTI) to measure each leg's GRF during bipedal and single leg stance (Fig. 1). The KAM was calculated in the tibia frontal plane [2] by multiplying the GRF and its distance perpendicular to the knee center (i.e., the midpoint between medial and lateral epicondyles). We compared the peak dynamic KAM and static KAMs and the static KAM to joint alignment and KOOS JR.

Results

The peak dynamic KAM obtained in the gait lab (in % of the patients' height times bodyweight) decreased from 2.4-6 to 1.6-4.4 between preoperative and 6-weeks postoperative (Fig. 2).

The static radiographic KAM obtained from the EOS exams matched the peak dynamic KAM, especially postoperatively during single leg stance (Fig. 3). Changes in bipedal static KAM were associated with changes in mechanical hip-knee-ankle angle. Higher KAM was associated with lower KOOS JR preoperatively but not postoperatively.

Discussion

It is important to analyze implant position and its effects on medial-lateral load distributions during gait. The radiographic static KAM is a promising surrogate of dynamic joint loading and can complement PROMs and joint alignment measurements. Future studies will include more patients, longer follow-up, and analyze additional biomechanical markers, like knee flexion moment.

References [1] AJRR Annual Report, 2023; [2] Shull et al., J Biomech, 2013

Figures

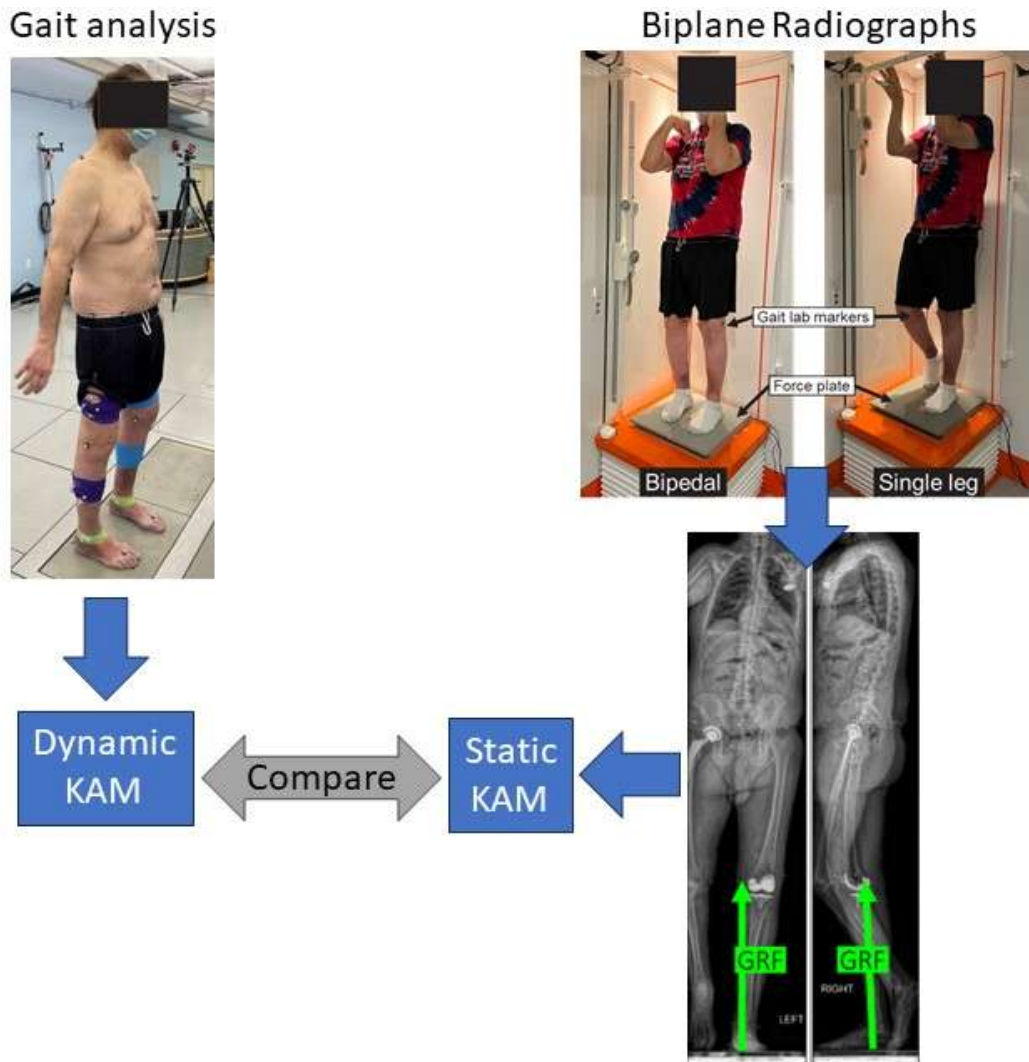


Fig. 1 – Gait and radiographic analysis to measure the dynamic and static KAM.

[Figure 1](#)

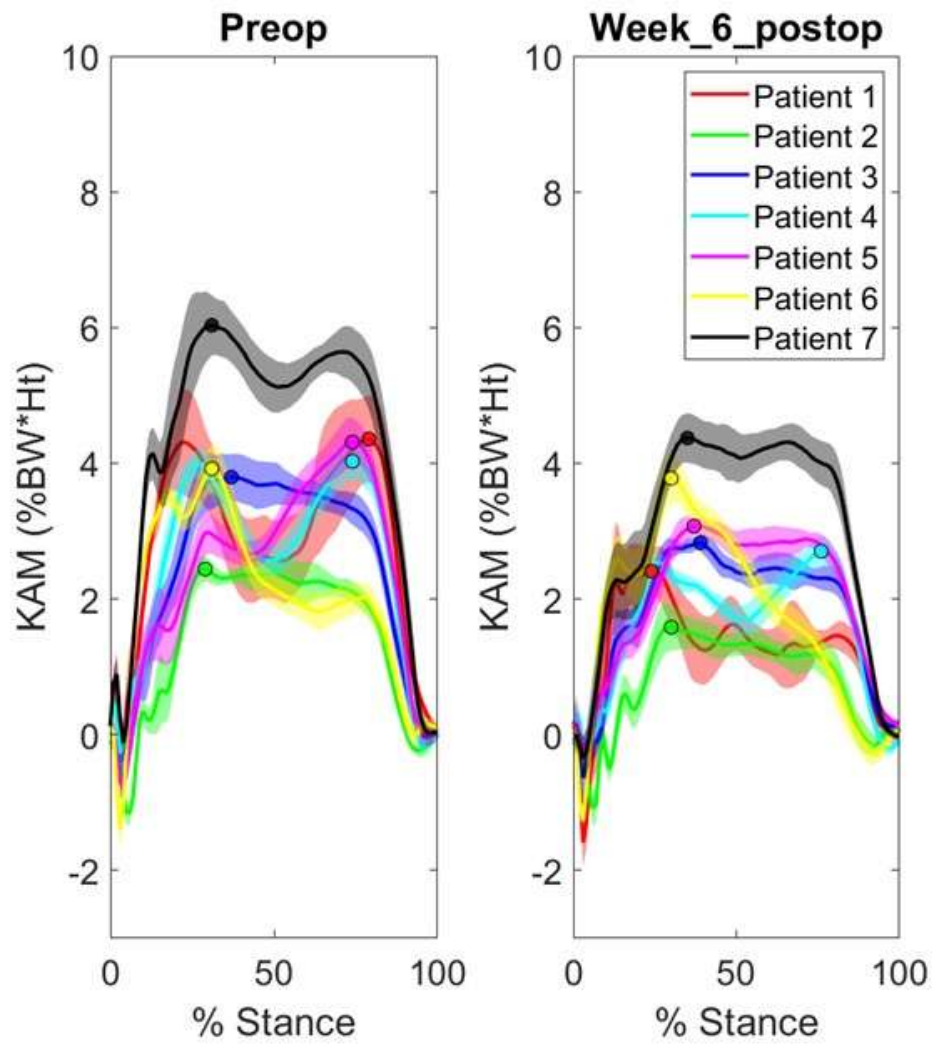


Fig. 2 – Preoperative and 6 weeks postoperative dynamic KAM

[Figure 2](#)

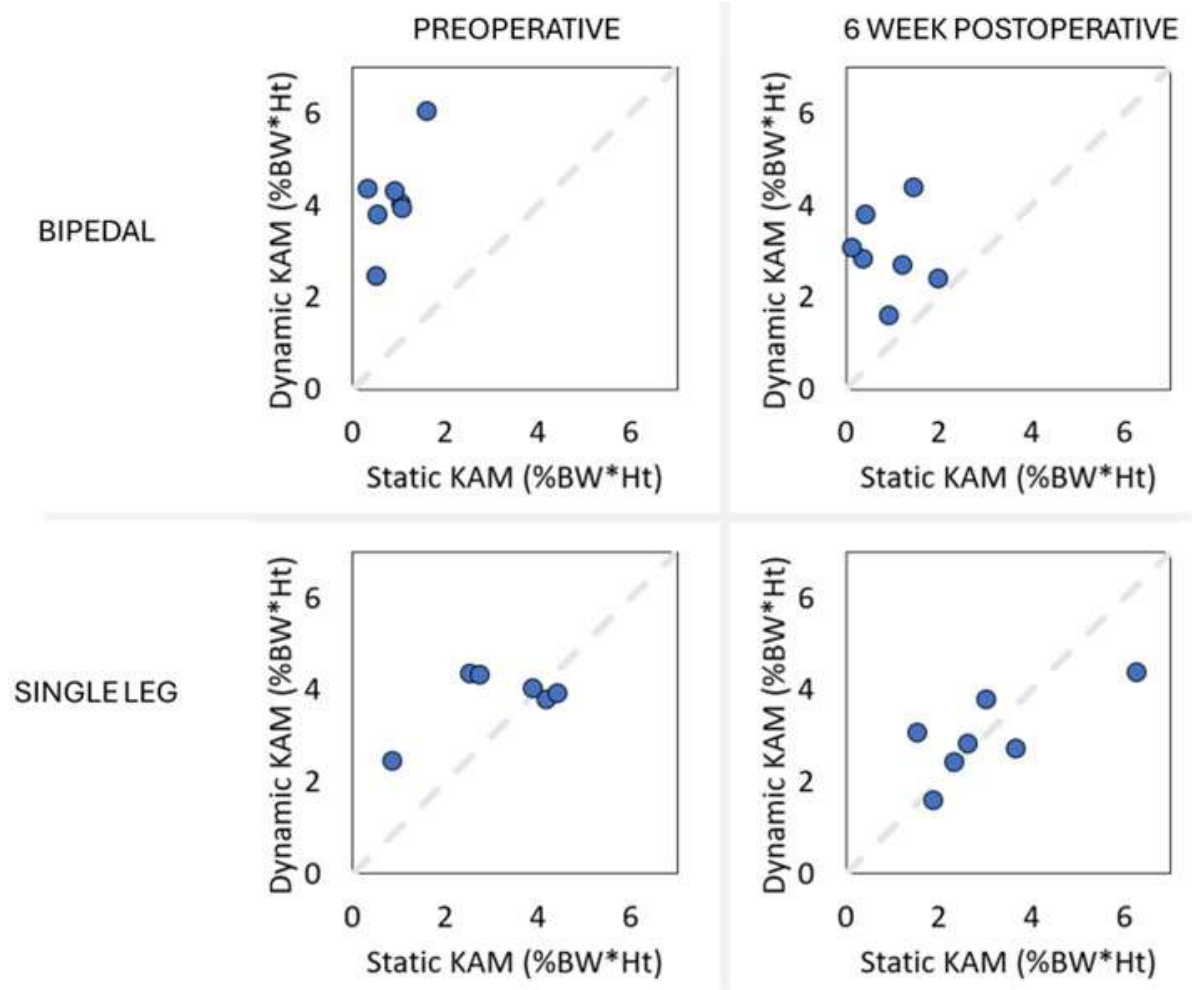


Fig. 3 – Static vs peak dynamic KAM

[Figure 3](#)

Introduction of Orthosonic™ Scanning for Creating Three-Dimensional Bones in Minutes for Component Sizing and Pre-Operative Planning

Russell McKissick - Tennessee Orthopaedic Alliance - Murfreesboro, USA

*Manh Ta - Stryker Corporation - Fort Lauderdale, USA

Steven MacDonald - London Health Sciences Centre - London, Canada

Richard Komistek - The University of Tennessee - Knoxville, USA

INTRODUCTION

Robotic surgery has become prevalent in Orthopaedics, with approximately 20% of total knee arthroplasty (TKA) performed in the United States now employing some form of enabling technology. All major implant manufacturers have acquired robots for either pre-operative or intra-operative planning and surgical execution. Either MRI or CT scans have been used for creating three-dimensional (3D) bones. MRI's are expensive and CT scans involve added radiation exposure to the patient, while both involve discomfort and even claustrophobia for the patient. Recently, 3D ultrasound technology (JointVue, LLC), defined as Orthosonic™, has been introduced where patient's knees can be scanned at the time of their pre-surgery appointment. The objective of this study was to evaluate the 3D Orthosonic™ scan to assess ease of use, surgeon and patient's feedback, accuracy of knee implant component sizing and procedural remuneration.

METHODS

Twenty-two subjects, implanted with a Journey II BCS TKA, underwent an Orthosonic™ scan during their pre-surgery visit to their orthopaedic surgeon. The Orthosonic™ scan is unique as it utilizes raw ultrasound radiofrequency signals (a-mode) and electromagnetic trackers to create a point cloud in a-mode (other ultrasound technology uses b-mode). Initial registration involves identifying three landmarks on the femur tibia. Designated areas, shown in red (Figure 1), are displayed and painted over to generate a point cloud representing the bone surface. Statistical shape modeling reconstructs 3D femoral and tibial bone models (Figure 2). These bones are then input to the pre-operative surgical planner to determine components sizes, alignment, and bone cuts for the procedure (Figure 3). The RMS error for bone creation is 0.92 mm for the femur and 1.07 mm for the tibia, compared to CT scans.

RESULTS

Twenty of the 22 subject scans were within one size for pre-operative component sizing. Challenges were encountered in two cases with landmark definition and scanning of the posterior condyles. Surgeon and patient feedback was excellent, with the surgeon found it easy to introduce ultrasound to his clinic and patients impressed by seeing their bones created in real-time. The surgeon provided an enhanced office visit by showing patients their bones and the surgical plan in 3D. Insurance reimbursement for each procedure was \$301.00. Surgeon feedback led to improvements in ease of use, particularly in landmarking and the scan time was shortened to five minutes, while maintaining the same accuracy.

DISCUSSION

Orthosonic™ has now been used in an orthopaedic clinic, proving to be accurate for creating 3D bones for component sizing and enhancement of surgeon-patient pre-

operative planning. Surgeon feedback has driven enhancements, notably in automated landmarking and scan time reduction (5-7 minutes) in Orthosonic™ 2.0.

Other Orthosonic™ ultrasound units have been placed in hospitals and surgeon clinics so that additional feedback can be obtained to enhance the accuracy and experience for both the surgeon and the patient.

Figures

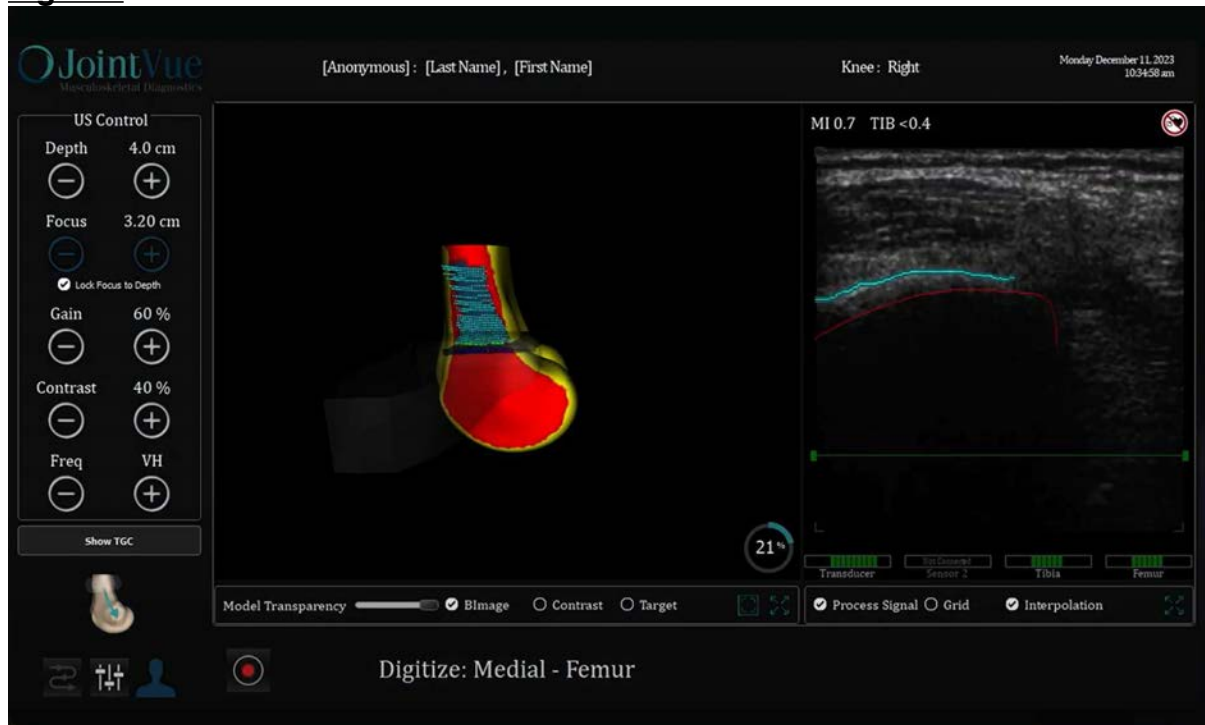


Figure 1



Figure 2

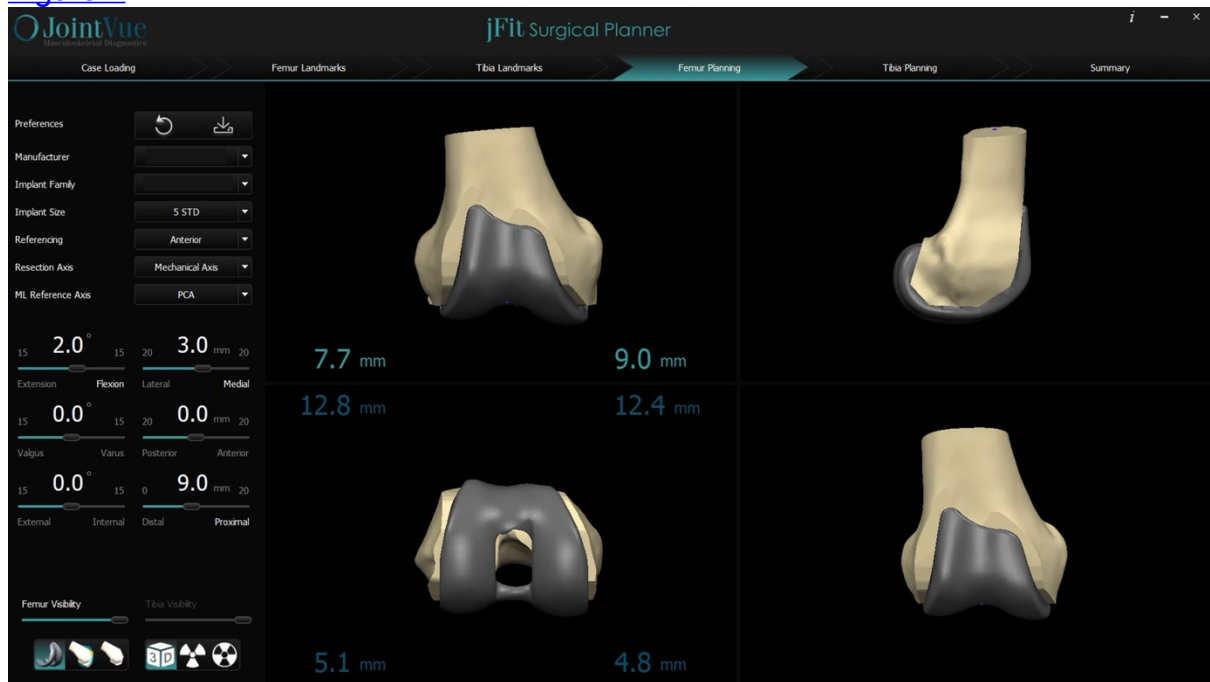


Figure 3

A Novel Method of Determining Bone Mineral Density From Pre-Surgical CT Scans to Aid in Surgical Planning

*Jared Weir

Sebastien Lustig - Hôpital de la Croix Rousse - Lyon, France

Alan Brett - Stryker - Newbury, United Kingdom

Niall Maguire - Stryker - Newbury, United Kingdom

Introduction

Patients with reduced Bone Mineral Density (BMD) may have worse outcomes after joint replacement surgery.

Concern surrounds the use of cementless implants, which rely on press-fit fixation in the surrounding bone. Where

BMD is reduced, fixation is greatly enhanced by the addition of cement. Cementless implants are often only

indicated for younger patients with higher BMD. Assessment of BMD is not commonly performed prior to surgery.

Quantitative CT (QCT) scans may be used to measure BMD by calibrating Hounsfield Units (HU) to BMD values,

but robotic surgery planning CT scans do not include BMD calibration phantoms.

Here we describe automated

BMD calibration based on air, fat and the aluminum motion-detection rod included in Mako robotic knee

arthroplasty CT images.

Methods

Image voxels containing air were identified using histogram analysis. The rod surface was identified using Active

Appearance Model (AAM) search and eroded by a 4mm radius to exclude partial voxels and beam hardening.

Median voxel intensity was used as the rod HU value. Normals to the AAM segmented femur bone surface were

sampled until a discontinuity was detected representing a soft-tissue boundary to air, bone or cartilage. A two-

gaussian mixture was used to model the histograms of fat and muscle tissue along this normal path. Mean of the

lower gaussian peak was reported as fat HU value. 133 CT knee arthroplasty planning images contained a

commercial BMD phantom (Mindways, TX) used to determine the average BMD equivalent values of air, fat and

rod as calibration standards. We used 10 iterations of 10-fold cross-validation to compare calibration from the

phantom or air-fat-rod standards in trabecular bone at femur and tibia.

Results

An example of rod and fat identification is shown in Figure 1. Trabecular bone BMD from phantom calibration were

highly correlated with BMD values calculated using the air-fat-rod standards for both femur and tibia ($r \approx 0.98$).

Bland-Altman analysis showed negligible bias of $\sim 0.3 \text{ mg/cm}^3$ (Figure 2). The SD of differences is 9.9 mg/cm^3 ,

suggesting an upper bound of precision of 9 mg/cm^3 (precision error for Mindways

phantom is $3.6\text{mg}/\text{cm}^3$), which produces a $\text{CoV}=7.2\%$ at mean $\text{BMD}=125\text{mg}/\text{cm}^3$.

Conclusion

Accurate volumetric BMD values may be derived at the knee from CT images acquired for robotic arthroplasty planning. This information may be useful in informing surgical decision about the use of cementless implants, particularly in postmenopausal women or patients that have received androgen blocking therapy as part of treatment for cancer, who may be at risk of osteoporosis.

Figures

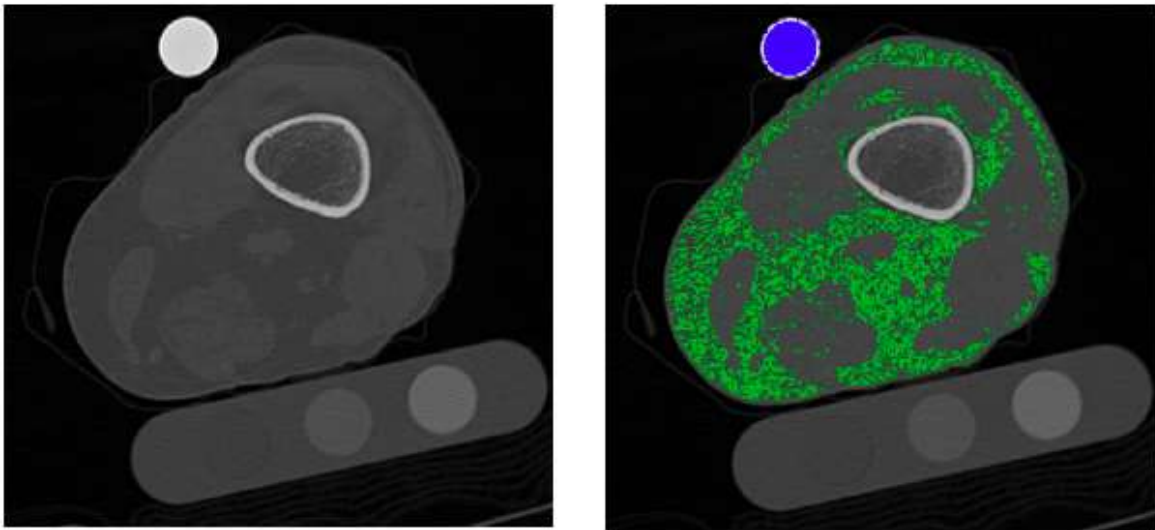


Figure 1: Left: axial slice through the femur with rod above and BMD phantom below. Right: after detection, rod is labelled in blue and fat is labelled in green.

[Figure 1](#)

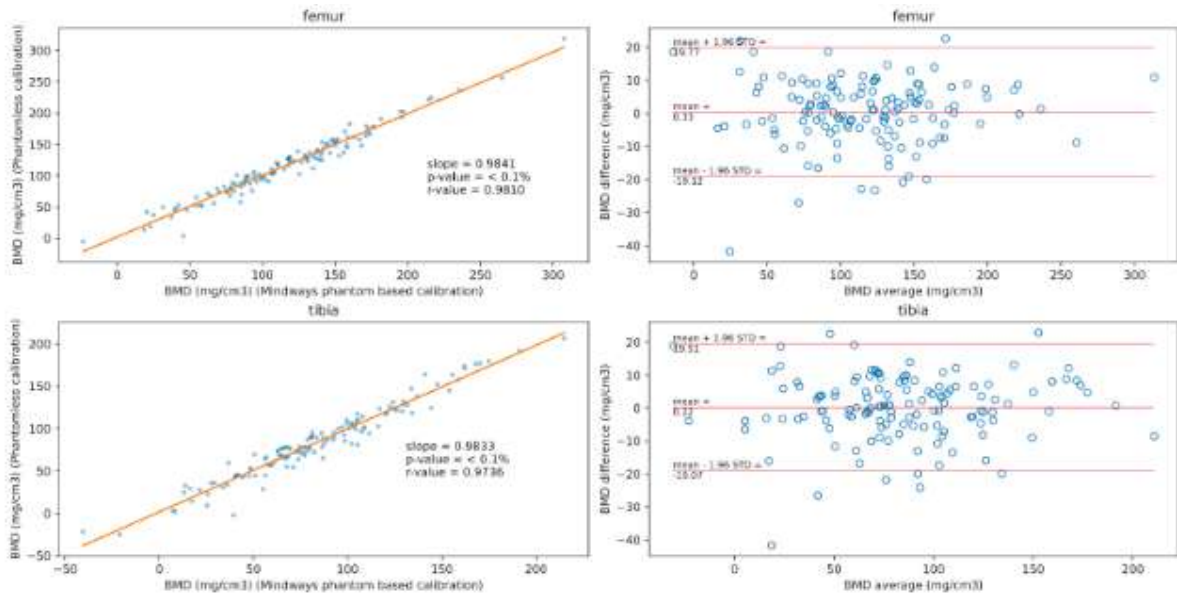


Figure 2: Comparison of trabecular bone BMD from phantom calibration and air/fat/rod calibration. Left: correlation of femur (top) and tibia (bottom). Right: Bland-Altman plots of agreement for femur and tibia.

[Figure 2](#)

Analysis of Discrepancy Between Kellgren-Lawrence(K-L) Grade and Intraoperative Cartilage Status in Patients Undergoing Total Knee Arthroplasty (TKA)

Cho min soo - Seoul, Korea (Republic of)

Seung-Baik Kang - Boramae Medical Center/ Seoul National University College of Medicine - Seoul, South Korea

Moon Jong Chang - SMG-SNU Boramae Medical Center - Seoul, South Korea

Tae Woo Kim - Seoul National University College of Medicine, SMG-SNU Boramae Medical Center - Seoul, South Korea

*Jisu Park - SMG-SNU Boramae Medical Center - Seoul, Korea (Republic of)

Sung Jun Jang - Seoul National University College of Medicine Boramae Medical Center (SMG-SNU Boramae Medical Center) - Seoul, Korea (Republic of)

Hyunkwon Kim - SMG-SNU Boramae Medical Center - Seoul, Korea (Republic of)

*Hyung Min Lee - Seoul National University Boramae Hospital - Seoul, Korea (Republic of)

Background : The K-L grade is one of the most useful indicator in determining the necessity of TKA. TKA is typically performed in patients with high K-L grade, suggesting a strong association with cartilage defects. However, several studies have reported the discrepancy between K-L grade and intraoperative cartilage status.

Purpose : This study aimed to (1) analyze the incidence of discrepancy between K-L grade and intraoperative cartilage status in patients undergoing TKA, and (2) determine preoperative radiologic factor that can predict discrepancy between K-L grade and intraoperative cartilage status.

Materials and Methods : Patients who underwent TKA at a single institution from February 2022 to October 2023 were assessed. K-L Grade and osteophyte size on the medial femoral condyle (MFC) were evaluated in both AP and Rosenberg view using picture archiving and communication system (PACS). The presence of femoral condylar flattening, and the convexity of MFC were also evaluated. MFC flattening was defined as positive when the flattened length of the articular surface of MFC was more than 10mm. MFC convexity was considered as positive when the distance from the line connecting the medial edge to the lateral edge of MFC to the apex of MFC was 2.5mm or less. Intraoperative cartilage status was assessed based on International Cartilage Repair Society (ICRS) grade using intraoperative photos.

Results : A total 879 patients underwent TKA was evaluated, and 86 patients (9.8%) appeared K-L Grade III in both AP view and Rosenberg view. Among patients with K-L Grade III, 33 patients (38.4%) were classified as ICRS grade III, while 53 patients (61.6%) were classified as ICRS grade IV. The average size of osteophytes measured in ICRS grade IV group was significantly larger than that of ICRS III group (AP view : 12.81 ± 6.37 mm vs 7.6 ± 3.91 mm, $p < 0.05$, Rosenberg view : 12.86 ± 6.29 mm vs 8.60 ± 4.89 mm, $p < 0.05$). The cut-off value of osteophyte for the discrepancy between K-L grade(III) and intraoperative ICRS grade(IV) was 10.31mm. MFC straightening was observed in 35 patients, with an average straightened length of $11.37 (\pm 1.69)$ mm. Also positive of MFC convexity was found in 13 patients, with an average distance of $1.91 (\pm 0.36)$ mm.

Conclusion : Concomitant huge osteophyte of femoral condyle greater than 10mm was defined as a predictor for the discrepancy between K-L grade (III) and intraoperative cartilage status (ICRS IV) in patients undergoing TKA. The result of this study can be helpful to evaluate the real cartilage status using K-L grade, and determine appropriate candidate for TKA.

Advanced Candidate Identification for Medial Partial Knee Arthroplasty: a Machine Learning Approach Using CT Data

Michael Bell - Stryker - Mahwah, USA

Sietske Witvoet - Stryker - Amsterdam, Netherlands

Alison Long - Stryker - Newbury, United Kingdom

Michael Bowes - Imorphics - Manchester, United Kingdom

Sebastien Lustig - Hôpital de la Croix Rousse - Lyon, France

*Jared Weir

Introduction

The integration of data-driven strategies in orthopedics is revolutionizing decision-making. Successful Medial

Partial Knee Arthroplasty (mPKA) relies on precise selection of candidates with particular anatomical damage, a

task traditionally reliant on 2D preoperative imaging, not optimal for visualizing key anatomical details. Our

study utilizes advanced 3D measurement of pre-operative computer tomography (CT) scans to develop and

validate a machine-learning model that predicts patient suitability for mPKA with heightened accuracy.

Methods

We conducted a retrospective analysis of 153 robotic-assisted knee arthroplasties who had pre-operative CT

scans. 43 patients were selected for mPKA, based on established criteria, using radiographs and physical

examination; the remainder underwent total knee arthroplasty. We extracted five disease-specific measures from

CT scans utilizing existing computer vision models: B-score, a measure of osteoarthritis severity (see Figure 1),

and four C-scores, indicating joint-space width and probability of cartilage loss (see Figure 2). These were

combined with age, BMI and sex. Logistic regression models were employed for binary classification of mPKA

suitability, using stratified 5-fold cross-validation with an 80-20 training-test split and feature ablation on the

demographic variables, as shown in Figure 3.

Results

All models exhibited robust performance in predicting mPKA candidacy in the test dataset, with an average area

under the curve ranging from 0.77 ± 0.05 to 0.80 ± 0.06 . Notably, B-score (weight: -0.64 ± 0.08 ($p < 0.001$), odds-

ratio: 0.53) and medial tibiofemoral C-score (weight: -1.13 ± 0.14 ($p = 0.002$), odds-

ratio: 0.32) were the only significant features.

Conclusion

This machine-learning model, leveraging accurate 3D measurement from CT images, effectively differentiates

mPKA candidates. Significant predictors of mPKA were lower overall severity of osteoarthritis (lower B-score)

and decreased medial joint-space (lower medial tibiofemoral C-score), indicating a higher probability of medial cartilage loss. Interestingly, age, BMI and sex had no effect on selection of candidates. The implementation of this new model could significantly aid surgeons in identifying appropriate candidates for mPKA.

Figures



Figure 1: B-Score. As OA progresses, each knee bone exhibits a characteristic shape change, involving the growth of osteophytes around the cartilage plates, and a spreading and flattening of the subchondral bone surface. B-score is the distance along a vector which captures this OA shape change in the femur, recorded as a z-score.

Figure 1

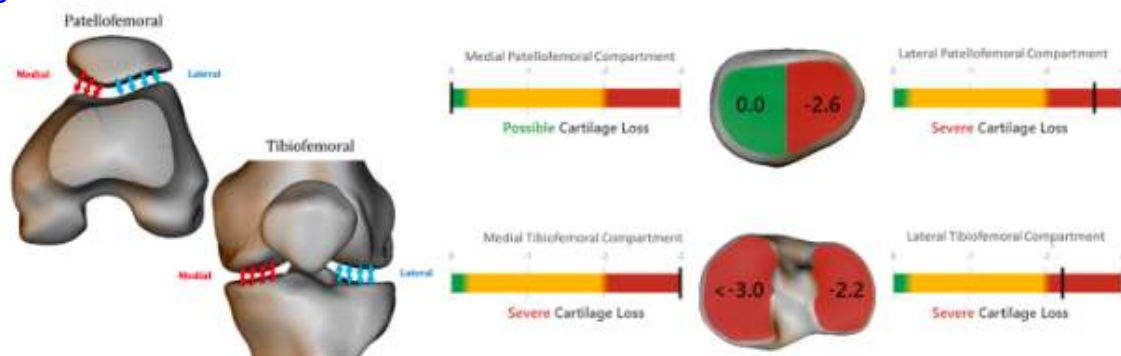


Figure 2: C-Score (cartilage loss probability) is a validated assessment of 3D joint space width (3DJWSW) which correlates strongly with cartilage thickness in MRI scans. Measurements in each of the four compartments of the knee are provided, after adjusting for gender differences, and displayed as a single score for each compartment.

Figure 2

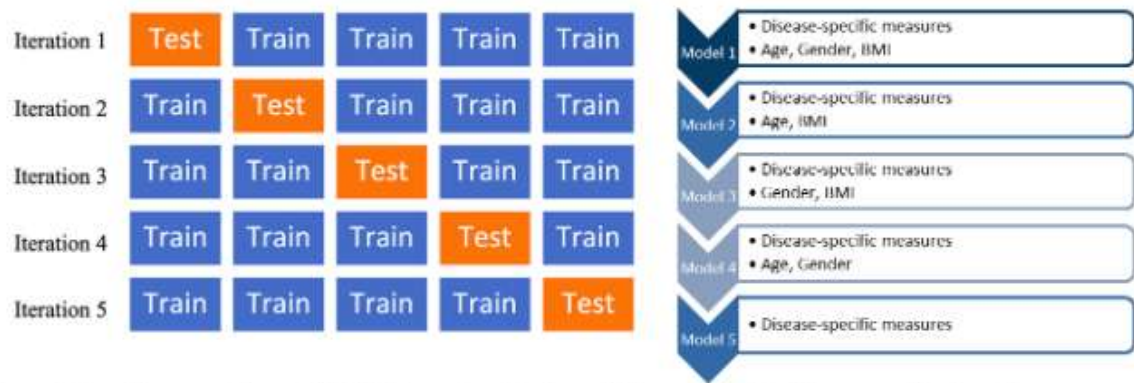


Figure 3: Logistic regression models for binary classification utilising stratified 5-fold cross-validation with an 80-20 training-test split, and feature ablation on the demographic variables

[Figure 3](#)

Similar Outcomes With Cylindrospheric and Subhemispheric Modular Dual Mobility Implants in Primary Total Hip Arthroplasty

*Alana Prinos - Langone Orthopedic Hospital - New York, USA

Catherine Digangi - NYU Orthopedic Hospital - New York, USA

Akram Habibi - NYU Langone Orthopedic Hospital - New York, United States of America

Sophia Antonioli - NYU Langone - New York, USA

Morteza Meftah - NYU Hospital for Joint Diseases - New York, USA

Matthew Hepinstall - NYU Langone Health - New York, USA

Introduction

Modular dual mobility (modDM) implants were introduced to decrease dislocations after total hip arthroplasty (THA) while maintaining the option for screw fixation of the acetabular shell, but there are substantial design differences between available options. “Subhemispheric” constructs prioritize impingement-free range of motion (ROM), whereas “cylindrospheric” DM components prioritize “jump distance”. The aim of this study was to compare rates of dislocation and other mechanical complications between cylindrospheric and subhemispheric modDM implants.

Methods

We retrospectively reviewed 742 primary THAs performed with modDM implants between June 2016 and December 2022 at an urban academic health system. Surgeons used modDM selectively in patients thought to be at higher risk of dislocation. Patients were included in this analysis if they underwent a unilateral THA for osteoarthritis and the operating surgeon selected a modDM implant. Two cohorts were created based on implant design: there were 342 cylindrospheric constructs (MDM, Stryker) and 400 subhemispheric constructs (OR30, Smith & Nephew or G7, Biomet). Dislocations, collected via ICD-10 codes, and reoperations were validated by chart reviews. Rates of dislocation and implant revision were compared using Chi-square and Independent Samples t-tests.

Results

There were 2 (0.6%) dislocations in the cylindrospheric cohort and 6 (1.5%) in the subhemispheric cohort ($p=0.23$). Although use of a cylindrospheric implant was associated with lower odds of dislocation (OR 0.39), this difference was not statistically significant with the numbers available (95% CI 0.078-1.93, $p=0.25$). There were 12 (3.5%) implant revisions in the cylindrospheric cohort and 18 (4.5%) in the subhemispheric cohort ($p=0.49$). In the cylindrospheric cohort, 3 of the 12 revisions were for aseptic loosening, 1 for osteolysis, and 1 for malposition. In the subhemispheric cohort, 2 of the 18 implant revisions were for aseptic loosening, 0 for osteolysis, and 2 for malposition. There were 0 revisions for dislocation in the cylindrospheric cohort and 2 (0.5%) in the subhemispheric cohort ($p=0.190$), both for intraprosthetic dislocation.

Conclusion

There were no statistically significant differences in dislocations or implant revisions between modDM designs across this cohort of 742 patients. Nonetheless, the confidence interval for odds of dislocation included the possibility of a greater than 10-fold reduction in dislocation with use of one design. This study was not powered to exclude a clinically important difference, despite a relatively large cohort size. Multicenter and/or national registry investigations may be necessary to compare

rates of mechanical complications between designs, as selective utilization limited modDM case volume even at a busy academic health system.

Figures

Table 1. Postoperative Outcomes, Stratified by modDM Implant Design

	Cylindrospheric (Stryker MDM) (n=342)		Subhemispheric (R3 and G7) (n=400)		P-value
	M SD	Range	M SD	Range	
Dislocations - no. (%)	2 (0.6)	-	6 (1.5)	-	0.229
Total Revisions – no. (%)	12 (3.5)	-	18 (4.5)	-	0.494
Revisions for fracture – no. (%)	6 (1.8)	-	5 (1.3)	-	0.571
Revisions for aseptic loosening – no. (%)	3 (0.9)	-	2 (0.5)	-	0.531
Revisions for wear/osteolysis – no. (%)	1 (0.3)	-	0 (0)	-	0.279
Revisions for malposition/impingement/failure – no. (%)	1 (0.3)	-	2 (0.5)	-	0.657
Revisions for dislocation – no. (%)	0 (0)	-	2 (0.5)	-	0.190
Revisions for infection – no. (%)	1 (0.3)	-	7 (1.8)	-	0.055
Days to Revision	351.8±384.4	4-1062	133.5±260.8	2-1050	0.074

Figure 1

Table 2. Univariate Odds Ratio Analysis for Dislocation by modDM Implant Design

	Dislocation Odds Ratio [CI]	P-value
Use of Cylindrospheric Dual Mobility Implant (compared to Subhemispheric Dual Mobility Implant)	0.386 [0.077-1.926]	0.246

Figure 2

Table 3. Univariate Odds Ratio Analysis for Revisions for Mechanical Failure by modDM Implant Design

	Revisions for Mechanical Failure Odds Ratio [CI]	P-value
Use of Cylindrospheric Dual Mobility Implant (compared to Subhemispheric Dual Mobility Implant)	1.026 [0.310-3.393]	0.966

*Mechanical Failure includes aseptic loosening, wear/osteolysis, malposition/impingement/failure, and dislocation

Figure 3

Influence of Dual Mobility Insert Design on Locking Strength Under Pull-Out and Cam-Out Testing Conditions

*Ahmad Faizan - Stryker - Mahwah, USA

Ananthkrishnan Gopalakrishnan - Stryker Orthopaedics - Mahwah, USA

Venus Vermani - Stryker - Gurugram, India

Sahil Khanna - Stryker - Gurugram, India

Geoffrey H Westrich - Hospital for Special Surgery - New York, USA

Introduction

Dual mobility (DM) designs combine the stability of a large femoral head with low wear characteristics of a smaller articulation to help mitigate the risk of dislocation. Several DM designs incorporate a 22 mm or 28 mm femoral head that is captured in the polyethylene insert. A new DM insert was designed for smaller size acetabular components that allows a 28 mm head instead of the 22 mm metal head. As such, the wall thickness is less than the legacy design. To better understand the effects on locking strength, this study compared the new, thinner DM insert with a 28 mm head to the thicker legacy DM insert.

Methods

Two DM insert designs were used in this study (new insert and legacy insert). Axial pull-out and cam-out tests were performed on both insert designs. A total of eight samples from each group were evaluated for both tests. For the axial pull-out test, the 28 mm head was assembled to the DM polyethylene insert using the compression device from the surgical protocol. This assembly was then impacted onto the trunnion statically using a 2000N load a 5mm/min rate. The head was then axially extracted from the DM insert at a rate of 0.5mm/sec until it disengaged from the polyethylene (Figure 1A). For the cam-out testing, a 28 mm head was again assembled to the DM polyethylene insert using the compression device from the surgical protocol and then the head/insert assembly was impacted onto the stem. This construct was then inserted into the fixture setup (Figure 1B), and a landmark was made on the stem 100 mm from the head center along the stem axis. A load was applied at a rate of 0.5mm/sec to the stem through the testing machine's crosshead and the stem moved such that it impinged on the edge of the polyethylene insert and then with continued applied force, torque was generated such that the femoral head was levered out from the polyethylene insert. Non inferiority statistical tests were performed for both pull-out and cam-out values.

Results

The pull-out strength values were normalized to the pull-out values for the legacy insert design as shown in Figure 2 (left). Similarly, the cam-out strength values were normalized to the cam-out values for the legacy insert design as shown in Figure 2 (right). For both tests, the newer design was non-inferior to the legacy design ($p < 0.05$).

Discussion

Axial pull-out and cam-out tests were used to compare the locking strength of the femoral head in two DM insert designs. These two tests represent two different failure modes, but the clinically significant failure mode that is observed in vivo is the cam-out mode that may result in intraprosthetic dislocation of the head from the DM polyethylene insert. The data presented in this study shows that both pull-out and cam-out strength values for the new insert were equivalent or greater than the legacy design, therefore, providing confidence that the new thinner DM design should be

able to withstand intraprosthetic dislocation as well as or better than the legacy design (95% confidence).

Figures

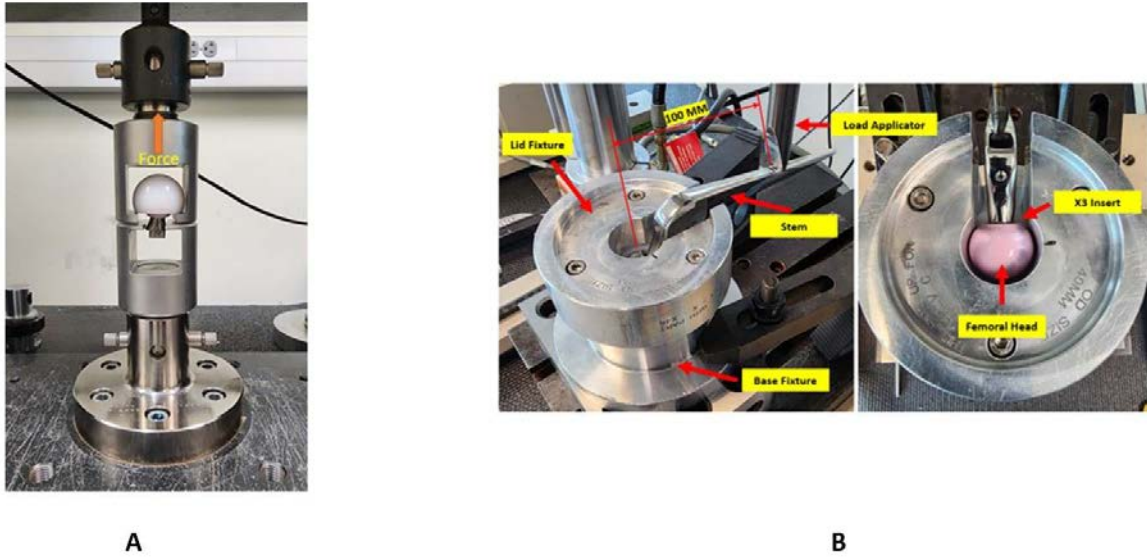


Figure 1A & 1B: Axial pull-out (A) and cam-out (B) test setups.

Figure 1

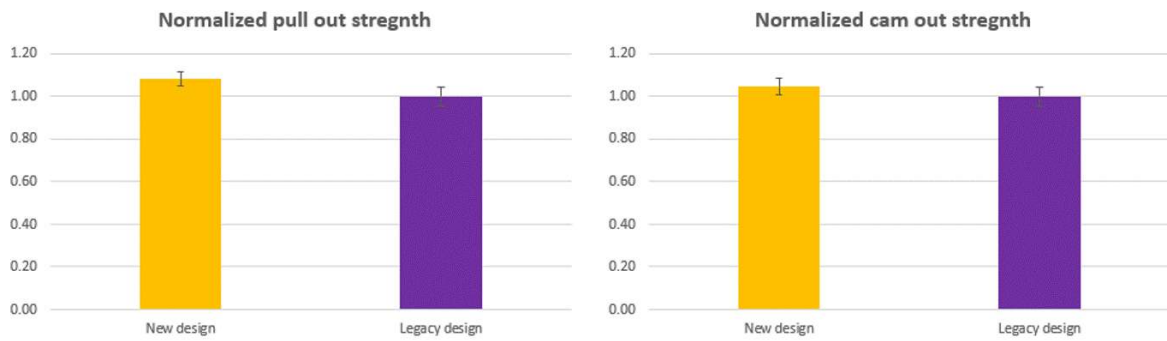


Figure 2: Normalized pull-out and cam-out values.

Figure 2

Investigating Component Impingement Risk Following Total Hip Arthroplasty in Vivo During Activities of Daily Living

*Shahnaz Taleb - Western University - London, Canada

Jordan Broberg - Western University - London, Canada

James Howard - London Health Sciences Centre - London, Canada

Brent Lanting - London Health Sciences Centre - London, Canada

Matthew Teeter - Western University - London, Canada

Introduction: Component-on-component impingement in total hip arthroplasty may lead to limited range of motion and function, pain, dislodgement of the modular liner or loosening of the implant due to increased stress on the liner rim, accelerated metal wear, subluxation, and dislocation. Because of its consequences, many clinical studies are looking at methods to reduce risk of impingement following hip arthroplasty. However, the assessment of component impingement is largely limited to qualitative imaging evaluation of the hip joint, finite element analyses, and cadaver studies, which do not accurately reflect the true prevalence of impingement in non-failed implants. The objective of this study is to employ radiostereometric analysis (RSA) to measure component impingement in vivo at various activities of daily living (ADLs) in patients who have undergone total hip arthroplasty (THA).

Methods: Eight participants six months to one year post-operation who underwent THA through the direct anterior approach were recruited. All received the same cementless metal-on-polyethylene implant system. RSA examinations were taken in nine positions simulating ADLs: standing neutral, external rotation, internal rotation, gait (loading response phase), step over, upstairs (weight acceptance phase), downstairs (controlled lowering phase), and frog leg (knees flexed at 30°, hip externally rotated by 45°). The RSA exams were used to measure the distance between the femoral neck and the inner circumference of the polyethylene liner. A 1 mm threshold was used to indicate impingement based on a prior phantom study, with neck-liner distances approaching 1 mm being defined as a higher risk of impingement.

Results: Neck-liner distances were 4.40 – 12.56 mm in standing neutral, 4.23 – 13.09 mm in external rotation, 9.44 – 22.07 mm in internal rotation, 10.31 – 17.23 mm in gait, 9.99 – 19.09 mm in step over, 9.12 – 18.75 mm in upstairs, 5.60 – 18.20 mm in downstairs, 8.70 – 14.13 mm in frog leg, and 10.22 – 20.13 mm in supine positions. There was a statistically significant effect of ADL position on neck-liner distance ($p = 0.038$), where activities of highest and lowest risk were external rotation and supine positions, respectively. No participants displayed impingement (neck-liner distance <1 mm) in any activity.

Conclusion: Neck-liner distances vary between patients and ADLs, thus indicating potential differences in impingement risk during ADLs following THA. As additional participants are recruited, component sizing, acetabular cup position and spinopelvic mobility will be considered to explore potential protective factors against component impingement.

Two-Year Outcomes of a Novel Dual-Mobility System in Revision Total Hip Arthroplasty

*Muhammad Haider - NYU Orthopedic Hospital - New York, USA

Michelle Richardson - NYU Langone Orthopedics - New York, USA

Nehir Parikh - Rothman Institute - Philadelphia, USA

Akram Habibi - NYU Langone Orthopedic Hospital - New York, United States of America

Benjamin Schaffler - NYU Orthopedic Hospital - New York, USA

Sophia Antonioli - NYU Langone - New York, USA

Chad Krueger - Rothman Orthopaedic Institute - Philadelphia, USA

P Maxwell Courtney - Rothman Orthopaedic Institute - Philadelphia, USA

Ran Schwarzkopf - NYU Langone Medical Center Hospital for Joint Diseases - New York, USA

Catherine Digangi - NYU Orthopedic Hospital - New York, USA

Background: Revision total hip arthroplasty (rTHA) is projected to increase substantially in volume. Dual-mobility (DM) implants, composed of a femoral head articulated within an outer polyethylene liner and an articulating outer acetabular shell, have gained popularity for their potential to reduce hip instability and dislocations due to the larger DM femoral head options. This study aimed to evaluate early outcomes and survivorship of a novel DM implant for rTHA.

Methods: This was a retrospective, multicenter study to assess clinical outcomes of 199 patients undergoing rTHA with a novel DM implant from April 2018 to July 2023. Patient demographics, clinical outcomes and implant survivorship were collected and analyzed. Primary outcomes included 90-day readmissions, cause for readmission, all-cause revisions, cause for revision and overall implant survivorship. Preoperative and postoperative Hip Disability and Osteoarthritis Score for Joint Replacement (HOOS, JR) were also analyzed.

Results: 108 patients achieved minimum 1-year of clinical follow-up and 50 patients achieved minimum 2-years of clinical follow-up. Patients who received the novel DM implant were a mean of 67.3 years old, with a majority of the patients being women (58.0%) and of white race (68.0%). Mean BMI of patients was 29.5. 8 patients (4.0%) experienced a 90-day orthopedic-related readmission, with the most common causes being cellulitis (n=3, 1.5%) and dislocation (n=3, 1.5%). One patient (0.5%) had revision of the acetabular component due to instability. Patients experienced significant improvements in mean HOOS, JR scores at all postoperative time points, surpassing the minimally clinically important difference for HOOS, JR (18.0).

Conclusions: This novel DM acetabular implant demonstrated excellent survivorship of the acetabular component at 1 and 2 years (99.5%, for both) of follow-up in complex rTHA cases, with low rates of instability and no reported episode of metallosis. Patients demonstrated clinically significant improvements in HOOS, JR at 2-years post-op.

Figures

Table 1. Baseline Characteristics

Demographic	rTHAs (n=199)
Mean Age (years) [range]	67.4 [29-94]
Sex, n (%)	
Men	84 (42.2)
Women	115 (57.8)
Race, n (%)	
White	135 (67.8)
African American	31 (15.6)
Asian	3 (1.5)
Other	30 (15.1)
Mean BMI (kg/m ²) [range]	29.5 [16.5-54.4]
Smoking Status, n (%)	
Never	162 (81.4)
Current	37 (18.6)
ASA Class, n (%)	
0	4 (2.0)
1	3 (1.5)
2	73 (36.7)
3	118 (59.3)
4	1 (0.5)
Procedure Laterality	
Right	98 (49.2)
Left	101 (50.8)

rTHA; revision Total Hip Arthroplasty, BMI; Body Mass Index, ASA; American Society of Anesthesiologists

[Figure 1](#)

Table 2. Clinical and Patient-Reported Outcomes

Outcome	rTHAs (n=199)
90 Day Orthopedic Related Readmissions (n, %)	8 (4.0)
Readmission Cause	
Deep Infection	1 (0.5)
Cellulitis	3 (1.5)
Dislocation	3 (1.5)
Hematoma	1 (0.5)
Acetabular Revisions	1 (0.5)
Revision Cause	
Dislocation	1 (0.5)
Mean HOOS, JR (SD)	
Preoperative	51.15 (15.18)
6 weeks	61.51 (17.68)
3 months	70.00 (18.98)
1 year	72.69 (22.60)
2 years	75.00 (21.98)
Δ Preop to 6 weeks	10.36 (16.43)
Δ Preop to 3 months	18.85 (17.08)
Δ Preop to 1 year	21.54 (18.89)
Δ Preop to 2 years	23.85 (18.58)

rTHA; Revision Total Hip Arthroplasty, HOOS, JR; Hip Disability and Osteoarthritis Outcome Score, Joint Replacement, SD; Standard Deviation

[Figure 2](#)

Figure 1: rTHA Survival from Acetabular Revision

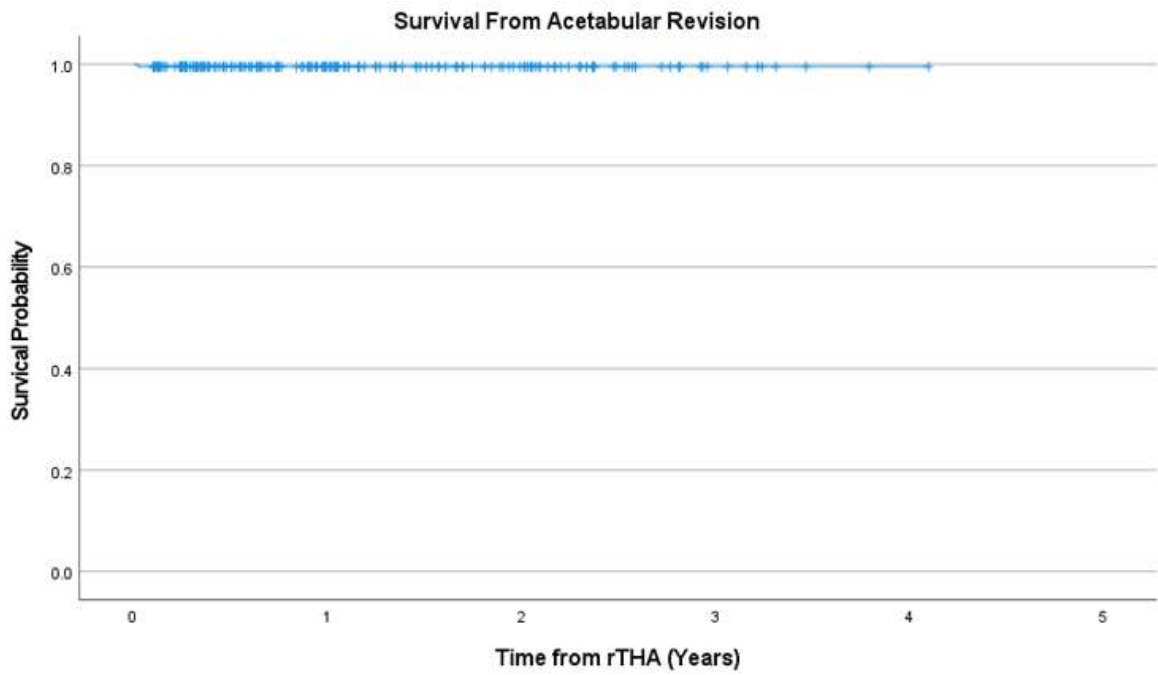


[Figure 3](#)

Predictive Factors for Making Optimal Surgical Decision in Patients With Knee Osteoarthritis: Analysis of Correlation With Plain Radiographs Findings With Wear Patterns and Anterior Cruciate Ligament

Cho min soo - Seoul, Korea (Republic of)

Seung-Baik Kang - Boramae Medical Center/ Seoul National University College of Medicine - Seoul, South Korea

Moon Jong Chang - SMG-SNU Boramae Medical Center - seoul, South Korea

Tae Woo Kim - Seoul National University College of Medicine, SMG-SNU Boramae Medical Center - Seoul, South Korea

Jisu Park - SMG-SNU Boramae Medical Center - Seoul, Korea (Republic of)

Sung Jun Jang - Seoul National University College of Medicine Boramae Medical Center (SMG-SNU Boramae Medical Center) - Seoul, Korea (Republic of)

Hyunkwon Kim - SMG-SNU Boramae Medical Center - Seoul, Korea (Republic of)

*Hyung Min Lee - Seoul National University Boramae Hospital - Seoul, Korea (Republic of)

Background : Total Knee Arthroplasty(TKA) and Unicompartmental knee arthroplasty (UKA) are common treatment options for symptomatic knee osteoarthritis(OA). Especially in cases where OA is confined to the medial compartment with intact Anterior Cruciate Ligament (ACL), UKA can be considered. Therefore, preoperative evaluation with MRI is frequently considered necessary prior to undergoing UKA. However, MRI may not be routinely performed due to cost considerations. Furthermore, it is known that surgical outcomes of posteromedial OA are not as favorable as those of anteromedial OA.

Purpose : This study aimed to identify factors on plain radiographs that can predict the necessity of MRI preoperatively and the surgical outcomes from a cost-effective standpoint.

Materials and Methods : Patients who underwent TKA at a single medical institution by single surgeon during July to December 2023 were analyzed. Plain radiographs were used to evaluate the Lateral Distal Femoral Angle(LDFA), Medial Proximal Tibial Angle(MPTA), Anatomical Hip-Knee-Angle(aHKA),and Joint Line Obliquity Angle(JLOA) in AP view, Posterior slope(PS) and presence of posterior wear(PW) in lateral view. Intraoperative photos were used to assess the wear pattern of the medial tibia and the integrity of the ACL. The medial compartment of the tibia was divided into four sections from anterior to posterior, labeled as A, B, C and D. If section A was included, it was considered as anteromedial OA(AMOA), when section D was included, it was considered as posteromedial OA(PMOA). ACL integrity was considered intact if it showed continuity of more than 75%.

Results : A total 195 patients underwent TKA was involved. 113 patients had intact ACL while 82 patients did not. 60 patients were observed with AMOA, while 36 patients were observed with PMOA. In the intact ACL group, the mean posterior slope was $8.70(\pm 3.50)^\circ$, and was $9.90(\pm 3.83)^\circ$ in the ACL deficient group. A significant correlation was found with ACL integrity and presence of posterior wear in plain radiograph. In both AMOA and PMOA groups also showed a significant correlation with posterior slope. The mean posterior slope was $7.47(\pm 3.79)^\circ$ in

AMOA group and $12.21(\pm 3.44)$? in PMOA group. Additionally, a significant correlation was found between ACL integrity and wear pattern. ($P < 0.05$).

Conclusion : Considering TKA and UKA options for patients with knee OA, certain findings on plain radiographs such as an excessive posterior slope or the presence of posterior wear may indicate insufficient ACL integrity or suggest posteromedial OA, both of which could predict poor prognosis with UKA. In such cases, recommending TKA than UKA without additional evaluation like MRI can assist in making cost-effective decisions.

Hiding in Plain Sight: MRI Indications for Total Hip Arthroplasty in Patients Without Radiographic Evidence of Severe Arthritis

*Benjamin Domb - American Hip Institute - Des Plaines, USA

Benjamin Kuhns - American Hip Institute Research Foundation - Chicago, USA

Yasemin Kingham - American Hip Institute Research Foundation - Chicago, USA

Tyler McCarroll - American Hip Institute Research Foundation - Chicago, USA

Ady Kahana - American Hip Institute Research Foundation - Chicago, United States of America

Roger Quesada-Jimenez - American Hip Institute Research Foundation - Chicago, USA

Ali P. Parsa - American Hip Institute - Des Plaines, USA

Veer Shah - American Hip Institute Research Foundation - Chicago, USA

Background: Hip arthroplasty is generally contraindicated in the setting of preserved radiographic joint space. Despite this reservation, there are limited indications for arthroplasty in patients that have failed conservative measures. The purpose of this study was to retrospectively evaluate a standardized preoperative MRI classification system as a decision-making tool for patients with intact joint space undergoing arthroplasty or hip preservation.

Methods: Following IRB approval, patients with a preserved joint space joint space (Tonnis grade <2, Joint Space Width >3mm) undergoing primary total hip arthroplasty with a preoperative hip MRI were included in the study. The arthroplasty cohort was then propensity matched by Tonnis Grade (1:1) and Joint Space Width to a population of patients undergoing hip preservation. Four fellowship trained hip preservation surgeons reviewed the preoperative MRI according to the Scoring of Hip Osteoarthritis in MRI (SHOMRI) grading system (Figure 1). Grading discrepancies were resolved in conference with a board-certified musculoskeletal radiologist familiar with this scoring system. SHOMRI scores were compared between the arthroplasty and hip preservation cohorts with an emphasis on articular cartilage, subchondral edema, and subchondral cystic change. Minimum 2-year postoperative outcome scores were collected for each group for the modified Harris Hip Score (mHHS), pain Visual Analog Scale (VAS), and Satisfaction.

Results: There were 27 patients included in both the arthroplasty and hip preservation cohorts. There were no significant differences in age, gender, BMI, joint space width, or Tonnis grade between each group. There was high inter-observer reliability between reviewers with ICC values greater than 0.7 for the total SHOMRI score as well as all component sub-scores (Figure 2). Patients undergoing arthroplasty had significantly greater acetabular cartilage, femoral cartilage, acetabular subchondral edema, and acetabular subchondral cystic changes compared to patients undergoing hip preservation ($p < 0.01$; figure 3). There were no significant differences in outcome scores between the hip preservation and arthroplasty cohorts with high rates of satisfaction for both at a minimum of two years postoperatively.

Conclusion: The SHOMRI scoring system can successfully distinguish between populations of patients undergoing hip preservation or arthroplasty in patients with similar appearing preoperative radiographs with intact joint space. Both groups had improved outcomes following their respective procedures.

Figures

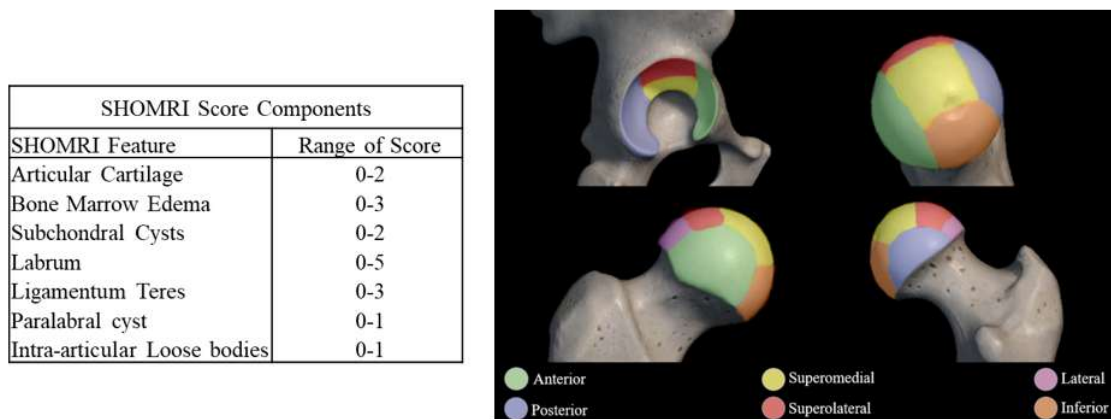


Figure 1: Scoring of Hip Osteoarthritis on MRI (SHOMRI) grading scale. The acetabulum is divided into 4 zones while the proximal femur is divided into 6 zones. Each zone is grade for each SHOMRI sub feature with a maximum score of 100.

Figure 1

SHOMRI Grade	ICC	95% CI
Femoral Head Cartilage	0.90	0.84-0.94
Acetabular Cartilage	0.89	0.84-0.94
Femoral Head Edema	0.96	0.93-0.98
Acetabular Edema	0.94	0.90-0.96
Femoral Head Cyst	0.86	0.79-0.92
Acetabular Cyst	0.73	0.61-0.83
Labrum	0.93	0.89-0.96
Ligamentum Teres	0.81	0.71-0.88
Paralabral Cyst	0.93	0.89-0.96
Loose Body	0.86	0.79-0.91

Figure 2: Reliability of the Scoring of Hip Osteoarthritis on MRI (SHOMRI) grading scale components across 4 graders.

Figure 2

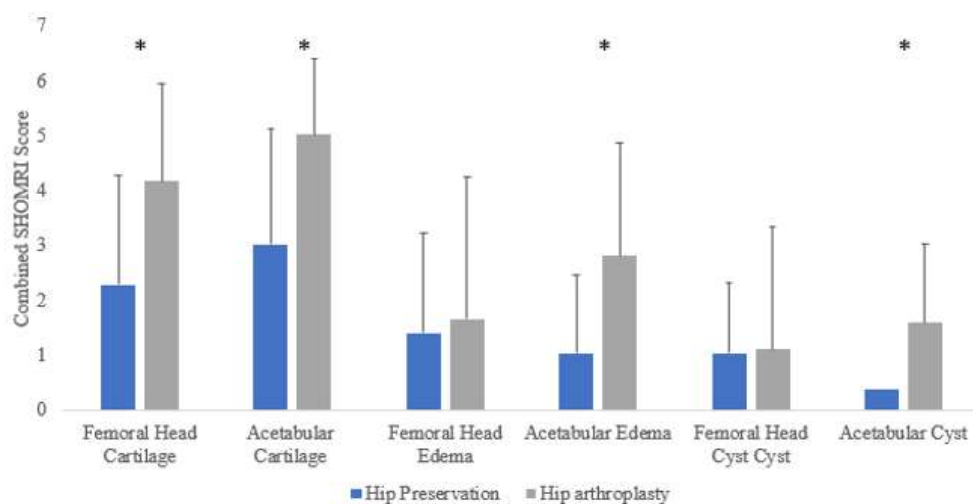


Figure 3: Combined SHOMRI score differences for the acetabular and femoral sub-regions. *Significant difference in SHOMRI score between the arthroplasty and hip preservation populations ($p < 0.01$).

[Figure 3](#)

Weight-Bearing CT Assessment Following Cementless Total Knee Arthroplasty

*Mathew G Teeter - Schulich School of Medicine and Dentistry, Western University and London Health Sciences Centre - London, Canada

Jane Lin - Western University - London, Canada

Mariam Zamani - Western University - London, Canada

Edward Vasarhelyi - Western University - London, Canada

Brent Lanting - London Health Sciences Centre - London, Canada

Background: Weight-bearing CT scanners are growing in availability and provide the capability of three-dimensional imaging while a joint is under load. The total knee arthroplasty (TKA) field is trending towards more personalized alignment and the use of cementless implants that rely on bone ingrowth. We hypothesized that weight-bearing CT could be used to assess the bone-implant interface, measure joint alignment, and measure bone density around cementless TKA.

Methods: Forty patients who underwent primary TKA approximately 3 years previously and received one of two cementless implant systems were recruited, including two subjects with bilateral TKA, for a total of 42 knees. Patient cohorts were matched based on sex, age (± 5 years), and post-operative hip-knee-ankle angle ($\pm 1.5^\circ$). There were ten men and ten women per implant design. All subjects underwent examination of their knee with weight-bearing CT while standing, thereby loading the indicated knee. A metal artifact reduction algorithm was implemented in the image reconstructions. The bone-implant interface was examined for radiolucencies. Lateral distal femoral angle (LDFA), medial proximal tibial angle (MPTA), hip-knee-ankle angle (HKA), and joint line obliquity (JLO) were measured on full length radiographs and the weight-bearing CT exams by two observers. Greyscale values representing bone density were assessed in five identically sized regions of interests in both the femur and the tibia.

Results: No radiolucent lines were appreciated beyond the zone that could be attributable to metal artifact with either implant design. The mean differences between the full-length radiograph and weight-bearing CT measurements were 4.3 deg for LDFA ($p < 0.0001$), 0.9 deg for MPTA ($p = 0.021$), -3.4 deg for HKA ($p < 0.001$), and 5.2 for JLO ($p < 0.001$). Within the tibia, greyscale values were lower ($p < 0.0001$) under the anterolateral peg compared to the other three pegs, and lower ($p < 0.0005$) under the keel than under the four pegs. Within the femur, there were no differences in greyscale values between regions ($p > 0.323$). Good interobserver agreement was found for alignment (95% ICC: 0.87) and femoral greyscale values (95% ICC: 0.87), and excellent agreement was found for tibial greyscale values (95% ICC: 0.97).

Discussion: Cementless TKA can be assessed post-operatively using weight-bearing CT, providing the measurement capabilities of conventional CT for implant position and bone density in a functional, loaded joint position. While there was good interobserver repeatability for alignment measurements with weight-bearing CT, there were differences from full-length radiographs, similar to the differences between full length and short film radiographs. This may indicate that weight-bearing CT systems that can perform full limb scans would be more valuable in assessing TKA alignment.

Limb Coronal Alignment Does Not Predict Transepicondylar Axis to Posterior Condylar Axis Variation in Primary Total Knee Arthroplasty

Utkarsh Anil - NYU Langone Orthopedic Hospital - New York, USA

Catherine Digangi - NYU Orthopedic Hospital - New York, USA

Charles Lin

Matthew Hepinstall - NYU Langone Health - New York, USA

Morteza Meftah - NYU Hospital for Joint Diseases - New York, USA

*Armin Arshi - New York University Langone Health - New York, United States of America

INTRODUCTION

Femoral rotation in total knee arthroplasty (TKA) plays an essential role in flexion gap balance and patellofemoral tracking. The impact of coronal mechanical axis alignment on the femoral rotation axis is less well understood. The purpose of this study is to understand the relationship between femoral rotation axes and coronal alignment.

METHODS

We identified 287 consecutive patients undergoing primary TKA with a preoperative planning CT scan. The surgical transepicondylar axis (sTEA) and posterior condylar axis (PCA) were identified and the angle between them was measured. The angle between the mechanical axis of the femur and tibia were used to measure the coronal alignment of the limb. Statistical analyses were performed in R.

RESULTS

The mean native coronal alignment in this analysis was 4.4 deg Varus (range 12 deg Valgus to 30 deg Varus). There were 193 patients with >2 deg Varus and 36 patients with >2 deg Valgus. There were no statistically significant differences between the two groups in gender (78% vs 65% Male, $p=0.14$), age (68.4 ± 10.39 vs 68.1 ± 8.97 , $p=0.7$) or BMI (30.4 ± 5.75 vs 32.2 ± 5.62 , $p=0.08$). On average, the sTEA was 2.9 deg external rotated to the PCA (range 3deg internal to 9 external). The difference between sTEA and PCA in the varus group was on average 3.3 ± 2.07 deg versus 2.6 ± 1.97 deg in the valgus group. This difference was not statistically significant.

CONCLUSION

There is significant variation in the femoral rotation axes between patients ranging sTEA being 3deg internally rotated to 9deg externally rotated. There was no significant relationship between overall limb coronal alignment and magnitude of femoral rotation axes variation.

3D vs 2D Preoperative Planning: Can More Information Yield Better Outcomes?

*Jarrod Nachtrab - University of Tennessee - Knoxville, USA

Thang Nguyen - University of Tennessee - Knoxville, USA

Michael LaCour - University of Tennessee - Knoxville, USA

Richard Komistek - The University of Tennessee - Knoxville, USA

Introduction

Traditional total hip arthroplasty (THA) preoperative planning involves overlaying component models onto a two-dimensional (2D) radiograph, incorporating morphological parameters such as Dorr Type, offsets, leg lengths, etc. More recently, three-dimensional (3D) planning using CT data has allowed surgeons to gain more information intraoperatively compared to 2D templating, particularly with respect to out-of-plane orientation of the components. The objective of this research is to use both 2D and 3D preoperative planning tools to determine and compare the femoral stem alignment of a single stem system across all three Dorr Types.

Methods

The EMPHASYS (DePuy Synthes, Warsaw IN) stem system was analyzed using a previously published and validated 3D planning tool that provides supplemental planning information [1]. Two different 3D fit algorithms were incorporated, one that focused on aligning the head center locations and one that focuses on the stem fit within the canal. The 2D fit algorithm was designed to replicate that of planning a THA using only a frontal-plane x-ray. After planning, the distance from the anatomical head center to the implanted head center (head distance), the implanted version angle, and the bone removal volume within the canal were determined. All fit methods were analyzed in 3D for comparison.

Results

It was determined that 3D preoperative planning reduced head distances (Table 1) and version angle differences (Table 2) by accounting for coronal plane information gathered by combining the Dorr bone-type classification system with out-of-plane information such as femoral bowing angles and anatomical version angles. When planning in 2D, out-of-plane information such as the femoral bowing angles were not considered, leading to increased amounts of cortical reaming ($p=1.8E-5$) as seen in Table 3, component misalignment regarding head distances ($p=0.03$), and possible malrotation of the entire leg postoperatively due to changing the anatomical version angle.

Conclusion

Two-dimensional templating using the Dorr classification system offers surgeons valuable information, but current advancements with 3D information give surgeons a more complete picture of a hip joint for THA surgery. These advanced 3D preoperative planning tools could be clinically beneficial for patients, as this study demonstrates improved alignment potential when components are planned and placed in a 3D environment. This may lead to increased patient satisfaction when combined with robotic surgery.

References

1. Ta MD. Development and Implementation of a Computational Surgical Planning Model for Pre-Operative Planning and Post-Operative Assessment and Analysis of Total Hip Arthroplasty. University of Tennessee, 2019.

Figures

		Anatomical Head Center to Implanted Head Center		
		3D Anatomic	3D Canal	2D
A	AVG ± ST Dev	0.4 ± 0.2	3.0 ± 1.5	9.3 ± 2.4
	[Min - Max]	[0.2 - 1.0]	[0.8 - 5.3]	[4.9 - 12.9]
B	AVG ± ST Dev	0.5 ± 0.2	2.8 ± 1.3	6.4 ± 2.7
	[Min - Max]	[0.1 - 0.9]	[0.8 - 6.1]	[0.6 - 10.4]
C	AVG ± ST Dev	0.6 ± 1.1	3.2 ± 2.0	6.5 ± 2.9
	[Min - Max]	[0.2 - 5.2]	[0.8 - 9.7]	[0.1 - 11.1]
Total	AVG ± ST Dev	0.5 ± 0.7	3.0 ± 1.6	7.4 ± 3.0
	[Min - Max]	[0.1 - 5.2]	[0.8 - 9.7]	[0.1 - 12.9]

Figure 1

Version Angle [°]	Anatomical	3D Anatomic	3D Canal	2D
AVG ± ST DEV	8.5 ± 4.3	8.4 ± 4.3	8.0 ± 6.3	-3.7 ± 5.9
[MIN - MAX]	[0.8 - 17.2]	[0.8 - 17.0]	[-7.0 - 23.1]	[-18.1 - 9.1]

Figure 2

Bone Removal [cm³]		3D Anatomic	3D Canal	2D
A	AVG ± ST Dev	0.0 ± 0.0	0.0 ± 0.0	0.6 ± 0.4
	[Min - Max]	[0.0 - 0.0]	[0.0 - 0.0]	[0.0 - 1.6]
B	AVG ± ST Dev	0.0 ± 0.0	0.0 ± 0.0	0.2 ± 0.3
	[Min - Max]	[0.0 - 0.1]	[0.0 - 0.0]	[0.0 - 0.9]
C	AVG ± ST Dev	0.0 ± 0.1	0.0 ± 0.0	0.2 ± 0.4
	[Min - Max]	[0.0 - 0.3]	[0.0 - 0.0]	[0.0 - 1.9]
Total	AVG ± ST Dev	0.0 ± 0.0	0.0 ± 0.0	0.4 ± 0.4
	[Min - Max]	[0.0 - 0.3]	[0.0 - 0.0]	[0.0 - 1.9]

[Figure 3](#)

Avoiding Arthroplasty - the Impact of Acetabular Orientation on Femoral Head Coverage and Hip Range of Motion

*Philip Noble - Institute of Orthopedic Research and Education - Houston, USA

Shuyang Han - University of Texas Health Science Center at Houston - Houston, USA

Nicholas Dunbar - Houston, United States of America

James Baker - University of Texas Health Science Center - Houston, USA

Maddison Brenner - University of Texas - Houston, USA

Chuheng Xing - University of Texas - Houston, USA

Angus Brooks - University of Texas Health Science Center at Houston - Bellaire, USA

Alexis Aboulafia - University of Texas Health Science Center - Houston, USA

Alfred Mansour III - University of Texas Health Science Center - Houston, USA

Introduction

Acetabular reorientation is performed in symptomatic dysplastic hips to improve function and prevent or delay joint degeneration leading to THA. As the morphology of the dysplastic hip is highly variable, preoperative planning of these procedures is difficult without 3D computer-based tools enabling individual adjustment of each component of acetabular orientation. In this study we examine the effect of changing acetabular inclination, flexion and anteversion on acetabular coverage of the femoral head and hip range-of-motion.

Methods:

Fourteen 3D patient-specific hip models were reconstructed from pre-operative CT scans of patients diagnosed with hip dysplasia. Each model was placed in a standard coordinate system with neutral pelvic tilt and femoral rotation. A standard Bernese periacetabular osteotomy (PAO) was simulated with correction of acetabular inclination (LCEA) to 30°. Twelve surgical plans were simulated by independently adjusting the anteversion: (change: 0°, 5°, 10°, 15°) and flexion (change: 0°, 5°, 10°) of the acetabulum. The neutral runs were repeated after changing acetabular inclination by $\pm 5^\circ$ (LCEA = 25° and 35°). After each rotational adjustment, the new position of the femoral head within the acetabulum was calculated by finding the position of maximum conformity in the region of articular contact. Once this was determined, we measured the 3D femoral head coverage (total and by quadrants) and the maximum internal rotation of the hip in 90° of flexion.

Results:

An inverse relationship was observed between head coverage and hip ROM.

Changes in each component of acetabular orientation led to a corresponding shift in the combination of antero-lateral head coverage and hip ROM. Variations in each component led to small changes in total head coverage and larger changes in the antero-lateral quadrant of the articular surface. The impact of each component was:

1. 10° change in Inclination (LCEA: 25-35°): AntLat Coverage: +33±5%; Change in ROM: -8.6±1.4°

2. 10° change in Flexion (0-10°): AntLat Coverage: +26±7%; Change in ROM: -7.7±3.8°

3. 10° increase in Anteversion (0-10°): AntLat Coverage: -6.5±4.5%; Change in ROM: +3.7±3.0°

Conclusions:

1. Small changes in the inclination and flexion of the acetabulum lead to dramatic increases in head coverage with loss of hip motion.
2. Loss of joint motion is much more predictable with changes in inclination than flexion.
3. Increasing acetabular anteversion leads to a slight reduction in head coverage and a variable increase in joint motion.

Because of the variability of head coverage and ROM, predictive models enabling patient-specific preoperative planning are needed to optimize the outcome of acetabular osteotomies performed to delay joint degeneration and hip arthroplasty.

Figures

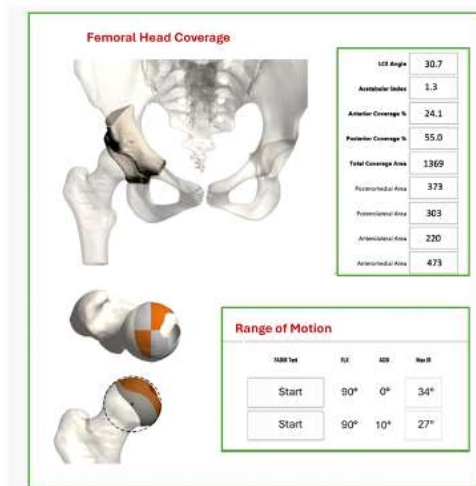


Figure 1. Interactive computer display showing the orientation of the acetabulum and the corresponding values of femoral head coverage and hip range of motion.

[Figure 1](#)

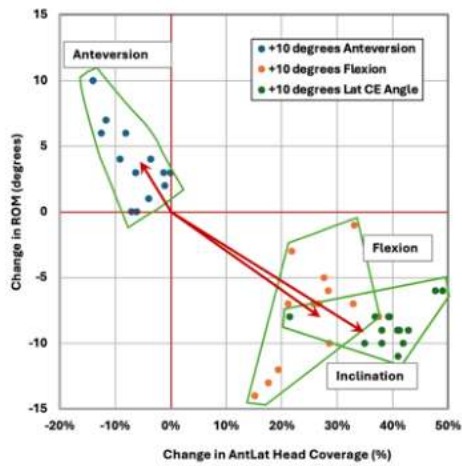


Figure 2. Changes in Antero-lateral head coverage and hip range-of- motion produced by rotating the acetabulum by 10 degrees of Inclination, Flexion and Anteversion from an initial starting point of 0 degrees flexion and anteversion and a lateral center edge angle of 30 degrees. The arrows correspond to the average values for all cases combined.

[Figure 2](#)

Mixed Reality-Guided Performance of Bernese Periacetabular Osteotomy: Proof of Concept

*Alexander F Heimann - New England Baptist Hospital - Boston, USA

Jens Kowal - USA

Stephen Murphy - New England Baptist Hospital - Boston, USA

Patrick Lane - Surgical Planning Associates - USA

Andrew Amundson - Surgical Planning Associates - Medford, USA

Moritz Tannast - University of Bern - Bern, Switzerland

Introduction

Mixed Reality has the potential to improve accuracy and reduce required dissection for the performance of peri-acetabular osteotomy. The current work assesses initial proof of concept of MR guidance for PAO.

Methods

A PAO planning module, based on preoperative computed tomography (CT) imaging, allows for the planning of PAO cut planes and repositioning of the acetabular fragment. 3D files (holograms) of the cut planes and native and planned acetabulum positions are exported with the associated spatial information. The files are then displayed on mixed reality head mounted device (HoloLens2, Microsoft) following intraoperative registration using an FDA-cleared mixed reality application designed primary for hip arthroplasty (HipInsight). PAO was performed on both sides of a bone model (Pacific Research). The osteotomies and acetabular reposition were performed in accordance with the displayed holograms. Post-op CT imaging was performed for analysis. Cutting plane-accuracy was evaluated using a best-fit plane and 2D angles ($^{\circ}$) between the planned and achieved supra (SA)- and retroacetabular (RA) osteotomy and retroacetabular and ischial osteotomies (IO) were measured.

To evaluate the accuracy of acetabular reorientation, we digitized the acetabular rim and calculated the acetabular opening plane. Absolute errors of planned and achieved operative inclination and anteversion ($^{\circ}$) of the acetabular fragment, as well as 3D lateral-center-edge (LCE) angles were calculated.

Results

The mean absolute difference between the planned and performed osteotomy angles was $3 \pm 3^{\circ}$.

The mean absolute error between planned and achieved operative anteversion and inclination was $1 \pm 0^{\circ}$ and $0 \pm 0^{\circ}$ respectively (Fig. 1). Mean absolute error between planned and achieved 3D LCE angle was $0.5 \pm 0.7^{\circ}$.

Conclusion

Mixed-reality guidance for the performance of pelvic osteotomies and acetabular fragment reorientation was feasible and highly accurate. This solution may improve the current standard of care by enabling reliable and precise reproduction of the desired acetabular realignment.

Figure 1. 3D Model of the acetabular reorientation plan with the target fragment orientation in 15° operative anteversion and 25° operative inclination (left). Postoperative CT-based 3D Model of the achieved fragment orientation in 16° operative anteversion and 25° operative inclination using Mixed Reality-guidance (right).

Figures

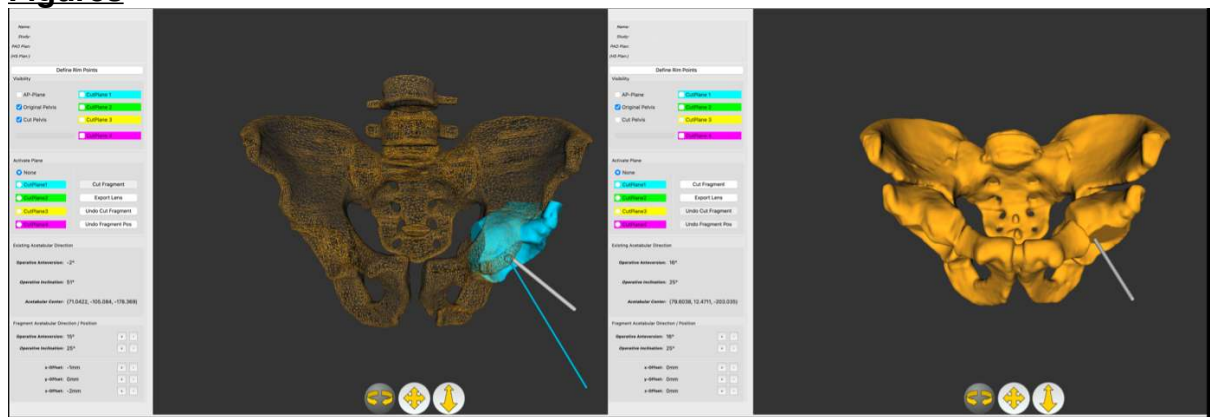


[Figure 1](#)

Determining the Minimal Clinically Important Difference and Substantial Clinical Benefit Following Revision Reverse Shoulder Arthroplasty

*Garrett Jackson - Chicago, United States of America

Ali Mohamed - FAU - Boca raton, USA

Anna Redden - FAU - boca raton, USA

Jared Kushner - Charles E. Schmidt Florida Atlantic University - Boca Raton, USA

Aghdas Movassaghi - Michigan State University - East Lansing, USA

Howard Routman - Atlantis Orthopedics - Atlantis, USA

Diego L Lima - Cleveland Clinic Florida - Weston, USA

Vani Sabesan - Cleveland Clinic Florida - Weston, USA

Jacob Calpey - Charles E. Schmidt College of Medicine Florida Atlantic University - Boca Raton, USA

Introduction: Reverse shoulder arthroplasty (RSA) has become a common procedure due to its expanded indications and popularity. The concern with this growth is the increased complications with RSA that may lead to more revision surgery. Given revision surgery has increased complexity and difficulty in recovery for patients, understanding outcomes can help guide patients and surgeons in this decision-making. This study aimed to determine the minimum clinically important difference (MCID) and substantial clinical benefit (SCB) following revision RSA (rRSA) using the anchor-based approach.

Methods: A retrospective review of all patients who underwent rRSA from 2007 to 2020 by a single fellowship-trained orthopedic surgeon was performed. Patient demographics, ROM, Simple Shoulder Test (SST), Constant-Murley score, American Shoulder and Elbow Surgeon (ASES) score, University of California at Los Angeles (UCLA) shoulder score, Shoulder Pain and Disability Index (SPADI), and the Shoulder Arthroplasty Smart (SAS) score, were collected preoperatively and postoperatively at the last follow-up visit. MCID and SCB were calculated using the anchor-based method. Analyses were performed using paired- and independent-sample t-tests and logistic regressions were used to identify potential predictors for meeting MCID and SCB.

Results: A total of 91 patients were included in this analysis. The cohort had a mean age of 67.8 years and a mean body mass index (BMI) of 29.7 kg/m². A majority of the cohort was male (51.7%) and Caucasian (93.2%). The MCID was found to be 3.4 for SST, 26.7 for CMS, 28.6 for ASES, 12.5 for UCLA, -35.3 for SPADI, 17.7 for SAS, 56° for forward flexion, 47° for abduction and 9° for external rotation. The SCB was found to be 6.2 for SST, 32.4 for CMS, 39.2 for ASES, 16.2 for UCLA, -54.1 for SPADI, 27.6 for SAS, 76° for forward flexion, 61° for abduction and 10.9° for external rotation. MCID or SCB was achieved by 72.5% of patients. Of these, 28.5% (n=26) of patients met MCID and 43.9% (n=40) met SCB at a mean follow-up of 22.7 months. Age, sex, and BMI were not found to be significantly associated with meeting MCID or SCB.

Conclusions: This study sets thresholds for the MCID and SCB following rRSA. Patient satisfaction after revision RSA indicated by MCID and SCB is shown to be directly correlated with higher patient-reported outcome scores at final follow-up and not significantly impacted by patient-specific factors. This information is

beneficial for orthopedic surgeons as it can help to set and guide the expectations of patients undergoing revision reverse shoulder arthroplasty.

Is Implant Wear and Corrosion in Anatomic and Reverse Total Shoulder Arthroplasty Associated With Radiographic Evidence of Aseptic Loosening?

*Colton Mowers - Rush Medical College - Chicago, United States of America

Deborah Hall - Rush University Medical Center - Chicago, USA

Jennifer Wright - Rush University Medical Center - Chicago, USA

Tyler Williams - Rush University - Chicago, USA

Gregory Nicholson - Rush University Medical Center - Chicago, USA

Grant Garrigues - Rush University Medical Center - Chicago, USA

Robin Pourzal - Rush University Med Ctr - Chicago, USA

BACKGROUND:

Recent advances in surgical techniques and implant design both anatomic total shoulder arthroplasty (TSA) and reverse total shoulder arthroplasty (RSA) implants have allowed for enhanced patient specificity, reducing pain, restoring mobility, leading to improved implant survival and long-term outcomes for patients. Despite these advances, there has been little attention given to the causes of aseptic loosening—a primary cause of failure. While wear particle induced osteolysis and subsequent aseptic loosening is well-defined in the literature in hip (THA) and knee (TKA), there remains a paucity of research for the shoulder (TSA). The incidence of revision shoulder arthroplasty is increasing annually, with an estimated 10,290 patients undergoing revision TSA or RSA in the U.S. alone. This emphasizes the importance of elucidating key factors leading to implant failure. The goal of this study was to identify potential relationships between implant wear and radiographic evidence of loosening in aTSA and rTSA.

METHODS:

We studied a cohort of 108 consecutively retrieved TSA implants (8 manufacturers) consisting of 70 aTSA and 38 rTSA components with various stem lengths after excluding infection cases and revision implants. Radiographic assessment of radiolucencies was performed using Gruen zones along the humeral stems and for aTSA pegged/keeled glenoid components. Scapular notching was evaluated for rTSA components according to Sirveaux classifications. Reason for failure was recorded from patient charts. A qualitative damage score for polyethylene (PE) bearing wear (0-14) and metal bearing wear (0-3) was performed using stereoscope microscopy. Damage of male/female modular taper surfaces was scored analog to the Goldberg scale (1-4). Pearson/Spearman correlations were conducted to determine the relationship between wear and radiographic findings and reason for revision.

RESULTS:

The aTSA group had a higher median PE wear score than rTSA (9 vs. 5, respectively, $p < 0.001$). For aTSA, PE wear positively correlated with the diagnosis of glenoid loosening ($p = 0.032$), metal wear was also positively correlated with glenoid loosening ($p = 0.011$) and trended with radiolucency scores for keeled and pegged glenoids ($p = 0.12$, $p = 0.059$, respectively). Male taper damage positively correlated with radiographic radiolucency scores for short stems ($p = 0.001$), while female taper

damage only exhibited a trend ($p=0.07$). For rTSA, there was a positive correlation between PE wear and Sirveaux classification due to rim damage caused by notching. Neither PE nor metal wear correlated with radiographic findings or diagnosis of loosening. Female/male taper damage was positively correlated with the diagnosis of glenoid loosening ($p<0.001$, $p=0.002$, respectively).

CONCLUSION:

PE wear may play a role in the loosening of the glenoid component in aTSA. This result is corroborated by our previous findings in a smaller cohort (ISTA 2023) exhibiting a severe presence of particle-laden macrophages within aTSA periprosthetic tissues indicating risk of osteolysis. However, the same study did not exhibit any significant metal particle presence within periprosthetic tissue. Thus, damage to taper surfaces likely occurred secondary to loosening and not vice versa. While rTSA did not exhibit a relationship between wear and loosening, we suspect the PE wear score to be insufficient to capture such relationship.

The Effect of Humeral Distalization in Reverse Total Shoulder Arthroplasty on Muscle Function, Scapular Strain, and Joint Load During Simulated Active Motion: An Ex-Vivo Biomechanical Study

*David Axford - Western University - London, Canada

Robert Potra - Mathys Medical - Sydney, Australia

Richard Appleyard - Macquarie University - Sydney, Australia

Janos Tomka - Macquarie University - Sydney, Australia

Desmond Bokor - Macquarie University Hospital - Sydney, Australia

Sumit Raniga - RothlMcFarlane Hand and Upper Limb Centre - London, Canada

Louis Ferreira - University of Western Ontario - London, Canada

Introduction

Reverse total shoulder arthroplasty (RTSA) was introduced to treat rotator cuff tear arthropathy, and since then, its utilization has expanded. The Grammont style prosthesis is characterized by medialization of the humerus and joint center. Humeral distalization restores deltoid tension, but excessive lengthening can cause deltoid pain and increase scapular fracture risk. To date, the biomechanical effects of isolated humeral distalization in RTSA has not been studied. Therefore, the purpose of this study was to use an ex-vivo shoulder motion simulator to examine the effect of humeral distalization on muscle function, acromial strain, and joint load.

Methods

Eight cadaveric specimens (48 ± 14 years) were mounted to an ex-vivo shoulder motion simulator (Figure 1A) that performed scapular plane abduction (SPA) and internal-external rotation (IER) of the shoulder for four joint conditions: intact, +0mm, +2.5mm, and +5mm RTSA distalization. Joint load was measured using an instrumented glenosphere (Figure 1B) and maximum principal strain in four locations [1] along the acromion and scapular spine was measured throughout motion (Figure 2A). Repeated measures analysis of variance was used to compare muscle function (excursion, force, and muscle work), scapular strains, and joint load across conditions.

Results

All RTSA states had significantly higher lateral and posterior deltoid excursions than the intact shoulder ($p < .05$). The superior cuff showed diminished abduction function while the inferior rotator cuff demonstrated increased adduction function (negative excursion and work) with RTSA implantation ($p < .05$) (Figure 3). This observation was also associated with progressive distalization, although not significant. During internal rotation, inferior subscapularis excursion was lower for all RTSA states ($p < .01$), and muscle work was less with +5mm distalization than intact ($p = .018$). Infraspinatus external rotation force was lower than intact for all RTSA states ($p < .05$). During SPA, RTSA scapular strains were significantly higher than intact at low elevation ($p < .05$) but not at high elevation (Figure 2B). Overall, strain in zone 3B was significantly higher than intact for all RTSA states and motions ($p < .05$). Progressive distalization showed small increases in scapular strains, although not significant. Finally, humeral distalization did not have a significant effect on joint loads.

Conclusions

This is the first biomechanical study to investigate the effect of isolated humeral distalization in RTSA on muscle function, scapular strains, and joint loads during simulated ex-vivo shoulder motion. RTSA implantation resulted in increased deltoid

activity during SPA with decreases in rotator cuff function. The differences between humeral distalization states were small and not significant.

References

[1] Kerrigan, A. M., Reeves, J. M., Langohr, G. D. G., Johnson, J. A., and Athwal, G. S., 2021, "The Influence of Reverse Arthroplasty Humeral Component Design Features on Scapular Spine Strain," *J Shoulder Elbow Surg*, 30(3), pp. 572–579.

Figures

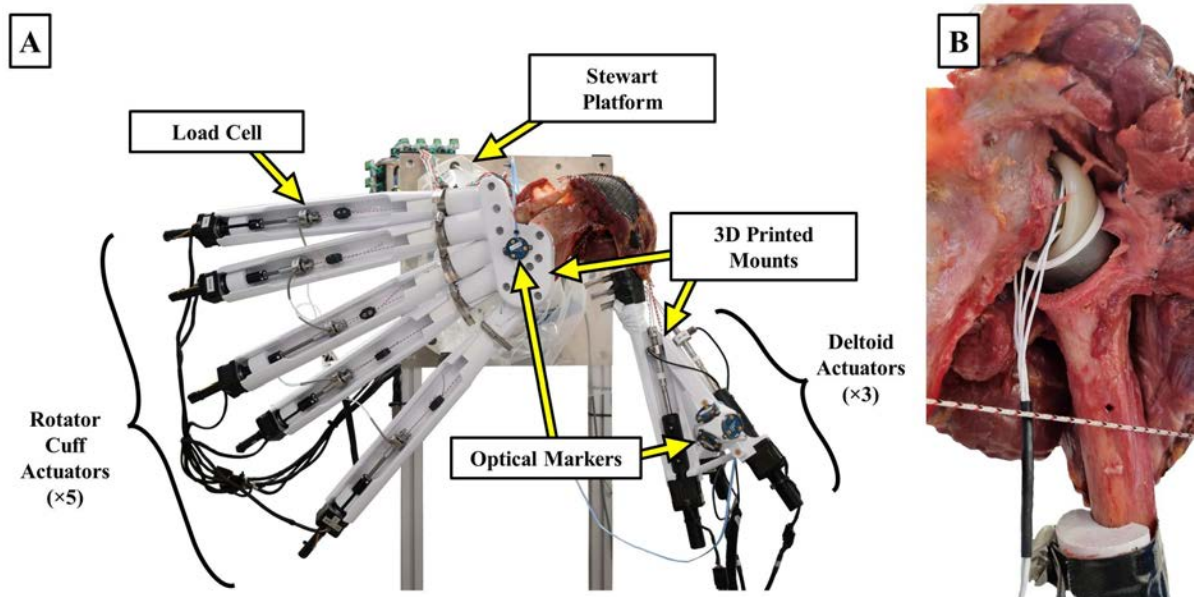


Figure 1: (A) Ex-vivo shoulder motion simulator. A specimen-specific 3D-printed scapular mount secured each specimen to a Stewart platform that simulated upward rotation of the scapula during motion. Three computer-controlled actuators were connected to the three aspects of the deltoid and five actuators were connected to five aspects of the rotator cuff. A load cell at the end of each actuator measured tendon load and optical markers tracked joint kinematics. (B) Joint compression and center of pressure were measured using an instrumented glenosphere.

Figure 1

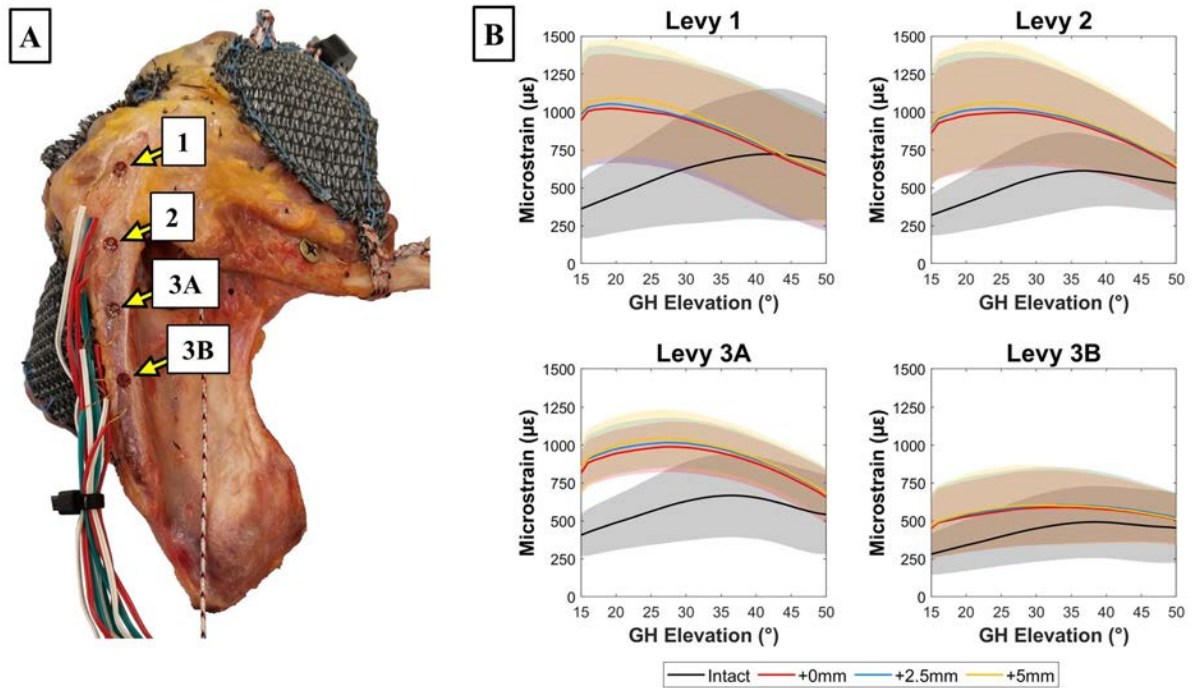


Figure 2: (A) Maximum principal strain was measured in four regions of the acromion and scapula spine as described by Kerrigan et al. [1] using triaxial strain gauge rosettes. (B) Maximum principal strains ($N=8$, Mean \pm SD) measured in each of the four regions (1, 2, 3A, and 3B) for each joint condition (intact, +0mm, +2.5mm, +5mm distalization) during scapular plane abduction.

Figure 2

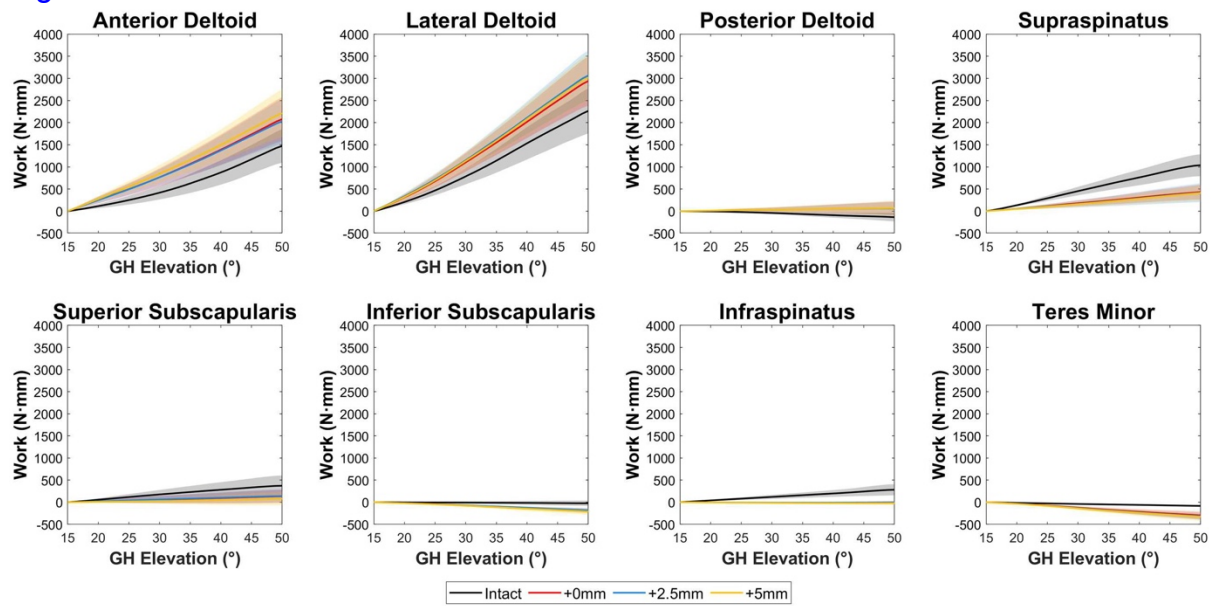


Figure 3: Average muscle work during scapular plane abduction ($N=8$, Mean \pm SD) for each joint condition (intact, +0mm, +2.5mm, +5mm RTSA humerus distalization). Positive work means that the muscle is an agonist to the motion and negative work means that the muscle is an antagonist.

Figure 3

Design and Characterization of a Clinical AMF System for Uniform Heating of Prosthetic Knee Implants

*Varun Sadaphal - Solenic Medical - Addison, USA

Bibin Prasad - Solenic Medical - Addison, USA

Suri Le - Cobalt Product Solutions - Plano, USA

Robert Oakley - Cobalt Product Solutions - Plano, USA

Mikel Serralde - Aava Technologies - Plano, USA

Isaiah Baker - 8Fold Mfg - Addison, USA

Andrei Mitrofan - 8Fold Mfg - Addison, USA

Jared Smothermon - Aava Technologies - Plano, USA

Kevin McCoy - Aava Technologies - Plano, USA

Jeff Garrett - Cobalt Product Solutions - Plano, USA

John Tepper - Solenic Medical - Addison, USA

Rajiv Chopra - Solenic Medical - Addison, USA

Treating prosthetic joint infection (PJI) involves highly-invasive surgical procedures with great impact on quality of life for patients. PJIs occur due to biofilm formation around the implant. This process sets up an altered microenvironment for bacteria to thrive unhindered by the body's natural immunologic protective response and antibiotic treatment. Studies have reported that heat can reduce biofilm on implant surfaces and can also increase its sensitivity to antibiotics. AMF provides a method for non-invasive targeted heating of metal implants without surgical intervention. Although promising, its application encompasses numerous engineering challenges. This study explores design challenges to generate a system capable of efficiently delivering a therapeutic dose of AMF to a primary knee implant and the development of a clinical device for human trials. Based on prior in-vitro, large animal, and computational studies, a complex AMF coil pattern generating 5 mT at 215 kHz was required to reach 75°C average surface temperature within 2 min on the knee implant with uniform distribution. Construction of the system required electrical currents on the order of 200 A, specialized litz wire, use of resonance and matching circuits, handling of up to 10 KV peak circuit voltage, dynamic tracking of thermal resistive changes of the tank circuit, and a means to position the coil accurately over the knee. The magnetic field of the constructed system was measured and validated against simulated magnetic field calculations. The surface temperature distribution of clinical knee implants was measured with infrared imaging, and found to agree within $\pm 5\%$ of equivalent simulations (Figure 1). Overall, this study shows successful engineering of a clinical system (Figure 2) for AMF heating of prosthetic knee implants, and it is in the process of obtaining approval for human feasibility studies.

Figures

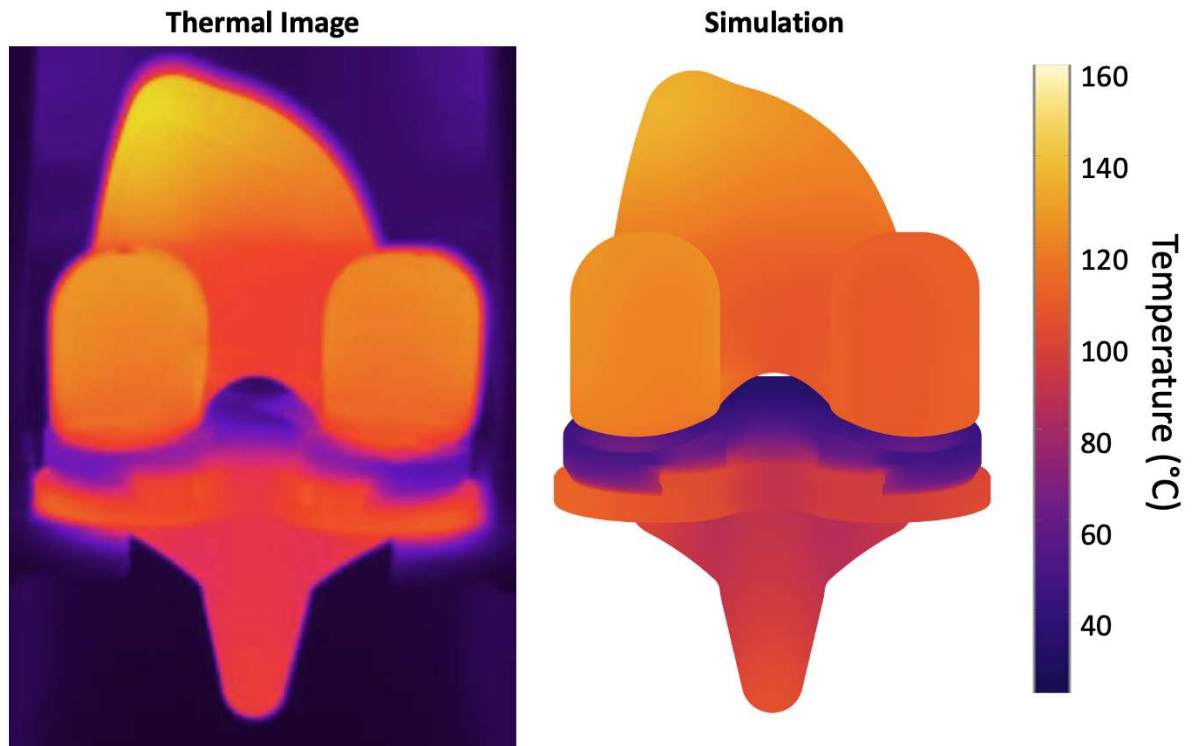


Figure 1

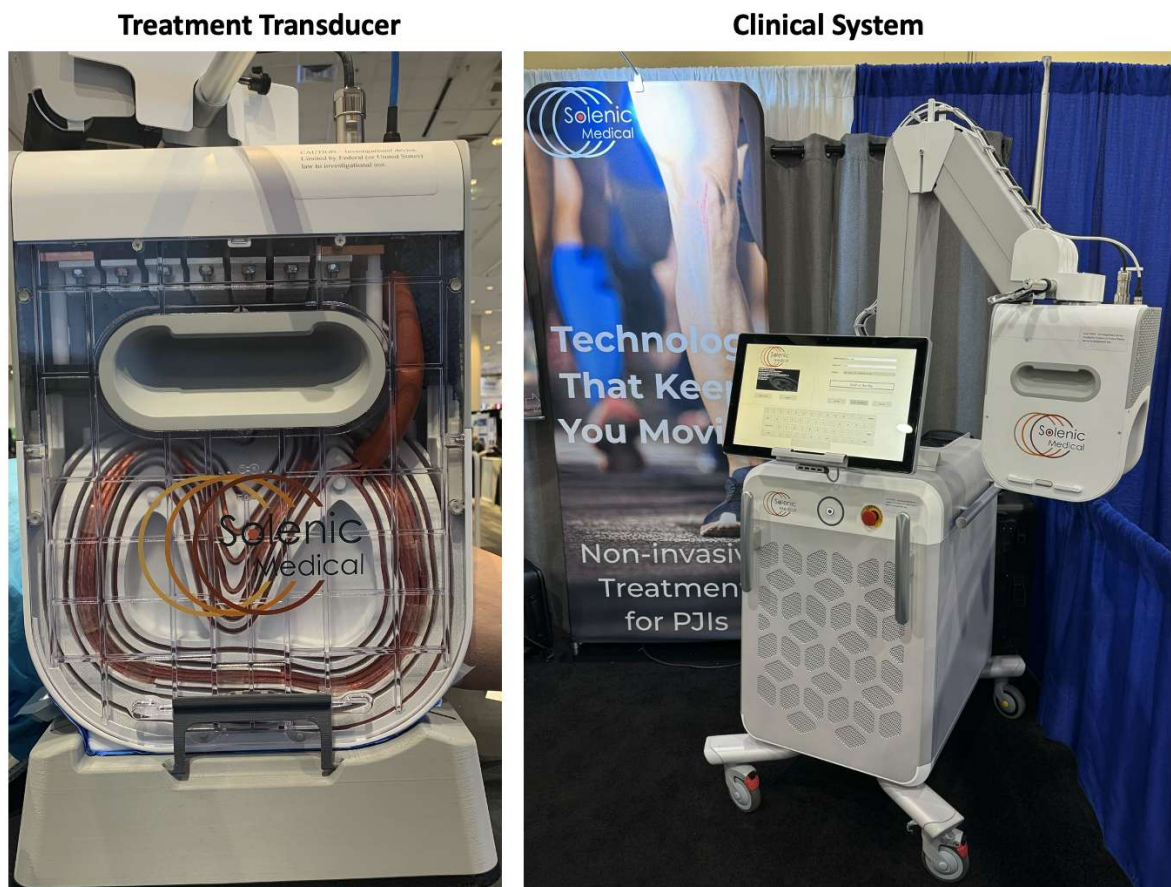


Figure 2

Preclinical Evaluation of a Chip-Integrated Implantable Biosensor for Infection Detection

Bruno Gil Rosa - Imperial College London - London, United Kingdom

*Thomas Hall - Imperial College London - London, United Kingdom

David Freeman - Imperial College London - London, United Kingdom

Damien Ming - Imperial College London - London, United Kingdom

Sasza Nabilla - Imperial College London - London, United Kingdom

Frederic Cegla - Imperial College London - London, United Kingdom

Richard van Arkel - Imperial College London - London, United Kingdom

INTRODUCTION: Infection is the second most common complication of arthroplasty^{1,2}. Its effects are devastating: five-year survivorship post-infection is worse than four of the five most common cancers³, and the cost of prolonged hospitalization, diagnostic testing, and reoperation amounts to \$100,000+ per deep infection⁴. Prophylactic antibiotics are discouraged amidst the ‘looming global crisis of antimicrobial resistance’⁵ and there is ‘no one single perfect test’ for rapid infection detection⁶. In this study, we evaluated a smart implant with a chip-integrated lactate biosensor (Figure 1) as a tool to prompt early intervention in an ex vivo model of living bone.

METHODS: The biosensor was fabricated with a third-generation lactate enzyme (LactaZyme, DirectSens, Austria) on a 1-mm working electrode, encased with an amperometric circuit in a 3D-printed titanium orthopaedic implant (8 × 15 mm), and read wirelessly via a smartphone (Samsung Galaxy A53). Sensitivity to lactate (an infection biomarker⁷), plus acetaminophen and ascorbic acid (potential confounders), was measured in serial dilutions. Infection detection in living bone was evaluated in a bioreactor model⁸: samples inoculated with *Staphylococcus epidermidis* were referenced against sterile controls.

RESULTS: The sensitivity, current density and limit-of-detection levels achieved by the lactate biosensor within a physiologically relevant range were 1.25 $\mu\text{A}\cdot\text{mM}^{-1}$, 1.51 $\mu\text{A}\cdot\text{M}^{-1}\cdot\text{mm}^{-2}$, and 66 μM respectively. The sensor was insensitive to acetaminophen. Sensitivity to ascorbic acid was half that of lactate, but physiologic ascorbic acid concentrations are typically an order magnitude lower, hence not of clinical concern. In the ex vivo model with living bone, *Staph. epi.* was detected within five hours of implantation, whilst the control sample led to no change in the sensor readings.

CONCLUSION: This study has demonstrated detection of an infection biomarker in living bone with a chip-integrated implantable biosensor. The sensor was insensitive to potentially confounding molecules at physiological concentrations, demonstrating a pathway towards earlier detection of infection.

ACKNOWLEDGEMENTS: This research was supported by United Kingdom Research and Innovation through an EPSRC Doctoral Prize Fellowship and an Impact Acceleration Account award.

REFERENCES:

1. American Joint Replacement Registry. 2023 Annual Report, 2023.
2. National Joint Registry, 20th Annual Report, 2023.
3. Lum *et al.*, J Arthroplasty, 2018;33(12):3783-3788.
4. Khan *et al.*, Ann Med Surg (Lond). 2022;77:103655.
5. Tsang and Simpson, Bone Joint Res, 2020;9(12):870-872.
6. Higgins *et al.*, J Clin Microbiol, 2022;60:e02196-21.

7. Watson and Heard, J Intensive Care Med, 2010;25(5):301-302.

8. Kohli *et al.*, Front Bioeng Biotechnol, 2023;11:1054391.

KEYWORDS: Smart Implants/Sensors & Instruments; Periprosthetic Joint Infection; Digital Health; Bioreactor.

Figures

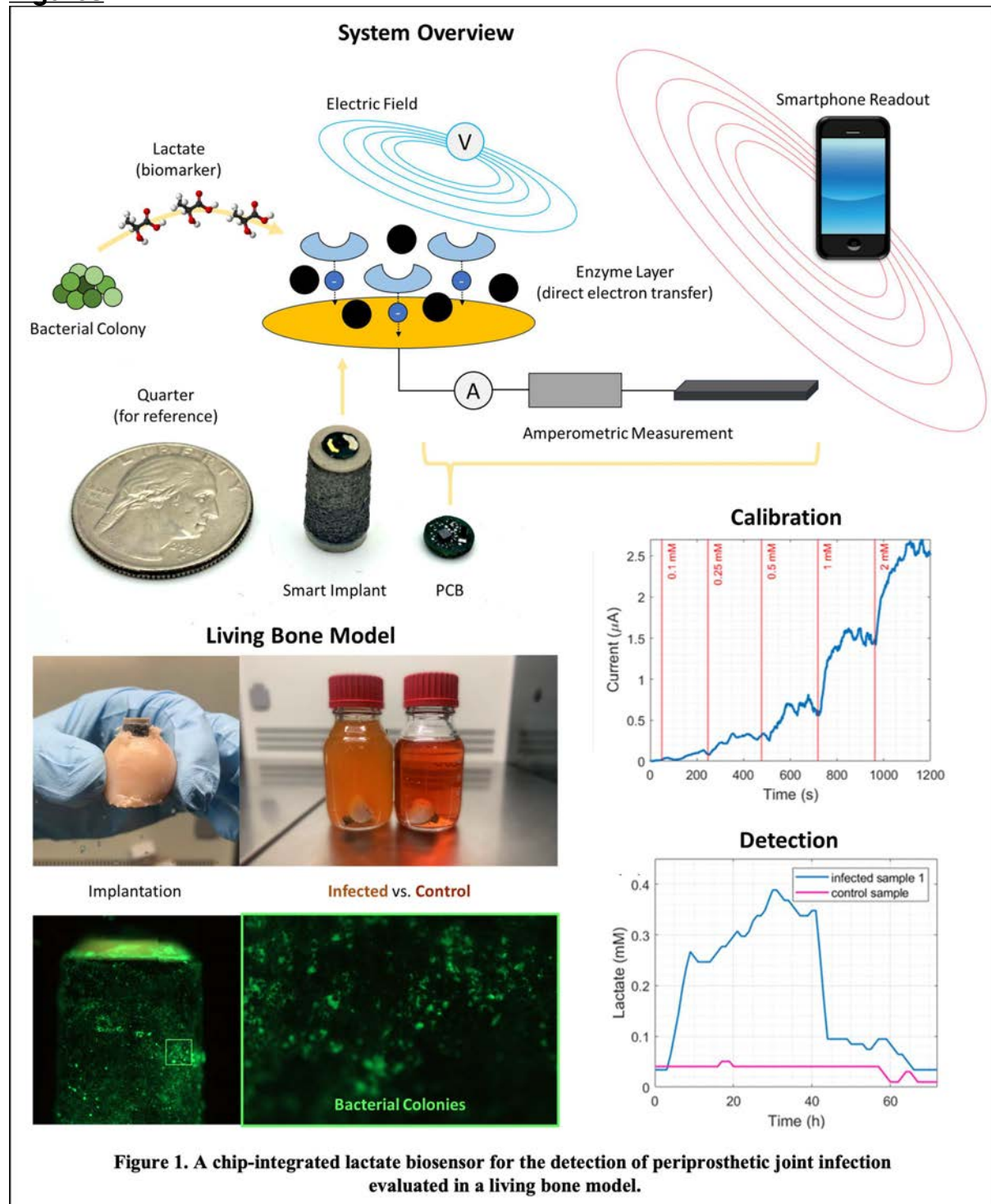


Figure 1

Platelet-Rich Plasma Injections Within 6 Months of Total Knee Arthroplasty Increase the Risk of Postoperative Surgical Site Infections

*Matthew Magruder - Maimonides Medical Center - Brooklyn, USA

Ameer Tabbaa - x, United States of America

Gabriel Lama - Maimonides Medical Center - Staten Island, United States of America

Orry Erez - Maimonides Medical Center - Brooklyn, USA

Introduction

Platelet-rich plasma (PRP) injections for the treatment of knee osteoarthritis has demonstrated beneficial effects on pain and function, but remains controversial. Nonetheless, PRP usage has been increasing in the last decade, many of which are given just prior to total knee arthroplasty (TKA). However, there is little data that have evaluates TKA postoperative outcomes following recent PRP injections.

Methods

A retrospective query was performed using a National database from January 2010 to March 2021. Patients who underwent TKA for osteoarthritis with a history of a PRP injection (CPT code 0232T) were identified. Patients were then segregated into three groups, those who received PRP injections: (1) < 6 months prior to surgery (PRP 0-6); (2) between 6 and 12 months before surgery (PRP 6-12); and (3) > 12 months before surgery (PRP >12). We did not use a no-PRP group because PRP is not covered by insurance, and the “no PRP” patient population would be significantly different from the those that received PRP injections likely uncontrollable ways. We conducted propensity score-matching for each combination of the three groups based on age, sex, obesity, diabetes mellitus (DM), smoking status and rheumatoid arthritis (chosen because they are common risk factors for postoperative infection). Matching was successful between the three groups (Table 1). Outcomes included 90-day and 2-year superficial surgical site infection (SSI), 90-day and 2-year prosthetic joint infection (PJI) and, 90-day and 2-year revisions, and 90-day readmissions. Multivariate logistical regressions calculated odds ratios (ORs), 95% confidence intervals, and *P*-values (significance threshold <0.05).

Results

The incidence and risk of each outcome can be viewed in Table 2. There were no significant differences in any outcome measure between the PRP 0-6 group and PRP 6-12 group (Table 3). Furthermore, there were no significant differences between the PRP 6-12 and PRP >12 groups (Table 3). When comparing PRP 0-6 and PRP >1 year groups, odds of 2-year SSI were significantly higher in the PRP 0-6 group (OR 7.74; *P* = 0.022). In addition, 90-day SSI trended towards being significantly higher in the 0-6 group compared with PRP >1 year (OR 7.9; *P* = 0.11). There were no significant differences in odds in any other complication.

Discussion

We present a retrospective analysis of postoperative surgical site infection risk following TKA patients who received a PRP injection. We demonstrate there to be a significant increase in the 2-year SSI risk in the group who received injections within 6 months prior to surgery, and a strong trend toward significance at 90 days. Importantly, we did not demonstrate an increased risk of PJI in any comparison of timepoints. This contrasts with the literature regarding preoperative corticosteroid injections, which have demonstrated increased risk of PJI when given prior to TKA. This difference may be due to the potent immunosuppressive nature of the

corticosteroids, in contrast to the mechanism of PRP. Many PRP injections are concentrated with immune cells (i.e. leukocyte-rich PRP) and could represent a protective measure against deep infection in the right patient population.

Comparison of Wound Irrigation Solutions Using an Ex Vivo Human Bone Organ Culture Model: Insight Into Antibacterial Effectiveness

*Hugh Jones - UT Health Science Center at Houston - Houston, USA

Mark Coggins - University of Texas Health Science Center at Houston - Bellaire, USA

Angus Brooks - University of Texas Health Science Center at Houston - Bellaire, USA

Catherine Ambrose

Steven Schroder - University of Texas Health Science Ctr - Houston, USA

David Doherty - The University of Texas Health Science Center - Houston, USA

Kenneth Mathis - The Methodist Hospital - Houston, USA

Robert Frangie - University of Texas - Houston, United Kingdom

David Rodriguez - University of Texas - Houston, USA

Background: It is estimated that by 2030 the number total knee arthroplasties (TKA) will reach 3.5 million. As this number grows, the number of TKA revisions increase with some estimates being as high as 12%. There are several mechanisms of TKA failure with infection being the leading factor (29.3%). Use of intra-operative irrigation solutions which balance antimicrobial efficacy and host cell toxicity can be an effective strategy in reducing infection. In this study we evaluate 7 irrigation fluids using a human *ex vivo* organ culture methodology to best replicate the infection site. The solutions evaluated use an array of technologies and antimicrobial agents, including acids and surfactants, chlorhexidine gluconate (CHG), benzalkonium chloride (BZK), polyhexamethylene biguanide (PHMB), and povidone iodine (PI).

Methods: Viable human femoral heads were collected during total hip arthroplasty. Cancellous bone cores were harvested and inoculated with *S. aureus* in media best replicating human serum. Half of the cores were treated with the irrigation solutions and the remaining patient matched cores were washed in saline. CFU counts were compared both acutely and 24 hours after treatment. Other treated cores were incubated in a dynamic bioreactor system that provided the biochemical and mechanical environment for bone. These specimens were metabolically and histologically compared to saline controls.

Results: PHMB and CHG containing solutions showed acute reductions greater than 3-log. After 24 hrs of incubation, PHMB and acetic acid/ethanol formulations reduced by over 6-log (Figure 2). The acetic acid/ethanol based solution had significantly less metabolic activity than the control. No other significant difference were found between the remaining groups.

Conclusions: While standard *in vitro* cell culture has a place, use of more complex and relevant models, such as the *ex vivo* bone model described here, can provide more insight as the biochemical environment impacts both bacterial metabolic activity and antimicrobial agent efficacy.

Figures

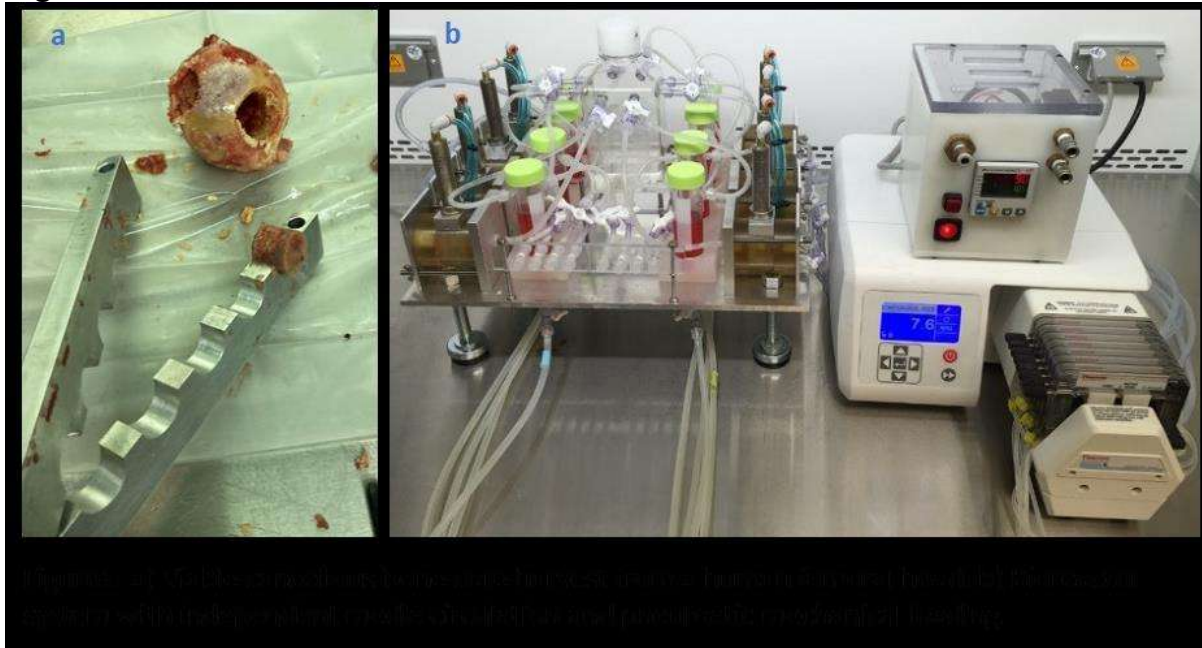


Figure 1

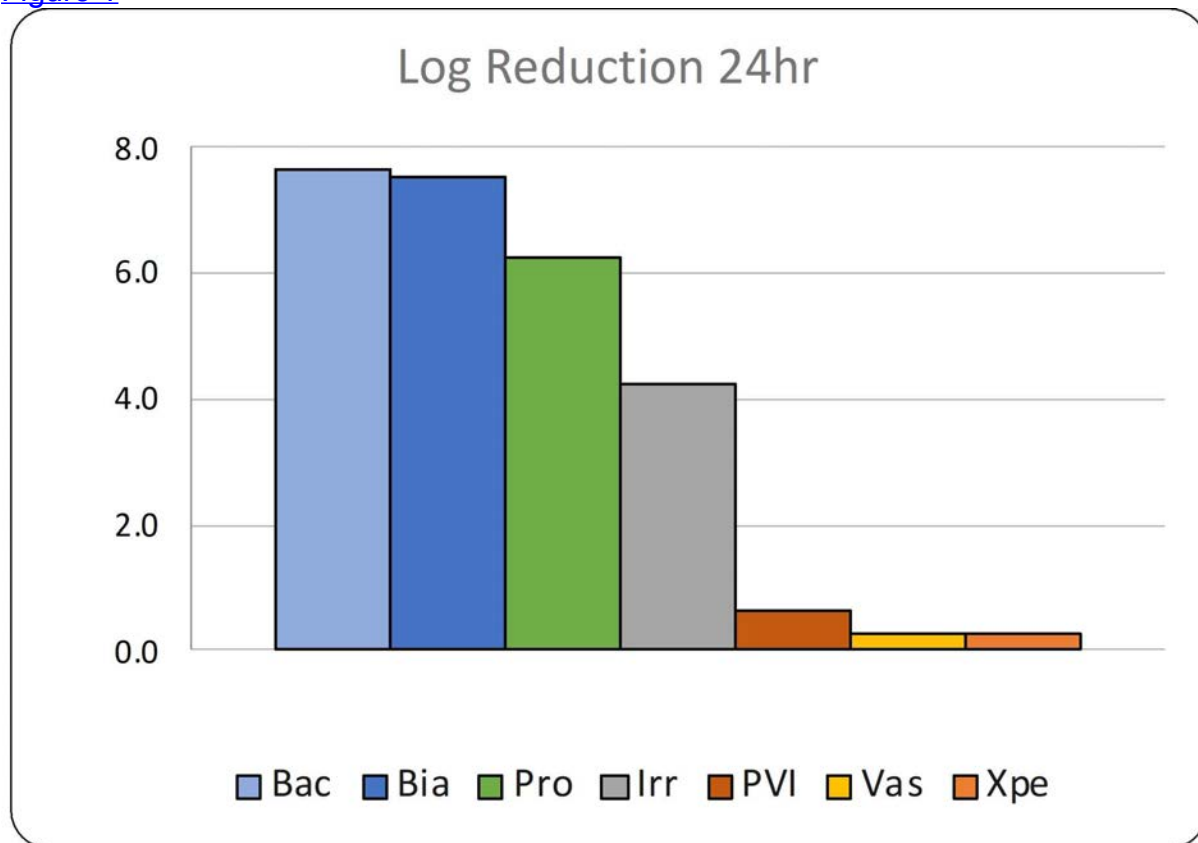


Figure 2. Chart showing log reductions of each irrigation fluid 24 hours after treatment.

Figure 2

A Workflow-Efficient Approach to Pre- and Post-Operative Assessment of Weightbearing 3D Knee Kinematics

*Scott Banks - University of Florida - Gainesville, USA

Gokce Yildirim - Vent Creativity - Weehawken, USA

George Jachode - Imaging Engineering, LLC - Gainesville, USA

John Cox - Imaging Engineering, LLC - Gainesville, USA

Andrew Jensen - Vent Creativity - New York, USA

Oren Anderson - Imaging Engineering, LLC - Gainesville, USA

J. Dean Cole - Orlando Health - Orlando, USA

Oliver Kessler - Center for Orthopaedics and Sport - Zurich, Switzerland

Introduction: Knee kinematics during daily activities reflect disease severity pre-operatively and are associated with clinical outcomes after total knee arthroplasty (TKA). It is widely believed measured kinematics would be useful for pre-operative planning and post-operative assessment. Despite decades-long interest in measuring 3D knee kinematics, no methods are available for routine, practical clinical examinations.

We report a clinically practical method utilizing machine-learning enhanced software and upgraded c-arm fluoroscopy for the accurate and time-efficient measurement of pre- and post-TKA 3D dynamic knee kinematics.

Methods: Using a common c-arm with an upgraded detector and software, we perform a 5-second horizontal sweeping pulsed fluoroscopic scan of the weightbearing knee joint. The patient's knee is then imaged using pulsed c-arm fluoroscopy while performing standing, kneeling, squatting, stair or chair and gait motion activities. Fully autonomous software uses limited-arc cone beam reconstruction methods to create 3D models of the femur and tibia/fibula bones, with or without implants, and then performs model-image registration to quantify the 3D knee kinematics with accuracy comparable to previously reported methods.

Results: The proposed protocol can be accomplished by an individual radiology technician in 5-10 minutes and does not require additional equipment beyond a stair or chair. The image analysis can be performed by a computer onboard the upgraded c-arm or in the cloud, before loading the examination results into the PACS and EMR systems.

Discussion: Weightbearing kinematics affect knee function pre- and post-TKA. It has long been exclusively the domain of researchers to make such measurements. We present an approach that leverages common, but digitally upgraded, imaging hardware and novel software to implement an efficient examination protocol for accurately assessing 3D knee kinematics. With these capabilities, it will be possible to include dynamic 3D knee kinematics as a component of the routine clinical workup for patients with diseased or replaced knees.

Articulation and Axial Rotations of Normal and CR TKA Knees During Flexion

*Guoan Li - Orthopaedic Bioengineering Research Center, Newton-Wellesley Hospital - Newton, USA

Background: Axial tibial rotation of the knee with flexion is recognized as a characteristic motion pattern that can affect the knee joint function. Numerous studies have reported that it is a challenge to restore normal axial tibial rotation using a contemporary total knee arthroplasty (TKA). Our objective is to investigate the mechanisms that limit axial tibial rotations of TKA knees by comparing the tibiofemoral articular motions of normal and TKA knees during a weightbearing flexion.

Materials and Methods: We measured in-vivo kinematics of 20 healthy knees and 11 patients with a unilateral CR TKA in our previous studies using a validated dual fluoroscopic imaging system (DFIS) (**Fig. 1a**). The articular contact distances on both the medial and lateral femoral condyles and tibial surfaces were analyzed at every 15° flexion interval along the flexion path from 0° to 105° (**Figs. 1b,c**). In this paper, we calculated asymmetric articulations using the differences between the medial and lateral articular distances of both femoral condyles and tibial surfaces at each flexion interval and compared the articulation asymmetry and axial tibial rotations of normal and TKA knees.

RESULTS: Both normal and TKA knees had longer articulation distances on medial than on lateral femoral condyles, the articular contact distances of the normal knees were significantly longer than TKA knees on medial femoral condyles (**Fig. 2a**), but shorter on lateral condyles at low flexion intervals ($p < 0.05$) (**Fig. 2b**), indicating that the asymmetric articulations on femoral condyles of normal knees are larger than on TKA knees. The asymmetric articulations on tibial surfaces are similar for both knees. Internal tibial rotations were $6.8 \pm 4.5^\circ$ for normal and $1.5 \pm 2.2^\circ$ for TKA knees at the flexion interval of 0°-15° (**Fig. 2c**). Total internal tibial rotations of the normal knees consistently increased with flexion and reached a peak of $18.4 \pm 7.8^\circ$, while the TKA knees had a maximal internal tibial rotation of $5.5 \pm 3.5^\circ$ (**Fig. 2d**).

DISCUSSION: This study analyzed biomechanical factors that could limit axial tibial rotations of the knee after a CR TKA during a weightbearing flexion. The data revealed that the TKA knees cannot restore the asymmetry of tibiofemoral articulations compared to the normal knees during the flexion. Consequently, the axial tibial rotations of the TKA knees were significantly reduced compared to the normal knees along the flexion path. Therefore, future investigations should focus on improvement of tibiofemoral articulations of the TKA knees to restore normal axial tibial rotations.

SIGNIFICANCE/CLINICAL RELEVANCE: This study revealed the physiological mechanisms that limit the axial tibial rotations of the knee after a CR TKA. The data could be instrumental for future improvement of TKA designs and surgical implantation techniques to restore normal knee functions.

Figures

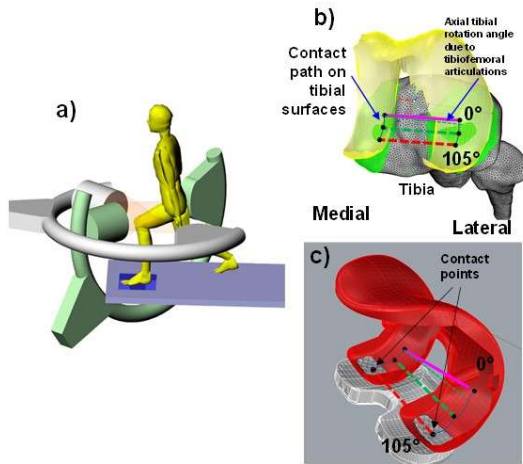


Fig. 1. (a) The dual fluoroscopic imaging system (DFIS) set up for measurements of knee joint positions during weightbearing flexion. (b) In-vivo normal and (c) TKA knee contact positions at different flexion angles along the flexion path reproduced using 3D models of the knee.

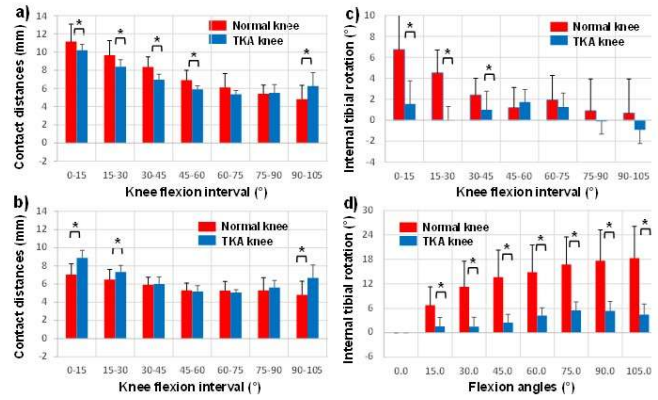


Fig. 2. Articular contact distances (Mean±SD) on the (a) medial and (b) lateral femoral condyles of the normal and TKA knees. Internal(+) and external(-) tibial rotations (c) at all flexion intervals and (d) along flexion path of the knee. A *** indicates that the data are significantly different between the normal and TKA knees ($p < 0.05$).

Figure 1

Reliable Predictions of Knee Kinematics Through Validated Knee Computer Models Are Important to Help Improve Clinical Outcomes After TKA

*Eik Siggelkow - Zimmer GmbH - Winterthur, Switzerland

Marc Bandi - Zimmer GmbH - Winterthur, Switzerland

Kyle Snethen - Zimmer Biomet - Warsaw, USA

Introduction: Surgical robots and virtual tools are widely applied during total knee arthroplasty (TKA) resulting in more accurate placement of implant components. Computer models are commonly used to determine optimal component placement by predicting knee function. However, a correct prediction relies on the accuracy of model derived data. This study compares and validates the resulting kinematics/laxities of implanted knee computer models against independent experimental data sets.

Methods: Experiments: In-vitro experiments on seven human post-mortem knee specimens were performed using a six degrees of freedom (DOF) industrial robot equipped with a six DOF force torque sensor. Implanted knee joints (PCL sacrificing, Persona®Medial-Congruent®, Zimmer Biomet, Warsaw, IN, USA) performed by practicing surgeons using the current surgical technique, were evaluated. Passive knee kinematics while performing laxity tests (varus-valgus (VV) $\pm 12\text{Nm}$, anterior-posterior (AP) $\pm 100\text{N}$, 44N compression) at several flexion angles (extension, 15° , 30° , 60° , 90° , 120°) and knee kinematics during a simulated lunge activity were determined.

Simulation: Virtual knee computer models (Abaqus/Explicit) were created for four separate knee specimens and virtually implanted following the same surgical technique utilized during the experiments. Computer models consisted of 3D geometry of the femur, tibia and fibula bone based on CT and MRI scans including the passive soft tissue contributions. Similar to the robot experiments, laxity testing and activity evaluations were performed.

Resulting kinematics in terms of femorotibial relative translation were analyzed for each experimental and virtual simulation by tracking the medial and lateral femur flexion facet centers (FFCs).

Results: Laxity: Averaged AP and VV-laxity were similar between the physical experiments and simulations (Figure 1 and 2) in magnitude and trend over flexion (RMSE VV med/lat = $2.2\text{mm}/1.1\text{mm}$, RMSE AP = 1.5mm). Averaged medial joint opening during VV-laxity testing was lower for the simulation. Lunge: Femorotibial AP-kinematics were similar in trend and magnitude between simulation and experiment (RMSE = 1.8mm , Figure 3). The simulation resulted in a more anterior femur position during high flexion.

Conclusion: Knee computer models can predict similar laxities and activity kinematics compared to in-vitro experiments. Differences in medial compartment laxities and femoral AP position at high flexion during lunge can be contributed to components placement differences which underlines the importance of correct component placement to achieve accurate predictions. However, since neither the component placements nor specimen specific anatomy was matched between simulation and experiment, taking the level of result agreement into account, the simulations showed a high robustness. This enables the application of simulations beyond specimen/patient specific models.

Figures

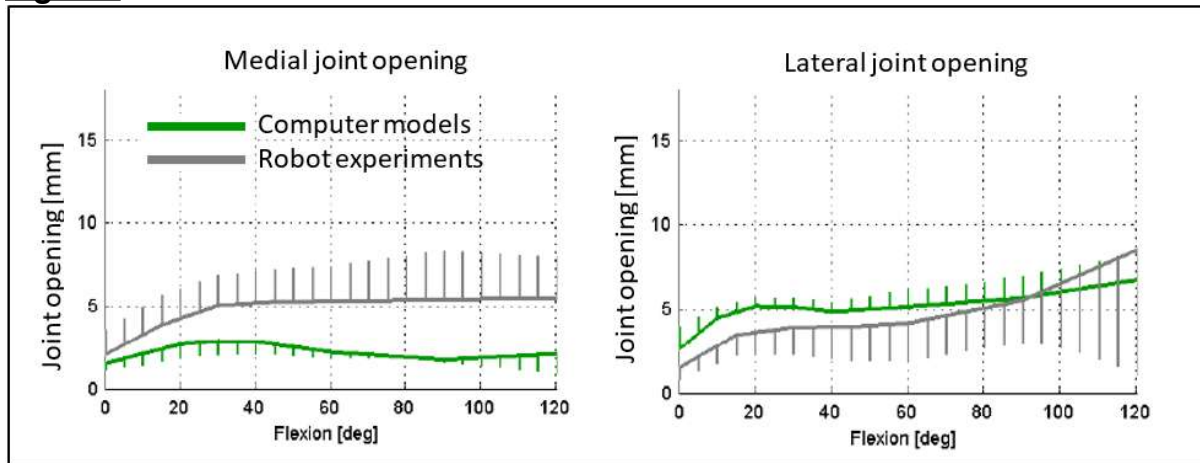


Figure 1. medial and lateral joint opening during varus – valgus laxity testing at several flexion angles

Figure 1

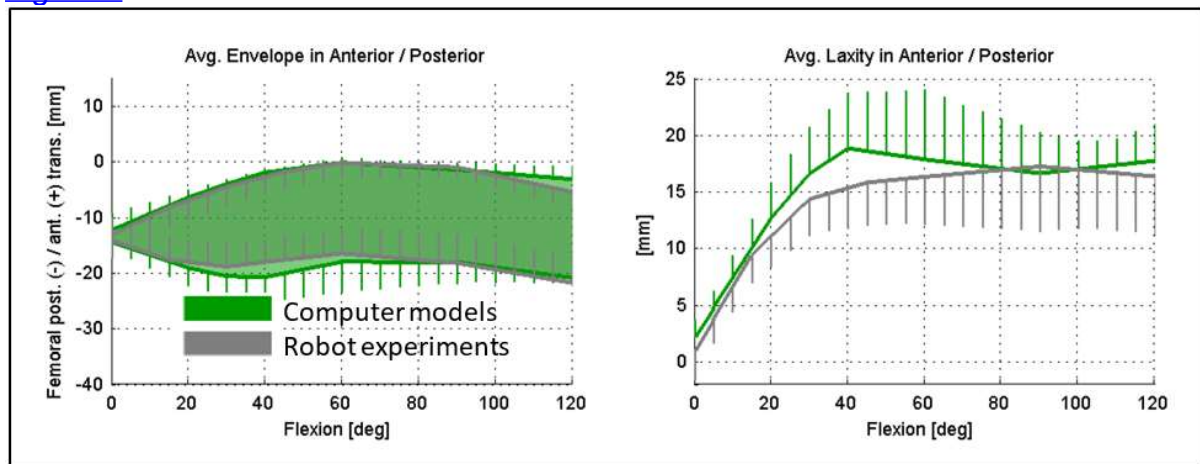


Figure 2. Femorotibial relative anterior-posterior envelope of motion and laxity at several flexion angles

Figure 2

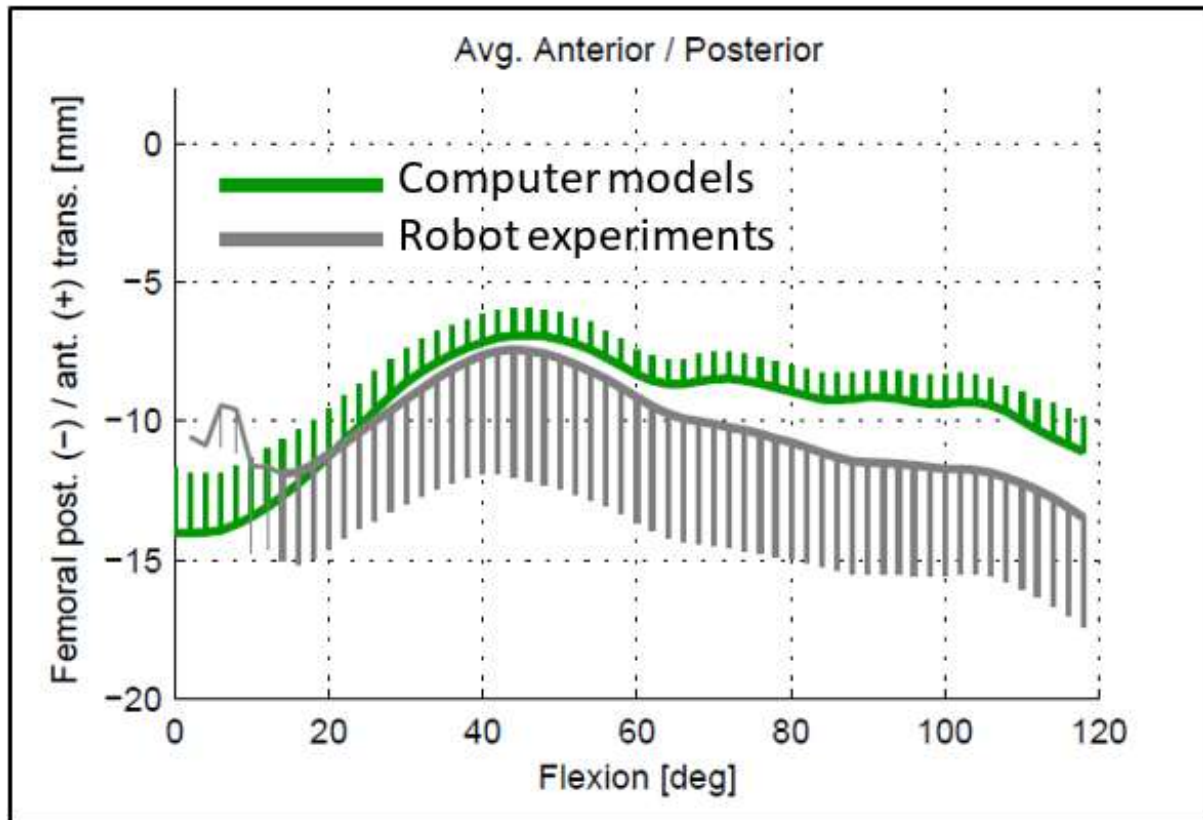


Figure 3. Femorotibial anterior-posterior kinematics during ADL of lunge

[Figure 3](#)

Investigating the Influence of Implant Geometry on Autonomous Kinematics Measurements

*Andrew Jensen - University of Florida - Gainesville, USA

Scott Banks - University of Florida - Gainesville, USA

Kerry Costello - University of Florida - Florida, United States of America

Introduction: Total joint replacements have been studied for decades to understand their in-vivo kinematics, which is crucial for implant design, post-operative assessment, and predicting wear and failure patterns. Recent advancements in computer vision and machine learning have enabled autonomous measurement of total knee arthroplasty (TKA) kinematics using single-plane fluoroscopy. However, applying the same techniques to reverse total shoulder arthroplasty (rTSA) has yielded suboptimal results, particularly along the internal/external rotation axis. This study investigates the fundamental shape aspects of each arthroplasty system to understand the performance differences in autonomous kinematics measurements between TKA and rTSA implants.

Methods: Representative 3D models of rTSA humeral and glenosphere implants, as well as TKA femoral and tibial implants, were obtained from a manufacturer. Binary silhouettes of each implant were rendered to an image plane using an in-house CUDA camera model. The Invariant Angular Radial Transform Descriptor (IARTD) was used to quantify the sensitivity of projected 2D shapes to changes in their 3D orientation. Shape differences were calculated using the central difference equation on the IARTD vector produced from two different orientations, with a grid of sampled orientations spanning $\pm 30^\circ$ with a step size of 5° for each axis.

Results: The humeral implant exhibited the lowest mean shape sensitivity along the internal/external rotation axis (δy) among all implant types. The glenosphere implant showed low sensitivity along the $y = 0$ axis, while the tibial implant displayed low sensitivity along the $x = 0$ axis, corresponding to the "symmetry trap" phenomenon. The femoral implant had the highest average sensitivity overall.

Discussion: The findings correspond closely with the challenges encountered in autonomous kinematics measurement using JointTrack Machine Learning (JTML). The humeral implant's low shape sensitivity, particularly along the internal/external rotation axis, aligns with the difficulties observed in JTML optimization. Similarly, the tibial implant's low sensitivity along the internal/external rotation axis is consistent with the concept of symmetry traps, where two different 3D orientations result in an identical projected shape. The study highlights the limitations of using Euler angles in the optimization process and suggests exploring alternatives such as optimizing directly on the Special Orthogonal group $SO(3)$. Additionally, incorporating bony landmarks and intensity-based metrics could help disambiguate challenging implant poses.

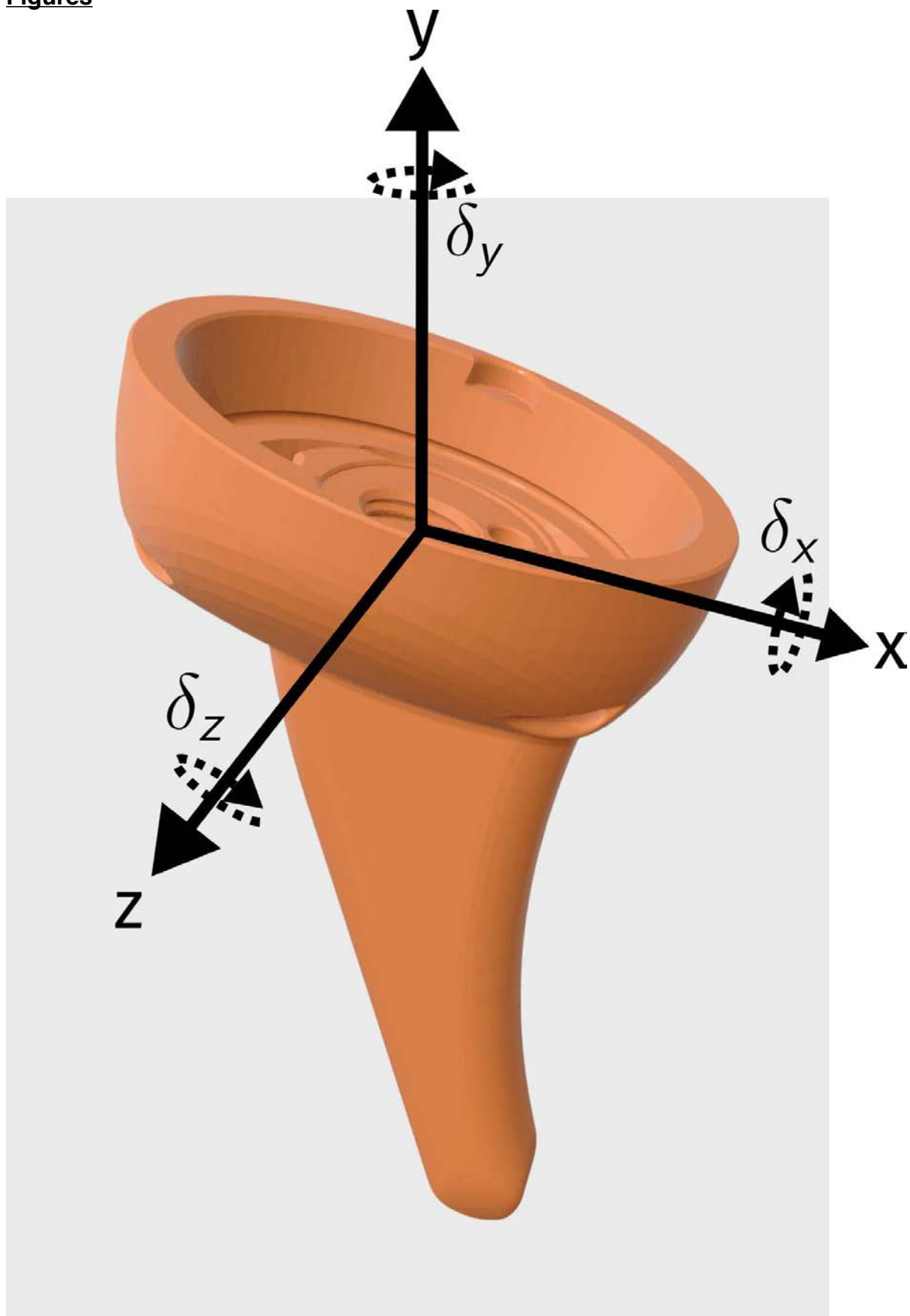
Conclusion: This study demonstrates intrinsic differences between implant types regarding projected 2D shape sensitivity, which align with the difficulties encountered in autonomous kinematics measurement. Small orientation changes yielded negligible 2D variability for near-symmetrical geometries and axes, limiting the data extractable solely from single-plane fluoroscopic silhouettes. Incorporating additional image information, such as bone, and employing precise anatomical constraints could enable robust clinical tracking despite unavoidable ambiguity along select dimensions.

Figure 1: Rotation axis and rotation perturbations on a representative rTSA humeral implant.

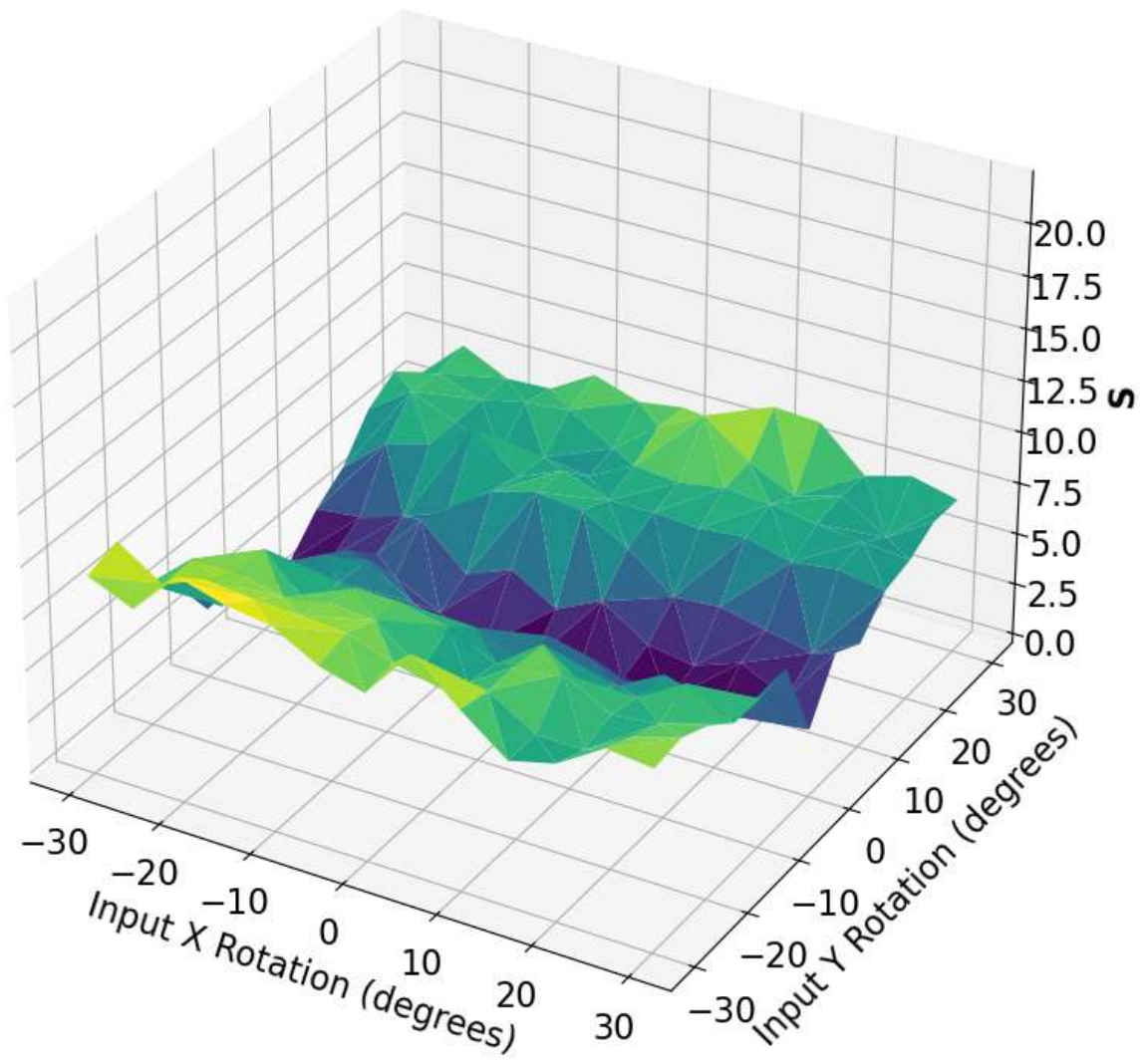
Figure 2: Glenosphere shape sensitivity about the implant's x-axis. The "valley" along $y=0$ is indicative of the near-spherical nature of the implant along that rotation axis.

Figure 3: Tibial shape sensitivity along the implant's y-axis. The valley along $x=0$ represents the "symmetry trap" phenomena reported in mediolaterally symmetric implants during kinematics measurements.

Figures



[Figure 1](#)



[Figure 2](#)

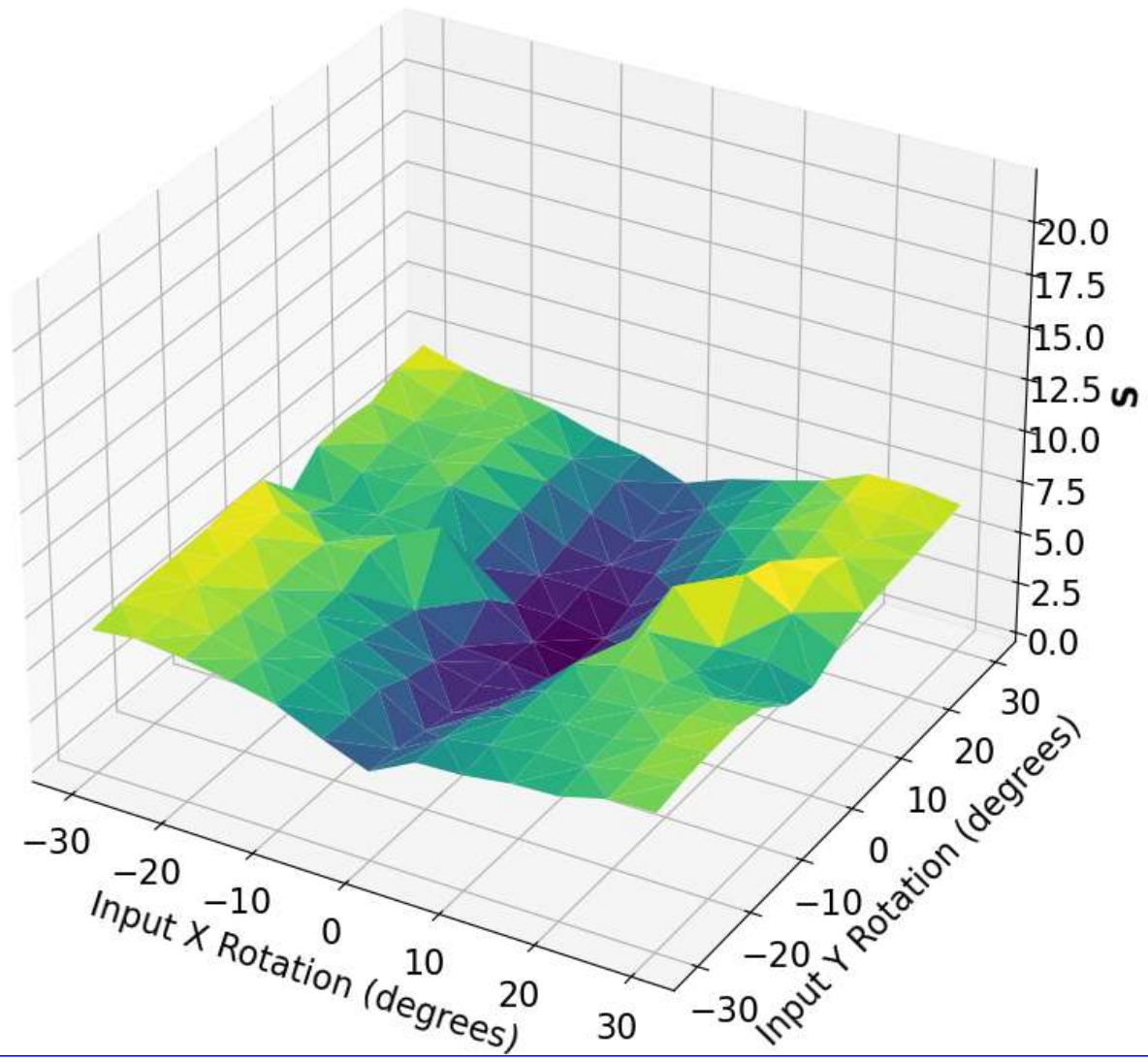


[Figure 3](#)

Bilateral Frontal Plane Lower Limb Alignment From Markerless Motion Capture During Gait Is Correlated Across Severity of Knee OA but Not Post-TKA

*[Elise Laende](#) - Queen's University - Kingston, Canada

Jereme Outerleys - Queen's University - Kingston, Canada

Kevin Deluzio - Queen's University - Kingston, Canada

Introduction

The low burden of data collection with markerless motion capture offers the potential for clinical assessments of orthopaedic patients that incorporate kinematic data. While much gait analysis has been performed unilaterally historically, bilateral data from markerless motion capture provides the opportunity to consider the status of both limbs in biomechanical analyses. The objective of our analysis was to compare bilateral gait waveform data in participants with varying combinations of knee osteoarthritis (OA), post-total knee arthroplasty (TKA), and asymptomatic joints, using principal component analysis (PCA) for the knee joint angle waveforms in the frontal and sagittal planes.

Methods

Orthopaedic patients were recruited from clinic visits. Two advanced practice physiotherapists provided a clinical status assessment (considering x-ray findings, function, and pain) for both knees (as mild, moderate, or severe OA, or asymptomatic, or previous TKA). Additional asymptomatic participants were recruited from the community. Gait was assessed during over-ground walking at a self-selected speed in the clothes and shoes they had worn that day. Markerless motion capture was recorded using 8 commercially available synchronized video cameras (Sony RX0-II) recorded at 60 Hz with 1/125 shutter speed and processed using Theia3D (Theia Markerless Inc., version v2023.1.0.3161p9). PCA was applied to the gait waveforms and principal component (PC) scores, capturing the maximum variability in the waveform data, were calculated for knee joint angles in the frontal plane (knee varus/valgus, stance only) and sagittal plane (knee flexion/extension, whole stride). Simple linear regression was applied to determine correlations of the PC scores for the two sides for all combinations of knee joint statuses. Mild and moderate knee OA were collapsed into a single category ("MildMod").

Results

614 knees in 307 individuals were included. In individuals with a TKA on one side, the frontal plane first principal component (PC1, magnitude of knee varus/valgus alignment during stance) was not correlated with the other side, but for all other combinations of clinical status, there were statistically significant correlations, with stronger correlations for the same clinical status on both sides (Fig. 1). In the sagittal plane, PC2 (associated with stiff knee gait) was significantly correlated across all groups.

Conclusions

Despite different degrees of knee OA severity, frontal plane gait waveform PC1 scores, capturing varus/valgus alignment, were significantly correlated for all combinations of unreplaced joints, including asymptomatic and severe knee OA. This indicates a level of patient-specific frontal plane alignment in both limbs that is retained across severities of knee OA. Frontal plane alignment, however, was not correlated between replaced and non-replaced joints, likely indicative of TKA placement in a standard neutral alignment. The correlations in alignment between sides have implications for TKA placement in patient-specific frontal plane

alignments, as these findings suggest that both pre-operative and contralateral alignment measures could be considered in defining patient-specific TKA alignment targets.

Figures

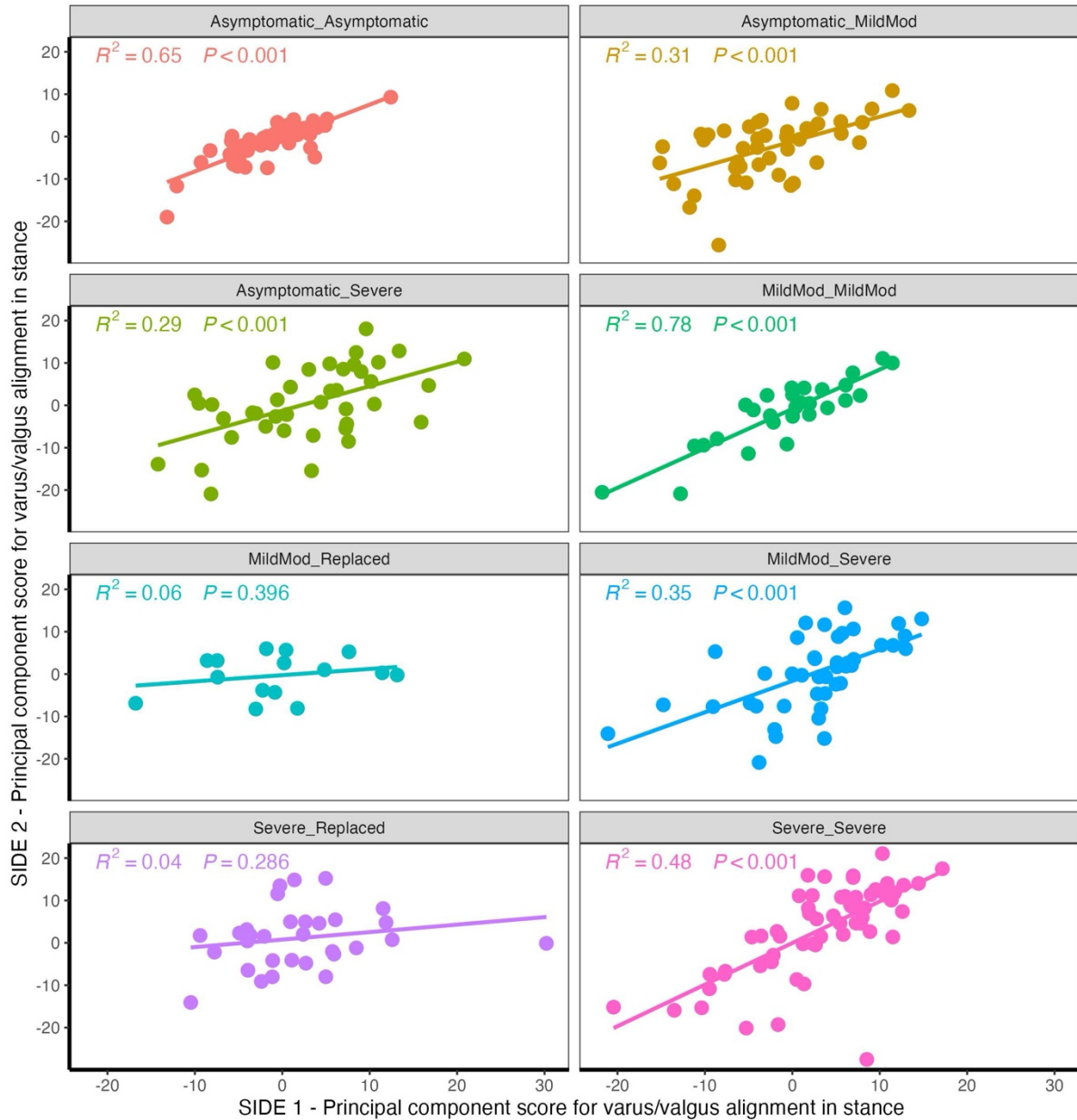


Fig. 1 : Correlations between frontal plane PC scores (magnitude of knee varus/valgus alignment during stance) of both legs for all combinations of clinical status. "Replaced" = post-TKA, "MildMod" = mild or moderate OA.

Figure 1

Knee Contact Forces in OA Patients During Gait

*Mario Lamontagne - University of Ottawa - Ottawa, Canada

Alexandre Pelegrinelli - State University of Londrina - Londrina, Brazil

Danilo S. Catelli - University of Ottawa - Ottawa, Canada

Erik Kowalski - University of Ottawa - Ottawa, Canada

Felipe A. Moura - State University of Londrina - Londrina, Brazil

Purpose

The objective of this study was to characterize and examine the overall tibiofemoral contact forces (TFCF), as well as those specifically within the medial and lateral knee compartments, during gait in individuals affected with knee osteoarthritis (OA) compared to healthy control subjects.

Methods

A cross-sectional investigation involved 14 individuals diagnosed with severe knee OA alongside 14 control subjects. Analysis was conducted on five gait cycles during the stance phase, performed at a self-selected speed. Gait data was captured using a synchronized motion capture system and force platforms installed in a 10-meter walkway. A modified musculoskeletal model [1] estimated total tibiofemoral contact forces (TFCF) and those within the medial and lateral compartments. Joint angles and net joint moments for each degree of freedom were determined through inverse kinematics and inverse dynamics tools, respectively, while muscle forces were computed using a static optimization approach. TFCF was calculated utilizing the *JointReaction* analysis in OpenSim [2]. Temporal series results were compared employing Statistical nonparametric mapping (SnPM) for independent samples, with significance set at $P < 0.05$.

Results

No significant differences in gait speed were observed between the groups: OA group recorded a speed of 1.27 (1.02; 1.35) m/s, while the control group recorded 1.24 (1.15; 1.40) m/s. However, in the OA group, the 1st peak in the medial TFCF compartment was notably smaller compared to controls, ranging between 8% and 22% ($P = 0.006$). Additionally, in terms of total TFCF, the OA group displayed a more pronounced valley between peaks in contrast to controls, with a difference ranging from 38% to 54% ($P = 0.001$) (Figure 1).

Conclusion

The OA group demonstrated a diminished peak of absorption in the medial compartment, leading to a reduction in compressive force in this area, which is typically the most affected in OA. This decline could be attributed to a gait strategy involving a medialization of the lower limb in the frontal plane, consequently transferring the compressive force to the lateral side of the knee. Furthermore, the total contact force was elevated between peaks in the OA group, indicating increased overload during the stance phase, potentially linked to cartilage degeneration and joint pain. Although the peaks of TFCF were similar between groups, OA patients exhibited decreased force in the medial compartment while displaying higher sustained loading throughout the stance phase.

References

1. Pelegrinelli ARM, Catelli DS, Kowalski E, Lamontagne M, Moura FA. Comparing three generic musculoskeletal models to estimate the tibiofemoral reaction forces during gait and sit-to-stand tasks. *Med Eng Phys.* 2023; 122:104074.
2. Delp SL, Anderson FC, Arnold AS, Loan P, Habib A, John CT, Guendelman E, Thelen DG. OpenSim: Open-source Software to Create and Analyze Dynamic Simulations of Movement. *IEEE Transactions on Biomedical Engineering.* 2007.

Figures

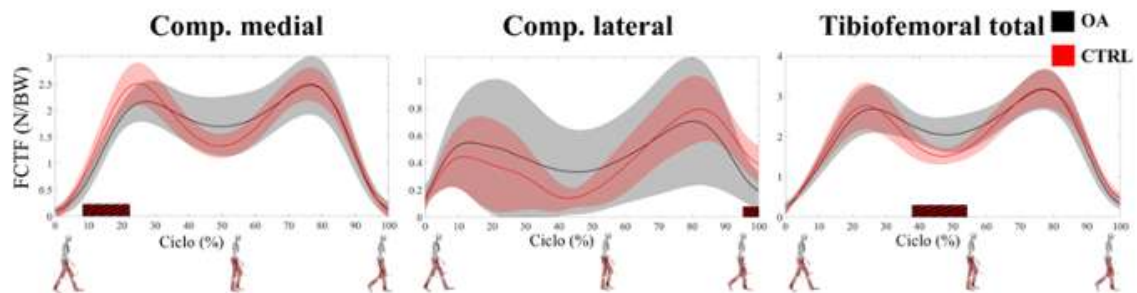


Fig 1: Tibiofemoral contact forces on the medial (left) and lateral (central) compartments, as well as total contact force (right). The rectangles at the bottom represent the moments during the gait cycle with differences between the groups. TFCF: Tibiofemoral contact force; N/BW: Newton/body weight.

[Figure 1](#)

In Vivo Assessment of Robotically Performed Total Knee Arthroplasty for Posterior-Cruciate and Bi-Cruciate Retaining and Substituting Implants

Michael Tim Yun Ong - Prince of Wales Hospital - Sha Tin, Hong Kong

Patrick Shu-Hang Yung - Prince of Wales Hospital the Chinese University of Hong Kong - Sha Tin, Hong Kong

Garett Dessinger - The University of Tennessee - Knoxville, USA

Richard Komistek - The University of Tennessee - Knoxville, USA

*Michael LaCour - University of Tennessee - Knoxville, USA

Introduction

Ligament management during total knee arthroplasty (TKA) is historically difficult, particularly involving the ACL. Recently, novel implants that retain or substitute for the ACL have been developed, as robotically assisted surgery has enabled improved cut precision, making difficult operations more reasonable. The objective of this study is to compare in vivo, weight bearing kinematics for bi-cruciate stabilized (BCS), posterior stabilized (PS), bi-cruciate retaining (BCR), and posterior cruciate retaining (CR) TKAs. To the authors' knowledge, this is the first study to directly compare all four implant types with surgeries performed in their respective robotic platforms.

Methods

Sixty-nine patients were implanted by the same surgeon using the corresponding robotic surgical technique. Twenty patients were implanted with Smith & Nephew Journey II BCS TKAs, 14 with Stryker Triathlon PS TKAs, 20 with the Journey II BCR TKAs, and 15 with the Triathlon CR TKAs. Subjects were analyzed using 3D-to-2D fluoroscopic image registration while performing both deep knee bend (DKB) and step up (SU) activities. In all cases, medial and lateral condylar motion (negative: posterior rollback) as well as femorotibial axial rotation (positive: external femorotibial rotation) were determined.

Results

Lateral condyle motion is shown in Figure 1. Interestingly, the functionality of both anterior and posterior cams is evidenced: during the first 30° of flexion, the anterior cam of the JII BCS TKA pushes the femur anteriorly. During mid-flexion and into deeper flexion, both systems have their posterior cam engaged, thus these motion patterns are similar. For both retaining implants, the CR TKA has less condylar rollback and more anterior sliding compared to the BCR implant, although both systems are less than their respective stabilized implant.

Medial condyle motion is shown in Figure 2. Notably, both Journey II systems are shifted anteriorly compared to the Triathlon systems, again evidencing anterior cam or ACL function. Femorotibial axial rotation is shown in Figure 3. Both Journey systems experience more axial rotation than their respective Triathlon systems, with the CR displaying instances of reverse axial rotation in early flexion.

In all cases, the anhyseretic nature of a flexion activity (DKB) and an extension activity (SU) is evidenced, as the extension curves for SU are nearly identical to the flexion curves of DKB.

Conclusion

This study confirms successful functionality of ACL management in the Journey II systems. While robotic tools allow increased precision for component placement, retention or substitution for the ACL enabled knee kinematics that more closely resemble the normal knee.

Figures

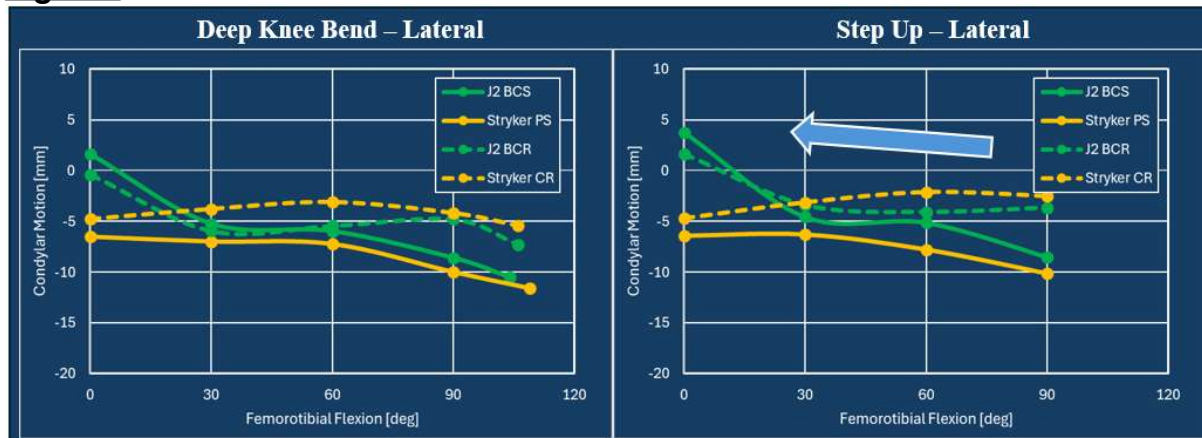


Figure 1

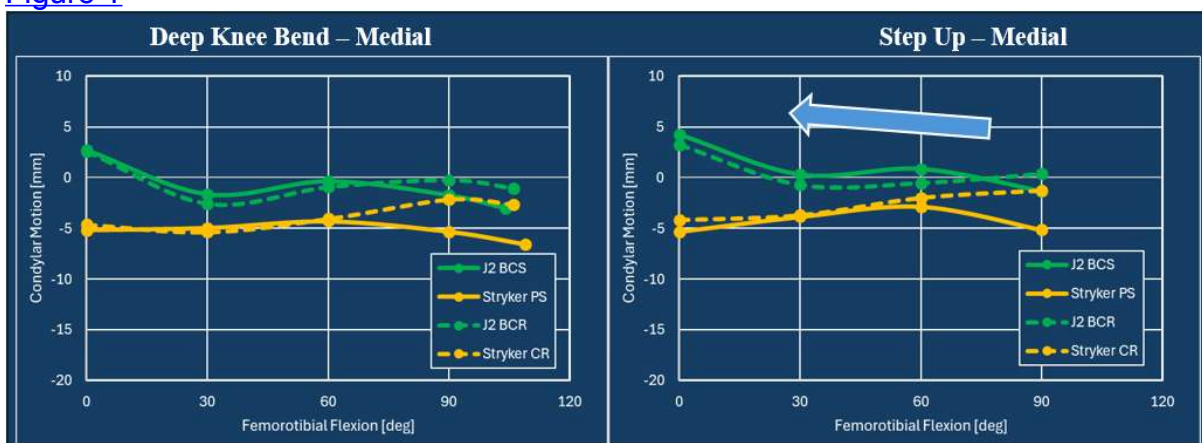


Figure 2

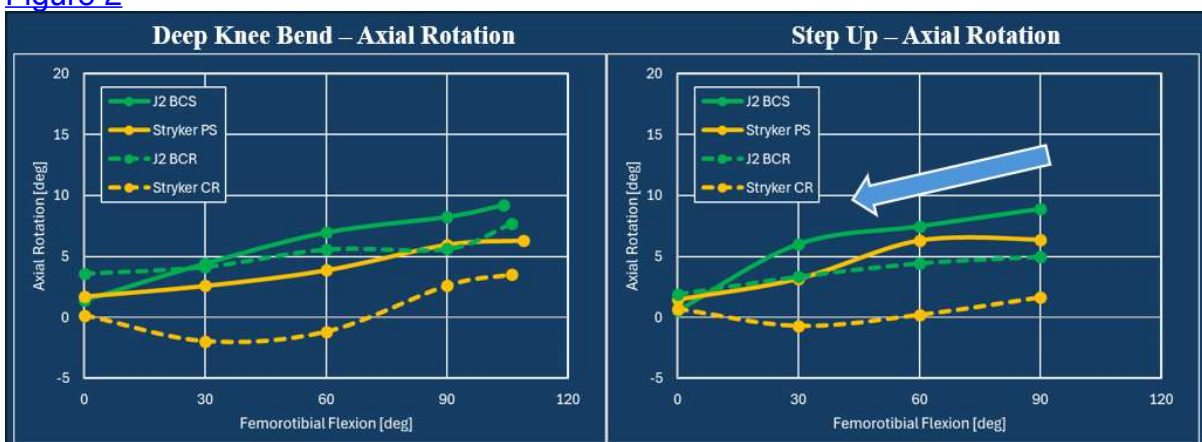


Figure 3

Improvement in Gait Five Years After Ceramic-on-Ceramic Hip Resurfacing Arthroplasty

*Amy Maslivec - Imperial College London - London, United Kingdom
Brogan Guest - Imperial College London - London, United Kingdom
Justin Cobb - Imperial College - London, United Kingdom

Introduction

Ceramic-on-Ceramic Hip Resurfacing Arthroplasty (cHRA) has demonstrated better physical activity and functional outcomes compared to Total Hip Arthroplasty (THA) and shown to restore gait function to near normal levels 12 months post-operatively. However, little is known about whether these functional improvements are sustained five years after surgery. This study examined physical activity levels and gait function of patients with cHRA using subjective and objective measures pre-operatively, one year and five years post-operatively.

Methods

41 unilateral patients (Age: 54.7, Male:31, Female:10, BMI:26.4) of a cHRA with a posterior approach completed patient reported outcome measures (PROMs) (Oxford Hip Score (OHS), EQ5D and MET score) and completed an instrumented treadmill gait analysis at three time points: pre-operatively, one year and five years post-operatively. Top walking speed (TWS), ground reaction force (GRF) profile and gait symmetry were measured. Motion capture analysis was used to record sagittal and frontal gait kinematics five years post-operatively. All gait data were compared to 35 age, gender and BMI matched healthy controls. Statistical Parametric Mapping (SPM) was used for analysis.

Results

PROMs significantly improved from pre-operatively to one year post-operatively and remained significantly unchanged from one to five years post-operatively (OHS: 27, 48, 48; EQ5D: 0.6, 1, 1; MET (6.69, 10.25, 11.31). TWS increased by 20% from pre-operatively to one year post-operatively (5.8 vs 7.03km/hr, $p=0.00$) and only a 1% difference between one and five years (7.0 vs 6.9km/hr, $p=0.67$). Pre-operatively, patients demonstrated an asymmetric GRF profile as SPM showed significantly higher loading of the non-affected leg. At one year and five years post-operatively, SPM revealed no significant GRF differences between legs and therefore a symmetrical gait profile (Figure 1). When comparing the affected leg at one year post-operatively compared to pre-operatively, patients increased loading of the affected leg at heel strike (1.12 vs 1.17, $p=0.01$) and produced a stronger push-off (1.02 vs 0.97). Push-off significantly improved at five years compared to one year post-operatively (1.02 vs 1.06, $p=0.02$) (Figure 2). GRF profile at one and five years post-operatively was comparable to healthy controls. SPM showed hip range of movement in the sagittal and frontal planes at five years post-operatively was comparable to healthy controls (Figure 3).

Conclusion

These mid-term gait results of Ceramic-on-Ceramic Hip Resurfacing Arthroplasty appear promising, indicating a return to a near-normal gait pattern and improved overall quality of life. These positive findings may be attributed to the absence of an intramedullary stem, avoiding stiffening of the femur, thus allowing higher physical activity levels and a near-normal gait pattern.

Figures

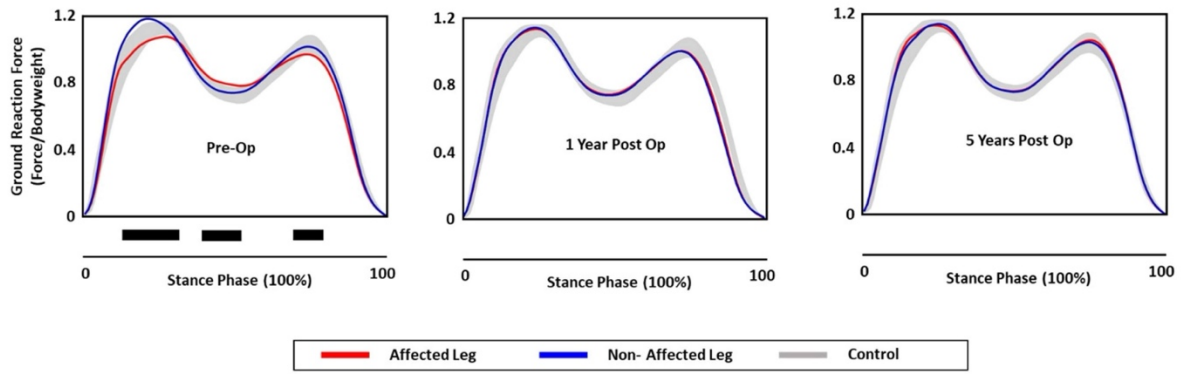


Figure 1. SPM analysis of GRF profile between affected and non-affected leg pre-operatively, one year and five years post-operatively. Horizontal black bars indicate significant difference between limbs.

Figure 1

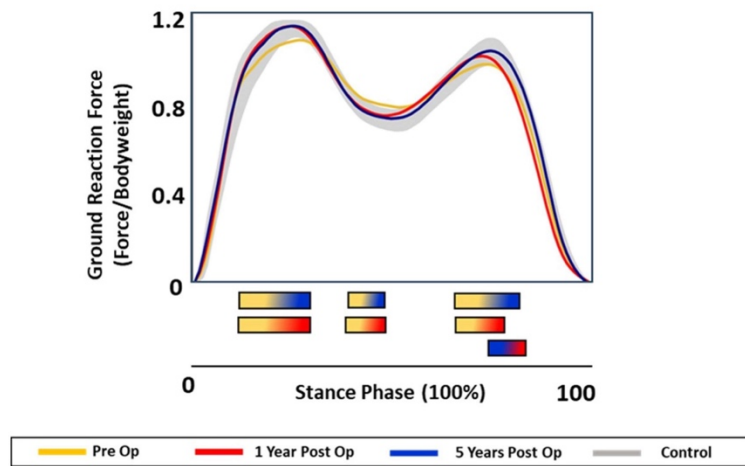


Figure 2. SPM analysis of GRF profile for the affected leg pre-operatively, one year and five years post-operatively. Horizontal bars indicate where the comparisons are, represented by the two colours of the bar. For example, yellow and red represent the comparison between pre-operatively and one year post-operatively.

Figure 2

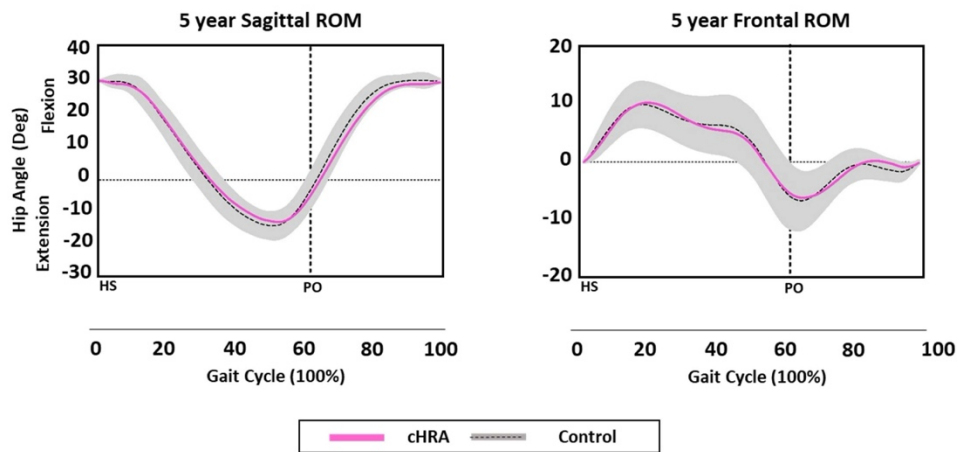


Figure 3. SPM analysis of hip angle of the affected leg in the sagittal and frontal planes compared to a healthy control group with normative range. HS=heel strike, TO=toe off.

[Figure 3](#)

Accelerated and Real-Time Aging of Cemented Ceramic Resurfacing Heads

*Danielle De Villiers - MatOrtho Ltd - Leatherhead, United Kingdom

Simon Collins - MatOrtho Limited - Leatherhead, United Kingdom

Introduction

Current Metal-on-Metal (MoM) hip resurfacing devices most commonly use hybrid fixation: a cemented head and cementless cup. Newer devices under clinical development/trials do not have the history of these established fixation methods. Ceramics offer a more biocompatible material than CoCrMo MoM implants and produce less wear. Direct fixation of the ceramic with cement is however relatively untested clinically, particularly in the short and long term. This study considers cementation of a ceramic resurfacing head comparing the fixation strength up to 2 years using real time and accelerated aging.

Methods

Fifteen 40mm diameter Biolox delta resurfacing heads were cemented onto prepared sawbones blocks. These were split into five groups to be tested at different time points: immediately following implantation, 30 days stored in saline at 37°C, 2 years stored in saline at 37°C, 2 years stored dry at room temperature, 37 days stored in saline at 80°C (equivalent to 2 years). Fixation strength was assessed by measuring torsional strength. After each storage period the heads were attached to a custom-made fixture and torque applied until failure.

Results

The average torque to failure in the implants tested following 'implantation' was 16.62Nm. Following 30 days of storage, the torque to failure did not change. After 2 years of storage the torque to failure was recorded as 20Nm regardless of storage condition. The heads which were subjected to accelerated aging at 80°C saw a dramatic decline in torque to failure to 3Nm.

Conclusions

The immediate and real time fixation strength of cemented ceramic was 6 times the jogging torque in an individual weighing 72.3kg which is sufficient for clinical use. The accelerated aging samples showed a reduction in fixation strength which was determined to be due to the increased temperature being above the glass transition temperature of the cement. This highlights the importance of careful consideration of accelerated aging techniques. Real time aging better mirrors the in vivo experience with over 600 implants now at 2 years and no reports of bonding failure and up to 5.5 years without failure of the cement-ceramic bond.

Figures



[Figure 1](#)

Table 1: Average torque to failure after different storage conditions

Condition	Average torque (Nm) (sd)
Implantation	16.62 (1.8)
30 days at 37°C	16.32 (1.76)
2 years at 37°C	21.96 (1.89)
2 years at room temperature	19.26 (0.87)
37 days at 80°C	3

[Figure 2](#)

15 Year Minimum Follow-Up of Hip Resurfacing Male Patients: A Review of Outcomes

*Anand Saluja - Hospital for Special Surgery - New York, United States of America

Zachary Wong - Texas College of Osteopathic Medicine - Fort Worth, USA

Jonathan Spaan - Hospital for Special Surgery - New York, United States of America

Louis Andrew Jordan - Hospital for Special Surgery - New York, United States of America

*Edwin Su - Hospital for Special Surgery - New York, USA

Introduction:

Hip resurfacing arthroplasty (HRA) has been shown to be a suitable alternative to total hip arthroplasty (THA), especially in active individuals seeking a return to high impact activity. With favorable clinical outcomes and positive survivorship in patients at short to medium-term follow-up, the longevity of HRA has become more of a relevant concern, especially when comparing it to the longstanding procedure of THA. However, the extent of long-term follow-up for HRA is limited, as the majority of the current literature stops at 10 years. As such, the purpose of this study was to evaluate long-term survivorship of HRA with a minimum 15-year follow-up.

Methods:

A retrospective review of hip resurfacing arthroplasties in both males and females performed by a single surgeon between 2006-2008 were included. Patient demographics, HOOS JR, HHS, VAS, and UCLA activity scores as well as implant survival and subject satisfaction were collected and analyzed. Minimum 15-year follow-up PROMs and subject satisfaction surveys were analyzed, and a Kaplan Meier Survivorship Analysis was utilized to assess implant survivorship.

Results:

A total of 320 male patients (357 hips) out of 470 (543 hips) with a minimum 15-year follow up (68.1% patient follow-up) were included. The mean age of male patients at surgery was 51.5 ± 7.5 and mean BMI was 27.5 ± 3.8 . The mean cup size was 56.6 (50-64) and the mean head size was 50.5 (44-58). The mean scores for HOOS JR, HHS, VAS, and UCLA activity scores in male patients at final follow-up were 97.5 ± 6.7 , 96.7 ± 8.3 , 0.3 ± 0.9 , and 7.9 ± 1.9 , respectively. Patients reported 99.3% subject satisfaction with the procedure, excluding revisions. There was an implant survivorship of 93.4%, and the Kaplan-Meier Survival Rate for subjects free from revision at 200 months was 92.2%. 5 deaths were reported before reaching final follow-up.

Conclusion:

High PROMs scores, implant survival, and subject satisfaction scores indicate that metal on metal HRA exists as a successful option for male patients with a mean age of 51.5 ± 7.5 at minimum 15-year follow up.

Insights Into Long-Term Performance and MRI Profiles in M2a-Magnum Cup Metal-on-Metal Total Hip Arthroplasty

*Ryo Orito - Kansai Rosai Hospital - Hyogo, Japan

Wataru Ando - Osaka University Graduate School of Medicine - Suita, Japan

Shoya Abe - Itami City Hospital - Itami City, Japan

Ema Nakahara - Osaka University - Suita, Japan

Takeshi Ogawa - Kansai Rosai Hospital - Amagasaki, Japan

Tsuyoshi Koyama - Kansai Rosai Hospital - Amagasaki, Japan

Takayuki Tsuda - Kansai Rosai Hospital - Amagasaki, Japan

Kenji Ohzono - Amagasaki Chuo Hospital - Amagasaki, Japan

Introduction: The M2a-Magnum Cup is recognized for its robust fixation achieved through a porous plasma spray coating and rotational stability provided by fins, allowing for use in large-diameter femoral heads. Metal-on-metal total hip arthroplasty (MoM THA) using a large diameter femoral head is expected to have wear resistance and prevent dislocation. However, concerns persist regarding metal-related complications, notably pseudotumor formation and adverse reactions to metal debris (ARMD). In this study, we investigated the outcomes of primary MoM THA employing the M2a-Magnum Cup at our institution, assessing the results over an 8-year postoperative period.

Methods: Among 102 patients and 106 hips subjected to primary MoM THA with the M2a-Magnum Cup between 2006 and 2013, we retrospectively studied 75 patients and 79 hips for which follow-up data beyond 8 years postoperatively were available, yielding a follow-up rate of 74.5%. The femoral head diameter was 6 mm smaller than the cup's outer diameter. The cohort consisted of 26 male and 49 female patients, diagnosed with osteoarthritis (N=61), osteonecrosis of the femoral head (N=15), rheumatoid arthritis (N=2), Rapidly Destructive Coxarthropathy (N=12). The mean age at surgery was 65.5 years (range: 34-86 years), with a mean follow-up duration of 136.6 months (range: 97-211 months). The evaluation included hip function assessed using the Japanese Orthopedic Association (JOA) Score, clinical assessment based on complications (dislocation, infection, ARMD), implant survival rate, and radiographic examination findings (cup installation angle, presence of initial gap, and radiolucent line). Additionally, MRI findings (Anderson classification) were assessed for cases undergoing MRI examinations.

Results: The mean JOA score improved significantly from 47.7 to 89.5 at the last follow-up. Complications included 4 cases of dislocation (5.0%), 3 cases of infection (3.8%), and 6 cases of ARMD (7.6%), with revision surgeries required in 6 cases (7.6%). The implant survival rate was 92.4% with revision surgery (Fig.1). Notably, all instances of dislocation were concurrent with ARMD. Radiographically, the mean acetabular cup anteversion and inclination were 27.6° and 37.6°, respectively (Fig.2). The initial gap and radiolucent lines resolved within 5 years postoperatively, with no instances of loosening detected on radiographic examinations during follow-up. MRI findings at 2-5 years and over 5 years postoperatively revealed abnormal findings, particularly in cases of pseudotumor development (Table 1).

Conclusion: M2a-Magnum Cup demonstrated stable fixation. However, the development of pseudotumors, even in MoM THA utilizing large-diameter heads, highlights the need for careful postoperative attention and management.

Figures

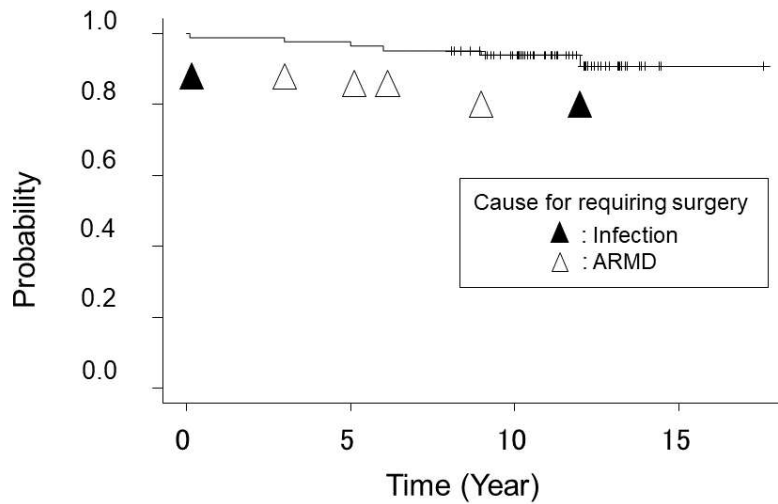


Fig. 1
Cumulative survival of 79 prostheses with Revision surgery as failure event. The small vertical spikes represent censored data

Figure 1

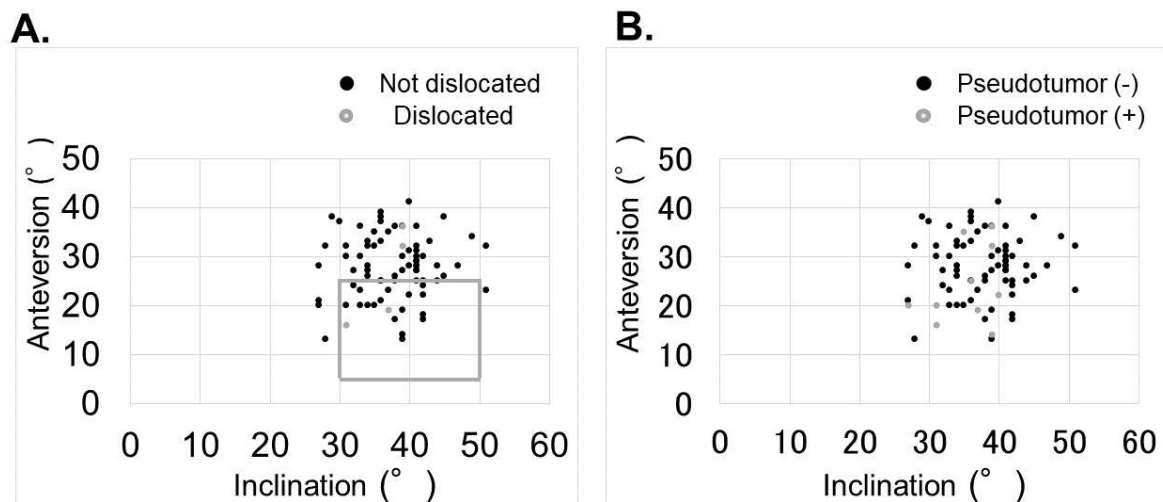


Fig. 2
(A) Relationship of the dislocation cases with the acetabular inclination and anteversion angle.
(B) Relationship of the complications of the pseudotumor with the acetabular inclination and anteversion angle.

Figure 2

Table 1. Results of the MARS MRI evaluations according to the Anderson classification.

Anderson grade	2-5 years	Over 5years
A	56 (81%)	37 (75%)
B	0 (0%)	1 (2%)
C1	7 (10%)	5 (10%)
C2	6 (9%)	7 (14%)
C3	0 (0%)	0 (0%)
Total	69 (100%)	50 (100%)

[Figure 3](#)

Is Femoral Component Malposition Acceptable in Metal on Metal Hip Resurfacing ?

*Lafayette Lage - Clinica Lage - sao paulo, Brazil

Gustavo Lage - Clinica Lage - São Paulo, Brazil

Introduction: Metal on metal hip resurfacing is an ideal prosthesis to save bone stock since any hip replacement is temporary. Femoral component malposition in hip resurfacing can cause early failure through early femoral neck fracture. Proper component position is necessary for the short- and long-term success of hip resurfacing.

Methods: A 38 years old male patient with bilateral femoral head osteonecrosis due to pulse corticosteroid therapy for treatment of cluster headache was submitted to the implantation of a hybrid 48x54 mm Cormet hip resurfacing from Corin on his right hip on December 12nd, 2003 and the same implant on his left hip on February 2nd, 2004. The left femoral component was in a “unacceptable varus position” which was noted only on the day after on control X-ray.

The post op of this hip was made with progressive weight bearing for 12 weeks in order to protect the femoral neck from an early fracture and medication was introduced in order to enhance bone strength.

Follow up was done routinely and only 19 years later he presented with pain and fracture of the femoral neck.

Revision was performed with no difficulty replacing only the femoral component with a uncemented femoral stem and a dual mobility ceramic – polyethylene head.

Metal ions levels were normal during these 19 years and no metallosis was found.

Full weight bearing was permitted and recovery was fast.

He had a good recovery and the films, pictures, and lab results will be presented.

Conclusion: The authors present a rare case of late femoral neck fracture. Metal on Metal hip resurfacing showed good resistance in long terms even in a mispositioned femoral implant.

Figures



[Figure 1](#)



[Figure 2](#)

Birmingham Hip Resurfacing: Clinical and Radiographic Outcomes With Minimum 2 Years Follow Up and Sub-Analysis of Navigation vs Non-Navigation

*Benjamin Domb - American Hip Institute - Des Plaines, USA

Roger Quesada-Jimenez - American Hip Institute Research Foundation - Chicago, USA

Ady Kahana - American Hip Institute Research Foundation - Chicago, United States of America

Elizabeth Walsh - American Hip Institute Research Foundation - Chicago, USA

Tyler McCarroll - American Hip Institute Research Foundation - Chicago, USA

Mark Schinsky - American Hip Institute Research Foundation - Chicago, United States of America

Background Hip resurfacing (HR) is a promising option for active individuals with hip osteoarthritis (OA). The integration of navigation technology offers real-time assessment of component placement and limb alignment during surgery, which could potentially enhance precision and improve clinical outcomes. The focus of our study is on the short-term clinical outcomes of HR with navigation, as well as the accuracy of acetabular implant placement in both the frontal and sagittal planes.

Methods: Data was retrospectively analyzed for patients who received HR between 2010-2021. Eligible patients completed x-rays and minimum 2-year follow-up questionnaire for the following patient-reported outcomes (PROs): modified Harris Hip Score (mHHS), Harris Hip Score (HHS), Forgotten Joint Score (FJS), Visual Analogue Scale (VAS), Satisfaction, and Hip Disability and Osteoarthritis Outcome Score, Joint Replacement (HOOS-JR). Hips were propensity-matched in a 1:1 ratio based on the use of navigation, age, and body mass index (BMI). The percentage of hips that met the Minimal Clinically Important Difference (MCID) for mHHS and VAS was noted. Component placement analysis was conducted based on the safe zone defined by Lewinnek, Callanan, and Relative Acetabular Inclination Limit (RAIL).

Results 76 hips were matched, 38 per group. No differences were observed in PROs or the percentage of hips reaching MCID between the groups. The NAV group was 28,8 and 6,8 times more likely to be within the Callanan and Lewinnek safe zones, respectively. Based on RAIL system, the non-NAV group had 1 hip outside the 95% confidence interval safe zones and 10 hips outside the 99% confidence interval safe zones. In comparison, the NAV group had 0 and 2 hips outside the safe zones, respectively.

Conclusion: HR is an effective treatment for physically active individuals with OA. Comparable improvements in PROs were observed in both groups over a minimum 2-year follow-up. Navigation-assisted surgery enhances the accuracy of acetabular component positioning, with a higher likelihood of cup placement within the safe zones.

The Effect of Surgical Approach on Gait Following Hip Resurfacing Arthroplasty

*Rima Nasser - Imperial College - London, GB

Amy Maslivec - Imperial College London - London, United Kingdom

Justin Cobb - Imperial College - London, United Kingdom

Introduction: The use of the direct anterior approach (DAA) for total hip arthroplasty (THA) has significantly increased over the past few years. This approach spares the gluteal muscles and has been shown to give THA patients slightly more normal gait biomechanics. Hip Resurfacing Arthroplasty (HRA) is an alternative to THA which allows patients to resume higher levels of activity post operatively. HRA has commonly been performed using the posterior approach (POS) involving an incision through the gluteus maximus and detachment of external rotators. The purpose of this study was to examine how the surgical approach may affect gait biomechanics following HRA.

Methods: Twenty-two hip resurfacing patients assigned to two groups based on surgical approach, 12 DAA and 20 POS patients completed a gait analysis using an instrumented treadmill and motion capture post-operatively (1-1.4 years). Top walking speed (TWS), Ground Reaction Force (GRF), spatiotemporal gait variables and hip range of movement (ROM) were recorded. Data was also compared to data from a group of 20 age, gender, and BMI matched group of healthy controls.

Statistical parametric mapping (SPM) was used for analysis.

Results: The TWS was 7 km/h for all three groups. The normalised step length was 89.5cm and the step width was a little over 8 cm for the DAA and control groups vs 88cm and 9 cm for the POS group. The cadence was 52 steps/min for the POS and control groups and 50 for the DAA group. For DAA patients, hip sagittal ROM was 47° and frontal ROM 16.6° whereas the posterior group had 45° of sagittal ROM and 17.6° of frontal ROM. SPM analysis revealed the POS had significantly more abduction of the hip in the swing phase of the gait cycle (64-68%, $p=0.01$). (Figures 1&2)

Conclusion: Gait analysis at 1 year follow-up showed that HRA patients with either DAA or POS demonstrated gait function very similar to healthy controls. (Figure 3) The small differences in gait noted between the patients who underwent different approaches and healthy controls are unlikely to be clinically relevant.

Pioneering Pre-Incision and Pre-Resection Joint Balancing Technologies

*Manh Ta - Stryker Corporation - Fort Lauderdale, USA

Thang Nguyen - University of Tennessee - Knoxville, USA

Steven MacDonald - London Health Sciences Centre - London, Canada

Richard Komistek - The University of Tennessee - Knoxville, USA

INTRODUCTION

Joint balancing stands as a critical determinant of success in total knee arthroplasty (TKA). Presently, this procedure is primarily conducted intra-operatively due to limitations in imaging modalities. However, the advent of 3D ultrasound technology, exemplified by Orthosonic™ (JointVue, LLC), offers a promising paradigm shift. It enables radiation-free, real-time 3D bone reconstruction and joint balancing during pre-surgery visits at the surgeon's office. This study aims to introduce a pre-incision and pre-resection joint balancing approach utilizing Orthosonic™'s software suite.

METHODS

The Orthosonic™ software suite (Figure 1), developed by JointVue, LLC, utilizes raw RF signal in a-mode and electromagnetic (EM) trackers to construct a point cloud representation of knee bones. Statistical shape modeling facilitates the generation of patient-specific 3D bone models immediately post-scan. Subsequently, passive knee bone kinematics is captured using EM trackers, providing insights into full range motion from full extension to 90 degrees of flexion. These 3D bone models and kinematics are imported into jFit (JointVue, LLC), a pre-operative surgical planning software, enabling determination of component sizes, alignment, pre-incision, pre-resection joint balancing, and necessary bone cuts for TKA, all accomplished pre-operatively during a patient's office visit.

RESULTS

The Orthosonic™ software suite successfully generates patient-specific 3D bone models with reported root mean square (RMS) accuracies of 0.92 mm for the femur and 1.07 mm for the tibia, compared to CT scans. Native knee laxity and alignment are captured (Figure 2), facilitating optimization of implant component positions and sizes, alongside pre-incision and pre-resection laxity assessment (Figure 3). Surgeons can review implant planning, including joint balancing, prior to surgery using jFit. Patients receive a printout of their planned implant components post-pre-surgery visit, enhancing their understanding and expectations.

DISCUSSION

Orthosonic™ software suite pioneers pre-incision and pre-resection joint balancing technologies. It stands as the first technology allowing surgeons to reconstruct patient-specific 3D bone models and conduct pre-incision and pre-resection joint balancing. While a portion of the Orthosonic™ suite has obtained FDA clearance, the pre-incision and pre-resection joint balancing component awaits clearance. JointVue, LLC is dedicated to rigorous development, verification, and validation processes before submitting a 510(k) application, reaffirming its commitment to advancing surgical outcomes and patient care.

Figures



Figure 1

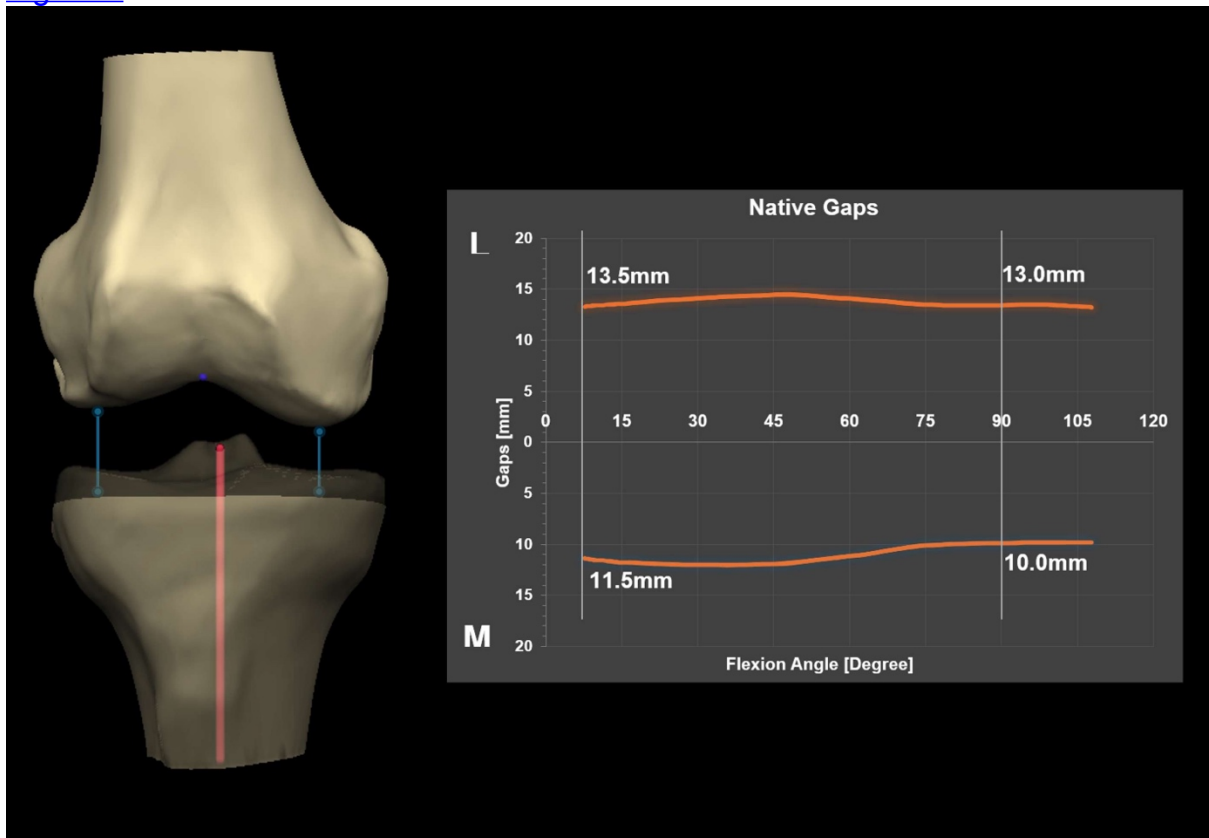


Figure 2

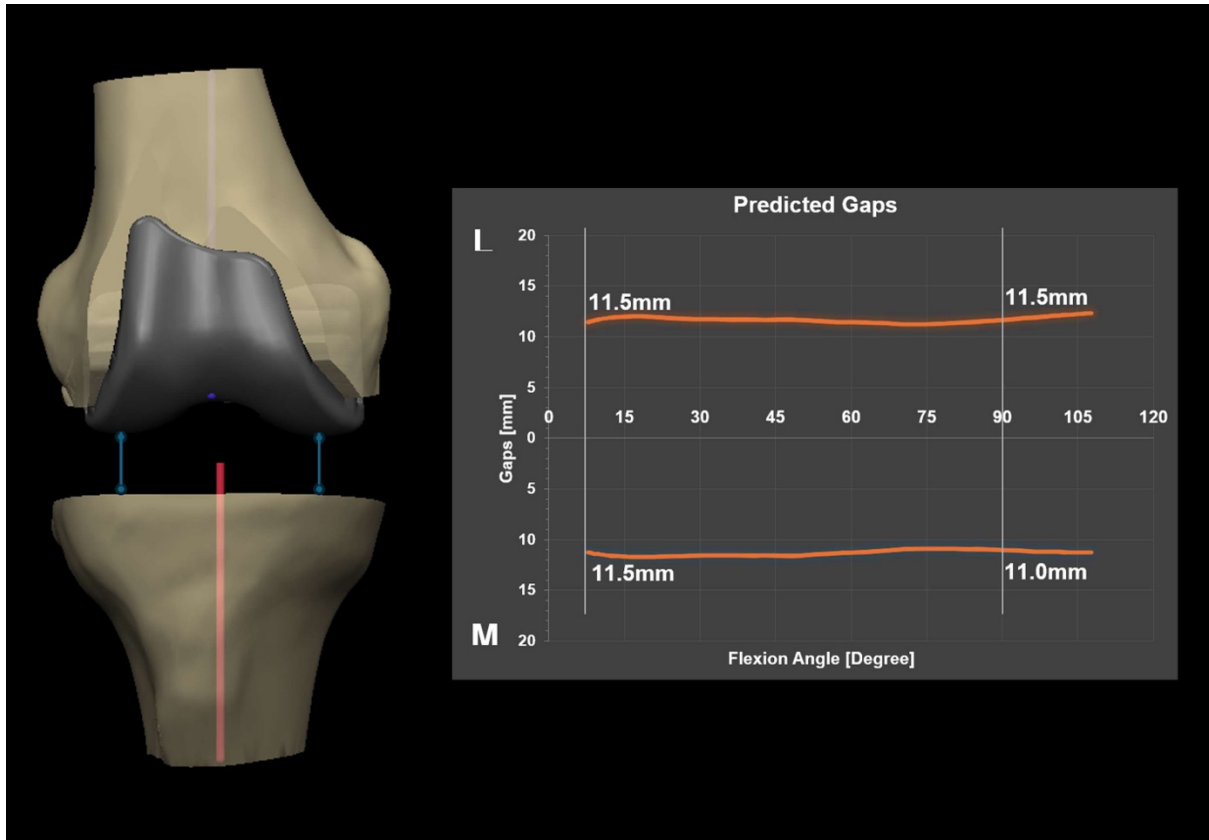


Figure 3

Novel Algorithm for Gap Balancing and Bone Cuts in Robotic Total Knee Replacements Significantly Improves Accuracy and Surgical Duration

Ryan Wai Keong Loke - National University of Singapore, Yong Loo Lin School of Medicine - Singapore, Singapore

Matthew Ng Song Peng - National University of Singapore, Yong Loo Lin School of Medicine - Singapore, Singapore

*Glen Zi Qiang Liao - Singapore General Hospital, Singapore - Singapore, Singapore

Background:

Robotic Total Knee Replacements (rTKR) have become increasingly popular in recent years. However, intra-operative manual planning of the positions of the femur and tibia implants in all possible degrees of freedom to achieve the surgeon's ideal targets and limits of bone cuts, gaps and alignment is challenging. The final manually defined solution may not be the most optimal, and surgical duration becomes extended significantly. The aim of our study is to demonstrate the effectiveness of utilising our novel algorithm clinically in terms of accuracy and surgical duration.

Methods:

We have developed a novel computational algorithm to achieve optimal positioning of rTKR implants in three-dimensional space. The initial set of parameters of the 3D positioning of the implants in relation to each other and the surgeon-defined target gaps and bone cuts are defined. The algorithm will then determine various permutations that give the ideal 3D positioning of the implants, to fulfil the targets with an accuracy of $\pm 0.5\text{mm}$, while also ranking them according to a set of surgeon-preference and evidence-based criteria. We compared the accuracy in achieving surgeon-defined target gaps between both groups, the intra-operative gap-balancing duration, and total surgical duration. Power analysis based on a pilot study showed that 44 patients were required.

Results:

A retrospective cohort study of 67 consecutive patients who underwent rTKR at a tertiary institution from November 2021 to December 2023 was performed. 25 patients (mean age 70.4 years ± 7.34) had our novel algorithm utilised intra-operatively, while 42 patients (mean age 70.5 years ± 6.90) did not. 92% of the rTKRs that used our algorithm achieved the surgeon-defined target gaps $\pm 1.5\text{mm}$, compared to 52% of rTKRs that were done manually ($P = 0.003$). The average difference between surgeon-defined target gaps and final achieved gaps was $1.08 \pm 0.51\text{mm}$ in the algorithm group, significantly lower than that in the non-algorithm group, which was $1.81 \pm 1.04\text{mm}$ ($P = 0.003$). Gap-balancing duration was significantly shorter: $1.16\text{min} \pm 0.11$ with algorithm use, compared to $14.49\text{min} \pm 8.31$ ($P < 0.0001$). Total surgical duration was also significantly lower with algorithm use, with a mean total surgical time of $38.4\text{min} \pm 14.94$ compared to $73.66\text{min} \pm 19.61$ ($P = 0.0002$).

Conclusions:

Our novel algorithm for gap-balancing in rTKRs significantly improves both accuracy of achieving the surgeon's target extension and flexion gaps, along with gap-balancing and overall surgical duration. This is highly promising for achieving both reproducibility and efficiency in rTKRs.

Total Knee Design to Achieve Anatomic Femoral-Tibial Motion and Laxity

***Peter Walker - New York University Langone Orthopedic Hospital - New York City, USA**

Peter S Walker - New York University - New York, USA

INTRODUCTION

Total knees with cruciate substitution have evolved through the Freeman-Swanson, Total Condylar, and Posterior Stabilized, to the Ultracongruent, Medial Pivot, Medially Congruent, and Dual Pivot (Kahlenberg et al 2021). There are two elements of kinematics: the neutral path of motion, namely a stable medial side and a progressive posterior displacement of the lateral femoral condyle during flexion (Dennis et al 2005) ; and laxity about that neutral path (Walker et al 2015; Bandi et al 2015), both anterior-posterior and internal-external. In the absence of one or both cruciates, the challenge is to closely reproduce anatomic kinematics. In most total knee designs, this is not achieved, particularly a stable medial side and lateral rollback (Angerame et al 2019). The purpose of this study was to determine if anatomic kinematics could be achieved by using a previous condylar design (Walker et al 2024) with the addition of an intercondylar offset cylindrical bearing.

METHODS

The femoral component replicated normal anatomy, modified with equal lateral and medial sagittal condyle radii. The center of the cylindrical femoral surface was offset relative to the condyles. Five different combinations of radii were tested. For motion evaluation, a Custom-Designed Test Rig was used which applied combinations of axial force, shear and torque, at flexion angles of 0, 30, 60, 90, 120 degrees. Displacements and rotations were measured. The test was based on the ASTM standard for total knee constraint. Comparisons were made with data of anatomic kinematics.

RESULTS

For the design with the closest to average anatomic data, AP laxities during flexion ranged from: Lat 3.9-6.2 mm, Med 3.0-4.0 mm. Rotational laxities ranged from 5.3 to 13.8 degrees. From 0-120 deg flexion, the lateral contact displaced from +8mm to -11mm, the medial contact displaced from +3 to -4mm.

CONCLUSIONS

The kinematics as measured by neutral path of motion, and laxity about the neutral path, showed an anatomic pattern. The lateral contact displaced progressively posterior with flexion. The medial side displaced only a few millimeters. There was AP and rotational laxity at each angle of flexion. Further close numerical resemblance to average normal could be achieved by optimizing various radii of the design. Alternatively customized kinematics could be achieved with different radii tibial surfaces. Such a design could achieve close to normal soft tissue lengths during flexion, a more normal feeling knee, and a higher flexion range.

Figures

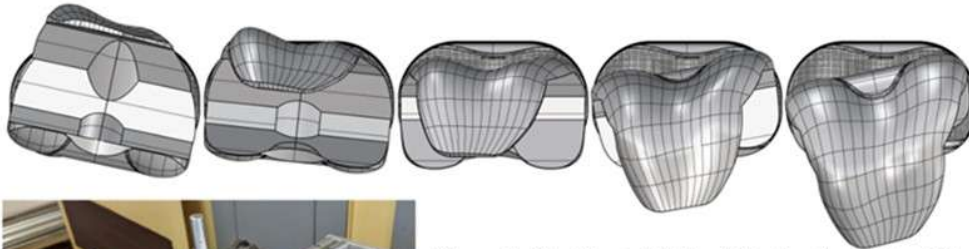


Figure 1. The Neutral Path of Motion from 0 to 120 degrees, showing progressive posterior lateral displacement, external femoral rotation, and a stable medial side. There are AP and rotational laxity about these neutral positions.

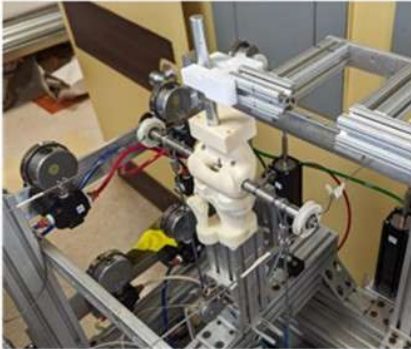


Figure 2. The Laxity Test Machine, showing the 3D printed Test Components. Axial compression, shear and torque are applied at a range of flexion angles. Displacements and rotations are measured.

[Figure 1](#)

Anterior-Posterior Constraint of Two Different Knee Inlay Designs in Mid-Flexion

*Saskia Anna Brendle - Aesculap AG / LMU Munich - Tuttlingen, Germany

Sven Krueger - Aesculap AG Research & Development - Tuttlingen, Germany

Joachim Grifka - Regensburg University Medical Center - 93077 Bad Abbach, Germany

Peter E. Mueller - Hospital of the Ludwig-Maximilians-University of Munich - Munich, Germany

William Mihalko - University of Tennessee - Germantown, USA

Berna Richter - Aesculap AG - Tuttlingen, Germany

Thomas M. Grupp - Aesculap AG - Tuttlingen, Germany

Various implant designs are currently available for total knee arthroplasty (TKA), each having a different conformity to generate different kinematics. However, it is not clear how the individual ligament situation influences the resulting anterior-posterior (AP) translation of different implant designs in mid-flexion. For this reason, the purpose of this study was to investigate the AP constraint of a symmetrical (CR/CS) and an asymmetrical, medial-stabilized (MS) inlay in the same knees during AP shear force and internal-external (IE) rotation moment.

In this in vitro study, fourteen fresh-frozen instrumented human cadaveric knees were tested on a six-degrees-of-freedom joint motion simulator (VIVO, Advanced Mechanical Technologies Inc., Watertown, USA). The specimens underwent cruciate-sacrificing TKA using the oneKNEE TKA system (Aesculap AG, Tuttlingen Germany), which allows the use of a CR/CS or MS inlay. In order to characterize the behaviour of each knee with both, a CR/CS and a MS inlay, AP shear forces of ± 80 N and ± 5 Nm IE rotation moments were sequentially applied at 45° flexion while maintaining an axial compression force of 200 N and all other forces and moments at 0 N / Nm. In order to track the relative position of femur and tibia during testing, each specimen underwent a complex 3D fitting process (ARAMIS 12M, Carl Zeiss GOM Metrology GmbH, Braunschweig, Germany). Tracking the relative positions of femur and tibia during testing allowed the projection of the flexion axis and the medial and lateral flexion facet centres (MFC and LFC) of the femoral component onto the tibial plane at different timepoints and therefore the measurement of condylar motion. The AP range of motion (ROM) of the projected MFC and LFC of each specimen was calculated for both inlays as the difference between the maximum and minimum AP force or IE rotation moment. Wilcoxon signed rank tests were used to compare the AP ROM medially and laterally between CR/CS and MS ($p \leq 0.05$).

The MS inlay resulted in a significantly lower AP ROM of the medial condyle compared to the CR/CS inlay during AP shear forces (Figure 1a and 2) and IE rotation moments (Figure 1b and 3). In contrast, the AP ROM of the lateral condyle with the MS inlay was significantly lower during AP shear forces and significantly higher during IE rotation moments compared to the CR/CS inlay.

The AP ROM of the medial and lateral condyles in mid-flexion is different between the individual specimens, but the AP ROM of the MFC is always smaller with the MS inlay than with the CR/CS inlay, showing the higher medial constraint of MS inlays.

Figures

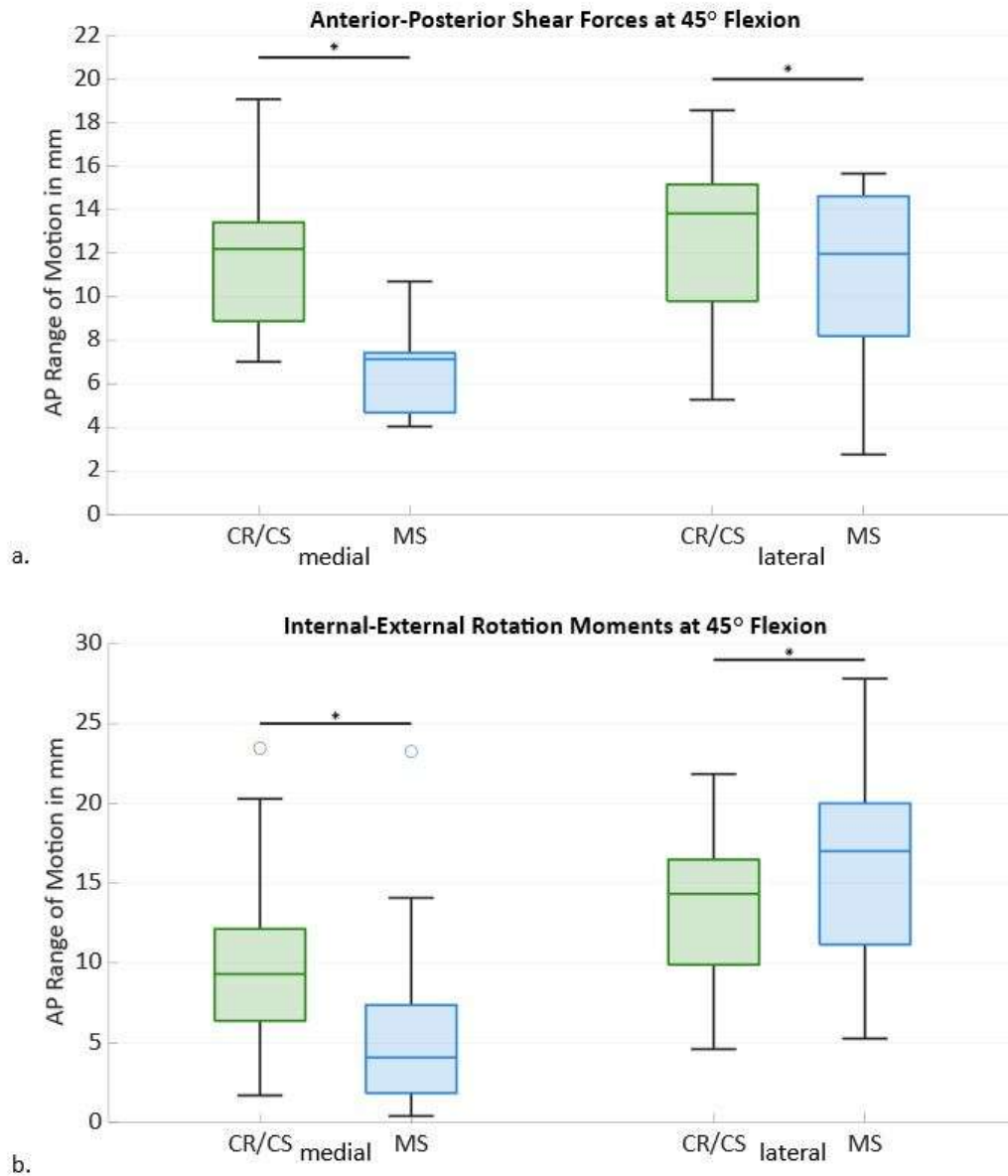


Figure 1. Boxplots of the medial and lateral anterior-posterior (AP) range of motion with CR/CS (green) and MS (blue) inlays during (a) AP shear forces and (b) internal-external rotation moments (n=14). Significant differences are marked with an asterisk ($p \leq 0.05$).

[Figure 1](#)

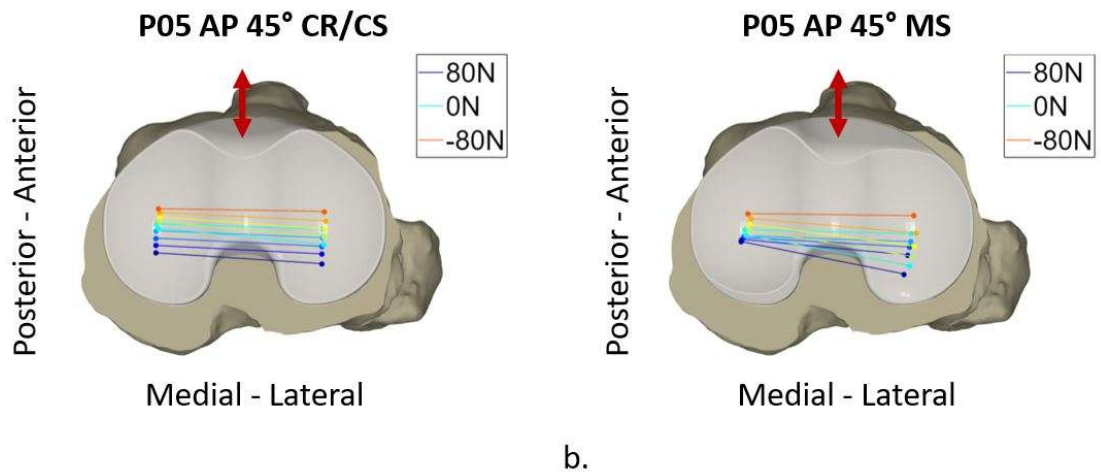


Figure 2. Projection of the flexion axis and medial and lateral flexion facet centers of the femoral component onto the tibial plane with ± 80 N anterior(-) posterior(+) shear force applied on the tibia at 45° of flexion showing the condylar motion with (a) a CR/CS inlay and (b) a MS inlay in specimen P05.

[Figure 2](#)

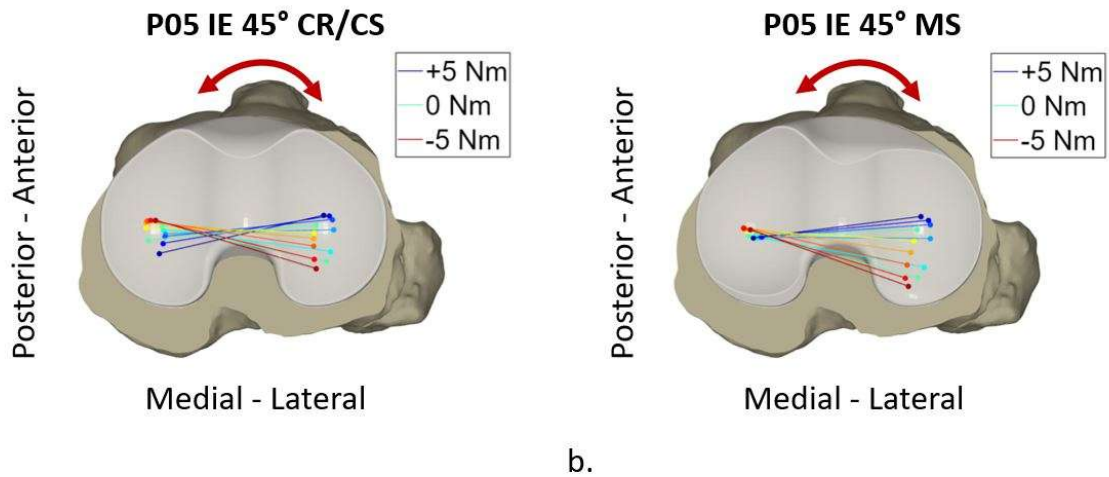


Figure 3. Projection of the flexion axis and medial and lateral flexion facet centers of the femoral component onto the tibial plane with ± 5 Nm internal(-) external(+) rotation moment applied on the tibia at 45° of flexion showing condylar motion with (a) a CR/CS inlay and (b) a MS inlay in specimen P05.

[Figure 3](#)

Accounting for Peripheral Osteophytes During Pre-Resection Balancing of a Total Knee Arthroplasty Helps to Mitigate the Risk of Mid-Flexion Laxity

*Joshua Roth - University of Wisconsin-Madison - Madison, USA

Matthew Blomquist - University of Wisconsin-Madison - Madison, USA

Introduction:

A vast majority of surgeons rely on knee laxities and/or gaps to assess soft tissue balance during knee arthroplasty. Those who use enabling technologies (e.g., robotic systems) can leverage a “pre-resection” balancing workflow in which they adjust the pre-operatively planned implant alignments based on a laxity assessment before making any bony resections. However, these pre-resection laxity assessments do not yet account for the effect that removal of peripheral osteophytes likely has on joint laxities [1]. Accordingly, **our objective** was to determine whether changes in joint laxities and gaps due to removal of peripheral osteophytes could be predicted based on the size of the osteophytes.

Methods:

We generated a virtual cohort of 1000 osteoarthritic knees with representative patient-to-patient variability in knee laxities and osteophyte sizes using a probabilistic framework [2] with a 12-degree-of-freedom, musculoskeletal model of the knee [3] (**Figure 1**). For each model in the cohort, we randomly sampled the size of the medial and lateral tibial osteophytes, represented as ellipsoidal wrap objects, based on a distribution reported previously [4]. To determine how removal of osteophytes changed knee laxities/gaps, we duplicated the first model set and removed both the anterior cruciate ligament and the osteophytes to mimic each knee post-bone resection.

For each model in each set, we performed forward dynamic simulations in OpenSim-JAM of varus-valgus (V-V) laxity assessments at 0° and 45° of knee flexion. We computed the increases in V-V laxities, and medial and lateral gaps between the two model sets by fitting multiple linear regressions to our data. The medial and lateral osteophyte sizes were the independent variables, and the change in either joint laxities or gaps between the pre- and post-resected knees was the dependent variable.

Results:

We found that removing medial osteophytes increased joint laxities and gaps by nearly an order of magnitude more than removing lateral osteophytes (**Figure 2, Table 1**). Specifically, we found the largest changes during a valgus laxity assessment at 45° flexion where removing 1 cm of osteophyte resulted in an average increase of 2.2° in valgus laxity and 1.6 mm in the medial gap.

Conclusion:

This study showed that removal of peripheral tibial osteophytes can have a clinically important effect on knee biomechanics, especially in mid-flexion where instability is most prevalent and most difficult to correct. Our ongoing work is focused on accounting for additional changes from pre-to-post resection (e.g., femoral osteophytes). The relationships from this study enable surgeons to predict post-resection laxities/gaps based on pre-operative imaging to mitigate the risk of over-resection and the additional surgical time that is then necessary to iteratively balance the knee.

References:

- [1] Pottenger, L. A., et al., Arthritis & Rheumatism, 1990. DOI: 10.1002/art.1780330612.
- [2] Smith, C. R., et al., Journal of Knee Surgery, 2016. DOI: 10.1055/s-0035-1558858.
- [3] Lenhart, R. L., et al., Annals of Biomedical Engineering, 2015. DOI: 10.1007/s10439-015-1326-3
- [4] Ishii, Y., et al., Journal of Orthopaedic Research, 2020. DOI: 10.1002/jor.24501.

Figures

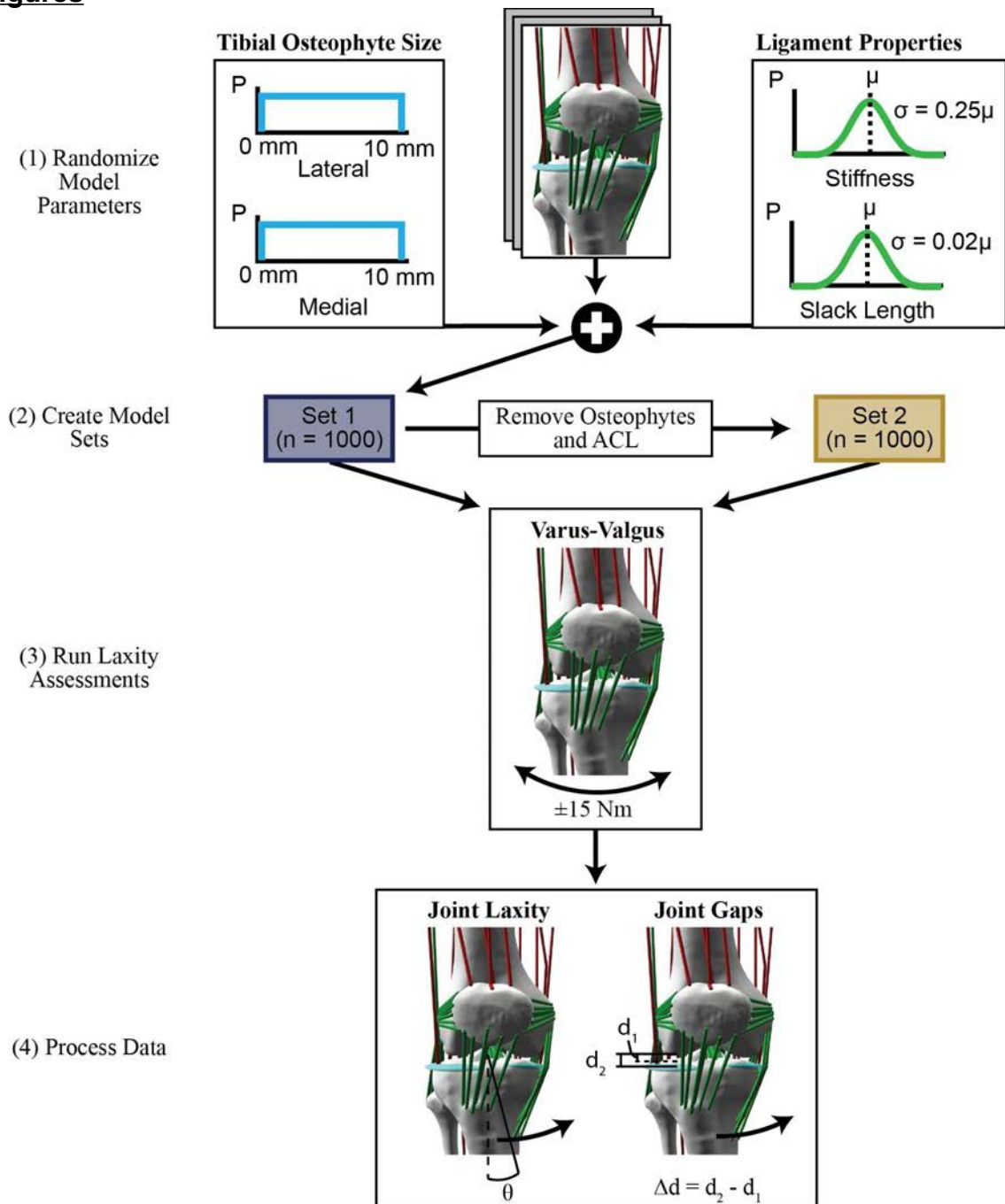


Figure 1: Flowchart shows the steps for creating models and performing laxity assessments to determine the effect of osteophytes on laxity and joint gaps. We randomly selected tibial osteophyte sizes and ligament properties to represent the wide variability in these properties in the osteoarthritis population. We created a baseline model set (Set 1) to mimic a pre-resection knee, and then we removed osteophytes and both bundles of the anterior cruciate ligament (ACL) to mimic a post-bone resection knee (Set 2). In both model sets, we ran varus-valgus laxity assessments and computed the change in joint laxity and medial and lateral joint gaps before and after a load was applied.

[Figure 1](#)

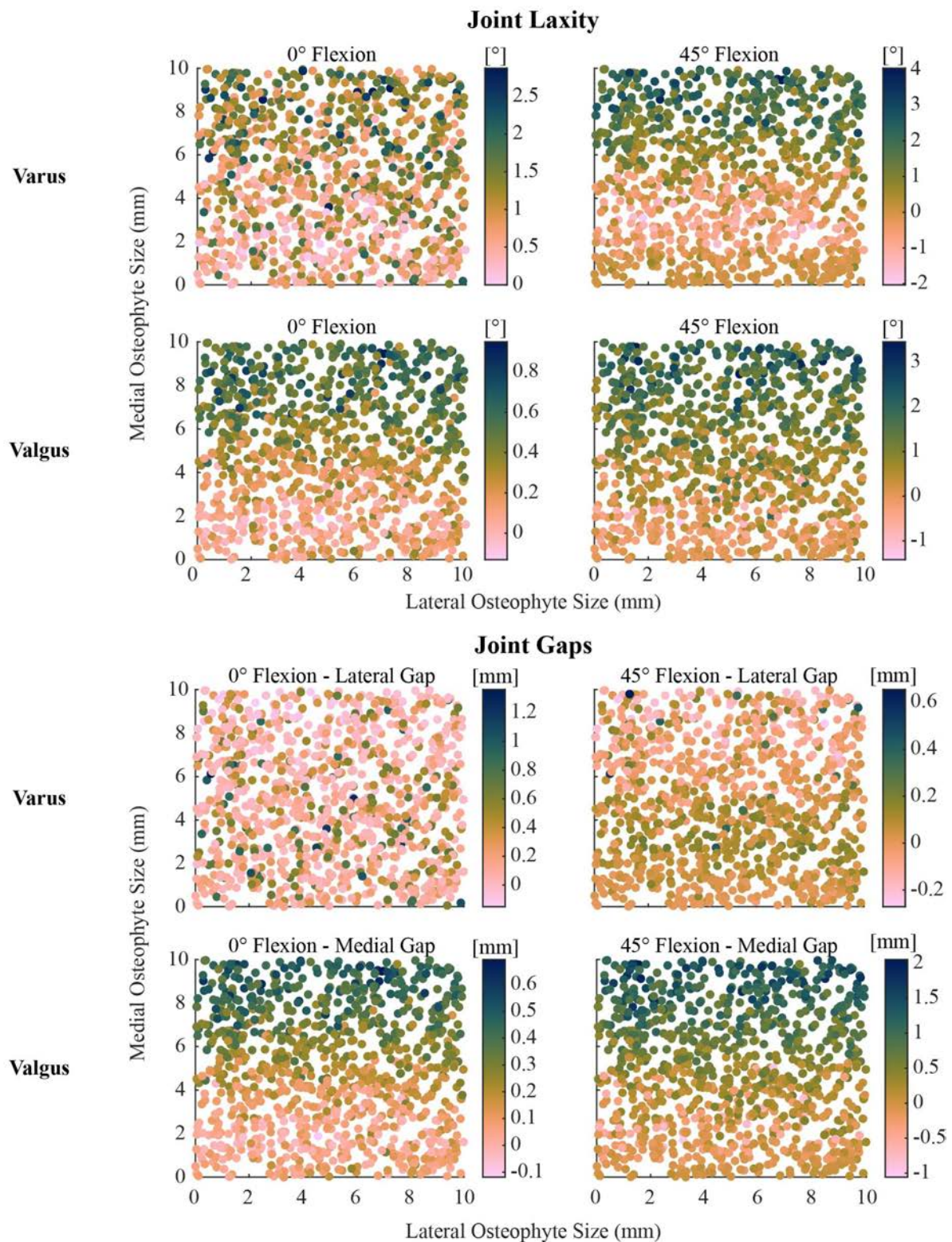


Figure 2: Scatter plots show the sensitivity of joint laxity and gap increase to the size of medial and lateral osteophytes removed. The horizontal axes show the sizes of the lateral osteophytes and the vertical axes show the sizes of the medial osteophytes. The scatter points are colored by the change in joint laxity (top) or change in joint gaps (bottom) between the two model sets.

[Figure 2](#)

Table 1: Results of multi-variable linear regressions with medial and lateral osteophyte sizes as the two independent variables and the change in joint laxity or joint gaps between the pre-resected and post-bone resected knees as the dependent variable.

Joint Laxity	Slope [°/cm]	Confidence Interval [°/cm]	p value
Varus, 0°			
Lateral	0.1	[-0.0, 0.2]	0.087
Medial	0.9	[0.8, 1.0]	<0.001
Varus, 45°			
Lateral	0.0	[-0.1, 0.2]	0.73
Medial	2.8	[2.6, 2.9]	<0.001
Valgus, 0°			
Lateral	0.1	[0.0, 0.1]	<0.001
Medial	0.6	[0.5, 0.6]	<0.001
Valgus, 45°			
Lateral	0.1	[0.0, 0.3]	0.007
Medial	2.2	[2.1, 2.3]	<0.001
Joint Gaps	Slope [mm/cm]	Confidence Interval [mm/cm]	p value
Varus, 0°			
Lateral	0.0	[-0.1, 0.1]	0.99
Medial	-0.1	[-0.2, -0.1]	<0.001
Varus, 45°			
Lateral	0.0	[-0.0, 0.0]	0.73
Medial	-0.1	[-0.2, -0.1]	<0.001
Valgus, 0°			
Lateral	0.0	[-0.0, 0.0]	0.13
Medial	0.5	[0.5, 0.5]	<0.001
Valgus, 45°			
Lateral	0.1	[0.0, 0.1]	0.008
Medial	1.6	[1.6, 1.7]	<0.001

[Figure 3](#)

Functional Knee Positioning Achieves Consistent Knee Balance in Total Knee Arthroplasty

*Azhar Ali - Stryker Orthopaedics - Mahwah, USA

Yogesh Mittal - The Orthopaedic Center - Tulsa, USA

Paul Jacob - Oklahoma Joint Reconstruction Institute - Oklahoma City, USA

Robert Marchand - Ortho Rhode Island - South County, USA

Introduction: Recently, functional knee positioning principles have been employed to personalize implant placement according to 3D CT-based implant planning, dynamic joint balancing, and robotic-execution of surgical plans [1]. While this process aims to restore knee balance, the accuracy of achieving planned knee laxity has not been well-established. The objective of this study was to compare a) pre-resection knee laxity before 3D implant adjustments, b) pre-resection knee laxity after 3D implant adjustments, and c) trialing knee laxity following bony resections in functionally-positioned, robotic-assisted TKA (RATKA) patients. Additionally, this study characterized knee balance by comparing the difference between medial and lateral laxity in extension and flexion.

Methods: A retrospective review was conducted for 777 patients from three hospital sites undergoing RATKA using functional knee positioning principles. Surgeons performed pre-resection and trialing knee laxity assessments by applying manual varus-valgus stress in extension (10°) and flexion (90°). The robotic system recorded medial and lateral compartment knee laxity as the distance between the femoral and tibial surgical plan during pre-resection and trialing. Planned laxity was defined as the pre-resection knee laxity after 3D implant adjustments were made based on initial laxity assessments. The average difference between final trialing and planned laxity was computed to determine the accuracy in restoring the planned knee laxity. Knee balance was calculated as the difference between the medial and lateral compartmental laxity in extension and flexion.

Results: Initial native knee laxities were highly variable, with compartment knee laxity as tight as -9.8 mm in the flexion medial compartment and as loose as 8.2 mm in the extension lateral compartment (Figure 1, left). Greater range of laxities were observed during flexion in both the medial and lateral compartments during these pre-resection assessments. The accuracy of achieving planned knee laxity was within an average of 1mm across all compartments (Figure 2b). Knee balance was restored during trialing with a reduction in mediolateral laxity differences by up to 52.9% in extension and 72.7% in flexion (Figure 2a).

Conclusion: Despite significant variability in native knee laxity, the 3D implant adjustments using functional knee positioning principles achieved accurate and consistent knee balance during trialing. The robotically-enabled surgeries successfully reproduced the planned knee laxity within an average of 1 mm across all knee compartments. The functional knee positioning principles, which aimed to individualize planned implant position and balance the knee prior to bone cuts, enabled consistent execution of knee balance regardless of implant size/type, patient pathology, and surgical workflow.

Figures

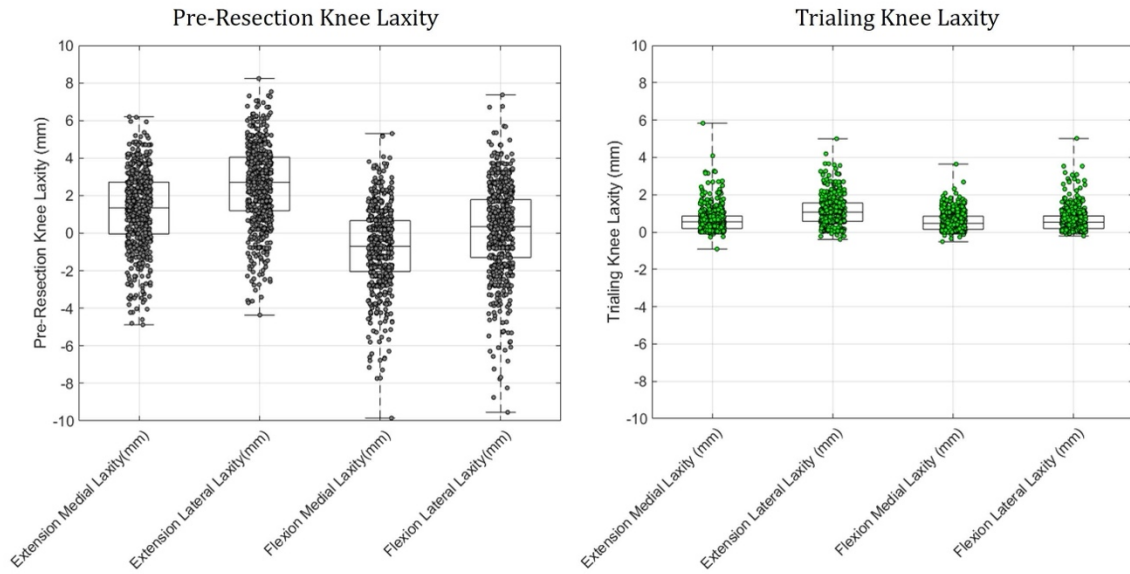


Figure 1: Medial and lateral compartment knee laxity in extension (10°) and flexion (90°) during pre-resection assessment (left) and trialing assessment (right) for 777 robotic assisted TKA patients aligned using functional knee positioning

Figure 1

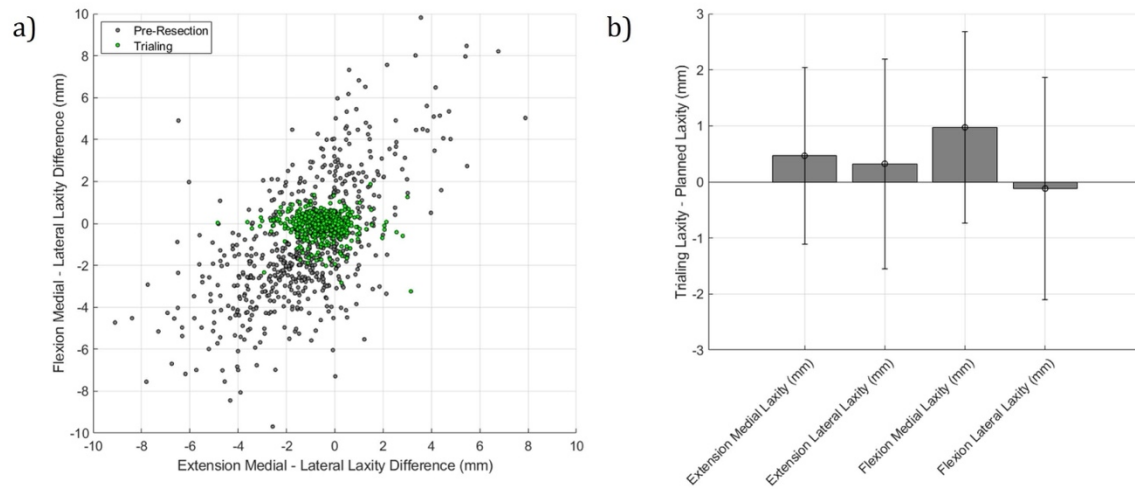


Figure 2: a) Knee balance measured as the difference between the medial and lateral compartmental laxity in extension and flexion during pre-resection and trialing assessments, b) average and standard deviation in difference between trialing and planned laxity for all compartments

Figure 2

CT-Measured Tibial Slope Will Not Optimize Ligamentous Reconstruction as Determined by NextAR

*John Mercuri - Geisinger - Scranton, USA

Massimiliano Bernardoni - Medacta International SA - Castel San Pietro, Switzerland

Daniele Ascani - Medacta International SA - Chiasso, Switzerland

Sanjiv Patel - Medacta USA - Nashville, United States of America

Introduction:

Tibial slope can be adjusted to balance a total knee arthroplasty (TKA). Traditional mechanical alignment targets are 0-3 degrees for posterior stabilized implants and 5-7 degrees for cruciate-retaining implants. Kinematic alignment recommends using the native slope of the medial tibial plateau which often exceeds 7 degrees. NextAR is an augmented reality, CT-based system that uses real-time, intra-operative information about ligament length to predict post-operative ligament behavior. This study evaluates whether the dynamic tibial slope measurements predicted by NextAR differed from the static, pre-operative CT measurements.

Methods:

Fifty-two consecutive cases were performed with NextAR. NextAR uses a predictive algorithm to demonstrate post-operative ligament length compared to their pre-operative state using CT acquired origins and insertions. Implant position is optimized before making bony cuts to achieve a patient-specific soft tissue envelop that recreates the natural, asymmetric laxities of the medial and lateral collateral ligaments (Fig. 1). The CT-measured slope of the medial tibial plateau is calculated in the planning stage. In this study, the slope values from the CT plans were compared to the intra-operative slope predictions that achieved an optimized ligamentous behavior.

Results:

Over 52 cases, NextAR predicted a mean tibial slope of 8.2 degrees (range 4.5-15) to recreate a patient-specific ligamentous behavior compared to a pre-operative CT mean of 9.1 degrees (range 1.8 to 16.8). This difference was not significant ($p=0.17$). The largest magnitude of deviation between the CT and NextAR measurements was 13.2 degrees, whereas the smallest was 0 degrees. Notably, 73.1% of patients had a difference between the CT and NextAR slopes of greater than 0.5 degrees, which is technologically relevant based on the tolerance of NextAR. Furthermore, 32.7% of patients had a difference of more than 3 degrees of tibial slope, 13.5% of patients had a difference of more than 6 degrees, 5.8% of patients had a difference of more than 9 degrees, and 2% of patients had a difference of more than 12 degrees. Lastly, 32.7% of patients had intraoperative NextAR predictions with greater slope values than the preoperative CT-measured values, whereas 67.3% of patients had lesser slope values.

Conclusion:

The average tibial slopes of the pre-operative CT scans and the intra-operative NextAR predictions were not significantly different (9.1 vs. 8.2 degrees) but both were of a higher value than traditional recommendations. About 73% of patients had NextAR predictions that differed from the CT measurements by greater than 0.5 degrees, which exceeds the tolerance of NextAR. Of greater clinical relevance, about 1/3 of patients had a difference of more than 3 degrees, which suggests that using the pre-operative CT-measured slope to optimize post-operative ligament behavior is inappropriate for a large number of patients. Moreover, approximately 2/3

of patients required intraoperative slope less than their pre-operative CT to adjust for bony wear of the osteoarthritic tibial plateau. However, one-third of patients actually required intraoperative slope adjustments greater than their CT measurements to recreate a patient-specific laxity of the prosthetic knee when in flexion.

Figures

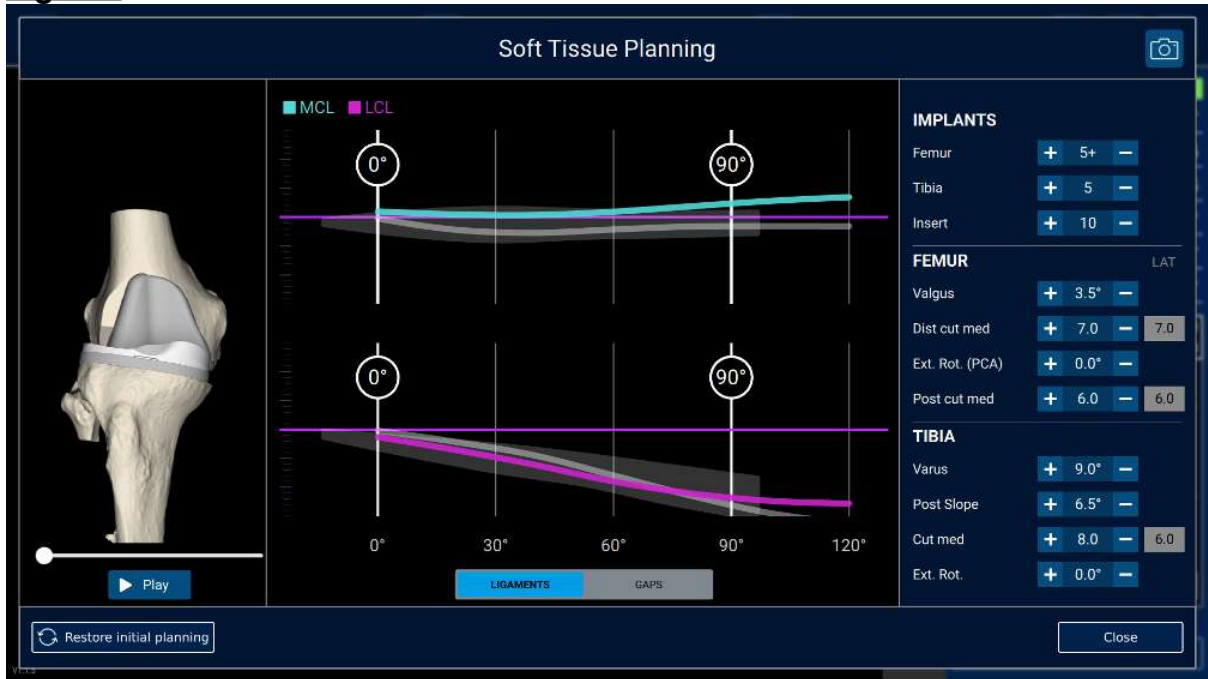


Figure 1

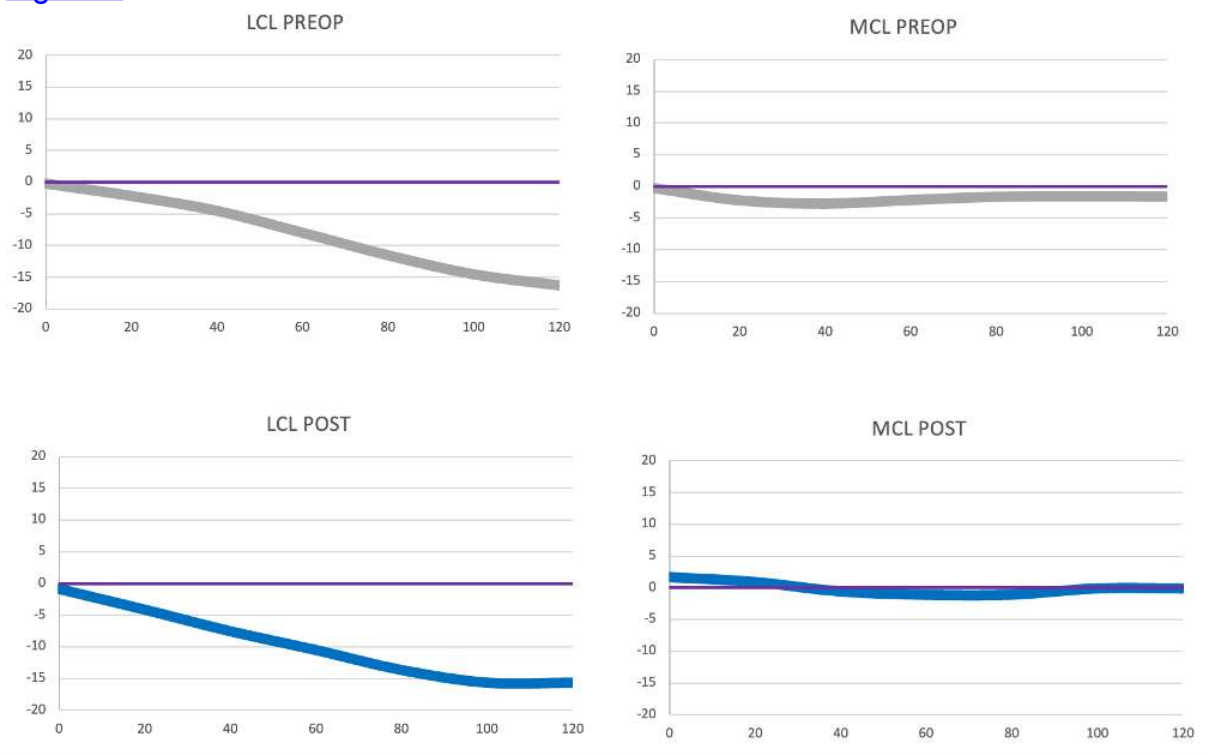


Figure 2

Predicting Post-Surgery Functional Outcomes Following Total Knee Arthroplasty

*Bradley Lambert - Houston Methodist Hospital - Houston, USA

Thomas Sullivan - Houston Methodist Hospital - Houston, USA

Terry Clyburn - Houston Methodist Hospital - Houston, USA

Kwan Park - Houston Methodist Hospital - Houston, USA

Stephen Incavo - Houston Methodist Hospital - Houston, USA

INTRODUCTION: Patient outcomes are often assessed at various time points before and following total joint replacement via either patient-reported outcome measures (PROMs) or functional assessments performed in clinical settings. The purpose of this study was to identify pre-operative factors that are correlated, and predictive of, post-operative assessments of patient mobility and physical function.

METHODS: Thirty-six patients (M=14, F=22; 66.7yr) undergoing primary TKA at a single institution underwent functional testing via a mobility outcomes testing battery (MOTB) developed by our laboratory prior to surgery (pre) as well as 6 months (6m) post-TKA. During mobility testing, patients performed the following: walking (3 meters), sit-to-stand, and ambulation up and down 4 stairs. Patients were scored on the following scale: 0=could not complete/attempt movement, 1=partial completion, 2=completion of movement. For each trial, patients rated their pain (VAS, 0-10). MOTB scoring incorporated both function and pain scores as follows for each movement: $\text{Function Score}(0-2) \times [(10 - \text{VAS})/10]$. A composite score for the entire MOTB (sum of test scores) was calculated and normalized to a maximal possible score of 100. Data for patient pre-operative demographics, comorbidities, limb alignment, PROMs (KOOS Jr, PCS, TSK-11) and blood labs were also collected along with DEXA assessments of body composition, and bone density. A t-test was used to compare MOTB scores between pre-surgery and 6m post-surgery. Multiple linear regression with stepwise removal was used to develop models that predict 6m post-operative total and movement-specific MOTB scores using the pre-operative data that were collected. Model selection for each assessment was based on the highest adjusted R^2 with the lowest level of variance inflation with a minimum model R^2 criteria of >0.5 . Type-I error was set at $=0.05$.

RESULTS: MOTB scores for all movements improved similarly by 6m (Walking 0.300.8, Sit-to-stand 0.290.9, stair ascension 0.430.10, stair descension 0.470.11, MOTB total score 22.14.5 $P<0.001$). Regression analysis revealed several pre-surgery variables to be significantly predictive of the 6-month post-surgery total MOTB score, as well as ascending and descending stairs ($P<0.01$). Predictive modeling for 6-month post-surgery walking and sit-to-stand performance was not observed to meet model development criteria ($R^2<0.5$) The final predictive models for total and stair ascension/descension MOTB scores were

6-Month Post-op Total MOTB Score (0-100)($R^2=0.502$, $SEE=14.9$)=
[Body Mass Index(kg/m²)*-2.651] +[Fat Mass Index(kgFM/m²)*2.939] +[Pre-op(0=varus, 1=valgus)*-10.597] +[Pre-op Sit-to-stand score(0-2)*-8.201] +[Pre-op stair ascension score(0-2)*9.956] +[Leg Length(cm)*1.463] +[Pre-op KOOS Jr. (0-100)*2.11] +10.573

6-Month Post-op Stair Ascension Score (0-2)($R^2=0.521$, $SEE=0.54$)=
[Height (cm)*-0.025] +[Body Mass Index(kg/m²)*-0.037] +[CAD/PVD (yes=1/no=0)*-0.524] +[Pre-op stair ascension score (0-2)*0.391] +[Leg Length(cm)*0.067] +[Lean Mass Index (kgLM/m²) *0.041] +[Pre-op (0=varus/1=valgus)*-0.17] +0.604

6-Month Post-op Stair Descension Score (0-2)($R^2=0.509$, $SEE=0.55$)=

$[\text{Body Mass Index}(\text{kg}/\text{m}^2) \times -0.037] + [\text{CAD/PVD}(\text{yes}=1/\text{no}=0) \times -0.594] + [\text{Pre-op stair ascension/descension average score}(0-2) \times 0.246] + [\text{Leg Length}(\text{cm}) \times 0.049] + [\text{Pre-op}(0=\text{varus}/1=\text{valgus}) \times -0.26] - 1.466$

CONCLUSIONS: These data provide considerable support for further predictive modeling for functional mobility screening following TKA. Such assessments may be utilized by clinicians to help patients manage expectations for their recovery. Prediction of functional capacity may also provide rehabilitation professionals in rehabilitation customization and to develop individualized functional milestones based on the prediction windows for MOTB assessments. Data collection remains ongoing for further model strengthening/development.

Promising Short-Term Outcomes for Robotic-Assisted Revision Total Knee Arthroplasty

*Kevin Chang - Northwell Health Huntington Hospital - Huntington, USA

Jonathan R. Danoff - Northwell Health, Northshore University Hospital - Manhasset, USA

Alekasandra Qilleri - 6. Donald & Barbara Zucker School of Medicine - Hempstead, USA

Alexandra Echevarria - Northwell Health - Great Neck, USA

Introduction

Revision total knee arthroplasty (TKR) is a complex surgery requiring extensive experience and skill. While robotic-assisted techniques have gained popularity in the last decade, their use for robotic-assisted revision total knee arthroplasty (RATKR) has only recently been published. Navigated techniques aim to virtually restore anatomic landmarks, facilitating tissue-balancing and joint-line restoration. This study compares short-term outcomes of RATKR to conventional TKR. We hypothesize that RATKR will accelerate return of function, measured in range of motion and time to ambulation.

Methods

This is a retrospective case-control study reviewing all TKR performed by an arthroplasty-fellowship-trained surgeon between 2017-2023. TKR performed prior to 2022 used conventional techniques and were compared to RATKR performed after 2022, using a newly published technique incorporating CT-guided navigation and MAKO-robotic assistance (Stryker, Mahwah, NJ). Patients undergoing revision for infection or fracture were excluded. Data collected included demographics, surgical and implant data, in-hospital physical therapy (PT) progress, and outcomes through 1-year.

Results

52 TKR cases were included with average age 67.1 years \pm 8y. Etiologies included 33 (63.5%) for loosening, 9 (17.3%) for second-stage reimplantation after infection eradication, 4 (7.7%) for polyethylene wear, 3 (5.8%) for instability, and 3 (5.8%) for component malposition/arthrofibrosis. 37 (71.2%) conventional TKR were compared to 15 (28.8%) RATKR. RATKR case time averaged 20 minutes less than conventional, $p=0.43$. More RATKR patients demonstrated ambulation of at least 100 feet by postoperative day (POD)1 ($p=.021$), but no differences were noted for PT clearance by POD2 ($p=0.11$) or discharge by POD3 ($p=0.11$). Significantly more RATKR cases (100%) achieved knee flexion past 90° at 2-week follow-up, compared to 75.6% conventional, $p=0.038$. All study patients achieved at least 110° knee flexion by 6-weeks. No medical, surgical, or pin-site complications, or need for revision surgery were found in the RATKR group through minimum 1-year. Two patients in the conventional group experienced complications including one deep vein thrombosis with pulmonary embolism within 30-days and another patient readmitted for local wound care within 90-days for gastrocnemius flap breakdown.

Discussion

TKR can be performed via conventional and robotic techniques with excellent functional success. In this study, RATKR did not add operative time to the revision surgery. RATKR may provide advantages in recovery, with more patients ambulating at least 100 feet on POD1 and achieving knee flexion past 90° by 2-weeks. There

were no construct failures in either cohort. Additional follow-up is needed to assess long-term outcomes, implant longevity, and patient-reported outcomes.

Revision TKA Using Robotic Assisted Surgery: Technical Challenges and Short Term Outcomes

*Arthur Malkani - Jewish Hospital - Louisville, USA

John Whitaker - University of Louisville - Louisville, USA

Erik Van Eperen - University of Louisville - Louisville, USA

Madhusudhan Yakkanti - Louisville Orthopaedic Clinic - Louisville, USA

Andrew Swiergosz - University of Louisville - Louisville, United States of America

Background: Successful revision of total knee arthroplasty (rTKA) is a technically challenging procedure for many reasons. Reestablishment of the joint line with successful gap balancing becomes more difficult to accomplish after a previously failed TKA. Robotic-assisted primary TKA has been established as more accurate at achieving these goals than manual TKA. The purpose of this paper is to demonstrate a reproducible surgical technique for using robotic assistance in rTKA and the potential benefits of this technique.

Methods: A single-center retrospective surgical technique guide of seven patients who underwent a robotic-assisted rTKA. All study participants had previous primary TKAs requiring revision. None of the patients included had infected primary TKA confirmed by knee aspiration and lab values.

Results: Seven patients had successful rTKA using robotic navigation. Total surgical time decreased significantly with subsequent rTKA procedures. No cases were aborted due to the inability to register the knee or other technical reasons. All cases had successful gap balancing and restoration of the joint line as confirmed by radiographic analysis.

Conclusion: rTKA using robotic navigation is an effective method for accurately reestablishing the native joint line, providing effective gap balancing, and assisting in soft tissue protection in the rTKA setting. This surgical method allows the incorporation of augments and the use of revision components while balancing the soft tissue envelope as you would in a primary TKA. Future research should be directed to comparing manual rTKA to robotic-assisted rTKA, and long-term follow-up of robotic rTKA is needed to validate the efficacy of robotic-assisted rTKA.

Clinical and Patient Reported Outcomes of a Novel Reverse Hybrid System in Total Knee Arthroplasty

*Muhammad Haider - NYU Orthopedic Hospital - New York, USA

Jonathan Katzman - NYU Langone - New York, United States of America

Casey Cardillo - NYU Orthopedic Hospital - New York, USA

Joshua Rozell - NYU Langone Orthopedic Hospital - New York, USA

Ran Schwarzkopf - NYU Langone Medical Center Hospital for Joint Diseases - New York, USA

Akram Habibi - NYU Langone Orthopedic Hospital - New York, United States of America

Benjamin Schaffler - NYU Orthopedic Hospital - New York, USA

Catherine Digangi - NYU Orthopedic Hospital - New York, USA

Sophia Antonioli - NYU Langone - New York, USA

Introduction

Reverse hybrid total knee arthroplasty (TKA) has gained popularity as a treatment option for patients with end-stage knee arthritis by offering the benefits of cementless tibial fixation and an anatomically designed cemented femoral component. This study aimed to evaluate clinical outcomes of patients treated with a novel reverse hybrid total knee system.

Methods

We conducted a retrospective, single-center review of 164 patients who received a reverse hybrid (cementless tibial component, cemented femoral component) system with a novel cementless tibial baseplate (CONCELOC™; Journey II, Smith & Nephew, Memphis, Tennessee) and had a minimum follow up of three months. Primary outcome measures included rates of all-cause revision, 90-day emergency department (ED) visits and readmissions, and the need for a manipulation under anesthesia (MUA). Survival from all-cause and aseptic revision was evaluated using the Kaplan-Meier method. Knee Osteoarthritis Outcome Score for Joint Replacement Scores (KOOS, JR) scores were evaluated preoperatively and three months postoperatively.

Results

Among the cohort there were 53 (32.3%) cruciate retaining and 111 (67.7%) bicruciate stabilized designed implants. Of the 156 (95.1%) patellas resurfaced, 34 (21.8%) were cemented. There were three orthopedic-related 90-day ED visits (1.8%) for knee pain, cellulitis and back pain. Two patients had orthopedic-related 90-day readmissions (1.2%) for cellulitis and deep infection. One patient (0.6%) underwent revision for peri-prosthetic joint infection. Survival from all-cause and aseptic revision was 99.4 and 100.0%, respectively. Five patients (3.0%) underwent MUA for stiffness. KOOS, JR scores improved by an average of 14.5 points at three months postoperatively, achieving the minimally clinically important difference.

Conclusions

This study suggests that this novel reverse hybrid total knee system is a safe and effective treatment option, with low rates of revision and manipulation and clinically significant improvement in PROMs. Future studies with longer follow-up are necessary to confirm the durability of this implant combination.

Patients Identified as Neutral Satisfied Patients Are, in Fact, Neutral, Questioning the Use of Dichotomizing to Satisfied or Dissatisfied.

*Jason Cholewa - Zimmer Biomet - Warsaw, USA

Mike Anderson - Zimmer Biomet - Lehi, USA

Roberta Redfern - Zimmer Biomet - Pemberville, USA

Introduction

Rates of patient satisfaction following total knee arthroplasty (TKA) are highly variable, with reported dissatisfaction ranging between 5% to 25%. Many patient satisfaction surveys contain a "neutral" or "neither satisfied nor dissatisfied" option. How neutral patients are dichotomized may be one source of ambiguity in the rate of TKA dissatisfaction. The purpose of this study was to clinically characterize neutrally satisfied patients and compare outcomes between satisfied, dissatisfied, and neutral patients.

Methods

This was a secondary analysis from data collected in a multicenter longitudinal cohort study comprised of TKA patients using a digital care management platform. Patients (n=2544) underwent primary TKA between November 2018 and October 2023. The five-item Knee Society Score satisfaction (KSS) survey was administered at 90 days post-operative, and dissatisfaction was defined as a composite score of less than 20, satisfied as a composite score equal to or greater than 30, and neutral as a composite score of 20 through 29. Patient-reported outcome measures (PROMs) were assessed pre-operatively and at one-, three-, six-, and twelve-months post-operative, and were compared between groups with pairwise comparisons.

Results

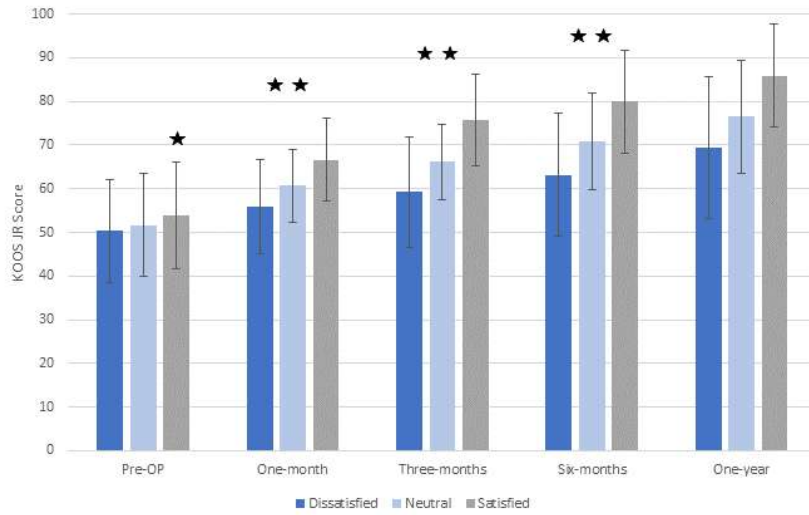
Approximately 58% of patients were satisfied (n=1486), 29.4% neutral (n=747) and 12.2% dissatisfied (n=311). Neutral and dissatisfied patients were younger, more likely to be female, and had lower pre-operative KSS scores compared to satisfied patients, though statistical differences were found between all groups. Pre-operative pain was significantly less in satisfied compared to neutral or dissatisfied patients. The change in Knee Osteoarthritis Score for Joint Replacement (KOOS JR) from pre-operative displayed significant differences between all groups at all time points, with greater improvements in satisfied vs. neutral patients, and neutral vs. dissatisfied patients (Figure 1). Similarly, satisfied patients experienced significantly greater improvements in pain and KSS at three months post-operative, and neutral patients improved more than dissatisfied patients (Figure 2).

Discussion

Neutral patients tended to be slightly more functional than dissatisfied patients but reported greater pain than satisfied patients before TKA. Following TKA, improvements in pain, ROM, and PROMs all followed a similar order, with neutral patients improving more than dissatisfied patients, but considerably less than satisfied patients. Neutral patients present with distinctively different clinical outcomes compared to satisfied or dissatisfied patients and should be classified separately as neutral.

Figures

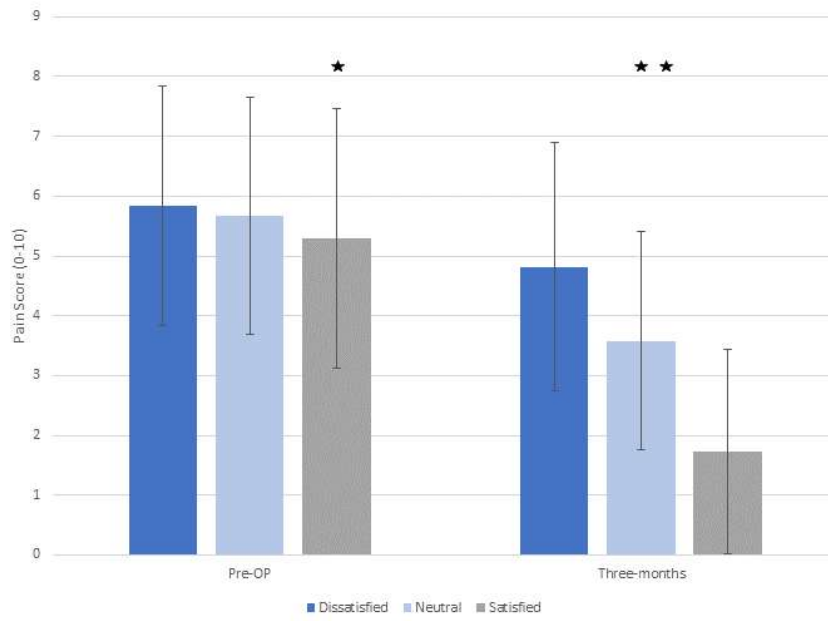
Figure 1. KOOS JR scores for satisfied, neutral, and dissatisfied patients through one-year post-operative



* Significantly different from dissatisfied and neutral; ** Significant differences between all groups

[Figure 1](#)

Figure 2. Pain scores for satisfied, neutral, and dissatisfied patients through three-months post-operative



* Significantly different from dissatisfied and neutral; ** Significant differences between all groups

[Figure 2](#)

Factors Associated With Increased Opioid Consumption Following Total Hip Arthroplasty

*Mads Koefoed Hansen - Hvidovre Hospital, CORH - Frederiksberg, Denmark
Andreas Fontalis - University College London Hospitals - London, United Kingdom
Fares Haddad - University College London Hospital - London, United Kingdom
Ricci Plastow - University College London Hospitals NHS Foundation Trust - London, United Kingdom
Adam Yasen - University College Hospital London - London, United Kingdom
Babar Kayani - University College Hospital London - London, United Kingdom

Abstract

Introduction: Effective postoperative pain management is imperative in Total Hip Arthroplasty (THA) to enable early mobilization and accelerate recovery pathways. This study investigated the patterns of in-hospital opioid consumption following THA and identified the factors associated with increased opioid usage.

Methods: In this large-scale, single-institution study, we analyzed data from 2,048 primary THAs between May 2019 and July 2023. We collected data on demographics, length of stay (LOS), type of anaesthesia, Post Anaesthesia Care Unit (PACU) admissions, 30-day readmissions, total opioid consumption (morphine equivalents), implant fixation techniques, surgical characteristics and pre- and post-operative haemoglobin (Hgb) levels. Factors associated with increased opioid consumption (patients above the third quartile in opioid consumption distribution) were identified through univariate and multivariate logistic regression models.

Results: The cohort included 1,260 (61.5%) female and 788 (38.5%) male patients. The median in-hospital opioid consumption was 88 mg (Q1, Q3: 39 mg, 211 mg). In the univariate model, significant predictors included age, ASA score, conventional surgical technique, general anaesthesia, pre- and post-operative Hb levels and the need for PACU admission. After adjusting for baseline demographics in the hierarchical multivariate logistic regression model, significant predictors of higher opioid utilization were ASA score (OR 1.492, 95% CI [1.193 – 1.866], $p < 0.001$), post-operative Hb levels (OR 0.981, 95% CI [0.970 – 0.992], $p < 0.001$), age (OR 0.989, 95% CI [0.981– 0.997], $p = 0.010$), general anaesthesia (OR 2.386, 95% CI [1.865 - 3.054], $p < 0.001$), and the need for PACU admission (OR 2.098, 95% CI [1.310 – 3.358], $p < 0.001$).

Discussion: The most significant correlations with higher opioid consumption were ASA score, younger age, lower levels of post-operative hemoglobin, the necessity for PACU admission and general anesthesia. It is essential to consider potential confounding factors related to opioid use, such as individual pain thresholds and daily variations in pain scores. Furthermore, larger-scale prospective studies and randomized controlled trials are required to expand on these findings.

Figures

Table 1. Demographic and baseline data of the studied cohort	
Variable	Absolute number (Percentage) Median [Quartile1, Quartile 3]
Gender	
Female	1260(61.5%)
Male	788(38.5%)
ASA rating	
1	224(11.6%)
2	1265(65.3%)
3	428(22.1%)
4	19(1%)
Anaesthesia type	
General	855(45.3%)
Spinal	1031(54.7%)
Implant fixation	
Uncemented	1508(82.6%)
Cemented	19(1%)
Hybrid (Cemented femur)	297(16.3%)
Hybrid (Cemented acetabulum)	2(0.1%)
Readmission within 30 days	122(6%)
Post anaesthesia Care Unit (PACU) admission	147 (7.2%)
Index of multiple deprivation (Quintiles)	
0-20 %	310(15.6%)
20-40%	574(28.8%)
40-60%	474(23.8%)
60-80%	373(18.7%)
80-100%	259(13%)
Month of admission	
January	150(7,3%)
February	145(7,1%)
March	151(7.4%)
April	148(7.2%)
May	220(10.7%)
June	247(12.1%)
July	219(10.7%)
August	153(7.5%)
September	184(9%)
October	142(6.9%)
November	178(8.3%)
December	119(5.8%)
Technique	
Robotic	355(17.3%)
Conventional	1693(82.7%)
Total Opioid usage (morphine equivalents)	88 (39.25, 211.93)
BMI	27.5 [24,2 ; 32]
Age	64 [53 ; 73]
Post anaesthesia Care Unit (PACU) Days	2 [2 ; 3]
Hb pre-operatively	136 [126 ; 144]

[Figure1](#)

Table 2. Binary logistic regression assessing predictors of higher opioid utilization (patients above the third quartile in opioid consumption distribution): a univariate analysis.

Variable	Odds ratio [95% CI]	P-value
Age	0.992 [0.985– 0.999]	P =0.026
Gender (Male)	0.822 [0.661 – 1.022]	P = 0.077
BMI	1.006 [0.991 – 1.020]	P = 0.440
Index of Multiple Deprivation (quintile)	1.006 [0.925-1.094]	P=0.887
Conventional technique	1.782 [1.308 – 2.426]	P < 0.001
General anaesthesia	2.816 [2.253-3.521]	P < 0.001
Need for PACU admission	2.788 [1.961 – 3.962]	P < 0.001
ASA	1.576 [1.319 – 1.882]	P < 0.001
Hb Pre-operatively	0.985 [0.978-0.991]	P < 0.001
Hb Post-operatively	0.981 [0.974 – 0.988]	P < 0.001
Year	0.623 [0.572 – 0.679]	P < 0.001

[Figure2](#)

Table 3. Binary logistic regression assessing predictors of higher opioid utilization (patients above the third quartile in opioid consumption distribution): a multivariate analysis.

Variable	Odds ratio [95% CI]	P-value
Age	0.989 [0.981– 0.997]	P =0.010
Gender (Male)	1.125 [0.847 – 1.493]	P = 0.418
BMI	1.003 [0.987 – 1.019]	P = 0.700
Conventional technique	1.059 [0.749 – 1.496]	P = 0.747
General anaesthesia	2.386 [1.865 - 3.054]	P < 0.001
Need for PACU admission	2.098 [1.310 – 3.358]	P = 0.002
ASA	1.492 [1.193 – 1.866]	P < 0.001
Hb Pre-operatively	1.004 [0.992-1.015]	P < 0.001
Hb Post-operatively	0.981 [0.970 – 0.992]	P < 0.001
Year	0.638 [0.579 – 0.703]	P < 0.001

[Figure 3](#)

2- to 17-Year Clinical Outcomes of 5352 Metal-on-Metal Hip Resurfacing Cases

***Dani Gaillard-Campbell - Midlands Orthopaedics & Neurosurgery - Columbia, USA**

Thomas P Gross - Columbia, USA

Introduction: This study aims to analyze and present 2- to 17-year clinical outcomes and implant survivorship data on a large, single-surgeon cohort of metal-on-metal (MoM) hip resurfacings with the Magnum-ReCap™ implant system.

Methods: The primary surgeon performed 6091 consecutive hip resurfacing surgeries from December 2004 to June 2021 using the Biomet Magnum-ReCap™ system. The first 739 cases utilized hybrid cemented fixation, comprised of cemented ReCap™ femoral component and an uncemented Magnum™ acetabular component. The 5352 resurfacing cases performed after March 2007 were fully uncemented.

Results: The combined 17-year implant survivorship with the Biomet Magnum-ReCap™ device in this consecutive single-surgeon series is 98.6%. The 15-year survivorship for the hybrid implant is 95.1%, and the 15-year survivorship for the UC implant is 99.1% ($p < 0.0001$). Raw failure rates differed significantly between the two implant types, with a 5.1% rate of failure in the cemented group and 1.1% overall rate of failure in the uncemented group ($p < 0.0001$). Metal ion test results were requested at 2 years postoperative. Of the patients tested, 97.3% of the hybrid cohort and 98.1% of the uncemented group had optimal ion levels. There have been no instances of adverse-wear related failure in any cases performed after 2009.

Conclusions: Since 2012, there is no statistically significant difference in resurfacing implant survivorship regardless of age, sex, or diagnosis in over 3765 cases. This study suggests that, with appropriate surgeon experience and technique, metal-on-metal hip resurfacing arthroplasty can be performed with desirable clinical outcomes and with a significantly lower risk of metal-wear related failures than is reported in the literature and major registries. At the time of publication, this study represents the largest single-surgeon series of metal-on-metal hip resurfacing with long-term data and the second-best long-term implant survivorship for any hip arthroplasty cohort published.

Figures

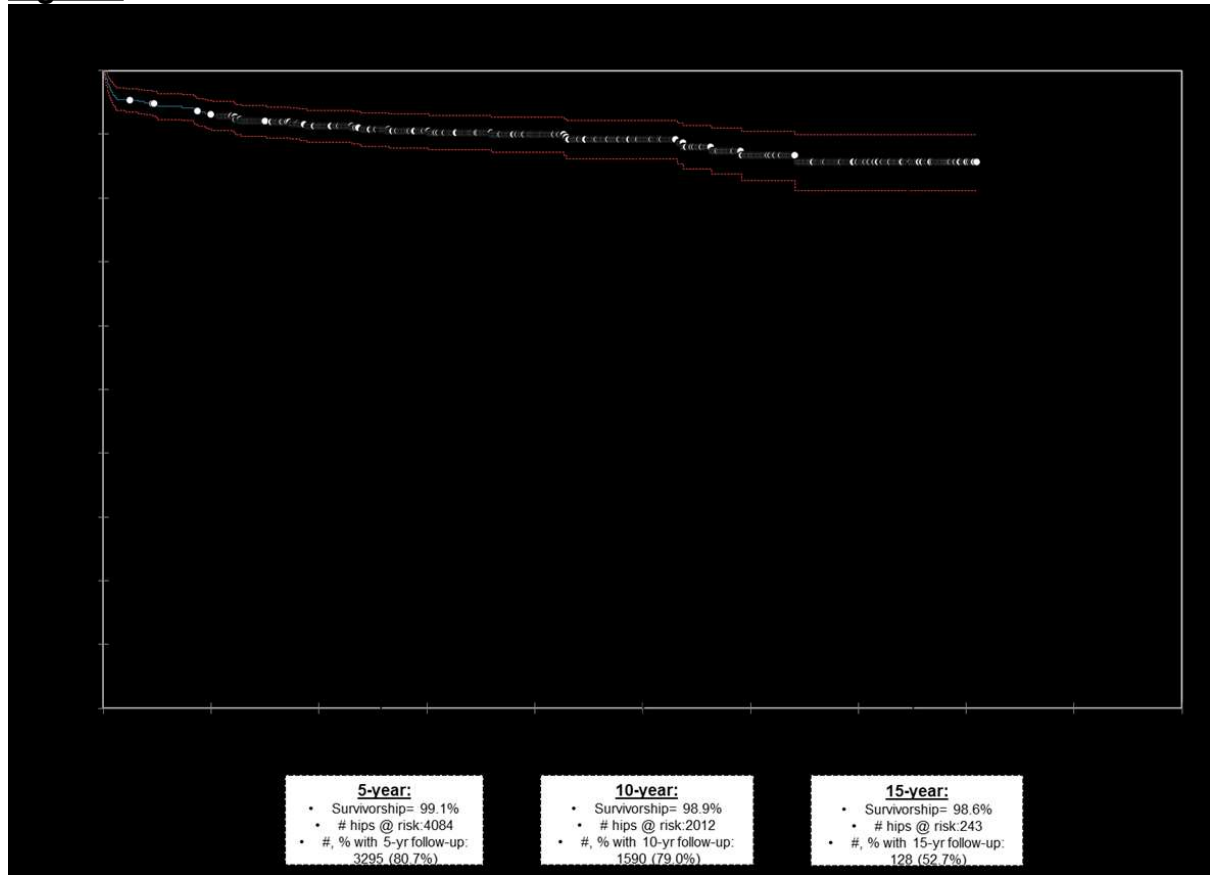


Figure 1

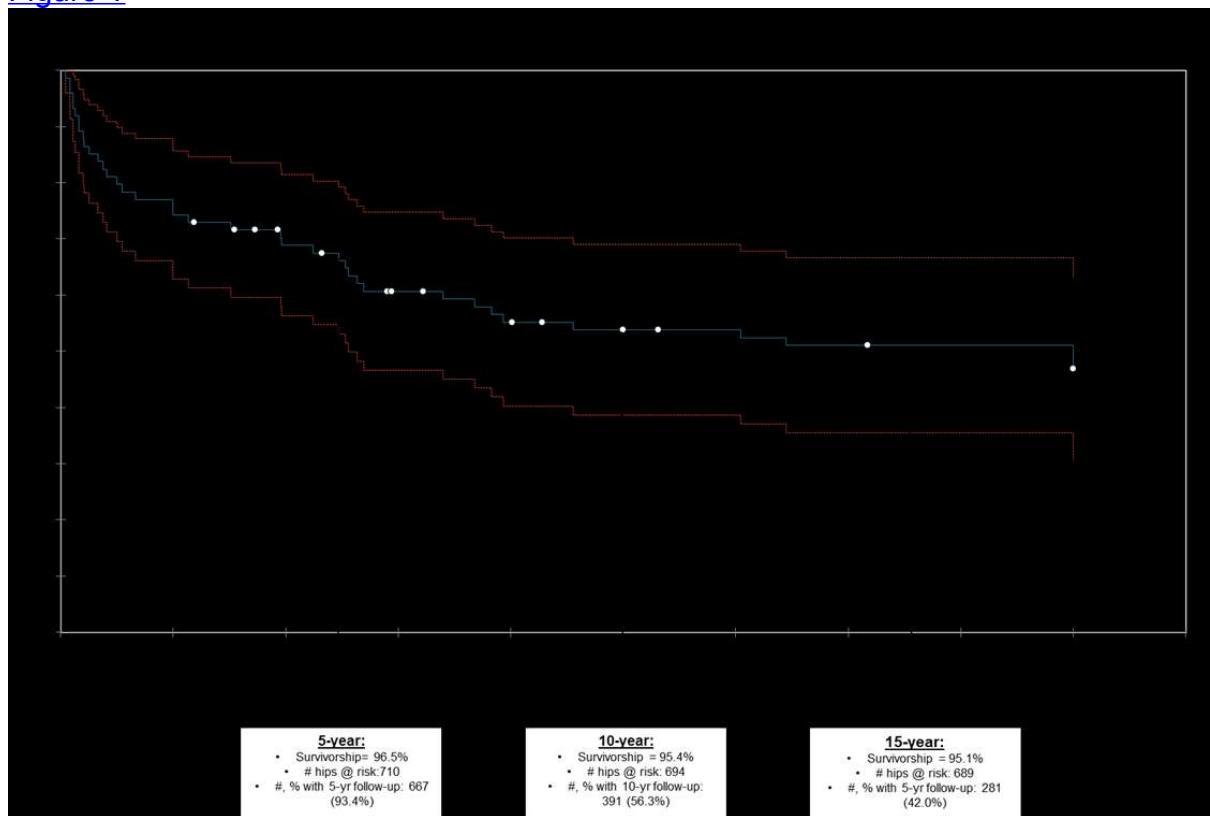


Figure 2

Findings From a Large Cohort of Modular Liner Metal-on-Metal Hip Replacements

Melissa Rupert - UCLA Bioengineering; The J. Vernon Luck, Sr., MD Orthopaedic Res - Los Angeles, USA

Sang-Hyun Park - Orthopaedic Institute for Children /UCLA - Los Angeles, USA

*Sophia Sangorgio - Orthopaedic Institute for Children/UCLA - Los Angeles, USA

Eddie Ebramzadeh - Orthopaedic Institute for Children and UCLA - Los Angeles, USA

Introduction

Despite numerous retrieval studies, the high failure rates for metal-on-metal (MoM) total hip arthroplasties reported have not been explained with one unifying theory. Some failures have been attributed to high articular wear, taper corrosion, edge loading, or metal hypersensitivity. For the Pinnacle MoM system, potential changes in manufacturing affecting implantations from 2007 onward have also been implicated. However, many revisions are not associated with any of these explanations. The purpose of the present study was to present the qualitative and quantitative findings from the retrieval investigation of a single metal-on-metal design with a modular acetabular component.

Methods

A total of 328 MoM hip replacement retrievals (Pinnacle Ultramet, DePuy, Warsaw, IN) were received between 2013 and 2018 by an independent academic retrieval laboratory through a voluntary post-market surveillance program. Features of wear, damage, and bony attachment were evaluated using a semi-quantitative scoring system. Taper corrosion was ranked using the Goldberg criteria. Linear and volumetric wear for the articular surfaces were quantified using metrology. All available tissues were sampled and examined for features of ALVAL and scored from 0-10 by a single observer. Further, devices were categorized by index surgery date, to investigate the possibility of any manufacturing changes.

Results

Index procedures were from 1999-2012, and dates of revision were from 2005-2018. The mean age at the index procedure was 61.2 ± 9.8 , and the median duration of implantation was 58.0 ± 29.7 . The most common bearing surface feature observed was light scratches. Overall, the median volumetric wear was low, 6.9mm^3 (range 0.5-568.4, Figure 1), with higher wear observed in cases with edge loading (Figure 2). 80% had a location of maximum linear wear depth $>75^\circ$, indicative of edge loading and possible malpositioning. Taper corrosion was predominantly scored as a 4 due to the presence of imprinting marks from micro-grooved femoral stems (62% of cases). 34 of the retrievals were submitted with tissue samples. Of those, the mean ALVAL score was 6.3 ± 1.9 . Wear rates for devices implanted before 2007 were comparable to those implanted from 2007 onward ($P=0.90$).

Discussion

While edge wear and subluxation were observed in many cases, particularly in those with high wear, the majority of cases had combined volumetric wear below 10mm^3 , typically cited as a threshold for technical measurement accuracy. These findings indicate that causes other than high articular wear, hypersensitivity, and potential manufacturing changes were responsible for the removal of these devices.

Figures

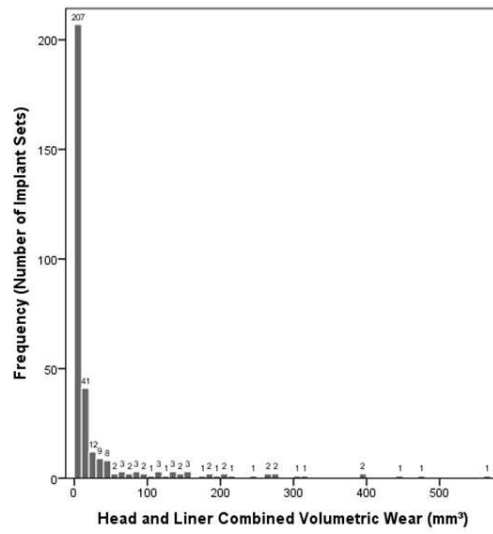


Figure 1

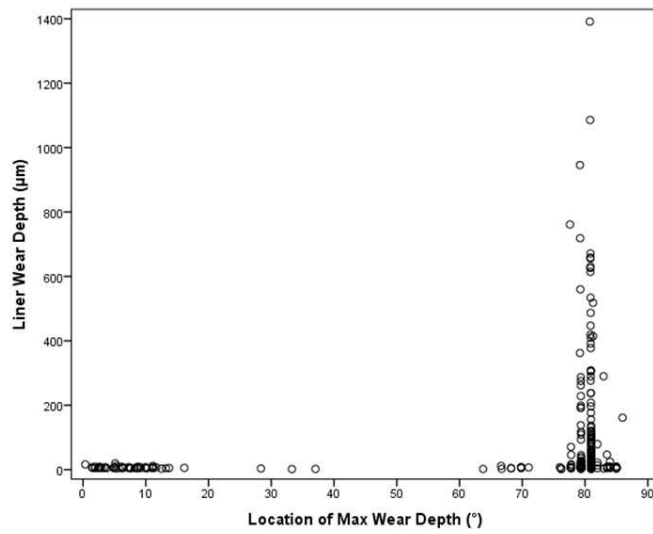


Figure 2

Category	Total
Total Retrievals	328
Male	121
Female	190
Unknown	17
Mean Age at Implantation (y)	61.2 ± 9.8
Mean Time Until Revision (mo)	58.0 ± 29.7
Heads	321
Liners	301
Shells (Separate from Liner)	47
Combined Liner and Shell	19
Femoral Stems	70
28mm Head	22
36mm Head	267
40mm Head	30
44mm Head	6

[Figure 3](#)

Correlation of Crosslinking Measured With the Trans-Vinylene Index and Wear as Measured by a Pin-on-Disc Test of Polyethylene Liners From Various Manufacturers Used in Total Hip Arthroplasty

*Peter Wahl - Kantonsspital Winterthur - Winterthur, Switzerland

Roman Heuberger - RMS Foundation - Bettlach, Switzerland

Andrea Pascucci - RMS Foundation - Bettlach, Switzerland

Thomas Imwinkelried - RMS Foundation - Bettlach, Switzerland

Markus Fuerstner - Bern University Hospital - Bern, Switzerland

Niels Icken - Cantonal Hospital Winterthur - Winterthur, Switzerland

Robin Pourzal - Rush University Med Ctr - Chicago, USA

Emanuel Gautier - HFR Fribourg - Cantonal Hospital - Fribourg, Switzerland

Emanuel Benninger - Cantonal Hospital Winterthur - Winterthur, Switzerland

Introduction: Highly cross-linked polyethylene (XLPE) is one of the most important progresses in total hip arthroplasty (THA), greatly reducing wear and requirement for revision compared to conventional polyethylene (CPE). Crosslinking is commonly achieved through irradiation. Irradiation dose and thermal treatment are the main material determinants of revision after THA identified so far for polyethylene.

However, how the degree of crosslinking varies between products and how this impacts tribological behaviour is still unclear. This study compares the degree of crosslinking and in vitro wear rates across a cohort of retrieved and unused polyethylene (PE) cups/liners from various manufacturers.

Methods: PE acetabular cups/liners were collected from one centre from April 2021 to April 2022. The trans-vinylene index (TVI) and the oxidation index (OI) were determined by Fourier-transformed infrared spectrometry. Wear was measured on pins 5 mm in diameter extracted from the cups/liners using a pin-on-disc test.

Results: Forty-seven PE specimens from eight manufacturers were included. The TVI was stable within each group and independent of time in vivo. A linear correlation ($r^2=0.995$) could be observed between the old and the current TVI standard, except for vitamin E infused PE (Fig. 1). No excessive oxidation interfered. The absorbed irradiation dose calculated from the TVI corresponded to product specifications for all but two products (Fig. 2). For one, an equivalent mean irradiation dose of 241% was observed, likely explained by higher crosslinking from electron irradiation compared to gamma irradiation. For another XLPE, much lower than expected (mean $41\% \pm 13\%$) doses were measured than indicated by the manufacturer. Lower wear was observed for higher TVI (Fig. 3). The one XLPE with unexpectedly low TVI showed wear more comparable to CPE. Despite adequate TVI, another vitamin E infused XLPE showed slightly higher in vitro wear than the others.

Conclusion: The TVI is a reliable measure of the absorbed dose of irradiation of PE and does not alter over time. Conversion from the old to the current standard is linear, except for vitamin E infused PE. Various brands differ by manufacturing details and consequently characteristics. Absorption and penetration of electron irradiation and gamma irradiation differ, potentially leading to different degrees of cross-linking. There is a non-linear, inverse correlation between TVI and in vitro wear. Irradiation doses calculated from the measured TVI deviated from specifications for one XLPE, which correlated with an inferior in vitro wear rate, comparable to CPE rather than the other XLPE.

Figure 1 – Correlation of the TVI₁₃₇₀ and the TVI₁₉₀₀ measured on the 47 polyethylene samples included.

Figure 2 – The TVI₁₃₇₀ value measured on all the samples was converted to the absorbed irradiation dose, using the calibration curve for remelted XLPE published previously. Results are grouped by product. All calculated irradiation doses were within specifications, respectively slightly higher than specifications, except for two products (higher for Durasul, lower for Highcross).

Figure 3 –Wear in dependence of the TVI₁₃₇₀, as determined in a modified pin-on-disc test.

Figures

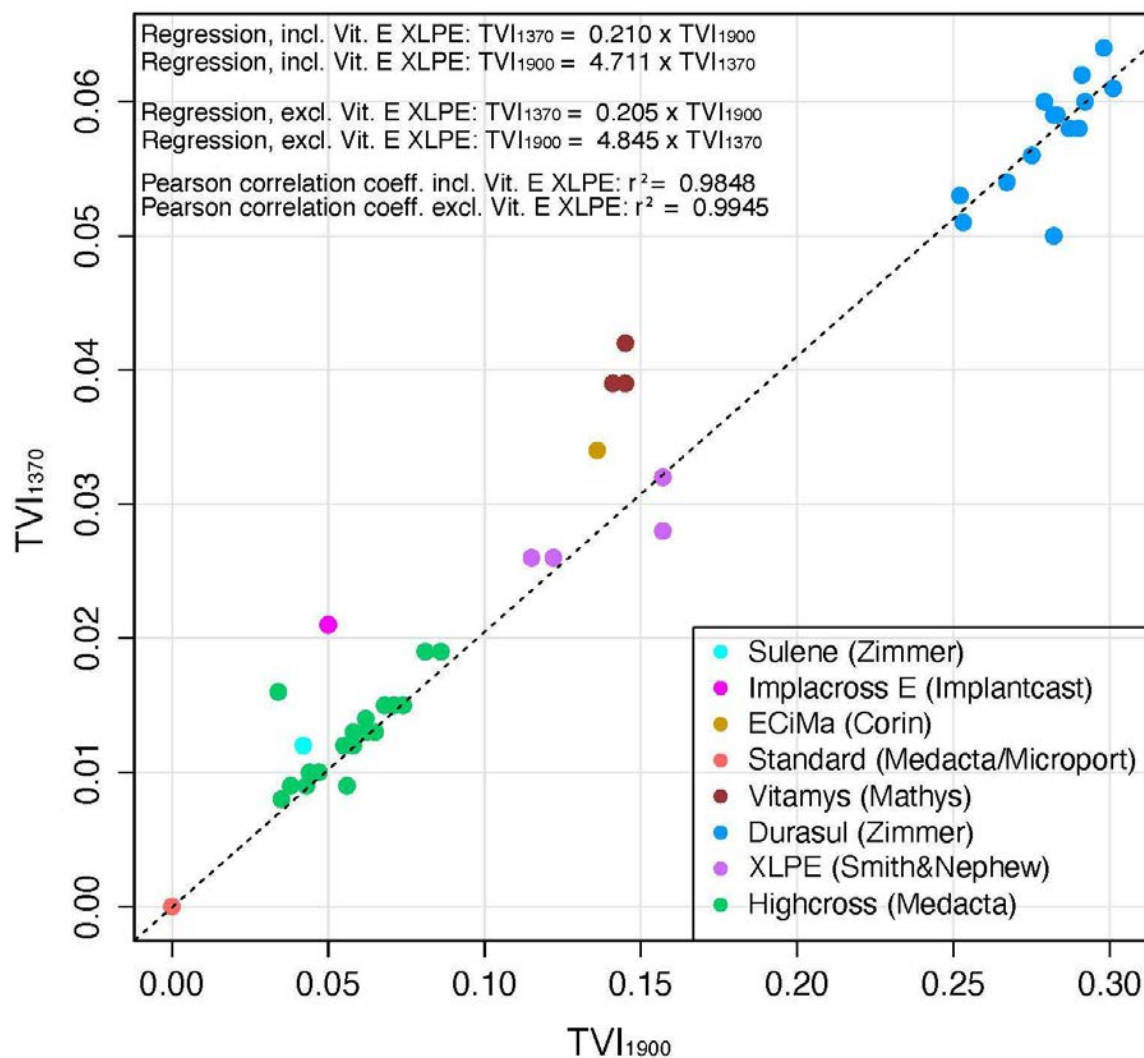
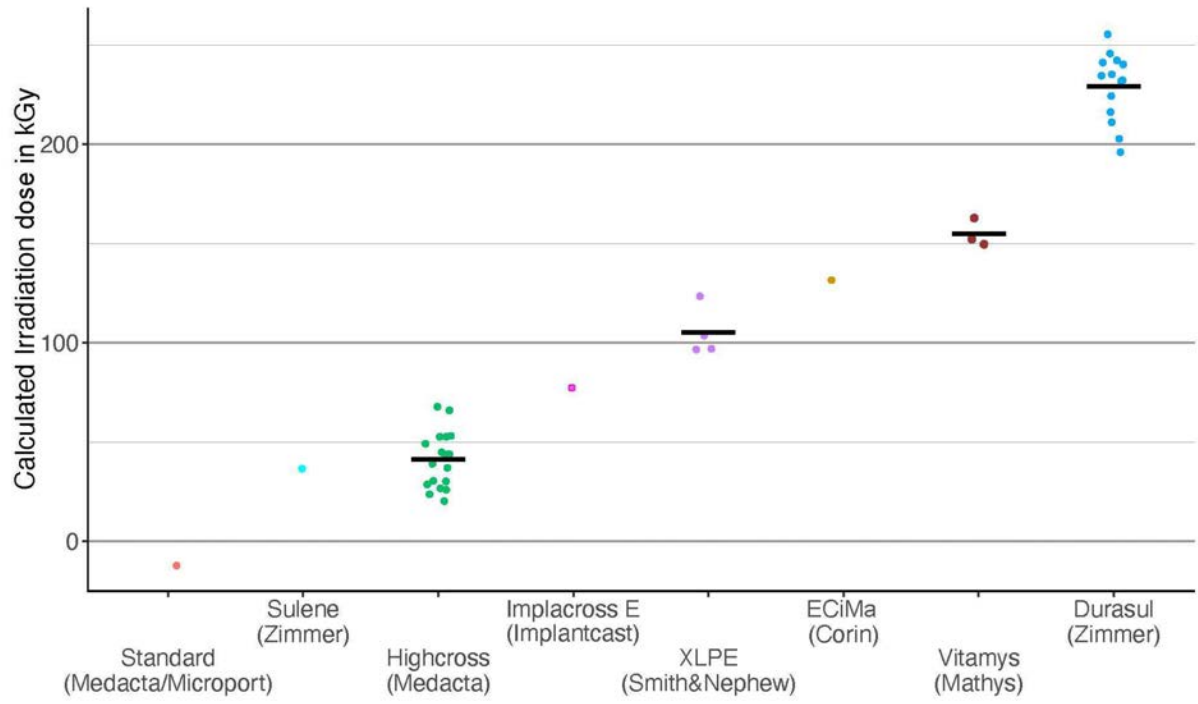


Figure 1



[Figure 2](#)

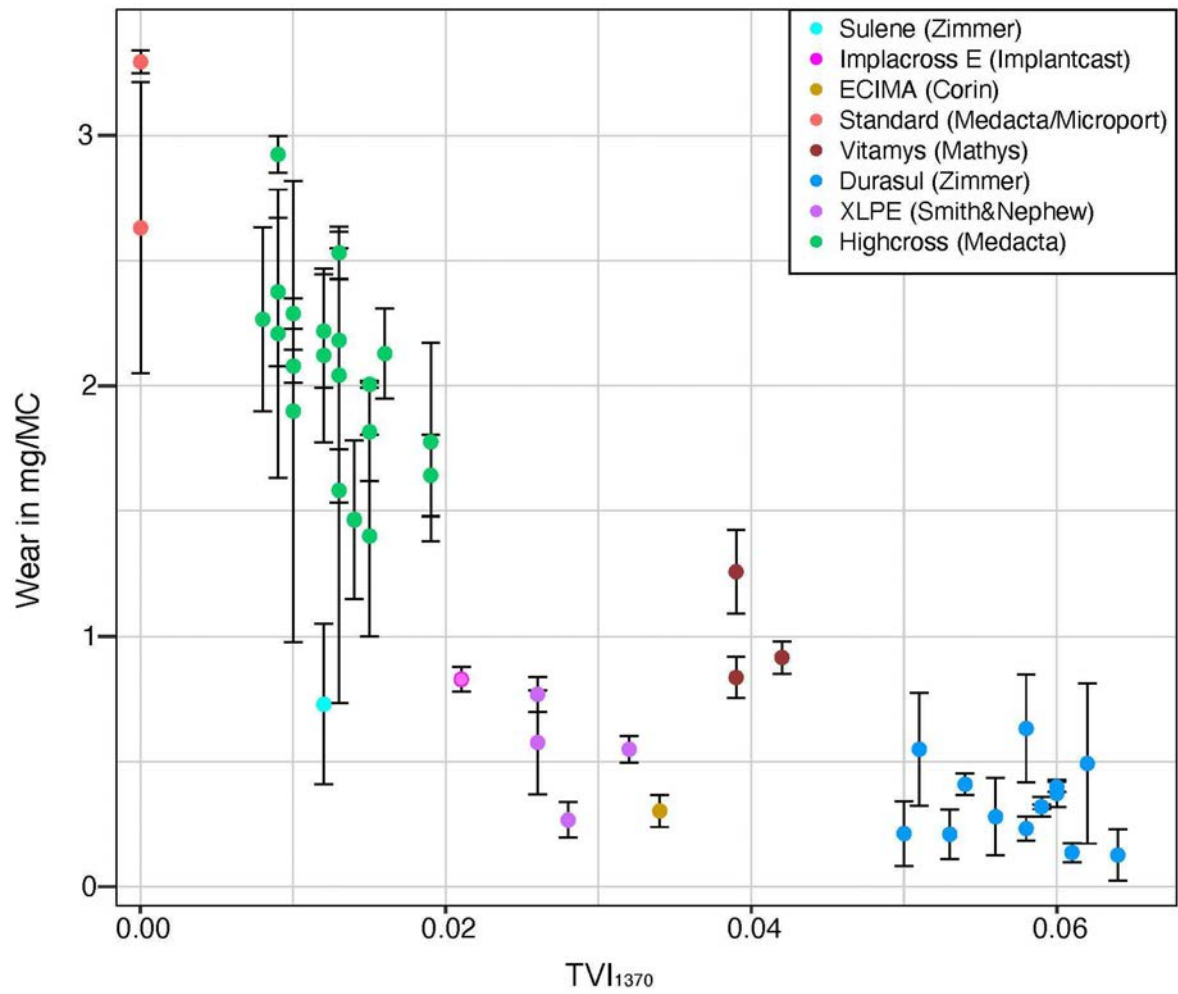


Figure 3

Silicon Nitride PEKK Composite Promotes Osteogenic Activity Compared to PEEK in Porous 3D Printed Specimens

*Paul DeSantis - Drexel University - Philadelphia, United States of America

Tabitha Derr - Drexel University - Philadelphia, USA

Ryan Bock - SINTX Technologies - Salt Lake City, USA

Noreen Hickok

Steven M. Kurtz - Drexel - Philadelphia, USA

INTRODUCTION: Aseptic loosening is a major post-surgery complication of total hip arthroplasty, and can be induced by relative motion at the interface and/or stress shielding in the bone. Polyetheretherketone (PEEK) has been proposed for use in implants, due to having a similar elastic modulus to bone, reducing stress shielding, but is also likely to fail at the interface due to its smooth surface and poor osseointegration. Polyetherketoneketone (PEKK), a relative of PEEK, differs in glass transition temperature and melt temperature, and its additional ketone group may influence its bioactivity. Silicon nitride (Si_3N_4), a synthetic non-oxide ceramic, has strong antibacterial and osseointegrative properties when compared to titanium and PEEK. Due to its ceramic nature, Si_3N_4 can be susceptible to brittle fracture on its own, however it is proposed that a composite material made from both Si_3N_4 and PEKK could have the potential to combine the favorable osseointegrative properties of Si_3N_4 , with then positive biomechanical properties of PEKK. This composite material would also have the advantage of being able to be 3D printed, meeting the needs of patient-specific geometries, useful in many arthroplasty procedures.

METHODS: PEEK, PEKK, and a composite material containing both Si_3N_4 and PEKK (Si_3N_4 -PEKK) were printed into porous discs with a 12.5 mm diameter, 2.5 mm height, and a diamond triply periodic minimal surface (TPMS) geometry with pores approximately 600 μm in size. Discs were sterilized, pre-incubated in Minimal Essential Media Alpha (supplemented with 10% fetal bovine serum and 1% penicillin-streptomycin) for 24 hours, and seeded with 30,000 MC3T3 E1 mouse pre-osteoblasts. After 7 days, media was supplemented with 5mM β -glycerophosphate and 50 $\mu\text{g}/\text{mL}$ of ascorbate to support osteogenic differentiation. After 24 and 72 hours, an MTT assay was performed to determine short term cell attachment and growth; at days 7, 14, and 21, an assay using fluorescein-diacetate (FDA) and 4-methylumbelliferone-phosphate (4-MUP) was used to determine normalized osteogenic activity; and at days 21 and 28, Alizarin Red stain was used to quantify cumulative mineralization on each surface. Statistical significance was determined using ANOVA with multiple comparisons ($\alpha=0.05$, $n=6$).

RESULTS: The number of cells on each surface after 24 and 72 hours are shown in Figure 1, with Si_3N_4 -PEKK having significantly more cell attachment than both PEEK and PEKK at 24 hours and significantly more than PEEK at 72 hours ($p<0.05$). In Figure 2, Alizarin Red was used to quantify cumulative mineralization and Si_3N_4 -PEKK was found to have significantly more mineralization than both PEEK and PEKK at both 21 and 28 day timepoints ($p<0.05$). The porous geometry of printed samples, as well as the surface texture of Si_3N_4 -PEKK are shown in Figure 3.

CONCLUSION: This testing confirms that a composite material of Si_3N_4 and PEKK can promote osseointegrative properties of porous printed samples *in vitro*. Future work is necessary to demonstrate that this effect is observed in an *in vivo* model, but shows promise as an improvement to neat PEEK and as an alternative to metal for use in hip arthroplasty.

Figures

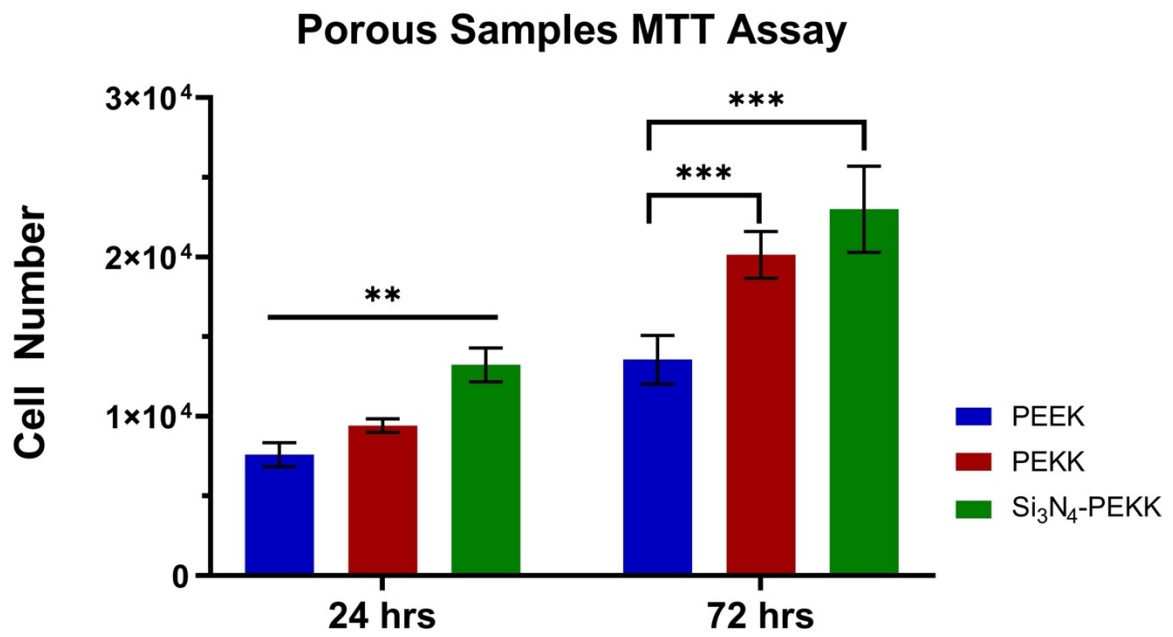


[Figure 1](#)

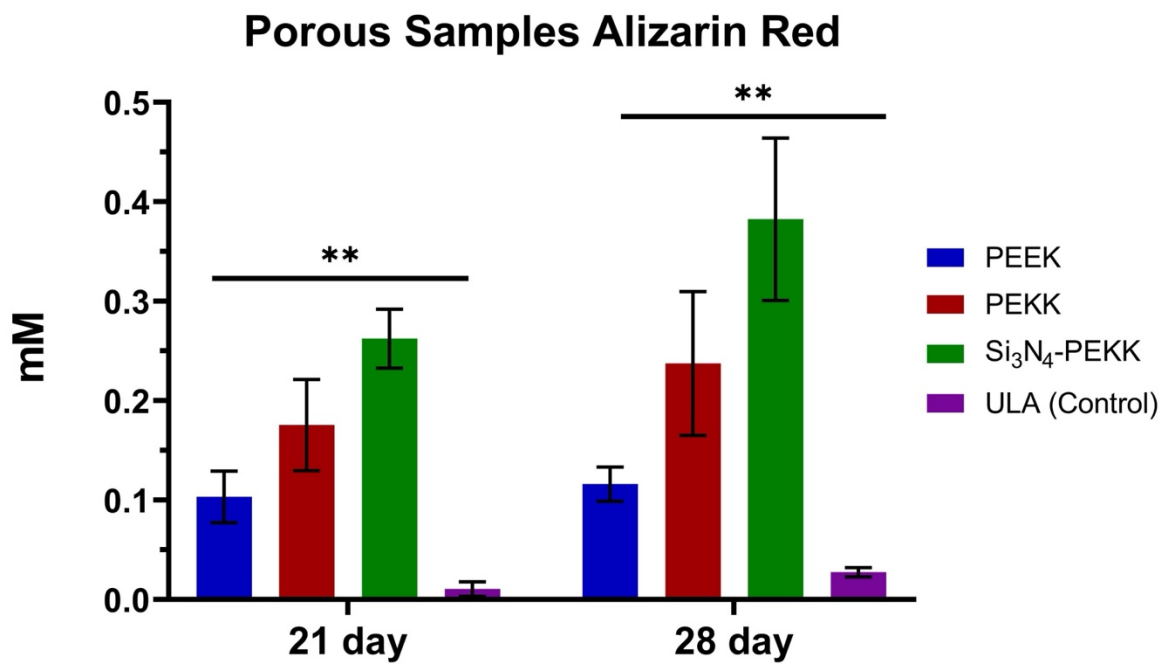


[Figure 2](#)

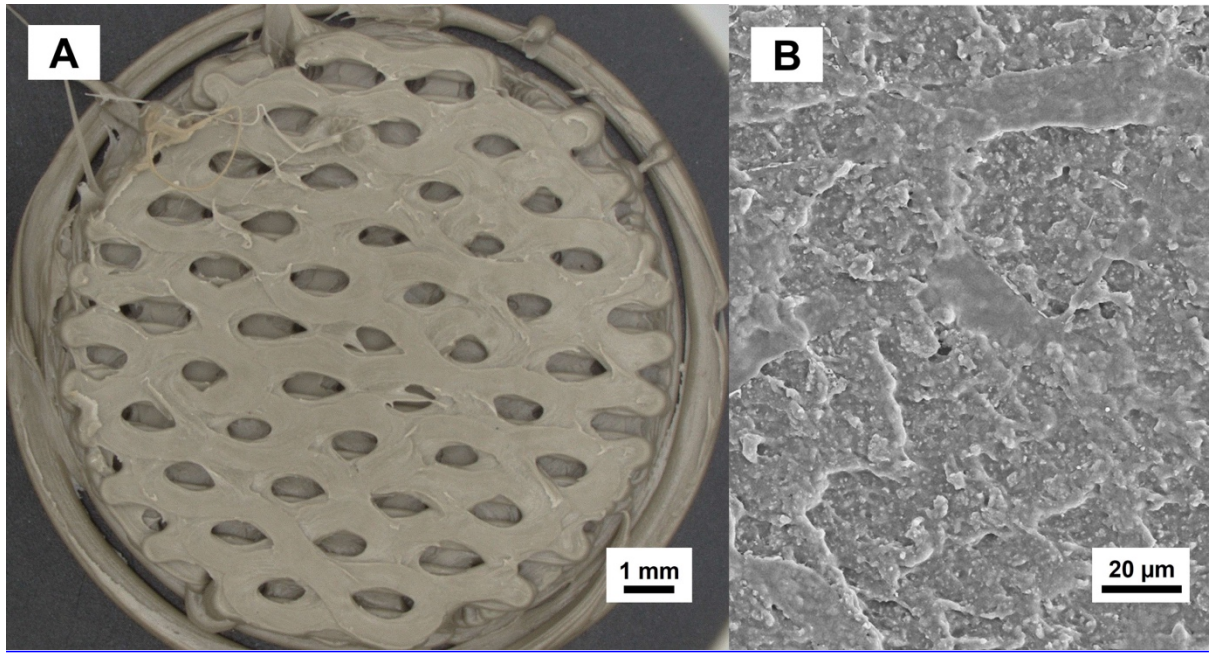


[Figure 3](#)

Next Generation Implant Design for Acetabular Reconstruction

*Sara De Angelis - University College London - London, GB

Anna Di Laura - Royal National Orthopaedic Hospital and Dept. MechEng at UCL - London, United Kingdom

Angelika Ramesh - University College London - London, United Kingdom

Johann Henckel - Royal National Orthopaedic Hospital - London, United Kingdom

Alister Hart - Royal National Orthopaedic Hospital - London, United Kingdom

Introduction

Acetabular osteolysis leading to component loosening is a major problem affecting the long-term survival of hip arthroplasty. The reconstruction of large acetabular defects is challenging due to the extent, location of osteolysis and the metal artefacts limiting the visualisation of bone on CT images.

Often, off-the-shelf solutions fail to provide an adequate fitting to the host bone. For this reason, excessive reaming of the bone is required to position the implant. This can lead to a high discrepancy between the planned and achieved position of the component.

We aimed to quantitatively evaluate the position and orientation of a series of next generation custom-made 3D printed implants.

- Our primary objective was to compute the difference between planned and achieved CoR.
- Our secondary objective was to calculate cup inclination and version angles.

Methods

This was a retrospective cohort study including seven patients with Paprosky type III defects who received a custom-made 3D printed cup by a single manufacturer. All cups were made of titanium and featured a built-in dome custom augment, specifically built to each patient's anatomy to fill the defects. Preoperative and postoperative three-dimensional (3D) reconstructions of bone and implant were created from computed tomography (CT) scans. The cup component was designed based on the 3D reconstruction of the diseased bone.

The outcome measures were:

1. The difference between the planned and achieved CoR in three planes (x medial-lateral direction, y inferior-superior direction, z anterior-posterior direction)
2. Cup inclination and version angles (radiographic definition).

Figure 1 illustrates the workflow described above.

Results

Seven custom-implants were included in the study.

1. The median (interquartile range [IQR]) discrepancy in CoR was found to be 2 mm (IQR: 1-4 mm) in the medial-lateral direction, 2 mm (IQR: 4-2 mm) in the inferior-superior direction and 1 mm (IQR: 2-(-2) mm) in the anterior-posterior direction.
2. Four components (57%) were positioned within 5 degrees of the planned cup inclination angle while three components (43%) were positioned within 5 degrees of the planned cup version angle. The median discrepancy (IQR) in cup inclination was 4 degrees (IQR: 11-1 degrees) while it was found to be 6 degrees (IQR: 9-3 degrees) for cup version.

An example case is shown in Figure 2.

Conclusions

New imaging techniques including CT scanning and 3D image reconstruction can help optimise implant design by more precisely filling the defect. The custom augments served as a guide for the positioning of the implant, facilitating the insertion of screws into the most optimal areas of the bone and eliminating the need for extensive bone preparation. The iliac flanges were designed to fit against the bone. The study demonstrated the feasibility of this next generation implant design in allowing for a minimal discrepancy between planned and achieved positions; however, further improvements can be made in the imaging, manufacturing and surgical implantation stages.

Figures

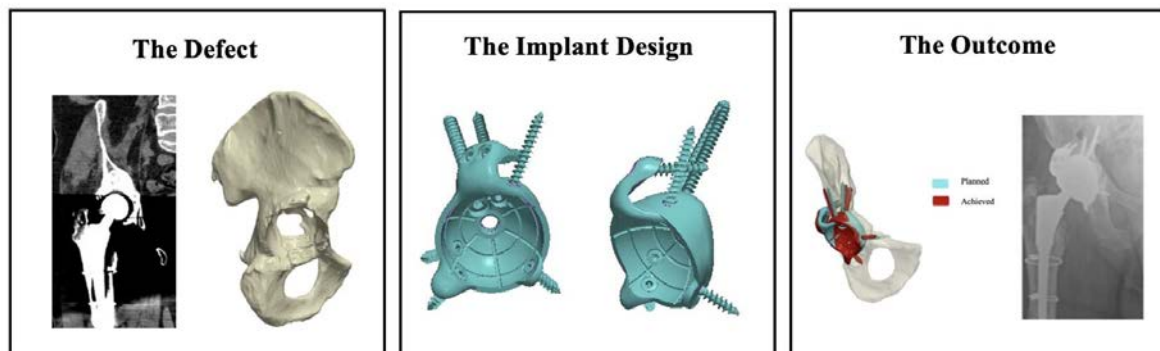


Figure 1: (Left) 3D reconstruction of the defect, (Middle) chosen implant design with screws, (Right) discrepancy between planned and achieved implant position.

Figure 1

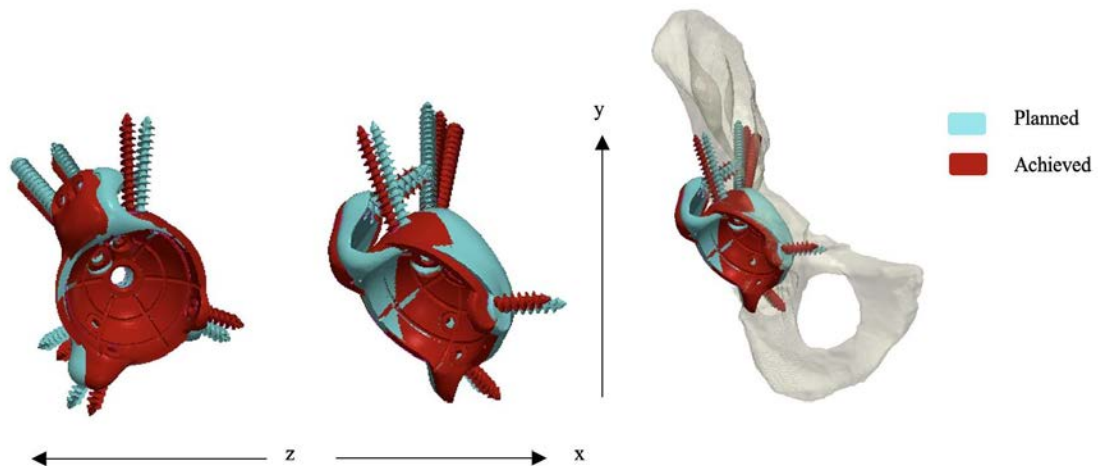


Figure 2: Discrepancy between planned and achieved implant position in the three planes.

Figure 2

Computational Model to Predict Primary Stability of a Patient Matched Glenoid Vault Reconstruction System

*Maged Awadalla - Zimmer Biomet - Warsaw, USA

Bradley Elliott - Zimmer Biomet, Inc. - Warsaw, USA

Robbin Monceaux - Zimmer Biomet - Warsaw, USA

Ravikumar Varadarajan - Zimmer Biomet - Warsaw, USA

Introduction

Reverse total shoulder arthroplasty (rTSA) in the presence of extreme glenoid bone loss is very challenging and often requires PMI® Patient-Matched Implants. PMI provides many potential benefits including precise implant fitting and restoration of the anatomical joint line [1,2]. Adequate glenoid implant primary fixation is essential to the long-term survivorship of these implants. This study aims to develop a computational model for simulating the primary fixation of PMI and to compare the results with those obtained experimentally.

Materials and Methods

The Comprehensive® glenoid Vault Reconstruction System (VRS) offers a PMI glenoid designed based on a CT scan of the patient scapula. Experimental testing (n# = 3) to evaluate primary fixation of the implant was conducted per ASTM F2028. A custom-made polyurethane foam block that recreates the geometry of a worst-case simulated glenoid defect in a cadaveric scapula was utilized. The implant was designed per Zimmer Biomet's standard VRS workflow (Figure 1) with the exception of porous coating, which was excluded to create a large gap between the implant and the supporting bone thus creating a worst-case [3]. The test involved three steps: pre-cyclic displacement, 10,000 cycles of dynamic loading, and post-cyclic displacement. The pre-cyclic/ post-cyclic test involved applying a 430N compressive load (applied axially) and 350N shear load (applied in both superior/inferior (SI) and anterior/posterior (AP) directions). A Finite Element Analysis (FEA) model (Figure 2) was created following published literature [5] to predict the glenoid displacement during the pre-cyclic test setup. The FEA results were compared against the experimental pre-cyclic displacement results.

Results

FEA results for pre-cyclic displacement were found to be within 6% of the experimental results. Experimental and FEA results for pre-cyclic displacement are shown in Figure 3. In the absence of porous coating, displacement in the SI direction was reduced by 89% relative to AP displacement. Including porous coating, although, it did reduce the overall micromotion, the ratio of reduction in SI displacement relative to AP remained at 71%.

Conclusions

This study highlights the importance of screw placement on VRS primary stability. Micromotion was increased in the AP direction compared to SI. This is primary due to lack of screw support in AP direction. This observation was also reported in prior studies on glenoid baseplates [6].

References

1. Dines D et al, 15th. ICSES. Congress, Rome, 2023.
2. Haikal ER et al, Clin. Shoulder. Elb. 27(1):108-116, 2024.
3. James J et al, J. Shoulder. Elbow. Surg. 22:1030–1036, 2013.
4. Achors K., JB. JS. Open. Access, 7(3):e22, 2022.
5. Dharia, M., Arthroplasty. Front. Physiol 9:1116, 2018.
6. Hoenig, M. et al, J. Shoulder. Elbow. Surg. 19:544–549, 2010.

Figures

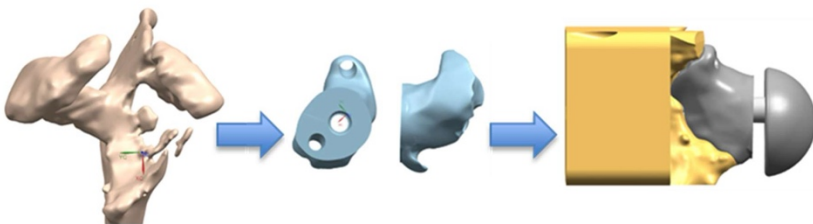
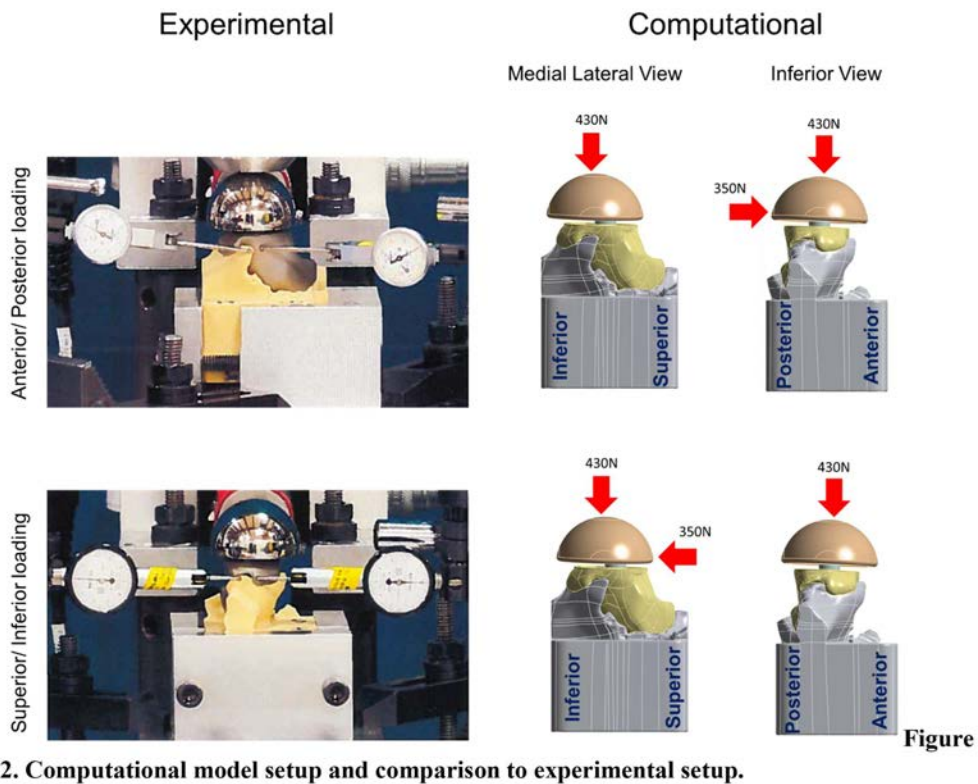


Figure 1. Process of making a custom VRS glenoid implant and polyurethane foam block that recreates the geometry of a worst case simulated glenoid defect in a cadaveric scapula.

[Figure 1](#)



2. Computational model setup and comparison to experimental setup.

Figure 2

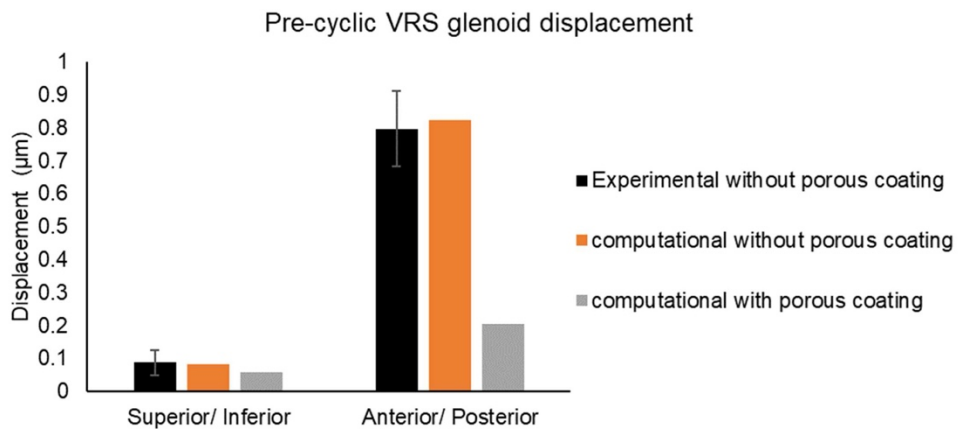


Figure 3. Influence of implant coating on pre-cyclic displacement compared to experimental data. Normalized micromotion data (normalized to maximum experimental value of micromotion + 1*SD), the graph compares the experimental data without porous coating to computation with and without coating.

Figure 3

Unsupervised Machine Learning Clustering of 3D CT Reconstructed Deltoids to Classify Deltoids Relevant to Shoulder Arthroplasty Clinical Outcomes

Hamidreza Rajabzadeh-Oghaz - Exactech, Inc - Gainesville, USA

Josie Elwell - Exactech, Inc - Gainesville, USA

Bradley Schoch - Mayo - Jacksonville, USA

Anshuman Singh - University of California, San Diego - San Diego, USA

Bruno Gobbato - Est cio - Jaragu  do Sul, Brazil

William Aibinder - Michigan, United States of America

David Berry - University of California, San Diego - San Diego, USA

Vikas Kumar - Exactech, Inc - Gainesville, USA

*Christopher Roche - Exactech - Gainesville, USA

Introduction

Clustering is an unsupervised machine learning (ML) approach used to classify complex datasets and identify groups of similar characteristics; as such, clustering could feasibly aid interpretability of radiomic analyses by identifying patterns within medical images and grouping together patient cohorts of similar radiomic measurements. The aim of this study is to perform a cluster analysis on the deltoid radiomics from CT scans of 1382 shoulder arthroplasty patients and determine if the identified cohorts of similar deltoids are associated with similar or different pre-operative and post-operative clinical outcomes.

Methods

A pre-trained CT-based ML segmentation algorithm was used to delineate deltoid image boundaries and create 3D deltoid masks from the pre-operative CT scans of 1382 shoulder arthroplasty patients treated with a single platform shoulder arthroplasty prosthesis (Equinox; Exactech, Inc., Gainesville, FL). After 3D deltoid model creation, a quantification technique extracts multiple radiomic features. A centroid-based k-means clustering algorithm was used on 3 deltoid image measurements along with patient age and gender. Five clusters (k=5) of patients were used, based on a prior conducted feasibility analysis of variance within clusters. Pre-operative range of motion and patient reported outcomes were quantified for each deltoid cluster cohort and post-operative outcomes were also characterized for all patients with 2-year minimum follow-up (average = 37.9 ± 14.0 months). Clinical outcomes were compared between clusters using a student's two-tailed t-test; $p < 0.05$ defined significance.

Results

5 deltoid clusters were identified as depicted in Figure 1 and described in Table 1. Clustering appeared to group deltoids by both gender and age. C2 had the largest and most spherical male deltoids and C0 had the smallest and least spherical male deltoids; whereas, C4 had the largest and most spherical female deltoids and C1 had the smallest and least spherical female deltoids. C3 had the least-flat deltoids and C4 had the most-flat deltoids. As described in Table 2, generally for both pre-operative and 2-year minimum clinical outcomes, C2 deltoids were associated with the most active motion and highest patient reported outcome scores; whereas, C1 deltoids were associated with the least active motion and lowest pre-operative patient reported outcome scores. Comparing outcomes for male clusters (C0 and C2), C2 deltoids had significantly better pre-operative and post-operative abduction

and forward elevation and significantly better post-operative Constant score, as compared to C0 deltoids. Comparing outcomes for female clusters, (C1, C3, & C4), C1 deltoids had significantly lower preoperative outcomes for all measures except ASES, as compared to C3 and C4 deltoids. Despite these differences, all 5 deltoid clusters demonstrated good clinical improvement and interestingly, C2 deltoids had the lowest average improvement across most outcome measures, despite having the best overall results.

Conclusions

The results of this study demonstrate that despite a wide range of variability within the image data, clustering identified multiple deltoid cohorts associated with both better and worse shoulder arthroplasty clinical outcomes. Future work should assess if additional deltoid image measurements and/or other data (e.g. rotator cuff image measurements, patient demographics/comorbidities) can be used to further stratify cohorts and identify edge-case patients.

Figures

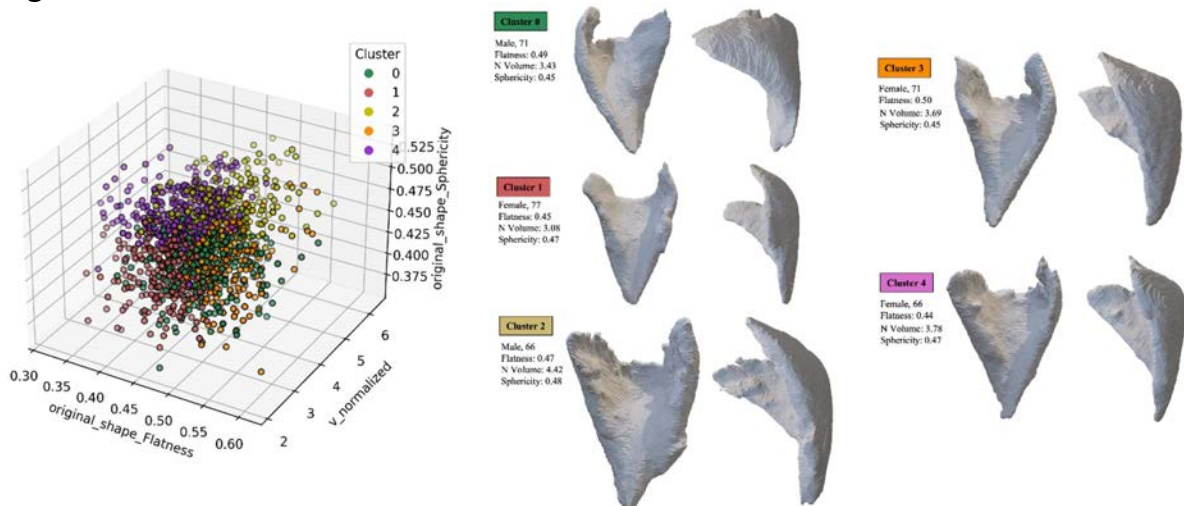


Figure 1. 3-D Scatter Plot of 5 Deltoid Clusters (left), with corresponding 3D CT Reconstructed Deltoids Representative (i.e. Near) of the Centroid of each of the 5 Deltoid Cluster Cohorts

Figure 1

Table 1. Distribution of Patient Demographics, Diagnoses, and 3D CT Deltoid Image Data Associated with each Identified Deltoid Cluster

	Age (years)	Gender (%Female)	aTSA%/rTSA%	OA %	RCT %	CTA %	Deltoid Volume Normalized by Scapular Volume	Deltoid Sphericity	Deltoid Flatness
Cluster 0 (n=297)	73.2 ± 6.1	0%	61 (20.5%) / 236 (79.5%)	63.6%	12.8%	31.0%	3.46 ± 0.47	0.441 ± 0.021	0.486 ± 0.040
Cluster 1 (n=288)	75.5 ± 5.9	99.7%	56 (19.4%) / 232 (80.9%)	72.6%	12.8%	20.1%	3.13 ± 0.41	0.434 ± 0.021	0.444 ± 0.031
Cluster 2 (n=267)	63.9 ± 7.1	2.6%	113 (42.3%) / 154 (57.7%)	73.4%	13.5%	21.3%	4.42 ± 0.55	0.478 ± 0.020	0.476 ± 0.037
Cluster 3 (n=203)	71.5 ± 6.9	100%	48 (23.6%) / 155 (76.4%)	64.5%	16.8%	31.0%	3.66 ± 0.48	0.443 ± 0.023	0.507 ± 0.031
Cluster 4 (n=327)	66.6 ± 8.0	99.7%	89 (27.2%) / 238 (72.8%)	66.4%	17.7%	21.7%	3.96 ± 0.53	0.476 ± 0.018	0.437 ± 0.034

Figure 2

Table 2. Comparison of Pre-operative and 2-Year Minimum Clinical Outcomes (Active Range of Motion and Patient Reported Outcome Measures) Associated with each Identified Deltoid Cluster

		Abduction	Forward Elevation	Internal Rotation Score	External Rotation	ASES	Constant	SAS
Pre-operative	Cluster 0 (n=297)	82.8 ± 37.6	94.3 ± 37.9	3.3 ± 1.8	23.2 ± 23.0	43.6 ± 16.1	43.5 ± 15.8	49.9 ± 11.7
	Cluster 1 (n=288)	74.5 ± 30.7	90.8 ± 33.6	2.9 ± 1.8	18.8 ± 21.7	34.9 ± 14.2	36.1 ± 14.3	44.3 ± 11.7
	Cluster 2 (n=267)	97.7 ± 37.2	110.2 ± 34.7	3.4 ± 1.8	22.8 ± 20.8	41.5 ± 15.2	46.5 ± 15.9	50.7 ± 11.2
	Cluster 3 (n=203)	80.3 ± 36.4	94.8 ± 39.3	3.6 ± 1.8	24.8 ± 22.0	39.2 ± 15.8	40.3 ± 14.4	48.6 ± 12.4
	Cluster 4 (n=327)	84.4 ± 36.1	96.8 ± 36.8	3.1 ± 1.9	22.7 ± 20.7	34.2 ± 15.0	37.8 ± 14.2	45.7 ± 12.5
T-Test (p-value)	C2 vs C1 (best v worst)	<0.0001	<0.0001	0.0007	0.0306	<0.0001	<0.0001	<0.0001
	C2 vs C0 (males)	<0.0001	<0.0001	0.6504	0.8121	0.1125	0.0491	0.4336
	C1 vs C3 & C4 (females)	0.0011	0.0500	0.0042	0.0032	0.2796	0.0260	0.0065
2-Year Minimum Latest Follow-up	Cluster 0 (n=193)	131.3 ± 27.1	143.8 ± 24.1	4.3 ± 1.7	43.8 ± 18.8	86.6 ± 15.5	71.7 ± 13.3	77.8 ± 10.7
	Cluster 1 (n=194)	123.9 ± 30.7	144.9 ± 27.4	4.6 ± 1.7	45.3 ± 18.2	84.3 ± 16.2	67.0 ± 14.2	78.4 ± 11.6
	Cluster 2 (n=181)	137.5 ± 25.8	150.7 ± 19.5	4.6 ± 1.6	47.3 ± 20.2	83.1 ± 19.1	73.9 ± 13.2	78.2 ± 11.6
	Cluster 3 (n=139)	129.3 ± 29.6	145.0 ± 28.1	5.0 ± 1.5	47.7 ± 19.6	82.8 ± 20.2	68.5 ± 14.9	79.1 ± 11.7
	Cluster 4 (n=232)	127.1 ± 33.4	140.9 ± 27.8	4.7 ± 1.7	45.9 ± 19.7	81.2 ± 18.7	67.6 ± 14.4	76.6 ± 13.5
T-Test (p-value)	C2 vs C1 (best v worst)	<0.0001	0.0296	0.8597	0.3264	0.4867	<0.0001	0.8658
	C2 vs C0 (males)	0.0346	0.0053	0.1032	0.0982	0.0553	0.1598	0.7416
	C1 vs C3 & C4 (females)	0.1733	0.3437	0.1495	0.4667	0.1198	0.5175	0.4401
Pre-to-Post-operative Improvement at 2-Year Minimum Latest Follow-up	Cluster 0 (n=193)	46.5 ± 35.6	46.0 ± 37.3	0.7 ± 2.0	19.4 ± 23.5	42.3 ± 20.0	26.4 ± 17.2	26.5 ± 13.8
	Cluster 1 (n=194)	47.0 ± 38.0	47.4 ± 37.1	1.4 ± 2.1	24.6 ± 23.7	47.3 ± 18.4	29.3 ± 16.0	31.5 ± 13.7
	Cluster 2 (n=181)	36.3 ± 36.8	36.8 ± 34.1	1.0 ± 2.0	23.4 ± 22.2	39.6 ± 23.4	24.8 ± 17.2	25.7 ± 13.6
	Cluster 3 (n=139)	49.0 ± 36.3	48.2 ± 39.2	1.1 ± 1.9	21.7 ± 22.0	43.5 ± 22.7	25.3 ± 17.5	29.4 ± 14.5
	Cluster 4 (n=232)	39.8 ± 42.6	41.9 ± 40.3	1.5 ± 2.3	20.9 ± 22.3	45.5 ± 21.5	27.4 ± 18.8	29.6 ± 16.7

[Figure 3](#)

Offset Between Proximal Humeral Canal Axis and Resection Center: An Automatic Morphological Analysis for Short Stem Implants Design and Positioning

*Axel Pavan - Limacorporate Spa - Cividale del Friuli, Italy

Cristiano Pizzamiglio - Limacorporate S.p.A. - Villanova Di San Daniele Del Friuli, Italy

Andrea Fattori - Lima Corporate - Villanova Di San Daniele del Friuli, Italy

Michele Pressacco - LimaCorporate Spa - Villanova di San Daniele del Friuli, Italy

Introduction: Short humeral stems with metaphyseal fixation are widely used in shoulder arthroplasty for bone stock preservation, easier revision and lower risk of periprosthetic fractures. Since the fixation occurs in the metaphysis, they should be centered within the endosteal bone cortex on the resection plane while being aligned with the proximal humeral canal axis (PHCA), avoiding diaphyseal implant-cortex contact to reduce the potential risk of stress-shielding observed with some designs. The aim of this study is to perform a morphological evaluation of the PHCA offset, in an anatomic cut, to provide guidance for implant design and/or positioning to improve placement and fitting.

Methods: Computed tomographies of 106 cadaveric humeri were segmented to create 3D models of periosteal and endosteal bone cortex. Humeral landmarks were automatically detected using the non-rigid registration algorithm provided by the Scalismo library. Relevant humeral coordinate systems were defined for each anatomy. Humeral head resection (NSA=135°, anatomic retroversion) was simulated and maximum circle inscribed in endosteal bone cortex on the resection plane (IC) was plotted. Diameter of IC (DialC) and center of IC (RC) were calculated. Finally, the offset between PHCA and RC (Fig. 1) was calculated. All the previous steps were carried out automatically, on each anatomy, using the open source-based FIGURA proprietary system (Enovis, US). The relationship between DialC and offset was studied. A constant-width binning was performed on DialC data leveraging Scott's rule, assuming a linear increase rate for metaphyseal diameter between sizes when designing an implant. The DialC bins were used to define DialC-Offset clusters (Fig. 2). Finally, the cluster's centroids allowed to compute a weighted linear regression.

Results: Results regarding binning, centroids and regression line are shown in Fig. 2. Fig. 3 reports the obtained centroid values. Considering that it is more common to have a linear increment in the implant diameter between the sizes, the linear regression of the clusters could be considered (see equation (1)).

$\text{Offset} = 0.24 \times \text{DialC} - 3.03 \quad (1)$

Conclusion: The results show an increase in the offset when DialC increases. Therefore, it is reasonable to design humeral short stem implants with an embedded variable offset or to consider this variability during the surgical technique to find the best trade-off between PHCA alignment and IC centering. When implant design does not embed this variability, a narrow stem design would provide more flexibility to correct stem position for a specific anatomy, without conflicting with endosteal bone cortex in both the diaphyseal and metaphyseal region.

Figures

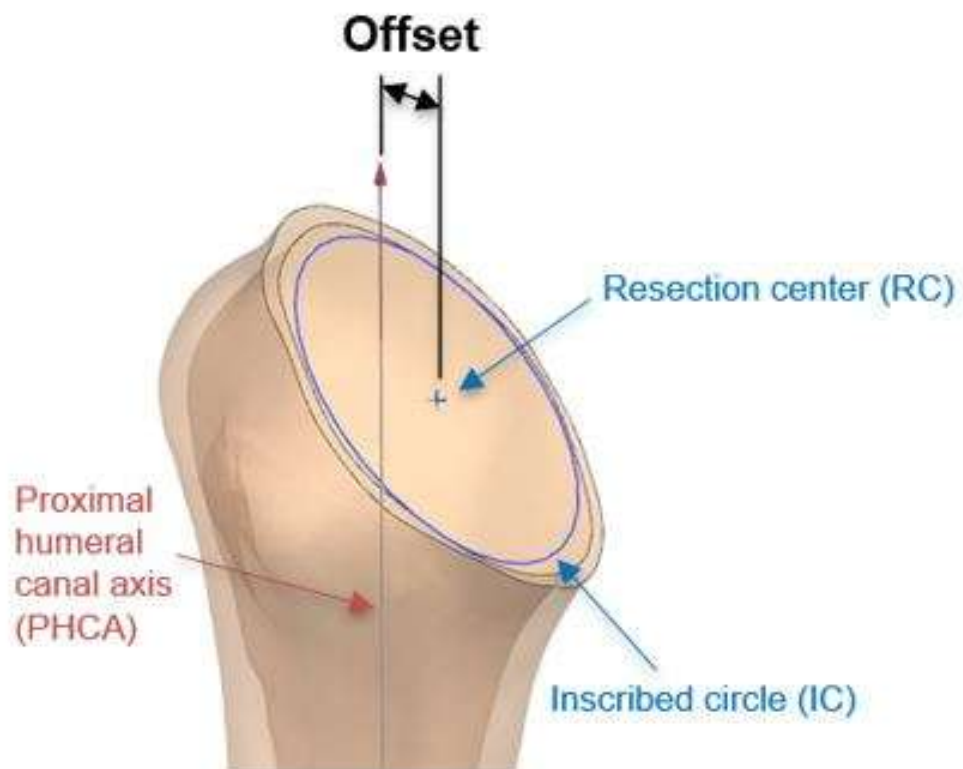


Fig. 1 Offset between proximal humeral canal axis and resection center

[Figure 1](#)

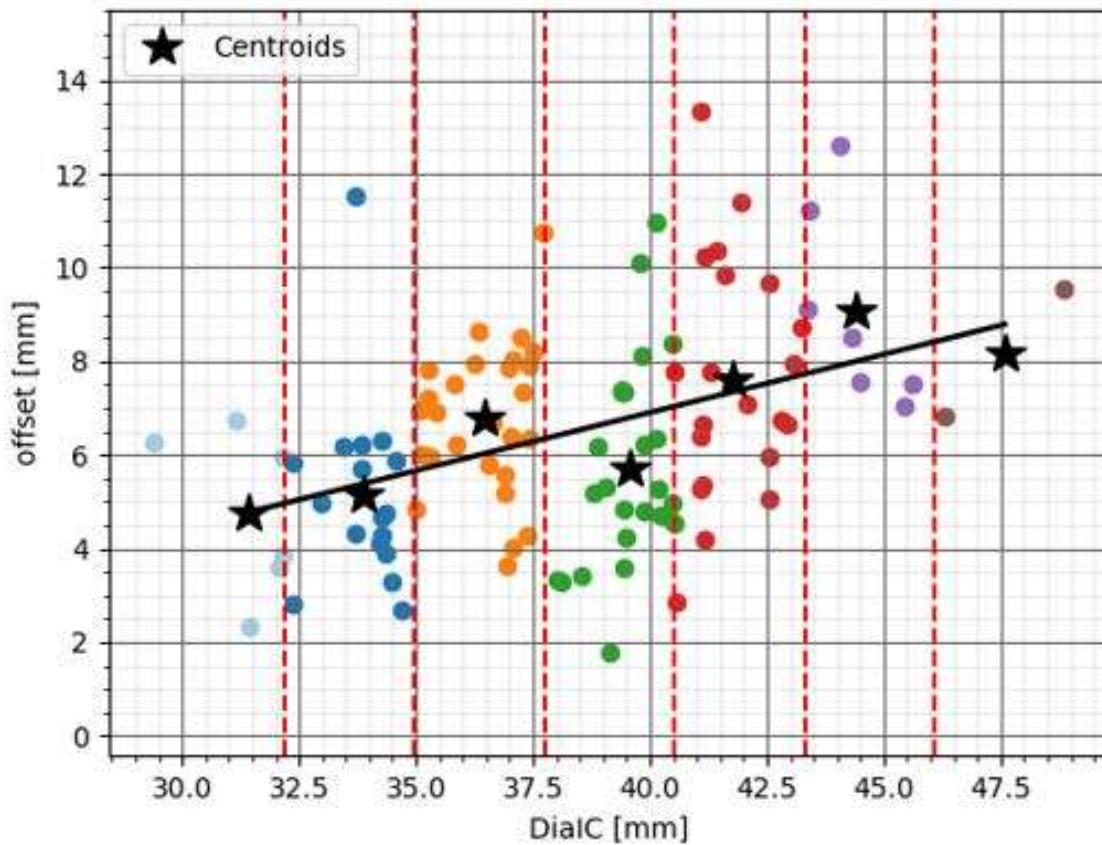


Fig. 2 Binning, centroids, and their linear regression

Figure 2

Centroid	DiaIC	Offset
Centroid 1	31.41	4.77
Centroid 2	33.86	5.15
Centroid 3	36.47	6.77
Centroid 4	39.56	5.70
Centroid 5	41.76	7.58
Centroid 6	44.39	9.08
Centroid 7	47.59	8.18

Fig. 3 Optimal centroid results

Figure 3

A Rapid Topographic U-Net for Detecting the Anatomic Neck in Arthritic Humeri: Enabling Automatic Shoulder Arthroplasty Planning

*Gregory Spangenberg - University of Western Ontario - London, Canada

Fares Uddin - King Hamad University Hospital - Busaiteen, Bahrain

Ahmed Habis - King Abdulaziz University - Jeddah, Saudi Arabia

Kenneth J. Faber - Western University / Hand and Upper Limb Clinic - London, Canada

G. Daniel G. Langohr - The University of Western Ontario - London, Canada

Introduction: The humeral anatomic neck is an important reference point for preoperative shoulder arthroplasty planning and accurate intraoperative placement of the humeral component. Osteophytes and deformity associated with osteoarthritis commonly obfuscate this landmark, can increase pre-operative planning time and complicate placement of the humeral component. 88% of all total shoulder arthroplasties (TSA) are performed to treat glenohumeral arthritis and the presence of osteophytes can affect surgical planning and navigation [1]. Among the automated methods for identifying the anatomic neck, none have effectively addressed the presence of osteophytes [2-3].

Methods: Computed tomography (CT) scans from 62 shoulders (37 healthy, 25 arthritic) were acquired from two CT scanners under various acquisition settings. Humeri were automatically segmented out of the CT scans and digitization of the true anatomic neck was performed by two upper limb orthopaedic surgeons. 20% of the humeri were then set aside to form a testing set. Humeri were transformed into single images using topographic image compression as shown in Figure 1. A U-Net model shown in Figure 2 was then trained to segment out and predict the location of the anatomic neck from the topographic images. Segmentation boundaries were transformed back to 3D and a plane was then fit to the true and the predicted anatomic neck for each humerus and the mean absolute error (MAE) between their centroids and normal vectors was calculated.

Results: The segmentation of the topographic images in the test set produced an F1 score of 0.933 and an IoU score of 0.875. The predicted anatomic neck plane derived from the segmentation boundary had mean absolute errors (MAE) of 3.23 ± 1.24 mm for the plane centroid and 5.58 ± 2.88 degrees for the normal vector, on arthritic humeri. For the healthy humeri test set MAEs were 2.56 ± 1.50 mm and 2.78 ± 1.84 degrees respectively. A comparison of performance between previous methods designed only for healthy humeri [2-3], and the present method which also works for arthritic humeri is shown in Figure 3.

Conclusion: This automated anatomic neck detection approach achieved excellent performance on healthy humeri and is the first model designed to work on arthritic humeri, which is found in most TSA cases. This model is available to use in the open-source python package *shoulder*.

References: [1] Tschannen et al. 2016. doi:10.1016/j.media.2016.02.008, [2] Westermann et al. 2015. pmid:26361437, [3] Kulyk et al. 2019. doi:10.1007/978-3-030-11166-3_3

Figures

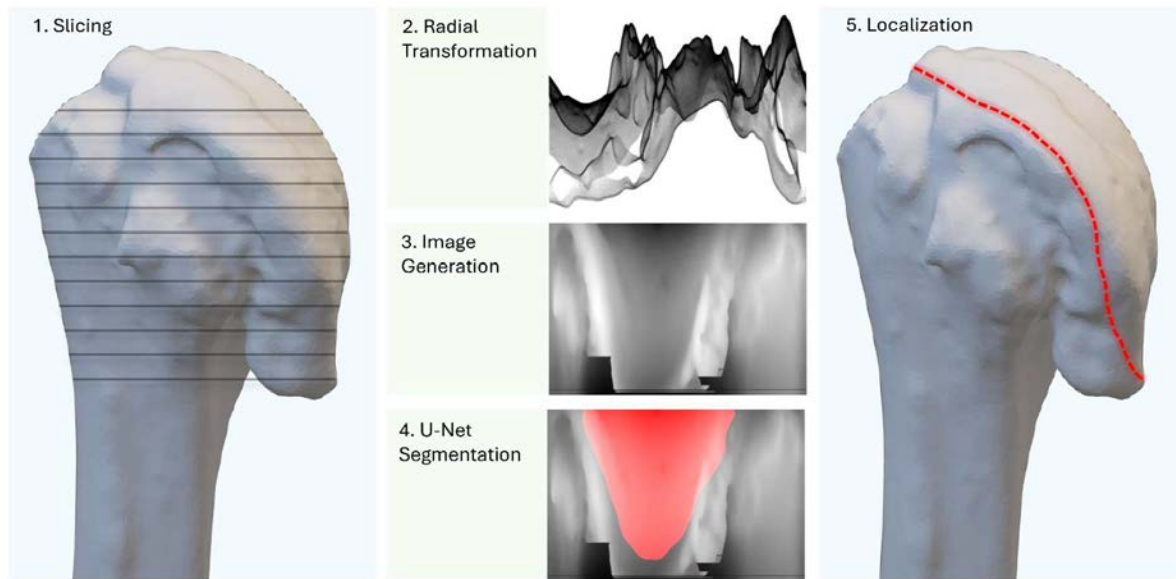


Figure 1. Topographic image compression for generating U-Net input images. 1) Segmented humerus CT is sliced. 2) Perimeter of each slice is transformed to radial coordinates. 3) Radial distance is normalized and stacked along z-height to form image. 4) Segmentation with U-Net 5) Boundary of segmentation transformed back to 3D

Figure 1

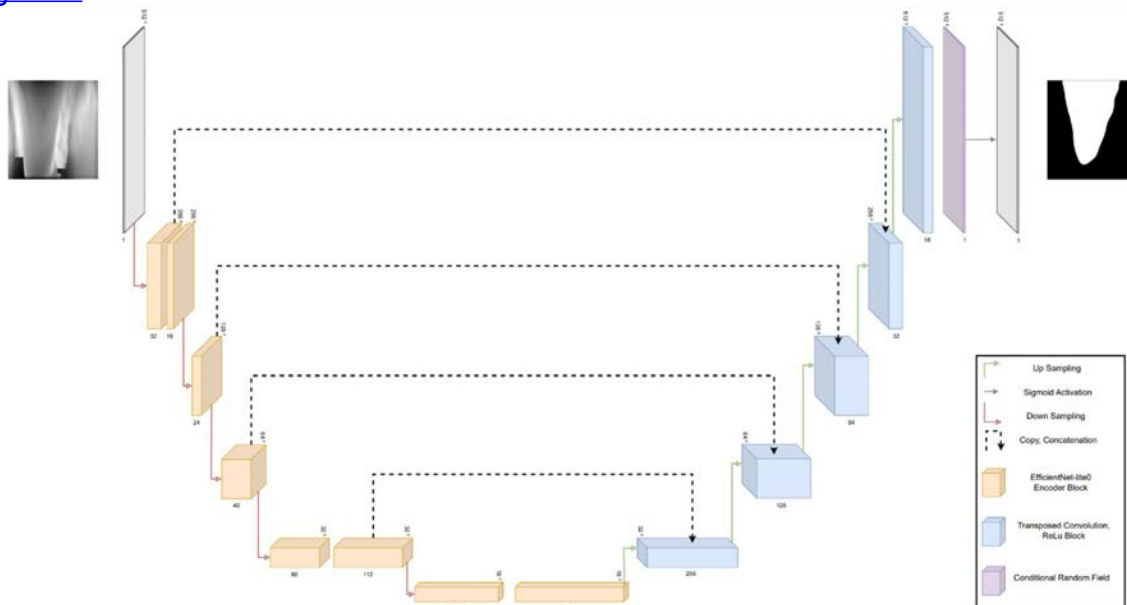


Figure 2. Architecture of Rapid Topographic U-Net with an EfficientNet-lite0 encoder and conditional random fields for binary segmentation

Figure 2

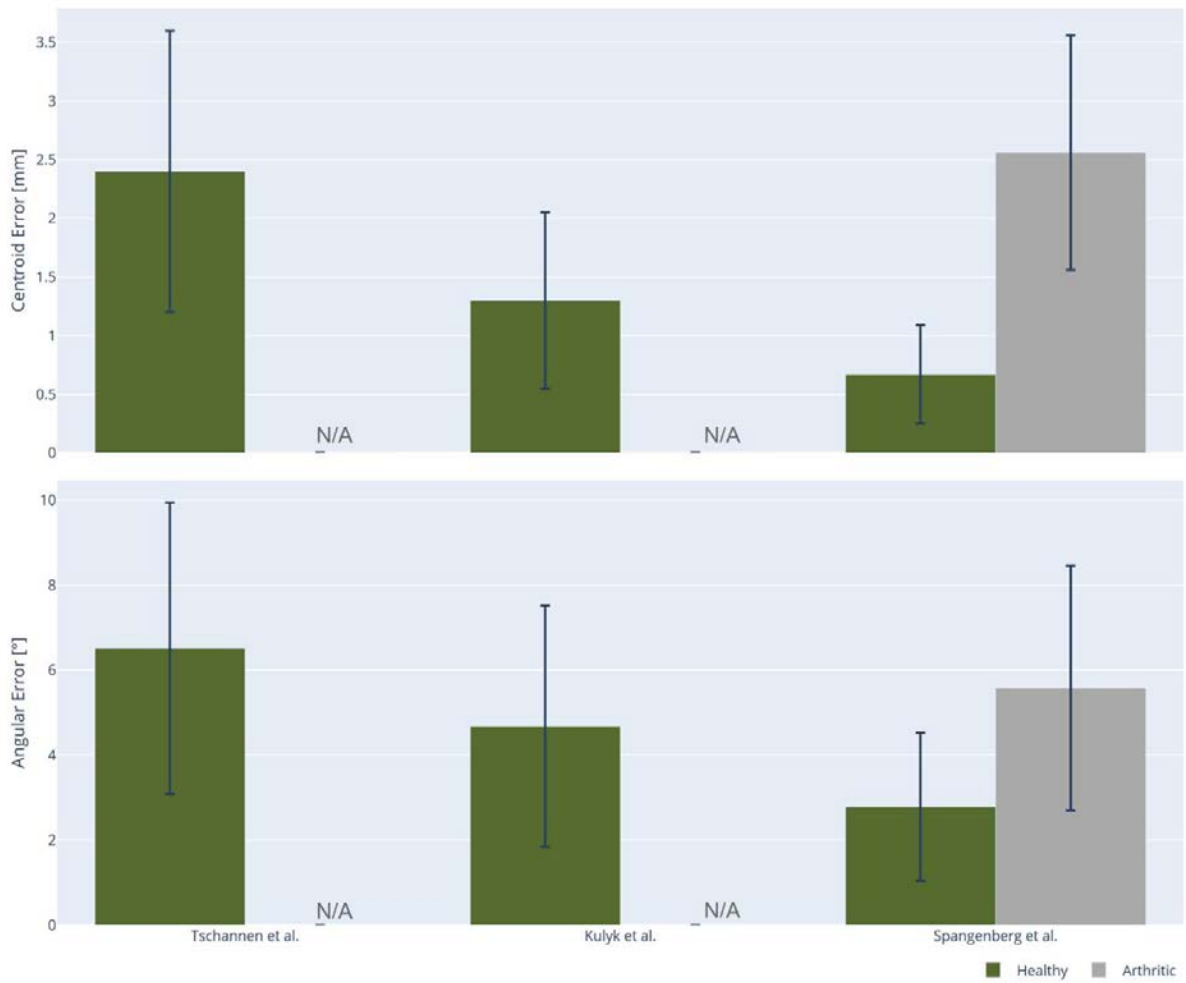


Figure 3. Comparison between current and prior works for anatomic neck plane (ANP) or articular margin plane (AMP) prediction errors.

[Figure 3](#)

Reduction of Metal Ion Release in Cemented Hip Stems by a Zirconium Nitride Multilayer Coating Simulating a Severe Stem Debonding Condition

*Thomas M. Grupp - Aesculap AG - Tuttlingen, Germany

Andreas M. Pfaff - Aesculap AG - Tuttlingen, Germany

Mevluet Sungu - Aesculap AG - Tuttlingen, Germany

Bernd Fink - Orthopaedic Clinic Markgroeningen, Markgroeningen - Markgroeningen, Germany

William Mihalko - University of Tennessee - Memphis, USA

Ana Laura Puente Reyna - Ludwig Maximilians University Munich - Munich, Germany

Introduction

Primary total hip arthroplasty (THA) is a very successful clinical treatment with excellent results over a 20 to 25 year period with low complication rates [Learmonth 2007, Evans 2015, AOANJRR 2023, 18th NJR 2021], but during the last decade metal ion and particle release has become an important subject in THA. Even though cobalt chromium alloys have shown a good clinical history and biocompatibility, in situ degradation is inevitable. Cemented hip stems out of CoCr28Mo6 alloy in a tribo-system with the surrounding bone cement mantle will undergo a process of wear and bio-corrosion by mechanisms such as fretting and fatigue, and will release metal ions and particles into the periprosthetic tissue. The stem-cement-interface experiences wear by low-amplitude oscillatory micro-motions under patient activities, resulting in metal ion release of cobalt, chromium and molybdenum [Gilbert 2014, Brown 2007, Buchhorn 2015].

Zirconium nitride (ZrN)-multilayer coating is clinically well established in total knee arthroplasty [AOANJRR 2023, Grimberg 2021, Luetzner 2022] and has demonstrated significant reduction in polyethylene wear and metal ion release [Reich 2010, Grupp 2013, Puente Reyna 2018].

The goal of our study was to analyze the biotribological behaviour and metal ion release of a ZrN-multilayer coating on a polished cobalt-chromium cemented hip stem, designed for patients with suspected metal ion hypersensitivity, in a demanding long-term test scenario of a severely debonded and toggling hip stem.

Methods

CoCr28Mo6 alloy hip stems with ZrN-multilayer coating (CoreHip®AS Aesculap AG) were tested versus an un-coated version. In a worst-case-scenario the stems with ceramic heads have been tested in bovine serum in a severe cement interface debonding condition under a cyclic load of 3,875 N for 15 million cycles. After 1, 3, 5, 10 & 15 million cycles the surface texture was analysed by scanning-electron-microscopy (SEM) and energy-dispersive x-ray (EDX). Metal ion concentration of Co, Cr, Mo was measured by inductively coupled plasma mass spectroscopy (ICP-MS) after each test interval.

Results

Based on SEM/EDX analysis, it has been demonstrated that the ZrN-multilayer coating keeps its integrity over 15 million cycles of severe stem cemented interface debonding without any exposure of the CoCr28Mo6 substrate. For the ZrN-multilayer coated hip stems, the cobalt ion concentration released by diffusion through the porosity of the multilayer coating was 14.0 µg/l after 1 million cycles, increased to 22.1 µg/l at 3 million cycles and ended with 23.9 µg/l at 15 million cycles. For the

uncoated CoCr28Mo6 hip stem, the cobalt ion concentration started with 767 $\mu\text{g/l}$ after 1 million cycles and ended with 3862 $\mu\text{g/l}$ after 15 million cycles (Figure 1).

Conclusion

The ZrN-multilayer coated polished cobalt-chromium cemented hip stem has shown to have a reduction of Co & Cr metal ion release by two orders of a magnitude, even under severe stem debonding and high interface micro-motion conditions. ZrN-multilayer coating on a polished cobalt-chromium cemented hip stem might be a suitable option for further minimization of Co & Cr metal ion release in total hip arthroplasty. Clinical evidence has to be proven as the next step.

Figures

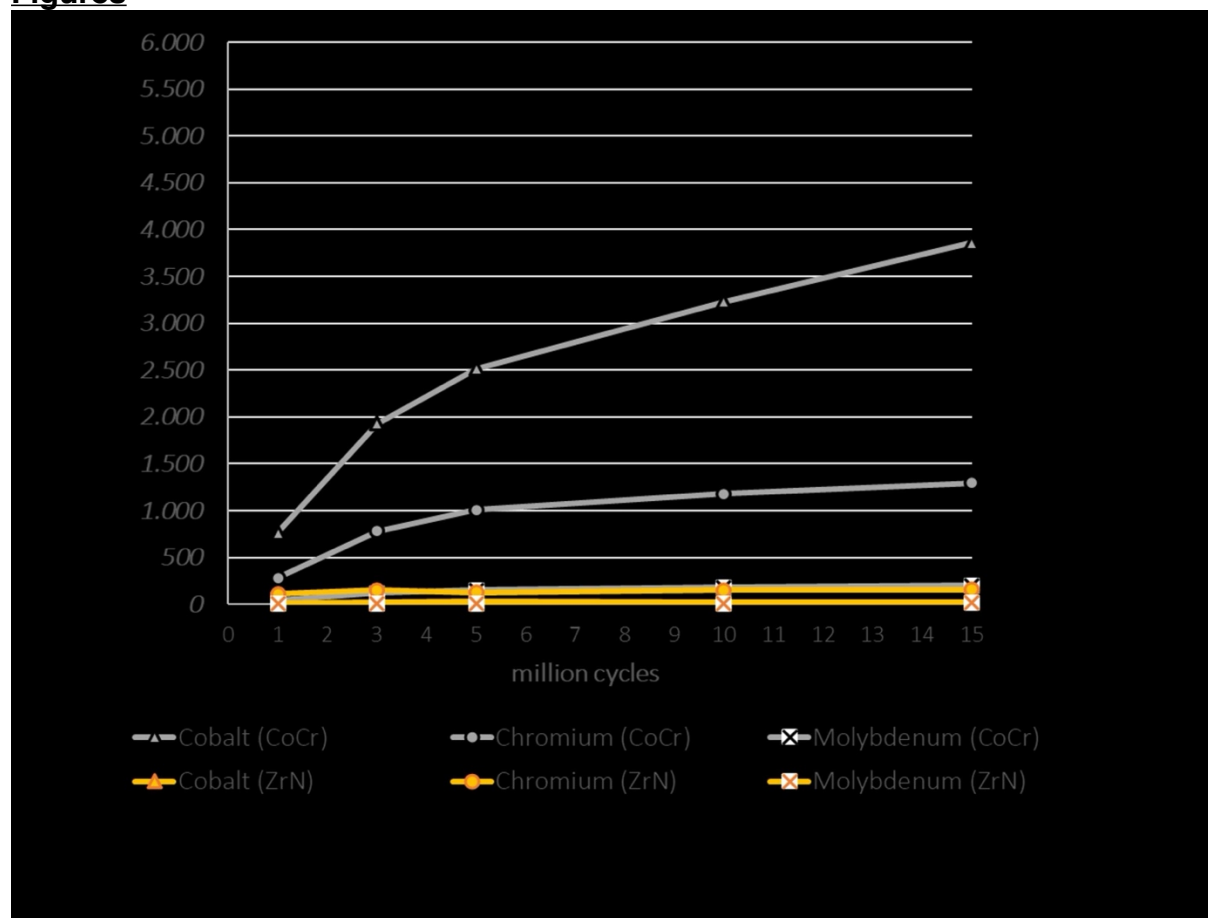


[Figure 1](#)

Concerning Crevice Corrosion in Metaphyseal Sleeves of Revision Total Knee Components

*Shabnam Aslani - Drexel University - Philadelphia, USA

Michael Kurtz - Clemson University - Charleston, USA

Christopher Pelt - University of Utah - Salt Lake City, USA

Joshua Rainey - University of Utah - Salt Lake City, United States of America

Michael James Archibeck - Albuquerque, USA

Jeremy Gililland - University of Utah - Salt Lake City, USA

James Smith - Drexel University - Philadelphia, USA

Jeremy Gilbert - Clemson University - Charleston, USA

Steven M. Kurtz - Drexel - Philadelphia, USA

Introduction: In revision total knee arthroplasty (TKA), metaphyseal sleeves help to mitigate bone loss and improve fixation. However, recent case reports document metallosis, adverse tissue reactions including pseudotumor-like masses, and corrosion at the taper-sleeve interface [1]. While metallosis and corrosion in metal-on-metal and modular total hip arthroplasties (THA) are well documented, such complications have rarely been reported in the context of TKA. This gap motivated us to investigate corrosion at the metaphyseal sleeve–femoral taper interface. We asked: (1) what is the prevalence of corrosion and (2) what damage modes and mechanisms occur?

Methods: Paired DePuy Synthes metaphyseal sleeves and femoral components (n = 11) were collected from a multi-center retrieval program. Implantation time was 2.37 ± 2.05 years and reasons for revision included loosening (n = 3), instability (n = 1), and infection (n = 6). The patients were 45% women. Femoral tapers and sleeves were classified using the Goldberg scoring method [2]. This system assigns scores of 1 for no corrosion, 2 for mild corrosion, 3 for moderate corrosion, and 4 for severe corrosion. Samples with severe corrosion were selected for further examination. First, femoral tapers were separated from the bearing condyles. Then, metaphyseal sleeves were sectioned using an abrasive cutoff wheel. Digital optical microscopy (DOM) and scanning electron microscopy (SEM) images were captured to identify different types of corrosion, and energy-dispersive X-ray spectroscopy (EDS) was performed to assess the chemical composition of oxide debris. Micrograph contrast and brightness were modified during and after SEM acquisition to highlight relevant features.

Results: Digital images show representative femoral components and metaphyseal sleeves before and after sectioning (Figure 1A-B). Note the black oxide debris on both taper and sleeve components. Most femoral tapers (73%, n = 8/11) and all (100%, n = 11/11) femoral sleeves showed visual evidence of corrosion (Figure 1C-D). Micrographs of the CoCrMo taper reveal mechanically assisted crevice corrosion (MACC, Figure 2A), pitting (Figure 2B) and etching (Figure 2C). Severe corrosion of the taper occurred in as little as 2.25 years. On the etched surface, raised white lines represent grain boundaries. A high magnification micrograph (20,000x) of the etching shows selective dissolution of a single crystal. The grain boundary is clear and distinct, and the inter-penetrating parallel lines represent crystallographic planes. Images of the sectioned Ti-6Al-4V sleeve show MACC, and a plate like oxide comprising of titanium, chromium, and molybdenum (Figure 3A-B). Additionally, we documented cell-like remnants within the sleeve (Figure 3C-D) approximately 5 μm in diameter.

Conclusion: All devices exhibited corrosion ranging from mild to severe at the taper-sleeve interface, with mild damage occurring the most. The main corrosion mechanism was MACC, manifesting as various chemically based corrosion damage modes. Both oxide composition and damage mode appearances were similar to those documented on retrieved THA components. While we identified cell-like features within the taper, it is unclear how patient biology affected the corrosion. Future work will investigate corrosion at the tibial sleeve interface.

References: [1] Rainey et al., Arthroplasty Today 2023; [2] Goldberg et al., CORR 2002.

Figures

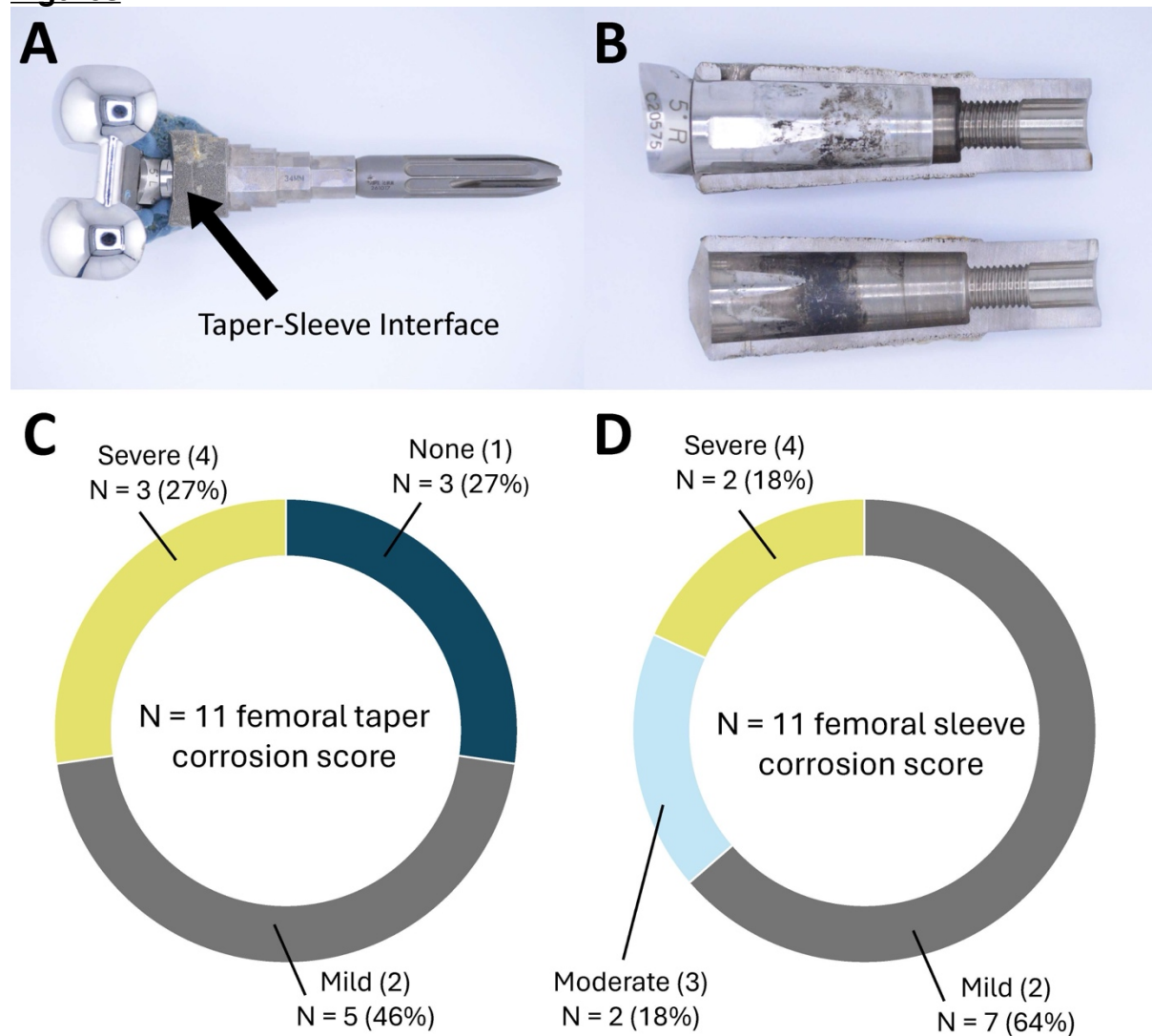


[Figure 1](#)

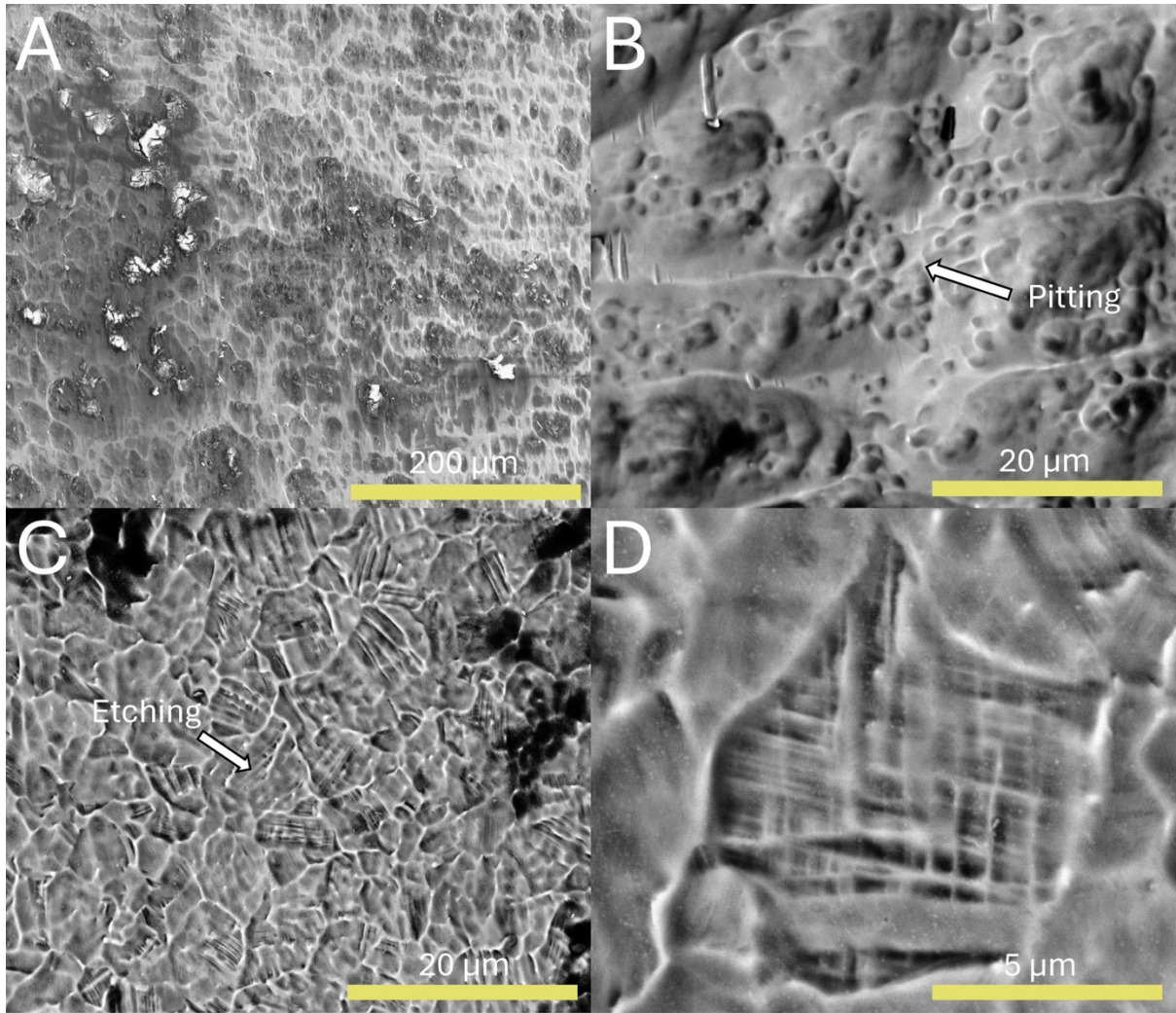


[Figure 2](#)

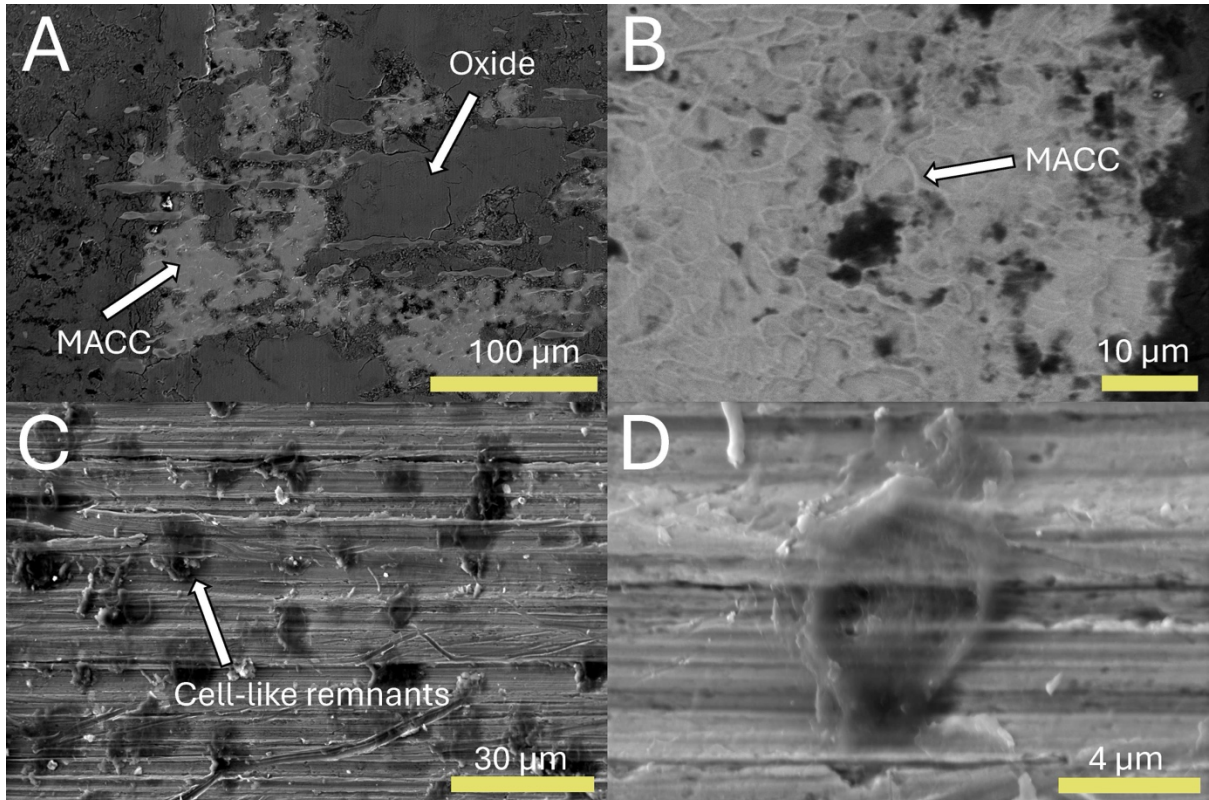


Figure 3

Titanium-Titanium Junctions in the Knee Corrode, Generating Damage Modes Identified in the Hip

*Michael Kurtz - Clemson University - Charleston, USA

Shabnam Aslani - Drexel University - Philadelphia, USA

James Smith - Drexel University - Philadelphia, USA

Hannah Spece - Drexel University - Philadelphia, USA

Greg Klein - Hartzband Center for Hip and Knee Replacement - Hackensack, USA

Steven Kurtz - Drexel University - Philadelphia, USA

Introduction: Total hip arthroplasty (THA) retrieval studies show crevice corrosion within titanium-titanium junctions [1-2]. Damage modes within these junctions are distinct from cobalt chrome-titanium interfaces and may be associated with device failure [3]. Despite the potential for corrosion, titanium-titanium stem-baseplate junctions remain ubiquitous in total knee arthroplasty (TKA). Compared to THA, same alloy TKA taper interfaces remain under-investigated. In this study, we asked: does corrosion chemically damage titanium-titanium TKA junctions, generating damage modes observed on THA retrievals? We hypothesized that cyclic loading within the baseplate taper would generate delamination, pitting, and selective dissolution, damage modes first identified on failed THA devices.

Methods: Fifty titanium-alloy baseplate and conical stem pairs (n = 100 components) were collated from a multi-center retrieval program and assessed using Goldberg corrosion scoring [4]. Threaded stems and cobalt chrome devices were excluded. A lasso regression model was used to identify associations between the Goldberg scores and patient data. Selected variables (gender, patient activity, standardized revision reasons) were further analyzed using non-parametric statistics. Moderate and severely corroded devices were imaged using both digital optical and scanning electron microscopy. Tibial baseplates were sectioned to allow for microscopy of the baseplate taper.

Results: Goldberg scoring (Figure 1) identified corrosion on 92% of the stems (n = 46/50) and on 98% of the baseplates (n = 49/50). Patient clinical data were not predictive of corrosion damage ($p > 0.05$). Digital images of a paired stem and baseplate (Figure 2A-B) reveal a limited contact area at the base of the trunnion and the taper bore where most corrosion occurred. Damage appeared mirrored, with corrosion debris, oxidation, and burnishing occurring at approximately the same location on both components. Micrographs of corroded regions (Figure 2C-D) revealed a chemical attack on the surface promoted by crevice corrosion. Severely corroded devices (Figure 3A-D) showed evidence of selective dissolution and pitting.

Conclusion: Most (95%) of the components we analyzed appeared visually corroded. We identified a crevice corrosion attack, including delamination, selective dissolution, and pitting. While the micrographs showed evidence of fretting, most of the corrosion we documented likely occurred from chemically based attacks, consistent with damage documented on titanium-titanium junctions in THA [2-3]. Though we found no association between the clinical data and corrosion severity, design may play a role: previous studies document significantly less corrosion on threaded tapers [5].

The clinical implications of this work remain to be seen. While bone cement mantles may prevent metal ion release into the surrounding tissue *in vivo*, cementless procedures are increasing. Additionally, a recent clinical study identifies corroded sleeve-stem TKA devices and evidence of local tissue reactions [6].

References: [1] Rodrigues et al., JBMR-B 2009; [2] Gilbert et al., JBMR-B 2012; [3] Carlson et al., JOA 2012 [4] Goldberg et al., CORR 2002; [5] Arnholt et al., JOA 2014; [6]. Rainey et al., Arthroplasty Today 2023.

Figures

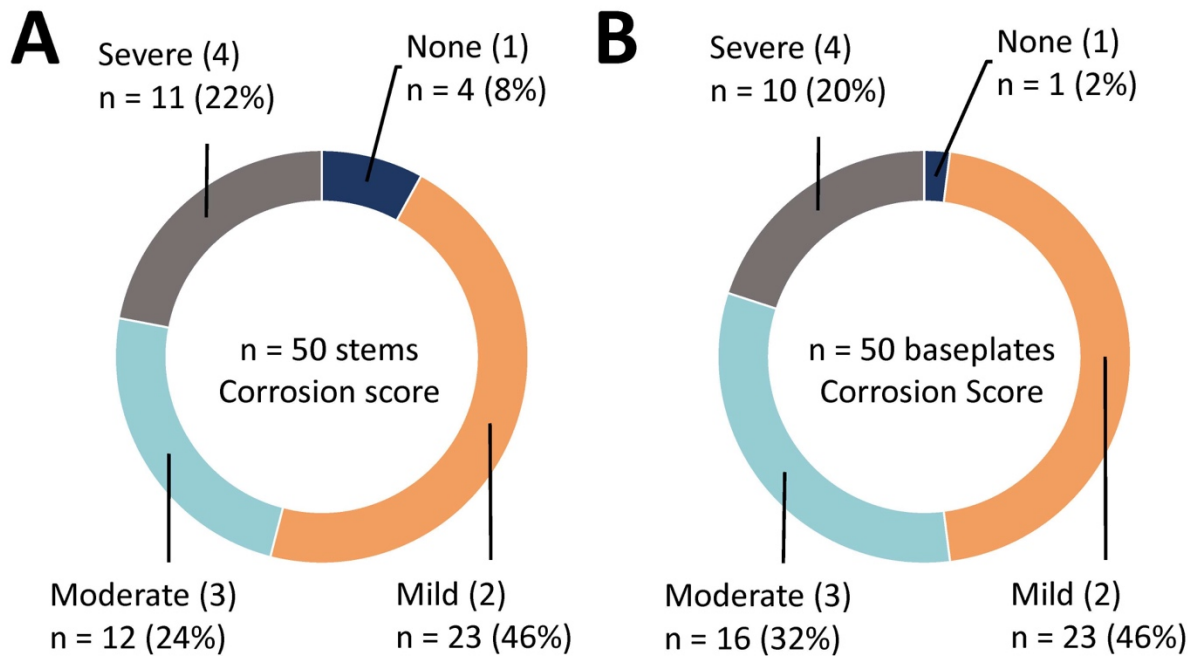


[Figure 1](#)

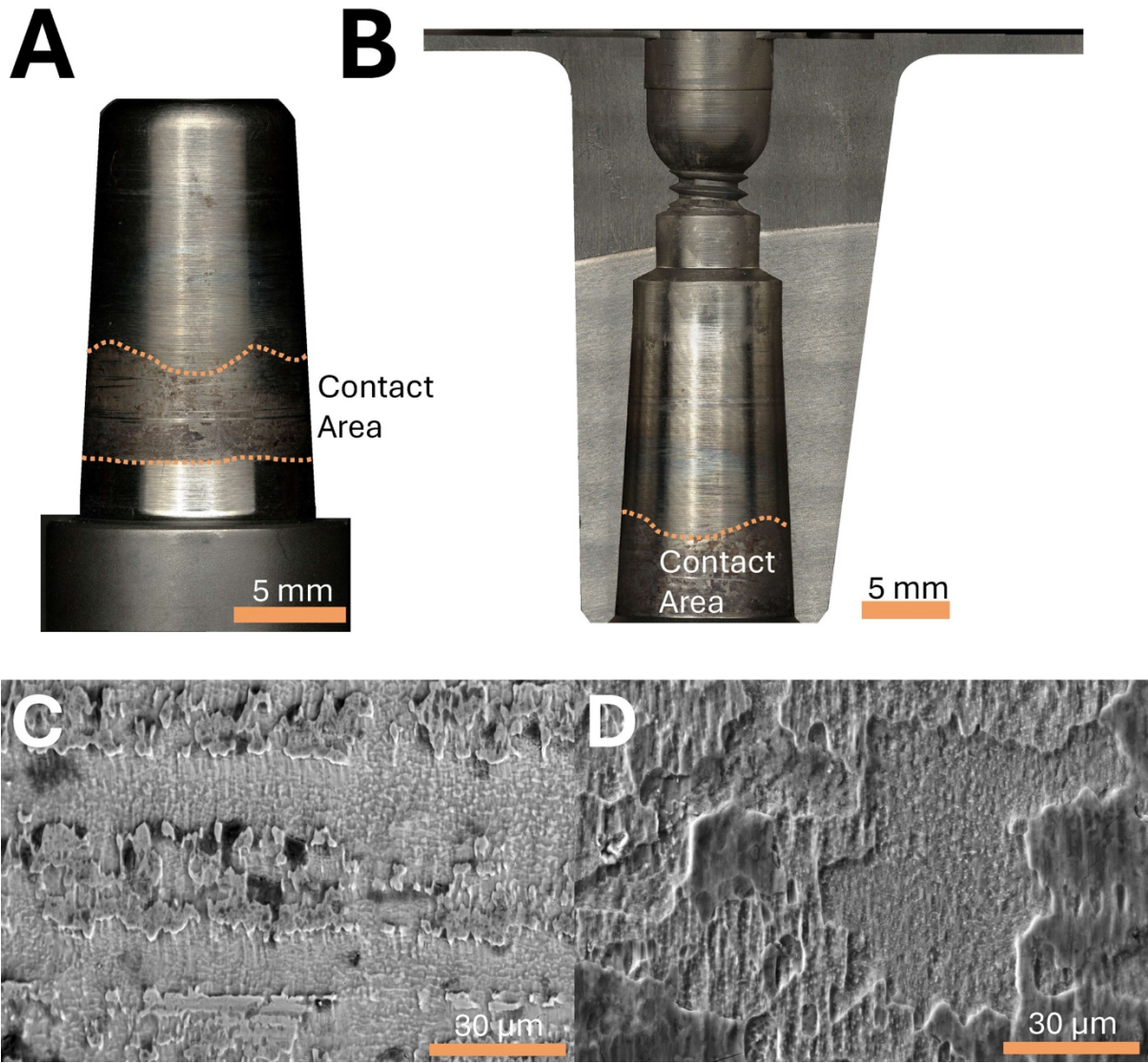


[Figure 2](#)

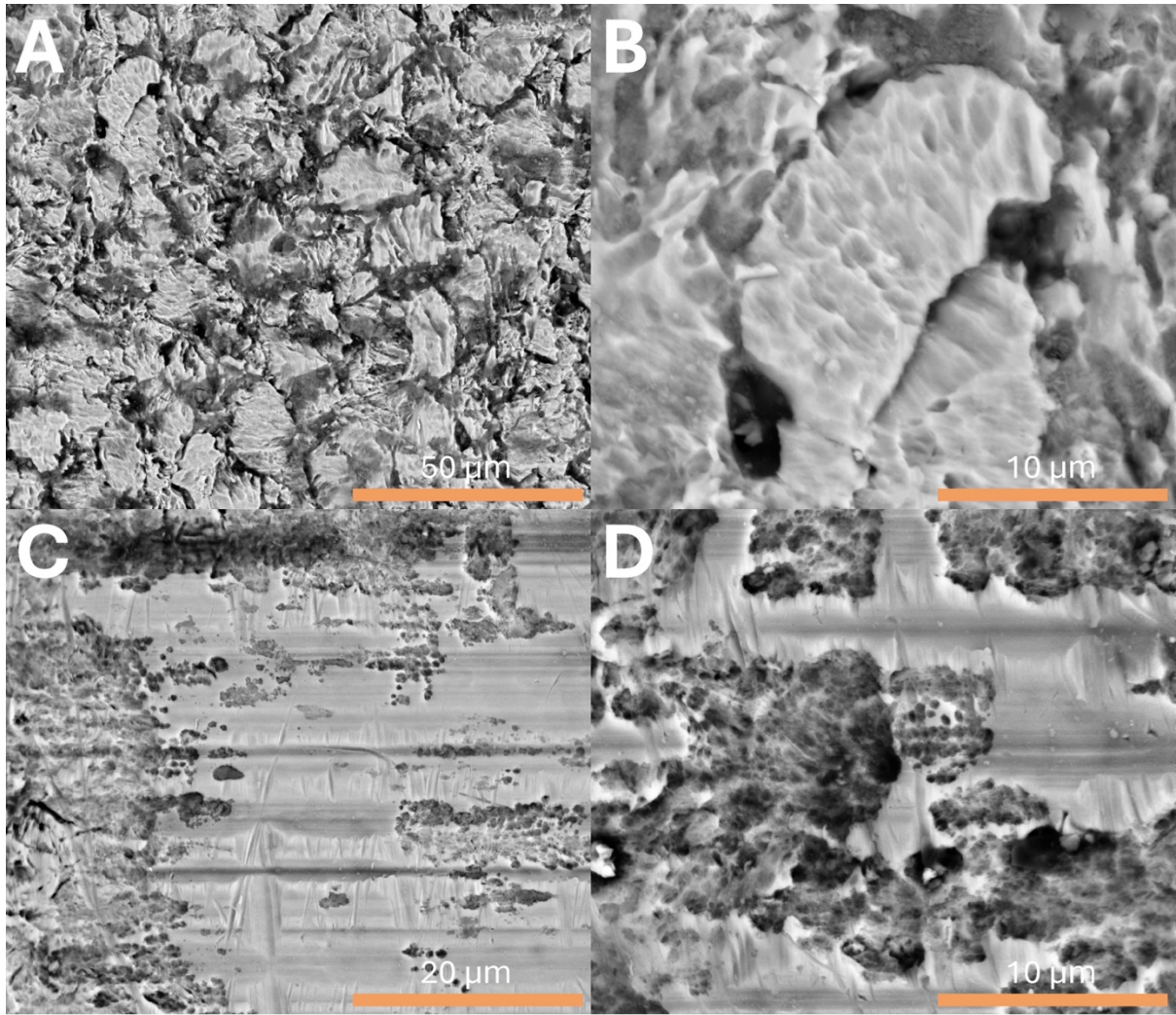


[Figure 3](#)

Corrosion in CoCrMo Modular Taper Junctions in Femoral Knee Component: A Retrieval Study

Hwaran Lee - Clemson University

Michael Kurtz - Clemson University - Charleston, USA

Greg Klein - Hartzband Center for Hip and Knee Replacement - Hackensack, USA

Steven M. Kurtz - Drexel - Philadelphia, USA

*Jeremy Gilbert - Clemson University - Charleston, USA

Introduction

Modularity is a longstanding feature in total hip arthroplasty, extensively studied for mechanically assisted crevice corrosion (MACC). In contrast, femoral knee components utilize modular junctions for stability, fixation, and alignment, particularly in revision devices. Unlike hip replacements, relatively few retrieval studies explore corrosion within these junctions. This retrieval study aims to document corrosion modes within the boss (hollow cylindrical component where the femoral implant taper resides) and compare the corrosion types and severity to hip replacements. We hypothesized that corrosion types in modular taper junctions of femoral knee components are similar to those of hip replacements.

Methods

Eight femoral knee components with cast cobalt-chrome-molybdenum (CoCrMo) alloy bosses (Fig 1) were collected at a multicenter retrieval program and shipped to our laboratory for retrieval analysis. Two boss elements (revised for infection after 16.25 and 8.5 years, respectively) were (1) transversely and (2) longitudinally sectioned (Fig 1) for imaging inside the boss. Various modes of damage (MACC and chemically based corrosion) in both intact and cross-sectioned surfaces were documented using digital optical microscopy (DOM, Keyence), scanning electron microscopy (SEM, Hitachi), and energy-dispersive X-ray Spectroscopy (EDS, Oxford Instruments).

Results

The cross-sectioned boss (seen in DOM) showed degradation in both the posterior and anterior views (Fig 2). Etched surfaces were predominantly found at proximal region, near the boss rim on both sides, as seen in DOM (Fig 2) and SEM images (Fig 3). Further analysis using SEM identified etching, pitting, fretting corrosion and selective dissolution (Fig 3). Corrosion was evident both in the contact region of the Ti-6Al-4V rod taper and below where the taper crevice was located (Fig 2). Etching revealed the dendritic microstructure of the cast alloy, with carbides present at interdendritic regions showing signs of corrosion adjacent to them. Darker regions seen in Fig. 3 consisted mainly of oxides containing Mo, Cr and Ti, filling the depressions arising on the damaged taper surface. Although fretting corrosion was observed at a scale of around 5 mm, it was not the predominant corrosion mode, unlike in hip replacements. Pitting corrosion, etching and selective dissolution were widespread across the surface on both the taper contact regions and the inner regions where no taper crevice was present. Lastly, cobalt selectively dissolved regions displayed a porous honeycomb appearance, corresponding to slip plane arrangements in the microstructure, indicating selective dissolution or dealloying based on decreased Co concentration in these areas.

Conclusion

The corrosion modes observed in the femoral boss junction have similarities to modular taper junctions of hip replacements, as determined through imaging and

chemical analysis. However, additional corrosion damage was detected beyond the direct taper contact region, indicating possibility of non-tribologically driven corrosion in these devices. These corrosion modes can be classified into chemically driven corrosion and MACC. This retrieval study will enhance our understanding of corrosion mechanisms in total knee arthroplasty.

Figures

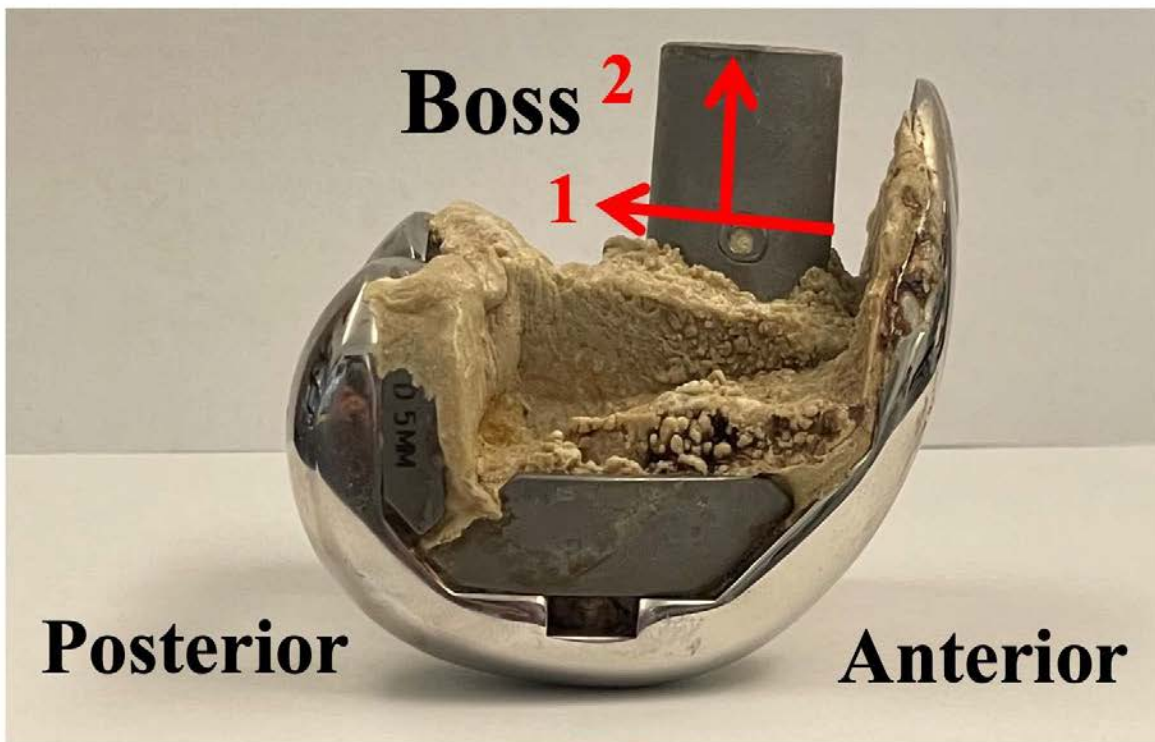


Fig 1. Femoral component with boss

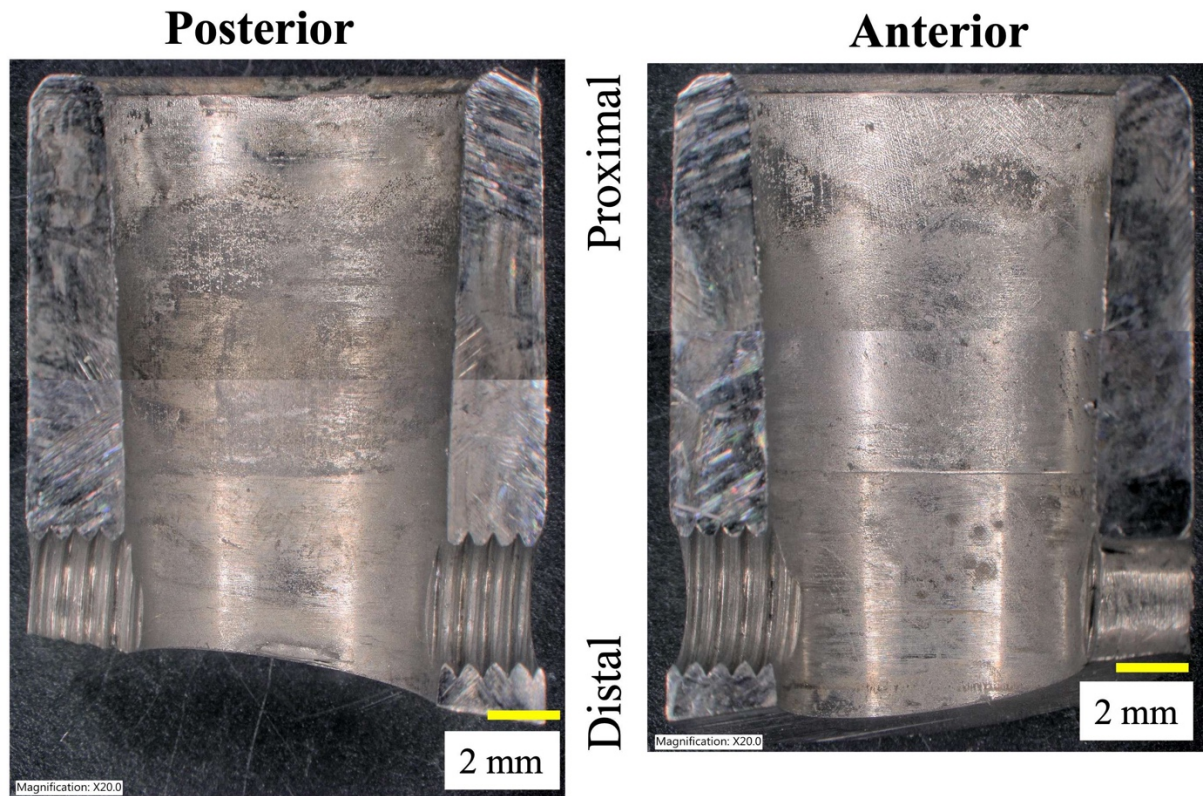


Fig 2. DOM images of cross-sectioned boss

Figure 2

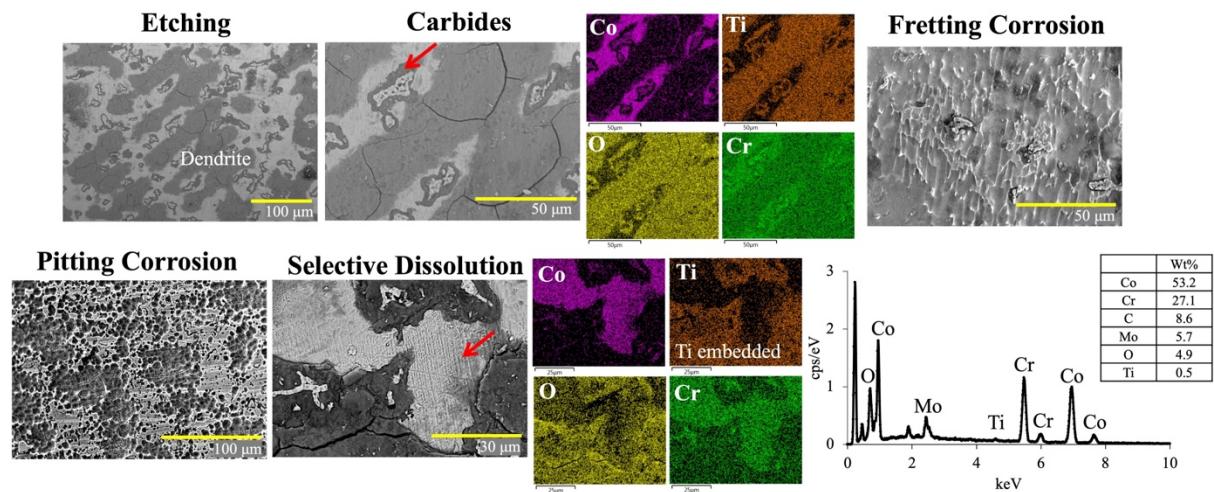


Fig 3. SEM images and EDS chemical analysis showing different types of corrosion in femoral boss

Figure 3

Does TKA Alter Synovial Fluid Properties? a Comparison of Necropsy TKA and Contralateral Knee Specimens

Bailey Bond - University of Tennessee Health Science Center - Memphis, USA

Michael Kurtz - Drexel University - Philadelphia, United States of America

Shabnam Aslani - Drexel University - Philadelphia, USA

Madison Brown - University of Tennessee Health Science Center - Memphis, USA

Steven Kurtz - Drexel University - Philadelphia, USA

Jeremy Gilbert - Clemson University - Charleston, USA

*William Mihalko - University of Tennessee - Memphis, USA

Introduction: A recent study reported moderate aseptic lymphocyte-dominated vasculitis-associated lesions (ALVAL) in 30% of revision total knee arthroplasty (TKA) patients [1]. *In vivo*, synovial fluid contacts cobalt-chromium-molybdenum (CoCrMo) implants and may transfer metal ions into the periprosthetic tissue. Previous studies identified both variable synovial fluid electrochemical properties and metal ion levels in necropsy TKA specimens [2]. This motivated us to compare synovial fluid properties in necropsy TKA and contralateral (native) knees. We asked: (1) will the physical and chemical properties of the TKA synovial fluid differ from the native knee synovial fluid; and (2) will these changes alter the synovial fluid's electrochemical properties?

Methods: Synovial fluid was collected from ten deidentified pairs of necropsy TKA and native knees following an IRB-approved protocol (Figure 1A-B, 22-09069-XP). For each knee, synovial fluid volume was recorded, and pH was measured using a compact pH meter. To assess electrochemical properties, synovial fluid was placed in an electrochemical cell. A machined CoCrMo rod (ASTM F1537) was used as the working electrode, Ag/AgCl was used as the reference electrode, and a platinum wire was used as the counter electrode. Open-circuit potential (OCP) was monitored for 60 minutes followed by electrochemical impedance spectroscopy (EIS). The resulting spectra were fit with a Randles-CPE model. Oxide polarization resistance (R_p) values were area-adjusted, and the inverse was taken to calculate the instantaneous corrosion rates. Nonparametric statistics (Mann-Whitney U) were performed using Excel and GraphPad Prism to determine differences in the synovial fluid volume, pH, and corrosion rates.

Results: Synovial fluid volume (Figure 2B) from TKA specimens (5.6 ± 2.5 mL) was significantly higher than the contralateral knees (1.6 ± 0.50 mL, $p=0.000$). We did not identify significant differences in pH (Figure 2C, $p=0.07$). The open circuit potential values for the specimens with total knee replacements and the contralateral specimens ranged from -0.15 to -0.35 V and -0.03 to -0.33 V, respectively. The instantaneous corrosion rates ($1/R_p$) for TKA specimens ($1.804E-7 \pm 7.49E-8$ $\text{?}^{-1}\text{cm}^{-2}$) were significantly higher (Figure 3) than the corrosion rates of the contralateral knees ($9.035E-8 \pm 5.58E-8$ $\text{?}^{-1}\text{cm}^{-2}$). Nine of the ten TKA specimens had a higher instantaneous corrosion rate than their native counterparts.

Conclusion: This study compared the physical and electrochemical properties of synovial fluid from necropsy TKA and native knee specimens. In the TKA group, synovial fluid volume and the median instantaneous corrosion rates of CoCrMo were significantly higher than in the native knee group. Future work will investigate a larger sample size and explore alternative circuit model fits for the EIS data.

References: [1] Rajamäki et al, Bone Joint Res, 2024. [2] Brown et al, ISTA Proceedings #8628, 2023.

FDA Disclaimer: The findings and conclusions in this abstract have not been formally disseminated by the Food and Drug Administration (USFDA) and should not be construed to represent any agency determination/policy. The mention of commercial products their sources, or their use in connection with material reported herein is not to be construed as either an actual or implied endorsement.

Figures

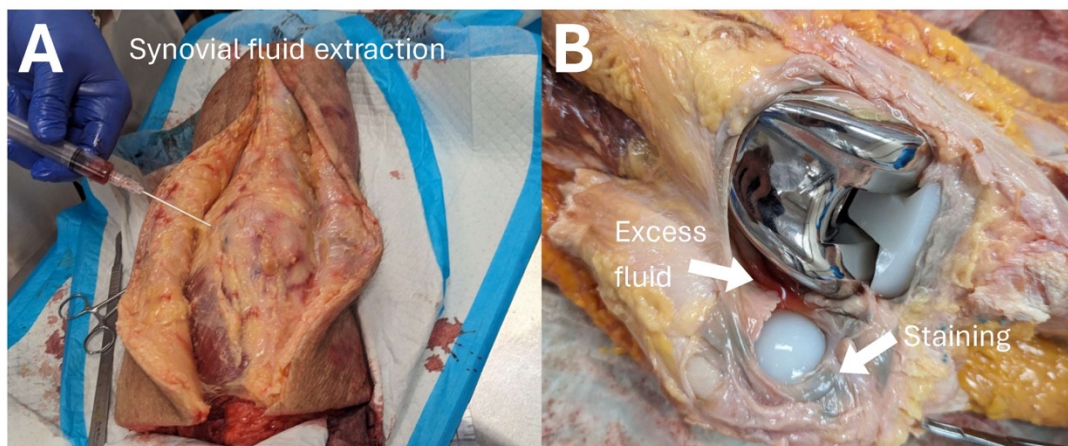


[Figure 1](#)

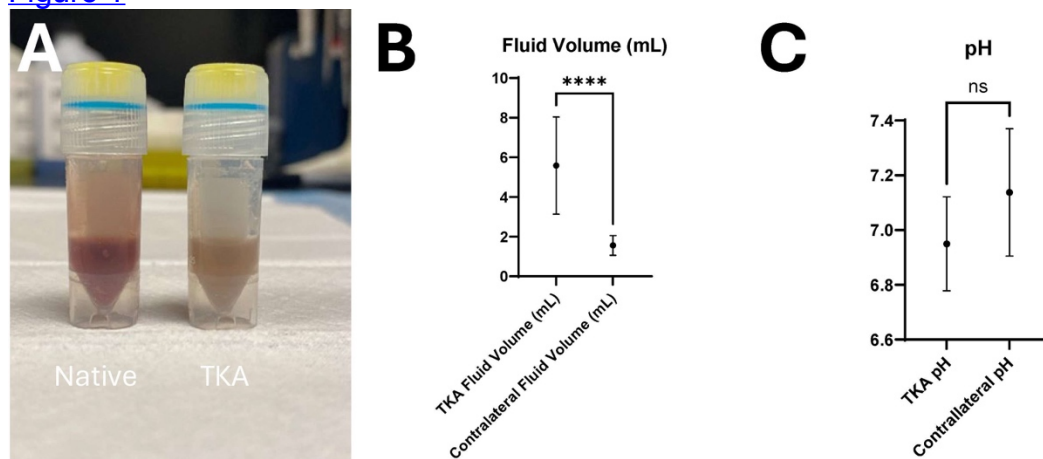


[Figure 2](#)

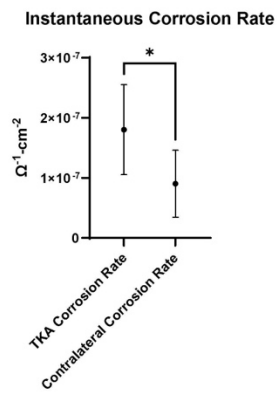


[Figure 3](#)

Is Wear Still a Concern in TKA With Contemporary Conventional and Highly Crosslinked Polyethylene Tibial Liners in the Long-Term?

*Devin Asher - Rush University Medical Center - Chicago, USA

Jennifer Wright - Rush University Medical Center - Chicago, USA

Deborah Hall - Rush University Medical Center - Chicago, USA

Hannah Lundberg - Rush University Medical Center - Chicago, USA

Douglas Van Citters - Dartmouth College - Hanover, USA

Joshua Jacobs - Rush University Medical Center - USA

Brett Levine - Rush University Medical Center - Chicago, USA

Robin Pourzal - Rush University Med Ctr - Chicago, USA

Introduction:

According to the American Joint Replacement Registry, polyethylene (PE) wear and osteolysis account for only 3% of TKA failure. However, retrieval evidence of conventional and highly crosslinked PE (HXPLPE) liners tells a different story. Severe wear, delamination, and prominent polished wear scars are evident in many tibial liners implanted for >6.5years. Polished wear scars are associated with sub-micron wear debris that contributes to the risk of osteolysis. While contemporary PEs, especially HXLPE, have solved the problem of early failure due to wear and osteolysis, long-term outcomes are still unclear. This study of retrieved tibial liners (>6.5years) aimed to determine the most prominent long-term failure reasons and their relationship with delamination and wear overall.

Methods:

A cohort of 107 (75 conventional/32 HXLPE) retrieved PE tibial liners with a median (min./max.) time in situ of 11.1 (6.6/23.6) years was studied. Liners were scored for delamination (0-none, 1- early onset, 2- gross delamination) (Fig.1). Linear wear on the medial and lateral sides was determined with a dial indicator apparatus. Separate wear rates were established with and without grossly delaminated cases for both conventional and HXLPE liners.

Results:

Across all liners, instability was the most common cause for failure, followed by aseptic loosening and PE wear (Fig.2A). Of liners in the top 3 failure categories, >80% had delamination (Fig.2B). Delamination occurred predominantly medially. With delaminated cases, there was no linear relationship between wear and time except for the lateral side of conventional liners (Fig.3A,B). By excluding delaminated surfaces, a linear relationship emerged except for the medial side of HXLPE liners. The median medial/lateral wear over time was 0.055/0.051 and 0.018/0.014 $\mu\text{m}/\text{year}$ for conventional and HXLPE liners, respectively (Figure 3C,D).

Conclusion:

The most dominant long-term TKA failure reason was instability, which appeared to be partly linked to delamination-driven gross wear of the articular surface for all liners. Excluding delamination, both conventional and HXLPE liners exhibited distinct wear scars with measurable material loss. While HXLPE showed lower wear compared to conventional PE, it must be considered that the smaller particles associated with HXLPE also carry higher osteolytic potential. While the diagnosis of osteolysis was rare for both liner types, the liners that reportedly failed due to aseptic loosening, pain, and inflammatory responses should be investigated histopathologically to rule out linkages to fine PE particles. Regardless, this study

shows that the impact of PE wear—delamination or sub-micron particle formation—on long-term TKA failure is currently underestimated.

Figures

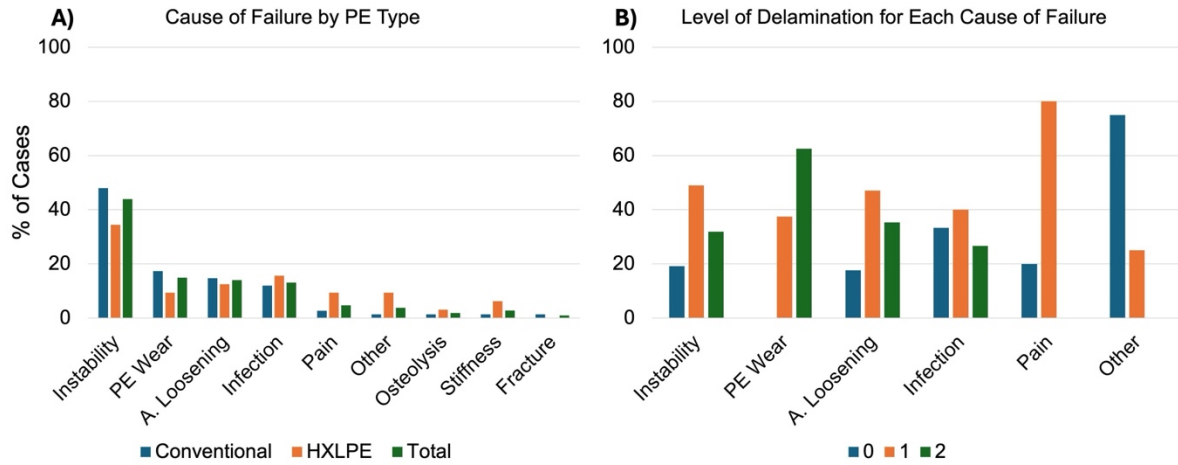


Figure 2. Distribution of causes of failure by PE type (A) and by delamination (B).

Figure 1

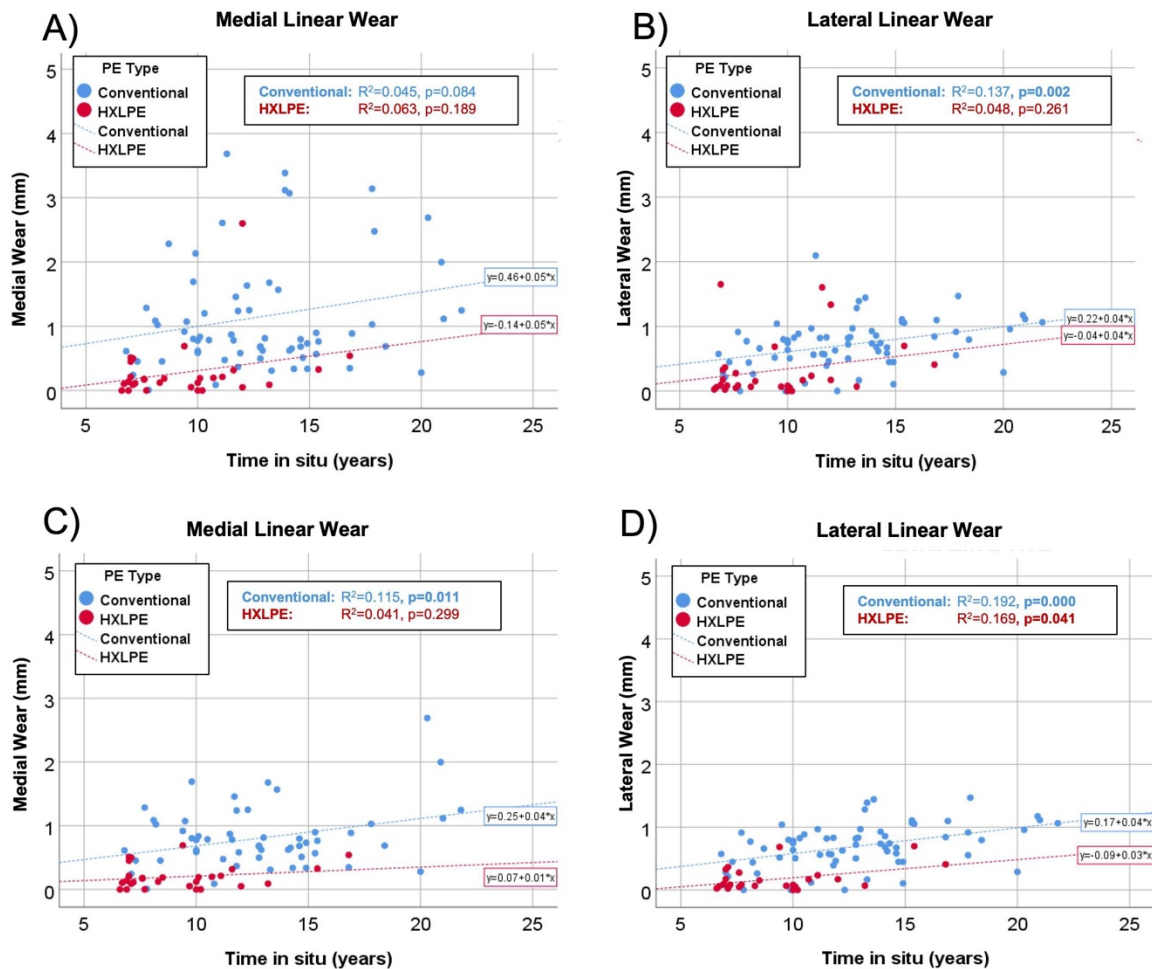


Figure 3. Medial and Lateral Linear Wear including (A&B) and excluding (C&D) all grossly delaminated cases.

Figure 2

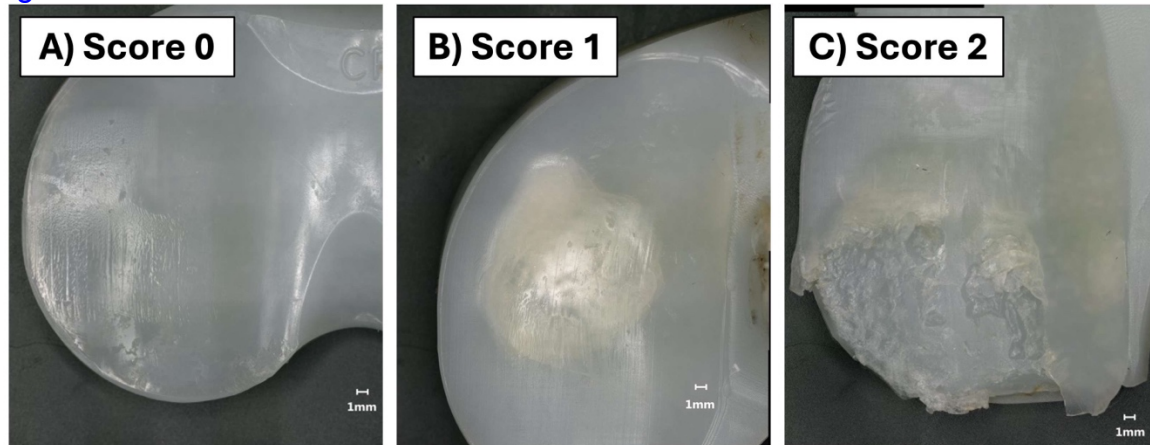


Figure 1. Examples of tibial liner bearing surfaces with A) no delamination (score 0), but other wear features such as polishing, pits and scratches, B) early onset of delamination characterized by areas with ‘milky’ appearance resulting from subsurface cracks, and C) severe delamination that resulted in gross material loss.

Figure 3

Migration of Retrieved Ball-and-Socket Cervical Disc Replacements

*Jenna Wahbeh - University of California, Los Angeles - Los Angeles, United States of America

Sang-Hyun Park - Orthopaedic Institute for Children /UCLA - Los Angeles, USA

Bryan Cornwall - University of San Diego - San Diego, USA

Edward Ebramzadeh - Orthopaedic Institute for Children/UCLA - Los Angeles, USA

Sophia Sangorgio - Orthopaedic Institute for Children/UCLA - Los Angeles, USA

Introduction: The porous coated motion (PCM) ball-and-socket cervical disc replacement (NuVasive, PCM; San Diego, CA) was developed to stabilize the spine and restore natural kinematics but has since been withdrawn from the market. The purpose of this study was to assess all retrieved PCM devices to identify the commonly reported reasons for removal, and to perform a qualitative and quantitative assessment of any damage.

Methods: Thirty-seven devices were received for post-market surveillance between 2013 and 2015. All available clinical and radiographic data including de-identified demographic information, reasons for removal, and time in vivo were documented. Following retrieval, each implant was non-destructively analyzed through visual examination, photographic documentation, and analytical measurements. Metrology was conducted on the polymeric surfaces.

Results: The mean time in vivo for all devices was 121 ± 115.6 days. The most commonly reported reason for removal was migration (N=17, Figure 1). The inferior component was observed to have migrated in 14 cases (Figure 2), no reports of superior component only migration, and migration of both components was observed in three cases (Figure 3). One device was removed due to improper sizing, and seven for unknown reasons. For devices that migrated, average time in vivo was 128.4 ± 119.7 days, compared to 69.5 ± 78.5 days, for all others ($P > 0.1$). Eleven superior and nine inferior endplates had evidence of bony ongrowth. Of these, only five had ongrowth on both endplates. The average outer surface R_a for all devices was $23.9 \pm 6.6 \mu\text{m}$, compared to $34.6 \mu\text{m}$, for a non-implanted device ($P < 0.1$), and there was no evidence of delamination. No devices had radiographic evidence of

osteolysis or bone resorption. There was one report of caudal vertebral body necrosis, and two observations of metallic wear debris. Surface damage was visible on the majority of the polyethylene components including polishing, pitting, and loss of machine lines, with a correlation noted between time in vivo and surface damage; however, metrology findings did not indicate any loss of dimension beyond manufacturing tolerances.

Conclusions: Findings from the present retrieval study are consistent with previously reported clinical data for the PCM.^{1,2} That is, these observations highlight the significance of transverse device migration as the most prevalent complication, deserving further biomechanical scrutiny. Interestingly, the inferior component (the polymeric “ball”) was reported to migrate more than the superior component. The biomechanics of this articulation type may lead to increased incidence of migration in patients. Future biomechanical evaluations should investigate the influence of device features, such as articulation type, on overall incidence of migration.

References:

1. Zavras AG, Sullivan TB, Singh K, Phillips FM, Colman MW. Failure in cervical total disc arthroplasty: single institution experience, systematic review of the literature, and proposal of the RUSH TDA failure classification system. *Spine J.* 2022 Mar;22(3):353-369. doi: 10.1016/j.spinee.2021.08.006. Epub 2021 Aug 20. PMID: 34419625.
2. Virk S, Phillips F, Khan S, Qureshi S. A cross-sectional analysis of 1347 complications for cervical disc replacements from medical device reports maintained by the United States Food and Drug Administration. *Spine J.* 2021 Feb;21(2):265-272. doi: 10.1016/j.spinee.2020.09.005. Epub 2020 Sep 20. PMID: 32966907.

Figures

Figure 1. Surgical Reason for Removal

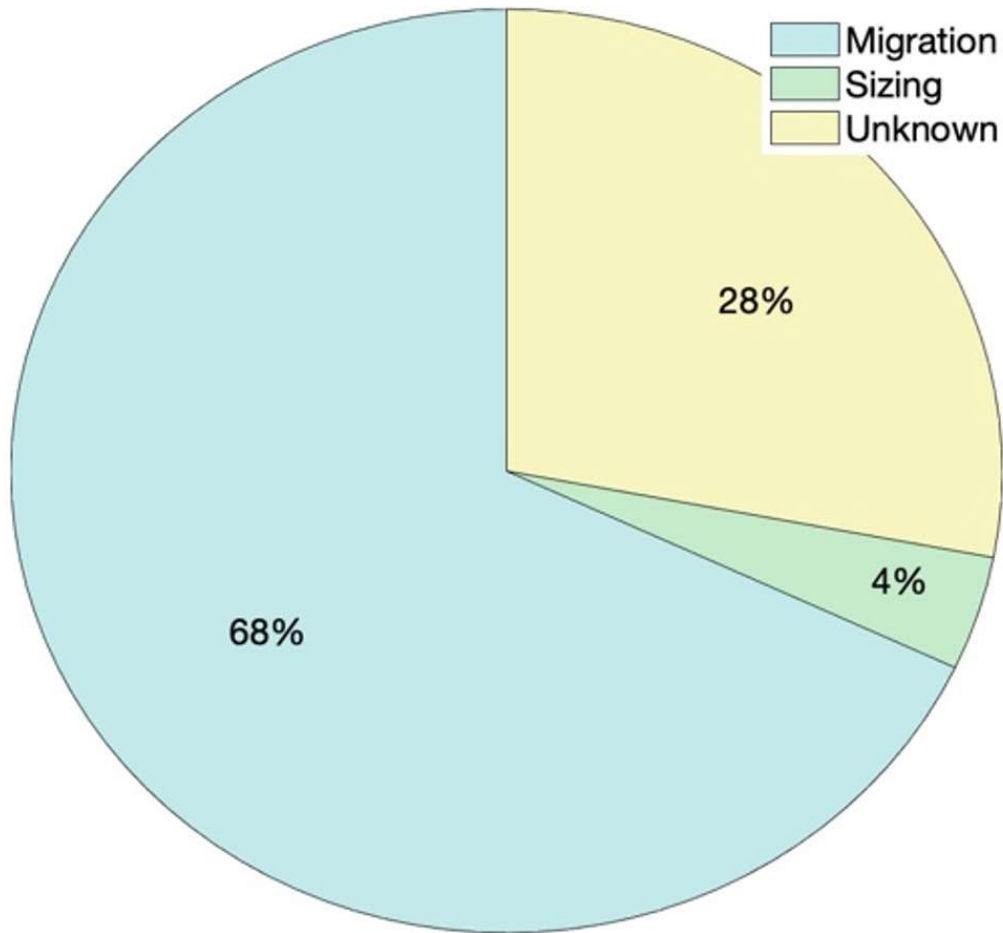


[Figure 1](#)

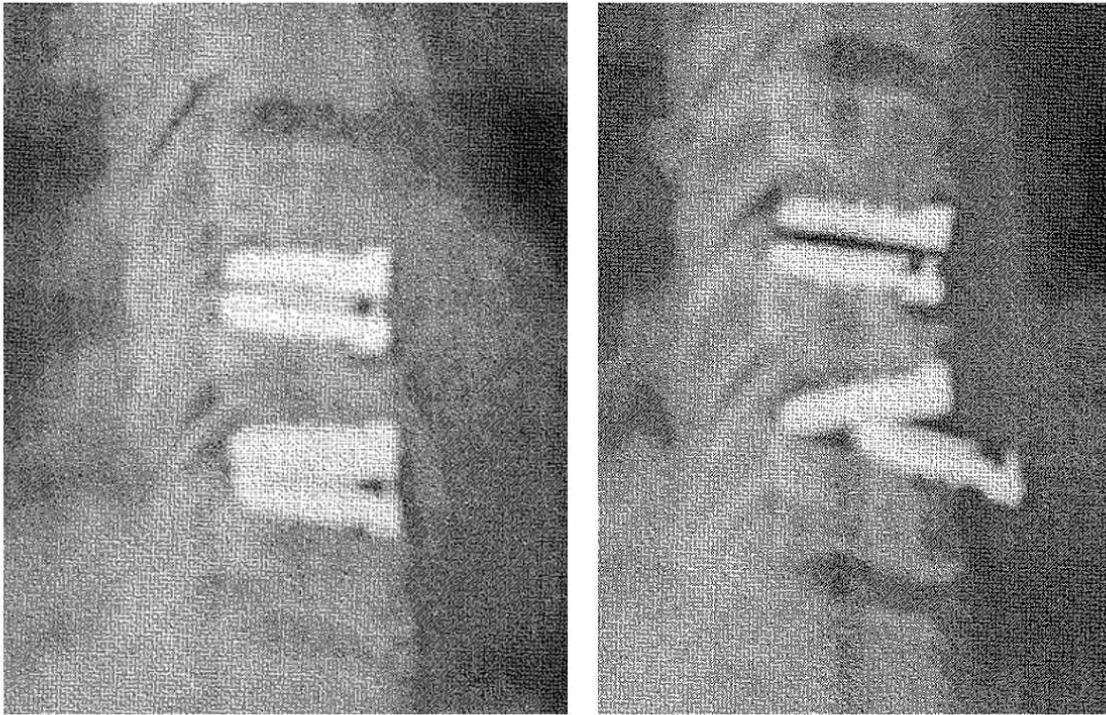


Figure 2. (Left) Pre-operative and (Right) Post-Operative radiographs from a device with reported migration of the inferior component only.

[Figure 2](#)

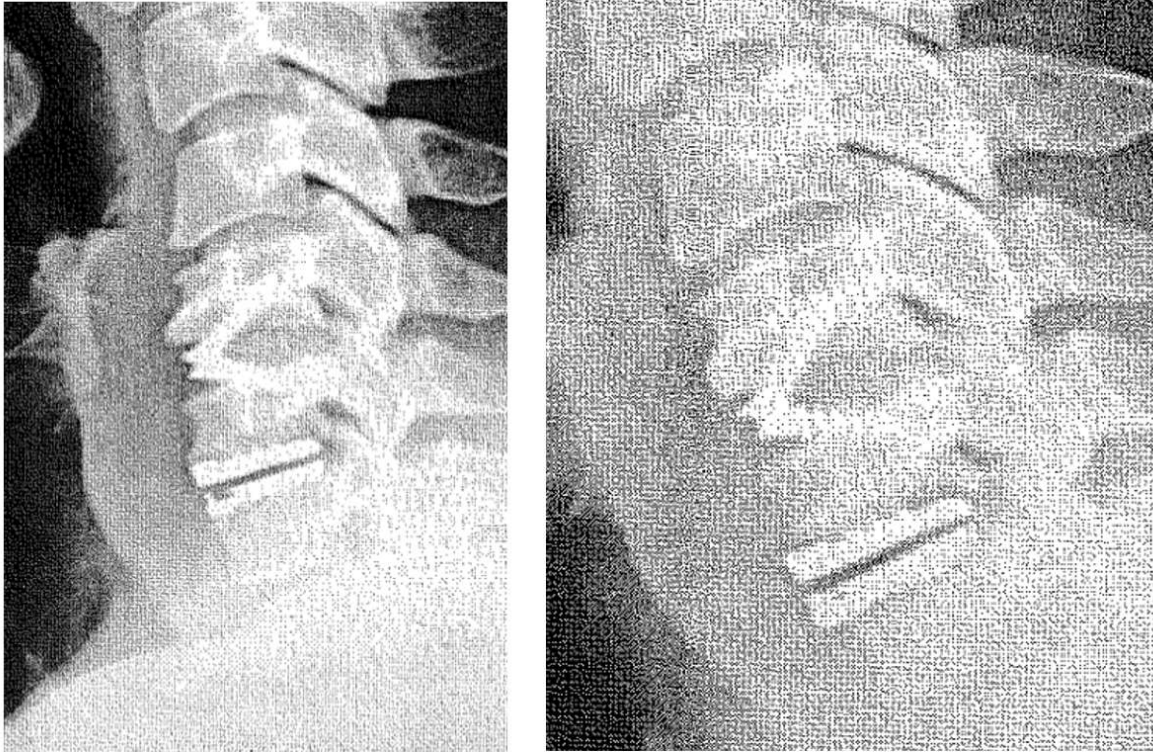


Figure 3. (Left) Pre-operative and (Right) Post-Operative radiographs from a device with reported migration of the inferior and superior component.

[Figure 3](#)

Comparison of ChatGPT Plus (Version 4.0) and Pretrained AI Model on Orthopaedic in-Training Exam

*[Matthew Magruder](#) - Maimonides Medical Center - Brooklyn, USA

Michael Miskiewicz - Renaissance School of Medicine at Stony Brook University Medical Center - Stony Brook, USA

Ariel Rodriguez - Maimonides Medical Center - Brooklyn, United States of America

Mitchell Ng - Maimonides Medical Center - Brooklyn, United States of America

Amr Abdelgawad - Maimonides Medical Center - Brooklyn, USA

Introduction: Recent advancements in large language model (LLM) artificial intelligence (AI) systems, like ChatGPT, have showcased ability in answering standardized examination questions, but their performance is variable. The goal of this study was to compare the performance of standard ChatGPT-4 with a custom-trained ChatGPT model taking the Orthopaedic Surgery In-Training Examination (OITE).

Methods: We used two different ChatGPT models in this investigation. The first was the standard ChatGPT Plus (version 4.0). The second model was a custom-trained model that incorporates the underlying power of the LLM but preferentially produces answers based on data designated to the AI – which we named “Orthopod”. Practice questions for the 2022 OITE, made available on the American Academy of Orthopaedic Surgery (AAOS) ResStudy website, were used for this study. Question stems were uploaded to both standard ChatGPT-4 and the custom-trained ChatGPT model, and the responses were documented as correct or incorrect. For questions containing media elements, screenshots were converted to PNG files and uploaded to ChatGPT. Analysis of variance (ANOVA) was performed to compare the performance of ChatGPT-4 to Orthopod on OITE questions based on question category. Pearson X^2 tests were used to determine if a correlation existed between the number of questions answered correctly and question order, as well as the presence of associated media.

Results: Two-hundred and seven questions were analyzed. ChatGPT and Orthopod answered 73.4% (152/207) and 71.0% (147/207) questions correctly, respectively (Figure 1). Both systems provided similar responses (either both correct or both incorrect) to 173 questions (83.57%). There was no statistically significant difference between the performance of ChatGPT ($p=0.194$) or Orthopod ($p=0.446$) based on question category (Table 1). There was no statistically significant difference between ChatGPT ($p=0.714$) or Orthopod’s ($p=0.206$) performance on questions with or without media. Similarly, there was no statistically significant difference between ChatGPTv4’s ($p=0.667$) or Orthopod’s ($p=0.115$) performance on first versus second order questions (Table 2). The sub-analysis on media-inclusion revealed no statistically significant difference in performance between ChatGPT ($p=0.383$) or Orthopod ($p=0.394$).

Conclusion: Both systems provided well-reasoned answers in response to multiple choice questions. The thoughtfully articulated responses and well-supported explanations offered by ChatGPT may prove to be a valuable educational resource for orthopedic residents. Regardless, enhancing the reliability of this LLM’s responses is essential. By integrating data from widely-used orthopedic textbooks into the initial training phase of Orthopod, we attempted to advance the reliability of information offered by ChatGPT, but ultimately were unsuccessful.

Figures

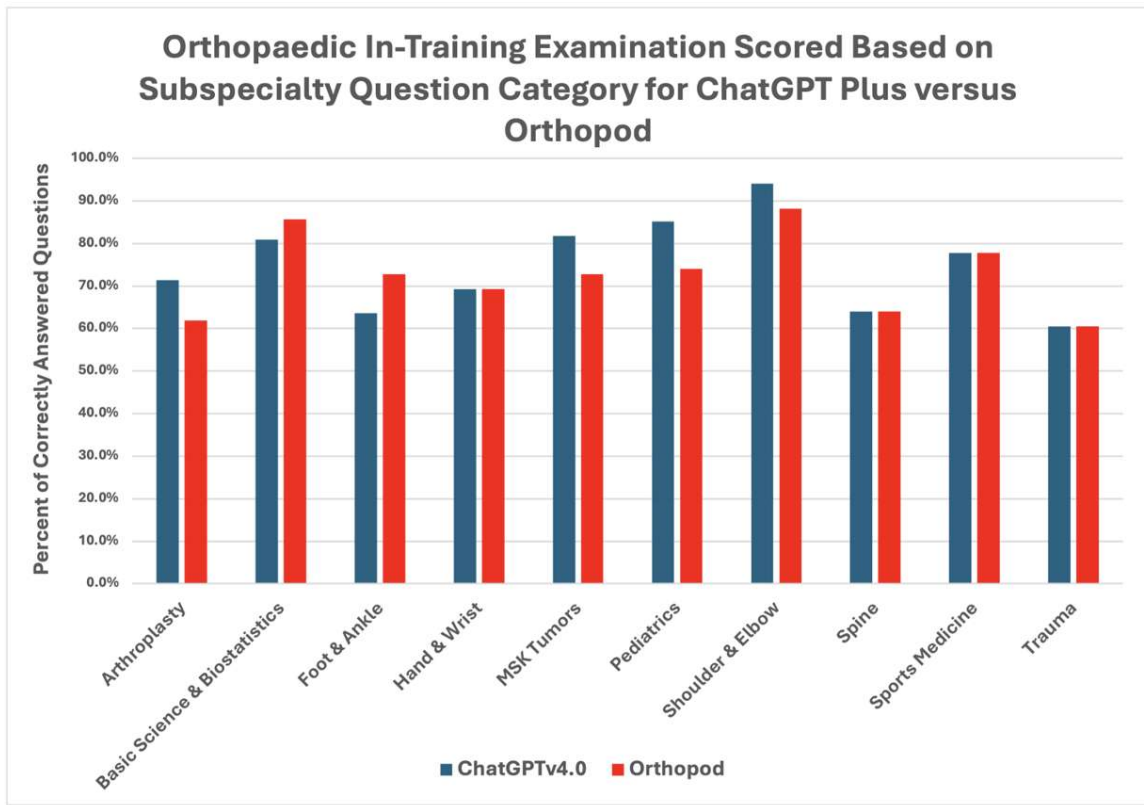


Figure 1: Bar graph displaying performance of ChatGPTv4 and Orthopod performance on OITE questions based on question category.

**Arthroplasty = adult reconstruction (hip & knee)*

**MSK Tumor = musculoskeletal tumors and disease*

**GPT = Generative Pretrained Transformer*

**Orthopod = custom pretrained GPT*

[Figure 1](#)

	ChatGPTv4.0			Orthopod		
	Number Correct	Percent	p-value	Number Correct	Percent	p-value
Arthroplasty	15	71.4%	0.194	13	61.9%	0.446
Basic Science & Biostatistics	17	81.0%		18	85.7%	
Foot & Ankle	7	63.6%		8	72.7%	
Hand & Wrist	9	69.2%		9	69.2%	
MSK Tumors	9	81.8%		8	72.7%	
Pediatrics	23	85.2%		20	74.1%	
Shoulder & Elbow	16	94.1%		15	88.2%	
Spine	16	64.0%		16	64.0%	
Sports Medicine	14	77.8%		14	77.8%	
Trauma	26	60.5%		26	60.5%	
Total	152	73.4%		147	71.0%	

Table 1: Summary performance of ChatGPTv4 versus Orthopod on OITE questions, based on question category.

**Orthopod = custom pretrained GPT*

[Figure 2](#)

	ChatGPTv4.0			Orthopod			Total
	Number Correct	Percent	p-value	Number Correct	Percent	p-value	
First Order	75	72.1%	0.667	79	76.0%	0.115	104
Second Order	77	74.8%		68	66.0%		103
Media	62	72.1%	0.714	57	66.3%	0.206	86
No Media	90	74.4%		90	74.4%		121

Table 2: Summary performance of ChatGPTv4 and Orthopod on (1) first versus second order questions and (2) questions with or without media.

**Orthopod = custom pretrained GPT*

[Figure 3](#)

Patient Specific Alignment and Laxity in TKA: A Neural Network Analysis

*Alex Orsi - Corin - Raynham, USA

Christopher Plaskos - Corin - Raynham, USA

Edgar Wakelin - OMNI Life Sciences - Raynham, USA

John Keggi - Orthopaedics New England - Middlebury, USA

Total knee arthroplasty (TKA) is the gold standard in treating end-stage knee osteoarthritis. Achieving consistent post-operative outcomes in TKA remains a hurdle, particularly in managing pain, which significantly impacts patient satisfaction and recovery. To address this, a neural network was developed to predict post-operative pain for TKA patients. The neural network takes patient demographics, pre-operative PROMS, joint anatomy, and soft tissue profile as inputs, and outputs a predicted Knee Injury and Osteoarthritis Outcome Score-12 (KOOS12) pain value. Data was extracted from an international joint replacement registry of patients who received a tibia first robotically assisted TKA with a digital joint tensioning device who completed pre-operative and post-operative questionnaires. A total of 914 patient outcomes from 368 individual patients were extracted from the registry. A fully connected neural network with 3 hidden layers was generated in AzureML using Keras. Optimization of neurons per hidden layer was performed using a sweep analysis in which the neurons per layer was varied between 10 – 2000. The mean squared error (MSE) and mean absolute error (MAE) were recorded. Initial training returned a model which converged over 68 epochs (MAE did not improve since epoch 18), Figure 1A. Sweep mode analysis returned a model with the lowest normalized MAE of 0.61 under the validation dataset with hidden layers of 2000, 500 and 300 neurons in the first, second and third hidden layer respectively. Using the optimized model, the test dataset reported a KOOS12 MAE of 8.1 points, and a correlation coefficient between the true KOOS 12 pain outcome and predicted outcome of 0.756, Figure 1B. An example patient was extracted from the test dataset and outcome predictions were generated from 3M to 2Yrs post-TKA, Figure 1C. Good predictions, although systematically lower than the ground truth, are observed at 3M, 1Yr and 2Yrs, with the greatest error at 6M post-op. An exploratory neural network was successfully developed to predict post-operative outcomes in TKA based on pre-operative patient information and intra-operative data. Using a test data set, the model was validated, and a mean absolute error well below the minimum clinically important difference for KOOS12 pain was observed. Neural networks such as the one developed here have the potential to provide real time patient specific intra-operative feedback to surgeons informing them on how to tailor their operations to optimize patient outcomes.

Figures

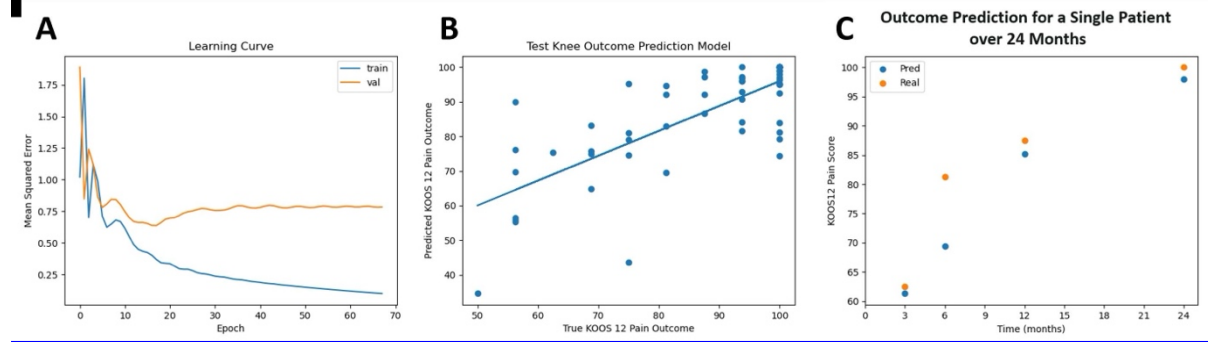


Figure 1

Automated SSM Landmarking With Region-Refinement Improves Landmarking Accuracy

*Marco Schneider - Formus Labs - Auckland, New Zealand

Duncan Bakke - Formus Labs - Auckland, New Zealand

Lilian Lim - FormusLabs - Auckland, New Zealand

Ju Zhang - Formus Labs - Auckland, New Zealand

Alex Carleton - FormusLabs - Auckland, New Zealand

Thor F Besier - University of Auckland - Auckland, New Zealand

Introduction

Landmarking plays a critical role in patient-specific orthopaedics and biomechanics. Errors in landmark selection carry forward to surgical planning and delivery. Manual landmarking is the gold standard but is time consuming and prone to intra- and inter-observer variability. Automated landmarking with statistical shape models (SSM) can improve reproducibility by morphing an atlas and its embedded landmarks to patient-specific geometry, but relies on achieving correspondence during both training and fitting. Augmentation of SSM methods can improve landmarking performance [1]. We aimed to develop an SSM landmarking algorithm with region-refinement (SSM-RR) and evaluate its accuracy to standard-SSM and manual methods.

Methods

CT scans of five patients (female, 56 ± 13 years) undergoing routine hip arthroplasty were automatically segmented to obtain 3D models of the pelvis and femur (Formus Labs, NZ). Three technicians performed manual landmarking of the femoral epicondyles (MEC & LEC), greater and lesser trochanters (GT & LT), femoral neck saddle (NS), anterior and posterior superior iliac spines (ASIS & PSIS), pubic symphysis (P_SYM) and tuberosity (P_TUB), and ischial spine (ISC_SPI) based on literature definitions [1]. The definitions were refined and manual landmarking repeated on one joint until the inter-observer difference was minimised. SSM-RR was implemented based on the refined definitions. Five hip joints were then manually landmarked and consensus was sought if a difference was observed. SSM-RR landmarks and standard-SSM landmarks were obtained and compared to consensus landmarks.

Results

Mean inter-observer difference in landmarks obtained with broad definitions was 5.3 ± 4.0 mm. After refinement, mean inter-observer difference was 0.7 ± 0.4 mm and consensus landmarks were obtained. Mean difference between the SSM-RR landmarks and consensus landmarks (2.9 ± 4.2 mm) was lower than the mean difference between the standard-SSM landmarks and consensus landmarks (4.6 ± 4.8 mm) ($p=0.032$). Greatest improvements were observed in the MEC, GT, LT, ASIS, PSIS, and PUB_TUB. The greatest difference was observed in the P_SYM (Figure 1).

Conclusion

The inter-observer difference in landmarks obtained with broad definitions was similar to literature reported values [2,3]. The SSM-RR method selected for landmarks that were closer to the consensus landmarks than the standard-SSM method ($p=0.032$), although both methods performed better than manual landmarking. Future work involves further improving the region-refinement algorithm such that all landmarks have lower differences than manual landmarking.

References

1. Kucha?, M., et al. (2021). *Int. J. Legal Med.*, 135
2. Victor, J., et al. (2009). *The knee*, 16(5)
3. Fischer, M. C., et al. (2019). *Scientific Reports*, 9(1)

Acknowledgements

Christina Leong and Jacob Mathews

Figures

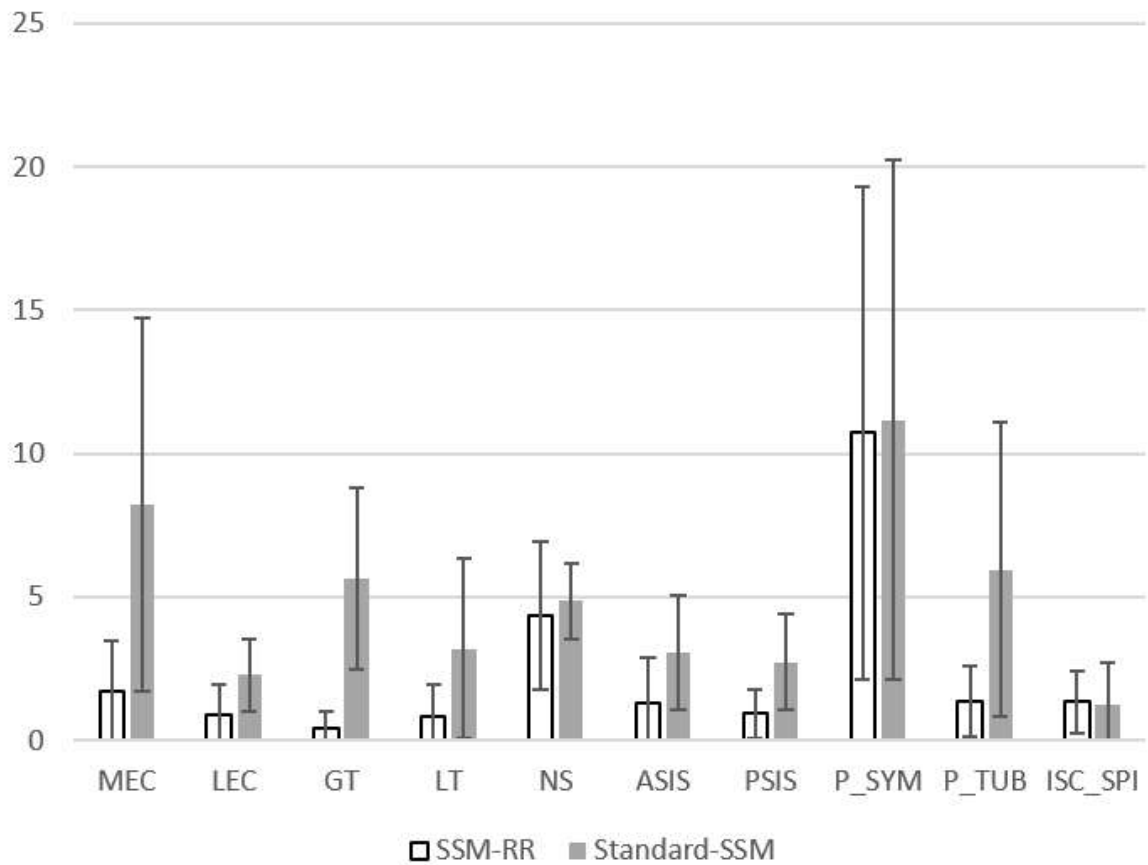


Figure 1. Mean differences between automated and consensus landmarks

[Figure 1](#)

Novel Dilation-Erosion Labeling Technique Allows for Rapid, Accurate and Adjustable Alignment Measurements in Primary TKA

*Aleksander Mika - Vanderbilt Orthopedics

Yehyun Suh - Vanderbilt University - Nashville, USA

Robert Elrod - Vanderbilt University - Nashville, USA

Martin Faschingbauer - Department of Orthopedic Surgery, RKU, University of Ulm - Ulm, Germany

Danile Moyer - Vanderbilt University - Nashville, USA

John Ryan Martin - Vanderbilt Health - Hendersonville, USA

Introduction:

Optimal implant position and alignment remains a controversial, yet critical topic in primary total knee arthroplasty (TKA). Future study of optimal implant position requires the ability to measure component positions at scale. While artificial intelligence possesses potential in this realm, current algorithms have limited accuracy, do not allow for oversight, and require extensive training time. Therefore, the purpose of this study was to develop and validate a machine learning model that can automate, with surgeon directed adjustment, implant position annotation.

Methods:

A retrospective series of 280 primary TKAs, performed in 160 patients was identified. The femoral-tibial angle (FTA), distal femoral angle (dFA), and proximal tibial angle (pTA) were manually annotated from the immediate post-op radiograph. We then trained a neural network to predict each annotated position. Training employed a novel label augmentation procedure of dilation, reweighting, and scheduled erosion steps (Figure 1). The model was compared against three previously described predication methods (Baseline 0, 1 and 2). Accuracy was then assessed using a validation set of 19 patients.

Results:

The training model significantly improved accuracy over baseline non-augmented training models. The model was significantly improved compared to Baseline 0 and Baseline 1 across all measures (dFA: $p < 1e-15$, pTA: $p < 1e-15$, FTA: $p < 1e-15$), and Baseline 3 for two of three measures (dFA: $p < 1e-9$, pTA: $p < 1e-9$, FTA: $p = 0.443$) (Figure 2) In the final model the mean squared prediction error (difference from clinician annotation) was 0.5 degrees for dFA, 0.1 degrees for FTA, and 0.6 for pTA (Figure 4).

Discussion:

Utilizing a novel machine learning algorithm, trained on a limited dataset of 280 TKAs, the accuracy of component position measurement was approximately 0.5 degrees. We believe this accuracy is well within the standard error of manual measurements and has substantial clinical implications for rapidly analyzing large datasets, use for intraoperative implant alignment, as well as identifying implant positions of other joint replacements. Furthermore, the proposed model outputs annotated, adjustable points from which the angles are calculated allowing for clinician oversight (Figure 3).

Figures

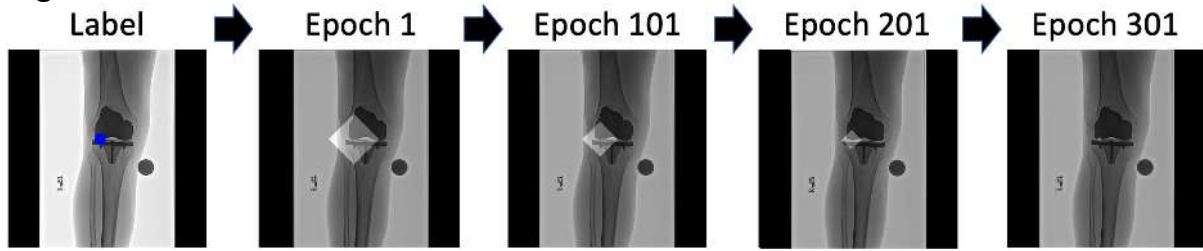


Figure 1

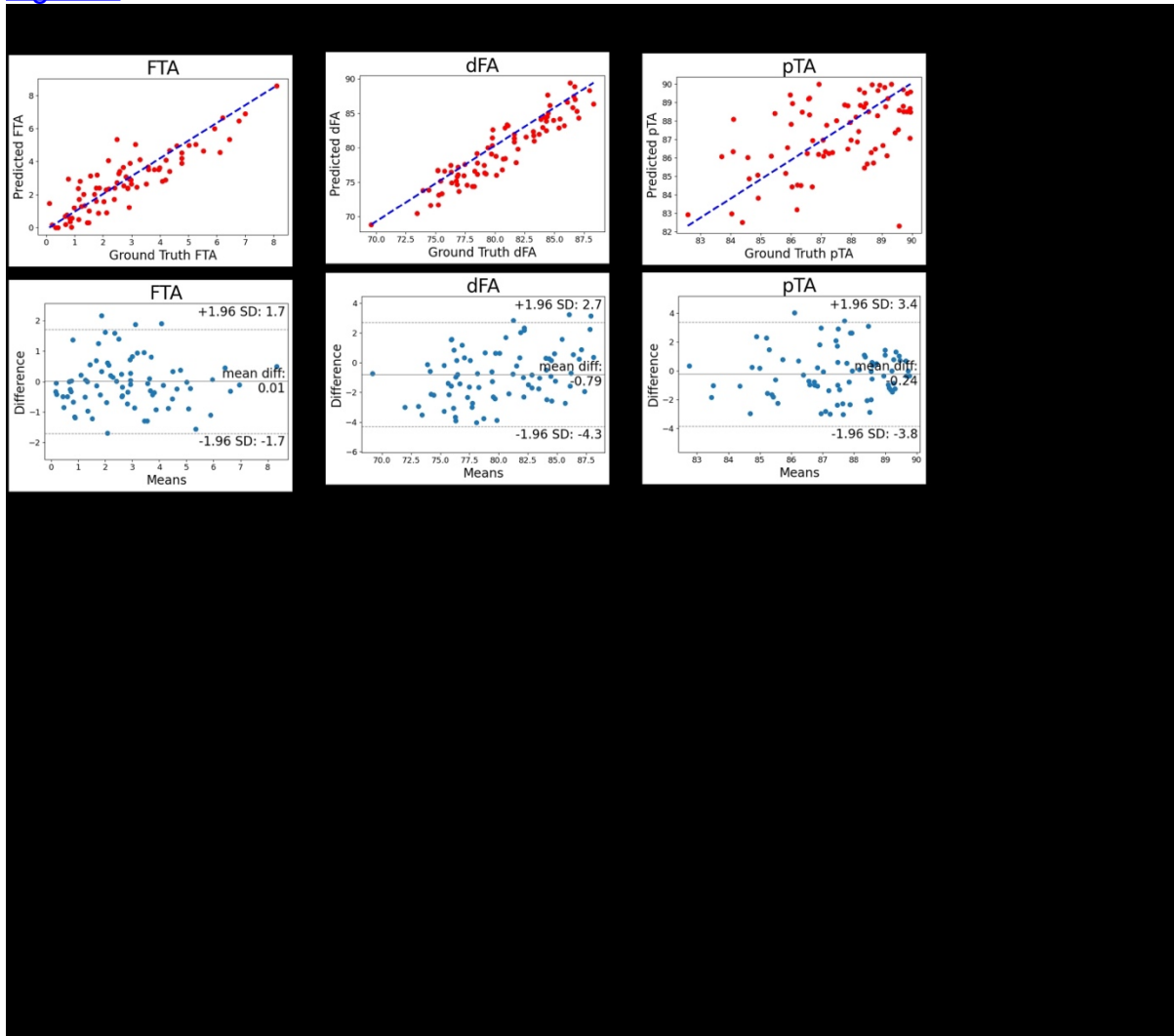


Figure 2

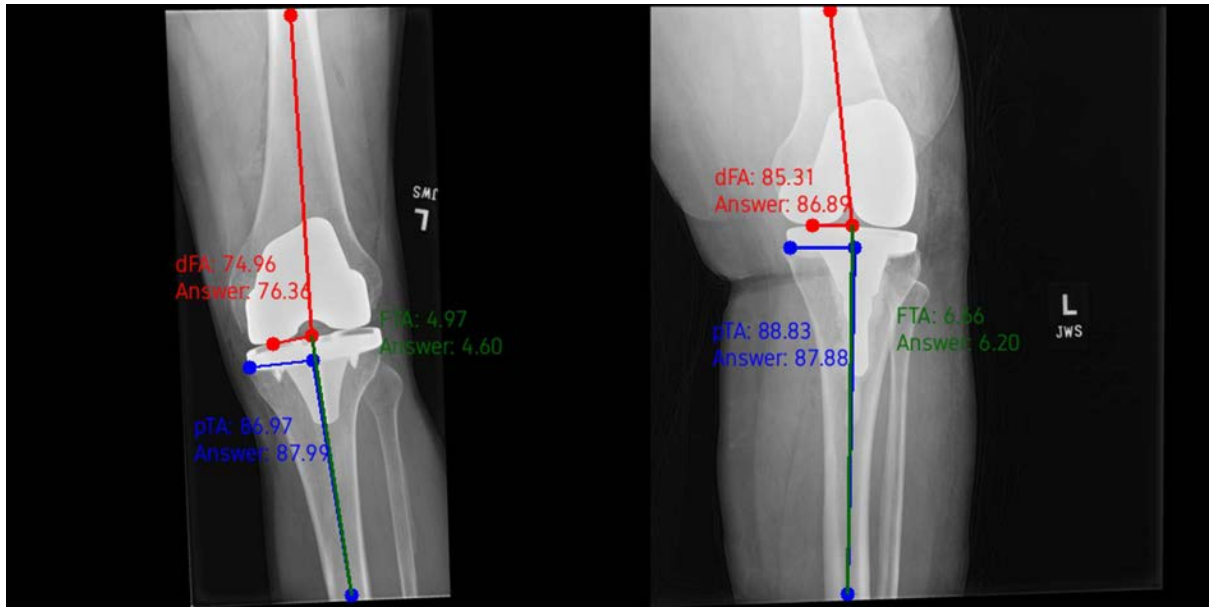


Figure 3

Predictive Modeling of Unplanned Hospital Inpatient Utilization in Osteoarthritis Patients

*[Lulla Kiwinda](#) - Duke University School of Medicine - Durham, USA

[Chuan Hong](#) - Duke University School of Medicine - Durham, USA

[Mikhail Bethell](#) - Duke University School of Medicine - Durham, USA

[Peiyu Li](#) - Duke University School of Medicine - Durham, USA

[Christian Pean](#) - Duke University - Durham, USA

Introduction. Despite the recognized influence of both comorbid conditions and social drivers of health (SDOH) on patient outcomes, gaps remain in our understanding of inpatient hospital utilization post-osteoarthritis diagnosis. This study aims to refine predictive models of inpatient utilization among osteoarthritis patients, considering a wide array of risk factors.

Methods. We conducted a retrospective cohort study using electronic health record (EHR) data from our institution. This study included patients who received a primary diagnosis of hip, knee, or shoulder osteoarthritis between 2016 and 2023 as defined by International Classification of Diseases 10th Edition. The primary outcome of interest was hospital readmission within 30-, 90-, and 365-days after diagnosis. A list of candidate predictors was curated by domain experts. Utilizing this curated list, we developed logistic regression models to identify risk factors associated with the likelihood of readmission. For each model, we divided the data with 50% for training and the remaining 50% for validation.

Results. A total of 31,042 patients were included in this study. Numerous clinical factors were found to be associated with the risk of inpatient utilization in osteoarthritis patients 30-, 90-, and 365-days after diagnosis, most notably race and insurance type (Figure 1). Black patients were 78% more likely to utilize inpatient hospital services within one year of osteoporosis diagnosis (OR: 1.792, CI: 1.389 to 2.313). Additional 1-year predictors of hospital inpatient utilization included active infections (OR: 2.222, CI: 1.622 to 3.046), alcohol use disorder (OR: 1.969, CI: 1.215 to 3.190), congestive heart failure (OR: 2.059, CI: 1.781 to 2.381), chronic high dose narcotic use (OR: 2.023, CI: 1.302 to 3.143), and depression (OR: 1.882, CI: 1.718 to 2.063). Similar patterns were observed for 30- and 90-days post-diagnosis (Figure 1). All models demonstrated robust and consistently good predictive performance across all periods, achieving area under the curve (AUC) ranging from 0.71 to 0.74 for 30-, 90-, and 365-days after diagnosis.

Conclusion. This study highlights the critical role of socio-economic and clinical factors in predicting hospital inpatient utilization for osteoarthritis patients. By leveraging predictive models that encompass a broad spectrum of risk factors, including significant comorbid conditions and SDOH factors, healthcare providers can more effectively identify and intervene with high-risk patients. This approach aligns with current trends towards condition-based management and aims to improve longitudinal patient outcomes while optimizing healthcare resource allocation.

Figures

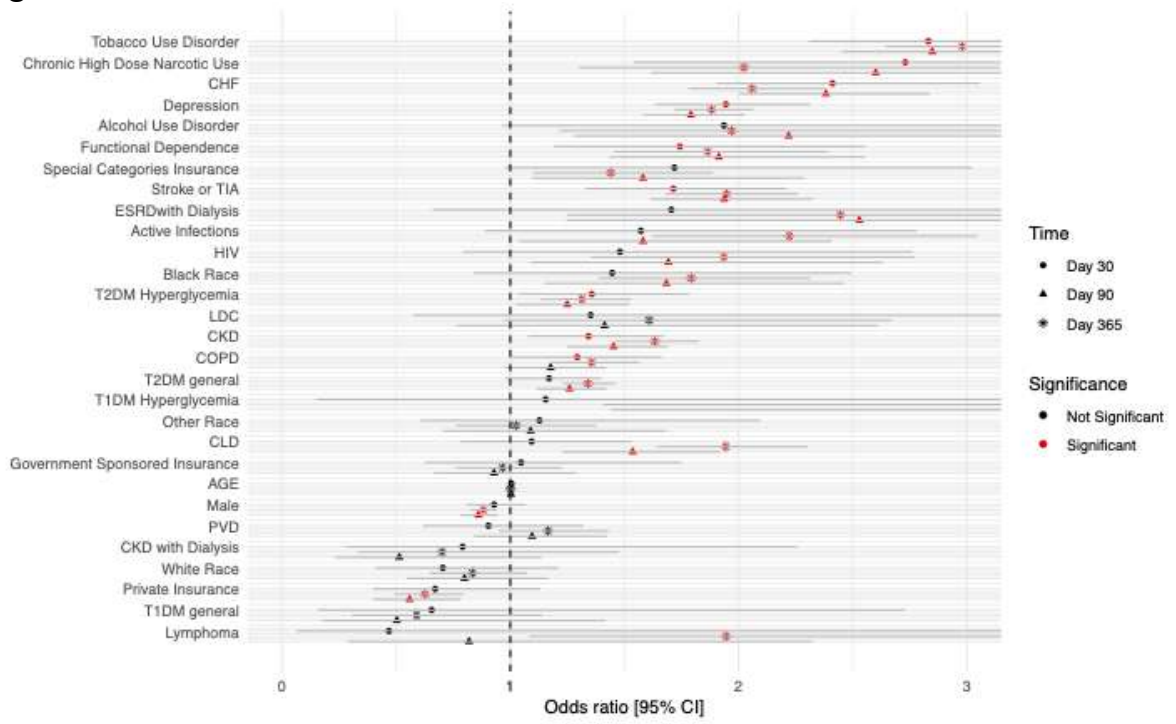


Figure 1

Activity Recognition Using Artificial Intelligence Techniques in a Cadaveric Knee Replacement Model Based on Dual Integrated IMU Devices

*Emma Donnelly - Western University - London, Canada

Ryan Willing - Western University - London, Canada

Lipalo Mokete - Charlotte Maxeke Johannesburg Academic Hospital, Johannesburg - Sandton, South Africa

Alex Conway - Moriana Innovations - Johannesburg, South Africa

Introduction

Total knee replacement (TKR) is a reliable treatment for end stage degenerative conditions of the knee. Patient reported outcome measures (PROMs) play a central role in patient centred assessment of the functioning of the TKR. However, PROMs are subject to limitations including floor and ceiling effects; hence, there is a need for objective measures. Wearable devices can generate objective data but are subject to inaccuracies. Inertial measurement units (IMUs) integrated into TKR implants have not only the potential to relay accurate objective quantitative activity data, but also qualitative data. The ability to seamlessly recognise and report specific activity can also enhance the ability to deliver patient specific rehabilitation protocols.

Methods

A standard off the shelf posterior stabilised cemented knee replacement with a blind chamber created on the lateral aspect of the femoral component and a standard tibial component with a modular augment containing a blind chamber on the lateral aspect was implanted with bone cement into a cadaveric knee using standard instrumentation. The femoral and tibial bone shafts were transected, potted, and attached to a 6-degree-of-freedom joint motion simulator (AMTI VIVO). Proprietary IMU devices comprising an accelerometer, a gyroscope, Bluetooth, and a micro lithium polymer battery were inserted into both blind cavities. The simulator reproduced various activities of daily living (ADL) based on in vivo measurements derived from OrthoLoad (www.OrthoLoad.com), including jogging 6km/h on a treadmill, knee bend, sitting down, stance, standing up, walking, walking downstairs and walking upstairs. Forces were reduced by 50%, and jogging, stair walking and walking activities were applied at half speed to avoid causing damage to the specimen. Accelerometer and gyroscope streamed data was recorded at 50 hertz and labelled according to the associated activity. An Artificial Intelligence (AI) multimodal deep learning model was constructed using a combination of networks and a late fusion network strategy. The AI model was trained to recognize ADLs using the labelled data, with 20% being used for training and the rest of the data set aside for deep learning. The activity recognition accuracy was then assessed.

Results

The overall accuracy of the AI model was 96.32% (jogging 6km/h treadmill:100%, knee bend:100%, sitting down:100%, stance:100%, standing up:100%, walking:93.55%, walking downstairs:93.55%, walking upstairs: 94.44%). The confusion matrix (Fig. 1) shows that the model performed perfectly for jogging, knee bend, stance, sitting and standing but confused walking with walking downstairs and vice-versa around 5% of the time, and similarly confused walking upstairs with walking downstairs.

Conclusion

Accelerometer and gyroscope data generated by dual IMU devices integrated in the femoral and tibial components of a TKR can accurately recognise specific types of knee activity based on our novel AI model. Our study focused on simulator generated data and involved a limited dataset. However, we believe it can be applicable with minor modifications of the AI model in the real world of TKR patients to convey objective qualitative activity data.

Figures

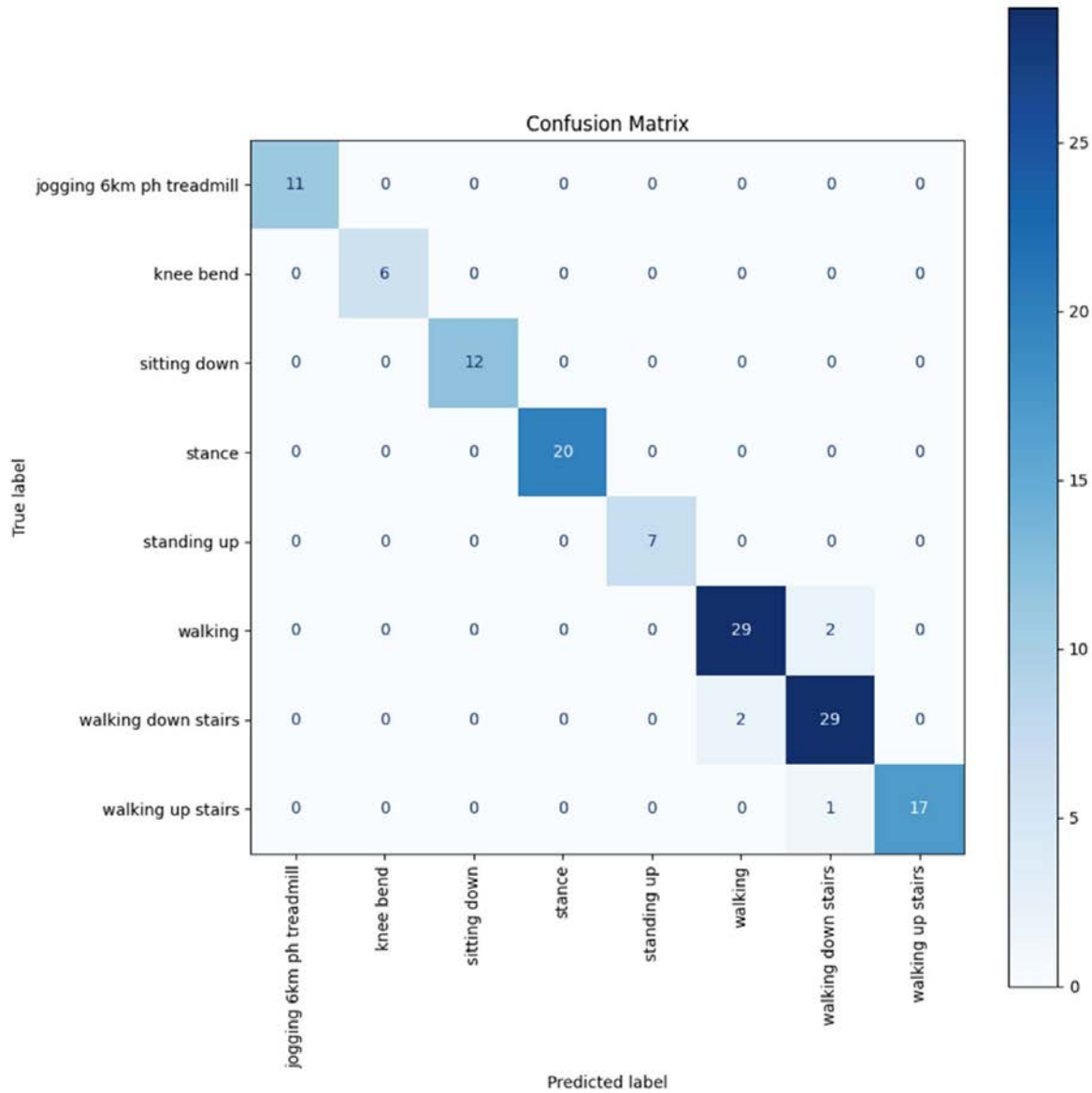


Figure 1. Model performance confusion matrix.

[Figure 1](#)

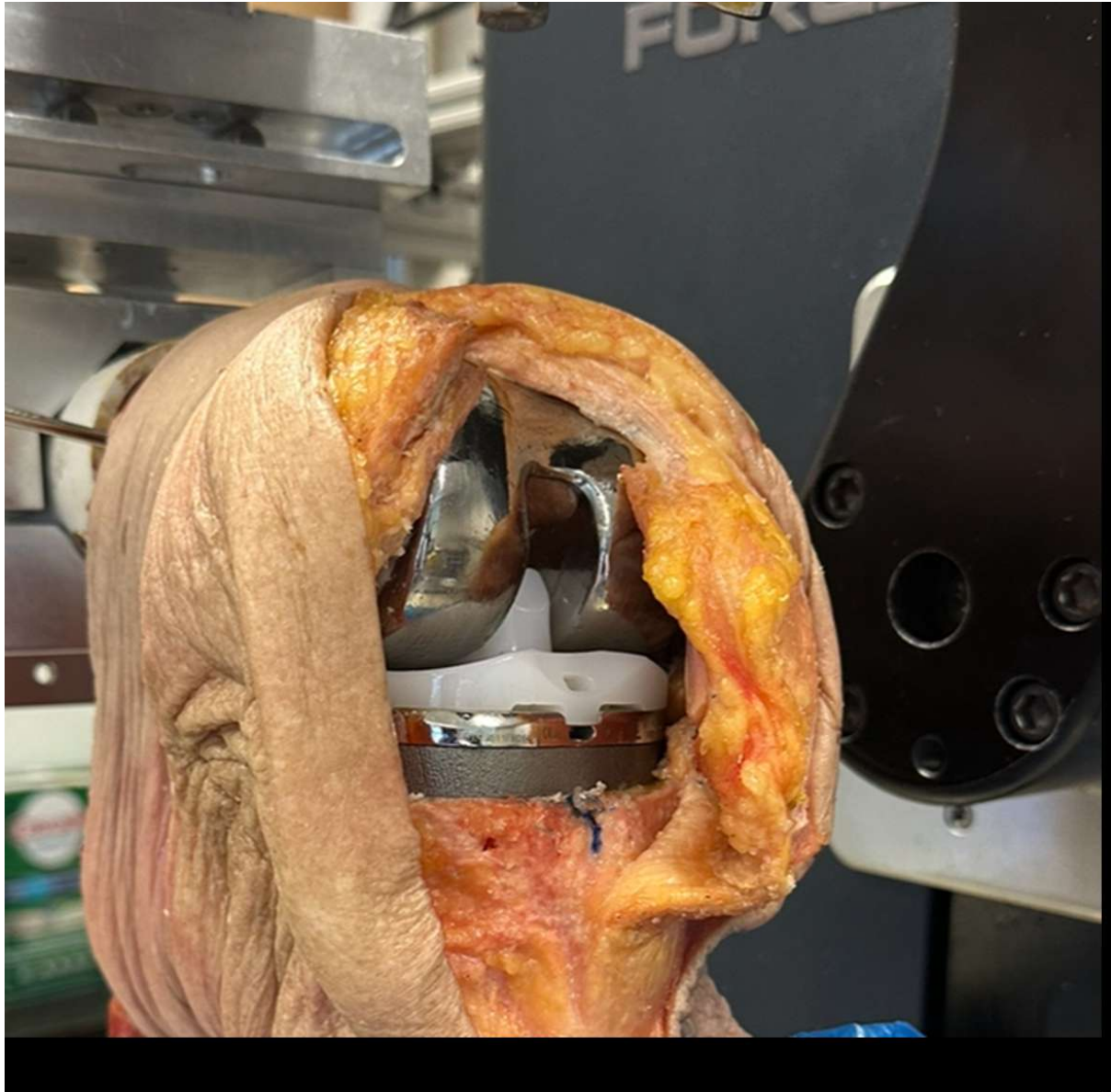


Figure 2. Experimental setup – modified posterior stabilized implant installed in cadaveric knee.

[Figure 2](#)

Development of Physiologically Relevant Loosening Tests: An Expansion of ASTM F2028-17

*[Samuel Perry](#) - University of Leeds - Leeds, GB

Andrew Robert Beadling - University of Leeds - Leeds, United Kingdom

Michael Bryant - University of Birmingham - Birmingham, United Kingdom

Imran Khan - Zimmer Biomet Inc - Swindon, United Kingdom

Richard M. Hall - University of Birmingham - Birmingham, United Kingdom

Saurabh Lal - Zimmer Biomet - Swindon, United Kingdom

INTRODUCTION: The number of primary shoulder arthroplasty procedures performed in England, Wales, and Northern Ireland increased from 3,880 in 2013, to 7,655 in 2019 [1]. However, while total shoulder replacements (TSRs) have been clinically successful, TSR revision rates remain higher than those for hips and knees [1,2]. ASTM F2028-17 was developed to standardise testing surrounding glenoid fixation and component loosening, a common failure mechanism with TSR; however, ASTM F2028-17 allows for a wide range of testing set-ups and input parameters. Furthermore, ASTM F2028-17 itself states that the axial force it suggests is significantly lower than those experienced in-vivo. The project aim was to develop an experimental framework that can account for significant limitations in the current gold standard for glenoid-loosening testing.

METHOD: A literature search surrounding in-vitro glenoid-loosening testing was conducted on MEDLINE to review the state of the art, yielding 137 results. Only in-vitro glenoid fixation studies were included with finite-element modelling studies excluded. The search output 37 relevant results, with 24 using a methodology comparable to ASTM F2028. Due to the flexibility of ASTM F2028-17, methodologies exhibited notable variations in loads, micro-motion measurements, and kinematics. Rarely was fixation assessed in bi-axially throughout cyclic loading, and loading parameters during post-test fixation tests varied from 50N to 350N [3]. Lubrication was scarcely utilised, but some methods maintained temperatures with air streams [4]. Test lengths were varied between 1,000 and 100,000 cycles, predominantly run at 0.5Hz. Methods lacked physiologically relevant loading and focused on sinusoidal kinematics.

RESULTS: A biomechanical framework was developed using a ProSim electro-mechanical single-station universal joint simulator (Simulation Solutions, UK), allowing advanced glenosphere baseplate fixation testing under ASTM F2028-17. The framework enables temperature-controlled lubrication alongside continuous micro-motion data collection. Four non-contact differential variable reluctance transducers (MicroStrain, USA) are anchored to the bone substitute, allowing analysis of baseplate tilt, and baseplate rotation or transverse fixation with a repeatability of $\pm 2\mu\text{m}$. The framework allows for complex, physiologically relevant testing. Publicly available motion captured data has been adapted for use on the universal simulator, allowing for the direct comparison between ASTM F2028-17 and activities of daily living (ADLs) on the loosening of glenoid components. The simulator is capable of providing 80° of internal/external rotation, 180° of flexion, and 45° of abduction. Furthermore, the fixtures allow for components adjusted such that flexion aligns with the dominant plane of elevation in any given profile. Up to 12KN of axial load, and $\pm 1.5\text{KN}$ in both transverse axes can be applied.

CONCLUSION: The developed framework will allow for both the replication of ASTM F2028-17 under ideal conditions, as well as novel testing under physiologically relevant loads and kinematics. Direct comparisons between the outputs obtained from ASTM F2028-17 and different ADLs will allow us to assess the efficacy of ASTM F2028-17 in imitating relevant loosening mechanisms. Furthermore, the impact of different ADLs on component loosening can be assessed.

REFERENCES: [1] National Joint Registry., 2023; [2] Chang et al., BJJ 2020; [3] Irlenbusch and Kohurt, Orthop Traumatol Surg Res 2015; Roche et al., JSES 2019

Figures



Figure 1: Rendering of the apparatus. The superior rockers can be orientated with respect to the component to apply flexion and abduction in the ideal plane. The inferior plate rotates to apply axial rotation.



Figure 2: A render showing a closeup of the fixtures. Micromotion fixtures are attached to bone substitute, and lubricant can be circulated through polymer components. An angled component allows for the glenoid version angle to be altered.

[Figure 2](#)

Novel Robotic Test Method to Compare Knee Stability With Different Prosthesis Designs

*Sander Holthof - Imperial College London - London, GB

Angela Brevio - Città Studi Hospital - Milan, Italy

Andrew Amis - Imperial College of London - London, UK

David Barrett

Michael Rock - DePuy Synthes Joint Reconstruction - Leeds, United Kingdom

Introduction

Instability after TKA is still a cause of patient dissatisfaction, affecting up to 22% of patients. Patient factors, implant design and surgical technique can contribute to instability. This study aimed to measure the effect of implant design on knee stability in a cadaveric setting, whilst minimizing effects of surgical technique and patient factors.

Method

8 fresh-frozen cadaveric knees were tested using a 6-DOF robotic arm, controlled by the simVITRO software. Skin and soft tissues were resected and the femur and tibia were potted into steel pots using polymethylmethacrylate. The tibial pot was attached to the robotic end effector and the femoral pot to a rigid base. The native knee was then flexed-extended from 0-90° flexion under 50N compressive force to find the 'passive flexion' arc and under 710N compressive force to find the loaded flexion arc, while minimizing secondary forces and moments. The following tibial loads were then added sequentially to the 710N tibial axial force: 90N anterior/posterior tibial force, 5Nm internal/external torque, 8Nm varus/valgus torque and the knee was flexed-extended again. Kinematics were measured in a trans-epicondylar axis system. A PCL-retaining TKA was carried. Three implant designs: Medially stabilised gradually reducing femoral radius (MSGrR), medially congruent multi radius (MCMR) and low conforming single radius (LCSR), internally modified to have the same bone-cuts, were then tested in each knee using the same loading conditions.

Results

Stability was defined as the difference from the loaded neutral path of flexion or extension when an external tibial load was applied.

Differences in AP stability were found between implanted knees and the intact knee, and also among the implanted knees, throughout flexion/extension (figures 1 and 2; Table 1). Results are reported prior to statistical analysis for N=6 as testing is ongoing.

Conclusion

The novel testing technique allowed direct comparison of three different implant designs within a loaded cadaveric knee, under continuous flexion and using force control. The test showed differences in AP stability between intact knees and the implants, especially in deeper flexion. Robotic testing can compare stability across the arc of loaded knee flexion with multiple implant designs in cadaveric tests. The differences between the implanted knee stabilities replicated those reported previously (Holthof et al, ISTA 2023) for tests of the isolated TKR components under the robotic continuous flexion/loading regime.

Figures

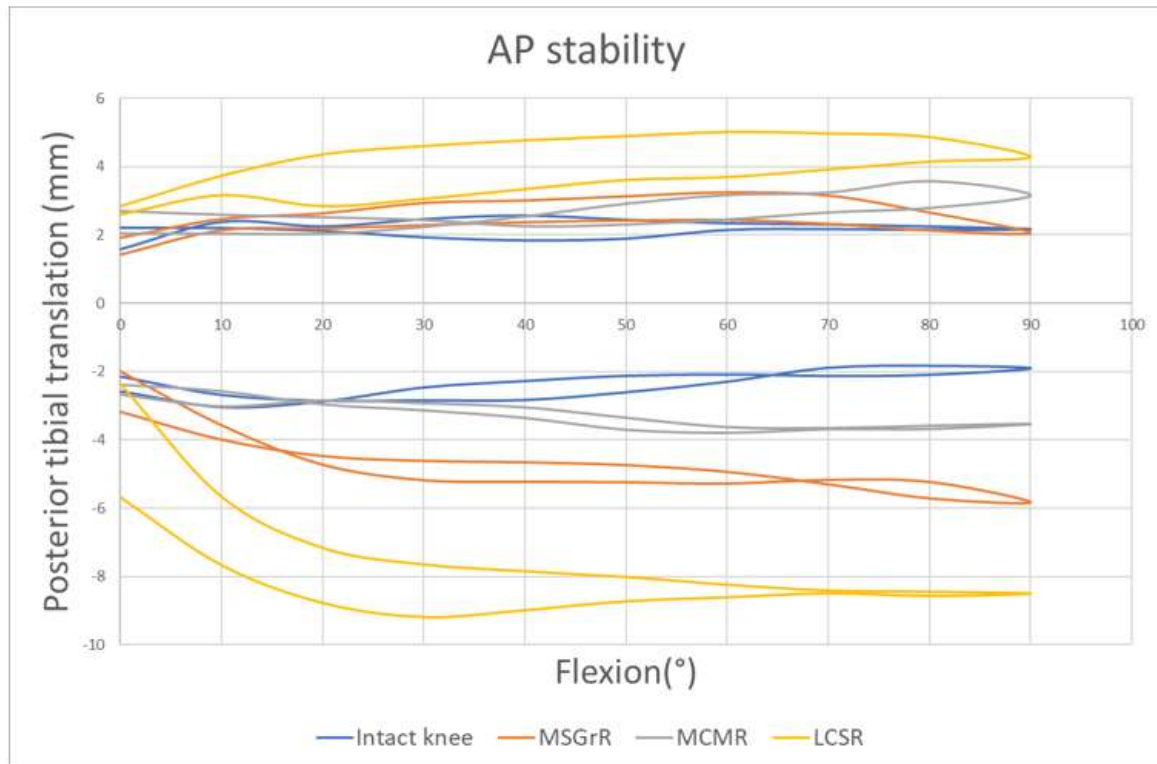


Figure 1: Mean AP stability for the intact knee and with each of the implants when flexing and extending (N=6). The low-constraint LCSR design shows greater hysteresis between flexing and extending motions due to tractive rolling.

[Figure 1](#)

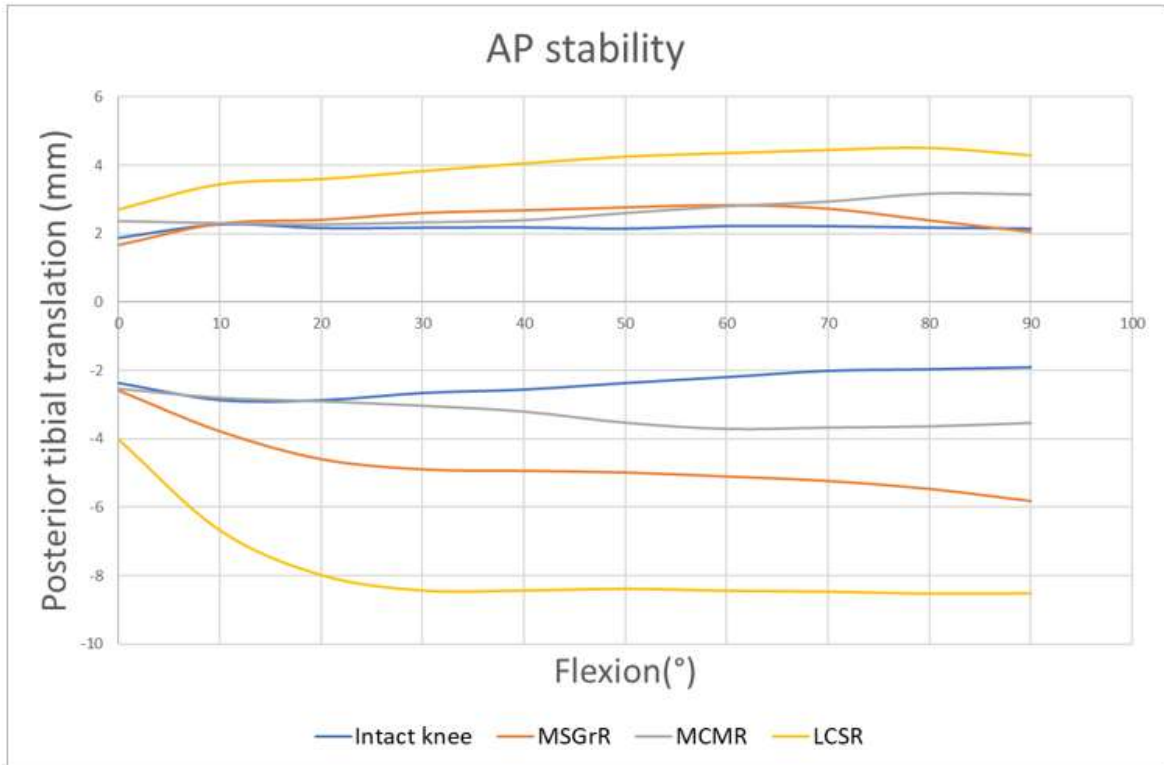


Figure 2: Average AP stability throughout flexion/extension, showing the means between the data for flexion and extension to eliminate tractive rolling effects (N=6). The replaced knee tended to be less stable than the native state in anterior tibial translation (increased femoral roll-back) as the knee flexed.

Figure 2

Implant tested	Anterior stability (mm)		Posterior stability (mm)	
	min	max	min	max
Intact knee	1.8	3.0	1.8	2.5
MSGrR	2.0	5.8	1.9	3.2
MCMR	2.4	3.8	2.0	3.6
LCSR	2.4	9.2	2.5	5.0

Table 1: AP stability throughout flexion for the intact knee and implants (N=6)

Figure 3

Cement Adhesion Testing IBED TiN Coating vs. Uncoated Ti6Al4V

*Jennifer Diederich - Total Joint Orthopedics - Salt Lake City, USA

Anna Sullivan - Total Joint Orthopedics - Salt Lake City, USA

Mike Rizk - Total Joint Orthopedics, Stratford Avenue South, Salt Lake City, UT - Salt Lake City, USA

Chris Weaber - TJO Inc. - Salt Lake City, USA

Carl Yelp - Total Joint Orthopedics - Salt Lake City, USA

Introduction: PMMA bone cement is commonly used in TKA and THA applications. The TJO Klassic Femur with Aurum, made from a Ti6Al4V substrate with IBED TiN coating, is used for cemented CR TKA applications. There is little to no available research surrounding the effect of various coatings and surface treatments on cement adhesion. The purpose of this study was to determine if IBED TiN coating influences cement adhesion.

Methods: Coupons were manufactured out of Ti6Al4V per ASTM F136 to match the cement pocket geometry and surface finish of the Aurum Femur. 10 pairs (20 coupons) were coated with IBED TiN and 10 pairs (20 coupons) remained uncoated. Palacos (Heraeus) PMMA bone cement was used following the manufacturer's instructions and mixed under a vacuum with a Zimmer cement mixing bowl. The coupons were split into two cement batches with 5 pairs of coated and uncoated coupons in each batch. Fixtures were manufactured to hold the coupons in place and compress them to their matching pair. The cement was cured overnight prior to tensile tests performed using a 5969 Instron with load rate of 0.25cm/min, with a test considered successful when the bonded coupons separated along the cement/coupon interface and maximum load recorded, see Figure 1.

Results: All 20 coupon pairs broke along a cement/coupon boundary, and it was random whether the cement adhered to the top or bottom coupon in the Instron jaws, see Figure 1. The results were consistent within cement Batch 1 with an average force of IBED TiN coated coupons slightly higher than that of the uncoated coupons (5kN vs 3.3kN). The results were not consistent within cement Batch 2. The average force of the IBED TiN coated coupons was 14kN compared to 1.30kN with the uncoated coupons, see Figure 2.

Conclusions: The IBED TiN coated coupons were shown to require higher tensile forces to separate the cement from the coupon than the uncoated coupons across the board. The inconsistencies between the two batches of cement could be due to the lack of a replicated OR environment (cement temperature, air temperature, etc.). However, due to the consistently higher tensile forces of the IBED TiN coated coupons for both batches of cement, it is reasonable to conclude that the IBED TiN coating has no negative effects on cement adhesion.



Figure 1. Left: Instron jaw setup. Right: Successful coupon break condition.

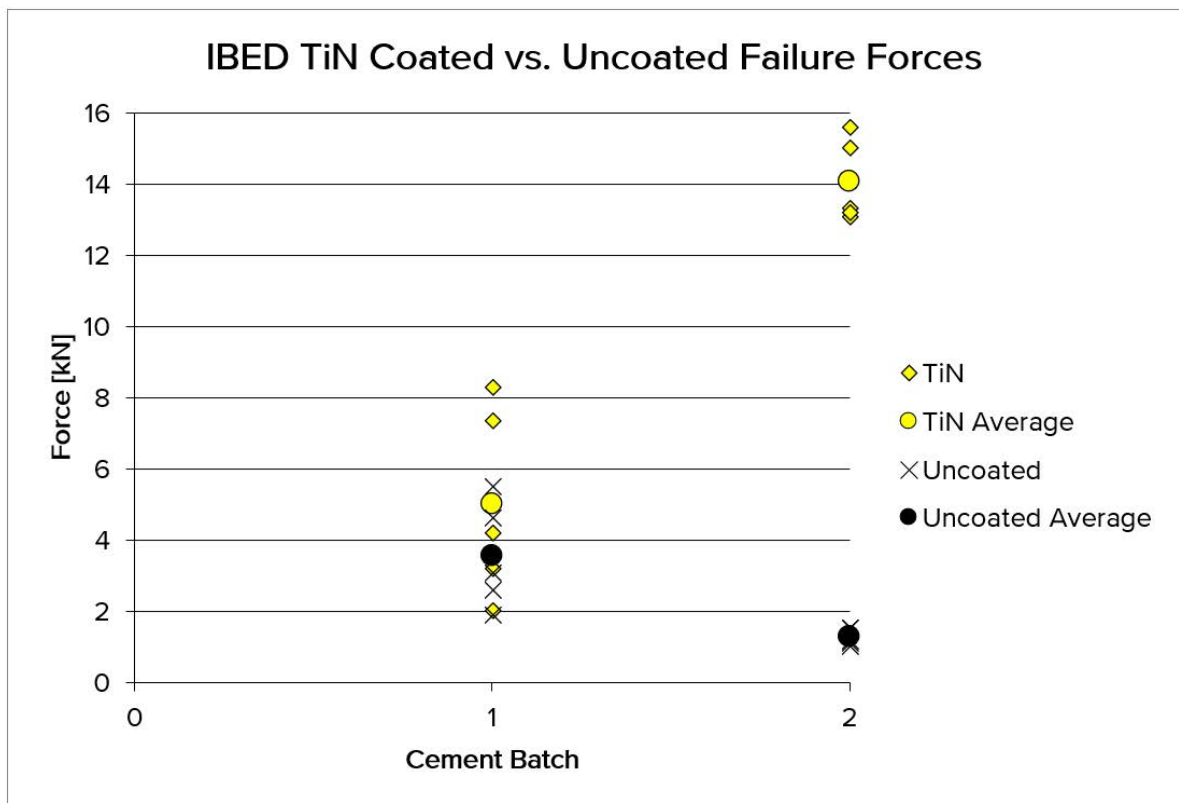


Figure 2. Tension force results.

Delamination Test of a Temporomandibular Joint Made of UHMWPE Fossa and Ti Alloy Mandibular Condyle

*Marcia Maru - Inmetro - Duque De Caxias, Brazil

Rafael Trommer - Inmetro - Duque De Caxias, Brazil

Ricardo dos Santos - Inmetro - Duque de Caxias, Brazil

Davis Machado Larrubia - OSTEOMED S.A. - Rio Claro, Brazil

Introduction

The temporomandibular joint (TMJ) is one of the articulating parts of the human body that can be replaced by an artificial joint, or a joint prosthesis, which is composed by two parts, one convex, the mandibular condyle, made of metal, and another one concave, the fossa, made of polymer.

As any joint that employs polymer, the durability of TMJ prostheses strongly depends on the delamination wear performance of the polymeric part. Delamination wear represents the ultimate failure of the artificial joint.

In this work, we proposed a test procedure for evaluating the delamination performance of a commercial TMJ prosthesis, for preclinical evaluation purpose. A multi-station hip joint simulator was adapted to simulate the sliding movement of the condyle over the polymer surface, under synovial liquid simulated lubrication.

Methods

The angular movement in the abduction-adduction direction of a hip simulator machine (AMTI-Boston) was changed to linear by an especially fabricated adapter, while the internal-external rotation and the flexion-extension movements were kept idle. Mandibular condyle specimens made of titanium alloy were adapted to be clamped in the simulator, to properly run against a flat plate made of UHMWPE (five replicates), which simulated the contacting surface of a fossa.

The main function of the TMJ is to facilitate movements of the lower jaw. This joint allows a range of movements of the lower jaw, namely translational plus rotational movements. The test was focused in simulating the translation of the condyle against the surface of the fossa. The normal load was kept constant to 280 N, and the oscillation frequency was 1 Hz to simulate the mastication up to 175 thousand cycles. Bovine serum was used to simulate the lubrication by synovial fluid in natural TMJ.

The possible occurrence of delamination of the polymeric contacting surface was investigated using optical microscope (Zeiss Axioscope). The wear depth was quantified by 3D profilometry (Taylor Hobson PGI830).

Results

The applied sliding movement, contact geometry and normal load did not cause delamination on the UHMWPE polymer (see Figure 1). The wear depth measured after the test was 100 micrometer.

Conclusion

The established test procedure for delamination wear was performed under extreme worst-case condition, provided by the high applied load and strictly sliding friction. It was evidenced that the commercial TMJ prosthesis does not delaminate under such worst-case operation.

Future work is underway, in which tests under more representative mastication loadings are being planned for simulating the wear of the TMJ prosthesis, and, this way, determine the durability of the TMJ prosthesis.

Figures

Delamination wear test of temporomandibular joint (TMJ)

Does the contact between fossa and condyle of TMJ delaminate?

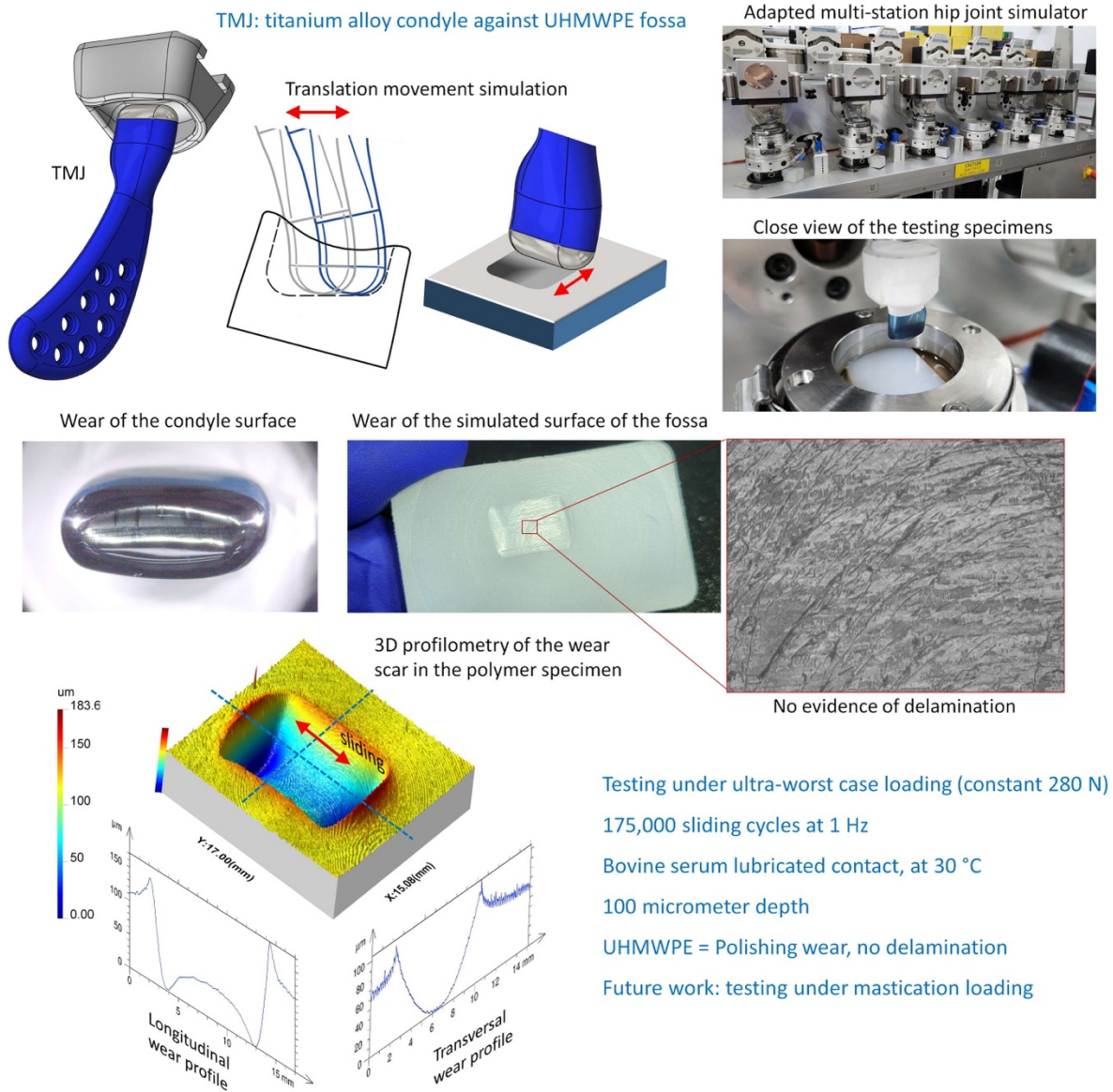


Figure 1

Validation of an Electromechanical Hip Simulator With a Metal-on-Polyethylene Total Hip Replacement

Raelene Cowie - University of Leeds - Leeds, United Kingdom

*Louise M. Jennings - University of Leeds - Leeds, United Kingdom

Introduction

The aim of this study was to compare two Prosim electromechanical simulators (Simulation Solutions, UK) under standard and edge loading conditions. EM13 is a first-generation electromechanical simulator [1,2]; EM16 is a new machine with additional functionality including the ability to introduce medial-lateral and anterior-posterior offsets to the cup. It was hypothesised that there would be no significant difference between UHMWPE wear and dynamic separation of the cup when similar hip replacements were tested on the two simulators.

Methods

Six 36 mm diameter metal-on-polyethylene hip replacements were set up in a 3-station electromechanical hip simulator (EM16). Three hip replacements were set up at 35° inclination angle (equivalent to 45° *in vivo*) and three at 55° inclination angle (equivalent to 65° *in vivo*). The hip replacements were tested using 25% bovine serum with 0.03% sodium azide as a lubricant first under standard conditions (ISO14242-1), then under edge loading conditions (ISO14242-4) as shown in Table 1. For each condition, 2 million cycles wear simulation was carried out. Wear of the UHMWPE liners was assessed gravimetrically every million cycles and the medial-lateral dynamic separation of the cup measured. The wear and dynamic separation of the hip replacements investigated in EM16 were compared to those from a previous generation electromechanical simulator (EM13) [2]. Statistical analysis was carried out using ANOVA with significance taken at $p < 0.05$.

Results

For EM16, the UHMWPE wear rate was higher at high inclination angles and with the introduction of edge loading, consistent with previous studies [2]. Under all conditions, a lower wear rate was measured in EM16 compared to EM13 with smaller 95% confidence intervals despite in some cases there being a smaller sample size (Figure 1). There was however no significant difference in UHMWPE wear rate between the two simulators for any of the conditions of interest ($p > 0.05$) [2]. At 35° inclination, the medial-lateral separation was significantly higher in EM13 compared to EM16 ($p = 0.04$); at 55° inclination, the separation was higher in EM16 compared to EM13 ($p < 0.001$), Figure 2 [2].

Conclusion

There were no significant differences in UHMWPE wear rates produced by the two simulators. There were however, significant differences in the dynamic separation of the hip replacements when tested under edge loading conditions thought to be influenced by variations in the medial-lateral spring rates and the weight of the assembly used to introduce medial-lateral and anterior-posterior offsets. This study highlights the importance of validation of new simulators.

1. Ali, M., et al, 2016. *JOEIM*, 230(5),pp.389-397.
2. Ali, M., et al, 2023. *Biotribology*, 33,p.100238.

Figures

Table 1: Input conditions, sample size and test duration for the two studies. EM16 was used in this study, the data from which is compared to a previous investigation in EM13 [2].

Simulator	Conditions	Spring rate (N/mm)	Medial-lateral offset (mm)	Sample size	Test duration (million cycles)
EM16	Standard		Concentric	N=3	2
	Edge loading	52	4	N=3	2
EM13	Standard		Concentric	N=3	2
	Edge loading	84	4	N=6	3

Figure 1

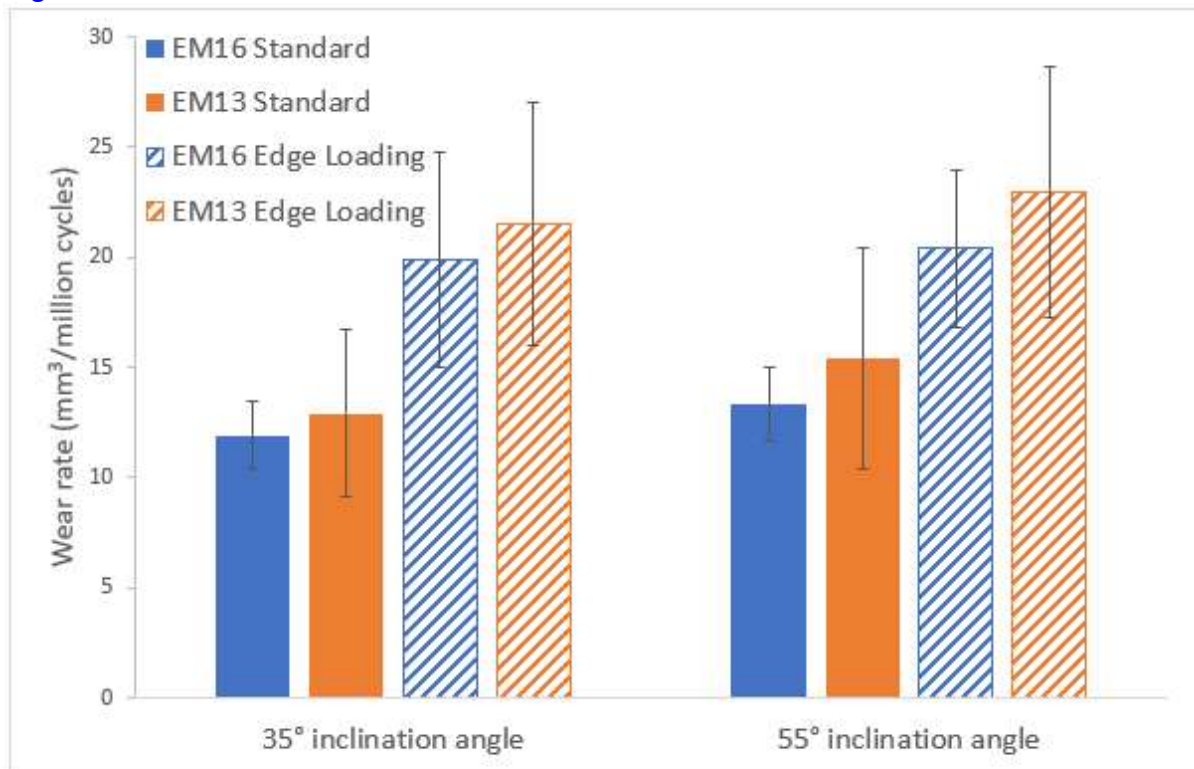


Figure 1: Mean wear rate (mm³/million cycles) ± 95% confidence limits of UHMWPE liners tested in EM16 with comparison to a previous study in EM13 [2].

Figure 2

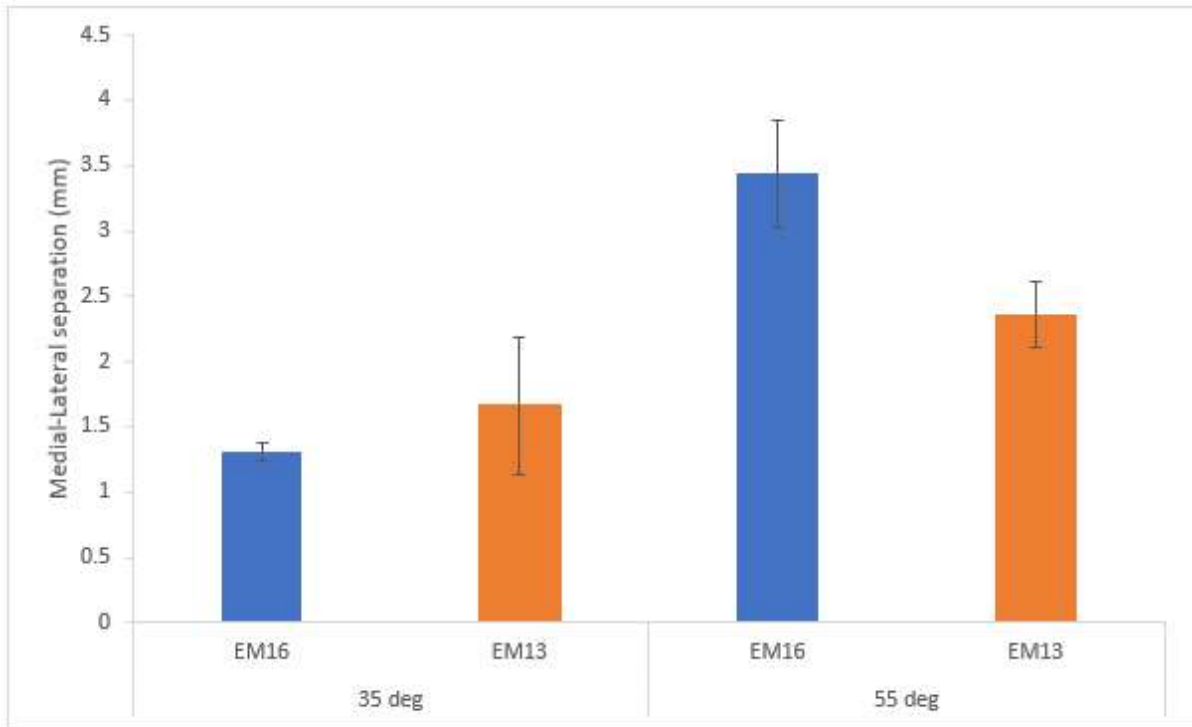


Figure 2: Mean medial-lateral separation of the cup (mm) \pm 95% confidence limits tested in EM16 with comparison to a previous study in EM13 [2].

[Figure 3](#)

Biomechanical Comparison of Two Extensor Mechanism Reconstruction Techniques

John Moon - University of Texas Health Science Center at Houston - Bellare, USA
Camryn Pletka - University of Texas Health Science Center at Houston - Bellaire, USA

*Hugh Jones - UT Health Science Center at Houston - Houston, USA

Shuyang Han - University of Texas Health Science Center at Houston - Houston, USA

Jonathan E. Gold - UTHealth - Houston, USA

Sabir K. Ismaili - UTHealth - Houston, USA

David Rodriguez - University of Texas - Houston, USA

Background

Extensor mechanism disruption is a devastating complication which can occur following total knee arthroplasty. Two methods of docking synthetic mesh in the tibia for extensor reconstruction are described in the literature but have not been compared. The purpose of this study was to evaluate and compare trough and intramedullary techniques of implanting mesh in a cadaveric model.

Methods

Synthetic mesh constructs were implanted using two techniques. A polypropylene mesh sheet (Marlex 26cm x 36cm) was folded in the longitudinal direction upon itself eight times and secured with a running locking stitch. Bone cuts were made to receive a tibial component on six matched pair of fresh frozen human tibiae.

Tuberosity trough technique

After cementing the tibial component, a 30mm x 15mm window was burred above the tuberosity. Cement was applied to the mesh construct and into the trough before seating the mesh within the cavity. After curing, a bicortical screw was passed obliquely through the construct.

Intramedullary technique

A 5mm x 25mm recess was burred through the anterior cortical rim. The mesh was inserted anteriorly into the medullary canal in line with the tibial crest, followed by a cemented tibial component with the keel posterior to the mesh.

Biomechanical testing

A modified materials testing machine (MTS) was used to apply tensile loads to the reconstruction while applying joint reaction forces. An auxiliary apparatus was constructed having a pneumatically controlled base that moved in the vertical direction. The tibia was mounted to the apparatus and a femoral component was mounted to the base. The base was loaded to apply a one body-weight joint reaction force. The proximal mesh was fed through a buckle clamp at the patellar level and attached to the MTS actuator via a steel cable and pulley system.

Passive reflective marker arrays were attached near the tibia insertion site, to the buckle clamp, and to the tibial base plate. A six-camera motion analysis system was used to track the displacement of the markers during testing.

Upon testing, each tibia was subjected to 25 cycles of preconditioning loads (650N) after which the specimens were loaded to failure.

Results

There were significant differences between the two surgical techniques. The stiffness of the tuberosity insertion method averaged 36.2 N/mm \pm 13.0. The under the tray technique was more stiff at 101.3 N/mm \pm 11.6 ($p=0.048$). The yield force for the

tuberosity and under the implant method was $510.8\text{N} \pm 87.3$ and $727\text{N} \pm 11.0$ ($p=0.087$) respectively. A large ultimate force to failure difference was found between the trough method ($698.6\text{N} \pm 90.8$) and the intramedullary method ($1132.7\text{N} \pm 36.3$) ($p=0.006$). Failure of the tuberosity method predominately occurred at the mesh insertion site whereas failure of the intramedullary technique was midway between the insertion and patellar buckle clamp. No measurable base plate lift-off was seen.

Conclusion

This study shows there is a biomechanical advantage to implanting under the tibial baseplate, with higher stiffness, yield force, and ultimate load to failure. Our model doesn't incorporate soft tissue/mesh ingrowth, it does compare insertion techniques where ingrowth has minimal effects.

Figures

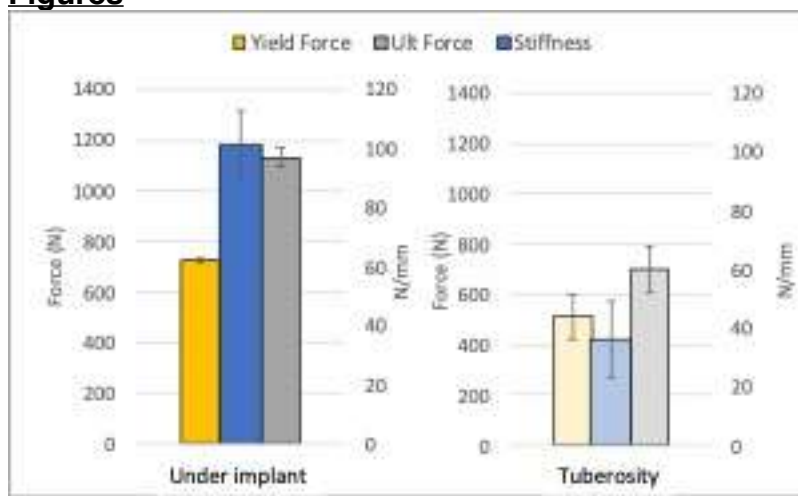


Figure 1



[Figure 2](#)

Do Cement Pockets Prevent Fluid Contamination of the Undersurface of Tibial Baseplates?

*Aleksander Mika - Vanderbilt Orthopedics

Bryce Biberstein - Vanderbilt - Nashville, USA

Jacob Wilson - Vanderbilt - Nashville, USA

John Ryan Martin - Vanderbilt Health - Hendersonville, USA

Hillary Mulvey - Vanderbilt - Nashville, USA

Introduction: Aseptic loosening remains one of the most frequent causes of implant failure following primary total knee arthroplasty (TKA). Prior literature has established that loosening often occurs at the implant-cement interface—likely secondary to lipid contamination. Some implant manufactures have incorporated cement pockets on the undersurface of tibial implants in order to improve fixation. The purpose of this study was to determine the impact of cement pockets on lipid contamination of the implant-cement interface.

Methods: Two contemporary tibial baseplates which have tibial cement pockets were utilized to create clear acrylic tibial base plate molds. For both implants, we created a version with and without cement pockets. These models were then used for an experimental cementing process after which, the degree of baseplate fluid contamination at the implant-cement interface was quantified. This was calculated as a percentage of the total baseplate surface area. .

Results: For implant A, the average percent surface area contamination was not significantly different with and without cement pockets, respectively (29.26% vs 29.63%, ($p=0.43$)). Similarly, for implant B, the average percent surface area contamination was not statistically significantly different with and without cement pockets, respectively (42.82% vs 30.36%, ($p=0.16$)).

Discussion: Lipid contamination of the implant-cement interface remains a primary mechanism of implant failure following primary TKA. We found that the addition of cement pockets does not decrease the percentage of implant fluid contamination. While these cement pockets may improve implant fixation, they do not reduce fluid/lipid contamination and alternative undersurface geometries and techniques should be considered to help limit lipid contamination.

Joint Reaction Forces on the Humerus: What Do We Know?

*Niloufar Shekouhi - Zimmer Biomet - Warsaw, United States of America

Christine Mueri - Zimmer Biomet - Winterthur, Switzerland

Philippe Favre - Zimmer Biomet - Winterthur, Switzerland

Jeffrey Bischoff - Zimmer, Inc. - Warsaw, USA

Introduction

Understanding glenohumeral joint reaction forces (GHF) is pivotal for shoulder implant testing, however, no consensus exists on loads to apply in anatomical/reverse conditions. This study aimed to review the literature on GHF in anatomic and reverse shoulder arthroplasty (RSA) during isolated motion and activities of daily living (ADL), reported by means of *in-vivo* measurements, musculoskeletal modeling (MSM) or cadaveric experiments.

Methods

A literature search was conducted in PubMed using “Humerus”, “Glenoid”, “Glenohumeral” or “Shoulder” with “joint forces” or “contact” and “activity of daily living”. Titles/abstracts were reviewed, excluding articles not relevant to shoulder biomechanics, not analyzing GHF (magnitude/direction), letters to editor, or focusing on patients with special needs (e.g., wheelchair propulsion).

Results

Anatomical GHF

Peak *in-vivo* GHF in unloaded abduction and forward flexion for a) angles of $\leq 90^\circ$ ranged from 51%-87% BW, aligning with MSM predictions (37%-102% BW), and b) beyond 90° , ranged from 65%-121% BW, demonstrating consistency with MSM/cadaver studies (30%-102% BW). *In-vivo* measurements for loaded abduction and forward flexion increased the GHF to 129%BW and 123%BW respectively.

Typical ADLs (e.g. combing, reaching) resulted in low GHF (up to 76% BW). Higher GHFs were observed in lifting weights (up to 130% BW) and sitting/standing using arms (up to 180% BW). Although a good agreement was observed between *in-vivo* measurements and MSM for isolated motions, MSM overestimated the GHFs during complex ADL relative to *in-vivo* measurements.

Reverse GHF

No *in-vivo* RSA measurements of GHF exist to date; GHF values come exclusively from MSM or cadaveric experiments.

For isolated motions, RSA reduced GHF by 20%-52% compared to anatomic. The presence of rotator cuff tears influenced the magnitude/direction of GHF. During ADL, peak GHFs ranged between 37%-90% BW. The limited data available on direction of GHFs acting on humerus suggest a load parallel to the humeral shaft (Table 1).

Conclusion

Understanding *in-vivo* loading conditions during ADL is essential for pre-clinical evaluation and improving implant design. GHFs in anatomic shoulder vary in magnitude and are highly dependent on elevation angle, speed of motion, and external load. However, the direction of the load is relatively consistent. Compared to anatomic, contemporary RSA reduced GHFs by 20%-52% during isolated motion; however limited data are available on the force magnitude/direction especially in ADL. Given the complexities associated with implant design, changes in the center of rotation due to humeral/glenoid lateralization, and rotator cuff

deficiencies, using anatomical loading for reverse implant testing may not be applicable.

Figures

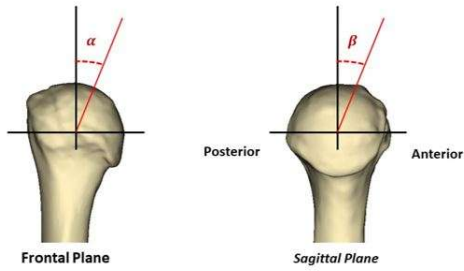


Figure 1. Typical examples of force directions acting on the humerus. α -angle shows the orientation of the peak GHF in the coronal plane, and β -angle shows the orientation in the sagittal plane.

Table 1. Ranges of load direction with respect to the humerus axis, acting on the humerus

Shoulder Arthroplasty Type	Activity	Ranges of load direction in the frontal plane (α -Angle)	Ranges of load direction in the sagittal plane (β -Angle)
Anatomic	Isolated motion	~30° on average	~20° on average
	ADL	26 – 40° on average	5 – 17° on average
Reverse	Isolated motion	Angle decreases as the rotator cuff deficiency increases (~0° with full tear)	Not available
	ADL	Not available	

Figure 1

Testing of Directly Applied Coating on Ceramic Substrates for Use in Acetabular Components.

*Danielle De Villiers - MatOrtho Ltd - Leatherhead, United Kingdom

Simon Collins - MatOrtho Limited - Leatherhead, United Kingdom

Introduction

State of the Art modular total hip replacement (THR) cups incorporate a metal outer shell typically coated in Titanium (Ti) and/or Hydroxyapatite (HA) and generally have both polyethylene and ceramic bearing options. This dual material design results in a thicker construct than necessary thus resulting in more acetabular bone being removed than needed or limiting the head diameter used. Applying a biocompatible fixation coating directly to the ceramic addresses this as the wall thickness can be substantially reduced. This direct-to-bone biocoating technology is novel and requires testing to indicate its safety and clinical performance. This study assesses the stability of such a Ti/HA coating applied to a ceramic substrate.

Methods

Bilox delta ceramic cups and discs were manufactured using usual processes. These were prepared and coated with either a Ti coating or a bi-layer Ti-HA coating applied by plasma spraying. Static tensile and static and dynamic shear tests according to ASTMs F1147, F1044, and F1160 and ISO 13779-4 were conducted on the coated discs. The cups coated with Ti-HA were subjected to pull-off adhesion tests (PAT) on both unaged and aged (134°C for 10 hours) cups. Additionally, a torsional test was developed bonding the head and cup and applying torsional loading until failure in three cups.

Results

The Ti and Ti-HA coatings on ceramics exceeded the 22 MPa criterion for static adhesion and the 20 and 15MPa criterion for static shear strength set out by the ASTM and ISO standards. In most cases, the results were double or triple this requirement. PAT testing on the cup also indicated strong adhesion of the coating with values over 50MPa ranging up to 76MPa and no change in adhesion following the equivalent of 10 years aging. Torsional testing recorded failure at the cement interface ranging from 35 to 102.5Nm.

Conclusions

Although the ASTMs test methods have been established for metal substrates, these methodologies can be used for direct coating on ceramics. These coatings have been shown to be stable and represent a potential use in other total hip replacement and hip resurfacing allowing for larger diameter bearings to be used for a given outer cup diameter. Early clinical data of over 1,000 of these cups is promising but long-term clinical data and monitoring is required to determine the clinical success *in vivo*.

Figures



[Figure 1](#)

Table 1: Static adhesion and static and dynamic shear results for the Ti and Ti-HA coating

Test	Ti Only	Ti-HA
Static adhesion tensile	64.5 +/- 5.4	28.5 +/- 1.1
Static adhesion shear	51.3 +/- 1.1	29.3 +/- 7.4
Dynamic adhesion shear	Survived 10 million cycles under 10MPa	Survived 10 million cycles under 10MPa

[Figure 2](#)

Impact of the Individual Femoral Degree of Freedom on the Restoration of the Trochlea - a Sensitivity Analysis

Prudhvi Tej Chinimilli - Exactech - Gainesville, USA

Leonard Duporte - Hopital Lapeyronie - Montpellier, France

Faustine Nogaret - Lapeyronie University Hospital of Montpellier - Montpellier, France

Scott Gulbransen - Exactech - Gainesville, USA

Gerard Giordano - Hopital Joseph Ducuing - Toulouse, France

Louis Dagneaux - Hopital Lapeyronie, Universit  de Montpellier - Montpellier, France

*Laurent Angibaud - Exactech, Inc. - Gainesville, USA

INTRODUCTION

Alignment philosophy in total knee arthroplasty (TKA) continues to be debated. A common ground about these different techniques relates to their focus on the femorotibial joint, at the potential detriment of the patellofemoral joint. The latest alignment techniques encompass the possibility of individually adjusting each of the six degrees of freedom (DOF) directly associated with the femorotibial joint. In this regard, this experimental study aimed to evaluate the individual impact of each femoral DOF on the position of the femoral component trochlea relative to the native trochlea.

METHODS

Four TKAs were performed using an enabling technology on four cadaveric specimens. During the TKA procedure, the native femoral trochlea was identified by the senior surgeon and then mapped by probing the identified surface. Similarly, after TKA implantation, the femoral component was mapped by probing. Subsequently, the cloud of points of the native trochlea and the femoral component were exported to a computer-aided design software and mesh surfaces were generated. Transversal cross sections of interest were established to characterize the anteroposterior (AP) and mediolateral (ML) offsets between the native trochlea and the prosthetic trochlea. From its neutral position (i.e., implanted position), the femoral component was digitally translated/rotated along/around each DOF by 2mm/  increment. For each of the simulated position/orientation, the AP and ML offsets were measured (Figure 1) and the impact of each DOF on these offsets was evaluated by assessing the sensitivity factor (SF) defined as the magnitude (i.e., absolute value of the slope) of the linear regression between the increment value and its impact on the offsets (Figure 2).

RESULTS

Regardless of the specimen, the DOF, and the offset, the R-squared values of each linear regression were consistently above 0.93, demonstrating the linear impact of each DOF on the offsets. As expected, both the AP and the ML translation DOFs had a direct impact on the AP offset and the ML offset, respectively, as demonstrated by an SF close or equal to 1. Both the flexion/extension and axial translation DOFs had a moderate impact on the AP offset, while the varus/valgus and axial rotation DOFs had minimal impact on the ML offset. The other SFs were negligible as being systematically below 0.1. The impact signature of each DOF was consistent (i.e., $SD < 0.11$) among the four specimens (Figure 3).

DISCUSSION

During TKA implantation, the impact of each femoral DOF on the restoration of the trochlea is unique and surgeons should be aware of this finding. For example, while it can be recommended to flex the femoral component to close the flexion gap, such change impacts the AP position of the prosthetic trochlea. In addition to the offset, further studies should encompass the impact of the DOFs on the angular orientation of the trochlea. There exists an opportunity for enabling technology to feature insights regarding the management of the patellofemoral joint in addition to the femorotibial joint.

Figures

Figure 1: Impact of the flexion/extension DOF on the AP and ML offsets for TKA #1; where the femoral component was incrementally rotated by -4° , -2° , $+2^\circ$, and $+4^\circ$ of flexion relative to the neutral position.

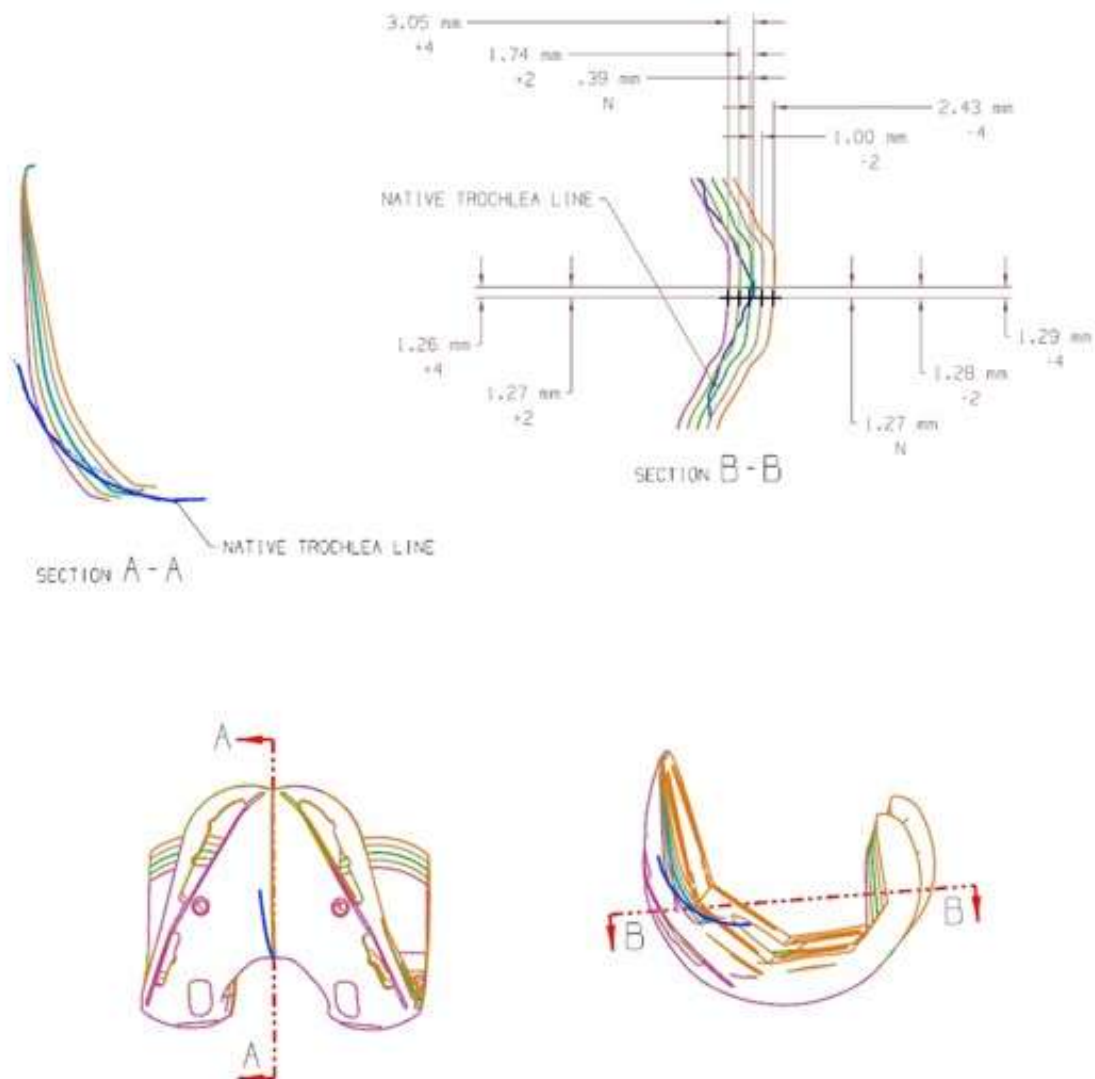


Figure1

Figure 2: Evaluation of the SF defined as the magnitude (i.e., absolute value of the slope) of the linear regression for each DOF for TKA#1

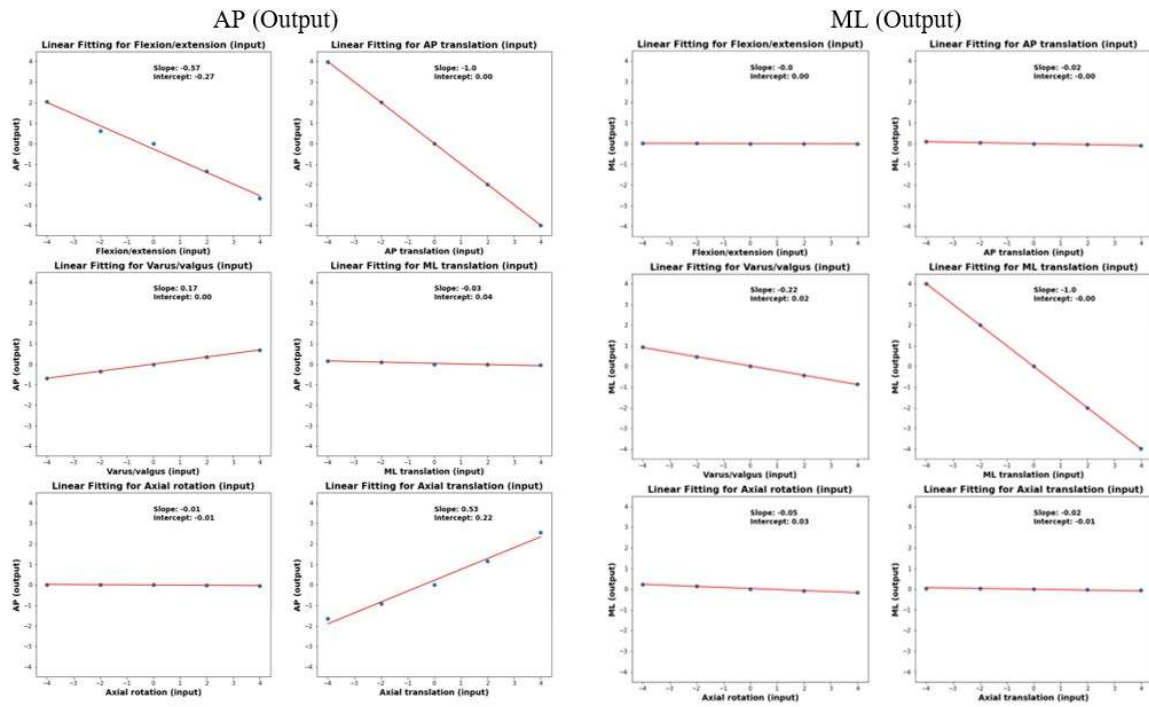


Figure2

Figure 3: Definition of the SF for each specimen and each DOF

DOF (Input)	SF for TKA#1		SF for TKA#2		SF for TKA#3		SF for TKA#4		Mean SF ± D	
	AP	ML	AP	ML	AP	ML	AP	ML	AP	ML
Flexion/extension	0.57	0	0.63	0.06	0.60	0.06	0.63	0.06	0.61 ± 0.03	0.05 ± 0.03
Varus/valgus	0.17	0.22	0.02	0.16	0.05	0.30	0.07	0.30	0.08 ± 0.06	0.25 ± 0.06
Axial rotation	0.01	0.05	0.03	0.12	0.05	0.22	0.07	0.33	0.04 ± 0.02	0.18 ± 0.11
AP translation	1	0.02	1	0.10	0.94	0.05	0.91	0.11	0.96 ± 0.04	0.07 ± 0.04
ML translation	0.03	1	0.05	1	0.11	0.99	0.13	0.99	0.08 ± 0.04	1 ± 0
Axial translation	0.53	0.02	0.44	0.04	0.49	0.03	0.55	0.16	0.50 ± 0.04	0.06 ± 0.06

Figure 3

Correlating Patient Reported Outcomes to External Peak Knee Adduction Moments and Surgical Techniques During Stair Descent

Alexis Nelson - UTHSC - Memphis, Select Country

Nuanqiu Hou - Campbell Clinic - Memphis, United States of America

Douglas Powell - University of Memphis - Memphis, USA

Marcus Ford - Campbell Clinic Orthopaedics - Germantown, USA

James Guyton - Campbell Clinic Orthopaedics - Germantown, USA

John Crockarell - Campbell Clinic Orthopaedics - Germantown, USA

Derek Dixon - Campbell Clinic Foundation - Germantown, USA

Teri Ross - University of Tennessee Health Science Center - Memphis, USA

William Mihalko - University of Tennessee - Memphis, USA

*Christopher Holland - Campbell Clinic - Memphis, USA

Disclosure: This study was funded by Medacta International.

Introduction: Patients who underwent kinematically aligned (KA) total knee arthroplasty (TKA) have been shown to have smaller knee adduction moments (KAMs) after surgery in comparison to those who underwent mechanically aligned (MA) TKA (Niki et al., 2018). However, whether the difference in knee joint biomechanics produces different patient reported outcomes (PROs) remain unclear. Our aim was to understand whether PROs correlates to external peak KAMs between MA and KA groups.

Methods: We included 27 patients who received a cruciate retaining Attune implant separated into two surgical alignment technique groups; MA (n=13) and KA (n=14). All patients underwent unilateral TKA and are at least one-year post-op. A three step instrumented staircase (1000Hz, AMTI Inc., Watertown, MA) and an 8-camera markerless motion capture system (200Hz, OptiTrack, NaturalPoint Inc., MA) were used to collect ground reaction forces and segment kinematics, respectively, during stair descent. An AI based reconstruction software (Theia Markerless, Inc., Version 2023, Kingston, ON) was used to identify segment kinematics. Patients completed the Knee Injury and Osteoarthritis Outcome Score for Joint Replacement (KOOS, JR.) and the Forgotten Joint Score-Knee (FJS) at the time of data collection. Visual3D Professional (HAS Motion, Version 2023.09.3, Canada) and MATLAB (The MathWorks, Inc., R2023b, Natick, MA) were used for data analysis. An independent sample t-test was used to compare surgical alignment techniques for external peak KAM, KOOS JR., and FJS scores. A two-way ANOVA was performed to correlate KOOS, JR. and FJS scores to external peak KAM and surgical techniques.

Results: There were no significant differences in age or BMI between MA and KA groups. Patients in both groups had compatible KOOS JR scores ($p=0.459$) and FJS score ($p=0.691$). Peak KAMs observed significant differences where the MA group had greater peak KAMs compared to the KA group to descend the stairs (MA=-0.14, KA=-0.75, $p=0.038$, Figure 1a). No significant differences were observed when correlating KOOS JR. scores ($F=0.436$, $p=0.512$, figure 1a, figure 1b) or FJS scores ($F=0.154$, $p=0.696$, figure 1c, figure 1d) to external peak KAMs and surgical techniques.

Conclusion: We aimed to study the relationship among PROs, knee joint biomechanics, and surgical techniques during stair descent. Significant differences were observed in KAMs during stair descent between MA and KA groups. We did not observe a significant correlation between PROs and surgical alignment techniques. A significant correlation was not observed between PROs and external peak KAM. The

difference in external peak KAMs did not impact PROs. To further our understanding, we will analyze the relationships between PROs and other biomechanical variables and muscle activation patterns.

Reference: Niki Y, Nagura T, Nagai K, Kobayashi S, Harato K. Kinematically aligned total knee arthroplasty reduces knee adduction moment more than mechanically aligned total knee arthroplasty. *Knee Surg Sports Traumatol Arthrosc.* 2018;26(6):1629-1635.

Figures

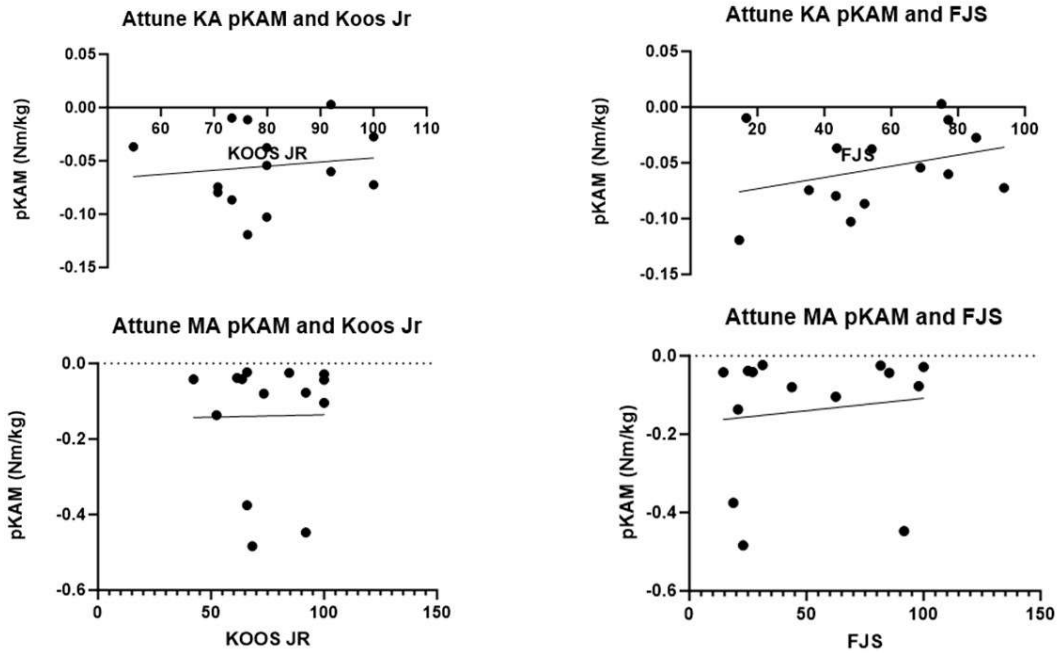


Figure 1

Long-Term Patient-Reported Outcomes of Hip Arthroplasty After Previous Hip Arthroscopy: A Matched Case-Control Study With a Minimum 10-Year Follow-Up

*Benjamin Domb - American Hip Institute - Des Plaines, USA

Roger Quesada-Jimenez - American Hip Institute Research Foundation - Chicago, USA

Elizabeth Walsh - American Hip Institute Research Foundation - Chicago, USA

Drashti Sikligar - American Hip Institute Research Foundation - Chicago, USA

Ady Kahana - American Hip Institute Research Foundation - Chicago, United States of America

Background: Previous hip arthroscopy may influence the outcomes of subsequent total hip arthroplasty (THA). The objective of this study is to perform a long-term comparative analysis between patients who underwent THA with a history of previous ipsilateral hip arthroscopy, compared to a benchmark matched control group.

Methods: Retrospective data was analyzed from patients who underwent primary THA and had a history of ipsilateral hip arthroscopy (THA-PA) between November 2010 and November 2013. Patients included had complete post-operative patient reported outcomes (PRO) and visual analog scale (VAS) pain scale with a minimum 10-year follow-up or reached an endpoint during the study period. Patients were matched in a 1:1 ratio based on body mass index (BMI), sex, use of robotic assistance, approach, and laterality to a benchmark control group of primary THA without previous hip arthroscopic surgery (THA-N-PA). Clinical hip arthroplasty outcome thresholds, complications, and revision surgery rates were compared between cohorts. A Kaplan-Meier analysis was performed to assess survivorship.

Results: 54 patients were included in the study group and were matched to a benchmark control group of THA-N-PA cases. Comparable and sustainable mean values were observed between the two groups at minimum 10-year follow up, for modified Harris hip score (mHHS), Harris hip score (HHS), Hip Disability and osteoarthritis outcomes for joint replacement (HOOSJR), forgotten joint score (FJS), VAS, and patient satisfaction ($p > 0.05$). Both groups reached PASS for FJS, HHS, and HOOS-JR at similar rates ($p > 0.05$). Patients in the study group exhibited a higher complication rate, with a relative risk of 2.8 ($P=0.033$), as well as an elevated risk for revision surgery, with a relative risk of 4.5 ($P=0.047$).

Conclusion: Patients in the THA-PA group showed comparable and sustainable mean values in all PROs, VAS scores, displayed high patient satisfaction, and favorable FJS scores compared to the benchmark control group at long-term follow-up. However, it is crucial to highlight that individuals in the study group exhibited a 2.8-fold increased risk of developing complications and a 4.5-fold higher risk of undergoing revision THA.

Midterm Outcomes of Primary Total Hip Arthroplasty With Simultaneous Gluteus Medius Repair With Nested Comparison

*Benjamin Domb - American Hip Institute - Des Plaines, USA

Roger Quesada-Jimenez - American Hip Institute Research Foundation - Chicago, USA

Yasemin Kingham - American Hip Institute Research Foundation - Chicago, USA

Tyler McCarroll - American Hip Institute Research Foundation - Chicago, USA

Ady Kahana - American Hip Institute Research Foundation - Chicago, United States of America

Background: Gluteus Medius (GM) tears are a recognized cause of pain and disability, with reported rates of approximately 20% in patients undergoing primary total hip arthroplasty (THA). It is established that patients who undergo THA without addressing GM pathology tend to experience inferior patient-reported outcomes (PROs). The aim of this study is to evaluate midterm outcomes in patients who underwent a primary THA with concomitant GM tear repair, as compared to a benchmark control group that did not have GM pathology.

Methods: Data was prospectively collected and retrospectively analyzed from patients who underwent a primary THA with a GM repair between 2015 and 2018. Patients were included if they had pre-operative and minimum five-year questionnaires completed for modified Harris Hip Score (mHHS), Harris Hip Score (HHS), visual analog scale (VAS), Veteran Rand 12-item health survey for physical and mental outcomes (VR-12), 12-item short form survey for physical and mental outcomes (SF-12); the Forgotten Joint Score-12 (FJS-12), Hip Disability, and Osteoarthritis Outcome Score Joint Replacement (HOOS- JR). The GM cohort was matched in a 1:1 ratio based on age at surgery, body mass index (BMI), sex, approach, and laterality to a control group of primary THAs without GM pathology. Thresholds for functional hip outcome were included for the analysis.

Results: 20 patients met the inclusion criteria and had complete pre-operative, intra-operative, and post-operative data. All patients were females. Both groups demonstrated significant and equivalent improvements for all PROs except for VR-12 Mental ($P=0.38$) and SF-12 Mental ($P=0.94$), which was comparable between the groups. Additionally, there was no significant difference between the groups in reaching the minimally clinically important difference (MCID) for hip arthroplasty.

Conclusions: GM tears are common among patients undergoing primary THA. Concurrent repairs provide comparable clinical outcomes to those seen in patients who did not have a GM pathology at the time of the THA. Given these findings, we recommend addressing and surgically repairing GM tears during the same surgical procedure.

Multi-Center Health Cloud Database: A Comprehensive Real-World Multi-Level Data Source for Outcomes Research in Orthopaedic Surgery

Ignacio Pasqualini - Cleveland Clinic - Cleveland, United States of America

Laura Yanoso-Scholl - Stryker Orthopaedics - USA

Anusha Guntupalli - Stryker - Amsterdam, Netherlands

Andrea Coppolecchia - Stryker - Mahwah, USA

*Nicolas Piuizzi - Cleveland Clinic - Cleveland, USA

Introduction: Measuring value in healthcare, defined as the health outcomes achieved relative to costs, is critical for improving patient care and allocating resources appropriately. Musculoskeletal disorders are a leading cause of disability worldwide, with joint replacement procedures alone costing over \$7 billion annually in the US. To help identify modifiable predictors of outcomes and enable evidence-based clinical decision making, real-world data from a large, representative patient population is important. We describe the development and characteristics of a comprehensive outcomes Health Cloud Database capturing patient-reported outcome measures (PROMs), surgical details, and clinical outcomes for orthopaedic procedures and its first research use cases.

Methods: The Health Cloud Database prospectively collects data from 382 facilities (hospital/ASC), of which 120 facilities and an unspecified subset of surgeons are actively contributing. Data is stored in a secure and HIPAA compliant Microsoft Azure cloud database and includes 845,972 cases from 2006-2024 (140,919 robotic procedures and 705,053 non-robotic procedures), including implants from multiple manufactures, with data collection ongoing. Over 500 variables are collected spanning patient demographics, comorbidities, surgical variables, PROMs, complications, readmissions, and other outcomes. PROMs are captured at multiple timepoints. For a subset of 33,815 robotic cases, additional pre- and intra-operative data is extracted from the robotic system. All data is deidentified to protect patient privacy following HIPAA/GDPR requirements.

Results: The most common procedures are listed in Table 1. The Health Cloud Database does include pre-op PROMs (including PROMIS Global10, EQ5D-5L, HOOS/KOOS JR, reduced WOMAC, Forgotten Joint Score and/or VAS Pain) for 179,903 cases and any post-op PROMs for 189,341 cases, with 1-year PROMs for 134,146 cases. Among the robotic cases, there were 20,911 (61.8%) total knee, 8,743 (25.9%) total hip, and 4,161 (12.3%) partial knee arthroplasties cases with data from the robotic system. Quarterly reports are generated to track outcomes and identify opportunities for quality and efficiency improvements.

Conclusion: The Health Cloud Database represents one of the largest and most comprehensive orthopaedic outcomes multi-level database to date, capturing both robotic and traditional procedures across dozens of facilities. The scale and richness of this data offers unparalleled opportunities for outcomes research, quality benchmarking, and clinical decision support. This database has been queried and integrated into analyses to gain insights on case time prediction and well as influence of surgical technique on patient length-of-stay, hospital revisits, and complications. Ongoing efforts may help further expand the database and leverage advanced analytics and AI models with the goal of generating insights that may aid in the improvement care for orthopaedic patients worldwide.

Functional Positioning Planning Attributes With Robotic Assisted TKA: Predictors of Outcomes

*Emily Hampp - Stryker - Mahwah, USA

Azhar Ali - Stryker Orthopaedics - Mahwah, USA

Michael Rodenbaugh - Stryker - Weston, USA

Akira Hada - Stryker - Weston, USA

Sidney Migliori - South County Health - Wakefield, USA

Robert Marchand - Ortho Rhode Island - South County, USA

INTRODUCTION: The introduction of CT-based robotic-arm assisted total knee arthroplasty (RATKA) offers surgeons the capability to plan individualized implant positioning and balance the knee without extensive soft tissue releases. However, the relationship between specific functionally-positioned RATKA planning attributes and clinical outcomes remains unexplored. This retrospective analysis aims to assess the statistical significance of functionally-positioned RATKA planning attributes using an upgraded software on patient-reported outcomes.

METHODS: This study retrospectively analyzed data from a prospectively collected dataset comprising 45 patients who underwent functionally-positioned RATKA from two surgeons at the same institution. All patients received a cruciate retaining RAKTA. The mean age of the cohort was 67.9 years (± 8), with 35.6% male and 64.4% female. Functional outcomes were assessed using the Forgotten Joint Score (FJS) completed by all patients at the 1-year postoperative mark. Additionally, Visual Analog Scale (VAS) pain scores were collected at 2 weeks, 6 weeks, and 3 months postoperatively, with scores available for 44, 37, and 42 patients, respectively. Multiple regression analysis was conducted for each of the 12 questions and total score in the FJS survey as well as the VAS pain scores at each postoperative interval. The analysis incorporated predictor values for medial congruency, lateral congruency, trochlear medial-lateral fit, tibial slope deviation from native, joint line restoration in extension, and joint line restoration in flexion. Predictors with p-values below 0.05 were considered statistically significant. Additionally, the median, first quartile, and third quartile were evaluated for each predictor value.

RESULTS: Tibial slope demonstrated significant predictive power ($p < 0.05$) for the total score and all 12 questions of FJS survey. Both tibial slope and lateral congruency were significant predictors ($p < 0.05$), specifically for the FJS question related to doing housework or gardening. For the VAS pain assessment, tibial slope and medial congruency emerged as significant predictors ($p < 0.05$) of pain levels at the 3-month postoperative mark. Additionally, lateral congruency was a significant predictor at the 2-week follow-up. Notably, while medial congruency exhibited a trend at the 2-week mark for the VAS pain assessment, it did not reach statistical significance ($p = 0.055$). For the remaining factors, p-values exceeded 0.05, indicating insufficient evidence to conclude those factors were related to the PROMs response. Median, first quartile, and third quartile values for each predictor are shown in Figure 1.

CONCLUSION: Tibial slope, as well as medial and lateral congruency, emerged as significant RATKA planning attributes influencing certain patient-reported outcome measures. Nevertheless, it is crucial to acknowledge limitations such as the small sample size and limited variability in certain predictor values. Additionally, while PROMs are valuable in assessing outcomes after TKA, they have certain limitations including floor and ceiling effects. Future investigations involving larger cohorts could offer a more comprehensive understanding of these relationships, thereby informing

more refined surgical approaches. The findings highlight the crucial role of functionally-positioned RATKA planning attributes in achieving favorable functional outcomes. Understanding the impact of specific planning attributes can inform surgical decision-making and may help improve patient outcomes.

Figures

Figure 1: Median, first quartile, and third quartile values for each predictor

Variable	N	Q1	Median	Q3
Medial Congruency (mm)	45	0.791	1.140	2.042
Lateral Congruency (mm)	45	2.032	2.574	3.406
Trochlear Medial-Lateral Fit (mm)	45	2.462	3.306	4.052
Tibial Slope, Deviation from native (degrees)	45	2.608	5.007	7.869
Joint Line Restoration, Extension (degrees)	45	-2.874	-0.619	2.396
Joint Line Restoration, Flexion (degrees)	44	-2.611	0.338	4.095

[Figure 1](#)

Early Clinical and Economic Outcomes of VELYS Robotic-Assisted Solution (VRAS) Compared to Manual Total Knee Arthroplasty

*Anshu Gupta - New Brunswick, United States of America

Philip Huang - OrthoIndy - Indianapolis, USA

Michael Cross - OrthoIndy - Indianapolis, USA

Dhara Intwala - Johnson & Johnson - New Brunswick, USA

Jill Ruppenkamp - Johnson & Johnson - New Brunswick, USA

Dan Hoeffel - Johnson & Johnson - New Brunswick, USA

Introduction

The VELYS Robotic-Assisted Solution (VRAS) manufactured by DePuy Synthes is one the latest entrants in the rapidly evolving field of robotic technology for TKA. VRAS is an imageless system, without reliance on preoperative CT scans, resulting in potential lower cost, preoperative preparation time and radiation exposure to the patient compared to other robotic systems [1]. The current VRAS specific evidence includes outcomes from single site [2,3] and/or is pre-clinical in nature [4,5]. Thus, the current study is designed to evaluate early post-operative clinical and economic outcomes of TKA with VRAS compared to manual TKAs in a large hospital billing database.

Methods

The Premier Healthcare Database [6] was analyzed to identify patients undergoing VRAS or manual TKA between September 1, 2021, and February 28, 2023. The primary outcomes for the study were the hospital follow up visits (revisits) and readmission rates within 90-day post TKA. Secondary outcomes include operating room time, discharge status and hospital costs. To control for the differences between the VRAS and manual TKA cohorts, a fine stratification and weighing (FSW) [7] methodology was used.

Results

A total of 1,180 VRAS TKA and 161,866 manual TKA cases were included in the study, with 866 VRAS and 128,643 manual TKA cases having 90-day follow-up data. A good balance was achieved between two cohorts using FSW method [Figure 1]. The rates of both all-cause and knee-related 90-day hospital revisits were significantly lower in the VRAS TKA cohort compared to the manual TKA cohort (13.86 vs. 17.19% and 2.66 vs. 4.81%, respectively, p -value <0.01). Similarly, the 90-day rate of knee-related readmission was significantly lower for the VRAS cohort (0.69 vs. 1.46%, p -value <0.01). We hypothesize that the reduction in hospital follow up visits and readmissions in the early postoperative period is related to an improved early recovery using VRAS compared to manual TKA. Most patients (96%) in both VRAS and manual TKA cohorts were discharged to home or home health services. VRAS procedures had slightly longer operating room time (4 minutes) than manual TKA procedures (137.96 vs. 133.67 minutes), most likely associated with the integration and set-up of robotic instrumentation. The 90-day all-cause cost of care was similar for both VRAS and manual TKA cohort (\$15,357 vs. \$14,944). In addition, the knee-related 90-day costs were similar for both cohorts (\$14,956 vs. \$14,547).

Conclusion

The study demonstrated lower number of follow up visits and readmission rates following total knee arthroplasty in patients treated with VRAS compared to manual surgery while having similar 90-day total hospital cost.

Figures

Covariate Balancing

Across Subclass

Sample ● Unadjusted ● Adjusted

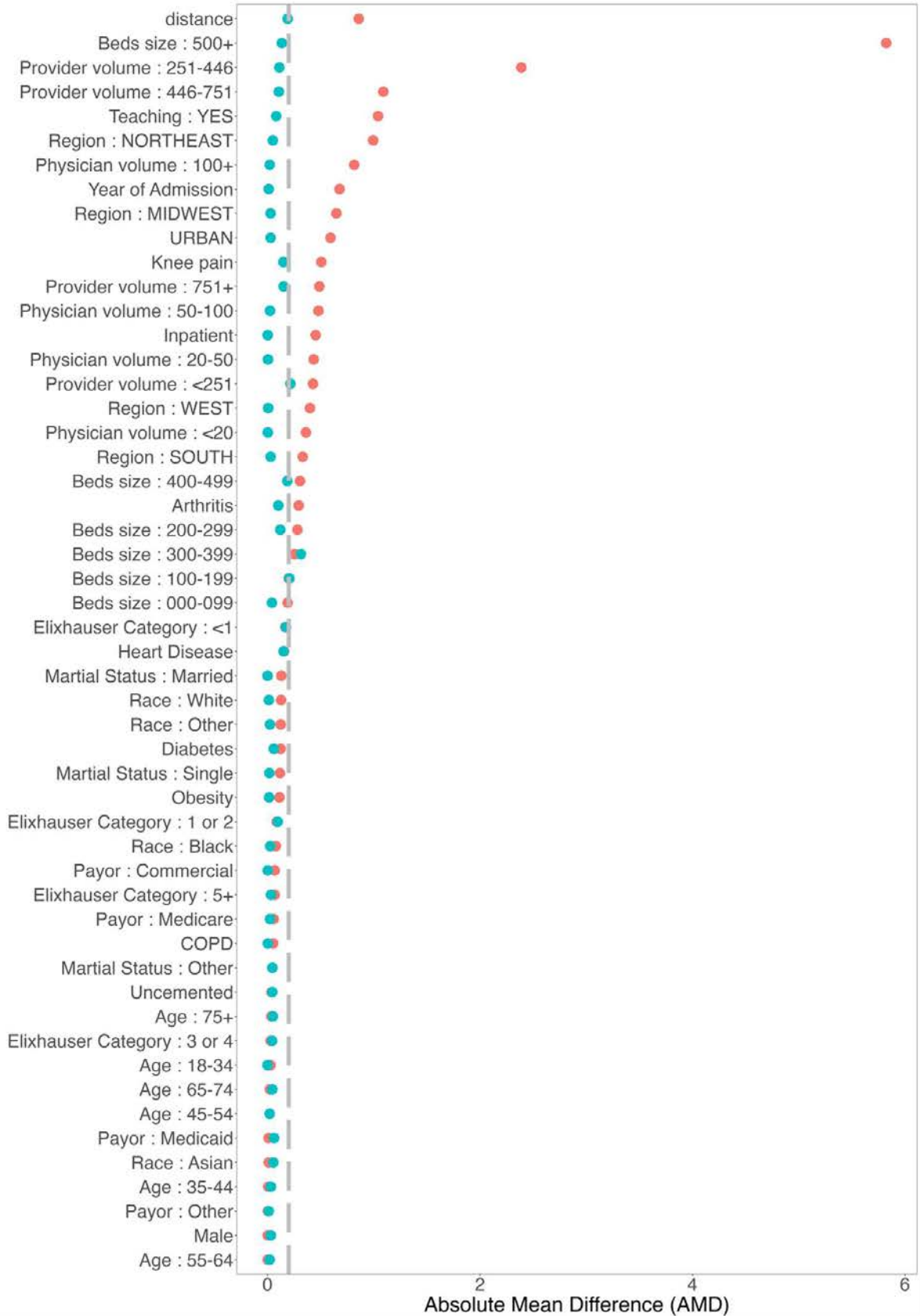


[Figure 1](#)

The Impact of Personality Traits on the Outcome of Total Knee Arthroplasty

*Alexander Giurea - Medical University of Vienna - Vienna, Austria

Georg Fraberger - Medical University Vienna - Vienna, Austria

Paul Kolbitsch - Medical University Vienna - Vienna, Austria

Richard Lass - Medical University Vienna - Vienna, Austria

Reinhard Windhager - Medical University Vienna - Vienna, Austria

Introduction: Ten to twenty percent of patients with total knee arthroplasty (TKA) are dissatisfied with their clinical outcome. Several reasons for dissatisfaction after TKA have been identified but until now no study was performed investigating personality traits as cause for patients satisfaction.

Aim of this study was to investigate if personality traits have an impact on patient`s satisfaction and clinical outcome after navigated TKAs, as navigated TKAs provide us with a cohort of patients with defined and compareable alignment of knee prostheses.

Methods: We investigated 80 patients with 86 computer navigated TKAs. All patients received the same implant type as well as the same implant fixation in a defined implant alignment. We asked for patients satisfaction and divided patients into two groups (satisfied or dissatisfied). 12 personality traits were tested in all patients using the Freiburg Personality Inventory (FPI-R). i.e.: life satisfaction, social orientation, performance orientation, inhibition, excitability, aggressiveness, strain, somatic distress, health worries, openness, extraversion, and emotional stability. Postoperative examination included Knee Society Score (KSS), Western Ontario and McMaster University Osteoarthritis Index (WOMAC), and the Visual Analogue Scale (VAS). Radiologic investigation was done in all patients.

Results: From 86 TKAs 84% of patients were satisfied, while 16% were not satisfied. Preoperative demographic data showed no differences between satisfied and dissatisfied patients. The FPI-R showed statistical significant influence of **four personality traits** on patient satisfaction: life satisfaction ($p = 0.006$) and performance orientation ($p = 0.015$) were significantly higher in satisfied patients whereas dissatisfied patients showed higher scores for somatic distress ($p = 0.001$) and emotional instability ($p = 0.002$). All clinical scores (VAS, WOMAC, and KSS) showed significantly better results in the satisfied patient group ($p < 0.01$). Radiological examination showed optimal alignment of all TKAs. There were no complications requiring revision surgery.

Conclusion: The results of our study show that personality traits may influence patients satisfaction and clinical outcome after TKA. Therefore patients personality traits may be a useful predictive factor for postoperative satisfaction after TKA and help to improve patient selection for successful TKA.

Development and Process of Psychometric Evaluation of a New Patient-Reported Outcome Measure for Patients Who Have Undergone Primary TKR Surgery

Samantha Birts - University of Leeds - Leeds, United Kingdom

Sheryl O'Farrell - Invibio Biomaterial Solutions - Thornton Cleveleys, United Kingdom

Lousie Strickland - Oxford University Hospitals NHS Trust - Oxford, United Kingdom

Crispin Jenkinson - University of Oxford - Oxford, United Kingdom

*Hemant Pandit - University of Leeds - Leeds, GB

Introduction:

Total Knee Replacement (TKR) is a common and effective intervention for the treatment of symptomatic end-stage arthritis. However, around 10-20% patients are not satisfied with the outcome of their TKR surgery despite demonstrating meaningful clinical improvements. Current Patient Reported Outcome Measures (PROMs) assess patient outcomes across multiple physiological and psychological domains; however do not necessarily report patient dissatisfaction and therefore potential factors contributing to dissatisfaction cannot be ascertained. This highlights the need for a novel and more sensitive PROM to explore patient dissatisfaction post-TKR surgery. The process of development and psychometric evaluation of the new PROM to assess patients' wellbeing and perceptions of TKR is reported here.

Methods:

Food and Drug Administration (FDA) guidance was adhered to in an iterative, multi-phased PROM development project. A comprehensive literature review guided the qualitative interviews with healthcare professionals (HCPs) in the Planning Phase and patient interviews in the subsequent Phase One. These identified opinions of key stakeholders helping generation of potential items which were tested in Phase Two in the form of Pilot Questionnaires (PQs) and interviews with patients. Phase Three then utilised exploratory factor analysis to aid item reduction and identify any relationships between the items. In Phase Three, the PQ along with the EQ-5D-5L and Oxford Knee Score (OKS), were administered to patients on one occasion between 3 months and 5 years post-TKR surgery. Patients who had bilateral TKRs were asked to complete the PQ and OKS twice in relation to each knee. Any patients who had suffered a complication post-TKR were excluded from any of the phases.

Results:

Development of the PROM included qualitative interviews with 20 orthopaedic HCPs in the planning phase, 23 patients in Phase One, and nine patients in Phase Two. Along with other commonly reported problems post-TKR, patients also identified issues such as clicking, heaviness, and discomfort in different environmental temperatures as contributors to their dissatisfaction. In Phase Three, 97 patients were enrolled, 22 of whom had undergone bilateral TKR, therefore 119 datasets were analysed. Two items were removed on initial testing due to significant floor effects. Further psychometric testing displayed high reliability and validity between items, therefore 32 of 34 items on the PQ remained and were subject to further testing. Three domains were identified, namely, "Physical mobility", "Discomfort" and "General Perceptions".. Spearman's Rank calculations showed sufficient correlation between 17 of the items to their respective domain, enabling the creation of a short-form version of the PROM. Further analysis will be completed to identify any potential correlations between the new questionnaire and OKS/EQ-5D-5L. The final phase will involve the validation of both questionnaires in a multi-centre clinical study in the UK.

Conclusion:

A new PROM highlights additional reasons for patient dissatisfaction following TKR surgery, thereby enabling healthcare providers to improve patient care and associated patient outcomes.

Reverse Shoulder Arthroplasty Provides Durable Outcomes Regardless of Diagnosis and Pathology

*Garrett Jackson - Chicago, United States of America

Aghdas Movassaghi - Michigan State University - East Lansing, USA

Hans Lapica - HCA Florida JFK Hospital - Atlantis, USA

Howard Routman - Atlantis Orthopedics - Atlantis, USA

Vani Sabesan - Cleveland Clinic Florida - Weston, USA

Antonio Da Costa - Florida Atlantic University, Charles E. Schmidt College of Medicine - Boca Raton, USA

Introduction: As surgical indications for reverse shoulder arthroplasty (RSA) have expanded, appropriate patient counseling and shared decision-making should be informed by clinical outcomes specific to each indication for RSA. While RSA has traditionally been indicated in patients with rotator cuff arthropathy (RCA), it has been employed increasingly in patients with osteoarthritis and in intact rotator cuff with better reported outcomes. To compare patient-reported outcomes (PROs) and postoperative range of motion (ROM) following RSA for patients with RCA compared to those with rotator cuff-intact GHOA.

Methods: All patients undergoing RSA from January 2015 to September 2019 by a single surgeon at a single institution were retrospectively identified through a prospectively collected database. Patients indicated for RSA secondary to GHOA without rotator cuff pathology were compared to patients indicated for RSA secondary to RCA. Patient-reported outcomes (PROs), including the Simple Shoulder Test (SST), American Shoulder and Elbow Surgeons (ASES), Shoulder Arthroplasty Smart (SAS) score, and University of California-Los Angeles (UCLA) scores, as well as active range of motion (ROM) were measured preoperatively and at a minimum 2-year follow-up, with outcomes between groups based on RSA indication compared.

Results: A total of 107 patients (n=71 RCA group, n=36 GHOA group) were identified, with no difference in patient demographics. No significant differences between groups were appreciated at the final follow-up based on SST ($p = 0.765$), ASES ($p = 0.437$), SAS ($p=0.782$), or UCLA ($p = 0.313$) scores, or ROM (all, $p<0.622$). Two patients (5.6%) in the GHOA group required revision RSA due to dislocation and loosening of the glenoid component.

Conclusion: Patients undergoing RSA for glenohumeral OA without rotator cuff pathology reported comparable patient reports outcomes and ROM values at a minimum 2-year follow-up compared to patients indicated for RSA secondary to RCA.

The Influence of Hyaluronic Acid on a Cartilage Wear Model for Hemiarthroplasty

*Markus Wimmer - Rush University - Chicago, USA

Francesca De Vecchi - Rush University Medical Center - Chicago, USA

AMANDINE IMPERGRE - Rush University Medical Center - Chicago, USA

Hemiarthroplasty, which involves the replacement of only one of the articular surfaces, allows the treatment of one-sided cartilage defects, as well as the replacement of individually degenerated bones in the wrist, hand, or foot. Its success, however, is variable with multiple influencing factors. In order to advance its performance, the development of a pre-clinical testing platform is important. This involves decisions about the kinematic and kinetic input, as well as the testing environment. In this study we investigated the effect of hyaluronan (HA), a high molar mass molecule within synovial fluid, when added to the testing medium of a ceramic-on-cartilage bearing couple.

Medical grade HA was mixed 1:1 with cell culture medium DMEM/F12 and compared with cell culture medium alone. Both media were used as lubricants in a previously published biotribometer with bovine cartilage as the articulating surface against alumina ceramics (BioloX Delta®, CeramTec GmbH, Germany) as the counterface. Since sulfated glycosaminoglycans (sGAGs) play a significant role in maintaining the cartilage's health, the release of sGAGs was chosen as wear outcome variable. Cartilage disks from 12 bovine stifle joints were articulated against 12 ceramic hip balls for 10 days in either medium. The sGAGs were measured using the DMMB assay from daily samples. For these measurements, samples were pooled for 1, 4, 7, and 10 days. In order to obtain a 'wear rate', the individual slopes of the sGAG release rates were then subtracted from the release rates of animal matched free-swelling control (FSC) samples. Additional cartilage health measures, e.g. cell viability and histological Mankin scores, were obtained as well.

The presence of HA in the medium produced lower and less variable sGAG release values. This was true for both articulated and FSC samples (Fig. 1). However, 'wear rates' were similar for both lubricants with 10.4 ± 2.8 vs. 11.4 ± 7.5 $\mu\text{g/mL}$ (mean $\pm 95\%$ C.I.; HA vs cell culture medium, respectively). For both lubricants, cell viability and Mankin scores stayed in acceptable ranges.

The presence of HA in medium had no measurable effect on cartilage wear when articulated against alumina; however, measurement variability dropped when HA was present in the medium. It is possible that HA, which binds at the surface of cartilage, retains sGAGs released from the matrix. Additional tests with other hemiarthroplasty materials need to follow.

Figures

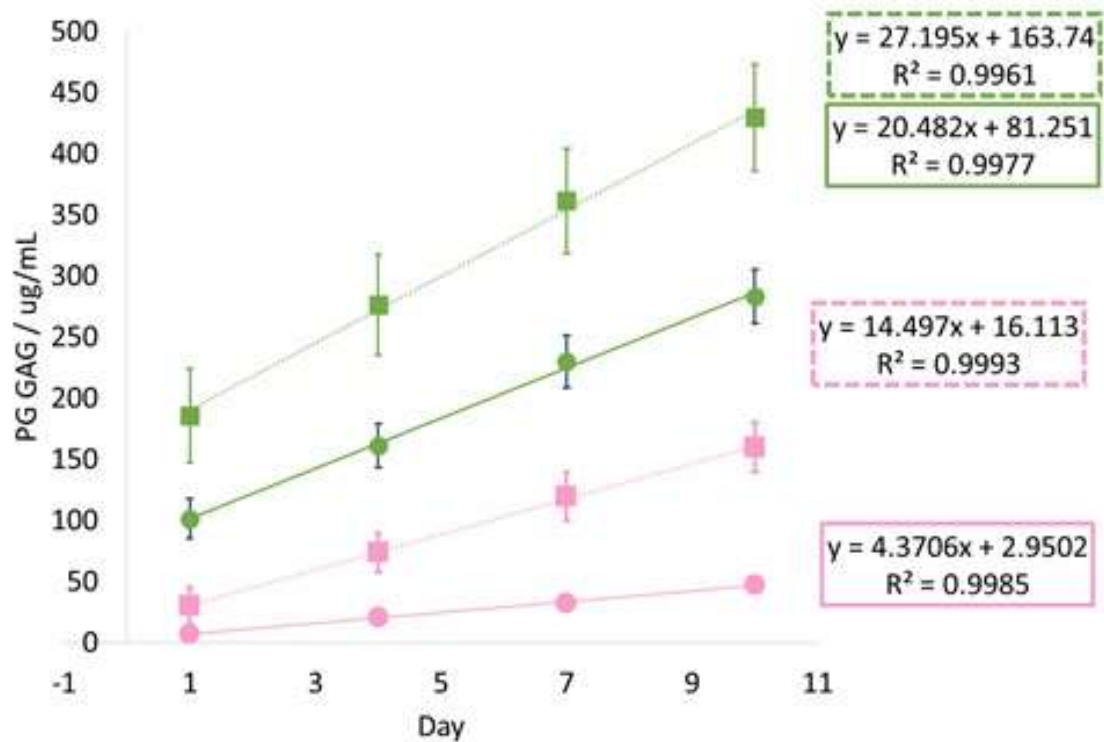


Figure 1: sGAG release over days of testing. Cell culture medium only (green) vs. cell culture medium with HA in (pink). Dashed lines indicate release during wear; solid lines release during free swelling.

[Figure 1](#)

Effects of Acetabular Cup Medialization on Muscle Function Vary Between THA Patients

Atul Kamath - Cleveland Clinic - Cleveland, USA

J. Bohannon Mason - Orthocolina - Charlotte, USA

Duncan Bakke - Formus Labs - Auckland, New Zealand

David Liu - Gold Coast Centre for Bone and Joint Surgery - Tugun, Australia

James Germano - Orlin and Cohen Orthopedic Group - New York, USA

Thor F Besier - University of Auckland - Auckland, New Zealand

*Marco Schneider - Formus Labs - Auckland, New Zealand

Introduction

Acetabular cup medialisation in total hip arthroplasty (THA) is known to affect moment arms of the abductor and adductor muscles, with the effect of medialization on muscle function on an 'average pelvis' recently characterized [1]. However, it is unclear how patient-specific variations in pelvic morphology influence this relationship. We investigated the effects of cup medialisation on abductors and adductors across a cohort of THA patients.

Methods

Pelves and femurs of 12 THA patients (7F/5M; 50-83 years) were automatically segmented from preoperative CT and fitted with implants by Formus Hip THA planning software (Formus Labs, NZ), then fitted with an articulated shape model of the lower limb to create patient-specific musculoskeletal models [2]. Post-operative models with varying medialisation were simulated by adjustment according to surgical plans and translating the cup from 5 mm lateral to 10 mm medial. All models were used to simulate sit-to-stand motion, estimating moment arms and muscle-tendon lengths for abductors and adductors throughout, presented as percentage change from native. Muscle moment arms were multiplied by their respective peak isometric force and summed to calculate Moment Generation Capacities [3].

Results

Abductor moment generation capacity increased by $10.9\% \pm 2.4\%$ with cup medialisation across the range tested (mean $R^2 > 0.99$, $p < 0.001$), or 0.7% increase per millimeter of translation (Figure 1). Adductor moment generation capacity reduced by $18.5\% \pm 1.9\%$ across the range tested (mean $R^2 < -0.99$, $p < 0.001$), or 1.2% decrease per millimeter of translation (Figure 2). Muscle-tendon length changes varied, with muscles paths aligned with the medial-lateral axis (e.g. piriformis, up to -9%) scaled in peak length more linearly than others (e.g. sartorius, up to $+1\%$).

Conclusion

The trends of medialising the cup on muscle function agreed with a generic model [3]. However, values varied between subjects by up to 20%. The relationship between increasing medialisation and change in moment generating capacity was linear, with large standard deviation between subjects for abductors ($\pm 2.4\%$ from a mean of 10.9%), and less deviation for adductors ($\pm 1.9\%$ from a mean of 18.5%). This reinforces the need for simulation of post-operative geometry when predicting patient-specific effects on postoperative soft tissue function.

References

1. Kamath, A. et al. (2023). ISTA 2023 Annual Congress
2. Rooks, N. et al. (2023). ISTA 2023 Annual Congress
3. Delp & Maloney (1993). J.Biomech 26.4-5

Figures

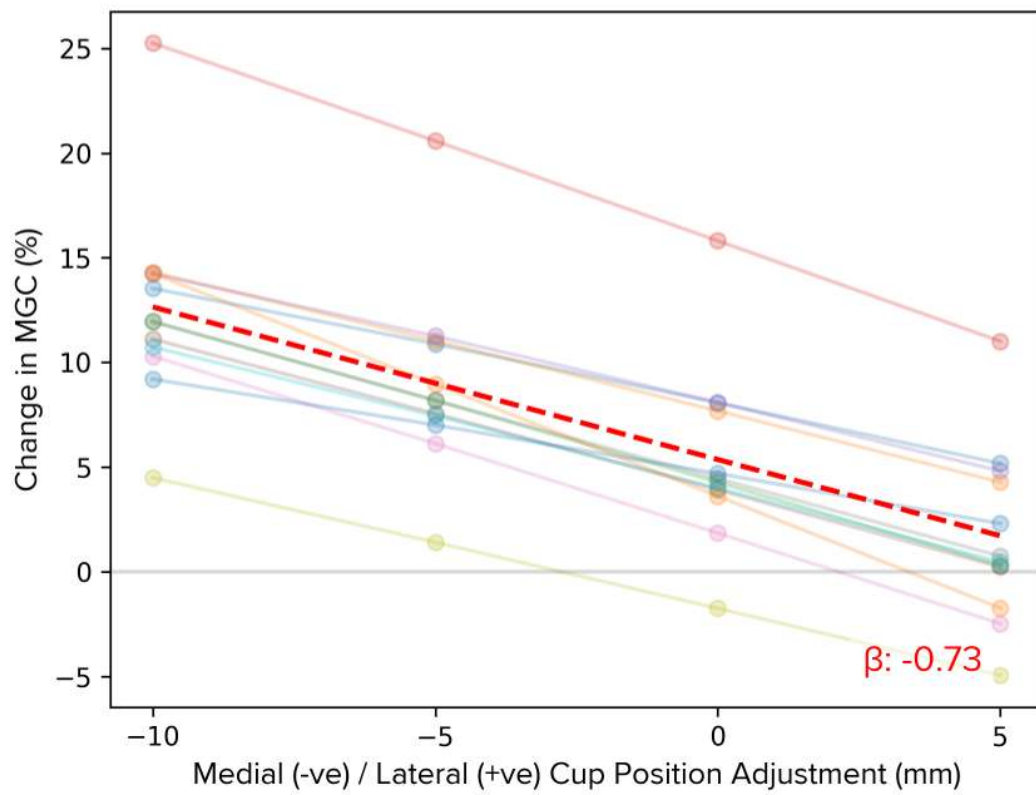


Figure 1. Effect of cup placement on hip abductor Moment Generation Capacity (MGC)

[Figure 1](#)

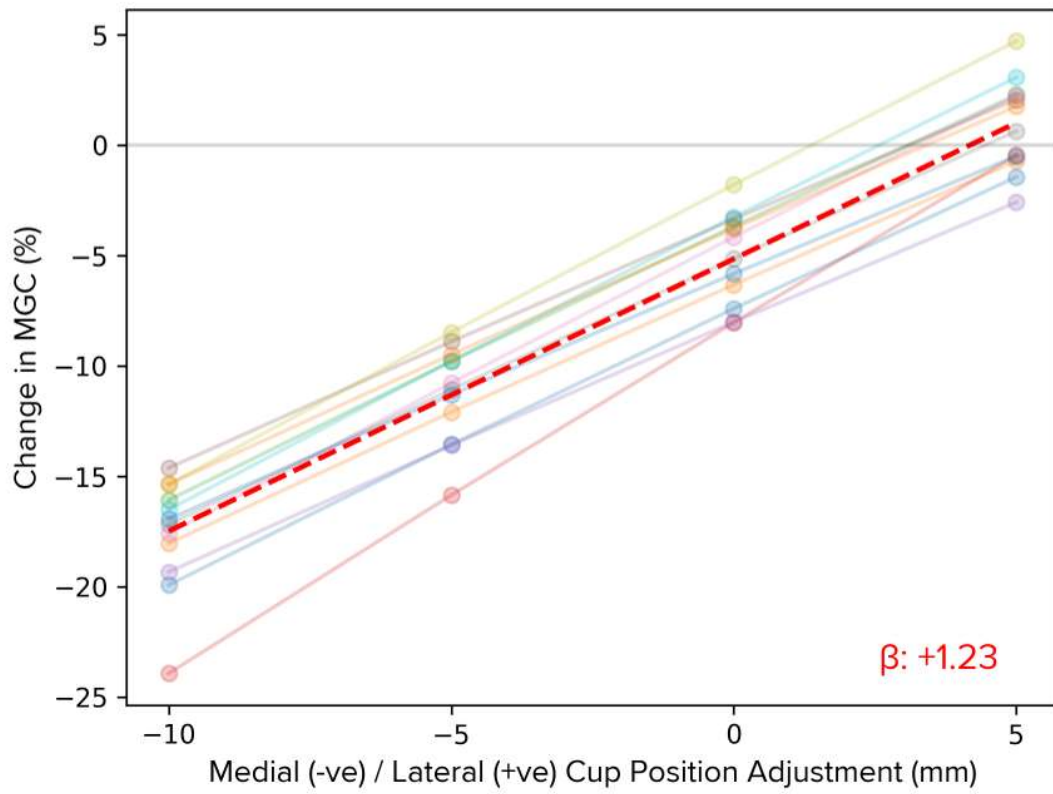


Figure 2. Effect of cup placement on hip adductor Moment Generation Capacity (MGC)

[Figure 2](#)

Clinical Results on Cup Placement Using the Mako Robotic System

Makoto Iwasa - Osaka University Graduate School of Medicine - Suita, Japan

*Hidenobu Miki - Osaka National Hospital - Osaka, Japan

Introduction: We investigated the clinical outcomes of cup placement in THA using the Mako system at our hospital.

Methods: A total of 104 primary THA cases performed from April 2022 to August 2023 by an expert surgeon using an anterolateral approach were included, 56 cases using the Mako system (group M) and 48 cases using the Navi system (group N). The mean age of the M and N groups was 66 years, the percentages of women and the mean body mass index were 93% and 84%, and 23.7 kg/m² and 24.2 kg/m², respectively, and no significant differences were observed. The assessment items were accuracy of clinical cup placement (absolute difference in cup angles before and after surgery), accuracy of cup display (absolute difference in cup angles during and after surgery), ratio of screws used, incidence of occult fracture, and ratio of cases with an initial gap of 2 mm or greater. The cup angle, anteversion, and inclination were measured using preoperative CT data and CT data obtained at 1 week postoperatively. The intraoperative angle was recorded as the angle displayed intraoperatively. Pre- and postoperative cup angles were measured using the Stryker Navigation System after aligning the pelvic coordinate system in the pre- and postoperative CTs. Initial gap was evaluated by the slice through the center of the head in the functional pelvic plane coronal section of the postoperative CT.

Results: Cup clinical placement accuracy was $1.4 \pm 1.7^\circ$ and $1.9 \pm 1.9^\circ$ for anteversion and $0.7 \pm 0.9^\circ$ and $1.5 \pm 1.6^\circ$ for cup inclination in the M and N groups ($p = 0.23$, $p > 0.01$). Cup inclination was $0.9 \pm 0.8^\circ$ and $1.8 \pm 1.5^\circ$ ($p = 0.50$, $p < 0.01$). The incidence of screw use and occult fracture was 1.8% and 8.3% in the M and N groups, and 5.4% and 4.2% in the M and N groups, respectively ($p = 0.18$, $p = 1.00$), with no significant difference in the percentage of patients with an initial gap of 2 mm or greater. The percentage of patients with an Initial Gap of 2 mm or greater was significantly different between 0% and 6.3% ($p = 0.04$).

Conclusion: The clinical results of cup placement in THA using the Mako system were good.

Neck Height Should Not Increase With Implant Size. Optimal Design of a New Collared, Metaphyseal-Filling, Triple-Taper Stem Using the CorinRegistry Statistical Shape Model

Elizabeth Cartwright - Corin - Cirencester, United Kingdom

Hanna Cacace - Corin - Raynham, USA

*Christopher Plaskos - Corin - Raynham, USA

Jonathan Bare - Melbourne Orthopaedic Group - Melbourne, Australia

Andrew Shimmin - Melbourne Orthopaedic Group - Melbourne, Australia

Travis Small - Saint Francis Health System - Tusla, USA

Michael P. Bradley - South County Hospital - Wakefield, USA

Jim Pierrepont - Corin - Pymble, Australia

Introduction – The use of collared, metaphyseal-filling THA stems has increased drastically. However, the optimal height of the prosthetic neck across the size range, relative to the medial calcar, remains unclear. We report on the use of a statistical shape model (SSM) to optimize the neck height across the size range of a new collared, metaphyseal-filling, triple-taper stem (Icona, Corin Ltd). We asked 1) how does the relationship vary between neck height from the medial calcar and increasing metaphyseal size in the native femur, and 2) how well does a stem designed to accommodate this relationship fit a diverse population of femoral anatomies undergoing THA.

Methods – A SSM was developed using preoperative CT data from the CorinRegistry. 2000 synthetic femoral geometries were then generated by randomly varying each principal mode of variation within ± 3 standard deviations of the mean. Internal metaphyseal mediolateral size was measured at the level of the lesser trochanter and neck length was measured from the head center to the medial calcar, defined 12.5mm superior to the lesser trochanter (figure 1). The association between these parameters was evaluated with the Pearson correlation coefficient. The final stem geometry was integrated into the OPSInsight™ 3D planning system and 30 clinical THA cases were planned by two users (15 cases each). Cases were selected to include a wide range of stem sizes (1-12) and anatomical variations.

Results – Neck height from the medial calcar did not increase with increasing metaphyseal size ($r=-0.085$, $r=0.142$, figure 2). This resulted in a stem design that had minimal increase in neck height across the size range, differing from competitive stems (figure 3). In all 30 clinical cases the stem could be optimally positioned within the proximal metaphysis while restoring the targeted leg length and offset within 1 mm. -4 mm, Neutral, +4 mm, and +8 mm heads were used in 3%, 57%, 23%, and 0% of cases, respectively.

Conclusions – Neck height from the medial calcar does not increase with internal metaphyseal diameter. Consequently, to avoid over lengthening in larger stems, neck height should grow minimally with increasing implant size, contrary to other common designs.

Figures

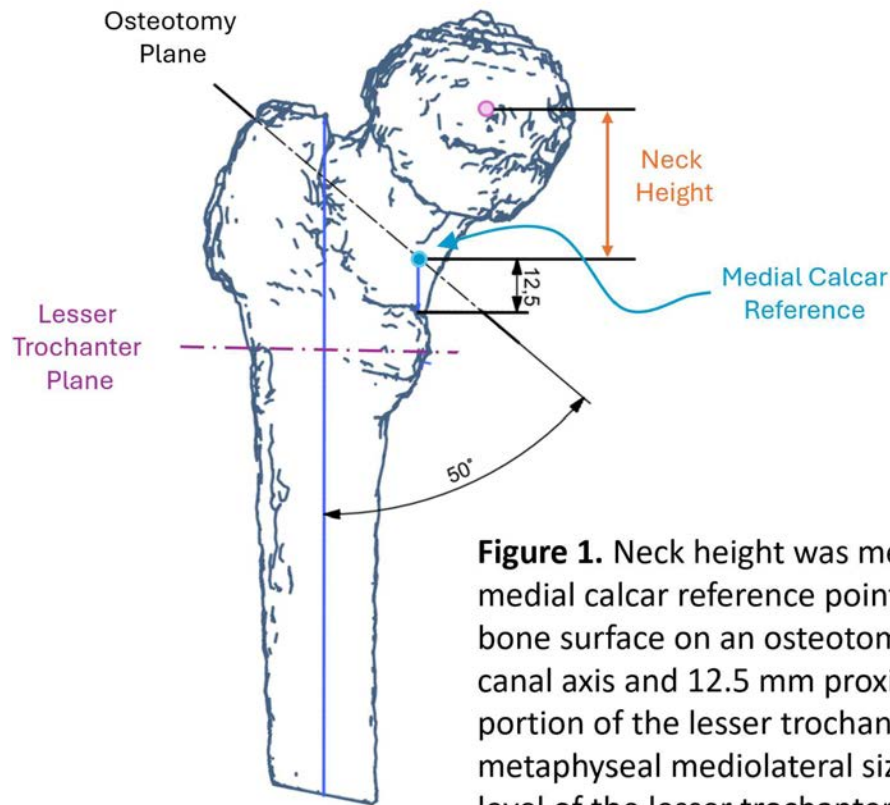


Figure 1. Neck height was measured from the medial calcar reference point located on the inner bone surface on an osteotomy plane 50° to the canal axis and 12.5 mm proximal to the upper portion of the lesser trochanter. Internal metaphyseal mediolateral size was measured at level of the lesser trochanter.

[Figure 1](#)

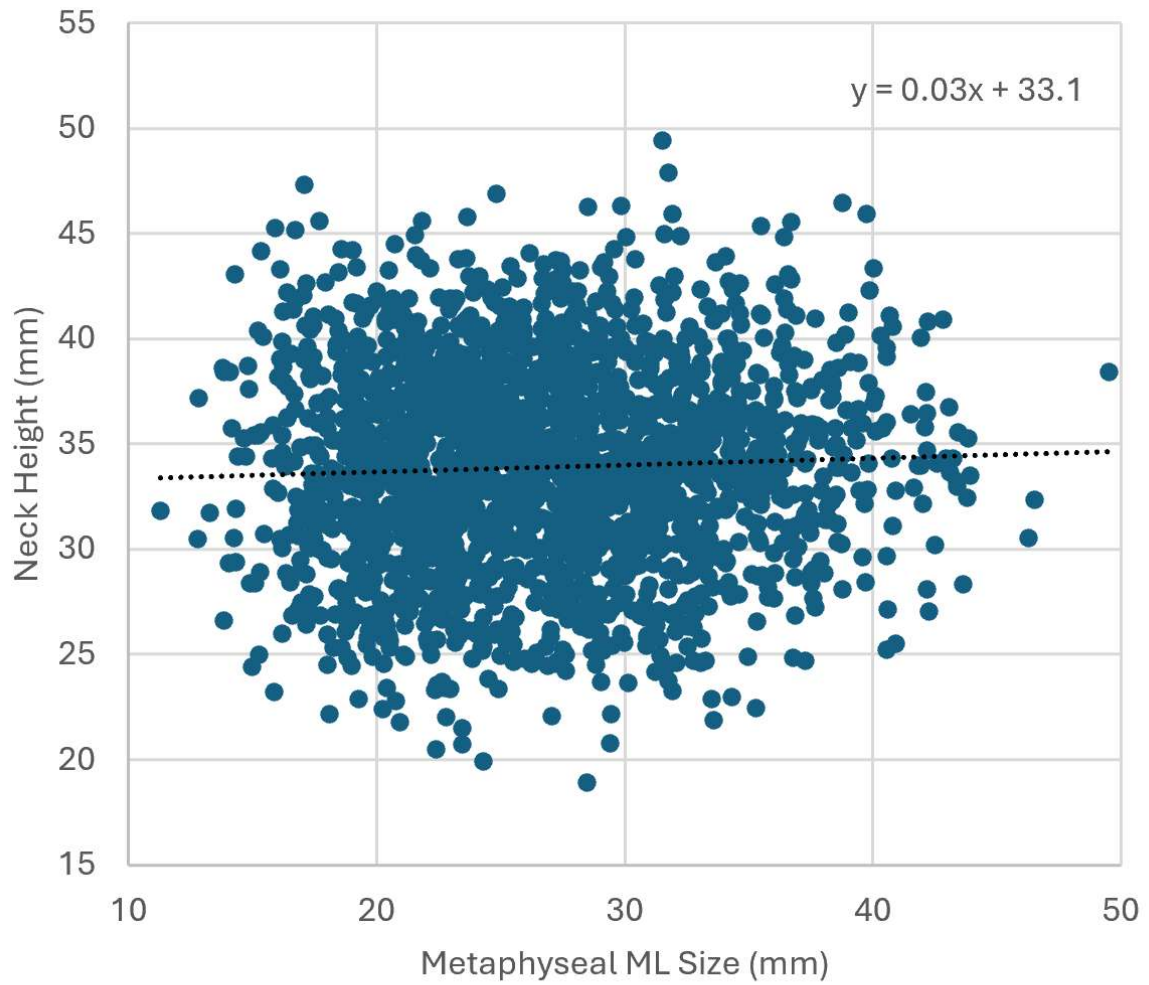


Figure 2. Neck Height was not associated with Metaphyseal Mediolateral (ML) Size.

[Figure 2](#)

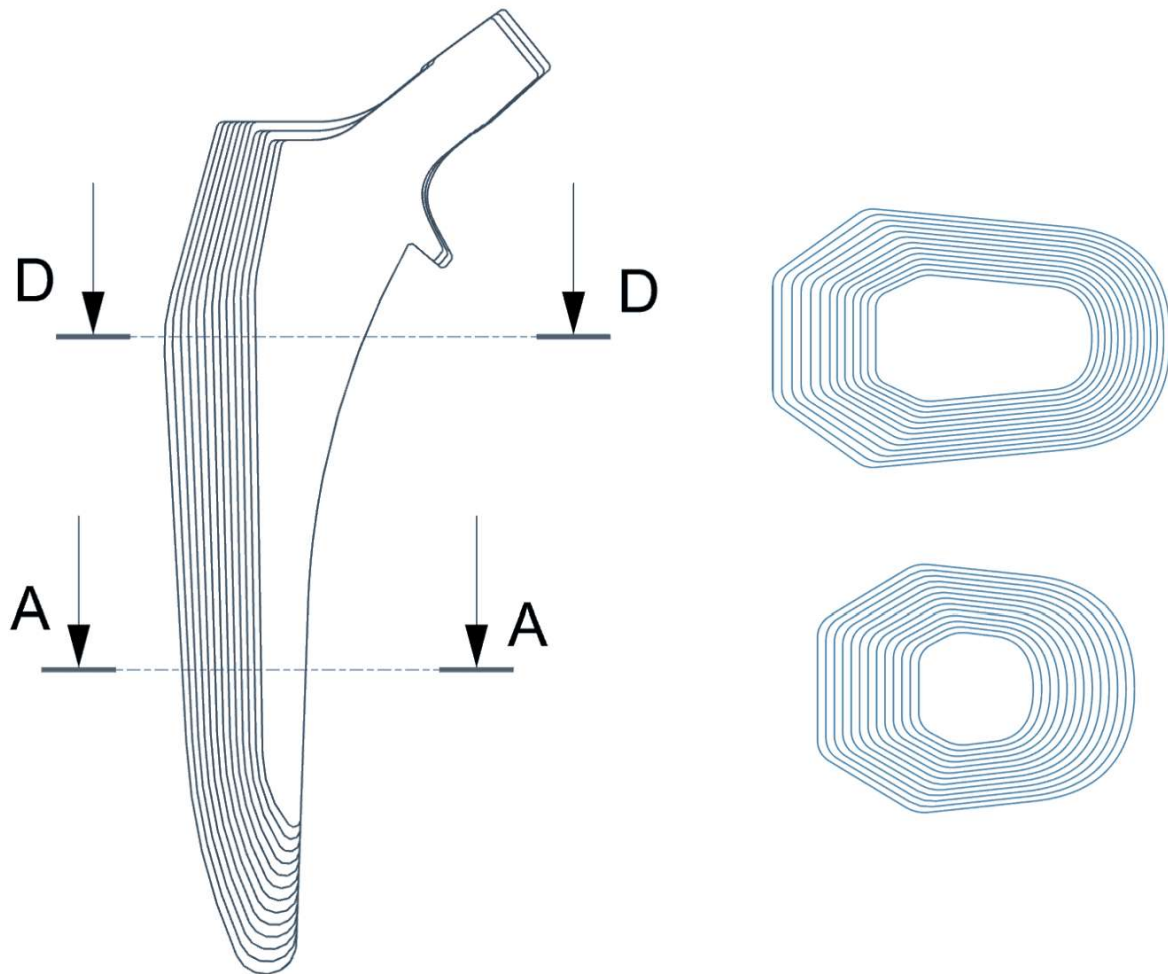


Figure 3. The Icona stem was designed to have minimal change in neck height from the medial calcar/collar junction across the size range.

[Figure 3](#)

Decoupled Impaction Increases Primary Cup Fixation in Cementless THA

***Adam Reynolds - Imperial College - London, GB**

Monil Karia - Imperial College London - London, United Kingdom

Jonathan Jeffers - Imperial College London - London, United Kingdom

Sarah Muirhead-Allwood - The London Hip Unit - London, United Kingdom

Hadi Alagha - Imperial College London - London, United Kingdom

Luyang Xu - Imperial College London - London, United Kingdom

Introduction: Cementless acetabular cups are traditionally installed by impacting the cup into a reamed undersized cavity using an introducer and mallet strikes. The objective is to achieve a strong press-fit and minimize the gap between the cavity floor and the implant for optimal mechanical fixation and bone ingrowth. However, the elastic rebound energy transferred to the implant during this process can compromise fixation by causing the cup to move out of the cavity. In previous studies, this 'wear' effect has been shown to reduce implant fixation, particularly if excess strikes are used. This study tests a new solution to mitigate the rebound energy by using a dynamically decoupling introducer.

Methods: Seven paired cadaveric hips were dissected and potted in bone cement. Each pair was reamed consistently with clinical practices, keeping the ream size constant between paired samples. One side of each pair was impacted using a traditional coupled introducer, while the other side used a dynamically decoupling introducer. A custom drop rig applied 10 medium-energy (4.5J) strikes to seat the implants. The implants were then removed using a single-axis tensile testing machine (Instron) to measure peak pull-out force.

Results: The mean peak pull-out force for the traditional coupled introducer was 1037N (SD 549N), while for the dynamically decoupled introducer, it was 1576N (SD 467N). The ratio paired t-test showed a significant difference in fixation strength between the methods ($t(7) = 2.9$, $p = 0.027$). On average, the dynamically decoupled introducer resulted in 65% higher fixation strength compared to the traditional method. These results are shown in Figure 1.

Conclusion: The dynamically decoupled introducer significantly improves the mechanical fixation strength of cementless acetabular cups in THA. This effect is expected to be even greater for either 1) high-energy strikes or 2) an excessive number of strikes used. Our method mitigates the effect of previously reported fixation degradation with excess strikes. This simple new design shows great potential for enhancing surgical outcomes and long-term implant stability, without affecting surgical workflow or increasing costs.

Figures

Acetabular Cup Fixation after 10 Strikes

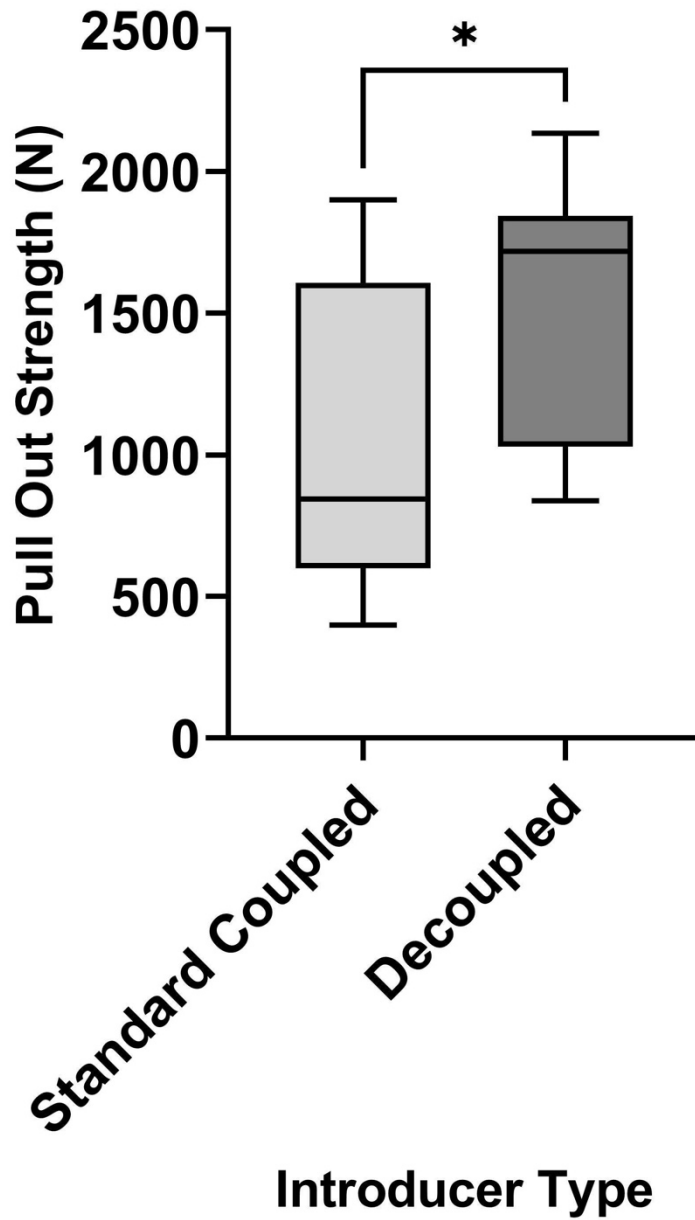


[Figure 1](#)

Statistical Shape Modelling Shows the High Variability of the Proximal Femoral Canal: Future Guide to Achieve Target Stem Anteversion

*Angelika Ramesh - London, GB

Johann Henckel - Royal National Orthopaedic Hospital - London, United Kingdom

Sara De Angelis - University College London - London, GB

Anna Di Laura - Royal National Orthopaedic Hospital and Dept. MechEng at UCL - London, United Kingdom

Alistair Hart - Royal National Orthopaedic Hospital - London, United Kingdom

Keywords: Statistical Shape Modelling, Principal Component Analysis, Intramedullary Femoral Canal

Introduction

The final position of a femoral stem component in uncemented total hip arthroplasty (THA) is dependent on both the shape of the femur and the design of the prosthetic stem.

Various design philosophies currently exist for an uncemented femoral stem, which include but are not limited to the tapered, cylindrical and anatomical designs. Despite their satisfactory long-term survivorship, the anatomically shaped stems fail to cover the wide range of shape variability of the intramedullary canal of the proximal femur. Delivering the intended stem version in uncemented THA is an unmet need.

We aimed to better understand the shape variations that characterise the intramedullary femoral canal and control the fit of the prosthetic stem. Our objective was to use Principal Component Analysis (PCA) to identify the main modes of variation.

Methods

This retrospective cohort study used 64 pre-operative pelvic CT scans of patients who underwent 3D planned hip replacement surgery. An image segmentation software was used to produce 3D reconstructions of the patient's femoral canal using an appropriate Hounsfield Unit (HU) threshold, and to build the SSM.

The images were standardised for length and orientation. A coordinate system was defined for each femoral canal, based on the posterior condylar axis and intertrochanteric crest, allowing for alignment in a fixed reference system before mean shape generation (Fig. 1). Each input femoral canal was then mapped onto the mean shape using point mapping.

PCA was used to extract the directions of variation (eigenvectors) and extent of change (eigenvalues) from the covariance matrix of the data.

The outcome measures were:

- The principal modes of variation;
- The variance/contribution of each mode.

Results

Five main modes of variation were identified through the PC analysis:

1) **canal size**; 2) **proximal torsion around the calcar**; 3) **femoral version**; 4) **varus/valgus orientation** and; 5) **distal femoral**

twist. These are in order of decreasing contribution to the overall variance.

Since the individual variance of mode 6 and onwards were less than 5%, it was assumed that the first 5 components captured the majority of the distinguishing features of the canal shape (accounting for 84% of the cumulative variance – Fig. 2).

The variance accounted by:

1. PC1 accounted for 36% of the cumulative variance (eigenvalue = 3.8×10^5).
2. PC2 accounted for 19% of the cumulative variance (eigenvalue = 1.9×10^5).
3. PC3 accounted for 15% of the cumulative variance (eigenvalue = 1.5×10^5).
4. PC4 accounted for 9% of the cumulative variance (eigenvalue = 8.9×10^4).
5. PC5 accounted for 6% of the cumulative variance (eigenvalue = 6.1×10^4).

Fig. 3 summarises the results of the PCA.

Conclusion

This study helps to better describe the variability in the intramedullary femoral canal shape in 3D. Its distinguishing features are identified as size, proximal torsion fixed at the calcar, femoral version, varus/valgus orientation and distal femoral twist.

A unique stem design which accounts for all of these patient characteristics does not yet exist, explaining the discrepancy commonly found between the intended and achieved prosthetic stem version. This information may be used to improve the planning and the delivery of anteversion of uncemented stems.

Figures

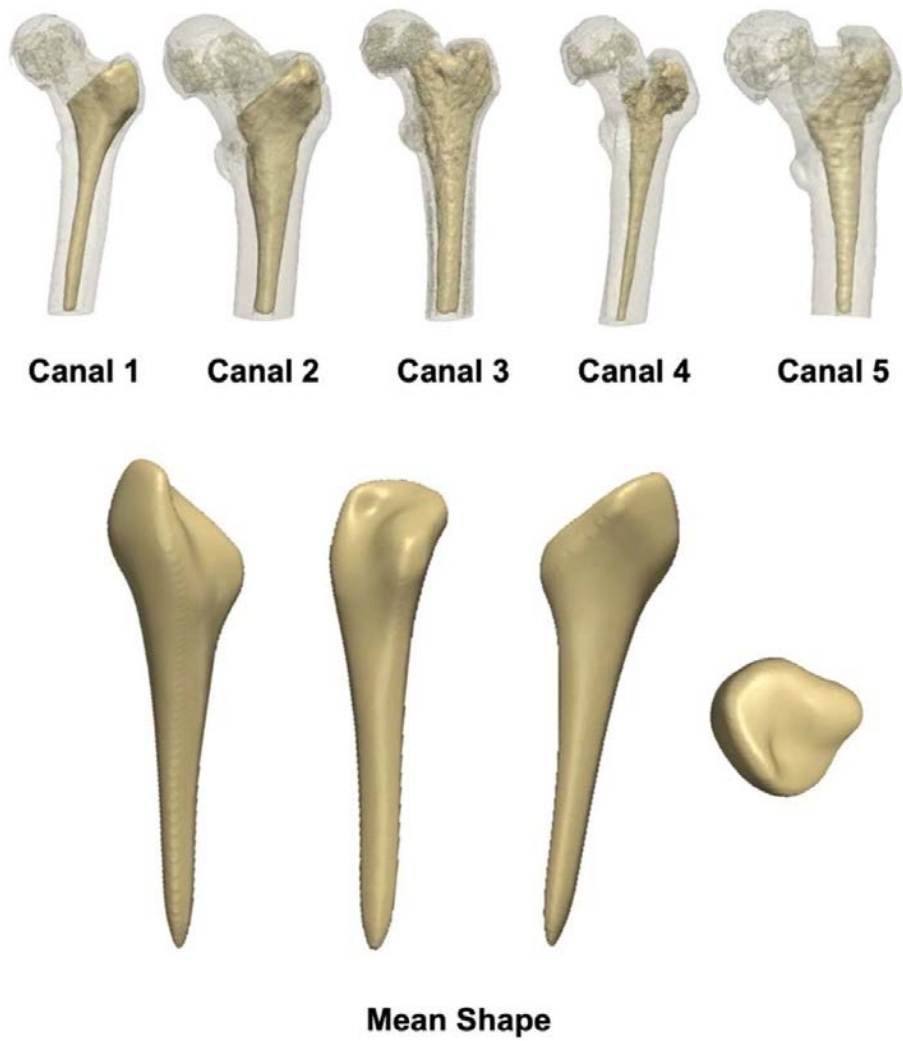


Figure 1. An illustration of five different femoral canals along with the mean shape generated from the 64 training inputs.

[Figure 1](#)

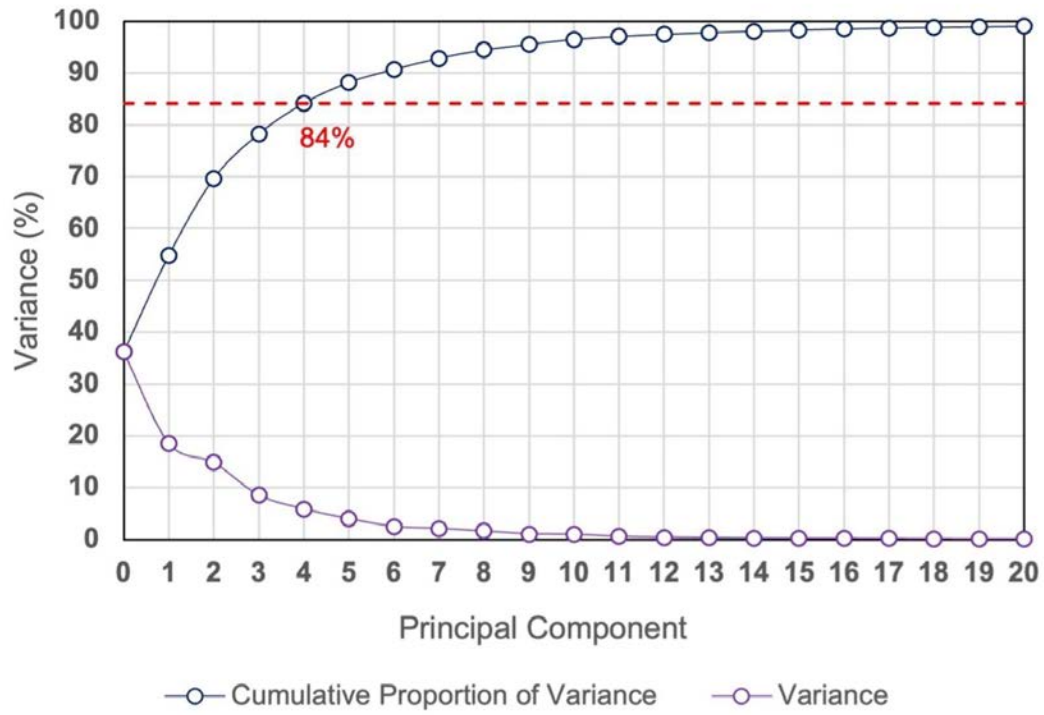


Figure 2. A Scree plot showing the cumulative and explained variance of each mode of the PCA.

[Figure 2](#)

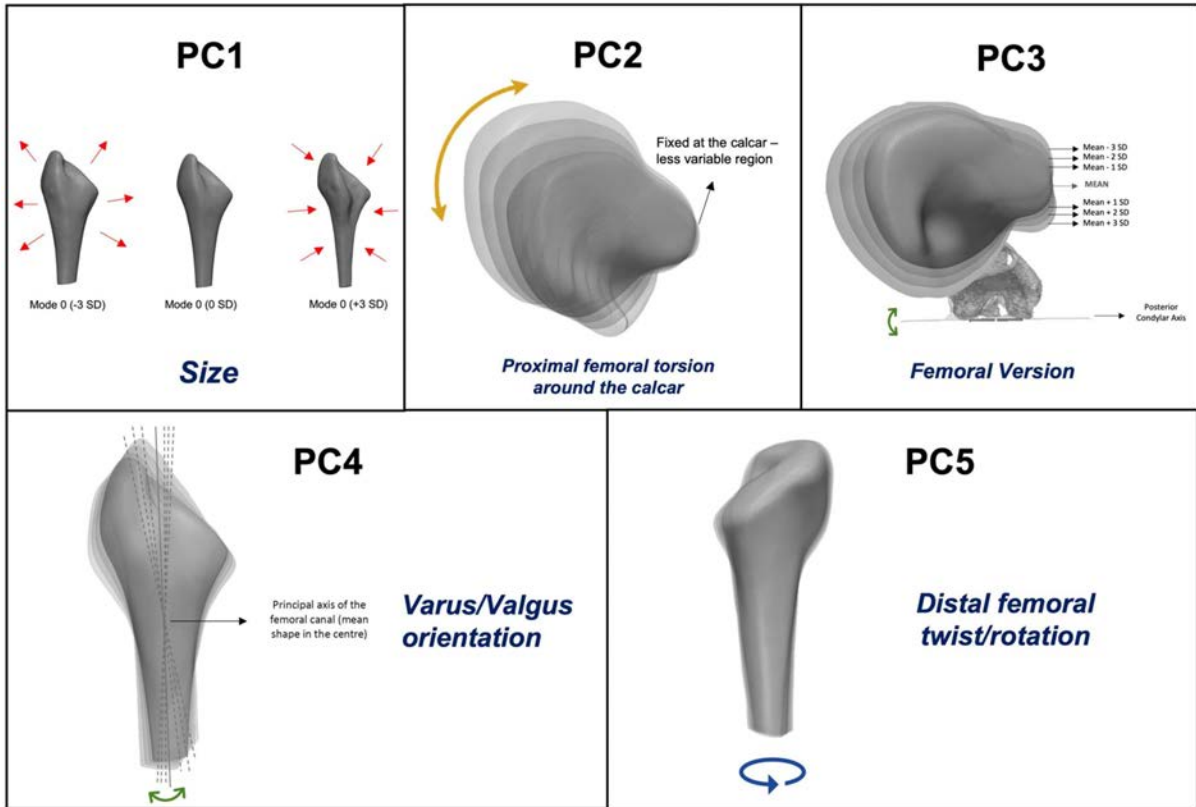


Figure 3. Results of the principal component analysis to illustrate 3D shape and size variations between the 64 femoral canal models. The first five modes of variation (PC1 – 5) as well as ± 3 SD models are displayed to track the main features changing within each mode. These are identified as: 1) Size; 2) Proximal femoral torsion around the calcar; 3) Femoral version; 4) Varus/valgus orientation and; 5) Distal femoral twist/rotation.

[Figure 3](#)

Is Vibratory Implantation an Alternative for Conventional Impaction of Acetabular Cups?

Yasaman Niki - Technische Universität Hamburg (TUHH) - Hamburg, Germany

*Gerd Huber - TUHH Hamburg University of Technology - Hamburg, Germany

Kambiz Behzadi - Behzadi Medical Device - Pleasanton, USA

Michael Morlock - TUHH Hamburg University of Technology - Hamburg, Germany

Introduction:

Total hip arthroplasty using uncemented components requires a compromise with regard to the implantation force. It has to be high enough to achieve sufficient primary implant stability due to the press-fit of the implant in an undersized bone cavity, but also small enough not to cause periprosthetic fractures (PPF). The ratio between the required implantation force and the load that could cause implant loosening depends on the friction coefficient between implant and bone coating. Vibratory implantation devices bear the potential to improve this ratio since dynamic relative movements might reduce the friction [1].

The aim of the study was to assess the effectiveness of vibratory cup implant insertion compared to an established implant insertion method.

Methods:

Nominal line-to-line and 1 mm over-sized implantation of acetabular cups (nominal diameter: 44 mm, Gription coating; Pinnacle, DePuy Synthes, UK) in porcine acetabula was performed (Figure 1) using a vibration device (60 Hz, Behzadi Medical Device, USA) and an established mechanical impactor (1 Hz, KINCISE, DePuy Synthes, USA). The applied impaction forces were recorded. Cups were impacted until the polar gap was below 2 mm or until additional strokes did not achieve further seating. The final cup position and the remaining polar gap were determined by aligning pre- and post-implantation laser scans. The cup lever-out moment served as a measure for primary stability (Z010, Zwick Roell, DE).

Results:

The actual diameter of the cup was 44.1 mm. The diameter of the reamers was 43.4 mm and 42.1 mm resulting in reamed cavities of 43.5 ± 0.3 and 42.5 ± 0.2 , respectively, so that the effective undersizing was 0.6 ± 0.3 mm and 1.6 ± 0.2 mm. Implantation with the vibratory device required almost 40% lower impaction forces at both press-fit levels, but complete seating could not be achieved, especially for the nominal press-fit of 1 mm. Furthermore, the primary stability was lower for the vibratory impaction for either press-fit (Figure 2).

Conclusion:

Bone fracture risk was reduced for the vibrational implant insertion, but on the cost of a reduction in primary stability. The outcome in porcine bone was similar to a previous study using polyurethane foams, suggesting that the viscoelasticity of bone may not play a crucial role during press-fit implant impaction [2].

It is unclear whether additional reaming by the implant was done or whether friction could be overcome during high frequency implantation.

The impaction method, the implant surface, the actual diameter of the cup and probably also the bone properties must always be considered together in order to find the optimal compromise between PPF and primary stability.

References:

[1] Nakasone et al., J. Arth. 2012

[2] Niki et al. BJR. 2024

Acknowledgements:

Provision of implants and surgical instruments by DePuy Synthes is kindly acknowledged.

Keywords:

acetabular cup, vibratory impaction, primary stability, animal bone model

Mallets Are Good for Implantation - Shakers for the Determination of Dynamic Properties

*Peter Schlieker - TUHH Hamburg University of Technology - Hamburg, Germany

Michael Morlock - TUHH Hamburg University of Technology - Hamburg, Germany

Gerd Huber - TUHH Hamburg University of Technology - Hamburg, Germany

Introduction: Since the beginning of cementless hip arthroplasty, mallets have been used for implantation, but (partially) automated implantation techniques are on a rise. Differences in blow characteristics may change the dynamics of the implantation.

Consequently, an enhanced understanding of the mechanical boundary conditions of the femur during impaction, which likely depends on the surrounding soft tissue, is necessary. The aim of this study was to select a methodology to determine the dynamic properties of the femur-tissue-system during surgery. Experiments on a mechanical substitute model should pave the way for experiments on body donors.

Methods: A substitute Voigt model for the femur in situ was built [1] (Fig. 1). The implemented stiffness (3.6 N/mm, 4.2 N/mm, 5.0 N/mm, 5.9 N/mm, all with a constant mass of 10.3 kg) and the implemented mass (0.3 kg, 5.3 kg, 10.3 kg, 15.3 kg, all with a constant stiffness of 4.2 N/mm) were varied to account for inter-specimen variability. The excitation of the substitute model was performed with an electrodynamic shaker (TV 51075-M, TIRA, GER; sinusoidal, increasing frequency: 1-100 Hz, 60 s) and a surgical mallet (0.9 kg). Force and acceleration were measured directly below the shaker (9321C, Kistler, CH; M354C03, PCB, NY). The surgical mallet was used in combination with an instrumented impactor (9333A, Kistler) to create a short impulse excitation, while the acceleration was measured below the impactor tip (350C03, PCB). Data acquisition was performed at 500 kHz (9222, NI, TX) and all measurements were repeated ten times ($n = 140$). The measured natural frequencies were calculated using a Bode plot in order to compare them with the known values based on the implemented components.

Results: The measurements with the shaker estimated the natural frequency of the substitute model with a deviation of 2.5% (IQR: 1.1% to 16.3%; $n = 70$). For the mallet the estimation was only possible for the group with the lowest weight and therefore the highest natural frequency ($f_0 = 12.3$ Hz; $n = 10$ out of 70). The deviation over all shaker measurements was smaller than for the one group of the mallet ($p < 0.001$, Fig. 2).

This difference between shaker and mallet is associated to the frequency spectra of the short force impulses of the metal on metal mallet blows, which were broad, but did not cover the low natural frequencies of the different configurations of the model as the shaker did.

Conclusion: Excitation and measurement with a shaker in the surgical environment is considerably more complex than with a mallet. However, due to the significantly better results, this effort should be taken in order to determine a baseline for the mechanical boundary conditions during hip implantation.

Although the excitation of the mallet was not suitable for modal analysis, it demonstrates why implantations with short force impulses work well: they are overcritical and consequently do not excite the whole dynamic femur-tissue-system.

References:

[1] Doyle et al., J BIOMECH 2019

Acknowledgement:

The partial funding by DePuy Synthes is kindly acknowledged.

Figures

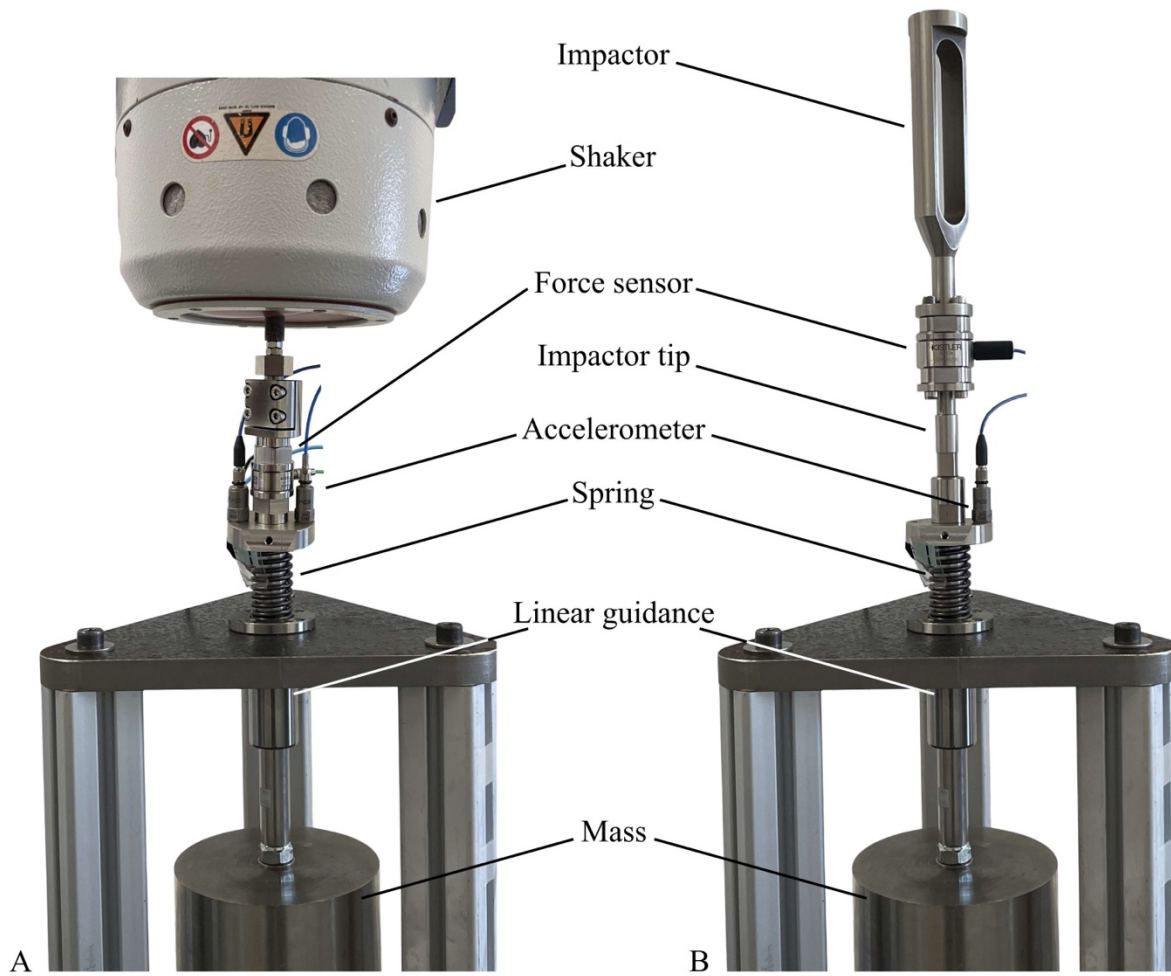


Figure 1: Experimental setup of the substitute model with (A) electrodynamic shaker and (B) instrumented impactor. The mass and the spring represent the femur with its surrounding tissue. The linear guidance was used to prevent buckling of the setup.

[Figure 1](#)

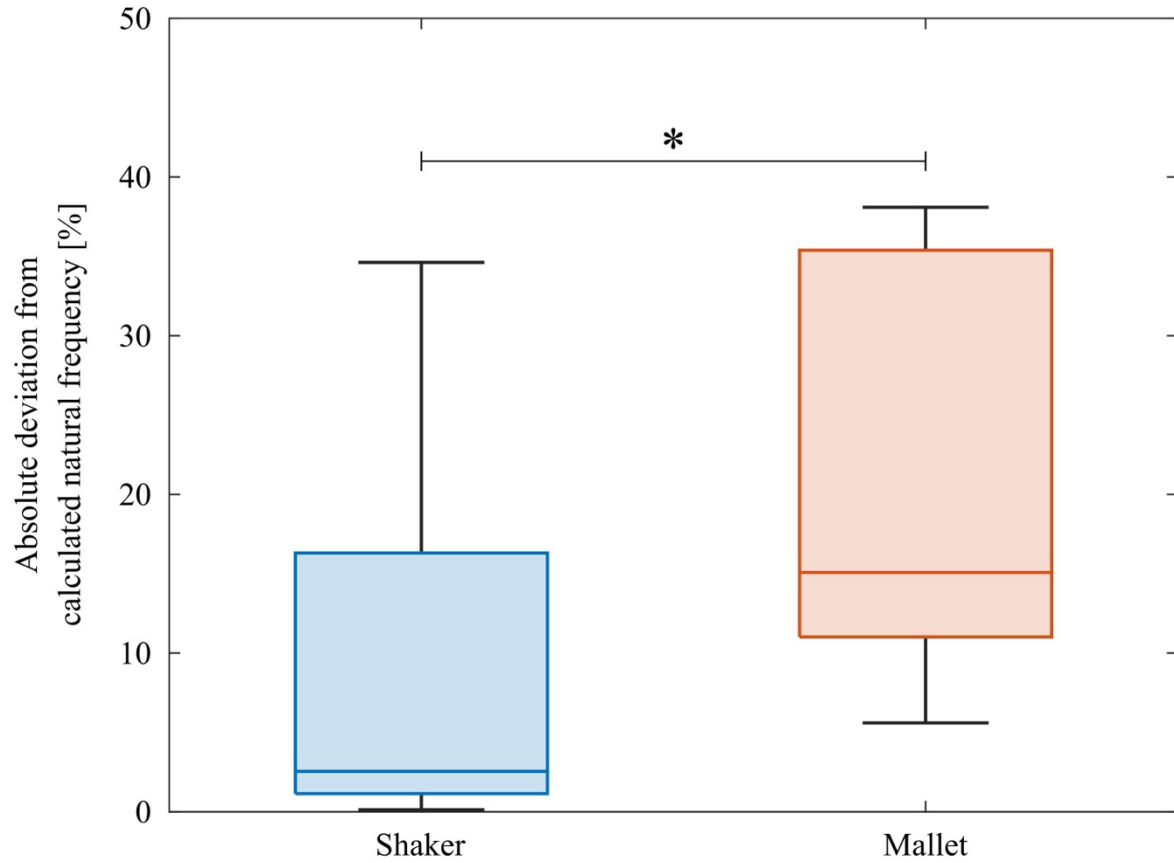


Figure 2: The absolute deviation from the calculated natural frequency was significantly smaller for the measurements with the shaker (all combinations of mass and stiffness, $n = 70$) than for the ones with the mallet (only one group with the highest natural frequency, $n = 10$).

[Figure 2](#)

Trapeziometacarpal Joint Contact Mechanics Pre- and Post-First Metacarpal Extension Osteotomy

*Max Campbell - Western University - London, Canada

Lauren Straatman - University of Waterloo - Waterloo, Canada

Assaf Kadar - St. Josephs Health Care - London, Canada

G Daniel Langohr - Canada

Hypothesis: The trapeziometacarpal (TMC) joint at the base of the thumb is one of the most affected joints by osteoarthritis in the hand. The biconcave-convex TMC saddle joint enables a wide breadth of motion yet is inherently susceptible to osteoarthritis as it lacks bony confinement, relying on ligamentous joint stabilization to support the joint. First metacarpal extension osteotomy has been a common surgical treatment of TMC osteoarthritis, aiming to correct the load direction in the arthritic joint and offload the high-stress volar compartment towards the dorsal compartment [1]. Previous cadaveric studies have examined the effect of extension osteotomy *in vitro*, but were limited in the range of osteotomies they could perform. This study aims to computationally evaluate how *in vivo* TMC joint contact area and stress changes after simulated osteotomy in a healthy cohort.

Methods: Three-dimensional models of four dominant TMC joints from healthy participants (mean age: 78 ± 4 years, sex: three female, one male) were constructed from CT data using Mimics image processing software. A segment fixed coordinate system was defined for the first metacarpal using *in vivo* joint proximity. A 50 N axial compressive force was applied to the first metacarpal distal articulation, simulating a four-kilogram lateral pinch. Next, 15°, 20°, 25°, and 30° extension osteotomies were performed virtually on each model, and the resulting change in joint contact area, peak first metacarpal volar beak cartilage contact stress, and overall joint peak cartilage contact stress was compared to the intact state.

Results: Following osteotomy, contact stress shifted dorsally on the first metacarpal, as shown by a reduction in volar beak contact stress pre- and post-osteotomy (Fig. 1). Osteotomy angles greater than 20° produced this effect, with no statistically significant difference detected in volar beak contact stresses pre- and post-15° osteotomy. There was no statistically significant difference in volar beak contact stress in osteotomy angles between 20°-30°. It was found that joint contact area and overall joint peak cartilage stress were unaffected by extension osteotomy (Fig. 2).

Conclusion: We have found that extension osteotomy angles greater than 20° effectively offloaded the volar compartment of the joint, supporting the findings of previous *in vitro* studies [1,2]. The findings from this work give clinicians more insight into the optimal extension osteotomy angle, improving the surgical technique.

References

[1] Pellegrini et al. *J. Hand Surg. AM.* 1996; 21(1): 16-23. [2] Koff et al. *J. Hand Surg. AM.* 2006; 31(3): 429-439.

Figures

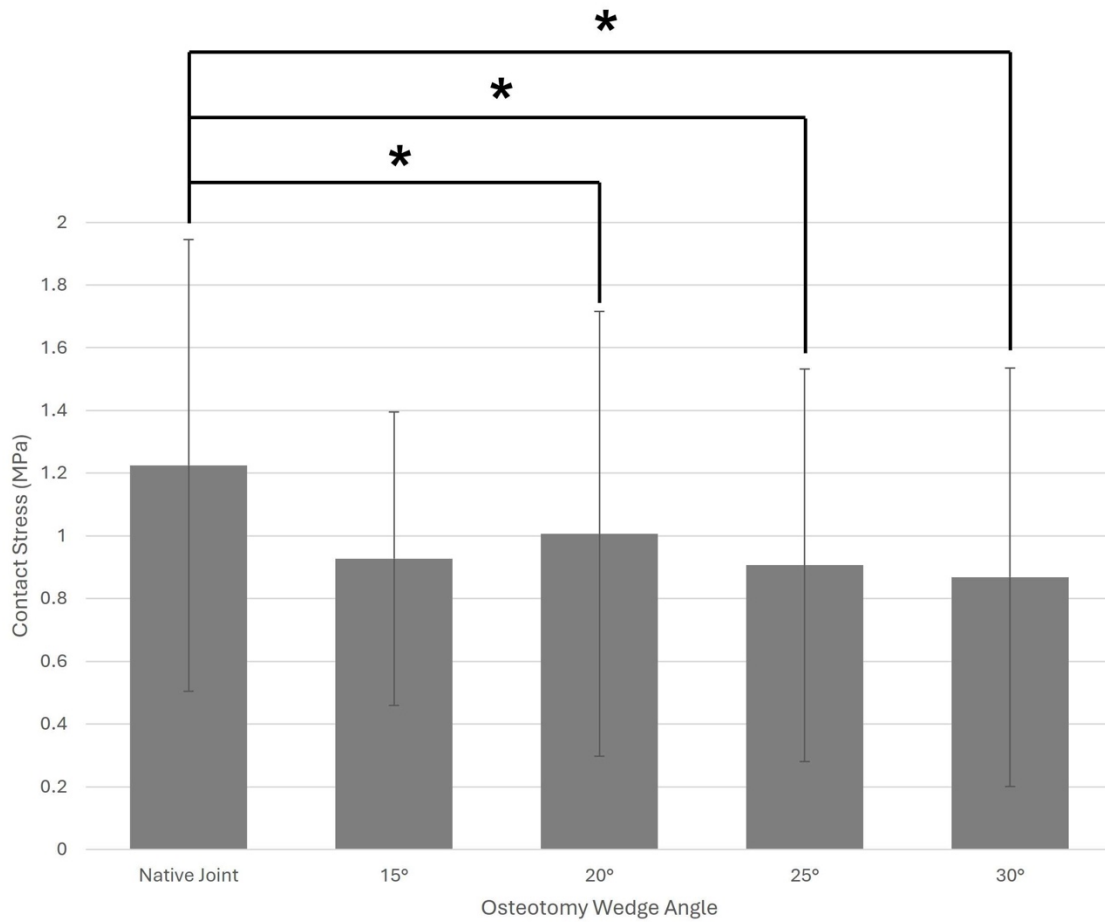


Fig. 1 Average peak cartilage contact stress in the first metacarpal volar beak for various osteotomy angles and the native joint.

**. $p \leq 0.05$, statistically significant difference from reference the native joint.*

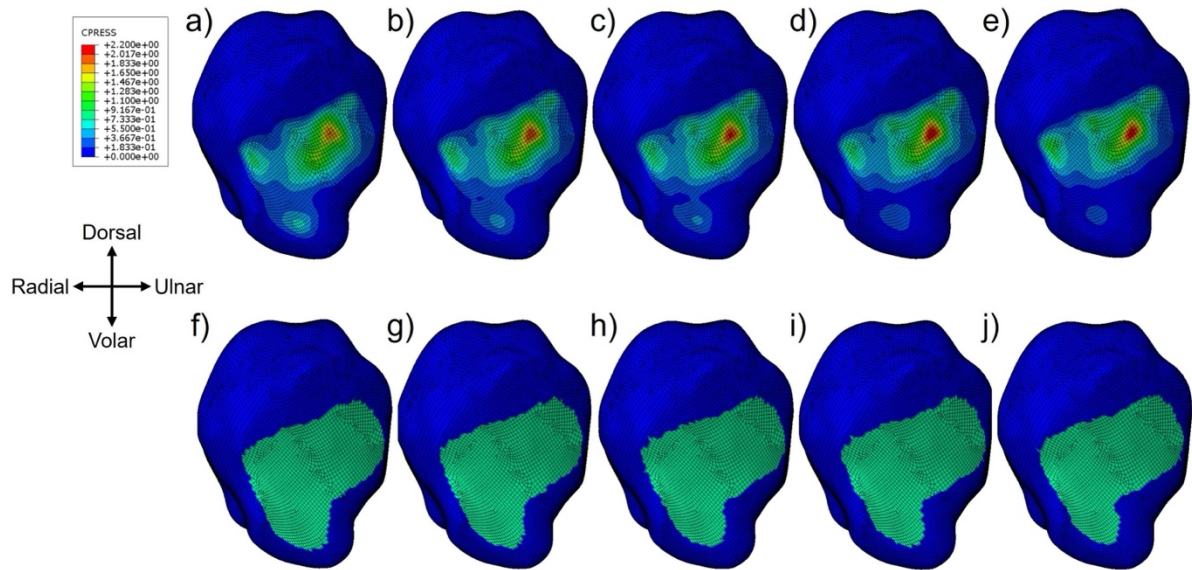


Fig. 2. Representative TMC joint contact stress (top, MPa) mapped on the proximal articulation of the first metacarpal in the a) native joint, and following b) 15° osteotomy, c) 20° osteotomy, d) 25° osteotomy, and e) 30° osteotomy. Joint contact area is also mapped (bottom) in the proximal articulation of the first metacarpal in the f) native joint, and following g) 15° osteotomy, h) 20° osteotomy, i) 25° osteotomy, and j) 30° osteotomy.

Figure 2

Wrist Kinetics Post-Scapholunate Dissociation: Experimental and Computational Analysis of Scapholunate Interosseous Ligament Injury

Wedam Nyaaba - University of Illinois at Chicago - Chicago, United States of America

Mark Gonzalez - Chicago, USA

Alfonso Mejia - University of Illinois at Chicago College of Medicine - Chicago, USA

Sunjung Kim - University of Illinois Chicago - Chicago, United States of America

Majd Mzeihem - American University of Beirut - Beirut, Lebanon

*

-

Introduction

Scapho-lunate dissociation leads to significant arthritis in the radiocarpal joint due to abnormal translation and joint angle deviation. This study aimed to investigate the critical deviations in the scapho-lunate joint caused by both partial and complete tears of the scapho-lunate ligament and further validate the degenerative findings through a CT-based Finite Element Analysis.

Method

The research study used eight specimens of wrist bones that were mounted on a customized rig. The objective was to study the impact of Scapholunate dissociation on the wrist. Sensors were used to measure contact pressure and motion sensors were attached to the scaphoid and lunate bones to track their movement during flexion. A finite element model was utilized to simulate wrist kinematics and investigate pressure distribution. Statistical analysis was conducted using the Friedman test with pairwise comparisons to determine the differences in movement and contact pressure among different conditions.

Result

The movement of the scaphoid and lunate bones significantly varied with ligament condition, showing increased scapholunate distance in distal and proximal directions and decreased in medial and lateral directions for complete tears. In addition, a significant lateral deviation of the scaphoid and lunate was found when the ligament was damaged. Lunate angles shifted from flexion to extension, while scaphoid angles did the opposite. Ligament tears reduced finger pressure without affecting wrist pressure (Table 1). The findings, confirmed by finite element analysis and experiments, accurately replicated scaphoid and lunate movements, with peak radiocarpal pressure significantly differing between intact and fully torn ligaments (Fig. 1 & 2) ($P < 0.05$).

Conclusion

According to our research, SLL damage significantly impacts the stability of the wrist joint, with a particular effect on the motion and angles of the scaphoid and lunate bones. Although there were no notable alterations in the contact pressure or joint surface area, our experimental findings were validated through finite element analysis and provided additional degeneration states of cartilage under these conditions.

Figures

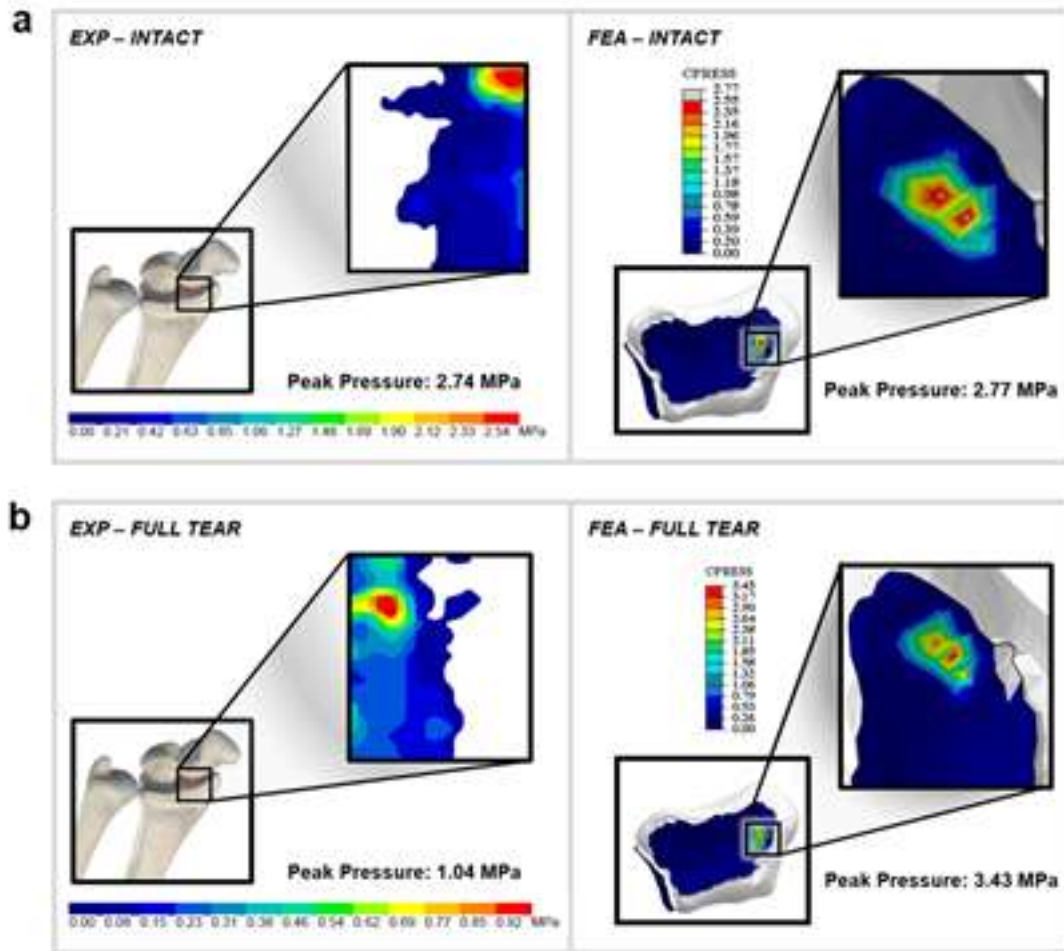


[Figure 1](#)

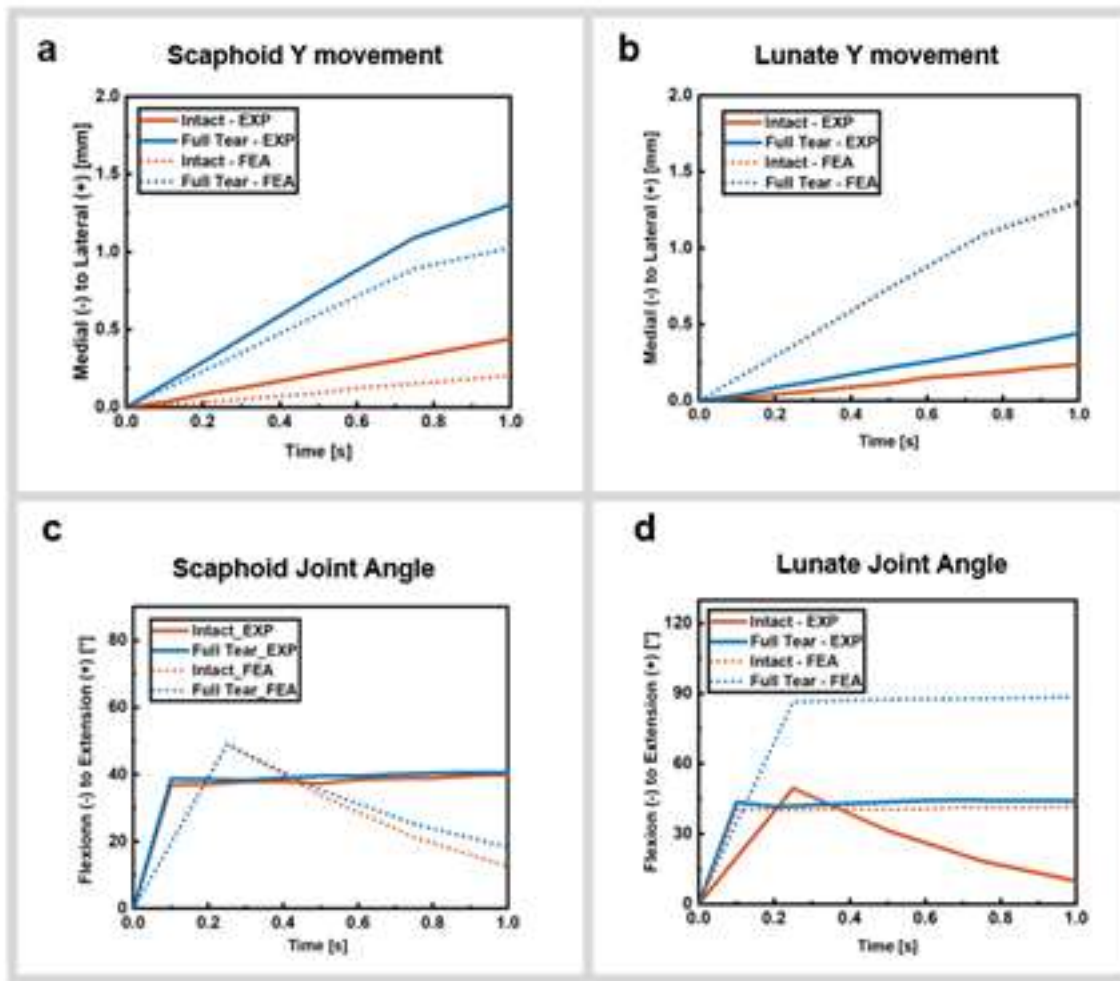


Figure 2

Scapholunate Gap	Fully Intact	Partial Tear	Full Tear	P-value
X Coord	-0.29 ± 0.34^a	0.17 ± 0.41^b	0.36 ± 0.66^b	<0.05
Y Coord	0.95 ± 0.37^a	0.11 ± 0.10^b	0.26 ± 0.14^c	<0.05
Z Coord	-2.30 ± 1.06^a	-1.35 ± 0.87^b	-1.03 ± 0.62^c	<0.05
Angle	Fully Intact	Partial Tear	Full Tear	P-value
Lunate	-15.7 ± 17.9^a	-20.4 ± 7.9^a	5.17 ± 5.32^b	<0.05
Scaphoid	27.3 ± 16.3^a	-37.0 ± 19.9^b	-25.5 ± 12.3^c	<0.05

^{a-c} Significance is represented by different letters, each denoting statistical significance within the analysis context.

Figure 3

Evaluation of Error Sources for an Image-Based Computer Assisted Surgical System for Total Ankle Arthroplasty

*Matthew Rueff - Exactech - Gainesville, USA

Zachary Tupper - Exactech - Gainesville, USA

Prudhvi Tej Chinimilli - Exactech - Gainesville, USA

Scott Gulbransen - Exactech - Gainesville, USA

Laureline Prouvost - Blue Ortho - Grenoble, France

Edward Haupt - Mayo Clinic - Jacksonville, USA

Matthew Hamilton - Exactech - Gainesville, USA

Laurent Angibaud - Exactech, Inc. - Gainesville, USA

Introduction

Computer Assisted Surgical (CAS) systems have been used successfully in joint arthroplasty to improve the accuracy of bony resections. The whole procedure is a suite of numerous surgical steps, and even using CAS systems, each of these steps may be associated with error such as mispositioning of the cutting block, play between the sawblade and the cutting slot due to the length and width of slot, or saw bending and skiving of the blade during the resection. The objective of this study was to evaluate error sources of the individual surgical steps for an image-based CAS system for total ankle arthroplasty (TAA).

Study Design & Methods

TAA was performed by a board-certified, fellowship-trained orthopedic surgeon on twelve artificial ankle joint specimens (PN1132-3, Pacific Research) using a CAS system (ExactechGPS, Blue-Ortho) featuring a dedicated ankle application. Video tracking was performed to confirm surgical technique was standardized for all specimens. Scans of each of the twelve specimens were performed before TAA using a structured light industrial scanner (Comet L3D, Steinbichler) used for assessing surface profiles with an accuracy better than 50 μ m. From the initial scan, a DICOM series representative of the CAS system recommended CT scan protocol was created from each model for segmentation, and a model coordinate system was created corresponding to the bony anatomy and mechanical axis of the specimen's tibia and talus. Bone resections were individually virtually planned and performed by the surgeon using template software to choose appropriate implant position and size relative to the bony anatomy. The resected bones were scanned and overlaid with the initial model for assessment of the error relative to the original plan. Opportunities for error were identified during positioning, execution, and verification (Figure 1).

Results

Mean and 95 % confidence intervals for positioning, execution and verification errors were less than 2mm and 2° (Figure 2 and 3). Average absolute errors for the tibia were: 0.30°/.26mm for positioning, 0.87°/.53mm for execution, 0.89°/.56mm for verification, and 0.74°/.59mm overall. Average absolute errors for the talus were: 0.82°/.52mm for positioning, 0.41°/.51mm for execution, 0.64°/.62mm for verification, and 1.13°/.67mm overall.

Conclusions

TAA performed with a CAS system resulted in overall error less than 2mm and less than 2° on all specimens. Design elements of the CAS system likely contribute to

the low observed error. The surgeon receives visual confirmation of the plan and resection confirmation throughout the procedure which allows for real-time adjustments. The positioning error on the tibia was lower in comparison to the talus because the tibial instrumentation allows adjustment of each degree of freedom individually, whereas the talar instrumentation required positioning of the foot in all degrees of freedom concomitantly. Future work should consider additional surgeon users, cadaver specimens with ankle arthritis and/or deformity, and comparison to patient-specific instrumentation (PSI) and traditional conventional techniques. There is future potential to remove the need for other fluoroscopy based checks for positioning guides which could reduce the burden on the user and reduce radiation exposure of the patient during TAA.

Figures

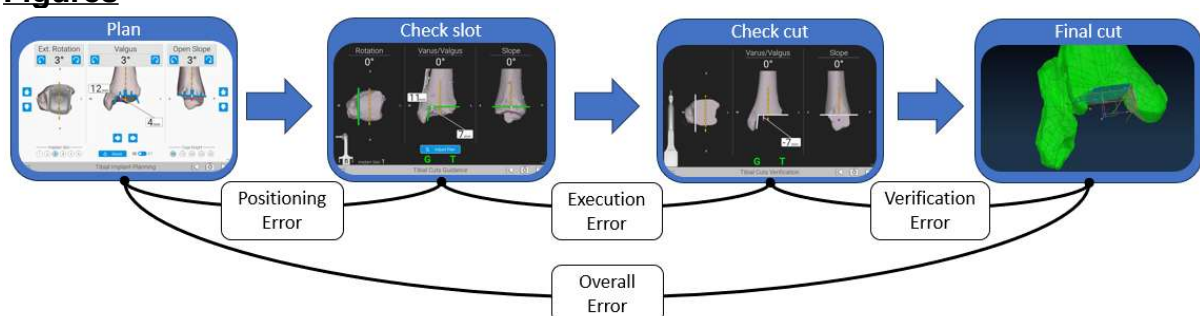


Figure 1: Flow of procedure and four investigated error sources in navigated TAA

Figure 1

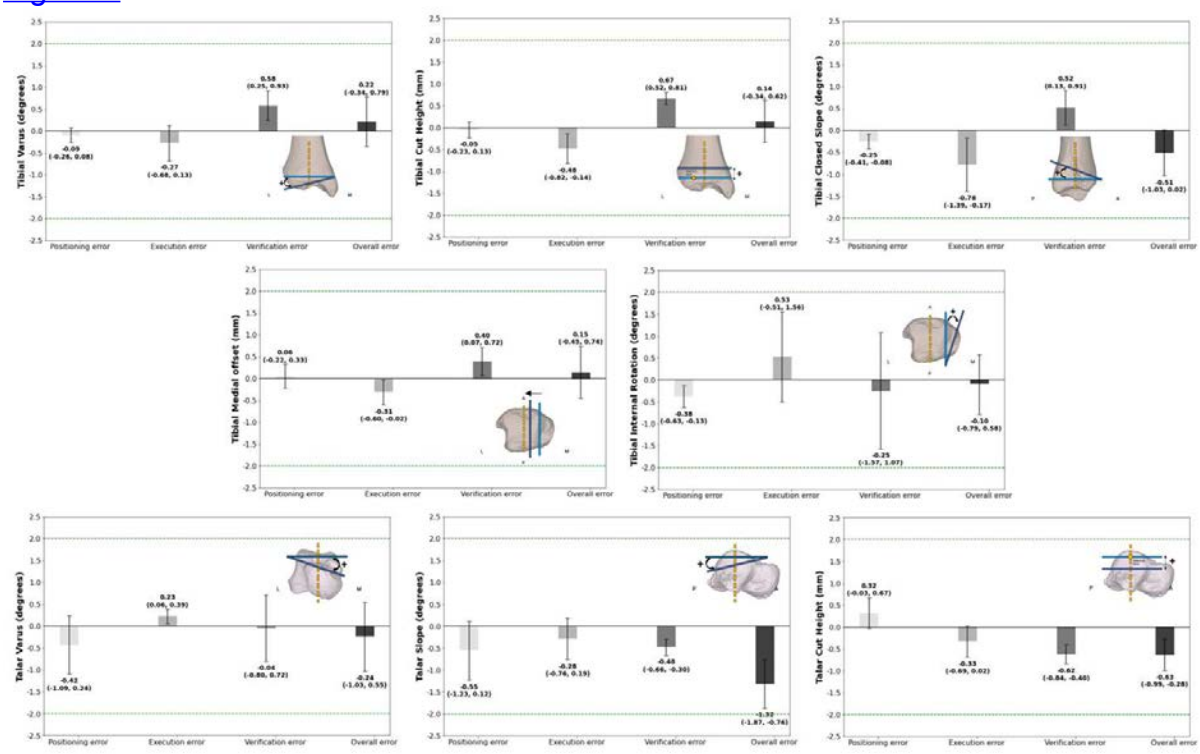


Figure 2: Error bar plots of Mean and 95% CI of error, Green lines at 2mm and 2°

Figure 2

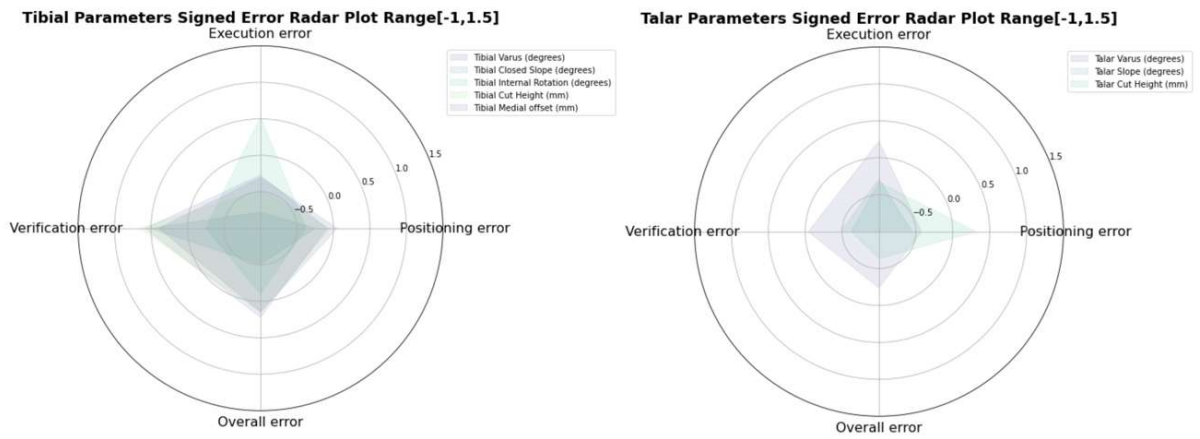


Figure 3: Radar plots of signed error (Range -1 to 1.5)

[Figure 3](#)

The 45 Most Cited Publications in Total Ankle Arthroplasty Revisions: A Bibliometric Analysis

*Thellma Jimenez Mosquera - NYU Langone Health - New York, United States of America

Grace Flynn - NYU Langone Health - New York, USA

Hugo Ubillus - NYU Langone Health - New York, USA

Raymond Walls - NYU Langone Health - New York, United States of America

INTRODUCTION: The understanding of total ankle arthroplasty (TAA) and optimal surgical management of end-stage ankle arthritis has significantly expanded over the last decade, evidenced by the increasing number of primary TAA surgeries being revised. Characterizing the most influential studies in total ankle replacement revision surgeries can clarify controversies regarding complications, identify core literature, and further collective knowledge for educational purposes. We conducted a comprehensive bibliometric analysis regarding revision total ankle arthroplasty to evaluate the significance and influence of these online sources.

METHODS: Using the search terms 'revision' AND 'total ankle replacement' OR 'TAR' OR 'total ankle arthroplasty,' we systematically searched through the top 45 most cited articles in The Science Citation Index Expanded subsection of the Web of Science Core Collection. Publication and study characteristics were extracted and reported using descriptive statistics for the total number of citations, citation rate, publication year, journal, implant type, and level of evidence. Spearman correlations were calculated to assess the relationship between citation data and the level of evidence.

RESULTS: 728 results were yielded from our initial search. 45 articles were published between 2004 and 2024, with 20% published in 2020. The top 45 cited papers had a mean of 11.35 citations (range: 0 to 68 citations), and the citation rate was 4.18 ± 7.6 citations per year. These articles were published across 16 different journals, mentioning 24 different implant types. The top three most frequently referenced implants were Agility (13 citations), STAR (13 citations), and Hintegra (12 citations). Most studies were level of evidence III (33, 73.3%), with the remaining articles classified as level of evidence IV. A significant positive correlation was found between the year of publication and citation rate ($r=0.38$, $p=0.009$).

CONCLUSION: This study provides a current landscape of the most cited articles in TAA revision surgeries. With the increase in these procedures over the past two decades, this study serves as the first historical landmark in the literature and a launching point for future research. As TAA becomes a more common option for end-stage arthritis, we anticipate a corresponding increase in revisions. Therefore, bibliometric analyses will play an important role for surgeons and future researchers in identifying foundational papers and research trends regarding this emerging procedure.

Effect of Patient Specific Alignment Total Knee Arthroplasty on Coronal Alignment of the Ankle Joint in Patients With Varus Knee Deformity

*Ittai Shichman - Tel-Aviv Sourasky Medical Center - Tel Aviv, Israel

Amer Hallak - Tel Aviv Sourasky Medical Center - Tel Aviv, Israel

Itay Ashkenazi - NYU Langone Health - New-York, United States of America

Yaniv Warschwaski - Tel Aviv Sourasky Medical Center - Tel Aviv, Israel

Aviram Gold - Tel Aviv Sourasky Medical Center - Tel Aviv, Israel

Nimrod Snir - Tel Aviv Sourasky Medical Center - Tel Aviv, Israel

Keywords: Patient Specific Alignment, Coronal Alignment, Ankle Joint

Background

Varus or valgus knee deformities influence and amplify ankle coronal alignments. The impact of Total knee Arthroplasty (TKA) on ankle joint alignment has not been entirely illustrated. Patient-specific alignment (PSA) is a surgical philosophy that aims to restore soft tissue balance, function and native anatomy within validated boundaries to restore restrictive native kinematics.

Objectives

Therefore, this study aimed to investigate the postoperative consequences of patient-specific alignment on the coronal alignment of the ankle in varus knee deformity patients who underwent PSA TKA. We hypothesized that greater preoperative varus malalignments would correlate with greater postoperative ankle coronal alignment change.

Study Design & Methods

This prospective study assessed patients who underwent imageless navigation assisted robotic TKA using a single implant design for primary osteoarthritis between January 2022 and February 2023. Preoperative and postoperative full-length standing AP X-ray imaging were used to measure Hip-Knee-Ankle (HKA), Tibial Plafond Inclination (TPI), Talar inclination (TI), and Tibiotalar Tilt (TTT) angles. Patients were subsequently divided into groups of varus ($<10^\circ$, N=59) and severe varus ($>10^\circ$, N=26) according to the preoperative HKA angle.

Results

Significant changes in preoperative and postoperative HKA angles were found in the neutral varus (4.6° vs 3.5° , $p=0.021$) and severe varus (14.4° vs 6.7° , $p<0.001$) groups. Minimal changes between preoperative and postoperative TPI, TI, TTT angles were found, greater in the severe varus group, however did not reach statistical significance. Delta change from pre to postoperative HKA was significantly higher for the severe varus group (7.7° vs 1.8° , $p<0.001$). Delta change of TPI, TI and TTT did not differ between groups.

Conclusions

TKA coronal alignment affects coronal alignment of the ankle. Patient specific alignment of varus knee deformity preserves or minimizes substantial coronal alignment changes of the ankle joint. These findings may add to the benefits of patient specific alignment TKA techniques.

Figures

METHODS – Measurements

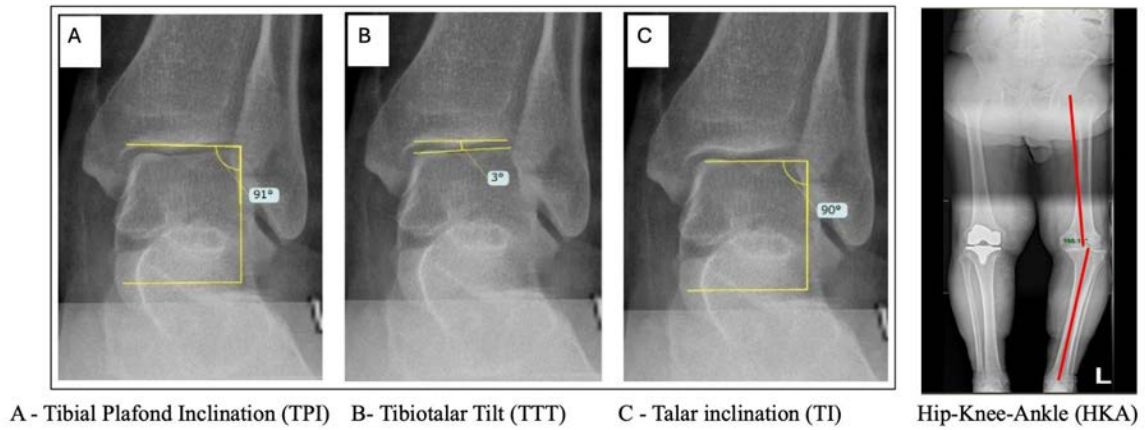


[Figure 1](#)

A Rare Case of Metallosis on Metal on Metal Hip Resurfacing

*Lafayette Lage - Clinica Lage - sao paulo, Brazil

Gustavo Lage - Clinica Lage - São Paulo, Brazil

Introduction: Metal on metal hip resurfacing is an ideal prosthesis to save bone stock since any hip replacement is temporary. Its implantation for sportsmen is ideal due to its stability and longevity.

Methods: The authors present a rare case of metallosis in a 73 years old male patient who used to be very active and played soccer twice a week. A hybrid Corin resurfacing prosthesis (54 mm uncemented acetabular component with a 48 mm cemented femoral component) was implanted on his right hip on June 4th, 2004 and a Corin cementless resurfacing prosthesis (both 54 mm acetabular and 48 mm femoral components were uncemented) was implanted on his left hip on June 8th, 2004 although both hips could be uncemented due to osteoarthritis and the femoral components.

Just after both surgeries he was diagnosed with primary testicle cancer with lung metastasis. One testicle was removed and was introduced just after.

A few months later the cementless femoral component became varus after a strong ball kick during the soccer game. His left leg became 15 mm shorter but he had no pain. He was examined by professor Harlam C. Amstutz at that time who indicated revision of the femoral component but the patient refused to do since he was feeling ok and simply raised 15 mm his shoe sole and used inserts in his tennis and special soccer shoes and kept playing soccer twice a week.

After 15,5 years he returned referring pain in his left hip and was submitted to revision one month later.

Surgical findings showed a huge cystic lesion and blood test with increased metal ions.

He had a good recovery and the films, pictures, and lab results will be presented.

Conclusion: Metal on Metal hip resurfacing showed good resistance in long terms even in a mispositioned femoral implant.

Figures
067

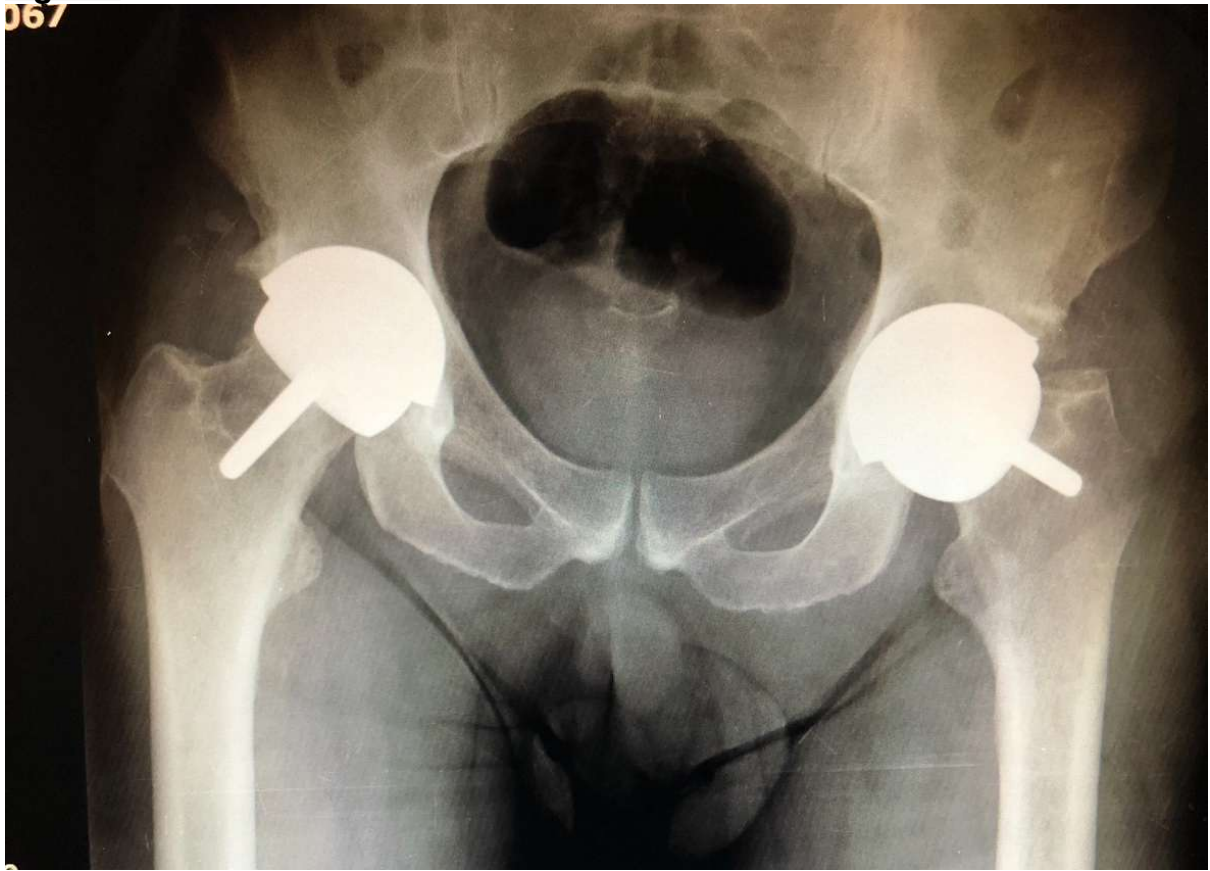


[Figure 1](#)

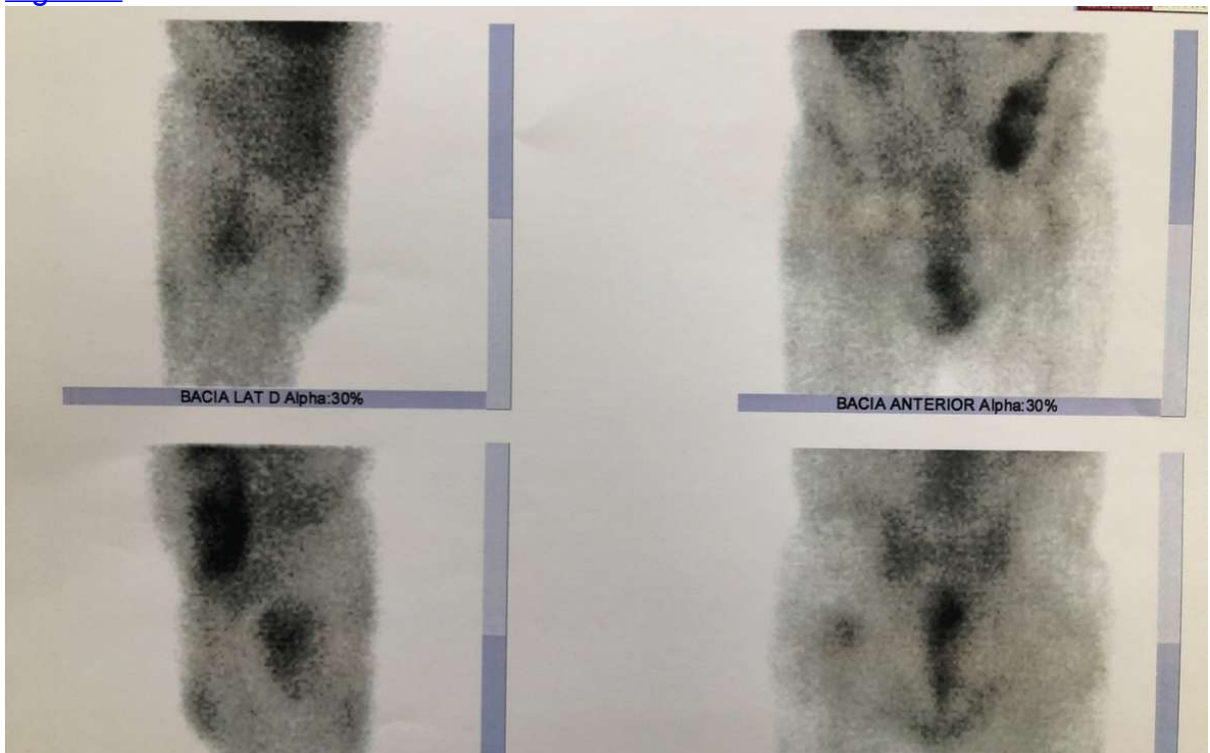


[Figure 2](#)



[Figure 3](#)

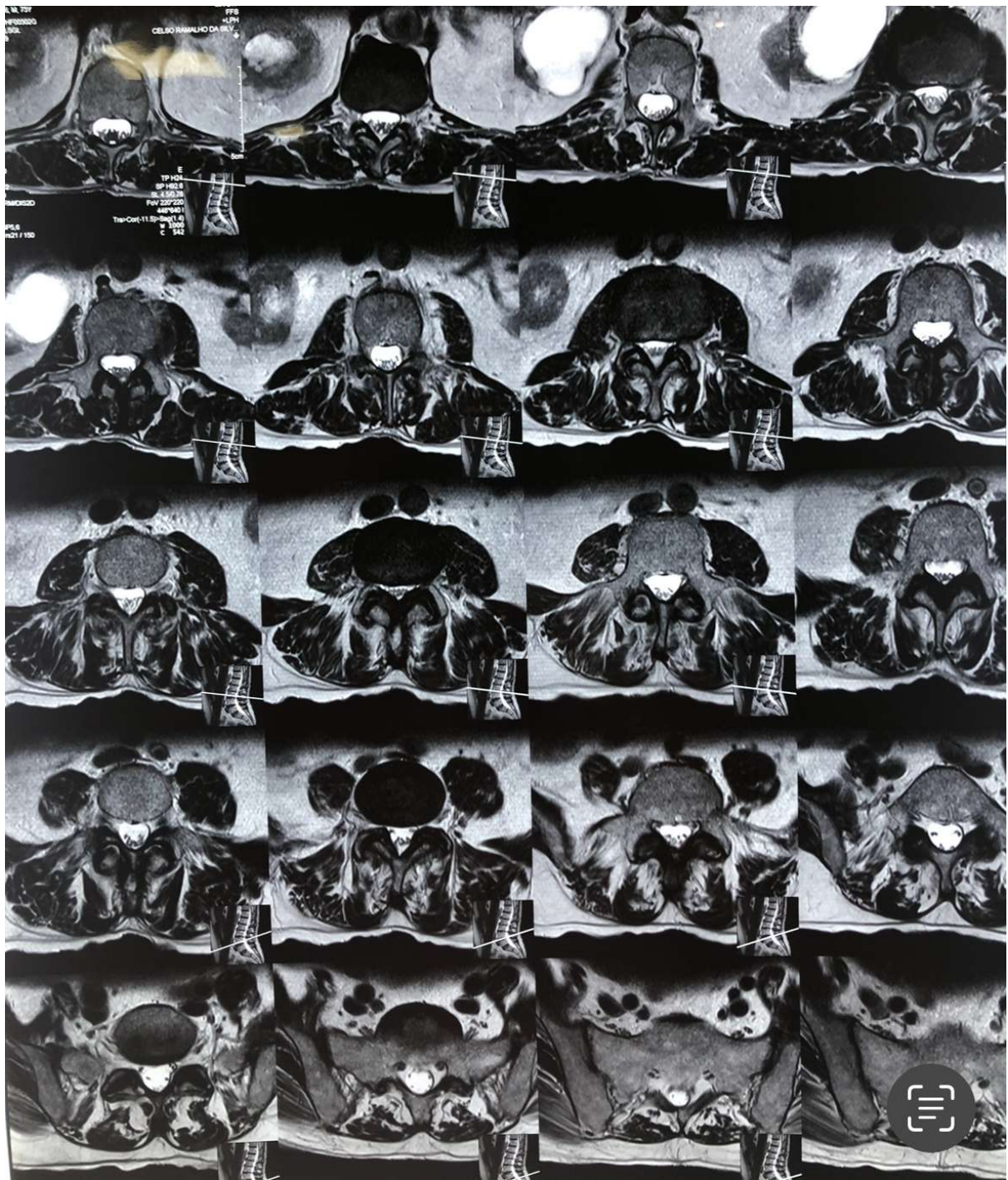


Figure 4

Association of Acetabular Cup Uncoverage With Groin Pain Following Total Hip Arthroplasty

*Gerard Smith - Corin - Sydney, Australia

Maeve Kelaher - The University of Sydney - Sydney, Australia

Jim Pierrepoint - Corin - Cirencester, United Kingdom

Christopher Plaskos - Corin - Raynham, USA

Michael O'Sullivan - Mater Clinic - Wollstonecraft, Australia

Suboptimal positioning of the acetabular cup, particularly when it results in anterior uncoverage, is a known precursor to iliopsoas tendinitis, which may necessitate revision surgery. Although the link between cup uncoverage and groin pain is established, comprehensive understanding of the specific thresholds, prevalence, and the contributory impact of spinopelvic mobility remains underexplored. This study aims to quantify the effects of acetabular cup uncoverage and spinopelvic mobility on groin pain, with the goal of enhancing preoperative strategies and reducing the risk of postoperative complications.

A retrospective analysis of post-operative CT scans was performed on 299 THA patients, including 137 asymptomatic controls and 162 patients reporting groin pain, sourced from a multi-center international medical imaging database. Measurements of acetabular cup uncoverage (Figure 1) in axial and sagittal CT slices were conducted (RadiAnt, Poland). By convention, cup uncoverage is denoted as positive (+). A logistic regression model calculated odds ratios to evaluate the association of groin pain with various degrees of uncoverage. This model also generated predicted probabilities for Receiver Operating Characteristic (ROC) and area under the curve (AUC) analysis to assess diagnostic performance. Pelvic tilt (PT) was measured using the anterior pelvic plane, with anterior tilt defined as positive. Lumbar flexion (LF) was defined as the change in lumbar lordotic angle between standing and flexed seated positions.

Patients reporting groin pain had higher sagittal (2.1 ± 8.1 mm vs -3.2 ± 4.9 mm, $p < 0.0001$) and axial (-0.4 ± 6.5 mm vs -5.0 ± 2.9 mm, $p < 0.0001$) uncoverage than the asymptomatic controls (Figure 2). Sagittal and axial uncoverage over 5 mm were associated with an increased odds of groin pain of 5.4 (95% CI: 2.8-8.7, $p < 0.001$) and 28.9 (95% CI: 6.8-119.5, $p < 0.001$) times, respectively. The ROC curve analysis indicated an AUC of 0.76, with a sensitivity of 62% and specificity of 87%. Significant associations were observed in spinopelvic parameters, with the groin pain group exhibiting more posterior standing pelvic tilt ($-4.1 \pm 7.6^\circ$ vs $-1.9 \pm 6.8^\circ$, $p = 0.020$), a greater Δ PT from standing to seated ($6.2 \pm 14.8^\circ$ vs $2.2 \pm 14.7^\circ$, $p = 0.033$), and reduced LF ($39.3 \pm 17.5^\circ$ vs $44.7 \pm 13.7^\circ$, $p = 0.005$) compared to the asymptomatic controls. Gender was the only demographic factor found to be significant ($p = 0.007$). Cup uncoverage is associated with groin pain following THA, wherein patients with 5 mm or more of uncoverage in the sagittal or axial planes had significantly higher odds of reporting groin pain postoperatively. Our findings emphasise the need for precise preoperative planning combining lateral spinopelvic mobility assessments with 3D placement to enhance outcomes and minimise revisions.

Figures

Uncoverage Measurements in the Sagittal and Axial Planes

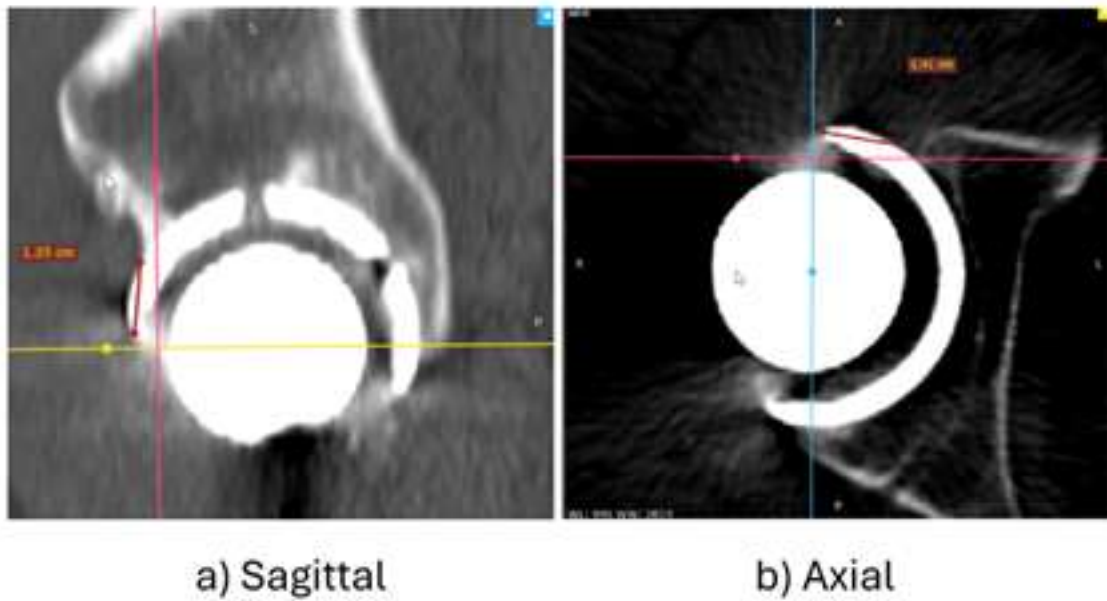


[Figure 1](#)

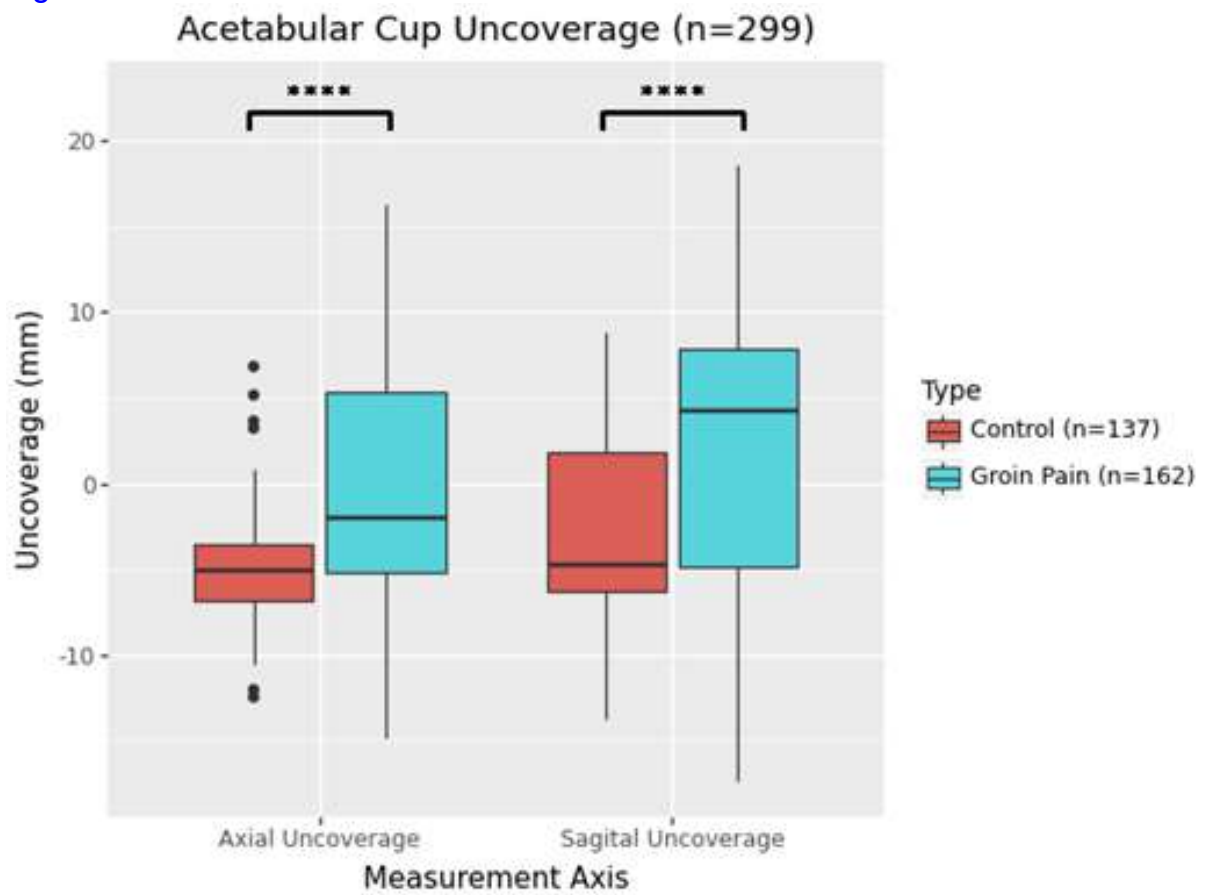


[Figure 2](#)

Sagittal Spinal Malalignment in Patients With Iliopsoas Tendonitis Following THA

*Joshua Twiggs - University of Sydney - Sydney, Australia

Brad Miles - 360 Knee Systems - Pymble, Australia

Max Hardwick-Morris - University of Sydney - Sydney, Australia

William Walter - Specialist Orthopaedic Group - North Sydney, Australia

Jitendra Balakumar - Melbourne Orthopaedic Group - Melbourne, Australia

Introduction: Iliopsoas tendonitis occurs in between 5-30% of patients after hip arthroplasty^[1, 2] and is mainly attributed to impingement between the acetabular cup and iliopsoas. In this study, which was motivated by the work of Okamoto et al. who found relationships between the psoas muscle index, pelvic incidence (PI) minus lumbar lordosis (LL), and a patient perceiving their hip as artificial, we report on spinopelvic parameters in patients who were diagnosed with, and treated for, iliopsoas tendonitis after hip arthroplasty.

Method: This retrospective study included a cohort of 24 patients who experienced iliopsoas tendonitis after total hip arthroplasty (THA) and a cohort of 13 patients who experienced iliopsoas tendonitis after hip resurfacing arthroplasty (HRA). All patients had previously had postoperative functional radiography taken. This included a standing x-ray, which was then measured for pelvic tilt (PT), PI, and LL. This permitted calculation of the PI-LL spinopelvic metric. Using this metric, a value of between -10° and 10° is defined as having 'normal' sagittal spinal alignment, a value of greater than 10° is defined as having flatback deformity, and a value of less than -10° is defined as having Hyperlordosis.

Results: In the symptomatic THA cohort, the mean standing PT was -3.0° (-19.8° to 13.3°), the mean PI was 56.0° (39.7° to 76.9°), the mean LL was 57.1° (33.1° to 82.0°), and the mean PI-LL was -1.1° (-21.8° to 29.7°). 14 (58%) patients were outside the normal PI-LL range with 6 patients have $PI-LL > 10^{\circ}$ and 8 patients with $PI-LL < -10^{\circ}$. In the symptomatic HRA cohort, the mean standing PT was -3.3° (-12.5° to 4.7°), the mean PI was 52.2° (35.1° to 65.2°), the mean LL was 49.7° (-2.9° to 74.0°), and the mean PI-LL was 2.5° (-9.5° to 38.0°). There was only one (7%) patient outside the normal PI-LL range (38°). The comparison between the THA and HRA cohort for standing PT, and PI – LL are displayed in Figure 1 and Figure 2, respectively.

Conclusions: The aim of our study was to investigate the prevalence of sagittal spinal malalignment in patients with iliopsoas tendonitis. Interestingly, over half of the THA cohort were outside the 'normal' range for PI-LL, but unexpectedly, there was a greater incidence of Hyperlordosis than flatback deformity. It is unclear if there is a direct link between iliopsoas tendonitis and sagittal spinal malalignment, particularly due to the low incidence of outliers in the HRA cohort potentially showing that sagittal spinal malalignment is more closely linked to age, and which direction causality is running. However, further research is warranted.

Figures

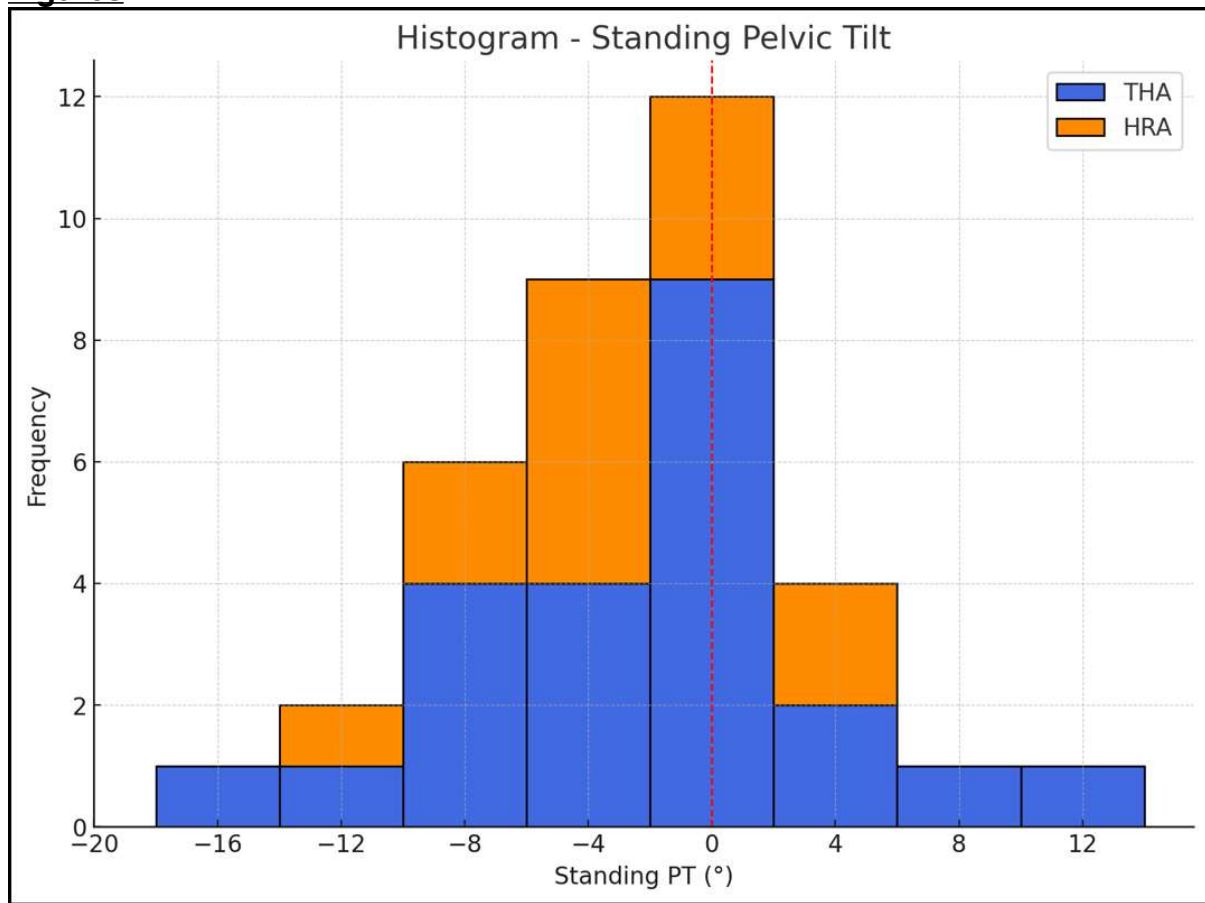


[Figure 1](#)

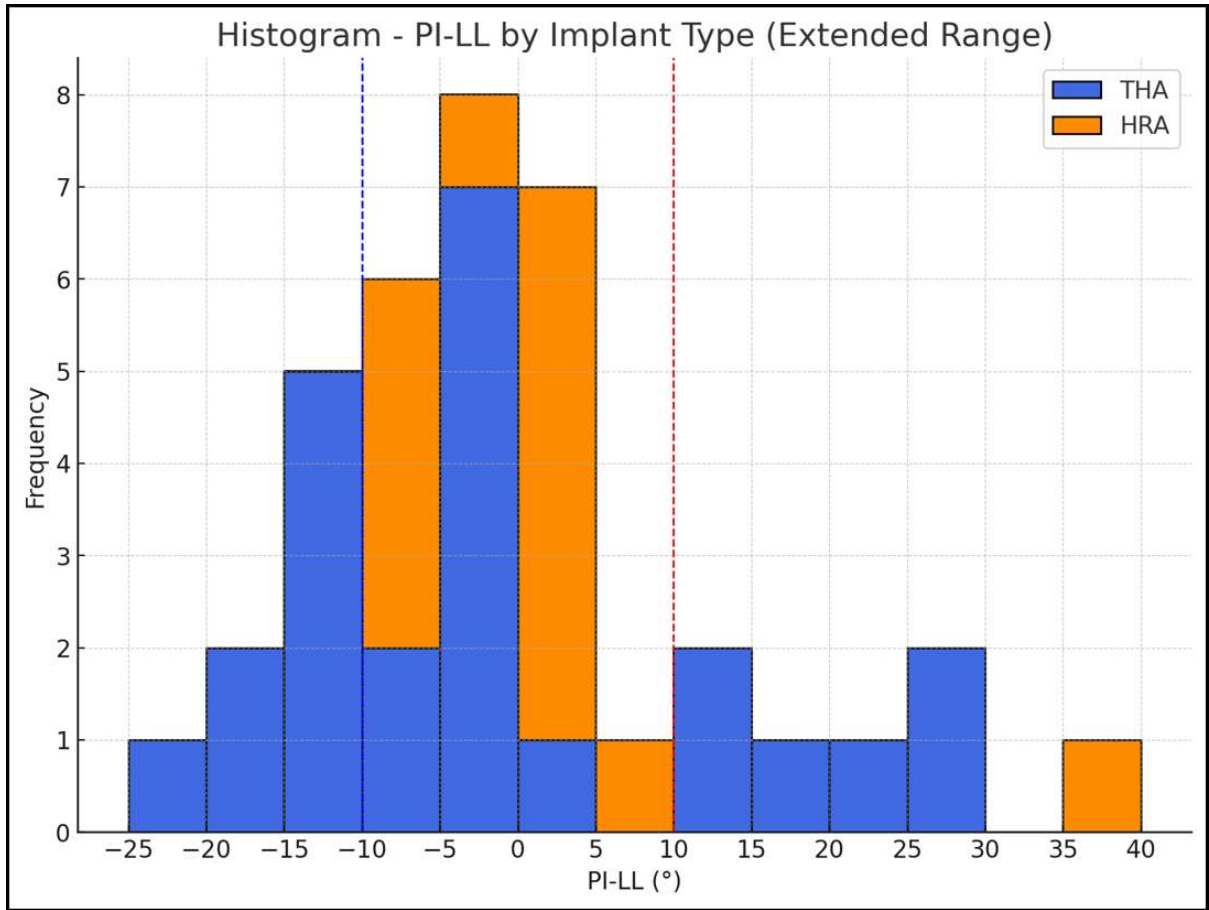


Figure 2

Risk Factors for Wound Complications in Direct Anterior Total Hip Arthroplasty: A 10-Year Analysis

*Muhammad Haider - NYU Orthopedic Hospital - New York, USA
Benjamin Schaffler - NYU Orthopedic Hospital - New York, USA
Amit Manjunath - NYU Langone Health - New York, United States of America
Michelle Richardson - NYU Langone Orthopedics - New York, USA
Akram Habibi - NYU Langone Orthopedic Hospital - New York, United States of America
Roy Davidovitch - NYU Langone Health - New York, USA
Matthew Hepinstall - NYU Langone Health - New York, USA
Joshua Rozell - NYU Langone Orthopedic Hospital - New York, USA
Catherine Digangi - NYU Orthopedic Hospital - New York, USA
Sophia Antonioli - NYU Langone - New York, USA

Background: The purpose of this study was to identify risk factors associated with wound complications following DAA THA and to evaluate the incidence of these wound issues when negative pressure wound therapy (NPWT) was used as the primary surgical dressing.

Methods: We reviewed 725 patients from five different surgeons at a single institution who underwent THA through a DAA from 2011-2023. Medical records were reviewed for demographics, comorbidities, surgical details, and a broad set of criteria denoting wound complications or dehiscence. Risk factors for wound complications were identified using univariate and multivariate analyses. Secondary outcomes included PJI, 90-day emergency room visits, readmission, and all-cause revision rates.

Results: 83 (11.4%) patients developed a wound complication based on criteria. Univariate analysis demonstrated that increased BMI (mean 30.4 vs. 27.8, $P<0.001$), surgical time (138.0 vs. 108.5 mins, $P<0.001$), longer hospital length of stay (50.4 vs. 40.6 hours, $p=.013$) and DAA surgeon experience of less than 1 year ($p=0.012$) were associated with wound complications. Multivariate analysis further demonstrated BMI and longer surgical time as risk factors and additionally demonstrated negative pressure wound therapy was associated with higher rates in high-risk patients (OR 2.1 [1.2-3.9], $p=0.016$). Wound complication patients had higher rates of 90-day emergency room visits (10.8 vs. 4.4%, $P=0.018$), more readmissions (15.7 vs. 3.9%, $P<0.001$), and more all-cause revision (19.3 vs. 2.8%, $P<0.001$) and PJIs (13.3 vs. 0.5%, $P=0.005$).

Conclusions: Obesity, length-of-stay, longer surgical time, and surgeon DAA experience less than one year were identified as risk factors for wound complications following DAA THA in our series. Prophylactic use of NPWT did not mitigate the risk of wound complications and was associated with increased risk in our cohort. Patients with wound complications had higher rates of PJI, readmission, and reoperation.

Figures

Table 1: Baseline Demographics for cohorts

Patient Variable	No Wound Complication (n=642)	Wound Complication (n=83)	P-Value
Mean Age (Years, range)	65.5 (21-97)	64.4 (21-84)	0.370
Sex (Female, %)	404 (62.9)	49 (59.0)	0.283
Mean BMI (kg/m ² , range)	27.8 (17.3-43.1)	30.4 (16.1-55.0)	<0.001*
Mean CCI (SD)	3.1 (2.5)	3.3 (2.5)	0.604
Mean Albumin (g/dL, range)	4.3 (3.5-5.1)	4.2 (3.4-4.9)	0.159
Active Diabetes Diagnosis (n, %)	43 (6.7)	8 (9.6)	0.218
Race (n, %)			
White	504 (78.5)	62 (74.7)	0.881
Black	53 (8.3)	8 (9.6)	
Asian	15 (2.3)	2 (2.4)	
Other	70 (10.9)	11 (13.3)	
Smoking Status (n, %)			
Never	358 (55.8)	39 (47.0)	0.116
Former	267 (41.6)	39 (47.0)	
Current	17 (2.6)	5 (6.0)	
ASA (n, %)			
I	46 (7.2)	4 (4.8)	0.030*
II	423 (65.9)	46 (55.4)	
III	170 (26.5)	31 (37.3)	
IV	3 (0.5)	2 (2.4)	

BMI; body mass index, CCI; [Charlson Comorbidity index](#), SD; Standard Deviation, ASA; American Society of Anesthesiologists

[Figure 1](#)

Table 2: Univariate analysis of Perioperative factors

Surgical Variable	No Wound Complication (n=642)	Wound Complication (n=83)	P-Value
Anesthesia Type (n, %) Regional General	575 (90.4) 67 (9.6)	68 (78.5) 15 (21.5)	0.035*
Anticoagulant Use (n, %) None DOAC Clopidogrel	621 (96.7) 18 (2.8) 3 (0.5)	79 (95.2) 3 (3.6) 1 (1.2)	0.527
Surgical Time (Mins, SD)	108.5 (34.5)	138.0 (103.9)	<0.001*
Estimated Blood Loss (mL, SD)	258.0 (112.3)	258.5 (115.9)	0.974
Wound Dressing (n, %) None PICO PREVENA	568 (88.5) 44 (6.9) 30 (4.7)	62 (74.7) 7 (8.4) 14 (16.9)	<0.001*
Length of Stay (Hours, SD)	40.6 (32.2)	50.4 (41.1)	0.013*
Discharge Disposition (n, %) Home SNF ARF	594 (92.5) 27 (4.2) 21 (3.3)	73 (88.0) 7 (8.4) 3 (3.6)	0.224

SD; Standard Deviation, Mins; Minutes, mL; Milliliters, SNF; Skilled Nursing Facility, ARF; Acute Rehabilitation Facility, DOAC; Direct Oral Anticoagulant

[Figure 2](#)

Table 3: Clinical Outcomes based on Presence of Wound Complications

	No Wound Complication (n=642)	Wound Complication (n=83)	P-Value
90-day ED Visit (n, %)	28 (4.4)	9 (10.8)	0.018*
90-day Readmission (n, %)	25 (3.9)	13 (15.7)	<0.001*
All-cause Revisions (n, %)	18 (2.8)	16 (19.3)	<0.001*
Revision Cause (n, %)			0.005*
Loosening	1 (0.2)	1 (1.2)	
Dislocation	9 (1.4)	0 (0)	
PPF	5 (0.8)	4 (4.8)	
PJI	3 (0.5)	11 (13.3)	

ED; Emergency Department, PPF; Peri-prosthetic Fracture, PJI; Peri-prosthetic Joint Infection

Table 4: Multivariate Regression for Odds of Developing a Wound Complication. BMI, NPWT use and surgical time remain significant risk factors for wound complication when other comorbidities are controlled.

Variable	OR [95% CI]	P-Value
Age	1.0 [0.97-1.0]	0.859
Male Sex	1.1 [0.65-1.76]	0.778
BMI	1.06 [1.01-1.11]	0.016*
CCI	1.0 [0.93-1.2]	0.574
ASA > 2	1.4 [0.81-2.4]	0.230
Diabetes	0.8 [0.4-1.8]	0.578
General Anesthesia	1.5 [0.7-2.9]	0.289
NPWT Use	2.0 [1.1-3.7]	0.024*
Surgical Time (Mins)	1.01 [1.003-1.014]	0.004*
Surgeon Experience > 1 Year	0.44 [0.16-1.17]	0.100

OR; Odds Ratio, CI; Confidence Interval, BMI; Body Mass Index, CCI; Charlson Comorbidity Index, ASA; American Society of Anesthesiologists, NPWT; Negative-Pressure Wound Therapy, Mins; Minutes

Figure 3

The Impact of Race and Gender on Complications and Healthcare Resource Utilization Following Shoulder Arthroplasty

*Garrett Jackson - Chicago, United States of America
Vani Sabesan - Cleveland Clinic Florida - Weston, USA
Anna Redden - FAU - boca raton, USA

Atharva Rohatgi - Charles E. Schmidt Florida Atlantic University - Boca Raton, USA
Carlos Fernandez - JFK / U Miami Orthopedic Surgery Program - Lantana, USA
Aghdas Movassaghi - Michigan State University - East Lansing, USA
Matthew McKinley - Florida Atlantic University, Charles E. Schmidt College of
Medicine - Boca Raton, USA

Introduction:

Racial disparities currently exist in the realm of healthcare that can have a significant impact on patient outcomes and access to quality care. Previous studies have indicated that Black patients are more likely to experience delays in treatment and increased surgical complications. Hispanic patients have more comorbidities and increased complications when undergoing orthopaedic surgeries. The purpose of this study was to analyze the effect of racial disparities on patient outcomes and healthcare resource utilization following Shoulder Arthroplasty (SA).

Methods:

A large healthcare network database was queried to identify 1,721 SA patients in the regional healthcare system between 2017-2021. Demographics, comorbidities, gender and race were collected. Race was defined as White, Black, Hispanic, Asian, and Other. Postoperative medical complications included sepsis, infection, disruption of the surgical wound, procedure-related complications, and embolism and thrombosis. Postoperative surgical complications included instability, dislocation, aseptic loosening, periprosthetic joint infection, periprosthetic fracture, hardware failure, revision, and wear and osteolysis. Patient outcomes collected include length of stay, readmission status at 30 and 90 days postoperatively, and ER visit within 90 days. Logistic regression and odds ratio point estimate analysis was utilized to assess for associations.

Results:

Of the 1,721 patients identified, 61.35% were female (n = 1,056) with an average age of 71 years and an average BMI of 29.47. The cohort included 7.79% Black (n=134), 29.98% Hispanic (n=516), 0.5% Asian (n=8), 0.9% Other (n=16), and 60.8% White (n=1,047). The average length of stay was 3.43 days, with 5.4% (n = 93) experiencing postoperative medical complications and 6.4% patients (n=111) experiencing postoperative surgical complications. There were no racial or gender disparities found for either postoperative medical or surgical complications. When assessing postoperative hospital readmission status, 8.6% (n = 148) were readmitted within 30 days and 20.3% (n = 349) were readmitted within 90 days in the cohort. Furthermore, 7.2% (n = 123) visited the ER within 90 days of surgery. Males were 17% more likely to be readmitted within 30 days ($p < .01$) and 13% more likely to be readmitted within 60 days ($p < .01$). Hispanic patients were 16% less likely to be readmitted within 60 days ($p = .01$) and 14% less likely to be readmitted within 90 days ($p = .02$) when compared to White patients. Race and gender were not significantly associated with ER visits within 90 days.

Conclusions:

Our results indicate no racial or gender disparities were found among patients undergoing SA when analyzing postoperative medical and surgical complications. Alternatively, males were more likely to be readmitted within 60 days from surgery and Hispanic patients were less likely to be readmitted within 90 days from surgery. Results from this large cohort study suggest that perhaps gender and race are factors to be considered in hospital-specific efforts in healthcare utilization. Further research is needed on the cultural impact of healthcare resource utilization and complications and to define specific link between race and determinants of health, socioeconomic status, access and outcomes after SA.

Diagnosis and Treatment of an Aseptic Loosening in a Triple-Cup-Construct Revision Hip Arthroplasty Due to Wear in the Interface of the Second and Third Cup

*Andrej Nowakowski - Kantonsspital Baselland - Bruderholz, Switzerland

Michael Robert Klauser - Kantonsspital Baselland - Bruderholz, Switzerland

Georg-Antonio Bernecker - Kantonsspital Baselland - Bruderholz, Switzerland

Introduction: Groin pain after multiple hip surgeries is often difficult to classify, especially when there are additional pathologies (e.g. hernias) in the differential diagnosis. In such situations, the usual diagnostic tools (SPECT-CT) to confirm/ rule out loose components may also be unspecific. Our aim was to highlight that in cup-in-cup revisions, clinical findings and joint test infiltration are crucial alongside imaging.

Case presentation: We present an 82-year-old patient with immobilizing hip pain under stress and during movement. The patient had undergone a primary total hip arthroplasty in 1986, followed by two total revision hip arthroplasty in 1992 and 2013. In each of these replacement surgeries, the acetabular cup was left in place and a new acetabular cup was cemented into the old one. The initial referral was made to our colleagues in the Department of Visceral Surgery, who diagnosed an inguinal hernia. Since the clinical findings and patient's history didn't suite for a symptomatic hernia, they introduced the patient to the Orthopaedic Depatement. Therefore, we took conventional radiographs, and performed a SPECT-CT scan witch were all not specific enough to lead to the correct diagnosis. Only combined with a test infiltration of the joint followed by an almost complete pain relief led to the correct diagnosis of a new aseptic loosening of the stem and cup due to wear.

Results: The clinical diagnosis was confirmed intraoperatively, one shell was no longer jammed in the multiple construct. The third cup (PE Flachprofil), which was cemented into the second cup (Morscher cup), could be easily tipped out with the PE remnants and anchoring holes still present. The mesh remnant of the second Morscher cup could also be completely removed with a light pull. Accordingly, we removed the remaining PE remnants and were able to cement a double mobility cup into the initial mash. Post-surgery, the patient was pain free and excellent mobilization in line with expectations after multiple previous operations with no signs of limping.

Conclusion: In individual cases, a cup-in-cup-in-cup revision may be an option. However, it should be noted that wear can occur at any interface, especially if the PE is not completely removed. In such cases, clinic and test infiltration may be more helpful than imaging (false negative SPECT-CT) in making the correct diagnosis, especially in the case of an asymptomatic inguinal hernia that was subsequently treated surgically.

Revision Rates After Single-Level Cervical Disc Arthroplasty Versus Anterior Cervical Discectomy and Fusion: An Observational Study With 5-Year Minimum Follow-Up

Adam Gordon - Maimonides Medical Center - Brooklyn, USA

Faisal Elali - SUNY Downstate Health Sciences University - Brooklyn, Select Country

Nikhil Vasireddi - Case Western Reserve University School of Medicine - Cleveland, USA

Matthew Magruder - Maimonides Medical Center - Brooklyn, USA

Hrishik Epuru - Maimonides Medical Center - Brooklyn, USA

Manas Gumedelli - Maimonides Medical Center - Brooklyn, USA

Nitish Polishetty - Maimonides Medical Center - Brooklyn, USA

Paul Mastrokostas - Maimonides Medical Center - Brooklyn, USA

*Mitchell Ng - Maimonides Medical Center - Brooklyn, United States of America

Objectives: Prospective studies have compared patient reported outcomes, adjacent segment degeneration, and long-term revisions between CDA and ACDF. Despite these high-level evidence studies, well-powered, large investigations have not been adequately reported. The aims were to compare rates and risk factors for all-cause 5-year revisions for patients undergoing primary single-level cervical disc arthroplasty (CDA) or Anterior Cervical Discectomy and Fusion (ACDF).

Methods: The 2010 to 2021 PearlDiver database was queried for patients undergoing primary single level CDA or ACDF for degenerative cervical spine pathology. Further inclusion criteria consisted of patients having a minimum of 5-year follow-up. Patients undergoing CDA were 1:5 ratio matched to patients undergoing ACDF by age, sex, individual comorbidities, and overall Elixhauser comorbidity index (ECI). Objectives were to compare the rates of all-cause 5-year revisions for those undergoing single level CDA versus ACDF and assess the risk factors associated with requiring a revision surgery. Trends in utilization of each surgery was compared by different subspecialty (neurosurgery vs orthopedic surgery). Multivariate logistic regression models were used to calculate odds ratios (OR) of revision surgery within 5 years of the primary procedure while controlling for age, sex, and individual comorbidities comprising the ECI. P values less than 0.001 were significant.

Results: After successful ratio matching, a total of 32,953 patients underwent single level CDA (N=5,640) or ACDF (N=27,313) with 5-Year minimum follow-up. The incidence of all cause revision within 5 years was 1.24% for CDA and 9.23% for ACDF (P<0.001). After adjustment, patients undergoing single level ACDF has significantly higher odds of all-cause revisions within 5 years (OR: 8.09; P<0.0001). Additional patient specific factors associated with revisions were a history of reported drug abuse (OR: 1.51; P<0.0001), depression (OR: 1.23; P<0.0001), cardiac arrhythmias (OR: 1.21; P=0.0008), hypertension (OR: 1.20; P=0.0006), and tobacco use (OR: 1.18; P=0.0003).

Conclusions: In this observational study of nearly 33,000 single level cervical spine surgeries with minimum 5-year follow-up, all-cause revision rates were significantly lower for patients undergoing CDA. Surgeons may use this data to counsel patients on nationwide reported revision rates up to 5-years from single level CDA or ACDF.

Total Hip Arthroplasty Decreases the Risk of Fall at High Fall Risk Patients With Hip

*Takamune Asamoto - Nagoya University - Nagoya, Japan

Yusuke Osawa - Nagoya University - Shizuoka, Japan

Hiroto Funahashi - Nagoya university - Nagoya, Japan

Keiji Otaka - Nagoya university - Nagoya, Japan

Yasuhiko Takegami - Nagoya University - Nagoya, Japan

[INTRODUCTION] Total hip arthroplasty (THA) improves the function of patients with hip osteoarthritis (HOA), and THA may reduce the falls of patients at high risk of falling.

[MATERIALS AND METHODS] We surveyed female patients undergoing THA for HOA from September 2019 to August 2021. We utilized the 5-item version of the Fall Risk Index (FRI) to assess fall risk. The questionnaire consists of five questions. A history of falls is assigned 5 points, while the other questions are each worth 2 points (back bending, use of cane, decrease in walking speed, taking more than 5 types of medication). A FRI score of 6 or higher indicates a high risk of falls. We conducted assessments one day before and one year after surgery, comparing FRI scores and the incidence of falls in the year preceding and following surgery. Additionally, we compared the high-risk group (FRI \geq 6) with the low-risk group (FRI $<$ 6) at one year post-THA. We collected data on age, body mass index (BMI), Japanese Orthopaedic Association (JOA) score, Japanese Orthopaedic Association Hip-Disease Evaluation Questionnaire (JHEQ), and perceived leg length discrepancy (P-LLD) both before and after THA. Statistical analyses were performed using paired t-tests, Student's t-tests, and Pearson's chi-square test, with significance set at $p < 0.05$.

[RESULTS] Sixty-nine patients with HOA were identified as being at high risk of falls. The mean FRI-5 score was 7.8 ± 2.1 before THA, which decreased to 4.7 ± 3.2 after THA ($p < 0.01$). The number of patients experiencing falls within one year decreased from 29 (42%) preoperatively to 16 (16%) postoperatively ($p < 0.01$). After THA, there were 29 patients in the high-risk group and 40 in the low-risk group. The mean age was 69.1 ± 9.5 years in the high-risk group and 64.3 ± 8.8 years in the low-risk group, with the high-risk group being significantly older ($p = 0.03$). Mean BMI did not differ significantly between the high-risk group (24.3 ± 4.6 kg/m²) and the low-risk group (23.6 ± 3.9 kg/m²) ($p = 0.48$). Other side osteoarthritis was present in 9 patients in the high-risk group and 8 in the low-risk group, with no significant difference. The JOA score before THA was 54.6 ± 12.6 in the high-risk group and 52.1 ± 12.6 in the low-risk group ($p = 0.42$), which improved to 82.9 ± 8.3 in the high-risk group and 86.2 ± 9.7 in the low-risk group postoperatively ($p = 0.14$). JHEQ scores showed a significant difference between the high-risk group (45.7 ± 16.6) and the low-risk group (57.6 ± 18.8) after THA ($p < 0.01$). Post-THA, 17 patients in the high-risk group and 9 patients in the low-risk group reported P-LLD ($p < 0.01$). Logistic regression analysis revealed that older age (OR: 1.34, 95% CI: 1.09-1.63, $p < 0.01$) and P-LLD after THA (OR: 13.2, 95% CI: 6.31-54.2, $p < 0.01$) were risk factors for persistent fall risk.

[CONCLUSION] THA reduces both fall risk assessment scores and the incidence of falls within one year.

Comparing TKA Implant Design for External Peak Knee Adduction Moments and Movement Strategies During Stair Ascent

Alexis Nelson - UTHSC - Memphis, Select Country

Nuanqiu Hou - Campbell Clinic - Memphis, United States of America

Douglas Powell - University of Memphis - Memphis, USA

Marcus Ford - Campbell Clinic Orthopaedics - Germantown, USA

James Guyton - Campbell Clinic Orthopaedics - Germantown, USA

John Crockarell - Campbell Clinic Orthopaedics - Germantown, USA

Derek Dixon - Campbell Clinic Foundation - Germantown, USA

Teri Ross - University of Tennessee Health Science Center - Memphis, USA

William Mihalko - University of Tennessee - Memphis, USA

*Christopher Holland - Campbell Clinic - Memphis, USA

Disclosure: This study was funded by Medacta International.

Introduction: The ultimate objectives of total knee arthroplasty (TKA) are to improve mobility and quality of life and relieve pain. Implant designs have evolved to improve patient outcomes, but functional deficits are still reported from patients post-TKA in the performance of daily activities. Despite the breadth of studies on TKA, our understanding of implant design on knee joint biomechanics during activities of daily living, specifically stair ascent, remains limited. Therefore, our purpose was to analyze two implant designs (Attune and Medacta) on the effect of knee adduction moments (KAM) and movement strategies to ascend the stairs.

Methods: We included 15 patients who received a cruciate retaining Attune implant and 8 who received a Medacta implant. All patients underwent unilateral TKA and are at least one-year post-op. A three step instrumented staircase (1000Hz, AMTI Inc., Watertown, MA) and an 8-camera markerless motion capture system (200Hz, OptiTrack, NaturalPoint Inc., MA) were used to collect ground reaction forces and segment kinematics, respectively, during stair ascent. An AI based reconstruction software (Theia Markerless, Inc., Version 2023, Kingston, ON) was used to identify segment kinematics. Visual3D Professional (HAS Motion, Version 2023.09.3, Canada) and MATLAB (The MathWorks, Inc., R2023b, Natick, MA) were used for data analysis.

Results: There were no significant differences in age or BMI between Attune and Medacta groups. Patients in both groups had compatible patient reported outcome scores. No asymmetry was observed in KAMs. External peak KAM ($p=0.070$) and mean KAM ($p=0.21$) were not significantly different between groups (Figure 1). We did not observe a significant difference in lateral trunk lean, peak ankle eversion, peak knee valgus nor peak knee varus angles.

Conclusion: We aimed to study the impact of implant designs on knee joint biomechanics during stair ascent. No significant differences in KAMs nor movement strategies were observed during stair ascent between Attune and Medacta groups. Future work will investigate other activities of daily living such as rising from a chair to understand potential differences in implant designs.

Figures

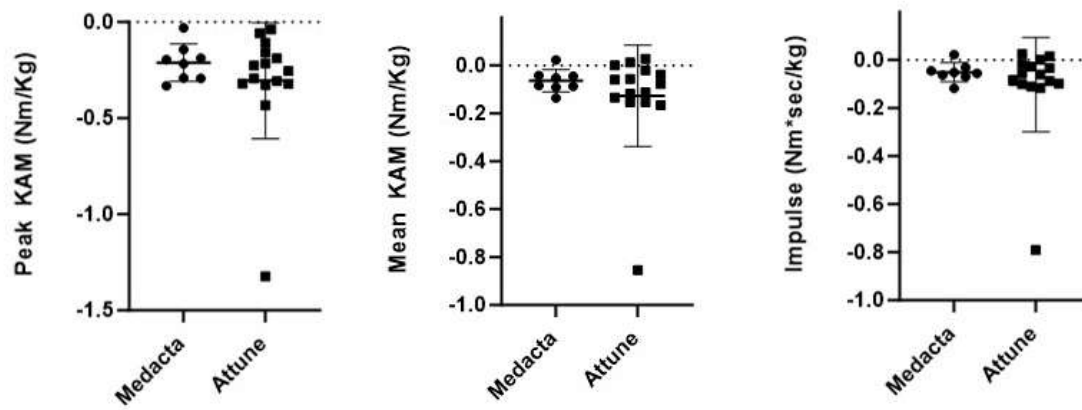


Figure 1

Combinations of Minor Acetabular Rotations Have a Major Impact on Femoral Head Coverage and Hip Range of Motion After Hip Preserving Osteotomies

*Philip Noble - Institute of Orthopedic Research and Education - Houston, USA

Nicholas Dunbar - Houston, United States of America

Shuyang Han - University of Texas Health Science Center at Houston - Houston, USA

Carey Clark - University of Texas Health Science Center - Houston, USA

Roshan Mara - University of Texas - Houston, USA

Maddison Brenner - University of Texas - Houston, USA

Chuheng Xing - University of Texas - Houston, USA

Angus Brooks - University of Texas Health Science Center at Houston - Bellaire, USA

Alexis Aboulafia - University of Texas Health Science Center - Houston, USA

Alfred Mansour III - University of Texas Health Science Center - Houston, USA

Introduction

Acetabular reorientation osteotomies are performed in symptomatic dysplastic hips to prevent or delay joint degeneration leading to THA. During these procedures, surgeons rotate and translate the acetabulum to increase the coverage of the femoral head, primarily in the antero-lateral and postero-lateral quadrants. The present study was undertaken to determine whether specific combinations of acetabular inclination, anteversion and flexion can be targeted to provide the best balance of head coverage and joint motion to delay conversion to hip arthroplasty.

Methods:

Fourteen 3D patient-specific hip models were reconstructed from pre-operative CT scans of patients diagnosed with hip dysplasia. Each model was placed in a standard coordinate system with neutral pelvic tilt and femoral rotation. A standard Bernese periacetabular osteotomy (PAO) was simulated with correction of acetabular abduction to a Lateral Center Edge Angle (LCEA) of 30°. Twelve surgical plans were simulated by independently adjusting acetabular anteversion: (change: 0°, 10°) and flexion (change: 0°, 10°), in addition to a combined rotation of 10° Flexion + 10° anteversion. For each plan, we measured the 3D femoral head coverage (total and by quadrants) and the maximum hip internal rotation motion at 90° of flexion. All runs were repeated after changing acetabular abduction to 25 and 35 degrees (LCEA). The results of each simulation were compared to the antero-lateral coverage of the normal hip (55%±9%; range:40-70%) and the change in hip range-of-motion (ROM) compared to acetabular reorientation to 30° (LCEA), without flexion or anteversion.

Results:

There were large variations in head coverage and hip ROM between combinations of components of acetabular rotation. No single combination led to acceptable values of head coverage and hip motion in every case. The percentage of acceptable outcomes (AntLat coverage: 40-70%, loss of ROM £10°) ranged from 7-71% (average:48%). The preoperative plans with the highest yield of acceptable outcomes were:

1. LCEA = 30° plus 10° anteversion (coverage: 55±12%; Change in ROM: -2.6±5.0°), and

2. LCEA =25° plus 10° anteversion and 10° of flexion (coverage: 57±15%; Change in ROM: 0.0±6.0°).

Conversely, the combination of LCEA =35° plus 10°of flexion resulted in the worst outcomes in all, but one case (coverage: 78±11%; Change in ROM: -9.0±3.8°). Values of head coverage and hip ROM for each of these 3 plans are depicted in Fig.2.

Conclusions:

1. The specific combination of acetabular rotations selected to correct the orientation of the dysplastic acetabulum has a major effect on coverage of the femoral head and the range of motion of the joint.

2. The combination of lateralization and flexion of the acetabular fragment should be avoided because of the risk of over-coverage and loss of motion.

3. As no single combination of rotational components is applicable to all cases, patient-specific preoperative planning is recommended to determine the best procedure for each case.

Figures

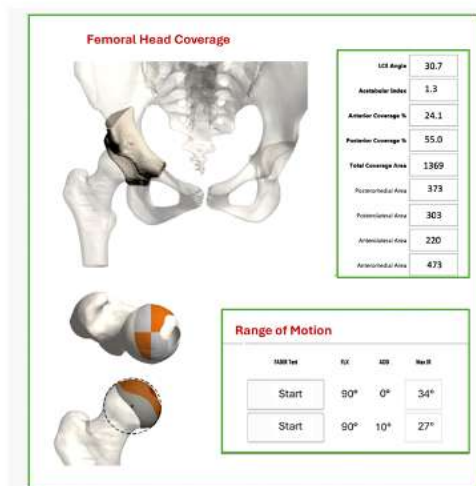


Figure 1. Interactive computer display showing the orientation of the acetabulum and the corresponding values of femoral head coverage and hip range of motion.

[Figure 1](#)

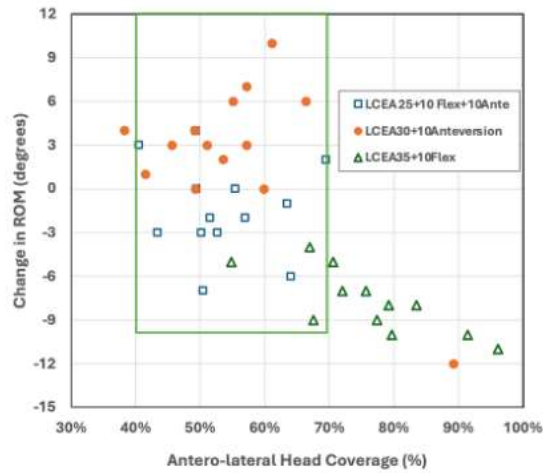


Figure 2. The relationship between antero-lateral head coverage and the change in hip range-of-motion resulting from 3 different surgical plans consisting of different combinations of acetabular rotations. The area within the green box represents the range of clinically acceptable outcomes. The change in hip ROM is calculated with respect to a standard plan (LCEA=30degrees, 0 flexion, 0 Anteversion).

Figure 2

Assessment of the Position of Anterior Inferior Iliac Spine Position in the Pelvis of Developmental Dysplasia of the Hip

*Hiroto Funahashi - Nagoya university - Nagoya, Japan

Yasuhiko Takegami - Nagoya University - Nagoya, Japan

Yusuke Osawa - Nagoya University - Shizuoka, Japan

Takamune Asamoto - Nagoya University - Nagoya, Japan

Keiji Otaka - Nagoya university - Nagoya, Japan

Hiroshi Asai - Nagoya university - Nagoya, Japan

Background?

The anterior inferior iliac spine (AIIS) is known as a site of bony impingement in flexion after total hip arthroplasty (THA), but in the pelvic morphology of developmental dysplasia of the hip (DDH), the iliac wing including the AIIS is usually different for the pelvic normal morphology. The objective of this study is to examine whether the distinct pelvic morphologies associated with pOA and DDH contribute to the observed differences in dislocation rates following THA.

Methods

A total of 990 hips underwent primary THA at our institution between 2011 and 2021. Among them, 418 hips were divided by sex and matched by propensity scores based on body height and weight, thus the cases were assigned as follows; male with pOA group was 27 hips, male with DDH group was 27 hips, female with pOA group was 38 hips and female with DDH group was 38 hips. In anatomical pelvic plane, the position of AIIS was defined as follows; the inferior iliac distance (IID) was defined horizontal distance from TD to AIIS, the inferior tear drop distance (ITD) was defined vertical distance from TD to AIIS and the inferior acetabulum distance (IAD) was defined anteroposteriorly distance from the most ventral position of acetabulum to AIIS. The measured parameters were compared to DDH and pOA by sex using student-t-test. The cup was positioned at an inclination and anteversion of 40° and 20° and set at the anatomical hip position. The stem were positioned at anteversion of 30° to simulate the femoral component in all cases. The ROM was measured at the impingement during flex with abduction 0°. The one-way analysis of variance were used to compare ROM. The Fisher's exact test was used to compare the impingement types by sex.

Results

In male, DDH had longer IID (DDH 36.9 ± 5.8 ; pOA 45.5 ± 6.1 ; $p \leq 0.001$) and longer ITD (DDH 54.7 ± 4.7 ; pOA 50.5 ± 6.8 ; $p \leq 0.001$) than pOA. In female, DDH had longer IID (DDH 31.5 ± 10.0 ; pOA 36.2 ± 4.7 ; $p \leq 0.001$) and longer ITD (DDH 52.1 ± 6.2 ; pOA 49.6 ± 5.4 ; $p \leq 0.001$) than pOA. IAD was no significantly in males (DDH 13.9 ± 3.6 ; pOA 14.3 ± 5.6 ; $p = 0.781$) and females (DDH 13.3 ± 6.6 ; pOA 12.8 ± 4.0 ; $p = 0.663$). Male with pOA group was significantly less flexion angle than other groups (ANOVA: $p \leq 0.001$, male with pOA 116.2 ± 10.8 versus male with DDH 125.5 ± 10.5 ; $p = 0.005$, male with pOA versus female in pOA 124.0 ± 9.8 ; $p = 0.014$, male in pOA versus female in DDH 126.0 ± 9.5 ; $p \leq 0.001$). Male had significantly frequently impingement on AIIS than females (83.3%, $p = 0.003$).

Conclusion

Compared to the position of AIIS with pOA, the position of AIIS with DDH is located more medial and cephalad from the position of TD and is a factor in limiting ROM during flexion after THA, especially in male.

Novel CT-Based 3D Assessment of Proximal Femoral Bone

*Ahmad Faizan - Stryker - Mahwah, USA

Ilissa Hamilton - Stryker - Mahwah, USA

Kyle Alpaugh - Massachusetts General Hospital - Boston, USA

Introduction:

Periprosthetic femur fracture (PFF) is a dreaded complication of total hip replacement (THR). PFF remains prevalent cause of revision surgery.¹ Bone quality has been identified as a risk factor for PFF.² Radiographic assessment of bone quality has been the “gold standard” for surgical planning and implant selection but is limited to its qualitative and subjective nature.^{3,4} Adjunctive CT-based planning for modern THR presents an unexplored opportunity to provide a quantitative 3D assessment of bone quality. The purpose of this study was to perform a novel CT-based 3D assessment of proximal femoral bone quality.

Methods:

CT scans of normal population in a bone database (SOMA, Stryker, Mahwah, NJ) were stratified by age and gender. Females: (age < 44 years, n= 49; age range 45-54 years, n=34; ages 55-64 years, n= 27; ages 65-74 years, n= 53; ages >75 years, n=63). Males: (age < 44 years, n= 49; age range 45-54 years, n=52; ages 55-64 years, n= 53; ages 65-74 years, n= 48; ages >75 years, n=51). All CT scans of each age and gender group were averaged to generate a mean DICOM for analysis. Bone density was assessed by measuring Hounsfield Units (HU). HU<136 was osteopenic/osteoporotic bone. HU>700 was cortical bone.^{5,6} Mean DICOM files were parsed by HU value into three regions. These regions were exported as 3D files, assigned a distinct color, and sectioned in the coronal plane and through the lesser trochanter in CAD software. To understand quantitative differences in > 75 years patients, HU values were extracted for each patient over a cross section through lesser trochanter and a two sample t test was performed.

Results:

Figure 1 depicts an increasing trend in the amount of osteoporotic bone in the coronal plane among both female and male populations as age increases. Figures 2 demonstrates a preferential increase in the amounts of osteoporotic bone in the posteromedial femur at the level of the lesser trochanter (LT). There was a statistically significant difference ($p=0$) between the HU values of the 75+ years group of female and male population. This correlates to the cross-sectional images of the mean DICOM, indicating a significant loss of high density (high HU value) cortical bone in older women.

Discussion:

We describe a novel method to assess the density distribution in proximal femur in a large population. 3D reconstruction and parsing of this data shows the regions with low HU values grow with age across both genders in normal population; however, the effect is slightly more pronounced in females. Cross sectional assessment at the level of the LT appears to show that the posteromedial bone is most affected by these age related changes. This method of bone quality assessment may have future applications on surgical planning and understanding potential periprosthetic fracture risk.

Figures

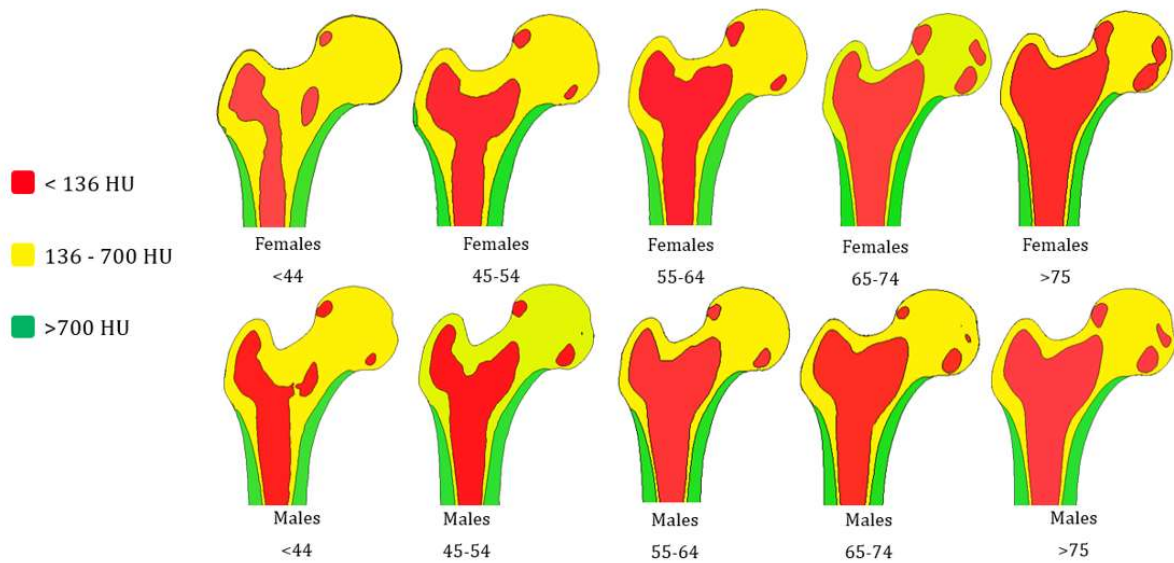


Figure 1: Density mapping of the proximal femur illustrating an increasing amount of osteoporotic bone by age.

Figure 1

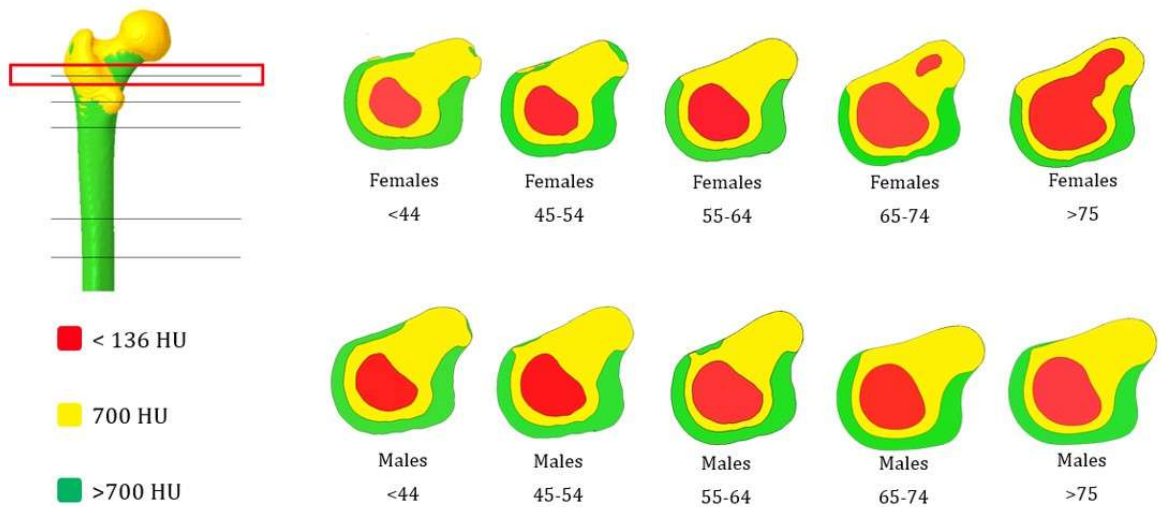


Figure 2: Cross sectional density distribution by age subgroup at the lesser trochanter level.

Figure 2

Unused 3D Femoral Morphology: Can They Lead to Better THAs?

*Jarrod Nachtrab - University of Tennessee - Knoxville, USA

Thang Nguyen - University of Tennessee - Knoxville, USA

Michael LaCour - University of Tennessee - Knoxville, USA

Richard Komistek - The University of Tennessee - Knoxville, USA

Introduction

With the introduction of 3D preoperative planning in total hip arthroplasty (THA), surgeons can access more information when planning a THA, but many surgeons are still only using 2D x-ray information to develop their preoperative plans. The objective of this study was to utilize three-dimensional (3D) bone morphology data to determine supplemental alignment information that may improve postoperative outcomes when applied to THA planning and implant design.

Methods

In this study, 60 cadaveric bones were segmented and classified by external evaluators using the Dorr system. A previously published 3D preoperative planning tool [1] utilized the femoral head center and shaft axis to determine the following parameters for the bone models: anatomical neck angle in frontal plane, anatomical neck version angle in transverse plane (anteversion=positive and retroversion=negative), and femoral shaft bowing angle in sagittal plane (Figure 1). Similar data pertaining to each stem, specifically stem neck angle, was also gathered for comparison with the anatomical data.

Results

For the native morphology, the average anatomical neck version angle was $8.5 \pm 4.3^\circ$ anteversion, (0.8-17.2° anteversion). Similarly, the average femoral bowing angle was found to be $5.3 \pm 2.6^\circ$ (0.5-10.5°) in the anterior direction. Finally, the average femoral neck angle with respect to the shaft in the frontal plane was $127.3 \pm 10.2^\circ$ (106.3-147.7°).

When comparing Dorr types, Type A femoral bones had an average neck angle of $127.2 \pm 10.6^\circ$ and exhibited the highest average femoral bowing angle at $6.4 \pm 1.8^\circ$. Interestingly, Type C bones had the highest femoral bowing angle for a specific subject at 10.5° . Type B exhibited the highest average anatomical neck version angle with $9.85 \pm 3.71^\circ$ anteversion.

The stem system used in this study had a neck angle of 130° , but it also exhibited a variable offset that allows it to fit a greater range on neck angles. Among all 60 femurs in the study, 16 had a neck angle less than 120° , 36 ranged from $120-140^\circ$, and 8 had a neck angle greater than 140° . The neck version and femoral bowing angle were not considered for the stem system. This correlates to 24 (>1/3) femurs in this study having a neck angle that did not fit the analyzed stem system.

Conclusion

With traditional frontal plane planning, out-of-plane information cannot be considered. Thus, out-of-plane data such as version angles and bowing angles can lead to unintended component alignments and potential issues within the canal. Future implant designs and surgical techniques should account for out-of-plane information to improve patient outcomes.

References

1. Ta MD. Development and Implementation of a Computational Surgical Planning Model for Pre-Operative Planning and Post-Operative Assessment and Analysis of Total Hip Arthroplasty. University of Tennessee, 2019.

Figures

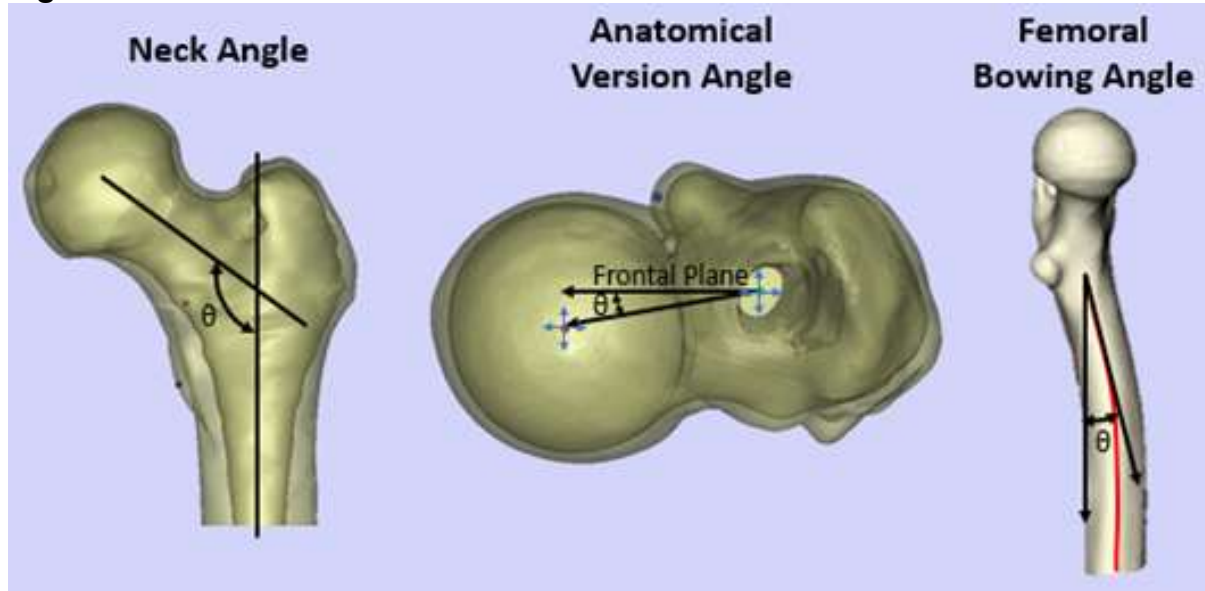


[Figure 1](#)

3D Distal Femur Phenotype Classification

*James Crutcher - Swedish Orthopedic Institute - Seattle, United States of America
Ronald Connors-Ehlert - Stryker - Mahwah, USA

Introduction:

Contemporary knee replacement is increasingly trending towards a more personalized surgical procedure, recognizing significant variation in native knee alignment and bony anatomy. Knee phenotype classifications have been developed, but most are based on 2-dimensional (2D) imaging. CT-based navigation and robotic technologies have illustrated that there is 3-dimensional (3D) variation in native knee anatomy, considering the coronal, sagittal, and axial planes. The purpose of this study is to describe a 3D phenotype classification of distal femoral anatomy incorporating the coronal and axial planes.

Methods:

A CT scan database of 1065 non-diseased subjects was studied to measure the range of the distal lateral femoral angle (DLFA) and the posterior condylar angle (PCA) across the cohort. A classification was developed to describe 9 3D phenotypes of distal femoral anatomy based on 3 ranges of the DLFA ($< 3^\circ$, $3-5^\circ$, $> 5^\circ$) and 3 ranges of the PCA ($< 2^\circ$, $2-4^\circ$, $> 4^\circ$). The 3D phenotype classification was applied to subsets of the group based on gender and ethnicity (Caucasian and Asian). The classification was also applied to data acquired from a consecutive series of 220 CT-based preoperative total knee replacement (TKA) plans, sorted by limb alignment.

Results:

Significant variation was found in the distal femoral anatomy as described by the 3D phenotype classification in both study groups. The most common 3D phenotype (18.3%) was Type 1 (DLFA $< 3^\circ$ /PCA $< 2^\circ$), and the least common phenotype (5.35%) was Type 3 (DLFA $< 3^\circ$ /PCA $> 4^\circ$). Type 1 was the most common in males (23.7%) as compared to 9.86% of females. Type 5 (DLFA $3-5^\circ$ /PCA $2-4^\circ$) was the most common in females (14.2%) as compared to 11.5% of males. Type 1 was the most common (19.6%) in Caucasians as compared to 11.7% of Asians. In the TKA CT group, there was significant variation when sorted by limb alignment, with varus knees most commonly (24%) Type 2 (DLFA $< 3^\circ$ /PCA $2-4^\circ$), and valgus knees most commonly (25%) Type 8 (DLFA $> 5^\circ$ /PCA $2-4^\circ$).

Conclusion:

This CT-based study found significant variation in the 3D distal femoral anatomy of normal and diseased subjects when considering the DLFA and the PCA, and this variation is described with a new 3D phenotype classification. Differences were found when the phenotype classification was applied to subsets based on gender, ethnicity, and limb alignment. Recognition of this anatomical variation as described by a 3D phenotype classification could be an important consideration when applying more personalized techniques to knee replacement surgery.

Automatic Muscle Attachment Estimation Compared to MR-Derived Manual Selection

Nancy Kim - Auckland Bioengineering Institute - Auckland, New Zealand

*Marco Schneider - Formus Labs - Auckland, New Zealand

Duncan Bakke - Formus Labs - Auckland, New Zealand

Thor F Besier - University of Auckland - Auckland, New Zealand

Madison Wissman - Washington University School of Medicine in St Louis - St. Louis, United States of America

Michael Harris - Washington University in St Louis - St Louis, United States of America

Introduction

Muscle attachment sites determine lines of action and moment arms of the muscle, which influence muscle and joint force estimates [1,2], and are important for predicting patient-specific function. Musculoskeletal models typically represent muscles as line-segments, with attachment sites derived from a generic template, scaled to match the dimensions of a subject. The use of subject-specific geometry and attachments has been shown to improve estimates of muscle function and joint-centres. It is unknown how well statistical shape-model (SSM) based scaling predicts muscle attachment points, particularly for clinical cohorts. We evaluated the disparities between automatically obtained SSM-fit and manually-selected muscle attachment sites defined from magnetic resonance (MR) images of hip dysplasia patients (DDH). In addition we compared the results to regional attachment sites from a SOMSO-PLAST® model.

Methods

MR images of the lower limb were obtained for 20 females with DDH (age: 16 to 39 yrs) and segmented to generate patient-specific 3D models of the pelvis and femur with 80 manually-selected muscle attachment points (manual-points). A lower-limb SSM [3] augmented with regional attachment sites obtained from a digitised SOMSO-PLAST® model and embedded with attachment points based on the MAP client (auto-points) was fitted to the segmented MR images to obtain 20 patient-specific musculoskeletal models. The Euclidean distances (mean, standard deviation) between the manual-points and the SSM-points were measured.

Results

The average difference between the auto-points and manual-points was 17 ± 10 mm for the pelvis and 29 ± 44 mm for the femur. The muscle on the pelvis with the greatest mean difference was the Gracilis muscle (32mm), and the muscle with the largest standard deviation in attachment was the Gluteus Medius (± 11 mm). The femoral attachment of the Adductor Magnus muscle had the greatest mean difference with the largest standard deviation of 38 ± 26 mm (Figure 1). Large discrepancies were apparent for muscles with large attachment sites (Figures 2 & 3).

Conclusion

Differences were found between automatically and manually selected attachments, which may lead to variation in muscle lines of action and joint contact force estimates. These differences highlight the need for more robust methods of identifying muscle attachments, particularly those with broad origins or insertions and in patient cohorts that have bone morphology that is ill represented by a model. Comparisons across models built through different approaches must be done

carefully. SSM fitting of muscle attachment regions offers a potential solution to this challenge.

References

1. Gerus P. et al. J Biomech. 2013;46(16):2778-86.
2. Martín-Sosa, E. et al. (2019). PlosOne, 14(9), e0222491.
3. Rooks, N. et al. (2023). ISTA 2023 Annual Congress.

Figures

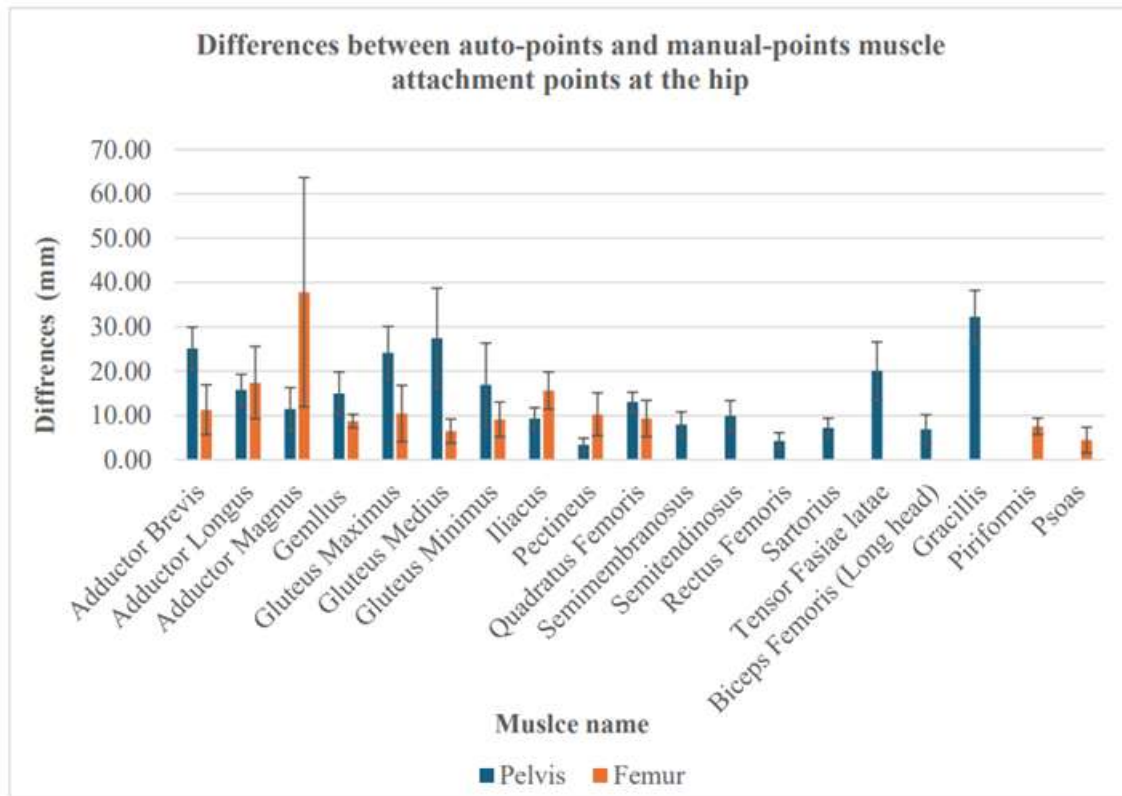


Figure 1. Differences between mean of manual-points and auto-points of hip dysplastic cohorts focusing on the hip muscles

[Figure 1](#)

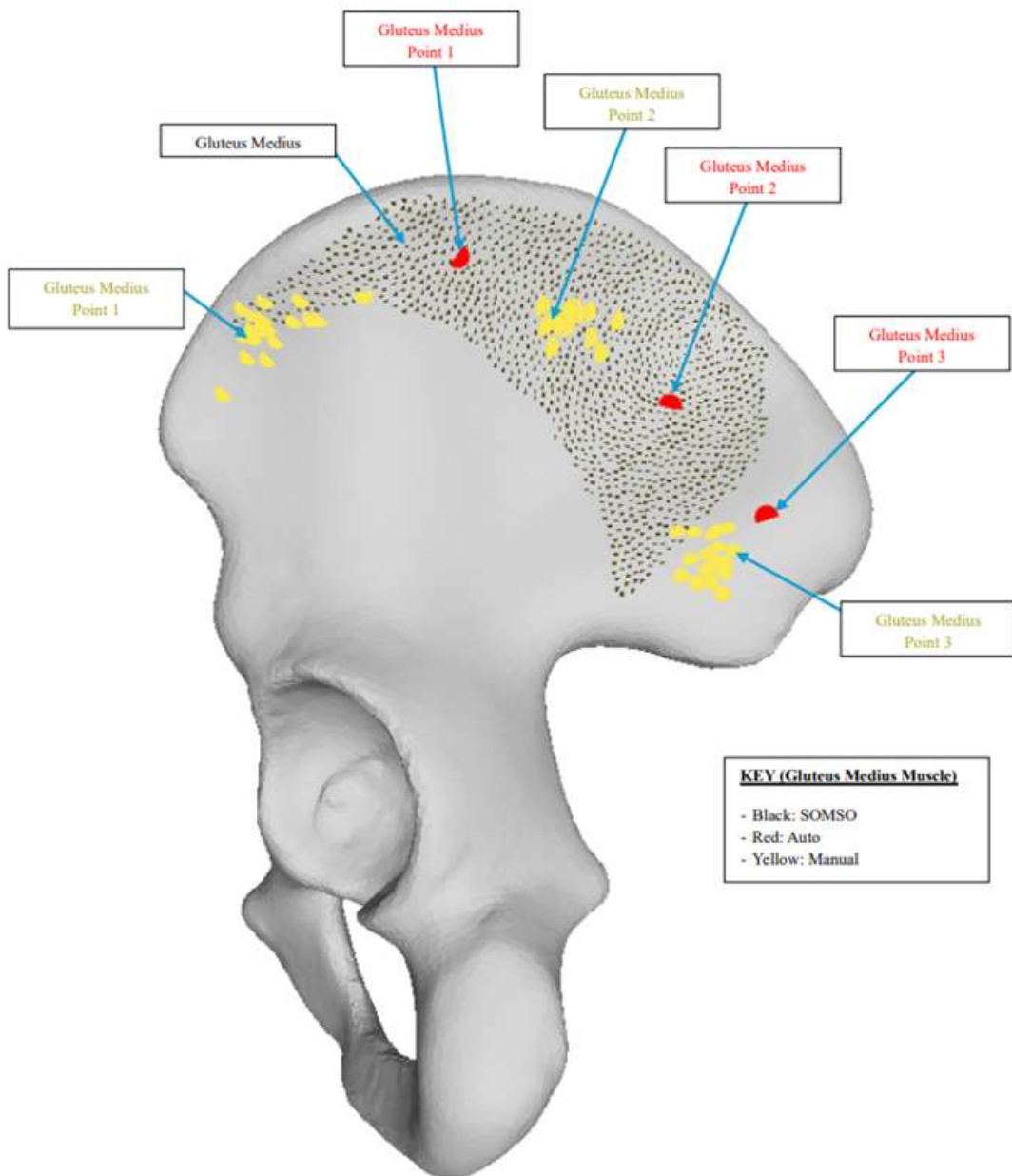


Figure 2. Left pelvis with Gluteus Medius muscle including all SOMSO, auto, and manual muscle points

[Figure 2](#)

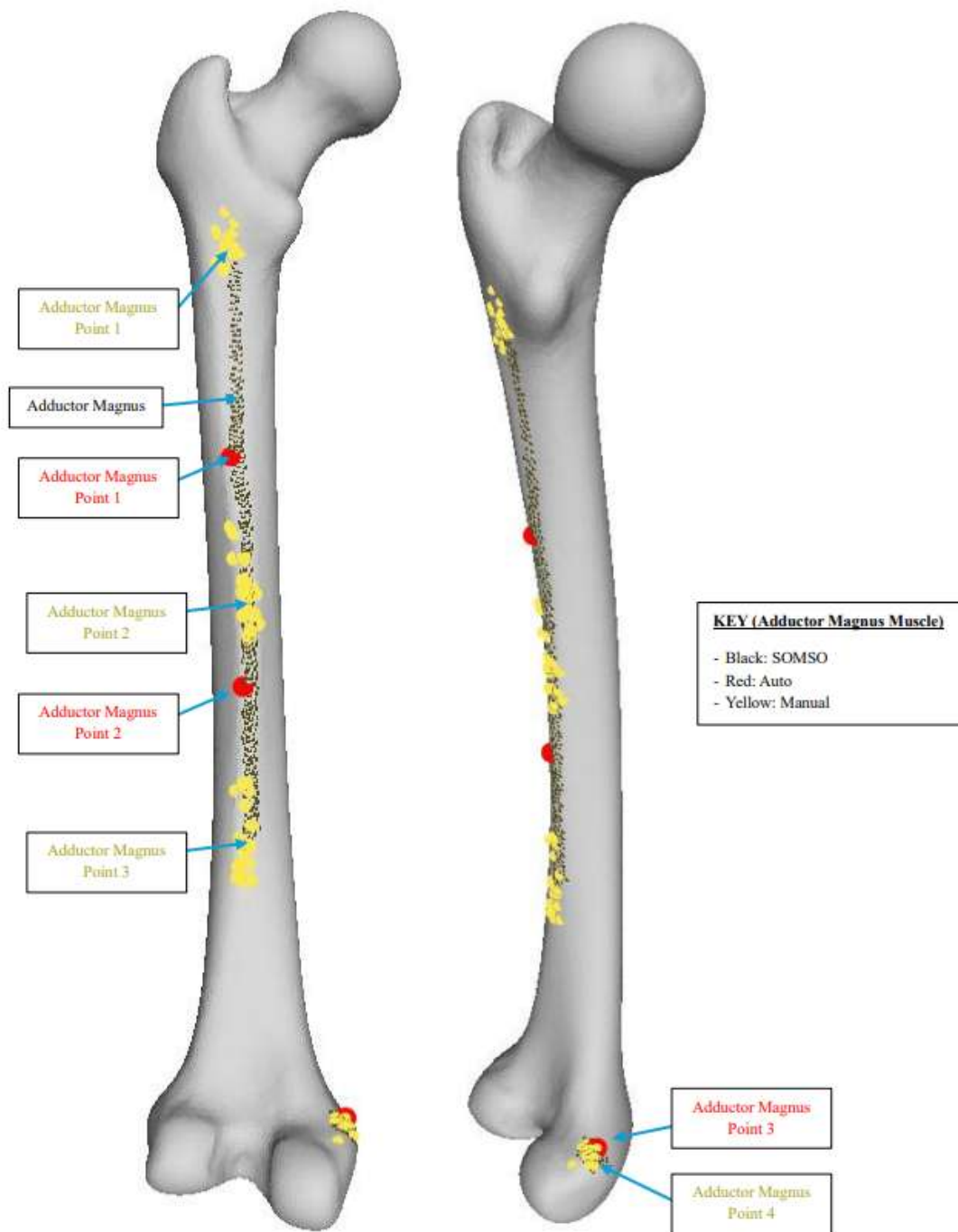


Figure 3. Left femur with Adductor Magnus muscle including all SOMSO, auto, and manual muscle points at two different views

[Figure 3](#)

Numerical Methods for Estimating Muscle Activities With Co-Contractions

Taiga Ishii - University of Hyogo - Himeji, Japan

*Masaru Higa - Himeji, Japan

Introduction: Understanding muscles activities is important for knowing the conditions of orthopedics prostheses within the body. Since it is challenging to directly measure muscle force inside the body, muscle activities are typically estimated using musculoskeletal computer software. However, there are few reports that consider co-contractions of antagonist muscles in the current estimation of muscle activities using musculoskeletal models. The aim of this study is to propose a novel method for estimating muscle activities during a simple exercise considering co-contractions.

Methods: Knee joint flexion exercises were performed on one male healthy subject. There exercises involved bending the subject's right knee joint to 90 degrees over 3 seconds with a leg standing posture. Five trials were performed for three types of exercises first, natural exercise with relaxation, second, exercise with maximum effort and third, exercise with moderate effort. No external force or moment was applied during the exercises. Surface electromyography (EMG) was utilized to measure muscle activities in five muscles (biceps femoris long head, rectus femoris, vastus medialis, vastus lateralis, gastrocnemius) during the knee flexion exercises. Knee joint kinematics were also measured using a motion capture system (Optitrack, NaturalPoint, Corvallis, USA). Musculoskeletal model analysis software (OpenSim 3.3) and numerical calculation software (MATLAB, Mathworks, Inc.) were used to estimate the muscle activities of the muscle activities during the movements. The calculation method was to minimize the sum of the muscle activation squared during the first condition and to maximize the sum of the muscle activities squared during the third condition. The muscle activation during the second condition was estimated by combining the minimized and maximized muscle activation then compared with the measured values.

Results: In the EMG measurements, there are clear co-contractions under the second and third conditions. In the estimations, minimization and maximization enabled us to estimate the muscle activities during the first and the second conditions respectively. A combination of the minimization and the maximization enabled an estimation of muscle activities under the third condition considering co-contraction. However, the accuracy of estimating the agonist muscle of the knee flexion movement was not as high as that of the antagonist muscle.

Conclusion: This study successfully estimated muscle activities considering co-contractions. Therefore, it is expected that the minimization and maximization methods presented in this study will improve the understanding of muscle activities.

Figures

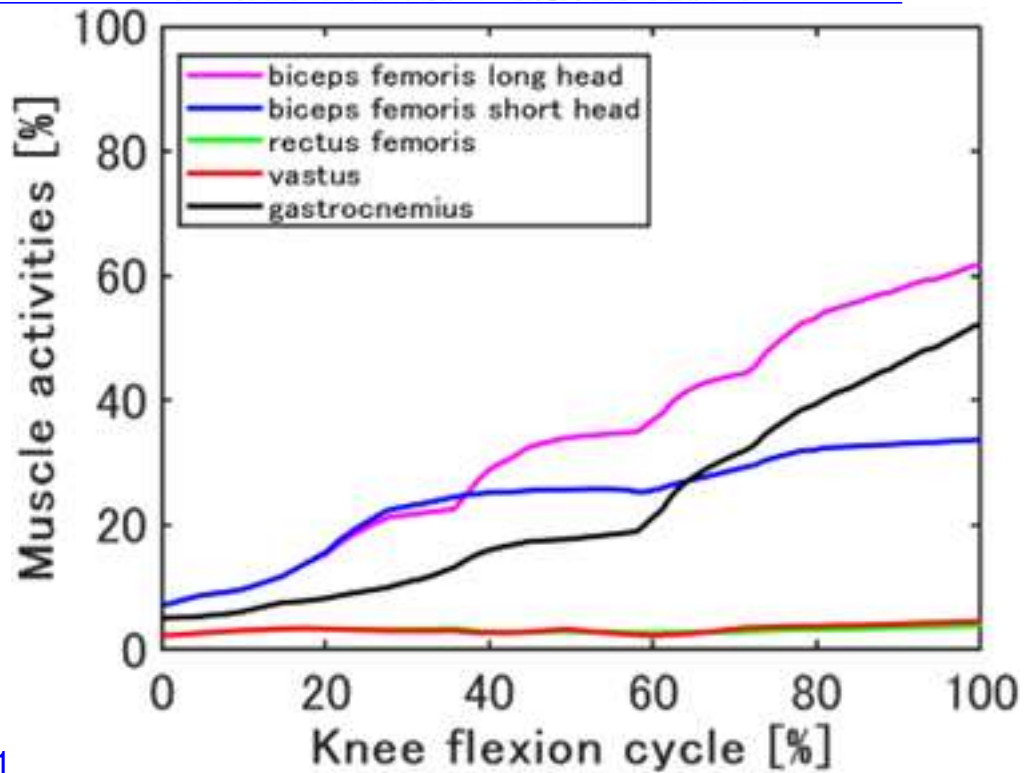
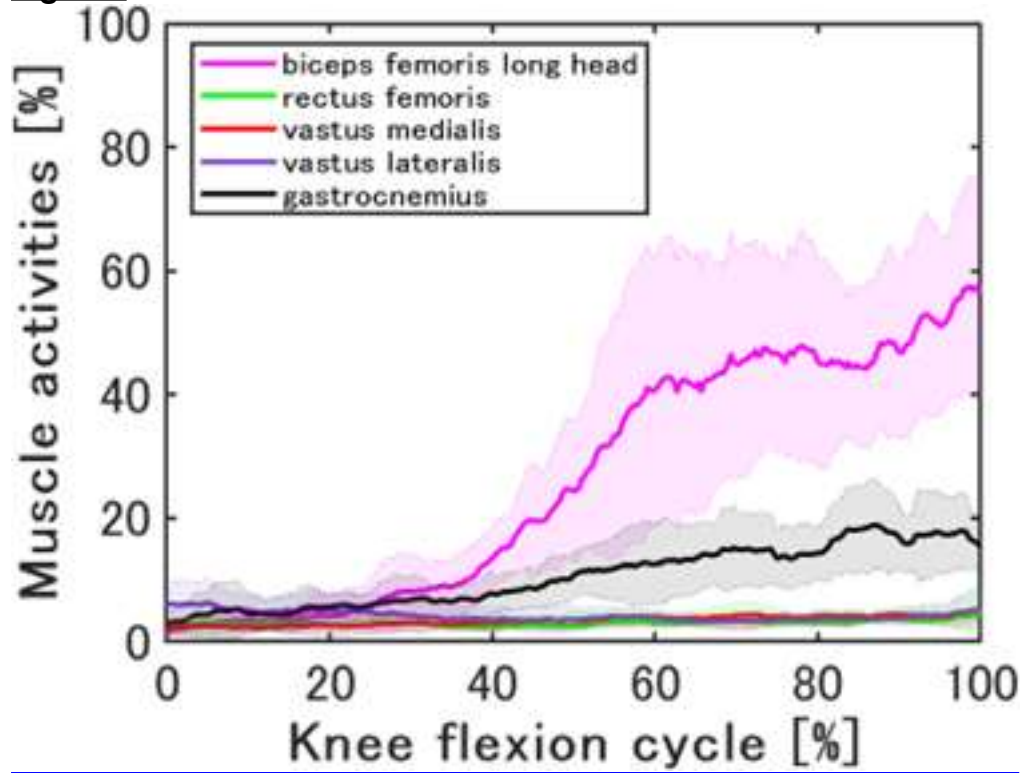


Figure 1

Figure 2

Quadriceps Muscle Action Assessment

*Gokce Yildirim - Vent Creativity Corporation - Weehawken, USA

Simon Talbot - Western Health - Melbourne, Australia

Introduction: Quadriceps muscle alignment relative to the femoral flexion axis has been shown to affect patient's ability to perform daily activities. External misalignment, forcing the patella to track laterally is shown to hinder patient mobility. This new automated measurement tool aims to measure the alignment to give surgeons actionable data to align patellofemoral joint for soft-tissue or arthroplasty interventions.

Methods: Standing CT data is used to generate previously validated intensity point clouds models¹. Four known quadriceps maltracking patient scans and four normal cadaver scans were analyzed to determine the effectiveness of the automated system to identify and measure quadriceps angle relative to the posterior femoral plane. Femoral inner canal points were collected, and the resulting axis was used to determine the rotation of the vector which points to the patellar tendon quadriceps attachment. The angle between the quadriceps vector and the posterior femoral plane vector was measured for each patient (Figure 1).

Results: Control and maltracking groups had statistically significant variation in angulation of the quadriceps tendon line of action. Average angle increased by 5 degrees for maltracking patients (Figure 2).

Conclusion: Quadriceps line of action can be attributed to success of sports medicine or arthroplasty surgeries. Detection of maltracking can help surgeons plan procedures that can potentially regain the corrected mechanical contributions for improved activities of daily living.

Figures

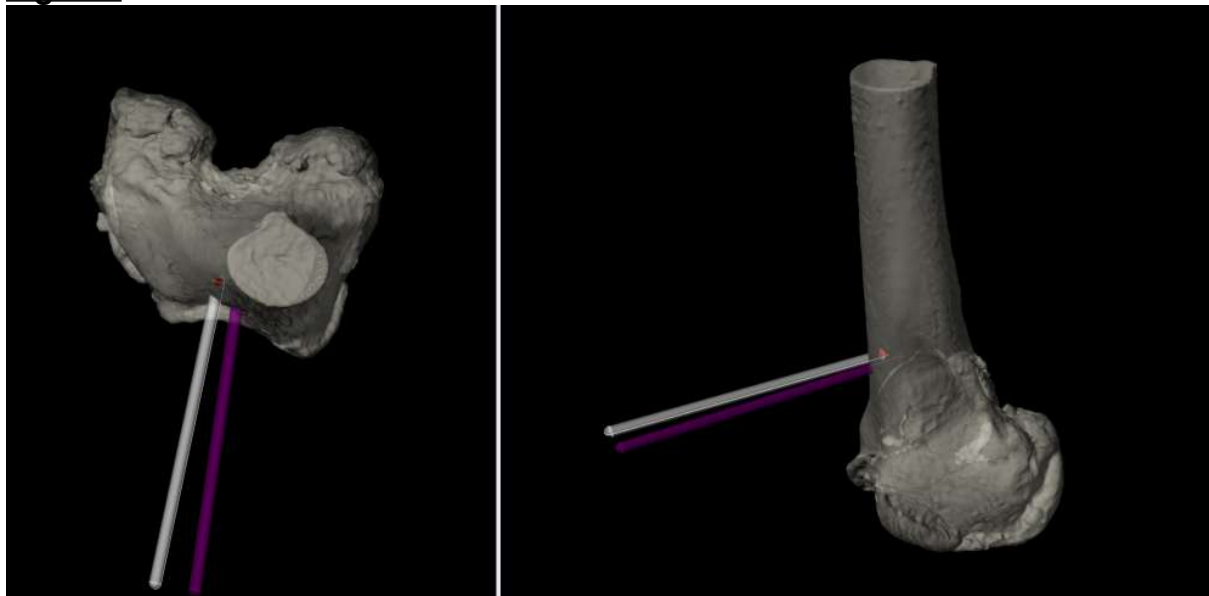


[Figure 1](#)

Femur	Angle (ext+)	Femur	Angle (ext+)
control 1	9.67	1	20.8
control 2	10.99	2	14.27
control 3	11.37	3	12.46
control 4	10.09	4	13.19
Average	10.53		15.18
STD	0.79		3.82

[Figure 2](#)

The Quadriceps Vector Has the Same Direction in Knees of People From India as in Caucasian and Japanese People Despite Different Bone Morphology

Chi Fangzhou - Niigata - Niigata, Japan

Shigeru Takagi - Niigata University - Niigata City, Japan

Tomoharu Mochizuki - Niigata University - Niigata, Japan

Osamu Tanifuji - Niigata University - Niigata, Japan

Shin Kai - Niigata University - Niigata, Japan

Rajesh Malhotra

*J (John) Blaha - University of Michigan - ANN ARBOR, USA

Introduction: Correct alignment of knee components contributes to the longevity and function of total knee arthroplasty. The authors published three studies reporting the accuracy and reliability of using the three-dimensional quadriceps vector for alignment in CT scans of Caucasian and Japanese study participants. In all cases the quadriceps vector was directed from the top of the patella to the middle of the femoral neck. The literature describes considerable difference in the morphology of bone in the lower extremity of East Asian people compared with that of Caucasian or Japanese people.

Methods: We conducted an imaging study to determine the quadriceps vector in a sample of 14 patients (CT scans, 7 men, 7 women) from India. The same measurement methods were used for this cohort as previous studies.

Results: The quadriceps vector for the Indian cohort was found to be directed from the top of the patella toward the femoral neck, as in Caucasian and Japanese CT scans.

In the Indian knees, the passing point of the vector was found to be anterior (31.3 ± 7.4 mm) and lateral (35.9 ± 19.9 mm) to the femoral head. When projected to the coronal plane, the quadriceps vector was different to the mechanical axis by $5.0 \pm 1.7^\circ$; to the anatomic axis by $1.8 \pm 1.0^\circ$ and to the spherical axis $1.2 \pm 0.8^\circ$.

Conclusion: As in the previously published studies, the quadriceps vector was found to be most parallel to the spherical axis (center of the femoral head to the center of the spherical medial condyle) projected onto the coronal plane. These data suggest that using the quadriceps vector for alignment can be applied to the human lower extremity regardless of morphology. Experience with aligning the medial-pivot knee prosthesis using the quadriceps vector without reference to another alignment paradigm has demonstrated excellent reliability in alignment and should produce excellent reliable clinical results.

Figures

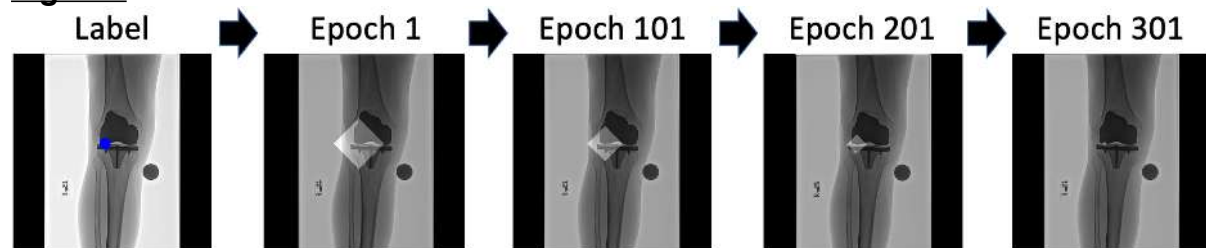


Figure 1

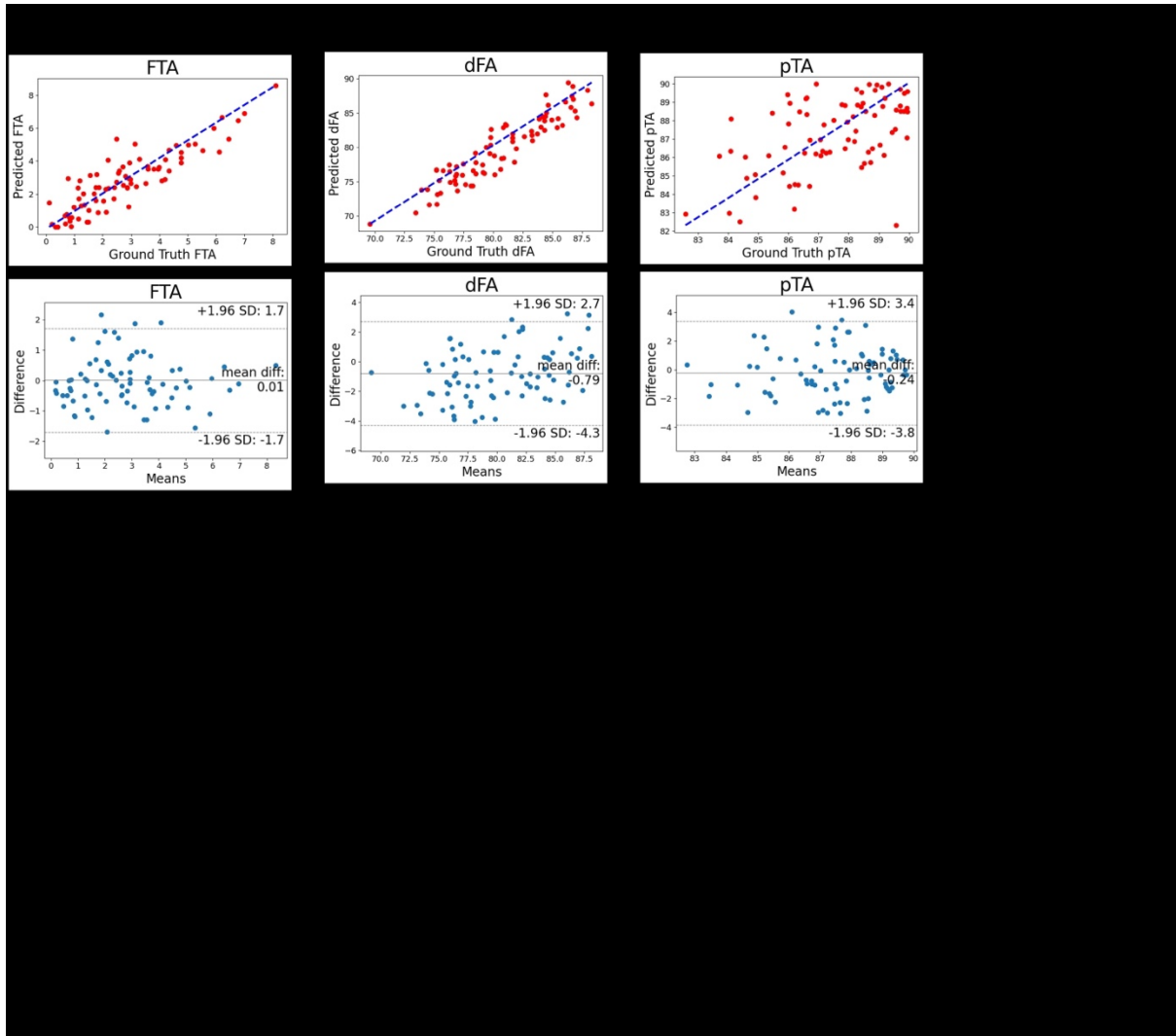


Figure 2

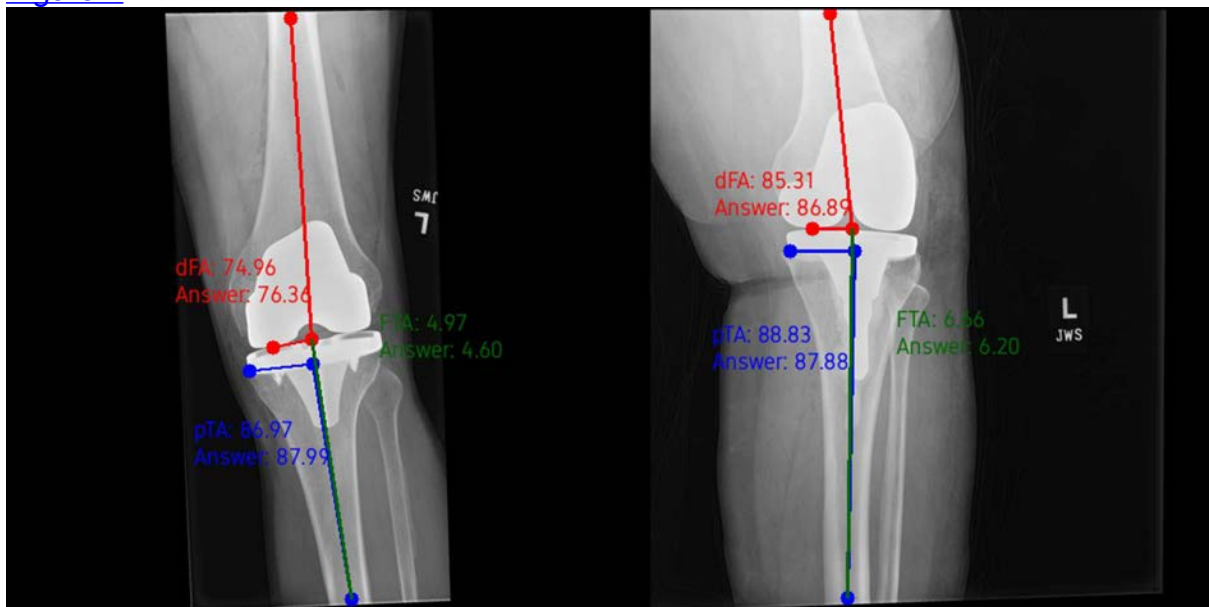


Figure 3

Understanding the Effect of Interscalene Blocks on Pulmonary Function: Can We Prevent Complications?

*Garrett Jackson - Chicago, United States of America

Vani Sabesan - Cleveland Clinic Florida - Weston, USA

Devin John - HCA JFK/University of Miami Orthopaedic Surgery Residency Program - Atlantis, USA

Aghdas Movassaghi - Michigan State University - East Lansing, USA

Howard Routman - Atlantis Orthopedics - Atlantis, USA

Jacob Calpey - Charles E. Schmidt College of Medicine Florida Atlantic University - Boca Raton, USA

Introduction: Interscalene nerve blocks (ISB) are a mainstay for multimodal pain management in shoulder surgery, successfully impacting the reduction of opioid medications. While ISBs have been shown to be safe and effective, they carry a risk of transient phrenic nerve paralysis in up to 100% of cases. Despite this negative impact that may occur on pulmonary function, currently, there are no specific risk factors or guidelines for patient selection or concerns with the use of ISB. The purpose of this study was to analyze patient risk factors leading to postoperative decreased pulmonary function following the administration of ISB for shoulder surgery.

Methods: Patients who received a liposomal bupivacaine ISB prior to undergoing shoulder surgery by a single shoulder fellowship-trained orthopedic surgeon were identified between October and November 2022. After institutional review board approval, patients were assessed at baseline for demographics, pulmonary history, brief resilience scale (BRS) survey, Charlson comorbidity index (CCI), Clinical Frailty Scale (CFS), and Frailty Index for Elders (FIFE). Patients were assessed for postoperative shortness of breath (SOB) and complications at two and eight weeks postoperatively.

Results: One patient was excluded due to lack of mental capacity to complete the surveys, leaving a total of four patients (50% female) with a mean age of 70.2 years, BMI of 29.6, and BRS of 16.5/30. All patients were Caucasian. Surgical procedures included primary reverse total shoulder arthroplasty (RTSA; n=1 patient), revision RTSA for a periprosthetic fracture (n=1 patient), and open reduction with internal fixation for proximal humerus fracture (n=2 patients). Three patients, all > 65 years of age, experienced SOB postoperatively, had a CCI ≥ 3 , and had one chronic respiratory-related illness (asthma, chronic obstructive pulmonary disease, or obstructive sleep apnea). Two patients that experienced SOB postoperatively were frail (FIFE = 4 and 5; CFS = 4 and 5), while one patient was at risk for frailty (FIFE = 2) but managing well (CFS = 3). Two patients did not report SOB until postoperative day one or later and all three patients reported symptoms lasting for 48-72 hours. The patient who did not experience SOB was < 65 years of age, had no chronic respiratory illness, and had a CCI of 2, FIFE of 0, and CFS of 1. One patient experienced pneumonia five weeks after surgery, prompting readmission.

Conclusion: Frail, elderly patients with respiratory-related illnesses, may be at greater risk of experiencing SOB following an ISB for shoulder surgery. Surgeons

can utilize this information to identify high-risk patients who may be more susceptible to postoperative SOB and potential complications.

Survivorship and Clinical Outcomes for a Platform Epiphysis Component Used in Reverse Shoulder Arthroplasty: A Multi-Center Registry Review

Maarten de Vos - Tergooi Hospital - Hilversum, Netherlands

Jacob Stueve - Kansas City Orthopaedic Institute - Leawood, USA

Sean Croker - Depuy Synthes - West Chester, USA

*David Fawley - DePuy Synthes - Warsaw, USA

Introduction

Reverse shoulder arthroplasty has continued to gain popularity. A legacy reverse shoulder system was designed as an evolution of the legacy Delta 1 implant and released in 2006. There are some data available to support survivorship and outcomes of this system, however, there is benefit to understanding the performance of these implants in standard of care settings. The aim of this evaluation was to retrospectively assess complications and revisions for a single platform epiphysis used in reverse shoulder arthroplasty.

Methods

We conducted a retrospective multicenter registry case review from a company-sponsored standard of care registry, filtering to include all implanted cases of a single platform epiphysis. Clinical assessments were summarized at standardized registry visit windows.

Results

A total of 109 reverse shoulders with the same epiphysis component were implanted across 2 sites (1 US, 1 Netherlands). Primary diagnosis was osteoarthritis in 37 (34.6%), complete cuff tear in 36 (33.6%), avascular necrosis in 3 (2.8%), dislocation in 2 (1.9%), acute fracture in 1 (0.9%) and other in 28 (26.2%). Mean age was 71.2 years, 67 (62.6%) were female and BMI averaged 28.4 (R 17.9 to 51.9). Overall, 1 (0.9%) revision was reported due to infection. Two additional shoulder complications were reported: one seroma scar of the registry shoulder treated with aspiration and oral medication, and one urinary tract infection due to catheter use that caused low blood pressure and required oral medication.

Conclusion

Our study shows low numbers of revisions and complications for a single platform epiphysis used in reverse shoulder arthroplasty. Continued study of this design would be beneficial.

How Much Do We Actually Use Our Wrists? Harnessing Wearable Motion Sensors to Determine Baseline Wrist Motion Values in Real-World Settings for Use in Preclinical Testing of Wrist Arthroplasty Devices

*Ryan Chapman - University of Rhode Island - Kingston, United States of America

J.J. Trey Crisco - Brown University - Providence, USA

Introduction: Wrist osteoarthritis is common (~45M Americans), yet total wrist arthroplasty (TWA) is infrequent and less successful than other joints (<1000 annually, $\geq 20\%$ failure rate). TWA's limited success is partly attributable to poorly established information regarding loads and range of motion (ROM) utilization. While wrist ROM during activities of daily living (ADLs) in laboratory/clinical settings are well-established, similar long duration data "in-the-wild" does not exist. Accordingly, we conducted a prospective study evaluating bilateral wrist motion using wearable inertial measurement units (IMUs) in healthy individuals during one day of free living activities.

Methods: After IRB approval, 10 healthy participants (5M, 21.1 ± 2.8 yrs) were bilaterally instrumented with IMUs (dorsal wrists/hands) via straps (Figure 1A). Temporally synchronized, inertial data were continuously stored on each IMU ($f_s=128\text{Hz}$, ~8-12 hours). Subjects returned IMUs at the end of the day for offline processing. Raw data were low pass filtered (LPF; Butterworth, 5th order, $f_c=5\text{Hz}$). IMU tilt was computed using 3D accelerometer data (Figure 1B). As a first attempt quantifying long-duration kinematics, sagittal wrist angle was computed subtracting hand tilt from wrist tilt. Continuous sagittal angles were LPF (Butterworth, 5th order, $f_c=2\text{Hz}$). Maximum, minimum, and average angles computed. Continuous angle data were subdivided (1s intervals). Average wrist angle in each interval was computed and binned in 5° increments. Transitions between angle bins were considered discrete movements. Total/discrete movement time in each 5° bin were computed.

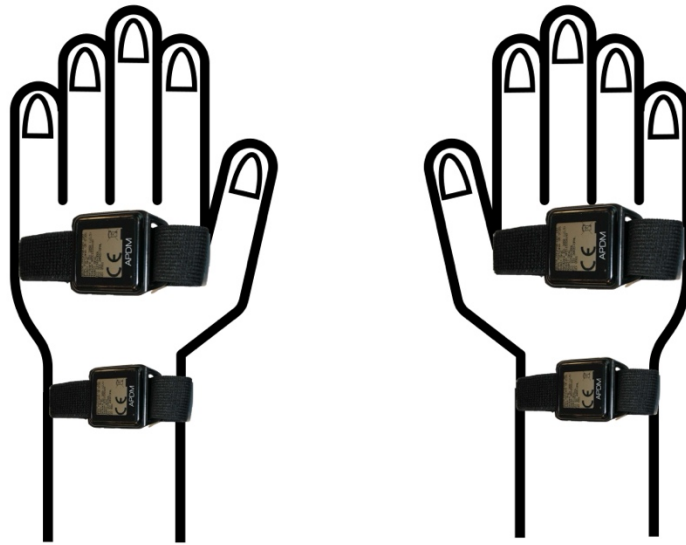
Results: An example subject's wrist flexion/extension highlights frequent motion bilaterally but more left wrist variability (Figure 2). Maximum flexion/extension were 63.8°/59.3° and 57.7°/58.4° for left and right wrists, respectively. Average angle was 3.4°/2.1° of flexion for left/right wrists, respectively. Total binned data showed >96% was spent between $\pm 30^\circ$ (Figure 3). Most time (>50 min) was spent 0-5° flexed and 5-10° extended for the left/right wrists, respectively. Discrete movements were more symmetrical left vs. right with >99% occurring between $\pm 40^\circ$.

Conclusion: Wearable IMUs are convenient, easily deployed devices for evaluating biomechanics "in-the-wild." Although wrist ROM during discrete ADLs is well-established, no such information exists for long durations in real-world settings. We believe these are the first long duration wrist kinematic data in healthy adults. The vast majority of time was spent between $\pm 40^\circ$. While individuals were capable of high wrist flexion/extension (~60-65°), angles over 40° occurred <0.5%. These results serve as preliminary data for further testing to develop preclinical guidelines for evaluating wrist implants as well as for assessing patient motion before/after TWA.

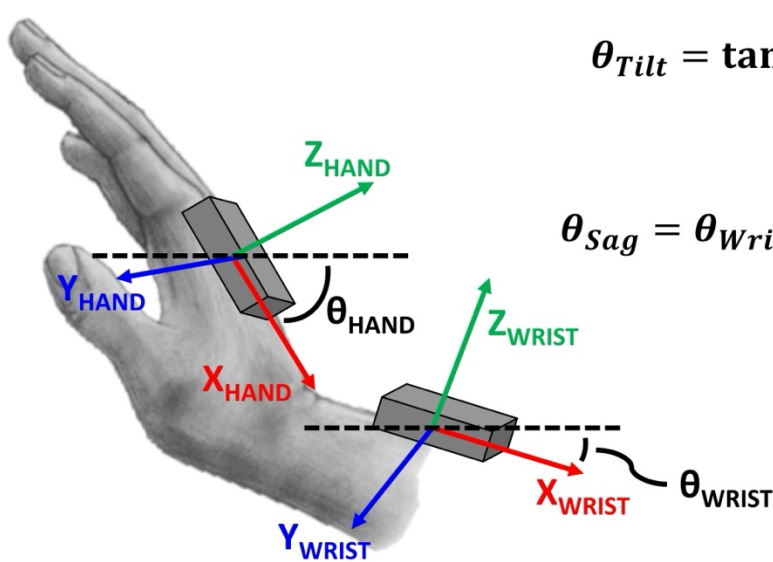
Keywords: Wearable, Kinematics, Range of Motion, Motion Capture, Biomechanics, Wrist

Figures

A



B



$$\theta_{Tilt} = \tan^{-1} \left(\frac{\vec{a}_x}{\sqrt{\vec{a}_y^2 + \vec{a}_z^2}} \right)$$

$$\theta_{Sag} = \theta_{Wrist_Tilt} - \theta_{Hand_Tilt}$$

Figure 1

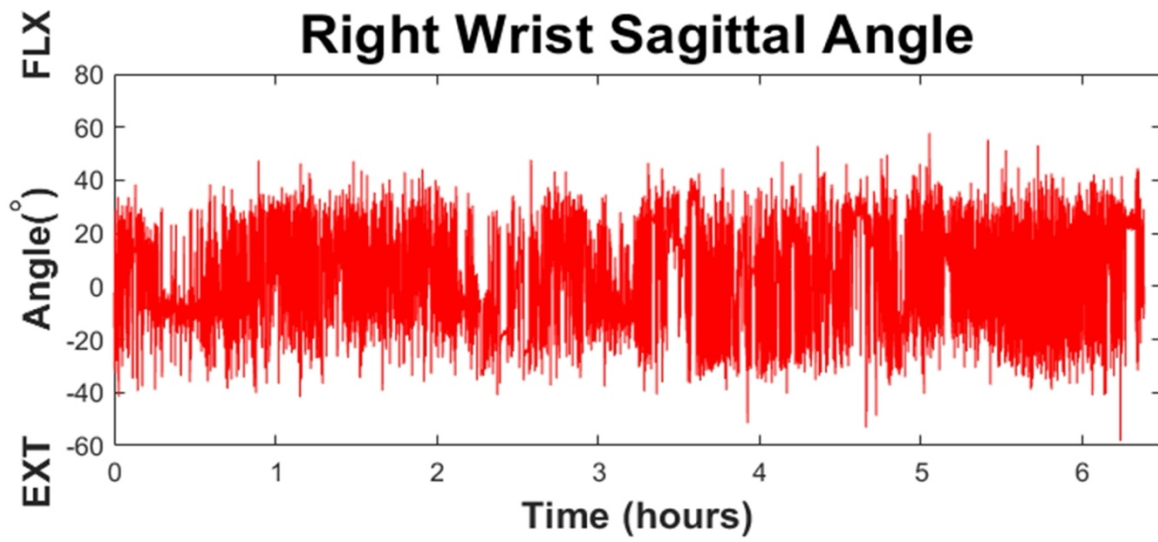
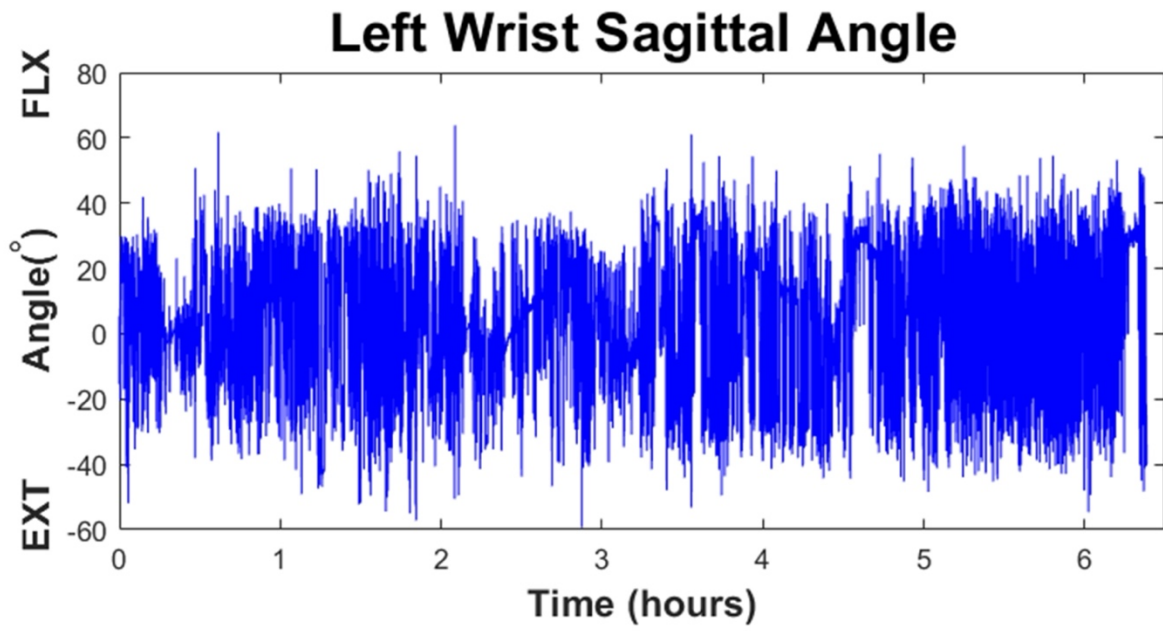


[Figure 2](#)

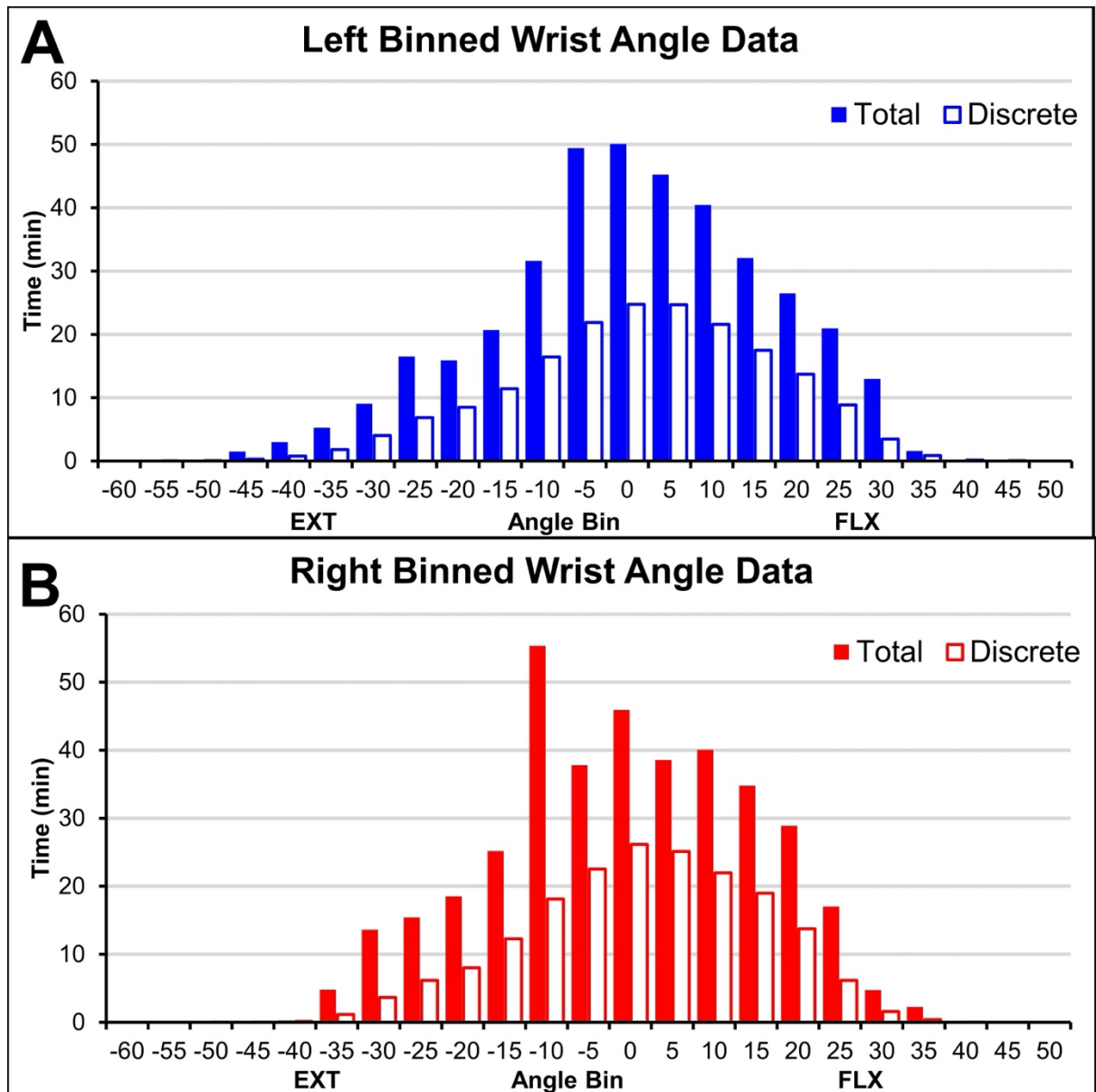


Figure 3

Survivorship and Clinical Outcomes for a Modular Lateralized Shoulder Epiphysis Used in Reverse Shoulder Arthroplasty: A Multi-Center Registry Review

*David Fawley - DePuy Synthes - Warsaw, USA

Amon Ferry - Arizona Sports Medicine Center - Scottsdale, USA

Rudolf Hoellrich - Slocum Research & Education Foundation - Eugene, USA

Sean Croker - Depuy Synthes - West Chester, USA

Introduction

In order to address the proper head center for the needs of each patient, lateralized options have been provided within a legacy shoulder system. The aim of this evaluation was to retrospectively assess survivorship and outcomes of the 145-degree epiphysis option implanted in reverse shoulder arthroplasty.

Methods

We conducted a retrospective multicenter registry case review from a company-sponsored registry. Clinical assessments were summarized at standardized registry visit windows. Kaplan-Meier (KM) survivorship was performed with revision of any component as the endpoint, with two separate censoring assumptions. First, unrevised subjects were censored at the last clinical follow-up [clinical assumption (CA)], and second at the date of database extract [registry assumption (RA)]. Survivorship was not calculated at timepoints where <40 shoulders were available for follow up.

Results

A total of 175 reverse shoulders were implanted across 2 US sites. Primary diagnosis was complete cuff tear in 104 (59.4%), partial cuff tear in 45 (25.7%), osteoarthritis in 19 (10.9%), and other in 7 (4%). Mean age was 70.6 years (R 47-88), 81 (46.3%) were female and BMI averaged 28.5 (R 16.9 to 44.7). Overall, 3 (1.7%) revisions were reported. Reasons for revision (N; % of reported cases) were chronic dislocation (1; 0.6%), pain/stiffness (1; 0.6%), and unstable shoulder (1; 0.6%). Additional complications included dislocation which was treated with closed reduction/manipulation and eventual revision; and a mid-shaft periprosthetic humeral fracture during insertion of the intermedullary rod guide, which was treated with open reduction and internal fixation. All-cause survivorship was 98.25% at 1 and 2 years for the RA. KM estimates are presented in Figure 1 and Figure 2.

Conclusion

Our study shows appropriate survivorship and complications for a 145-degree epiphysis used in reverse shoulder arthroplasty. Continued study of this design would be beneficial.

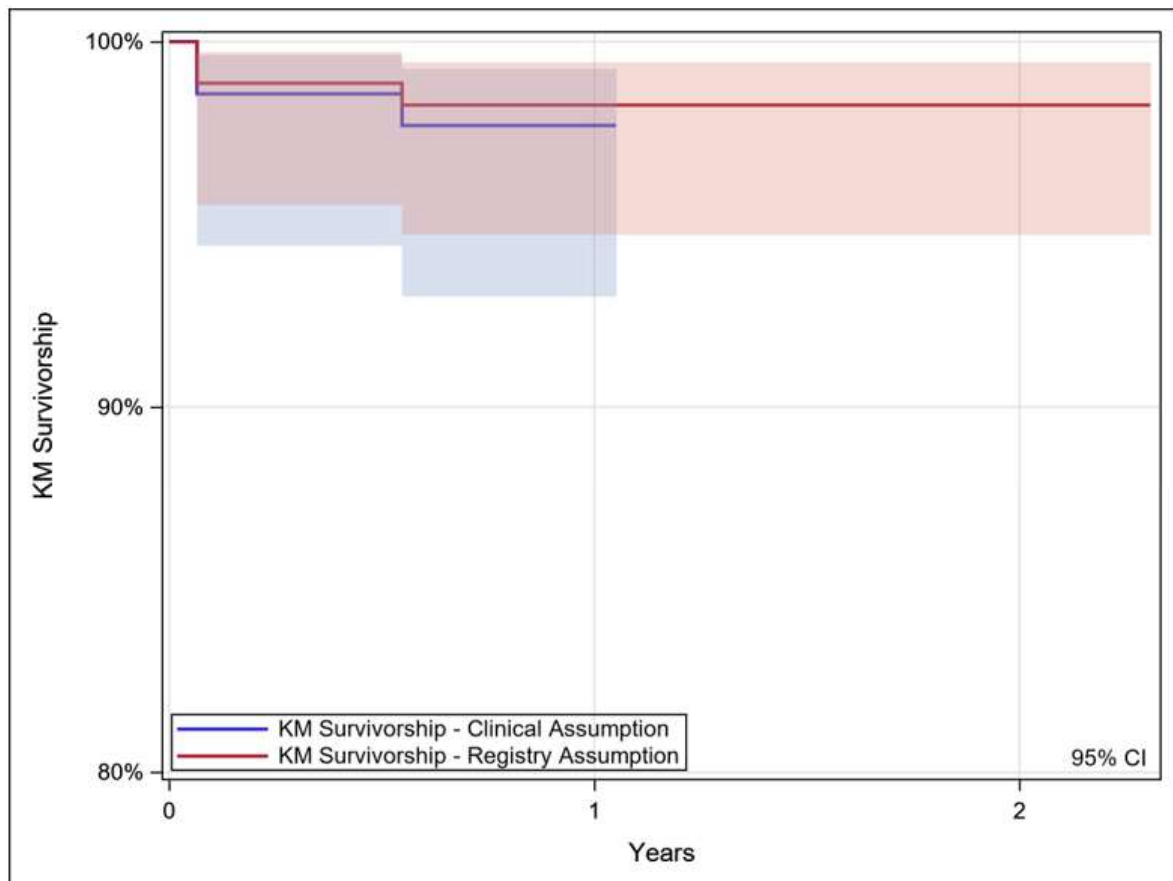
Figures

Figure 1 – Kaplan Meier Device Survivorship Estimates (Any component, any reason)

All Shoulders (N=175)	1 Year	2 Year
	KM Survivorship (95% CI) n with Later Follow-up	
All Cause Revision - CA	97.69% (92.97, 99.25%) n = 69	<40 shoulders
All Cause Revision - RA	98.25% (94.68, 99.43%) n = 155	98.25% (94.68, 99.43%) n = 73
Cumulative Revised	3	3

[Figure 1](#)

Figure 2 – KM Device Survival Estimates (Clinical and Registry Assumptions)



[Figure 2](#)

Porcine Carpal Biomechanics: Feasibility as a Preclinical Animal Model for the Human Wrist Joint

*J.J. Trey Crisco - Brown University - Providence, USA

Rohit Badida - Brown University - Providence, USA

Quianna Vaughan - Brown University - Providence, USA

Edward Akelman - Brown University - Providence, USA

Madison Altieri - Brown University - Providence, USA

Introduction: Arthroplasties that involve the hip, knee, or shoulder provide higher success rates than wrist due to years of in vitro, preclinical animal models and in vivo research. Previous studies evaluating ACL repair, bone fracture, and cartilage damage, have used porcine models because of the resemblance of the porcine knee in bony anatomy, bone mineral density, morphology, and healing to humans.

Advancing successful treatments for carpal instabilities are hindered due in part to limited preclinical animal models. The purpose of this study is to evaluate the Yucatan minipig (YP) as an animal model for the human wrist by quantifying carpal biomechanics in vitro during intact and ligament transection conditions.

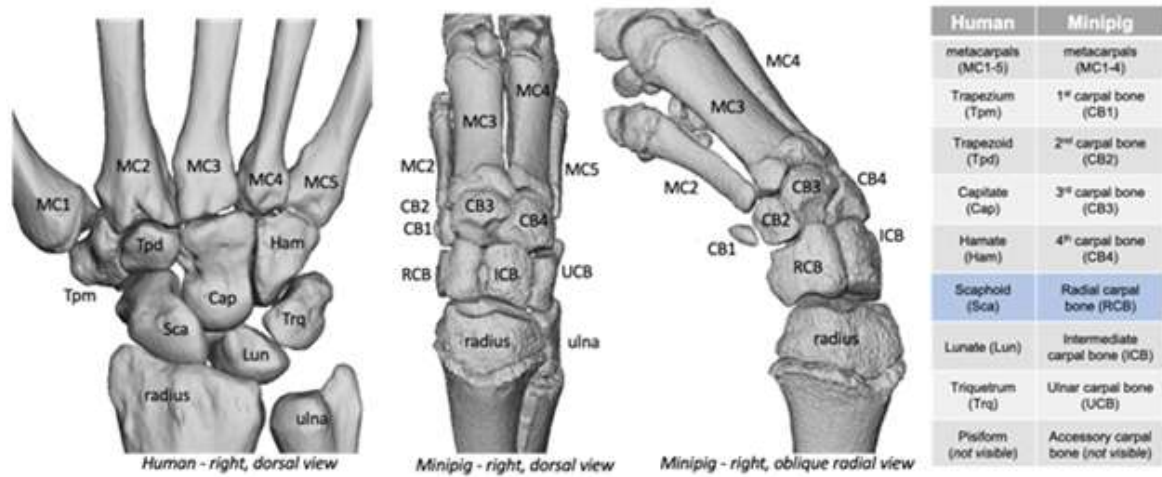
Methods: Gross anatomical review of the YP revealed that the carpus includes 8 individual carpal bones in two distinct rows, each with a unique size and geometry, bound together by a system of connective tissues (Fig. 1). Of the ligaments identified in the YP carpus, two were postulated to be homologous to the critical stabilizers of the human carpus; the radial intermediate ligament (RIL- homologous to the scapholunate interosseous ligament) and dorsal intercarpal ligament (DIC). ROM and stiffness were determined (n=12) using a six-axis robot in 28 directions. The testing was implemented in three conditions – intact, and after sequential transection of the RIL and the DIC. Mixed models evaluated the differences in kinematics as a function of testing direction, ligament condition, and sex. The difference in ROM between male and female specimens were consistently less than 1°, thus reported results were not stratified by sex.

Results & Discussion: The intact ROM envelope was elliptical in shape and oriented toward ulnar flexion with highest ROM about 15° from flexion-extension axis (Fig. 2). The carpus was most stiff in radial deviation and least stiff in ulnar flexion. Transection of RIL and DIC did not alter the ROM envelope orientation, however, significant ROM increase (p<0.05) was observed in flexion, extension and radial deviation following transection of both RIL and DIC. Supination of the YP carpus was significantly lower than pronation (p<0.05) in all three conditions. Volar translation was significantly higher (p<0.05) than dorsal translation in all three conditions.

Conclusions: This study provided insight into the influence of the carpal anatomy and biomechanics that maintains the stability of the porcine wrist and assesses the feasibility of whether it can be used as a preclinical animal model for the treatment of the degenerative wrist.

Acknowledgments: Supported in part by the National Institute of Arthritis and Musculoskeletal and Skin Diseases of the National Institutes of Health under Award Number R21AR08213. The content is solely the responsibility of the authors and does not necessarily represent the official views of the National Institutes of Health.

Figures



Human	Minipig
metacarpals (MC1-5)	metacarpals (MC1-4)
Trapezium (Tpm)	1 st carpal bone (CB1)
Trapezoid (Tpd)	2 nd carpal bone (CB2)
Capitate (Cap)	3 rd carpal bone (CB3)
Hamate (Ham)	4 th carpal bone (CB4)
Scaphoid (Sca)	Radial carpal bone (RCB)
Lunate (Lun)	Intermediate carpal bone (ICB)
Triquetrum (Trq)	Ulnar carpal bone (UCB)
Pisiform (not visible)	Accessory carpal bone (not visible)

Figure 1. Renderings from CT studies of the human and Yucatan minipig wrist, comparing the skeletal anatomy. The minipig carpus has bone homologues for all of the human carpal bones but lacks a thumb metacarpal (MC1). The pisiform and accessory carpal bone are both sesamoid bones, not true carpals, on the ulnar side and are not visible in these renderings.

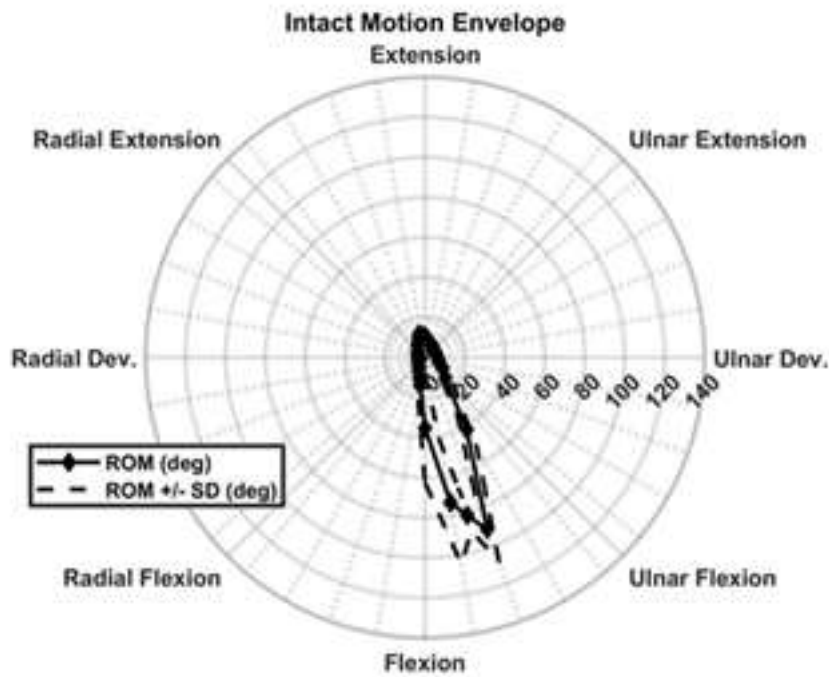


Figure 2. Envelope of the average (solid line) Intact ROM (\pm SD (dashed line) (deg)) across the 28 directions of forelimb motion.

[Figure 1](#)
[Figure 2](#)

Analyzing Prosthetic Radial Head 3D Topography

Srinath Kamineni - UK College of Medicine - Lexington, United States of America

*Anika Yadav - UK College of Medicine - Florence, United States of America

Background: In today's market, there are many prosthetic options for radial head arthroplasty that attempt to mimic the radial head's natural shape. However, machining technology has, in the majority, limited these prostheses to a symmetrical shape. This paper will compare the asymmetrical shape of the human radial head to several prostheses.

Method: We collected and analysed 11 commercially available radial head prostheses, along with a human cadaveric radial head. Using three dimensional topographic analysis, with an articulated digitizer, we compared the diameter, wall height, and radius of curvature. Statistical analysis with a student T test was performed with significance set at <0.05

Results: Only 2 of the 11 were statistically similar in fit ($p<0.025$) to the natural radial head in all dimensional categories, when utilizing non-standardized sizing, with two other implants mis-matched in the radius of curvature category only. When prostheses were standardized to the long and short axis of the human radial head only one implant was statistically similar to the human radial head ($p<0.025$), with two others mis-matched by only the short axis radius of curvature.

Conclusions: Our results suggest that a symmetrically machined radial head implant can closely match the capitellar articulation of a human radial head. However, manufacturer implant sizes made available to the market and the proximal radio-ulnar articulation have not been addressed and require more investigation to optimize radial head replacements. Of clinical relevance is that matching the prosthetic radial head to the long axis of the human radial head may achieve a better overall dimensional match, but over-sizes the short-axis diameter.

Figures

Table 1

	d (mm)	h1 (mm)	h2 (mm)	r (mm)		d (mm)	h1 (mm)	h2 (mm)	r (mm)
human long	16.5300	1.9200	1.9200	20.2700	human short	14.9500	1.9200	1.9200	15.7300
Avanta MONO	16.5300	1.0771	0.7846	37.1574		14.9500	0.9741	0.7096	33.6058
Avanta b1	16.5300	1.2196	0.6577	36.8567		14.9500	1.1030	0.5948	33.3338
Biomet F	16.5300	1.4672	1.5743	23.2198		14.9500	1.3269	1.4238	21.0004
Corin	16.5300	2.6090	2.8064	13.9679		14.9500	2.3596	2.5382	12.6328
Pritchard	16.5300	3.3653	3.3962	11.7932		14.9500	3.0436	3.0716	10.6659
radial head01	16.5300	2.7487	2.5518	14.2126		14.9500	2.4860	2.3079	12.8541
Sorbie	16.5300	1.3516	1.5297	24.4287		14.9500	1.2224	1.3834	22.0937
Stratec	16.5300	1.5821	1.8822	20.5849		14.9500	1.4308	1.7023	18.6173
Stryker	16.5300	2.1674	2.1450	16.9184		14.9500	1.9603	1.9400	15.3013
Tornier	16.5300	0.6940	1.1373	37.7584		14.9500	0.6277	1.0286	34.1493
Wright	16.5300	1.1684	1.2365	29.0063		14.9500	1.0567	1.1183	26.2337
Std Dev	1.0100	0.3200	0.3200	4.6100		0.9900	0.3200	0.3200	1.6300
<2.2414 Std Devs	14.2662	1.2028	1.2028	9.9371		12.7310	1.2028	1.2028	12.0765
>2.2414 Std Devs	18.7938	2.6372	2.6372	30.6029		17.1690	2.6372	2.6372	19.3835

Figure 1

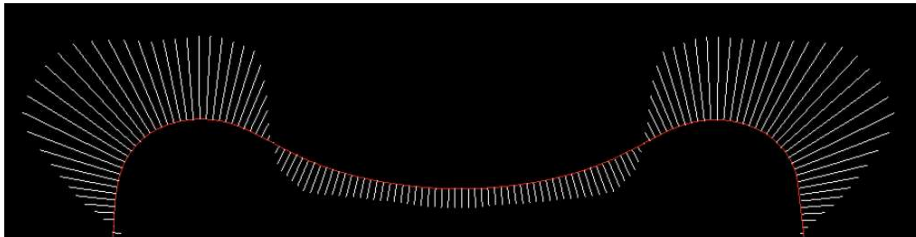


Figure 4 – Stryker

Figure 2

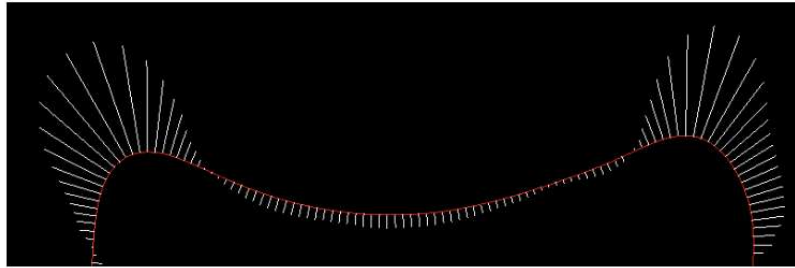


Figure 5 – Human head, short axis

[Figure 3](#)

Distribution of Coronal Plane Alignment of the Knee in German Patients With Knee Arthritis

*Anoop Chandrashekar - Vanderbilt - Nashville, United States of America

Courtney Baker - Vanderbilt - Nashville, USA

Stephen Engstrom - Vanderbilt University Medical Center - Nashville, USA

Gregory Polkowski - Vanderbilt University Medical Center - Nashville, USA

Martin Faschingbauer - Department of Orthopedic Surgery, RKU, University of Ulm - Ulm, Germany

John Ryan Martin - Vanderbilt Health - Hendersonville, USA

Introduction: The Coronal Plane Alignment of the Knee (CPAK) classification proposes 9 phenotypes of knee alignment. Deep learning algorithms have been developed to classify health and arthritic knees according to CPAK. However, no models have been published in post-operative knees. The aim of this study was to develop a deep learning model to determine post-operative knee CPAK classifications.

Methods: Long leg radiographs (LLR) from 566 German patients who had undergone total knee arthroplasty (TKA) were manually annotated to measure mechanical hip-knee-ankle (mHKA) angles, mechanical lateral distal femoral angle (LDFA), and mechanical medial proximal tibial angle (MPTA). A machine learning model was trained using 455 LLR to recognize anatomic landmarks necessary to measurement alignment. The model was then tested on 111 LLR to automatically calculate mHKA, MPTA, and LDFA. Bland-Altman plots were used to measure agreement in the measurements obtained from manual and automated measurement. Kappa statistic was used to determine agreement in CPAK classification from manual and automated measurement.

Results: The mean difference between the manually and automatically measured mHKA, LDFA, and MPTA were 0.133° (95% agreement interval -1.44° to 1.17°), 0.377° (-6.82° to 6.21°), and 1.15° (-4.36° to 3.58°) respectively. Cohen's Kappa demonstrated substantial agreement in CPAK classification by the manual and automated methods ($\kappa = 0.717$, $p < 0.001$).

Conclusions: We describe a novel machine learning model for analyzing post-operative LLRs to classify patient knees according to the CPAK classification system with excellent results. Further research should examine the effect post-operative CPAK classification may have on outcomes from TKA.

Tibial Components Placed in Constitutional Varus Following TKA: A Minimum 5-Year Survivorship Analysis

*Arthur Malkani - Jewish Hospital - Louisville, USA

John Whitaker - University of Louisville - Louisville, USA

Gavin Clark - Royal Perth Hospital - Perth, Australia

Serene Lee - Perth Hip & Knee - Perth, Australia

Dermot Collopy - Perth Hip and Knee Clinic - Perth, Australia

Langan Smith - UofL Health - Louisville, United States of America

Rohat Bhimani - University of Louisville - Louisville, United States of America

Introduction:

The concept of kinematic alignment incorporates the technique of reproducing the patient's constitutional tibial varus in order to establish the native joint line and medial joint space. Tibial components placed in varus has been controversial due to concerns of tibial subsidence and loosening. The purpose of this study was to evaluate mid-term survivorship following total knee arthroplasty (TKA) with tibial components placed in 3 degrees or greater of constitutional varus alignment.

Methods:

This was a retrospective review of 265 patients, with a minimum 5-year follow-up, who underwent a primary robotic-assisted TKA (RA-TKA) with tibial components placed in constitutional varus. The study group included 154 male and 111 female patients. Mean patient age was 66 years (range 36 to 91, SD=8.5). There were 231 cemented and 34 cementless implants. The mean postoperative tibial varus alignment was 4.0 degrees (range -3.0 to -6.4, SD=1.2). The mean femoral valgus alignment was 1.1 degrees (range -3.7 to 7.9, SD=1.9) and the mean overall limb alignment was 2.9 degrees of varus (range -2.5 to -6.7, SD = 1.8). Outcome measures included complications, revisions, along with PROMs.

Results:

The mean increase in FJS-12 and KOOS-JR postoperatively were 62.4 (SD=24.9) and 42.0 (SD=16.4), respectively. Six patients required revision TKA: prosthetic joint infection (2), traumatic extensor mechanism rupture (2), instability (1), and arthrofibrosis (1). Three patients required non-revision intervention for stiffness. There was no incidence of aseptic loosening, subsidence, or fracture of either the tibial or femoral components. Survivorship at 5 years with all-cause failure as the end point in this series was 98%.

Conclusion:

Tibial components placed in constitutional varus using RA-TKA to achieve the desired goal of approximating the native joint line demonstrated 98% survivorship at 5 years with no cases of aseptic tibial or femoral component failure. The use of RA-TKA to achieve well balanced gaps and target alignment through bone cuts and implant positioning appears promising. Further follow-up is needed to determine if long-term survivorship can be maintained with varus tibial component alignment.

Does Increased v-v Moment Affect the Tibial Micromotion of a v-v Constrained Insert?

*Chase Maag - DePuy Synthes - Warsaw, USA
Ryan Knowles - University of Denver - Denver, USA
Amit Mane - DePuy Synthes - Warsaw, USA

Introduction: Total knee arthroplasty (TKA) is a common treatment for knee osteoarthritis [1]. In cementless TKA, the initial fixation of a cementless tibial tray to the host bone is crucial for successful bony ingrowth, and the magnitude of interface micromotions can depend on the type of implant used. The kinetics across the joint can alter due to various reasons, such as ligament laxity, placement errors, or implant conformity. Post-TKA instability in the coronal plane can change the contact mechanics in the medial and lateral compartments of the knee, thereby changing the varus-valgus (V-V) moment across the joint. This study aimed to computationally understand the effect of the V-V moment on tibial tray micromotion during stair descent activity in a V-V constraint insert.

Methods: This study developed two loading profiles: Normal Step-Down and Increased V-V (2xV-V) Step-Down, using a validated finite element lower limb model [2]. Step-down boundary conditions (BCs) were extracted from the Orthoload database and applied to the lower limb model [3]. The baseline BCs were considered normal, while the 2xV-V loading profile had the V-V moment doubled. Micromotion was investigated using a validated finite element cadaveric tibial micromotion model [4]. Each loading profile was applied to an asymmetric insert with V-V constraint. The peak change in the distance between six points on the tray and bone was considered the micromotion of the construct (3 on tray; 3 on bone), (Fig. 1).

Results: The 2xV-V loading condition changed the micromotion by 8.7%, -49.8%, and -78.1% for the medial, central, and lateral point pairs, respectively (Fig. 2). Components of the micromotion had significantly different contributions to the overall micromotion during the cycle. The 2xV-V loading condition increased the micromotion in the M-L axis, but it reduced in the S-I and A-P axes (Fig. 3).

Discussion: The purpose of this study was to understand the effect of increased V-V loading on the micromotion of an asymmetric insert with V-V constraint using a computational FE model. The micromotion was found for 3 colinear point pairs and the maximum distance change over the loading cycles were found. The 2xV-V loading increased the M-L axis micromotion but it did not increase along the A-P and S-I axes, which could be due to the increased loading leading to stabilized the construct in the lateral compartment. While the M-L axis micromotion increased for the 2xV-V loading condition, the overall micromotion of the construct reduced. Thus, the micromotion may not be overly sensitive to increased V-V torque in an asymmetric insert with V-V constraint.

References: 1. Sloan M, et. al. - 2018; 2. Fitzpatrick et. al. – 2014; 3. Bergman et. al. – 2008 4. H. Yang, et. al. - 2022.

Figures



Figure 1. Cadaveric Micromotion Measurement Points

Figure 1

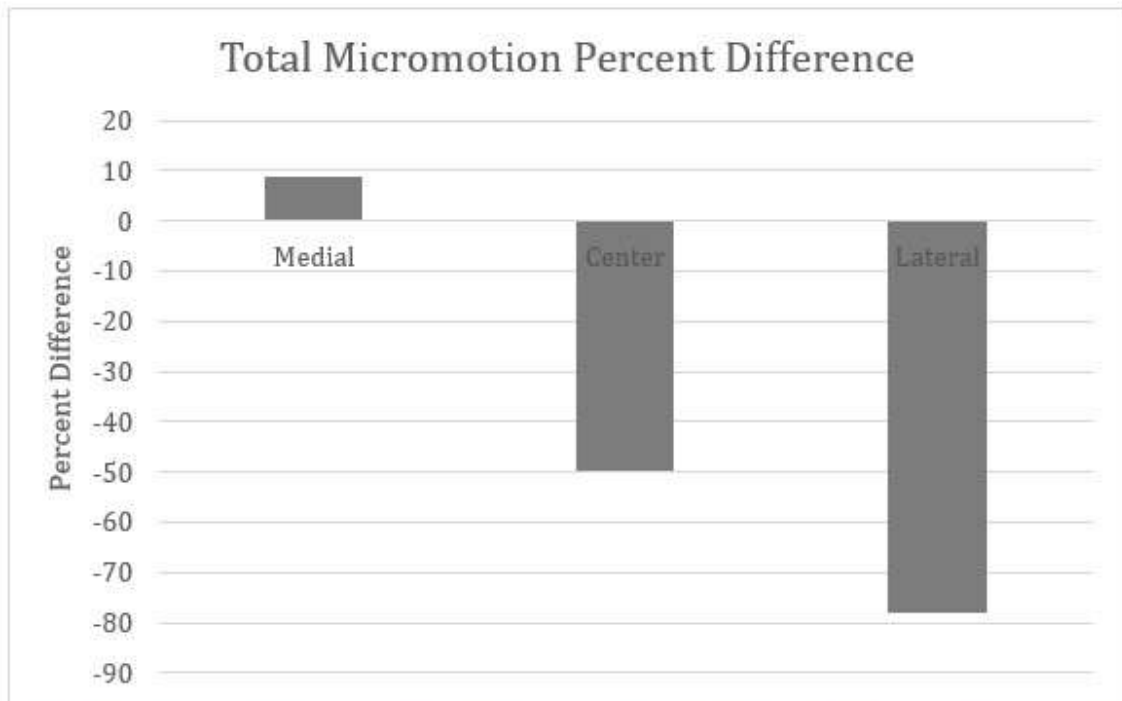


Figure 2. Percent Difference of total micromotion (Percent difference from Normal micromotion)

Figure 2

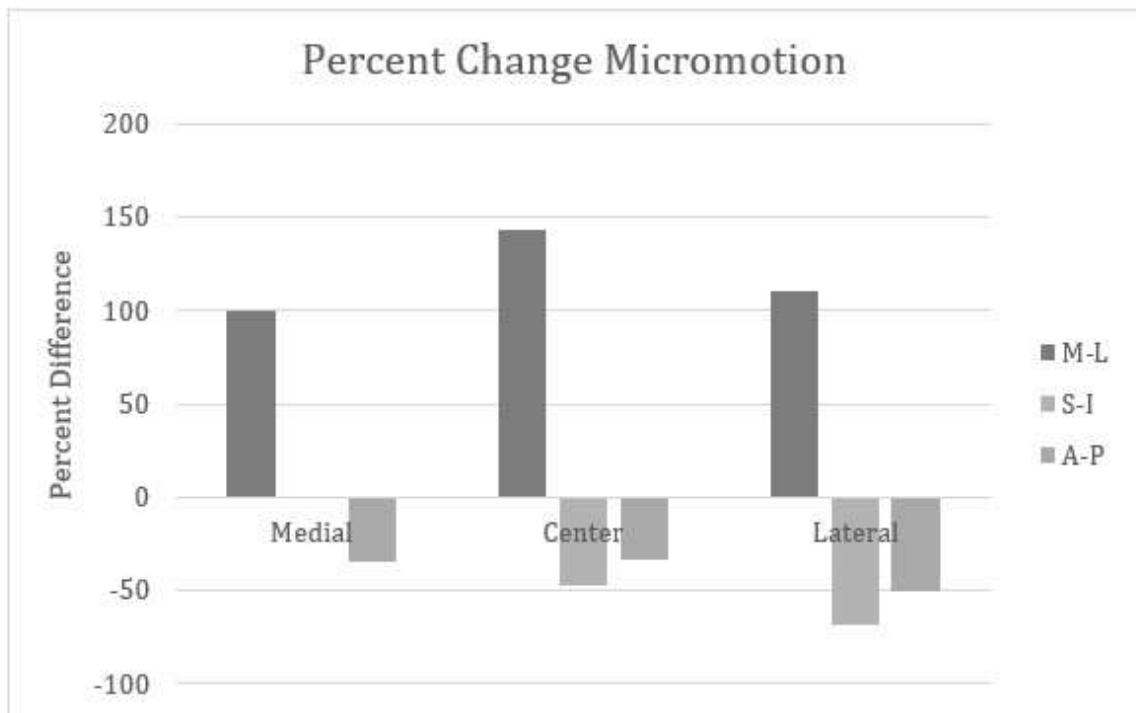


Figure 3. Percent Difference of independent axis (Percent difference from Normal micromotion)

[Figure 3](#)

Intact and Total Knee Arthroplasty Joint Kinematics During Activities of Daily Living

*Emma Donnelly - Western University - London, Canada

Ryan Willing - Western University - London, Canada

Brent Lanting - London Health Sciences Centre - London, Canada

Introduction

Robotic-assisted (RA) surgery is seeing greater use in orthopedics, specifically with its continued growing popularity for total knee replacement (TKR). Sufficient evidence supports claims that RA surgery improves implant alignment accuracy [1]–[3]. There have been fewer studies, however, on the impact of this on resulting joint behaviors, such as laxity and kinematics during activities of daily living, under controlled laboratory conditions. Therefore, this study investigates joint kinematics in intact knees and TKR knees following conventional and RA surgery under loads simulating activities of daily living (ADL).

Methods

The knees of eight (8) full-lower body specimens (5 males, 3 females, aged 52-76) underwent TKR surgery. For each pair, one joint replacement was done using conventional manual methods, while the contralateral side used an RA system. Regardless of surgical method, mechanical alignment, and a cruciate retaining rotating platform (CR PR) implant system were used. An additional six (6) specimens (3 males, 1 female, aged 65-90) comprised the intact cohort. The knee joints from all specimens were isolated and mounted onto a six degree-of-freedom joint motion simulator. Simulated loads representative of gait, stair ascent, and stair descent were applied to the joint; these were based on the Orthoload (<https://orthoload.com/>) dataset [4] but reduced by 75% to prevent specimen damage and slowed to 25 seconds per cycle. Optical markers were affixed to the femur and tibia, from which tibiofemoral joint kinematics were computed using modified Grood & Suntay conventions [5], [6]. For each ADL, statistical parametric mapping (SPM, one-way ANOVA with post hoc tests) was performed to compare the three cohorts (conventional vs RA vs intact) in terms of anterior/posterior (AP), varus/valgus (VV) and internal/external rotation (IE) kinematics.

Results

During gait, TKR knees had smaller AP translations than the intact knees to varying degrees depending on the activity. Both TKR cohorts had AP translations statistically significant from intact during the stance phase of gait (Fig. 1). Differences in AP translations between cohorts were also observed during stair ascent during the swing – or pull-up – phase (Fig. 2). During the weight acceptance phase of stair descent (Fig. 3) only RA TKR knees had statistically different AP translation to the intact cohort. No other statistically significant differences were found.

Conclusion

Differences in AP kinematics with respect to intact can likely be attributed to the prosthesis design used, and that the intact specimens were from different donors than the (paired) TKA cohort. The fact that RA yielded significantly different kinematics across longer durations of the motion cycles is perhaps a result of their being less variability in surgical outcomes using this technique. Ultimately, the similarity between conventional and RA results suggests that, overall, kinematics differences between approaches are minor compared to the effect of prosthesis design.

References

- [1]Cho et al., *Int. Orthop.*, 2019; 43(6):1345-54.
- [2]Agrawal et al., *Arthroplasty*, 2022; 4(1):6.
- [3]Song et al., *Clin Orthop Relat Res*, 2013; 471(1):118-26.
- [4]Bergmann et al., *PLoS ONE*, 2014; 9(1): e86035.
- [5]Dabirrahmani et al., *Med. Eng. Phys.*, 2017; 39(1):113-16.
- [6]Grood & Suntay, *J. Biomech. Eng.*, 1983; 105(2): 136-44.

Figures

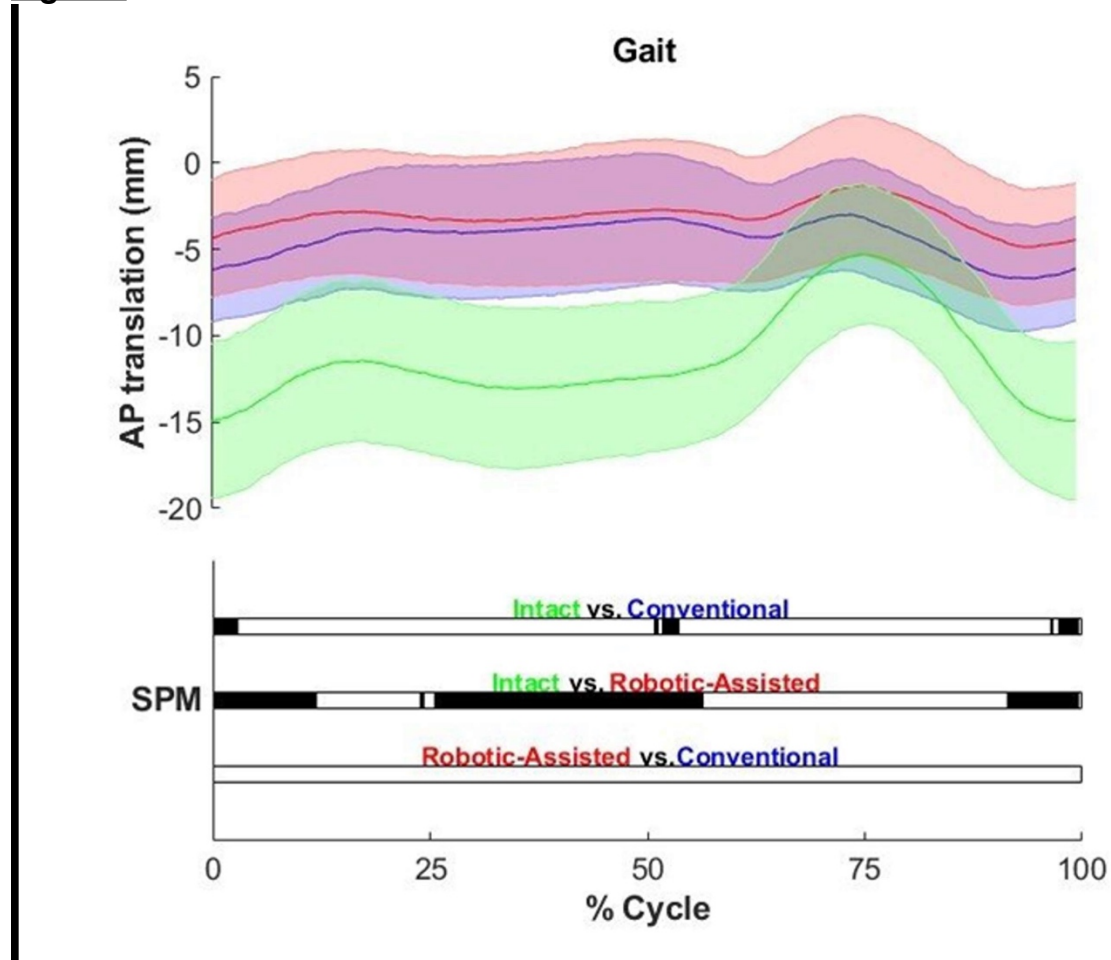


Figure 1: Mean \pm SD of anterior-posterior (AP) translation of the tibia with respect to the femur during gait in conventional TKA, Robotic-assisted TKA and intact knees.

[Figure 1](#)

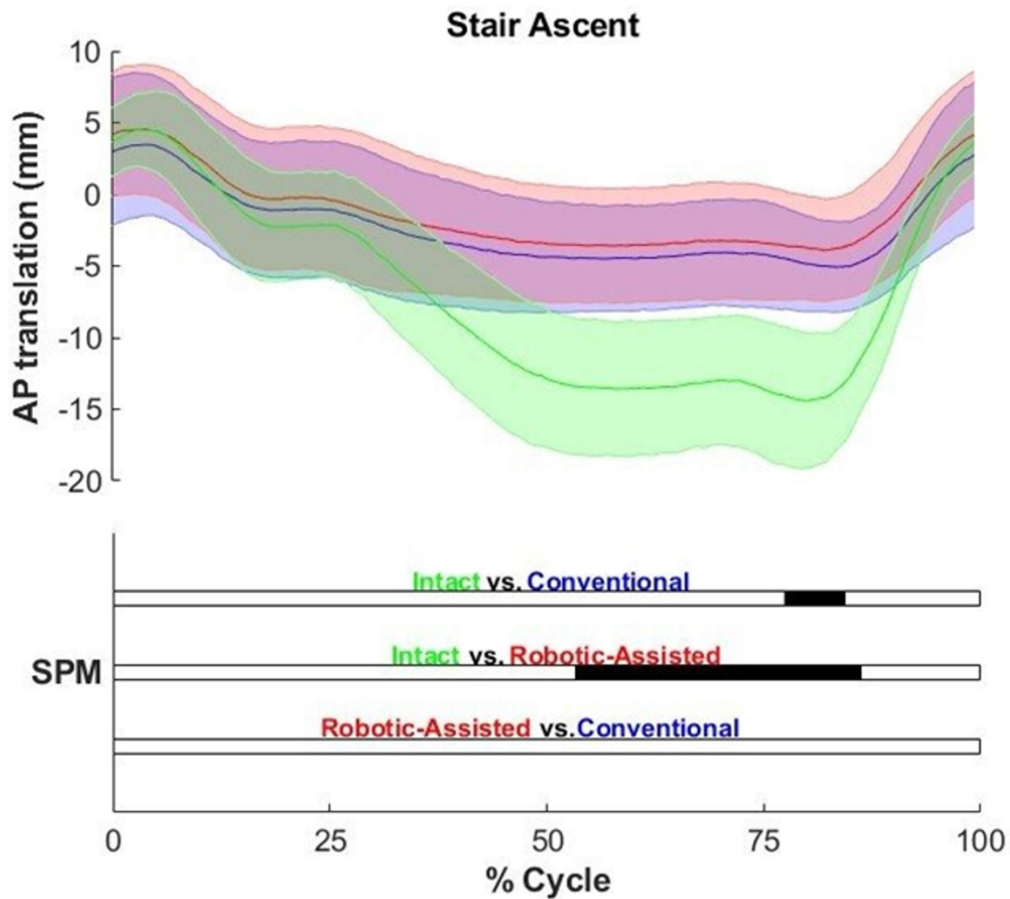


Figure 2: Mean \pm SD of anterior-posterior (AP) translation of the tibia with respect to the femur during stair ascent in conventional TKA, Robotic-assisted TKA and intact knees.

[Figure 2](#)

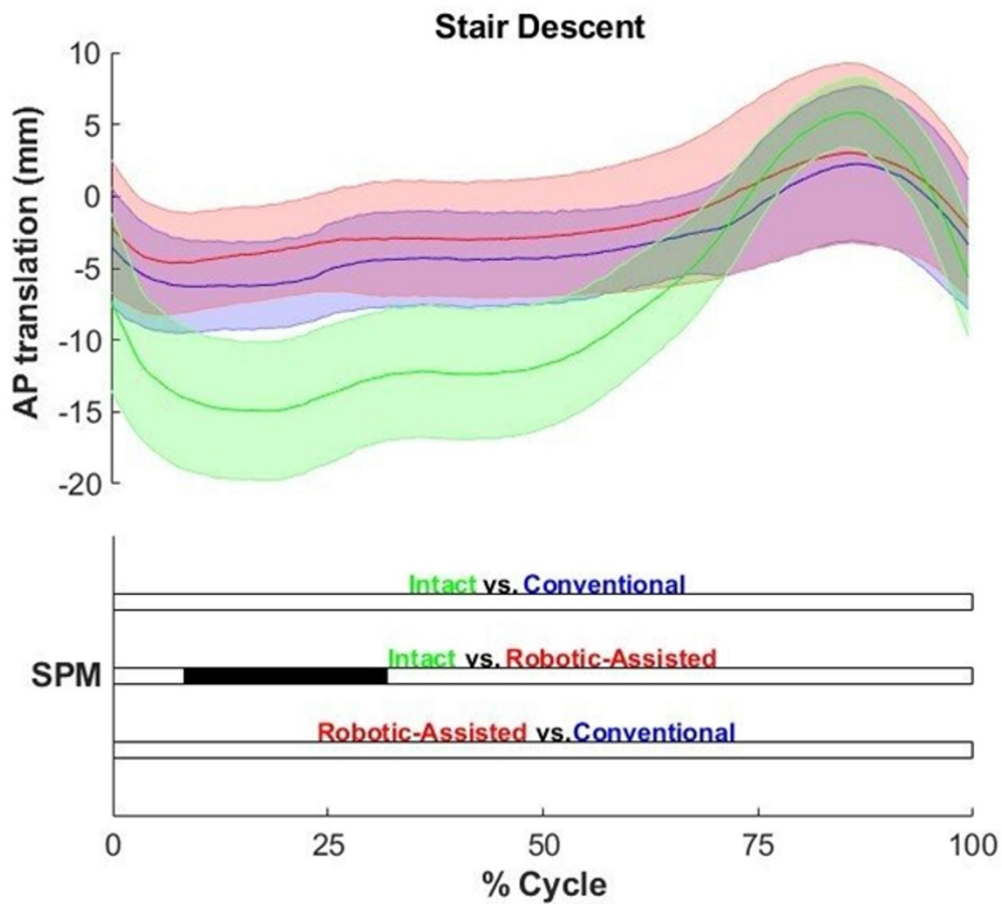


Figure 3: Mean \pm SD of anterior-posterior (AP) translation of the tibia with respect to the femur during stair descent in conventional TKA, Robotic-assisted TKA and intact knees.

[Figure 3](#)

Anatomical Phenotyping of the Knee for TKA Planning: Beyond the Coronal Plane

*Ishaan Jagota - 360 Med Care - Sydney, Australia

Jonathan Bare - Melbourne Orthopaedic Group - Melbourne, Australia

Andrew Shimmin - Melbourne Orthopaedic Group - Melbourne, Australia

Joshua Twigg - University of Sydney - Sydney, Australia

Brad Miles - 360 Knee Systems - Pymble, Australia

Introduction:

The Coronal Plane Alignment of the Knee (CPAK) classification system^[1] has seen growing use in describing knee phenotypes based on the Joint Line Obliquity (JLO) and arithmetic Hip-Knee-Ankle (aHKA) alignment in total knee arthroplasty (TKA) planning. It has been proposed that CPAK phenotypes could be used for subject specific surgical planning. However, the growing use of 3D image based navigation raises the question of whether a 2D classification captures the complex 3D anatomical variations and axial plane alignments present in individual patients. This study investigates the degree to which 2D CPAK classifications are representative of 3D anatomical variations in patient geometry.

Method:

Data was aggregated from 7,450 knees from 6,235 patients operated on from August 2015 to January 2024 who had a pre-operative CT scan segmented and landmarked from the 360MedCare CT database. From these landmarks, the Joint Line Obliquity (JLO) and arithmetic Hip-Knee-Ankle (aHKA) were calculated to determine CPAK Group. In addition, from the 3D reconstruction the Transepicondylar Axis to the Posterior Axis (TEA angle), the Trochlear Groove to the Posterior Axis (Trochlear angle) and the angle between Insall's axis connecting the medial third of the tubercle and posterior collateral ligament attachment on the tibia and Cobb's axis between the centres of the plateau (Tibial Rotation angle) were calculated. Correlations between these axial measurements and the JLO and aHKA were calculated and any systematic differences in axial offsets based on CPAK group determined.

Results:

The distribution of the CPAK classifications for the 6,235 patients' data used in the analysis was similar to those originally described in the CPAK classification, with our database finding 2,577 (34.6%) of patients fit into the most populous group II of neutral aHKA/apex distal JLO (32.2% in the original study^[1]).

Correlations between axial measurements and CPAK aHKA and JLO measurements were all statistically significant but low in strength, indicating low clinical relevance. The highest strength correlation was between the JLO measurement and the Tibial Rotation angle with $r = -0.23$ indicating a weak relationship, with most axial plane variation not captured by the CPAK grouping.

Conclusion:

Statistically significant correlations between CPAK grouping and axial measurements of the femoral and tibial angles were observed in end stage osteoarthritic tibia and femora, but the relationships were not strong, indicating inter-patient variation dominated. CPAK categorical give a concise and readily interpretable description of the coronal plane phenotype but does not capture the full picture of 3D variation in patient geometry.

References:

[1] MacDessi, S. J., Griffiths-Jones, W., Harris, I. A., Bellemans, J., & Chen, D. B. (2021). Coronal plane alignment of the knee (CPAK) classification: a new system for describing knee phenotypes. *The bone & joint journal*, 103(2), 329-337.

Blinded Assessment of Soft-Tissue Balance Using an Advanced Knee Simulator Model

*Kevin Abbruzzese - Stryker - Mahwah, USA

Vincent Alipit - Stryker - Mahwah, USA

Andre Freligh - Stryker Orthopaedics - MAHWAH, United States of America

Michael Dunbar - Dalhousie University - Halifax, Canada

Jared Weir

Michael Mont - Sinai Hospital of Baltimore - Baltimore, USA

Sally LiArno - Stryker Orthopaedics - Bergenfield, USA

Introduction:

Ensuring proper soft tissue balance is imperative for successful total knee arthroplasty (TKA), as imbalances can lead to patient dissatisfaction, instability, and stiffness. Achieving optimal outcomes in TKA relies on restoring the natural balance within the soft-tissue envelope surrounding the knee. However, conventional soft tissue balancing techniques often involve subjective assessments, predominantly based on a surgeon's tactile evaluation of ligament laxity. This study investigates a surgeon's ability to discern appropriate insert thickness during a blinded manual laxity assessment.

Methods:

An advanced knee simulator model (AKS) was created using a patient's 3D Computed Tomography scan undergoing left TKA with varus deformity and moderate osteophytes. The AKS underwent robot-assisted total knee arthroplasty (RATKA), utilizing an 11mm tibial insert to achieve balance. Surgeons conducted manual laxity assessments on balanced model with unrestricted visual and proprioceptive feedback. They then repeated the assessment while blinded to the joint, using a knee stocking to obscure ligaments and TKA components. Inserts ranging from 9-14mm with 1mm increments were then randomized and evaluated. Eight high-volume surgeons identified the random insert over three rounds, totaling 15 blinded trials per surgeon. Accuracy and precision were recorded, excluding the 11mm insert.

Results:

Surgeons demonstrated a combined average accuracy of 0.58 ± 0.27 for all randomized rounds with a range of 0.4-0.87, Figure 1. No learning effects were observed over the course of the three rounds for each surgeon, as accuracy did not increase per round, Figure 2. The distribution of errors indicated a margin of error beyond 1mm in 40% of cases, Figure 3.

Discussion:

Soft tissue balance relies on individual proprioception, which inherently varies in terms of accuracy and precision. High-volume surgeons displayed varying levels of accuracy and precision during blinded laxity assessments. While they effectively detected gross laxity changes based on proprioceptive feedback, their accuracy in identifying insert thickness resolution was inconsistent. This variability underscores the need for objective measures, such as the passive knee drop test, to ensure reproducible results in soft tissue balance assessment during TKA.

Figures

JR-GSNPS-ARTI-1029135

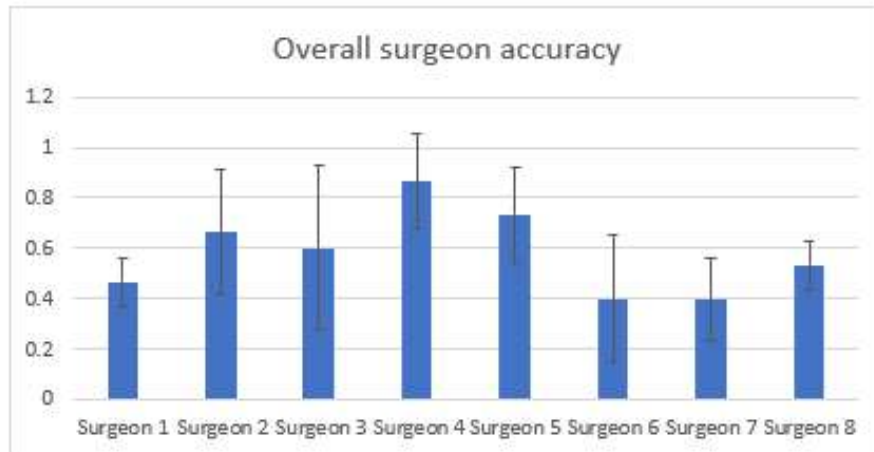


Figure 1. Overall accuracy per surgeon based on blinded randomized laxity assessment

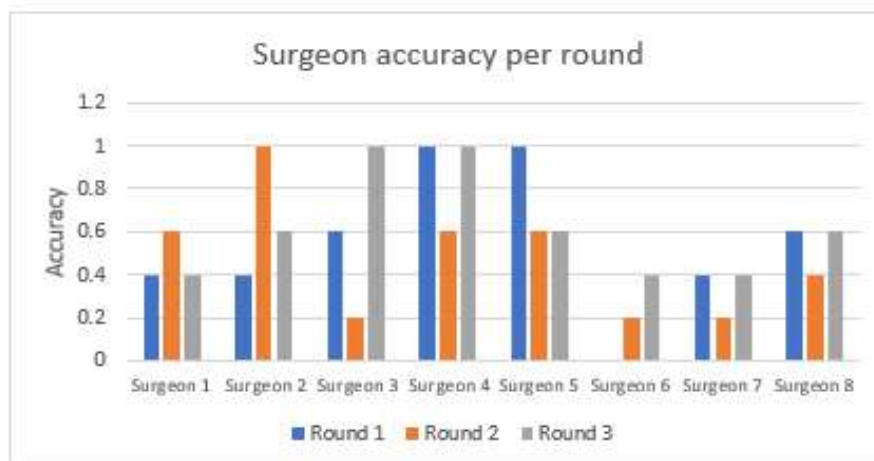


Figure 2. Estimate of learning as overall accuracy per surgeon laxity assessment per round



Figure 3. Error distribution (mm) for incorrect response

[Figure 1](#)

Correlational Analysis of CPAK-Based Coronal Alignment and Patellofemoral Joint Status: Enhancing Surgical Planning and Management in Total Knee Arthroplasty

*Amir Pourmoghaddam - Memorial Bone and Joint Research Foundation - Houston, USA

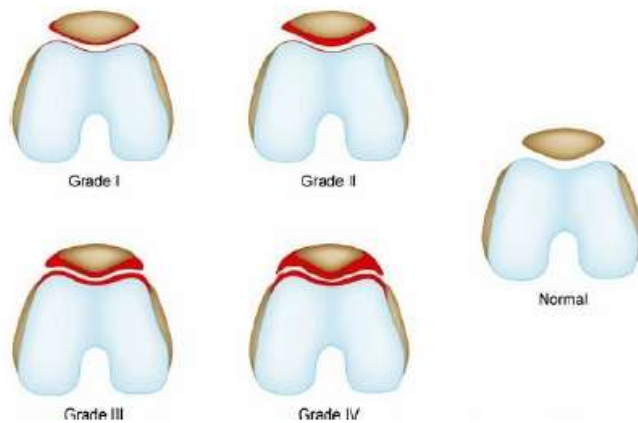
Danielle DeMoes - Inov8 Orthopedics - Houston, USA

Stefan Kreuzer - INOV8 Orthopedics - Houston, USA

Total Knee Arthroplasty (TKA), utilized for end-stage osteoarthritis (OA), has up to 20% patient dissatisfaction. Efforts aim to enhance surgical methods, patient optimization, and intraoperative conditions, customizing procedures and balancing ligaments to reduce revisions and enhance satisfaction. Conventional knee alignment terms fail to capture joint line dynamics. Coronal Plane Alignment of the Knee (CPAK) offers a nuanced understanding based on leg alignment and joint line position. Though helpful for preoperative planning, CPAK excludes the patellofemoral joint (PFJ). While traditionally, knee OA focused on the tibiofemoral joint (TFJ), the PFJ's importance grows apparent. PFJ disorders increase stress, leading to cartilage deterioration. Malalignment raises contact pressure, asymmetry, and facet-specific OA, as per the Sperner classification. Numerous strategies exist for knee OA treatment, but alignment objectives, surgical methods, and patient criteria remain uncertain. Achieving ideal coronal alignment in TKA is challenging, with a lack of consensus on optimal alignment, hindering comparisons. Refined surgical techniques offer promise for precise planning. Malalignment contributes to PFJ wear, yet CPAK overlooks the PFJ. This study aims to correlate specific PFOA grades with CPAK classifications, suggesting an interplay between joint health and alignment. Customizing alignment goals based on individual conditions could enhance outcomes and restore natural knee function.

This study involved 130 participants. Data were systematically gathered from each patient, including the grading of both CPAK and Femoral OA. The data collection process adhered to the guidelines of an Institutional Review Board (IRB)-approved database. A three-way loglinear analysis was performed to determine a hierarchical unsaturated model for the associations between CPAK, Medial Femoral OA scoring, and Lateral Femoral OA scoring. An unsaturated model was chosen using SPSS Statistics' hierarchical loglinear model selection procedure with a backwards elimination stepwise procedure. This produced a model that included all main effects and two two-way associations of CPAK*MedFOA and CPAK*LatFOA. The model had a likelihood ratio of $\chi^2(48) = 33.13$, $p = .973$. Partial likelihood ratio χ^2 are presented in Table 1 and loglinear parameter estimates in Table 2.

Figures



The Sperner classification of patellofemoral osteoarthritis delineates five grades:

Grade 0: No degenerative changes observed.

Grade 1: Definitive subchondral sclerosis with minimal osteophytes on the patella.

Grade 2: Clear presence of osteophytes on the patella.

Grade 3: Narrowing of the patellofemoral joint space, with osteophytes evident on both the patella and femoral condyles.

Grade 4: Constricted joint space accompanied by significant osteophytes and a distorted patella.

[Figure 1](#)

Parameter	Estimate	Z	Sig.
Constant	2.273	7.903	0.000
[CPAK = IV]	-0.229	-0.528	0.597
[CPAK = V]	-0.717	-1.342	0.180
[MedFOA = Grade 0]	-2.015	-2.677	0.007
[MedFOA = Grade 1]	-0.629	-1.436	0.151
[MedFOA = Grade 2]	-1.099	-2.127	0.033
[MedFOA = Grade 3]	-1.322	-2.349	0.019
[LatFOA = Grade 0]	-3.091	-3.023	0.003
[LatFOA = Grade 1]	-1.992	-3.237	0.001
[LatFOA = Grade 2]	-1.992	-3.237	0.001
[LatFOA = Grade 3]	-1.482	-2.991	0.003
[CPAK = IV] * [MedFOA = Grade 0]	-1.076	-1.031	0.303
[CPAK = IV] * [MedFOA = Grade 1]	-1.769	-2.596	0.009
[CPAK = IV] * [MedFOA = Grade 2]	-1.587	-2.011	0.044
[CPAK = IV] * [MedFOA = Grade 3]	-1.076	-1.402	0.161
[CPAK = V] * [MedFOA = Grade 0]	-18.308	-0.005	0.996
[CPAK = V] * [MedFOA = Grade 1]	-2.262	-2.025	0.043
[CPAK = V] * [MedFOA = Grade 2]	-19.224	-0.005	0.996
[CPAK = V] * [MedFOA = Grade 3]	-19.001	-0.005	0.996
[CPAK = IV] * [LatFOA = Grade 0]	3.186	2.866	0.004
[CPAK = IV] * [LatFOA = Grade 1]	2.634	3.614	0.000
[CPAK = IV] * [LatFOA = Grade 2]	1.887	2.457	0.014
[CPAK = IV] * [LatFOA = Grade 3]	1.258	1.835	0.067
[CPAK = V] * [LatFOA = Grade 0]	3.091	2.571	0.010
[CPAK = V] * [LatFOA = Grade 1]	1.992	2.258	0.024
[CPAK = V] * [LatFOA = Grade 2]	1.769	1.943	0.052
[CPAK = V] * [LatFOA = Grade 3]	-17.223	-0.006	0.996

Figure 2

Effect	df	Partial Association ($\chi^2(df)$)	Sig.
CPAK *MedFO	8	15.361	0.052
CPAK*LatFOA	8	26.8	0.001
MedFOA*LatFOA	16	11.334	0.788
CPAK	2	20.178	0
MedFOA	4	133.238	0
LatFOA	4	16.895	0.002

Figure 3

Evaluation of a Self-Powered Knee Implant Under Simulated Gait Loading

*Adam Garry Redgriff - Western University - London, Canada

Yizhao Li - Western University - London, Canada

Sherry Towfighian - Binghamton University - Binghamton, USA

Ryan Willing - Western University - London, Canada

Introduction: Although “smart” implants are capable of monitoring prosthesis health, few can assess joint contact forces post-total knee arthroplasty (TKA), with none reaching commercial availability. Self-powered triboelectric generators (TEGs) are capable of both sensing joint forces and harvesting energy to power telemetry circuits. However, the correlation between the voltages measured by TEGs and the actual applied forces is complex and not directly linear, and therefore should be observed under controlled loading conditions representative of activities of daily living (ADL) to refine sensing algorithms. Previous studies have examined TEG responses to ADL loads, but only assessed a two-sensor configuration under select compressive loading conditions. This study examines the voltages produced using a four-quadrant TEG design and assesses these voltages under loading conditions that more accurately represent gait.

Methods: Joint contact forces for a right knee during normal gait were defined using Orthoload’s Standard Loads Knee Joint dataset [1]. Force and moment magnitudes for each DoF were scaled to 25% of their original value, resulting in a maximum compressive force of ~500 N. These loads were applied to the TEG harvester using a 6-DoF joint motion simulator (AMTI VIVO). The harvester package contains four separate TEG quadrants and is housed between the ultra-high molecular weight polyethylene (UHMWPE) bearing and tibial tray of a commercially available cruciate-retaining TKA system (Fig 1). Voltages were measured with a Keithley 2410 source-meter for each quadrant during four loading conditions: (i) Fixed - Vertical compression with all other DoF fixed. (ii) Free - Vertical compressive loading with all DoF in force control, allowing them to move to maintain 0 N or 0 Nm with knee flexion angle set to zero degrees. (iii) 5-DoF Extension - 5-DoF in force control with ADL loads but without flexion. (iv) 6-DoF - 5-DoF in force control with ADL loads and physiological flexion/extension motions.

Results: The largest peak voltages from all four harvester quadrants were generated during the 6-DoF (iv) condition (Table 1). Prescribing 5-DoF ADL loads while locked in extension produced the lowest magnitude peak voltages. Voltage magnitudes were similar during the Fixed and Free vertical compressive loading conditions. On average, peak voltages were larger in medial quadrants compared to lateral quadrants across all testing conditions.

Conclusion: This study evaluates the voltage generated from a four-quadrant TEG harvester package under loading conditions representative of gait. Different peak voltages were measured for the different loading conditions. These results indicate that, to accurately estimate the response of a TEG in a TKA, accurate 6-DoF loading conditions need to be considered. Peak voltages from the TEG were most pronounced during the 6-DoF condition; indicating that uniaxial loading conditions that mimic vertical compression but neglect loads in other directions will underestimate the voltage (harvestable energy).

References: Hossain, N. A., Yamomo, G. G., Willing, R., & Towfighian, S. (2021). Characterization of a Packaged Triboelectric Harvester Under Simulated Gait Loading for Total Knee Replacement. *IEEE/ASME Transactions on Mechatronics*, 26(6), 2967-2976. <https://doi.org/10.1109/TMECH.2021.3049327>

Figures

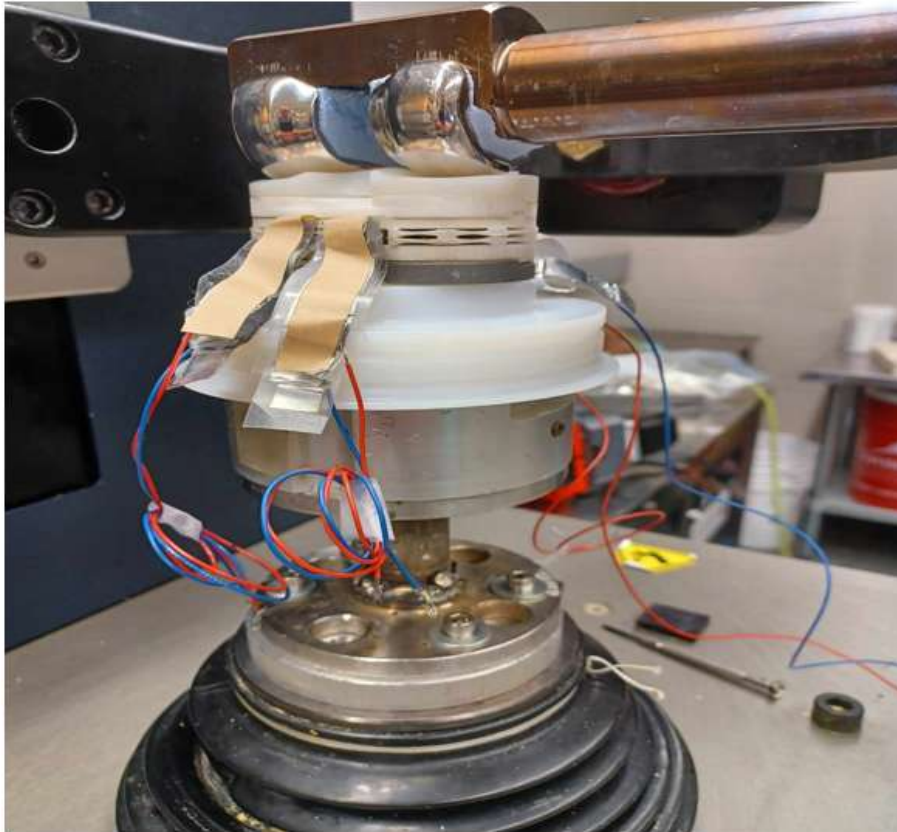


Figure 1: Experimental setup of TENG energy harvester mounted on the VIVO Joint Simulator

Figure 1

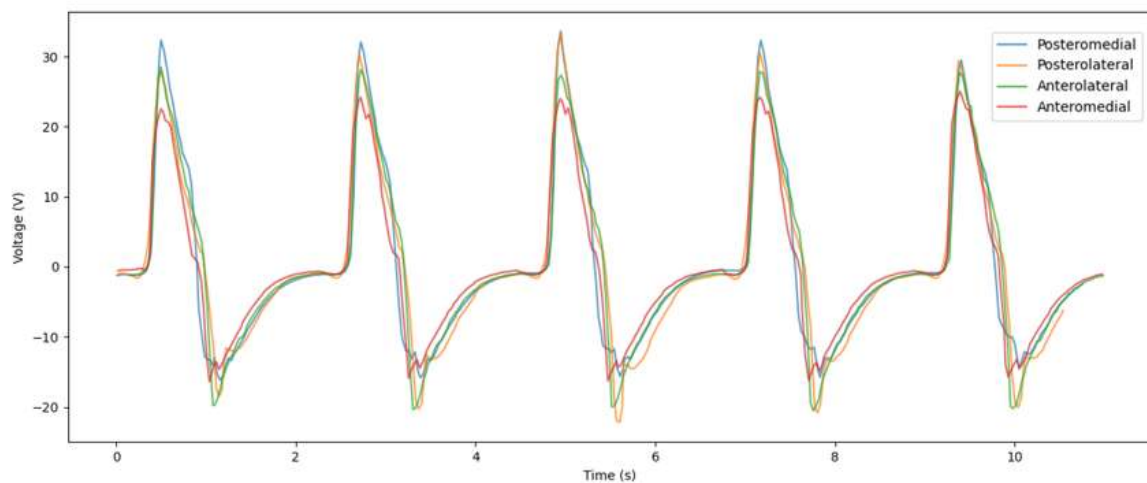


Figure 2: Voltages for each harvester quadrant generated from normal gait joint loads for a right knee with a maximum compressive force of 487 N through full flexion range of motion.

Figure2

Condition	Medial (V)		Lateral (V)	
	Anterior	Posterior	Anterior	Posterior
Fixed	24.6	22.8	20.3	22.7
Free	24.9	22.3	23.6	23.3
6-DoF loads in Extension	21.9	20.7	18.9	19.4
6-DoF loads through Flexion	25.0	34.3	28.8	34.2

Table 1: Comparison of peak voltage measurements from each harvester quadrant for all four loading conditions.

[Figure 3](#)

Load to Shear Failure of Cemented Patellar Components in Well-Functioning Postmortem Total Knee Arthroplasties

*Sara Sacher - Hospital for Special Surgery - New York, United States of America

Drake Lebrun - Hospital for Special Surgery - New York, USA

Elexis Baral - Hospital for Special Surgery - New York, USA

Breana Siljander - Hospital for Special Surgery - New York, USA

Robert Hopper - Anderson Orthopaedic Research Institute - Alexandria, USA

Ryan Breighner - Hospital for Special Surgery - New York, USA

Hollis Potter

C. Anderson Engh - Alexandria, USA

Douglas E Padgett - Hospital for Special Surgery - New York, USA

Timothy Wright - Hospital for Special Surgery - New York, USA

Introduction: Anterior knee pain and patellofemoral complications are common causes of dissatisfaction after total knee arthroplasty (TKA)¹. Shear forces on the patella can produce wear and lead to patella component failure^{2,3}. Cemented patellar components demonstrate inferior fixation and increased fibrous tissue compared to tibial or femoral components⁴. However, no studies have been conducted on postmortem patellar components with well-functioning TKAs. The objectives of this study were to 1) evaluate the durability of patellar component fixation by evaluating the mechanical load to shear failure of cemented patellar components in well-functioning postmortem TKAs, and 2) determine the influence of clinical and radiographic factors on load to shear failure.

Methods: 9 patellae were harvested from postmortem well-functioning knees obtained at the Anderson Orthopaedic Research Institute (AORI). Magnetic resonance images (MRI) were acquired, graded for implant integration, and classified into 4 interface groups: normal, fibrous tissue, fluid interface, and osteolysis. High-resolution peripheral quantitative computed tomography (HR-pQCT) and computed tomography (CT) images were acquired for bone mineral density (BMD) and bone quality measurements. 3D-printed alignment jigs were used to define the shear plane across the patella-implant interface. Specimens were mounted in polyvinyl chloride pipes and fixed with resin-based epoxy (Bondo body filler). Specimens were loaded with isolated shear stress (axial displacement of 5 mm / minute) using a v-block attached to a servo-hydraulic test frame (MTS systems Corp, Eden Prairie, Minnesota) until failure occurred (Fig. 1). Load-displacements curves were recorded (WaveMatrix, Instron). Linear regressions were used to analyze effects of clinical and radiographic factors on load to failure. T-tests assessed differences in load to failure between groups.

Results: The mean load to failure was 1479.3 ± 229.4 N. The components failed in a lever-like mechanism with the superior aspect of the patella initially debonding and pegs remaining intact (Fig. 2). Load to failure was lower with decreased implant integration of the inferior aspect of the patella (Figure 3) ($R^2 = 0.83$ $p < 0.001$). Load to failure trended lower in patellas with an MRI classification of "fibrous tissue" in the inferior and medial aspect of the patella compared to "normal" tissue ($p = 0.07$). Load to failure was not significantly influenced by surface damage or BMD. HR-pQCT analysis is forthcoming and will be included in future reports.

Conclusion: Load to shear failure of well-functioning postmortem TKA patellar components was higher than previous work^{5,6}. Well-functioning patellar implants may be better fixed than time-zero lab samples, demonstrating the difficulty in simulating patellar component fixation in vitro.

References: ¹El-Othmani et al, JBJS Rev. 2023; ²Mann et al, J Orthop Res 2019, ³Mann et al, Comput Methods Biomech Biomed Engin 2014; ⁴Debbi et al, J Arthroplasty 2023; ⁵Wagner et al, Am J Orthop 2013; ⁶Beck et al, JOA 2021.

Figures

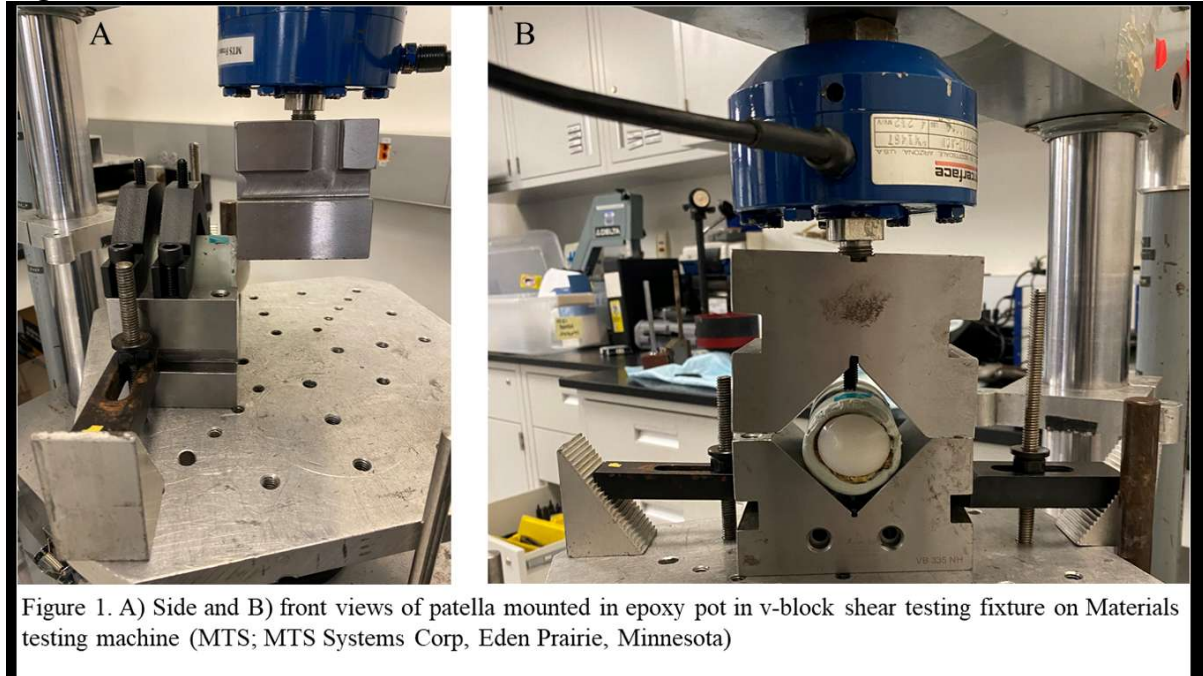


Figure 1. A) Side and B) front views of patella mounted in epoxy pot in v-block shear testing fixture on Materials testing machine (MTS; MTS Systems Corp, Eden Prairie, Minnesota)

Figure 1

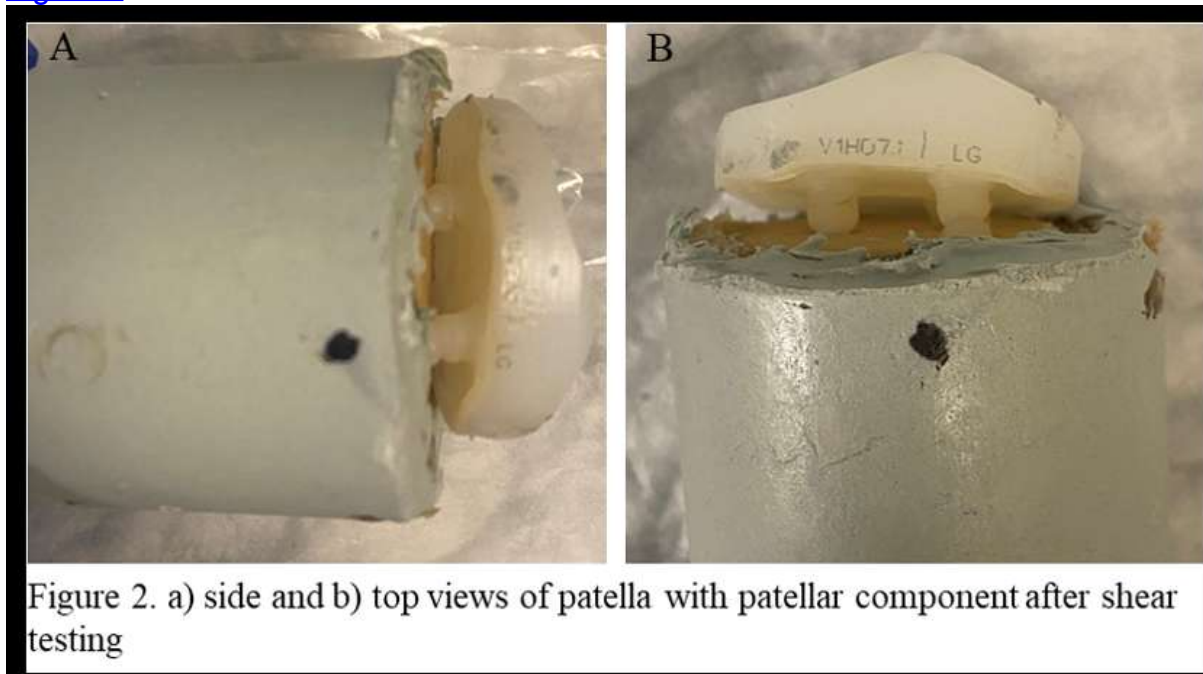


Figure 2. a) side and b) top views of patella with patellar component after shear testing

Figure 2

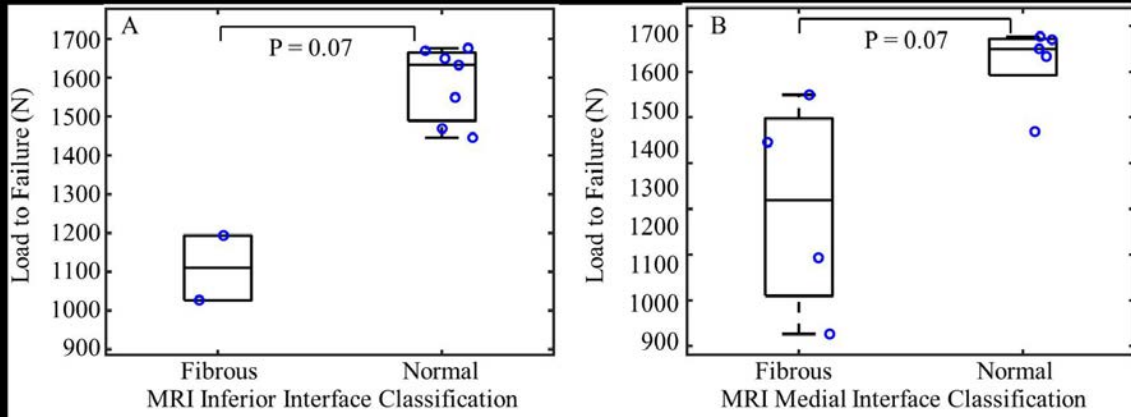


Figure 3. Boxplot of ultimate load to failure in patellas with the MRI classification of “fibrous” tissue in the inferior aspect vs. patellas with a classification of “normal” tissue in the A) inferior and B) medial facet

[Figure 3](#)

Muscle and Knee Contact Forces During Sit-to-Stand in Patients One Year After Unilateral Total Knee Arthroplasty

*Erik Kowalski - [University of Ottawa - Ottawa, Canada](#)

Alexandre Pelegrinelli - [State University of Londrina - Londrina, Brazil](#)

Danilo Catelli - [University of Ottawa - Ottawa, Canada](#)

Geoffrey F Dervin - [Ottawa, Ontario, CAN](#)

Mario Lamontagne - [University of Ottawa - Ottawa, Canada](#)

Introduction

Many patients report no limitations while walking after total knee arthroplasty (TKA). However, more limitations exist during more demanding tasks, such as rising from a chair, as 49.4% and 7.8% of patients report mild or moderate limitations, respectively[1]. The reported differences may be due to different contact loads the knee experiences during various activities of daily living (ADLs). Rising from a chair or sit-to-stand movements are among the few ADLs with in vivo data, creating greater peak knee contact force (KCF) on the lateral component of the knee[2, 3], which may create difficulties in patients after TKA. It also requires bilateral support in which both feet are in contact with the ground, so if patients compensate with their non-operated limb, it may be sensitive enough to evaluate movement asymmetries. The purpose of this study was to compare knee kinematics, kinetics, muscle forces, and KCF on the operated and non-operated limbs during sit-to-stand in patients after TKA with either a medial ball-and-socket (MBS) or posterior stabilized (PS) implant and compared them to a group of similarly aged controls (CTRL).

Methods

Eighteen TKA patients were randomized to either an MBS (n=9, females=4, age=64.5±6.5 years, BMI=25.8±2.7 kg/m², months post-op=12.6±0.5) or PS (n=9, females=4, age=63.1±8.6 years, BMI=29.3±3.8 kg/m², months post-op=13.7±2.8) implant and were compared with nine controls (females=4, age=63.2±4.4 years, BMI=25.1±3.0 kg/m²). Patients visited the biomechanics lab approximately 12 months after TKA, where knee biomechanics were measured as they performed a sit-to-stand task. A musculoskeletal model and static optimization estimated lower limb kinematics, knee kinetics, muscle forces, and KCFs. The normalized sit-to-stand cycle was compared among the groups using statistical nonparametric mapping, and peak between-limb differences were compared using discrete statistics.

Results

The PS group required greater forward lean during the sit-to-stand task, causing greater spine flexion, posterior pelvic tilt, and decreased hip flexion on the operated limb (Figure 1). PS and MBS groups favored their non-operated limb, resulting in less range of motion throughout the lower limb, lower knee kinetics, muscle forces, and KCFs on the operated limb. The MBS and PS groups had reduced medial compartment KCF compared to the controls (Figure 2). The control group did favor their dominant limb over their non-dominant limb.

Conclusion

Post-operative rehabilitation should continue to promote greater use of the operated knee to have more symmetry between operated and non-operated limbs but also target improving strength and mobility at the hip and ankle joint.

References

- [1] Singh JA, Lewallen DG. Patient-level improvements in pain and activities of daily living after total knee arthroplasty. *Rheumatology (Oxford, England)*. 2014;53:313-20.
- [2] Kutzner I, Bender A, Dymke J, Duda G, von Roth P, Bergmann G. Mediolateral force distribution at the knee joint shifts across activities and is driven by tibiofemoral alignment. *The bone & joint journal*. 2017;99-B:779-87.
- [3] Moewis P, Trepczynski A, Bender A, Duda GN, Damm P. Loading of the Knee Joint After Total Knee Arthroplasty. Springer International Publishing; 2022. p. 65-76.

Figures

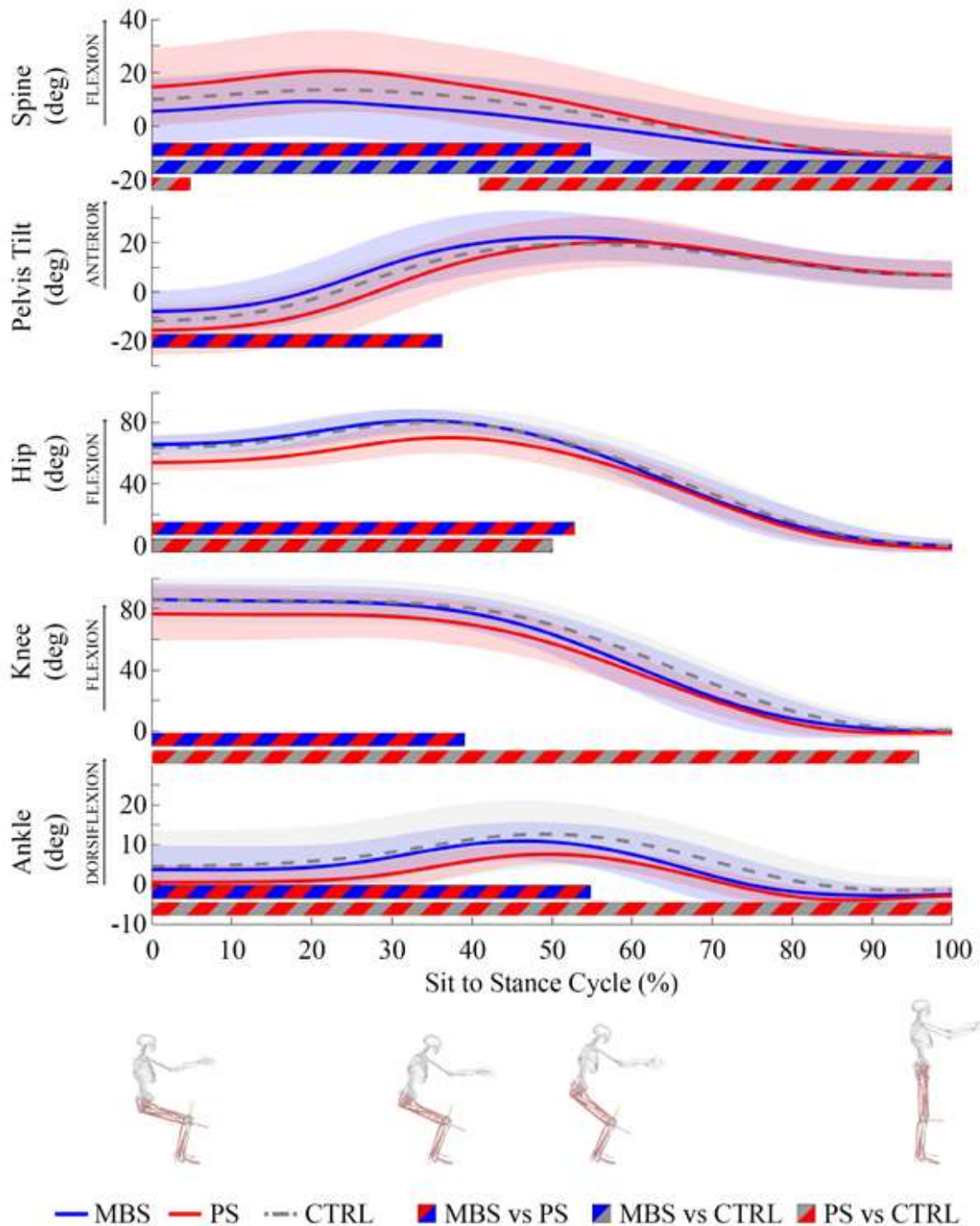


Figure 1: Sagittal plane joint angles for the spine, pelvis, hip, knee, and ankle during the sit-to-stand task for the operated limb in the MBS (blue) and PS (red) groups, and average between both limbs for the CTRL (grey) group. SnPM results are displayed below each figure and indicate significant ($p < .05$) differences between MBS and PS (red/blue), MBS and CTRL (blue/grey), and PS and CTRL (red/grey). MBS = medial ball-and-socket, PS = posterior stabilized, CTRL = control, SnPM = statistical non-parametric mapping, BW = body weight.

Figure 1

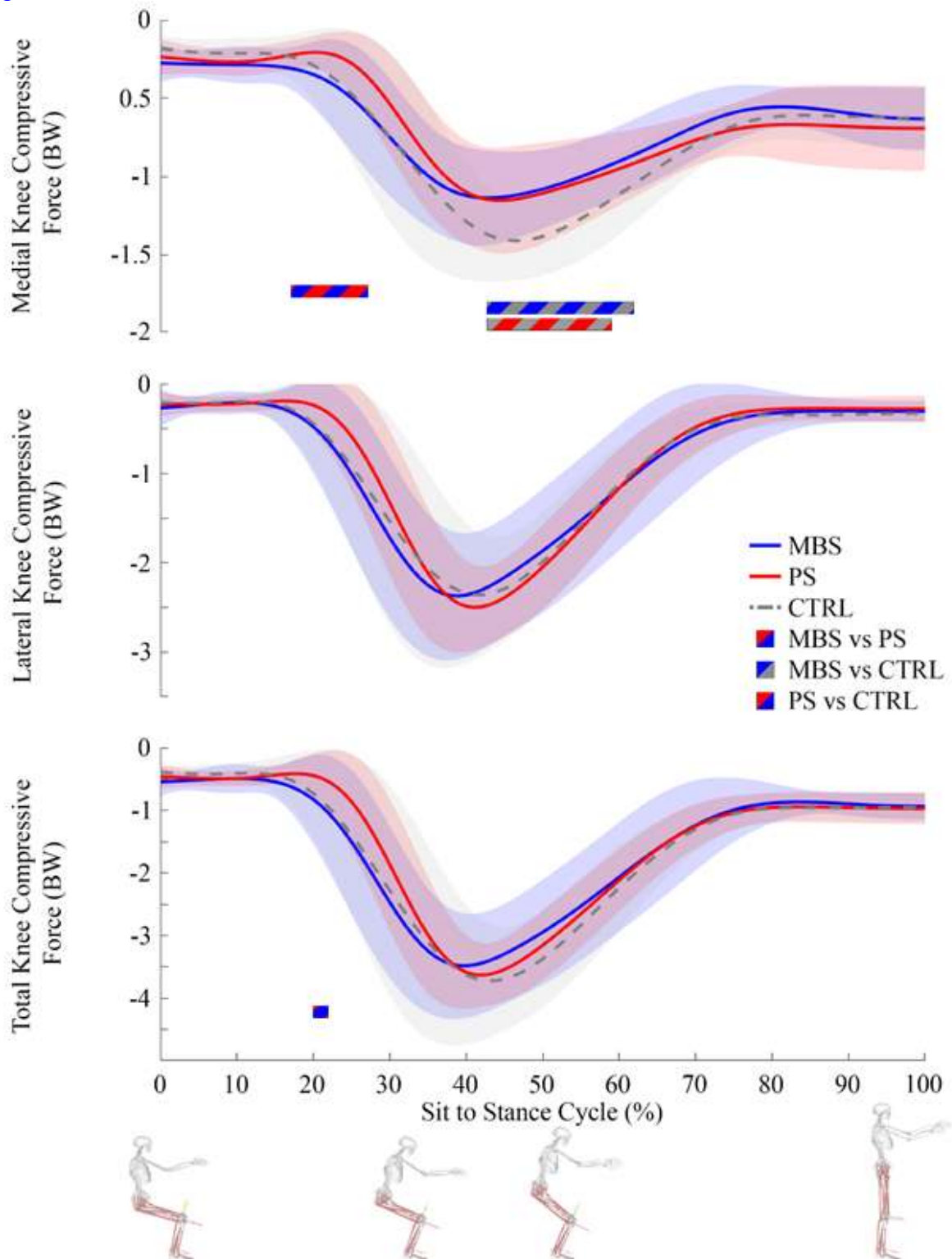


Figure 2: Knee contact forces during the sit-to-stand task for the operated limb in the MBS (blue) and PS (red) groups, and average between both limbs for the CTRL (grey) group. SnPM results are displayed below each figure and indicate significant ($p < .05$) differences between MBS and PS (red/blue), MBS and CTRL (blue/grey), and PS and CTRL (red/grey). MBS = medial ball-and-socket, PS = posterior stabilized, CTRL = control, SnPM = statistical non-parametric mapping, BW = body weight.

Figure 2

Experimental Estimates of the Forces and Moments Which Could Compromise Reregistration of Reference Frames in Navigated or Robotic Arthroplasty

Alexander Eischeid - University of Nebraska Medical Center - USA

Joel Weisenburger - The University of Nebraska Medical Center - Omaha, USA

*Hani Haider - UNMC - Omaha, USA

FA reference frame is rigid constellation of tracked infrared-reflective, active LED or other markers identified by a 3D-tracking system. A bone or surgical instrument can be tracked with a reference frame only after a 3D registration process calculating a relationship (transformation) between the two. After registration, it is assumed/essential that the reference frame does not shift/tilt relative to the tracked object. However, if a surgical tool is accidentally dropped, or the surgeon inadvertently bumps into a reference frame, a time-costly repeat registration may be required, if detected; if not, the consequences can be worse. Standardized tests (e.g. ASTM F3107) have started to emerge to assess how susceptible reference frames attached to a patient's bone using pins or screws, are to loosening/shifting under static forces ranging 10-30N. To date, no data has been available for what forces/moments may occur during arthroplasty surgery. This study is the first to measure comprehensive data for this purpose.

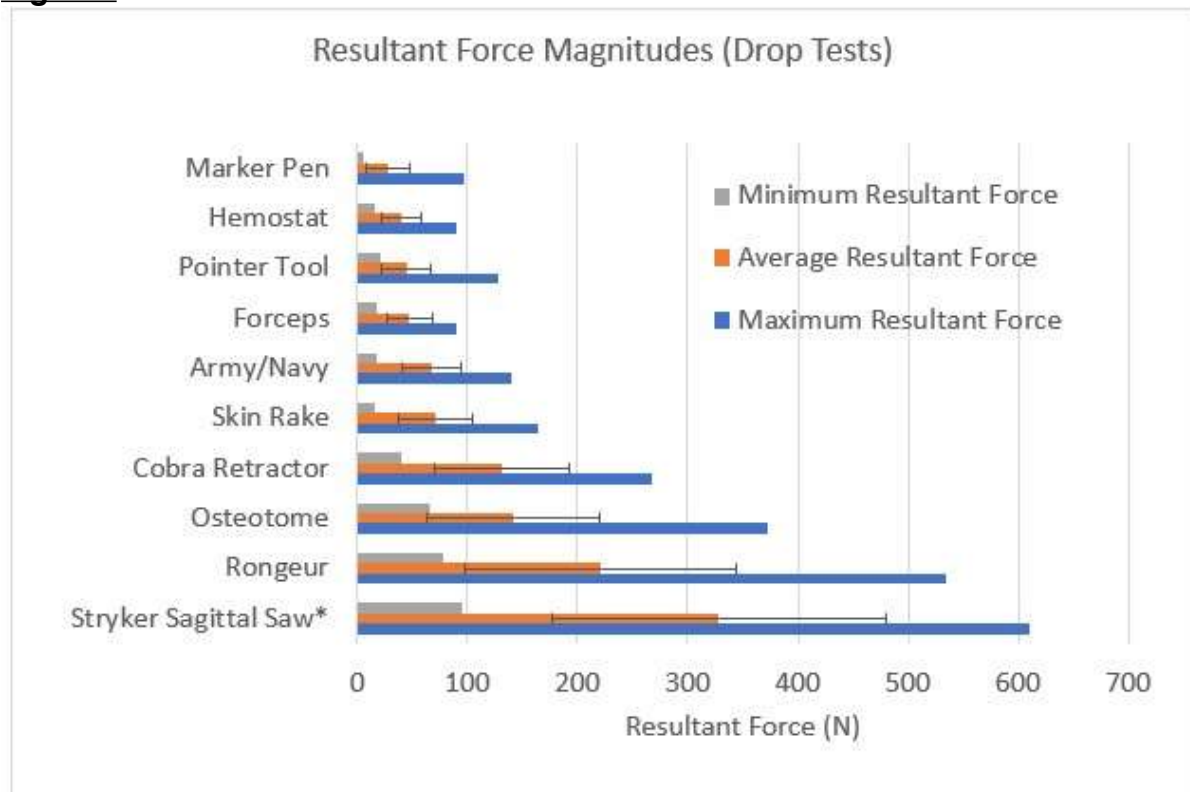
Nine commonly used total knee replacement (TKR) surgical instruments varying in size and weight were dropped from a height of 200mm onto a surrogate reference frame rigidly connected to a 6 degree-of-freedom load cell. The load cell was used to acquire/log at 326Hz, sufficient to capture impact of three orthogonal linear forces and torques. Each surgical instrument was dropped 25 times, randomly varying the orientation of the instrument in every drop. A sagittal saw was also dropped from a height of 50mm. Four volunteers wearing surgical gloves and gowns were also asked to brush/bump the surrogate reference frame 25 times with randomly varying speed and direction while articulating hand/arm movements common in TKR surgery. The three forces and moments were vector summed to yield a resultant force and moment for each interaction. The minimum and maximum resultant force and moment, as well as the average and standard deviation were reported for each instrument and volunteer.

In the brush/bump testing of all volunteers, the average force measured was 31.1 ± 25.0 N and a maximum of 92.0N. The average torque was 3.57 ± 3.21 Nm with a maximum of 11.4Nm.

The resulting forces and torques from drop testing showed much higher variation due to varying weight and size of the nine instruments (all detailed in Figs. 1 and 2). Dropping a large/heavy instrument like a "rongeur" caused an average force of 222 ± 123 N, and 8.70 ± 4.67 Nm torque, reaching 535N and 20.0Nm maxima respectively. Forces/torques from dropping a sagittal saw even from a smaller distance of 50mm exceeded those of the rongeur from the full 200mm drop. The lowest drop forces/torques were for the marker pen and a "hemostat" instrument, averaging 30-40N in force and <2Nm in torque, with maxima <100N force and <3.5 Nm torque respectively.

The brush/bump forces/torques showed that the highest ASTM force (30N) as modest instead of unrealistically harsh. Further sobering was the forces/torques from the instrument drop tests which were much higher. Do they mean that a reference frame attached to a bone will need re-registration regardless of what instrument is dropped on it?

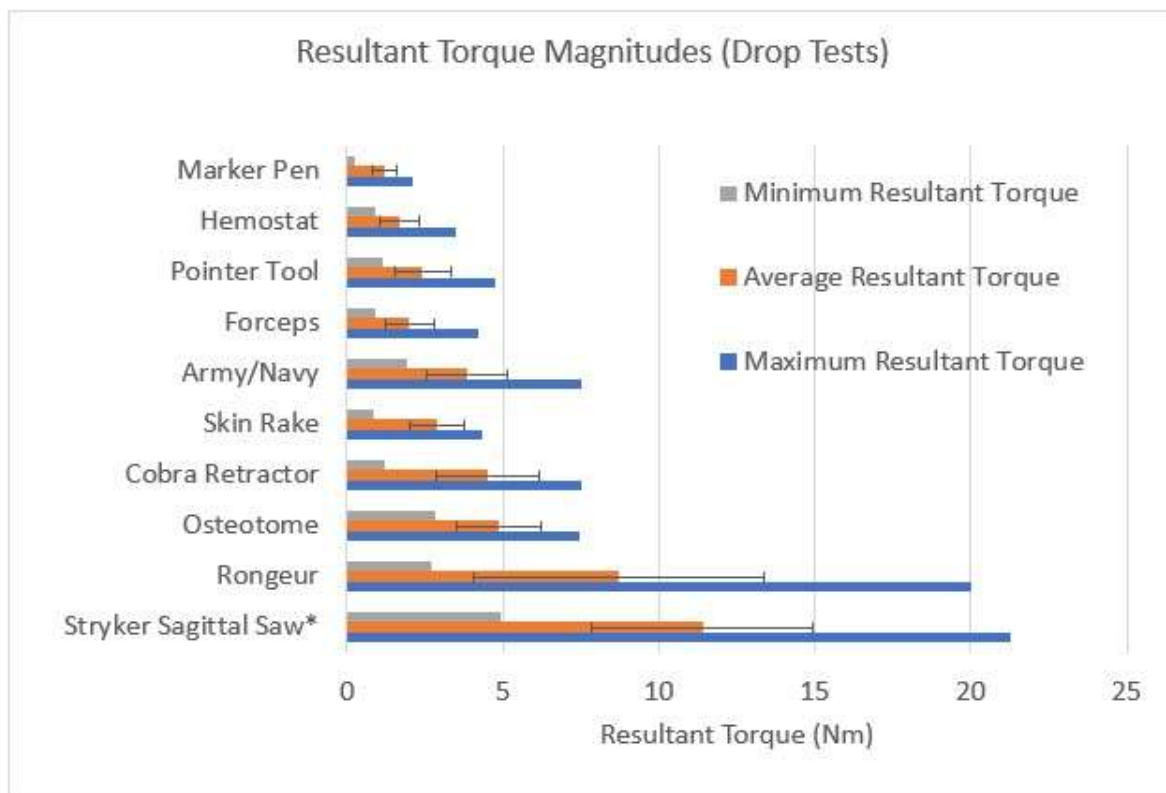
Figures



*Stryker Sagittal Saw was dropped from a reduced height of 5 cm to prevent oversaturation of the load cell and damage to the saw

Figure 1: Resultant force peaks by each instrument from 25 drops from 200mm height. (Error bars represent one standard deviation.)

[Figure 1](#)



*Stryker Sagittal Saw was dropped from a reduced height of 5 cm to prevent oversaturation of the load cell and damage to the saw

Figure 2: Resultant torque peaks by each instrument from 25 drops from 200mm height. (Error bars represent one standard deviation.)

[Figure 2](#)

How Does Subchondral Bone Remodeling Affect the Trajectory of the Bone Saw in the AP Trajectory? a Bone Foam Model Evaluation

*Devin Asher - Rush University Medical Center - Chicago, USA

Craig Silverton - Henry Ford Hospital - Detroit, USA

Erickson Andrews - Henry Ford Health system - Detroit, USA

Tahsin Rahman - Henry Ford Health System - Detroit, USA

Robin Pourzal - Rush University Med Ctr - Chicago, USA

Jonathan Shaw - Henry Ford Health System - Detroit, USA

Introduction:

Subchondral bone remodeling and sclerosis is a key finding associated with the pathogenicity of osteoarthritis of the patellofemoral joint. This is commonly terminally treated via total knee arthroplasty (TKA). One key element to successful TKA, especially those inserted using press-fit components, is a sufficiently flat surface to maximize implant adherence and survivability. This study aims to evaluate the effects of subchondral sclerotic bone on the deviation of the cutting plane when preparing the tibial plateau during TKA using bone foam models.

Methods:

Tibial bone with subchondral, sclerotic bone was simulated in bone foam models (Sawbone) with pressurized bone cement added to the posterior ¼ of the medial plateau. (Figure 1). A Stryker 2108 Series sagittal blade was used through a conventional closed extramedullary tibial resection guide to cut sawbones of normalized high or low density (HD & LD) (Figure 2). HD and LD models were each cut by one of four surgeons for a total of 8 cuts. Using a VHX 600 Digital Microscope from Keyence, z-height deviations in the AP trajectory were measured on the lateral and medial sides of each sample. Comparisons of the median AP trajectory on the medial and lateral side in HD and LD models were performed with the Mann-Whitney test.

Results:

Across surgeons and in both bone density models, medial side median height deviation was found to be significantly greater than that of the lateral side (HD: $p < 0.005$, LD: $p < 0.05$) (Fig. 2). On average, when comparing medial and lateral side sawblade trajectory, there was a difference in height of $+254.47\mu\text{m}/+231.90\mu\text{m}$ (HD/LD).

Conclusion:

A significant difference in the Z-height deviation when comparing medial and lateral surfaces was observed. This deviation could potentially cause enough difference to disturb the adhering surface when fitting tibial components during TKA, leading to a shorter life of the implant, and ultimately, more and more frequent revisions. While the connection to TKA failure is yet to be discovered, this study provides grounds for consideration to further investigate.

Figures



Figure 1. Image of the Bone Models displaying the pressurized cement insert “sclerosis”.

[Figure 1](#)



Figure 2. Bone model in conventional closed extramedullary tibial resection guide setup for cutting.

[Figure 2](#)

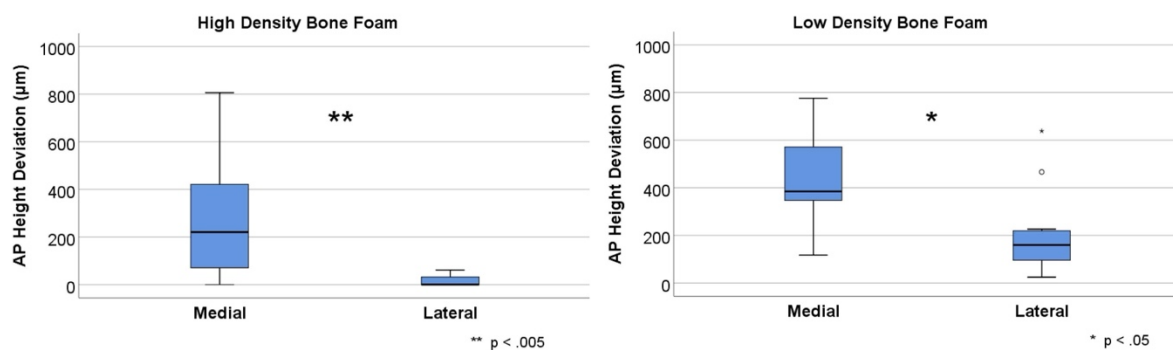


Figure 3. AP Height Deviation by laterality in high-density bone models (A) and low-density bone models (B).

[Figure 3](#)

Analyzing the Effects of Tibial Plate Positioning on TKA Femorotibial Mechanics Using a Dynamic Mathematical Model of the Knee

*Caleb Chesney - University of Tennessee - Knoxville, USA

Michael LaCour - University of Tennessee - Knoxville, USA

Richard Komistek - The University of Tennessee - Knoxville, USA

Bradley Meccia - University of Tennessee - Knoxville, United States

INTRODUCTION

While technological advancements in robotics have improved the precision of total knee arthroplasty (TKA), there remains room for improvement regarding accurate positioning targets and understanding the effects of misalignment, particularly with the tibial tray. There is a lack of consensus regarding proper internal/external (I/E) tray rotation [1], and bone cuts are subject to 1 mm of error even with surgical robotics, which is further exacerbated by potential bending of bone saws up to 2° [2]. The objective of this research is to use mathematical modeling to investigate the effects of tibial tray position on femorotibial mechanics for three medially stabilized TKA systems.

METHODS

A single subject was virtually implanted with Medial Stabilized (DePuy Inc.), Medial Congruent (Zimmer Biomet Inc.), and Condylar Stabilized (Stryker Inc.) cruciate retaining TKAs, implanted in Mechanical Alignment with 6° posterior tibial slope. Subjects underwent a deep knee bend to 120° flexion using a validated mathematical model [3]. Tibial alignment variations included $\pm 4^\circ$ adjustments to varus/valgus (V/V) cuts, 3° increments of slope cuts, and $\pm 5^\circ$ adjustments to I/E rotation (Figure 1). Parameters of interest include medial/lateral condylar positions (MCP/LCP), femorotibial axial rotation, and MCL, LCL, and PCL strains.

RESULTS

Both I/E and V/V rotations affected MCP and LCP. I/E rotations yielded 5 mm of lateral variability and 6 mm of medial variability, while V/V rotations yielded 5 mm of lateral variability but less medially (Figure 2). Overall, the Medial Stabilized TKA demonstrated posterior rollback, the Medial Congruent TKA demonstrated mid-flexion variability, and the Condylar Stabilized TKA experienced paradoxical anterior sliding.

Both changes also yielded approximately 10° of variability in axial rotation (more in Medial Congruent and Condylar Stabilized TKAs). V/V rotations also yielded changes to MCL and LCL strains, with valgus cuts generating increased MCL and decreased LCL tension, and varus vice versa (Figure 3). Ligament strains for all systems were similar, with the Medial Stabilized TKA showing more MCL stability and the lowest LCL tension.

DISCUSSION

Proper internal/external rotation of the tibial tray has the least consensus and can be difficult to plan yet in this study demonstrated the largest effect on femorotibial mechanics. Tibial slope does not appear to have a significant impact, which has been documented previously [3]. While varus/valgus alignment has an impact on both kinematics and ligament tensions, these may be accounted for via proper ligament releases and balancing. Overall, more consensus is needed regarding proper tibial tray positioning, particularly for internal/external rotation.

REFERENCES

- [1] Indelli PF, Graceffa A, Marcucci M, Baldini A. "Rotational alignment of the tibial component in total knee arthroplasty." *Ann Transl Med.* 4(1):3. (2016 Jan). doi: 10.3978/j.issn.2305-5839.2015.12.03. PMID: 26855939; PMCID: PMC4716934.
- [2] Hasegawa M, Tone S, Naito Y, et al. "Comparison of accuracy and early outcomes in robotic total knee arthroplasty using NAVIO and ROSA." *Sci Rep*, 14, 3192 (2024). doi: 10.1038/s41598-024-53789-4
- [3] Khasian M, Meccia BA, LaCour MT, Komistek RD. "Effects of posterior tibial slope on a posterior cruciate retaining total knee arthroplasty kinematics and kinetics." *The Journal of Arthroplasty*, 36 (7), 2379-2385 (2021). doi: 10.1016/j.arth.2020.12.007

Figures

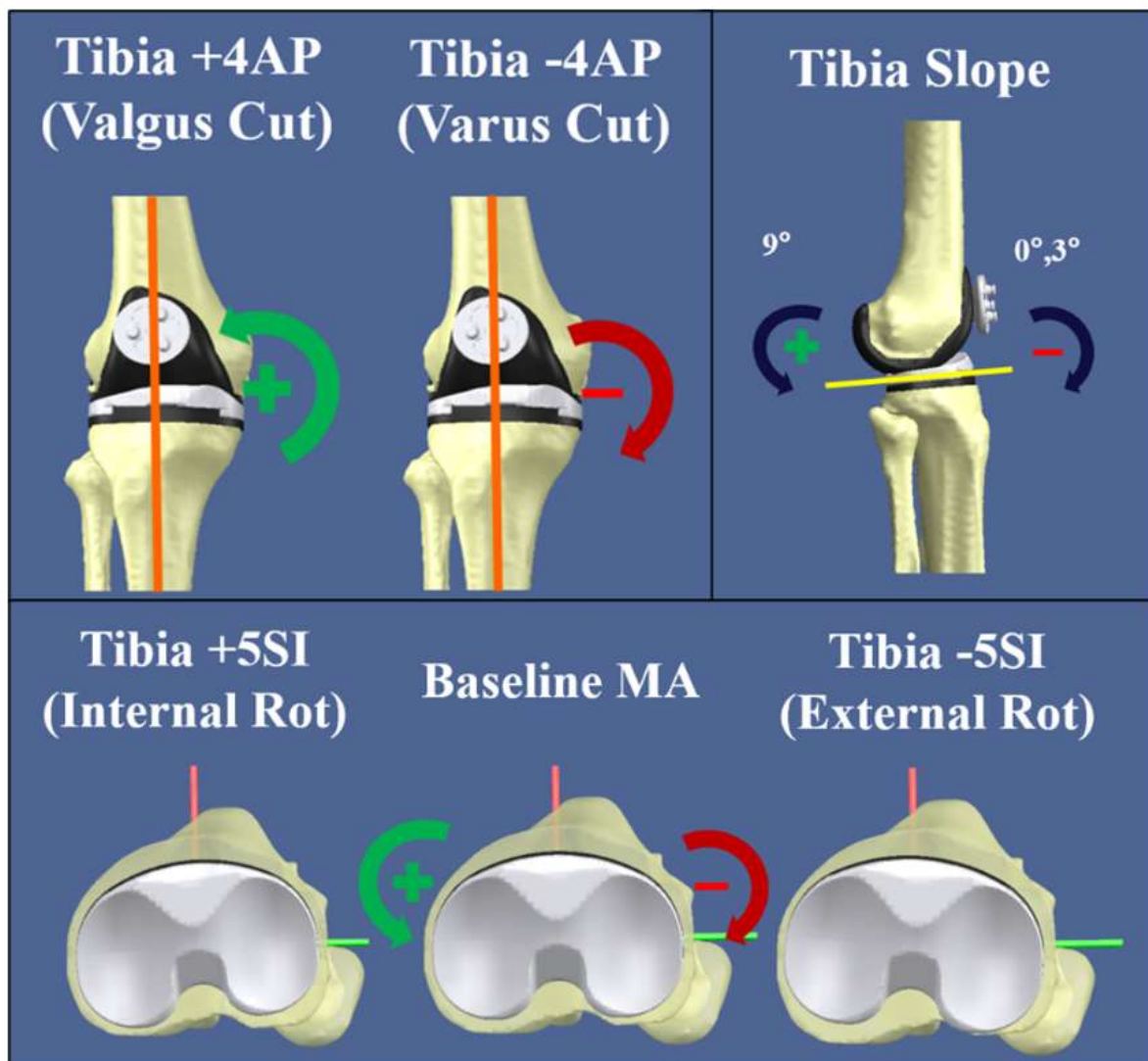


Figure 1: Visualization of all adjustments and directions made to the tibial tray.

[Figure 1](#)

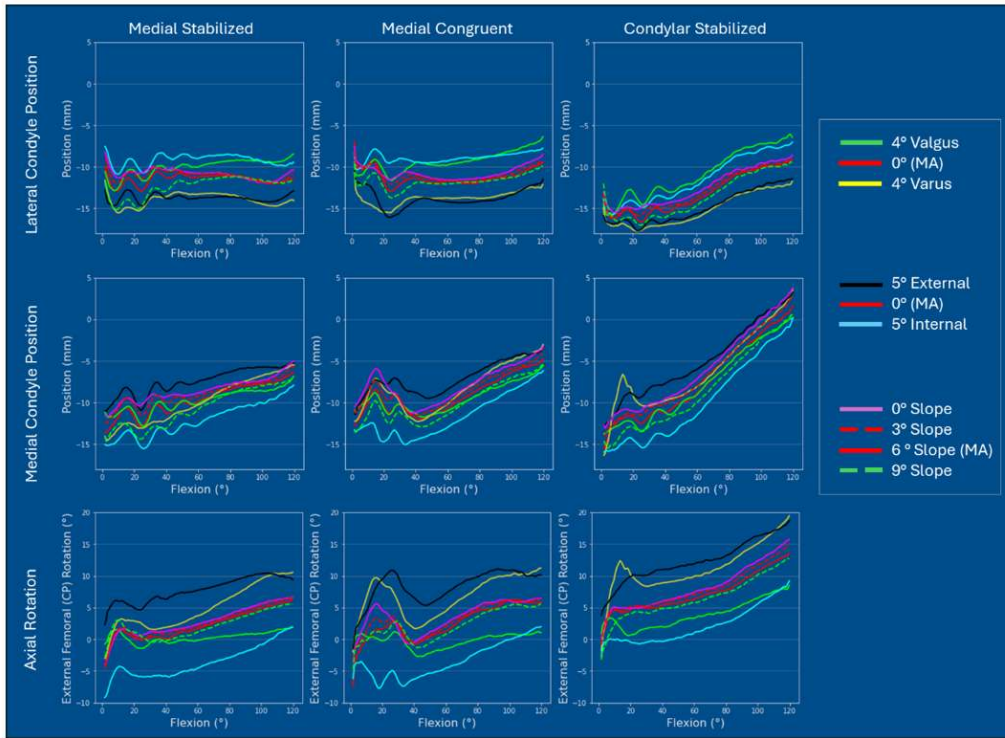


Figure 2. Primary Kinematic Outputs (MCP, LCP, Axial Rotation) versus Flexion. Plots are arranged with LCP on the top row, MCP in the middle, and Axial Rotation on the bottom. Positive indicates anterior translation for MCP and LCP, and positive indicates external femorotibial axial rotation.

Figure 2

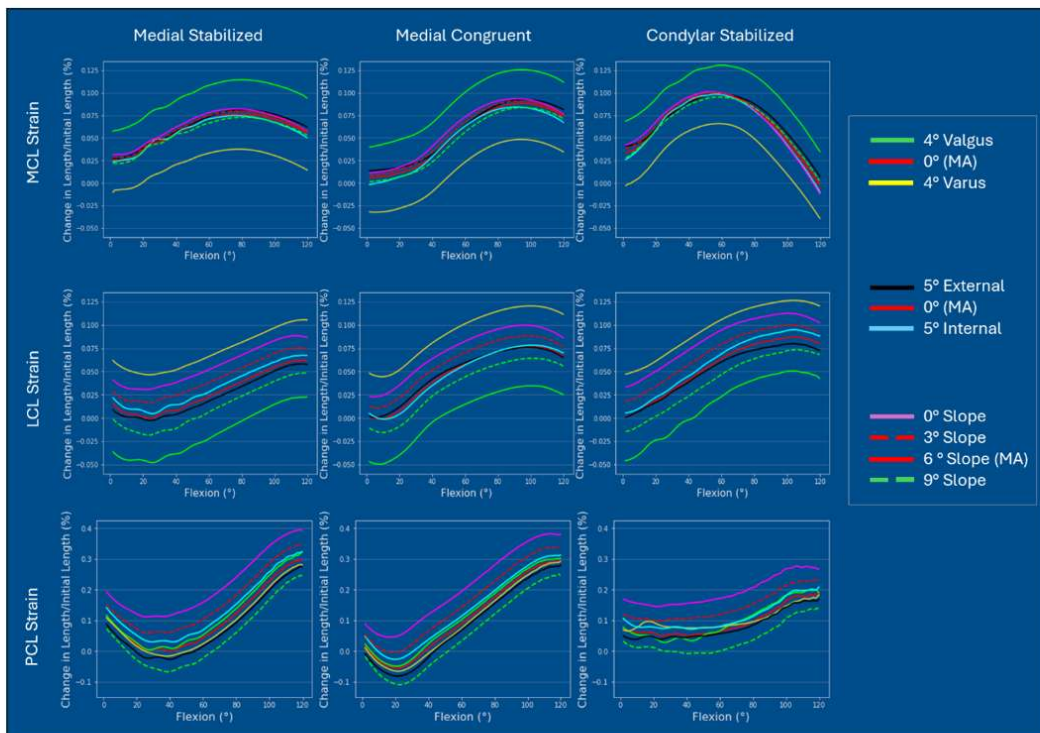


Figure 3. Ligament strains versus Flexion. Plots are arranged with MCL on the top row, LCL in the middle, and PCL on the bottom.

Figure 3

Investigation of a Spatial Computing Device for Knee Stiffness Modulation in Total Knee Arthroplasty

*Kevin Abbruzzese - Stryker - Mahwah, USA

Mark Cass - Stryker - Menlo Park, USA

Akshansh Chaudhry - Stryker - Menlo Park, USA

Sally LiArno - Stryker Orthopaedics - Bergenfield, USA

Introduction:

Virtual reality interfaces provide a non-pharmacological technique to create immersive experiences that can modulate cognitive and physical responses. The ability to use virtual reality technologies to create immersive environments that engage users has demonstrated positive means to reduce pain and anxiety during medical procedures [1]. Knee osteoarthritis is a degenerative disease which results in severe pain with reduced function and increased knee stiffness and may be associated with catastrophizing and muscle guarding to reduce pain [2]. A pendulum knee drop (PKD) test was performed to evaluate knee stiffness changes where a spatial computing device (SCD) was used to assess the ability to induce relaxation based on changes in range of motion (ROM).

Methods:

To assess knee stiffness changes, the PKD test was performed on six consenting subjects in three conditions: Reality, SCD, and Reality Retest. In the Reality condition, subjects were asked to relax without the use of a spatial computing device to serve as the control. In the SCD condition, subjects wore a spatial computing device (Apple Vision Pro, Cupertino, Ca) and interacted with a virtual meditation application. The third condition represented a retest of the Reality condition without the virtual reality intervention, administered after the SCD condition. An IMU sensor system was placed on the left shank to record the knee ROM. The thigh rested on a table and the shank was suspended and dropped from a 45-degree reference position and allowed to oscillate until rest. Ninety trials were performed, five for each condition for all subjects. The log decrement ratio was calculated for each condition as the ratio of successive peaks of the ROM [3]. An ANOVA test was performed to assess significance between conditions with a 95% confidence interval.

Results:

The PKD technique determined differences between conditions based on observed stiffness values (Figure 1). Significant differences were detected in knee stiffness between the Reality and SCD conditions, where the SCD condition resulted in lower log decrement values ($p < 0.001$). The Retest condition resulted in a significant increase in log decrement values when administered after the SCD test condition ($p < 0.005$). No significant differences were observed for the Reality and Reality Retest conditions. SCD test condition resulted in lower standard deviations (0.06) compared to Reality (0.14) and Reality Retest (0.23).

Discussion:

The PKD technique objectively assessed knee stiffness changes across multiple conditions. The initial feasibility assessment in the limited population demonstrates that spatial computing devices may be able to create an immersive environment to induce relaxation effects with greater reproducibility in measurements. The decrease

in knee stiffness based on changes in the log decrement values suggest that virtual reality meditation with a SCD may induce relaxation effects and improve diagnostic techniques like the PKD. Future work includes additional assessments to increase sample size and determine the impact of various immersive environments on the ability to modulate knee stiffness.

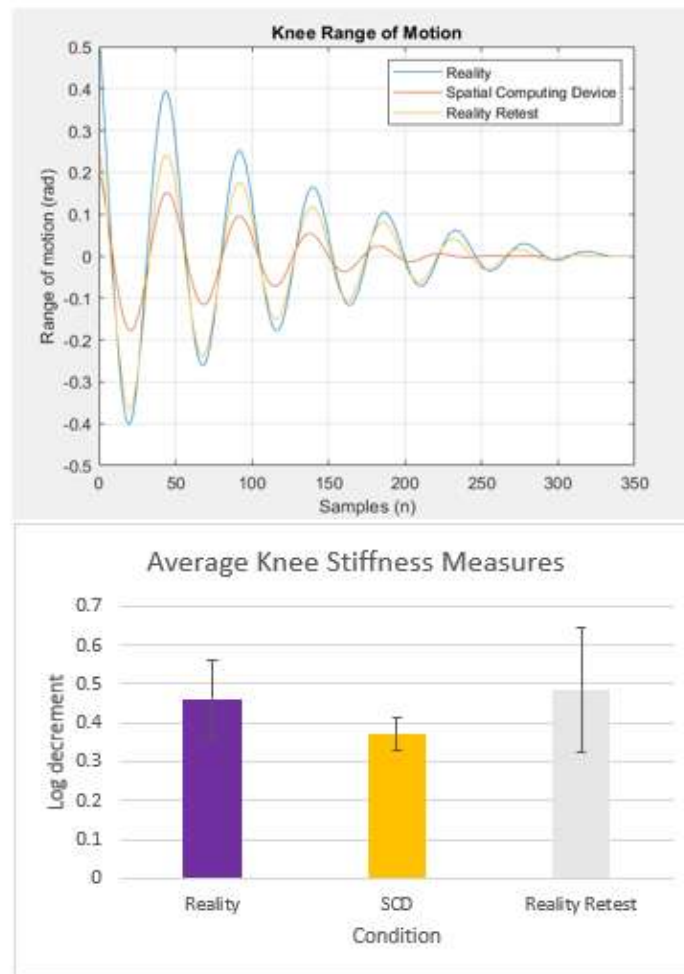


Figure 1. Knee range of motion response (top) with average log decrement values per condition (bottom)

References:

- [1]. Kjeldgaard Pedersen L, Fisker LYV, Rölfing JD, Ahlburg P, Veien M, Vase L, Møller-Madsen B. Virtual reality increases pressure pain threshold and lowers anxiety in children compared with control and non-immersive control-A randomized, crossover trial. *Eur J Pain*. 2023 Aug;27(7):805-815. doi: 10.1002/ejp.2108. Epub 2023 Mar 21. PMID: 36897663.
- [2]. Olugbade T, Bianchi-Berthouze N, Williams ACC. The relationship between guarding, pain, and emotion. *Pain Rep*. 2019 Jul 22;4(4):a770. doi: 10.1097/PR9.0000000000000770. PMID: 31579861; PMCID: PMC6728010.
- [3]. Abbruzzese, K. (2023). Knee Stiffness Evaluations Using an Advanced Total Knee Arthroplasty Simulator Model for Loaded Ligament Assessments. *ISTA 2023*

Figure 1

Preoperative Patient Gait Kinematics May Impact Total Knee Arthroplasty Outcomes: Insight Into Bearing Design

*Alex Fuentes - Emovi - Montreal, Canada

Rémi Courteille - École de Technologies Supérieure - Montreal, Canada

Evan R Deckard - Indiana Joint Replacement Institute - Indianapolis, USA

Alix Cagnin - Emovi Inc - Montreal, Canada

Nicola Hagemeister - Ecole de technologie superieure - Montreal, Canada

Laurence CHEZE - Université Claude Bernard Lyon 1 - Lyon, France

Scott Banks - University of Florida - Gainesville, USA

Michael Meneghini - Indiana School of Medicine - Fishers, USA

Introduction: It is widely held that mimicking the native knee pivot pattern is essential for achieving optimal function after total knee arthroplasty (TKA). While consensus exists regarding a medial pivot during deep flexion, considerable divergence of opinion persists regarding pivot behavior during tasks involving lower degrees of flexion, particularly in weight-bearing. While fluoroscopic studies on healthy knees report a predominant central or lateral pivot during stance, medial pivot patterns are observed during early flexion in the vast minority. This study aimed at exploring whether the patient's preoperative knee pivot pattern during gait (stance phase) affects outcomes after TKA utilizing a conforming bearing designed to guide kinematic motion.

Methods: Twenty-three (23) individuals received the same dual-pivot type bearing (EMPOWR 3D Knee®, DJO Surgical, TX) designed to facilitate a central/lateral pivot in early knee flexion and a medial pivot in greater flexion. Three-dimensional knee kinematics were captured in clinic using the KneeKG™ system (Emovi, Canada) during treadmill walking before and 4 months after surgery (Fig.1). Knee pivot motion was assessed by projecting the transepicondylar axis (TEA) in the transverse plane throughout stance. The tibial plateau was normalized from -1 (lateral condyle) to +1 (medial condyle) and divided in four zones: the lateral (from -1.4 to -0.20), central (-0.20;+0.20), medial (+0.20;+1.4), and extra-articular (<-1.4 or >+1.4). The center of rotation (i.e., intersection of two consecutive TEA projections) was determined throughout the gait cycle to characterize the pivot pattern (translation, lateral, medial, or central; Fig.2). The predominant pattern was determined independently in four stance sub-phases (i.e., loading, mid-stance, end-stance, push-off). Patient-reported outcomes were collected (satisfaction, KOOS-JR, walk pain) and Chi-square/Student T-tests were used to compare patient preoperative and postoperative pivot patterns within the gait cycle and correlate to PROMs with statistical significance set at $p<0.05$.

Results: The cohort was 65.2% women, with a mean age of 67.3 years. The majority of patients exhibited a preoperative and postoperative kinematic pivot pattern of central or lateral pivot during early flexion stance. This group reported better satisfaction levels ($p<0.05$; Table 1) and a statistical trend towards higher improvements in KOOS-JR from pre- to post-op (+21.8pts vs. +10.1pts; $p=0.076$) compared to the sub-group of patients (representing 26.1% of the cohort) which exhibited a predominant medial pivot pattern pre-TKA and a prevalent non-medial pivot post-surgery. 83.3% of this sub-group showed a changed in their pivot pattern behavior after surgery.

Conclusion: This preliminary study provides new insights and begins to answer the question of whether preoperative native knee pivot motion influences postoperative

outcomes after TKA. Results show that patients preserving their own native pivot pattern with a conforming bearing TKA presented better satisfaction level at 4 months. These findings support previous surgical navigation studies highlighting the potential value of preoperative kinematic assessment, more specifically assessing the pivot pattern, as it may ultimately influence personalized surgical decision-making. Due to study limitations, further analyses on larger cohorts and with longer follow-ups are needed to better understand these findings.

Figures



Fig-1. A knee kinesiology exam in a clinical setting.

Figure 1

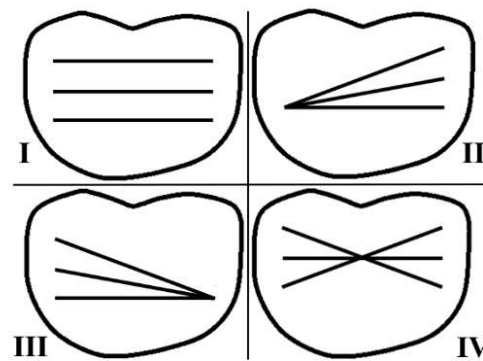


Figure 2 - Knee pivot motion patterns - Superior view of the transverse plane (anterior side at the top, left knee; I: antero-posterior translation, II: lateral pivot, III: medial pivot, IV: central pivot).

Figure 2

Table 1 – Between-group differences on patient-reported outcomes at 4-month follow-up.

*: p<0.05	Medial pivot pre-TKA	Central/lateral pivot pre-TKA	T-test / Khi2 (p-value)
Satisfaction	2.4 (1.0;3.8)	1.5 (1.1; 1.9)	0.042*
Walk pain	2.0 (0.0;4.3)	0.9 (0.3;1.6)	0.134
Delta walk pain (<i>post-op score minus pre-op score</i>)	-4.4 (-7.3;-1.5)	-3.4 (-5.0;-1.8)	0.458
KOOS-JR	66.2 (59.1;73.3)	73.4 (68.1;79.1)	0.097
Delta KOOS-JR (<i>post-op score minus pre-op score</i>)	+10.1 (-3.4;23.7)	+21.8 (14.3;29.3)	0.076
Patients who achieved PASS-KOOS-JR (threshold targeted at 1-year follow-up)	40.0%	76.9%	0.176

Likert Satisfaction: 1 = Very Satisfied, 2 = Satisfied, 3 = Neutral, 4 = Dissatisfied, 5 = Very Dissatisfied. Walk pain: (ranges 0-10, 0 = no pain, 10 = worst pain). PASS: Patient acceptable symptom state = patients who reported a KOOS-JR score >71.

Figure 3

Does Cruciate Ligament Substitution and Implant Asymmetry Make a Difference for Total Knee Arthroplasty Kinematics?

*Lauren Smith - University of Tennessee, Knoxville - Knoxville, USA

Richard Komistek - The University of Tennessee - Knoxville, USA

Michael LaCour - University of Tennessee - Knoxville, USA

Introduction:

The non-implanted knee differs in comparison to typical total knee arthroplasty (TKA) designs in both asymmetry as well as functionality of the anterior cruciate ligament (ACL) and a posterior cruciate ligament (PCL). While surgeons may choose to implant either posterior stabilized (PS) or bi-cruciate stabilized (BCS) TKAs to substitute for one or both cruciate ligaments, the effect of symmetry vs. asymmetry in substituting TKA designs has not been widely analyzed. Therefore, the objective of this research study is to determine if TKA asymmetry and/or anterior ligament stabilization can lead to more normal-like kinematics and clinical benefit for patients.

Methods:

In vivo femorotibial kinematics for 64 subjects were evaluated in this retrospective study. Overall, ten subjects had a normal, non-implanted knee, 20 had a BCS TKA, and 34 had one of two different PS TKAs. All three TKAs had varying degrees of symmetry incorporated into the design, and all were implanted by the same surgeon and were analyzed using fluoroscopy during a deep knee bend (Table 1). The kinematic parameters assessed for each subject were lateral and medial anterior/posterior (LAP, MAP) condylar position and axial rotation.

Results:

At full extension, the BCS subjects demonstrated a more anterior position of both condyles compared to both PS TKAs. The BCS TKA was statistically more anterior than both PS TKA #1 ($p < 0.0001$) and the PS TKA #2 ($p = 0.0328$). Both the normal knee and BCS TKA experienced statistically more posterior femoral rollback (PFR) of the lateral condyle during early flexion than PS TKA #1 ($p < 0.0001$) and PS TKA #2 ($p < 0.0001$). The PS TKAs in this study having asymmetry experienced greater amounts of PFR and weight-bearing flexion compared to the symmetrical PS TKA. Detailed motion patterns can be seen below (Figure 2).

Discussion:

In early flexion, the anterior cam/post positions the femoral component more anterior, and all TKAs experienced PFR when the posterior cam engaged the post. Accordingly, in early flexion, the BCS TKA displayed higher amounts of PFR of both condyles, as one would expect to see in the normal knee. The asymmetric designs achieved greater rollback and axial rotation compared to the symmetric designs. Because of the anterior cam/post interaction with the BCS TKA, they demonstrated a more anteriorized position at full extension, likely attributed to the design accounting for ACL functionality. It appears that asymmetry with respect to joint lines and condylar geometries may yield more normal-like kinematics, much like the normal knee.

Assessment of Knee Ligaments Behavior in Cadaveric Study: Comparing Mechanical Alignment (MA) and Kinematic Alignment (KA) Using Augmented Reality Guidance NextAR in Total Knee Arthroplasty

*Daniele Ascani - Medacta International SA - Chiasso, Switzerland

Massimiliano Bernardoni - Medacta International SA - Castel San Pietro, Switzerland

Introduction

Two predominant alignment approaches stand out in the field of total knee arthroplasty (TKA): mechanical alignment (MA) and kinematic alignment (KA) (1). MA involves a perpendicular cut of the proximal tibia, KA takes a three-dimensional approach, aiming to restore the patient's constitutional alignment (2). This study compares the effects of MA and KA on femorotibial kinematics, specifically focusing on their influence on knee ligament behavior. The NextAR TKA augmented reality system enables real-time measurement of knee ligament length (3). A cadaveric study was conducted to determine which alignment method best replicates the natural behavior of knee ligaments in a healthy knee.

Method

Ten healthy frozen knees were scanned to obtain the CT scan images and create the 3D models, then the native alignment of each knee was categorized by using the CPAK classification (4). NextAR TKA system was used to register the preoperative length of the medial collateral ligament (MCL) and lateral collateral ligament (LCL) throughout a passive flexion/extension movement manually performed by expert surgeons. A 3D preoperative planning has been performed on one specimen for each side: the right knee was planned with an MA alignment, whilst the left knee with a KA alignment. The two knees were operated by using by using the NextAR TKA system to accurately execute the preoperative planning and measure the ligaments' length before and after the prosthesis, for both knees a medial pivot design Medacta SpheriKA implant was implanted.

Results

The CPAK classification showed that 60% of the knees were CPAK II and the rest CPAK I, the native behavior of the ligaments showed that MCL pattern is very similar and it showed an isometric elongation with an average variation in mm of 3%, whilst the LCL showed a variable change of 14% from extension to flexion. A 3D preoperative planning was performed on both sides of a CPAK I type specimen (LDFA=89.5, MPTA=82.0, aHKA=-7.5, JLO=171.5): the right side was planned with a MA alignment whilst the left with KA. The results showed a significant difference on the postoperative curves of the ligaments behavior:

	MCL (%)		LCL (%)	
	EXT	FLEX	EXT	FLEX
MA	4.48	2.99	6.72	5.73
KA	0.67	1.12	1.56	3.22

Table 1 – Difference in % of the variation between preoperative and postoperative length MA Vs KA

Conclusion

The lateral collateral ligament (LCL) became laxer throughout the range of motion (ROM) allowing the roll back of the lateral condyle of the femur which is specific for each patient. The medical collateral ligament (MCL) looks isometric during the flexion extension movement. Based on the findings, KA combined with a MS implant supports the reproduction of physiological knee ligaments' behavior. The increased internal rotation and precise medial pivot point associated with KA contribute to this effect. These results underscore the importance of alignment choices in TKA, emphasizing the need for individualized approaches to optimize knee ligament behavior and overall joint function. Augmented reality guidance, such as NextAR TKA, can play a crucial role in achieving precise alignment during surgery.

Figures

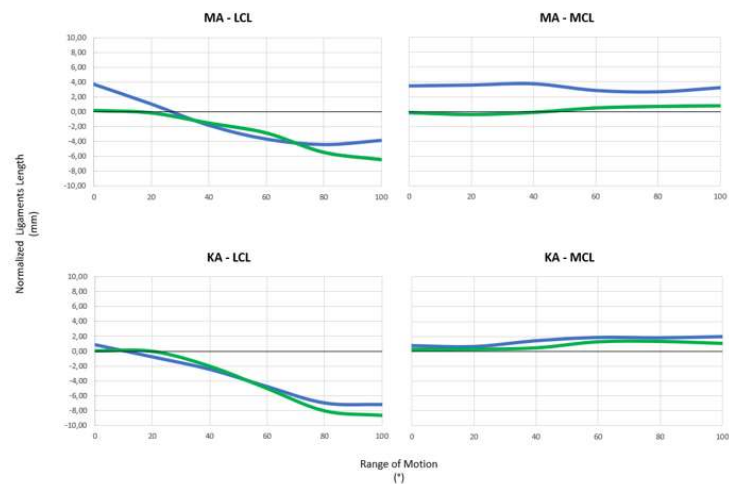


Figure 1 – The figure shows the pattern of the ligament' length in mm, the length has been normalized so the 0 values is the length registered ad 0° of flexion

Figure 1

Surgical Alignment Techniques and Implant Designs After Total Knee Arthroplasty Has Little Effects on Muscle Strength

*Nuanqiu Hou - Campbell Clinic - Memphis, United States of America

Alexis Nelson - UTHSC - Memphis, Select Country

Douglas W. Powell - University of Memphis - Memphis, USA

Marcus Ford - Campbell Clinic Orthopaedics - Germantown, USA

James Guyton - Campbell Clinic Orthopaedics - Germantown, USA

John Crockarell - Campbell Clinic Orthopaedics - Germantown, USA

Christopher Thomas Holland - Campbell Clinic Orthopaedics - Tennessee, United States of America

Derek Dixon - Campbell Clinic Foundation - Germantown, USA

Teri Ross - University of Tennessee Health Science Center - Memphis, USA

William Mihalko - University of Tennessee - Memphis, USA

Disclosure: This study was funded by Medacta International.

Introduction: Total knee arthroplasty (TKA) patients' functional reported outcomes can be affected by the surgical alignment technique performed by the surgeon and the implant design utilized on their TKA. Previous work has suggested that alignment outside of the mechanical axis results in an altered performance from the quadricep muscle group (Sogabe et al., 2009). No previous work has analyzed the effect of implant design on muscular performance. Therefore, our purpose was to analyze two surgical alignment techniques (mechanical (MA) and kinematic (KA) alignment) and two implant designs (Attune and Medacta) on the effect of muscular strength and performance.

Methods: Preliminary data of 18 cruciate retaining TKA patients were recruited with either a mechanical or kinematic alignment with an Attune (DePuy Synthes, West Chester, PA, USA) or Medacta (Medacta International, Switzerland) implant at least one-year post-op. All patient groups were similar in sex distribution, age, BMI, and patient reported outcomes (KOOS, JR and FJS). The isometric extensor/flexor (quadricep/hamstring) muscle performance were measured at 30-, 60- and 90- degrees knee joint flexion angles using a HUMAC NORM isokinetic dynamometer (Computer Sports Medicine, Inc, Stoughton, MA, USA) according to manufacturer's instructions. Five trials were performed in flexion and extension at each isometric angle. The isokinetic extensor/flexor muscle performance was performed at 60 degrees per second with five continuous trials. The dynamometer recorded torque and position at (100 Hz). Custom software (MATLAB, 2021a) was utilized to analyze peak torque from the dynamometer in each testing condition. Independent sample t-tests were used to compare groups (surgical alignment technique and implant design) in each condition. Alpha was set at 0.05.

Results: Muscle strength was compared in two surgical alignment techniques (MA and KA) and two implant designs (Attune and Medacta) in one isokinetic (60 deg/sec) and three isometric (30, 60, 90) conditions. For surgical alignment techniques, differences were observed at 30 degrees isometric extensor strength between MA and KA. For KA patients, extensor peak torque was greater compared to the MA patient group (Figure 1, KA=106.0 Nm, MA=73.6 Nm p=0.013). No other differences were observed comparing surgical alignment techniques. For implant design, differences were observed at 30 degrees isometric extensor strength between the Attune and Medacta implant groups. For the Attune group, peak extensor torque was

greater compared to the Medacta group (Figure 1, Attune=106.0 Nm, Medacta=64.4 Nm $p<0.01$). No other differences were observed comparing implant designs.

Conclusion: When comparing surgical alignment techniques and implant designs, we found that muscle strength was similar between the groups. We observed differences at 30 degrees isometric extensor strength in both the surgical alignment techniques and implant design groups where the Attune KA group exhibited greater difference in peak isometric extensor strength regardless of alignment or design.

References: Sogabe A, Mukai N, Miyakawa S, Mesaki N, Maeda K, Yamamoto T, Gallagher P M, Schragger M, Fry A C. Influence of knee alignment on quadriceps cross-sectional area. J Biomech 2009; 42(14): 2313-7.

Figures

Extension

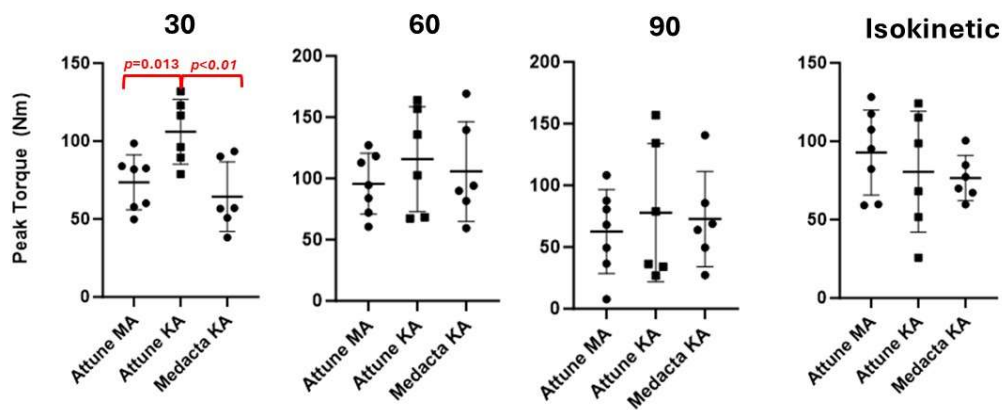


Figure 1

Strong Associations Between Robotic Functional Intraoperative Planning and Dynamic Alignment Behavior After Total Knee Arthroplasty

Sebastien Lustig - Hôpital de la Croix Rousse - Lyon, France

Clement Favroul - Hôpital de la Croix Rousse - Lyon, France

*Alix Cagnin - Emovi Inc - Montreal, Canada

Laurence CHEZE - Université Claude Bernard Lyon 1 - Lyon, France

NICOLA HAGEMMEISTER - École de technologie supérieure - Montreal, Canada

Alex Fuentes - Emovi - Montreal, Canada

Cecile Batailler - Lyon, France

Introduction: Total knee arthroplasty (TKA) aims at optimising implant positioning and soft tissue balance to restore knee function. While emerging technologies like image-based robotic-assisted systems allow personalized intraoperative planning, it is not well understood how it ultimately impacts the knee alignment dynamic behavior post-surgery, especially during weight-bearing tasks. Since dynamic alignment behavior has been linked to clinical outcomes and patient satisfaction post-TKA, this study aimed at exploring the associations between robotic functional intraoperative planning and dynamic knee alignment during gait post-TKA.

Methods: Nineteen (19) patients who underwent primary TKA were included. Functional positioning technique was used for all knees which received the same cruciate-substituting implant (Triathlon® CS cruciform, Stryker). This technique utilizes a robotic-assisted surgical system (MAKO 1.0, Stryker, United States) allowing an individualized intraoperative planning based on X-Ray and CT scan images, aiming at conforming with patient anatomical characteristics. This functional planning is followed by soft tissue balancing in extension and flexion before any bone resections (Figure 1). Intraoperative planning variation was assessed using robotically measured gaps, including medial-lateral extension and flexion gaps, differences between medial and lateral gaps, and planned lower limb coronal alignment. Three-dimensional knee kinematics were captured 6 months post-TKA through a knee kinesiography exam (KneeKG® system, Emovi, Canada) during treadmill walking. Associations between intraoperative planning measures and dynamic alignment in the coronal plane were assessed using bivariate Pearson correlations. Considering the exploratory nature of this study, significance thresholds were set at $p < 0.1$.

Results: There was 63.2% of women and the mean age was 69.7 years (95%CI:65.9;73.6). Mean values of intraoperative measures and their associations with dynamic alignment markers during gait are presented in Table 2. Two intraoperative planning measures showed moderate to very strong associations (i.e., $0.502 \leq |r| \leq 0.815$) with knee alignment dynamic behaviour at heel strike, during stance, and during swing (all $p \leq 0.08$). Functional intraoperative plans delivering lower medial gap and greater lateral gap (i.e., compared to medial) in flexion exhibited significantly higher dynamic varus alignment post-TKA (Figure 3), while associations with extension gap measures were not quite significant. Interestingly, the planned lower limb alignment was not associated with dynamic alignment during walking after surgery.

Conclusion: Results suggest that robotic functional intraoperative planning is strongly associated with dynamic knee alignment behavior post-TKA. While additional studies are needed to better characterize the links between intraoperative parameters and dynamic alignment post-surgery, this constitutes a first step towards

establishing more accurate plans to achieve desired knee function post-TKA. Further research should explore similar associations with preoperative kinematics to ultimately help define patient-specific targets which could maximize outcomes and satisfaction with more individualized surgeries.

Figures

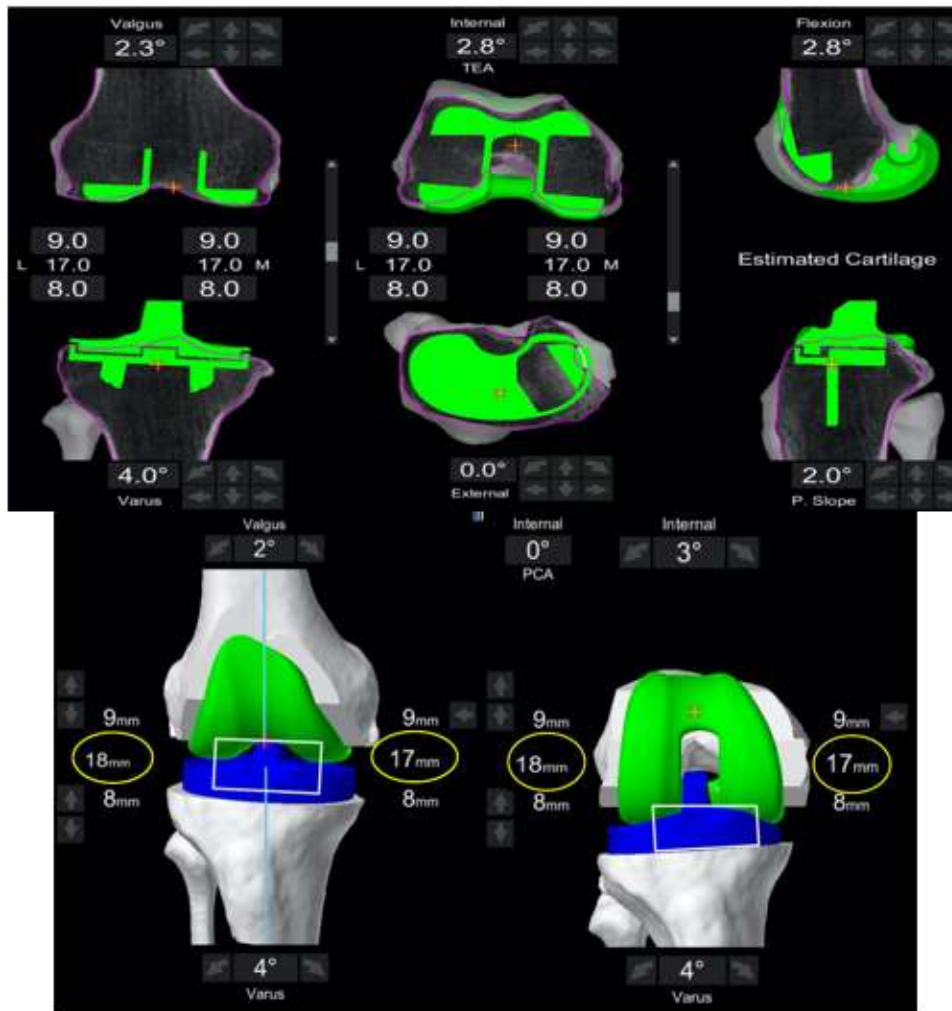


Figure 1. Example of a functional intraoperative planning and delivered gap measures.

[Figure1](#)

Table 2. Mean values of intraoperative measures and their associations with dynamic alignment markers post-TKA.

*: p<0.1 **: p<0.01	Mean values (95% confidence interval)	Dynamic alignment at heel strike	Mean alignment during stance	Maximum malalignment during swing
	<i>mm</i>	<i>Pearson r (p-value)</i>	<i>Pearson r (p-value)</i>	<i>Pearson r (p-value)</i>
Extension gap				
Lateral	21.3 (20.1;22.6)	0.028 (p=0.93)	-0.130 (p=0.67)	0.203 (p=0.51)
Medial	18.5 (17.3;19.8)	-0.332 (p=0.27)	-0.455 (p=0.12)	-0.311 (p=0.30)
Lateral/medial difference	2.8 (0.8;4.7)	0.237 (p=0.44)	0.217 (p=0.48)	0.336 (p=0.26)
Flexion gap				
Lateral	17.8 (16.5;19.1)	-0.064 (p=0.84)	-0.470 (p=0.11)	0.127 (p=0.68)
Medial*	16.4 (15.0;17.7)	-0.668 (p=0.01)**	-0.815 (p<0.001)**	-0.503 (p=0.08)*
Lateral/medial difference*	1.4 (-0.3;3.0)	0.502 (p=0.08)*	0.302 (p=0.32)	0.517 (p=0.07)*
Planned lower limb coronal alignment [varus (+)]	1.9° (0.6;3.2)	0.225 (p=0.44)	0.303 (p=0.29)	0.091 (p=0.76)

Figure 2

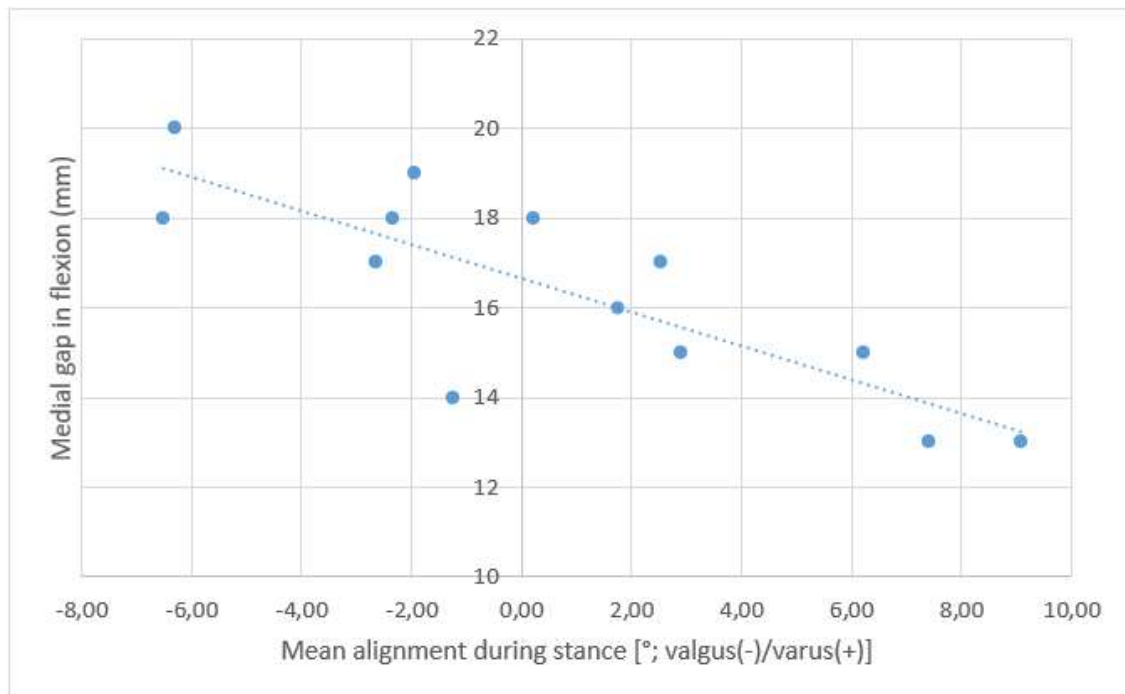


Figure 3. Very strong association between medial gap in flexion and mean alignment during stance.

Figure 3

Comparing TKA Surgical Alignment Techniques for External Peak Knee Adduction Moments, Adduction Impulse and Movement Strategies During Stair Ascent

Alexis Nelson - UTHSC - Memphis, Select Country

*Nuanqiu Hou - Campbell Clinic - Memphis, United States of America

Douglas W. Powell - University of Memphis - Memphis, USA

Marcus Ford - Campbell Clinic Orthopaedics - Germantown, USA

James Guyton - Campbell Clinic Orthopaedics - Germantown, USA

John Crockarell - Campbell Clinic Orthopaedics - Germantown, USA

Christopher Thomas Holland - Campbell Clinic Orthopaedics - Tennessee, United States of America

Derek Dixon - Campbell Clinic Foundation - Germantown, USA

Teri Ross - University of Tennessee Health Science Center - Memphis, USA

William Mihalko - University of Tennessee - Memphis, USA

Disclosure: This study was funded by Medacta International.

Introduction: Little research has been done on the effect of surgical technique on biomechanical outcomes; however previous research has shown that kinematic alignment (KA) has significantly greater patellofemoral and tibiofemoral contact stresses compared to mechanical alignment (MA) surgical technique (Ishikawa et al., 2015). Further, postoperative alignment of more than 3 degrees varus may result in accelerated wear, risk of implant failure and overall affects implant longevity (Ritter et al., 2011). All the above creates disagreement in the field on the practice of KA in TKA and there is a greater need for research in this area to understand the risks of surgical alignment techniques on functional outcomes post TKA. Therefore, our purpose was to analyze KA and MA techniques on the effect of knee adduction moments (KAM), impulse and movement strategies to ascend the stairs.

Methods: We included 28 patients who received a cruciate retaining Attune implant separated into two surgical alignment technique groups; mechanical alignment (MA, n=14) and kinematic alignment (KA, n=14). All patients underwent unilateral TKA and are at least one-year post-op. A three step instrumented staircase (1000Hz, AMTI Inc., Watertown, MA) and an 8-camera markerless motion capture system (200Hz, OptiTrack, NaturalPoint Inc., MA) were used to collect ground reaction forces and segment kinematics, respectively, during stair ascent. An AI based reconstruction software (Theia Markerless, Inc., Version 2023, Kingston, ON) was used to identify segment kinematics. Visual3D Professional (HAS Motion, Version 2023.09.3, Canada) and MATLAB (The MathWorks, Inc., R2023b, Natick, MA) were used for data analysis.

Results: There were no significant differences in age or BMI between Attune and Medacta groups. Patients in both groups had compatible patient reported outcome scores. The MA cohort had significantly larger external peak KAM ($p=0.0043$, Figure 1a) and mean KAM ($p=0.031$, Figure 1b) compared to KA cohort during stair ascent. We did not observe a significant difference in knee adduction/abduction impulse ($p=0.122$, Figure 1c), peak ankle inversion ($p=0.290$), lateral trunk lean ($p=0.680$) and peak knee valgus angle ($p=0.066$) between the alignment groups.

Conclusion: We aimed to study the impact of surgical alignment technique on knee joint biomechanics during stair ascent. We observed significant differences in KAMs where MA had larger external peak KAM, and mean KAM compared to KA. Future work will investigate muscle activation patterns, specifically of the quadriceps group,

to understand the activation patterns behind the altered movement strategy between MA and KA groups.

References:

Ishikawa M, Kuriyama S, Ito H, Furu M, Nakamura S, Matsuda S. Kinematic alignment produces near-normal knee motion but increases contact stress after total knee arthroplasty: A case study on a single implant design. *Knee* 22(3):206-212, 2015.

Ritter MA, Davis KE, Meding JB, Pierson JL, Berend ME, Malinzak RA. The effect of alignment and bmi on failure of total knee replacement. *J Bone Joint Surg Am* 93(17):1588-1596, 2011.

Figures

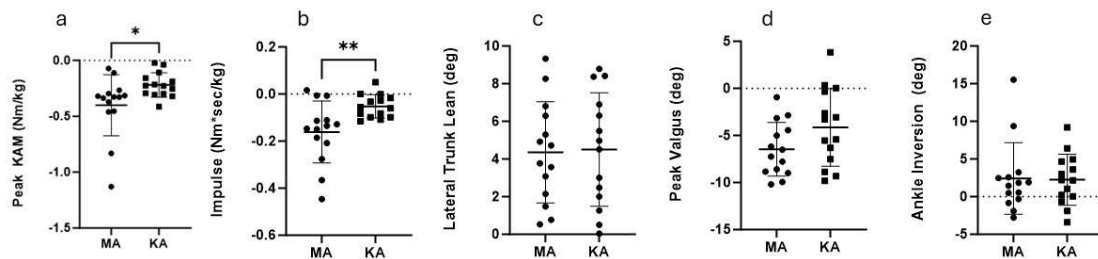


[Figure 1](#)

Variability of Alignment and Bone Resections in Robotically Balanced Total Knee Arthroplasty

*Catherine Digangi - NYU Orthopedic Hospital - New York, USA

Matthew Hepinstall - NYU Langone Health - New York, USA

Christian Oakley - NYU Langone Health - New York, USA

Michael Sybert - NYU Langone Health - New York, USA

Sophia Antonioli - NYU Langone - New York, USA

Akram Habibi - NYU Langone Orthopedic Hospital - New York, United States of America

Morteza Meftah - NYU Hospital for Joint Diseases - New York, USA

Patrick Meere - NYU Hospital for Joint Diseases - New York, USA

Introduction

Image-based robotic-assisted total knee arthroplasty (RA-TKA) allows surgeons to start with patient-specific 3-dimensional measured-resection plans based on mapping of the bone surface. This will allow adjustment of the plans intraoperatively based on objective assessment of ligament laxity and gap balance. The aim of this study was to identify ranges of implant alignment and bone resections with RA-TKA.

Methods

We retrospectively reviewed 530 primary Mako (Stryker) TKA cases performed from November 2022 to December 2023. The cohort was divided by their native arithmetic hip-knee-ankle angle (aHKA) into varus, neutral, and valgus groups. Demographics, clinical characteristics, and intraoperative data were collected and compared using Chi-square, ANOVA, and Independent Sample t-tests. Separate analyses were performed for cruciate-retaining (CR) and posterior-stabilized (PS) implants.

Results

There were 214 (40.4%) varus, 202 (38.1%) neutral, and 114 (21.5%) valgus cases in the study cohort, with 91.3% using CR implants. The varus, neutral, and valgus cohorts had mean preoperative aHKAs of 4.9, 0.2, and -4.8 degrees, respectively. Planned transverse rotation relative to the transepicondylar axis was lowest in the valgus cohort compared to varus and neutral (0.5 vs. 2.4 vs. 2.0, $P<0.001$). Planned resections of the lateral distal femur and of the medial posterior femur were greater in the varus group compared to neutral and valgus (5.6 vs. 4.6 vs. 3.5, $P<0.001$; 9.9 vs. 9.4 vs. 8.6, $P<0.001$). There were significant differences between cohorts in planned tibia resections, laterally and medially. The sum of planned resections in extension laterally, were 11.9, 10.8, and 9.0 millimeters for varus, neutral, and valgus, respectively ($P<0.001$); Medially, resections for varus, neutral, and valgus were 10.8, 11.8, and 12.2 millimeters ($P<0.001$). The sum of resections in flexion were similarly associated with significant differences, medially and laterally. Metric variability was high for all values for sums of resection in both extension and flexion across aHKA cohorts.

Conclusion

This study demonstrated trends in intraoperative planned alignment and resection metrics across various preoperative coronal knee alignments and prosthesis design. These findings contribute to the understanding of RA-TKA and may inform surgical decision-making in achieving optimal outcomes.

Figures

Table 1. Targeted metrics, Stratified by Preoperative Coronal Alignment

	Varus (n=214)			Neutral (n=202)			Valgus (n=114)			P-value
	M	SD	Range	M	SD	Range	M	SD	Range	
Preoperative aHKA (°) ¹	4.9± 2.2		2.1 – 12.8	0.2± 1.1		-2 – 2	-4.8± 2.1		-12.5 – -2.1	<0.001
Planned Coronal Alignment (°) ¹										
Limb	2.9± 1.7		-2 – 6.2	0.9± 1.4		-4 – 4.4	-1.3± 1.5		-4.9 – 2.2	<0.001
Distal Femur	0.7± 1.2		-3.5 – 4	-0.3± 1.2		-4.5 – 2.5	-1.4± 1.2		-4.5 – 2	<0.001
Proximal Tibia	2.2± 1.1		-1 – 5.1	1.1± 1.2		-1 – 4	0.0± 1.0		-2 – 3.5	<0.001
Planned Transverse Rotation (°) ²										
Femoral TEA	2.4± 1.8		-3 – 6	2.0± 1.8		-4 – 6.5	0.5± 1.9		-5.2 – 5	<0.001
Femoral PCA	5.0± 2.0		-0.8 – 9.5	4.6± 2.1		-1.2 – 9.9	3.7± 2.0		-0.4 – 10	<0.001
Planned Sagittal Alignment (°)										
Femoral Flexion ³	3.9± 1.4		0 – 7.5	4± 1.5		0.5 – 8	4.1± 1.5		0 – 8	0.654
Tibial Slope ⁴	3.2± 0.8		0 – 5.5	3.1± 0.8		1 – 5.8	3.2± 0.7		1 – 5.5	0.950
Distal Femur Resection (mm)										
Lateral	5.6± 1.5		0.5 – 9.5	4.6± 1.5		1 – 8.5	3.5± 1.3		0.5 – 7	<0.001
Medial	7.1± 1.6		1.5 – 11	7.3± 1.2		4 – 10	7.4± 1.2		4.5 – 11	0.223
Posterior Femur Resection (mm)										
Lateral	5.8± 1.7		0.5 – 10	5.6± 1.8		1.5 – 11.5	5.7± 1.7		1.5 – 9.5	0.738
Medial	9.9± 1.6		5 – 13.5	9.4± 1.5		4 – 14.5	8.6± 1.4		5 – 12.5	<0.001
Tibia Resection (mm)										
Lateral	6.3± 1.2		2 – 10	6.2± 1.3		1 – 10	5.5± 1.5		2 – 10	<0.001
Medial	3.7± 1.4		0 – 8	4.5± 1.3		1 – 9	4.8± 1.4		1 – 7.5	<0.001
Sum of Extension Resections (mm)										
Lateral	11.9± 1.9		6.5 – 17.5	10.8± 1.8		6 – 15.5	9.0± 1.8		4.5 – 14	<0.001
Medial	10.8± 2.1		3.5 – 17.5	11.8± 1.7		7 – 16	12.2± 1.6		8 – 16.5	<0.001
Sum of Flexion Resections (mm)										
Lateral	12.0± 1.9		5.5 – 17.5	11.9± 1.9		6 – 17	11.2± 1.9		6.5 – 16	<0.001
Medial	13.7± 1.8		7.5 – 17	13.9± 1.6		8.5 – 19	13.4± 1.7		7 – 18	0.019

M, mean; SD, standard deviation; mm, millimeters; aHKA, arithmetic hip-knee-ankle; TEA, transepicondylar axis; PCA, posterior condylar axis

¹ Varus measurements are greater than 0; valgus measurements are less than 0. ² External measurements are greater than 0; internal measurements are less than 0. ³ Flexion measurements are greater than 0; extension measurements are less than 0. ⁴ P slope measurements are greater than 0; a slope measurements are less than 0.

Range values are maximum and minimum. Metric variability was determined by SD from mean and characterized as **low** (greater than or equal to 1.5) and **high** (greater than 1.5).

Figure 1

Table 2. Targeted Metrics, Stratified by Implant Design and Preoperative Coronal Alignment

	Varus			Neutral			Valgus		
	CR		PS	CR		PS	CR		PS
	(n=191)	(n=23)		(n=189)	(n=13)		(n=104)	(n=10)	
Preoperative aHKA Alignment (°) ¹	M SD	M SD	P-value	M SD	M SD	P-value	M SD	M SD	P-value
Planned Coronal Alignment (°) ¹									
Limb	3±1.1	2.2±1.4	0.027	0.9±1.4	0.7±1.4	0.618	-1.3±1.4	-1.8±1.6	0.315
Distal Femur	0.8±1.2	0.3±1.2	0.082	-0.3±1.2	0.1±1.0	0.323	-1.4±1.2	-1.4±1.3	0.950
Proximal Tibia	2.2±1.1	1.9±1.2	0.148	1.2±1.2	0.6±1.0	0.110	0.1±1.0	-0.4±0.8	0.163
Planned Transverse Rotation (°) ²									
Femoral TEA	2.4±1.8	1.9±1.7	0.180	2.1±1.8	1.5±1.4	0.265	0.5±2.0	0.8±1.4	0.651
Femoral PCA	5±2.0	4.6±2.0	0.343	4.8±2.1	2.9±2.4	0.002	3.7±2.0	3.3±2.1	0.504
Planned Sagittal Alignment (°)									
Femoral Flexion ³	3.9±1.4	4±1.5	0.853	4±1.5	4.3±1.4	0.395	4.1±1.5	4±1.9	0.814
Tibial Slope ⁴	3.3±0.6	1.9±1.1	<0.001	3.2±0.6	1.8±1.4	0.004	3.3±0.6	2.1±1.0	0.004
Distal Femur Resection (mm)									
Lateral	5.5±1.5	5.8±1.2	0.473	4.6±1.5	5.1±1.8	0.208	3.4±1.4	4.2±0.9	0.074
Medial	7.1±1.7	7±1.4	0.705	7.3±1.2	7.4±1.0	0.680	7.3±1.2	7.9±1.4	0.160
Posterior Femur Resection (mm)									
Lateral	5.8±1.7	5.2±1.6	0.094	5.6±1.8	6.2±1.9	0.297	5.7±1.7	5.4±1.7	0.603
Medial	10±1.5	9.2±2.0	0.014	9.5±1.5	8.5±1.1	0.036	8.6±1.4	7.9±1.8	0.108
Tibia Resection (mm)									
Lateral	6.3±1.2	6.1±1.4	0.479	6.3±1.2	5.7±1.8	0.122	5.6±1.5	4.6±1.1	0.028
Medial	3.8±1.3	3.1±1.5	0.013	4.6±1.3	3.6±1.0	0.009	4.9±1.4	3.8±1.4	0.017
Sum of Extension Resections (mm)									
Lateral	11.9±1.9	11.9±1.2	0.891	10.8±1.8	10.8±1.6	0.969	9±1.8	8.8±1.6	0.662
Medial	10.9±2.2	10±1.7	0.062	11.9±1.7	11±1.2	0.094	12.2±1.5	11.7±1.8	0.319
Sum of Flexion Resections (mm)									
Lateral	12.1±1.9	11.3±1.8	0.047	11.9±1.9	11.8±2.3	0.969	11.3±1.9	10±2.0	0.032
Medial	13.8±1.7	12.2±2.3	0.003	14±1.6	12.2±1.2	<0.001	13.5±1.6	11.7±2.3	<0.001

M, mean; SD, standard deviation; mm, millimeters; aHKA, arithmetic hip-knee-ankle; TEA, transepicondylar axis; PCA, posterior condylar axis; CR, Cruciate-retaining; PS, Posterior-stabilized

¹Varus measurements are greater than 0; valgus measurements are less than 0. ²External measurements are greater than 0; internal measurements are less than 0. ³Flexion measurements are greater than 0; extension measurements are less than 0. ⁴P.slope measurements are greater than 0; a.slope measurements are less than 0.

Range values are maximum and minimum. Metric variability was determined by SD from mean and characterized as **low** (greater than or equal to 1.5) and **high** (greater than 1.5).

Figure 2

Prediction of Coronal Alignment in Robotic-Assisted Total Knee Arthroplasty With Artificial Intelligence

Catherine Digangi - NYU Orthopedic Hospital - New York, USA

Joseph A. Bosco IV - Washington & Lee University - Lexington, USA

*Morteza Meftah - NYU Hospital for Joint Diseases - New York, USA

Daniel Waren - NYU Langone Health - New York, USA

Cody Watson - Washington & Lee University - Lexington, USA

Sophia Antonioli - NYU Langone - New York, USA

Akram Habibi - NYU Langone Orthopedic Hospital - New York, United States of America

Introduction

Robotic-assisted technologies provide the ability to avoid soft tissue release in a majority of cases utilizing more accurate bony cuts during total knee arthroplasty (TKA). However, the ideal limb alignment is not yet established. The aim of this study was to predict postoperative Coronal Plane Alignment of the Knee (CPAK) using corresponding native bony measurements.

Methods

This study analyzed a retrospective cohort of 530 primary robotic-assisted TKAs (Mako, Stryker) performed from November 2022 to December 2023. Medial proximal tibial angle (MPTA) and lateral distal femoral angle (LDFA) measurements were determined from the robotic system. We utilized machine learning to predict appropriate target LDFA and MPTA values from preoperative LDFA and MPTA measurements. In the preprocessing stage, the dataset was split into input and target sets using the preoperative and planned LDFA and MPTA values, then split again into testing, training, and validation sets of sizes 30%, 66.5%, and 3.5%, respectively. Normalization of LDFA and MPTA alignments was performed using the min-max scaler operation on the training set with feature range [-1, 1] and repeated separately for the input and target distributions. A neural network of hidden dimensions (16, 8, 4) (Figure 1) was trained via supervised learning to predict planned LDFA and MPTA values from preoperative LDFA and MPTA measurements.

Results

The model converged after 104 epochs and batch size 4 (Figure 2) with mean squared error $\pm 1.82^\circ$. The model's regression agrees with the hypothesized change in preoperative to planned coronal alignment: valgus measurements (x-axis, right) are translated to neutral/aligned targets (y-axis, middle) while varus alignments (x-axis, left) are translated to varus alignment of lesser severity (y-axis, bottom) (Figure 3). Evaluative statistics demonstrate this method for planning knee morphologies is significantly more accurate than making predictions about the mean (RMSE 1.440; R-squared 0.444; Nash Sutcliffe 0.579).

Conclusion

This study's model provides accurate predictions for target knee alignment morphologies. Future work is warranted to evaluate this method's usefulness for planning robotic TKA.

Figures

Figure 1. Neural Network Model Architecture

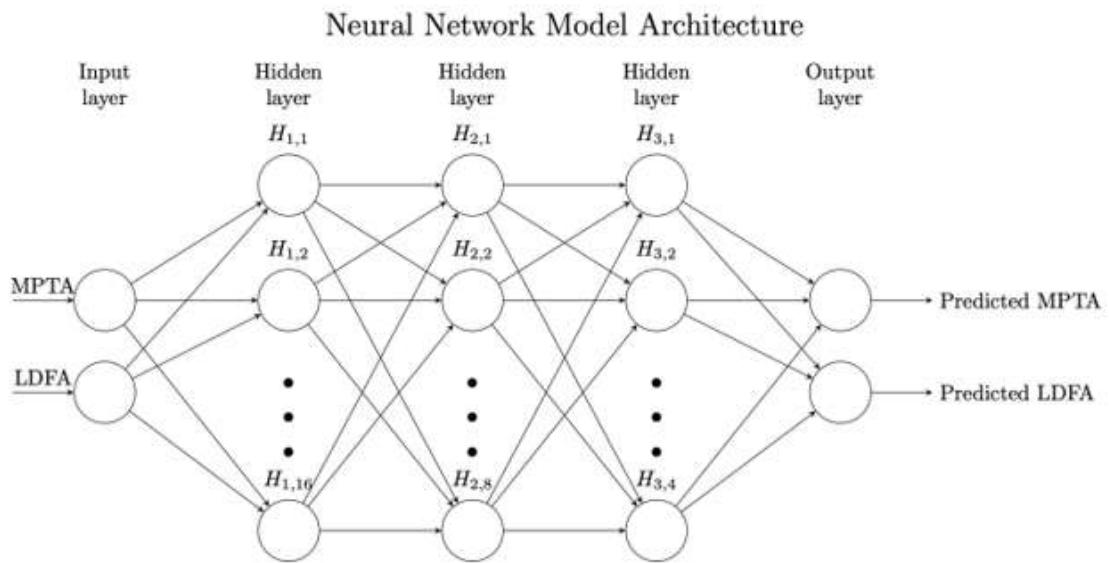


Figure 1

Figure 2. MLP Regressor Loss Curve

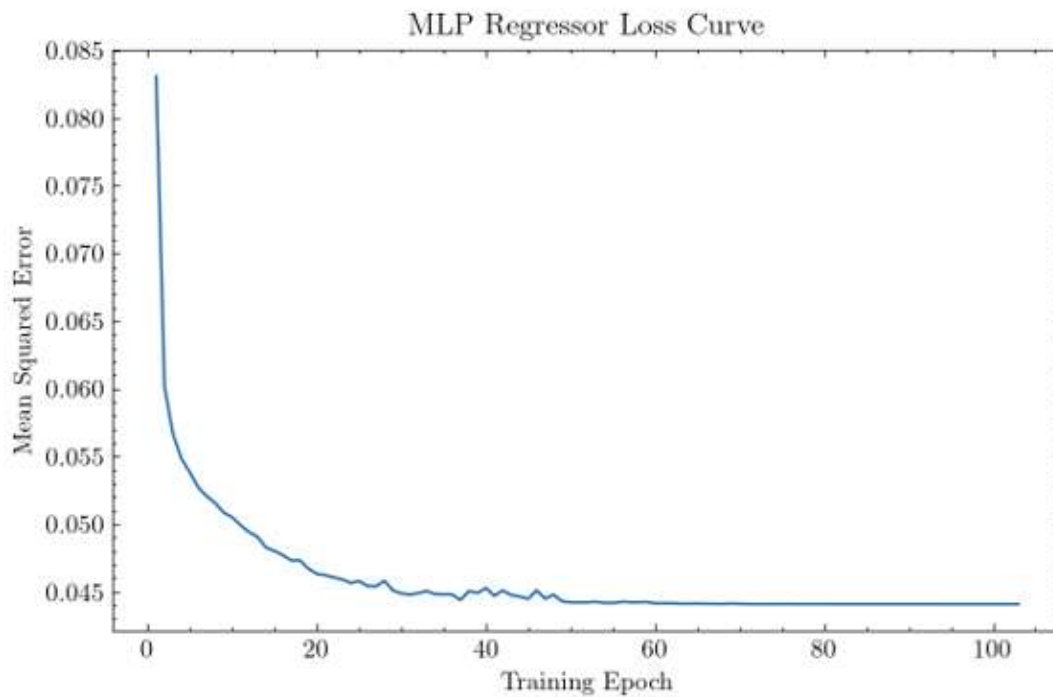


Figure 2

Figure 3. Prediction of Planned aHKA from Preoperative aHKA

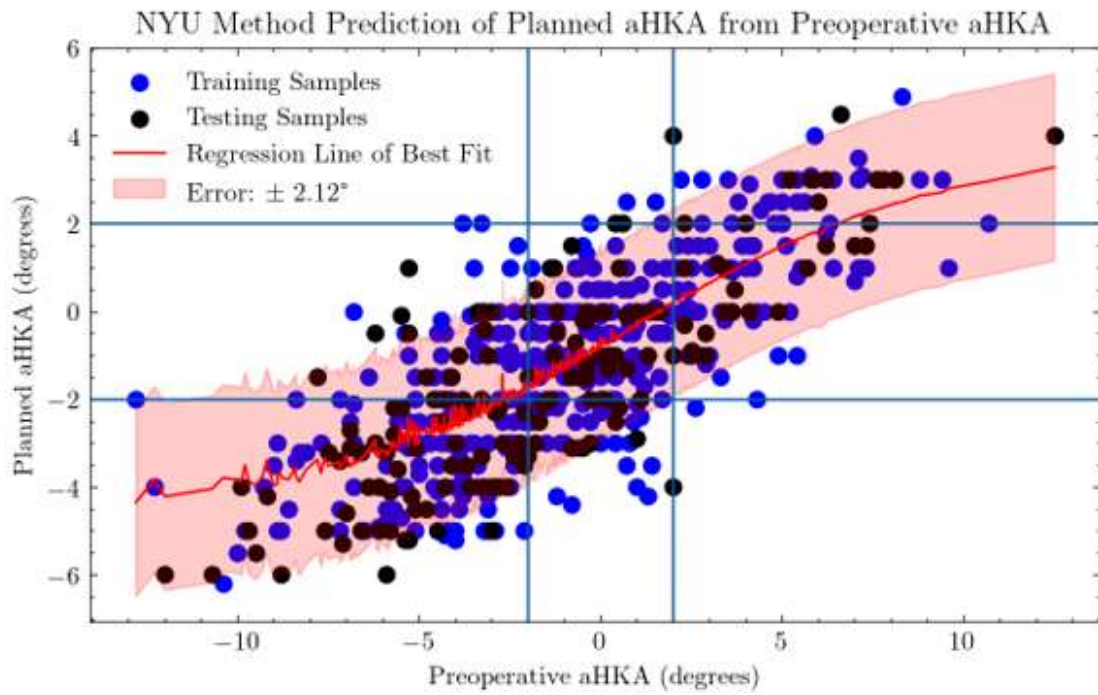


Figure 3

Comparison of Mechanical Versus Kinematic Alignment in Kinematic Outcomes in TKA Subjects Using a Forward Mathematical Model of the Knee

*Caleb Chesney - University of Tennessee - Knoxville, USA

Michael LaCour - University of Tennessee - Knoxville, USA

Richard Komistek - The University of Tennessee - Knoxville, USA

Bradley Meccia - University of Tennessee Knoxville - Knoxville, USA

INTRODUCTION

While Mechanical Alignment (MA) has long been the gold standard for total knee arthroplasty (TKA), Kinematic Alignment (KA) has recently gained popularity, aiming to recreate the anatomical joint line by matching bone resection to the thickness of the implant and adjusting bone cuts for soft tissue balancing. However, there is lack of consensus on whether it is superior to MA [1] [2], as some have reported difficulty balancing either varus [3] or valgus [4] knees in KA. The objective of this study was to use a validated mathematical model to analyze MA and KA alignments for patients with preoperative varus and valgus knees.

METHODS

Four subjects were included in this study, with two varus and two valgus deformities, defined as a joint line orientation greater than $\pm 2^\circ$ from a normal joint line. All subjects were implanted using both calipered KA and traditional MA alignment techniques using three cruciate-retaining systems: DePuy Attune (CR #1), Zimmer-Biomet Persona (CR #2), and Stryker Triathlon (CR #3). Subjects performed a deep knee bend to 120° flexion. Parameters of interest include medial/lateral condylar position, femorotibial axial rotation, strains in the MCL, LCL, and PCL.

RESULTS

KA for varus and valgus knees reported opposite trends compared to their respective MA. For example, KA of a varus knee resulted in a more anteriorized lateral condyle and posteriorized medial condyle, generating decreased axial rotation, with CR #1 in MA experiencing a stable medial condyle with lateral rollback, and external rotation of all scenarios. KA of a valgus knee resulted in posteriorized lateral condyles and anteriorized medial condyles (sliding with CR #3; alternating anterior/posterior motion patterns with CR #2), generating increased axial rotation. However, KA of valgus knees also generated excess slack in the MCL and tension in the LCL, with a particularly high increase in LCL tension with CR #2. In all cases, KA generated slight decreases in PCL tension.

DISCUSSION

Given how KA techniques try to balance the ligaments via bone cuts, knees with excess deformities may require significant bone resections to achieve ligament balancing. Otherwise, excess tension in the collateral ligaments may prevent full range of motion. Furthermore, these preoperative deformities have likely already caused abnormal ligament tension preoperatively, so it may be impossible to successfully balance knees without restrictions or other techniques. Given the reliance that KA has on preoperative morphology, it may be advantageous to use careful selection criteria when treated patients with excess deformities.

REFERENCES

- [1] <https://doi.org/10.1016/j.jos.2023.08.001>.
- [2] <https://doi.org/10.1097/md.00000000000008157>
- [3] <https://doi.org/10.1007/s00167-022-07073-5>
- [4] <https://doi.org/10.3390/jcm13051302>

Figures

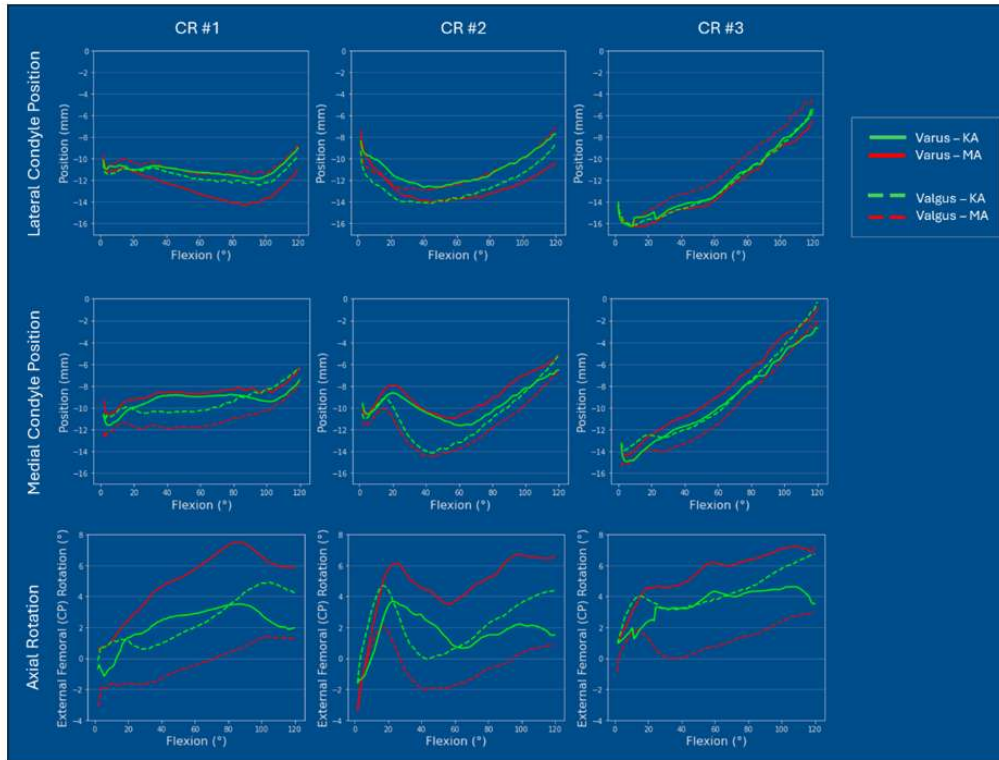


Figure 1. Primary Kinematic Outputs (MCP, LCP, Axial Rotation) versus Flexion. Plots are arranged with LCP on the top row, MCP in the middle, and Axial Rotation on the bottom. Positive indicates anterior translation for MCP and LCP, and positive indicates external femorotibial axial rotation.

[Figure 1](#)

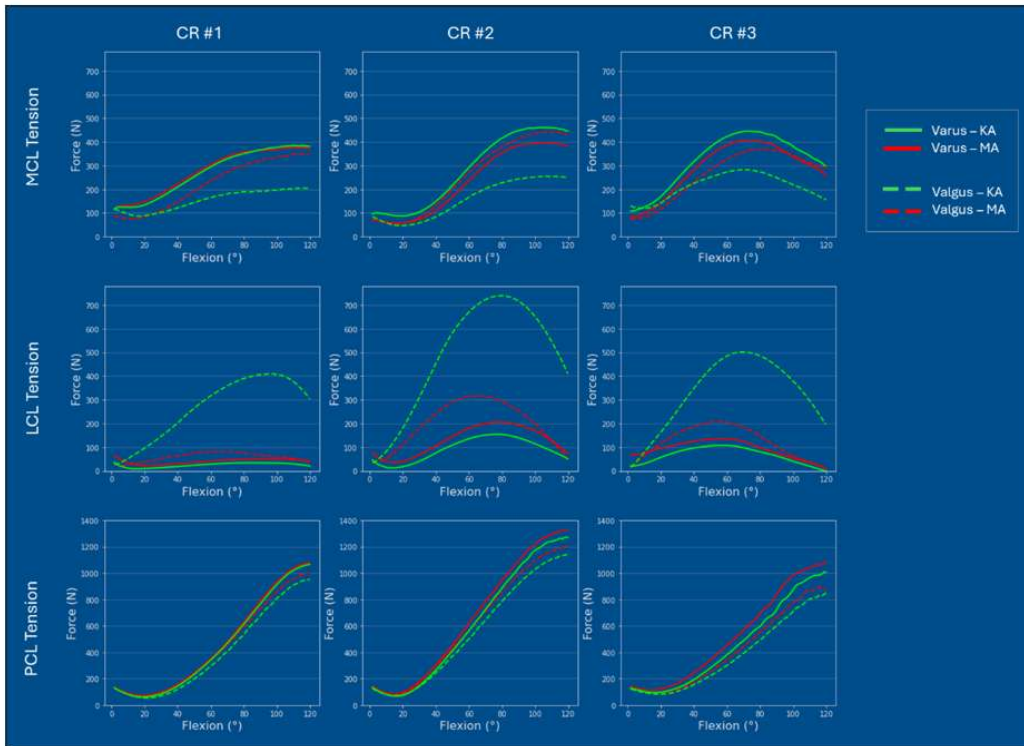


Figure 2. Ligament tension versus Flexion. Plots are arranged with MCL on the top row, LCL in the middle, and PCL on the bottom.

[Figure 2](#)

Inverse Kinematic Alignment Decreases Joint Line Obliquity Compared to Kinematic Alignment

*Joseph Maratt - Forté Sports Medicine & Orthopedics - Carmel, United States of America

Lucian Warth - Forte Sports Medicine & Orthopedics - Carmel, USA

Chris Curless - Forte Orthopedic Research Institute - Carmel, USA

Rachel Brennan - Forte Orthopedic Research Institute - Carmel, USA

Introduction:

Kinematic alignment in TKA has shown promise in improving outcomes by more closely recreating pre-arthritic tibiofemoral relationships and avoiding soft tissue releases. However, there is concern about the degree of intentional tibial varus and resulting joint line obliquity adversely affecting the longevity of the construct. We set out to evaluate joint line obliquity in calipered kinematic alignment (cKA) and inverse kinematic alignment (iKA) techniques.

Methods:

We collected alignment and balancing data during 198 consecutive robot-assisted TKAs utilizing an iKA technique. In the initial planning, implants were positioned with cKA principles to achieve shape matched equal resections accounting for cartilage loss of the medial and lateral distal femur, posterior condyles and proximal tibia. Balance was achieved utilizing iKA principles - changing the femoral component position to achieve an equal extension gap, sagittal profile concentricity of the medial femoral condyle to implant geometry and matching the trochlear geometry resulting in a 1-2 mm larger lateral flexion gap. For the simulated cKA analysis, balance was achieved by changing the tibia position only.

Results:

86% of cases did not have an equal extension gap during ligament testing with the initial cKA resection plan. The extension gap was smaller medially (M=1.9mm, SD=1.4mm). In the iKA plan, balance in extension was achieved by decreasing femoral valgus (M=2.1°, SD=1.2°) and increasing the tibial varus (M=0.5°, SD=0.9°). As expected of the simulation, HKA (M=-2.6°, SD=2.4°) was unchanged between the executed iKA plan and simulated cKA plan. In the executed iKA plan, joint line obliquity was 1.6 degrees (p<.001, 95% CI 1.44-1.87) lower than the simulated cKA plan.

Conclusions:

Inverse kinematic alignment technique with pre-resection balancing results in significantly less joint line obliquity and less tibial component varus than femur first calipered kinematic alignment. This approach may achieve the goals of kinematic alignment with fewer varus outliers.

Portable Navigation Enables Accurate Coronal and Sagittal Alignment in Total Knee Arthroplasty Performed by Less Experienced Surgeons.

*Keisuke Matsukura - Asahikawa Medical University - Asahikawa, Japan

Satomi Abe - Asahikawa Medical University - Asahikawa, Japan

Hiroshi Ito - Asahikawa Medical College - Asahikawa, Japan

Portable Navigation Accurately Aligns Coronal and Sagittal Plane Osteotomies in TKA for Uncertified Physicians

Introduction: Alignment in total knee arthroplasty (TKA) has been the subject of much discussion, and the amount of bone resection must be more precise and the techniques must be easy to perform. To evaluate the effectiveness of portable navigation (hereafter referred to as "NAVI"), we compared the component position before and after using navigation, and further compared them between certified surgeons (S group) and less experienced surgeons with fewer than 50 cases of surgeries (R group).

Method: The subjects were primary PS-type TKA cases performed with medial parapatellar approach, with mechanical alignment as the goal. Component positions were evaluated based on the postoperative X-rays. Outliers were defined as component angles exceeding α -angle 92-97 degrees, β -angle 87-93 degrees, γ -angle 0-3 degrees, and the δ -angle 83-90 degrees. 300 knees using intramedullary or extramedullary guides were compared to 100 knees using NAVI (KneeAlign2®). Additionally, we compared S group (2 surgeons) who performed TKA using NAVI (160 knees) with R group (4 surgeons) who also performed TKA using NAVI (36 knees).

Results: The outlier rates before NAVI were α 13%, β 10%, γ 13%, and δ 19%, while after NAVI, they were α 8%, β 6%, γ 25%, and δ 7% (figure 1). The mean unilateral surgery time was significantly different between S group and R group ($P < 0.0001$). Although, there was no difference in component angles between S group ($\alpha 94 \pm 1^\circ$, $\beta 89 \pm 1^\circ$, $\gamma 2.3 \pm 2.0^\circ$, and $\delta 86 \pm 2^\circ$) and R group ($\alpha 93 \pm 2^\circ$, $\beta 89 \pm 2^\circ$, $\gamma 1.6 \pm 1.4^\circ$, and $\delta 86 \pm 2^\circ$), there was a significant difference in CTA (S group: $1.6 \pm 1.4^\circ$, R group: $2.4 \pm 2.0^\circ$, figure 2) ($P < 0.001$). The outlier rates of S group were α 10%, β 6%, γ 15%, and δ 8%, while those of R group were α 11%, β 8%, γ 8%, and δ 8% (figure 3).

Conclusion: The rotation of the femoral component was more accurate for experienced surgeons, but accurate component position in the coronal and sagittal planes was possible even for less experienced surgeons when using navigation. Furthermore, to further reduce outliers, it was considered necessary to understand and master the characteristics of navigation, including draping around the hip joint, registration sites on the lower leg, and reconfirmation of the amount of bone resection before cutting.

Figures

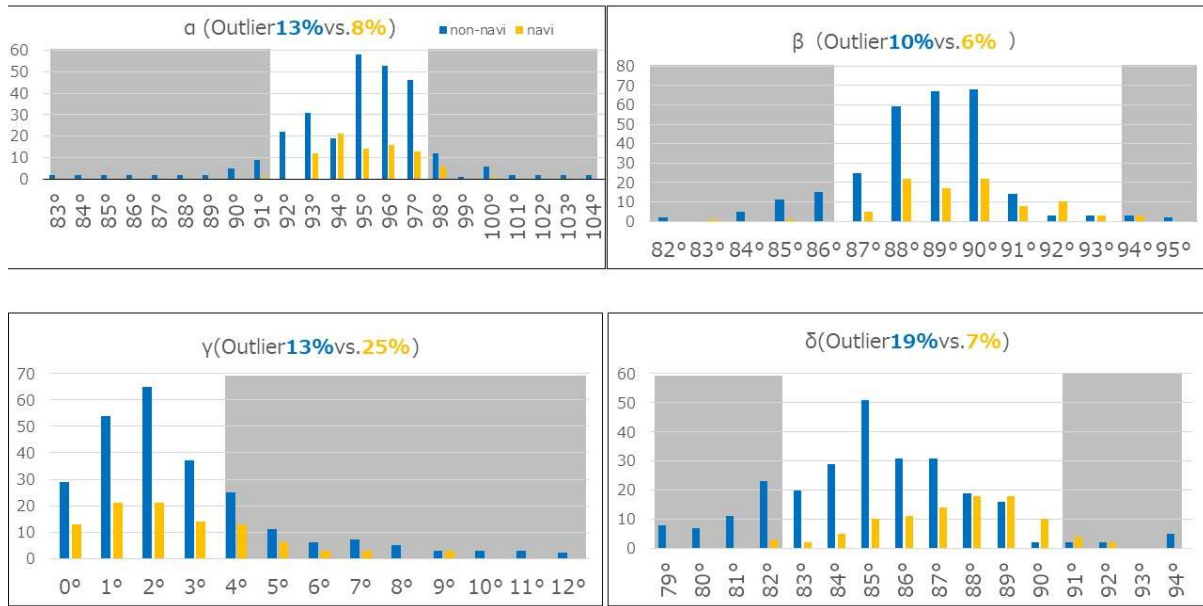


Figure 1

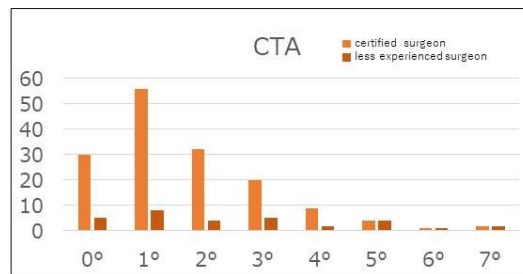


Figure 2

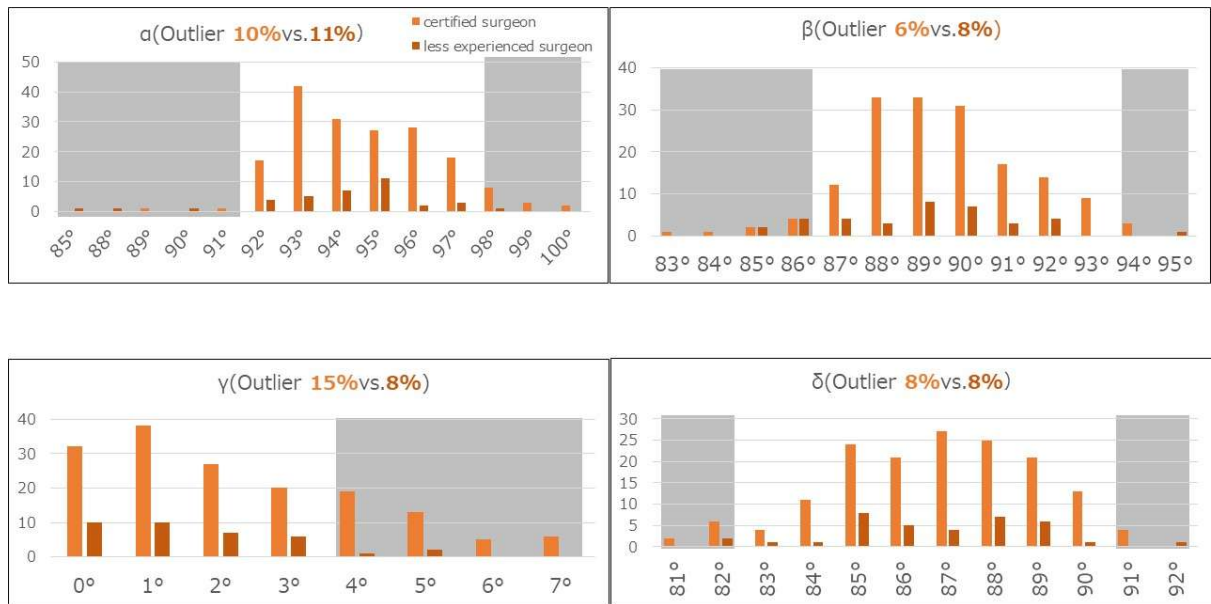


Figure 3

What Is the Best Way to Identify Femoral and Tibial Anatomic Landmarks for Component Alignment? a Cadaver-Based Study

*Melanie Caba - Stryker Corporation - Mahwah, United States of America

Azhar Ali - Stryker Orthopaedics - Mahwah, USA

Antonia Chen - Brigham and Women's Hospital - Boston, USA

Michael Mont - Sinai Hospital of Baltimore - Baltimore, USA

James Crutcher - Swedish Orthopedic Institute - Seattle, United States of America

Ormonde Mahoney - Athens Orthopedic Clinic - Athens, USA

Laura Yanoso-Scholl - Stryker Orthopaedics - USA

Emily Hampp - Stryker - Mahwah, USA

Sarah Shi - Stryker - Mahwah, USA

Introduction:

Femoral and tibial component malalignment in total knee arthroplasty (TKA) has been associated with postoperative complications such as instability, patient dissatisfaction, and early component failure. Therefore, precise placement of components in the desired rotational alignment is important to help achieve optimal clinical results. The placement of femoral and tibial components are determined by reference points from bony landmarks relative to native anatomy. Previous studies have demonstrated that manually identifying reference points on bony landmarks are inconsistent, but few studies have compared manual identification to computed tomography (CT) measurements. The purpose of this study was to compare variation between identification of femoral and tibial landmarks executed manually and using CT scans.

Methods:

Two evaluator groups identified femoral and tibial bony landmarks (defined in Figure 1) of six cadaveric knees. The groups included three experienced arthroplasty surgeons, who intra-operatively identified bony landmarks on the cadavers (manual identification), and three CT-scan evaluators, who identified the landmarks digitally on the cadavers corresponding CT scans (CT identification). All landmarks were identified three times while rotating between specimens for randomization and the data was collected utilizing a robotic system. The three-dimensional locations of each identified landmark was converted into a distance value and variation between each landmark was analyzed. A two-sample *t*-test was used to evaluate statistical significance.

Results:

In this cadaveric study, CT identification was associated with decreased variation for all landmarks when compared to manual techniques (Figure 2), and CT identification had a significant decrease in variation for the anterior trochlear groove ($p < 0.001$), medial posterior femoral condyle ($p = 0.010$), lateral posterior femoral condyle ($p = 0.021$), medial epicondyle ($p = 0.006$), lateral tibial plateau ($p = 0.029$), and lateral malleolus ($p = 0.028$).

Conclusion:

In this cadaveric study, the use of CT identification for femoral and tibial landmarks demonstrated less variability for all landmarks compared to manual identification, which may lead to more consistent implant component placement. Further studies are needed to determine the influence of landmark variation on component positioning.

Figures

Figure 1: Bony landmarks and reference landmark definitions

	Landmark	Point Selections	Point Selection Definition
Femur	Whiteside's Line	<ul style="list-style-type: none"> • Anterior Trochlear Groove • Intercondylar Notch 	<ul style="list-style-type: none"> • most anterior point of trochlear groove • most distal point of trochlear groove
	Posterior Condylar Axis	<ul style="list-style-type: none"> • Medial Posterior Femoral Condyle • Lateral Posterior Femoral Condyle 	<ul style="list-style-type: none"> • most posterior point of the medial condyle • most posterior point of the lateral condyle
	Transepicondylar Axis	<ul style="list-style-type: none"> • Medial Epicondyle • Lateral Epicondyle 	<ul style="list-style-type: none"> • point in the bony sulcus on the medial femur • the most proud point on the lateral bony protuberance
Tibia	Tibial Tubercle	<ul style="list-style-type: none"> • Tibial Tubercle 	<ul style="list-style-type: none"> • middle 1/3 of tibial tubercle
	Joint Line	<ul style="list-style-type: none"> • Medial Tibial Plateau • Lateral Tibial Plateau 	<ul style="list-style-type: none"> • 2/3 posterior placement of medial tibial plateau • 2/3 posterior placement of lateral tibial plateau
	Tibial Ankle Center	<ul style="list-style-type: none"> • Medial Malleolus • Lateral Malleolus 	<ul style="list-style-type: none"> • the most proud point on the distal medial tibia • the most proud point on the distal lateral fibula

[Figure 1](#)

Figure 2: Variation of distance results for CT and manual identification of landmarks.

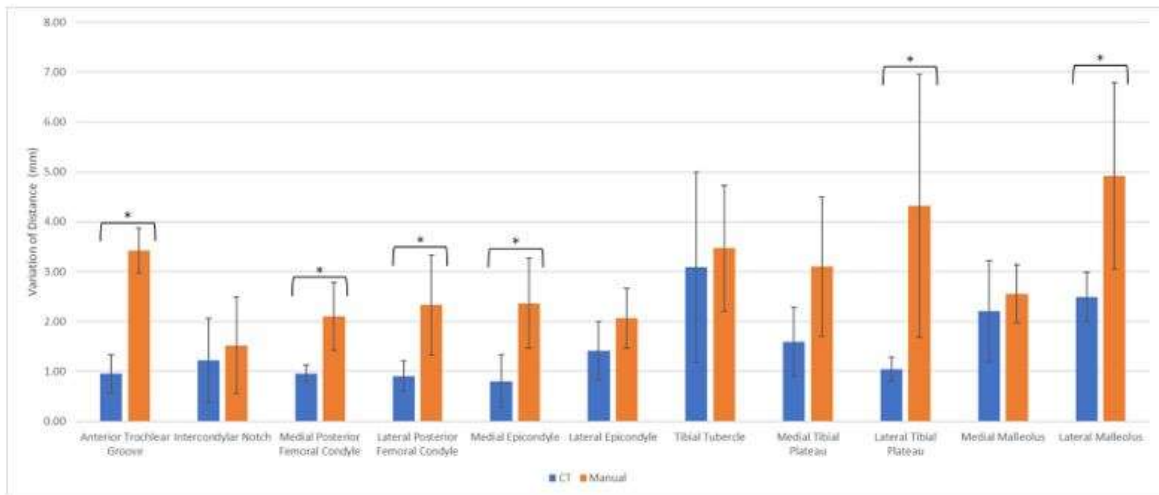


Figure 2

Oxidation and Crosslink Density of Retrieved Highly Crosslinked Polyethylene Total Hip and Total Knee Inserts After Long-Term Implantation

*Aarti Shenoy - Hospital for Special Surgery - New York, USA

Nathaniel T. Ondeck - Hospital for Special Surgery - New York, USA

Louise O Connor - Hospital for Special Surgery - New York, USA

Elexis Baral - Hospital for Special Surgery - New York, USA

William Querido - Temple University - Philadelphia, USA

Nancy Pleshko - Temple University - Philadelphia, USA

Timothy Wright - Hospital for Special Surgery - New York, USA

Introduction: Highly crosslinked polyethylene (XLPE) was introduced as a more wear-resistant and tougher alternative to ultra-high molecular weight polyethylene (UHMWPE). XLPE demonstrates superior wear resistance and fracture toughness due to higher crosslink density achieved through increased irradiation doses [1]. A study in total knee arthroplasty (TKA) tibial inserts has shown that crosslink density deteriorates and XLPE oxidation increases after a mean implantation time of 18 months [2]. We aim to investigate crosslink density (XLD) and oxidation index (OI) changes in retrieved total hip liners and tibial inserts after long-term implantation. **Methods:** 16 (out of 575) XLPE hip liners and 13 (out of 602) XLPE tibial inserts revised between 2020-2023 were identified by chart review from our IRB-approved institutional retrieved implant repository. Mean implantation time for the hip liners was 161 ± 39.32 months and for the tibial inserts was 119 ± 28.09 months. All tibial inserts were posterior-stabilized (PS) designs. All implants included have been in situ for the longest time and also stored at -18°C within 6 months of revision to minimize ex vivo oxidation effects. Samples were visually assessed for surface damage. A cylinder was cored from the apex of each hip liner and sectioned into two halves, representing inner and outer bearing surfaces to measure XLD. Hip liners were sectioned at the apex for OI measurements. $3 \times 3 \times 3 \text{mm}^3$ samples were created from tibial insert condylar regions at 'loaded' and 'unloaded' regions identified using digital microscopy. XLD measurements will be conducted following ASTM F2214. OI will be measured along the sectioned face. OI will be measured along the sectioned face using Optical Photothermal Infrared (O-PTIR) spectroscopy. Spearman's correlations will be used to assess statistical relationships between patient demographics and OI, and XLD.

Results: The reasons for revision are summarized in Figure 1a for the hip liners cohort and in Figure 1b for tibial inserts cohort. None of the hip liners show any delamination and only one shows evidence of minor scratching. Among the tibial inserts, XLD and OI measurements are ongoing.

Conclusion: The improved mechanical and wear properties of first and second generation XLPE components must be evaluated through longer-term follow-up studies as long-term implanted components start to become available in retrieved implant repositories such as at our institution.

References:

[1] Muratoglu O et al., *Biomat.*, 1999, 20(16), pp 1463-70

[2] Liu et al., *Clin Orth Rel Res*, 2017; 475, pp 128-136

Figures

Reason for Revision	N
instability	8
infection	3
osteolysis	1
aseptic loosening	1
trunnionosis/fracture	3

Reason for Revision	N
Broken post	4
Ligament laxity	1
Infection	3
Aseptic loosening	2
Recurrent effusions	1

[Figure 1](#)

[Figure 2](#)

Oxidation Assessment on the Surface and Subsurface of Total Knee Arthroplasty Tibial Inserts Revised Within Less Than 5 Years

*Enrico Fava - Federal University of Santa Catarina - Florianópolis, Brazil

Amanda Fullgraf Petry - Universidade Federal de Santa Catarina - Florianópolis, Brazil

Carlos Rodrigo De Mello Roesler - Universidade Federal de Santa Catarina - Florianópolis, Brazil

Gean Vitor Salmoria - Universidade Federal de Santa Catarina - Florianópolis, Brazil

Alan De Paula Mozella - Instituto Nacional de Traumatologia e Ortopedia Jamil Haddad São Cristóvão - Rio de Janeiro, Brazil

Patricia Ortega Cubillos - UFSC - Florianopolis, Brazil

Introduction: The oxidation process on tibial inserts is directly related to sterilization, crosslinking, and packaging processes. The oxidation study on revised prostheses with less than five years is necessary for the comprehension of its impact on early revision and how the control of the cited processes is imperative to ensure the prosthesis' success.

Methods: Five tibial inserts from three different manufacturers were evaluated for ketone oxidation index (KOI) in their surface (depth zero) and two subsurfaces (depth 200 and 400 μm) regions (Figure 1 and Figure 2). All samples had a length of implantation between three- and five-years' time. First manufacturer was Depuy Synthes Sigma, samples A1, A2, and A3 all of them crosslinked with annealing and remelting post processing; second manufacturer was Exactech Optetrak Logic, sample B1 conventional polyethylene; final manufacturer was Implantcast ACS, sample C1 conventional polyethylene with annealing post processing. Polymer slices for FTIR assessment were collected from three regions on the condyles, on the axial plane. KOI was calculated as the reason between the areas under the peaks of the FTIR spectrum located at 1720 cm^{-1} and 1370 cm^{-1} (Figure 3). The resulting oxidation indexes were compared utilizing one-way ANOVA and multiple comparisons tests.

Results: For the surface, B1 presented the highest KOI, followed by A1 and the other samples. On subsurface one, A1 presented the highest index, followed by A2 and A3 and then B1 and C1. On subsurface two, only C1 stood out, with the lowest oxidation. The difference between the A samples group could be related to the unknown shelf life of the samples, while B1's value could be associated with packaging problems disclosed by the manufacturer in 2022¹. Average oxidation remained at acceptable levels for the length of implantation, between 0.21 and 0.72 for the samples. Found literature varies greatly, from very low oxidation indexes (less than 0.1) for both conventional and crosslinked inserts (SPECE *et al.*, 2019), to higher values around 1.0 for the presented length of implantation (Reinitz *et al.*, 2015). Literature on greater lengths of implantation may reach values up to 9.0 (Manescu *et al.*, 2022).

Conclusion: Although the found KOI from the samples is near the limit for expecting mechanical properties degradation, aside from punctual measurements above 1.0, the samples results are in agreement with what is reported by most contemporary literature. The high values on B1 and A1 demonstrate the importance of proper packaging and knowing or limiting maximum shelf life for such components.

Figures

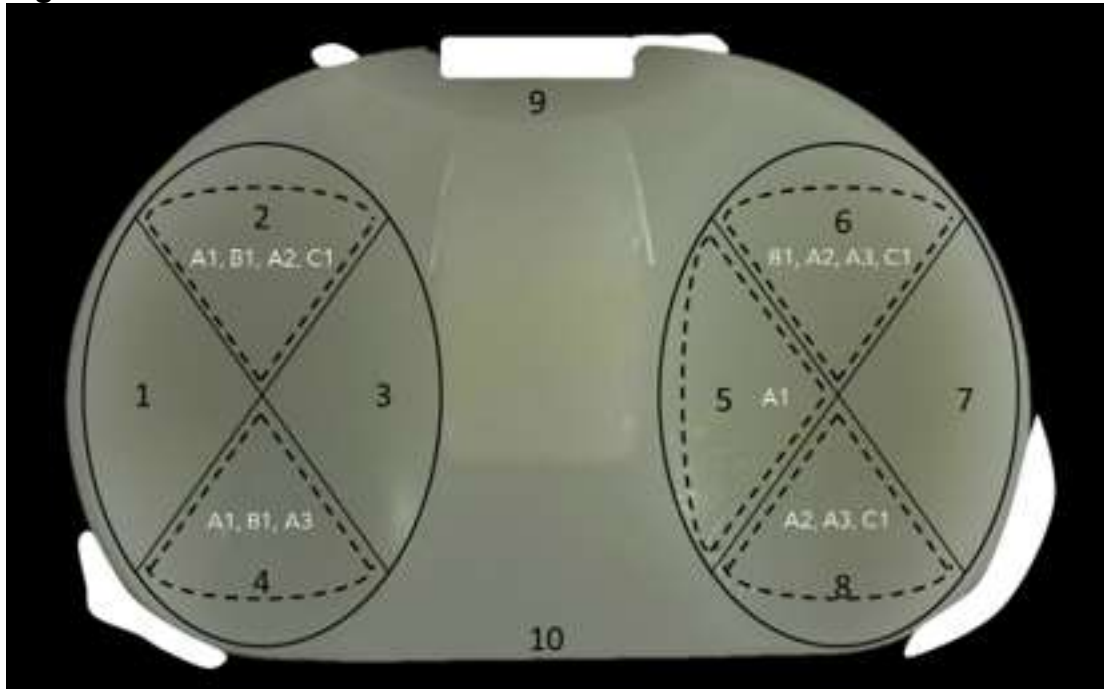


[Figure 1](#)

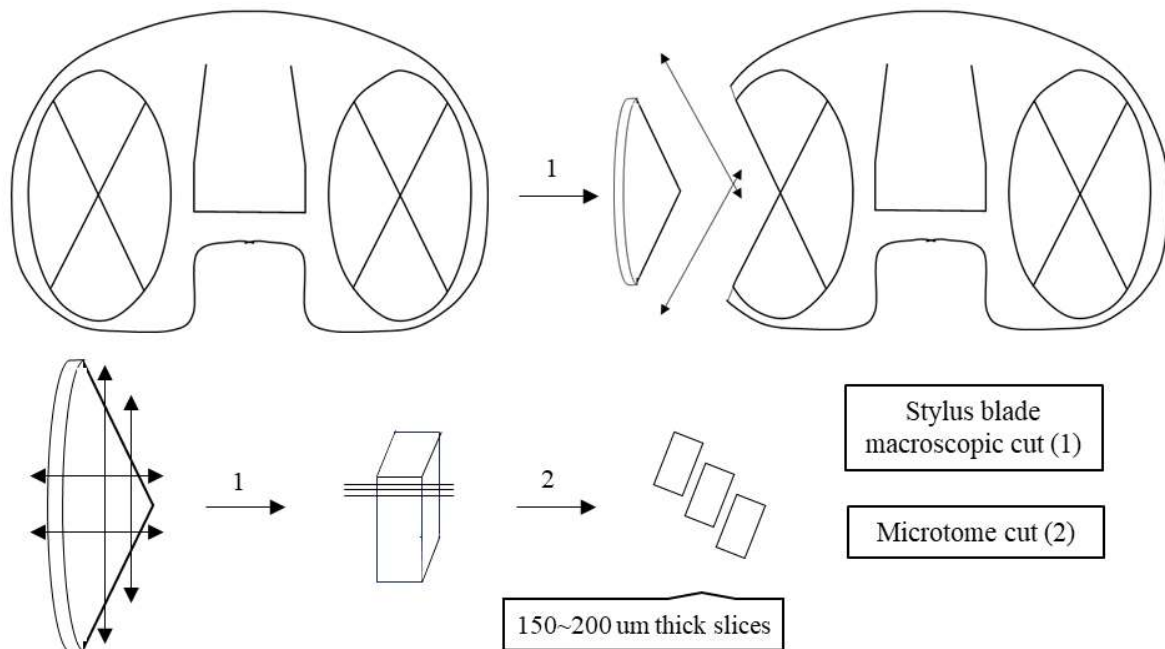


[Figure 2](#)

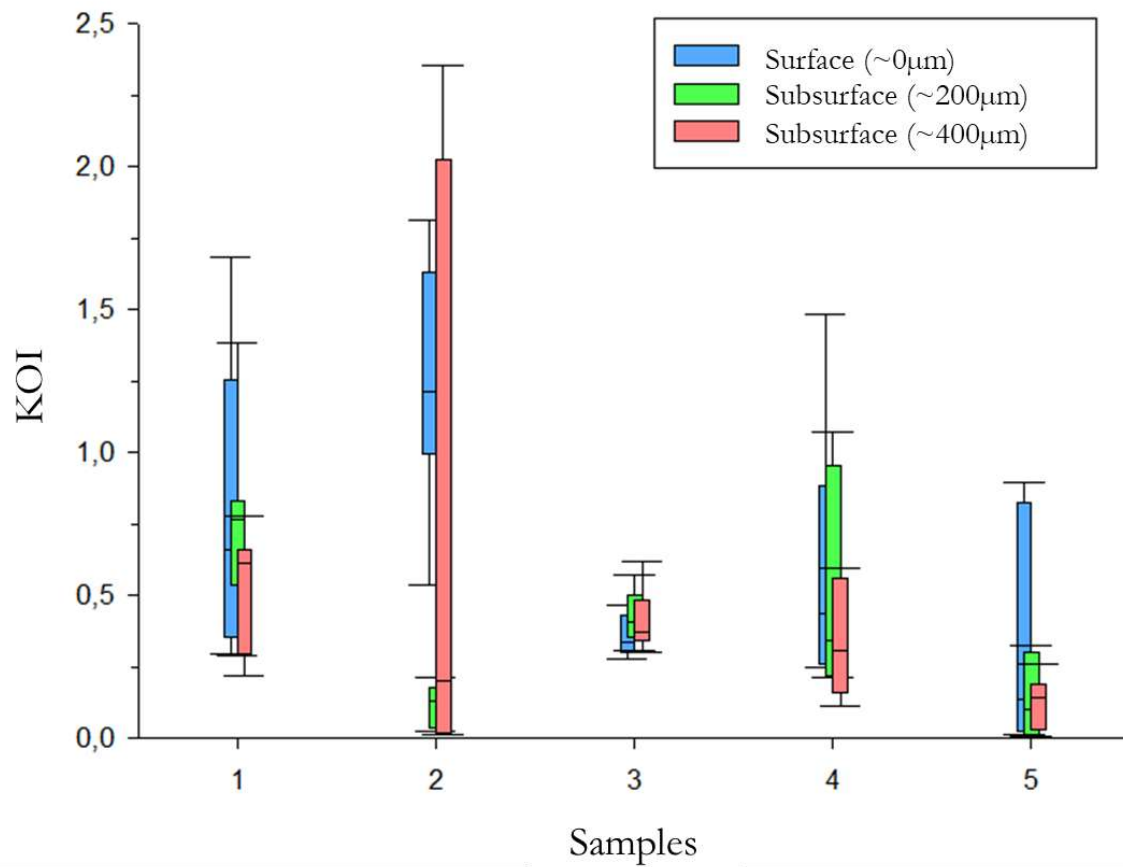


Figure 3

Comparative Analysis of Polyethylene Wear Particle Shape Generated Under Standard and Edge Loading Conditions in a Metal-on-Polyethylene Total Hip Replacement

*Amisha Desai - University of Leeds - Leeds, GB

Raelene Cowie - University of Leeds - Leeds, United Kingdom

Samantha Paterson - University of Aberdeen - Aberdeen, United Kingdom

Louise M. Jennings - University of Leeds - Leeds, United Kingdom

INTRODUCTION: Metal-on-polyethylene is the most used bearing couple in total hip replacement however, wear debris induced osteolysis, leading to aseptic loosening remains a primary indication for revision [1]. The osteolytic potential of debris may vary depending on the materials, the wear debris size and shape as well as the wear volume, which may in turn be influenced by implant positioning [2, 3]. The aim of this study was to investigate the influence of edge loading on the wear particle shapes in a metal-on-polyethylene total hip replacement.

METHODS: Six commercially available cobalt chrome heads (36mm diameter) were coupled with UHMWPE cups in a hip simulator (EM16, Simulation Solutions, UK). Three bearing couples were subjected to standard gait loading and motions (ISO 14242-1) and three were investigated under edge loading conditions with a combination of high cup inclination angle and medial-lateral translational offset (ISO 14242-4) [Table 1], using 25% (v/v) bovine serum as a lubricant. Serum samples were collected from each of the standard and edge loading bearing couples to give a total of n=4 samples for each condition. Samples underwent digestion using an acid-based method and sequential filtration through 10, 1, 0.015 micron size filters as outlined in ISO17853. A section of each filter was coated with platinum or iridium and imaged using a Scanning Electron Microscope between 700 and 90K times magnification. A minimum of 90 particles per serum sample were analysed using Mountains® 9 software. The mean aspect ratio and form factor was calculated for each experimental group. Statistical analysis to compare experimental groups was carried out using a Student's t test with significance taken at $p < 0.05$.

RESULTS: The resulting UHMWPE wear debris was a similar shape under both standard and edge loading conditions [Figure 1] with no significant difference in aspect ratio (3.43 ± 0.41 and 3.87 ± 1.26 for standard and edge loading group respectively; $p = 0.22$) or form factor (0.42 ± 0.02 and 0.43 ± 0.02 for standard and edge loading group respectively; $p = 0.91$) between experimental groups.

CONCLUSION: The present study has shown that edge loading had no effect on particle shape. This study is the first to characterise the shape of polyethylene particles generated under edge loading conditions. Future work will analyze the wear particle size distributions.

REFERENCES:

[1] <https://www.njrcentre.org.uk/njr-annual-report-2022/>

[2] Fisher et al (2000). JOEIM, 214(1), 21-37

[3] Ali, M. et al. (2017). Orthopaedic Proceedings, 99(SUPP_3), 12

Figures

Table 1: Study conditions and wear rates of UHMWPE cups

Experimental group	Test conditions			UHMWPE wear rate \pm 95% confidence limits (mm ³ /million cycles)
	Cup inclination angle (°)	Head medial-lateral translational offset	Swing phase load (N)	
Standard conditions ISO 14242-1	45	0 mm – Concentric	300	11.9 \pm 1.5
Edge loading conditions ISO 14242-4	65	4 mm	70	20.4 \pm 3.6

Figure 1

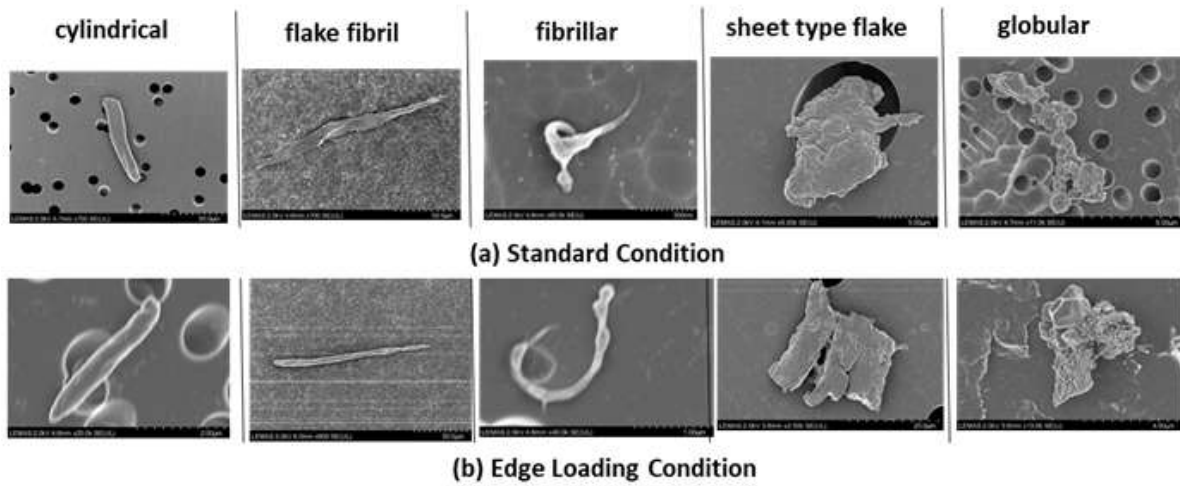


Figure 1: Typical morphologies of UHMWPE debris

Figure 2

Wear in Reverse Shoulder Arthroplasty: An in Vitro Comparative Study in Clean Conditions on Highly Cross-Linked Vitamin E UHMWPE Components in Standard and Inverted Configuration

*Andrea Fattori - Lima Corporate - Villanova Di San Daniele del Friuli, Italy

Gabriele Vidoni - LimaCorporate SpA - Villanova di San Daniele del Friuli, Italy

Thomas Ferro - Limacorporate - Villanova di San Daniele del Friuli, Italy

Michele Pressacco - LimaCorporate Spa - Villanova di San Daniele del Friuli, Italy

Introduction.

Reverse Shoulder Arthroplasty (RSA) is an effective treatment for rotator cuff deficient arthritic shoulders; indications for RSA have been recently expanded and is currently used also to treat young patients with functional cuff, with more active and longer life expectancy, which poses concerns about wear-related durability of the RSA pairs. Recently, the use of vitamin E highly cross-linked polyethylene (E-XLPE) has been introduced in the shoulder to enhance long term durability. However, especially in medialized configurations, wear due to the scapular notch (SN) might still be a concern. A possible solution is the inversion of bearing materials by using polyethylene glenospheres, with the aim to avoid reverse cup's polyethylene degradation due to notching on the scapular neck. The aim of this study is to compare wear performances of two RSA pairs in clean conditions in standard (CoCrMo glenosphere) and inverted (polyethylene glenosphere) configurations.

Methods.

As no standard was available for wear testing of RSA components, an internal protocol was defined based on available bibliographic references. Each pair was composed by CoCrMo and aged E-XLPE components of the Prima System (Enovis, US) in standard and inverted configuration, respectively a $\Phi 42$ mm CoCrMo glenosphere with a E-XLPE retentive liner and a $\Phi 44$ mm E-XLPE glenosphere with a CoCrMo liner (Fig.1). The protocol simulates cyclically circumductions at two abduction positions (Fig.2), includes edge loading and enhances potential creep and deformation that might arise in critical thinner polyethylene glenosphere's areas. Each pair was tested with minimum 4 samples for 5M cycles in clean condition.

Results.

The results of the wear test showed 29.4% less wear for the inverted configuration (Fig.3). There were no signs of deformation onto the articular surfaces of the polyethylene glenospheres or the reverse cups.

Discussion and Conclusions.

Materials inversion in RSA has shown to be effective to reduce SN in clinical practice. In this study, inverting the materials presented better wear results in clean condition, even though greater surfaces were exposed in the standard configuration (retentive liner). The tests did not simulate impingement of the reverse liner with bone, which has been shown to induce a significant amount of wear in explanted polyethylene reverse cups and to be associated with SN phenomena. For this reason, inversion of materials in RSA can provide an advantage in terms of polyethylene wear and durability; additionally, having a metal reverse cup allows for enhancing its design by allowing lower minimum thickness within its articular surface.

Figures



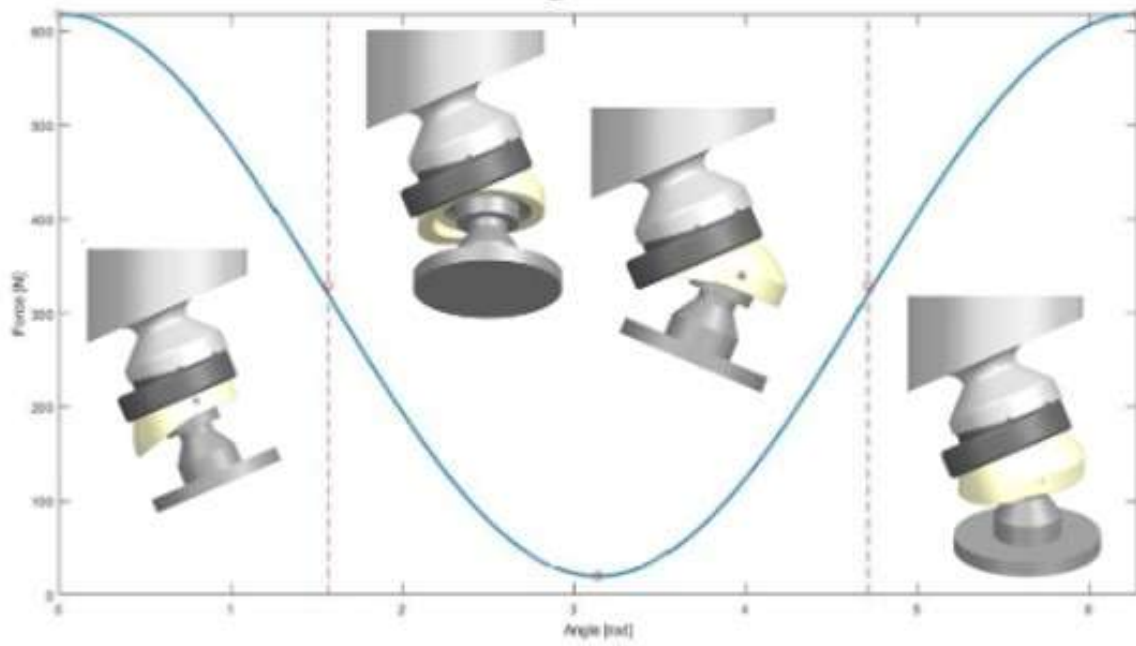
Configuration		Reverse liner	Glenosphere
Inverted		Ø44 Long Lateralized <u>CoCrMo</u>	Ø44 Concentric <u>LimaVit</u>
Standard		Ø42 Short 0°, Retentive - <u>LimaVit</u>	Ø42 Concentric - <u>CoCrMo</u>

Fig.1: Tested components

[Figure 1](#)

Test Configuration A



Test Configuration B

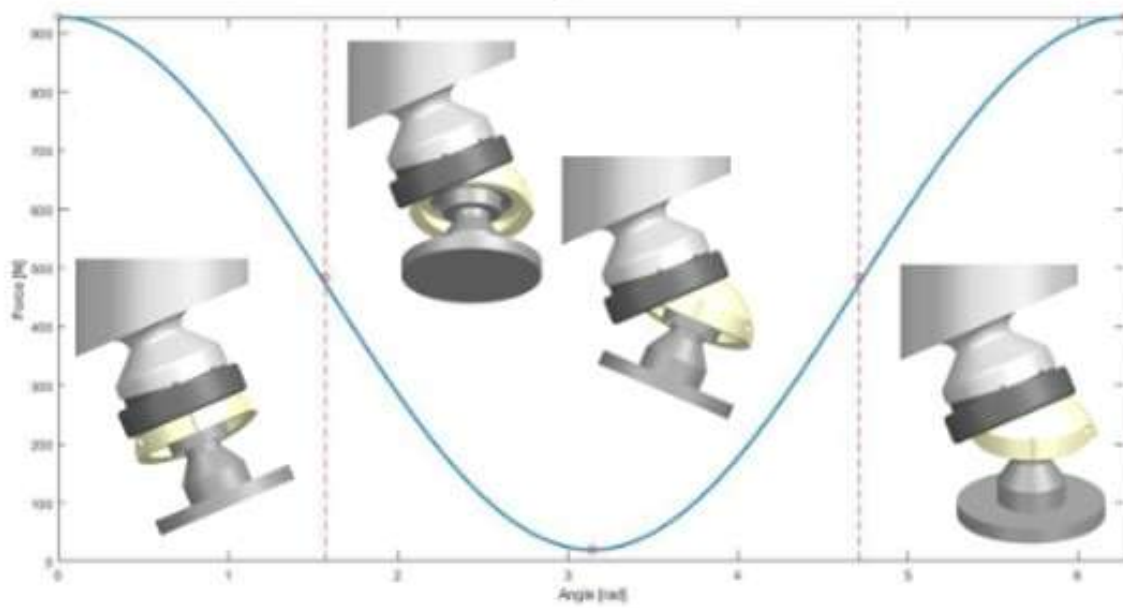


Fig.2: Wear setup and cycles

[Figure 2](#)



Fig.3 Results

[Figure 3](#)

Influence of EDTA on Friction and Its Effectiveness to Reduce Solid Precipitation on Lubricants Used in Arthroplasty Wear Testing

Alexander Eischeid - University of Nebraska Medical Center - USA

Mercedes Renken - UNMC - Omaha, USA

Joel Weisenburger - The University of Nebraska Medical Center - Omaha, USA

*Hani Haider - UNMC - Omaha, USA

Diluted bovine calf serum is used as a standard lubricant simulant in wear-testing of arthroplasty implants. ASTM and ISO standard wear testing methods (e.g. F732-17) allow some additives to serum to reduce solid-precipitation and microbial-growth. Ethylenediaminetetraacetic acid (EDTA) is commonly used as an additive in many labs, but it is not standardized. With wear testing “coming of age,” it was time to clearly evaluate the influence of EDTA on serum lubricants. Can it potentially add a confounding variable to the implant wear results from different labs, by adding or reducing friction?

In this study, we measured friction coefficients of lubricants with varying EDTA concentrations and assessed EDTA’s effectiveness in serum preservation. We used a custom in-house-built pin-on-disk friction-measuring machine, which could cover a wide range of compressive stresses (up to 20 MPa) but unique in using near-frictionless air-bearings to isolate/measure tiny friction coefficients (0.03-0.09) of arthroplasty material couples. Like other tribometers, the test machine load cells continuously measured and logged frictional and compressive forces between a loaded pin against a rotating disk. We used 6 mm diameter cylindrical GUR-1020 ultra-high molecular weight polyethylene (UHMWPE) pins. These articulated against 35 mm diameter, 12.7 mm thick, cobalt-chrome alloy (CoCr) disks polished to an orthopaedic grade finish ($R_a < 0.05 \mu\text{m}$). Nine human synovial fluid samples and a mixed blend of all nine samples from separate (IRB approved) patients undergoing joint replacement surgery were tested to provide extra base-level “controls” for friction coefficients for comparison. In the bovine serum tests, the lubricant was diluted with deionized water to protein contents of 20 and 30 g/L, with varying EDTA concentrations (0 to 10 g/L). Friction testing was conducted at 5 and 10 MPa stress levels representative of medium knee and high hip physiological stresses respectively, at 25 mm/s articulation speed. We assessed the effectiveness of EDTA for serum preservation over 21 days by measuring the mass of resulting precipitation separated through centrifugation of 1 mL aliquots of agitated liquid.

Adding EDTA resulted in a 68.8% decrease in serum precipitate formation after 21 days ($p < 0.01$), so its addition was functionally effective. The friction of the serum lubricant without EDTA was more or less on par to that of human synovial fluid, with some exception, as the higher stress produced slightly less friction in serum (Fig. 1). Adding EDTA to the serum and increasing its concentration increased the friction coefficient, plateauing at 25% higher coefficient when the EDTA concentration reached 7.45 g/L (ASTM F732-17) (Fig. 2). This increase of friction with EDTA did not vary with time (Fig. 3). At 10MPa stress, adding EDTA at 7.45 g/L brought the friction coefficient of diluted serum closer to that of human synovial fluid.

All in all, adding EDTA was verified to reduce solid precipitants in a wear testing diluted serum lubricant, and if anything, provided for nominal harshness and not lenience regarding friction of metal-on-UHMWPE.

Figures

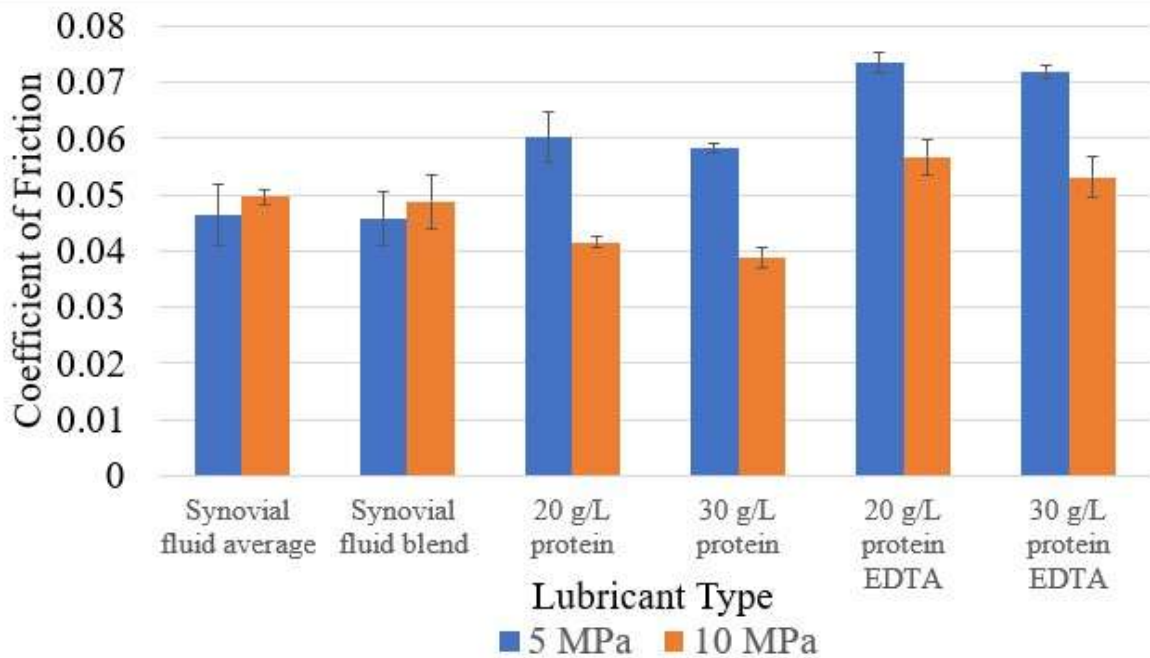


Fig. 1: Variation of coefficient of friction with lubricant type at two stress levels. (EDTA concentration was 7.45 g/L per ASTM F732.) (Standard dev. bars shown.)

Figure 1

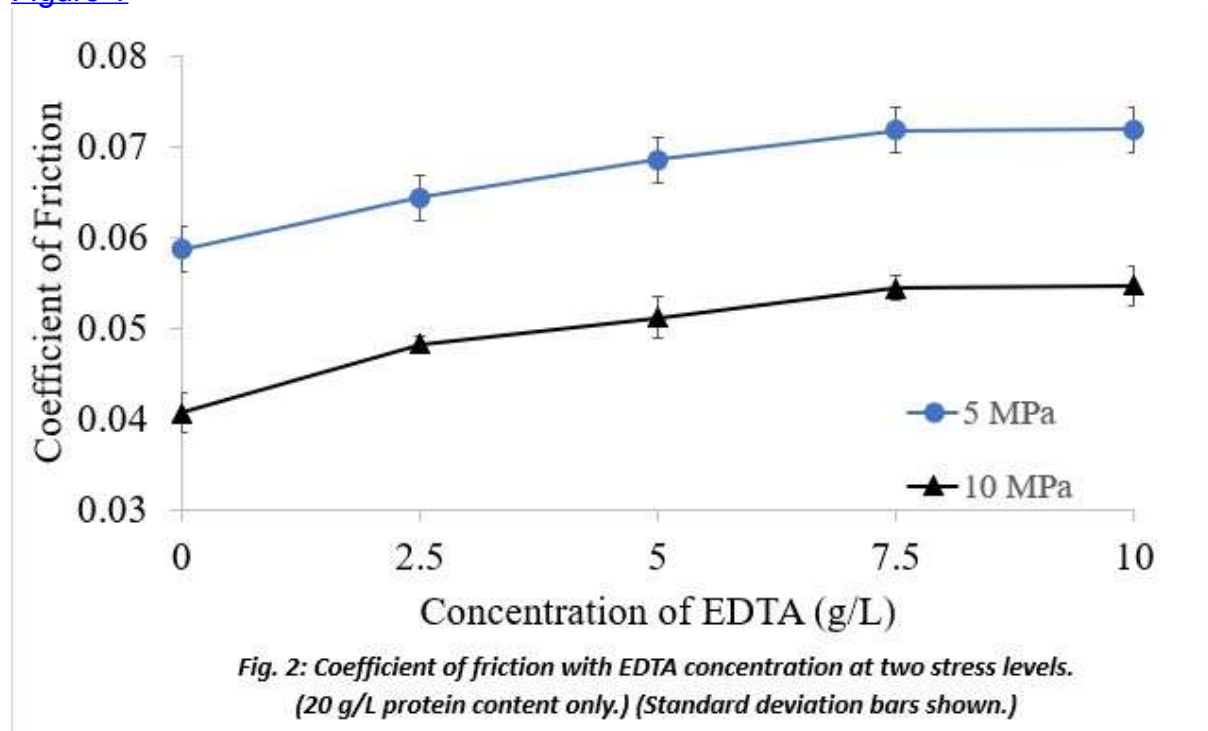


Fig. 2: Coefficient of friction with EDTA concentration at two stress levels. (20 g/L protein content only.) (Standard deviation bars shown.)

Figure2

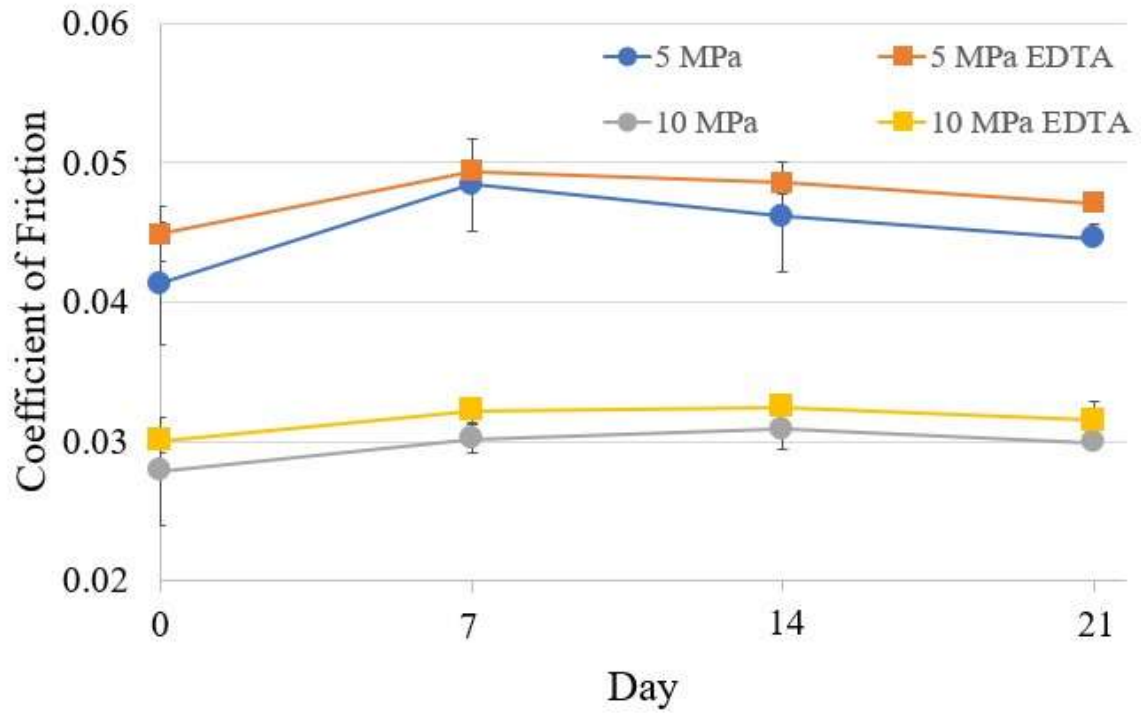


Fig. 3: Coefficient of friction of 20 g/L protein concentration bovine calf serum without and with EDTA (7.45 g/L) over a time period of three weeks. (Standard deviation bars shown.)

[Figure 3](#)

Delamination and Oxidation in Exactech Patellar Components: To Revise or Not to Revise

*Aarti Shenoy - Hospital for Special Surgery - New York, USA

Peter Hsiue - Hospital for Special Surgery - New York, United States of America

Elexis Baral - Hospital for Special Surgery - New York, USA

Geoffrey H Westrich - Hospital for Special Surgery - New York, USA

Thomas Sculco - Hospital for Special Services - New York, USA

Douglas E Padgett - Hospital for Special Surgery - New York, USA

Timothy Wright - Hospital for Special Surgery - New York, USA

Introduction: A recall is in effect since 2022 for ultra-high molecular weight polyethylene (UHMWPE) tibial components manufactured by Exactech Inc. due to early onset oxidation-related wear and resulting osteolysis caused by packaging issues [1]. The recall does not include the patellar components manufactured from the same polyethylene material. Surgical observations within our institute suggest there might be similar levels of wear and articular damage in these components as seen in tibial inserts. This study aims to investigate patellar component damage by visually assessing articular surface damage in retrieved components and measuring oxidation using a novel spectroscopy method as an assessment of mechanical deterioration.

Methods: 62 patellar components revised between 2017-2023 were identified from our IRB-approved institutional implant retrieval system. Each component was divided into four zones oriented along superior-inferior and medial-lateral axes. Two independent observers visually graded each component for presence and severity of damage modes (scratching, pitting, surface deformation, burnishing, delamination, abrasion, embedded debris, scale 1-4) in each zone based on the Hood scoring method for polyethylene components [2]. Average damage scores are reported across all damage zones for each component. Oxidation indices (OI) for 30/62 patellar components will be obtained using Optical Photothermal Infrared (O-PTIR) spectroscopy. O-PTIR results will be validated with results obtained by standard Fourier-transformed infrared (FTIR) spectroscopy oxidation analysis. Spearman's correlations will be used to assess statistical relationships between patient demographics and OI, and between damage scores and OI.

Results: The most prevalent damage mode across all 62 patellar components was burnishing and surface deformation (Figure 1), most prevalent in the medial and lateral zones in all components. Delamination was observed to some extent in 59/62 (95.16%) components. Average delamination score was 5.69 ± 2.01 across all four zones, distributed uniformly across all four zones. Preliminary O-PTIR results (n=1) show an oxidation index (OI) of 3.1 at undamaged articular surface and an OI of 5 at a delaminated region on the same component (Figure 2).

Conclusion: Revised Exactech patellar components appear to demonstrate delamination damage associated with accelerated oxidation based on visual assessment. Previous studies have established an OI > 3 is indicative of mechanical deterioration of UHMWPE [3]. Further investigation of oxidation index in these patellar components, particularly on visibly undamaged regions, is imperative before clinical recommendations can be made regarding patellar component revision in these cases.

References:

[1] FDA website. *Recalls of Medical Devices database* (updated 01/13/2024). accessed on 01/15/2024

[2] Hood R.W. et al. *J Biomed Mater Res* 1983; 17: pp. 5

[3] Currier B.H. et al. *J Arthroplasty* 2007; 22: pp. 721-731

Figures

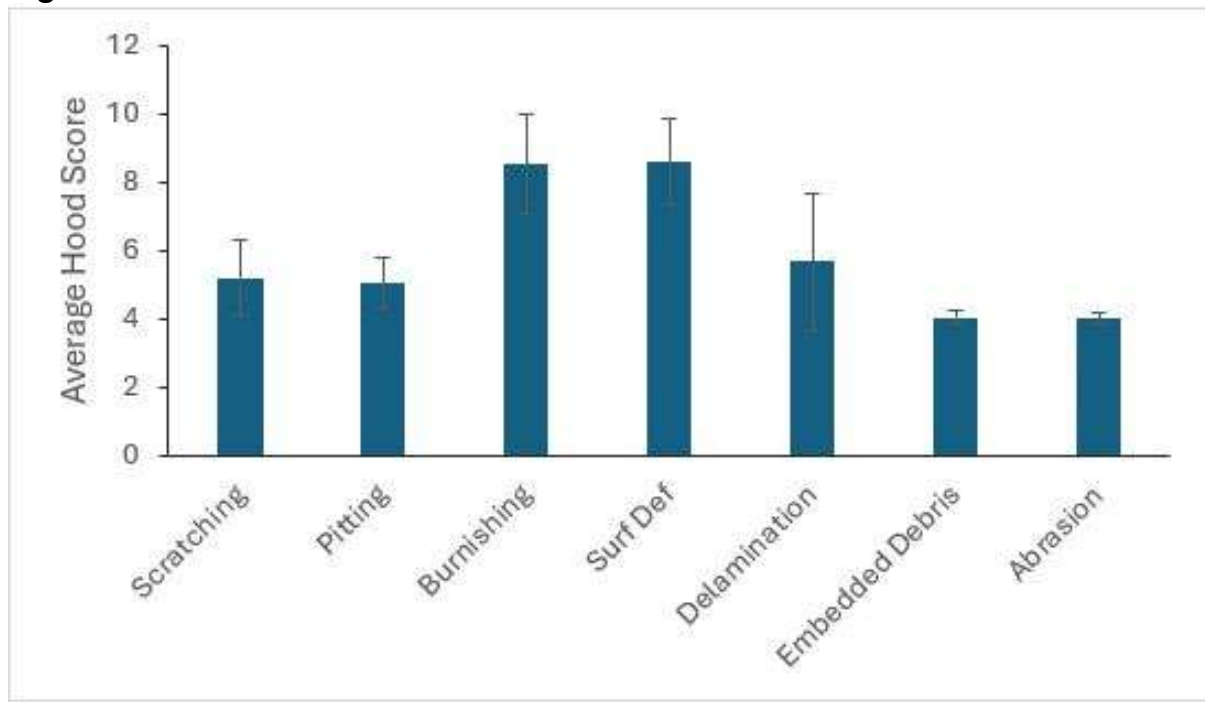
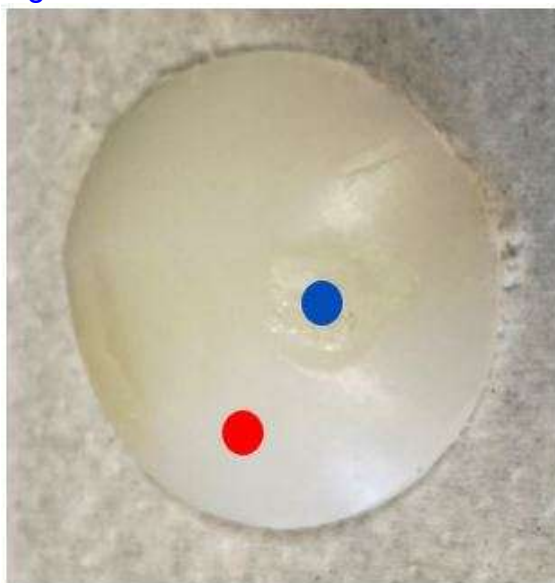


[Figure 1](#)



Oxidation index (OI)

1744/1370 ratio

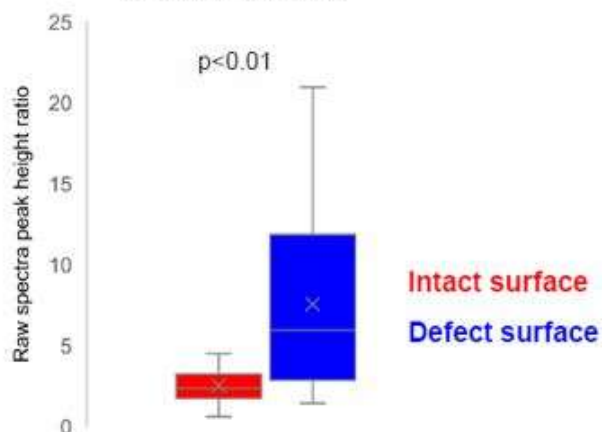


[Figure 2](#)

Electrosurgery Induced Subsurface Damage and Hardness Changes of Ti-6Al-4V Implant Alloy

Mohsen Karshenas - Clemson University - Charleston, United States of America

*Jeremy Gilbert - Clemson University - Charleston, USA

Peter Kurtz - Clemson University - Charleston, USA

Introduction: Electrocautery is frequently used in orthopedic surgeries. However, its proximity to metal implants can cause electrical arcing, resulting in high-temperature phenomena such as oxidation, residual stress generation, cracking, and melting [1]. This can reduce fatigue strength of the Ti-6Al-4V femoral stem [2].

Our research questions are: (1) How does electrocautery damage (ECD) alter the implant alloy microstructure underneath the damage? (2) How does ECD affect hardness? We hypothesize that the heat-affected zone (HAZ) underneath the surface damage experiences microstructural changes and has high hardness that varies with depth.

Methods: ECD was induced on a Ti-6Al-4V disk in monopolar cutting mode at multiple sites (n=6) using an output power range of 150 Watts for 2s with a CONMED System 2450 electro-surgical generator (Utica, NY). The ECD sites were sectioned through the middle of the damaged areas using a low-speed diamond cutting wheel (Beuhler, Isomet). Digital optical microscopy (DOM), scanning electron microscopy and energy dispersive spectroscopy (SEM/EDS) of the alloy was performed. Hardness tests were performed using a 17 mm instrumented diamond tip at a constant load (78 mN) which imparted scratches as a function of depth (n=9 / location). The diameter of the scratch defined a spherical contact area which was divided into the load to obtain the hardness (in GPa). Statistical analysis of hardness versus depth into the surface was performed using ANOVA methods ($p < 0.05$), correlating the observed damage characteristics with hardness variations.

Results: The cross-sectioned damage observed on the Ti-6Al-4V alloy (Fig. 1A) shows molten resolidified particles (top), and cracks (Fig. 1B). SEM/EDS analysis (Fig. 2) showed oxidation layers, transferred silicon and iron, and intermixing of alloying elements. Further into the alloy, up to 300 μm or more, there is a heat-affected zone (HAZ) where rapid heating and cooling induces phase transformations, including the formation of a needle-shaped martensite microstructure (α') in the primary α grain (Figs. 1B and 2). Hardness tests (Fig. 3) indicated statistically significant changes ($p < 0.05$) in the hardness in the HAZ from 3 GPa to 9 GPa, penetrating 250 to 300 μm into the depth, potentially decreasing fatigue strength.

Conclusion: Electrocautery-induced damage during orthopedic surgeries includes surface oxidation, local melting, intermixing, and cracking. The generated heating energy also causes microstructural alterations in the near-surface zones, such as melt and heat-affected zones (HAZ) into the depth. A melted/oxidized and intermixed layer on the top, and a needle-shaped martensite microstructure with high hardness properties down to 200 μm were observed. These changes can render the surface susceptible to initiating fatigue cracks, confirming our hypotheses. However, further research is needed to fully understand the extent of microstructural alterations and their implications.

References: 1. Gilbert et al, J Arthroplasty, 2017. 2. Zobel et al. , 2. Aepli et al, J Bone & Joint Surgery, 2019.

Figures

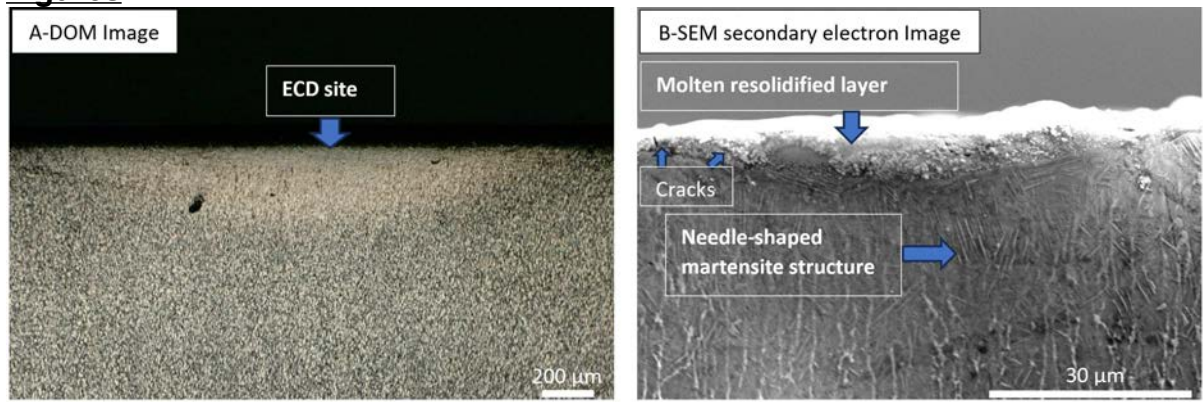


[Figure 1](#)

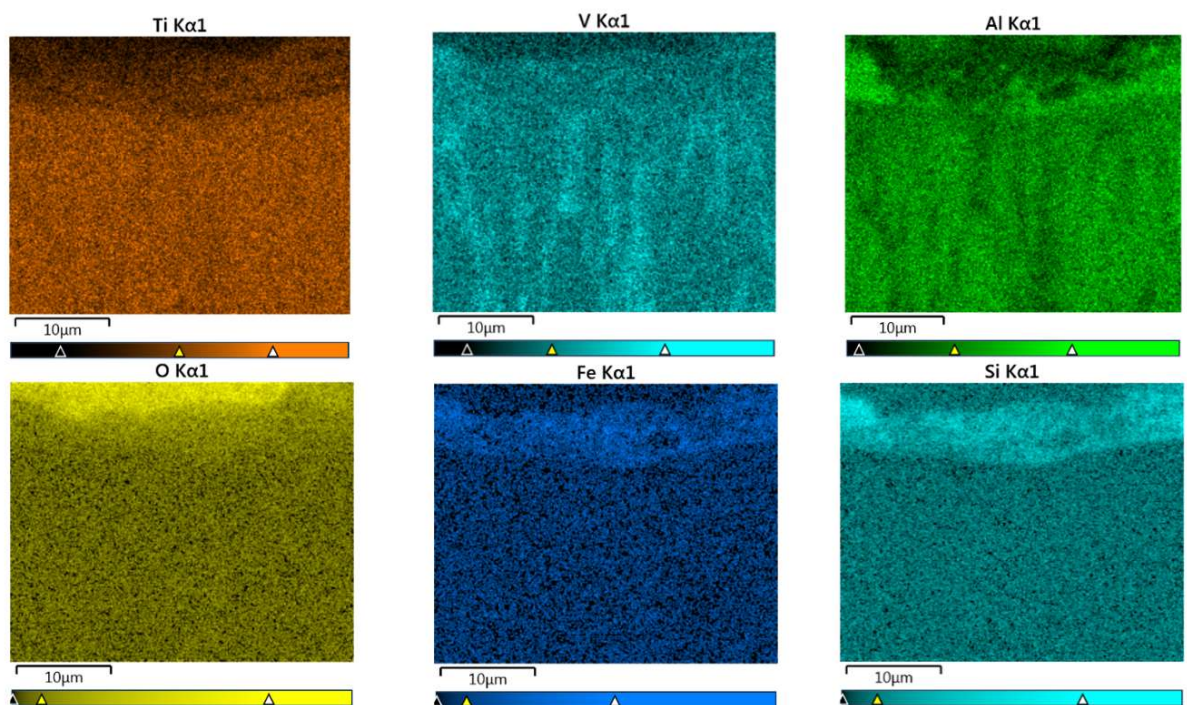
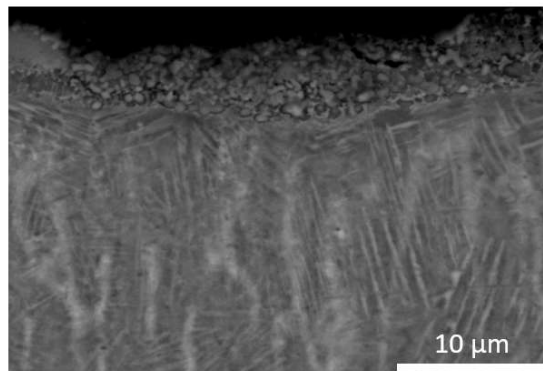


[Figure 2](#)

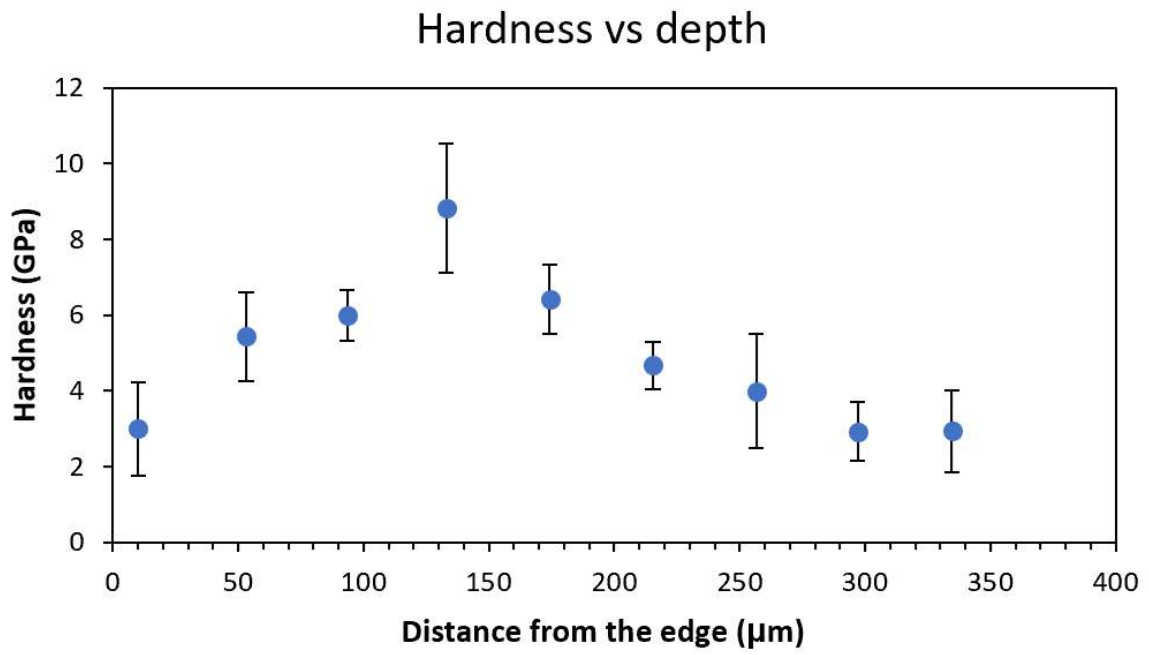


[Figure 3](#)

Effects of Adverse Loading on Metal on Polymer Total Hip Replacements

*Ben Clegg - Luleå University of Technology - Luleå, Sweden

Nazanin Emami - Luleå University of Technology - Luleå, Sweden

Samuel Perry - University of Leeds - Leeds, GB

Richard Hall - University of Leeds - Leeds, United Kingdom

Michael Bryant - University of Leeds - Leeds, United Kingdom

Andrew Robert Beadling - University of Leeds - Leeds, United Kingdom

INTRODUCTION: Preclinical wear examinations using ISO-14242 [1] are regularly conducted to assess the wear performance of total hip replacements (THR), including adverse conditions specified by ISO-14242-Part 4 that enact micro separation and edge loading. This mechanism is generally seen to increase wear behaviour on hard-on-hard (HoH) bearings [2], whereas hard-on-soft (HoS) such as metal on polymer and/or ceramic on polymer (MoP & CoP) [3] have reduced wear in these 'adverse' conditions. These assessments rely on basic wave forms that may not fully capture the wide range of in vivo loading conditions encountered across varied patient activities. This study aims to compare the effects of clinically representative gait profiles on the wear rates of MoP hip replacement bearings.

MATERIALS & METHOD: Ø32mm HC CoCrMo (Aesculap, Germany) femoral heads were articulated against moderately crosslinked (50kGy) polyethylene acetabular liners (Aesculap, Germany) (n=3) on electromechanical hip simulators (ProSim, SIMSOL, UK), capable of applying beyond ISO-standard patient derived activities of daily living. The components were fixtured and mounted on the simulator and lubricated with Bovine Calf Serum (BCS) diluted to a protein concentration of 30g/L, as per ISO 14242-1 [3].

The devices were subjected to 2-Mcycles of standard ISO-14242-1 [1] walking kinematics and loading to enact a running in period. Subsequently 1-Mcycle of patient derived jogging was applied, followed by a 1-Mcycles of a jogging profile under a stop-dwell-start configuration. These profiles were derived from motion capture of THR patients, resolved via multi-body musculoskeletal model (AnyBody Technology) to calculate the rotations and contact forces [4]. Frictional forces at the bearing were resolved via a six-axis load cell fitted to the simulator, and cumulative wear was assessed gravimetrically every 0.5-Mcycles.

RESULTS: Figure 1 shows the volumetric wear and cumulative wear loss for the acetabular cups during the course of the experiment. The introduction of jogging leads to a two-fold increase in the wear volume, from approximately 15 /Mcycle under ISO walking, to just below 30 /Mcycle. There was no significant change in wear volumes with the addition of a dwell period to the jog, similar to results of Hadley et al. [5] adding a dwell period to an ISO gait.

CONCLUSIONS: The performance of a MoP bearing was assessed under 'daily living' loading regimes showing an increase in wear volume. With ISO-Part4 reducing overall wear in MoP bearings, this study shows that physiologically relevant profiles applied to hip simulator testing would aid pre-clinical testing to more accurately represent the effects of daily living within THR patients.

Figure 1: Mean volumetric and cumulative wear (mm³) comparison of ISO and Jogging profiles.

[1] O. O'Dwyer Lancaster-Jones *et al.*, 2018.

[2] J. J. Halma *et al.*, 2014.

[3] BS ISO, 14242-1:2014.

- [4] D. E. Lunn *et al.*, 2020.
- [5] M. Hadley *et al.*, 2018.

Figures

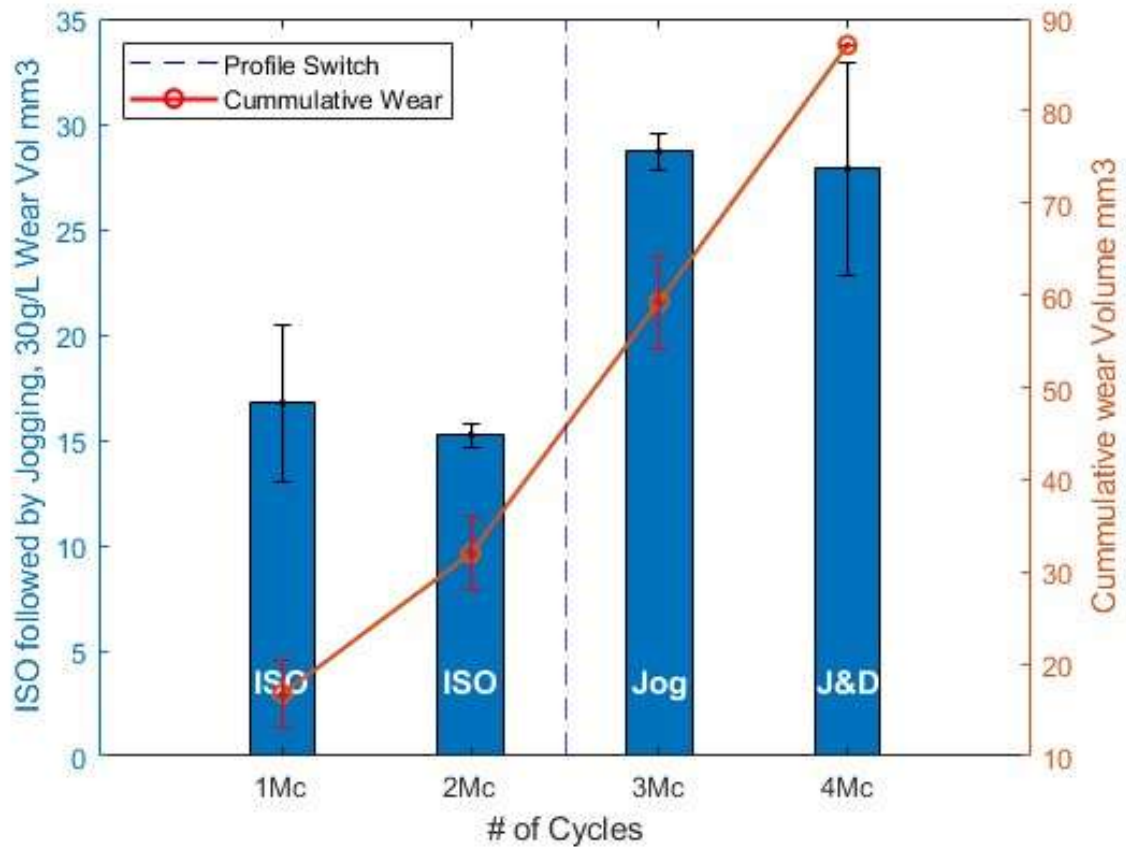


Figure 1

Morphological and Mechanical Properties of a Dual Layered Porous Plasma Spray Coating

*Aline Elquist - Smith and Nephew - Memphis, United States of America

Patrick Steiger - Smith and Nephew - Aarau, Switzerland

Marc Taylor - Smith & Nephew - Memphis, USA

INTRODUCTION: Dual layer porous plasma sprayed titanium and hydroxyapatite (PPS-Ti/HA) coatings provide a structure for biological fixation on implant devices. Many factors can influence the fixation of a device including porosity of the coating, pore size, coating thickness, and surface roughness. A thicker coating can improve press-fit and allow for increased bone ingrowth, however; impact on mechanical properties is also a consideration. The purpose of this study was to assess properties of a clinically successful coating with increased thickness.

METHODS: A PPS-Ti/HA dual layer coating was sprayed (Vacuum Plasma Spray) with the same parameters as the clinically successful coating used on the POLARSTEM™ implant with over 20 years of clinical history [1]; however, the thickness of the porous titanium layer was approximately doubled. The morphological properties of both porous coatings were characterized on three devices per ASTM F1854 [2] and compared using students t-test ($\alpha < 0.05$). Morphological properties compared include porosity, pore size measured by mean void intercept length (MVIL), HA coating thickness, and average surface roughness (Ra). The mechanical properties were characterized on coupons per ASTM standards F1147 [3] (tensile attachment strength (TAS), n=25), F1044 [4] (static shear, n=30 POLARSTEM™ coupons and n=11 increased thickness), and F1160 [5] (shear fatigue, n=5).

RESULTS: There was no statistically significant difference for porosity, pore size, average surface roughness, and static shear. The 3 μm difference in mean HA thickness observed between the two coatings was statistically significant, but not clinically meaningful. Both coatings were well above the FDA guidance of 22 and 20 MPa for TAS and static shear, respectively [6]. Both coatings ran-out at 10 MPa for 10 million cycles for shear fatigue. Values are plotted in Figure 1. Cross-sectional images of coatings are included in Figure 3.

CONCLUSION: Both coatings displayed similar morphology, high mechanical strength, and optimal HA coating thickness [7]. Due to the nature of pore size and porosity measurements per ASTM F1854, measurements on thinner PPS-Ti coatings may be disproportionally impacted by surface roughness (i.e., values may skew higher due to subtleties in measurement methodology). These results suggest that the thicker coating performs just as well, if not better than, the POLARSTEM™ coating clinically.

REFERENCES: [1] Fiquet, A., Noyer, D. "Polarsystem" Dual Mobility Hip Prosthesis and "Minimally Invasive Surgery" (MIS), <https://doi.org/10.1007/s11610-006-0004-4>. [2] ASTM F1854-15. [3] ASTM F1147-05R17E01. [4] ASTM F1044-05. [5] ASTM 1160-14 e1. [6] FDA Guidance Document, ID: FDA-2020-D-0957-0127. [7] Botterill, J., Khatkar, H., The Role of Hydroxyapatite Coating in Joint-Replacement Surgery – Key Considerations, [J Clin Orthop Trauma](#). 2022 Apr 22;29:101874.

Figures

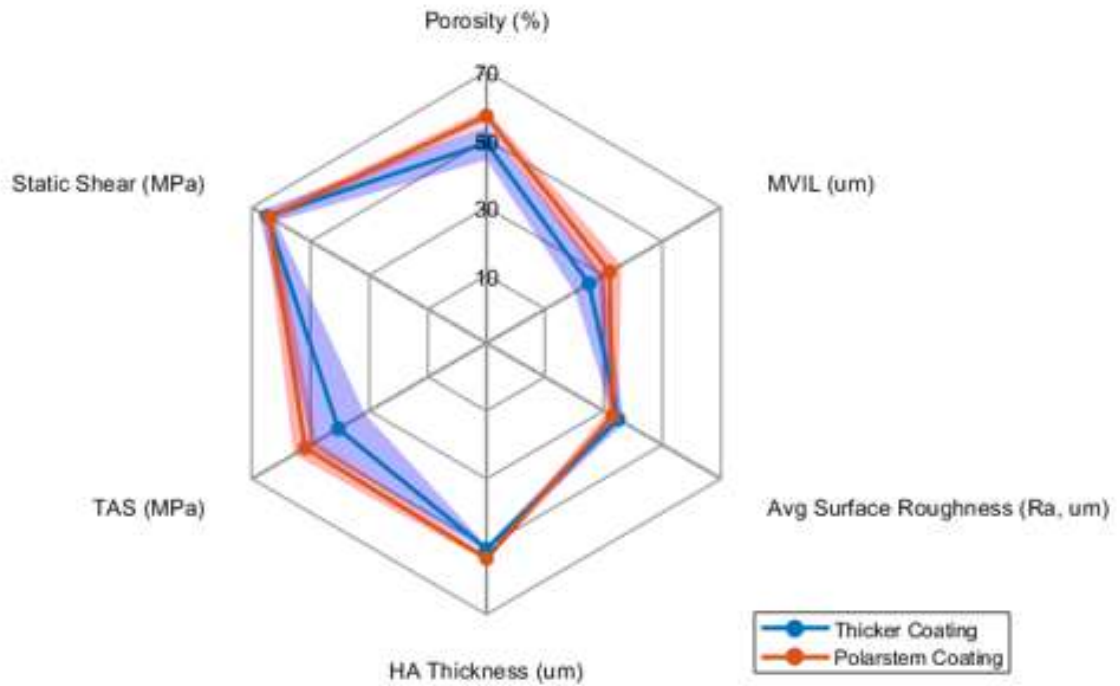


Figure 1: Plot of values measured to characterize coatings. Shaded areas represent standard deviation.

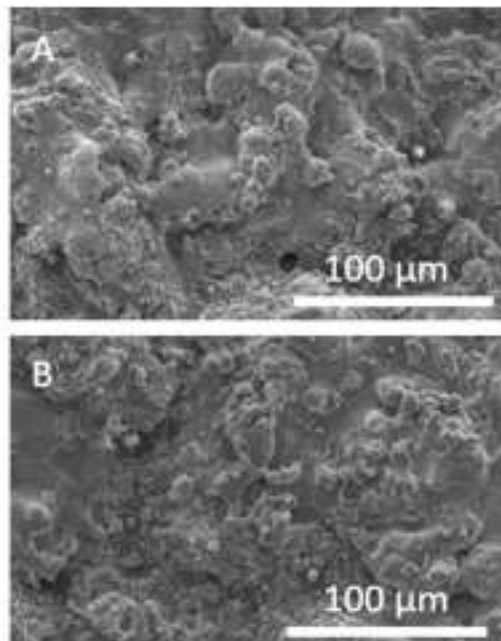


Figure 2: Surface images of (A) the POLARSTEM™ coating and (B) the coating with increased PPS-Ti

[Figure 1](#)
[Figure2](#)

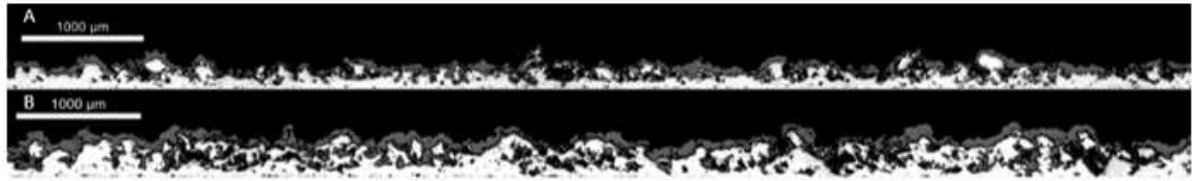


Figure 3: Cross-sectional images of (A) the POLARSTEM™ coating and (B) the coating with increased PPS-Ti thickness. High contrast (white) – PPS-Ti, lower contrast (grey) – HA top coating

[Figure 3](#)

The Iatrogenic Bone Trauma and Soft Tissue Injury (BOSTI) Classification System: A Prospective Cohort Study Comparing Robotic-Arm Assisted Versus Conventional Total Hip Arthroplasty

*Mohammed Wazir - University College London University Hospitals - London, United Kingdom

Fabio Mancino - University College London Hospitals NHS Foundation Trust - London, United Kingdom

Fares Haddad - University College London Hospital - London, United Kingdom

Babar Kayani - University College Hospital London - London, United Kingdom

Introduction:

The primary objective of this study was to develop a validated classification system for assessing iatrogenic bone trauma and soft tissue injury during total hip arthroplasty (THA). The secondary objective was to compare macroscopic bone trauma and soft tissue injury in conventional THA (CO THA) versus robotic-arm assisted THA (RO THA) using this classification system.

Methods:

This study included 30 CO THAs versus 30 RO THA performed by a single surgeon. Intraoperative photographs of the osseous acetabulum and periacetabular soft tissues were obtained prior to implantation of the acetabular component. The intraoperative photographs were used to develop the proposed classification system. Interobserver and intraobserver variability of the proposed classification system were assessed.

Results:

The iatrogenic bone trauma and soft tissue injury (BOSTI) classification system provides a score between 28-100 points that summates bone trauma scores from the four acetabular quadrants and periacetabular muscle damage. The classification system had an interclass correlation coefficient of 0.90 (95% CI: 0.86-0.93) for interobserver agreement and 0.89 (95% CI: 0.84-0.93) for intraobserver agreement. RO THA was associated with improved BOSTI scores ($p=0.004$) and more pristine acetabular surfaces in the superior anterior ($p=0.001$) and superior posterior quadrants ($p<0.001$) of the acetabulum compared with CO THA. RO THA had a non-statistically significant trend towards reduced muscle injury to the gluteus maximus ($P=0.52$); gluteus medius ($p=0.78$) obturator internus ($P=0.56$); piriformis ($P=0.42$); superior gemellus ($P=0.23$); inferior gemellus ($P=0.78$); quadratus femoris ($P=0.12$), and vastus lateralis ($P=0.41$) compared with CO THA.

Discussion:

The proposed BOSTI classification is a reproducible grading system for stratifying iatrogenic bone trauma and soft tissue injury during THA. Patients undergoing RO THA had improved BOSTI scores and reduced acetabular bone trauma compared with CO THA. Furthermore, RO THA was associated with reduced periacetabular muscle injury compared with CO THA, although this did not reach statistical significance.

Size-Up, Size-Down: Accuracy of Component Sizing With Computerized Tomography & Robotic-Assisted Total Knee Arthroplasty

*James Henry - Northwell Health, Huntington Hospital - Huntington, USA

Brienne Paradis - 3. University of New England College of Osteopathic Medicine - Biddeford, USA

Alekasandra Qilleri - 6. Donald & Barbara Zucker School of Medicine - Hempstead, USA

Nadia Baichoo - Orlin & Cohen Orthopaedic Group - Rockville Center, USA

Keith R. Reinhardt - Northwell Health, South Shore University Hospital - Bay Shore, USA

James Slover - Northwell Health, Lenox Hill Hospital - New York City, USA

Jonathan R. Danoff - Northwell Health, Northshore University Hospital - Manhasset, USA

James Germano - Orlin and Cohen Orthopedic Group - New York, USA

Background: Templating prior to total knee arthroplasty (TKA) can help to improve surgical efficiency and potentially improve alignment and outcomes. The purpose of this paper is to evaluate the ability of CT-based preoperative templating to accurately predict implant sizes.

Methods: 724 Stryker MAKO robotically assisted total knee arthroplasty cases were retrospectively evaluated from a prospectively collected database between January 2020 to October 2023. Cases were performed by one of three arthroplasty fellowship trained orthopaedic surgeons from a health system that includes an academic level one trauma center, ambulatory surgery center, and community hospital. 391 out of the 724 cases were preoperatively templated independently by the surgeon and the company representative (MPS). The remaining 333 cases were only templated prior to incision by the MPS. Final implant size of the tibial and femoral components were compared to preoperative templates.

Results: The MPS was able to preoperatively predict final tibial and femoral implants within one size in 97.4% and 97.9% of cases, respectively. A surgeon and MPS combined preoperative templating increased accuracy to predict final tibial and femoral implants within one size in 98.9% and 99.5% of cases, respectively. Height and weight were positively correlated with final implant size ($p < 0.001$).

Conclusion: Non-surgeons can reliably predict implanted components in CT-base preoperative templating in the majority of cases, which is further enhanced by surgeon review and adjustments. In no cases in our series were the final size components implanted greater than two sizes larger or smaller. Our findings suggest there is opportunity to avoid waste by processing fewer trial implants and transporting fewer components. This would likely decrease overall case cost and improve efficiency in the operating room.

High in-Vivo Accuracy of a Novel Robotic-Arm-Assisted System for Total Knee Arthroplasty: A Retrospective Cohort Study

*Faseeh Zaidi - University of Auckland - Auckland, New Zealand

Michael Goplen - University of Alberta - Edmonton, Canada

Connor Fitz-Gerald - Auckland City Hospital - Auckland, New Zealand

Scott Bolam - University of Auckland - Auckland, New Zealand

Michael M Hanlon - Auckland City Hospital - Auckland, New Zealand

Jacob T Munro - University of Auckland - Auckland, New Zealand

Andrew Paul Monk - University of Auckland - Auckland, New Zealand

Introduction: Recent technological advancements have led to the introduction of robotic-assisted total knee arthroplasty (TKA) to improve the accuracy and precision of bony resections and implant position. However, the *in vivo* accuracy is not widely reported. The primary objective of this study is to determine the accuracy and precision of a cut-block positioning robotic arm.

Methods: This was a retrospective cohort study of adult patients who underwent primary TKA with various workflows and alignment targets by three arthroplasty-trained surgeons with previous experience using the ROSA® Knee System (Zimmer Biomet, Montreal, Quebec, Canada). Accuracy and precision were determined by measuring the difference between various workflow time-points, including the final pre-operative plan, validated resection angle, and post-operative radiographs. The mean difference between the measurements determined accuracy, and the standard deviation represented precision. Post-operative complications were recorded at 3-months follow-up.

Results: A total of 77 patients were included in the final analyses. The accuracy and precision for all angles comparing the final planned resection and validated resection angles was $0.90^\circ \pm 0.76^\circ$. The proportion within 3° ranged from 97.9% to 100%. The accuracy and precision for all angles comparing the final intra-operative plan and post-operative radiographs was $1.53 \pm 1.07^\circ$. The proportion of patients within 3° was 93.2%, 95.3%, 97.3%, and 94.6% for the distal femur, proximal tibia, femoral flexion, and tibial slope angles when the final intra-operative plan was compared to post-operative radiographs. No patients had a post-operative complication at the final follow-up.

Conclusions: The ROSA Knee System has acceptable accuracy and precision of coronal and sagittal plane resections with few outliers at various steps throughout the platform's entire workflow in vivo.

Comparison of Accuracy and Short-Term Results Between MAKO and Manual Technique

Chan Young Lee - Chonnam National University Hwasun Hospital - Hwasun-Gun, Jeollanam-Do, South Korea

*Kyung-Soon Park - Center for Joint Disease, Chonnam National University Hwasun Hospital - Hwasun-gun, South Korea

TAEK-RIM YOON - Chonnam national university hwasun hospital - Gwang-ju, Korea (Republic of)

Introduction

The purpose of this study is to compare the accuracy of acetabular cup placement and the short-term outcomes and complications between the MAKO THA system and manual THA.

Methods

This retrospective study involved 17 patients who underwent THA by MAKO Hip system and 229 patients who underwent THA by manual manner from December 2022 to December 2023. The approach of all operation was modified minimally invasive two incision technique. For MAKO THA group, pre-operative acetabular cup planning was specified by each patient and we used Trident® acetabular cup with polyethylene liner. For manual THA group, pre-operative acetabular cup planning was 20 degrees of anteversion and 40 degrees of inclination and we used Bencox®, Lima®, Ecofit®, and G7® acetabular cup with ceramic or dual mobility liner. We checked periprosthetic fracture and measured cup anteversion at post-operative 3 days by computed tomography. We compared the two groups based on the differences between the angles planned pre-operatively and the actual angles measured post-operatively. And each follow-up, we checked bone-ingrowth and complications like component loosening, infection, dislocation, and periprosthetic fracture.

Results

The average age was 67.5(54-84) years old in MAKO group, and 63.0(26-90) years old in manual group. The anteversion angle of acetabular cup was 20.2 ± 3.8 degrees in MAKO group and 26.8 ± 9.6 degrees in manual group. The difference from pre-operative planning was 3.1 ± 2.7 degrees in MAKO group and 9.6 ± 6.7 degrees in manual group for anteversion. The abduction angle of acetabular cup was 39.6 ± 2.0 degrees in MAKO group and 37.0 ± 5.1 degrees in manual group. The difference from pre-operative planning was 1.6 ± 1.2 degrees in MAKO group and 4.8 ± 3.5 degrees in manual group for abduction angle. There was significant differences in accuracy for acetabular cup placement between two groups.

Conclusion

With MAKO Hip system, we can make more accurate acetabular component position than manual principle. It can be a good option for patients who have complex anatomy or have risk factors of dislocation.

Validation of Coronal Alignment in a Robotic Total Knee Arthroplasty System

***Anoop Chandrashekar - Vanderbilt - Nashville, United States of America**

John Ryan Martin - Vanderbilt Health - Hendersonville, USA

Logan Locascio - Vanderbilt University School of Medicine - Nashville, USA

Peter Chan - University of Texas- Southwestern - Dallas, USA

Gregory Polkowski - Vanderbilt University Medical Center - Nashville, USA

Martin Faschingbauer - Department of Orthopedic Surgery, RKU, University of Ulm - Ulm, Germany

Introduction: Numerous robotic systems have been developed for total knee arthroplasty (TKA), aimed at aiding surgeons in attaining precise and optimal knee alignment. This study sought to validate intraoperative robotic measurements of femoral and tibial component coronal alignment by comparing them with pre-operative and post-operative hip-to-ankle radiographs.

Methods: This study included 59 unique patients undergoing primary total knee arthroplasty (TKA), and their long leg radiographs (LLR) were analyzed. The femoral and tibial component coronal alignment was measured using a previously developed and validated deep learning model. The measurements obtained from the robotic output and the deep learning model were compared to evaluate their accuracy.

Results: Pre-operative coronal alignment of the lower extremity as measured by the robotic system was highly correlated with measurements from pre-operative LLR (Pearson $r^2=0.68$). Additionally, intra-operative and post-operative coronal alignment of femoral and tibial implants were not significantly different ($p= 0.1191$ and $p=0.9547$, respectively) and strongly correlated with one another (Pearson $r^2=0.48$ and Pearson $r^2=0.62$ respectively). The mean difference in femoral alignment was 0.43° of varus and the mean difference in tibial alignment was 0.012° of valgus.

Conclusions: The findings of this study suggest that there were no significant differences in the coronal alignment of TKA when assessed intraoperatively by the robotic system compared to LLR, signifying the system's high accuracy. Nonetheless, given the distinct proprietary technological features among various robotic total knee systems, the precision of coronal alignment could fluctuate across systems. Consequently, additional investigations are warranted to verify the accuracy of alternative systems.

Robotic vs. Conventional Shoulder Arthroplasty: Impact of Surgical Variability on Preoperative Bone Density Estimates

Ghislain Maquer - Zimmer Biomet - Winterthur, Switzerland

*Ingmar Fleps - Warsaw, United States of America

Mirella Lopez Picazo - 3DShaper Medical - Barcelona, Spain

Thomas Duquin - Univesity at Buffalo - Buffalo, USA

Taku Hatta - Joint Surgery Sports Clinic Ishinomaki - Ishinomaki, Japan

John Sperling - Mayo Clinic - Rochester, USA

Jean-Guillaume Abiven - Zimmer Biomet - Montreal, Canada

Chloe Landry - Zimmer Biomet - Montreal, Canada

Ludovic Humbert - 3D-Shaper Medical - Barcelona, Spain

Jeffrey Bischoff - Zimmer, Inc. - Warsaw, USA

Philippe Favre - Zimmer Biomet - Winterthur, Switzerland

Introduction: Bone mineral density (BMD) is a determinant of implant stability that can be extracted from computed tomography (CT) scans used in preoperative planning. Yet, discrepancies between planning and surgery might affect the reliability of preoperative BMD estimate. This study addresses two questions:

1. What impact has surgical variability on preoperative BMD estimate, with respect to conventional and robotic shoulder arthroplasty?
2. If deviations between planned and actual resections are known, can we improve the estimate?

Methods: A matched-pair study for anatomic and reverse shoulder arthroplasties was conducted on 69 cadaver humeri, with one side operated with conventional instrumentation and the other with the surgical robot. All resections were planned on preoperative CT scans. Actual resections were measured on postoperative CT scans. The difference between planned and actual resections was computed (Figure 1).

Additionally, CT scans of 45 humeri acquired with a BMD phantom were calibrated. The “Planned” cohort was created by resecting each humerus through the anatomical neck. “Conventional” and “Robotic” cohorts were generated by simulating 100 resections distributed via a Latin hypercube sampling around the planned resection within the respective accuracy ranges (Figure 2).

For each humerus, BMD was computed in a 30mm-thick of trabecular bone directly below the resection for planned cases (BMD_{plan}), and cases resulting from conventional (BMD_{conv}) and robotic (BMD_{robo}) surgeries. Multilinear models accounting for resection’s inclination, version, height and BMD_{plan} as independent variables were then created, resulting in two “corrected” metrics: $BMD_{conv_{corrected}}$ and $BMD_{robo_{corrected}}$ (Figure 2).

Results: The preoperative estimate (BMD_{plan}) was already highly predictive of the postoperative measurements, but deviations (ie. residual errors) were significantly higher with conventional instrumentation. It was shown that including surgical variability in a multilinear model further reduced these deviations (Figure 3).

Conclusion: The position and orientation of the resection and the density of the bone that would support the humeral implant are strongly related. Resection made with a surgical robot are closer to the plan compared to conventional instrumentation and therefore improves the reliability of preoperative BMD estimates. A multilinear model can predict the density at the actual implantation site, provided that the

discrepancy between plan and final surgery is known, which would be the case using the robot's recorded postoperative values.

Keywords: Total Shoulder Arthroplasty, Bone Density, Surgical Planning, Robotic Surgery

Acknowledgments: This study was funded by the Eurostars grant #1521.

Figures

Accuracy	Conventional surgery (18 TSA / 18 RSA)	Robotic surgery (16 TSA / 17 TSA)
Height (mm)	$H = 2.6 \pm 1.6$	$h = 1.2 \pm 0.8$
Inclination ($^{\circ}$)	$I = 5.5 \pm 3.6$	$i = 3.7 \pm 3.2$
Version ($^{\circ}$)	$V = 10.7 \pm 7.3$	$v = 3.9 \pm 2.8$

Figure 1

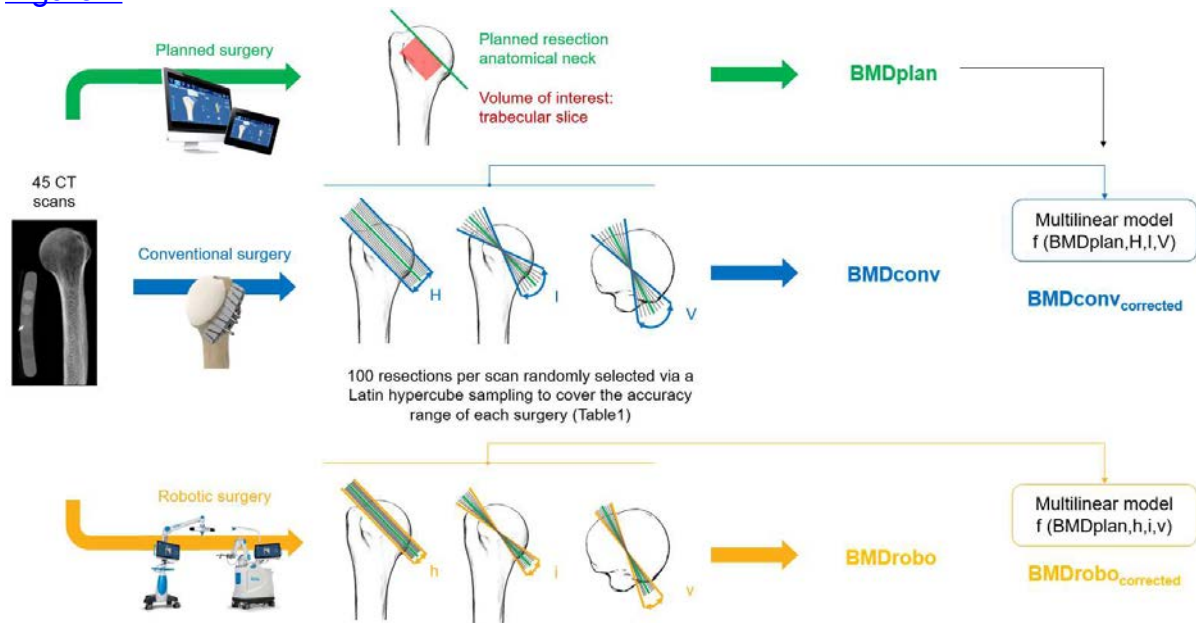


Figure2

Relation between <i>BMDplan</i> and:		R^2	$SD_{\text{residual_error}} \text{ mg/cm}^3$
Question 1	<i>BMDconv</i>	0.98	5.04
	<i>BMDrobo</i>	0.99	2.47
Question 2	<i>BMDconv_corrected</i>	0.99	3.92
	<i>BMDrobo_corrected</i>	0.99	2.08

Figure 3

Access to Robotic Spine Surgery in the Continental United States: A Geospatial Analysis

*Mitchell Ng - Maimonides Medical Center - Brooklyn, United States of America

Paul Mastrokostas - Maimonides Medical Center - Brooklyn, USA

Leonidas Mastrokostas - Maimonides Medical Center - Brooklyn, USA

Ahmed Emara - Cleveland Clinic - Cleveland, USA

Ian Wellington - University of Connecticut - Hartford, USA

Ahmed Saleh - Maimonides Medical Center - Brooklyn, USA

Jad Monsef - SUNY Downstate Medical Center - Brooklyn, USA

Objective: Robotic-assisted spine surgery has significantly improved surgical precision and outcomes. This study builds on existing literature by examining geospatial disparities in access to robotic spine surgery. The aims of this study are to: 1) analyze the current access to robotic spine surgery across the United States, 2) identify the types of medical centers affiliated with robotic spine surgeons, and 3) highlight disparities in access.

Methods: We utilized provider-finding functions from major medical equipment manufacturers to identify robotic spine surgeons and categorized affiliated hospitals. Geospatial analyses combined with socioeconomic indicators, Rural-Urban Continuum Codes, and the Area Deprivation Index (ADI) provided insights into access disparities. Multivariate logistic regression and Student's t-tests were used to identify county-level variables associated with hotspots and coldspots. Statistical significance was set at the 0.05 level.

Results: Ninety-one robotic spine surgeons were identified. Robotic spine surgeons were pre-dominantly affiliated with nonteaching hospitals (50.55%), followed by minor teaching (38.46%) and major teaching (10.99%) hospitals. Access hotspots are in the Northeast and Southeast, with rural areas showing 22% lower odds of being hotspots (OR=0.78, $p<0.001$). Factors increasing the odds of being a hotspot include higher disability prevalence (OR=1.19, $p<0.001$), lack of insurance (OR=1.18, $p<0.001$), and older median age (OR=1.17, $p<0.001$). Educational attainment and ADI, despite being significant, had lower predictive values for access.

Conclusion: Disparities in access to robotic spine surgery are influenced by socioeconomic, demographic, and geographic factors. The pre-dominance of surgeons in nonteaching hospitals and affluent areas highlights market forces in healthcare access. Addressing economic hurdles and demonstrating cost-effectiveness of robotic surgery are crucial for broader access.

Manual vs Robotic Patellofemoral Arthroplasty Outcomes: A Single Center MARCQI-Based Study

*Alexander Ziedas - Ascension Providence Hospital - Southfield, USA

Adam Miller - Ascension Providence Hospital - Southfield, USA

Elliot Biddle - Ascension Providence Hospital - Southfield, USA

Michael Laker - Ascension Providence Hospital - Southfield, USA

Jefferey Michaelson - Ascension Providence Hospital - Southfield, USA

Todd Frush - Ascension Providence Hospital - Southfield, USA

David Markel - Providence Hospital and Medical Center - Southfield, USA

Introduction

Patellofemoral arthroplasty (PFA) is effective for the treatment of isolated patellofemoral osteoarthritis. Historically, all PFA were performed manually. However, robotic-assisted PFA has become increasingly popular. The purpose of this study was to determine whether a robotic-assisted technique influenced outcomes and revision rates. We hypothesized that robotic-assisted PFA would have improved 90-day complication and revision rates.

Methods

A prospectively maintained statewide arthroplasty registry, the Michigan Arthroplasty Registry Collaborative Quality Initiative (MARCQI), was queried for all primary PFAs from January 2014 to December 2022 performed at a single hospital. Manual and robotic cohorts were compared for 90-day complications including emergency department visits, readmissions, returns to the OR, two-year revision rates, and overall revision rates. Chi-square and Fisher's exact tests were used for categorical data and t-tests for continuous data.

Results

Of 75 PFAs identified (mean age 53.0 ± 12.9 years, 78% female), 19 were manual and 56 robotic. All robotic procedures utilized the Mako robot (Stryker Orthopaedics). There were no statistically significant differences between manual and robotic cohorts relative to age, BMI, gender, race, surgical time, 30-day events, 90-day events or revision rate. Similarly, the specific nature of the 30 and 90-day events did not correlate with technique (Table 1). Manual PFA had a longer mean length of stay (30.9 ± 14.4 vs 20.6 ± 17.7 hours, $p=0.025$). There were no revisions for manual PFA. Three robotic PFAs were converted to total knee arthroplasty (TKA) for progression of osteoarthritis. Robotic PFA revision rate was 5% ($p=0.5667$). Mean time to robotic PFA conversion was 4.5 ± 2.7 years. Cumulative percent revision (CPR) of all PFAs at five years was 7.37% (Figure 1). Logistical regression modeling showed that patients undergoing manual PFA were more likely to experience 90-day events (OR 3.84, $p=0.04$, Figure 2).

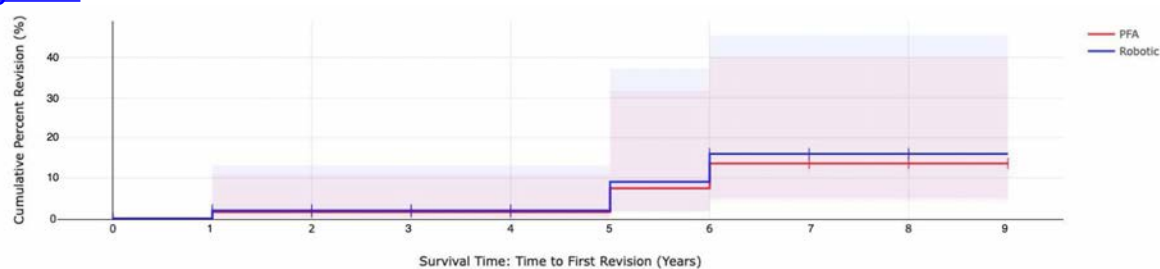
Conclusion

Manual PFA were prone to more 90-day events and longer length of stay than robotic PFA. Robotic PFA may minimize postoperative events without changing revision rate. Interestingly the PFA revision rate herein exceeded that of the reported MARCQI revision rates for unicompartmental knee arthroplasty (UKA) and TKA.

Figures

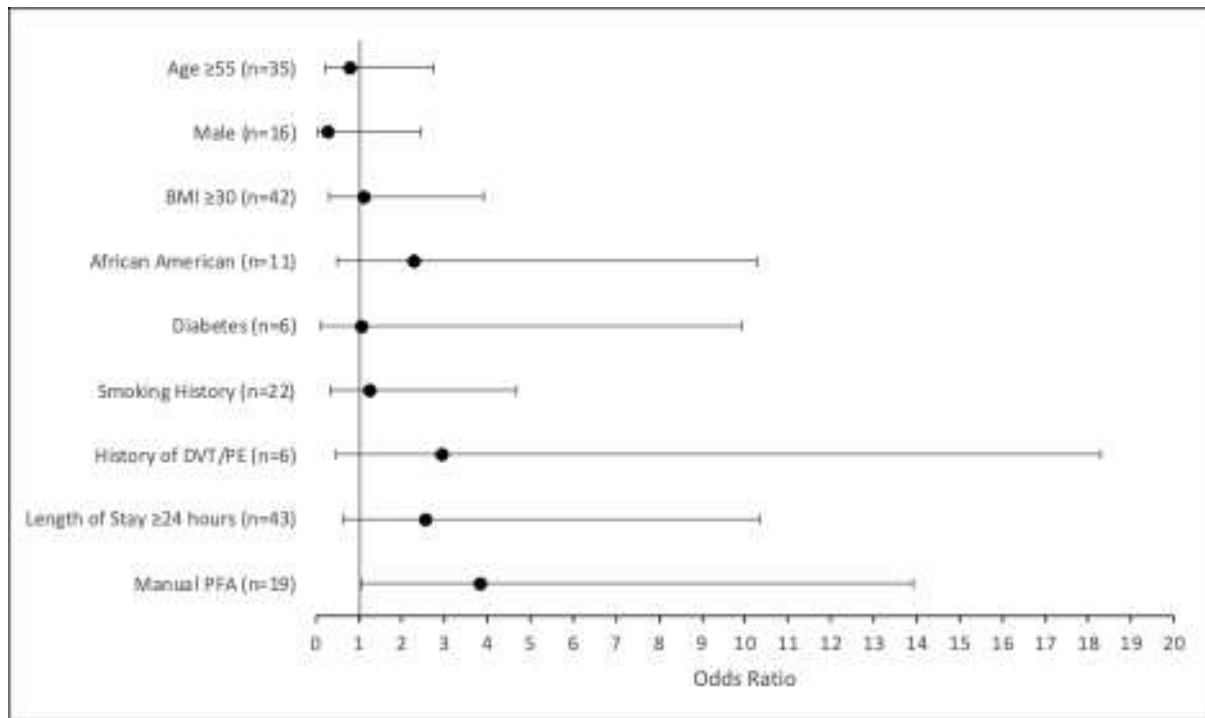
Outcome	Manual PFA			Robotic PFA			P-value
	Total	Count	%	Total	Count	%	
30-day Event	19	1	5%	56	3	5%	0.9874
90-day Event	19	6	31%	56	6	10%	0.0636
2-year revision	19	0	0%	56	0	0%	1
Overall Revision	19	0	0%	56	3	5%	0.5667
Conversion to TKA	19	0	0%	56	3	5%	0.5667
ED Visit	19	3	15%	56	2	3%	0.0963
Joint Related Readmission	19	1	5%	56	1	1%	0.4812
Unrelated Readmission	19	0	0%	56	0	0%	1
Wound Issues	19	1	5%	56	2	3%	0.7451
MUA	19	0	0%	56	2	3%	0.4037
PE/DVT	19	0	0%	56	0	0%	1
Return to OR	19	1	5%	56	3	5%	0.613
PJI	19	1	5%	56	1	1%	0.9874

Figure 1



	N	1 year	5 years	9 years
CPR All PFA	75	1.58 (10.73, 0.22)	7.37 (31.68, 1.58)	13.55 (39.99, 4.06)
CPR Manual	19	0	0	0
CPR Robotic	56	1.96 (1.3, 0.27)	8.96 (37.23, 1.87)	15.96 (45.49, 4.86)

Figure 2



[Figure 3](#)

Navigated Instrumentation Improves Reproducibility of Laxity Acquisition During a Total Knee Arthroplasty

*François Boux de Casson - Blue-Ortho - Meylan, France

Laurent Angibaud - Exactech, Inc. - Gainesville, USA

Florian Kerveillant - Blue-Ortho - Meylan, France

Leonard Duporte - Hopital Lapeyronie - Montpellier, France

Gerard Giordano - Hopital Joseph Ducuing - Toulouse, France

Louis Dagneaux - Hopital Lapeyronie, Université de Montpellier - Montpellier, France

Introduction:

In total knee arthroplasty (TKA), laxity assessment is crucial for joint balance and bone cut planning, but its reproducibility and reliability may vary with the acquisition method and operator experience. This experimental study compares laxity measurements reproducibility between two acquisition methods.

Methods:

Five operators (3 senior and 2 junior surgeons) measured laxity during navigated TKA with a posterostabilized prosthesis. This study included 8 knees (4 cadaveric specimens). Each operator assessed knee joint laxity through the full flexion arc, first manually manipulating the limb in varus and valgus, then using an instrumented method with a distractor inserted between the tibial cut and the native femur, repeating the process six times per knee. Reproducibility of measurements was evaluated via inter-operator and intra-operator intra-class correlation coefficients (ICC), varying with method and operator experience.

Results :

The four women specimens, aged 79 to 96 (mean 90 ± 7.9), comprised two with genu valgum, one with genu varum, and one normoaxed. A total of 960 gap acquisitions were recorded with the CAOS system to evaluate both techniques across the motion arc. The instrumented method had a significantly greater inter-operator ICC than the manual method for the lateral laxity (0.92 versus 0.25; $p < 0.0001$) [Fig 1] and the medial laxity (0.87 versus 0.60; $p = 0.02$) [Table 1]. For the manual method, the lateral laxity acquired under varus stress was less reproducible than the medial laxity acquired under valgus stress (0.25 versus 0.60; $p = 0.01$), while the instrumented method showed no difference (0.92 versus 0.87; $p = 0.8$) between the two compartments [Table 2]. For both manual and with the distractor, the seniors had better inter-operator ICCs than the juniors, although this was not significant (manually 0.55 versus 0.39; $p = 0.1$, with the distractor 0.92 versus 0.90, $p = 0.3$). The intra-operator ICC was significantly higher with the instrumented method than with the manual method for laxity assessment in all tests (0.78 versus 0.51; $p < 0.0001$) and for the lateral compartment (0.84 versus 0.40; $p < 0.0001$), but not for the medial compartment (0.71 versus 0.63; $p = 0.07$).

Conclusion:

The instrumented method, with an intra-articular distractor, improved knee laxity acquisition reproducibility, minimizing the impact of experience and acquisition challenges inherent in maintaining varus force during flexion compared to the manual method. The controlled force application by the distractor, along with its ease of use in the neutral position, could contribute to gap acquisition reproducibility. Using a distraction device with navigation enhanced knee laxity measurement reproducibility compared to manual varus/valgus acquisitions.

Figures

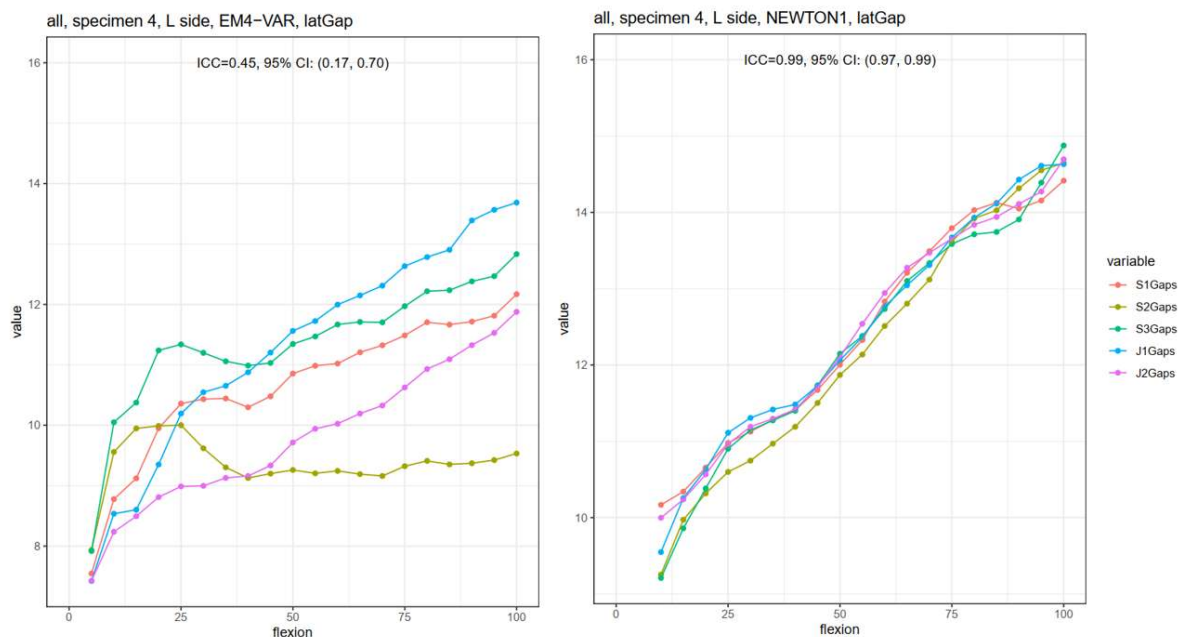


Figure 1. Lateral compartment gaps measured by the manual method (Left) and instrumented method (Right) for specimen 4, left knee.

Figure 1

	Conventional Technique	Instrumented Technique	1-sided t-test
	mean ICC (95% CI)		
Inter-operator			
All tests	0.43 (0.23, 0.60)	0.90 (0.76, 0.96)	p<.0001
Varus tests (lat. gaps)	0.25 (0.09, 0.43)	0.92 (0.81, 0.97)	p<.0001
Valgus tests (med. gaps)	0.60 (0.37, 0.76)	0.87 (0.71, 0.95)	p=.002
Intra-operator			
All tests	0.51 (0.33, 0.70)	0.78 (0.64, 0.88)	p<.0001
Varus tests (lat. gaps)	0.40 (0.22, 0.60)	0.84 (0.71, 0.92)	p<.0001
Valgus tests (med. gaps)	0.63 (0.44, 0.80)	0.71 (0.57, 0.84)	p=.07

Table 1: Inter-operator and Intra-operator Intraclass Correlation Coefficient (ICC) per Technique of Laxity Measurements for All Tests, Varus Tests and Valgus Tests.

Figure 2

	Inter-operator		2-sided t-test
	mean ICC (95% CI)		
	Varus tests (lat. gaps)	Valgus tests (med. gaps)	
Conventional Technique	0.25 (0.09, 0.43)	0.60 (0.37, 0.76)	p=.01
Instrumented Technique	0.92 (0.81, 0.97)	0.87 (0.71, 0.95)	p=.8
	Juniors	Seniors	
Conventional Technique	0.39 (0.08, 0.62)	0.55 (0.27, 0.72)	p=.3
Instrumented Technique	0.90 (0.66, 0.96)	0.92 (0.78, 0.97)	p=.1
Intra-operator			
	Varus tests (lat. gaps)	Valgus tests (med. gaps)	
Conventional Technique	0.40 (0.22, 0.60)	0.63 (0.44, 0.80)	p<.0001
Instrumented Technique	0.84 (0.71, 0.92)	0.71 (0.57, 0.84)	p=.01
	Juniors	Seniors	
Conventional Technique	0.53 (0.34, 0.71)	0.50 (0.32, 0.69)	p=.7
Instrumented Technique	0.75 (0.61, 0.87)	0.79 (0.66, 0.89)	p=.2

Table 2: Inter-operator and Intra-operator Intraclass Correlation Coefficient (ICC) Between Measurement of Lateral and Medial Gaps and between Juniors and Seniors Surgeons.

[Figure 3](#)

Accuracy of Robotic Assistance in Unicompartmental Knee Arthroplasty: A Cadaveric Study Comparing VELYS Robotic Assisted Solution to Conventional Instrumentation

*Gary Doan - DePuy Synthes - Raynham, USA

Ian Leslie - DePuy Synthes Joint Reconstruction - Leeds, United Kingdom

Patrick Curtis - DePuy Synthes Joint Reconstruction - Warsaw, USA

Daniel Hoeffel

Richard Southgate - Northwestern Medical Group - Lake Forest, USA

David F Dalury - Baltimore, USA

Introduction:

Robotic assistance has proven to enhance the precision of bone preparation, minimize the variability in outliers, and increase the reproducibility of limb alignment in unicompartmental knee arthroplasty (UKA). As a result, the utilization of robotic assisted techniques in UKA is progressively growing. A UKA application is in pre-clinical development for the VELYS Robotic Assisted Solution (VRAS). The purpose of the study was to assess the accuracy of VRAS compared to conventional instrumentation for UKA in a cadaveric study.

Methods:

Forty pelvis-to-toe cadaveric specimens were used in this study. Six different surgeons performed bilateral UKA with robotic-assisted surgery on one leg and conventional instrumentation on the contralateral leg, alternating sides as to avoid handed or side bias. Optical arrays were implanted in cadavers either for the purpose of the robotic-assisted technique or for collecting data using conventional instruments. Preoperative CT scans were performed and intraoperative targets for femoral coronal alignment (FCA), femoral sagittal alignment (FSA), femoral internal external alignment (FIE), tibial coronal alignment (TCA) and tibial sagittal alignment (TSA), distal femoral resection depth (DFRD), posterior femoral resection depth (PFRD), transverse tibia resection depth (TTRD), and hip-knee-ankle (HKA) angle were established. After the bone preparation steps, the bone remnant thicknesses were measured using a digital caliper, trials were implanted, long leg alignment was measured via the optical arrays, and the resected bones were CT scanned. The native and resected bones were segmented from the pre-operative and post-operative CT scans, respectively, and registered together to align the two geometries. The surgical plan for each case was recreated, and the resection angles of the bone surfaces and HKA angles of the knee were quantified in-silico and compared to the surgical plan. The absolute error between each resection angle, resection depth, and HKA angle were calculated.

Results:

For VRAS the mean absolute error of the FCA (1.82 Vs. 2.75 $p=0.022$), FSA (1.21 Vs. 4.43 $p>0.001$), FIE (1.35 Vs. 4.02 $p>0.001$), TCA (1.57 Vs. 2.54 $p=0.002$) and TSA (1.22 Vs. 2.25 $p=0.002$) were significantly reduced compared to manual. There was no significant difference in the mean absolute error of the DFRD (0.56 Vs. 0.77 $p=0.051$), PFRD (0.69 Vs. 0.65 $p=0.221$), TTRD (1.05 Vs. 1.31 $p=0.060$), and HKA (1.07 Vs. 1.37 $p=0.090$).

Conclusion:

The VRAS system for UKA was found to have significantly improved resection angle accuracy compared to manual instrumentation. This may lead to improved control of UKA component positioning.

Figures

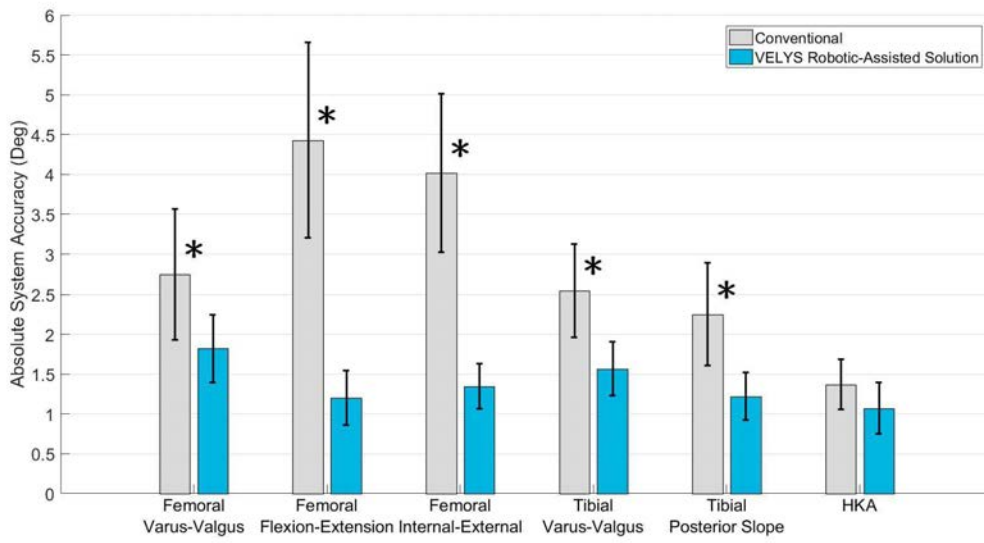


Figure 1

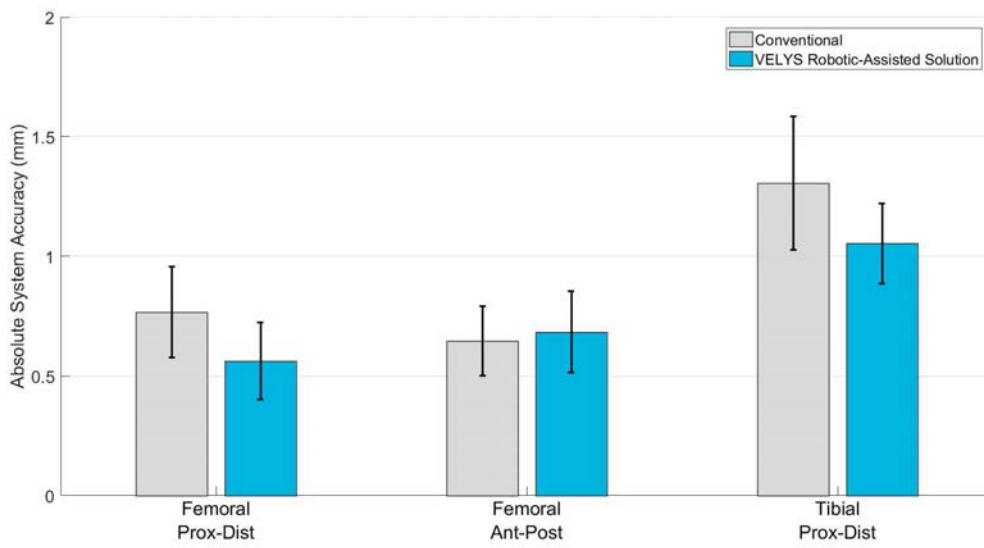


Figure 2

How Accurately Can a Miniaturized Navigation Device Assess the Intra-Operative Sagittal Position of the Pelvis?

*Tristan Jones - Naviswiss Inc - Tampa, United States of America

Stefan Kreuzer - INOV8 Orthopedics - Houston, USA

Stephen Raterman - Florida Medical Clinic - Tampa, USA

Danielle DeMoes - Inov8 Orthopedics - Houston, USA

Miroslava Rangel - Naviswiss Inc - Denver, USA

INTRODUCTION

Recently, a great deal of literature has focused on understanding the functional dynamics of patient specific sagittal pelvic rotation, such that surgeons can customize component positioning when performing total hip arthroplasty (THA). Such surgical customizations are executed while the patient is on the operating table, therefore requiring an understanding of the relative orientation of the pelvis intra-operatively, with respect to those more functional postures (standing and / or seated). The purpose of this study was to evaluate the effectiveness of a miniaturized navigation device to accurately assess the intra-operative sagittal position of the pelvis in the supine position.

METHODS

A navigated imageless workflow (Naviswiss, AG) was used to identify and landmark the anterior pelvic plane (APP) intra-operatively, in a group of 30 patients undergoing THA via a direct anterior approach. Landmarks were registered using a calibrated blunt tip pointer and the sagittal tilt of the pelvis was measured and recorded within the logfiles of the navigation device. Further, an intra-operative lateral X-ray was taken immediately prior to registration process, which was later landmarked and measured to provide an objective radiographic measure of sagittal tilt for comparison. These two sagittal rotation measurements were then compared and correlated with anthropometric data.

RESULTS

Mean error between the two measurement methodologies was 1.8° (min 0, max 13), with 2 outliers outside of 5° . The correlation coefficient between the landmark based imageless navigation and intra-operative lateral X-ray measurement was strong at 0.92. A weak correlation (0.31) was found between the magnitude of measurement discrepancy and BMI.

CONCLUSION

A miniaturized navigation device can provide an accurate assessment of sagittal pelvic tilt in the supine position on the operating table. Intra-operative use of this device may provide a reliable method to understand pelvic tilt at the time of surgery and therefore allow the surgeon to deliver customized and functional component orientations, patient specifically.

Navigation Accuracy of a Novel Mixed Reality Platform for Orthopedic Surgery

*John Cooper - Columbia University - New York, USA

Winona L. Richey - PolarisAR - Miami, USA

INTRODUCTION

Surgical navigation systems have improved precision and patient outcomes in orthopedic surgery. However, conventional navigation systems are costly, have a large footprint, and require line of sight to a camera away from the surgical field. Here we present and evaluate a novel navigation platform where state-of-the-art instrument tracking, computing, and displays are all integrated into an augmented reality headset [Fig. 1].

METHODS

The mixed reality surgical platform for total knee arthroplasty was evaluated according to the latest update (F2554-22) to the ASTM consensus standard recognized by the U.S. FDA for positional accuracy of computer assisted surgical systems. Analysis investigated the platform's ability to locate points and planes with the disposable tracked tools across the tracking volume, including rotational and positional extremes. Testing also extended the ASTM standard to include additional rotation tests and an evaluation procedure for planar accuracy metrics.

RESULTS

Point localization accuracy achieved 0.5 ± 0.3 mm bias (mean \pm standard deviation) and 0.4 ± 0.3 mm precision, summarized across more than 2,700 points. Paired distance error, or inter-point distance error, was 0.5 ± 0.3 mm evaluated in over 395,000 combinations of Stylus measurements. Plane localization accuracy achieved $0.3\pm 0.1^\circ$ bias and $0.1\pm 0.1^\circ$ precision across more than 25,000 measurements. Paired angular error, or inter-plane angle error, was $0.1\pm 0.2^\circ$ evaluated at over 13.9 million combinations of planar measurements. The tracking subsystem localized over 99.5% of points with positional accuracy better than ± 2 mm and localized over 99.5% of planes with angular accuracy better than $\pm 1^\circ$ [Fig. 2].

CONCLUSION

Tracking errors were sub-millimeter and sub-degree, demonstrating this novel mixed reality surgical platform is accurate and reliable, providing accuracy comparable to modern robotic-assisted orthopedic surgery systems. This open-platform, imageless system has a reduced footprint, reduced toolkit, and data overlaid holographically directly onto the surgical scene, while still allowing live tracking of femur and tibia and providing a comprehensive set of metrics with state-of-the-art accuracy.

Figures

Figure 1

The complete surgical platform including reusable instruments (a-g), disposable screws (h), disposable tracked instruments (i-l), and the Head Mounted Device – Microsoft HoloLens 2.

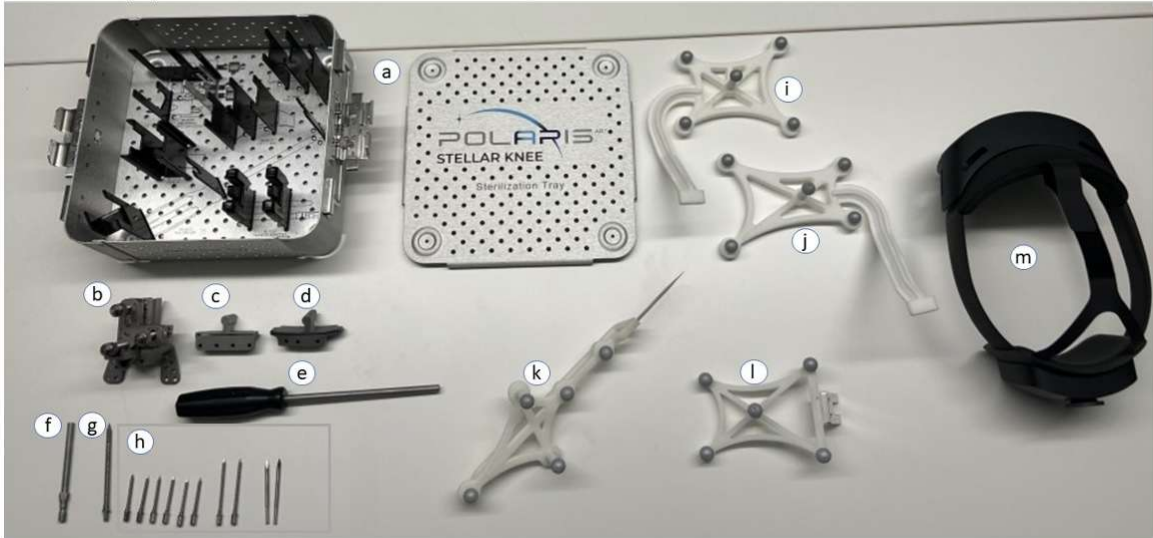


Figure 1

Figure 2

Absolute tracking error across extended ASTM testing, where the orange line is the median, and the whisker caps show the 0.25 and 99.75 percentiles. Data outside this central 99.5% are plotted as “x”es. Point data is collected with a Stylus tool, and plane data is collected with a Fin tool, with errors shown at left and right respectively.

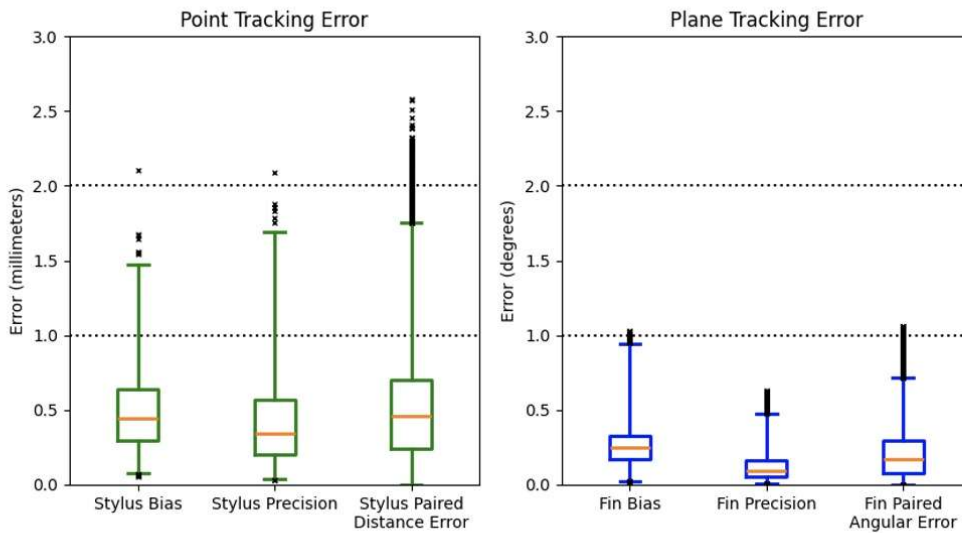


Figure 2

Boney Compaction Surrounding Cementless TKA Implants and the Effect of Robotic Surgery

Emma Donnelly - Western University - London, Canada

Jaques S. Milner - University of Western Ontario - London, Canada

David Holdsworth - Western University - London, Canada

*Ryan Willing - Western University - London, Canada

Brent Lanting - London Health Sciences Centre - London, Canada

Introduction: Successful long-term fixation of cementless total knee arthroplasty (TKA) tibial components depends on achieving accurate prosthesis alignment and appropriate bone-implant contact mechanics; both of which are influenced by surgical technique. Surgical robotics can improve the accuracy of the cuts which determine prosthesis alignment; however, robotic systems which directly control motion of the oscillating saw can also yield cleaner cuts. When the tibial component is impacted into the proximal tibia, uniform compaction of bone beneath the implant is desirable, and a cleaner bone-implant interface may promote this. Thus, the objective of this study was to compare bony compaction beneath the tibial component in paired tibiae using conventional versus robotic surgical approaches.

Methods: Full lower bodies from 16 donors (8 males, 8 females, aged: 37-77) received TKAs, with the left and right legs randomized to have bone cuts performed using conventional (manual) versus robotic approaches. The proximal tibiae were prepared to receive cementless, rotating-platform tibial components that featured a cylindrical central stem and four small peripheral pegs. Prior to impaction of the tibial components, each leg was imaged using a GE Locus Ultra micro-computed tomography system with a resolution of 0.154 mm. The tibial component was impacted into the tibia before the joint was mounted onto a joint motion simulator for biomechanical analyses which included up to ~500 N of compression (reported elsewhere). The tibial component extraction force was then recorded (1 mm/s). The tibiae were then re-imaged using the same uCT settings. Changes in bone density were evaluated across the cut surface via computed differences in matched 1×1×8 mm density-averaged sample volumes. Bone density across pre-impaction and post-removal cut planes was compared using Wilcoxon matched pair signed rank tests for each tibiae duo. Comparison of mean cut plane bone density between conventional, and robot assisted techniques was performed using a paired difference t-test.

Results: For ten pairs, the tibiae with cuts done using the robotic system required a greater pull-out force than the conventional counterpart by a mean of 63±48N. In the remaining cases the average required force was 145±176N larger for the tibiae with conventional cuts; though this includes two outliers. Across all tibiae, the pre-impaction/post-removal mean bone density increase was 0.019 g/cm³ (SD = 0.033). When compared by surgical technique, tibiae in which the robot assisted technique was used showed a greater increase in mean bone density (M = 0.026 g/cm³, SD = 0.038) over those in which the conventional method was used (M = 0.012 g/cm³, SD = 0.025). The mean of the paired differences between the two different techniques was 0.014 g/cm³ (SD = 0.031, p = 0.09).

Conclusion: Higher pullout forces and larger bone density increases occur in tibiae that have undergone robot assisted tibial cuts suggesting that bony compaction

beneath the tibial component is more substantial with this technique than when the conventional surgical method is used; however, this technique may experience more variability.

Figures

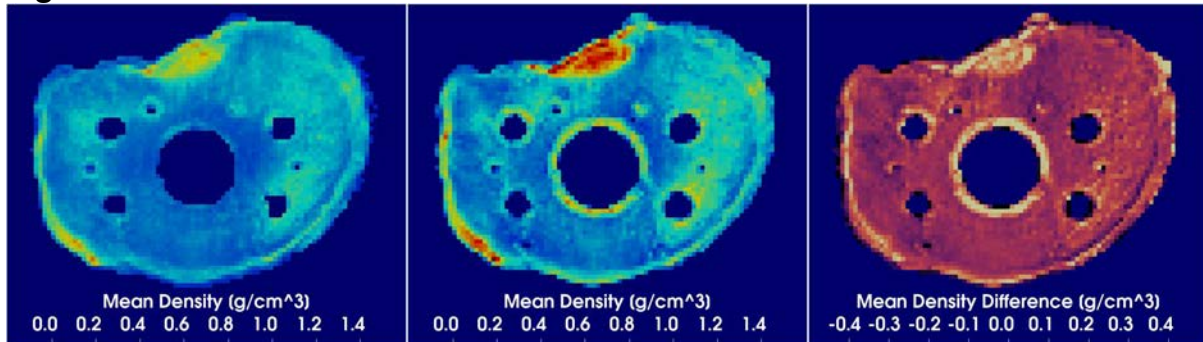


Figure 1. Changes in bone density pre-impaction versus post-removal were calculated after co-registering uCT volumes and estimating density using established density vs uCT number relationships.

Figure 1

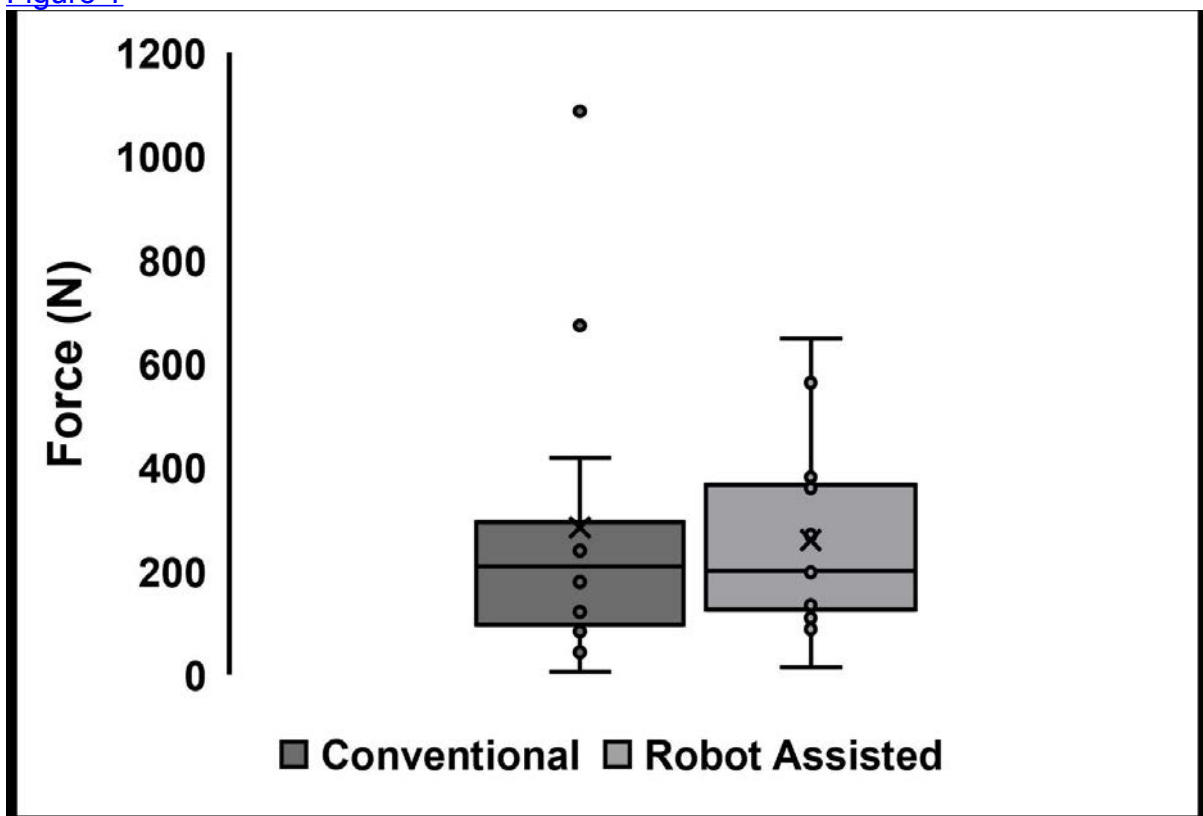


Figure 2. Differences in peak pull-out forces between the conventional and RA TKA tibial components.

Figure 2

Bone Density Median Paired Differences

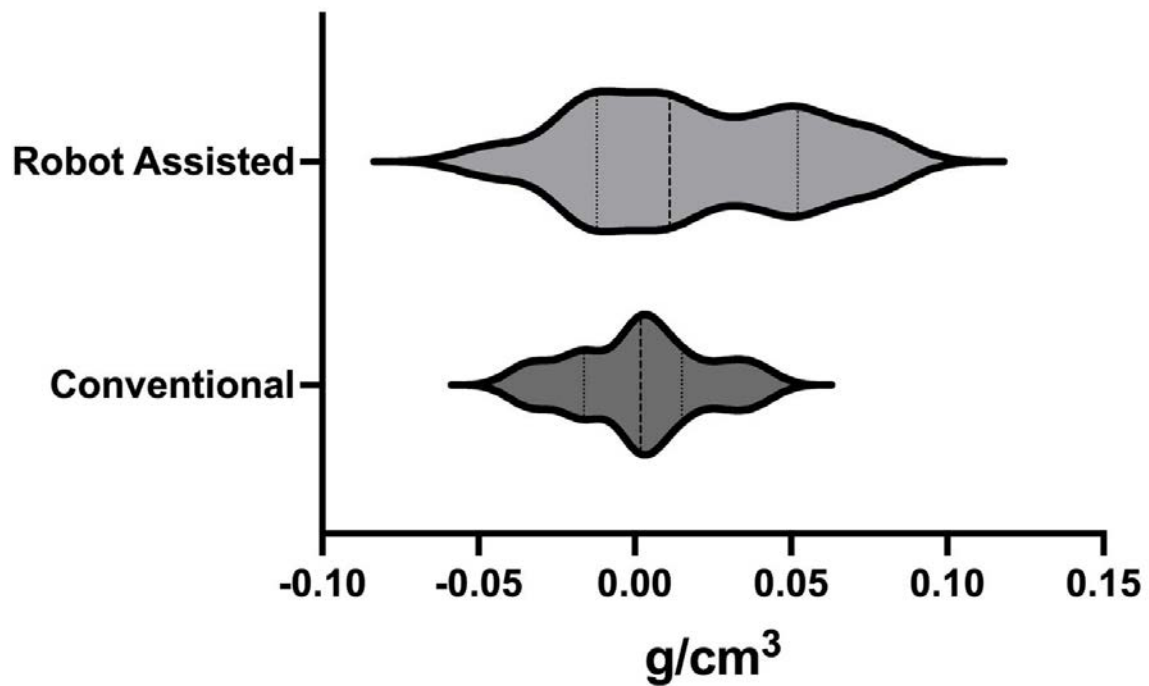


Figure 3. Changes in median bone density pre-impaction versus post-removal with TKA cuts made using conventional versus robot assisted techniques.

[Figure 3](#)

Evaluation of the Learning Curve Associated With Advanced Intra-Operative Planning for Total Knee Arthroplasty

*François Boux de Casson - Blue-Ortho - Meylan, France

James Huddleston

Wen Fan - Exactech - Gainesville, USA

Amaury Jung - Blue Ortho - La Tronche, France

Laurent Angibaud - Exactech, Inc. - Gainesville, USA

Prudhvi Tej Chinimilli - Exactech - Gainesville, USA

Introduction

New total knee arthroplasty (TKA) technologies can improve procedures and outcomes but may affect surgeons' habits. On the other hand, their adoption may impact surgeons' habits. Recent developments enable the intra-operative planning of the bone cut parameters in terms of size, alignment and soft-tissues considerations. This study aimed to assess surgeons' learning curve with new technologies and its correlation with the time for the initial 50 surgeries.

Methods

This study retrospectively reviewed a cloud-based database, housing case logs from surgeries performed using an instrumented computer-assisted surgery (CAS) system. This system enables comprehensive assessment of knee joint laxities across the full range of motion with a constant distraction force, allowing for advanced intraoperative planning of femoral cut parameters (size, alignment, and soft-tissue considerations). The first 50 cases of each selected surgeon were analyzed. The CAS system recorded the time spent on intraoperative planning setup. The learning curve was evaluated using cumulative summation analysis (CUSUM) of this time. The CUSUM values were plotted chronologically to assess surgeon-specific learning curves. The ideal curve would show a bell-shaped pattern, with the asymptote indicating competency attainment. The inflection point on the CUSUM graph marks the transition from learning to proficiency. Learning phase duration was analyzed per surgeon and globally (mean \pm SD), and its Pearson correlation with the time taken for the initial 50 surgeries was examined. Independent samples Student t-tests were applied for continuous variable comparisons, assuming equal variance, or corrected t-tests if not. Statistical significance was set at $p < 0.05$.

Results

A total of 450 cases performed by 9 individual surgeons were considered, corresponding to surgeries performed worldwide from August 2021 to April 2023, so a total period of 597 days with a mean by surgeons of 239 ± 98 days to perform their 50 first cases. The CUSUM learning phase varied from 2 to 11 cases, with a mean of 6.4 ± 2.8 cases. For all surgeons combined, the total intraoperative planning mean time in the learning phase was 82 seconds longer than in the proficiency phase (132 vs. 49 sec; $p < 0.0001$) but, individually, this difference was only significant for 5 of the 9 surgeons. The correlation coefficient between the learning phase and completion time for the first 50 cases was 0.75 ($p = 0.0203$, 95% CI 0.17 to 0.94).

Conclusion

CUSUM analysis offers a refined assessment of learning progression. Recent studies on robot-assisted TKA using CUSUM demonstrated learning curves for total operative time, ranging from 11 to 43 cases for high-volume surgeons (>70 cases). Interestingly, post-learning curve, operative times did not significantly differ from conventional techniques. Another robotic system showed an average of 8.7 cases. In

this study, adoption was swifter, averaging 6.4 cases to proficiency. Unlike prior studies comparing overall operative time, we focused solely on the duration of the intraoperative planning stage, where the technology was integrated. Our findings reveal a more than 50% reduction in average planning time after the learning phase. Furthermore, correlation analysis indicates that faster completion of the initial 50 cases is associated with a shorter learning curve.

Figures



Figure 1: Example of CUSUM for planning time per case, surgeon 7.

[Figure 1](#)

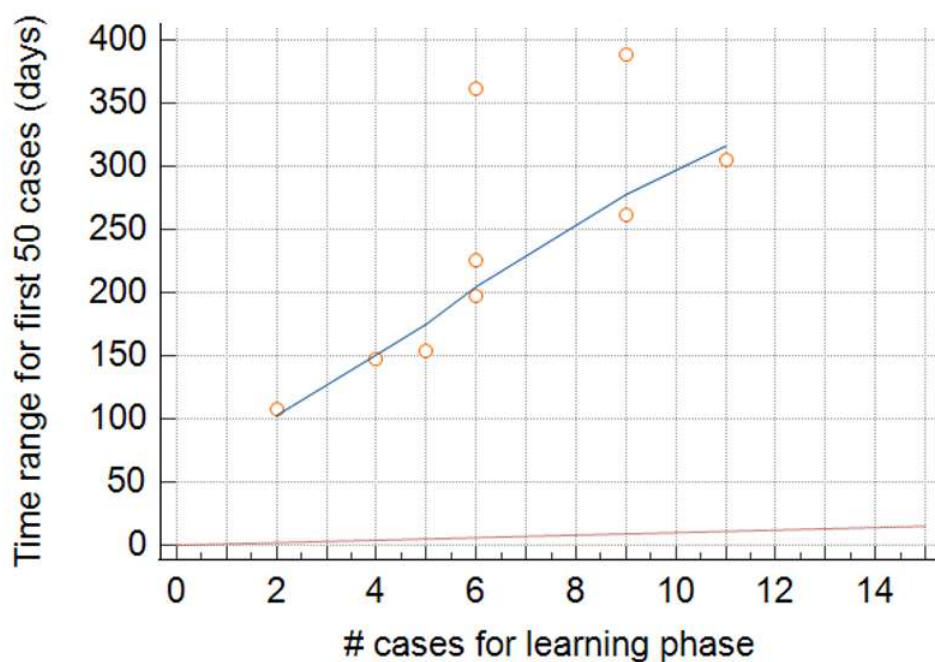


Figure 2 Relationship between the duration of first 50 surgeries and learning curve number of cases

Figure 2

	Time required to perform the first 50 surgical procedures (days)	Number of cases for the learning phase (CUSUM)
Surgeon 1	305	11
Surgeon 2	154	5
Surgeon 3	197	6
Surgeon 4	389	9
Surgeon 5	148	4
Surgeon 6	362	6
Surgeon 7	262	9
Surgeon 8	108	2
Surgeon 9	225	6
Mean (SD)	239 (98)	6.4 (2.8)

Table 1: Duration of first 50 cases and learning phase.

Figure 3

Learning Curve for a New Novel, Miniaturized, Imageless Navigation Technology for TKA.

*Abigail Priestley-Collins - Naviswiss Inc - Denver, USA

George Branovacki - Midwest Orthopaedic Consultants - Orland Park, USA

Introduction

Computer-assisted navigation systems (CAS) continue to be utilized in total knee arthroplasty (TKA) procedures, which are increasingly conducted in outpatient surgery settings. Despite universal advancements in system operation and workflow, successful adoption still depends heavily on system efficiency and the surgical learning curve. This study aims to evaluate the learning curve for implementing a miniaturized handheld navigation system in an ambulatory surgical center (ASC) setting.

Method

A retrospective review was conducted on the first 27 cases completed using the Naviswiss Knee (Naviswiss AG) image-less TKA solution, by a single surgeon. Following initial registration and pre-op range of motion assessment (Registration), the proximal tibia and distal femoral resections were planned in real time. After completion of all resections, implant trials were completed with a final range of motion trial. All registration times were saved and collected using the time stamps contained in the case log files, while patient information, complications and tourniquet times were collated from the surgical records.

Results

The mean timespan across which the navigation system was 'operational' (from first registration to final range of motion assessment) was 20.25 minutes (range 14.51 - 31.33). This time period showed a reduction from a mean of 24.22 minutes across the first 5 cases to a mean of 19.34 minutes for the following 22 cases. The mean time to execute the initial registration process was 2:47 minutes (range 1:38 – 8:39). Across the first 5 cases, the mean registration time was 4:05 minutes, with a mean tourniquet time of 46 minutes. For the next 22 cases, the mean registration time accelerated to 2:29 minutes, while the mean tourniquet time decreased to 38.82 minutes. Patients had an average BMI of 33.5. There were no post-op complications.

Conclusion

This miniaturized imageless TKA navigation system proved to integrate well with a single surgeon in a busy ASC setting. Mean system operation time, registration time and tourniquet time all reduced significantly after the first 5 cases, which may be considered the learning curve for the imageless workflow with this system.

Resurfacing Unicondylar Knee Arthroplasty Should Be the Gold Standard for Patients Over 70 Years Old With Single-Compartment Degeneration of the Knee.

*Robert Eberle - Maxx Orthopedics - Apex, USA

Martin Redish, MD - ParkRidge Bone & Joint - Chattanooga, USA

INTRODUCTION

The reported use of Unicondylar Knee Arthroplasty (UKA) has been controversial over the years. UKA is a less-invasive procedure, resulting in faster rehabilitation, greater preservation of bone stock, reduced blood loss, and a lower risk of infection in comparison with Total Knee Arthroplasty (TKA). This is more important in the elderly patient where surgical objectives are not the same as in younger patients. The purpose of this study was to revisit the 10-year results of the previously reported UKA patients, comparing the younger (<70yo) versus older (\geq 70yo) patient cohorts' results.

METHODS

We retrospectively reviewed consecutive patients with isolated medial or lateral osteoarthritis who underwent cemented UKA resurfacing with the Repicci II UKA system. The original paper reported an average age at surgery of 70.5 years. Using this as a guide, we divided the database at patient age at surgery of 70 years. Descriptive statistics were used to summarize the two cohorts. The "Forgotten Joint Score" (FJS) and the "Oxford Knee Score" (OKS) were used to assess the patient outcomes through 10-years minimum follow-up between both study cohorts.

RESULTS

The "young" cohort (< 70) had an average age at surgery of 59.9 ± 6.5 years, and included 184 patients (173 medial, 11 lateral). Of the 184 patients, not included for review were 17 lost to follow-up, 5 deceased, 1 incapacitated patient, and 12 patients revised leaving 149 patients for review at 10-years follow-up. The "elderly" cohort (\geq 70) had an average age at surgery of 81.5 ± 8.5 years, and included 176 patients (166 medial, 10 lateral). Of the 176 patients, 38 were lost to follow-up, 72 deceased, 2 incapacitated patients, and 1 patient revised status post traumatic fracture thus leaving 63 patients for review at the 10-year follow-up. The average FJS was 67.1 ± 30.0 in the young cohort and was 72.8 ± 27.1 in the elderly. These were not statistically different ($p = 0.18$) Likewise, the average OKS were 38.9 ± 9.8 for the young cohort and 40.7 ± 7.2 in the elderly cohort and not statistically different ($p = 0.14$).

CONCLUSION

From our 10-year follow-up of resurfacing UKA, the results as determined by the FJS and the OKS were statistically similar between young and elderly patient cohorts when split at 70 years of age at surgery. There was an increased expected loss of patients to death in the elderly cohort. However, these patients had well-functioning UKA components at the time of death. We hypothesize that in elderly patients greater than 70 years of age which present with single compartment knee degeneration and the presence of multiple comorbidities and need for rapid recovery, that the use of resurfacing, all-poly inlay tibial UKA may be the standard for care. The authors question the use of TKA these patients when sacrificing two perfectly functional knee compartments, the ACL, and possibly the PCL as well. The authors hope that

this review instigates further discussion and warrants a serious evaluation of TKA versus resurfacing UKA in the elderly.

Constraint of Modern Posterior Stabilized Total Knee Replacements

*Joel Weisenburger - The University of Nebraska Medical Center - Omaha, USA

Kevin Garvin - Univ of Nebraska Med Ctr - Ortho Dept. - Omaha, USA

Carlos Rodrigo De Mello Roesler - FAPEU - Florianopolis, Brazil

Maria Eduarda Quissini - Federal University of Santa Catarina - Florianópolis, Brazil

Hani Haider - UNMC - Omaha, USA

The anterior-posterior (AP) and internal-external (IE) rotation constraint after Knee Replacement depend on the TKR design and materials, presurgical anatomy, and implant surgical alignment and ligament tuning. The implant constraint is provided by the implant's articular surface geometry and the bearing's viscoelastic and frictional characteristics.

In previous studies we have shown that even when indicated for the same patient, different designs of Poster-Cruciate-Ligament (PCL) Retaining (CR) TKRs have widely differing constraint; surprising when all those CR TKRs were claimed to be optimally constrained by their own manufacturer. In this study we tested a set of PCL sacrificing (PS) TKRs and hypothesized that they ought to offer similar constraint levels, unless they surprise us too.

We tested five PS and two CR TKR designs of comparable middle size. We used an MTS test machine with custom fixtures providing 6 degrees of freedom (DOF) motions with four controllable force/motion axes and virtually friction-free slides and bearings for the other axes. With a 712 N (1 bodyweight) constant compressive load, the AP tests varied AP force/displacement to their extremes in either direction in three loops while leaving IE, varus-valgus (VV) rotation and Medial-Lateral (ML) translation free. We recorded thousands of measurements of all forces, torques and displacements whether controlled or secondary. In the IE constraint tests, we varied IE rotation angle/torque under compression and left all other motions including AP to be free. Both the AP and IE tests were repeated at flexion angles of 0°, 15°, 90° and the maximum flexion of each TKR (typically 110°-140°). Articulating surfaces were lubricated with diluted bovine calf-serum. The AP force vs. displacement plots and IE Torque vs. angle plots are shown in Figs. 1 and 2. The resulting average constraint was estimated as the slope of a least-squares-error line through the hysteretic constraint plots, and the peak forces and torques together with the displacements & rotations where they occurred were all tabulated (Fig. 3).

The AP constraint at 0° flexion ranged from a low of 14.9 N/mm to a 3x higher 44.4 N/mm. All PS TKR AP tests at showed an anterior force-spike as the tibial bearing post's anterior side engaged the femoral box. The CR designs showed less constraint (9.29, 12.9 N/mm) and no force-spike (no post). The IE constraint ranged from 0.043 to 0.420 Nm/°, a 10-fold variation. At 15° flexion some posts still impinged on some PS designs on the anterior and posterior sides. By 90° and higher flexion, the AP motion was drastically curtailed to the posterior side of the tibial bearing, limited by the post on all PS designs. In all tests on all the TKR designs the IE constraint decreased at higher flexion, a goal typically intended by most TKR designs/geometries.

Our study demonstrated that even for contemporary PS TKR designs indicated for the same patient, not only significant but huge differences exist in both AP and IE constraint, yet none of such differences are explicitly stated quantitatively to aid the choice of which TKR to use.

Figures

AP Force vs. AP Displacement Curves

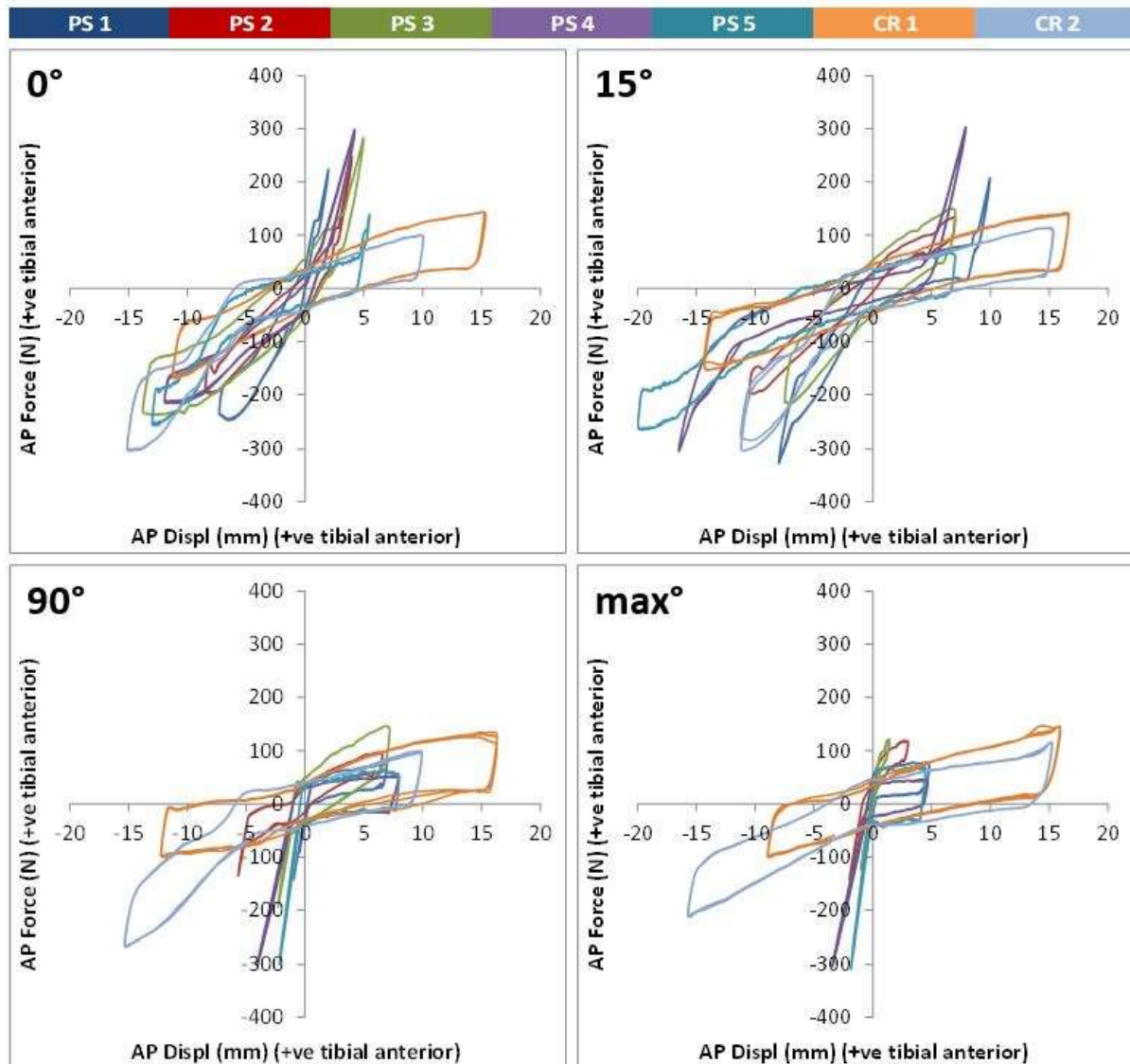


Fig. 1: AP force vs. AP displacement constraint test at 4 flexion angles. The key at the top indicates the color in which that TKR's curve is displayed.

[Figure 1](#)

IE Torque vs. IE Rotation Curves

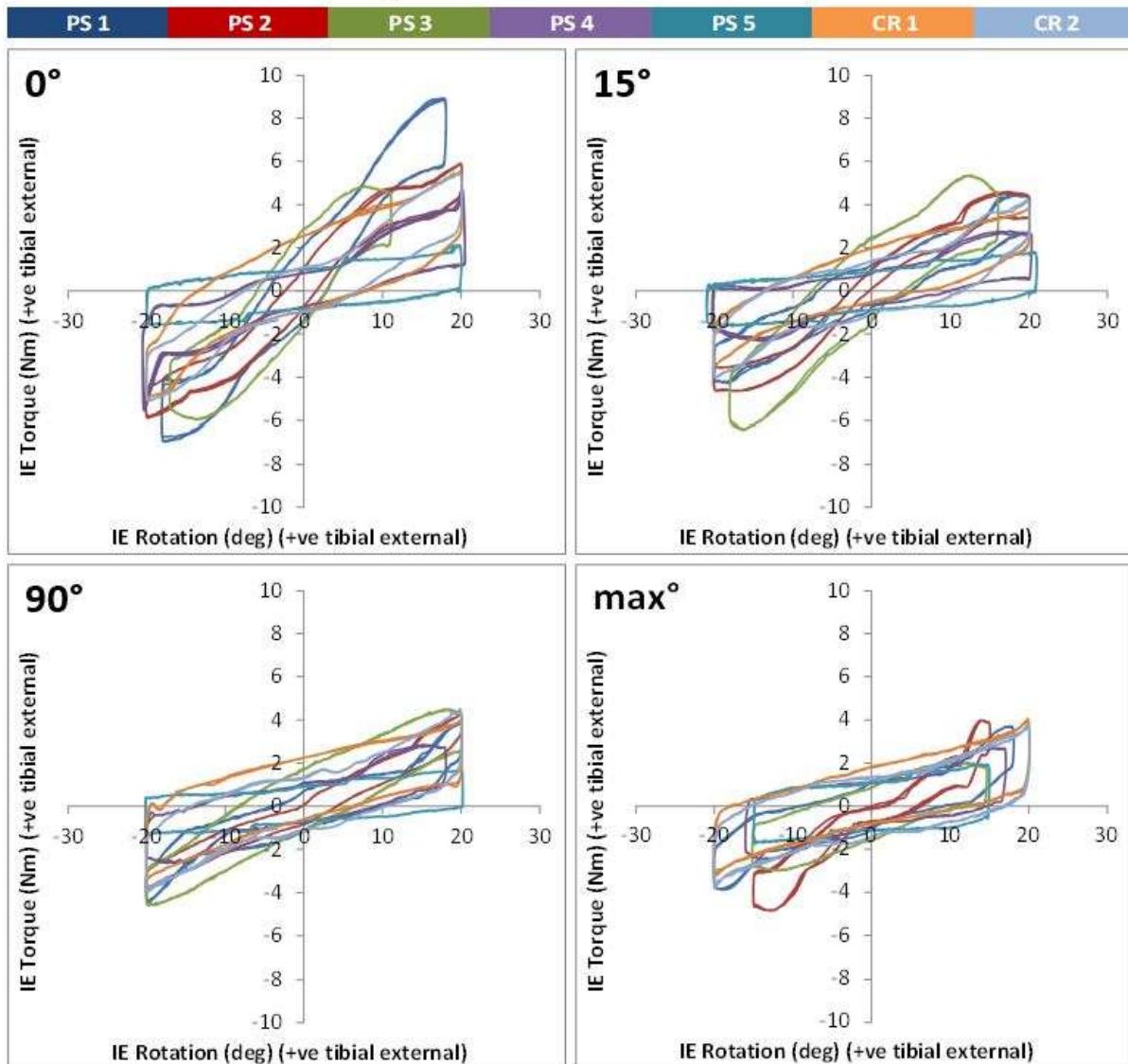


Fig. 2: IE torque vs. IE rotation constraint test at 4 flexion angles. The key at the top indicates the color in which that TKR's curve is displayed.

[Figure 2](#)

Flexion angle	Test Type	Units	PS 1		PS 2		PS 3		PS 4		PS 5		CR 1		CR 2	
			max	min	max	min	max	min	max	min	max	min	max	min	max	min
0°	AP	Peak ± AP Force (N)	224	-248	249	-198	283	-238	299	-216	139	-256	141	-166	98.4	-301
		Corresponding AP Displ. (mm)	1.98	-6.51	3.97	-8.02	4.98	-12.5	4.22	-11.1	5.49	-12.9	14.7	-11.2	9.41	-14.5
		Avg. AP Constraint (N/mm)	44.4		26.9		20.5		25.3		14.9		9.29		12.9	
	IE	Peak ± IE Torque (Nm)	8.92	-6.93	5.89	-5.86	4.84	-5.96	4.66	-5.47	2.11	-1.56	5.51	-4.90	5.42	-5.07
		Corresponding IE Angle (°)	17.5	-17.5	20.0	-20.0	7.82	-13.8	20.2	-20.4	19.6	-17.9	20.0	-20.0	19.4	-19.5
		Avg. IE Constraint (Nm/°)	0.420		0.295		0.351		0.131		0.043		0.171		0.199	
15°	AP	Peak ± AP Force (N)	208	-327	133	-198	150	-218	304	-304	67.1	-264	139	-151	113	-301
		Corresponding AP Displ. (mm)	9.98	-7.99	6.98	-10.3	6.81	-7.12	7.91	-16.5	6.41	-19.6	15.9	-13.5	14.7	-10.5
		Avg. AP Constraint (N/mm)	20.6		17.9		21.1		13.3		10.4		7.34		12.3	
	IE	Peak ± IE Torque (Nm)	4.48	-4.28	4.60	-4.65	5.37	-6.40	2.76	-2.30	1.80	-1.64	3.78	-3.42	4.21	-4.00
		Corresponding IE Angle (°)	18.4	-18.3	17.5	-17.0	12.6	-16.3	17.6	-14.4	20.6	-17.6	20.0	-20.0	20.0	-20.0
		Avg. IE Constraint (Nm/°)	0.180		0.249		0.290		0.078		0.043		0.119		0.129	
90°	AP	Peak ± AP Force (N)	82.4	-146	97.1	-134.7	146	-194	51.5	-300	64.6	-300	134	-98.1	98.2	-265
		Corresponding AP Displ. (mm)	6.71	-0.99	6.28	-5.69	6.83	-2.28	7.06	-4.03	6.65	-2.17	14.9	-11.5	9.31	-15.3
		Avg. AP Constraint (N/mm)	16.5		13.6		23.8		21.2		17.7		5.96		10.7	
	IE	Peak ± IE Torque (Nm)	3.87	-4.41	4.24	-3.85	4.50	-4.59	2.86	-2.64	1.66	-1.28	3.94	-3.34	4.49	-3.94
		Corresponding IE Angle (°)	20.0	-19.5	20.0	-19.9	18.0	-18.9	15.2	-15.2	19.6	-19.6	20.0	-20.0	20.0	-20.0
		Avg. IE Constraint (Nm/°)	0.135		0.170		0.193		0.093		0.033		0.105		0.122	
Max°	Maximum Flexion (°)		125		120		125		110		110		140		140	
	AP	Peak ± AP Force (N)	78.4	-124	119	-142	121	-124	46.0	-305	71.1	-309	146	-98.7	114	-210
		Corresponding AP Displ. (mm)	4.58	-0.99	2.68	-1.99	1.40	-0.99	4.05	-3.44	4.12	-1.86	14.7	-8.97	15.2	-15.7
		Avg. AP Constraint (N/mm)	25.3		45.8		98.5		35.6		38.9		6.62		7.39	
	IE	Peak ± IE Torque (Nm)	3.69	-3.88	3.99	-4.86	2.03	-2.98	2.73	-2.45	1.94	-1.71	4.02	-3.22	3.78	-3.78
		Corresponding IE Angle (°)	17.5	-18.7	13.9	-12.7	12.0	-11.8	15.3	-13.7	13.8	-14.8	20.0	-20.0	20.0	-20.0
Avg. IE Constraint (Nm/°)		0.127		0.233		0.123		0.080		0.043		0.097		0.094		

Fig.3: Maximum and minimum forces and torques measured during AP and IE constraint testing, as well as the corresponding displacements at which they occurred. Constraint values are also shown in N/mm and Nm/°.

Figure 3

Using Stressed HKA for Alignment in Varus Knees Show Signs of Early Recovery.

*Adam Henderson - Zimmer Biomet - Winterthur, Switzerland

Eyal Kazin - Zimmer Biomet - London, United Kingdom

Karl Surmacz - Zimmer Biomet - Swindon, United Kingdom

Mike Anderson - Zimmer Biomet - Lehi, USA

Simon Plasman - Zimmer Biomet - Wemmel, Belgium

Introduction

Personalized alignment is an increasingly popular concept in total knee arthroplasty (TKA). However, bounds for Hip Knee Ankle Angle (HKA) remain debated, partially due to the absence of sensitive outcome measures. Robotic assisted TKA provides initial laxity information that can be used to derive an estimate for constitutional alignment and accurately apply this plan. Functional gait data obtained from a digital care management platform can subsequently be utilized to objectively evaluate the influence of surgical decisions.

Methods

Anonymized intra- and post-operative data from a commercial database of patients were analyzed (n=9,647). A subpopulation analysis was performed focusing on patients who had a minimum valgus laxity greater than 2° and a maximum varus laxity less than 10° varus (n=960) during their stress test. The majority of patients were male (54.7%) and the mean age was 66.4 years. Data were captured from the robotic system's log files and a digital care management platform using a smartphone's gait metric analysis.

The theoretical native alignment was calculated as one degree more varus than the maximum valgus as this partially unloaded the medial collateral ligament. The knees were split into a group that matched the native alignment within two degrees and those nonmatching. Differences between the groups were compared using the change between the pre-operative and post-operative gait metrics between groups at 15-, 30-, and 90-day post-operative time. The differences in medians of the distributions were assessed using Mann-Whitney U tests and differences in distributions using Kolmogorov-Smirnov two sample tests at a significance level of < 0.05.

Results

The patients that had their implants close to matching the native alignment showed a statistically significant faster recovery in terms of relative performance of gait speed (p=0.03; Figure 1) and asymmetry (p=0.04; Figure 2) at 15 days postoperative. The difference in alignment strategy were apparent but less pronounced at 30 days, and negligible at 90 days. We found similar findings when examining males and females separately as well as different age ranges.

Discussion

These analyses present a simple method that can be used to set an initial target for final HKA that could result in a slightly faster recovery in the early post-op period. The study shows this change as a beneficial nudge toward personalized treatment; however, more evidence is needed to substantiate these findings as well as looking closer at different surgical philosophies and how they change the joint line obliquity.

Figures

Figure 1. Violin plot showing alignment strategy vs gait speed across gender at 15 days post-operative (Left) and 90 days post-op (Right).

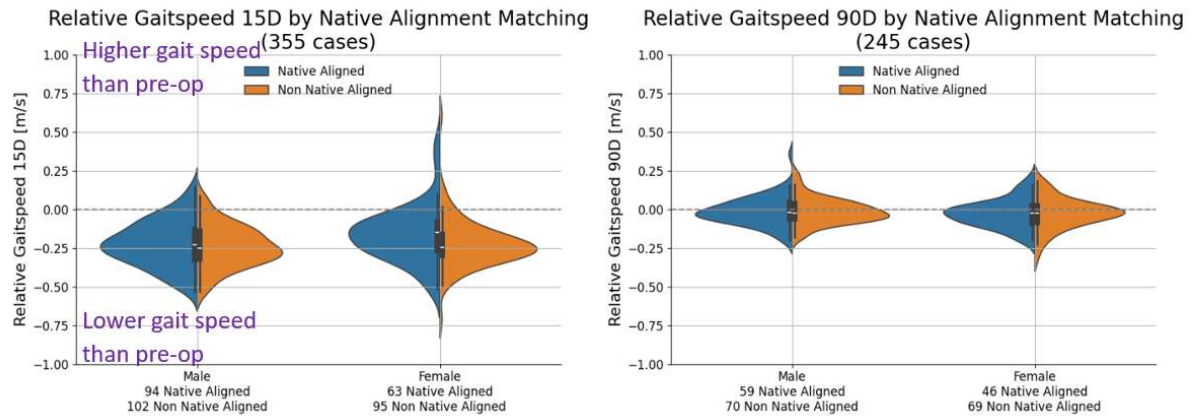


Figure 1

Figure 2. Violin plot showing alignment strategy vs in gait asymmetry across gender at 15 days post-operative (Left) and 90 days post-op (Right).

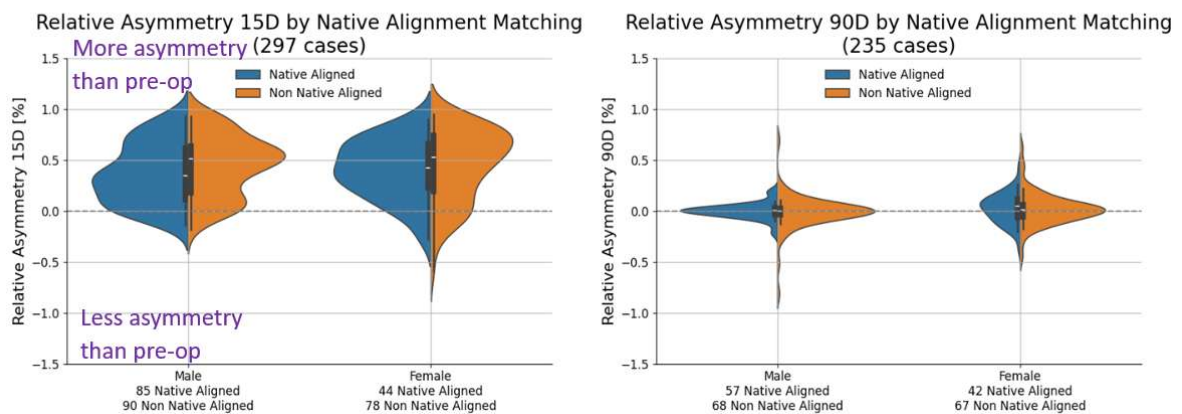


Figure 2

TKA Joint Line Obliquity Post-Op Comparisons for External Knee Adduction Moments During Stair Descent

*Alexis Nelson - UTHSC - Memphis, Select Country

Nuanqiu Hou - Campbell Clinic - Memphis, United States of America

Douglas W. Powell - University of Memphis - Memphis, USA

Marcus Ford - Campbell Clinic Orthopaedics - Germantown, USA

James Guyton - Campbell Clinic Orthopaedics - Germantown, USA

John Crockarell - Campbell Clinic Orthopaedics - Germantown, USA

Christopher Thomas Holland - Campbell Clinic Orthopaedics - Tennessee, United States of America

Derek Dixon - Campbell Clinic Foundation - Germantown, USA

Teri Ross - University of Tennessee Health Science Center - Memphis, USA

William Mihalko - University of Tennessee - Memphis, USA

Disclosure: This study was funded by Medacta International

Introduction: Knee joint alignment is thought to impact knee joint biomechanics and influence patient outcomes after total knee arthroplasty (TKA). Achieving neutral alignment was shown to produce optimal clinical outcomes (Fang et al., 2009). However, recent studies demonstrated that restoring patients' natural lower extremity alignment lead to improved patient reported outcomes (Howell et al., 2013) and reduced knee adduction moments (Niki et al., 2018). Our aim was to understand whether the difference between preoperative and postoperative knee joint alignment impacts biomechanical variables during stair descent.

Methods: We included 58 patients who received cruciate retaining implants. All patients underwent unilateral TKA and are at least one-year post-op. A three step instrumented staircase (1000Hz, AMTI Inc., Watertown, MA) and an 8-camera markerless motion capture system (200Hz, OptiTrack, NaturalPoint Inc., MA) were used to collect ground reaction forces and segment kinematics, respectively, during stair descent. An AI based reconstruction software (Theia Markerless, Inc., Version 2023, Kingston, ON) was used to identify segment kinematics. Joint line convergence angle was measured using anteroposterior weight bearing radiographs. Visual3D Professional (HAS Motion, Version 2023.09.3, Canada) and MATLAB (The MathWorks, Inc., R2023b, Natick, MA) were used for data analysis. An independent sample t-test was used to compare external peak and mean knee adduction moment and impulse between patients who had a change in knee joint alignment and those who maintained the same knee joint alignment postoperative.

Results: A change in knee joint alignment was observed in 34 patients. 24 patients maintained their natural alignment postoperative. There were no significant differences in age or BMI between groups. We did not observe a significant difference in external mean knee adduction/abduction (Figure 1b, $p=0.0502$), external peak knee adduction moment (Figure 1a, $p=0.234$), and adduction/abduction impulse (Figure 1, $p=0.172$).

Conclusion: We aimed to understand the impact that knee joint alignment changes had on knee joint biomechanics. Whether patients' natural knee joint alignment was maintained did not significantly impact external peak knee adduction moment nor impulse.

Reference:

Fang, D. M., Ritter, M. A., & Davis, K. E. (2009). Coronal alignment in total knee arthroplasty: just how important is it? *J Arthroplasty*, *24*(6 Suppl), 39-43.

Howell, S. M., Papadopoulos, S., Kuznik, K. T., & Hull, M. L. (2013). Accurate alignment and high function after kinematically aligned TKA performed with generic instruments. *Knee Surg Sports Traumatol Arthrosc*, *21*(10), 2271-2280.

Preclinical Development of Endoprosthetic Implants for Replacement of Lost Limbs

*Dustin Crouch - University of Tennessee-Knoxville - Knoxville, United States of America

David E Anderson - University of Tennessee-Knoxville - Knoxville, USA

Stacy M. Stephenson - University of Tennessee Graduate School of Medicine - Knoxville, USA

Introduction: As many as 45% of amputees abandon limb prostheses [1] partly because they fail to restore natural function and appearance. This is not surprising since all existing prostheses are worn externally, and most are physically detached from neuromuscular tissues. Therefore, to address limitations of existing prostheses, we are developing orthopedic endoprosthetic implants that are completely enclosed within living skin and physically attached to muscles for direct neuromuscular control of endoprosthesis motion. A practical target for first-in-human use is the thumb (Fig. 1A) since it is critical for hand function and requires relatively low skin coverage. Recently, we have developed endoprosthesis prototypes and performed in vivo testing in a New Zealand White rabbit hindlimb below-knee amputation model. This model was chosen because the size and load magnitudes are relevant to that of the human thumb.

Methods: Foot and shank segments of the device prototype were modeled in computer-aided design software (Solidworks, Dassault Systemes), 3D printed in 316 Stainless Steel, molded within a biomimetic silicone (BIO M340, Elkem), and joined with a polyethylene hinge pin. We tested three different prototypes in order of increasing size and complexity to assess skin wound healing: a linear, 2-cm-long unjointed stem [2], an angled unjointed foot-ankle endoprosthesis [3], and a jointed foot-ankle muscle-driven endoprosthesis (Fig. 1B). The triceps surae and tibialis cranialis muscles were attached across the ankle joint using artificial tendons that consisted of braided, silicone-coated polyester suture. Prototypes were implanted at the time of amputation and completely enclosed in a contiguous skin flap that was salvaged from the amputated segment. In rabbits with jointed foot-ankle muscle-driven endoprostheses, we measured hindlimb biomechanics during hopping gait using an infrared motion capture system (Motive, OptiTrak) and pressure sensing mat (Strideway, Tekscan).

Results & Discussion: The skin fully healed and closed in 3 of 6 rabbits with the unjointed stem [2], in 3 of 3 rabbits with the angled unjointed foot-ankle implant [3], and in 4 of 5 rabbits with the jointed foot-ankle implant (Fig. 1C). Preliminary data during hopping gait showed that stance time (Fig. 2A), normalized peak vertical ground contact force (Fig. 2B), and ankle joint total range of motion (Fig. 3) generally decreased from pre- to post-surgery but improved over time post-surgery. Passive ankle range of motion in the jointed foot-ankle implant was limited due to fibrous encapsulation. Future research directions include (1) optimizing the device-tissue interface, (2) testing in various amputation scenarios, and (3) designing the thumb endoprosthesis in preparation for clinical trials.

Acknowledgements: UTK Office of Laboratory Animal Care. NIH R61AR078096 and K12HD073945, NSF CAREER 1944001.

References: [1] Salminger et al. (2022), *Disabil Rehabil* 44(14); [2] Hall et al. (2021) *Ann Biomed Eng* 49(3). [3] Crouch et al. (2022) *Bioeng* 9(8).

Figures

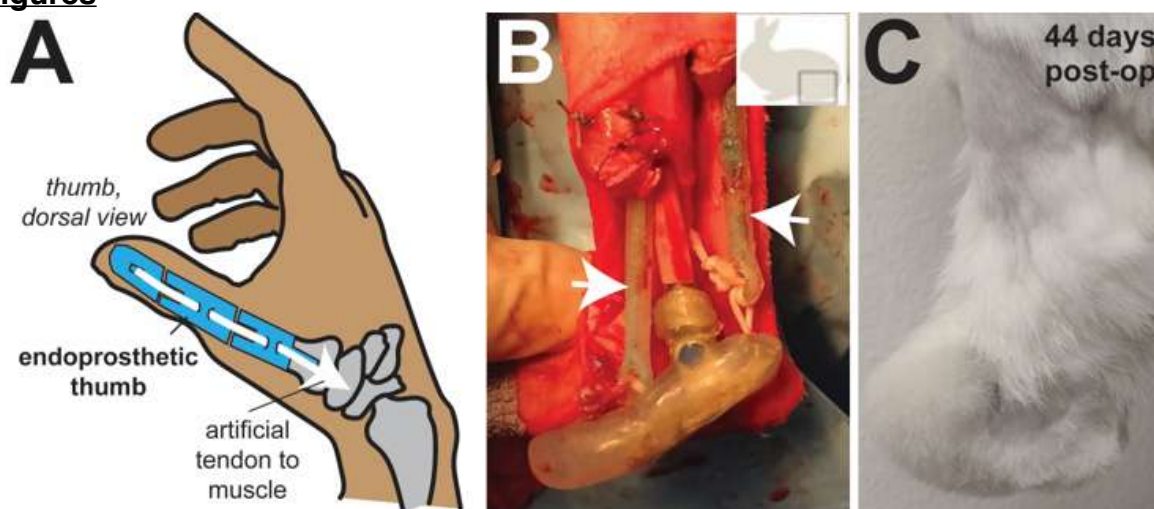


Figure 1: (A) **Jointed**, muscle-driven endoprosthesis thumb concept. (B) Jointed foot-ankle muscle-driven endoprosthesis prototype in rabbit hindlimb ankle just before enclosing with skin flap. Arrows indicate silicone-coated polyester artificial tendons. (C) Rabbit hindlimb with jointed foot-ankle endoprosthesis 44 days post-surgery.

[Figure 1](#)

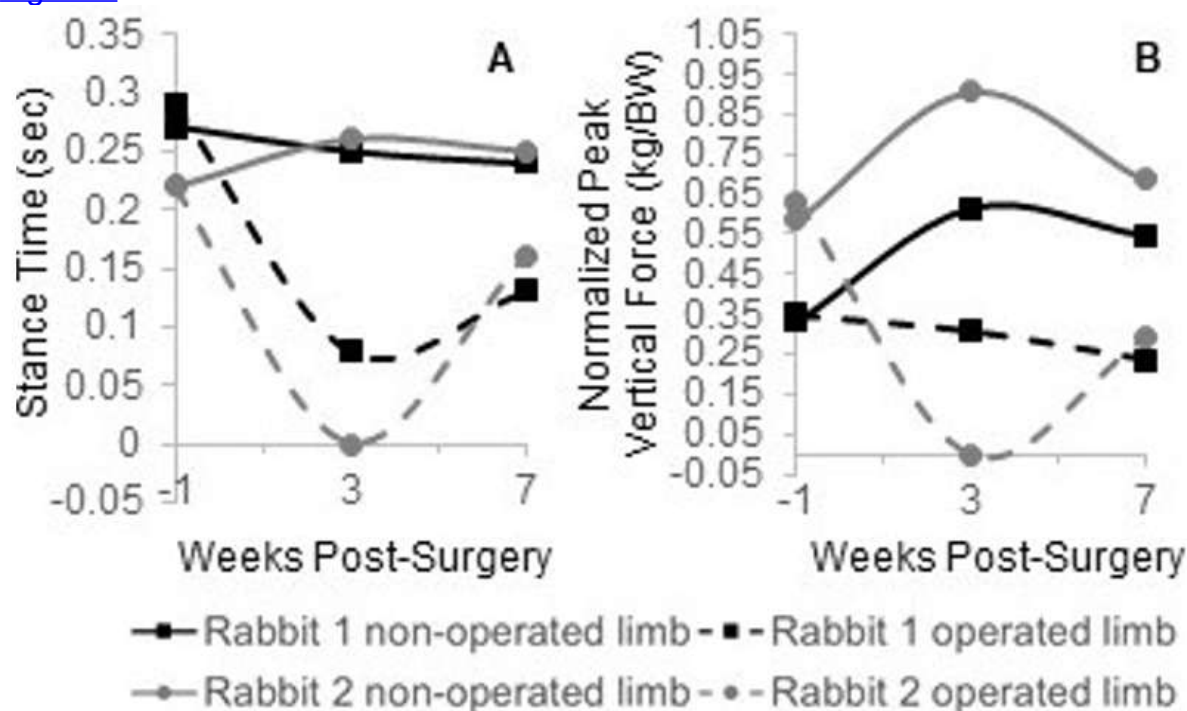


Figure 2: A) Stance time and B) Normalized peak vertical force, averaged across 9 - 11 gait cycles at each timepoint.

Figure 2

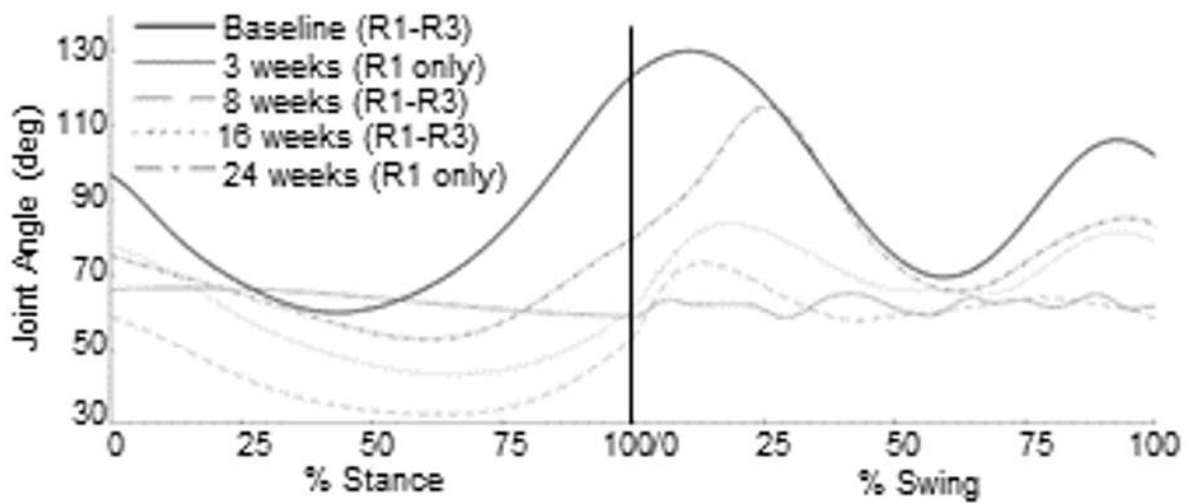


Figure 3: Ankle joint angle over stance and swing phase of gait for different timepoints. Three and 24-weeks post-surgery are for rabbit 1 only. The other timepoints are averages for the 3 rabbits.

Figure 3

Differences in Cementless Total Elbow Arthroplasty Stem Design Depending on Degree of Bone Loss

*Yupin Shi - Hospital for Special Surgery - New York, United States of America

Joseph Lipman - Hospital for Special Surgery - New York, USA

Fernando Quevedo Gonzalez - Hospital for Special Surgery - New York, USA

Timothy Wright - Hospital for Special Surgery - New York, USA

Robert Hotchkiss - Hospital for Special Surgery - New York, USA

Introduction:

Total elbow arthroplasty (TEA) is generally performed with cemented implants; however, cementless fixation may be an attractive choice due to the increased longevity of biologic fixation. Previous work characterized the geometry of various cemented elbow stems [1] and classified the bone defect for cemented TEA analysis [2] but no similar work was done for cementless TEA. Understanding how the amount and location of bone loss affect the optimal design for cementless stem geometry can assist us in developing design principles tailored to specific bone anatomies.

Methods:

We identified 29 cementless humeral stems including 5 standard stems (all Lima) and 24 patient-specific stems (11 Lima, 5 Latitude, 4 Discovery, 3 Coonrad/Morrey, and 1 Osteonics), and 30 cementless ulnar stems including 12 standard stems (all Lima) and 18 patient-specific stems (5 Lima, 5 Latitude, 5 Discovery, 3 Coonrad/Morrey) implanted from March 1998 to March 2024 at our institution. To determine whether a relationship exists between the preoperative bone loss and the implant design, the extent of preoperative bone loss was measured on preoperative radiographs and classified into three types with decreasing amount of bone loss: damaged bone without metaphysis (type I), damaged bone with metaphysis (type II), and intact bone (type III). The stems were classified into two types according to their diaphyseal and metaphyseal characteristics (Fig. 1): smooth diaphysis with wedged metaphysis (wedged stem), and fluted diaphysis with conical metaphysis (fluted stem). The diameter, length, and ingrowth area were measured on available CAD models. Stem dimensions were compared using T-tests with a significance of 0.05.

Results:

Nine humeri were classified as type I, two as type II, and eighteen as type III. All type I humeri and one type III humerus received fluted stems, while all type II and the rest of type III humeri received wedged stems (Fig.2). Fluted stems in type I humeri were designed to be longer (107mm-155mm vs. 90mm-102mm, $p=0.0003$) and have a larger diameter (7mm-14mm vs. 6mm-9mm, $p=0.0008$) to engage more contact with the endosteal surface for initial fixation, and have greater ingrowth area (877mm²-2084mm² vs. 427mm²-1199mm², $p=0.001$) to achieve more potential bone ingrowth for long-term fixation than wedged stems in type III humeri.

Three ulnae were identified as type I, three as type II, and twenty-four as type III. All type I ulnae and one type III humerus received fluted stems, while all type II and the rest of type III ulnae received wedged stems (Fig.2). Fluted stems in type I ulnae with less metaphysis for bone ingrowth were designed to have less ingrowth area (196mm²-470mm² vs. 410mm²-1243mm², $p=0.02$).

Conclusion:

Fluted stems were used more often in type I humerus and ulna and wedged stems were used more often in type II&III bones. Humeral fluted stems were generally

longer and had a larger diameter and greater ingrowth area than wedged stems. Ulnar fluted stems had less ingrowth area than wedged stems.

References:

[1] Evans et al Clinical Mat 1988 [2] Morrey et al J Bone Joint Surg 2007

Figures

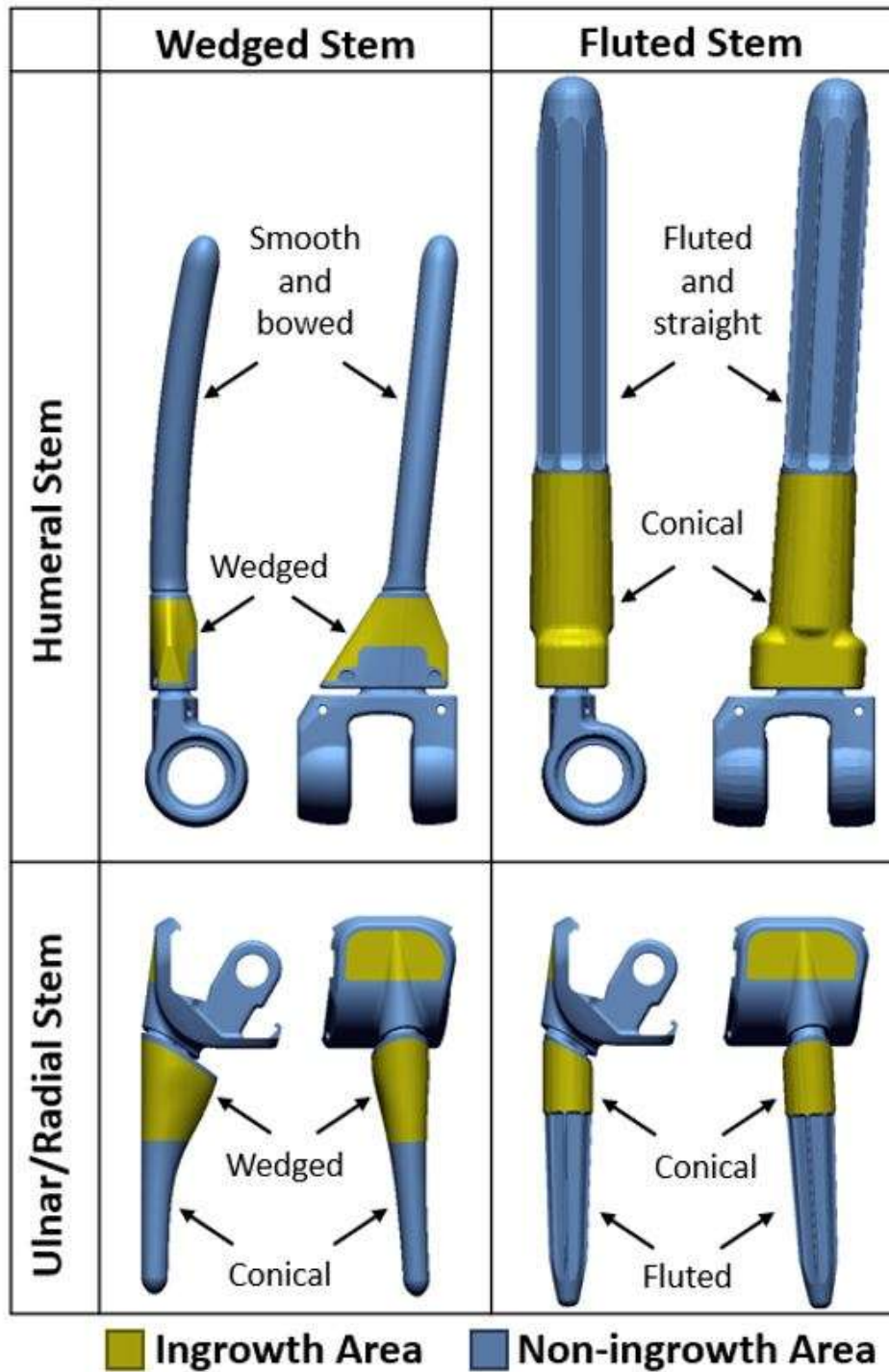


Fig.1 – Examples of humeral wedged stem & fluted Stem and ulna wedged stem & fluted Stem with ingrowth and non-ingrowth Area.

Figure 1

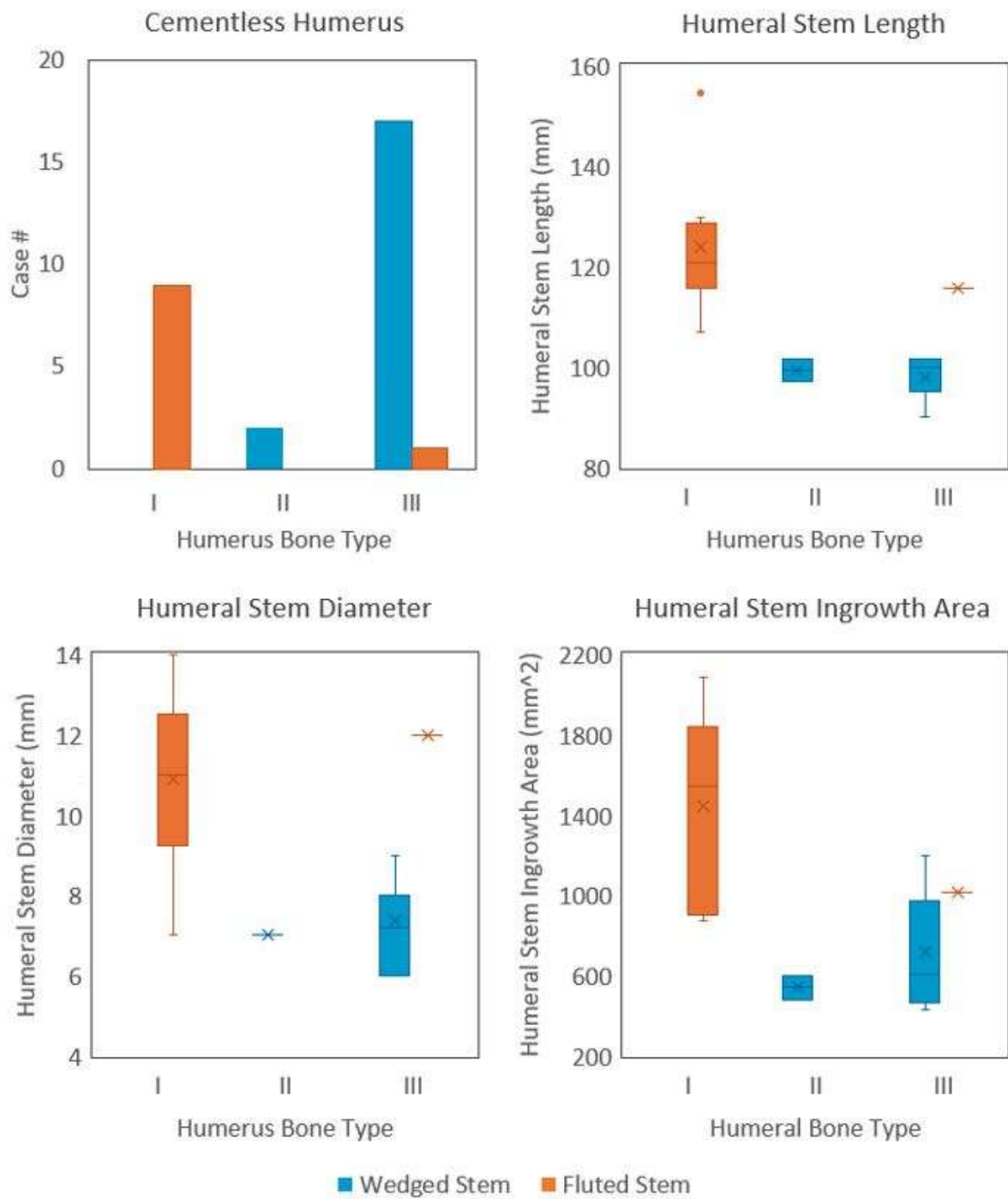


Fig.2 – The number of cases, stem length, stem diameter, and stem ingrowth area of wedged and fluted humeral stems implanted in type I, II and III humerus.

Figure 2

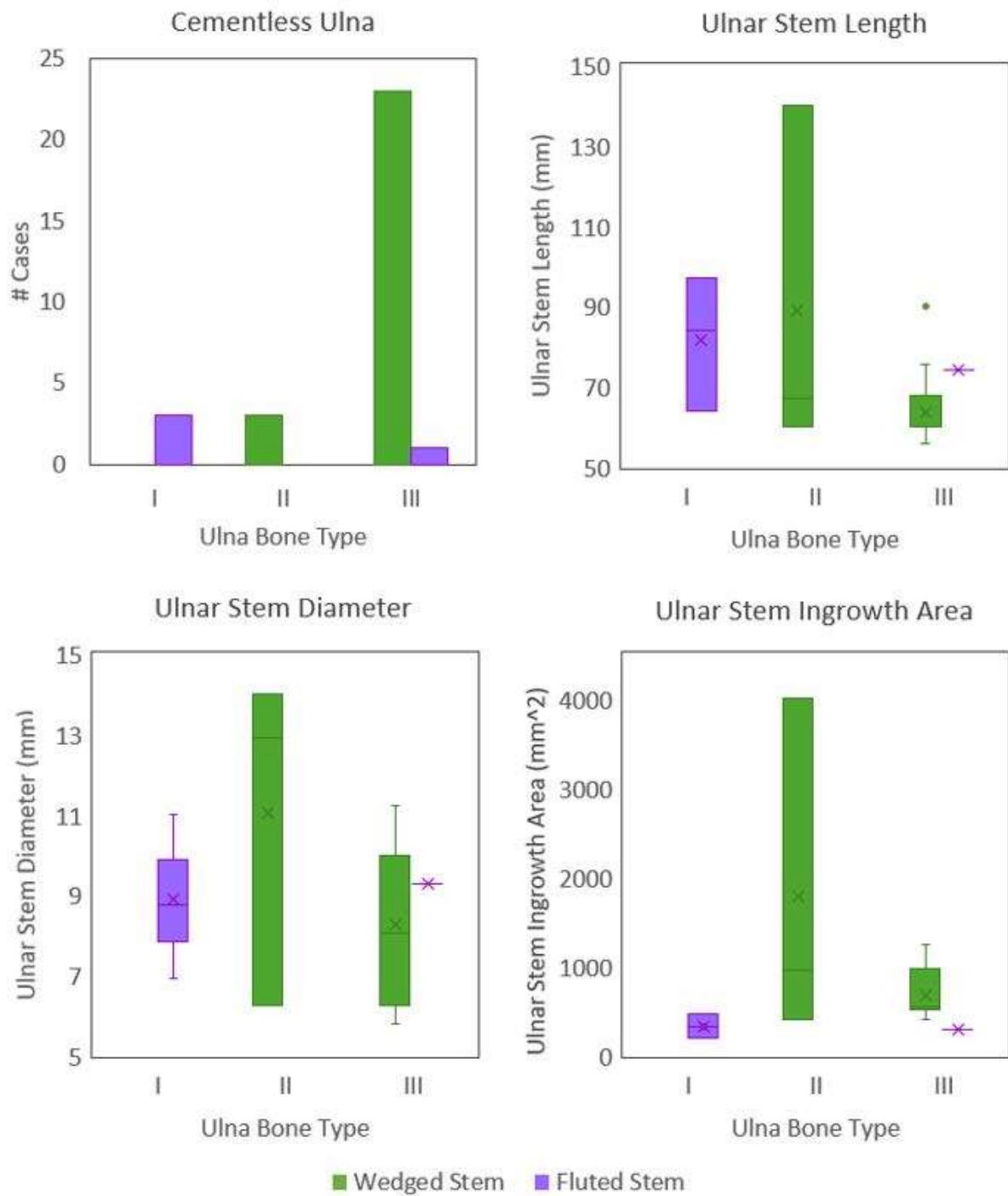


Fig.3 – The number of cases, stem length, stem diameter, and stem ingrowth area of wedged and fluted ulnar stems implanted in type I, II and III ulna.

[Figure 3](#)

Development of an Implantable Trapezium Replacement for Measuring in Vivo Loads at the Base of the Thumb

*J.J. Trey Crisco - Brown University - Providence, USA

Julia Henke - Brown University - Providence, USA

Daniel McDermott - Brown University - Providence, USA

Amy Morton - Brown University - Providence, USA

Josephine Kalshoven - Brown University - Providence, USA

Douglas Moore - Brown University - Providence, USA

Rohit Badida - Brown University - Providence, USA

INTRODUCTION: A functional and pain-free thumb is critical to accomplishing many activities of daily living. The thumb is also a common site for both acute trauma and the repetitive workplace injury and osteoarthritis. Investigators have used musculoskeletal modeling to understand and mitigate workplace-associated injuries. Notably, for this project, a common surgical treatment for thumb base osteoarthritis is the removal of the trapezium carpal bone (Fig. 1A). Understanding the loads at the base of the thumb during activities of daily living would advance and validate musculoskeletal modelling, and inform the approaches to clinical treatments, especially arthroplasty design and the scope of preclinical testing for FDA clearance. The ultimate goal for this project is to develop an instrumented replacement trapezium capable of measuring the loads in vivo. In this abstract we present two strain gage-based load sensor design options and report on the accuracy associated with two different approaches to calibration and with strain gauge drop out.

METHODS: An initial ("Tube") design was based on previous designs implemented in successful instrumented total knee arthroplasty implants that measure the loads across the knee joint during activities of daily living. The Tube design incorporated a central sensing column with 3 circumferentially placed rosette strain gages (Fig. 1B). Although well-established for larger joints, this approach affords limited space for internal electronics, due to the small size of the trapezium (17x15x25mm³). A subsequent design iteration used a diaphragm as the sensing element with five gauges bonded to the underside of the Diaphragm (Fig. 1C), designed to be welded to a container that houses the electronics (inductive power receiver, signal conditioner, amplifier and bluetooth data transmission). Calibration was performed with a 6 DOF load cell and using a supervised neural network. Loading along the longitudinal axis of the first metacarpal (F_y) was set as the most critical outcome measure. Accuracy was defined as the 95% CI of the limits of agreement (LOA) using a Bland-Altman analysis.

RESULTS: The 95% CI LOA in F_y was significantly less in the Diaphragm design (1.9 N) than in the Tube design (19.7 N). Strain gauge removal had variable effects, depending on sensor design and the number and locations of the gauges removed. For example: Removing individual gauges in the Diaphragm design increased the 95% CI LOA for F_y by 3.0 N, 3.9 N, and 5.0 N, respectively. On the other hand, removal of 2 of the 9 gauges in the Tube design (separately) increased the 95% CI LOA for F_y to 25.8 N and 28.1 N.

CONCLUSIONS: We present a novel design for a trapezium replacement instrumented to measure loads across the thumb carpometacarpal joint. An instrumented trapezium capable of measuring loads at the base of the thumb will be immensely valuable to clinicians, researchers, and implant designers who need accurate load data to understand the role of joint loading in thumb pathophysiology,

to refine musculoskeletal models, to standardize pre-clinical testing, and to develop more effective and cost-effective surgical treatments.

ACKNOWLEDGEMENTS: This research was funded in part by NIH/NIAMS R21AR077201.

Figures



Fig. 1A. Palmar view of the skeletal hand segmented from a CT volume image. The trapezium carpal bone (Tpm) will be replaced with the load sensing Tpm in patients undergoing trapeziectomy for severe osteoarthritis.

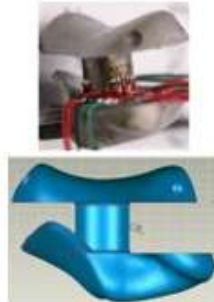


Fig. 1B. Tube design showing strain gauges for benchtop calibration.



Fig 1C. The underside of the distal component of the Diaphragm design instrumented with 5 strain gauges (L). An exploded view of the components of the Diaphragm design: distal articulating surface, diaphragm, container, and trapezium body with proximal articulating surfaces (R, top to bottom).

[Figure 1](#)

Formal Risk-Informed Validation of a Finite Element Model for Lumbar Spine Total Joint Replacement Under Normal and Impingement Conditions

Steven Rundell - Explico, Inc. - Novi, USA

Ron Yarbrough - 3Spine - Chattanooga, USA

*Steven Kurtz - Drexel University - Philadelphia, USA

Introduction: A novel total joint replacement (TJR) that treats degeneration in the anterior, middle, and posterior columns of the lumbar spine has been previously assessed under *in vitro* Mode I and Mode IV conditions [1]. In the present study, we relied on these previous wear tests to establish a relationship between finite element model (FEM)-based bearing stresses and *in vitro* wear metrics. The purpose of our modeling effort was to “simulate the simulator” and address the following question of interest: What are the bearing stresses for the L-TJR during Mode 1 (best-case, non-impingement) and Mode 4 (impingement) wear-test simulator duty-cycle boundary conditions?

Methods: The FEM is a solid mechanics simulation of the bilateral cranial and caudal components of the LTJR under wear testing boundary conditions (i.e., loading and displacements of the duty cycle). The model was based on CAD geometry of the *in vitro* wear testing setups described previously [1] and were analyzed using ANSYS LS-DYNA (vR15) (Fig. 1). The FEM was formally validated using the risk informed credibility assessment framework established by ASME V&V40-2018 that was adopted in 2023 FDA Guidance (Fig. 2). The context of use (COU) for the FEM is to assess the sensitivity of the L-TJR to misalignment in the coronal and axial planes. The model risk was assessed as low based on its COU for relative risk assessment comparing against two wear test scenarios with accepted low risk [1].

Results: The credibility plan included six verification and three validation activities, including direct comparison against MicroCT penetration maps from Mode I and Mode IV testing as “ground truth.” FEM results were compared with pre- and post-test microCT scans that were overlaid to create penetration maps (Fig. 3 d) [1]. The FEM was consistent with physical Mode I and IV penetration maps. In simulated Mode I conditions, the peak contact stress was 39 MPa and occurred at or near to 100% of the duty cycle. The simulation of Mode IV impingement resulted in higher contact pressures, internal stresses, and plastic strain (Fig. 3a-c). The peak contact pressure for the long implant was 83.8 MPa and 102.4 for the short design.

Discussion: The results of this study support that the LTJR FEM is credible for its context of use (COU). This study is also novel for adopting the ASME V&V 40 standard framework and FDA’s latest guidance for formal validation of a LTJR FEM. Bartel et al. [2] reported maximum contact pressures ranging from 40 to 60 MPa for contemporary TKA, which is generally greater than what was reported in the current model under Mode I conditions (39 MPa). Overall, these prior TKA results are reasonably analogous to those for the LTJR under Mode I (non-impingement) conditions. In contrast, the Mode IV (impingement) stress values provide an upper bound for risk assessment of future misalignment assessments using this validated FEM.

References: 1. Siskey et al., *Bioengineering*, 10(10), 2023; [2] Bartel et al., *CORR*, 1995.

Figures

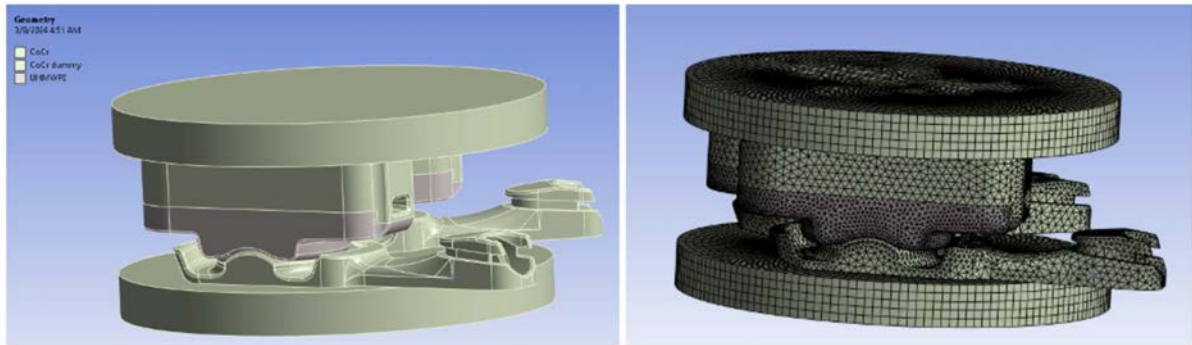


Figure 1 CAD surfaces and FEM Model of the in vitro wear simulator [1].

Figure 1

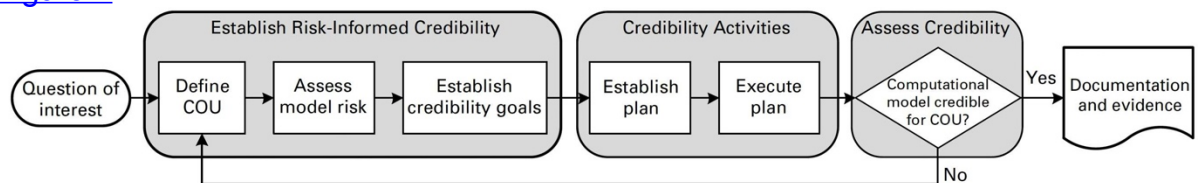


Figure 2 Process Flow Diagram of the Risk Informed Credibility Assessment

Figure 2

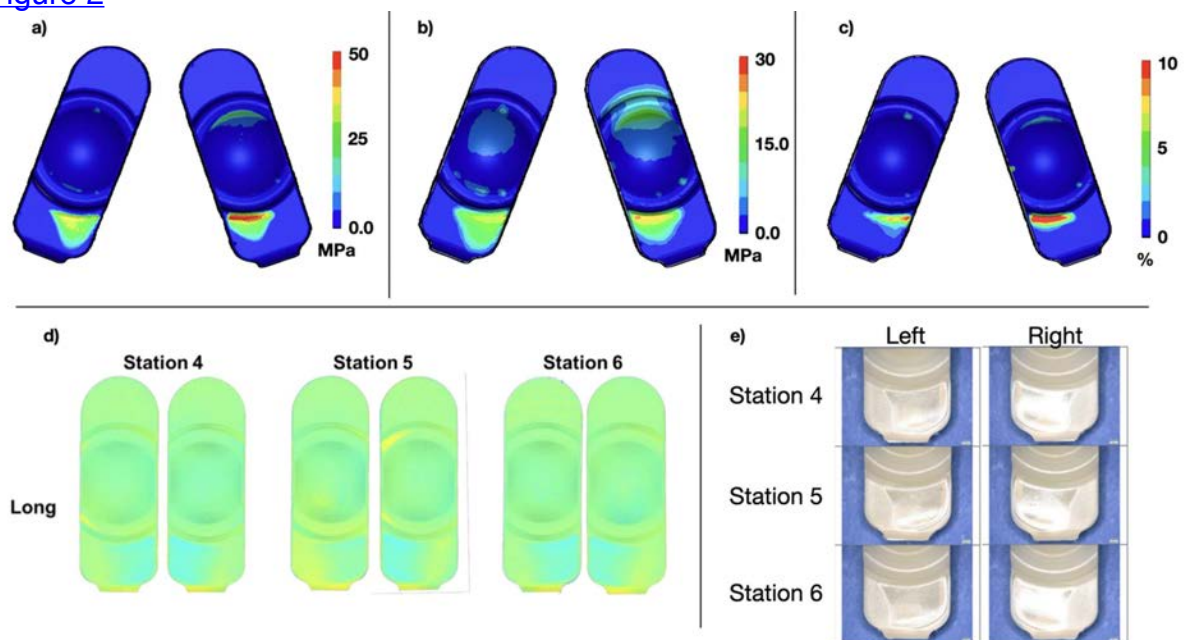


Fig. 3. Cumulative contours of maximum contact pressure across the Mode IV duty cycle (a), cumulative maximum von Mises stress (b), and cumulative plastic strain. Penetration maps based on microCT scans (d) and photo documentation (e) after 1 million cycles of Mode IV duty cycles is also shown.

Figure 3

Safety and Tribology of a Design Optimized Ceramic Bearing for a Cervical Total Disc Replacement

*Lucia Kölle - ETH Zürich - Zürich, Switzerland

Gregory Pryce - University of Leeds - Leeds, United Kingdom

Andrew Robert Beadling - University of Leeds - Leeds, United Kingdom

Michael Bryant - University of Birmingham - Birmingham, United Kingdom

Benedikt Helgason - ETH Zurich - Zurich, Switzerland

S J Ferguson - Zurich, Switzerland

Richard M. Hall - University of Birmingham - Birmingham, United Kingdom

Introduction

Arthroplasty using Total Disc Replacements (TDRs) is commonly performed on the cervical spine. However, reoperation rates are significant: 5.2% in the index level at 7-year follow-up (1). Pre-clinical testing should be completed in a manner that represents activities of daily living and adverse events. Tribology data is essential for computer simulations of systems containing articulating TDRs, however depends on many factors including geometry. Therefore, this study aims to investigate the tribology of a TDR bearing as well as safety in adverse events. To this end, advanced preclinical testing of a novel TDR bearing is performed.

Methods

A ball-in-trough bearing design for a ceramic cervical TDR was computationally optimized to replicate the native segmental moment-rotation curve during coupled flexion/extension-anterior/posterior translation motion (2). Samples of the bearing were manufactured from zirconia-toughened alumina ceramic (Figure 1) and tested in a six-degree-of-freedom joint simulator in diluted calf serum (20g \pm 2g protein/l) at body temperature (37°C (+/-2°C) (Figure 2). Friction measurements were made with load- and motion profiles simulating daily living: (a) +/- 7.5° flexion/extension; (b) +/- 6° lateral bending. Both were applied under 100N static axial load (5 samples, 200 cycles). Safety in adverse events was evaluated with three subluxation test conditions: (a) 6.5mm anteriorly with parallel endplates; (b) 6.5 mm posteriorly with endplates at 12° extension and (c) 5mm laterally with parallel endplates. Displacement applied at 6 mm/min under 100N static axial load (5 samples, 10 cycles).

Results

The dynamic friction coefficients during pure flexion/extension and lateral bending were $\mu = 0.16 \pm 0.01$ (mean \pm SD) and $\mu = 0.16 \pm 0.06$ (mean \pm SD) respectively (Figure 3). Subluxation testing indicated that resistance to subluxation was sufficient (>2x the typically required 20N in FDA Summary of safety and effectiveness data) (Figure 3). Surface roughness was comparably low (Ra: superior part: 21.91 \pm 2.5nm; inferior part: 35.38 \pm 12.3nm) but radial clearance was considerably higher than intended (0.24 \pm 0.05mm, instead: 0.07mm), which likely increased friction.

Conclusion

Friction values of the manufactured ball-in-trough samples were comparable to or higher than those reported for ceramic-on-ceramic hip replacements but lower than those reported for TDRs with other bearing materials. Furthermore, this study indicated that the proposed bearing design is sufficiently resistant to subluxation.

References:

1. Badhiwala et al., J. Spine Surg. 6, 2020.
2. Kölle et al., Presented Abstracts: ISTA 2023.

Acknowledgements:

Funding: European Union’s Horizon 2020 programme: Marie Skłodowska-Curie grant agreement No 812765.

Figures

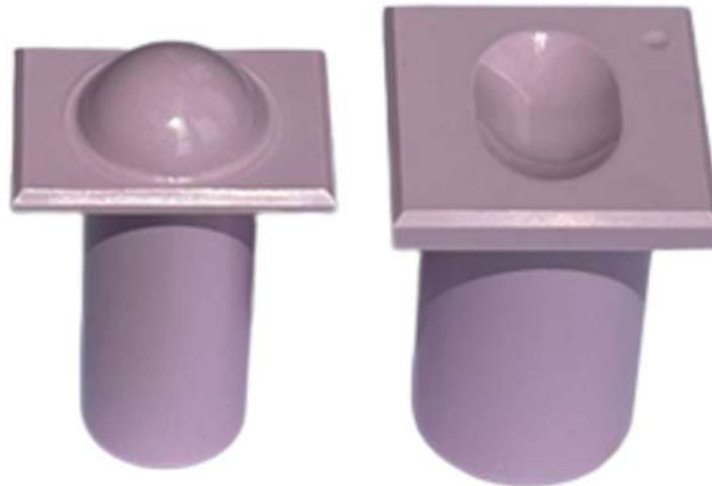


Figure 1: Ceramic sample. Left: superior part, right: inferior part. The bearing surfaces are polished. The small deepening on the inferior part (on the top right in this picture) marks the posterior side. The cylinders provide secure mounting in the testing device.

Figure 1

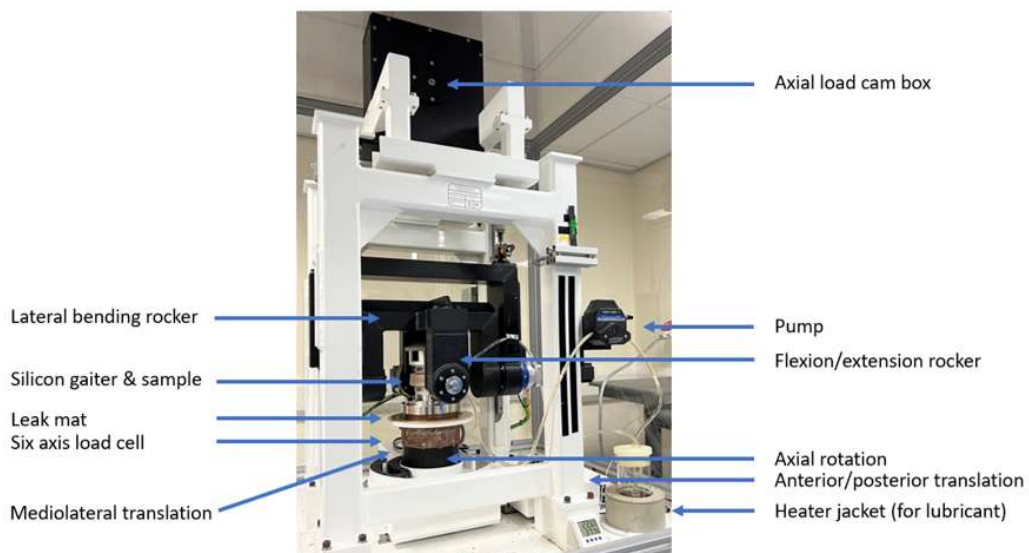


Figure 2: Universal Joint Simulator (Prosim 1-Station Universal Simulator, Simulation Solutions Ltd, UK). The silicone gaiter is fixed to the Polyoxymethylene fixtures. The heater jacket maintains the desired temperature of the lubricant and the pump transports it to the silicone gaiter under constant flow.

Figure 2

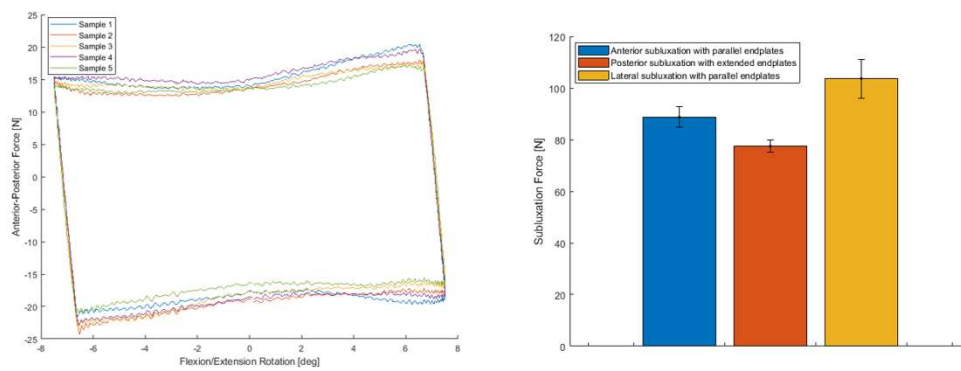


Figure 3: Friction loop of the flexion/extension test (Top Left). Subluxation forces measured during subluxation experiments (Top Right). The 180th-189th cycles were evaluated, except for the subluxation tests, for which the eight cycles were evaluated.

[Figure 3](#)

Hyperspectral Chemical Imaging Reveals Spatially Varied Degradation of Artificial Nucleus From M6-C Cervical Disc

*Songyun Liu - University of Illinois at Chicago - Chicago, USA

Donna Ohnmeiss - Texas Back Institute - Plano, USA

Dino Samartzis - Rush University Medical Center - Chicago, USA

Deborah Hall - Rush University Medical Center - Chicago, USA

Guyer Richard - Texas Back Institute - Plano, USA

Alexander Satin - Texas Back Institute - Plano, USA

Scott Blumenthal - Texas Back Institute - Plano, USA

Robin Pourzal - Rush University Med Ctr - Chicago, USA

Introduction: Cervical neck pain is on the rise worldwide. Intervertebral disc degeneration is a factor attributed to neck pain. Anterior cervical discectomy and fusion (ACDF) has been the gold-standard for the management of neck pain with/without radiculopathy. The use of cervical total disc replacement (CTDR) preserves the motion at individual level and mitigates drawbacks, such as elevated intradiscal pressure, compared to traditional ACDF procedure. Among FDA-approved CTDRs, M6-C™ is unique by allowing all six degree-of-freedom. Recently, high revision rates due to ossification, osteolysis and/or implant failure have been reported in a 6.5-11 years follow-up study that demonstrated potential risks of long-term complications. To date, the majority of outcome studies of the M6-C™ device have been for single-level use; whereby, multi-level applications and their outcomes remain largely unknown. Our study is a report of a case whereby a patient underwent application of the M6-C™ device from C4-C7 which resulted in instrumentation failure and removal. Our goal was to characterize material degradation from implant components, primarily of the artificial nucleus, of the M6-C™ device.

Methods: The patient was symptoms free for 16 years, but the implants were removed after 17 years due to C7 radiculopathy, numbness, and weakness. The pre-op radiographic imaging showed significant remodelling of the bones at all three levels (C4-C7). A severe osteolytic lesion can be seen at endplates between C5-C6 level (**Fig.1**). The collapse of the disc led to compressing of the oesophagus with abnormal soft tissue mass. The retrieved individual artificial nucleus was imaged using light microscope to assess the deformed surface topography, and then sliced into 10- μ m sections in the A-P direction using a microtome. The cross-sections were analysed using Fourier Transform Infrared (FTIR) spectroscopic imaging.

Results: The artificial nucleus was made of poly-carbonate urethane (PCU). The initial microscopic assessment revealed strong plastic deformation along with pitting on both superior and inferior surfaces (**Fig.2**). Significant losses of the 1258 cm^{-1} carbonate oxygen linkage and 1740 cm^{-1} carbonyl peak heights were attributed to chemical changes in the soft segment not only at the surface, but also reaching deep inside the bulk part of the nucleus (**Fig.3A**). Under polarized light, a unique contour of birefringence can be seen (**Fig.3D**). Some debris were found embedded in the section and identified as polyethylene particles (**arrowed; Fig.3F**).

Conclusion: This study demonstrates the severe deformation and *in vivo* chemical degradation of the artificial nucleus. While the implants performed well for a long duration, material degeneration contributed eventually to failure. Besides the degradation of the nucleus, polyethylene particles were found that likely originated from the rubbing of the PE fibers that hold the nucleus in place against the titanium alloy endplate component. Such particles may contribute to particle induced

osteolysis. A 5-year clinical outcome study on single level use of this device showed favorable outcomes compared to ACDF treatment in the US, yet other studies posted worrisome on the long-term complications. Routine clinical follow-up to monitor the implant condition, as well as retrieval analysis on surgically retrieved implant and periprosthetic tissues are warranted.

Figures

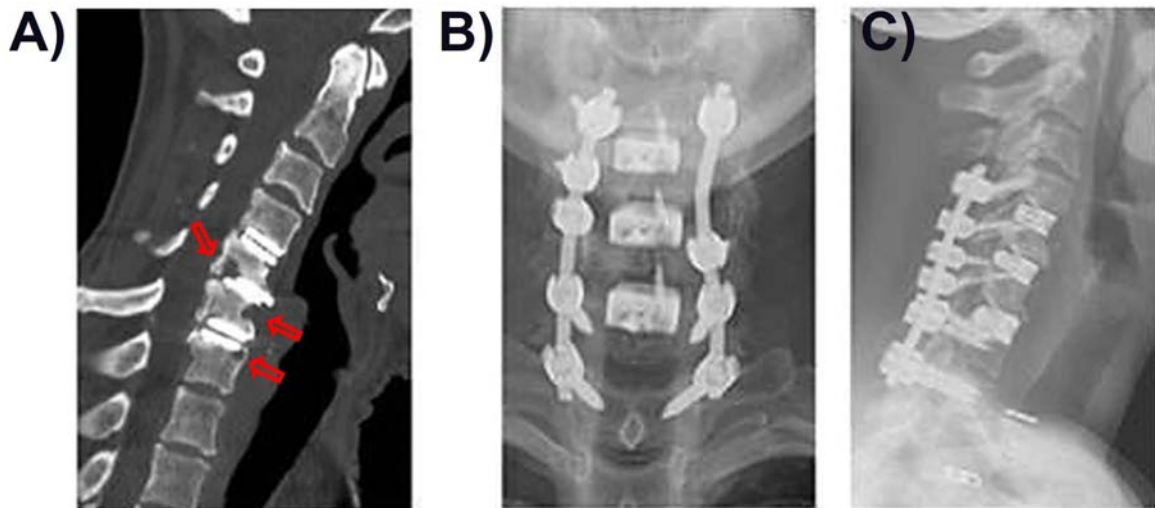


Figure 1 A) Pre-op radiographic imaging of the patient with failed CTDR at C4-C7 level. Strong bone remodeling and osteolytic lesion can be seen at all three levels. B) and C) Post-op X-rays of the patient underwent implant removal, ACDF, and posterior cervical fusion.

[Figure 1](#)

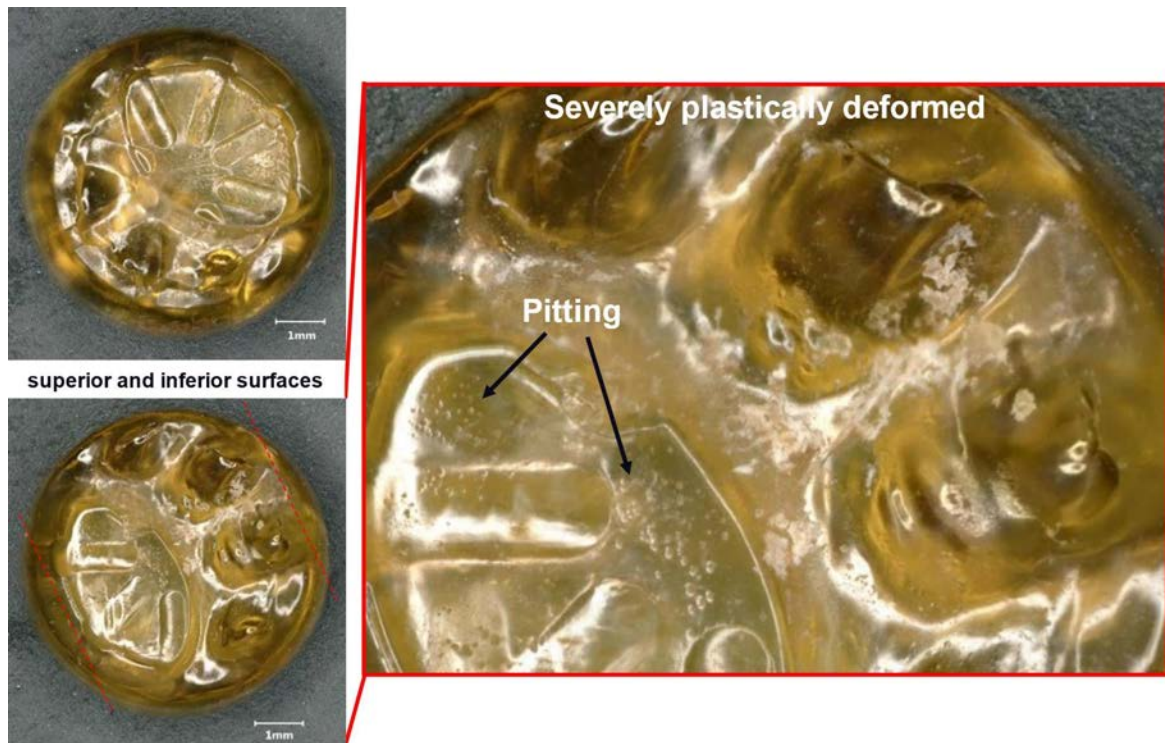


Figure 2 Representative light microscopic image on the surface of retrieved artificial nucleus. The component was made of PCU, and designed to be compliant. Yet, the retrieved component was appeared to be hard and present a yellowing discoloration compared to pristine one. Typical plastic deformation patterns (*e.g.* pitting and surface fatigue) is apparent. The red-dash lines represent the cross-section direction for subsequent FTIR imaging analysis.

[Figure 2](#)

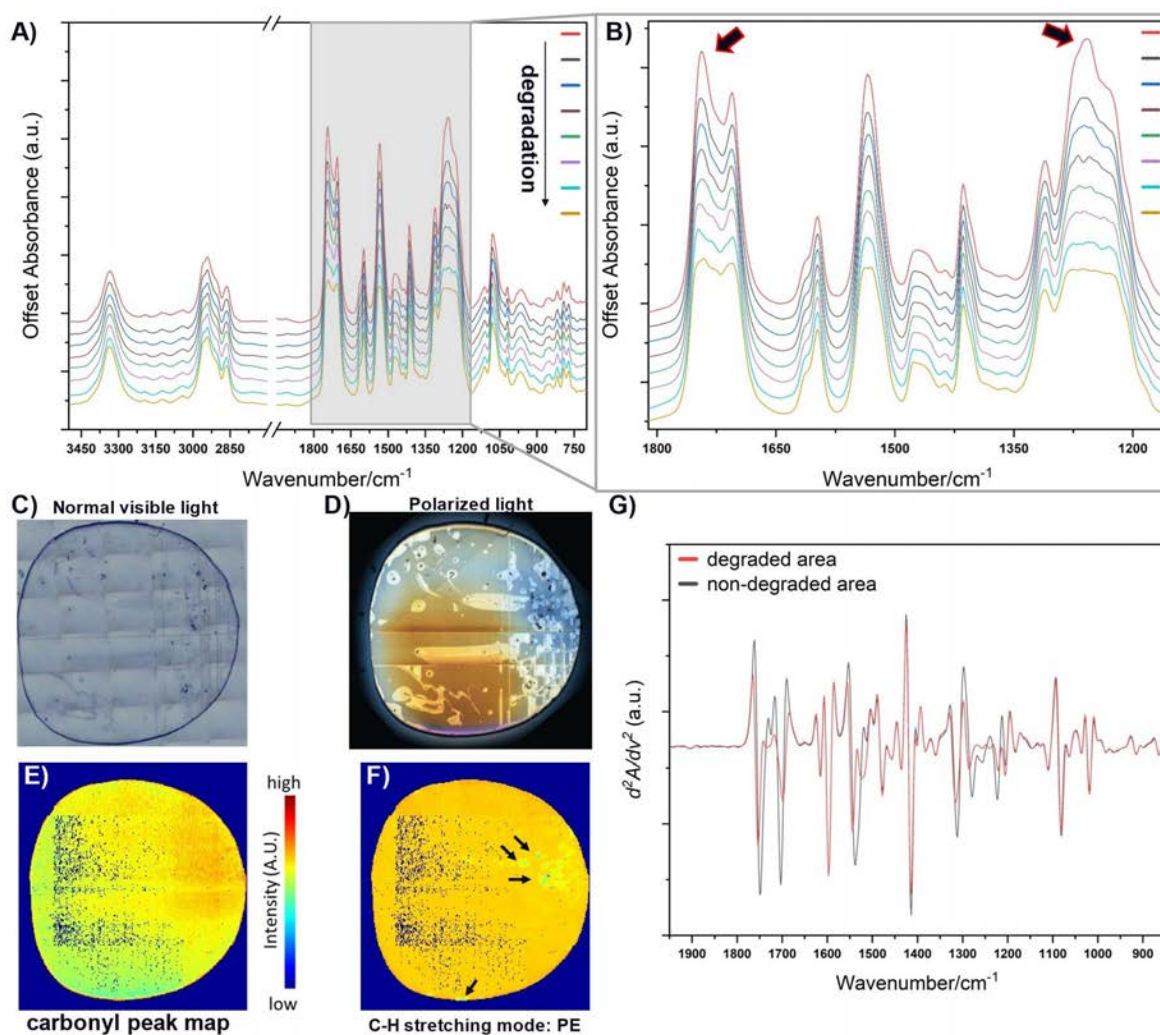


Figure 3 Micro-spectroscopic analysis of the cross-section of artificial nucleus. The thin section has been placed on a BaF₂ disc, which is Infrared transparent. **A)** a series of stacked spectra showing the spectral features variation due to in vivo degradation. All spectra have been normalized to 1597 cm⁻¹ (*i.e.*, C=C stretching in aromatic ring), which has been shown to remain unchanged by bio-degradation in the literature. The significant losses of the 1258 cm⁻¹ carbonate oxygen linkage (*i.e.*, C=O) and 1740 cm⁻¹ carbonyl (*i.e.*, O-C-O) peak heights were attributed to chemical changes in the soft segment showing in the blow-up in **B)**. **C)** Light microscopy of the thin section for FTIR analysis. **D)** Under polarized light, a unique contour of birefringence can be seen. It is likely due to the stress induced photoelasticity effect. **E)** The FTIR imaging can reveal the spatially varied carbonyl peak intensity as a metric showing the degradation profile. The warmer the color means more to its original status. **F)** The embedded particulate debris, showing as black dots, that can be seen in **C)** were identified as polyethylene (PE), which may be transferred during microtome from the outer surface. The polyethylene debris (black-arrowed) could be originated from the wear of the PE artificial anulus. **G)** The 2nd derivative plot of the spectra from a degraded area and non-degraded area, respectively. The fine spectral variation can be appreciated with improved spectral resolution.

Figure 3

Composite Lumbar Spine Surrogate Biomechanical Variability During Multi-Laboratory Collaborative Testing

*Jenna Wahbeh - University of California, Los Angeles - Los Angeles, United States of America

Emma Coltoff - Wake Forest School of Medicine - Winston-Salem, USA

Jeremy G Loss - Lerner Research Institution - Cleveland, USA

Siril Teja Dukkupati - McGill University - Montreal, Canada

Kalle Chastain - Hospital for Special Surgery - Brooklyn, United States of America

Matthew Pelletier - University of New South Wales - Sydney, Australia

Tian Wang - University of New South Wales - Randwick, Australia

Philip J. Brown - Wake Forest School of Medicine - Winston-Salem, USA

Mark Driscoll - McGill University - Montreal, Canada

Sophia Sangorgio - Orthopaedic Institute for Children/UCLA - Los Angeles, USA

Edward Ebramzadeh - Orthopaedic Institute for Children/UCLA - Los Angeles, USA

Kate Meyers - Hospital for Special Surgery - New York, USA

William Walsh - University of New South Wales - Randwick, Australia

Bryan Cornwall - University of San Diego - San Diego, USA

Brian Kelly - Barrow Neurological Institute - Phoenix, USA

Robb Colbrunn - Cleveland Clinic - Cleveland, United States of America

INTRODUCTION: Novel spine arthroplasty devices require rigorous biomechanical evaluation to ensure reliability and efficacy. Composite spine models serve as a valuable tool for this process, providing a standardized testing model that negates the risks and complications associated with cadaveric testing and may allow for outcome comparison between laboratories. Although there is currently a composite spine model commercially available, it has not been widely validated by third party users. Therefore, the objective of this study was to assess the variability in testing outcomes across lumbar spine surrogates between multiple spine biomechanics laboratories using the same prescribed loading conditions.

METHODS: Five L2-L5 Sawbones synthetic lumbar spinal surrogates were tested by seven participating laboratories. The models were tested consecutively by each lab using the individual laboratories' testing environment. Each lab conducted pure moment testing with the same peak moments applied on the surrogates under flexion-extension (FE), lateral bending (LB), and axial rotation (AR). This resulted in a mixture of trapezoidal and sinusoidal loading schemes, testing rigs, bending measurement methods, and fixturing choices (Table 1). The joint translations and rotations were calculated by each participating lab and reported back in a joint coordinate system (JCS).

RESULTS: All labs reported the rotation angles in FE, LB, and AR for the full spine kinematics of each of the five lumbar composite models. Averages were calculated for the six primary testing directions: flexion ($14.8 \pm 2.7^\circ$), extension ($9.9 \pm 1.7^\circ$), left lateral bending ($11.2 \pm 1.6^\circ$), right lateral bending ($11.8 \pm 1.6^\circ$), left axial rotation ($4.5 \pm 1.0^\circ$), and right axial rotation ($3.8 \pm 0.8^\circ$). For these specimens, full left to right lateral bending ranged from 17.1° to 24.1° , full left to right axial rotation ranged from 6.6° to 9.7° , and full flexion-extension ranged from 18.3° to 26.6° (Figure 1).

CONCLUSION: Significant differences were measured between the reported rotations for each surrogate. Variations in the measured rotations highlight the need to identify underlying sources of variability, such as equipment, procedures and loading protocols. A level of inherent specimen variability was expected; however, significant differences were noted between specimens, indicating variability among the specimens themselves. Future works should delve into the lumbar composite surrogates and explore their ability to produce reliably comparable results. By quantifying rotational variability, this study enhances the reliability and comparability of data obtained through interlaboratory studies, ultimately advancing the development and preclinical evaluation of spinal arthroplasty devices.

ACKNOWLEDGEMENTS: The authors would like to acknowledge Sawbones for funding and support of the transportation of the spine surrogates between the participating labs.

Figures

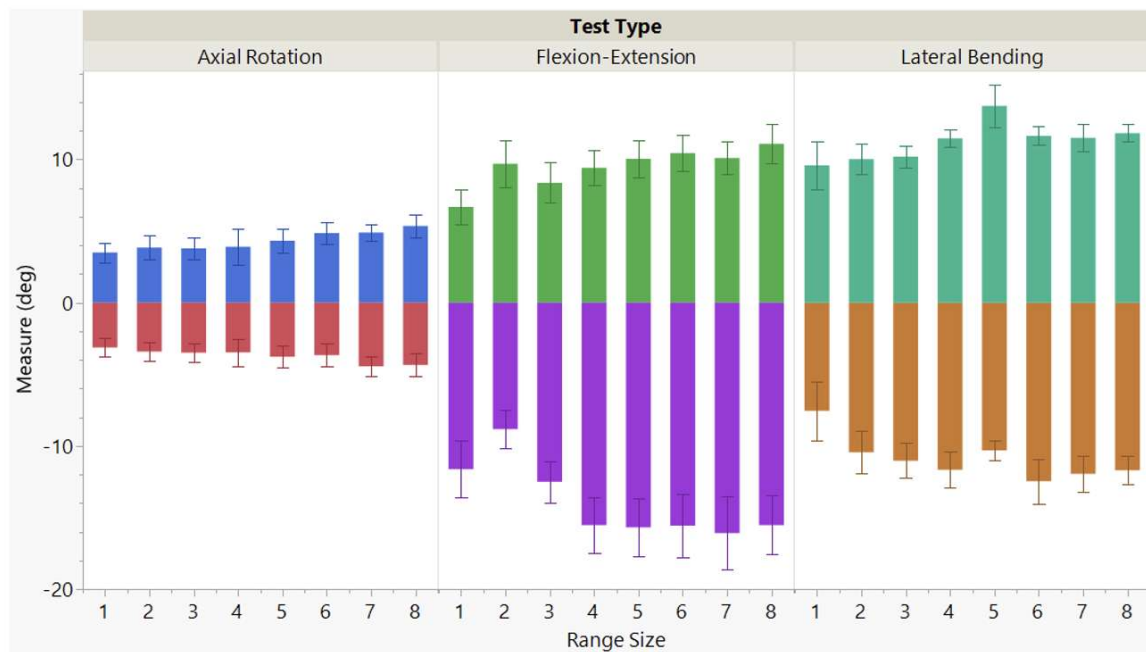


Figure 1. AR, FE, LB Range Variation Across Testing

[Figure 1](#)

Summary Equipment Table					
Test Rigs	Load Cell	Measurement Method	Software	Testing Approach	Specimen Removal
Robotic Arm (4) -KUKA (3) -Denso (1)	ATI (4)	NDI (4)	simVITRO (4)	Primary: Trapezoidal Secondary: Sinusoidal (2)	No specimen removal/resetting during testing (5)
Universal Testing Systems (UTS) (2) -Instron (1) -MTS (1)	AMTI (1)	Motion Analysis Corp (2)	NDI (1)	Primary: Sinusoidal Secondary: Trapezoidal (3)	Specimen removal/resetting during testing (2)
Custom Gantry Robot (1)	JR3 (1)	From Testing Rig (1)	Omron (1)	Sinusoidal Only (2)	
	Instron (1)		Instron (1)		

Table 1. Inter-laboratory Equipment Summary

[Figure 2](#)

Temporal Variation in Artificial Composite Spinal Surrogates Through Inter-Laboratory Spine Biomechanics Testing

Jenna Wahbeh - University of California, Los Angeles - Los Angeles, United States of America

Emma Coltoff - Wake Forest School of Medicine - Winston-Salem, USA

Jeremy G Loss - Lerner Research Institution - Cleveland, USA

Siril Teja Dukkupati - McGill University - Montreal, Canada

Kalle Chastain - Hospital for Special Surgery - Brooklyn, United States of America

Matthew Pelletier - University of New South Wales - Sydney, Australia

Tian Wang - University of New South Wales - Randwick, Australia

Philip J. Brown - Wake Forest School of Medicine - Winston-Salem, USA

Mark Driscoll - McGill University - Montreal, Canada

Sophia Sangorgio - Orthopaedic Institute for Children/UCLA - Los Angeles, USA

Edward Ebramzadeh - Orthopaedic Institute for Children/UCLA - Los Angeles, USA

Kate Meyers - Hospital for Special Surgery - New York, USA

William Walsh - University of New South Wales - Randwick, Australia

Bryan Cornwall - University of San Diego - San Diego, USA

Brian Kelly - Barrow Neurological Institute - Phoenix, USA

*Robb Colbrunn - Cleveland Clinic - Cleveland, United States of America

INTRODUCTION: Biomechanical testing of spine arthroplasty devices has evolved greatly, marked largely by advancements in testing equipment and techniques. Composite spine surrogates have been developed to address challenges associated with cadaveric specimens, yet their consistency and reproducibility has not been explored. Therefore, the goal of this study was to evaluate longitudinal changes in these surrogates through a multi-laboratory approach, specifically assessing time-dependent variations in repeated testing and overall performance over time.

METHODS: Seven laboratories conducted pure moment testing on five L2-L5 Sawbones synthetic lumbar spine surrogates. Each lab conducted pure moment testing on each of the surrogates under single plane bending. Three cycles of each rotation were done at each lab, for a total of 64 cycles of testing, per specimen. Labs reported range of motion (ROM) was measured for the total spinal length (L2-L5) and for each functional spinal unit (L3-L4). Additionally, laboratories noted any degradation to the surrogate models on a scale of 1 to 5 for individual factors relating to specimen condition (1=poor and 5=excellent). Specifically, factors that were assessed for overall quality were: rigid blocks, facet joints, transverse processes, and L3 and L4 lumbar fixtures.

RESULTS: The mean ROM did not vary substantially over time in any plane. Furthermore, consistency improved, as the standard deviations tended to decrease over time (0.7° to 0.6° for AR, 1.5° to 2.2° for Flexion, 1.4° to 1.3° for Extension, 1.0° to 0.8° for LB) (Figure 1). The overall integrity of the L3-L4 lumbar fixtures did not degrade substantially, with only one L4 lumbar fixture crack after 3 testing laboratories. However, the facet joints saw consistent degradation over the course of testing, decreasing from a mean initial score of 5 to a final score of 2 (Figure 2). Finally, the transverse processes remained relatively intact, apart from one case in which the processes experienced a 5mm tear after the first 9 cycles of testing which progressed to 15mm by the time it reached the final lab for testing.

CONCLUSION: While some surrogate spines showed visible deterioration over time, ROM remained relatively stable over time, indicating that overall performance was not compromised. It is noteworthy that significant degradation was evident after just 64 cycles of pure moment testing, intended to be nondestructive. This raises concerns about the long-term durability of these surrogate models. Further studies should assess the surrogate's performance under prolonged testing conditions to ensure their suitability for continued use.

ACKNOWLEDGEMENTS: The authors would like to acknowledge Sawbones for their funding support of the transportation of the spine surrogates between the participating labs.

Figures

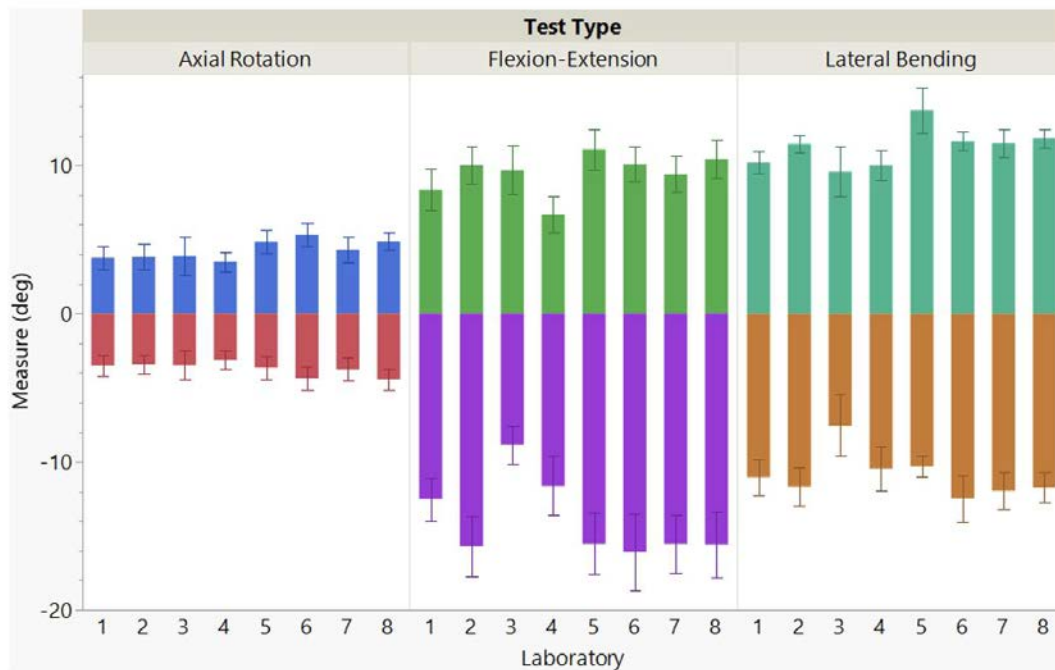


Figure 1. Rotational ranges of L2-L5 specimens for Axial Rotation, Flexion/Extension, and Lateral Bending in sequential time order.

Figure 1

Patient-Reported Outcome Measures Provide Little Value for Long-Term Clinical Surveillance in Joint Arthroplasty: A Systematic Review and Meta-Analysis

*[Hannah Spece](#) - Drexel Implant Research Center - Philadelphia, USA

Michael Kurtz - Drexel University - Philadelphia, United States of America

Nicolas Piuze - Cleveland clinic - Cleveland, United States of America

Steven Kurtz - Drexel University - Philadelphia, USA

Introduction

Patient reported outcome measures (PROMs) are an essential tool for evaluating joint arthroplasty success and supporting shared decision making between clinicians and patients. Currently, there is a growing emphasis on PROMs collection and reporting in the U.S. and Europe. However, the robustness and clinical relevance of long-term PROMs have been called into question, as a patient's evolving health status over time may be difficult to distinguish from the arthroplasty's performance. In this study we asked: 1) How complete is PROMs data at 5+ follow-up for total knee arthroplasty (TKA) and total hip arthroplasty (THA); and 2) To what extent do PROM scores change between early (1-2 year) and longer (5+ year) term follow-up?

Methods

We conducted a systematic review using PRISMA guidelines. Searches were conducted using PubMed and Embase. Randomized controlled trials that focused on TKA or THA and reported PROMs for preoperative, postoperative, and 5+ year follow-up timepoints were included.

Basic study details and joint-specific PROM information were recorded along with the number of patients evaluable at follow-up. Attrition rates were calculated. Data presented groupwise were combined for each study.

We used meta-analyses to determine the mean difference in PROM scores from preoperative to early follow-up (1-2 years) timepoints and from early follow-up to final follow-up. All analyses were performed using Cochrane RevMan Web using a random-effects model.

Representative studies were selected for further analysis. Scores were plotted over time, then the derivative of the plots was calculated, showing the mean rate of change for each PROM over time.

Results

A total of 406 unique studies were identified, and 20 (16 TKA, 4 THA) were included for review. The most frequently reported PROMs were Oxford Knee Score (OKS, n=10 studies) and Western Ontario and McMaster Universities Osteoarthritis Index (WOMAC, n=8 studies) for TKA, and UCLA activity score (n=4 studies) and Harris Hip Score (n=3 studies) for THA. The follow-up rate based on patients evaluable at follow-up averaged 68% for TKA (mean follow-up 7.9y) and 78% for THA (mean follow-up 7.8y). Actual response rates were lower.

Early TKA score changes (preoperative to early follow-up) averaged 16.3 points for OKS and 25.1 for WOMAC (Figures 1 and 2). Score changes from early to final follow-up dropped to an average 1.3 points for OKS and 3.1 for WOMAC. Final follow-up averaged 7.0 years. A similar meta-analysis was not possible for THA studies due to missing data.

Across the reviewed, we commonly observed that PROM scores plateaued after 1-2 years. Representative plots (Figure 3) show this for OKS, Knee Society Score, and

WOMAC PROMs. Notably, the change in PROMs with respect to time ($dScore/dt$) approaches 0 between 1-2 years.

Conclusion

Our review and meta-analysis do not support the utility of long-term PROMs. Not only is the rate of missing data unacceptably high, but the sensitivity of these outcome measures (in terms of showing score changes) becomes critically diminished after short-term follow-up. Ultimately, the use of long-term PROM requirements should be abandoned in favor of more robust measures of success.

Figures

Oxford Knee Score

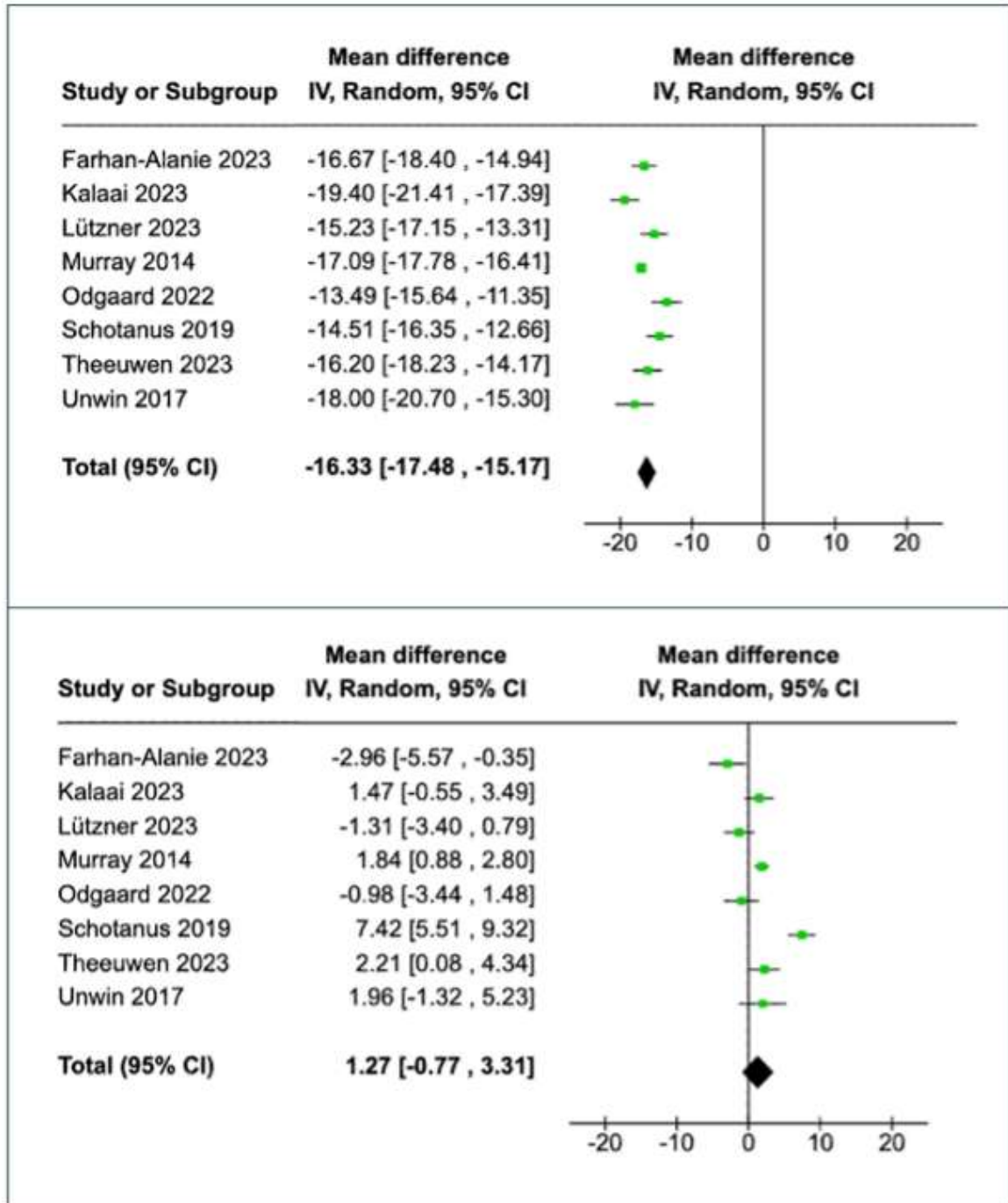


[Figure 1](#)

WOMAC

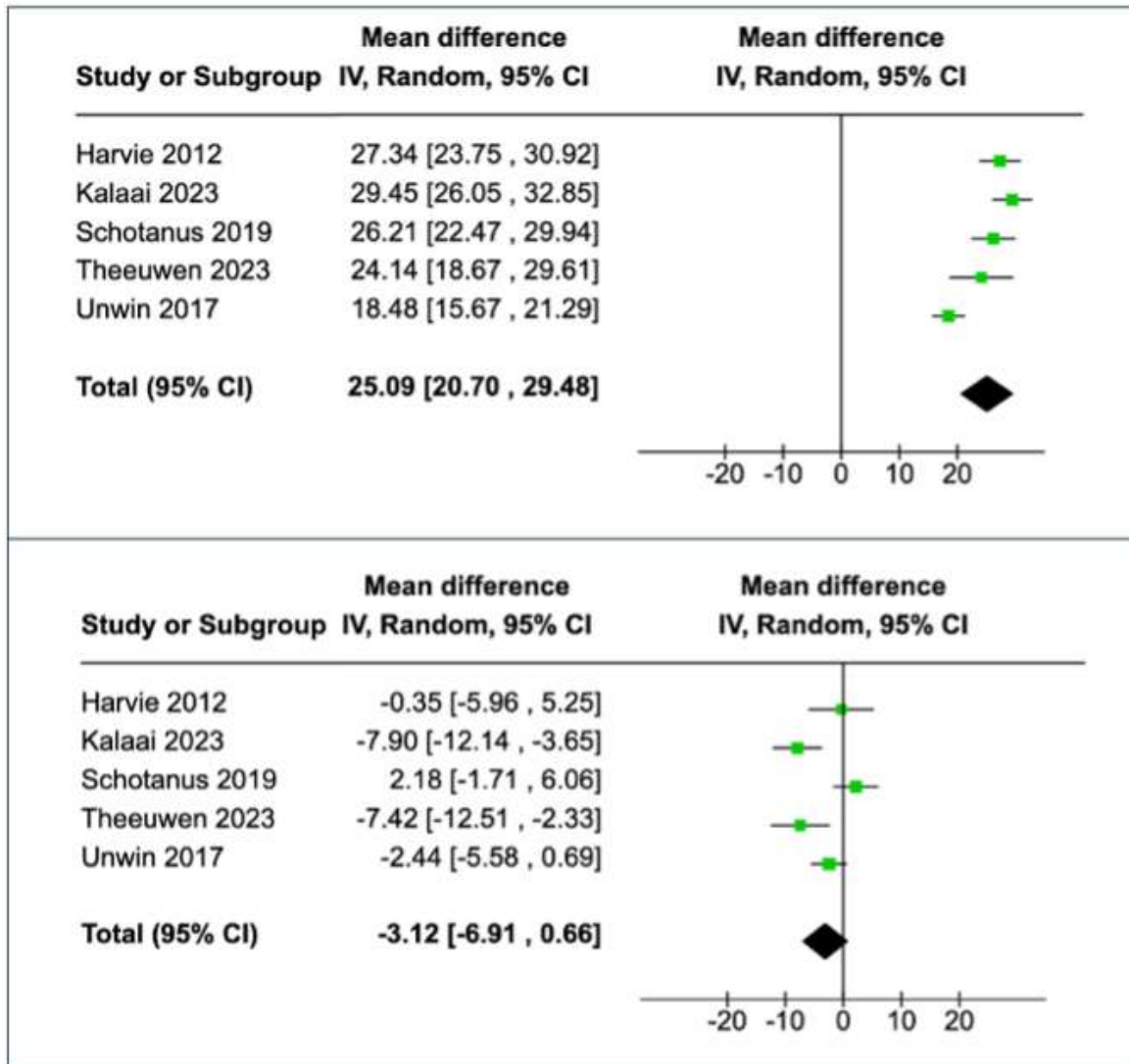


Figure 2

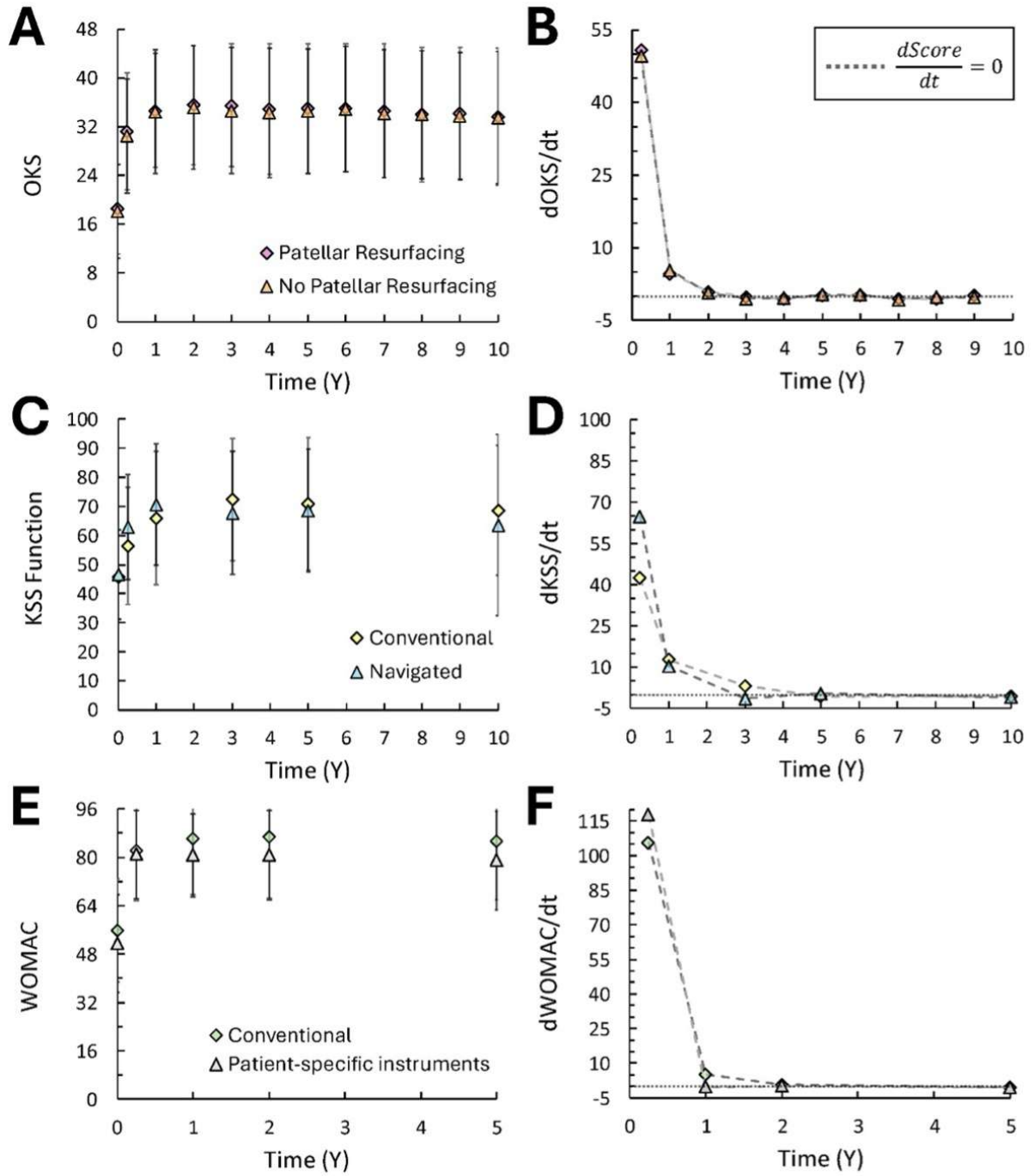


Figure 3

Outcomes in Patients Undergoing Primary Total Hip Arthroplasty With History of Prior Hip Arthroscopy

*Hayley Raymond - NYU - New York, United States of America

Brian A. Perez - NYU Langone Orthopedic Hospital - New York, USA

Muhammad Haider - NYU Orthopedic Hospital - New York, USA

Sophia Antonioli - NYU Langone - New York, USA

Akram Habibi - NYU Langone Orthopedic Hospital - New York, United States of America

Ran Schwarzkopf - NYU Langone Medical Center Hospital for Joint Diseases - New York, USA

Diren Arsoy - NYU Langone Orthopedic Hospital - New York, USA

Catherine Digangi - NYU Orthopedic Hospital - New York, USA

Introduction

As the number of hip arthroscopies (HA) performed rises, further research is needed on total hip arthroplasty (THA) following HA. This study aimed to compare clinical and patient-reported outcomes for patients undergoing THA with and without history of HA.

Methods

We retrospectively reviewed 168 patients who underwent unilateral, primary THA following ipsilateral HA from 2012 to 2024. Patients were propensity matched 10:1 to THA patients without history of ipsilateral HA. Cohorts were matched with respect to age, sex, race, smoking status, ASA score, BMI, and CCI (Table 1). Operative data as well as HOOS, JR and PROMIS scores were collected. Logistic regression analyses were used to assess the impact age, sex, race, smoking status, BMI, ASA, CCI, and prior HA on revision and 90-day orthopedic readmissions.

Results

Patients with prior history of HA had shorter LOS ($P=0.039$, Table 2) and operative times ($P=0.001$, Table 2). HA patients were discharged home at a greater rate ($P=0.010$, Table 2). HA patients had higher rates of subsequent revision surgery (5.4% vs. 2.6%, $P=0.041$, Table 2). On multivariate analysis, prior hip arthroscopy was associated with higher odds of revision (OR 2.21, 95% CI 1.05-4.67, $P=0.038$, Table 3). No difference was seen in 90-day readmission rates between both groups (Table 2). At two-year follow up, HA patients had lower PROMIS mobility scores ($P=0.039$, Table 4). All other patient reported outcomes were similar among both groups at final follow-up (Table 4).

Conclusion

In our study, patients with a history of HA exhibited inferior outcomes including increased revision rates and lower rates of reported mobility. Patients should be counseled with regards to inferior outcomes and further studies are needed to explain our findings.

Figures

Table 1. Baseline characteristics for matched groups

	No Hip Scope (n = 1,680)	Hip Scope (n = 168)	P-value
Mean Age (SD)	51.05 (11.88)	50.65 (11.55)	0.674
Sex, n (%)			
Female	1,086 (64.6)	107 (63.7)	0.872
Male	594 (35.4)	61 (36.3)	
Race, n (%)			0.053
White	1,027 (61.1)	111 (66.1)	
Black	247 (14.7)	12 (7.1)	
Asian	69 (4.1)	6 (3.6)	
Other	337 (20.1)	39 (23.2)	
Smoking Status, n (%)			0.263
Never	907 (54.0)	87 (51.8)	
Former	539 (32.1)	63 (37.5)	
Current	234 (13.9)	18 (10.7)	
ASA Score, n (%)			0.212
1	262 (15.6)	18 (10.7)	
2	1,139 (67.8)	125 (74.4)	
3	275 (16.4)	24 (14.3)	
4	4 (0.2)	1 (0.6)	
Mean BMI (SD)	28.13 (5.93)	27.94 (5.51)	0.685
Mean CCI (SD)	1.26 (1.53)	1.46 (1.66)	0.096

ASA, American Society of Anesthesiologists; BMI, Body mass index; CCI, Charlson Comorbidity Index; SD, Standard deviation.

[Figure 1](#)

Table 2. Clinical outcomes for matched groups

	No Hip Scope (n = 1,680)	Hip Scope (n = 168)	P-value
Mean LOS (hours) [SD]	45.84 (38.32)	39.43 (37.67)	0.039
Mean Operative Time (min) [SD]	104.30 (36.23)	97.77 (23.14)	0.001
Discharge Disposition, n (%)			0.010
Home	1,594 (94.9)	168 (100.0)	
ARF	25 (1.5)	0 (0)	
SNF	61 (3.6)	0 (0)	
90-Day Orthopedic Readmissions, n (%)	45 (2.7)	6 (3.6)	0.316
Mean Days to Orthopedic Readmissions (SD)	27.73 (16.45)	17.00 (7.48)	0.124
Any Revision, n (%)	43 (2.6)	9 (5.4)	0.041
Mean Days to Revision (SD)	440.81 (779.08)	368.11 (579.96)	0.793

ARF, Acute rehab facility; SNF, Skilled nursing facility; LOS, Length of stay; SD, Standard deviation.

Figure 2

Table 3. All dependent variables entering the logistic regression mode and their adjusted odds ratio for any revision.

	Odds Ratio (95% CI)	P-value
Age	1.010 (0.983-1.038)	0.470
Sex (female vs. male)	1.376 (0.727-2.606)	0.327
Race		
Black vs. White	1.900 (0.915-3.948)	0.085
Asian vs. White	1.189 (0.273-5.178)	0.818
Other vs. White	1.033 (0.473-2.255)	0.936
Smoking Status		
Former vs. Never	1.149 (0.623-2.120)	0.656
Current vs. Never	1.037 (0.436-2.465)	0.934
BMI	0.966 (0.917-1.017)	0.188
ASA		
2 vs. 1	1.409 (0.531-3.744)	0.491
3 vs. 1	2.182 (0.690-6.902)	0.184
4 vs. 1	0 (0)	0.999
CCI	1.053 (0.873-1.270)	0.589
Prior hip scope vs. no hip scope	2.211 (1.046-4.674)	0.038

ASA, American Society of Anesthesiologists; BMI, Body mass index; CCI, Charlson Comorbidity Index; CI, Confidence interval

Figure 3

Table 4. Patient Reported Outcome Measures for Patients Undergoing Primary Total Hip Arthroplasty With or Without Prior Hip Arthroscopy

	No Hip Scope (n = 1,680)	Hip Scope (n = 168)	P-value
Mean HOOS, JR (SD)			
Preoperative	45.99 (16.74)	48.14 (14.11)	0.566
6 weeks	63.11 (15.70)	63.36 (17.82)	0.944
3 months	67.19 (24.12)	69.95 (13.50)	0.614
1 year	62.98 (30.11)	68.38 (27.74)	0.518
2 years	64.82 (31.30)	66.16 (19.20)	0.878
Mean PROMIS Pain Intensity (SD)			
Preoperative	55.09 (6.86)	52.37 (6.49)	0.029
6 weeks	47.58 (6.95)	51.36 (7.29)	0.015
3 months	44.42 (7.97)	45.63 (10.22)	0.488
1 year	45.66 (8.79)	47.60 (10.38)	0.323
2 years	47.44 (9.03)	48.40 (9.82)	0.668
Mean PROMIS Pain Interference (SD)			
Preoperative	65.12 (6.61)	62.76 (7.80)	0.053
6 weeks	60.16 (7.88)	61.99 (7.44)	0.291
3 months	54.91 (9.00)	58.20 (8.55)	0.085
1 year	55.45 (9.96)	58.45 (9.23)	0.167
2 years	57.46 (10.23)	58.37 (9.62)	0.709
Mean PROMIS Physical Function (SD)			
Preoperative	36.58 (6.84)	37.26 (6.03)	0.726
6 weeks	34.60 (8.67)	35.18 (8.80)	0.830
3 months	42.96 (7.62)	42.39 (8.97)	0.793
1 year	43.00 (9.09)	41.77 (8.38)	0.633
2 years	41.74 (10.52)	42.32 (8.31)	0.842
Mean PROMIS Mobility (SD)			
Preoperative	37.23 (5.69)	40.11 (6.65)	0.045
6 weeks	38.92 (5.41)	35.25 (4.96)	0.030
3 months	43.86 (7.15)	41.20 (8.56)	0.286
1 year	46.55 (8.86)	39.20 (8.31)	0.025
2 years	46.07 (8.69)	38.18 (8.24)	0.039
Mean PROMIS Physical Health (SD)			
Preoperative	39.06 (7.44)	40.81 (6.68)	0.264
6 weeks	43.15 (6.84)	41.36 (6.24)	0.281
3 months	45.57 (7.87)	43.75 (8.85)	0.305
1 year	45.09 (8.30)	42.27 (8.23)	0.117
2 years	44.76 (8.47)	42.41 (9.30)	0.297
Mean PROMIS Mental Health (SD)			
Preoperative	46.97 (8.52)	47.97 (9.17)	0.583
6 weeks	50.62 (8.06)	48.74 (6.99)	0.337
3 months	50.49 (9.30)	48.43 (8.98)	0.330
1 year	50.96 (9.38)	45.75 (9.15)	0.011
2 years	49.97 (9.35)	45.51 (11.55)	0.081

HOOS, JR, Hip dysfunction and Osteoarthritis Outcome Score for Joint Replacement; PROMIS, Patient-Reported Outcomes Measurement Information System; SD, Standard deviation.

Figure 4

Patients Having Primary Total Joint Arthroplasty at ASCs Receive Higher Opioid Prescriptions at Discharge Than Those at HOPDs or Hospitals

*Simarjeet Puri - Detroit, United States of America

Harjot Uppal - Ascension Providence - Southfield, USA

Martin Weaver - Ascension Providence Hospital - Southfield, USA

Giresse Melone - University of Michigan - Ann Arbor, USA

Richard Hughes - University of Michigan - Ann Arbor, USA

Elizabeth Dailey - University of Michigan - Ann Arbor, USA

David Markel - Providence Hospital and Medical Center - Southfield, USA

Introduction: Opioid use and overuse reached epidemic proportions in the United States leading to interventions in the postoperative period. The Michigan Arthroplasty Registry Collaborative Quality Initiative (MARCQI) released guidelines for opioid prescriptions in March 2019 for opioid naïve patients after primary total hip (THA) and knee arthroplasty (TKA), recommending ≤ 240 oral morphine equivalents (OMEs) for THA and ≤ 320 OMEs for TKA. These led to a significant decrease of OME prescriptions across the state. More recently, changes to Medicare's inpatient only rule have allowed arthroplasty cases to move to ambulatory surgery centers (ASCs) and to hospital outpatient departments (HOPDs). Our goal was to assess MARCQI OME guideline adherence after primary TJA at ASCs, HOPDs, and hospitals.

Methods: Using MARCQI data, 33,993 patients were identified as opioid naïve and undergoing a primary THA or TKA between July 1, 2021 and June 30, 2022. Of the 13,252 THA: 10.8% (1,429) were performed in ASCs, 5.2% (685) in HOPDs, and 84% (11,138) in hospitals. For the 21,741 primary TKA: 10.9% (2,373) were performed in ASCs, 4.5% (980) in HOPDs, and 84.6% (18,388) in hospitals. Cohorts were not significantly different in terms of age, sex, or body mass index. However, the inpatient hospital cohort had more patients with American Society of Anesthesiology Class 3 and 4 ($p < 0.001$) and lower rates of private health insurance ($p = 0.04$).

Results: THA at an ASC had the lowest rate of guideline compliance. However, guideline adherence was poor for both THA and TKA at the ASCs compared to those at HOPDs or hospitals (THA: ASC 56% vs HOPDs 89% vs Hospitals 83%, $p < 0.001$; TKA: ASC 71% vs HOPD 81% vs Hospital 87%, $p < 0.001$).

Conclusion: ASC patients are selected for the ability to discharge home. Yet, opioid naïve patients receiving primary total joint arthroplasty at Michigan ASCs received more opioid prescriptions at discharge than patients undergoing the same procedures at HOPDs and hospitals. This is an area for improvement that may reflect educational gaps or a prescribing learning curve.

Is Robotic Assisted Unicompartmental Knee Arthroplasty Effective in Elderly Patients? Early Outcomes of a Single Centre Prospective Study

*Shantanu Patil - SRM Medical College, SRM Institute of Science and Technology - Kattankulathur, India

Ashok Kumar P. S. - CHENNAI, India

Vikas Rai - SIMS Hospital - Chennai, India

Kalaivanan Kannian - Asian Joint Reconstruction Institute AJRI @SIMS Hospitals - Chennai, India

Pichai Suryanarayan - India

Vijay C Bose - AJRI - chennai, India

Introduction:

Unicompartmental knee Arthroplasty(UKA) has been an effective and established treatment option for patients with isolated unicompartmental anteromedial osteoarthritis. As a procedure with lower surgical morbidity, reduced hospital stay, UKA presents a practical solution for elderly patients (>60 yrs. age) who have multiple pre-existing comorbidities. Safety and efficacy of UKR in an older population remains an emerging area of research. Key to success lies in appropriate patient selection.

Robotic assistance has been proven to increase surgical precision by Accurate component positioning, Better limb alignment, optimised soft tissue balancing with Precise and refined bone cuts. The purpose of this study is to evaluate the efficacy and functional outcome of robotic assisted UKR in elderly patients with unicompartmental osteoarthritis and to evaluate the role of ACL and Patello femoral arthritis in the outcome.

Although many studies have stressed on better joint line restoration after UKA, very few studies assessed PROM in UKA. It is crucial to assess how well UKA serves the patient's goals rather than strictly taking objective measures alone.

Materials and Methods:

Patients diagnosed with isolated medial compartmental OA and suitable for UKA were included in our study, age of 60 years was used to define elderly. 107 Patients above 60 yrs. age identified from institutional database were divided into two groups Group A (Between 60-70yrs) and group B (> 70 yrs.). All patients were investigated with preoperative scanograms along with Anteroposterior, lateral and stress radiographs of the affected knee. Oxford Knee Score, Knee Society Score 2011 satisfaction scores were recorded preoperatively and postoperatively at 6 weeks, 3 months, 6 months, 1 year and 3 year. All surgeries were performed by senior surgeons trained in robotic technology.

Intraoperatively, grading of ACL, PFJ and medial facet done using the Oxford knee UKR form. Only cemented, fixed bearing implants were used. Figure 1 Summarises the Intraoperative protocol along with Pre- and Post-surgical alignment radiographs.

Results:

The results are summarised in Figure 2. At 3 year follow up, OKS is slightly better in < 70 yrs. group. Among the components of the Oxford Knee score, Greatest improvement was seen in Pain Severity & Limp. No significant difference was seen in post-operative satisfaction (p value=0.766)

The number of Grade 2 & 3 ACLs was significantly higher in Group B. Distribution of Trochlea and Medial Facet cartilage status was comparable between the 2 groups. One patient had pin tract infection, which settled after 1 week of oral antibiotics. There were No revisions in this cohort till last follow-up. (Figure3)

Conclusion:

Elderly patients undergoing UKA can experience similar satisfaction & slightly lower PROM as their younger counterparts which can be attributed to activity levels and higher prevalence of comorbidities in elderly age group. Damage to the articular cartilage of the Patello-femoral Joint and Status of ACL had no influence on outcome. Our study may help clinicians provide valuable prognostic information to elderly patients and guide preoperative counselling.

Figures

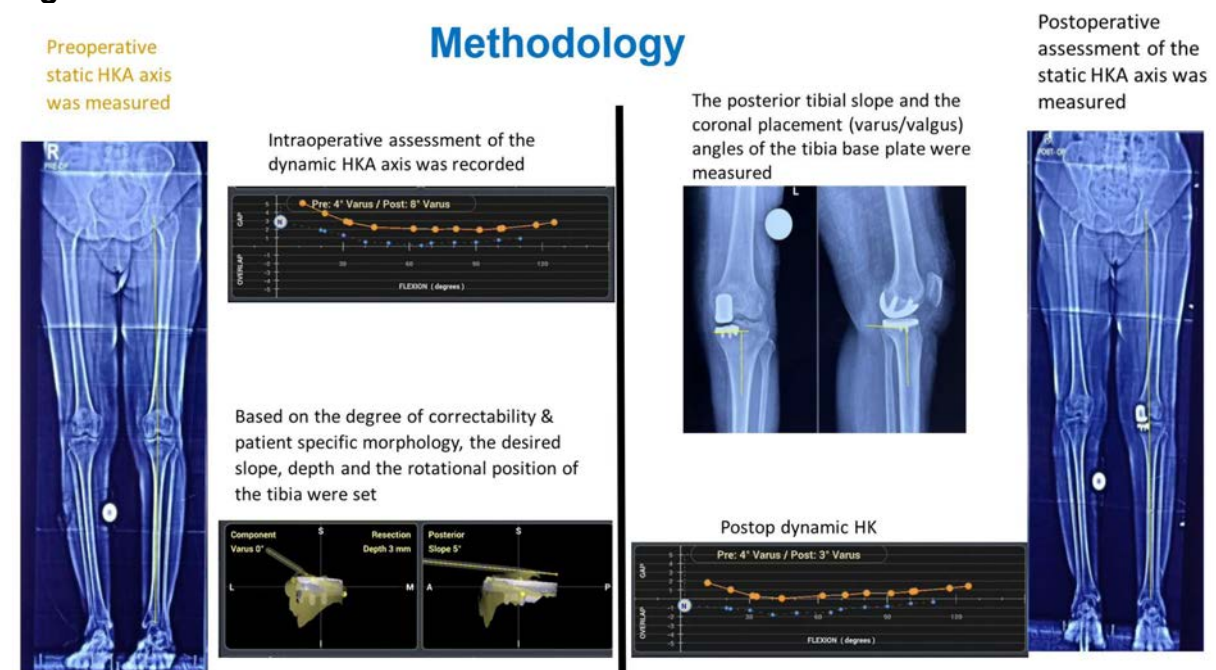


Figure 1

Parameters	Group A 60-70 yrs	Group B > 70 yrs	P value
Number of Knees	73	34	
Age(yrs)	63.25 ± 6.36	74.04 ± 3.00	
Gender(M:F)	11:62 M:F	32:13 M:F	
BMI	29.14 ± 4.43	28.02 ± 4.48	
Oxford Knee Score			
Preoperative	24.99 ± 0.99	25 ± 1.13	0.006 [†]
Postoperative (3 Yrs)	45.12 ± 2.05	44.06 ± 1.25	
Satisfaction Score (KSS 2011) %			
Preoperative	15.51 ± 3.44	11.88 ± 2.2	0.766 [†]
Postoperative (3 Yrs)	36.71 ± 3.04	36.88 ± 1.92	

Table 1 Demographics and PROMS

ACL Status	Group A 60-70 yr	Group B (> 70 Yr)	P value
Grading			< 0.002
Normal	16.44 %	11.76 %	
Synovial Damage	71.23 %	44.11 %	
Longitudinal Splits	12.33 %	41.18 %	
Friable and Fragmented	0%	2.94 %	

Table 2 ACL Status

Grading	Trochlea		Medial Facet	
	Group A (60-70 yr)	Group B (> 70 Yr)	Group A (60-70 yr)	Group B (> 70 Yr)
Normal	13 (17.8%)	5 (14.7%)	5 (6.8%)	2 (5.9%)
Superficial Damage	27 (36.99%)	16 (47.06%)	33 (45.21%)	17 (50%)
Partial Thickness Cartilage Loss	23 (31.51%)	11 (32.35%)	32 (43.84%)	13 (38.24%)
Focal Thickness Cartilage Loss	5 (6.85%)	1 (2.94%)	3 (4.11%)	1 (2.94%)
Extensive Thickness Cartilage Loss	5 (6.85%)	1 (2.94%)	0 (0%)	1 (2.94%)
P value	< 0.84		< .704	

Table 3 Trochlea and Medial Facet status

Figure 2

Pre & Post Static Alignment

Pre HKA -8.4 ± 3.6 Post HKA -4.0 ± 3.0



Target was 4.0°

Pre & Post Dynamic Alignment

Pre HKA -6.9 ± 2.9 Post HKA -4.2 ± 2.6



Target was 50% correction of the deformity



ACL and PFJ Status during Surgery



Post Surgical ROM

Figure 3

Does the Use of a Tourniquet Influence Five-Year Outcomes Following Total Knee Arthroplasty? Results of a Randomized Controlled Trial

*Jonathan Katzman - NYU Langone - New York, United States of America

Alana Prinós - Langone Orthopedic Hospital - New York, USA

Hayley Raymond - Langone Orthopedic Hospital - New York, USA

Casey Cardillo - NYU Orthopedic Hospital - New York, USA

Morteza Meftah - NYU Hospital for Joint Diseases - New York, USA

Akram Habibi - NYU Langone Orthopedic Hospital - New York, United States of America

Ran Schwarzkopf - NYU Langone Medical Center Hospital for Joint Diseases - New York, USA

Catherine Digangi - NYU Orthopedic Hospital - New York, USA

Sophia Antonioli - NYU Langone - New York, USA

Background:

Intraoperative tourniquet application during total knee arthroplasty (TKA) is a commonly employed practice among orthopedic surgeons to improve surgical field visibility and minimize blood loss. While the short-term effects of tourniquet use on pain management have been extensively studied and found to be minimal, its influence on longer-term outcomes remains underexplored. This randomized controlled trial seeks to evaluate the potential impact of tourniquet utilization on TKA outcomes with a follow-up period of up to five years.

Methods:

This single-center randomized controlled trial enrolled 227 patients undergoing primary, elective, unilateral TKA. Patients were randomly assigned preoperatively to two groups: TKA with intraoperative tourniquet ($n=112$) and TKA without intraoperative tourniquet ($n=115$). Data on patient demographics, perioperative variables, clinical outcomes, and patient-reported outcome measures (PROMs) such as Knee injury and Osteoarthritis Outcome Score for Joint Replacement (KOOS, JR) and Patient-Reported Outcomes Measurement Information System (PROMIS) scores were collected and compared between the groups.

Results:

All demographic variables were comparable between the groups. The tourniquet cohort exhibited a trend towards less blood loss (161.7 vs. 131.8 mL, $P=0.098$), shorter operative time (95.7 vs. 97.8 minutes, $P=0.264$), and slightly higher postoperative day one Visual Analog Scale (VAS) pain scores (3.6 vs. 3.1, $P=0.197$), although none of these differences reached statistical significance. Mean lengths of stay (2.1 vs. 2.0 days, $P=0.837$) and home discharge rates (92.0 vs. 88.7%, $P=0.340$) were similar across groups. Three 90-day readmissions were recorded, all occurring in the group without tourniquet application (0% vs. 2.7%, $P=0.081$). Active range of motion at last follow up did not significantly differ between the groups. All-cause revision rates at five years were comparable between the tourniquet and non-tourniquet groups (3.6 vs. 4.3%, $P=0.734$). Kaplan-Meier survivorship analysis demonstrated similar implant survival between the cohorts at five years ($P=0.769$). There were no significant differences in KOOS JR, PROMIS pain intensity, PROMIS pain interference, or PROMIS physical health scores at three months, six months, one year, and last follow up postoperatively.

Conclusion: The use of an intraoperative tourniquet was not associated with differences in clinical or patient-reported outcomes following total knee arthroplasty up to five years. These findings suggest that there may not be an optimal tourniquet strategy for TKA.

Figures

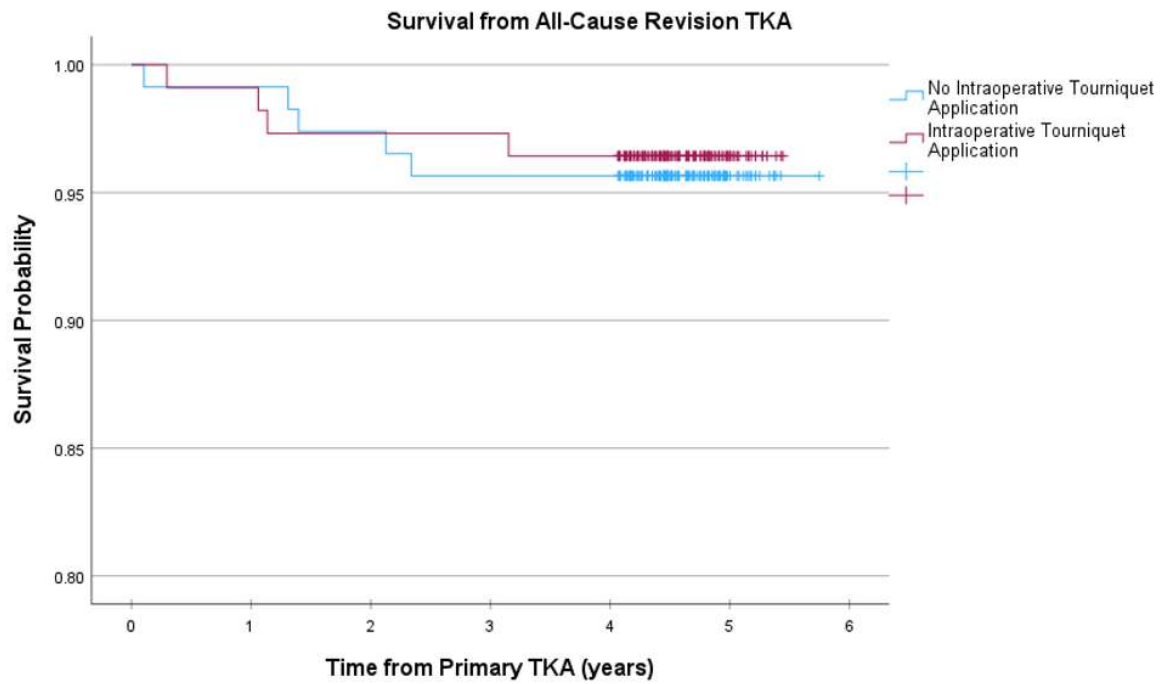


Figure 1

Increased Risk of Flexion Impingement and Posterior Instability Following Total Hip Arthroplasty

Linden Bromwich - Macquarie University - Sydney, Australia

*Christopher Plaskos - Corin - Raynham, USA

Nathanael Heckmann - Keck School of Medicine of USC - Los Angeles, USA

Stephen McMahon - Monash University - Melbourne, Australia

Andrew Shimmin - Melbourne Orthopaedic Group - Melbourne, Australia

Jonathan Bare - Melbourne Orthopaedic Group - Melbourne, Australia

Jim Pierrepont - Corin - Pymble, Australia

Introduction:

Posterior instability during deep flexion is a commonly identified risk factor in total hip arthroplasty (THA), which can lead to posterior edge loading, anterior impingement and/or dislocation of the implants. The purpose of this study was to investigate the risk of posterior instability due to adverse spinopelvic mobility (SPM) before and after THA.

Methods:

This study evaluated 555 patients undergoing THA under 9 Australian Surgeons at multiple centres between May 2015 and July 2021. The mean age at surgery was 66 years old (range: 24 to 89), with 57% of the cohort females. Patients received functional radiographs in standing and flex-seated pre-operatively, and at one year post THA (mean time between surgery and post-op imaging was 13 ± 2 months).

Anterior Pelvic Plane Tilt (PT), Lumbar Lordosis (LL) and the Pelvic Femoral Angle (PFA) were measured in each position. Changes in postural positions (?) and the Hip User Index (HUI) were calculated at each timepoint.

The risk of flexion impingement was determined by Δ PT from standing to deep seated of 20° or more (Δ PT $\geq 20^\circ$), Figure 1. Patients were broken into 4 risk groups based on whether they had pre- or post-op flexion risk. Logistic regression modelling was conducted to predict post-op flexion risk and the classifier model was tuned using Receiver-Operator-Characteristic curve (AUC) analysis.

Differences in rates of flexion risk from pre- to post-op between groups were assessed with Chi-squared tests, and Welch's two-sample t-tests compared means of continuous variables.

Results:

Pre-operatively, 13% of patients were at risk of flexion impingement (Table 1, Groups 3 and 4), which increased to 29% post-operatively (Table 1, Groups 2 and 4) ($p < 0.001$).

A total of 23% of patients developed a flexion risk post-operatively not present pre-operatively (Table 1 Group 2). Patients in this group had higher Δ PT (27° vs 6°), less LF (37° vs 42°), larger Δ PFA (110° vs 88°) and greater HUI (76% vs 68%) post- vs pre-operatively (all $p < 0.001$).

Compared with the group that displayed no flexion risk both pre- and post-op (Group 1), patients in this group (Group 2) had a higher change in Δ PT pre- to post-operative (20° vs 7°), tended to be older (69 vs 64), were more likely to be female (71% vs 48%) and had lower lumbar flexion both pre- (42° vs 48°) and post-operatively (37° vs 45°) (all $p < 0.001$), Table 1.

A classifier model has been developed and optimised to detect post-op flexion risk based on pre-operative parameters with a balanced accuracy of 73% (Sensitivity: 76.0%, Specificity: 69.5%) and an AUC of 80%, Figure 2.

Conclusion:

Post-operatively, nearly one in four patients exhibited a flexion risk ($?PT \geq 20^\circ$) between seated and standing positions which was not identified pre-operatively, elevating their risk for posterior instability. At risk patients tended to be older, female and have a stiffer spine pre-operatively than those that showed no flexion risk both pre- and post-op.

Figures

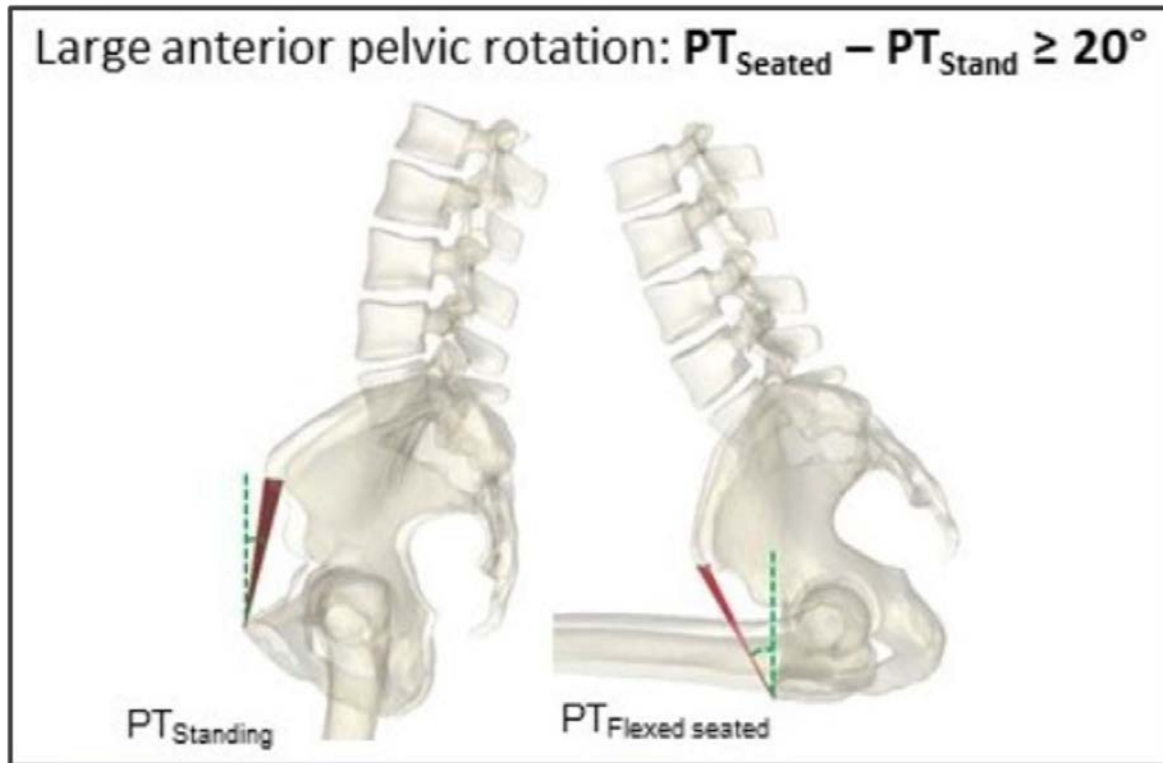


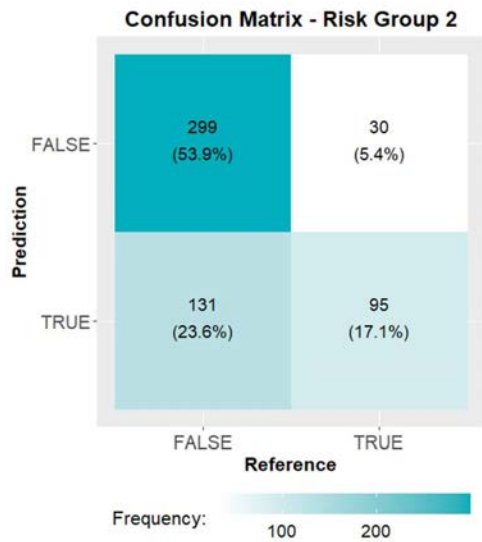
Figure 1 The risk of flexion impingement was determined by $\Delta PT \geq 20^\circ$.

[Figure 1](#)

Table 1: Mean spinopelvic measurements by flexion risk group

Class	Group 1: No Risk	Group 2: Post Risk	Group 3: Pre Risk	Group 4: Both Risk	All Data
Δ P \geq 20° Risk Pre	FALSE	FALSE	TRUE	TRUE	-
Δ P \geq 20° Risk Post	FALSE	TRUE	FALSE	TRUE	-
(n) Patients	357	125	39	34	555
% Total	64%	23%	7%	6%	100%
% Female	48%	71%	77%	82%	57%
Age At Surgery	64	69	70	73	66
Δ PT Pre	-1°	6°	26°	27°	4°
Δ PT Post	6°	27°	10°	30°	12°
Δ PT Post-Pre	7°	20°	-15°	3°	8°
PT Stand Post-Pre	-2°	-2°	1°	0°	-2°
PT Seated Post-Pre	5°	18°	-15°	3°	7°
LF Pre	48°	42°	36°	33°	45°
LF Post	45°	37°	37°	30°	41°
Δ PFA Pre	81°	88°	105°	109°	86°
Δ PFA Post	92°	110°	95°	113°	98°
HUI% Pre	63%	68%	75%	77%	66%
HUI% Post	68%	76%	73%	79%	71%

[Figure 2](#)



Accuracy:	71%
Sensitivity:	76%
Specificity:	70%
Balanced Accuracy:	73%

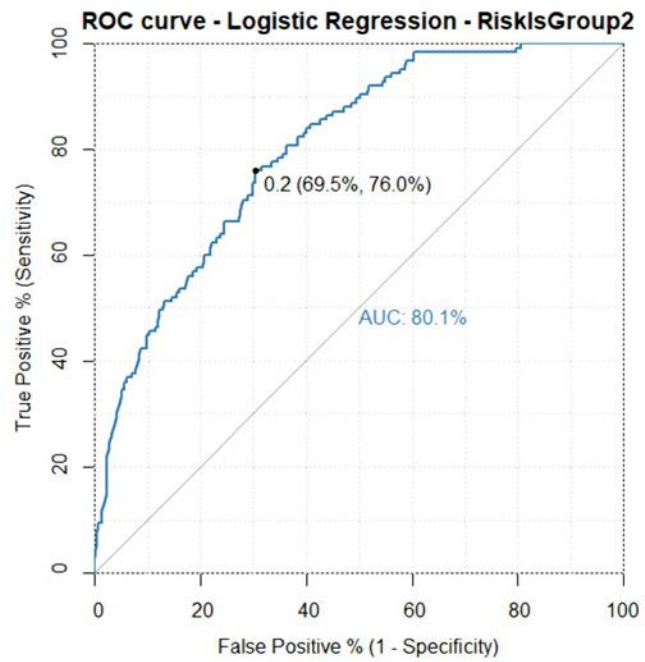


Figure 2. Confusion matrix and ROC-AUC classifier results for predicting patients who are at risk for impingement in flexion postop but not preop.

Figure 3

Targeted Prehabilitation Approach Guided by a Knee Kinesiography Exam Can Improve Function and Realign Expectations in Total Knee Arthroplasty Candidates

Pierre Ranger - Hopital Jean-Talon - Montreal, Canada

*Alix Cagnin - Emovi Inc - Montreal, Canada

Bianca Marois - Emovi - Montreal, Canada

Jean-Philippe Lajoie - Centre de médecine sportive de Laval - Laval, Canada

Alex Fuentes - Emovi - Montreal, Canada

Introduction: Up to 20% of patients are dissatisfied after total knee arthroplasty (TKA). Residual functional deficiencies and unmet expectations are recognized as significant factors in poorer TKA outcomes. Studies have advocated the importance of better preoperative care to address these issues to achieve optimal functional outcomes and satisfaction. Research has established the efficacy of a home-based exercise and education program, guided by a knee kinesiography exam, in non-surgical management of knee osteoarthritis. This study investigates whether implementing a similar targeted approach in prehabilitation for TKA candidates can yield similar outcomes.

Methods: This study was carried out in a private orthopaedic ambulatory surgical center (ASC) in Canada. Following the orthopaedic consultation, all patients eligible for TKA were invited to participate. A knee kinesiography exam with the KneeKG® system (Emovi, Canada) was performed at the ASC on the same day to accurately assess knee function during walking and identify knee biomechanical markers relevant to prehabilitation and TKA surgery (Figure-1). Following the exam, participants underwent a 45-minute education session, including explanation of the identified biomechanical markers, their possible underlying musculoskeletal causes, and the extent to which they could be impacted by conservative and surgical interventions. Patients were taught exercises designed to target these markers and given access to online instructional videos. A follow-up call was conducted 2 weeks after to adjust, if necessary, the nature and intensity of the exercises. The Knee Osteoarthritis and Injury Outcome Score for Joint-Replacement (KOOS-JR) and short Hospital for Special Surgery TKA Expectations were completed at baseline and 1 week before surgery. Patients who followed usual care completed the KOOS-JR one week prior to their surgery (controls). T-tests (paired and independent) were used to assess intra-/inter-group differences before surgery.

Results: Thirty (30) patients participated (prehabilitation: N=14, control: N=16). There was 56.7% of women (mean age: 69.1yrs (95%CI:65.5;72.7), BMI: 30.4kg/m² (27.4;33.3)). Patients followed the prehabilitation program for 8 weeks and most (79%) reported high adherence, performing their exercises at least several times/week. Prehabilitation group reported significant improvement in KOOS-JR (+15.4% from baseline score, p=0.019) leading to higher scores compared to controls going into surgery (59.1 vs 50.2, p=0.058). Pain while going up/down stairs, standing upright, and ability to bend/pick up objects were the items with the most improvement from prehabilitation (all 0.01≤p≤0.08). Incidentally, 30% of patient expectations in prehabilitation group were realigned (17% were reduced, 13% increased). Expectations regarding improved ability to walk, perform daily activities and climb stairs were the most frequently increased following the tailored exercises and education (for 18%, 20%, 27% of patients respectively), while participating in

recreational activities and sports were frequently reduced (25% and 20% respectively).

Conclusion: Results underscore the efficacy of a targeted prehabilitation and education approach guided by a knee kinesiography exam to improve patient function and realign their expectations towards TKA. While the approach showed value as an educational aid and supportive tool to promote self-management and empower patients to have more realistic expectations regarding their postoperative recovery, further investigation is needed to evaluate its impact on postoperative outcomes and satisfaction.

Figures



Fig-1. A knee kinesiography exam in a clinical setting.

[Figure 1](#)

Inertial Measurement Units Reveal Functional Differences Between Anterior and Posterior Approach in Hip Arthroplasty Patients

*Kate Moyle - University of Auckland - Auckland, New Zealand

Thor F Besier - University of Auckland - Auckland, New Zealand

George Grammatopoulos - The Ottawa Hospital - Ottawa, Canada

Isabel Horton - The Ottawa Hospital - Ottawa, Canada

Introduction

Traditional patient-reported outcome measures (PROMs) are subjective with a known 'ceiling effect' [1], which makes it challenging to differentiate outcomes of surgical approach or implant variation. Walking gait can be assessed using inertial measurement units (IMUs), providing easy, clinic-based measurement of spatiotemporal characteristics [2] and impact load asymmetry [3]. Improvements in walking speed have been shown following total hip arthroplasty (THA) [2], but comparisons between surgical approaches remain unexplored. We illustrate the capabilities of IMUs to assess early patient progress following THA and compare direct anterior and posterior surgical approaches.

Methods

A total of 66 THA patients (mean age: 62 ± 17 years) were recruited to the study, and their walking gait was assessed pre-operatively and at 2-weeks, 6-weeks, and 3-months following surgery using either a direct anterior approach (DAA, $n=47$) or a posterior approach ($n=19$). Patients walked at a self-selected pace, and spatiotemporal data were calculated from two ankle-worn IMUs (VICON-IMeasureU) using a validated algorithm [4]. We also recorded Oxford Hip Score (OHS), PROMIS-10 and EuroQol-5-dimension (EQ-5D) PROMs. Gait velocity, stride length, and impact load asymmetry between DAA and Posterior cohorts were compared using a repeated-measures ANOVA.

Results

All patients increased their stride length and walking speed between two- and six-weeks post-operation (Figure 1A). On average, the gait velocity of DAA patients increased by 0.25 m/s ($p < 0.01$), while posterior patients increased by 0.21 m/s ($p = 0.025$). Variations in impact load between operated and non-operated limbs correspond to individual differences in walking gait (Figure 1B). However, DAA patients had lower impact asymmetries six weeks and three months following surgery, indicating earlier operative joint loading and improved gait compared to Posterior patients. PROMs failed to identify differences in recovery between the two surgical groups at six weeks and three months post-operation ($p = 0.69$), compared to IMU data ($p = 0.04$) (Figure 1C).

Conclusion

Changes in IMU-measured gait were detected at six weeks post-THA surgery for both DAA and Posterior approaches, indicating a return to joint function. However, walking speed was still below an age-matched asymptomatic mean, as previously reported [2]. PROMs could not distinguish between the surgical groups during rehabilitation, suggesting a potential lack of sensitivity in capturing early progress. Individual changes in function are relevant to the surgeon to indicate early-stage problems in rehabilitation, and these data provide an important reference for future benchmarking. We are expanding this dataset with further comparison of surgical techniques.

References

1. Hamilton, D. F. et al. 2016. Bone Jt. Res. 5, 87–91.

2. Kaufmann, M. et al. 2023. J Orthop. Res. 41, 759–770.
3. Bolam, S. et al. 2021. Sensors. 21, Epub 2021/08/11.
4. Trojaniello, D. et al. 2014. J Neuroeng Rehab. 11.

Figures

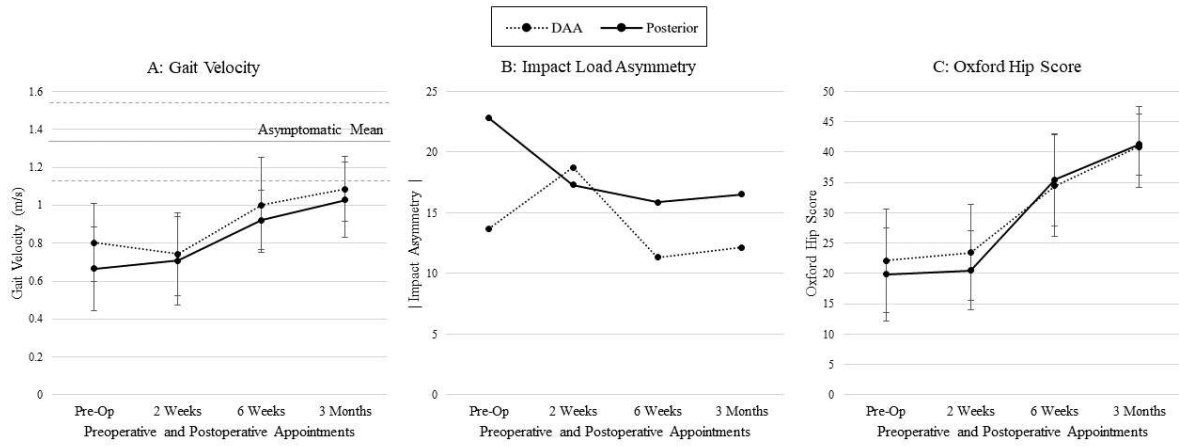


Figure 1. Mean IMU-measured gait velocity, mean absolute IMU-measured gait impact load asymmetry, and mean Oxford Hip Scores over rehabilitation periods following differing THA approaches (anterior vs posterior).

Figure 1

Impact of Proximal Stem Fill on Humeral Loosening and Stress Shielding

Maged Awadalla - Zimmer Biomet - Warsaw, USA

*Christine Mueri - Zimmer Biomet - Winterthur, Switzerland

Adam Henderson - Zimmer Biomet - Winterthur, Switzerland

Lukas Connolly - Zimmer Biomet - Winterthur, Switzerland

Ghislain Maquer - Zimmer Biomet - Winterthur, Switzerland

Jeffrey Bischoff - Zimmer, Inc. - Warsaw, USA

Philippe Favre - Zimmer Biomet - Winterthur, Switzerland

Introduction

Diaphyseal referencing stems are sometimes associated with higher risk of intraoperative fracture and stress shielding [1]. To address these clinical issues, metaphyseal-engaging stems provide a smaller distal stem diameter and rely on a larger proximal volume for fixation. However, the impact of proximal stem volume on fixation and stress shielding are not well understood. The goal of this study was to evaluate humeral loosening and stress shielding in a virtual population for a stem with a wider proximal volume and compare to a clinically successful stem with a slender proximal volume (both with metaphyseal fixation).

Methods

Forty-five humeral CT scans were reconstructed and virtually implanted with each of the device types (slender and wider proximal volume). Implant tilt, sizing (nominal, under-, oversized) and stem length (long/short) were varied for each device, resulting in over 300 finite element models (Fig.1). Physiological joint reaction and muscle forces representing three abduction positions were applied after being scaled to subject body weight. Interface conditions simulated short (frictional for humeral loosening) and long (bonded for stress shielding) term fixation. Bone-implant interface micromotion (humeral loosening) and change in cortical strain energy density between the intact and implanted states (stress shielding) were compared between the two devices.

Results

Micromotion was consistently lower for the wider proximal filling stem across all stem sizes (Fig.2), independent of surgical and loading conditions. For both device types, increased micromotion was observed with undersized stems. Stem length did not significantly influence micromotion, attributed to the dominant role of metaphyseal fixation of both devices as compared to diaphyseal fixation.

No difference in average stress shielding potential was found between the two devices (Fig.3) in any region around the humeral stem (as reflected in Gruen zone), independent of the implant tilt and sizing. Resorption was more likely in the calcar region (GZ6) for both devices and found in 1/3 of cases, while bone deposition was predicted in the proximal lateral/greater tubercle region (GZ1).

Conclusion

Modifying an implant design to improve one outcome may impact the risk of another clinical outcome. Modeling has shown a design with a wider proximal profile may improve primary stability, without significantly impacting the risk for stress-shielding. The population-based computational approach allows a direct comparison of two devices on the same cohort (which is not possible *in vivo*) and provides performance indicators before long term clinical data become available.

References

[1] Schnetzke et al., Obere Extremität 2019,14:139–148

Figures

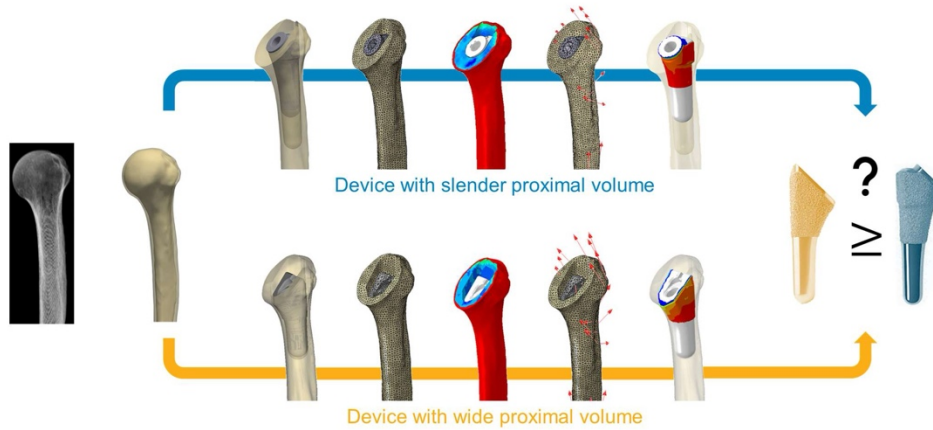


Figure 1. Methodology for evaluation of loosening and stress shielding in a virtual cohort.

Figure 1

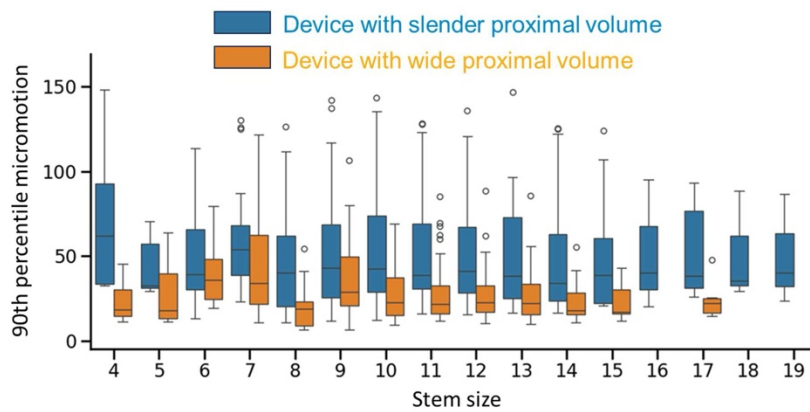


Figure 2. Micromotion for the two stem families by stem size, with nominal, under- and oversized stems.

Figure 2

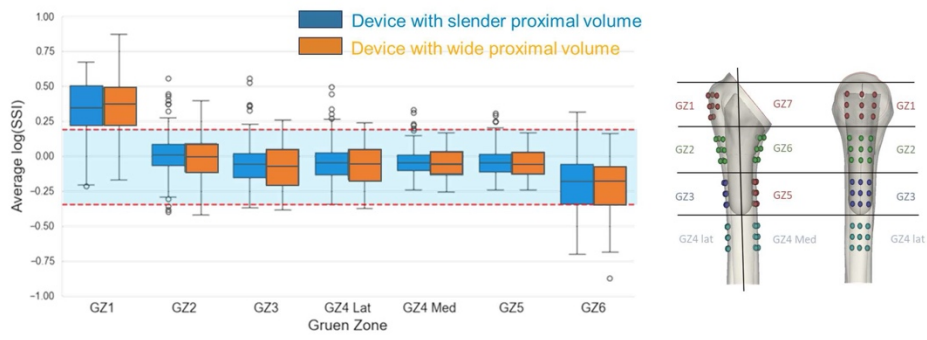


Figure 3: Average stress shielding index (SSI) per Gruen zone. The blue corridor indicates steady state, values above the corridor indicate bone deposition and values below the corridor indicate bone resorption potential.

[Figure 3](#)

Is a Lateral Facetectomy the Solution for Unresurfaced Patellae?

Nathan Lenz - Smith & Nephew - Memphis, USA

*William Fugit - Bartlett, United States of America

Introduction: Patellar resurfacing in total knee arthroplasty (TKA) continues to be a controversial topic with some surgeons preferring to resurface to avoid postoperative anterior knee pain and secondary resurfacing, while others do not resurface due to complications including fracture and patellar component failure. However, lateral facetectomy of the patella provides a simple treatment for patellae without the need for resurfacing [1]. The purpose of this study was to compare ligament strain and patella kinematics through simulations of TKAs with and without a lateral facetectomy for unresurfaced patella.

Methods: 66 cadaveric patellae were segmented and organized into the three Wiberg classification types [2]. Each patella had a duplicate with a lateral facetectomy. To keep the facetectomy consistent, each patella had 1/3-1/2 of the lateral facet removed parallel to the patellar ridge, then at 45° from the tip of the patellar ridge the lateral face was cut to match the patella to the trochlea of the femoral component to avoid catching and crepitus [Fig. 1] [3]. Each patella, with and without a lateral facetectomy, was then simulated with JOURNEY II BCS in LifeMOD through a full deep knee bend up to 160° of flexion, with the same soft tissue conditions for each simulation [Fig. 2]. Ligament strains and patellar kinematics were tracked within the software. A two-way ANOVA with a Tukey's Post-Hoc test was performed between the different Wiberg types and with or without a lateral facetectomy on the collected data.

Results: Lateral facetectomy resulted in a decrease in lateral retinaculum strain and creating more lateral versus medial tilt for all three Wiberg types [Fig. 3]. Retinaculum strains and patella tilt were significantly different ($p < 0.05$) for the Wiberg types when the patella was intact especially between types 1 and 3, but after lateral facetectomy no significant differences ($p > 0.05$) remained. A significant change was observed when a lateral facetectomy was performed on any patella type, with larger changes for patella type 2 and 3, specifically for lateral retinaculum strain and patellar tilt.

Conclusion: This study resulted in positive effects to an unresurfaced patella with a lateral facetectomy, specifically with a decrease in Lateral Retinaculum strain and more consistent patellar tilt. The results also showed that before a lateral facetectomy there are large differences in ligament strain and patellar kinematics between the Wiberg types, but with a lateral facetectomy it results in a more consistent and similar outcome between all three types. The data revealed significant changes for all Wiberg types after a lateral facetectomy, which determined that the positive effects of a lateral facetectomy is not exclusive to a Wiberg type. However, the changes were larger for the type 2 and 3 patellae, which may correlate lateral facet length to positive effects of a lateral facetectomy.

[1] Zhang et al. JOA. 2012;27:1442-7.

[2] 2. Wiberg AOS. 1941;12:319-410.

[3] Lakstein et al. JOA. 2014;29:2146-9.

Figures

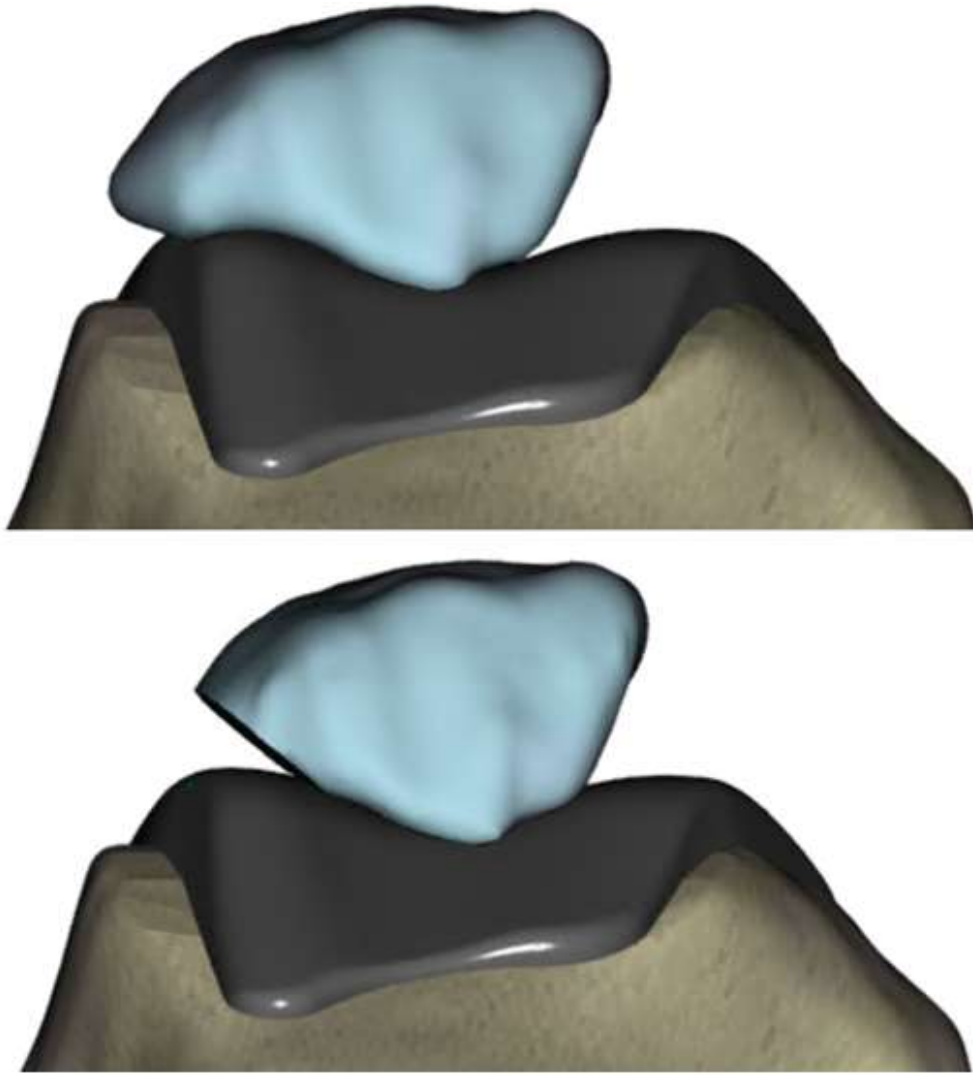


Figure 1. Skyline view of a Wiberg Type 3 patella before a lateral facetectomy (top) and after (bottom).

[Figure 1](#)

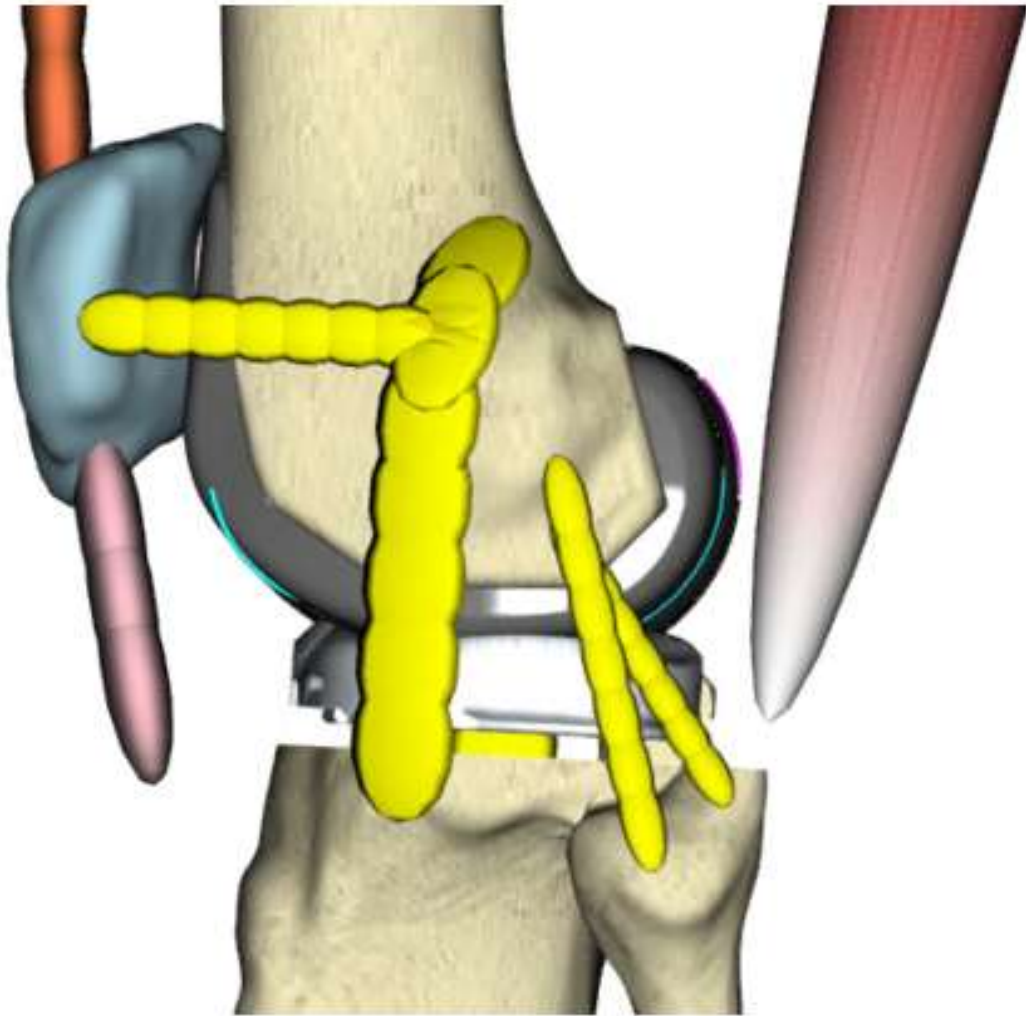


Figure 2. LifeMOD computerized model setup for deep knee flexion simulation.

Figure 2

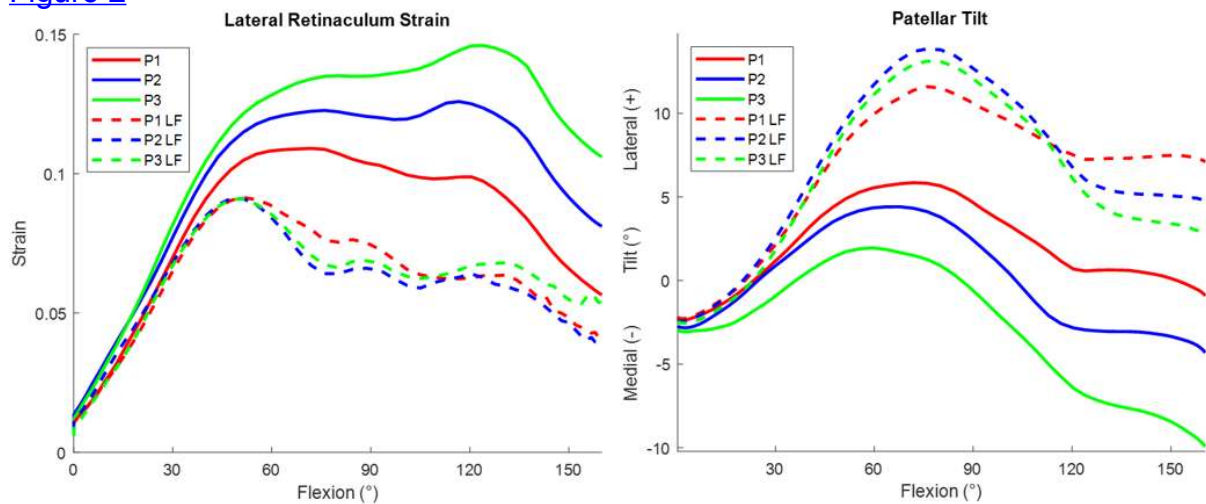


Figure 3. Average Lateral Retinaculum strain for each Wibeig Patella type with and without a lateral facetectomy (LF) (left). Average Patellar Tilt for each Wibeig Patella type before and after a lateral facetectomy (right).

Figure 3

Matching Trochlear Congruity to the PCA in Total Knee Replacement

*James Crutcher - Swedish Orthopedic Institute - Seattle, United States of America

Introduction:

Contemporary knee replacement is embracing new alignment philosophies including kinematic alignment, anatomic alignment, and functional alignment as alternatives to traditional mechanical alignment. These new alignment strategies introduce variable degrees of femoral component rotation to balance the flexion gap, which have an effect on the congruity of the prosthetic trochlea with the native trochlea, when using modern monolithic femoral components. CT-based navigation and robotic technologies have introduced 3-dimensional (3D) pre-operative plans that allow evaluation of femoral component placement in an axial view. The purpose of this study is to examine how often matching femoral component rotation to the posterior condylar axis (PCA) creates incongruity with the native trochlea.

Methods:

220 consecutive CT-based 3D pre-operative total knee replacement (TKA) plans were reviewed. A standardized axial view of the distal femur 10 mm proximal to the distal medial femoral condyle was used to measure the PCA, as well as the degree of femoral component rotation required to optimize trochlear congruity, both relative to the trans-epicondylar axis (TEA), in all cases. A matching score was computed by adding the PCA to the trochlear congruity angle. A good match was defined as $< 4^\circ$, a moderate match as $4-6^\circ$, and a poor match as $>6^\circ$. The matching scores were also sorted by gender and pre-operative limb alignment.

Results:

There was a good match ($<4^\circ$) between the PCA and trochlear congruity in 107 (49%) cases; a moderate match ($4-6^\circ$) in 55 (25%) cases; and a poor match ($>6^\circ$) in 58 (26%) cases. In 23 (10%) cases, the mismatch was $>8^\circ$. There was some disparity when the results were sorted by gender, with 21 males (19%) having a poor match, as compared to 37 females (34%). A good match occurred in 46% of varus knees, 52% of valgus knees, and 81% of neutral alignment ($\pm 2^\circ$) knees.

Conclusion:

This CT-based study found significant variation in matching the PCA and optimal trochlear congruity when evaluating a 3D pre-operative plan in a standardized axial view. A poor match was identified in 26% of the study group. There was some disparity when the results were sorted by gender and pre-operative limb alignment. These results imply that optimization of the 3D positioning of a monolithic femoral component may require some compromise of trochlear congruity and/or flexion gap balance, or an alternative femoral component design, in some cases.

Does Melatonin Improve Sleep Following Primary Total Hip Arthroplasty: A Randomized, Double-Blind, Placebo-Controlled Trial

*Muhammad Haider - NYU Orthopedic Hospital - New York, USA

Kyle Lawrence - NYU Orthopedic Hospital - New York, USA

Thomas Christensen - NYU Langone Health - New York, USA

Akram Habibi - NYU Langone Orthopedic Hospital - New York, United States of America

Benjamin Schaffler - NYU Orthopedic Hospital - New York, USA

Ran Schwarzkopf - NYU Langone Medical Center Hospital for Joint Diseases - New York, USA

William Macaulay - Center for Hip & Knee Replacement - New York, USA

Joshua Rozell - NYU Langone Orthopedic Hospital - New York, USA

Sophia Antonioli - NYU Langone - New York, USA

Catherine Digangi - NYU Orthopedic Hospital - New York, USA

Background:

Sleep impairment following total hip arthroplasty (THA) is common and may decrease patient satisfaction and early recovery. We aimed to assess whether melatonin use could promote healthy sleep and reduce sleep disturbance in the acute period following THA.

Methods:

Patients undergoing primary, elective THA between July 2021 and March 2024 were prospectively enrolled and randomized to receive either 5mg of melatonin nightly or placebo for 14 days postoperatively. Participants recorded their nightly pain on the visual analogue scale (VAS), number of hours slept, and number of nighttime awakenings in a 14-day sleep diary starting the night of surgery (postoperative day [POD] 0). Sleep disturbance was assessed preoperatively and on POD14 using the patient reported outcome measurement information system sleep disturbance (PROMIS-SD) form (with higher scores representing greater sleep disturbance). Epworth Sleepiness Scores (ESS) were collected on POD14 to assess sleep quality.

Results:

139 patients successfully completed the study protocol, with 64 patients in the placebo group and 75 patients in the melatonin group. Melatonin patients experienced significantly more hours of sleep on POD 2 (placebo: 5.7 ± 2.4 , melatonin: 6.5 ± 1.7 , $P = 0.017$) and averaged over POD 1 to 3 (placebo: 5.7 ± 2.0 , melatonin: 6.1 ± 1.6 , $P = 0.136$), although this was not statistically significant. Both groups demonstrated comparable hours of sleep from POD4 and onward. Fewer night-time awakenings in the melatonin group were observed on POD 2 (placebo: 3.1 ± 2.0 , melatonin: 2.7 ± 1.5 , $P = 0.282$), although this was not statistically significant. The melatonin group demonstrated significantly lower postoperative PROMIS-SD scores (placebo: 56.3 ± 9.2 , melatonin: 52.5 ± 9.3 , $P = 0.040$). Although not statistically significant, the melatonin group demonstrated lower postoperative ESS scores (placebo: 6.8 ± 4.5 , melatonin: 6.0 ± 4.0 , $P = 0.348$).

Conclusion:

Melatonin may promote longer sleep in the immediate postoperative period after THA, although these benefits wane after POD 3. Disturbances in sleep should be expected for most patients, although melatonin may have an attenuating effect. Melatonin is safe and can be considered for THA patients experiencing early sleep disturbances postoperatively.

Figures

Table 1: Baseline Characteristics

Demographic	Placebo (n=64)	Melatonin (n=75)	P-Value
Mean Age (years) [range]	62.6 [24-83]	62.7 [32-85]	0.949
Sex, n (%)			0.497
Men	24 (37.5)	27 (36.0)	
Women	40 (62.5)	48 (64.0)	
Race, n (%)			0.750
White	46 (71.9)	54 (72)	
African American	6 (9.4)	10 (13.3)	
Asian	3 (4.7)	5 (6.7)	
Hispanic/Latino	5 (7.8)	3 (4.0)	
Other	4 (6.3)	3 (4.0)	
Insurance, n (%)			0.933
Commercial	37 (57.8)	41 (54.7)	
Medicare	23 (35.9)	29 (38.7)	
Medicaid	4 (6.3)	5 (6.7)	
BMI (kg/m ²) [range]	29.0 [18.6-55.0]	29.5 [15.5-49.4]	0.687
Smoking Status, n (%)			0.815
Never	40 (62.5)	46 (61.3)	
Former	22 (34.4)	25 (33.3)	
Current	2 (3.1)	4 (5.3)	
ASA Class, n (%)			0.921
1	11 (17.2)	11 (14.7)	
2	44 (68.8)	53 (70.7)	
3	9 (14.1)	11 (14.7)	
Mean CCI (SD)	3.0 (2.8)	2.5 (2.2)	0.236
Primary diagnosis, n (%)			0.166
OA	61 (95.3)	75 (100.0)	
Post-Traumatic OA	1 (1.6)	0	
AVN	2 (3.1)	0	

BMI; body mass index, CCI; [Charlson Comorbidity Index](#), SD; Standard Deviation, ASA; American Society of

Anesthesiologists, OA; Osteoarthritis, AVN; Avascular Necrosis

Figure 1

Table 2: Primary Outcomes of Placebo and Melatonin Groups

	Placebo	Melatonin	P-Value
Average Hours Slept (SD)			
POD1	4.9 ± 2.6	5.3 ± 2.3	0.353
POD2	5.7 ± 2.4	6.5 ± 1.7	0.017*
POD3	6.3 ± 2.1	6.5 ± 1.6	0.535
POD1-3	5.7 ± 2.0	6.1 ± 1.6	0.136
POD4-6	6.4 ± 2.0	6.4 ± 1.5	0.967
POD7-9	6.4 ± 1.8	6.6 ± 1.5	0.485
POD10-14	6.6 ± 1.7	6.7 ± 1.4	0.507
Average # Nightly Awakenings (SD)			
POD1	3.1 ± 2.3	3.2 ± 1.9	0.717
POD2	3.1 ± 2.0	2.7 ± 1.5	0.282
POD3	2.7 ± 1.4	2.7 ± 1.6	0.899
POD1-3	2.9 ± 1.6	2.9 ± 1.4	0.959
POD4-6	2.6 ± 1.4	2.6 ± 1.4	0.784
POD7-9	2.3 ± 1.2	2.4 ± 1.4	0.745
POD10-14	2.2 ± 1.2	2.1 ± 1.1	0.435
PROMIS Sleep Disturbance (SD)			
Preoperative	53.9 ± 7.9	53.2 ± 9.8	0.692
Postoperative	56.3 ± 9.2	52.5 ± 9.3	0.040*
Delta	2.1 ± 9.8	0.3 ± 9.8	0.346
Patients (%) with increased sleep disturbance	23 (51.1%)	28 (49.1%)	0.923

POD; postoperative day, PROMIS; patient-reported outcome measure information system

Figure 2**Table 3: Secondary Outcomes of Placebo and Melatonin Groups**

	Placebo	Melatonin	P-Value
Average Nightly Pain Score (SD)			
POD1	4.7 ± 2.7	5.4 ± 2.6	0.148
POD2	4.3 ± 2.4	4.8 ± 2.7	0.226
POD3	4.0 ± 2.3	4.3 ± 2.5	0.535
POD1-3	4.3 ± 2.3	4.8 ± 2.4	0.200
POD4-6	3.5 ± 2.1	3.7 ± 2.4	0.498
POD7-9	2.9 ± 2.1	3.0 ± 2.3	0.788
POD10-14	2.4 ± 1.9	2.1 ± 2.0	0.369
Average Epworth Sleepiness Score (SD)	6.8 ± 4.5	6.0 ± 4.0	0.348

POD; postoperative day, SD; standard deviation

Figure 3

Evaluating the Precision of Joint Centre Reconstruction in Total Hip Arthroplasty and Its Effect on Post-Operative Axial Rotation of the Femur

*Gerard Smith - Corin - Sydney, Australia
Christopher Plaskos - Corin - Raynham, USA
Douglas Dennis - Colorado Joint Replacement - Denver, USA
Jim Pierrepont - Corin - Pymble, Australia

In total hip arthroplasty (THA), accurate reconstruction of the centre of rotation (COR) is essential for joint stability, range of motion, and implant longevity. It is hypothesized that an inaccurately restored COR has the potential to alter femoral rotation, leading to complications such as altered gait and increased risk of dislocation. This study aims to assess the deviations between preoperatively planned and intraoperatively delivered CORs, referencing the native preoperative position, and potential influence on post-op axial rotation of the femur.

This study retrospectively analysed 938 THAs in 938 patients who underwent staged bilateral THA in the CorinRegistry (53% female, mean age 64 ± 10). Each case was planned using OPSInsight™ (Corin, Cirencester, UK) 3D preoperative planning platform between June 2019 and August 2023. Each patient underwent two CT scans: 1) prior to the initial surgery and 2) before the second stage procedure (average time between imaging was 12 ± 10 months). 3D models of the pelvis and proximal femur were created using medical image segmentation software.

Automated registration of the pelvis (Figure 1) and proximal femur models generate 3D transformation matrices, enabling the mapping of post-operative landmarks to the pre-operative reference frame. The preop and postop COR of the femur was determined by fitting a sphere to the native (worn) and implanted femoral heads, respectively. To determine the acetabular COR, the femoral head centre was transferred to the pelvis using the relative position of the femur and pelvis in the CT scan. Positive change in global AP anterior offset is defined by the cumulative difference between the anteriorization of the femoral COR and the posterization of the pelvic COR. The effect of change in global AP anterior offset on change in femoral internal rotation (relative to the CT coronal plane) was assessed using linear regression. Additionally, differences in femoral rotation for low (< -5 mm), average (-5 to 5 mm), and high (> 5 mm) changes in global anterior offset were assessed Tukey's post-hoc test.

The achieved COR was medialized by 4.6 mm on the acetabulum and 5.1 mm on the femur relative to the native head centre, Table 1. Similarly, the achieved femoral and acetabular CORs were shifted proximally by 2.8 mm and 0.4 mm respectively, resulting in an average increase in hip length of 3.2 mm.

Change in global AP offset was moderately correlated with change in femoral internal rotation ($R = 0.5$), with a regression slope indicating an average increase in femoral internal rotation of 0.6° per millimetre increase in global anterior offset ($p < 0.0001$, Figure 2A). Changes in femoral internal rotation of -1.8° , 5.0° and 10.0° were reported across low, average, and high anterior offset change groups, respectively ($p < 0.0001$, Figure 2B).

The COR is medialized by approximately 5 mm on average in THA, which may reduce muscle moment arms but increase torque acting at the bone-stem interface. Global AP offset increased by > 5 mm in 24% of cases, resulting in an average increase in femoral internal rotation of 10° . Future studies should investigate the effects of these large changes in COR and AP offset on the biomechanics of the hip joint.

Figures

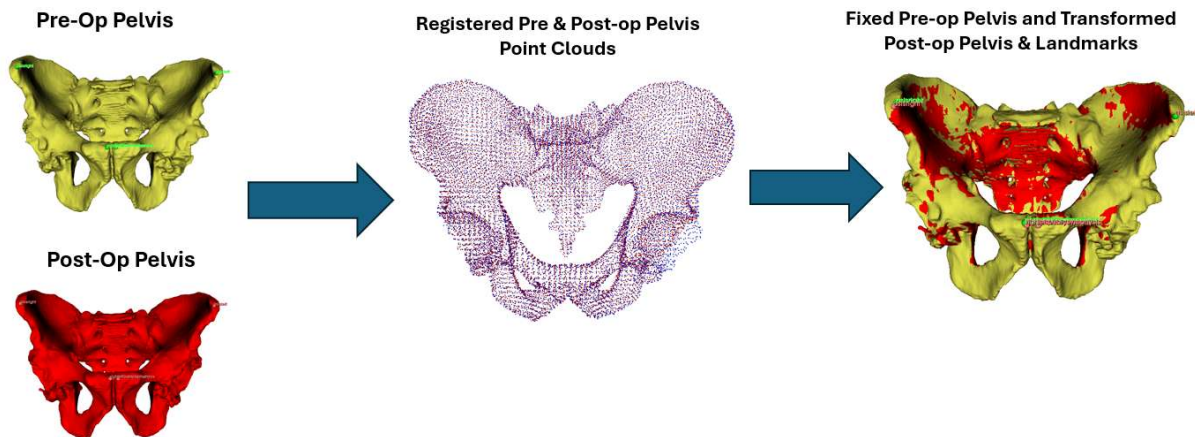


Figure 1

	Femur Head Centre (Mean ± SD)			Pelvis Centre (Mean ± SD)		
	AP	ML	IS	AP	ML	IS
Planned vs Native	0.6±2.3	2.9±3.1	2.2±2.5	-2.3±2.0	5.1±3.9	0.5±2.3
Achieved vs Native	-0.8±5.8	5.1±4.4	2.8±3.9	-1.7±2.3	4.6±4.2	0.4±2.7
Achieved vs Planned	-1.4±5.5	2.2±4.1	0.6±3.7	0.6±2.1	-0.6±3.1	-0.1±2.5

Figure 2

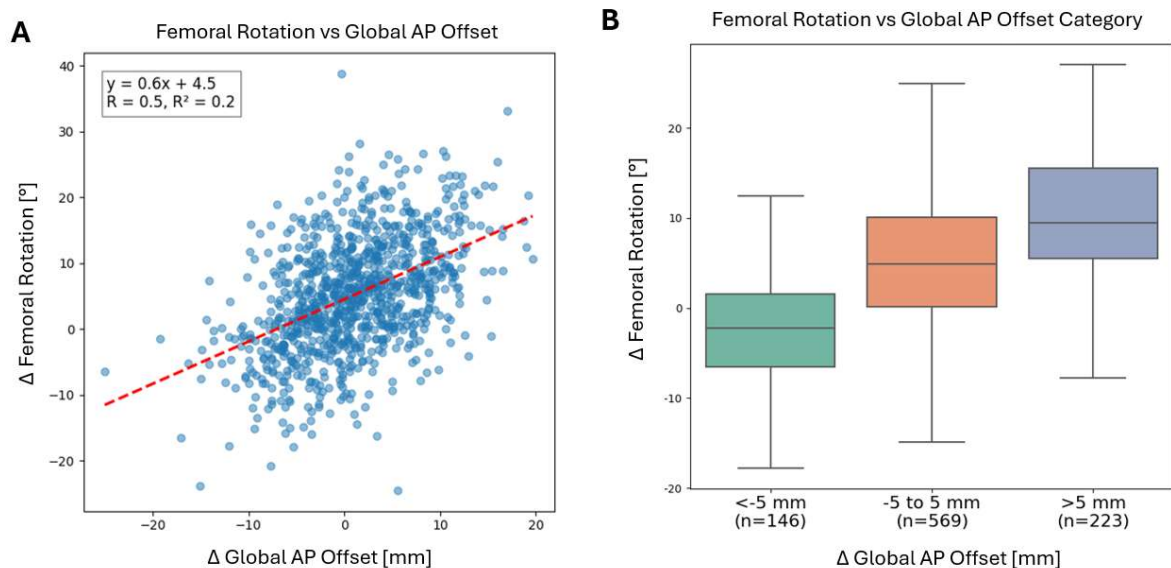


Figure 3

Computational Anatomical Reconstruction of Abnormal Patellar Geometries Based on Statistical Shape Modelling (SSM)

*Maria Moravidou - Imperial College London - London, GB

Rima Nasser - Imperial College - London, GB

Justin Cobb - Imperial College - London, United Kingdom

Richard van Arkel - Imperial College London - London, United Kingdom

Introduction:

Patellar component design in knee arthroplasty is less investigated than femoral and tibial components. Recent findings indicate that its design also influences knee biomechanics, and as such there is interest in more anatomical, or even customised patellar components. However, little is known about patellar morphology, and abnormal patellar bony anatomy often seen in patients with severe patellofemoral arthritis poses an obstacle to customised design. This study aimed to apply and validate a Statistical Shape Model (SSM)-based technique for establishing normal patellae from those with defects.

Methods:

The research sample included 50 patellae (25 female, mean age 63, range 43-77), which were segmented with Mimics from Magnetic Resonance Imaging (MRI) data obtained from the Osteoarthritis Initiative (OAI) database.

The establishment of point-to-point correspondences and reconstruction of virtual anatomical defects were performed using Scalismo. Initially, one randomly selected mesh served as the template mesh, which underwent a two-step rigid alignment with the other 49 patella, and then non-rigid registration using a gradient-based optimization. The performance of the SSM was assessed using compactness and generality metrics.

Evaluation of the SSM's reconstruction ability was conducted through leave-one-out cross-validation analysis. For this, a patella was randomly selected to be a test case. A virtual anatomical defect, that effectively removed the lateral portion of the patella, was computationally annotated on it. This defect removed the region of the patella that is typically most deformed in the case of severe osteoarthritis. Two sizes of defect were analysed: a small defect, which removed 1/3 of the distance between the patella ridge and the most lateral aspect of the patella, and a large defect, removing 2/3 of this distance. An SSM trained on the remaining 49 patella was then non-rigidly fitted to the remaining 'healthy' portion of the test patella, and the missing bone area was reconstructed. The reconstructed patella was quantitatively compared to the native patella. This process was repeated until all patellae had served as the test case.

Results:

The most prominent mode of shape variation of the patella represented its size, followed variation in its proximal and distal morphology (Figure 1). Compactness metrics revealed that only 25% of variation was described by the first mode, and 20 modes were required to capture 90% of the total shape variation (Figure 2a).

Generality metrics showed that the resulting SSM described unlearned shapes with a mean absolute error of 0.5mm (Figure 2b).

The average absolute distance between the reconstructed and native patella was (mean \pm standard deviation) 0.3 ± 0.1 mm for small defects and 0.4 ± 0.1 mm for large defects (Figure 3a). The maximum absolute distance between the reconstructed and native patella was (mean \pm standard deviation) 2.1 ± 0.6 mm for small defects and 2.4 ± 0.6 mm for large defects (Figure 3b).

Conclusion:

An SSM-based reconstruction technique has been demonstrated to reconstruct virtual patellar defects with low error, similar to that associated with PSI guides and

robotic surgery. These findings suggest that SSM could potentially serve as an aiding tool in the surgical planning of patellar reconstruction and custom design.

Figures

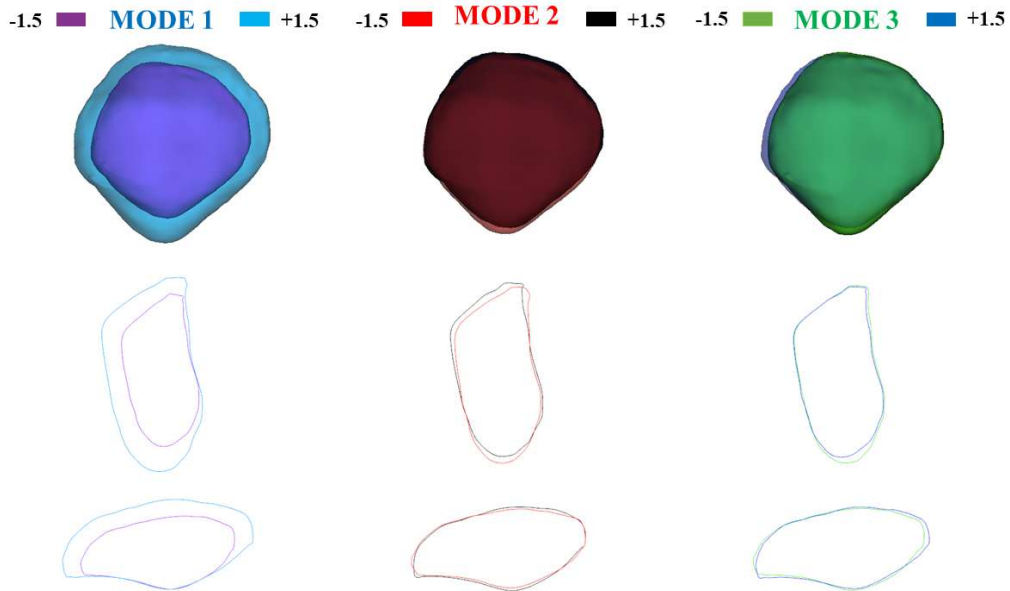


Figure 1: Illustration of the anatomical shape variation of the patellar bone using the first three modes of variation in coronal, sagittal, and axial views, with each view represented at \pm SD (Standard Deviation).

Figure 1

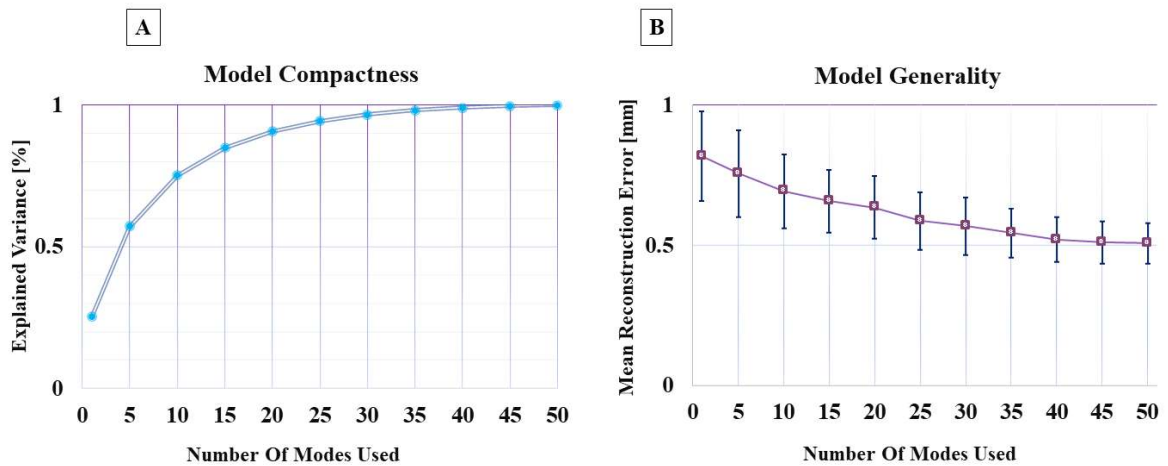


Figure 2: SSM performance through a) compactness and b) generality metrics.

Figure 2

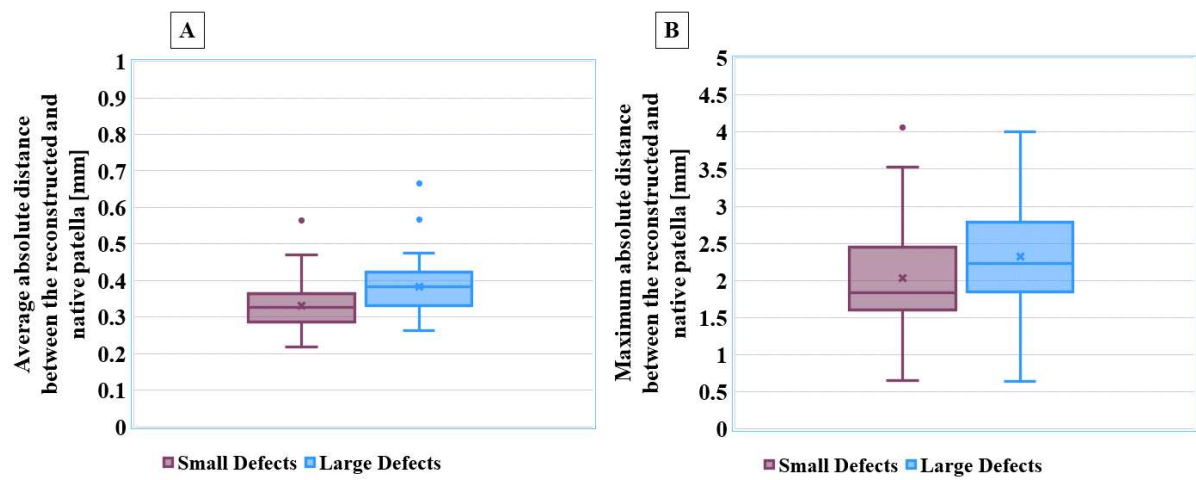


Figure 3: Cross-validation results for the SSM-based reconstruction algorithms expressed as a) average absolute and b) maximum absolute distances between the reconstructed and native patella for small and large defects.

[Figure 3](#)

Clinical Accuracy of Patient-Specific Humeral and Glenoid Guides in Total Shoulder Arthroplasty

*Estelle Liu - 360 Med Care - Sydney, Australia

Joshua Twiggs - University of Sydney - Sydney, Australia

Brad Miles - 360 Knee Systems - Pymble, Australia

Benjamin Kenny - Greenslopes Hospital - Brisbane, Australia

Introduction:

Accurate positioning of the humeral and glenoid component is crucial for successful total shoulder arthroplasty (TSA), impacting implant longevity, stability, and range of motion. Component malalignment has been linked to various complications, emphasising the need for precise surgical techniques and advanced planning. Despite this, there is a scarcity of studies evaluating computer-assisted technologies for humeral component positioning. This study aimed to assess the accuracy of humeral and glenoid component positioning using patient-specific instruments (PSI) in a clinical setting.

Methods:

42 patients undergoing primary TSA were included. All patients received a CT scan, which was used for preoperative planning and PSI design. Patients were stratified into normal (up to B1) or severe (B2 onwards) glenoid wear according to the Walch classification. The aetiology for TSA was determined as cuff tear arthropathy (CTA) or osteoarthritis (OA) based on radiologic features and clinical presentation. Postoperative CT scans were used to assess the achieved version and neck-shaft angle of the humeral component, and version and inclination of the glenoid component. Humeral version was only calculated for patients with a CT scan extending to the distal humerus, which was available for 18 patients.

Results:

The mean deviation between planned and achieved humeral version, humeral neck-shaft angle, glenoid version and glenoid inclination were $3.1^{\circ} \pm 2.1^{\circ}$, $2.3^{\circ} \pm 1.4^{\circ}$, $1.7^{\circ} \pm 1.5^{\circ}$ and $1.4^{\circ} \pm 1.4^{\circ}$, respectively (Figures 1-2). Two humeral components and one glenoid component were implanted with greater than 5° deviation from the planned neck-shaft angles and inclination, respectively, and considered outliers. The mean deviation in glenoid version was greater in males compared to females ($p=0.019$), with a greater variance in deviation for glenoid inclination ($p=0.046$) (Figure 3). No statistically significant difference was found between the deviations when comparing between patients based on TSA diagnosis, or between patients with normal or severe glenoid wear for any orientation.

Conclusion:

To the best of our knowledge, this is the first study to evaluate the accuracy of humeral guides in vivo. The primary finding is that a preoperatively planned humeral component can be precisely executed with PSI in 95% of cases and glenoid component in over 97% of cases. The non-significance observed in the accuracy between patients stratified for glenoid wear and diagnosis for TSA, suggests that PSIs can be designed and used accurately, independent of patient morphology, osteophytic growth and disease progression. A higher deviation in glenoid accuracy in males may be attributed to the challenges of exposure in patients with a larger anatomy and muscle mass.

Figures

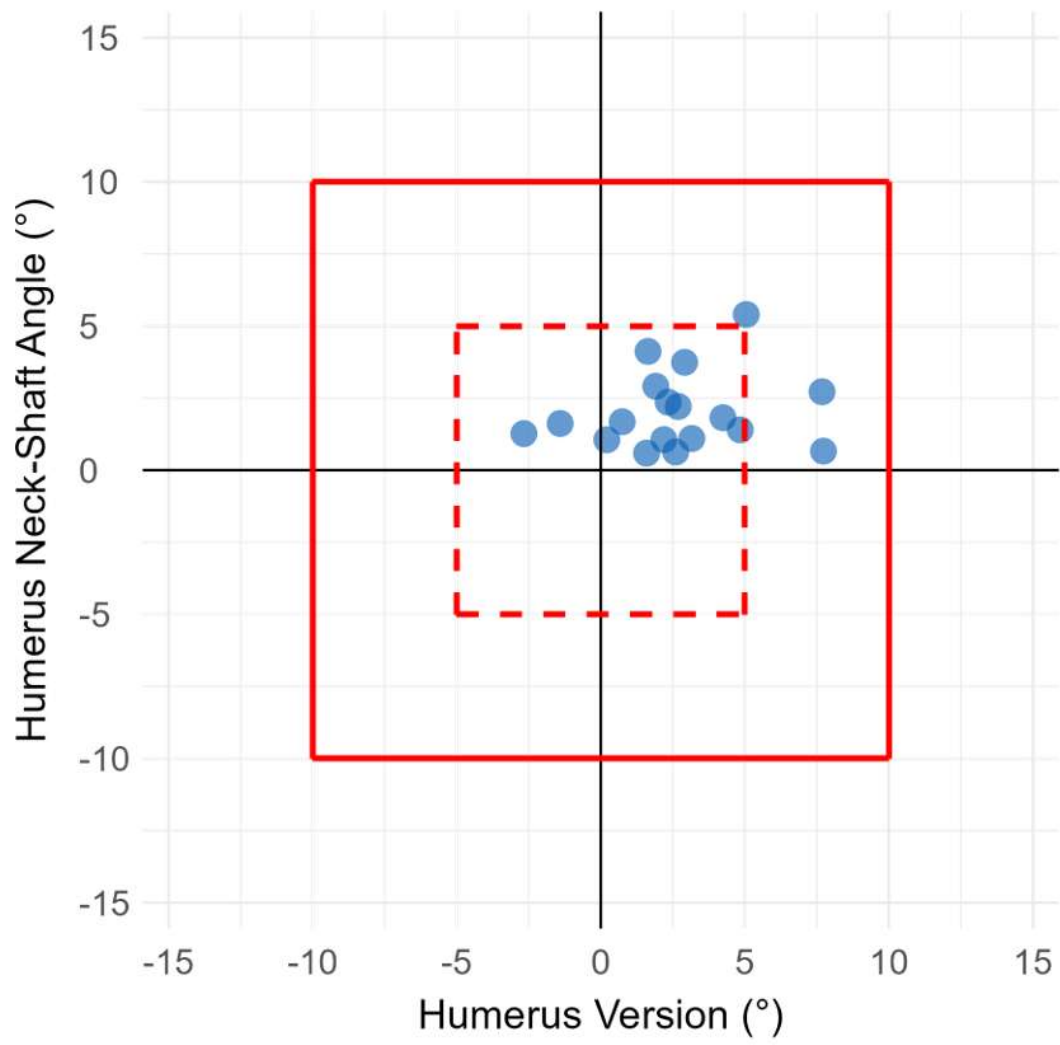


[Figure 1](#)

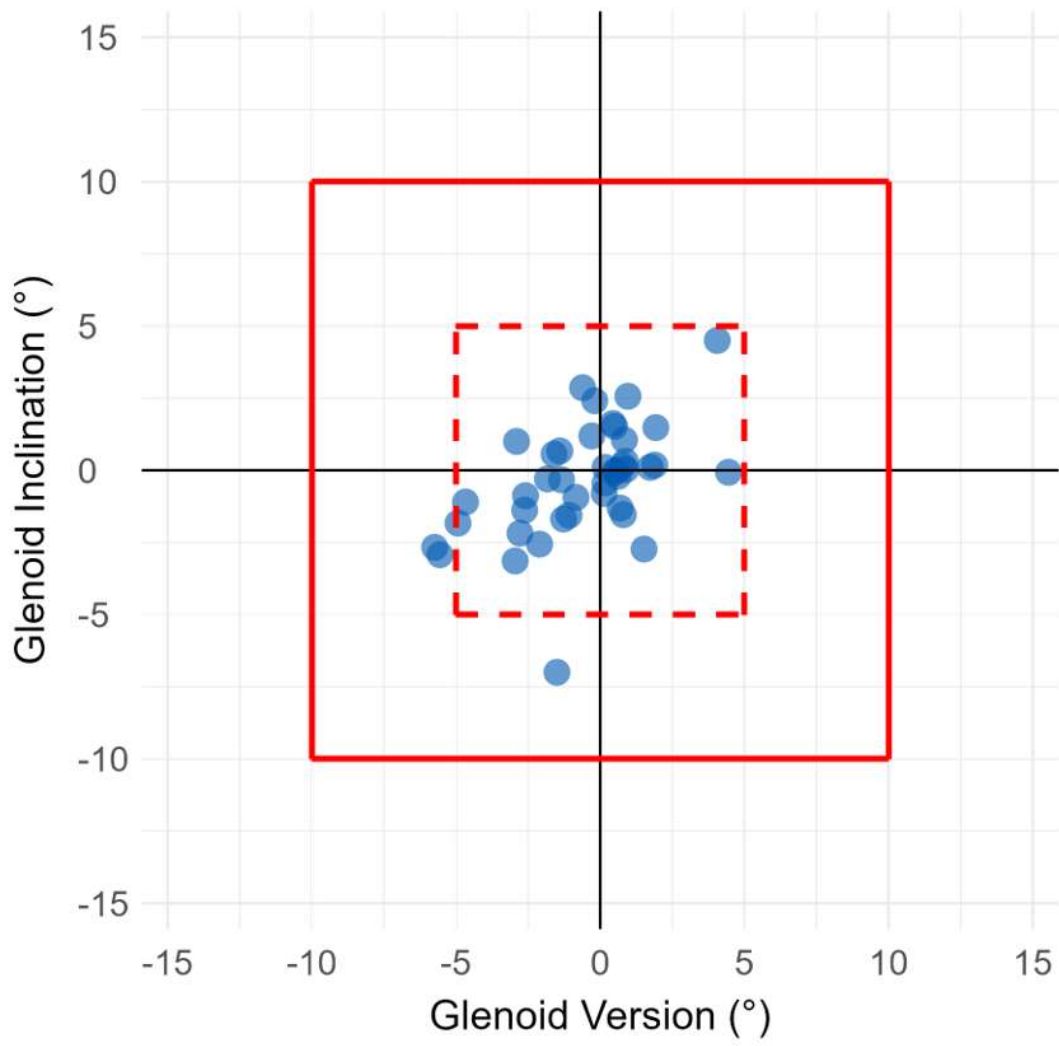


[Figure 2](#)

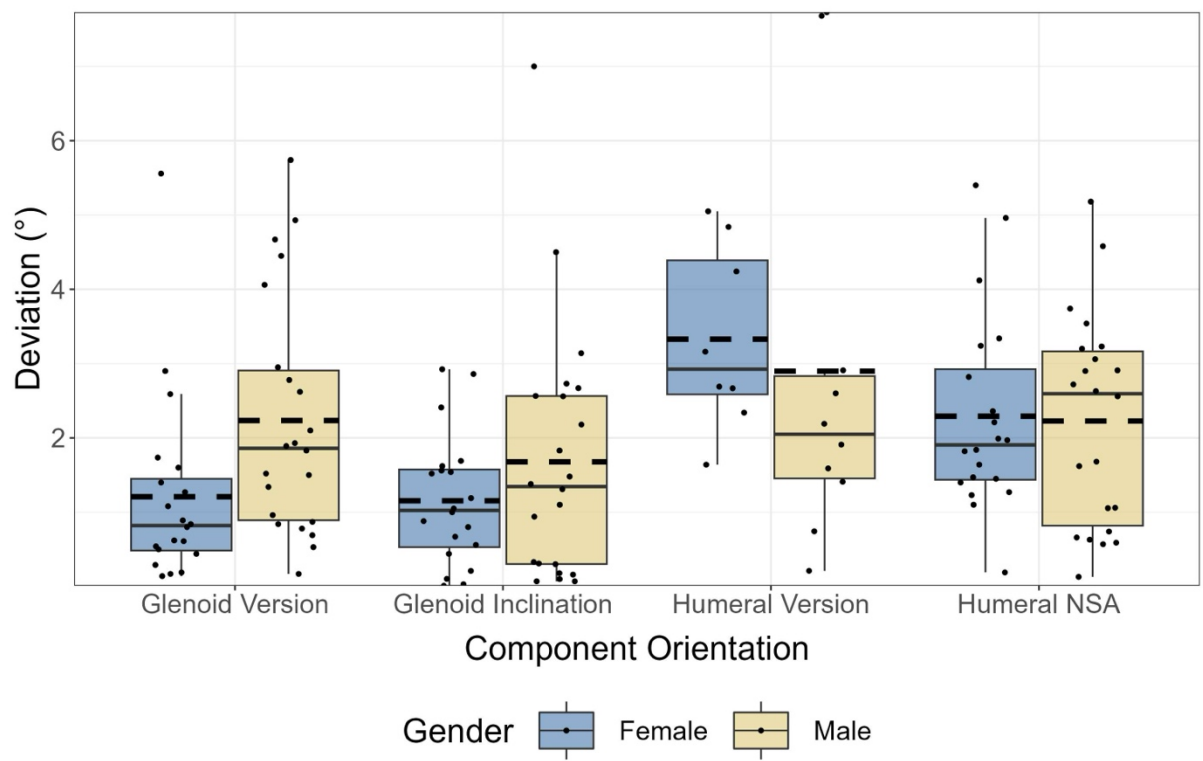


[Figure 3](#)

Accuracy of a Mixed Reality Surgical Platform for Total Knee Arthroplasty

*John Cooper - Columbia University - New York, USA

Aaron Young - PolarisAR - Miami, USA

Jacob B. Brenza - PolarisAR - Miami, USA

Mike E. King - PolarisAR - Miami, USA

Winona L. Richey - PolarisAR - Miami, USA

INTRODUCTION

Computer-assisted navigation has improved surgeons' ability to achieve accurate implant placement in total knee arthroplasty (TKA). Conventional navigation systems are large and costly while smaller systems do not provide the full gamut of guidance from landmarking, pre-resection assessment of soft-tissue laxity, and bone resection planning, execution, and validation. Here we present and evaluate a novel platform where instrument tracking, computing, and displays are all integrated into an augmented reality headset, allowing this comprehensive guidance in a small, efficient footprint [Fig. 1].

METHODS

Accuracy of this novel mixed reality system was evaluated in a cadaveric simulated use study with four pelvis-to-toe specimens. Depth and angular errors are reported across eight knees for proximal tibial, distal femoral, and posterior femoral resections by comparing platform-navigated resection metrics to calipered resection depths and post-operative CT measured angles. Ground truth measurements were compared to the surgeon-accepted metrics displayed by the platform prior to resection [Fig. 2].

RESULTS

All simulated use depth and angular absolute errors were below 2mm and 2° with 83% of depth and angular errors were at or below 1mm and 1°. Depth errors averaged -0.2 ± 0.8 mm (mean \pm standard deviation) with a 95% confidence that 90% of data lies within the interval of [-1.8mm, 1.4mm]. Angular errors averaged $0.3 \pm 0.7^\circ$ with a 95% confidence interval of [-1.2°, 1.8°] at 90% reliability. Absolute errors averaged 0.7 ± 0.4 mm and $0.6 \pm 0.5^\circ$ for depths and angles respectively.

CONCLUSION

This novel mixed reality platform achieves sub-millimeter and sub-degree average errors, providing both a workflow and accuracy that are comparable to modern robotic-assisted TKA systems. This imageless, open platform for TKA surgical guidance requires only an augmented reality headset with no additional equipment footprint, minimal tooling, and data overlaid holographically onto the surgical scene, while still providing a comprehensive, robust surgical workflow with state-of-the-art accuracy.

Figures

Figure 1

The complete surgical platform including reusable instruments (a-g), disposable screws (h), disposable tracked instruments (i-l), and the Head Mounted Device – Microsoft HoloLens 2.

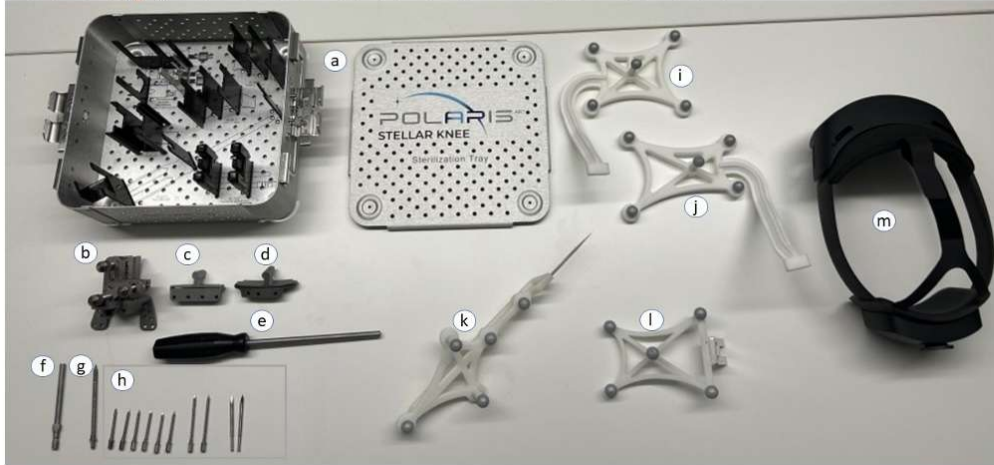


Figure 1

Figure 2

Surgeon's view through the headset during a cadaveric procedure showing the alignment of the planned and navigated resection planes, shown in the center bottom as green and white planes respectively. Alignment of the resection plane is precisely adjusted with mechanical tools and quantified in the center holographic display.

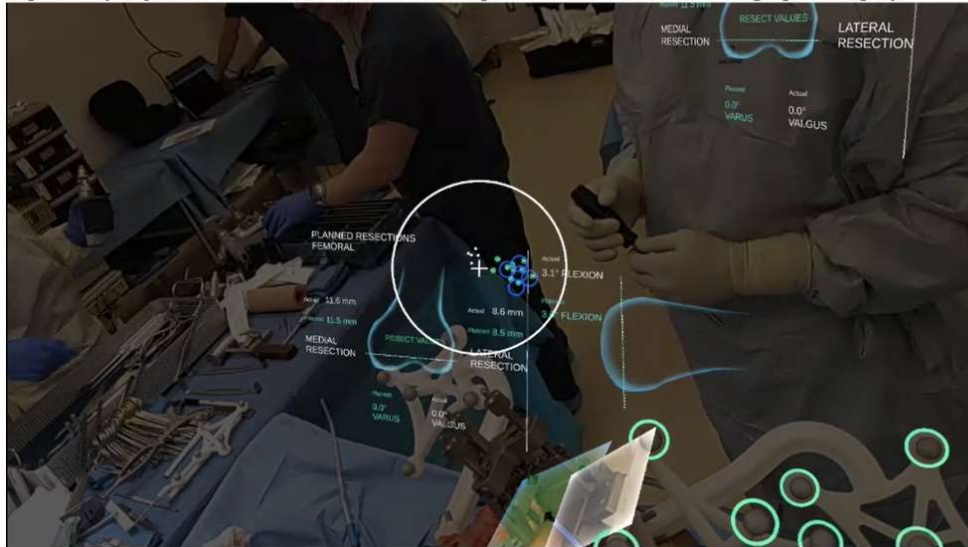


Figure 2

Mixed Reality-Guidance for Accurate Cup Positioning During Total Hip Arthroplasty

*Alexander F Heimann - New England Baptist Hospital - Boston, USA

Stephen Murphy - New England Baptist Hospital - Boston, USA

Dan Sun - Tufts University - Boston, USA

William Murphy - Harvard Medical School - Boston, USA

Introduction:

Optimal positioning of the acetabulum is an important factor in total hip arthroplasty (THA) to secure a stable prosthesis with an impingement-free range of motion and optimal wear characteristics. Surgeons increasingly recognize the importance patient-specific morphological and dynamic characteristics in defining ideal cup positioning. In the past, a variety of different surgical navigation systems, including image-free, fluoroscopy-guided, CT-based, and robotic-assisted procedures, have been proposed to improve the accuracy of conventional THA. More recently, mixed reality guided THA (MR-THA) has been developed. Based on a comprehensive, patient-specific planning module, this solution relies on the intraoperative display of holograms via a head mounted display (HMD) to guide the surgeon during the THA procedure. The purpose of this study was to evaluate the clinical accuracy of cup alignment during MR-THA.

Methods:

IRB-approved, single-center, retrospective, observational study in 40 patients (40 hips). All hips underwent preoperative CT-based planning in a custom-designed planning software allowing for patient-specific goals for operative anteversion and inclination of the acetabular cup with respect to the anterior pelvic plane (APP). The software additionally enabled leg-length and offset-adapted planning of the femoral stem with automated calculation of femoral anteversion. Upon completion of the planning, 3D holograms of the patient's pelvis, cup, liner, impactor and planned screw hole locations were exported and loaded on an HMD prior to surgery. During surgery in the lateral decubitus position using a minimally invasive approach with a superior capsulotomy, automated holographic registration was performed using a smart mechanical navigation tool with an affixed image tracker, that was docked to the patient in a pre-planned position. The hologram of the cup impactor in the target position was then displayed in real-time on the HMD. Manual alignment of the cup impactor with the hologram then allowed the surgeon to identify the desired cup position (Fig. 1). All cases were performed by the senior author. After surgery, all patients underwent simultaneous biplanar radiographic imaging. Based on this, a validated measurement method then allowed for calculation of the achieved cup orientation. To validate the clinical accuracy of the MR-THA navigation system, the mean absolute target error was calculated.

Results:

For operative anteversion, the mean absolute target error was $0.7 \pm 1.1^\circ$ (95% CI $0.3 - 1.0^\circ$; range $[0^\circ - 4^\circ]$). For operative inclination, the mean absolute target error was $1.1 \pm 1.2^\circ$ (95% CI $0.7 - 1.4^\circ$; range $[0^\circ - 4^\circ]$). Demographic patient information is summarized in table 1.

Conclusion:

The studied MR-guided THA planning and navigation system allowed for highly accurate, patient-specific placement of the acetabular cup. The accuracy was well within reported mean absolute target errors for other navigation and robotic systems

for THA. Further studies may provide additional data on the accuracy of MR-THA and potential clinical benefits arising from increased precision in acetabular component placement.

Figures



[Figure 1](#)

Acetabular cup positioning absolute target error (°) with 10 degrees safe zone (blue)

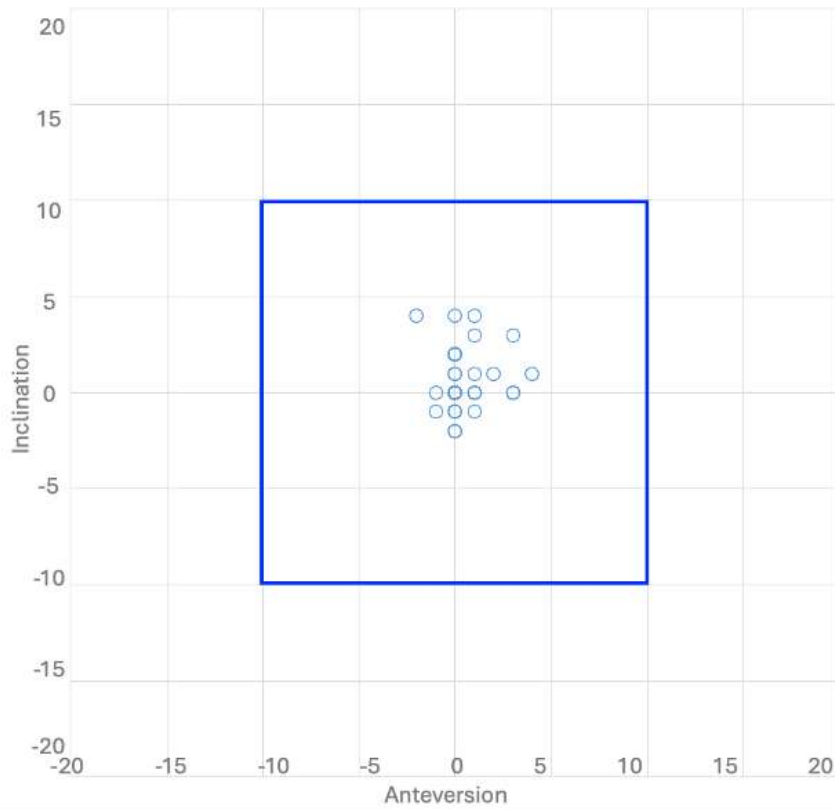


Figure 2

Table 1. Patient demographics

Female sex, n (%)	19 (48)
Age in y, mean ± SD (95% CI)	65 ± 8 (63 – 68)
Height in m, mean ± SD (95% CI)	1.73 ± 0.10 (1.70 – 1.76)
Weight in kg, mean ± SD (95% CI)	82.0 ± 18.8 (76.2 – 87.8)
BMI in kg m ⁻² , mean ± SD (95% CI)	27.1 ± 4.6 (25.7 – 28.6)
Right side, n (%)	21 (53)
Previous contralateral THA, n (%)	18 (45)

SD = standard deviation. CI = confidence interval. BMI = body-mass-index. THA = total hip arthroplasty.

Figure 3

Utilizing Machine Learning and Morphing Algorithms for 3D Reconstruction of Implanted Knee Models

*Viet Dung Nguyen - The University of Tennessee, Knoxville - Knoxville, United States of America

Richard Komistek - The University of Tennessee - Knoxville, USA

Michael LaCour - University of Tennessee - Knoxville, USA

Introduction: Accurate reconstruction of implanted and non-implanted component models plays a pivotal role in enhancing total knee arthroplasty preoperative planning, optimizing implant design, and improving surgical outcomes. Traditional methods of constructing these models often rely on manual image segmentation techniques, which are labor-intensive and prone to human error. To address these challenges, this study proposes a novel approach that leverages machine learning (ML) algorithms and morphing techniques for precise, automated reconstruction of three dimensional (3D) implanted knee models from 2D x-ray images.

Method: Four specifically-oriented fluoroscopy or x-ray images of the patient's knee joint are first collected, as shown in Figure 1. Subsequently, a convolutional neural network (CNN), based on YOLO model [1], is trained by 6,000 manual segmentation images to automatically segment the femur contour of the implanted components. This automated segmentation process significantly reduces the time and effort required for manual delineation while ensuring high accuracy and reliability, as shown Figure 2.

Following the segmentation stage, a previously-published morphing algorithm [2] is employed to generate a personalized 3D model of the implanted knee joint, This algorithm utilizes segmented data as well as biomechanical principles to simulate the shape of the knee joint, considering factors such as implant position, size, and orientation. By integrating morphological data with implant-specific parameters, the reconstructed models more accurately reflect implant geometry.

Results: The effectiveness of the proposed approach is validated through comprehensive evaluations, including comparisons with known CAD models (Figure 3) and existing reconstructed models. Based on comparisons with twelve known 3D ground truth models, the ML-based segmentation method showcases remarkable reconstruction accuracy and consistency, with an average RMS error of 0.57 ± 0.13 mm. Notably, the most significant errors, averaging 2.77 ± 0.85 mm, occur at the inner surface of the reconstructed model, as depicted in Figure 3.

Conclusion: Overall, this research advances the field of orthopedic surgery by providing a robust framework for the automated reconstruction of implanted knee models. By incorporating novel machine learning and morphing algorithms, clinicians and researchers can gain valuable insights into patient-specific geometry, implant biomechanics, and surgical planning, ultimately leading to improved patient outcomes and enhanced quality of care.

Reference

[1] J. Redmon and A. Farhadi, "YOLOv3: An Incremental Improvement," arXiv:1804.02767 [cs], Apr. 2018, arXiv: 1804.02767. [Online]. Available: <http://arxiv.org/abs/1804.02767>

[2] Nguyen, V. D., LaCour, M. T., Dessinger, G. M., & Komistek, R. D. (2023). *Advancements in total knee arthroplasty kinematics: 3D implant computer aided design model creation through X-ray or fluoroscopic images*. Clinical

Figures

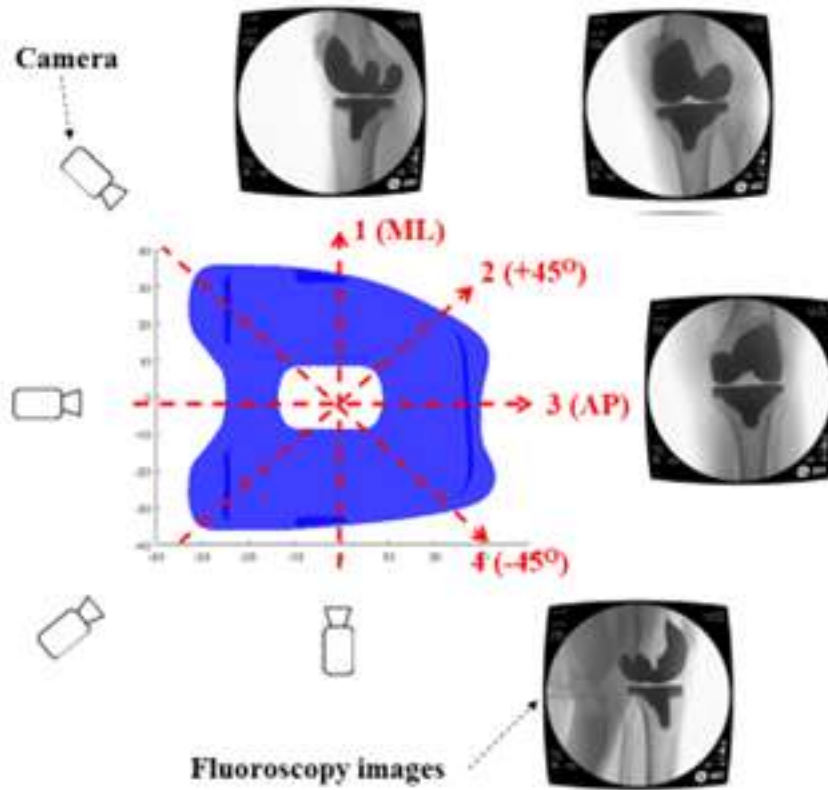


Figure 1

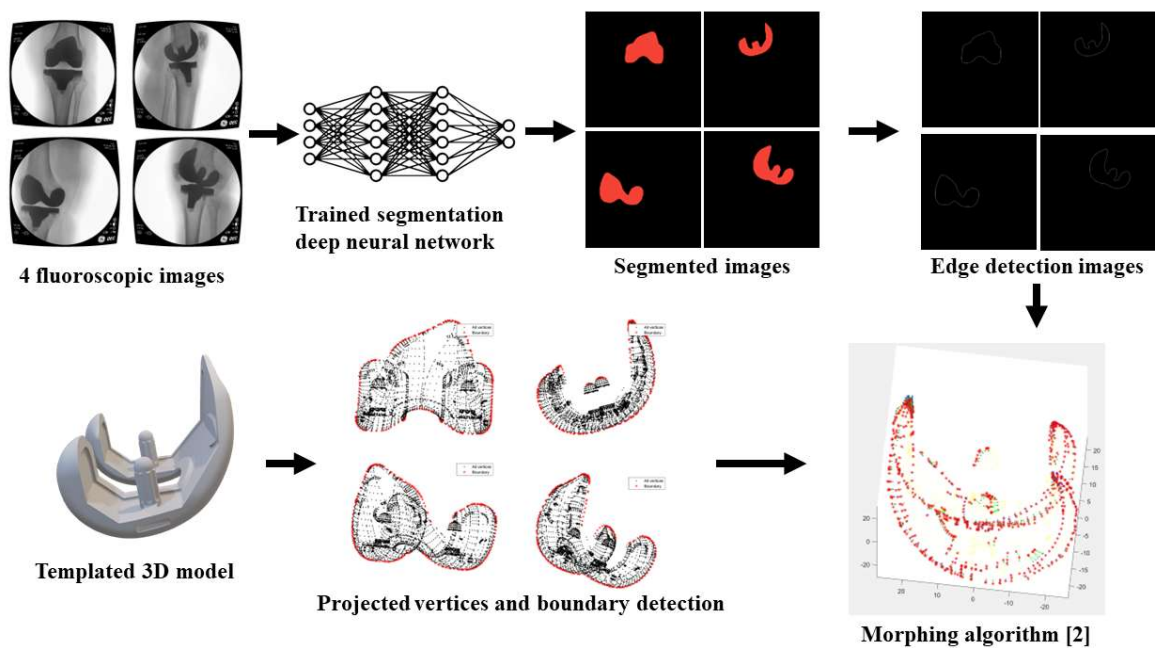
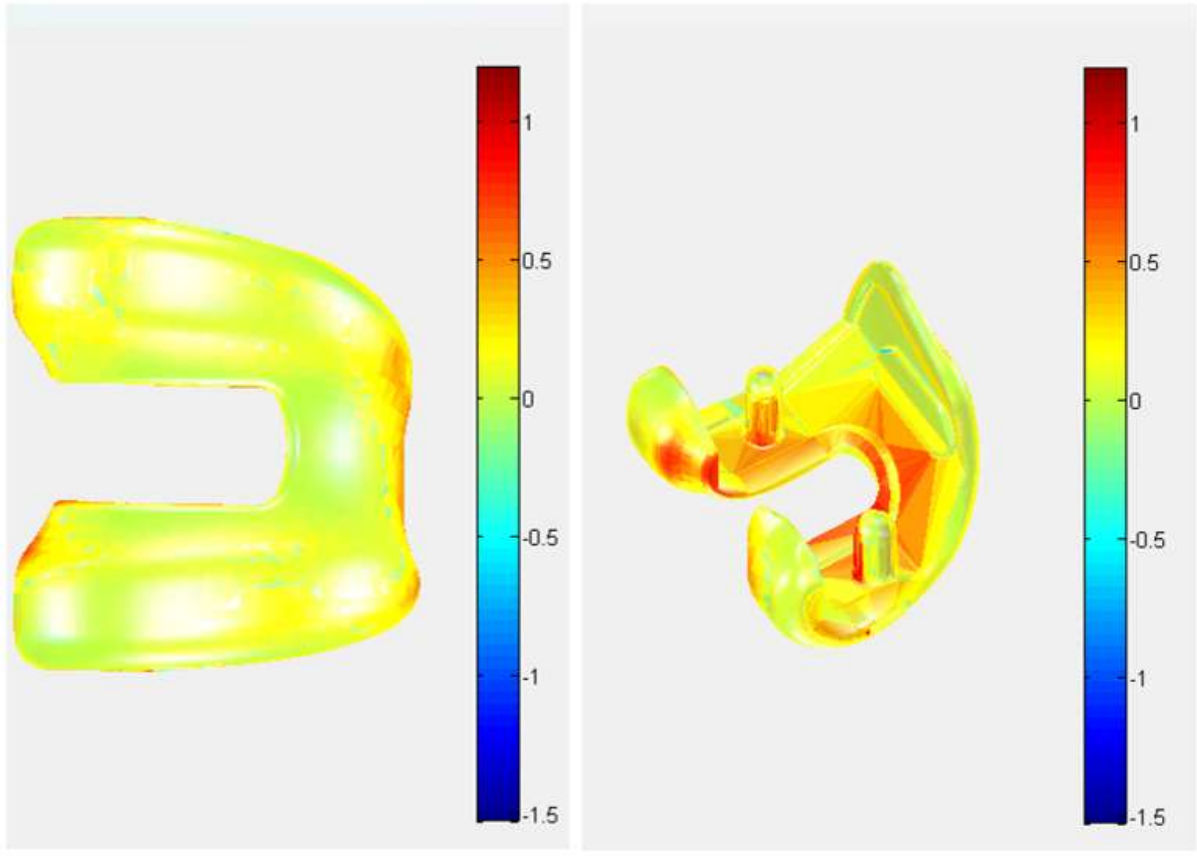


Figure2



[Figure 3](#)

Is Change in Walking Asymmetry Correlated With Changes in Quality of Life in Patients Undergoing Total Joint Arthroplasty?

*Jason Cholewa - Zimmer Biomet - Warsaw, USA

Mike Anderson - Zimmer Biomet - Lehi, USA

Roberta Redfern - Zimmer Biomet - Pemberville, USA

Introduction

Total joint arthroplasty is well known to improve function and quality of life (QoL) for patients with end-stage osteoarthritis. However, little is known regarding the relationship between specific gait metrics and the improvement in QoL following total knee arthroplasty (TKA) or total hip arthroplasty (THA). Our aim was to quantify the relationship between improvement in walking asymmetry and QoL as measured by the Euro-QoL-5-Dimension-5-Level (EQ5D5L) from pre-operative levels.

Methods

This study is a secondary analysis of data collected during a multicenter, prospective longitudinal cohort trial. All participants provided written informed consent and downloaded a smartphone care management platform prior to undergoing TKA or THA. Participants completed the EQ5D5L and EQVAS pre-operatively as well as at three and 12 months post-operatively. Change in scores were calculated for each post-operative period from baseline. Walking asymmetry as collected by smartphones were evaluated only if at least 5 pre-operative days of data were available, and four of seven days centered at each post-operative period were collected. Change in asymmetry from baseline was calculated for each patient. Pearson correlations were calculated for change in asymmetry with the corresponding change in EQ5D5L and EQVAS scores at each post-operative time point. Generalized linear models were created to control for demographic variables including age, body mass index, pre-operative anxiety, pre-operative pain, and sex.

Results

In total, 422 THA patients provided data pre-operatively and at 3 months post-operative; 266 had complete data available at one year following THA. Pearson correlations between change in EQ5D5L and change in asymmetry were weak, but highly significant at both times ($r=-0.16$, $p=0.0009$ and $r=-0.14$, $p=0.02$), however change in EQVAS scores were not correlated with change in walking asymmetry. Multivariate models demonstrated that only pre-operative pain ($\beta=0.06$, $p<0.0001$) and change in walking asymmetry at one year ($\beta=-0.26$, $p=0.04$) were associated with change in QoL. Similar results were observed in the TKA ($n=958$) population ($r=-0.23$, $p<0.0001$ and $r=-0.16$, $p=0.0008$). While age, sex, pre-operative anxiety, and pre-operative pain were associated with change in QoL, change in asymmetry exhibited the strongest effect ($\beta=-0.20$, $p=0.006$).

Discussion

Walking asymmetry may be related to mobility difficulties and thus general health-related quality of life. Improvements in walking asymmetry collected by a smartphone-based care management platform were significantly associated with patient-reported changes in QoL one year after total joint arthroplasty.

The Efficacy of Cement-Augmented Pedicle Screw for Osteoporotic Vertebral Fracture

*Atsunori Ohnishi - Itami city hospital - Itami, Japan

Toru Minami - Itami city hospital - Itami, Japan

Takaaki Nakai - Itami city hospital - Itami, Japan

Junzou Hayashi - Itami city hospital - Itami, Japan

Tsuyoshi Nakai - Itami city hospital - Itami, Japan

Introduction: Spinal fixation for osteoporotic vertebral fractures sometimes leads to complications including screw loosening and subsequent vertebral fractures. Since cement-augmented pedicle screws were introduced in Japan in 2020, their postoperative clinical outcomes have been under investigation due to their potential to reduce such complications. This report examines the efficacy of cement-augmented screws in five patients, focusing on two illustrative cases.

Methods: Five consecutive patients (one male and four females, age 59-84) who underwent posterior fixation with cement-augmented pedicle screw for osteoporotic vertebral fracture since July 2022 and were followed for at least 1 year after surgery were included in this study. We investigated screw loosening and subsequent vertebral fracture after surgery.

Case Summaries: Case 1 detailed a 78-years-old female with T11 vertebral fracture. She underwent T10-L1 posterior fixation, T11 vertebroplasty, and T11-12 laminectomy. There were no new postoperative vertebral fractures, and pain control was excellent. Case 2 detailed an 85-year-old female with an L3 vertebral fracture. She underwent L2-3 TLIF and L1-3 posterior fixation. Two months postoperatively, a new vertebral fracture at L1 was observed. She experienced significant back pain during activities, and 8 months postoperatively, underwent T12-L1 laminectomy and additional T10-L1 posterior fixation.

Result: In our five cases, three of five patients had new postoperative vertebral fractures, two of which patients required reoperations. Screw loosening was observed 10%.

Discussion: These studies indicate the ongoing risk of subsequent vertebral fractures despite the use of cement-augmented screws. However, in a previous study, the pullout strength of cement-augmented screws was reported to be 2.4 times higher than that of normal screws. These findings suggest that while cement-augmented screws offer an improved fixation method for osteoporotic vertebral fractures, the prevention of subsequent vertebral fractures remains a complex challenge. Further research is essential to optimize surgical strategies and enhance patient outcomes in this vulnerable population.

Design of a Tibial Component for Triboelectric Force Sensing in Total Knee Arthroplasty

*Yizhao Li - Western University - London, Canada

Adam Garry Redgrift - Western University - London, Canada

Sherry Towfighian - Binghamton University - Binghamton, USA

Ryan Willing - Western University - London, Canada

Introduction: The magnitude and distribution of loads that are transmitted through total knee arthroplasty components are important and worth measuring. Self-powered triboelectric generators (TEGs) can be employed to simultaneously measure joint forces and harvest energy to power telemetry circuits. TEGs rely on contact and separation between two interfaces that would be embedded within the tibial component to create a static electrical charge. Previous work employed leaf-spring-like structures 3D-printed from Ti6Al4V to provide the required compliance for contact and separation during activities of daily living but failed prematurely due to fatigue [1]. This study uses finite element (FE) models to assess alternative shapes and materials for a new compliant tibial component.

Method: The basic perimeter shape and bearing-facing geometry of an existing cruciate-retaining tibial prosthesis were reverse-engineered using 3D laser scanning. Based on the compliance requirement, a structure comprising a top flat plate with a convex-curved wall and a flat bottom plate (Fig. 1) was considered. The height of the wall was set to exactly accommodate the TEGs (5 mm), with the curvature of the wall set at half the height to minimize stiffness. Displacements and stresses resulting from simulated contact loads were estimated with FE modeling. The material and geometry (thickness of the top and bottom plates and curved wall) were determined through parametric simulations. The objective was to achieve a maximum displacement of 0.3 mm for a load of 2200N while ensuring that the maximum Von Mises stress of the tibial component and TEG remained below the material's allowable stress (yield strength/1.5).

Results: Polyether ether ketone (PEEK) was selected based on its Young's modulus, strength, and biocompatibility. The optimal design has a thickness of 2 mm for both top and bottom plates and a radial thickness of 1.5 mm for the wall. The displacement of the top plate was up to 0.36 mm for the total load of 2200 N and the maximum Von Mises stresses of the component (64.5 MPa) and TEG (0.18 MPa) were below their allowable stress (67MPa and 1.6 MPa) (Fig. 2).

Conclusion: The current study presents the design of a compliant tibial component for housing TEGs. The designed structure fulfills the displacement requirement while remaining within the mechanical failure stress limit. Its total thickness (9 mm) is half that of the previous prototype [1]. Future work is required to test the durability of the component in cyclic physiological loadings and test the amount of electric power, sensitivity, and repeatability of the TEGs integrated into the tibia component.

Reference: [1] Yamomo, G., Hossain, N., Towfighian, S., & Willing, R. (2021). Design and analysis of a compliant 3D-printed energy harvester housing for knee implants. *Medical engineering & physics*, 88, 59-68.

Figures

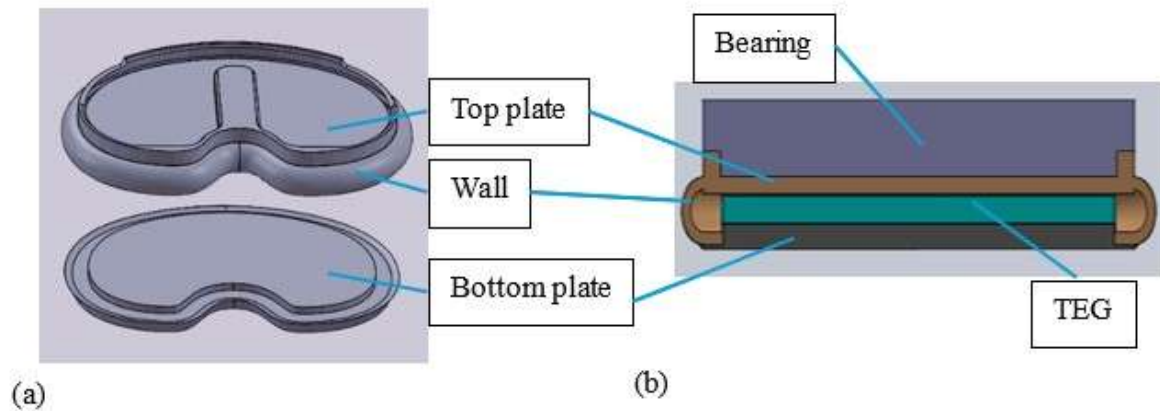


Figure 1 CAD models of the tibial component: (a) Exploded view of the tibial component; (b) Section view of the tibia component with the bearing and TEG for FE modeling.

Figure 1

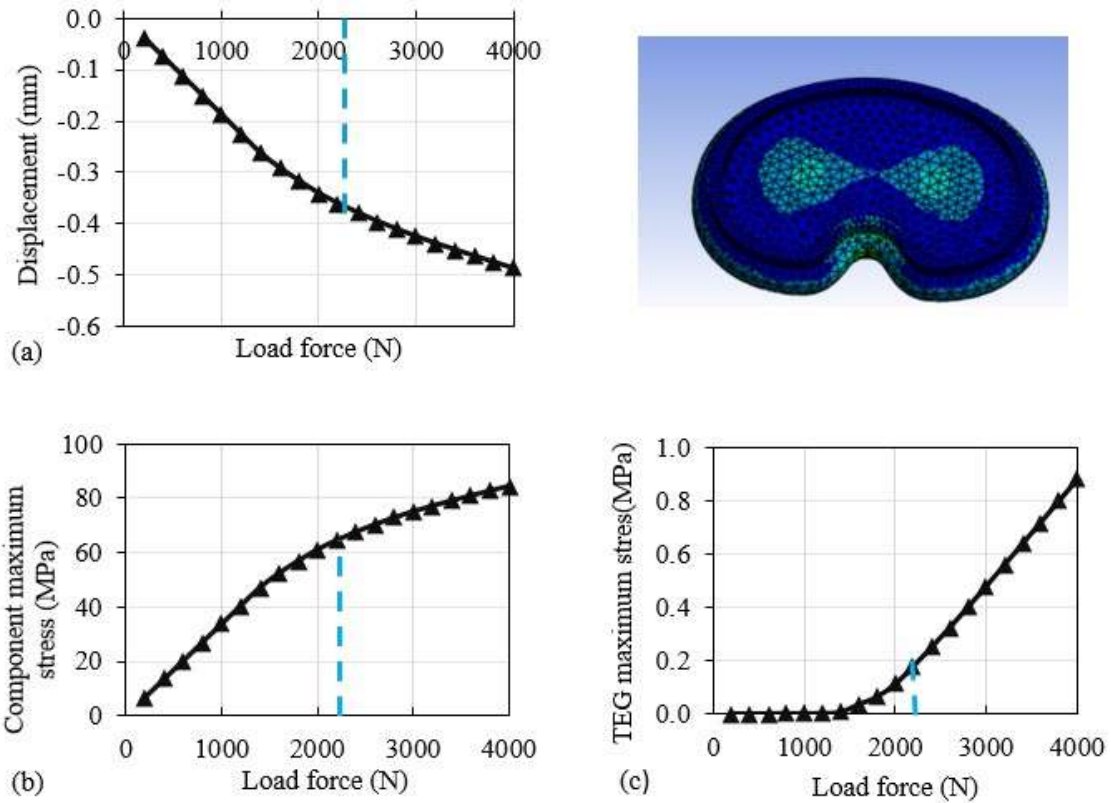


Figure 2 Maximum displacement of the top plate (a), maximum Von Mises stress of the tibial component (b) and TEG (c) for a load from 100 to 4000N. The blue dash lines indicate the values for 2200N loading.

Figure 2

How to Understand the Biomechanics of New Hip Stem Designs

*Hajinderjit Gill - University of Bath - Bath, United Kingdom

Elise Pegg - University of Bath - Bath, United Kingdom

Jennie McNab - Smith & Nephew - Memphis, USA

Mouhsin El-Chafei - Smith & Nephew - Memphis, USA

Edward Davis - The Dudley Group NHS Foundation Trust - Dudley, United Kingdom

INTRODUCTION: Understanding the biomechanical consequences of new stem designs remains a challenge, experimental methods are limited to simple loading, here we discuss an approach using a combination of experiment and Finite Element Analysis (FEA). A new stem (NEW), designed to proximally load the femur, was compared to a clinically available (CA) uncemented stem.

METHODS: In Phase 1, experimental loading of a composite femur before and after implantation was performed, and specimen specific FEA models of the intact and implanted condition were created. In Phase 2 a CT scan of a human femur was segmented and then virtually implanted with both stems(line-to-line), creating Intact, NEW and CA FEA models using the same modelling pipeline as Phase 1. A linear elastic approach was taken, stems were made from Ti64AL4 alloy ($E=113.8$ GPa, $\nu=0.36$). Distribution of physiological bone material properties was based on CT grayscale using equations from Hambli et. al.[1], giving rise to 72 values for Young's modulus (30 MPa to 26.7 GPa) with $\nu=0.3$. Muscle and joint contact forces (adapted from Stolk et al [2]) were applied to the femur simulating 10% gait cycle loading. (Fig. 1). A mesh convergence study was performed on implanted models where implant contact with bone was expected (1.2mm into bone surface and 0.6mm into stem surface).

RESULTS: The modelling pipeline was validated using experimental strain measurements. The expected reduction in proximal medial outer surface stresses were observed from Intact to implanted conditions, matching the experiment measurements (Figure 2). Considering the physiological loading of the bone adjacent to the stem, very similar patterns in strain were observed between the NEW and CA stems (Figure 3).

CONCLUSION: This approach allows a modelling pipeline to be validated, using simplified experimental loading. Physiological loading together with realistic bone representation can then be simulated in FEA models created using this pipeline. Here we have shown that a NEW stem, designed to proximally load the femur, gives rise to similar loading of the hosts bone to a clinically available stem.

REFERENCES: [1] R Hambli, S Allaoui. "A robust 3D finite element simulation of human proximal femur progressive fracture under stance load with experimental validation" *Annals of Biomedical Engineering* 41(12), 2013. [2] J Stolk, N Verdonschot, R Huiskes. "Hip-joint and abductor-muscle forces adequately represent in vivo loading of a cemented total hip reconstruction" *J Biomech* 34, 2001.

Figures

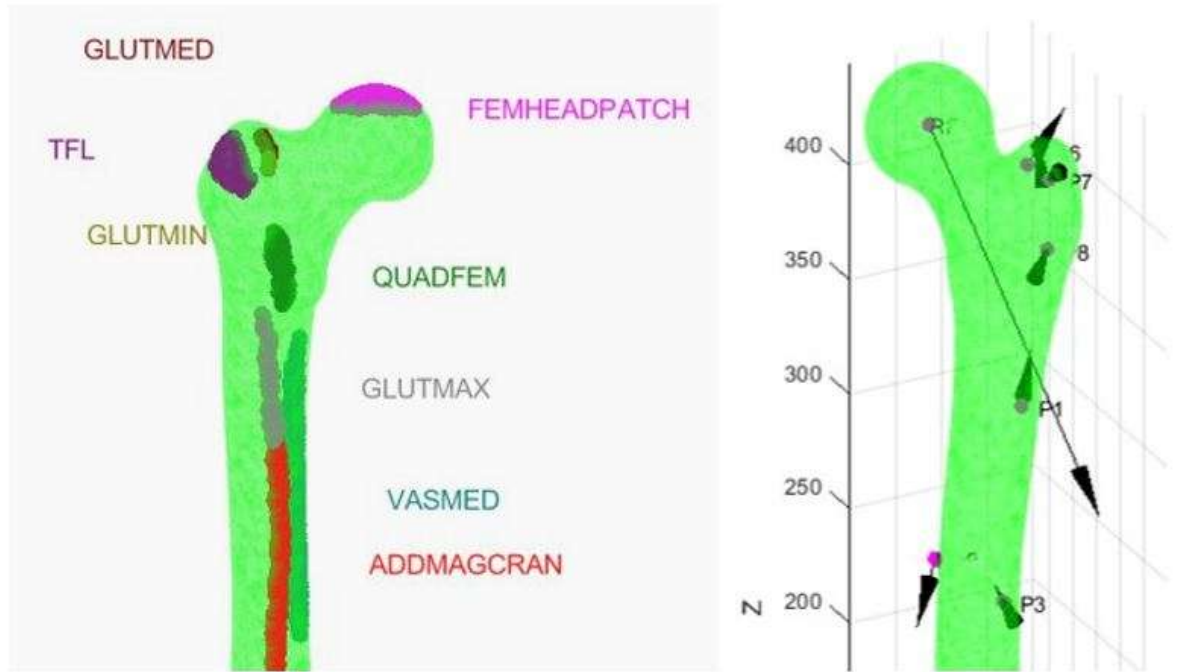


Figure 1

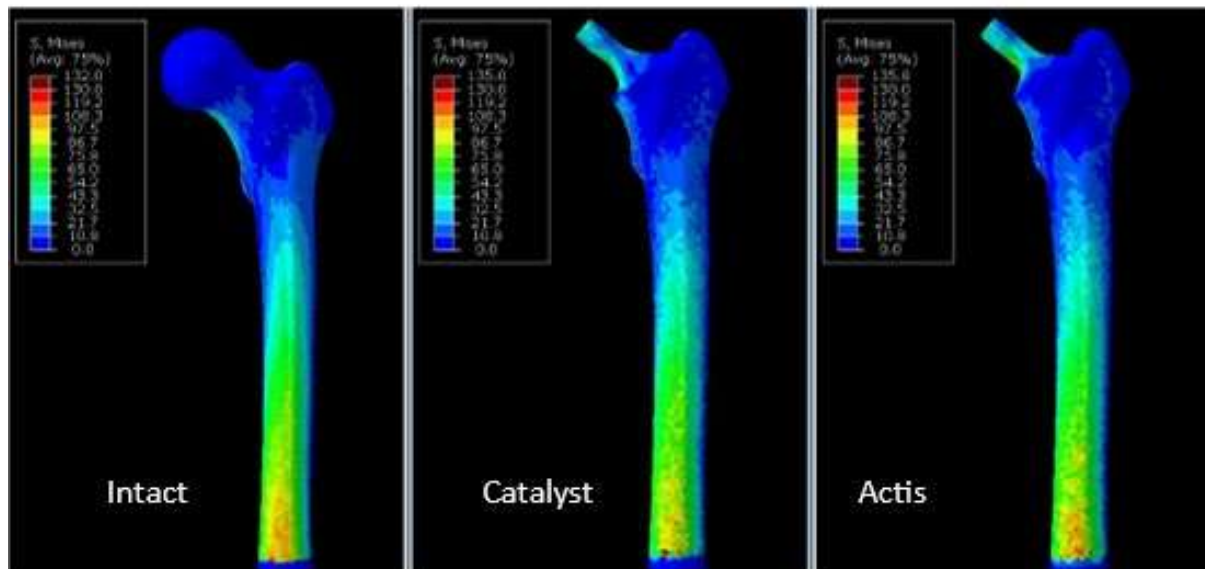


Figure 2

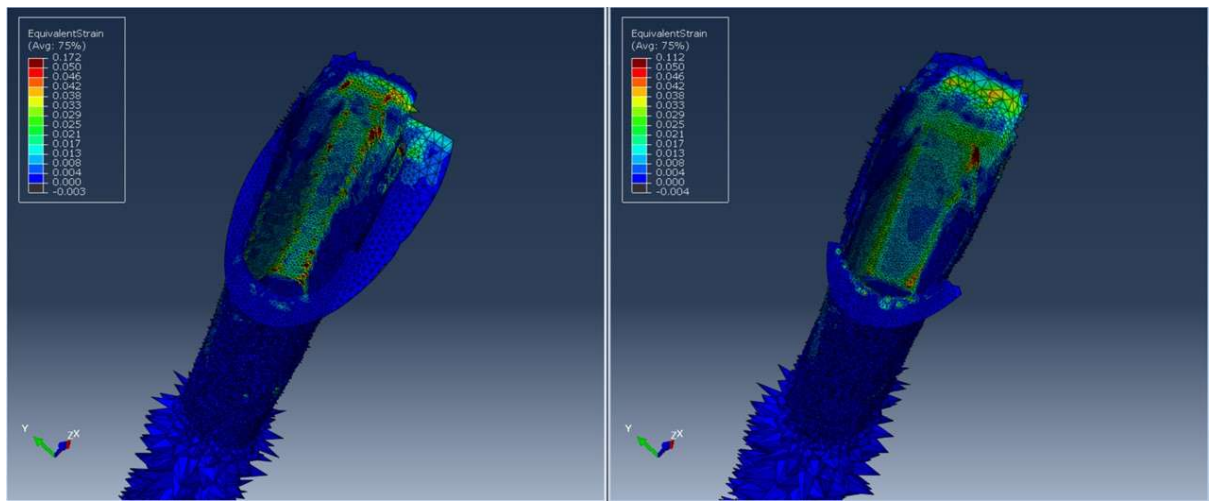


Figure 3

Increasing Use of Cemented Stems Is Associated With Reduced Early Fracture After Total Hip Arthroplasty: A Single Statewide Arthroplasty Registry Perspective

*Kevin Adik - McLaren - Flint, USA

Nathanael Adams - McLaren - Flint, USA

Ajay Srivastava - McLaren - Flint, USA

Richard Hughes - University of Michigan - Ann Arbor, USA

Huiyong T Zheng - MARCQI Coordinating center - Ann Arbor, USA

Brian Hallstrom - University of Michigan - Ann Arbor, USA

David Markel - Providence Hospital and Medical Center - Southfield, USA

Introduction

The Michigan Arthroplasty Registry Quality Collaborative Initiative (MARCQI) identified periprosthetic fracture as a common reason for early total hip arthroplasty (THA) revision. An initiative was started to address this complication, and the use of cemented stems was encouraged for at risk populations. This descriptive analysis describes the results of this effort.

Materials and Methods

MARCQI reports its quality data to participants through reports and in-person meetings. Reducing hip fracture was also included as a pay-for-performance incentives metric. MARCQI began collecting detailed data on implant fixation in 2017. The percent of stems cemented in the state has been analyzed by age, sex and year of surgery. The incidence of fracture within 90 days of surgery is reported by age and sex. Associations between cementing and fracture are reported.

Results

In analyzing fracture rate from 2012-2022, the percentage began to rise from 2012 and peaked at 1.26% in 2018. Since then, there has been a decline to <1% in 2022 (Fig 1). Patients >75yo saw the biggest increase (4.68% to 10.8% in men, 10.4% to 26.8% in women) (Fig 2). For women >75yo the peak fracture rate was 3.6% in 2018. There was an inverse relationship between use of cemented stems and early revision rates with a fracture rate of 1.65% in 2022 (Fig 3).

Discussion

There was a steady increase in fractures from 2012 to 2018, with the peak at 1.26%. Since 2018 there has been a steady decline with fracture rates falling to <1% in 2022. When stratifying the data by age and gender, the at risk populations become defined. There was a direct correlation between the use of cemented stems and decreased post-operative fracture rates, especially with elderly females. From 2017 to 2022 cementation rate in this demographic increased 16% and the fracture rate decreased by nearly 2%. Using MARCQI initiatives there has been an estimated 280 fewer revisions secondary to fractures in the State of Michigan. The data suggests that surgeons should consider increased use of cemented femoral stems.

Figures

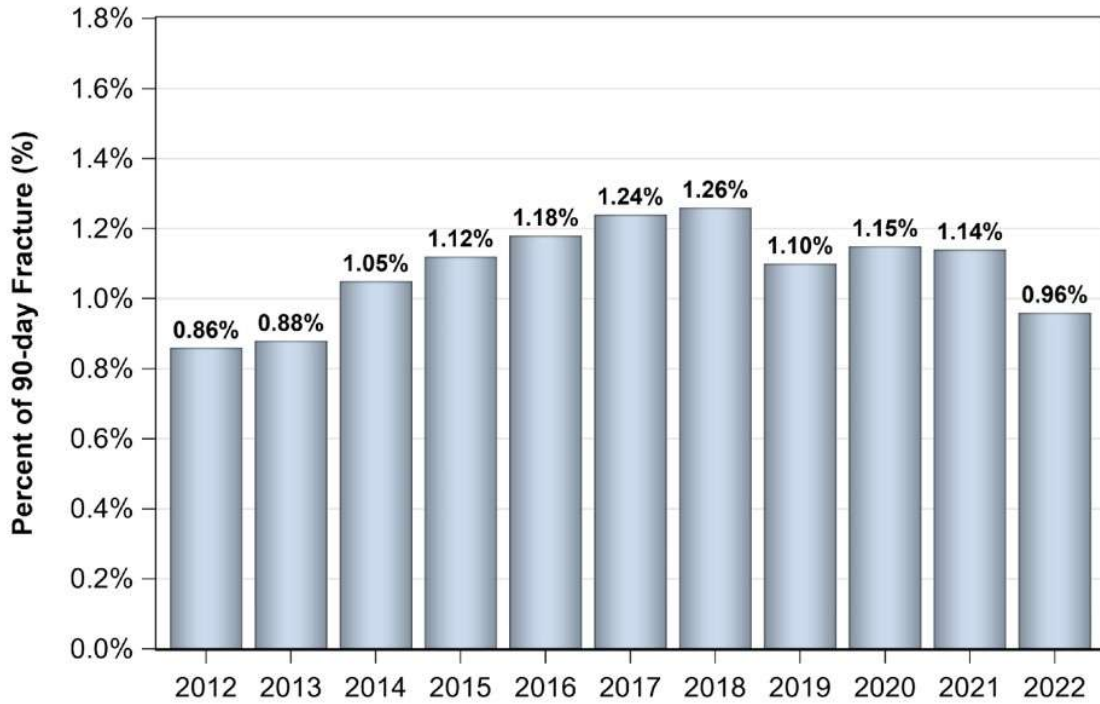


Figure 1

Figure 1

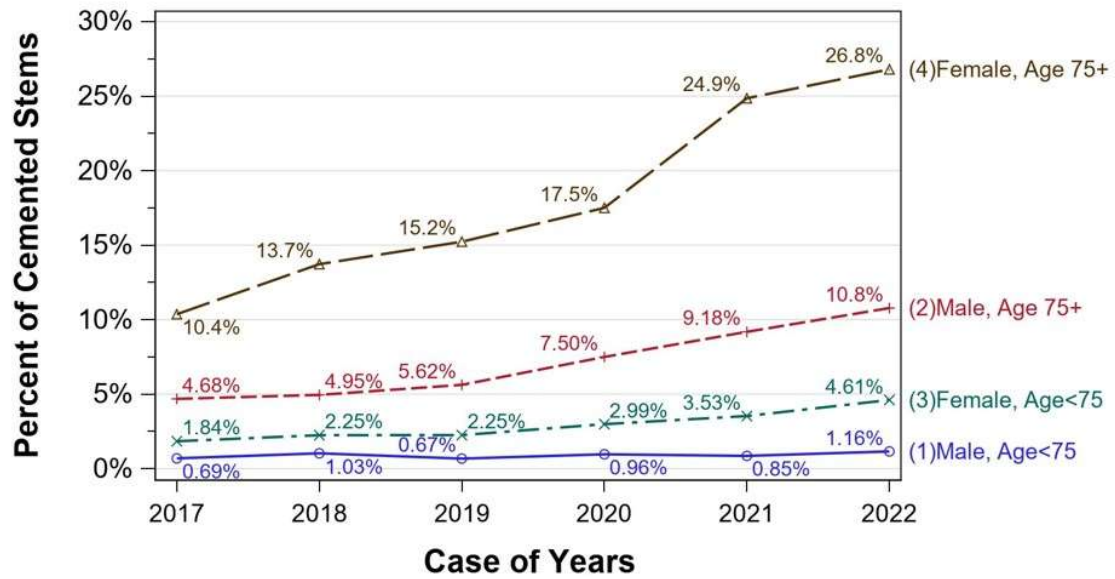


Figure 2

Figure 2

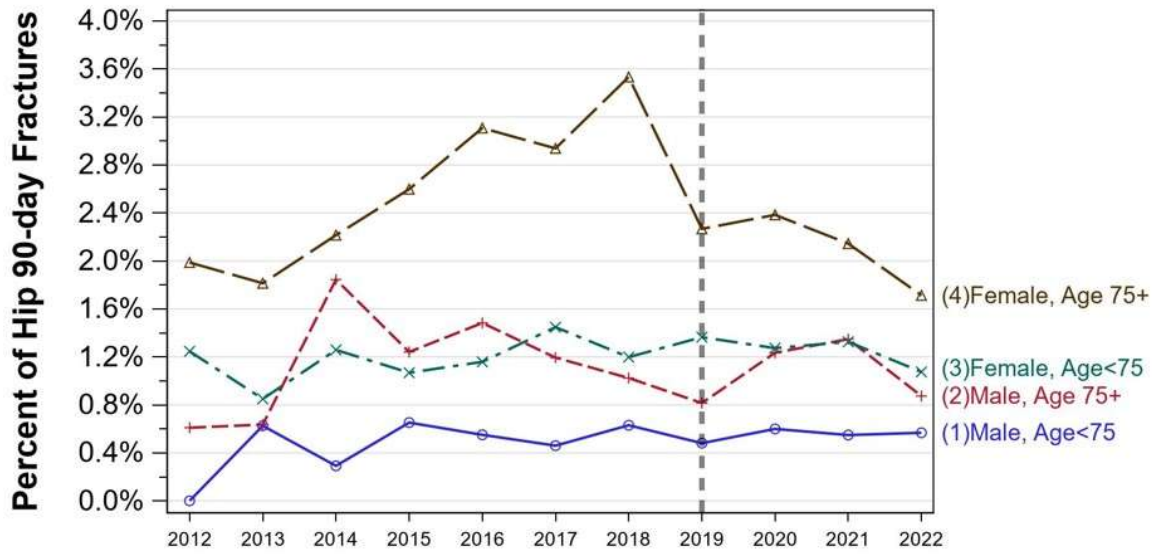


Figure 3

[Figure 3](#)

How Do Collared Double Taper Wedge Stems Reduce the Periprosthetic Fracture Risk?

*Katja Glismann - TUHH Hamburg University of Technology - Hamburg, Germany
Golzar Dakhili - TUHH Hamburg University of Technology - Hamburg, Germany
Michael Morlock - TUHH Hamburg University of Technology - Hamburg, Germany
Gerd Huber - TUHH Hamburg University of Technology - Hamburg, Germany

Introduction: Implant registries and studies clearly show that double taper wedge style collared cementless prostheses have a lower revision rate compared to collarless equivalents, particularly for periprosthetic fractures (PPF) [1-3]. The common explanation is the calcar-collar contact which prevents further migration of the stem into the femur and cleaving of the femur [3]. Axial compression of the cortical bone of the calcar might also positively influence PPF risk [4]. The aim of this study was to determine whether the lower migration in combination with an altered force flow into the femur results in higher fracture forces for collared stems.

Methods: Prostheses were implanted quasi-statically into porcine femurs (standard Corail n = 7; collared Corail n = 7, DePuy Synthes, England) using a material testing machine (0.1 mm/s, Z010, Zwick Roell, Germany) until failure (PPF) was observed visually or until the actuator displacement reached 40 mm. Digital image correlation (25 fps, Aramis3D, MV100; Carl Zeiss GOM Metrology GmbH, Germany) was used to record the strains at the anteromedial cortical bone and to identify the location of the principle strains (PS; 1. PS = maximum strain, 2. PS = maximum compression) [5].

Results: Femurs in the collared group exhibited three fracture mechanisms depending on the contact situation between the collar and the bone (Fig. 1). Fracture forces for collared stems were 131 % higher ($p = 0.001$), while the maximum strain on the cortical bone was quite similar for both stem types ($p = 0.456$; Fig. 2). Maximum compression was increased by up to 1045 % for the collared group ($p = 0.007$; Fig. 3). One femur in the collared group did not fracture (the force at the end of the test was used as fracture load).

Discussion & Conclusion: Different force flow can be achieved through a calcar-collar contact. Rising forces with collar contact lead to an increased compression of the femur until the increasing strain causes the bone to “burst” (fracture). Standard implants subside under rising forces and the critical strains are reached at a lower force level. The collar on double taper wedge stems reduces the risk of periprosthetic fractures by preventing the prosthesis from migrating into the femur while transmitting higher forces into calcar compression. Collared stems still can experience fractures at higher forces.

Acknowledgements: Institutional financial support by DePuy Synthes is kindly acknowledged.

References:

- [1] Lamb, Bone and Joint Journal, 2019
- [2] Konow, Bone and Joint Journal, 2021
- [3] AOANJRR Report, 2023
- [4] Torre, AAHKS, 2023
- [5] Hoffman, Hottinger, 1987

Figures

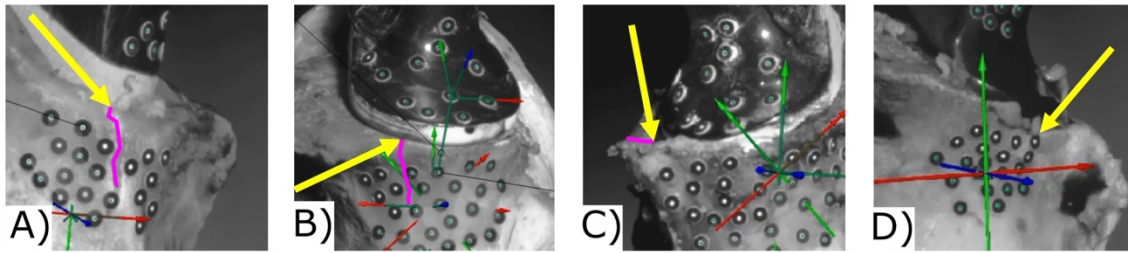


Figure 1: Different fracture types marked with yellow arrows (fractures highlighted in magenta): A) typical calcar crack during implantation of a collarless stem, B) calcar crack for partial calcar-collar contact without achieving complete contact between calcar and collar, C) stem in valgus resulting in contact of the collar with trabecular bone pushing forward and D) collar compressing the cortical bone in the contact area.

[Figure 1](#)

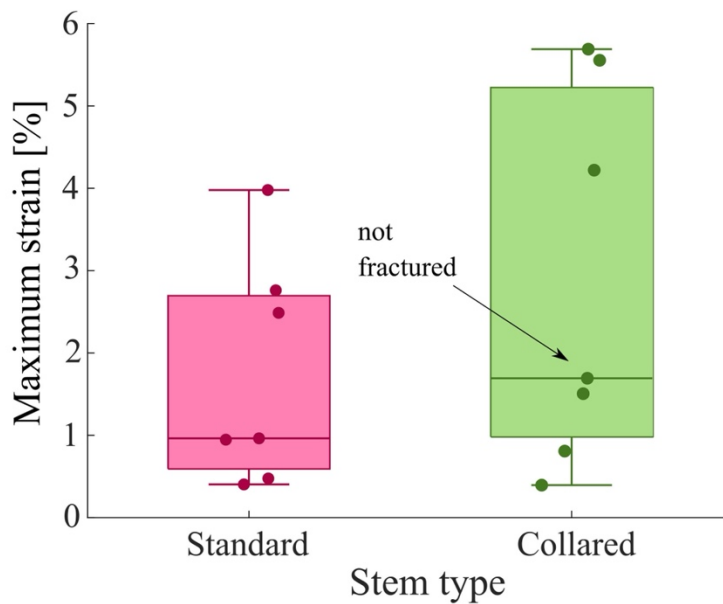


Figure 2: Maximum strains were not significantly different between the stem types.

[Figure 2](#)

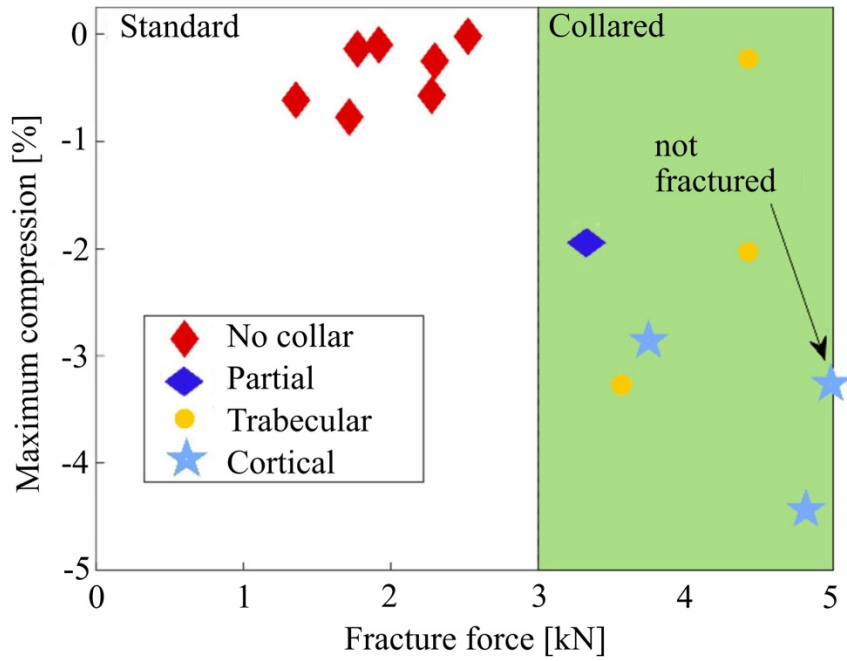


Figure 3: Higher maximum axial compression was reached for collared stems. The fracture force for collared stems was significantly higher than for collarless stems. Partial calcar-collar contact lead to the lowest fracture force among the collared stems.

[Figure 3](#)

Statistical Shape Modelling of the Pelvis Helps Minimise Leg Length Discrepancy in Primary THA

*Sara De Angelis - University College London - London, GB

Johann Henckel - [Royal National Orthopaedic Hospital - London, United Kingdom](#)

Angelika Ramesh - University College London - London, United Kingdom

Alister Hart - Royal National Orthopaedic Hospital - London, United Kingdom

Anna Di Laura - Royal National Orthopaedic Hospital and Dept. MechEng at UCL - London, United Kingdom

Introduction

Hip arthroplasty is often needed to restore hip joint function when acetabular distortion or bone loss are present. Restoration of the centre of rotation (CoR) allows for an improved kinematic of the hip and preservation of acetabular bone stock, decreasing the risk of long-term loosening.

Correcting limb length inequality while maintaining hip stability poses a significant challenge in total hip arthroplasty (THA). Restoration of the hip biomechanics, including offset and leg length, is a crucial objective of THA. Statistical shape modelling (SSM) can help guide the restoration of the CoR, the orientation of the component, an adequate offset, and an equal leg length by predicting anatomical information that is missing or impossible to capture with traditional modelling.

We aimed to aid the surgical planning of primary hip surgery. Our objective was to apply SSM to patients who previously underwent primary hip replacement.

Methods

This was a retrospective cohort study involving 50 patients who underwent primary hip replacement. An SSM was built on 100 healthy hemipelvises and used to virtually reconstruct the native pelvic morphology for all cases.

The SSM-based models were then compared to the postoperative computerised tomography (CT)-based reconstructions.

The outcome measure was the difference in CoR between the diseased hip and its SSM-based reconstruction.

We had previously validated the model for accuracy using healthy anatomies [1]. In this study, a discrepancy within 2 mm in the inferior-superior direction was considered satisfactory.

Results

The median (interquartile range [IQR]) difference in CoR between the diseased hip and its SSM-based reconstruction was found to be 9 mm (IQR: 8 mm).

The CoR of the diseased hips was found to have deviated on average 5 mm laterally, 5 mm superiorly and 5 mm anteriorly from its corresponding SSM-based model.

When validating the model, the median difference in CoR between the healthy hemipelvises and their SSM-based models was 5.69 mm (IQR: 6.37–3.77 mm). The median difference in CoR was 2.37 mm (IQR: 4.02–1.70 mm) in the medial-lateral direction, 1.75 mm (IQR: 3.84–0.55 mm) in the inferior-superior direction, and 3.24 mm (IQR: 4.03–0.96 mm) in the anterior-posterior direction.

Conclusion

The restoration of the hip CoR and leg length are key factors in achieving good clinical outcome. This is the first study to apply an SSM to patients who underwent primary hip replacement. SSM aids optimal reconstruction of the native anatomy [Fig.1]. SSM is an important tool to aid preoperative planning in primary, complex primary and revision THA.

References

[1] De Angelis S, Henckel J, Bergiers S, Hothi H, Di Laura A, Hart A. Statistical shape modeling of the large acetabular defect in hip revision surgery. *J Orthop Res.* 2023;41:2016-2025. doi:10.1002/jor.25547

Figures

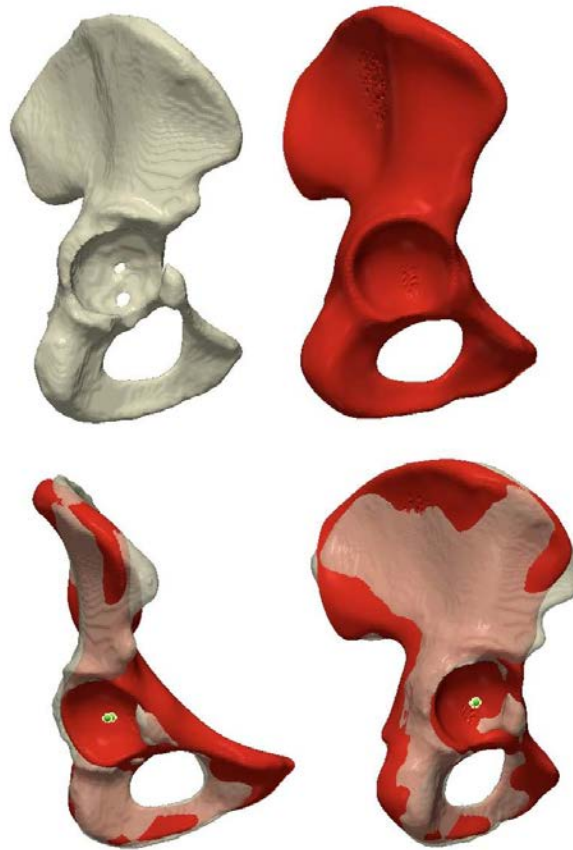


Figure 1: (Top-Left) 3D reconstruction of the defect, (Top-Right) SSM-based reconstruction, (Bottom-Left) Antero-posterior and (Bottom-Right) lateral view of difference in hip joint centre between the diseased hemipelvis and its corresponding SSM-based reconstruction.

[Figure 1](#)

Using 3D Preoperative Planning to Predict Stem Alignment, Sliding, and Edge Loading for Compaction Broach and Press Fit Stems

Thang Nguyen - University of Tennessee - Knoxville, USA

Jarrold Nachtrab - University of Tennessee - Knoxville, USA

Richard Komistek - The University of Tennessee - Knoxville, USA

*Michael LaCour - University of Tennessee - Knoxville, USA

INTRODUCTION

Component placement has long been debated in THA, as postoperative complications such as dislocation, edge loading, and hip separation remain unsolved. While significant research has been done on acetabular alignment, fewer investigations focus on stem position. This study uses three-dimensional (3D) preoperative planning tools to evaluate two different stem systems, a compaction broaching stem and a blade-style proximal press fit stem, to determine the effects that stem design has on postoperative alignment and edge loading.

METHODS

A previously validated 3D pre-operative planner [1] was used to place components in a virtual surgical environment to determine the best fit. The planner exports position and orientation information into a dynamic model that can be used to predict patient-specific biomechanics. The model initially aligns the stem axis with the proximal canal axis. As the stem is inserted into the canal, a contact detection algorithm between the cortical wall and stem surface is used to adjust component positioning until the desired position is reached.

The planner was used to predict contact mechanics for ten subjects (Figure 1). Each subject was implanted with both stems. Parameters of interest include the distance between the implanted non-implanted femoral heads, the amount of hip sliding, and the contact area to determine edge loading.

RESULTS

Both stem systems were able to place the femoral head less than 1 cm away from the preoperative femoral head, indicating good alignment accuracy potential. The average distance between head centers was 4.6 ± 2.7 mm (0.9 – 9.7 mm) regardless of stem type. The largest source of error among all stems was in the anterior/posterior direction, with the implanted femoral head sitting an average of 2.3 ± 2.7 mm more anteriorly than the native femoral head.

When evaluating comparisons between femoral head alignment, a positive (although weak) correlation exists between increased femoral head distances and increased hip sliding (Figure 2, $R^2 = 0.22$). Similarly, a negative correlation exists between increased femoral head distances and decreased contact area (Figure 3, $R^2 = 0.27$).

CONCLUSION

This study demonstrates that modern stem designs have good potential for accuracy. Still, there remains a need for improved planning and alignment tools. Even when 3D planning is used, the directions of misalignments in this study were largely in the anterior/posterior direction, which is the direction that 2D radiographs cannot assess. This study also revealed that stem misalignments may result in changes in stem anteversion, increases in hip sliding, and increases in edge loading.

REFERENCES

1. LaCour MT, Ta DM, Komistek RD, "Development of a hip joint mathematical model to assess implanted and non-implanted hips under various conditions," Journal of Biomechanics, vol. 112, no. 9, 2020.

Figures

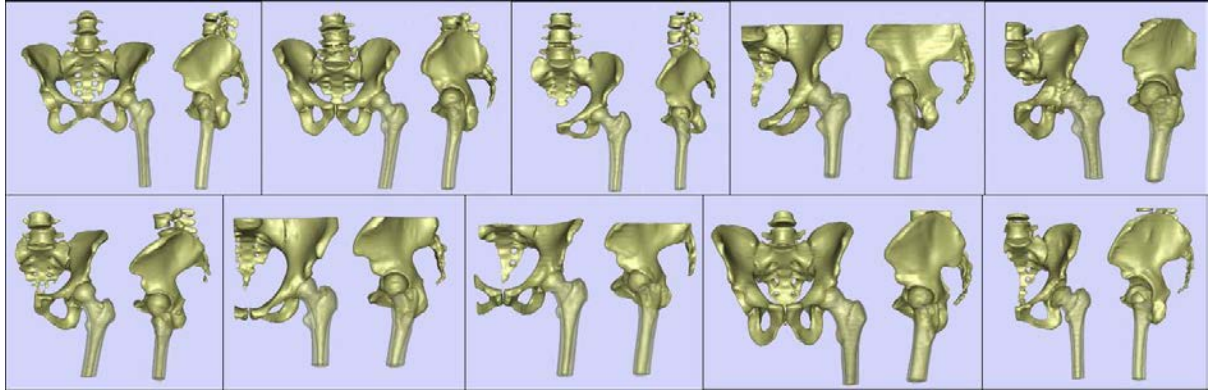


Figure 1

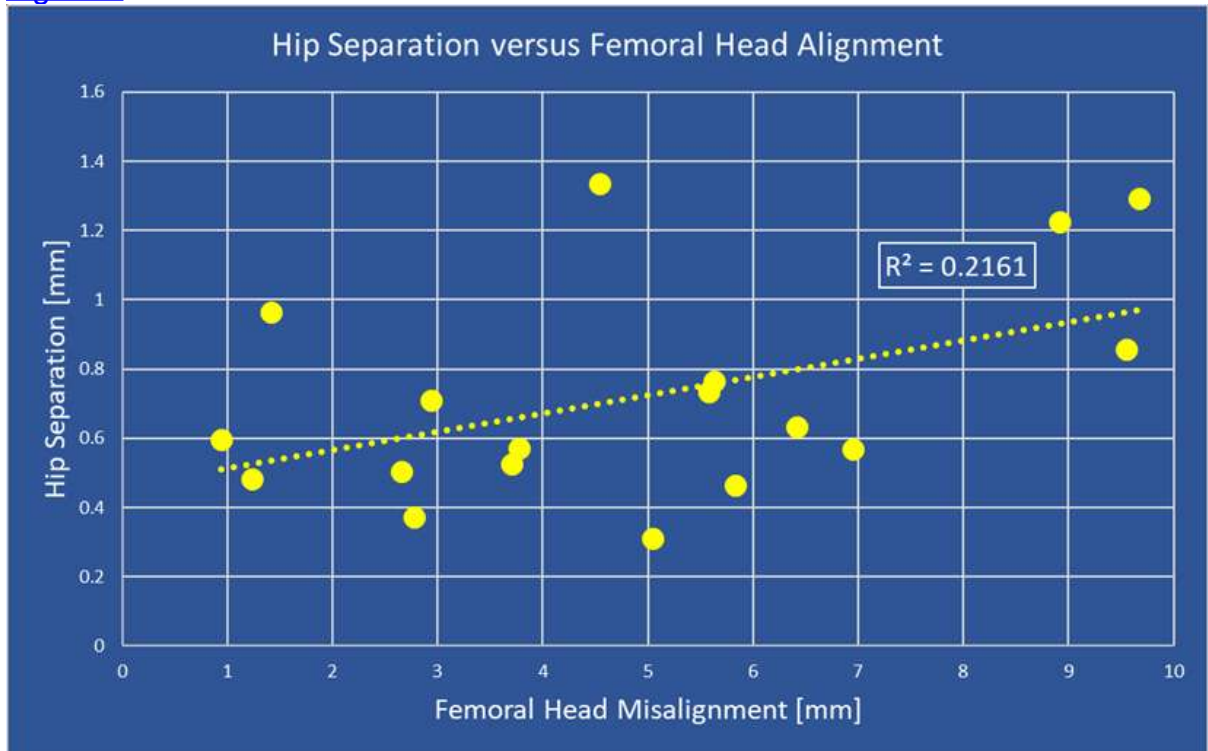
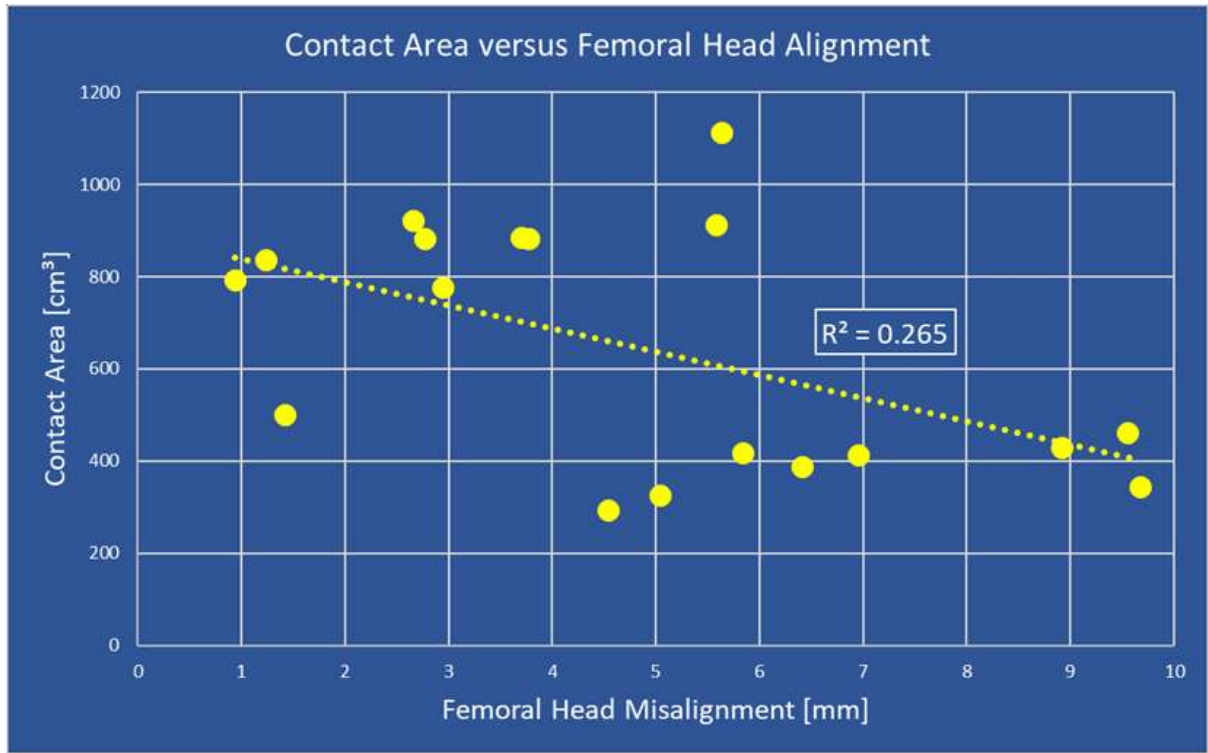


Figure 2



[Figure 3](#)

Re-Revision Risk of Modular and Monobloc Revision Stems After Revision Total Hip Arthroplasty

*Michael Morlock - TUHH Hamburg University of Technology - Hamburg, Germany

Alexander Grimberg - EPRD - Berlin, Germany

Klaus-Peter Gänther

Marc Michel - Peter Brehm - Germany

Carsten Perka - Charite University Hospital - Berlin, Germany

Yinan Wu - EPRD - Berlin, Germany

Implant fracture of modular revision stems is a major complication after total hip arthroplasty revision (rTHA). Studies looking at specific modular designs report fracture rates of 0.3% [1] to 0.66% [2] whereas fractures of monobloc designs are only reported anecdotally. It is unclear whether the overall revision rate of modular designs is higher and if, whether stem fractures or other revision reasons are responsible for this elevation.

Materials and Methods. Revisions occurring within 7 years after implantation of a revision stem ($n_0=14,752$; $n_7=924$) documented in the German arthroplasty registry EPRD were analysed using Kaplan-Meier survival analysis and Cox regression with design (modular: $n=17$, monobloc: $n=27$), body mass index BMI, Sex, Age, PPF as reason for the implantation, hospital surgical volume and Elixhauser Score as independent variables. A competing risk analysis of revision or death was performed. One stage and two stage procedures of known first revisions were analysed separately (1-stage: modular $n= 1,033$; monobloc $n= 750$; 2-stage: 188 / 136).

Results. Stem fracture was the reason for re-revision of modular stems in 2.4% of the re-revisions in males (fracture rate: 0.43%) and 0% for the monobloc stems. The reasons for revisions were predominantly infection, dislocation and loosening (Table 1). The risk for a first re-revision up to 7 years after implantation was similar for modular (18.1% [15.5%, 21.1%]) and monobloc stems (17.8% [14.4%, 21.9%]; $p=0.05$). Only the pre-obese group with a BMI of (25-30) showed a significantly increased risk of modular stem failure compared to the obese group (BMI 30-35; $p= 0.04$). The competing risk analysis of all data including up to 7 revisions of a patient revealed a higher risk of failure of modular revision stems ($p<0.001$; Figure 1). This was not the case for 2-stage revisions neither for first revisions nor for cases with multiple revisions ($p>0.9$). The risk of death was similar for both stem designs ($p=0.69$; Figure 1). Male patients tended to have a higher risk for revision in general ($p=0.052$).

Discussion. Fractures of modular revision stem as reason for revision contribute very little to the overall re-revision risk. In 2-stage revisions, no difference in overall re-revision rates between designs was observed. This might indicate that the differences between stem designs observed for 1-stage procedures, especially considering multiple revisions, are due to differences between the patient cohorts, not reflected by the parameters available for analysis or the individual surgeon choice. The analysis of revision reasons for revision surgeries based on registry data is difficult due to the complexity of the surgery and frequently incomplete data sets.

References

[1] Krueger DR et al., Bone Joint J. 2020;102-B(5):573-579.

[2] Herold F et al., Hip Int. 2021;31(3):398-403.

Figures

Main Reasons for Re-revision				
	modular stems		monobloc stems	
	female	male	female	male
Infection	16.5%	17.8%	15.6%	17.6%
Component loosening	7.2%	11.1%	9.7%	8.2%
Dislocation	19.4%	20.9%	17.1%	16.4%
Unknown	42.9%	38.1%	40.0%	40.6%

Figure 1: Main reasons for revision analysing all revision stem revisions recorded in the German Arthroplasty registry EPRD. Cases with up to 7 revisions are included. The large number of cases without a specified reason for revision make conclusions difficult.

Figure 1

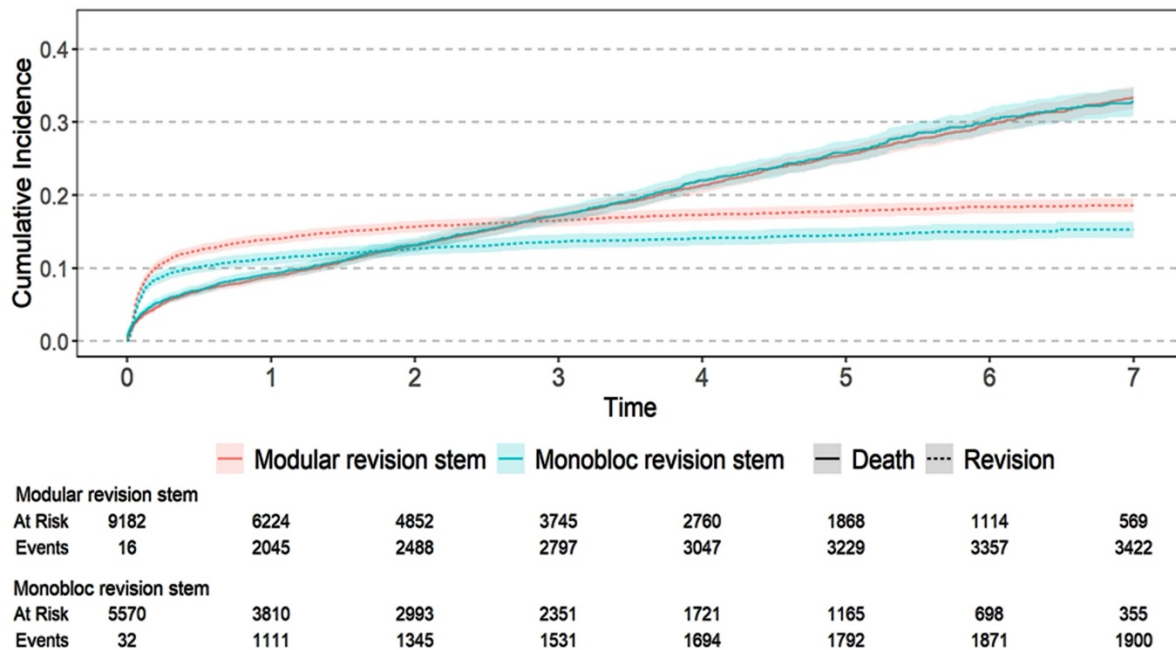


Figure 1: Competing risk of death or revision for all revision stem data in the German Arthroplasty registry EPRD. Cases with up to 7 revisions are included. About 3 years after implantation of a revision stem, the risk to die is higher than the risk for a revision. The risks of death is similar for either stem design ($p=0.69$), the risk of revision higher for modular stems ($p<0.001$).

Figure 2

Flexible Metaphyseal Cones in Total Knee Arthroplasty Revision: Evaluation of Clinical-Radiographic Results and Short-Term Survival in a Sample of 11 Patients

Giulio Maria Marcheggiani Muccioli - University of Bologna - Bologna, Italy

Domenico Alesi - IRCCS Istituto Ortopedico Rizzoli - Bologna, Italy

*Alberto Fogacci - Istituto Ortopedico Rizzoli - Bologna, Italy

Mirco Lo Presti - Rizzoli Orthopaedic Institute - Bologna, Italy

Stefano Zaffagnini - Researcher Istituti Ortopedici Rizzoli - Bologna University Sports - Bologna, Italia

Maria Pia Neri - Istituti Ortopedici Rizzoli - Bologna University - Bologna, Italy

Introduction:

The present study evaluated the short-term survival and clinical radiographic outcomes in a sample of patients undergoing revision total knee arthroplasty (rTKA) with a mobile bearing constrained prosthesis and flexible metaphyseal cones.

Methods:

Eleven patients (7M, 4F) with mean follow-up of 27 months operated between June 2015 and April 2023 were retrospectively recruited. Clinical scores (OKS, KSS, KOOS) and complications were recorded at the last outpatient follow-up.

Demographic and clinical parameters were collected from medical records. Knee alignment and prosthetic component placement were assessed radiographically.

Results:

The analyzed sample had a mean age of 71.5 years at the time of surgery, with a mean BMI of 27.6 kg/m². 64% of the patients had a grade III AORI bone defect and 34% a grade IIb AORI.

The revision causes were septic loosening in 73% of the cases (treated by two-stage revision) and aseptic loosening in 27% of the cases (18% one stage, 9% two stage). Both femoral and tibial cones were implanted in 36.4%, tibial only in 54.5% and femoral only in 9.1%.

At the final follow-up the mean OKS was 30.5 points (range 12-44 points), the clinical KSS was 66.5 points (range 41-87 points), the functional KSS was 57.3 points (range 20-80 points), the KOOS was 57.8% (range 32%-79%).

The radiographs showed in 81.8% correct implant positioning, while in 18.2% there was slight radiolucency at the interface between cement and tibial bone.

Wound dehiscence occurred in 27.2% and was treated with surgical cleaning and advanced medications. No failures, considered as revisions for any reason, were recorded.

Conclusion:

The present study analyzed the experience with the use of flexible cones in revision knee replacements. These devices allow the management of metaphyseal bone loss by ensuring optimal implant fixation and gradual dissipation of mechanical stresses from the epiphysis to the diaphysis. The clinical results obtained were satisfactory and, although at reduced follow-up, no implant failure was recorded.

The use of flexible cones represents a valuable tool for the management of severe bone loss during rTKA, ensuring good clinical and radiographic results. Future studies will evaluate the performance of these devices in the medium to long term.

Evolving Techniques in Revision Knee Arthroplasty: Comparative Analysis of Novel and Legacy Hinge Knee Implants Demonstrating Reduced Bone Removal

*Emily Hampp - Stryker - Mahwah, USA

Oliver Jenner - Stryker - Mahwah, USA

Julia Halligan - Stryker - Mahwah, USA

Nicolas Piuzzi - Cleveland Clinic - Cleveland, USA

Introduction:

In revision knee arthroplasty (RTKA), the preservation of healthy distal femoral bone is critical. The amount of bone removed in femoral implant revision depends on differences in resection profiles, especially in hinged implants, where the presence of a hinge mechanism can alter the bone cut profile compared to the original implant. Comparing the volumetric bone removal between different implant designs and clinical scenarios may inform surgical decision-making and enhance patient care. The purpose of this study was to compare the volumetric bone removal required when converting a clinically proven varus valgus constrained knee design [1] to: 1) a clinically proven hinged knee design (Hinge 1) [2]; and 2) a novel hinged knee design (Hinge 2) in three clinically relevant revision scenarios.

Methods:

A total of 733 femurs were identified from a large computed tomography (CT) database, belonging to skeletally mature individuals (sex: 392 M/340 F/1 Unidentified; mean age: 60 ± 16 years; mean BMI 25 ± 5.1 kg/m³). These femurs were divided into groups based on a medial-lateral and anterior-posterior implant sizing schema for the varus valgus constrained knee design [Fig. 1]. Mean composite bone models were generated for each group. Using CAD modeling software, planar resections of the distal femur were generated for the legacy revision knee system and two hinged knee designs. These resections were simulated for three clinically relevant scenarios of revising a varus valgus constrained knee to either a Hinge 1 or Hinge 2 design of the nearest size, including scenarios without distal augments, with 5mm distal augments, and with 10 mm distal augments [Fig. 2]. The volume of bone removed (mm³) was determined for each size conversion of each hinge design and clinical scenario. The percent decrease in bone removal between Hinge 1 and Hinge 2 was then compared and the mean percentage was determined across all size conversions evaluated for each clinical scenario [Fig. 3].

Results:

In this CAD analysis, the Hinge 2 design demonstrated a reduced volume of bone removal compared to the Hinge 1 design when revising the varus valgus constrained knee. The mean decrease in bone removal across all size conversions evaluated (Hinge 2 vs. Hinge 1) was 19%, 46%, and 35% for RTKA without distal augments, with 5mm distal augments, and with 10 mm distal augments, respectively.

Conclusion:

This CAD analysis highlights the reduced mean volume of bone removal observed across three clinically relevant scenarios for the Hinge 2 design over Hinge 1 in RTKA. Notably, in Hinge 2, the posterior chamfer bone cut is shifted posteriorly relative to the intramedullary canal axis (femoral boss), when compared to the clinically successful Hinge 1, which contributes to a reduction in bone removal during revision surgeries. These findings underscore the importance of considering implant design factors in surgical decision-making to preserve healthy bone during RTKA.

References:

[1] Stevens JM, et al. Eur J Orthop Surg Traumatol. 2019 Oct;29(7):1511-1517. doi: 10.1007/s00590-019-02449-9.
 [2] Wignadasan W, et al. Knee. 2021 Jan;28:72-80. doi: 10.1016/j.knee.2020.11.009.

Figures

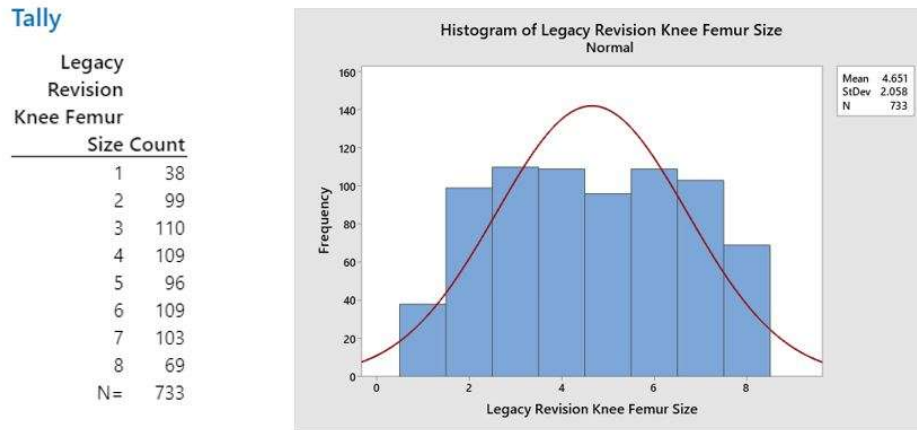


Figure 1. Histogram of the scans sorted into the appropriate Legacy Revision Knee femoral size schema

Figure 1

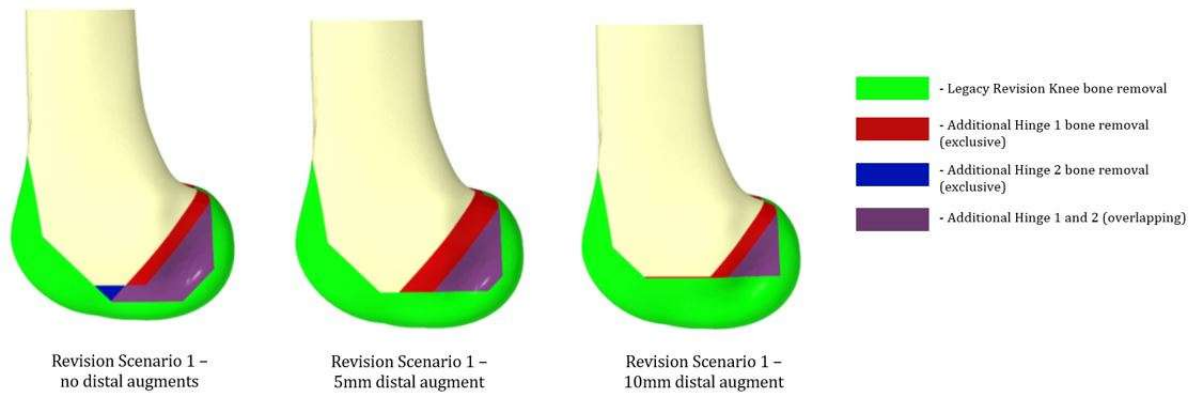


Figure 2. Bone removal comparison overlays

Figure 2

Figure 3. Percent decrease in bone removal between Hinge 1 and Hinge 2 designs for all size conversions and each clinical scenario evaluated.

Size Conversions			Percentage Decrease of Bone Removal (Hinge 1 vs Hinge 2)		
			No Augments	5mm Distal Augments	10mm Distal Augments
Legacy RTKA	Hinge 2	Hinge 1			
Size 1	Size 1	XS	-26%	16%	-21%
Size 2	Size 2	XS	1%	32%	15%
Size 3	Size 3	S	19%	46%	36%
Size 4	Size 4	S	33%	55%	50%
Size 4	Size 4	M	21%	47%	39%
Size 5	Size 5	M	28%	53%	47%
Size 6	Size 6	L	31%	56%	52%
Size 7	Size 6	L	30%	54%	47%
Size 7	Size 6	XL	28%	52%	45%
Size 8	Size 6	XL	24%	47%	39%
		Mean	19%	46%	35%

[Figure 3](#)

Association Between Postoperative Zonal Fixation of Hybrid Fixated Tibial Components in Revision Total Knee Arthroplasty and Subsequent Aseptic Loosening: Appropriate Metaphyseal Fixation Is Key

*Petra Heesterbeek - Sint Maartenskliniek - Nijmegen, Netherlands

Simon Van Laarhoven - Sint Maartenskliniek - Ubbergen, Netherlands

Gijs Van Hellemond - Ubbergen (Near Nijmegen), Belgium

Wim Schreurs - Radboud University Medical Center - Nijmegen, Netherlands

Sjoerd Nota - Sint Maartenskliniek - Ubbergen, Netherlands

Ate Wymenga - Sint Maartenskliniek - Nijmegen, Netherlands

Introduction

Tibial fixation in revision total knee arthroplasty (rTKA) is a challenge. It has been suggested that appropriate fixation in at least two of the three anatomic zones (epiphysis, metaphysis, and diaphysis) is essential for implant survival. However, clinical supporting data is lacking. In this retrospective case-control study, we investigated the relationship between zonal fixation of hybrid fixated rTKA and re-revision for aseptic loosening (rrTKA-AL).

Methods

All consecutive rTKAs with hybrid fixated tibial components (2006–2020) were screened for rrTKA-AL. A control group was randomly selected from the remaining cohort. Post-operative radiographs were scored in random order by three blinded observers for zonal fixation in the epiphysis (bone resection level below, at, or above fibular head; 0–2), metaphysis (number of sufficiently cemented zones; 0–4) and diaphysis (canal filling ratio [CFR]; %). The intraclass correlation coefficient (ICC) was calculated to quantify the agreement between observers. Multivariate logistic regression analysis was performed to assess the relationship between zonal fixation and rrTKA-AL.

Results

Thirty-three patients experienced a rrTKA-AL from a total of 1,173 hybrid fixated tibial components (2.8%). Patients with rrTKA-AL had a significantly lower epiphyseal bone resection level (OR 0.43; 95%CI 0.23–0.76; $p=0.006$), lower number of sufficiently cemented zones (OR 0.50; 95%CI 0.30–0.79; $p=0.004$), but no difference in CFR ($p=0.86$). Furthermore, patients with rrTKA-AL had more frequently previous revisions ($p=0.047$), a higher rate of a prior stemmed component ($p=0.011$) and a higher Anderson Orthopaedic Research Institute classification ($p<0.001$). Agreements of zonal fixation between observers was good (ICC 0.79–0.87).

Conclusion

Patients with rrTKA-AL had lower epiphyseal bone resection levels and a lower number of sufficiently metaphyseal cemented zones. These results emphasize the importance of appropriate metaphyseal fixation. With this information, orthopaedic surgeons can identify patients at risk for rrTKA-AL and optimise their surgical technique in revision knee surgery.

Comparison of Patients Profile Between Femoral Stem Fixation Methods in Primary Hip Revisions in Brazilian Patients Between the Years 2020 to 2024.

*Julia De Lira Kaszubowski - Federal University of Santa Catarina (UFSC) - Florianopolis, Brazil

Patricia Ortega Cubillos - UFSC - Florianopolis, Brazil

Amanda Dos Santos Cavalcanti - National Institute of Traumatology and Orthopaedics (INTO) - Rio de Janeiro, Brazil

Ari Digiacomio Ocampo More - Universidade Federal de Santa Catarina - Florianópolis, Brazil

Joao Antonio Matheus Guimaraes - INTO - Rio de Janeiro, Brazil

Lourenco Pinto Peixoto - INTO - Rio de Janeiro, Brazil

Carlos Rodrigo De Mello Roesler - FAPEU - Florianopolis, Brazil

INTRODUCTION

The cementation and revision rates of total hip arthroplasties have been studied in elderly and younger patients. 165 explants from primary hip revisions were analyzed in Brazil to characterize patient profiles regarding femoral stem cementation.

However, a crucial question remains: how does the choice between cemented and uncemented femoral stems in hip arthroplasties affect outcomes across different age groups in Brazil? This study aims to provide insights for orthopedic practice in the country.

METHODS

The cases collected between November of 2020 and March of 2024 were analyzed, all being from primary hip revisions. Patient and surgery data were compared for different fixation methods, including: age, implant survival in years, gender, indication for primary surgery, indication for the first revision and comorbidities. Statistical comparisons were made using Chi-square tests for categorical variables and Student's t-test for continuous variables with a p-value <0.05 considered statistically significant.

RESULTS

Out of the 165 explants analyzed, 71 were cemented and 94 uncemented. Average age in cemented total hip arthroplasty (THA) was 50 years, in uncemented THA was 47 years. For primary hip revision, average age in cemented prosthesis was 66 years, in uncemented was 61 years ($p=0,011$) (Figure 1). Average implant survival in cemented prosthesis was 15.4 years, uncemented was 13.8 years ($p=0,328$) (Figure 2).

In cemented prosthesis, 54.9% were from male patients, in uncemented 60.6% were male ($p=0,564$). Additionally, of the indication with available data the predominant indication for cemented THA was femoral neck fractures (36.4%), for uncemented was primary hip osteoarthritis (46.9%) ($p=0,322$). Primary surgery data is incomplete due to lack of patient histories.

Aseptic loosening was the most prevalent revision indication in cemented prostheses (29.5%) followed by infection (14.7%), in uncemented prostheses aseptic loosening was the second most prevalent indication of revision with 25.3% of the cases, while infection took the first place with 27.8% ($p=0,253$). Predominant comorbidities were Systemic Arterial Hypertension (SAH) and Diabetes Mellitus (DM), with 40.8% and 14.0%, respectively, in cemented, and 35.1% and 17.0%, respectively, in uncemented.

CONCLUSION

Based on the findings of this study, the only significant difference observed is the age of the patient in the revision of cemented or uncemented prostheses, with a noticeable preference for uncemented prostheses in younger patients. However, other factors such as bone quality, which may have some relation to this preference, could not be assessed in this study, emphasizing the need for further research in the field and understand the Brazilian standard of cementation when these prostheses were implanted.

Figures

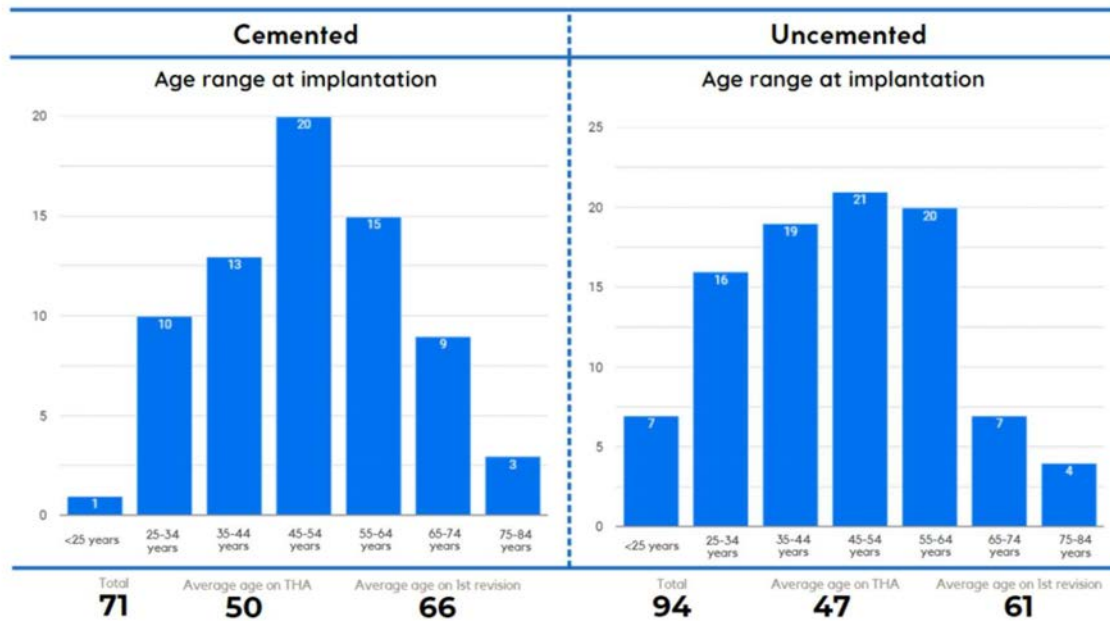


Figure 1 - Number of explants per age range at implantation for cemented and uncemented prosthesis.

[Figure 1](#)

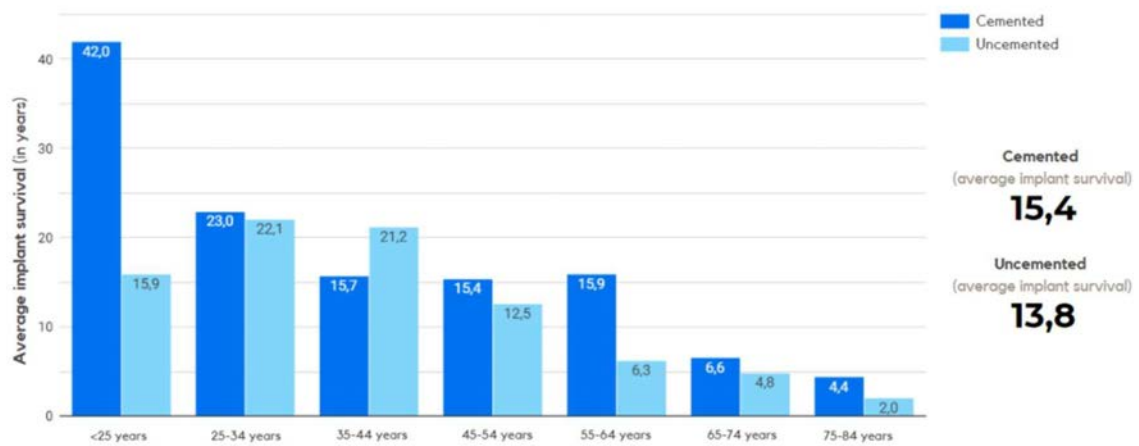


Figure 2 - Average implant survival in years for cemented and uncemented prosthesis per age range at implantation.

[Figure 2](#)

A Statistical Shape Model of Revision Tibia

*Bryan Kirking - Enovis - Austin, USA

Joshua Twigg - University of Sydney - Sydney, Australia

William Calov - 360 Med Care - Sydney, Australia

Nathaniel Pyle - DJO Surgical - Austin, USA

Introduction

Statistical shape modeling (SSM) in orthopedics can be useful in designing primary arthroplasty implants to produce detailed descriptions of anatomies that are complex and difficult to quantify. Given their usefulness, it could be helpful to expand their use into revision cases where the increased number of implant shapes, design features, and pathologies increases the anatomical complexity.

Method

A sample of 30 segmented tibia and fibula from an existing database of revision knee surgery CT scans were selected and then groomed using MeshLab.

Correspondence points were autogenerated in ShapeWorks Studio and then analyzed with python-sklearn to determine the principal components and loadings for each sample. Model performance was evaluated by calculating the RMS error between the input and reconstructed correspondence points, examining the explained variance, and visual inspection of the instances. The model was then used to instance the mean shape and the categorical shape by specifying target features (keel and round stems). Figure 1 illustrates the steps used to create the instances.

Results

Implant features observed in the sample included keels, stems, and pegs. The combination of keel and round stem occurred in fifteen cases and was used for the categorical instance. The SSM demonstrated an explained variance ratio of 99.0%. The overall mean RMS between correspondence points was 0.33 mm with the largest specimen specific mean RMS of 1.32 mm. Cross sectional views for both mean and the categorical instances are shown in Figure 1 and the surface reconstruction of the categorical round stem & keel instance is shown in Figure 2.

Conclusions

When using SSMs to generate instances, the mean of the loadings represents the central tendency and what is mostly likely to occur. However, taking a mean of shapes that maybe dissimilar produces a mathematical combination that may not be represented in the input data. The categorical instance was expected minimize deviations from the observed shapes by minimizing the combining of dissimilar features. Qualitatively, both instances were mostly similar, but the length of the stem feature is shorter in the mean instance compared to the categorical instance, which may be a result of combining stemmed and non-stemmed features in the mean.

Figures

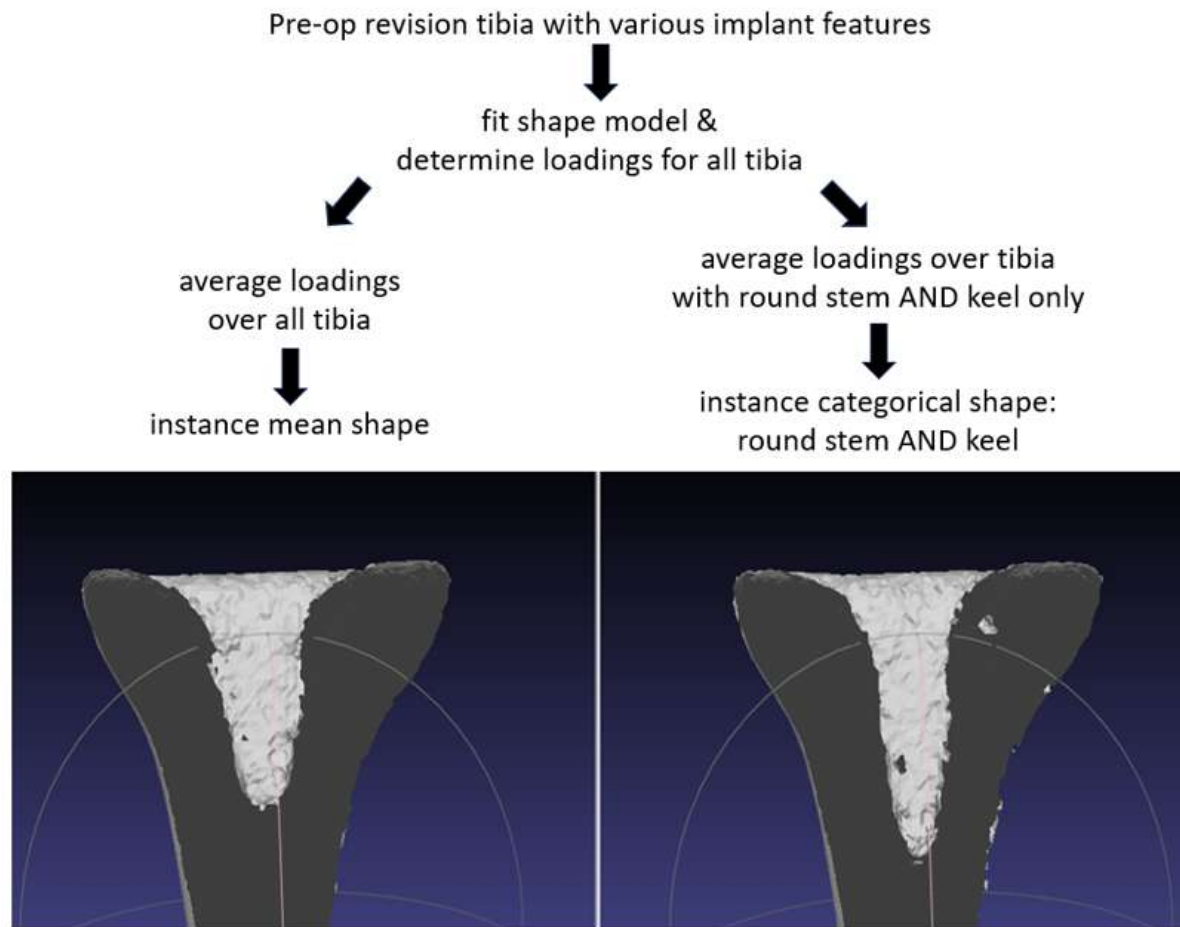


Figure 1. Model steps and cross sections of the mean (left) and the categorical (right) instances from the preop revision tibia statistical shape model.

[Figure 1](#)

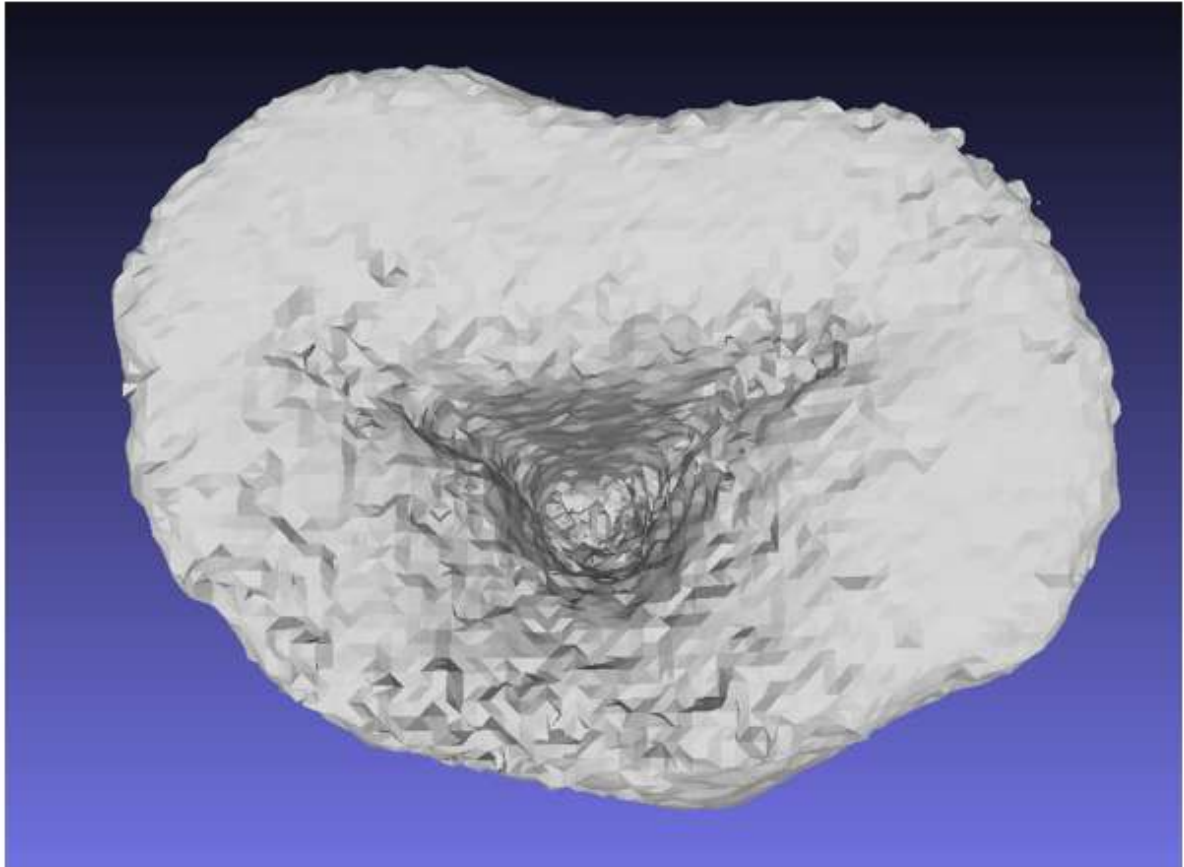


Figure 2. The categorical round stem & keel instance predicted by the preop revision tibia statistical shape model.

[Figure 2](#)

Unicompartmental Knee Arthroplasty Revised to Total Knee Arthroplasty Versus Primary Total Knee Arthroplasty: A Meta-Analysis of Matched Studies

*Mitchell Ng - Maimonides Medical Center - Brooklyn, United States of America

Kenneth Levy - CUNY School of Medicine - New York, USA

Matthew Magruder - Maimonides Medical Center - Brooklyn, USA

Afshin Razi - Maimonides Medical Center - Brooklyn, USA

Nikhil Vasireddi - Case Western Reserve University School of Medicine - Cleveland, USA

Paul Mastrokostas - Maimonides Medical Center - Brooklyn, USA

Hrishik Epuru - Maimonides Medical Center - Brooklyn, USA

Ruhani Sujlana - Maimonides Medical Center - Brooklyn, USA

Nitish Polishetty - Maimonides Medical Center - Brooklyn, USA

Background: Unicompartmental knee arthroplasty (UKA) offers a less invasive alternative to total knee arthroplasty (TKA), but is accompanied by a high revision risk. The aim of our study was to perform a meta-analysis comparing outcomes of UKA revised to TKA versus primary TKA, to assess if UKA is an effective treatment option, despite its potential need for revision.

Methods: Studies comparing matched cohorts of patients with UKA revised to TKA versus primary TKA were identified via the PubMed, Ovid EMBASE, and Scopus databases. The following outcome measures were compared between treatment modalities: postoperative reoperation or revision, total complications, range of motion, patient-reported outcome measures, and length of stay.

Results: Ten studies were included with 1,070 patients: 410 UKA to TKA and 660 primary TKA. At an average follow-up of 5.6 years in the UKA to TKA cohort and 5.7 years in the primary TKA cohort, there were no significant difference in risk of revision ($p = 0.81$), total complications ($p = 0.54$), range of motion ($p = 0.09$), or length of stay ($p = 0.31$). Both objective and functional Knee Society Score were significantly higher in patients with primary TKA ($p < 0.01$). However, there was no difference in Western Ontario and McMaster Universities Osteoarthritis Index (WOMAC) or pain scores ($p = 0.13$ and $p = 0.21$, respectively).

Conclusion: UKA revised to TKA produced comparable clinical and patient-reported outcomes to a primary TKA. UKA may be an effective treatment option in unicompartmental arthritis that would allow for improved functionality and satisfaction without the concern of outcomes deteriorating in patients where a revision becomes necessary.

Long-Term Outcome of Cementless Total Hip Arthroplasty After Rotational Acetabular Osteotomy

*Hiroshi Asai - Nagoya university - Nagoya, Japan

Yusuke Osawa - Nagoya University - Shizuoka, Japan

Yasuhiko Takegami - Nagoya University - Nagoya, Japan

Hiroki Iida - Nagoya University - Nagoya, Japan

Yuto Ozawa - Nagoya University - Nagoya, Japan

Hiroto Funahashi - Nagoya university - Nagoya, Japan

Hiroaki Ido - Nagoya University - Nagoya, Japan

Takamune Asamoto - Nagoya University - Nagoya, Japan

Shiro Imagama - Nagoya university - Nagoya, Japan

Introduction

Total hip arthroplasty (THA) after rotational acetabular osteotomy (RAO) is considered technically difficult because the rotated acetabular fragment results in anatomical deformities. It is known that inadequate RAO which results in Crowe type ? or ? dysplasia after surgery causes severe bone defects. The aim of this study is to investigate long-term outcome of cementless THA after RAO.

Methods

50 hips of 47 patients (3 male, 44 female) who underwent THA after RAO from April 2000 to October 2012 were included. They were followed for at least 10 years. The mean age at surgery was 58.4 and the mean follow-up time was 12.4 years. 12 cases underwent RAO combined with femoral valgus osteotomy. The mean period of time from RAO to THA was 12.4 years. Crowe type before the surgery was type? 27 joints, type? 18 joints, type? 5 joints. Harris hip score (HHS) before surgery and at the last follow-up, the positional relationship between tear drop and femoral head center, leg length discrepancy after surgery, complications and revision surgery were assessed. In addition, we compared Crowe type? (27 hips) and Crowe type ? and ? (23 hips) as subgroup analysis.

Results

HHS improved significantly from 57.2 preoperatively, to 84.5 postoperatively. Femoral head center moved 24.9 mm in a vertical direction and 33.8mm in a horizontal direction. Postoperative leg length discrepancy was 6.6mm. There were 2 cases who experienced dislocation, and no case needed revision surgery. Comparing preoperative Crowe type ? with type ? and ?, preoperative HHS did not differ significantly (57.9 vs 56.5) but postoperative HHS was significantly higher in Crowe type ? group. Femoral head center movement differed significantly (20.9mm vs 29.4mm in a vertical direction, 32.5mm vs 35.1mm in a horizontal direction). Postoperative leg length discrepancy also differed significantly (4.8mm vs 8.4mm).

Conclusion

This study showed cementless THA after RAO provides good long-term fixation of the implant. On the other hand, with regard to THA after inadequate RAO which causes superiorization and lateralization of the femoral head center, the femoral head center significantly locates superior and lateral and the leg length discrepancy is larger after surgery, which is considered to affect the hip function.

Relaxed vs Flexed Seated: Bridging the Gap Between Spinopelvic Mobility Assessment Methods in THA

*Linden Bromwich - Corin Group - Sydney, Australia
Christopher Plaskos - Corin - Raynham, USA
Jonathan Bare - Melbourne Orthopaedic Group - Melbourne, Australia
Stephen McMahon - Monash University - Melbourne, Australia
Andrew Shimmin - Melbourne Orthopaedic Group - Melbourne, Australia
Jim Pierrepont - Corin - Pymble, Australia

Introduction:

Both relaxed- and flexed-seated functional positions are used for assessing spinopelvic mobility (SPM) and instability risk in total hip arthroplasty (THA), although there is debate on which position is superior and how they relate to one another. This study characterizes the spinopelvic relationship between relaxed- and flexed-seated and the proportion of patients classified as at risk for each.

Methods:

1481 THA patients underwent preoperative standing, relaxed- and flexed-seated functional radiographs at one institution (mean [range] age: 65?[23 to 94] years, 49.8% female), Figure 1. Sacral Slope (SS) and Lumbar Lordosis (LL) and their change between standing and seated (Δ SS, Lumbar Flexion (LF)) were measured along with standing spinal alignment (Pelvic Incidence (PI)-LL). Pearson correlation (r) and coefficient of determination (R^2) assessed the relationship between positions. The proportion of patients classified as at risk using the 'simple hip-spine classification' [1] of 1A, 1B, 2A, 2B for relaxed-seated (where $1/2 = \text{PI-LL} </\geq 10^\circ$, $B/A = \Delta\text{SS} \leq/> 10^\circ$) was compared to modified one using flexed-seated risk factors ($1/2 = \text{PI-LL} </\geq 10^\circ$, $B/A = \text{LF} \leq/> 20^\circ$) using Pearson's Chi-squared test.

Results:

All parameters differed between relaxed- vs flex-seated: SS: 27° vs 46° , LL: 37° vs 11° , Δ SS 14° vs -5° , LF: 20° vs 46° , $p < 0.001$ for all, Figure 2. Relaxed- and flexed-seated parameters were significantly correlated: SS: $r = 0.66$, LL: $r = 0.67$, Δ SS $r = 0.67$, LF: $r = 0.63$, $p < 0.001$, but exhibited considerable variation: SS: $R^2 = 0.43$, LL: $R^2 = 0.47$, Δ SS $R^2 = 0.45$, LF: $R^2 = 0.40$, Figure 3. The proportions of patients classified in each risk group for relaxed- and flexed-seated differed significantly for each group: 1A: 52.3% vs 83.6%, 1B: 32.7% vs 1.4%, 2A: 7.8% vs 12.6%, 2B: 7.2% vs 2.4% (all $p < 0.001$). The total proportion of patients classified as having a stiff spine risk (groups 1B & 2B) between relaxed- and flexed-seated also differed significantly: 40% vs 4%. The overall dislocation rate was 0.68% at mean follow-up of 2 years. There was no significant difference in the percentage of dislocations within each group between the two classifications.

Conclusions:

Relaxed and flexed-seated positions yield different spinopelvic mobility parameters and hip-spine classification systems based on each will yield substantially different risk stratification proportions. The data presented here may help to yield a better understanding of the interrelationships between the two assessment methods.

References:

[1] Vigdorich JM, Sharma AK, Buckland AJ, Elbuluk AM, Eftekhary N, Mayman DJ, Carroll KM, Jerabek SA. 2021 Otto Aufranc Award: A simple Hip-Spine Classification for total hip arthroplasty : validation and a large multicentre series. Bone Joint J. 2021 Jul;103-B(7 Supple B):17-24.

Figures

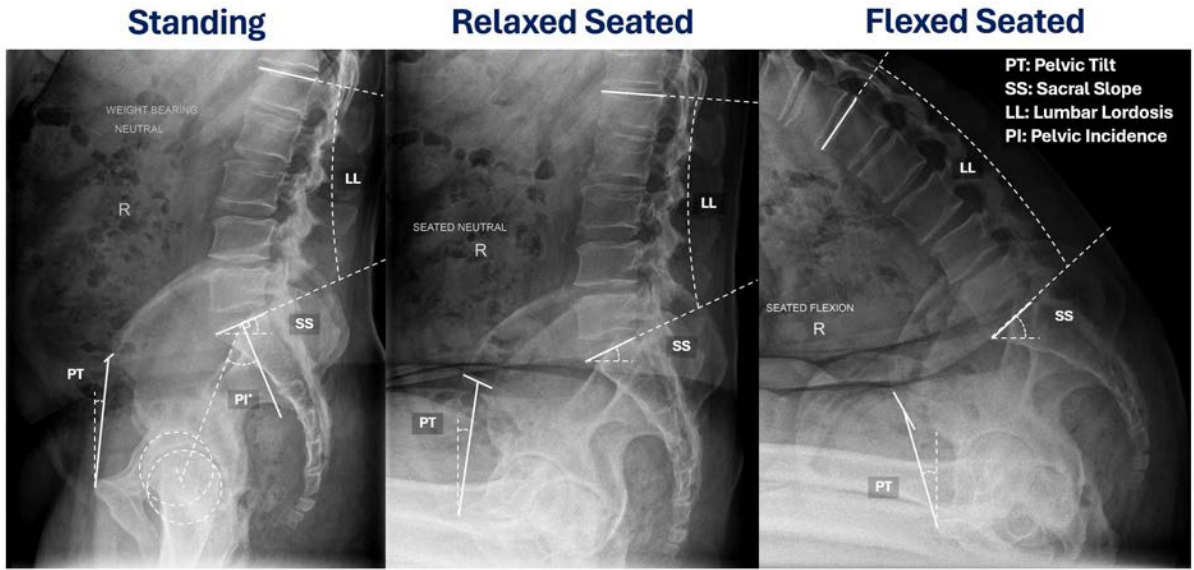


Figure 1

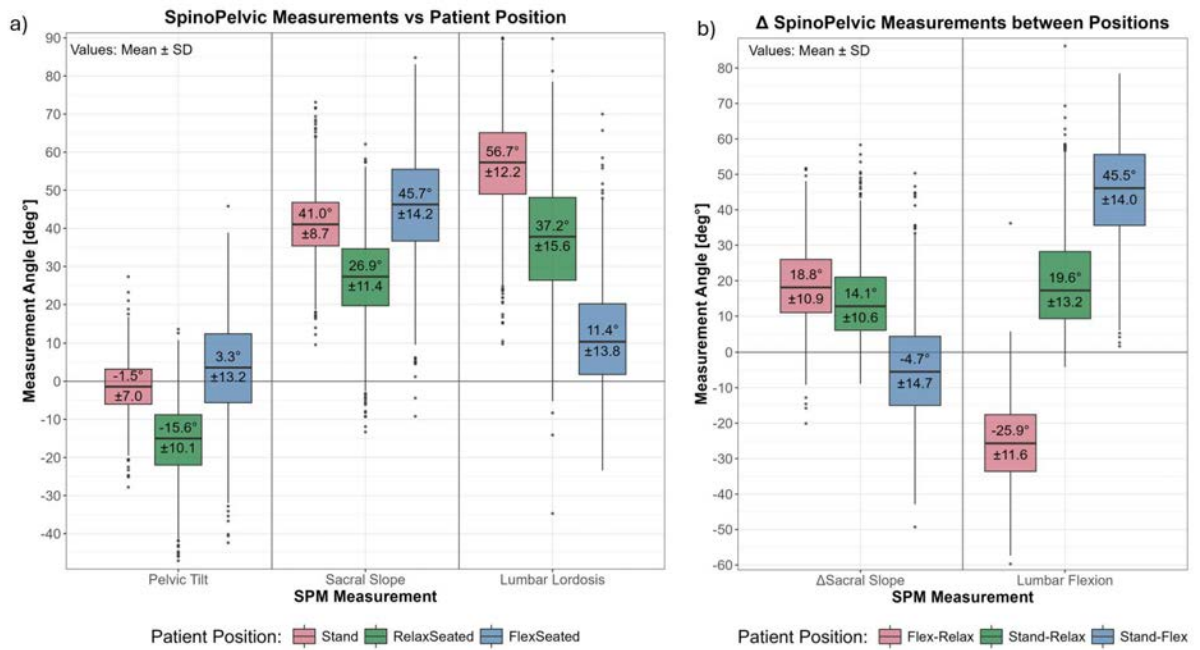
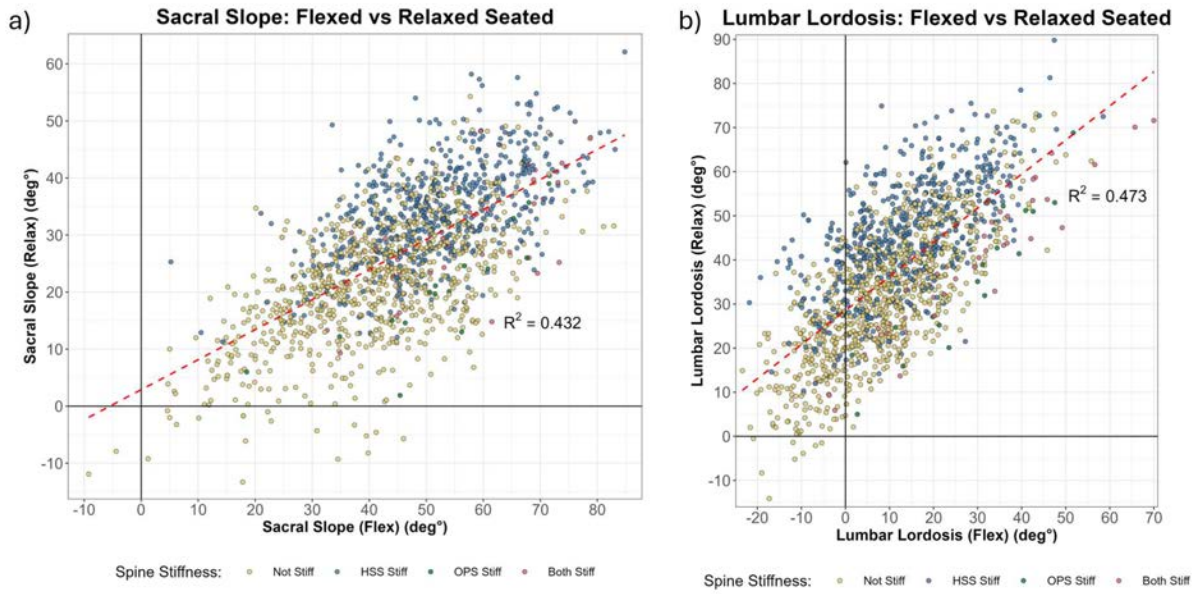


Figure 2



*HSS Stiff is determined from relaxed seated view ($\Delta SS < 10^\circ$), OPS Stiff is determined from flex-seated ($LF < 20^\circ$)

Figure 3

Improving Hip Resurfacing Outcomes in Women: A Retrospective Analysis of 1285 Cases

*Dani Gaillard-Campbell - Midlands Orthopaedics & Neurosurgery - Columbia, USA
Thomas P Gross - Columbia, USA

Background: Hip resurfacing arthroplasty offers many benefits over traditional total hip arthroplasty, including improved bone stock, more nearly-normal gait, reduced pain, and improved range-of-motion. However, resurfacing implant survivorship is lower in females than males in major orthopedic registries, often leading to surgeons selecting against women for hip resurfacing and limiting treatment options. To address this issue, we investigated the specific reasons for why resurfacing devices perform worse in women and formulated solutions for each.

Methods: We implemented a series of intra- and post-operative protocols to address the implant failure modes known to be more common in female than male resurfaced hips. The entirety of these interventions were in place by January 2010. We compare 3169 male and 1285 female hip resurfacing cases done consecutively from January 2010 to November 2021, with all cases having a minimum 2-year follow-up. All data was collected prospectively per standard of care..

Results: Kaplan-Meier implant survivorship was not statistically different at any postoperative time point between men and women. Thirteen-year Kaplan-Meier implant survivorship was 99.1% for men and 97.5% for women ($p=0.2$). Despite a greater number of high-risk diagnoses in the female group, there was no significant difference in rate of failure for any failure mode between the male and female cohorts. While mean HHS and UCLA activity score were greater for males than females, pain scores did not differ significantly between the two groups.

Conclusions: This study shows that - rather than selecting against arthroplasty patients on the basis of sex - failure modes unique to females can be addressed to significantly improve clinic outcomes and implant survivorship. Females with debilitating hip conditions may still be great candidates for hip resurfacing when appropriate changes to surgical technique and postoperative protocol are implemented.

Figures

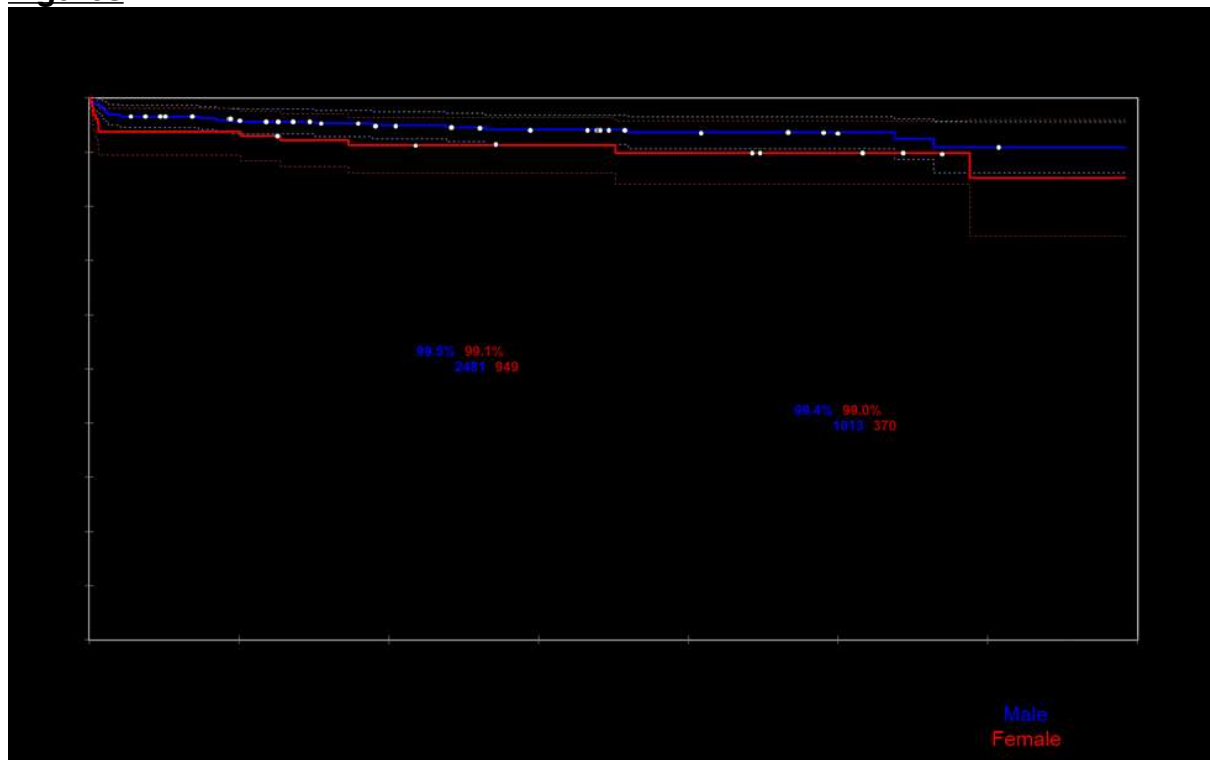


[Figure 1](#)

Early Performance of a Triple-Taper Metaphyseal Filling Collared Femoral Stem in a Multicenter Trial

*Ahmad Faizan - Stryker - Mahwah, USA

Filesha Haniff - Mahwah, United States of America

Hannah Pacheco - Stryker - Mahwah, USA

Han Wang - Stryker - Mahwah, USA

Dennis Nam - RUSH - Chicago, USA

Introduction

Triple tapered collared stems have been shown to have clinical benefits over non-collared stems, especially in the elderly population ¹. Early performance of a newly designed triple tapered collared stem is reported in this study. To understand the impact of surgical variables, the data is stratified by surgical techniques, technology assistance, fluoroscopy use, and patient demographics.

Methods

In this prospective multicenter study, 313 cases were enrolled (310 surgeries completed) at 11 sites (172 females and 138 males). Mean BMI and age were 29.7 and 63.2 years, respectively. 79 subjects completed 1 year follow up. Surgical approaches, use of robotic assistance, intraoperative fluoroscopy use, and adverse events were recorded for each procedure. Various PROMs such as Harris hip score and EQ5D scores were collected during follow up visits. Figure 1 depicts the patient population in various age groups. 153 patients were <65 years, 128 were 65 to 75, and 29 patients were >75 years old.

Results

Surgical approaches were the direct anterior (192 cases), posterolateral (104), anterolateral (10), and direct superior (4). Seventy-three cases were performed with robotic assistance vs. 237 cases without robotic assistance. 135 cases used intraoperative fluoroscopic guidance. Mean HHS score improved from 54.03 pre-op to 90.42 at 1 year follow up. Similarly, mean EQ5D VAS score improved from 68.6 to 84.6 between pre-op to 1 year follow up. There was no report of any intraoperative complications related to the device. A total of 2 stems were revised (as a result of a fall and joint infection respectively).

Discussion

Early clinical data in this trial shows that the metaphyseal filling collared stem was used in a wide variety of patients using various surgical techniques. Approximately, 10% cases were performed in patients over 75 years of age, with no early adverse events reported. Recently, this stem philosophy has been shown to reduce periprosthetic fractures in elderly population as compared to other non-collared stems¹. In addition, for cases where CT based robotic assistance was used, it eliminated the need for intraoperative fluoroscopy use in all but one case. In summary, early data is encouraging on this stem and long-term clinical outcomes and adverse events will be reported in future.

Figures

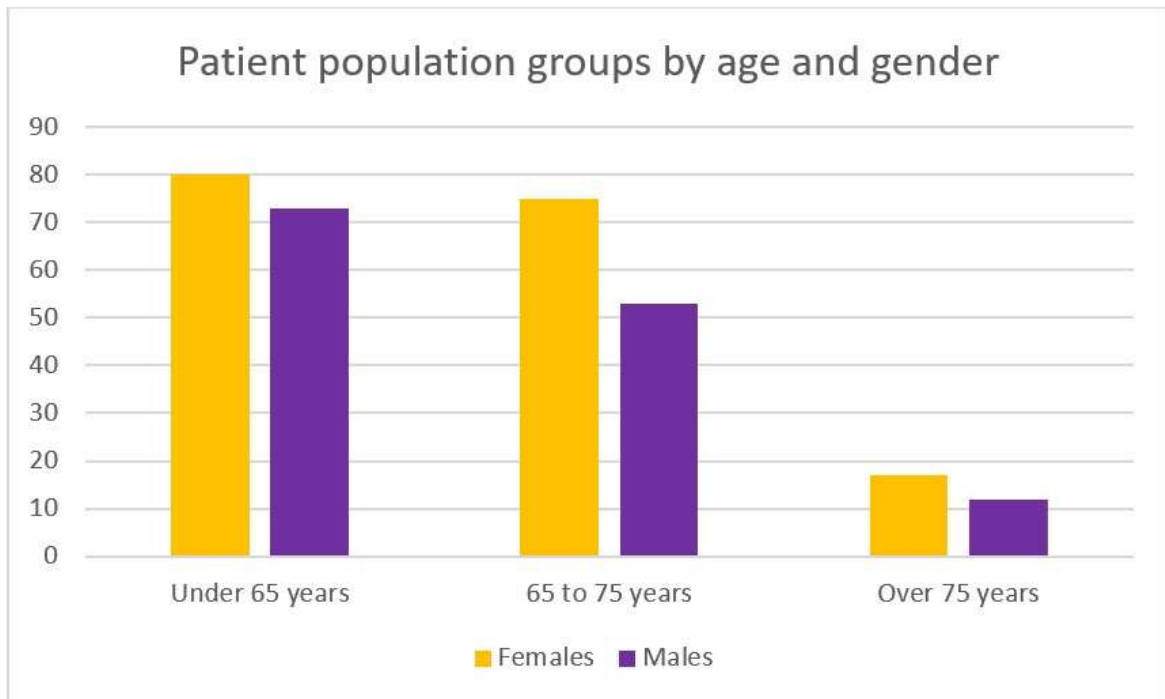


Figure 1: Patient population groups by age and gender

[Figure 1](#)

Femoral Stem Distal Fit Assessment With Novel Three-Dimensional Planning Software

David Rister - Smith & Nephew, Inc. - Cordova, USA

*Gokce Yildirim - Vent Creativity Corporation - Weehawken, USA

Rachel Alexander - Vent Creativity Corporation - Weehawken, USA

Femoral Stem Distal Fit Assessment with Novel Three-Dimensional Planning Software

Authors: David Rister¹, Gokce Yildirim², Rachel Alexander²

1:Smith+Nephew 2:VentCreativity

Introduction:

Utility of 3D preoperative templating for quantifying the contact of total hip constructs and automating landmarking, sizing, and placement in-silico has been explored in the literature¹. Fit of new stem designs has traditionally been assessed using with 2D radiologic imaging². Automated 3D templating potentiates new femoral stem fit assessment using existing femoral CT scan data. Distal fit of an investigational stem was assessed in this study.

Methods:

Investigational collared, short fit-and-fill stem CAD models were fit in 63 CT scans from North America, Asia, and Europe. Femoral cortical shells (CS) were generated based on point cloud density related to a scan threshold of 300 Hounsfield units (HU) defining the femoral canal (FC). The inner diameter of CS was measured at 3.0cm and 10.0cm distal to the lesser trochanter (LT) to assess canal calcar ratio (CCR) and isthmus diameter 10.0cm from LT to identify Dorr Type and narrow FCs ($\varnothing < 10\text{mm}$) prone to distal locking. Full femoral point clouds (FF) were used to measure the radial gap between stems and FCs at three levels below the porous coating level to assess the risk of distal fixation of the proximally fixed stem. A conservative limit of distal interference was established at 0.10mm at any point within the three distal sections.

Results:

The distribution of femoral Dorr score was 38.1% Type A, 55.6% Type B, and 6.3% Type C. Average femoral isthmus inner diameter was 12.8mm (SD 2.6mm), 12.4mm (SD 1.6mm), and 13.4mm (SD 1.2mm) for Types A, B, and C femurs, respectively ($AD > 0.641$, normal data). Scans were predominantly from North America (65.1%), then Asia (31.7%) and Europe (3.2%). All femurs passed criteria for good fit with 0 scans exceeding the maximum distal contact limit.

Discussion:

3D templating software may help predict potential unintended distal reaming and locking of novel femoral stem designs. Limitations include the lack of cadaveric or clinical validation of automated placement accuracy, suggesting further investigation of this method.

Bibliography:

1. Hart et al., EOR, Volume 5, December 2020, DOI: 10.1302/2058-5241.5.200046
2. Beverland, et al., JOA 35(2020) 3204-3207, DOI: 10.1016/j.arth.2020.05.066
3. Yildirim, et al., ISTA 2023, Novel Implant Planning Tool for Hip Stem Alignment

Unexpected Positive Cultures in Aseptic Revision Hip and Knee Arthroplasty: Prevalence and Outcomes at Mid-Term Follow-Up

*Mohammed Wazir - University College London University Hospitals - London, United Kingdom

Fabio Mancino - University College London Hospitals NHS Foundation Trust - London, United Kingdom

Joanna Baawa - University College London Hospital - London, United Kingdom

Fares Haddad - University College London Hospital - London, United Kingdom

Babar Kayani - University College Hospital London - London, United Kingdom

Background

The outcomes of patients with unexpected positive cultures (UPCs) during revision total hip arthroplasty (THA) and total knee arthroplasty (TKA) remain unknown. The objectives of this study were to establish the prevalence and infection-free implant survival in UPCs during presumed aseptic single-stage revision THA and TKA at mid-term follow-up.

Methods

This study included 297 patients undergoing presumed aseptic single-stage revision THA or TKA at a single treatment centre. All patients with at least three UPCs obtained during revision surgery were treated with minimum three months of oral antibiotics following revision surgery. The prevalence of UPCs, causative microorganisms, recurrence of PJIs and infection-free implant survival were established at minimum 5-years' follow-up (range 5.1 to 12.3 years)

Results

Of the 297 patients undergoing aseptic revisions, 37 patients (12.5%) had at least three UPCs obtained during surgery. The UPC cohort included 23 males (62.2%) and 14 females (37.8%), with mean age of 71.2 years (range, 47 to 82 years). Comorbidities included smoking (56.8%), hypertension (48.6%), diabetes mellitus (27.0%), and chronic renal impairment (13.5%). The causative microorganism included *Staphylococcus epidermidis* (49.6%); *Bacillus species* (18.9%); *Micrococcus species* (16.2%) and *Cutibacterium acnes* (16.2%). None of the study patients with UPCs developed further PJIs or required further surgical intervention during follow-up.

Conclusions

The prevalence of UPCs during presumed aseptic revision THA and TKA was 12.5%. The most common causative microorganisms were of low-virulence, and included *Staphylococcus epidermidis*, *Bacillus species*, *Micrococcus species* and *Cutibacterium acnes*. Microorganism-specific antibiotic treatment for minimum three months duration of UPCs in presumed aseptic revision arthroplasty was associated with excellent infection-free implant survival at mid-term follow-up.

Efficacy of a Vancomycin/tobramycin-Doped Dicalcium Phosphate Dehydrate (P-DPCD) Composite in a Mouse Pouch Infection Model Implanted With 3D-Printed Porous Titanium Cylinders

*Adam Miller - Ascension Providence Hospital - Southfield, USA

Michael Kaminski - Michigan State University College of Human Medicine - Grand Rapids, USA

Therese Bou-Akl - Providence-Providence Park Hospital - Southfield, USA

Paula Dietz - Ascension Providence Hospital - Southfield, USA

David Markel - The CORE Institute - Novi, USA

Introduction:

Prosthetic joint infection (PJI) remains a challenging problem. Various strategies have been applied to prevent implant-associated bacterial infections with varying levels of success. Intraoperative saline irrigation is commonly used as a preventative measure; however, bacterial infection and biofilm formation are generally not effectively treated with saline irrigation alone. This study evaluated the effect of antibiotic doped polymeric dicalcium phosphate dehydrate (P-DCPD) in a mouse pouch infection model implanted with 3D printed porous titanium (Ti) cylinders (400 μm pore size). The printing process for these cylinders is identical that used in commercial total joint replacement products.

Methods:

Air pouches were created in 30 female BalBc mice by subcutaneous injection of air (n=10 per group). Pouches were then implanted with either porous Ti cylinders only (negative control), Ti cylinders and *Staphylococcus aureus* (*S. aureus*) (1×10^6 colony forming units (cfu)) (positive control), or Ti cylinders preloaded with antibiotic-loaded P-DCPD and *S. aureus* (1×10^6 cfu) (treatment group). Mice were sacrificed 28 days after implantation. At sacrifice, pouches were washed with 3 ml of sterile saline, and the washout was collected for quantitative bacterial analysis (Figure 1). The Ti cylinders were also collected and sonicated for quantitative bacterial analysis (Figure 1).

Results:

There were no detectable bacteria in either the pouch washings or the Ti cylinder sonicate (0 cfu/ml) following treatment with antibiotic doped P-DCPD or in the negative control group. There was significantly less bacteria in the pouch washout of mice treated with antibiotic doped P-DCPD (0 cfu/ml) when compared to the positive control (1894 ± 2455 cfu/ml) ($P < 0.001$) (Table 1). Similarly, sonication analysis of the Ti discs showed significantly less bacteria in the treatment group when compared to positive controls (0 cfu/ml vs 22233 ± 33735 cfu/ml, $P = 0.002$) (Table 1).

Conclusion:

Porous Ti implants are vulnerable to bacterial infection and biofilm formation. Pre-treatment of these implants with Vancomycin and Tobramycin doped P-DCPD led to a significant reduction in bacterial infection in this mouse pouch model. In fact, there were no detectable bacterial colony forming units in any of the treated animals. Antibiotic doped PDCPD as an implant precoat may represent an effective means of decreasing or preventing PJI.

Figures

Table 1

WASH		
Group (#1)	Group (#2)	p-value
Ti cylinder only (0 cfu/ml)	Bacteria + Ti cylinder (1894 ± 2455 cfu/ml)	<0.001
Ti cylinder only (0 cfu/ml)	Bacteria + Ti cylinder + antibiotic doped P-DCPD (0 cfu/ml)	1.000
Bacteria + Ti cylinder (1894 ± 2455 cfu/ml)	Bacteria + Ti cylinder + antibiotic doped P-DCPD (0 cfu/ml)	<0.001
CUMULATIVE SONICATE		
Group (#1)	Group (#2)	p-value
Ti cylinder only (0 cfu/ml)	Bacteria + Ti cylinder (22233 ± 33735 cfu/ml)	0.002
Ti cylinder only (0 cfu/ml)	Bacteria + Ti cylinder + antibiotic doped P-DCPD (0 cfu/ml)	1.000
Bacteria + Ti cylinder (22233 ± 33735 cfu/ml)	Bacteria + Ti cylinder + antibiotic doped P-DCPD (0 cfu/ml)	0.002

Tukey HSD Post Hoc test. Mean bacterial amount with 95% confidence intervals in parentheses below group name. Significance set at P<0.05.

[Figure 1](#)

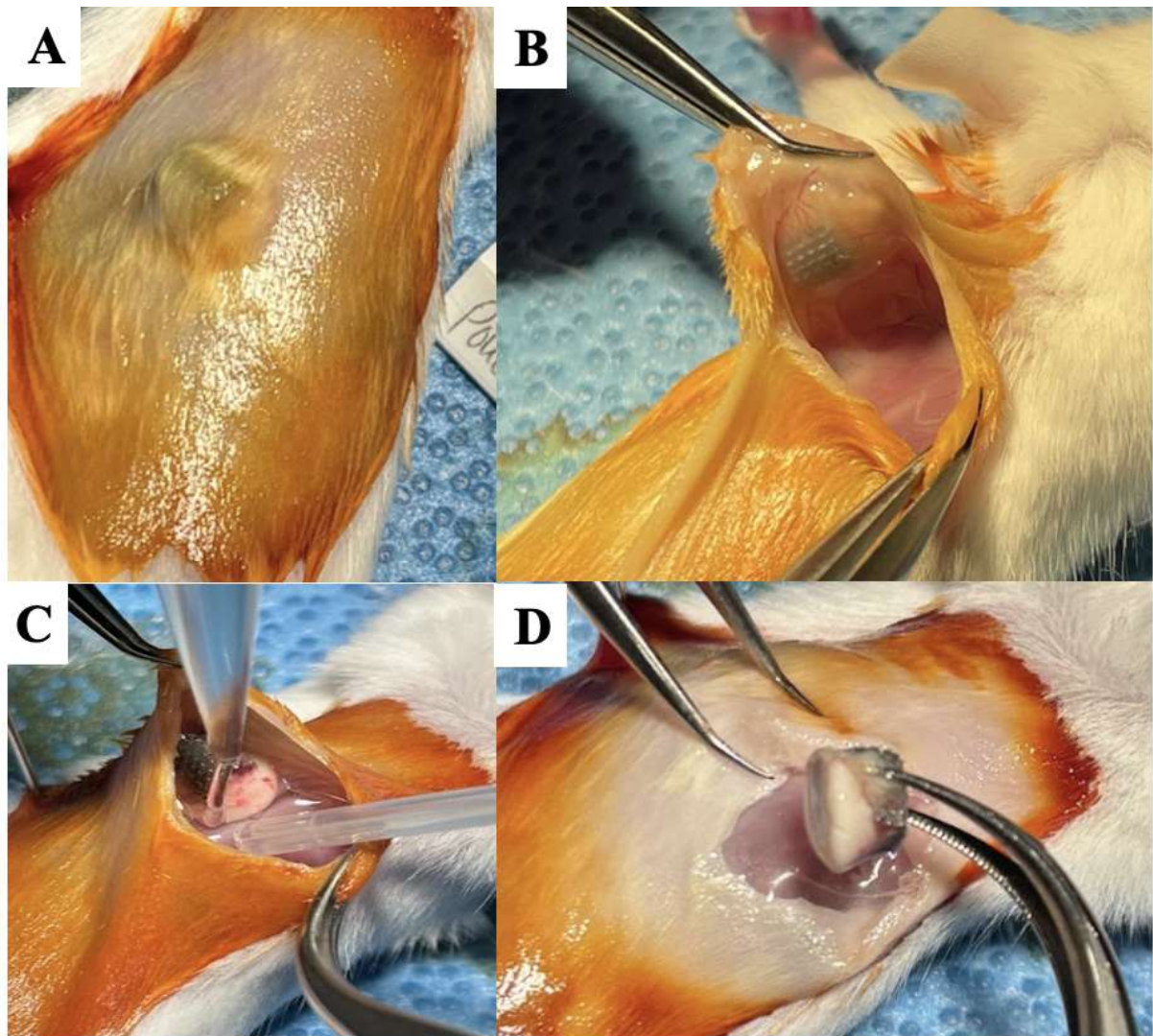


Figure 1: Gross images of surgical steps of the pouch cavity with saline wash and implant harvest 28 days after Ti cylinder implantation and bacterial inoculation. (A) Air pouch cavity with Ti cylinder visible inside. (B) Pouch cavity open with Ti cylinder visible inside. (C) Pouch cavity washout with saline and collection of washing. (D) Harvest of the Ti cylinder.

[Figure 2](#)

Effects of Intravenous Dexamethasone on Glycemic Control in Patients With Type 2 Diabetes Mellitus After Total Knee Arthroplasty: Prospective, Randomized Controlled Study

Sung Jun Jang - Seoul National University College of Medicine Boramae Medical Center (SMG-SNU Boramae Medical Center) - Seoul, Korea (Republic of)

Hyunkwon Kim - SMG-SNU Boramae Medical Center - Seoul, Korea (Republic of)

*Hyung Min Lee - Seoul National University Boramae Hospital - Seoul, Korea (Republic of)

Cho min soo - Seoul, Korea (Republic of)

Jisu Park - SMG-SNU Boramae Medical Center - Seoul, Korea (Republic of)

Tae Woo Kim - Seoul National University College of Medicine, SMG-SNU Boramae Medical Center - Seoul, South Korea

Moon Jong Chang - SMG-SNU Boramae Medical Center - Seoul, South Korea

Seung-Baik Kang - Boramae Medical Center/ Seoul National University College of Medicine - Seoul, South Korea

Background : The perioperative administration of intravenous (IV) dexamethasone is recognized as effective in minimizing postoperative pain and postoperative nausea and vomiting (PONV) and facilitate early recovery after Total knee arthroplasty (TKA). However, concerns persist regarding undesirable side effect resulting from administration of glucocorticoid during perioperative period especially in diabetic patients.

Purpose : This study aimed to determine whether the administration of dexamethasone before and in the immediate postoperative period in diabetic patients (1) increases blood glucose level and insulin requirements, (2) increases postoperative complications, such as surgical site infections and delayed wound healing, and (3) mitigates postoperative pain, nausea and vomiting.

Material & Methods : We randomized 81 diabetic patients undergoing TKA to receive two IV injection of 10mg dexamethasone (DEXA group, n = 41), or 2cc normal saline (No-DEXA, n = 40). Blood glucose levels were measured four times a day. Blood glucose curves were then generated from the operation day to postoperative day (POD) 5. The area under the blood glucose curve was calculated each day to evaluate postoperative blood glucose levels. Pain levels, incidence of PONV and severity of nausea were assessed at postoperatively 0 to 6 hours, 6 hours to the night of the operation day, and daily on POD 1 to 5. Postoperative complications including delayed wound healing and surgical site infection were assessed within 90 days following surgery.

Results : The DEXA group showed a significant higher blood glucose levels on the operation day and POD 1. Conversely, the blood glucose level was lower in the DEXA group on POD 2. No significant differences were observed between the two groups from POD 3 to 5. The insulin requirement was higher in the DEXA group on POD 1, but lower on POD 2. No significant differences were found on operation day, and from POD 3 to 5. Patients in the DEXA group reported lower pain during POD 1 to 3 and consumed less analgesics on POD 1. In severity and incidence of PONV, no significant differences were noted during the overall study period. There were no significant differences in wound complication and surgical site infection between two groups.

Conclusions : The administration of dexamethasone to diabetic patients undergoing TKA led to a transient elevation in blood glucose levels. However, it did not lead to alterations in insulin requirements or result in wound complications.

Appropriate Sequence and Timing of Ipsilateral Hip and Knee Arthroplasty

*Ameer Tabbaa - x, United States of America

Matthew Magruder - Maimonides Medical Center - Brooklyn, USA

Gabriel Lama - Maimonides Medical Center - Staten Island, United States of America

Ariel Rodriguez - Maimonides Medical Center - Brooklyn, United States of America

Introduction

Patients are progressively receiving more arthroplastic procedures as primary osteoarthritis rates have increased. However, there is limited research in terms of how to approach multi-joint replacement procedures and their effects on each other. The objective of this study was to determine if the timing of total hip arthroplasty (THA) in relation to ipsilateral total knee arthroplasty (TKA) affects the outcomes of TKA.

Methods

A retrospective query of a national administrative claims database was performed between 2010 and 2022, examining patients who underwent both THA and TKA on the same lower extremity. Four subsequent groups were formed: (1) a control group of patients who underwent a TKA without ever undergoing a THA- 9,780; (2) those who underwent TKA at least 2 years before THA- 2,110; (3) those who underwent TKA in the 2 years before THA- 1,956; and (3) those who underwent THA before TKA- 3,873. The groups were matched to based on age, gender, obesity, Charleston Comorbidity Index (CCI), smoking status, and rheumatoid arthritis, while excluding patients with connective tissue disorders. Multivariate logistical regressions were used to evaluate the following outcomes: 90-day and 2-year implant-related complications, 90-day readmissions, and 90-day and 2-year revisions. Patients in Group 2 had their 2-year post-operative outcomes merged with 2-year TKA complications following their THA surgery date.

Results

Compared to the control, patients who either underwent TKA within 2 years before ipsilateral THA or had a THA before an ipsilateral TKA demonstrated higher rates of periprosthetic fractures (OR: 3.01 & 3.20; $p=0.009$ & $p<0.0001$, respectively) and 90-day revision rates (OR: 2.53 & 1.92; $p=0.009$ & $p=0.037$, respectively). Patients who underwent TKA greater than or within 2 years before undergoing an ipsilateral THA had higher rates of 2-year aseptic loosening (OR: 3.29 & 1.79; $p<0.001$ & $p=0.043$, respectively). Patients who underwent TKA more than two years before undergoing ipsilateral THA had higher odds of instability (OR: 2.22, $p=0.012$), but had lower revision rates than the control group, the TKA within 2 years before ipsilateral THA, and the THA before ipsilateral TKA groups (OR: 0.23 vs 0.22 vs 0.29, $p= 0.04$ vs 0.019 vs 0.047, respectively). There were no significant differences in surgical and revision outcomes between patients undergoing TKA within two years before THA and those who underwent THA before TKA.

Conclusion

Having both TKA and THA on an ipsilateral leg brings about more complication to the TKA than having a TKA alone. Patients receiving a THA before an ipsilateral TKA have similar outcomes to patients who receive a TKA within two years before undergoing ipsilateral THA. Patients with a TKA greater than two years before a THA have lower 90-day revision rates and rates of periprosthetic fractures when compared to having a TKA within 2 years before an ipsilateral THA or having a THA before an ipsilateral TKA. If a patient demonstrates a significant history of

osteoarthritis and there's high clinical suspicion for the patient receiving ipsilateral TKA and THA, having a TKA at least 2 years before a THA helps to minimize complications.

Measuring the Quality of Periprosthetic Joint Infection Diagnosis: An Administrative Database Study

Daniel Buchalter - Hospital for Special Surgery - New York, USA

Andy Miller - Hospital for Special Surgery - New York, USA

Shinhye Kim - Hospital for Special Surgery - New York, USA

*Edward Grabov - Hospital for Special Surgery - New York, USA

Diana Chee - Hospital for Special Surgery - New York, USA

Amy Chin - Hospital for Special Surgery - New York, USA

Alexander Mclawhorn - HSS - New York, USA

Catherine MacLean - Hospital For Special Surgery - New York, USA

Introduction

The timely and accurate management of periprosthetic joint infection (PJI) remains a challenge. No published work evaluates compliance with diagnostic guidelines for PJI surgery. We assessed the quality of PJI diagnosis using an administrative claims database by determining whether erythrocyte sedimentation rate (ESR) and c-reactive protein (CRP) were obtained before any revision arthroplasty surgery, and whether ESR, CRP, and aspiration with cell count (CC) and culture were obtained before PJI surgery.

Methods

Using relevant International Classification of Disease Tenth Revision (ICD-10) and Current Procedural Terminology (CPT) codes, inpatient and outpatient Merative MarketScan claims data between 2019 and 2021 were queried for records with continuous enrollment 1-year prior, through 1-year after PJI surgery. Records were excluded if in the past year they had PJI surgery or a hospital visit, presented to the ER \leq 2 days from surgery, or if they were transferred from another hospital. Demographics, geography, payor status, and comorbidities were collected. CPT codes were used to identify those that had preoperative ESR, CRP, and aspiration with cell count and culture. Compliance with preoperative testing by gender, age, geography, and employment status were compared using Chi-squared tests.

Results

946 revision and 509 PJI eligible records were identified. In the revision and PJI cohorts, respectively, 464/946 (49.1%) and 225/509 (44.2%) were female, and 659/946 (69.7%) and 351/509 (69.0%) were 55-64 years old. In the revision cohort, 382 (40.4%) had no preoperative testing, and 481 (50.9%) had both ESR and CRP performed. In the PJI cohort, 186 (36.6%) had ESR, CRP, CC, and culture performed; 98 (19.3%) had three of these tests; 108 (21.3%) two; 37 (7.1%) one; and 80 (15.8%) none. For the revision and PJI cohorts with zero versus any number of tests performed, respectively, there were no significant differences by gender ($p=0.467$; $p=0.086$), age ($p=0.260$; $p=0.988$), geography ($p=0.074$; $p=0.608$), nor employment status ($p=0.847$; $p=0.375$).

Conclusion

This novel application of administrative claims data found that no preoperative inflammatory markers are sent for 40.4% of revision arthroplasty patients, and only 36.6% of PJI patients receive a complete, standard-of-care, preoperative workup. These findings demonstrate clear areas for improvement in the quality of care of PJI nationally.

Short-Term Outcomes of Robotic-Assisted 1.5-Stage Exchange Total Knee Arthroplasty for the Management of Periprosthetic Joint Infection

Alekasandra Qilleri - 6. Donald & Barbara Zucker School of Medicine - Hempstead, USA

*Kevin Chang - Northwell Health Huntington Hospital - Huntington, USA

Alexandra Echevarria - Northwell Health - Great Neck, USA

Jonathan R. Danoff - Northwell Health, Northshore University Hospital - Manhasset, USA

Introduction

Prosthetic joint infection (PJI) has long presented a challenge to arthroplasty surgeons. 1.5-stage exchange total knee arthroplasty (1.5-TKR) for management of PJI has garnered interest over traditional 2-stage approaches given advantages of early ambulation and potential for single surgery with similar efficacy in clearance of infection. A recently published robotic-assisted 1.5-TKR revision (1.5-RATKR) technique has demonstrated utility in assisting surgeons performing this procedure. The purpose of this study is to compare the short-term outcomes of 1.5-RATKR and conventional 1.5-TKR. We hypothesize that 1.5-RATKR will show faster return of physical function, measured in knee range of motion and time to ambulation.

Methods

This retrospective case-control study reviews all 1.5-TKR performed by a single arthroplasty fellowship-trained surgeon between 2017-2023. 1.5-TKR performed using conventional techniques before 2022 were compared to 1.5-RATKR performed after 2022 using a novel technique using CT-guided navigation and Stryker MAKO robotic assistance (Stryker, Mahwah, NJ). Data collected included patient demographics, surgical and implant data, in-hospital physical therapy (PT) progress, and short-term outcomes through minimum of 6 months.

Results

Twenty-two 1.5-TKR for PJI were included with average patient age 73.3 years \pm 10 years. 11 conventional 1.5-TKR were compared to 11 1.5-RATKR. 100% of cases showed eradication of the diagnosed infection at 6 months. There were no significant differences in 1.5-RATKR versus 1.5-TKR in rates of PT clearance by postoperative day 2 (18.1% vs 9.1%, $p=1.0$), hospital length of stay (5.1 days \pm 1.8days vs 6.8 days \pm 4.4days, $p=0.24$), or 2-week knee range of motion past 90 degrees (91% vs 73%, $p=0.59$), respectively. No pin site complications or reoperations occurred in the 1.5-RATKR group. In the conventional cohort, one case required revision at 2 years for anterior knee pain with a previously unresurfaced patella, one case developed a new PJI over 1 year later with an unrelated organism after clearance of original infection, and one case required irrigation and debridement with implant retention within 90 days for superficial wound dehiscence. No patients required revision for implant failure secondary to loosening.

Discussion

1.5-TKR and 1.5-RATKR are viable techniques in management of acute and chronic PJI, with 100% eradication of infection in both cohorts. Robotic-assisted techniques may assist surgeons with more accurate joint-line restoration and coronal and sagittal balancing. No patients in the robotic cohort required revision surgery and functional outcomes showed similar short-term outcomes between groups. Additional follow up is needed to assess long-term outcomes and implant longevity.

A Novel, Cordless, Non-Powered, Continuous Negative Pressure Wound Dressing: Optimizing Total Hip Arthroplasty

*Robert Eberle - Maxx Orthopedics - Apex, USA

Asit Shah - Englewood Health - Englewood, USA

Saira Shah - University of Wisconsin - Madison, USA

INTRODUCTION

Negative pressure wound dressings (NPWDs) are well established across various surgical disciplines, with known mechanisms of action and benefits for wound care and healing. However, continuous NPWDs commonly utilize a powered unit that either tethers the patient to a wall power outlet or requires wearing a battery powered unit. We introduce the use of a self-contained, non-powered, continuous NPWD for primary total hip arthroplasty (THA). The purpose of this case series was to report on the feasibility, patient compliance, and result of the use of this system for primary THA.

MATERIALS AND METHODS

A consecutive series of 35 non-selected patients presenting with osteoarthritis (OA) underwent elective primary THA. There were 23 (66%) females and 12 (34%) males with an average age at surgery of 68.7 years \pm 12.1 years (range: 43 years to 93 years). Twenty (57%) were left hips and 15 (43%) right hips. Average patient body mass index (BMI in g /cm²) was 27.8 \pm 4.8. Patients' average Hgb A1C was 5.5 \pm 0.4 with 2 patients diagnosed with DM-II (controlled with meds). Pre-operative HOOS-JR patient reported outcome measures (PROMs) were administered (raw score total range: 0 to 24 where 0 is best) with an average of 22.6 \pm 0.5. All surgeries were performed by senior author (AS) through a posterior approach for THA. Following wound closure, all patients received the single use, NPseal® surgical dressing (Guard Medical, Miami, FL), which delivers continuous non-powered negative pressure wound therapy (NPWT). The NPseal features a simple pinch pump that applies and maintains negative pressure (-75 to -125mm that may promote wound healing). At the 2-week post-operative follow-up, patient compliance with the NPseal was reviewed and wounds assessed.

RESULTS

All patients were reviewed post-operatively, and the NPseal NPWDs were in place and intact at follow-up. Upon visual assessment, all wounds were found to be progressing without evidence of any surgical site complications, adverse, or serious adverse events. Regarding the use of the NPseal NPWD, patient queries reported the ease of use and compliance with monitoring and maintaining the negative pressure gradient during recovery. Patient age, gender or pre-operative co-morbidities had no adverse correlation to current state of assessed wound healing.

DISCUSSION AND CONCLUSION

We report the results of a single surgeon, case series involving a single use surgical NPWD which delivers continuous non-powered NPWT. The use of the NPseal NPWD is well established across other surgical disciplines and has recently been introduced for use across orthopedic surgical application. We found that the use of the NPseal NPWD is feasible in primary THA. The limitations of this case series include a small sample size, single surgeon use, and not including a control group.

However, this was intended to be a feasibility study to answer the minimal questions about the device application, patient compliance, general wound outcome, and patient satisfaction in primary THA. We conclude that the purpose of this feasibility study was met and that further use and study of the NPseal NPWD in primary THA, and other orthopedic applications, is warranted.

Comparative Analysis of Aidify's Knee Care Aids and General ChatGPT in Providing Knee Replacement Information: A Blinded Study

Evan Bloom - NYU Grossman Long Island School of Medicine - Garden city, USA

*timur seckin - NYU

Jan Albert Koenig - Winthrop University Hospital - Rockville Centre, USA

James D Capozzi - New York, USA

Gregory H Sirounian - NYU Grossman Long Island School of Medicine - Garden City, USA

Omid Barzideh - NYU Orthopedic Hospital - New York, USA

Introduction: With the evolving landscape of digital healthcare solutions, personalized artificial intelligence (AI) assistants have become pivotal in enhancing patient education and post-operative support. Aidify, at the forefront of healthcare innovation, has developed AI-driven Care Aids tailored for various medical disciplines, aiming to optimize patient care through intelligent assistance. This study evaluates the effectiveness of Aidify's Knee Care Aids against general ChatGPT responses in addressing common knee replacement queries.

Methods: This study employed a double-blinded methodology, engaging four arthroplasty surgeons to evaluate responses to 10 common knee replacement questions. These questions were answered by both Aidify's Knee Care Aids and general ChatGPT, with surgeons blinded to the source of each response. Responses were rated on a 5-point Likert scale, ranging from strong disagreement or concern regarding patient safety to strong endorsement of the response as being thorough and exceeding typical advice. The scale was designed to capture the surgeons' confidence in the safety, accuracy, and practice-specific relevance of the responses. This approach allowed for an unbiased comparison of the perceived value and safety of the information provided by the two AI systems.

Results: The average response rating for Care Aids was 4.025, marginally higher than ChatGPT's 3.95, indicating a preference for the customized Care Aids' responses. Notably, no Care Aid responses were rated at the lowest two levels of the Likert scale, demonstrating a high level of acceptance. In contrast, ChatGPT's responses included one rated as potentially harmful (Level 1) and twelve as non-specific or disagreeable (Level 2 and 3). This comparison highlights the tailored and safer approach of Aidify's Care Aids in delivering patient education.

Conclusion: The study demonstrates Aidify's Care Aids' ability to offer more preferred responses to knee replacement queries than general AI platforms like ChatGPT. The findings suggest that personalized AI assistants can enhance the quality of patient care by providing more accurate and practice-specific information. This advancement aligns with Aidify's mission to empower healthcare professionals with personalized virtual assistants, indicating a promising direction for the future of AI in healthcare. The study's outcomes support further exploration and development of AI-driven solutions in enhancing patient education and support, contributing to the broader goals of improved patient satisfaction and outcomes in the healthcare sector.

Keywords: Aidify, AI-driven Care Aids, ChatGPT, knee arthroplasty, patient education, digital healthcare solutions.

GPT-4 as a Source of Patient Information for Cervical Disc Arthroplasty: A Comparative Analysis Against Google Web Search

*Mitchell Ng - Maimonides Medical Center - Brooklyn, United States of America

Paul Mastrokostas - Maimonides Medical Center - Brooklyn, USA

Leonidas Mastrokostas - Maimonides Medical Center - Brooklyn, USA

Ahmed Emara - Cleveland Clinic - Cleveland, USA

John Houten - Maimonides Medical Center - Brooklyn, USA

Ahmed Saleh - Maimonides Medical Center - Brooklyn, USA

Afshin Razi - Maimonides Medical Center - Brooklyn, USA

Hrishik Epuru - Maimonides Medical Center - Brooklyn, USA

Ruhani Sujlana - Maimonides Medical Center - Brooklyn, USA

Nitish Polishetty - Maimonides Medical Center - Brooklyn, USA

Objectives: ChatGPT, an AI chatbot, has seen widespread use with over 100 million weekly users seeking online information. Previous studies have aimed to assess the quality of answers provided by AI chatbots related to various pathologies and treatment modalities. However, to the best of our knowledge, no studies have analyzed how GPT-4 compares to Google in quality of answers generated regarding cervical disc arthroplasty (CDA). To compare Google and GPT-4 in terms of 1) question types, 2) initial response readability, 3) ChatGPT's ability to modify responses for increased readability, and 4) numerical response accuracy for the top 10 most FAQs related to CDA.

Methods: "Cervical disc arthroplasty" was searched on Google and GPT-4 on December 18, 2023. The top 10 FAQs were recorded and analyzed using the Rothwell system for categorization and JAMA criteria for source quality. Readability was assessed by Flesch Reading Ease and Flesch-Kincaid grade level. GPT-4 was also prompted to revise text for low-literacy readability. We used Student's t-tests for statistical comparisons, setting significance at $p < 0.05$.

Results: FAQs from Google predominantly related to technical details and evaluation of surgery, paralleling GPT-4's focus, which also included indications/management. No significant differences were found in readability between GPT-4 and Google, displaying a similar Flesch-Kincaid grade level (13.06 vs. 12.24, $p = 0.410$) and Flesch Reading Ease score (36.87 vs. 40.05, $p = 0.528$). Upon prompting GPT-4 to improve the readability of its responses, GPT-4 showed a lower Flesch-Kincaid grade level (6.58 vs. 13.06 vs. 12.24, $p < 0.001$) and a higher Flesch Reading Ease score (76.20 vs. 36.87 vs. 40.05, $p < 0.001$). JAMA scores indicated no quality difference between sources (2.00 vs. 2.00, $p = 1.000$). Numerically, 60% of responses differed, with GPT-4 suggesting a broader recovery period for CDA.

Conclusions: This study highlights GPT-4's potential to enhance patient education through the provision of information on CDA. While the initial readability of GPT-4's responses was comparable to Google's, with a similar collegiate-level complexity, GPT-4 demonstrated a remarkable ability to simplify responses upon request, significantly lowering the Flesch-Kincaid grade level. This suggests that GPT-4 could fill gaps in online resources, particularly benefiting users with lower health literacy. Moreover, the study revealed discrepancies in numerical answers between Google and GPT-4, underscoring the need for consistent and accurate medical information online. Despite limitations such as potential biases due to personalized search results and the paid nature of GPT-4, the findings advocate for further refinement of AI chatbots to better align with patient language and understanding. The study calls for ongoing efforts to ensure that AI tools like GPT-4 not only provide accurate

medical information but also present it in a manner that is accessible to all users, thereby supporting informed healthcare decisions.

CODEX AI: Clinical Orthopaedic Data Extraction - Using Large Language Models for Improved Clinical Data Capture and Coding in Clinical Notes

*Joshua Rozell - NYU Langone Orthopedic Hospital - New York, USA

Kush Attal - NYU Grossman School of Medicine - New York City, USA

Lefko Charalambous - NYU Langone Orthopedic Hospital - New York City, USA

Unmet Need (Problem Statement): Electronic health records (EHR) are notoriously poorly suited to the needs of modern healthcare. In addition, documentation is one of the most time-consuming and disliked aspects of medical practice.¹ Moreover, the free-text nature of many notes makes it difficult to track discrete endpoints such as patient-reported-outcomes (PROs). With increasing requirements by regulators and payors to track outcomes, healthcare systems are burdened to create their own expensive custom solutions for tracking outcomes.² Also, clinical research organizations can benefit from improved data collection from free-text notes. Taken together, there is a significant unmet clinical need for a turnkey solution to create free-text clinical notes and translate them into structured datasets.

Solution: Our team is creating a custom-built large language model (LLM) using Retrieval Augmented Generation (RAG) which will be able to read and write clinical notes and provide structured datasets. RAG is a technique that plugs an external database to LLMs to keep them up-to-date. First, a retrieval model retrieves the most relevant information from a stored database (e.g., relevant past operative notes from the LLM's training dataset) for a query (e.g., capture data for this hip arthroplasty operative note). Afterwards, these retrieved op notes are sent with the query to the LLM, producing more accurate and contextually relevant responses compared to LLMs alone. With this, the model will be able to write clinical notes as instructed and read novel clinical text for relevant data points such as PROs and procedures. Importantly, this model will be able to make recommendations based on the notes, such as phrasing changes to optimize prior-authorization clearance, recommending CPT billing codes, and highlighting sections of notes justifying those recommendations.

The Current Market (Brief comparison of competitors and what our competitive advantage is): Commercial competitors include Fathom AI and Galeai. Notably, our model is unique because it annotates segments of notes with the reasoning behind its decision. Additionally, our model is built on a unique, growing dataset, consisting of high-quality clinical notes with associated verified billing codes. Competitor companies can only suggest codes based on natural language processing, but our model is validated with notes known to meet the rigorous free-text standards for associated codes.

Strategy (Development strategy, go to market strategy, reimbursement strategy): Our business strategy will focus on a three-prong market—insurance companies, clinical research organizations, and healthcare providers. We will offer insurance companies automated language model tools to parse the healthcare record for the required criteria for prior authorizations. CROs will leverage our tool to extract structured data from free-text clinical notes. Clinicians can utilize the tool to both write notes and receive billing code recommendations. All tools will be offered via a standard subscription service model.

1. Gaffney A, Woolhandler S, Cai C, et al. Medical Documentation Burden Among US Office-Based Physicians in 2019: A National Study. *JAMA Intern Med.* 2022;182(5):564–566. doi:10.1001/jamainternmed.2022.0372
2. Deans CF, et al. New CMS Merit-Based Incentive Payment System Value Pathway After Total Knee and Hip Arthroplasty: Preparing for Mandatory Reporting. *J Arthroplasty.* 2024;39(5):1131-1135. doi:10.1016/j.arth.2024.01.037

GPT-4 as a Source of Patient Information for Anterior Cervical Discectomy and Fusion: A Comparative Analysis Against Google Web Search

*Mitchell Ng - Maimonides Medical Center - Brooklyn, United States of America

Paul Mastrokostas - Maimonides Medical Center - Brooklyn, USA

Leonidas Mastrokostas - Maimonides Medical Center - Brooklyn, USA

Matthew Magruder - Maimonides Medical Center - Brooklyn, USA

Ahmed Emara - Cleveland Clinic - Cleveland, USA

Ian Wellington - University of Connecticut - Hartford, USA

Ahmed Saleh - Maimonides Medical Center - Brooklyn, USA

Jad Monsef - SUNY Downstate Medical Center - Brooklyn, USA

Afshin Razi - Maimonides Medical Center - Brooklyn, USA

Objectives: ChatGPT, an AI chatbot developed by OpenAI, is used by over 100 million weekly users for its ability to provide insightful answers to various queries. Previous studies have aimed to assess the quality of answers provided by AI chatbots related to various pathologies and treatment modalities. However, to the best of our knowledge, no studies have analyzed how GPT-4 compares to Google in quality of answers generated regarding a common spinal pathology such as ACDF. This study aims to compare Google and GPT-4 in terms of 1) question types, 2) response readability, 3) source quality, and 4) numerical response accuracy for the top 10 most frequently asked questions (FAQs) about anterior cervical discectomy and fusion (ACDF).

Methods: "Anterior cervical discectomy and fusion" was searched on Google and GPT-4 on December 18, 2023. Top 10 FAQs were classified according to the Rothwell system. Source quality was evaluated using *JAMA* benchmark criteria and readability was assessed using Flesch Reading Ease and Flesch-Kincaid grade level. Differences in *JAMA* scores, Flesch-Kincaid grade level, Flesch Reading Ease, and word count between platforms were analyzed using Student's t-tests. Statistical significance was set at the 0.05 level.

Results: FAQs from Google were varied, while GPT-4 focused on technical details and indications/management. GPT-4 showed a higher Flesch-Kincaid grade level (12.96 vs. 9.28, $p=0.003$), lower Flesch Reading Ease score (37.07 vs. 54.85, $p=0.005$), and higher *JAMA* scores for source quality (3.333 vs. 1.800, $p=0.016$). Numerically, 6 out of 10 responses varied between platforms, with GPT-4 providing broader recovery timelines for ACDF.

Conclusions: This study demonstrates GPT-4's ability to elevate patient education by providing high-quality, diverse information tailored to those with advanced literacy levels. As AI technology evolves, refining these tools for accuracy and user-friendliness remains crucial, catering to patients' varying literacy levels and information needs in spine surgery.

Patient Experiences With a Smartphone Application (Post Op) in Elective Arthroplasty

Gagandeep Mahi - Kettering General Hospital - Coventry, GB

*Faizal Rayan - Kettering General Hospital - Kettering, United Kingdom

Myrto Vlazaki - University Hospitals of Leicester NHS Trust - Leicester, United Kingdom

Srinivasan Shyamsundar - Kettering General Hospital - Kettering, United Kingdom

Hamidreza Khairandish - Kettering General Hospital - Kettering, United Kingdom

Introduction: The widespread adoption of smartphones has facilitated the development of innovative applications to enhance patient experiences in the rapidly evolving domain of digital health technologies. The introduction emphasises the extensive global use of cellphones and their potential uses in healthcare, as shown by the "Post Op" smartphone application as a notable therapeutic mobile application. This system prioritises postoperative assistance and emphasises data recording, adherence to national standards, and a user-friendly interface. The study seeks to evaluate the app's effectiveness in achieving these objectives, with a particular focus on its ability to improve patient experiences and recovery protocols and its continuous improvements based on user feedback.

Methods:

A cohort of patients at Kettering General Hospital (KGH) who underwent elective joint arthroplasty surgeries over the past one to twelve months was interviewed over the phone using a meticulously created, organised, and standardised questionnaire to gather their feedback on the "Post Op" smartphone application.

Results:

A total of 42 consecutive patients, consisting of 22 total hip replacement (THR) patients and 20 total knee replacement (TKR) patients, who had undergone elective joint arthroplasty procedures at a district hospital- Kettering General Hospital, United Kingdom were surveyed for the study. The "Post Op" mobile application garnered overwhelmingly positive feedback from the respondents, whose median age was 66. The average score for ease of use was 5.31 on a scale ranging from 1 to 6. The only two patients who scored lower were the ones who encountered difficulties with photography. Nevertheless, the app's overall performance, particularly in uploading photos, received an average rating of 4.78. Almost ninety-eight percent of respondents expressed willingness to recommend the app despite encountering technical challenges. They emphasised the program's positive impact on boosting recovery confidence and reducing unnecessary doctor appointments. Narrative responses underscored the simplicity of use, the level of support provided, and the promptness of communication with medical personnel. Patients who underwent elective arthroplasty frequently express positive feedback regarding the "Post Op" programme, emphasising its potential benefits for postoperative care.

Conclusion:

To summarise the study recognises the achievements of the locally developed software and identifies areas for potential enhancement, providing valuable information on the impact of the "Post Op" smartphone application on postoperative care of elective arthroplasty patients. The "Post Op" mobile application connects the hospital and the patient's residence. It serves as a virtual connection between patients and their professional team, preventing them from experiencing a sense of abandonment after being discharged from the hospital. Home recovery aids in

achieving the global healthcare objective of minimising hospital stays and overall financial implications associated with avoidable hospitable visits. Further research and iterative modifications are being looked into, in order to enhance patient experiences and ensure that the app complies with healthcare regulations for adoption at a wider scale.

The Utilization of the Pixee Knee+ Augmented Reality-Assisted Navigation System in Total Knee Arthroplasty

*Safa Kassab - Orthopedic Specialists of Oakland County - Bloomfield, USA

Jacob Waitzman - Wayne State University - Detroit, USA

Background: Total Knee Arthroplasty (TKA) requires precise alignment for optimal post-operative outcomes and prosthesis longevity. Recently, augmented reality (AR) has emerged as a promising technology in surgical procedures, including TKA. This study evaluates the feasibility and accuracy of the Knee+ Augmented Reality-Assisted Navigation (ARAN) system by Pixee Medical Company in an Ambulatory Surgical Center (ASC) setting.

Methods: Our study involved 17 consecutive TKA patients treated with the Knee+ ARAN system at an ASC from August 2022 to October 2022. Demographic data, including sex, age, ASA score, height, weight, and BMI, were recorded.

Postoperative measurements of the mechanical distal femoral angle (MDFA), mechanical distal tibial angle (MDTA), posterior tibial slope (PTS), and femoral-tibial angle (FTA) were compared to the ideal intraoperative angles. Outliers were defined as deviations greater than 3° from the planned angles.

Results: In this study, 15 out of 17 TKAs utilizing the Pixee Knee+ ARAN system were analyzed. All mean post-operative CT measurements were within clinically acceptable ranges. The study also found that surgeries using the Knee+ system had a longer incision-to-closing time relative to the control group, averaging 48.33 minutes versus 40.90 minutes respectively. These results indicate clinically acceptable accuracy and precision in alignment with the Knee+ ARAN system, albeit with a slight increase in surgery duration.

Conclusion: The first study evaluating the Knee+ ARAN system in an ASC setting indicates its suitability for outpatient centers, highlighting its precision, portability, and cost-effectiveness. Larger studies utilizing outcome measures can further assess the system's advantages and disadvantages.

Figures

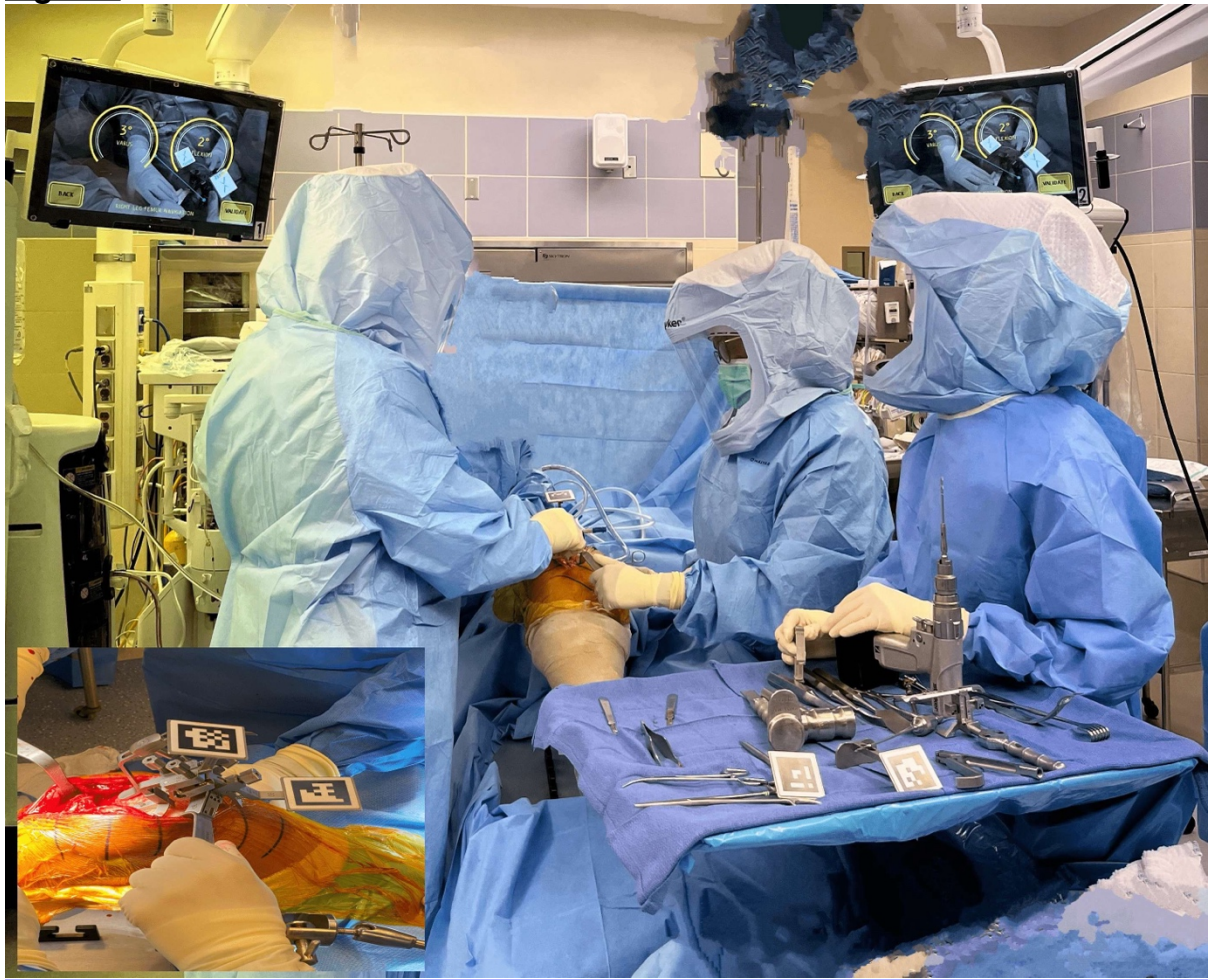


[Figure 1](#)



[Figure 2](#)



[Figure 3](#)

Development of a Deep Learning Model for Determining Post-Operative Coronal Plane Alignment of the Knee (CPAK) Classification

*Anoop Chandrashekar - Vanderbilt - Nashville, United States of America

Courtney Baker - Vanderbilt - Nashville, USA

Stephen Engstrom - Vanderbilt University Medical Center - Nashville, USA

Gregory Polkowski - Vanderbilt University Medical Center - Nashville, USA

Martin Faschingbauer - Department of Orthopedic Surgery, RKU, University of Ulm - Ulm, Germany

John Ryan Martin - Vanderbilt Health - Hendersonville, USA

Introduction: The Coronal Plane Alignment of the Knee (CPAK) classification proposes 9 phenotypes of knee alignment based on constitutional alignment and joint line obliquity. There is evidence that proposes that knee phenotypes may have geographic, racial, and sexual variation. The aim of this study was to describe the knee phenotypes of patients with arthritis seeking treatment total knee arthroplasty in Germany.

Methods: Long leg radiographs (LLR) from 566 German patients were manually annotated to measure mechanical hip-knee-ankle (mHKA) angles, mechanical lateral distal femoral angle (LDFA), and mechanical medial proximal tibial angle (MPTA).

Results: Across the 566 knees included, the average mHKA, LDFA, and MPTA in the cohort was 5.53° (SEM= 0.219), 83.5° (SEM= 0.146), and 85.2° (SEM= 0.416) respectively. 406 patients had CPAK Group 3 knees, and 160 patients had Group 1 knees. No other phenotypes were observed in the cohort.

Conclusions: CPAK is a pragmatic classification system to describe knee alignment. Previous research has identified that classification may depend on several epidemiological patient factors.

We applied the classification system to a German cohort to further validate and strengthen the system.